Soil Sampling and Methods of Analysis

Second Edition

Edited by
M.R. Carter
E.G. Gregorich

Canadian Society of Soil Science

Soil Sampling and Methods of Analysis

Second Edition

In physical science the first essential step in the direction of learning any subject is to find principles of numerical reckoning and practicable methods for measuring some quality connected with it. I often say that when you can measure what you are speaking about, and express it in numbers, you know something about it; but when you cannot measure it, when you cannot express it in numbers, your knowledge is of a meagre and unsatisfactory kind; it may be the beginning of knowledge, but you have scarcely in your thoughts advanced to the state of science, whatever the matter may be.

Lord Kelvin, Popular Lectures and Addresses (1891–1894),
vol. 1, *Electrical Units of Measurement*

Felix qui potuit rerum cognoscere causas.

Happy the man who has been able to learn the causes of things.

Virgil: Georgics (II, 490)

Soil Sampling and Methods of Analysis

Second Edition

Edited by
M.R. Carter
E.G. Gregorich

Canadian Society of Soil Science

CRC Press
Taylor & Francis Group
6000 Broken Sound Parkway NW, Suite 300
Boca Raton, FL 33487-2742

Printed in the United States of America on acid-free paper
10 9 8 7 6 5 4 3 2 1

International Standard Book Number-13: 978-0-8493-3586-0 (Hardcover)

Library of Congress Cataloging-in-Publication Data

Soil sampling and methods of analysis / edited by M.R. Carter and E.G. Gregorich. -- 2nd ed.
p. cm.
Includes bibliographical references and index.
ISBN-13: 978-0-8493-3586-0 (alk. paper)
ISBN-10: 0-8493-3586-8 (alk. paper)
1. Soils--Analysis. 2. Soils--Sampling. I. Carter, Martin R. II. Gregorich, E. G. III. Title.

S593.S7425 2007
631.4'1--dc22 2006102606

Visit the Taylor & Francis Web site at
http://www.taylorandfrancis.com

and the CRC Press Web site at
http://www.crcpress.com

PREFACE

This volume is an update of the book, *Soil Sampling and Methods of Analysis*, first published in 1993. The aims of this second edition remain the same as those of the earlier edition—to provide a compilation of soil analytical and sampling methods that are commonly used, straightforward, and relatively easy to use. The materials and procedures for these methods are presented with sufficient detail and information, along with key references, to characterize the potential and limitation of each method.

As methods develop, so do their degree of sophistication. Taking these developments into account, the second edition includes several chapters that serve as ''primers,'' the purpose of which is to describe the overall principles and concepts behind a particular type or types of measurement, rather than just methods alone.

All of the chapters retained from the earlier edition have been modified and updated. The second edition also introduces new chapters, particularly in the areas of biological and physical analyses, and soil sampling and handling. For example, the ''Soil Biological Analyses'' section contains new chapters to reflect the growing number and assortment of new microbiological techniques and the burgeoning interest in soil ecology. New chapters are offered describing tools that characterize the dynamics and chemistry of soil organic matter. A new section devoted to soil water presents up-to-date field- and laboratory-based methods that characterize saturated and unsaturated soil hydraulic properties.

This second edition of *Soil Sampling and Methods of Analysis* comprises 7 sections and a total of 85 chapters and 2 appendices written by 140 authors and co-authors. Each section is assembled by two section editors and each chapter reviewed by at least two external reviewers. We are grateful to these people for their diligent work in polishing and refining the text and helping to bring this new volume to fruition. We particularly thank Elaine Nobbs for her support in working with the many authors involved in writing this book.

We offer this new edition of *Soil Sampling and Methods of Analysis* in the belief that it will continue as a useful tool for researchers and practitioners working with soil.

M.R. Carter and E.G. Gregorich
Editors

CANADIAN SOCIETY OF SOIL SCIENCE

The Canadian Society of Soil Science is a nongovernmental, nonprofit organization for scientists, engineers, technologists, administrators, students, and others interested in soil science. Its three main objectives are

- To promote the wise use of soil for the benefit of society
- To facilitate the exchange of information and technology among people and organizations involved in soil science
- To promote research and practical application of findings in soil science

The society produces the international scientific publication, the *Canadian Journal of Soil Science*, and each year hosts an international soil science conference. It sponsored the first edition of *Soil Sampling and Methods of Analysis* (Lewis Publishers, CRC Press, 1993) and also promoted the publication of the popular reference book *Soil and Environmental Science Dictionary* (CRC Press, 2001). The society publishes a newsletter to share information and ideas, and maintains active liaison and partnerships with other soil science societies.

For more information about the Canadian Society of Soil Science, please visit www.csss.ca.

EDITORS

M.R. Carter holds degrees in agriculture and soil science from the University of Alberta and obtained a PhD in soil science from the University of Saskatchewan in 1983. Since 1977, he has held agricultural research positions with Agriculture and Agri-Food Canada (AAFC) and is currently a research scientist at the AAFC Research Center, Charlottetown, Prince Edward Island. Dr. Carter is a fellow and past-president of the Canadian Society of Soil Science, and past editor of the *Canadian Journal of Soil Science*. He edited the first edition of *Soil Sampling and Methods of Analysis*, (CRC Press, 1993) and also edited *Conservation Tillage in Temperate Agroecosystems* (CRC Press, 1994) and *Structure and Organic Matter Storage in Agricultural Soils* (CRC Press, 1996). In collaboration with Dr. Gregorich, he edited *Soil Quality for Crop Production and Ecosystem Health* (Elsevier, 1997) and *Soil & Environmental Science Dictionary* (CRC Press, 2001). Dr. Carter presently serves as editor-in-chief for the international scientific journal *Agriculture Ecosystems & Environment*.

E.G. Gregorich is a research scientist with Agriculture and Agri-Food Canada at the Central Experimental Farm in Ottawa, Canada. His work focuses on soil biochemistry, particularly carbon and nitrogen cycling in soil. He is a fellow and past-president of the Canadian Society of Soil Science, and has served the Soil Science Society of America as chair of the soil biology and biochemistry division. Dr. Gregorich has been a member of the International Panel on Climate Change, has conducted field studies in Scotland, New Zealand, and Antarctica, and directs a Canadian international development project in Vietnam. He has served as associate editor for the *Journal of Environmental Quality*; *Agriculture, Ecosystems & Environment*; *European Journal of Soil Science*; and the *Canadian Journal of Soil Science*. This is the third book on which he and Dr. Carter have collaborated as editors.

CONTRIBUTORS

D. Acosta-Mercado
Department of Biology
University of Puerto Rico
Mayaguez, Puerto Rico

J.A. Addison
School of Sustainability and Environment
Royal Roads University
Victoria, British Columbia, Canada

S.M. Adl
Department of Biology
Dalhousie University
Halifax, Nova Scotia, Canada

D.W. Anderson
Department of Soil Science
University of Saskatchewan
Saskatoon, Saskatchewan, Canada

Denis A. Angers
Agriculture and Agri-Food Canada
Quebec, Quebec, Canada

H. Antoun
Department of Soils and Agrifood Engineering
Laval University
Quebec, Quebec, Canada

J.M. Arocena
College of Science and Management
University of Northern British Columbia
Prince George, British Columbia, Canada

V.L. Bailey
Biological Sciences Division
Pacific Northwest National Laboratory
Richland, Washington, United States

G.H. Baker
Entomology
Commonwealth Scientific and Industrial Research Organization
Glen Osmond, South Australia, Australia

J.A. Baldock
Land and Water
Commonwealth Scientific and Industrial Research Organization
Glen Osmond, South Australia, Australia

B.C. Ball
Scottish Agricultural College
Edinburgh, Scotland, United Kingdom

M.H. Beare
New Zealand Institute for Crop and Food Research
Christchurch, New Zealand

E.G. Beauchamp
Department of Land Resource Science
University of Guelph
Guelph, Ontario, Canada

V.M. Behan-Pelletier
Agriculture and Agri-Food Canada
Ottawa, Ontario, Canada

N. Bélanger
Department of Soil Science
University of Saskatchewan
Saskatoon, Saskatchewan, Canada

Normand Bertrand
Agriculture and Agri-Food Canada
Quebec, Quebec, Canada

R.P. Beyaert
Agriculture and Agri-Food Canada
London, Ontario, Canada

H. Bolton, Jr.
Biological Sciences Division
Pacific Northwest National Laboratory
Richland, Washington, United States

Jeff Braidek
Saskatchewan Agriculture and Food
Saskatoon, Saskatchewan, Canada

E. Bremer
Symbio Ag Consulting
Lethbridge, Alberta, Canada

J.A. Brierley
Agriculture and Agri-Food Canada
Edmonton, Alberta, Canada

P.C. Brookes
Agriculture and Environment Division
Rothamsted Research
Harpenden, Hertfordshire, United Kingdom

M.S. Bullock
Holly Hybrids
Sheridan, Wyoming, United States

B.J. Cade-Menun
Department of Geological and Environmental Sciences
Stanford University
Stanford, California, United States

C.A. Campbell
Agriculture and Agri-Food Canada
Ottawa, Ontario, Canada

J. Caron
Department of Soils and Agrifood Engineering
Laval University
Quebec, Quebec, Canada

M.R. Carter
Agriculture and Agri-Food Canada
Charlottetown, Prince Edward Island
Canada

Martin H. Chantigny
Agriculture and Agri-Food Canada
Quebec, Quebec, Canada

M.J. Clapperton
Agriculture and Agri-Food Canada
Lethbridge, Alberta, Canada

F.J. Cook
Land and Water
Commonwealth Scientific and Industrial Research Organization
Indooroopilly, Queensland, Australia

F. Courchesne
Department of Geography
University of Montreal
Montreal, Quebec, Canada

H.P. Cresswell
Land and Water
Commonwealth Scientific and Industrial Research Organization
Canberra, Australian Capital Territory
Australia

J.A. Crumbaugh
Canadian Forest Service
Natural Resources Canada
Edmonton, Alberta, Canada

J.L.B. Culley
Agriculture and Agri-Food Canada
Ottawa, Ontario, Canada

M.P. Curran
British Columbia Ministry of Forests
Nelson, British Columbia, Canada

Denis Curtin
New Zealand Institute for Crop and Food Research
Christchurch, New Zealand

Y. Dalpé
Agriculture and Agri-Food Canada
Ottawa, Ontario, Canada

Pauline Défossez
French National Institute for Agricultural Research
Laon, France

J.R. de Freitas
Department of Soil Science
University of Saskatchewan
Saskatoon, Saskatchewan, Canada

C.F. Drury
Agriculture and Agri-Food Canada
Harrow, Ontario, Canada

K.E. Dunfield
Department of Land Resource Science
University of Guelph
Guelph, Ontario, Canada

M. Duquette
SNC-Lavalin
Montreal, Quebec, Canada

B.H. Ellert
Agriculture and Agri-Food Canada
Lethbridge, Alberta, Canada

J.A. Elliott
Environment Canada
Saskatoon, Saskatchewan, Canada

D.E. Elrick
Department of Land Resource Science
University of Guelph
Guelph, Ontario, Canada

R.E. Farrell
Department of Soil Science
University of Saskatchewan
Saskatoon, Saskatchewan, Canada

Ty P.A. Ferré
Department of Hydrology and Water Resources
University of Arizona
Tucson, Arizona, United States

C.T. Figueiredo
Department of Renewable Resources
University of Alberta
Edmonton, Alberta, Canada

T.A. Forge
Agriculture and Agri-Food Canada
Agassiz, British Columbia, Canada

C.A. Fox
Department of Renewable Resources
Agriculture and Agri-Food Canada
Harrow, Ontario, Canada

J.J. Germida
Department of Soil Science
University of Saskatchewan
Saskatoon, Saskatchewan, Canada

Tee Boon Goh
Department of Soil Science
University of Manitoba
Winnipeg, Manitoba, Canada

C.D. Grant
School of Earth and Environmental Sciences
University of Adelaide
Glen Osmond, South Australia, Australia

E.G. Gregorich
Agriculture and Agri-Food Canada
Ottawa, Ontario, Canada

M. Grimmett
Agriculture and Agri-Food Canada
Charlottetown, Prince Edward Island
Canada

P.H. Groenevelt
Department of Land Resource Science
University of Guelph
Guelph, Ontario, Canada

Umesh C. Gupta
Agriculture and Agri-Food Canada
Charlottetown, Prince Edward Island
Canada

C. Hamel
Agriculture and Agri-Food Canada
Swift Current, Saskatchewan, Canada

X. Hao
Agriculture and Agri-Food Canada
Lethbridge, Alberta, Canada

S.C. Hart
School of Forestry and Merriam-Powell Center for Environmental Research
Northern Arizona University
Flagstaff, Arizona, United States

A. Hartmann
National Institute of Agronomic Research
Dijon, France

W.H. Hendershot
Department of Renewable Resources
McGill University
Sainte Anne de Bellevue, Quebec, Canada

Ganga M. Hettiarachchi
School of Earth and Environmental Sciences
University of Adelaide
Glen Osmond, South Australia, Australia

D.W. Hopkins
Scottish Crop Research Institute
Dundee, Scotland, United Kingdom

H.H. Janzen
Agriculture and Agri-Food Canada
Lethbridge, Alberta, Canada

R.G. Kachanoski
Department of Renewable Resources
University of Alberta
Edmonton, Alberta, Canada

Klaus Kaiser
Soil Sciences
Martin Luther University
Halle-Wittenberg, Halle, Germany

Karsten Kalbitz
Soil Ecology
University of Bayreuth
Bayreuth, Germany

Y.P. Kalra
Canadian Forest Service
Natural Resources Canada
Edmonton, Alberta, Canada

A. Karam
Department of Soils and Agrifood Engineering
Laval University
Quebec, Quebec, Canada

Thomas Keller
Department of Soil Sciences
Swedish University of Agricultural Sciences
Uppsala, Sweden

J. Kimpinski
Agriculture and Agri-Food Canada
Charlottetown, Prince Edward Island
Canada

Peter J.A. Kleinman
Pasture Systems and Watershed Management Research Center
U.S. Department of Agriculture
University Park, Pennsylvania
United States

C.G. Kowalenko
Agriculture and Agri-Food Canada
Agassiz, British Columbia, Canada

D. Kroetsch
Agriculture and Agri-Food Canada
Ottawa, Ontario, Canada

H. Lalande
Department of Renewable Resources
McGill University
Sainte Anne de Bellevue, Quebec, Canada

David R. Lapen
Agriculture and Agri-Food Canada
Ottawa, Ontario, Canada

F.J. Larney
Agriculture and Agri-Food Canada
Lethbridge, Alberta, Canada

R. Lessard
Environmental Division
Bodycote Testing Group
Edmonton, Alberta, Canada

B.C. Liang
Environment Canada
Gatineau, Quebec, Canada

N.J. Livingston
Department of Biology
University of Victoria
Victoria, British Columbia, Canada

D.H. Lynn
Department of Integrative Biology
University of Guelph
Guelph, Ontario, Canada

J.D. MacDonald
Agriculture and Agri-Food Canada
Quebec, Quebec, Canada

D.G. Maynard
Pacific Forestry Centre
Natural Resources Canada
Victoria, British Columbia, Canada

R.A. McBride
Department of Land Resource Science
University of Guelph
Guelph, Ontario, Canada

W.B. McGill
College of Science and Management
University of Northern British Columbia
Prince George, British Columbia
Canada

G.R. Mehuys
Department of Renewable Resources
McGill University
Sainte Anne de Bellevue, Quebec, Canada

A.R. Mermut
Department of Soil Science
University of Saskatchewan
Saskatoon, Saskatchewan, Canada

J.C. Michel
INH–INRA–University of Angers
Angers, France

Jim J. Miller
Agriculture and Agri-Food Canada
Lethbridge, Alberta, Canada

J.O. Moir
Department of Soil Science
University of Saskatchewan
Saskatoon, Saskatchewan, Canada

D.D. Myrold
Department of Crop and Soil Science
Oregon State University
Corvallis, Oregon, United States

R. Naasz
Department of Soils and Agrifood
Engineering
Laval University
Quebec, Quebec, Canada

I.P. O'Halloran
University of Guelph
Ridgetown, Ontario, Canada

D.C. Olk
U.S. Department of Agriculture
Agriculture Research Service
National Soil Tilth Laboratory
Ames, Iowa, United States

D. Paré
Natural Resources Canada
Canadian Forest Service
Quebec, Quebec, Canada

L.E. Parent
Department of Soils and Agrifood
Engineering
Laval University
Quebec, Quebec, Canada

G.W. Parkin
Department of Land Resource Science
University of Guelph
Guelph, Ontario, Canada

G.T. Patterson
Agriculture and Agri-Food Canada
Truro, Nova Scotia, Canada

Dan Pennock
Department of Soil Science
University of Saskatchewan
Saskatoon, Saskatchewan, Canada

Caroline Preston
Pacific Forestry Centre
Natural Resources Canada
Victoria, British Columbia, Canada

D. Prévost
Agriculture and Agri-Food Canada
Quebec, Quebec, Canada

P. Qian
Department of Soil Science
University of Saskatchewan
Saskatoon, Saskatchewan, Canada

D. Reyes
Department of Renewable Resources
McGill University
Sainte Anne de Bellevue, Quebec, Canada

W.D. Reynolds
Agriculture and Agri-Food Canada
Harrow, Ontario, Canada

Guy Richard
French National Institute for Agricultural Research
Olivet, France

Philippe Rochette
Agriculture and Agri-Food Canada
Quebec, Quebec, Canada

L. Rock
Agriculture and Agri-Food Canada
Lethbridge, Alberta, Canada

P.M. Rutherford
College of Science and Management
University of Northern British Columbia
Prince George, British Columbia, Canada

S. Sauvé
Department of Chemistry
University of Montreal
Montreal, Quebec, Canada

J.J. Schoenau
Department of Soil Science
University of Saskatchewan
Saskatoon, Saskatchewan, Canada

Andrew N. Sharpley
Crop, Soil and Environmental Sciences
University of Arkansas
Fayetteville, Arkansas, United States

S.C. Sheppard
ECOMatters Inc.
W.B. Lewis Business Centre
Pinawa, Manitoba, Canada

B.C. Si
Department of Soil Science
University of Saskatchewan
Saskatoon, Saskatchewan, Canada

Myrna J. Simpson
Department of Physical and Environmental Sciences
University of Toronto
Toronto, Ontario, Canada

J.O. Skjemstad
Land and Water
Commonwealth Scientific and Industrial Research Organization
Glen Osmond, South Australia, Australia

J.L. Smith
U.S. Department of Agriculture
Agriculture Research Service
Washington State University
Pullman, Washington, United States

Y.K. Soon
Agriculture and Agri-Food Canada
Beaverlodge, Alberta, Canada

P. St-Georges
Agriculture and Agri-Food Canada
Ottawa, Ontario, Canada

C. Swyngedouw
Environmental Division
Bodycote Testing Group
Calgary, Alberta, Canada

M. Tenuta
Department of Soil Science
University of Manitoba
Winnipeg, Manitoba, Canada

Y.-C. Tien
Agriculture and Agri-Food Canada
London, Ontario, Canada

H. Tiessen
Inter-American Institute for Global Change Research
Sao Jose dos Campos
Sao Paulo, Brazil

E. Topp
Agriculture and Agri-Food Canada
London, Ontario, Canada

G. Clarke Topp
Agriculture and Agri-Food Canada
Ottawa, Ontario, Canada

T. Sen Tran
Institute of Research and Development in Agroenvironment
Quebec, Quebec, Canada

M.-C. Turmel
Department of Geography
University of Montreal
Montreal, Quebec, Canada

A.J. VandenBygaart
Agriculture and Agri-Food Canada
Ottawa, Ontario, Canada

Ken C.J. Van Rees
Department of Soil Science
University of Saskatchewan
Saskatoon, Saskatchewan, Canada

R.P. Voroney
Department of Land Resource Science
University of Guelph
Guelph, Ontario, Canada

C. Wang
Agriculture and Agri-Food Canada
Ottawa, Ontario, Canada

Jennifer L. Weld
Department of Crop and Soil Sciences
The Pennsylvania State University
University Park, Pennsylvania, United States

G. Wen
Lemington, Ontario, Canada

O.O.B. Wendroth
Department of Plant and
Soil Sciences
University of Kentucky
Lexington, Kentucky, United States

J.P. Winter
Nova Scotia Agricultural College
Truro, Nova Scotia, Canada

N. Wypler
Leibniz-Centre for Agricultural
Landscape Research
Institute for Soil Landscape Research
Müncheberg, Germany

X.M. Yang
Agriculture and Agri-Food Canada
Harrow, Ontario, Canada

Thomas Yates
Department of Soil Science
University of Saskatchewan
Saskatoon, Saskatchewan,
Canada

N. Ziadi
Agriculture and Agri-Food Canada
Quebec, Quebec, Canada

TABLE OF CONTENTS

I. SOIL SAMPLING AND HANDLING

Section Editors: G.T. Patterson and M.R. Carter

Chapter 1
Soil Sampling Designs

Dan Pennock and Thomas Yates

University of Saskatchewan

Saskatoon, Saskatchewan, Canada

Jeff Braidek

Saskatchewan Agriculture and Food

Saskatoon, Saskatchewan, Canada

1.1 INTRODUCTION

Sampling involves the selection from the total population of a subset of individuals upon which measurements will be made; the measurements made on this subset (or sample) will then be used to estimate the properties (or parameters) of the total population. Sampling is inherent to any field research program in soil science because the measurement of the total population is impossible for any realistic study. For example, even a single 10 ha field contains about 100,000 1 m^2 soil pits or 1×10^7 10 cm^2 cores, and sampling of the entire population would be more of an unnatural obsession than a scientific objective.

Sampling design involves the selection of the most efficient method for choosing the samples that will be used to estimate the properties of the population. The definition of the population to be sampled is central to the initial formulation of the research study (Eberhardt and Thomas 1991; Pennock 2004). The sampling design defines how specific elements will be selected from the population, and these sampled elements form the sample population.

There are many highly detailed guides to specific sampling designs and the statistical approaches appropriate for each design. The goal of this chapter is to present the issues that should be considered when selecting an appropriate sampling design. In the final section, specific design issues associated with particular research designs are covered. Suggested readings are given in each section for more in-depth study on each topic.

1.2 APPROACHES TO SAMPLING

1.2.1 Haphazard, Judgment, and Probability Sampling

Sample locations can be chosen using (a) haphazard sampling, (b) judgment sampling, or (c) probability sampling. Haphazard, accessibility, or convenience sampling involves a series of nonreproducible, idiosyncratic decisions by the sampler and no systematic attempt is made to ensure that samples taken are representative of the population being sampled. This type of sampling is antithetical to scientific sampling designs. Judgment sampling (also termed purposive sampling [e.g., de Gruijter 2002]) involves the selection of sampling points based on knowledge held by the researcher. Judgment sampling can result in accurate estimates of population parameters such as means and totals but cannot provide a measure of the accuracy of these estimates (Gilbert 1987). Moreover the reliability of the estimate is only as good as the judgment of the researcher. Probability sampling selects sampling points at random locations using a range of specific sample layouts, and the probability of sample point selection can be calculated for each design. This allows an estimate to be made of the accuracy of the parameter estimates, unlike judgment sampling. This allows a range of statistical analyses based on the estimates of variability about the mean to be used, and is by far the most common type of sampling in soil science.

1.2.2 Research Designs Using Judgment Sampling

Pedogenetic and soil geomorphic studies focus on determining the processes that formed the soil properties or landscapes under study and the environments that controlled the rates of these processes. Pedon-scale studies are closely associated with the development of soil taxonomic systems, and focus on vertical, intrapedon processes. Soil geomorphic studies are the interface between quaternary geology and soil science, and soil geomorphologists focus on lateral transfer processes and the historical landscape evolution.

Both types of studies involve the identification of soil and/or sediment exposures that are highly resolved records of the sequence of processes that have formed the soil landscape. The researcher locates these exposures by using his judgment as to the landscape positions where optimum preservation of the soil–sediment columns is most likely. The development of the chronological sequence can be done with a detailed analysis of a single exposure; no replication of exposures is required.

Surveys are designed to define the extent of spatial units. Soil surveyors map the distribution of soil taxonomic units and provide descriptive summaries of the main properties of the soils. In soil survey the association between soil classes and landscape units is established in the field by judicious selection of sampling points (termed the free survey approach). This type of judgment sampling can be an extremely efficient way of completing the inventory. Contaminant surveys are most typically undertaken by private-sector environmental consultants, and the specific objective may range from an initial evaluation of the extent of contamination to the final stage of remediation of the problem. Laslett (1997) states that consultants who undertake these surveys almost always employ judgment sampling and place their samples where their experience and prior knowledge of site history suggest the contamination might be located. In many jurisdictions the sampling design may also be constrained by the appropriate regulatory framework.

1.2.3 Research Designs Using Probability Sampling

Inventory studies share the common goal of measuring the amount of a property or properties under study and the uncertainty surrounding our estimate of the amount. For example, in agronomic sampling we may wish to estimate the amount of plant-available nutrients in a given field; in contaminant sampling the goal may be to estimate the amount of a contaminant present at a site. In comparative mensurative experiments, comparisons are drawn among classes that the researcher defines but cannot control—for example, sampling points grouped by different soil textures, landform positions, soil taxonomic classes, and drainage class. Their location cannot be randomized by the researcher, unlike imposed treatments such as tillage type or fertilizer rates where randomization is essential. In manipulative experiments the treatments can be directly imposed by the researcher—ideally as fixed amounts that are applied precisely. Many studies are hybrid mensurative–manipulative designs—for example, the measurement of yield response to different fertilizer rates (imposed treatment) in different landform positions (characteristic or inherent treatment). The role of sampling in inventory, mensurative, and manipulative designs is very similar—to allow statistical estimation of the distribution of the parent population or populations. In inventory studies the statistical estimates may be the end point of the study.

Pattern studies are undertaken to assess and explain the spatial or temporal pattern of properties. Two main types of pattern studies exist: (a) the quantification of the spatial and temporal variability in properties and (b) hypothesis generation and testing using point patterns. In pattern studies the initial goal may be a visual assessment of the pattern of observations in time or space, and statistical estimation of the populations may be a secondary goal.

Geostatistical and other spatial statistical studies are undertaken to model the spatial pattern of soil properties, to use these models in the interpolation of values at unsampled locations, to assess the suitability of different spatial process models, or to assist in the design of efficient sampling programs.

1.3 STATISTICAL CONCEPTS FOR SAMPLING DESIGN

1.3.1 Measures of Central Tendency and Dispersion

The key characteristics of the distribution of attributes are measures of its central tendency and the dispersion of values around the measure of central tendency. In the initial stage of study formulation the researcher defines the population, which is composed of the sampling units and one or more attributes measured on these sampling units. Each attribute has a distribution of values associated with it, which can be characterized by parameters such as the population mean (μ) and variance (σ^2). A sample of the sampling units is drawn from the population, and statistics such as the sample mean ($\bar{x}$) and variance (s^2) are calculated, which serve as estimates of the population parameters. Calculations of these statistics are readily available and will not be repeated here. The number of samples taken is denoted as n. For sample populations that are more or less normally distributed the arithmetic mean ($\bar{x}$) is an appropriate measure of central tendency. The variance (s^2) is a common measure of the deviation of individual values from the mean and its square root; the standard deviation (s)

reports values in the same units as the mean. The coefficient of variation (CV) is a normalized measure of the amount of dispersion around the mean, and is calculated by

$$\mathrm{CV} = (s/\bar{x})100 \tag{1.1}$$

Sample populations in the soil science commonly show a long tail of values to the right of the distribution (i.e., they are right-skewed). In this case a log normal or other right-skewed distribution should be used.

The mathematical properties of the normal distribution are well understood and the probability that the true population mean lies within a certain distance of the sample mean can be readily calculated. For sample populations the estimated standard error of the sample mean is

$$s(\bar{x}) = s/\sqrt{n} \tag{1.2}$$

For a sample population that has a large sample size or where the standard error is known and that approximates a normal distribution, the true mean will be within ± 1.96 standard errors of the sample mean 95 times out of 100 (i.e., where the probability $P = 0.05$). The range defined these limits are the 95% confidence interval for the mean and these limits are the 95% confidence limits. The value 1.96 is derived from the t distribution, and values of t can be derived for any confidence limit. For sample populations based on a small sample size or where the standard error is not known the value of 1.96 must be replaced by a larger t-value with the appropriate degrees of freedom. A probability of exceeding a given standard error (α) may be selected for any sample distribution that approximates the normal distribution and the appropriate confidence limits calculated for that distribution.

1.3.2 Independence, Randomization, and Replication

The goal of sampling is to produce a sample that is representative of the target population. If the choice of samples is not probability based then a strong likelihood exists that the sample will not be representative of the population. For example, selection of sampling locations convenient to a farmyard (instead of distributed throughout the field) may lead to overestimates of soil nutrients due to overapplication of farmyard manure near the source of the manure through time. The use of probability-based sampling designs (i.e., the designs discussed in Section 1.4) confers a design-specific independence on the sample selection process, which satisfies the need for independence of samples required by classical statistical analysis (a theme developed in great detail by Brus and de Gruijter 1997).

Replication is an important consideration in mensurative and manipulative experiments. In a manipulative study, replication is the repeated imposition of a set of treatments (e.g., fertilizer or pesticide rates). In a pattern or mensurative study, replication is the repeated, unbiased selection and sampling of population elements in a particular class—for example, the selection of multiple 5×5 m slope elements in a field that have markedly convex downslope curvatures. Replication provides an estimate of the experimental error, and increasing replication improves precision by reducing the standard error of treatment or class means (Steel and Torrie 1980). Correct identification and sampling of replicates is critical for estimating the parameters of the class the sample is drawn from and is required for statistically correct procedures. Pseudoreplication (Hurlbert 1984) occurs when a researcher assumes a very general effect from a limited sampling and often occurs because the target population has not been clearly defined at the outset of the research.

Randomization is a consideration in manipulative designs. Steel and Torrie (1980, p. 135) summarizes the need for randomization:

> "... it is necessary to have some way of ensuring that a particular treatment will not be consistently favored or handicapped in successive replications by some extraneous sources of variation, known or unknown. In other words, every treatment should have an equal chance of being assigned to any experimental unit, be it unfavorable or favorable."

Randomization is implemented by ensuring the random placement of treatment plots within a field design; the repeated imposition of the same sequence of treatments in a block of treatments may cause an erroneous estimate of the experimental error. The random order of treatment placement is achieved using random number tables or computer-generated randomizations.

1.4 SAMPLE LAYOUT AND SPACING

Although many types of sampling designs exist (reviewed in Gilbert 1987; Mulla and McBratney 2000; de Gruijter 2002) only two main types (random and systematic) are commonly used in the soil and earth sciences. Inventory studies can be completed using any of the designs discussed in the following two sections. Pattern and geostatistical studies typically use transect or grid designs, as is discussed in more detail in Section 1.5.

1.4.1 Simple Random and Stratified Random Sampling

In simple random sampling all samples of the specified size are equally likely to be the one chosen for sampling. In stratified random sampling, points are assigned to predefined groups or strata and a simple random sample chosen from each stratum. The probability of being selected can be weighted proportionally to the stratum size or the fraction of points sampled can vary from class to class in disproportionate sampling. Disproportionate sampling would be used if the degree of variability is believed to vary greatly between classes, in which case a higher number of samples should be drawn from the highly variable classes to ensure the same degree of accuracy in the statistical estimates.

Stratified sampling (correctly applied) is likely to give a better result than simple random sampling, but four main requirements should be met before it is chosen (Williams 1984):

1. Population must be stratified in advance of the sampling.
2. Classes must be exhaustive and mutually exclusive (i.e., all elements of the population must fall into exactly one class).
3. Classes must differ in the attribute or property under study; otherwise there is no gain in precision over simple random sampling.
4. Selection of items to represent each class (i.e., the sample drawn from each class) must be random.

The selection of random points in a study area has been greatly facilitated by the widespread use of Global Positioning System (GPS) receivers in field research. The points to be sampled can be randomly selected before going to the field, downloaded into the GPS unit, and then the researcher can use the GPS to guide them to that location in the field.

TABLE 1.1 Sample Sizes Required for Estimating the True Mean μ Using a Prespecified Relative Error and the Coefficient of Variation

Confidence level	Relative error, d_r	Coefficient of variation (CV), %					
		10	20	40	50	100	150
0.80	0.10	2	7	27	42	165	370
	0.25			6	7	27	60
	0.50				2	7	15
	1.0					2	4
0.90	0.10	2	12	45	70	271	609
	0.25			9	12	45	92
	0.50				2	13	26
	1.0					2	8
0.95	0.10	4	17	63	97	385	865
	0.25			12	17	62	139
	0.50				4	16	35
	1.0					9	16

Source: Adapted from Gilbert, R.O., in *Statistical Methods for Environmental Pollution Monitoring*, Van Nostrand, Reinhold, New York, 1987, 320 pp.

Determination of Sample Numbers in Inventory Studies

A necessary and important step in the planning stages of a project is to determine the number of samples required to achieve some prespecified accuracy for the estimated mean. One approach is to use prior knowledge about the CV of the property under study to estimate sample numbers required to achieve a certain prespecified relative error. The relative error (d_r) is defined as

$$d_r = |\text{sample mean} - \text{population mean}|/\text{population mean} \tag{1.3}$$

The sample numbers required to achieve a specified relative error at a selected confidence level can be estimated from Table 1.1. For example, at a confidence level of 0.95 and a relative error of 0.25, 16 samples are required if the CV is 50% and 139 samples are required if the CV is 150%. Estimates of CV for different soil properties are widely available, and are summarized in Table 1.2.

1.4.2 Systematic Sampling

The most commonly used sampling design for many field studies is systematic sampling using either transects or grids. Systematic sampling designs are often criticized by statisticians but the ease with which they can be used and the efficiency with which they gather information makes them popular in the field of earth sciences. Ideally the initial point of the transect or grid and/or its orientation should be randomly selected. The major caution in the use of systematic sampling with a constant spacing is that the objects to be sampled must not be arranged in an orderly manner which might correspond to the spacing along the transect or the grid.

The choice of a transect or a grid depends on several factors. Certain types of research designs require particular types of systematic designs—as discussed below, wavelet analysis requires long transects whereas geostatistical designs more typically use grid designs. Grids are often used for spatial pattern studies because of the ease with which pattern maps can be derived from the grids. The complexity of landforms at the site is also a consideration.

TABLE 1.2 Variability of Soil Properties

Coefficient of variation			
Low (CV <15%)	**Moderate (CV 15%–35%)**	**High (CV 35%–75%)**	**Very high (CV 75%–150%)**
Soil hue and value[a]	Sand content[a]	Solum thickness[a]	Nitrous oxide flux[b]
pH[a]	Clay content[a]	Exchangeable Ca, Mg, K[a]	Electrical conductivity[b]
A horizon	CEC[a]	Soil nitrate N[b]	Saturated hydraulic conductivity[b]
Thickness[a]	% BS[a]	Soil-available P[b]	Solute dispersion coefficient[b]
Silt content[a]	$CaCO_3$ equivalent[a]	Soil-available K[b]	
Porosity[b]	Crop yield[b]		
Bulk density[b]	Soil organic C[b]		

[a] Adapted from Wilding, L.P. and Drees, L.R., in L.P. Wilding, N.E. Smeck, and G.F. Hall, (Eds.), *Pedogenesis and Soil Taxonomy. I. Concepts and Interactions*, Elsevier Science Publishing, New York, 1983, 83–116.

[b] Adapted from Mulla, D.J. and McBratney, A.B., in M.E. Sumner (Ed.), *Handbook of Soil Science*, CRC Press, Boca Raton, Florida, 2000, A321–A352.

For level and near-level landscapes either a transect or a grid can be used (Figure 1.1). The appropriateness of transects in sloping terrain depends in part on the plan (across-slope) curvature. Where no significant across-slope curvature exists each point in the landscape receives flow from only those points immediately upslope and a single transect can adequately capture the variations with slope position (Figure 1.2). A single transect will not, however, be sufficient if significant plan curvature exists. In this case a zigzag design or multiple, randomly oriented transects could be used, but more typically a grid design is used (Figure 1.3). It is important to ensure that all slope elements are represented in the grid

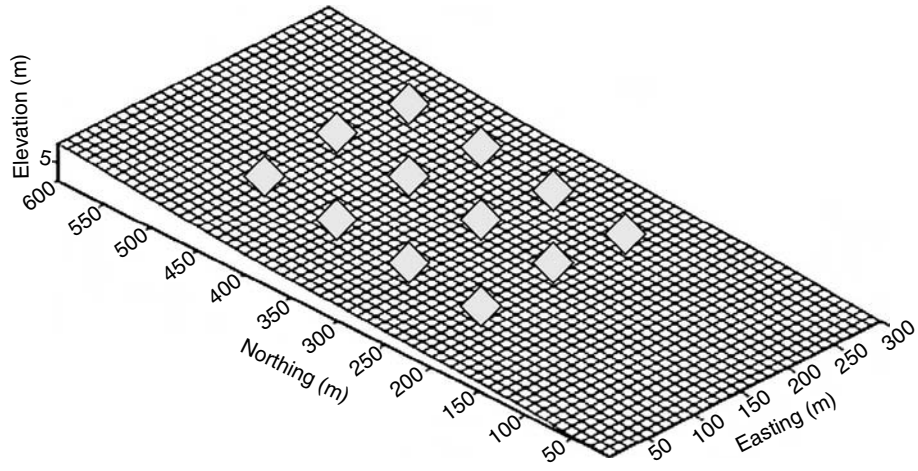

FIGURE 1.1. Example of a grid sampling layout composed of four parallel transects on a near-level surface form. Soil samples would be taken at each point labeled with a diamond shape.

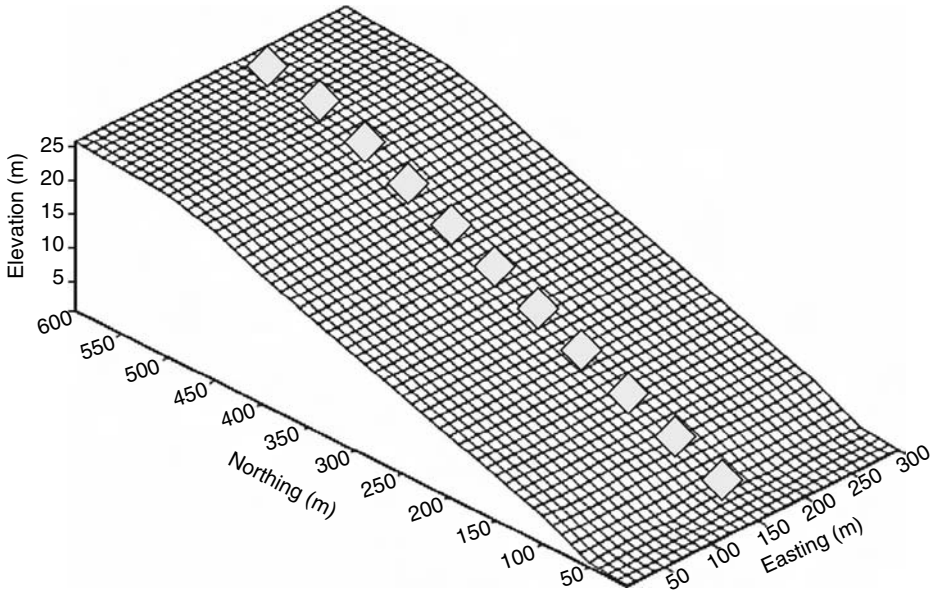

FIGURE 1.2. Example of a transect sampling layout on a sloping surface with no significant across-slope (plan) curvature. Soil samples would be taken at each point labeled with a diamond shape.

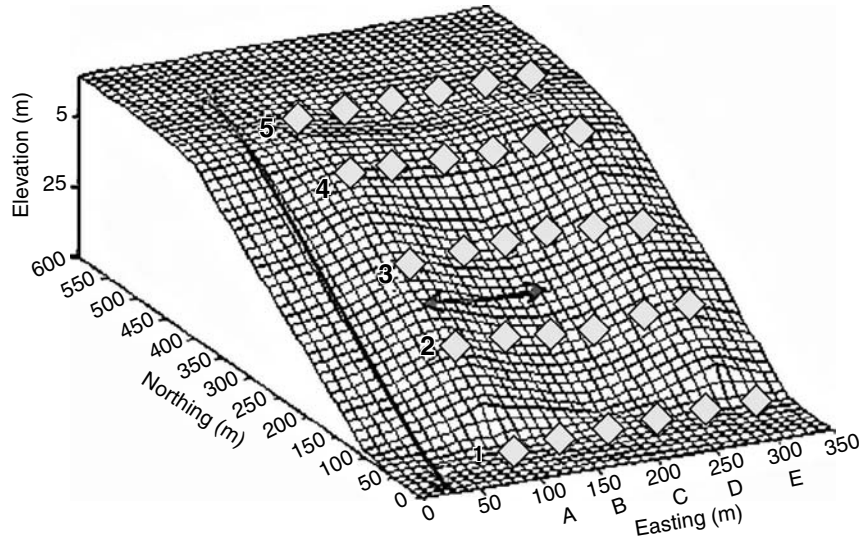

FIGURE 1.3. Example of a grid sampling layout composed of six parallel transects on a sloping surface form with pronounced across-slope curvature. The arrow-oriented downslope delineates the minimum downslope length of the long axis of the grid, and the arrow across the slope indicates the minimum length of the short axis of the grid. Soil samples would be taken at each point labeled with a diamond shape.

design. A rule of thumb is that the grid should extend from the level summit of the slope to the toeslope along the long axis of the slope and along at least one complete convergent–divergent sequence across the slope.

The distance between sampling points in either a transect or a grid should be smaller than the distance required to represent the variability in the field. For example, if the study area contains landforms whose tops and bottoms are equally spaced at 30 m, then a transect crossing these landforms should have sample locations spaced much shorter than this (e.g., 5 or 10 m). It is desirable to base sample spacing on prior knowledge of the area.

1.5 SAMPLING DESIGNS FOR SPECIFIC RESEARCH OBJECTIVES

1.5.1 Sampling Designs for Mensurative and Manipulative Experiments

In mensurative and manipulative designs a typical goal is to assess if the attributes sampled from different classes have different distributions or the same distribution, using difference testing. In the simplest type of hypothesis testing, two hypotheses are constructed: the null hypothesis (H_0) of no difference between the two groups and the alternative hypothesis of a significant difference occurring. The researcher chooses an α level to control the probability of rejecting the null hypothesis when it is actually true (i.e., of finding a difference between the two groups when none, in fact, existed in nature or a Type I error). Peterman (1990) states that the consequences of committing a Type II error (i.e., of failing to reject the null hypothesis when it is, in fact, false) may be graver than a Type I error, especially in environmental sampling. The probability of failing to reject the H_0 when it is, in fact, false is designated as β and the power of a test equals $(1-\beta)$. Calculation of power should be done during the design stage of a mensurative or manipulative experiment to ensure that sufficient samples are taken for a strong test of differences between the groups.

The use of nonstratified, systematic designs may be very inefficient for mensurative experiments. For example, in a landscape where 60% of the site is classified as one class of landform element and 5% is classified into a second class, a 100-point grid should yield approximately 60 points in the major element and 5 points in the second. The dominant element is probably greatly oversampled and the minor element undersampled. Appropriate sample numbers can be efficiently gathered by stratified sampling by a priori placement of points into the relevant groups or strata, and then a random selection of points is chosen within each stratum until the desired number is reached.

In manipulative designs the treatments are commonly applied in small strips (or plots). If the experimental unit is believed to be homogenous then the treatments can be randomly assigned to plots in a completely random design. More typically some degree of heterogeneity is believed to occur—for example, a slight slope or a gradient in soil texture exists across the plot. In this case the treatments are assigned to square or rectangular blocks. Each block typically contains one of each of the treatments being compared in the experiment, and the sequence of treatments in each block is randomly determined. This is termed as a randomized complete block design (RCBD), and is the most commonly used manipulative design. Many other types of manipulative designs have been developed for field experimentation (Steel and Torrie 1980) and the advice of a biometrician is invaluable for the design of these types of experiments.

1.5.2 Soil Sampling for Nutrient Inventories

These are a particular type of inventory study that are undertaken to provide average values of soil nutrient properties over a field or field segment (more commonly called soil testing). This average value is then often used as the basis for fertilizer recommendations in the next growing season. The accuracy with which soil test results reflect the true condition of soils in the field is more dependent on the way in which the sample is collected and handled rather than on error associated with the laboratory analysis (Cline 1944; Franzen and Cihacek 1998). As such, the sample used for laboratory analysis must be representative of the field from which it was taken and sample collection and sample handling must not cause a change to the soil properties of interest before the laboratory analysis.

The development of a sampling procedure must address the following points.

Division of the Field into Different Sampling Units

The farm operator must decide what level of detail is relevant to his or her field operations. Are there parts of the field that have different fertility patterns? Are these areas large enough to be relevant? Does the operator want to engage in site-specific management? Has the operator has the ability to vary fertilizer application rates to accommodate the field subsections identified?

Subsections of a field would commonly be identified by differences in topography (termed *landscape-directed soil sampling*), parent material, management history, or yield history. It may be impossible to subdivide a field into smaller units if the farm operator has no prior knowledge of the field, or if there is no obvious topographic or parent material differences. Under these conditions a grid sampling design has the potential to provide the greatest amount of spatial detail. However, a grid is also the most expensive sampling method and is not typically economically feasible for routine soil testing.

Where landscape-directed soil sampling can be implemented it has been shown to provide superior information on nutrient distribution and the identification of separate management units than that obtained via grid sampling. Landscape-directed soil sampling is particularly effective at assessing patterns of mobile soil nutrients.

Selection of Sampling Design and Sample Numbers

For each field or field subsection samples can be taken using a random sampling design, a grid sampling design, or a benchmark sampling design.

In random sampling individual samples are collected from locations that are randomly distributed across the representative portion of the field. These random locations can be generated with a GPS. A zigzag sampling pattern (Figure 1.4) is often used for field sampling. The sampler should avoid sampling atypical areas such as eroded knolls, depressions, saline areas, fence lines, old roadways and yards, water channels, manure piles, and field edges. Typically, all samples are combined and a composite sample is taken and submitted for laboratory analysis. Composite sampling is comparatively inexpensive since only one sample from each field or subsection of a field is sent for laboratory analysis. However, this design provides no assessment of field variability, and relies on the ability of the farm operator to identify portions of the field that may have inherently different nutrient levels.

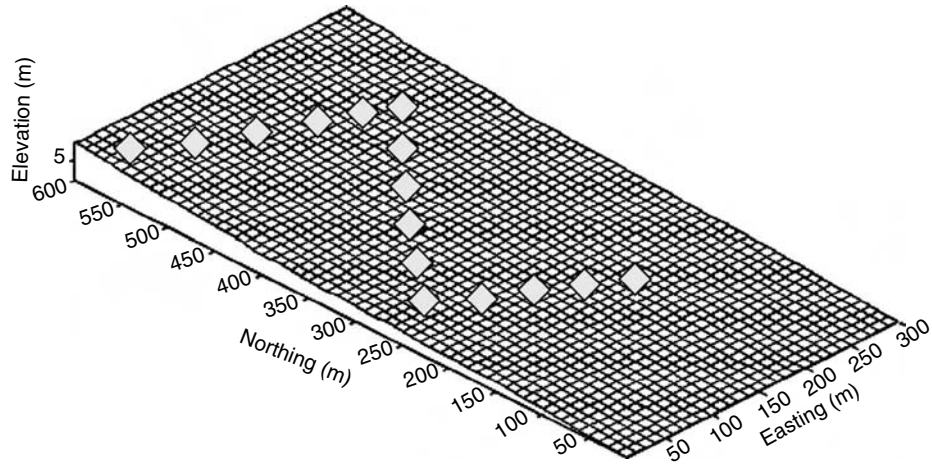

FIGURE 1.4. Example of a zigzag sampling layout on a near-level surface. Soil samples would be taken at each point labeled with a diamond shape.

Soil-testing laboratory guidelines consistently suggest that on average 20 samples be collected for each field or subsection of a field regardless of the actual area involved.

Grid Sampling

In this sampling design a grid system is imposed over each field or subsection of a field. One composite sample from each grid node is sent for laboratory analysis. The grid sampling design is the most expensive method employed in soil sampling but it can provide highly detailed information about the distribution of nutrient variability if the grid size is small enough.

Benchmark Sampling

In this design a single representative site (benchmark) is selected for each field or subsection of a field. The benchmark site should be approximately 1/4 acre or 30×30 m. Twenty or more samples should be randomly taken from within the benchmark and then composited. The farm operator can return to the same benchmark site in subsequent years for repeated testing. The advantage of this design is that year to year changes in nutrient status are more accurately reflected.

1.5.3 Sample Timing, Depth of Sampling, and Sample Handling

As a general rule, sampling for mobile nutrients should be taken as close to seeding as possible or when biological activity is low. Fall sampling should generally start after the soil temperature is less than 10°C at which time no further changes in the soil nutrient levels are expected. Spring sampling, before seeding, can be done as soon as the soil frost is gone.

Commonly used sample depth combinations are 0 to 15 cm (0″–6″) and 15 to 60 cm (6″–24″), or 0 to 30 cm (0″–12″) plus 30 to 60 cm (12″–24″). However, if the soil nutrient of interest is expected to be stratified by depth, as with water-soluble highly mobile nutrients, then additional sampling increments would help ensure accurate recommendations. If organic matter and/or pH measurements are of importance (particularly when evaluating potential herbicide residue carryover) then a 0 to 15 cm (0″–6″) sample should be taken.

To ensure that a uniform volume of soil is taken through the full depth of each sampling increment samples should be collected using soil probes and augers designed for this purpose. A wedge-shaped sample like that collected using a spade will not give consistent results. All probes should be kept clean and rust free. Avoid contamination at all stages of sample handling.

In many situations, a lubricant will need to be applied to the soil probe to prevent the soil sticking inside the probe. This lubricant will help to prevent compaction of the soil as the probe is pressed into the ground, and it will facilitate emptying the collected sample from the probe. Research by Blaylock et al. (1995) suggests that the commonly used lubricants will not affect soil test results other than the case of the micronutrients iron, zinc, manganese, and copper. The most commonly used lubricants include WD-40 lubricant, PAM cooking oil, and Dove dish-washing liquid.

1.5.4 Sampling for Geostatistical, Spectral, and Wavelet Analysis

The choice of geostatistical techniques over the approaches discussed above involves a fundamental decision about whether the sampling is design based or model based; potential users of the geostatistical approach are referred to Brus and de Gruijter (1997) (and the discussion papers following their article) and de Gruijter (2002) for a comprehensive discussion of the difference between the two approaches.

Geostatistics, spectral analysis, and wavelet analysis all address the spatial dependence in soil properties between locations. Thus the location of each sample point in space using GPS-determined spatial coordinates is critical information. Sample programs where this type of analysis is intended should include a topographic survey and generation of digital elevation model.

Sampling for Geostatistics

Spatial variability in soil properties can be separated into random and nonrandom components (Wilding and Drees 1983). The nonrandom variability is due to the gradual change of a soil property over distance. Knowledge of this nonrandom variation gained through the application of geostatistics can be useful in the design of efficient sampling programs and the estimation of the value of a soil property at unsampled locations. There are comprehensive discussions of geostatistics in Webster and Oliver (1990), Mulla and McBratney (2000), and Yates and Warrick (2002).

Geostatistics assume that the value of a soil property at any given location is a function of the value of that same property at locations nearby (spatial dependence). The distance and direction between locations determine the degree of spatial dependence between values of a soil property at those locations. The use of geostatistics thus requires that not only the value of a soil property be known, but the location as well. The primary geostatistical tools are the semivariogram and kriging. The semivariogram provides a measure of spatial dependency, the range, which can be used to determine optimum sample spacing or the extent of soil unit boundaries. Kriging is used to estimate the value of a soil property at a location where the value is unknown by using the known values at locations about the point of interest. Spatial dependence between two different soil properties can be explored using cross-semivariograms and cokriging techniques.

A common sample design to determine optimal sample spacing and soil boundary definitions is the linear transect. Calculations are simplest if equal spacing is maintained between

sample points; however, unequal spacing can be accommodated with more complicated mathematics. If the study area has recognizable topographic features then the transect should be directed perpendicular to the trend of these features.

Kriging techniques require that sample locations are taken on a grid. Sample locations are typically chosen by random selection from a set of predetermined grid intersections. In this case distances between locations are not equal. Efficient grid design and kriging may be based on a semivariogram constructed from preliminary sampling along a transect in the same area.

Geostatistics require the assumption of stationarity. Stationarity assumes that all values of a soil property within an area are drawn from the same distribution. This assumption is not always valid. As well, variation in a soil property may occur at more than one scale. For scale analysis and nonstationarity more advanced statistical techniques must be used.

Sampling for Spectral Analysis

In landscapes where landforms are repetitive such as a hummocky, rolling, or undulating terrains the continuous variation of soil properties may result in a data series with a repetitive cycle of highs and lows. The periodicity may be examined in the frequency domain using techniques referred collectively as spectral analysis (see McBratney et al. 2002 for a recent discussion of these techniques). The total variance of a data series is partitioned by frequency. The soil property is considered to cycle at a particular period if a significant portion of the variance is associated with the frequency represented by that period. Period is comparable to scale or distance much like the range from a semivariogram. Unlike a semivariogram, more than one scale can be identified. A cross spectrum can identify soil properties that cycle together and the coherency spectrum can identify scales at which two properties may be positively or negatively correlated in the same area.

The linear transect is the most common sample design used to amass a data series for spectral analysis. Sample spacing must be consistent. As for geostatistical methods the number of samples, the spacing, and the direction of the transect should be chosen to best represent the landscape features of the site.

Sampling for Wavelet Analysis

Both geostatistics and spectral analysis require the assumption of stationarity. Nonstationarity can occur, for example, due to changes in land use or geomorphology across the site, resulting in more than one population of values. A method of analysis that does not require the assumption of stationarity is wavelet analysis (see McBratney et al. 2002; Si 2003 for recent summaries of developments in this technique). A wavelet is a mathematical function that yields a local wavelet variance for each point in a data series. Like spectral analysis, wavelets portion the total variance of a data series according to frequency (scale), but unlike spectral analysis the total variance is also portioned according to space (location). A wavelet approach allows the ability to discern between multiple processes occurring in the field, the scale at which the processes are operating, and the location or distribution of these processes along the data series.

Like spectral analysis, wavelet analysis requires a data series collected from locations spaced equally along a linear transect. Wavelets are rescaled by powers of two and thus transects that contain a power of two data points (64, 128, 256, …) are best for computational speed (Si 2003). As a result, large transects are common when using

wavelet analysis. In cases where the number of transect locations is not a power of two, the data series can be padded with zero values to the nearest power of two. Transects of 128 points are large enough for detailed scale analysis, yet may be manageable by most research programs.

REFERENCES

Blaylock, A.D., Bjornest, L.R., and Lauer, J.G. 1995. Soil probe lubrication and effects on soil chemical-composition. *Commun. Soil Sci. Plant Anal*. 26: 1687–1695.

Brus, D.J. and de Gruijter, J.J. 1997. Random sampling or geostatistical modelling? Choosing between design-based and model-based sampling strategies for soil (with discussion). *Geoderma* 80: 1–44.

Cline, M.G. 1944. Principles of soil sampling. *Soil Sci*. 58: 275–288.

de Gruijter, J.J. 2002. Sampling. In J.H. Dane and G.C. Topp, Eds. *Methods of Soil Analysis, Part 4—Physical Methods*. Soil Science Society of America, Inc., Madison, WI, pp. 45–79.

Eberhardt, L.L. and Thomas, J.M. 1991. Designing environmental field studies. *Ecol. Monogr*. 6: 53–73.

Franzen, D.W. and Cihacek, L.J. 1998. *Soil Sampling as a Basis for Fertilizer Application*. North Dakota University Extension Service Publication SF990. Available at: http://www.ext.nodak.edu/extpubs/plantsci/soilfert/sf-990.ht (July 2006).

Gilbert, R.O. 1987. *Statistical Methods for Environmental Pollution Monitoring*. Van Nostrand Reinhold, New York, NY, 320 pp.

Hurlbert, S.H. 1984. Pseudoreplication and the design of ecological field experiments. *Ecol. Monogr*. 54: 187–211.

Laslett, G.M. 1997. Discussion of the paper by D.J. Brus and J.J. de Gruijter. Random sampling or geostatistical modeling? *Geoderma* 80: 45–49.

McBratney, A.B., Anderson, A.N., Lark, R.M., and Odeh, I.O. 2002. Newer application techniques. In J.H. Dane and G.C. Topp, Eds. *Methods of Soil Analysis, Part 4—Physical Methods*. Soil Science Society of America, Inc., Madison, WI, pp. 159–200.

Mulla, D.J. and McBratney, A.B. 2000. Soil spatial variability. In M.E. Sumner, Ed. *Handbook of Soil Science*. CRC Press, Boca Raton, FL, pp. A321–A352.

Pennock, D.J. 2004. Designing field studies in soil science. *Can. J. Soil Sci*. 84: 1–10.

Peterman, R.M. 1990. Statistical power analysis can improve fisheries research and management. *Can. J. Fish. Aquat. Sci*. 47: 2–15.

Si, B. 2003. Scale and location dependent soil hydraulic properties in a hummocky landscape: a wavelet approach. In Y. Pachepsky, D. Radcliffe, and H.M. Selim, Eds. *Scaling Methods in Soil Physics*. CRC Press, Boca Raton, FL, pp. 169–187.

Steel, R.G.D. and Torrie, J.H. 1980. *Principles and Procedures of Statistics. A Biometrical Approach*. McGraw-Hill, New York, NY, 633 pp.

Webster, R. and Oliver, M.A. 1990. *Statistical Methods in Soil and Land Resource Survey*. Oxford University Press, Oxford, 316 pp.

Wilding, L.P. and Drees, L.R. 1983. Spatial variability and pedology. In L.P. Wilding, N.E. Smeck, and G.F. Hall, Eds. *Pedogenesis and Soil Taxonomy. I. Concepts and Interactions*. Elsevier Science Publishing Company, New York, NY, pp. 83–116.

Williams, R.B.G. 1984. *Introduction to Statistics for Geographers and Earth Scientists*. Macmillan Publishers Ltd., London, 349 pp.

Yates, S.R. and Warrick, A.W. 2002. Geostatistics. In J.H. Dane and G.C. Topp, Eds. *Methods of Soil Analysis, Part 4—Physical Methods*. Soil Science Society of America, Inc., Madison, WI, pp. 81–118.

Chapter 2
Sampling Forest Soils

N. Bélanger and Ken C.J. Van Rees
University of Saskatchewan
Saskatoon, Saskatchewan, Canada

2.1 INTRODUCTION

The causes for forest soil variability are many. Spatial variability is a function of bedrock type and parent material, climate, tree species composition and understory vegetation, disturbances (e.g., harvesting, fire, windthrow), and forest management activities (e.g., site preparation, thinning, pruning, fertilization, vegetation management). For example, a second generation 50-year-old Radiata pine plantation grown on plowed alluvial sands in Australia would have lower spatial variability compared to mixed hardwoods developed from a shallow rocky till of the Precambrian (Canadian) Shield after harvest. The mixed hardwoods would likely show high variability in forest floor properties such as forest floor thickness due to tree fall (Beatty and Stone 1986; Clinton and Baker 2000) and the influence of different tree species (Finzi et al. 1998; Dijkstra and Smits 2002). Moreover, the fact that the soil is plowed in the pine plantation would likely reduce some of the soil variability that could have been created by the previous plantation (e.g., changes in soil properties when sampling away from the stem). In the mineral soil, it would be more difficult to assess nutrient pools compared to the pine plantation because of the problem of measuring bulk density and percentage of coarse fragments in the rocky till (Kulmatiski et al. 2003). It would also be more problematic to develop a replicated sampling scheme by depth in the natural forest because horizon thickness across the landscape evolves as a continuum with complex spatial patterns (e.g., Ae pockets along old root channels and thick FH material in pits).

All these sources of spatial variability must be considered in efforts to systematically sample and describe forest soil properties. This is why sampling strategies and methodologies must be selected with care and this chapter is dedicated to that goal; however, information regarding field designs and plot establishment can be found in Pennock (2004) or Pennock et al. (see Chapter 1).

2.2 SAMPLE SIZE

Developing a sampling scheme that represents the inherent variability and true value of the population mean in forest floor chemistry may require many sampling points. Calculating the sample size is important because a sample size that is too large leads to a loss of time, human

resources, and money, whereas a sample size that is too small leads to erroneous statistical testing. The margin of error (d) is the maximum difference between the observed sample mean and the true population mean. It can be calculated according to the following equation (Snedecor and Cochran 1980):

$$d = t_{\alpha}^{2} \frac{s}{\sqrt{n}} \tag{2.1}$$

where t_{α} is the Student t factor for a given level of confidence (generally 95%) and s is the coefficient of variation (CV) as a percentage of the mean value. The equation can be rearranged to solve the sample size needed to produce results to a specified p and margin of error:

$$n = \left[\frac{t_{\alpha} s}{d}\right]^{2} \tag{2.2}$$

In a field study designed to test the spatial variability of nutrient concentrations and pools in the forest floor, Arp and Krause (1984) sampled the forest floor at 98 locations in a 900 m^2 plot. They showed that concentrations and pools of KCl extractable NO_3-N and NH_4-N and extractable P on field-moist soils had the highest CV values and required as many as 1371 samples (i.e., KCl extractable NO_3-N pool) to decrease the margin of error on the population mean to 10% at a confidence level of 95% and $t_{\alpha} = 1.96$ ($\alpha = 0.05$). An accurate estimate of the mean content of a nutrient required more samples than that for measuring its mean concentration. This was due mostly to the large variation in forest floor weight and thickness in the study. Figure 2.1 shows margins of error obtained using CV values in Arp and Krause (1984) with 10, 15, and 20 sampling points and confidence level set at 95%. This simple exercise demonstrates that a margin of error of 5% is generally not possible using 10 sampling points, except for total C concentration and soil pH. For nutrient concentrations (except for NO_3-N, NH_4-N, and P on field-moist soils) and physical properties (i.e., moisture, thickness, and weight), a margin of error between 31% and 9.9%, 26% and 8.0%, and 22% and 7.0% is possible with 10, 15, and 20 sampling points, respectively, with forest floor weight having the highest margin of error and total N having the lowest. However, 20 sampling points are required to obtain a margin of error between 19% and 29% when these concentrations are transformed as pools. Similarly, McFee and Stone (1965) found that it was necessary to have 50 sampling points to have a 10% margin of error (confidence level of 95%) on the calculated mean of forest floor weight and thickness for forest plots in the Adirondacks. This supports the idea that the problem of assessing forest floor nutrient pools with a high level of confidence comes in large part from the high variability in forest floor weight and thickness. Results also show that it is not financially and logistically feasible to develop replicated field design testing treatment effects on concentrations and pools of KCl extractable NO_3-N and NH_4-N as well as water-extractable P pools on field-moist samples.

The number of sampling points required for a reliable representation of a plot's mean does not appear to be related to its size. Quesnel and Lavkulich (1980) and Carter and Lowe (1986) had smaller study plots (300 and 400 m^2, respectively) than Arp and Krause (1984), but the intensities of sampling required for obtaining a reasonable estimate of the plot's mean were similar. Interestingly, Carter and Lowe (1986) conducted the study with LF and H horizons as distinct samples and found that the LF horizons required fewer samples (3 to 10) than the H horizons (3 to 38 samples) for a reliable estimate of the population mean for total C, N, P, and S concentrations and pH (margin of error of 10% at a confidence level of 95%).

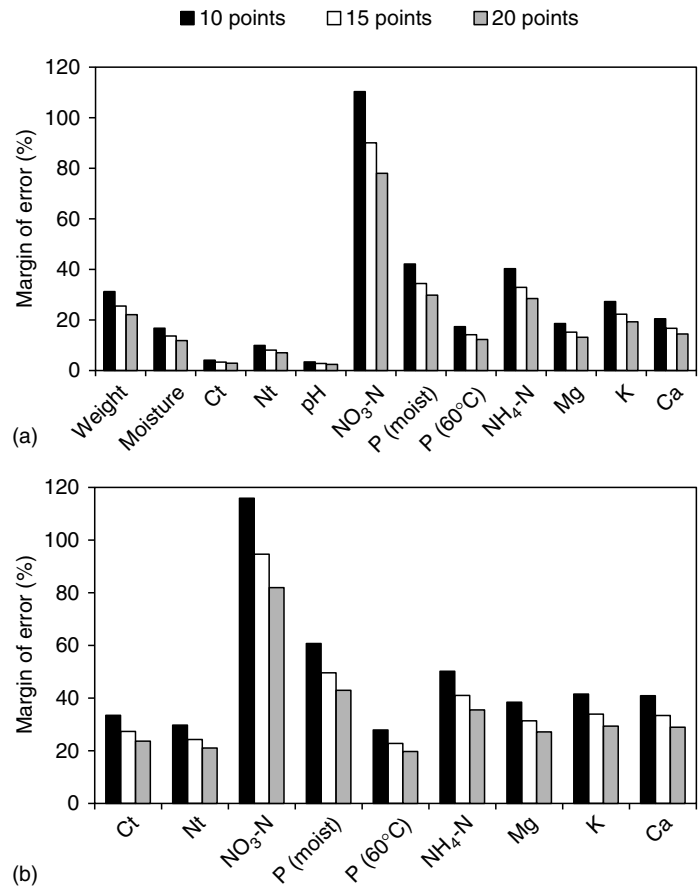

FIGURE 2.1. Margins of error of the population mean (forest floor (a) weight, moisture, pH and extractable nutrient, total C (Ct), and total N (Nt) concentrations as well as (b) extractable nutrient, Ct and Nt pools) obtained using coefficients of variation in Arp and Krause (1984) with 10, 15, and 20 sampling points with the level of confidence set at 0.95.

The results also suggested that 15 sampling points should be enough to characterize the population mean of total Mg, K, N, P, C, Cu, and Zn concentrations, lipid concentrations, pH and bulk density in LF, and H material within a margin of error of 20% at a confidence level of 95%. However, a more intensive sampling strategy was required for obtaining similar margins of error on the population mean of total Ca and Mn concentrations in the H material (81 and 47 samples, respectively) and total Al and Fe concentrations in LF material (41 and 50 samples, respectively).

In the mineral soil, the intensity of sampling required to obtain a reliable estimate of the population mean also appears to depend on the variable tested. Studying the variability of organic matter in the forest floor and mineral soil in a Tuscany forest, Van Wesemael and Veer (1992) sampled six 2500 m^2 plots and found that between 17 and 80 sampling points were required to have a 10% margin of error on the plots' population means (confidence level of 95%) of organic matter content in the first 5 cm of mineral soil compared to 33 to 235 sampling points for organic matter content in LF or FH horizons. This appears to fit with

the values of Arp and Krause (1984) who found that 114 samples were required to arrive at the same level of confidence for total C content in the forest floor. An accurate measure of the mean for soil pH, particle size, and moisture appears to be considerably easier: Ike and Clutter (1968) demonstrated that 1 to 12 sampling points in forest plots of the Georgia Blue Ridge Mountains were necessary to obtain a 10% margin of error on the population mean of pH, separate sand, silt and clay fractions, and available water and moisture. However, available P and exchangeable K concentrations required 15 to 32 samples per plot for the same margin of error, 14 to 76 samples per plot for exchangeable Mg concentration, and 153 to 507 for exchangeable Ca concentration.

2.3 SAMPLING METHODS

There are two generally accepted techniques for sampling the forest floor: soil cores or a square template. McFee and Stone (1965) used a sharp-edged steel cylinder with a diameter of 8.7 cm (59 cm^2) for coring the forest floor to quantify the distribution and variability of organic matter and nutrients in a New York podzol. Similarly, Grier and McColl (1971) used a steel cylinder with a diameter of 26.6 cm (556 cm^2). As an alternative to soil corers, Arp and Krause (1984) used a square wooden sampling template of 25 × 25 cm (625 cm^2) placed on the surface of the forest floor as a cutting guide. Others have used smaller or larger cutting templates (225 to 900 cm^2) and Klinka et al. (1981) suggested using a 10 × 10 cm template. A corrugated knife used on the inside edge of the frame will generally cut through the forest floor material with no difficulty and once the sample is cut on all sides, it is relatively simple to partition it from the mineral soil. Square sampling templates can also be constructed with heavier gauge metal and sharp edges can be added to the bottom of the frame in order to push or hammer (use hard plastic hammers or mallets) the frame into the forest floor until the mineral soil is reached. The litter can then be pulled from the frame. In some cases, a wooden cap can be built for the metal frames to assist in hammering into the forest floor. We believe this a convenient way of sampling the forest floor as it allows at the same time, after the measurement of thickness and determination of wet and dry mass, a measure of bulk density and water content.

The general rule of thumb for sampling the forest floor is that the larger the surface area being sampled, the greater chances you have of reducing microsite variability in the sample once it is air-dried, cleaned for roots and other woody material, and mixed in the laboratory. Therefore, it is recommended to use a sampling scheme that will cover, individually or bulked, at least 200 cm^2.

2.4 DIFFERENTIATING BETWEEN FOREST FLOOR AND Ah MATERIAL

Sampling of forest floor horizons varies among soil scientists and there are no accepted standards for how horizons should be sampled. Generally, LFH horizons are sampled as a whole (Bock and Van Rees 2002) or samples are taken from individual (i.e., L or F or H horizon) or combinations of horizons (i.e., FH horizon) (Olsson et al. 1996; Hamel et al. 2004), depending on the objective of the study. Normally, all layers are collected together (LFH) or the litter is collected individually (L + FH) for nutrient cycling studies or individually if one is investigating specific processes such as decomposition (e.g., Cade-Menun et al. 2000).

Sampling problems can occur when trying to distinguish between H horizons and Ah horizon sequences. In forest soils with an abrupt transition between the forest floor and the mineral

soil such as those classified as mor forest floors, it is relatively simple to distinguish the forest floor from the mineral soil. However, in forest soils with Mull and sometimes Moder forest floors (i.e., Chernozems and Melanic Brunisols), the F or H horizons are often not easily discernible from the mineral Ah horizon, thus making it more difficult to sample the forest floor layers separately. The incorporation of organic matter in the mineral soil therefore introduces a bias in forest floor sampling as some of the Ah material can be incorporated in the forest floor samples. The Expert Committee on Soil Survey (1987) defines the Ah horizon as ''A horizon enriched in organic matter, it has a color value one unit lower than the underlying horizon or 0.5% more organic C than the IC or both. It contains less than 17% organic C by weight.'' If correct sampling of the forest floor is an important issue for the study, then the most appropriate way to distinguish between the FH and Ah horizons is to carry out a presampling campaign and then conduct C analyses on the samples. Running a quick and fairly reliable loss-on-ignition (LOI) test should be very informative and allow separation between forest floor and mineral soil material: organic C constitutes 58.3% of the soil organic matter content and thus, LOI should not exceed 30% on Ah samples, whereas an LOI of 30% or more is expected from forest floor material depending on the amounts of mineral soil particles, coarse fragments, and charcoal incorporated in the material. If the cost for accessing the study site is high and there is no possibility for presampling and returning to the site after LOI testing, then a second option for separating FH horizons from Ah material is to rely on color and feel. Humus forms do vary and their taxonomy can be quite complex. In this respect, the reader is directed to Klinka et al. (1981) and/or Green et al. (1993) for an in-depth description of these horizons.

2.5 BULK DENSITY AND COARSE FRAGMENTS

Soil bulk density is a commonly measured parameter in forest soil studies to assess harvesting effects on forest soil quality such as compaction induced by logging or site preparation practices (e.g., Powers 1991; Aust et al. 1995). For forests growing on glacial till of the Precambrian Shield or other rocky soils, however, the presence of large rocks and coarse fragments makes it difficult to measure soil bulk density with standard techniques. In addition, quantifying the amount of coarse fragments is important for accurately calculating nutrient pools in soils (Palmer et al. 2002; Kulmatiski et al. 2003). There are a variety of forest soil sampling techniques to assess coarse fragments and bulk density ranging from the clod, core, pit, to the sand cone technique (i.e., Page-Dumroese et al. 1999; Kulmatiski et al. 2003). The intensive approach is to excavate a sample that is larger than the largest rock in the sample (see Chapter 66 of this book for a detailed description of the excavation and sand replacement method) while the extensive approach is to collect smaller sized samples over a large area using a corer.

Page-Dumroese et al. (1999) conducted a study where two different size cores (183 and 2356 cm^3) were compared to two pit excavation methods and one nuclear source moisture gauge for calculating bulk density. They found that bulk densities measured with the two excavation methods were 6% to 12% lower than those measured with the two core measurements and the nuclear gauge method. The nuclear gauge method gave the highest values of total and fine bulk densities and the small corer method produced the most variable results. Sampling with a corer produces higher values compared to the pit methods because compaction may occur during sampling. This was more apparent at the greater depth increments, probably because some compaction likely occurred during core insertion (Lichter and Costello 1994). To prevent this, it was suggested to remove the top mineral soil with an

auger or shovel and then hammering the corer to the desired soil depth. On the other hand, Page-Dumroese et al. (1999) also argued that the smaller corer may have provided samples too small to be representative of overall soil conditions: it is possible that the small core technique underestimates total bulk density because it does not account for large rocks with high densities. The larger size corer generally produced intermediate bulk density values, although estimates were low at the greater depths sampled because of incomplete filling or soil loss at the bottom of the core sampler. The accuracy of this method is likely increased for greater soil depths as rock fragments usually augment with depth.

Similarly, Kulmatiski et al. (2003) compared the ability of the core and excavation methods for detecting a 10% change in total C and N pools in forest soils of southern New England. They found that mean total C and N contents measured from the extensive core techniques were 7% higher than those measured from the intensive pit approach, but these differences were not statistically significant. The core techniques produced lower estimates of percentage C and N and bulk densities compared to the pit technique, but the core techniques also produced lower estimates of coarse fragments and higher soil volume values. Consequently, both techniques produced very similar estimates of total N and C soil pools. The 7% divergence between mean total C pools measured using the two techniques was reduced when coarse roots were added in the calculations, whereas coarse roots were not a significant portion of the total N pools and had no impact on estimates. The results also showed little variability of total C and N pools at a depth greater than 15 cm (assessed by the pit technique), meaning that deeper nutrient pools are insensitive to environmental factors such as tree species composition and topography. Moreover, Kulmatiski et al. (2003) suggested that the extensive core approach required less than one-half of the sampling time for determining the population mean (i.e., N and C pools) compared to the intensive pit approach and that a smaller number of samples was required for a low margin of error of the population mean. They recommended the use of the core techniques to calculate total N and C contents in the upper mineral soil horizons. However, one advantage of the pit technique is that it allows direct measurement of large rock fragments in the soil. For calculating total C and N pools in deeper soils with generally greater rock fragments, Kulmatiski et al. (2003) therefore recommended to extrapolate data from the upper mineral horizons to deeper soil by building regression models developed from a few local soil pits.

2.6 SAMPLING BY DEPTH OR DIAGNOSTIC HORIZONS?

Obtaining a reliable estimate of the population mean of a specific nutrient concentration in the mineral soil probably requires less sampling points than that in the forest floor (e.g., organic matter content in Van Wesemael and Veer (1992)). The number of sampling points is also probably less if the soil is sampled by diagnostic horizon compared to sampling by depth. More variability in soil properties is expected from sampling by depth because the sample is a mixture of soil material with different properties. For example, sampling Bhf horizons of sandy Ferro-Humic Podzols means that the soil material has at least 5% organic C and 0.4% pyrophosphate-extractable Fe and Al. However, if the mineral soil is sampled by depth, e.g., 20 cm increments, then Ae material (higher in Si and lower in Al, Fe, and C than the Bhf, see Table 2.1) is bound to be incorporated with Bhf material in the first increment and Bhf and Bf/BC material will be bulked in the second increment. In a study on jack pine growth, Hamilton and Krause (1985) showed a negative relationship between the depth of the eluvial material and tree growth. In podzols, roots develop most of their biomass in the forest floor and upper B horizons and not in the Ae material (e.g., Côté et al. 1998). Sampling by 20 cm increments in well-drained forest soils with a fully developed Ae horizon means

TABLE 2.1 Total Elemental Composition (Given as Percentage of Total Soil Matrix) of Ae and Bf Horizons of Podzols Developed under Balsam Fir in the Gaspé Peninsula of Quebec (Mean ± Standard Deviation with $n = 6$)

	Ae horizon	Podzolic B horizon
SiO_2	84.5 ± 4.18	53.3 ± 7.56
TiO_2	1.17 ± 0.16	0.68 ± 0.18
Al_2O_3	4.98 ± 1.08	11.2 ± 1.99
Fe_2O_3	0.62 ± 0.15	7.06 ± 1.79
MgO	0.24 ± 0.07	0.90 ± 0.35
CaO	0.08 ± 0.02	0.12 ± 0.05
Na_2O	0.69 ± 0.09	0.83 ± 0.18
K_2O	0.92 ± 0.24	1.34 ± 0.33
P_2O_5	0.05 ± 0.01	0.24 ± 0.08
LOI[a]	6.59 ± 3.05	24.5 ± 7.52

[a] LOI is loss-on-ignition. Total elemental composition does not sum up to 100% as trace elements are not shown here.

Note: Total iron present has been recalculated as Fe_2O_3. In cases where most of the iron was originally in the ferrous state, a higher total is the result.

that the arbitrary differences in soil morphology will govern the results of the chemical analyses. In this respect, significant correlation between tree nutrition/growth and mineral soil chemistry may be masked by the fact that the sampling scheme used is not representative of the capacity factor of the actual mineral soil to provide nutrients to the trees. Also, an admixture of soil material with different properties may camouflage the response of specific soil horizons to harvesting, acid deposition, etc., as some of the material incorporated in the sample may be in steady-state with the conditions created by the disturbance whereas the other material may not.

Note that there are also clear advantages of sampling soil by depth when conducting studies on soil changes over time. One of the best conceptual examples for demonstrating the benefits of sampling by depth is a study comparing soil C pools in a natural forest with a plantation established close by. The plantation is building a new forest floor (as it was plowed) and is likely shallower than that of the natural forest. Also, the natural sequence of horizons in the plantation is obviously different from that of the natural forest to a depth of about 5–8 cm. Therefore, as the sequencing of diagnostic horizons differs between the plantation and natural forest, sampling by depth is the best option for comparing soil C pools. Due to the horizontal variability, it is strongly recommended to sample the soil evenly across the whole sampling increment: sampling only a part of the full increment will indisputably result in artifacts. Examples of studies on long-term changes in forest soil properties that required this sampling strategy can be found in Eriksson and Rosen (1994), Parfitt et al. (1997), and Bélanger et al. (2004). Moreover, the reader will find a thorough discussion on sampling strategies to study temporal changes in soil C for agricultural soils in Ellert et al. (see Chapter 3).

2.7 COMPOSITE SAMPLING

In some forests, soil variability can be enhanced by forest processes such as tree falls to create ''pit and mound'' topography. These kinds of sites need different types of sampling strategies to account for changes in microtopography. In a study on ''pits and mounds'' in New York state hardwoods, Beatty and Stone (1986) made a composite sample from four 4.5 cm or five 2 cm diameter cores (total surface area 64 and 16 cm^2, respectively) at 0.5 or 1 m intervals across the microsites. Although these samples have a small surface area, the

sampling procedure is quite accepted considering that the study is conducted at the microsite scale and that more or larger samples were likely not needed over such a small area to calculate a valid population mean. Similarly, forest soil scientists are bulking forest floor samples for studies conducted at the plot scale, i.e., a set of samples coming from the same population (plot) are carefully mixed together so that they are equal in terms of weight or volume. Obviously, this is a tedious task to do in the field and unfortunately, it is often unclear whether proper mixing is done. Preferably, samples should be stored separately and bulking should be done in the laboratory after they have been air-dried and sieved.

A disadvantage of bulking the samples in a plot is that it does not allow for the calculation of the standard deviation or CV values. In an effort to assess the precision of the variables measured by bulking forest floor samples, Carter and Lowe (1986) compared the mean nutrient contents weighted by depth and bulk density using the 15 sampling points within a plot to the values obtained from analyzing a single sample obtained by bulking these 15 samples (as a function of depth and bulk density). Values from composite samples were all within one standard deviation of the mean, except for total P and Cu concentrations in LF material. Moreover, they investigated the relationships between the weighted means and the composite sample values across the six study plots and found that they were quite strong for most variables, suggesting that bulking samples can provide good estimates of the real population mean ($r > 0.90$, except for Ca and Al concentrations in LF, and Mn and C in LF and H horizons). Similarly, Bruckner et al. (2000) investigated the impact of bulking soil samples on microarthropod abundance on a Norway spruce plantation in Austria. It was assumed that the grinding action of soil particles during mixing would injure or kill part of the population and thus underestimate the population relative to a mean weighted from samples of the population analyzed individually. However, using a special mixing procedure of the extracts, Bruckner et al. (2000) came to the conclusion that no microarthropod was lost or damaged because a large number of samples were bulked in a systematic manner and mixed in equal amounts.

REFERENCES

Arp, P.A. and Krause, H.H. 1984. The forest floor: lateral variability as revealed by systematic sampling. Canada. *Can. J. Soil Sci*. 64: 423–437.

Aust, W.M., Tippett, M.D., Burger, J.A., and McKee, W.H. Jr. 1995. Compaction and rutting during harvesting affect better drained soils more than poorly drained soils on wet pine flats. South. *J. Appl. Forest* 19: 72–77.

Beatty, S.W. and Stone, E.L. 1986. The variety of soil microsites created by tree falls. *Can. J. Forest Res.* 16: 539–548.

Bélanger, N., Paré, D., Bouchard, M., and Daoust, G. 2004. Is the use of trees showing superior growth a threat to soil nutrient availability? A case study with Norway spruce. *Can. J. Forest Res.* 34: 560–572.

Bock, M.D. and Van Rees, K.C.J. 2002. Forest harvesting impacts on soil properties and vegetation communities in the Northwest Territories. *Can. J. Forest Res*. 32: 713–724.

Bruckner, A., Barth, G., and Scheibengraf, M. 2000. Composite sampling enhances the confidence of soil microarthropod abundance and species richness estimates. *Pedobiologia* 44: 63–74.

Cade-Menun, B.J., Berch, S.M., Preston, C.M., and Lavkulich, L.M. 2000. Phosphorus forms and related soil chemistry of Podzolic soils on

northern Vancouver Island. I. A comparison of two forest types. *Can. J. Forest Res.* 30: 1714–1725.

Carter, R.E. and Lowe, L.E. 1986. Lateral variability of forest floor properties under second-growth Douglas-fir stands and the usefulness of composite sampling techniques. *Can. J. Forest Res.* 16: 1128–1132.

Clinton, B.D. and Baker, C.R. 2000. Catastrophic windthrow in the southern Appalachians: characteristics of pits and mounds and initial vegetation responses. *Forest Ecol. Manag.* 126: 51–60.

Côté, B., Hendershot, W.H., Fyles, J.W., Roy, A.G., Bradley, R., Biron, P.M., and Courchesne, F. 1998. The phenology of fine root growth in a maple-dominated ecosystem: relationships with some soil properties. *Plant Soil* 201: 59–69.

Dijkstra, F.A. and Smits, M.M. 2002. Tree species effects on calcium cycling: the role of calcium uptake in deep soils. *Ecosystems* 5: 385–398.

Eriksson, H.M. and Rosen, K. 1994. Nutrient distribution in a Swedish tree species experiment. *Plant Soil* 164: 51–59.

Expert Committee on Soil Survey. 1987. The *Canadian System of Soil Classification*, 2nd edn. Agriculture Canada Publ. 1646, Supplies and Services, Ottawa, Canada, 164 pp.

Finzi, A.C., van Breemen, N., and Canham, C.D. 1998. Canopy tree–soil interactions within temperate forests: species effects on soil carbon and nitrogen. *Ecol. Appl.* 8: 440–446.

Green, R.N., Trowbridge, R.L., and Klinka, K. 1993. *Towards a taxonomic classification of humus forms*. Forest Science Monograph 29. Society of American Foresters, Bethesda, MD, 50 pp.

Grier, C.C. and McColl, J.G. 1971. Forest floor characteristics within a small plot in Douglas-fir in Western Washington. *Soil Sci. Soc. Am. Proc.* 35: 988–991.

Hamel, B., Bélanger, N., and Paré, N. 2004. Productivity of black spruce and jack pine stands in Quebec as related to climate, site biological features and soil properties. *Forest Ecol. Manag.* 191: 239–251.

Hamilton, W.N. and Krause, H.H. 1985. Relationship between jack pine growth and site variables in New Brunswick plantations. *Can. J. Forest Res.* 15: 922–926.

Ike, A.F. and Clutter, J.L. 1968. The variability of forest soils of the Georgia Blue Ridge Mountains. *Soil Sci. Soc. Am. Proc.* 32: 284–288.

Klinka, K., Green, R.N., and Trowbridge, R.L. 1981. *Taxonomic classification of humus forms in ecosystems of British Columbia. First approximation*. British Columbia Ministry of Forest, 53 pp.

Kulmatiski, A., Vogt, D.J., Siccama, T.G., and Beard, K.H. 2003. Detecting nutrient pool changes in rocky forest soils. *Soil Sci. Soc. Am. J.* 67: 1282–1286.

Lichter, J.M. and Costello, L.R. 1994. An estimation of volume excavation and core sampling techniques for measuring soil bulk density. *J. Arboric.* 20: 160–164.

McFee, W.W. and Stone, E.L., 1965. Quantity, distribution and variability of organic matter and nutrients in a forest podzol in New York. *Soil Sci. Soc. Am. Proc.* 29: 432–436.

Olsson, B.A., Bengtsson, J., and Lundkvist, H. 1996. Effects of different forest harvest intensities on the pools of exchangeable cations in coniferous forest soils. *Forest Ecol. Manag.* 84: 135–147.

Page-Dumroese, D.S., Jurgensen, M.F., Brown, R.E., and Mroz, G.D. 1999. Comparison of methods for determining bulk densities of rocky forest soils. *Soil Sci. Soc. Am. J.* 63: 379–383.

Palmer, C.J., Smith, W.D., and Conkling, B.L. 2002. Development of a protocol for monitoring status and trends in forest soil carbon at a national level. *Environ. Pollut.* 116: S209–S219.

Parfitt, R.L., Percival, H.J., Dahlgren, R.A., and Hill, L.F. 1997. Soil and solution chemistry under pasture and radiata pine in New Zealand. *Plant Soil* 191: 279–290.

Pennock, D.J. 2004. Designing field studies in soil science. *Can. J. Soil Sci.* 84: 1–10.

Powers, R.F. 1991. Are we maintaining productivity of forest lands? Establishing guidelines

through a network of long-term studies. In A.E. Harvey and L.F. Neuenschwander, compilers. *Proceedings—Management and Productivity of Western Montane Forest Soils*. General Technical Report. INT-GTR-280. April 10–12, 1990, USDA Forest Service, Washington, DC, pp. 70–89.

Quesnel, H.J. and Lavkulich, L.M. 1980. Nutrient availability of forest floors near Port Hardy, British Columbia, Canada. *Can. J. Soil Sci.* 60: 565–573.

Snedecor, G.W. and Cochran, W.G. 1980. *Statistical Methods*, 7th edn. Iowa State University Press, Ames, AI, 507 pp.

Van Wesemael, B. and Veer, M.A.C. 1992. Soil organic matter accumulation, litter decomposition and humus forms under Mediterranean-type forests in southern Tuscany, Italy. *J. Soil Sci.* 43: 133–144.

Chapter 3
Measuring Change in Soil Organic Carbon Storage

B.H. Ellert and H.H. Janzen

Agriculture and Agri-Food Canada

Lethbridge, Alberta, Canada

A.J. VandenBygaart

Agriculture and Agri-Food Canada

Ottawa, Ontario, Canada

E. Bremer

Symbio Ag Consulting

Lethbridge, Alberta, Canada

3.1 INTRODUCTION

Organic carbon (C) must be among the most commonly analyzed soil constituents, starting with the earliest soil investigations. Already in the nineteenth century, chemists were routinely analyzing soil C (e.g., Lawes and Gilbert 1885). Initially, these analyses were done to investigate pedogenesis and to assess soil productivity, both of which are closely linked to organic C (Gregorich et al. 1997). But more recently, scientists have been analyzing soil organic C (SOC) for another reason: to measure the net exchange of C between soil and atmosphere (Janzen 2005). Indeed, building reserves of SOC has been proposed as a way of slowing the rising atmospheric CO_2 concentrations caused by burning fossil fuel (Lal 2004a,b).

Measuring SOC to quantify soil C ''sinks'' requires more stringent sampling and analyses than measuring SOC to evaluate productivity. Where once it was sufficient to measure relative differences in concentration over time or among treatments, now we need to know the change in amount of C stored in Mg C per ha. Reviews of SOC measurement typically focus on the chemical methods of determining the SOC concentrations after samples have been brought to the laboratory. Here we emphasize soil sampling procedures and calculation approaches to estimate temporal changes in SOC stocks. Uncertainties along the entire chain of procedures, from designing the soil sampling plan, to sampling in the field, to processing and storing the samples, through to chemical analysis and calculating soil C stocks need to be considered (Theocharopoulos et al. 2004).

SOC is dynamic: newly photosynthesized C is added regularly in the form of plant litter, and existing SOC is gradually decomposed back to CO_2 by soil biota. Management or environmental conditions that change the relative rates of inputs and decomposition will effect a change in the amount of SOC stored. Rates of change in SOC (typically less than 0.5 Mg C ha^{-1} $year^{-1}$) are quite small, however, compared to the large amounts of SOC often present (as high as 100 Mg C ha^{-1}, or more, in the top 30 to 60 cm soil layer). Thus changes in SOC can only be reliably measured over a period of years or even decades (Post et al. 2001). Since the distribution of SOC in space is inherently variable, temporal changes (e.g., attributable to management practices, environmental shifts, successional change) must be distinguished from spatial ones (e.g., attributable to landform, long-term geomorphic processes, nonuniform management).

Temporal changes in SOC can be defined in two ways (Figure 3.1): as an absolute change in stored C (SOC at $t = x$ minus SOC at $t = 0$), or as a net change in storage among treatments (SOC in treatment A minus SOC in treatment B, after x years). The former provides an estimate of the actual C exchange between soil and atmosphere; the latter provides an estimate of the C exchange between soil and atmosphere, attributable to treatment A, relative to a control (treatment B). Both expressions of temporal change may be available from manipulative experiments with appropriate samples collected at establishment (assesses spatial variability) and at various intervals (say 5 to 10 years) thereafter.

This chapter provides selected methods for measuring the change in C storage, either absolute or net, typically for periods of 5 years or more. To be effective, the method needs to: measure *organic* (not total) C, provide estimates of C stock change (expressed in units of C mass per unit area of land to a specified soil depth and mass), be representative of the land area or management treatment under investigation, and provide an indication of confidence in the measurements. These methods are applicable, with minor modification, to a range of scales and settings, including benchmarks sites and replicated research experiments.

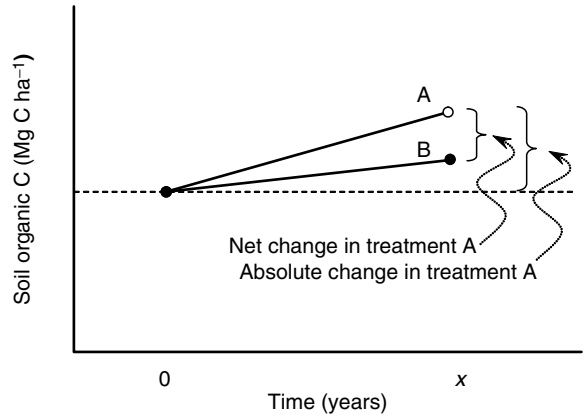

FIGURE 3.1. Illustration of hypothetical changes in soil organic C in two treatments, A and B. For treatment A, the absolute change is the difference in SOC at time = x, compared to that at time = 0. The net change is the difference between SOC in treatment A and that in treatment B, at time = x, assuming that SOC was the same in both treatments at time = 0. The latter approach is often used to measure the effect on SOC of a proposed treatment (e.g., no-till) compared to a standard "control" (e.g., conventional tillage).

3.2 SELECTING THE SAMPLING LOCATIONS AND PATTERN

Determining the optimum number and spatial arrangement of sampling points to estimate SOC storage remains as much an art as a science. Nevertheless, careful study of the site, along with clearly articulated objectives can improve the cost-effectiveness and precision of the estimates (VandenBygaart 2006).

3.2.1 Materials

1 Descriptions of soil properties, landscape characteristics, and agronomic history at the study site, from sources such as: soil maps and reports, aerial photos, scientific publications, cropping records, and yield maps.

3.2.2 Procedure

Two general approaches can be used in sampling a study area (e.g., a plot, field, watershed):

a Nonstratified sampling, where the entire study area is considered to be one unit, and sampled in a systematic or random manner.

b Stratified sampling, where the study area is first subdivided into relatively homogeneous units, based on factors such as topography (e.g., slope position), and each unit is sampled separately.

3.2.3 Nonstratified Sampling

1 Obtain an estimate of the likely sample variance and required accuracy for SOC at the study site, based on previously compiled information.

2 Using as much information as available, calculate the number of samples required using Equation 3.1. The required number of samples will increase as variability and the required accuracy increase (Figure 3.2) (Garten and Wullschleger 1999; Wilding et al. 2001). Required accuracy is expressed as in the same units used for the sample mean, and often is less than 10% of that value because even small changes in the mean imply appreciable pedosphere–atmosphere C exchange over large tracts of land.

3 Select an appropriate grid or linear sampling pattern, suited to the study site and sampling equipment.

3.2.4 Stratified Sampling

1 Subdivide the study site into areas likely to have similar SOC stocks, based on factors such as topography or management history.

2 Select the number of sampling sites within each subarea, using Equation 3.1, or Figure 3.2 as a guide, or by fixed allotment. In the latter case, for example, one or several sampling sites may be designated for each of three slope positions within a large research plot.

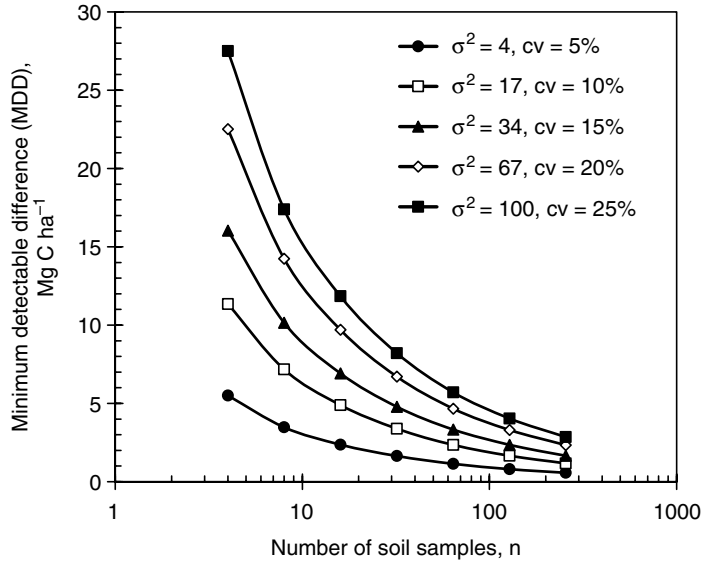

FIGURE 3.2. Decrease in the minimum detectable difference (MDD) between mean soil C at two sampling times for contrasting levels of variance as the number of samples collected at each time doubles (4, 8, 16, ...). The MDD was calculated for $\alpha = 0.05$ significance and $(1-\beta) = 0.90$ statistical power (i.e. probability of rejecting the null hypothesis when it really is false and should be rejected). The lines correspond to increasing variance (σ^2) selected for a hypothetical soil layer containing a mean of 40 Mg C ha^{-1} with the coefficient of variation (cv) increasing from 5% to 25%. (Adapted from Garten, C.T. and Wullschleger, S.D., *J. Environ. Qual.*, 28, 1359, 1999. With permission.)

3.2.5 Calculations

$$n_{\text{req}} = \frac{t^2 s^2}{(d \times \text{mean})^2} \tag{3.1}$$

where n_{req} is the required number of samples, t is the Student's t-value, at the desired confidence level (typically $1-\alpha = 0.90$ or 0.95), s^2 is the sample variance, d is the required accuracy or maximum acceptable deviation from the mean (e.g. $d = 0.10$), and mean is the arithmetic sample mean.

3.2.6 Comments

Sampling patterns and intensities will vary widely, depending on site characteristics and on other factors, notably economic considerations. Often, the number of samples required to achieve the desired sensitivity is exceedingly expensive, and the number of sampling points is somewhat arbitrarily reduced. As well, sampling intensity may have to be reduced in small plots, such as long-term experiments, where excessive soil removal may disturb the site to the extent that future research is jeopardized. But such compromises, if carried too far, may reduce the chance of measuring any differences with reasonable reliability. Studies with insufficient sampling points typically lack statistical power to assess treatment effects. Consequently, the ''cost'' of erroneous conclusions drawn from such data (when the data really are inconclusive) may greatly exceed the ''savings'' provided by reduced sample numbers.

Precisely measuring temporal changes in SOC first depends on identifying or minimizing spatial changes. Spatial changes can be minimized by pairing sampling locations in space (Ellert et al. 2001, 2002; VandenBygaart 2006). This approach allows for effective measurement of SOC changes in time at comparatively few sampling points, but measured C stock change values at these points are not necessarily representative of the entire study site. Conant and Paustian (2002) and Conant et al. (2003) have evaluated similar sampling strategies.

3.3 EXTRACTING AND PROCESSING SOIL CORES

The following procedure is intended for the extraction of soil cores, from agricultural plots or landscapes, for subsequent organic C analysis. It is provided as an illustration, recognizing that individual studies may require modification to satisfy specific objectives and local conditions.

3.3.1 Materials

1 Truck-mounted hydraulic soil coring device.

2 Soil coring tube, with slots 1 cm wide by 30 cm long, and a cutting bit with inside diameter of about 7 cm. The bit usually has slightly smaller diameter (by 1 to 4 mm) than the tube; this difference should be small enough to avoid soil mixing, but large enough to prevent sticking. In dry, coarse-textured soils with weak consolidation this difference should be reduced so there is enough friction to hold the core when the tube is pulled from the soil. The diameter of the coring bit should be measured accurately and recorded for future calculations of soil core density.

3 Piston to push the soil core out of tube. A simple piston can be constructed by attaching a rubber stopper to the end of a wooden dowel.

4 Knife, steel ruler, scissors, wire brush.

5 Aluminum foil trays ($\sim 24 \times 30 \times 6$ cm, used in steam tables for serving food), coolers for transporting trays from field, and heavy polyethylene bags ($\sim 30 \times 50$ cm) to contain trays of field-moist soil.

6 Analytical balance (3000 g capacity, resolution to 0.01*g*), moisture tins (8 cm diameter $\times$ 6 cm tall), drying oven (105°C).

7 Paper ''coffee'' bags with plastic lining and attached wire ties (e.g., Zenith Specialty Bag Co., 11 $\times$ 6 cm base $\times$23 cm height).

8 ''Rukuhia'' perforated drum grinder, with 2 mm perforations (Waters and Sweetman 1955); or another coarse soil grinder and a 2 mm soil sieve.

9 Equipment to measure soil sampling locations. This may be a simple surveyor's tape to measure locations relative to permanent marker stakes in long-term field experiments, or a Global Positioning System (GPS) receiver. For precise pairing (in space) of samples collected at sequential time intervals of several years, a two-stage measuring approach may be useful: the general location is measured relative to permanent reference points or is recorded using a simple GPS receiver,

and the position of the initial cores is marked by burying an electromagnetic marker originally developed to identify underground utilities (Whitlam 1998). Alternatively, high-resolution GPS is available in many regions.

3.3.2 Procedure

1 Before sampling, label paper bags with name, sampling date, location, and soil depth. These bags, eventually to be used for storing the air-dried soils, also serve as labels throughout the sampling process. Weigh the aluminum trays, one for each sample, and record the weight on the tray.

2 In the field, for each sampling point, lightly brush away surface residue and extract a core to a depth of at least 60 cm. Move the core from the vertical to a horizontal position (e.g., in a sectioning trough made of 10 to 15 cm diameter pipe cut lengthwise), and measure the depths of any visible discontinuities (e.g., depth of A_p horizon). Be prepared to discard cores that are unrepresentative (e.g., excessively compacted during sampling, evidence of atypical rodent activity, gouged by a stone pushed along the length of the core during sampling). It may prove useful to push the core (from the deepest end) out in increments, using the top end of the tube as a guide to make perpendicular cuts. Cut the core into carefully measured segments (for example: 0 to 10, 10 to 20, 20 to 30, 30 to 45, and 45 to 60 cm), and place segments into aluminum trays, avoiding any loss of soil. Repeat the procedure for a second core, about 20 cm apart, and composite with the first core segments. Place aluminum trays inside a polyethylene bag, along with the labeled paper bag, fold over polyethylene bag, and store in cooler before subsequent processing indoors.

3 In the laboratory, remove aluminum trays from the polyethylene bags and air-dry at room temperature. Except for very sandy soils, it will be much easier to grind the soils if the field-moist soil cores are broken apart by hand before air drying and subsequent grinding. Great care is required to avoid sample losses during processing and contamination by dust, plant material, paper, or other C-rich contaminants during drying. Wear rubber gloves when handling soil to avoid contamination.

4 Once samples are air-dry, record weight of sample + aluminum tray. Remove a small, representative subsample (e.g., 50 to 80 g, excluding stones and large pieces of plant residue), and determine air-dry moisture content by oven-drying for 48 h at 105°C. Alternatively, the weights of field-moist cores plus trays may be recorded immediately after removal from the polyethylene bag and before they are broken apart and air-dried. In this case, accurate field moisture contents are crucial to estimate the densities of core segments, but spillage when cores are broken apart and mixed may be less consequential than the case when cores are dried before weighing. Thoroughly mix soils before subsampling to determine field moisture content and possibly to retain a field-moist subsample for biological analyses.

5 Crush or grind entire samples to pass a 2 mm sieve, and screen out gravel >2 mm in diameter. All organic material in the sample should be included; if necessary, separately grind roots and other large organic debris to <2 mm, and mix into the sample. A ''Rukuhia'' perforated drum grinder (Waters and Sweetman 1955)

allows efficient, effective grinding of soil samples for SOC analysis. For each sample, remove and record the air-dry weight of gravel >2 mm in diameter.

6 Place coarsely ground samples in labeled ''coffee'' bags for storage under cool, dry conditions, before analysis. For permanent storage (longer than 1 year), soil samples should be placed in sealed glass or plastic jars, and kept under cool, dry, and dark conditions. If finely ground soil is required (e.g., for elemental micro-analysis), the coarsely ground (<2 mm) soil should be thoroughly mixed and subsampled before bagging.

3.3.3 Calculations

1 Air-dry moisture content

$$W_s = (M_{AD} - M_{OD})/(M_{OD} - M_{tin}) \tag{3.2}$$

where W_s is the water content of air-dry soil, by weight (g g^{-1}), M_{AD} is the mass of air-dry soil and tin (g), M_{OD} is the mass of oven-dry soil and tin (g), and M_{tin} is the mass of tin (g).

2 Density of core segment

The following calculation provides an estimate of the density of the soil core segments. This may not be identical to more exacting estimates of soil bulk density, because compaction or loose surface layers may thwart efforts to collect samples of a uniform volume without altering the original mass *in situ*. Despite this, core segment density is preferred over a separate bulk density measurement for calculating SOC stocks.

$$D_{cs} = [(M_{cs} - M_g)/(1 + W_s)]/[L_{cs}\pi R_b^2] \tag{3.3}$$

where D_{cs} is the density of core segment (g cm^{-3}), stone-free mass averaged over the entire sample volume, M_{cs} is the total mass of air-dry soil in the core segment, M_g is the mass of gravel (g), L_{cs} is the length of core segment (cm), and R_b is the core radius (cm), i.e., inside diameter of coring bit/2. If the sample is a composite of more than 1 core segment, then L_{cs} is the cumulative length. For example, if the sample contains two segments from 10 to 20 cm depth, then $L_{cs} = 20$ cm.

3.3.4 Comments

The procedure described above may be modified to make it applicable to individual study sites and objectives. Some of the important considerations include:

a *Sampling depth*

The sampling depth should, at minimum, span the soil layers significantly affected by the management practices considered. For example, it should include the entire depth of soil affected by tillage. The preferred depth may also vary with crop type; for example, studies including perennial forages may require deeper samples than those with only shallow-rooted annual crops. As the number of sampling depths increases, so does the effort and cost of sampling, processing and analysis. Detection of a given

change in soil C (e.g., 2 Mg C ha^{-1}) becomes more difficult as the change is averaged over increasingly thick soil layers containing increasing soil C. In such instances, it may be reasonable to calculate changes for a layer thinner (to a minimum of perhaps 30 cm) than that sampled, although it might have been preferable to shift resources from sampling deeper layers to sampling at more points. The best compromise may be to sample to below the zone of short-term agricultural influence, but not much deeper. Usually, the sampling depth should be at least 30 cm for annual vegetation and 60 cm or more for perennial vegetation.

b *Division of cores into segments*

The number and length of core segments depends on the vertical heterogeneity of SOC in the profile. Generally, the greater the gradient, the shorter should be the core segments. Often, the length of segments increases with depth because the SOC is less dynamic and more uniform at depth. Where possible, core segments might be chosen to correspond roughly to clear demarcations in the profile, such as tillage depth or horizon boundary. To facilitate comparisons among a fixed soil volume it is preferable to have at least one common sampling depth, but this is not essential for comparisons among a fixed soil mass.

c *Core diameter and number per sampling point*

The preferred core diameter and number of cores per sampling point depend on the sensitivity required and the amount of soil needed for analysis. Sampling larger volumes of soil makes the sample more representative, but also increases cost and disturbance of the experimental area. Soil coring may not be feasible in stony soils that are impenetrable, but larger cores may effectively sample profiles containing some gravel.

d *Core refilling*

The soil void left after removing the sample can be filled by a soil core from an adjacent area (e.g., plot buffers), thereby preserving the physical integrity of the sampling site. This replacement, however, is labor-intensive and introduces soil from outside the treatment area which could affect subsequent samplings. Without intentional replacement, core voids become filled by adjacent topsoil, so subsequent cores should be positioned far enough away to avoid areas most affected by removal of previous cores, but close enough to exclude excessive spatial variations.

e *Core location relative to plants*

Proximity to plants may affect sample SOC contents, especially at the soil surface where plant C is concentrated at the crowns and under perennial or tap-rooted vegetation with localized plant C inputs to soil. Cores should be positioned to avoid bias, for example, when about 1/3 of the soil surface area is occupied by plants, three cores could be collected: one beneath plants, and two more between plant rows or crowns. Often basal areas occupied by the crowns of crops planted in rows are small ($\ll$30%) relative to the interrow areas, so samples are collected exclusively from the interrow. In other cases, such approximations may introduce considerable bias.

f *Measuring total soil C stocks*

In earlier studies of SOC, largely from the perspective of soil fertility, recent plant litter in the sample was often removed by sieving and discarded. In studies of C sinks, however, the total C stock should be measured. The procedure described above includes recent litter directly in the sample. An alternative approach is to analyze the plant debris separately, but include it in the calculation of C stocks. Above-ground residue, if present in significant amounts, may also need to be considered in calculating total C stocks (Peterson et al. 1998).

g *Contamination from other C sources*

Care should be taken to avoid introducing extraneous C from oil used as lubricant in soil coring tubes, wax in sample bags, and coatings on foil trays. The sample drying area should be free of dust (e.g., from plant sample processing), insects, and rodents. Cross contamination (e.g., between carbonate-rich subsoil and organic matter-rich surface soil) should be avoided during processing.

h *Repeated measurements of SOC over time*

Temporal changes in SOC can be measured with higher sensitivity if successive samples are removed from close proximity to (though not directly on) previous soil cores (Ellert et al. 2001; Conant et al. 2003; VandenBygaart 2006). To do that, the original sampling locations can be recorded using the GPS receiver, or by burying an electronic marker in one of the voids left by core removal. At subsequent sampling times, soil cores can then be taken immediately adjacent to previous cores, often in a grid pattern within ''microplots'' (Figure 3.3). The pattern may be modified to accommodate additional sampling times or other site conditions

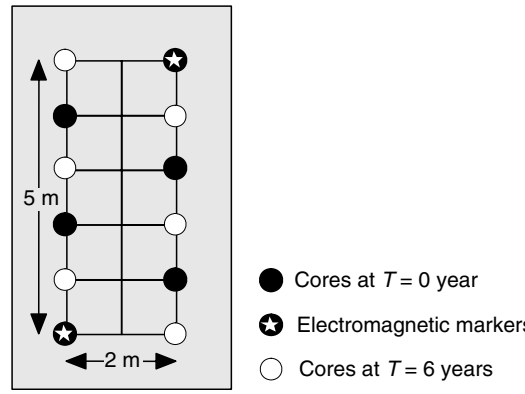

FIGURE 3.3. An example of the arrangement of soil cores within 4×7 m microplots intended for measuring temporal change in SOC stocks. (Adapted from Ellert, B.H., Janzen, H.H., and McConkey, B.G. in R. Lal, J.M. Kimble, R.F. Follett, and B.A. Stewart, (Eds.), *Assessment Methods for Soil Carbon*, Lewis Publishers, Boca Raton, Florida, 2001.)

(Conant et al. 2003; VandenBygaart 2006). To most efficiently assess temporal changes in soil C stocks, the number of cores within each microsite and of microsites within a field or plot may be adjusted for differences in variability at the microsite and field levels (Bricklemyer et al. 2005).

3.4 ESTIMATING ORGANIC C STOCKS IN SOIL

3.4.1 Materials

1 Fine soil grinder and small test sieves (No. 60 with 250 μm openings and No. 100 with 150 μm openings).

2 Carbon analyzer, using dry combustion and subsequent analysis of CO_2. (For information on analysis of total and organic C see Chapter 21.)

3.4.2 Procedure

1 Obtain a representative subsample of the previously stored air-dry soil samples, ideally using ''drop through'' sample riffles or centrifugal sample dividers, as needed to avoid a biased subsample. Variability introduced by simpler, more expedient approaches (e.g., small scoops from six distinct areas within a thoroughly mixed tray of air-dried, <2 mm soil) is easily quantified by collecting multiple subsamples from a few samples. Scooping from the tops of sample bags or jars is not recommended, because soil constituents tend to separate during bag or jar filling and sample handling.

2 For most microanalytical techniques the coarsely ground (<2 mm) sample will have to be finely ground using a roller or jar mill, ball-and-capsule mill, shatter-box or ring-and-puck mill, or a mortar and pestle (e.g., Kelley 1994; Rondon and Thomas 1994; McGee et al. 1999; Arnold and Schepers 2004). The preferred fineness depends on the amount of sample analyzed. If less than 0.1 g is to be combusted, the sample should be ground to pass through a 150 μm sieve. The entire subsample should be ground to pass through the designated sieve (verified by testing a representative subset of samples rather than every sample). Finely ground samples can be stored in glass vials.

3 Dry samples and standards at 60°C to 70°C for 18 h, and determine the organic C concentration (g C kg^{-1} soil) (see Chapter 21). It is critical that inorganic C be completely removed before analysis by addition of acid, or that inorganic C be analyzed separately and then subtracted from total C concentration to estimate organic C concentration (see Chapter 21). Ideally certified reference materials should be used to verify analytical accuracy, but standard soils with certified values for total and organic C remain rare (Boone et al. 1999). At minimum, standard soils prepared in-house or obtained from a commercial supplier should be used to calibrate analyses and monitor analytical precision.

4 Express the concentration in units of mg C g^{-1} dry soil (=kg C Mg^{-1} = % × 10).

3.4.3 Calculations

The SOC stock is the amount of organic C in a fixed layer of soil per unit area of land. Typically, it is expressed in units of Mg C ha^{-1} to a specified depth. Alternative units include kg C m^{-2} = Mg C $ha^{-1} \times 0.100$. The simplest way to calculate SOC stocks is to accumulate the products of concentration and core density to a fixed soil depth and volume (see calculation below). But this approach is subject to bias when comparing SOC across space or time if core density varies even slightly (Ellert and Bettany 1995). For example, when comparing SOC stocks in two treatments, if the average core density to the specified depth is 1.10 Mg m^{-3} in treatment A and 1.00 Mg m^{-3} in treatment B, then the SOC stocks in treatment A will be biased upward because it has 10% more soil in the layers compared. For that reason, SOC stocks should be calculated on an ''equivalent mass'' or ''fixed mass'' basis (see calculation below), unless core densities are very uniform.

SOC Stocks (Fixed Depth)

$$\mathrm{SOC_{FD}} = \sum_{1}^{n} D_{cs} C_{cs} L_{cs} \times 0.1 \tag{3.4}$$

where $\mathrm{SOC_{FD}}$ is the SOC stock to a fixed depth (Mg C ha^{-1} to the specified depth), D_{cs} is the density of core segment (g cm^{-3}), C_{cs} is the organic C concentration of core segment (mg C g^{-1} dry soil), and L_{cs} is the length of core segment (cm).

SOC Stocks (Fixed Mass)

1 For all samples, calculate the mass of soil to the designated depth:

$$M_{soil} = \sum_{1}^{n} D_{cs} L_{cs} \times 100 \tag{3.5}$$

where M_{soil} is the mass of soil to a fixed depth (Mg ha^{-1}).

2 Select, as the reference, the lowest soil mass to the prescribed depth from all sampling sites (M_{ref}).

3 Calculate the soil mass to be subtracted from the deepest core segment so that mass of soil is equivalent in all sampling sites:

$$M_{ex} = M_{soil} - M_{ref} \tag{3.6}$$

where M_{ex} is the excess mass of soil, to be subtracted from deepest core segment.

4 For each sampling site, calculate SOC stock to fixed mass:

$$\mathrm{SOC_{FM}} = \mathrm{SOC_{FD}} - M_{ex} \times C_{sn}/1000 \tag{3.7}$$

where $\mathrm{SOC_{FM}}$ is the SOC stock for a fixed mass of M_{ref} and C_{sn} is the SOC concentration in deepest soil core segment (mg C g^{-1} dry soil) (core segment = n).

Sample Calculations

Given the following three hypothetical soil cores:

	SOC concentration (g C kg^{-1} soil)			Density (g cm^{-3})		
Depth (cm)	Core 1	Core 2	Core 3	Core 1	Core 2	Core 3
0–10	20.0	22.0	19.0	1.04	1.10	0.99
10–20	17.4	16.3	17.1	1.17	1.27	1.20
20–40	14.3	15.2	13.9	1.30	1.35	1.25
40–60	12.2	11.9	12.1	1.40	1.45	1.42

SOC_{FD} to 40 cm is
78.3, 85.9, and 74.1 Mg C ha^{-1} for cores 1, 2, and 3, respectively.

For SOC_{FM}:
$M_{soil} = 4810$, 5070, and 4690 Mg ha^{-1} to 40 cm, for cores 1, 2, and 3, respectively.
Hence:
$M_{ref} = 4690$ Mg ha^{-1} (mass of soil core 3), and
$M_{ex} = 120$, 380, and 0 Mg ha^{-1}, for cores 1, 2, and 3, respectively.

Thus:
For core 1, $SOC_{FM} = 78.3 - 120 \times 14.3/1000 = 76.6$ Mg C ha^{-1}.
Similarly, $SOC_{FM} = 80.1$ and 74.1 Mg C ha^{-1}, for cores 2 and 3, respectively.
Thicknesses of the fixed masses $= 40 - M_{ex}/(D_{cs} \times 100) = 39.1$, 37.2, and 40.0 cm for cores 1, 2, and 3, respectively.

Comments

The approach described to estimate SOC stocks is applicable to sites where temporal changes are attributable to biological processes (chiefly the balance between soil C inputs and outputs), rather than geomorphic processes (soil erosion and deposition). The fundamental assumption is that soil mass is largely conserved among sampling times. At sites where this does not hold, other approaches are required to estimate lateral soil redistribution or net soil imports or exports, before temporal changes in SOC may be estimated. For example at sites with considerable mass additions or removals (e.g. waste application or soil export) survey techniques that enable sampling to a fixed subsurface elevation might be appropriate (Chang et al. 2007).

Numerous variations are possible in the calculation of SOC stocks by the ''fixed mass'' approach. For example, instead of using the SOC concentration of layer n in the correction (Equation 3.7), it may be more appropriate to use the weighted mean concentration in layers n and $n+1$. Or, rather than subtracting SOC in the correction, some researchers select a reference mass and *add* SOC, based on the SOC concentration of the layer below. In all cases, the method assumes that concentration value used is representative of the layer added or subtracted. For that reason, some researchers have used core configurations with a short segment just below the depth of interest. For example, if C stocks are to be estimated for the 0 to 20 cm layer, a 20 to 25 cm segment is isolated to be used for the ''fixed depth'' calculation.

Whether comparisons are based on a fixed soil depth or mass is immaterial for situations with soil redistribution, accumulation, or export. In such situations, it is practically impossible to distinguish between the effects of geomorphological processes (soil redistribution) and biological processes (plant C inputs and SOC decay). Only in rare instances (e.g., soils with a persistent and uniform marker layer, such as a fragipan) can soil deposition or erosion be inferred from routine soil sampling.

REFERENCES

Arnold, S.L. and Schepers, J.S. 2004. A simple roller-mill grinding procedure for plant and soil samples. *Commun. Soil Sci. Plant Anal.* 35: 537–545.

Boone, R.D., Grigal, D.F., Sollins, P., Ahrens, R.J., and Armstrong, D.E. 1999. Soil sampling, preparation, archiving, and quality control. In G.P. Robertson, D.C. Coleman, C.S. Bledsoe, and P. Sollins, Eds. *Standard Soil Methods for Long-Term Ecological Research*. Oxford University Press, New York, pp. 3–28.

Bricklemyer, R.S., Miller, P.R., Paustian, K., Keck, T., Nielsen, G.A., and Antle, J.M. 2005. Soil organic carbon variability and sampling optimization in Montana dryland wheat fields. *J. Soil Water Conserv*. 60: 42–51.

Chang, C., Ellert, B., Hao, X., and Clayton, G. 2007. Elevation-based soil sampling to assess temporal changes in soil constituents. *Soil Sci. Soc. Am. J*. 71: 424–429.

Conant, R.T. and Paustian, K. 2002. Spatial variability of soil organic carbon in grasslands: implications for detecting change at different scales. *Environ. Pollut*. 116: S127–S135.

Conant, R.T., Smith, G.R., and Paustian, K. 2003. Spatial variability of soil carbon in forested and cultivated sites: implications for change detection. *J. Environ. Qual*. 32: 278–286.

Ellert, B.H. and Bettany, J.R. 1995. Calculation of organic matter and nutrients stored in soils under contrasting management regimes. *Can. J. Soil Sci*. 75: 529–538.

Ellert, B.H., Janzen, H.H., and Entz, T. 2002. Assessment of a method to measure temporal change in soil carbon storage. *Soil Sci. Soc. Am. J*. 66: 1687–1695.

Ellert, B.H., Janzen, H.H., and McConkey, B.G. 2001. Measuring and comparing soil carbon storage. In R. Lal, J.M. Kimble, R.F. Follett, and B.A. Stewart, Eds. *Assessment Methods for Soil Carbon*. Lewis Publishers, Boca Raton, FL, pp. 131–146.

Garten, C.T. and Wullschleger, S.D. 1999. Soil carbon inventories under a bioenergy crop (switchgrass): measurement limitations. *J. Environ. Qual*. 28: 1359–1365.

Gregorich, E.G., Carter, M.R., Doran, J.W., Pankhurst, C.E., and Dwyer, L.M. 1997. Biological attributes of soil quality. In E.G. Gregorich and M.R. Carter, Eds. *Soil Quality for Crop Production and Ecosystem Health*. Elsevier, Amsterdam, pp. 81–113.

Janzen, H.H. 2005. Soil carbon: a measure of ecosystem response in a changing world? *Can. J. Soil Sci*. 85: 467–480.

Kelley, K.R. 1994. Conveyor-belt apparatus for fine grinding of soil and plant materials. *Soil Sci. Soc. Am. J*. 58: 144–146.

Lal, R. 2004a. Soil carbon sequestration to mitigate climate change. *Geoderma* 123: 1–22.

Lal, R. 2004b. Soil carbon sequestration impacts on global climate change and food security. *Science* 304: 1623–1627.

Lawes, J.B. and Gilbert, J.H. 1885. On some points in the composition of soils with results illustrating the sources of the fertility of Manitoba prairie soils. *J. Chem. Soc*. 47: 380–422.

McGee, E.A., Vohman, D.D., White, S.A., and Thompson, T.L. 1999. Rapid method for fine grinding soils for organic N and ^{15}N analysis. *Commun. Soil Sci. Plant Anal*. 30: 419–426.

Peterson, G.A., Halvorson, A.D., Havlin, J.L., Jones, O.R., Lyon, D.J., and Tanaka, D.L. 1998. Reduced tillage and increasing cropping intensity in the Great Plains conserves soil C. *Soil Till. Res.* 47: 207–218.

Post, W.M., Izaurralde, R.C., Mann, L.K., and Bliss, N. 2001. Monitoring and verifying changes of organic carbon in soil. *Climatic Change* 51: 73–99.

Rondon, M.A. and Thomas, R.J. 1994. A piston-action ball mill for the rapid preparation of plant and soil samples for the automated analysis of nitrogen (^{15}N) and carbon (^{13}C). *Commun. Soil Sci. Plant Anal.* 25: 435–445.

Theocharopoulos, S.P., Mitsios, I.K., and Arvanitoyannis, I. 2004. Traceability of environmental soil measurements. *Trends Anal. Chem.* 23: 237–251.

VandenBygaart, A.J. 2006. Monitoring soil organic carbon stock changes in agricultural landscapes: issues and a proposed approach. *Can. J. Soil Sci.* 86: 451–463.

Waters, D.F. and Sweetman, I.C. 1955. The Rukuhia soil grinder. *Soil Sci.* 79: 411–413.

Whitlam, R.G. 1998. Cyberstaking archaeological sites: using electronic marker systems (EMS) for a site datum and monitoring station. *Soc. Am. Archael. Bull.* 16(2): 39–47.

Wilding, L.P., Drees, L.R., and Nordt, L.C. 2001. Spatial variability: enhancing the mean estimate of organic and inorganic carbon in a sampling unit. In R. Lal, J.M. Kimble, R.F. Follett, and B.A. Stewart, Eds. *Assessment Methods for Soil Carbon.* Lewis Publishers, Boca Raton, FL, pp. 69–86.

Chapter 4
Soil Sample Handling and Storage

S.C. Sheppard
ECOMatters Inc.
Pinawa, Manitoba, Canada

J.A. Addison
Royal Roads University
Victoria, British Columbia, Canada

4.1 INTRODUCTION

This chapter deals with soil samples between when they are sampled and when they are analyzed. The key message is that sample handling and storage can profoundly affect analysis results, and no one way is suitable for all analytes. The issues related to soil sample handling and storage relate to the management of sample clump size, moisture content, temperature, and storage time.

With the increased availability of software to gather and interpret spatial information, there have been important advances in the past decade on methods to sample soils. Similarly, analytical capabilities have been remarkably enhanced, with greater sensitivity and more analytes. This includes notable advances in the characterization of soil organisms and biological attributes. However, there has been much less research and practical emphasis on the effects of handling and storage of soil samples. Nonetheless, there is abundant evidence that differences in handling and storage can profoundly affect the interpretation of results.

Perhaps the single most important role of analysis in soil science is to move beyond the reporting of absolutes, and toward the reporting of environmentally relevant measures. Absolute quantities, such as total elemental composition, total organic matter content, and even total porosity, are relatively simple to measure, and are relatively insensitive to effects related to sample handling and storage. However, these quantities are only partially relevant to what many researchers want to measure. Often, the more important measures are attributes such as the bioavailable or leachable elemental composition, and functional and biotic properties of the soil. For these more subtle measures, methods of sample handling and storage become critical. Examples from the literature include:

- Plant-available nitrogen (Craswell and Waring 1972; Wang et al. 1993; Verchot 1999; Fierer and Schimel 2002; Magesan et al. 2002; Riepert and Felgentreu 2002), phosphorus (Potter et al. 1991; Grierson et al. 1998; Turner and Haygarth 2003; Worsfold et al. 2005), potassium (Luo and Jackson 1985), and sulfur (Chaudhry and Cornfield 1971; David et al. 1989; Comfort et al. 1991)

- Speciation of metals and soil solution composition (Leggett and Argyle 1983; Lehmann and Harter 1983; Haynes and Swift 1985, 1991; Walworth 1992; Neary and Barnes 1993; Meyer and Arp 1994; Simonsson et al. 1999; Ross et al. 2001)

- Soil biological activity (Ross 1970; Zantua and Bremner 1975; Ross 1989; Van Gestel et al. 1993; Stenberg et al. 1998; Mondini et al. 2002; Allison and Miller 2005; Goberna et al. 2005)

- Studies of soil organic matter (Kaiser et al. 2001)

- Extraction of organic contaminants (Belkessam et al. 2005)

Without doubt, researchers must refer to the primary literature to identify the requirements and limitations for sample handling and storage specific to the analysis they undertake. It is not a default process; the researcher must be able to defend the sampling handling and storage decisions. Unfortunately, several researchers have shown that the effects of sample preparation and storage are not similar from soil to soil, so that inappropriate handling can jeopardize interpretation of results among different soils (e.g., Brohon et al. 1999; Neilsen et al. 2001).

The objective of this chapter is to provide guidance on sample handling, including compositing, reduction in clump size, and management of soil moisture. Table 4.1 gives an overview. The chapter also discusses two aspects of sample storage; storage between sampling and the primary analysis, and the long-term storage or archive of samples. Handling of samples of soil constituents separated in the field, such as soil pore water collected in lysimeters (e.g., Derome et al. 1998) is not discussed.

4.2 STEPS IN HANDLING AND STORAGE

The requirements for each sampling campaign will differ, but a typical sequence is as follows:

- Collect composite sample in the field or from the experimental system.

- If the sample is too large, reduce clump size, mix and package a portion of the composite to transport to the laboratory.

- Collect a subsample for determination of moisture content, the subsample is weighed, dried at 105°C, and reweighed.

- Dry remaining sample to a moisture content suitable for further sample handling.

- If appropriate and required, further reduce clump size, such as by grinding.

TABLE 4.1 Typical Attributes for Handling and Storage of Soil Samples

Analyte	Compositing and clump reduction	Moisture	Storage before analysis	Archival storage
Soil fauna: earthworms, nematodes, other invertebrates	Avoided, generally use minimally disturbed soil cores or clods (point samples, not composites)	Handle field-moist	Minimal time, refrigerated but not frozen	Not possible for primary analytes, suitable for some ancillary measurements
Microbial activities: respiration, functionality assays	May be minimally disturbed point samples or composites of gently ground soil	Field-moist or workable moisture content	Minimal time, refrigerated but not frozen	Not possible for primary analytes, suitable for some ancillary measurements
Microbial populations: enumeration, population types	Need for aseptic conditions often results in point samples (not composites)	Field-moist or workable moisture content	Minimal time, refrigerated but not frozen	Not possible for primary analytes, suitable for some ancillary measurements
Microbial attributes: PLFA, DNA	May be minimally disturbed point samples or composites of gently ground soil	Field-moist or workable moisture content	Varies with analysis, freezing may be appropriate	Varies with analyte, extremely low temperature freezing (−80°C) may be appropriate
Soil organic matter: structure, composition	Moderately aggressive grinding may be acceptable	Varies with analysis, may include oven drying	Varies with analysis	Varies with analysis
Bioavailability and chemical speciation	Moderately aggressive grinding may be acceptable	Workable moisture content	Minimal time, refrigerated may be ideal	Not possible for primary analytes, suitable for some ancillary measurements
Bulk physical properties: pore size distribution, bulk density	Avoided, generally use minimally disturbed soil cores or clods (point samples, not composites)	Field-moist or workable moisture content, but results reported on oven-dried basis	Indefinite if refrigerated, may change upon freezing	Indefinite if refrigerated, may change upon freezing
Mineralogical	Aggressive grinding acceptable as long as single grains are not crushed	Generally reported on an oven-dried basis	Indefinite in dried state	Indefinite in dried state
Physical: granulometry, total organic matter content	Aggressive grinding acceptable as long as single grains are not crushed	Generally reported on an oven-dried basis	Indefinite in dried state	Indefinite in dried state
Elemental analysis: total and strong-acid extractable	Aggressive grinding acceptable	Generally reported on an oven-dried basis	Indefinite as long as contamination avoided	Indefinite as long as contamination avoided

- Subsample as required for analysis.
- Prepare an archive sample.

4.3 COMPOSITING AND REDUCTION IN CLUMP SIZE

The intended outcome of compositing and reduction in clump size is to ensure the sample represents the whole. Compositing involves the gathering and mixing of a series of individual samples, typically from a series of sampling points across the landscape. Reduction in clump size is often required so that both compositing and subsampling for analysis represent a uniform material. See Schumacher et al. (1990) for detailed discussion of methods of sample splitting and subsampling.

One key issue is that the clumps be small enough that the composite sample or subsample contains a large number of them. This is a statistical issue. Allison and Miller (2005) described how variability in biological assays increased as the size of the analyzed subsamples decreases, and Liggett et al. (1984) commented that the size of subsample required to obtain consistent measurements of plutonium in soils was too large to be practical (in their case, variability among subsamples always dominated over field variation). As a general guideline, if a required composite sample is 1 kg of soil, a reasonable clump size might be $\sim$5 g (5 cm^3) or less. If a required subsample is 0.5 g, then the ''clump'' size might better be described as powder, ground as fine as practical within the limits required by the analysis. For example, Neary and Barnes (1993) and Wang et al. (1993) both recommended grinding to pass a $<$0.5 mm mesh if subsamples were to be $<$1 g.

The other key issue is that the process of breaking up the clumps does not disrupt the analytes. Some of this is self-evident; if one is sampling to measure soil macropore properties or soil fauna, then breaking up of clumps should be minimal and not aggressive. Craswell and Waring (1972) showed that grinding affected microbial mineralization rates in soil, and Neary and Barnes (1993) found that grinding, and especially mechanical grinding, affected extractable iron and aluminum concentrations. In contrast, if the analyte is total elemental concentration, quite aggressive grinding (hammer mill, mortar, and pestle) may be acceptable, as long as the grinder itself does not introduce contamination.

More controversial is the degree of grinding appropriate for measures of bioavailable element composition, or microbial attributes. As an example, tests of soil nutrient availability (soil fertility testing) were originally calibrated with soils that had very specific preparation, typically air-dried, hand-sieved to pass a 2 mm mesh, followed by volumetric (as opposed to mass-based) sampling for analysis. More aggressive drying and grinding affects the amount of nutrient removed by the selective extractants employed, increasing the extractable P by up to 165% in some soils (Turner and Haygarth 2003). Unfortunately, gentle manual preparation is expensive and, with the commercialization of soil fertility testing, more rapid and more aggressive grinding is now the norm. It is not clear if the underlying test response data have been recalibrated accordingly.

Another difficult issue in soil sample preparation is the decision of what to do with pebbles, roots, and anything else that behaves differently during sample preparation than the bulk soil matrix. Many researchers simply remove these nonconforming materials, but obviously their presence can significantly affect the interpretation of analytical results back to the field, if for no other reason than they represent a volumetric dilution of the soil matrix. As a default,

it may be an appropriate rule to remove pebbles larger than the required mesh size, but record their mass relative to the mass of the whole soil. This implies the full sample, apart from the pebbles, is ground to pass the mesh. For roots and organic debris, it may be appropriate to simply remove these as they could be considered ephemeral to the soil. For some analytes, the organic debris might be considered an important secondary subsample. This might be the case for analysis of lipophilic compounds or of fungal activities.

Subsampling organic soils and horizons can also be problematic, especially when materials such as decaying woody plants are present within the soil profile. Knife mills may be useful for grinding fibrous organic soils, if appropriate for the intended analysis.

4.4 SAMPLE MOISTURE CONTENT

The soil moisture content of stored samples is not only of importance for issues related to sample preparation (e.g., reduction of clump size) but can also profoundly affect the results of subsequent analyses. Many soils are physically impossible to handle when they are too wet, and clay soils can be very difficult to grind if they become too dry. One argument in deciding how much to dry the sample is that soils in their native setting are usually subject to wetting and drying processes, and so drying in the laboratory to moisture contents that can be found in the field seems defensible for many analytes.

The standard for measurement of soil mass is dried at 105°C for as long as required to reach a constant weight. For analyses of soil properties reported on a dry weight basis, this basis should be, and is usually assumed to be, the weight after drying at 105°C.

However, the 105°C temperature and the resultant low moisture content are very disruptive to many soil properties. It kills meso- and microbiota, denatures organic entities including soils enzymes, oxidizes some inorganic constituents, collapses clay interlayers, and can modify other soil solids. It is a suitable dryness for absolute measures such as total elemental composition and granulometric composition, and is suitable for some levels of grinding for some soils. For many other analytes, and for successful grinding of clay or organic soils, it is better to allow the soil to retain more moisture.

Nonetheless, if soil samples are not dried to 105°C and the results are to be presented per unit of soil dry weight, then the researcher should measure the soil moisture content of the soil ''as analyzed,'' and convert the results to the 105°C-dry basis. Very often, there is little difference in moisture content between air-dried and 105°C-dried, but they cannot be assumed to be equivalent.

Typical target moisture contents are:

- Field moist or ''as is'' moisture content, which can be extremely variable but necessary to avoid disruption if living organisms are to be extracted.

- Workable, a judgment by the researcher where the soil is allowed to dry to a moisture content that is typically between field capacity and air-dry, and the soil is just dry enough to allow gentle grinding, such as sieving, with no dust production. Microbial activity will be present, seeds may germinate, and refrigerated and dark storage should be considered. As the soil still contains living organisms, allowance for gas-exchange may be required, but the sample should be protected against excessive moisture loss.

Polyethylene bags may be suitable as they allow diffusion of oxygen and limit water loss. The actual moisture content should be confirmed whenever analyses are undertaken.

- Air-dried, where the soil is allowed to equilibrate with humidity in the air, resulting in soil that is nearly as dry as oven dry and can be aggressively ground (if required). Soils at this moisture content can be stored in water-permeable containers (e.g., cardboard boxes). Microbial activity is minimal and a flush of microbial activity is expected when the soil is rewetted. This is the most convenient moisture content, as long as it is consistent with the intended analyses (see examples in Table 4.1).

- Oven-dried at 105°C, where the soil is dry enough that it will accumulate moisture from the air. Soils at this moisture content must be stored in sealed containers or desiccators, and it may be necessary to redry the soils to assure they are at the required moisture content when used. The advantage of this moisture content is that it is the reference standard.

- Oven-dried to a temperature intermediate between air-dry and 105°C, which is generally a compromise between the rather slow process of air-drying and the damaging effects of 105°C. Temperatures of 30°C–40°C are arguably in the range of temperatures experienced at the soil surface in the field. Temperatures of 50°C–80°C are compromises.

Drying a soil, even at room temperature, causes a number of reactions. Living organisms either pass into a resting stage, or die. Dissolved inorganic materials will become more concentrated in the remaining pore water, and ultimately will form precipitates or perhaps gel-phase materials. Dissolved organic materials probably coagulate, both because they become concentrated and because the salt concentration of the pore water increases. Solid organic materials will deform when dry, uncover underlying mineral surfaces and may become very hydrophobic. Mineral-phase materials are generally resistant to modification until the soil becomes extremely dry or excessive heat is used.

Given these changes, it is obvious that moisture management must vary according to the required analysis (Table 4.1). Storage of air-dried or oven-dried samples is very convenient, and although dry storage will introduce gradual changes in some soil attributes, at least for the measurement of some soil chemical and physical properties these changes may be minimal. However, some types of chemical analyses are affected by drying. For example, some soil nitrogen fertility tests are influenced by drying, and as a result some commercial laboratories request soils not be dried before being sent to the laboratory. For most other large-scale operations, such as other soil fertility testing where large numbers of samples are required, air-dried or a low temperature oven-dried samples are the norm, for convenience as well as reasonable consistency.

An approach used by some to overcome the effects of drying is to rewet and incubate soil samples before analysis. The rationale is that air-drying and rewetting are natural occurrences, and so rewetting may be appropriate mitigation for the temporary effects of air-drying. Lehmann and Harter (1983) noted some recovery of copper sorption when soils were rewetted and incubated for 1 month. Haynes and Swift (1991) noted that extractability of metals could be restored with rewetting, whereas effects of drying on extractability of organic matter ‘‘was only slowly reversed following rewetting.’’

For biological, microbial, and enzyme assays, drying should generally be avoided or restricted to drying to a workable moisture content. Numerous studies have shown that drying and then rewetting the soil has a tremendous impact on biological properties, including microbially mediated soil chemical transformations (Van Gestel et al. 1993; Riepert and Felgentreu 2002). Although some studies have shown that rewetting and incubation of dried soil restores biological activity to at least some degree, it is also clear that different segments of the microbial population respond in different ways. Consequently the degree of recovery and the time taken for microbial population and functions to reestablish differs for different soils and for different microbial groups (e.g., Fierer and Schimel 2002; Pesaro et al. 2004).

4.5 EFFECTS OF TEMPERATURE AND DURATION OF STORAGE

As indicated in the introduction, there is no default storage method for all analytes and each researcher must be able to defend decisions made about sample storage. Any analysis of biological attributes or biologically mediated activities, and any analysis of volatile or labile constituents obviously require minimal storage time and specific conditions of temperature, moisture content, and container type. Analysis of nitrogen compounds and organic chemicals subject to biodegradation are notably among those where storage conditions are an issue (Stenberg et al. 1998; Rost et al. 2002).

In situations where a living soil fauna is of interest, soil samples should be stored at 5°C rather than frozen. The ability to withstand freezing temperatures in soil invertebrates is determined by a complex set of physiological and behavioral adaptations that are time dependent, so it is generally not reasonable to assume that soil samples can be safely frozen simply because the sample comes from an area subject to seasonal freezing. Edwards and Fletcher (1971) concluded that soil storage up to a week at 5°C should not cause any serious changes in the numbers of individuals or groups of soil fauna extracted from soil samples, but that after 28 day storage at 5°C, or even earlier at higher temperatures, significant changes were to be expected.

The appropriate temperature for storing soil samples required for determining microbial parameters, including the potential of the indigenous microbial flora to degrade contaminants, is controversial. Stenberg et al. (1998) concluded it was acceptable to store soils for microflora analyses at −20°C if the soils were from areas where they were normally frozen in winter. Indeed some test guidelines that measure microbial activity (e.g., OECD 2000) agree that if soils are collected from areas where they are frozen for at least 3 months of the year, then storage at −18°C for 6 months ''can be considered.'' However several other authors, including some working on soils from northern areas, stress that freezing soil samples causes significant and long-term changes in microbial abundance and activity and that certain groups are particularly sensitive to the effects of freezing (Zelles et al. 1991; Shishido and Chanway 1998; Pesaro et al. 2003). On the other hand other microbial assays (e.g., phospholipid fatty acid [PLFA]) generally require samples to be stored in a frozen state in order to minimize degradation of the fatty acids during storage.

4.6 ARCHIVAL STORAGE

Archival storage is intended to serve a number of objectives. The most immediate is to allow reanalysis of samples where the primary results are questioned. This is a form of replication of analysis. Relatedly, it is sometimes important to measure other attributes of a specific

sample in order to explain the primary results. For example, retrospective analysis of trace element content may confirm a hypothesis about differences in the initial analyses.

However, both these objectives relate to the initial reason to collect the samples. Archive samples serve other objectives as well, related to future research. An improved analytical method may become available, and reanalysis of archived samples is one way to validate the new method and relate the new and old methods. Alternatively, another research project may require a suite of soils with the specific attributes available in the archive samples.

Another key role for archived soils samples is to provide reference standards, and in the case of ecotoxicology assays to provide a diluent soil (Sheppard and Evenden 1998). Ehrlichmann et al. (1997) commented that in their reference soils, the toxicity of organic contaminants decreased with storage time, whereas the toxicity of metals increased with storage time. Riepert and Felgentreu (2002) investigated soils stored as reference soils for plant ecotoxicity bioassays, and concluded that ''soil kept as a laboratory standard under air-dried conditions over a long time period is not suitable [. . .] due to the [. . .] microbial situation,'' especially as related to nitrogen mineralization.

There is not a lot of information on how long an archive sample remains valid. Certainly samples lose biological validity fairly quickly, but will retain physical attributes such as granulometry indefinitely. In contrast, Bollen (1977) found that samples stored dry for 54 years retained their ability to respire and oxidize sulfur, some more and some less than when the samples were originally collected.

Perhaps the single most important aspect of archived soil samples, just as with any kind of archive, is the documentation. This must include provenance of the sample, collection details, preparation and storage conditions, and ideally the linkage to the researcher, and the primary analysis the researcher completed on the samples.

4.7 CONCLUSION

A review of the literature will immediately indicate that artifacts have been shown to arise from all types of soil sample handling and storage. No one protocol is suitable for all analytes. Convenient protocols such as air-drying and grinding have profound effects on physical, chemical, and biological attributes of soils. Even soil fertility testing for phosphorus and metals can be jeopardized by subtle differences in sample handling. Soil is a living material, and perhaps soil samples need the same care in handling that is afforded to tissue samples.

The most important message of this chapter is that sample handling and storage protocols are not by default. It is the responsibility of the researcher to consider and be prepared to defend the decisions taken.

REFERENCES

Allison, V.J. and Miller, R.M. 2005. Soil grinding increases the relative abundance of eukaryotic phospholipid fatty acids. *Soil Sci. Soc. Am. J.* 69: 423–426.

Belkessam, L., Lecomte, P., Milon, V., and Laboudigue, A. 2005. Influence of pre-treatment step on PAHs analyses in contaminated soils. *Chemosphere* 58: 321–328.

Bollen, W.B. 1977. Sulfur oxidation and respiration in 54-year-old soil samples. *Soil Biol. Biochem.* 9: 405–410.

Brohon, B., Delolme, C., and Gourdon, R. 1999. Qualification of soils through microbial activities measurements: influence of the storage period on INT-reductase, phosphatase and respiration. *Chemosphere* 38: 1973–1984.

Chaudhry, I.A. and Cornfield, A.H. 1971. Low-temperature storage for preventing changes in mineralizable nitrogen and sulphur during storage of air-dry soils. *Geoderma* 5: 165–168.

Comfort, S.D., Dick, R.P., and Baham, J. 1991. Air-drying and pretreatment effects on soil sulfate sorption. *Soil Sci. Soc. Am. J.* 55: 968–973.

Craswell, E.T. and Waring, S.A. 1972. Effect of grinding on the decomposition of soil organic matter. II. Oxygen uptake and nitrogen mineralization in virgin and cultivated cracking clay soils. *Soil Biol. Biochem.* 4: 435–442.

David, M.B., Mitchell, M.J., Aldcorn, D., and Harrison, R.B. 1989. Analysis of sulfur in soil, plant and sediment materials: sample handling and use of an automated analyzer. *Soil Biol. Biochem.* 21: 119–123.

Derome, K., Derome, J., and Lindroos, A. 1998. Techniques for preserving and determining aluminium fractions in soil solution from podzolic forest soils. *Chemosphere* 36: 1143–1148.

Edwards, C.A. and Fletcher, K.E. 1971. A comparison of extraction methods for terrestrial arthropods. In J. Phillipson, Ed. *Methods of Study in Quantitative Soil Ecology: Population, Production and Energy Flow*. IBP Handbook No. 18, Blackwell Scientific Publications, Oxford, U.K. pp. 150–185.

Ehrlichmann, H., Eisentrager, A., Moller, M., and Dott, W. 1997. Effect of storage conditions of soil on ecotoxicological assessment. *Int. Biodeter. Biodegr.* 39: 55–59.

Fierer, N. and Schimel, J.P. 2002. Effects of drying-rewetting frequency on soil carbon and nitrogen transformations. *Soil Biol. Biochem.* 34: 777–787.

Goberna, M., Insam, H., Pascual, J.A., and Sanchez, J. 2005. Storage effects on the community level physiological profiles of Mediterranean forest soils. *Soil Biol. Biochem.* 37: 173–178.

Grierson, P.F., Comerford, N.B., and Jokela, E.J. 1998. Phosphorus mineralization kinetics and response of microbial phosphorus to drying and rewetting in a Florida Spodosol. *Soil Biol. Biochem.* 30: 1323–1331.

Haynes, R.J. and Swift, R.S. 1985. Effects of air-drying on the adsorption and desorption of phosphate and levels of extractable phosphate in a group of acid soils, New Zealand. *Geoderma* 35: 145–157.

Haynes, R.J. and Swift, R.S. 1991. Concentrations of extractable Cu, Zn, Fe and Mn in a group of soils as influenced by air- and ovendrying and rewetting. *Geoderma* 49: 319–333.

Kaiser, K., Kaupenjohann, M., and Zech, W. 2001. Sorption of dissolved organic carbon in soils: effects of soil sample storage, soil-to-solution ratio, and temperature. *Geoderma* 99: 317–328.

Leggett, G.E. and Argyle, D.P. 1983. The DTPA-extractable iron, manganese, copper, and zinc from neutral and calcareous soils dried under different conditions. *Soil Sci. Soc. Am. J.* 47: 518–522.

Lehmann, R.G. and Harter, R.D. 1983. Copper adsorption by soils exposed to desiccation stress. *Soil Sci. Soc. Am. J.* 47: 1085–1088.

Liggett, W.S., Inn, K.G.W., and Hutchinson, J.M.R. 1984. Statistical assessment of subsampling procedures. *Environ. Int.* 10: 143–151.

Luo, J.X. and Jackson, M.L. 1985. Potassium release on drying of soil samples from a variety of weathering regimes and clay mineralogy in China. *Geoderma* 35: 197–208.

Magesan, G.N., White, R.E., Scotter, D.R., and Bolan, N.S. 2002. Effect of prolonged storage of soil lysimeters on nitrate leaching. *Agr. Ecosyst. Environ.* 88: 73–77.

Meyer, W.L. and Arp, P.A. 1994. Exchangeable cations and cation exchange capacity of forest soil samples: effects of drying, storage, and horizon. *Can. J. Soil Sci.* 74: 421–429.

Mondini, C., Contin, M., Leita, L., and De Nobili, M. 2002. Response of microbial biomass to air-drying and rewetting in soils and compost. *Geoderma* 105: 111–124.

Neary, A.J. and Barnes, S.R. 1993. The effect of sample grinding on extractable iron and aluminum in soils. *Can. J. Soil Sci.* 73: 73–80.

Neilsen, C.B., Groffman, P.M., Hamburg, S.P., Driscoll, C.T., Fahey, T.J., and Hardy, J.P. 2001. Freezing effects on carbon and nitrogen cycling in northern hardwood forest soils. *Soil Sci. Soc. Am. J.* 65: 1723–1730.

OECD 2000. Organisation for Economic Co-operation and Development (OECD) Guidelines for the Testing of Chemicals—Section 2: *Soil Microorganisms, Carbon Transformation Test*. Adopted Guideline #217, Adopted January 2000.

Pesaro, M., Nicollier, G., Zeyer, J., and Widmer, F. 2004. Impact of soil drying–rewetting stress on microbial communities and activities and on degradation of two crop protection products. *Appl. Environ. Microbiol*. 70: 2577–2587.

Pesaro, M., Widmer, F., Nicollier, G., and Zeyer, J. 2003. Effects of freeze–thaw stress during soil storage on microbial communities and methidathion degradation. *Soil Biol. Biochem.* 35: 1049–1061.

Potter, R.L., Jordan, C.F., Guedes, R.M., Batmanian, G.J., and Han, X.G. 1991. Assessment of a phosphorus fractionation method for soils: problems for further investigation. *Agr. Ecosyst. Environ*. 34: 453–463.

Riepert, F. and Felgentreu, D. 2002. Relevance of soil storage to biomass development, N-mineralisation and microbial activity using the higher plant growth test, ISO 11269-2, for testing of contaminated soils. *Appl. Soil Ecol*. 20: 57–68.

Ross, D.J. 1970. Effects of storage on dehydrogenase activities of soils. *Soil Biol. Biochem.* 2: 55–61.

Ross, D.J. 1989. Estimation of soil microbial C by a fumigation-extraction procedure: influence of soil moisture content. *Soil Biol. Biochem.* 21: 767–772.

Ross, D.S., Hales, H.C., Shea-McCarthy, G.C., and Lanzirotti, A. 2001. Sensitivity of soil manganese oxides: drying and storage cause reduction. *Soil Sci. Soc. Am. J.* 65: 736–743.

Rost, H., Loibner, A.P., Hasinger, M., Braun, R., and Szolar, O.H.J. 2002. Behavior of PAHs during cold storage of historically contaminated soil samples. *Chemosphere* 49: 1239–1246.

Schumacher, B.A., Shines, K.C., Burton, J.V., and Papp, M.L. 1990. Comparison of three methods for soil homogenization. *Soil Sci. Soc. Am. J*. 54: 1187–1190.

Sheppard, S.C. and Evenden, W.G. 1998. *Approach to Defining a Control or Diluent Soil for Ecotoxicity Assays*. ASTM Special Technical Publication 1333: 215–226.

Shishido, M. and Chanway, C.P. 1998. Storage effects on indigenous soil microbial communities and PGPR efficacy. *Soil Biol. Biochem.* 30: 939–947.

Simonsson, M., Berggren, D., and Gustafsson, J.P. 1999. Solubility of aluminum and silica in spodic horizons as affected by drying and freezing. *Soil Sci. Soc. Am. J*. 63: 1116–1123.

Stenberg, B., Johansson, M., Pell, M., Sjodahl-Svensson, K., Stenstrom, J., and Torstensson, L. 1998. Microbial biomass and activities in soil as affected by frozen and cold storage. *Soil Biol. Biochem.* 30: 393–402.

Turner, B.L. and Haygarth, P.M. 2003. Changes in bicarbonate-extractable inorganic and organic phosphorus by drying pasture soils. *Soil Sci. Soc. Am. J*. 67: 344–350.

Van Gestel, M., Merckx, R., and Vlassak, K. 1993. Microbial biomass responses to soil drying and rewetting: the fate of fast- and slow-growing microorganisms in soils from different climates. *Soil Biol. Biochem*. 25: 109–123.

Verchot, L.V. 1999. Cold storage of a tropical soil decreases nitrification potential. *Soil Sci. Soc. Am. J*. 63: 1942–1944.

Walworth, J.L. 1992. Soil drying and rewetting, or freezing and thawing, affects soil solution composition. *Soil Sci. Soc. Am. J*. 56: 433–437.

Wang, D., Snyder, C., and Bormann, F. 1993. Potential errors in measuring nitrogen content of soils low in nitrogen. *Soil Sci. Soc. Am. J*. 57: 1533–1536.

Worsfold, P.J., Gimbert, L.J., Mankasingh, U., Omaka, O.N., Hanrahan, G., Gardolinski, P.C.F.C., Haygarth, P.M., Turner, B.L., Keith-Roach, M.J., and McKelvie, I.D. 2005. Sampling, sample treatment and quality assurance issues for the

determination of phosphorus species in natural waters and soils. *Talanta* 66: 273–293.

Zantua, M.I. and Bremner, J.M. 1975. Preservation of soil samples for assay of urease activity. *Soil Biol. Biochem.* 7: 297–299.

Zelles, L., Adrian, P., Bai, Q.Y., Stepper, K., Adrian, M.V., Fischer, K., Maier, A., and Ziegler, A. 1991. Microbial activity measured in soils stored under different temperature and humidity conditions. *Soil Biol. Biochem.* 23: 955–962.

Chapter 5
Quality Control in Soil Chemical Analysis

C. Swyngedouw
Bodycote Testing Group
Calgary, Alberta, Canada

R. Lessard
Bodycote Testing Group
Edmonton, Alberta, Canada

5.1 INTRODUCTION

In analytical work, quality can be defined as the ''delivery of reliable information within an agreed span of time, under agreed conditions, at agreed costs, and with the necessary aftercare'' (FAO 1998). The agreed conditions include specifications as to data quality objectives (DQOs), which include precision, accuracy, representativeness, completeness, and comparability. These objectives are directly related to ''fitness of use'' of the data and they determine the degree of total variability (uncertainty or error) that can be tolerated in the data. The DQOs ultimately determine the necessary quality control (QC).

Quality management systems have been developed for analytical laboratories (USEPA 2004) and there are examples of these systems in the literature (CAEAL 1999). More information can be obtained from the International Organization for Standardization (ISO 17025).

Implementation of quality management implies the next level of quality—quality assurance (QA), defined as the ''assembly of all planned and systematic actions necessary to provide adequate confidence that an analytical result will satisfy given quality objectives or requirements'' (FAO 1998). The use of QA guarantees that the delivered product is commensurate with the intended use and ensures that data have scientific credibility, and thus permits statistical interpretations as well as management decisions to be made (AENV 2004).

All sampling and laboratory activities have one target: the production of quality data that is reliable, consistent, and has a minimum of errors. Thus, to ensure the integrity of QA a system of checks are needed to establish that quality management systems are maintained within prescribed limits providing protection against ''out of control'' conditions and ensuring that the results are of acceptable quality. To achieve this, an appropriate program

of QC is needed. QC includes ''the operational techniques and activities that are used to satisfy the quality requirements or DQOs'' (FAO 1998). Producing quality data is a major enterprise requiring a continuous effort. Approximately 20% of the total costs of analysis are spent on QA and QC.

This chapter focuses on some pertinent aspects of QC in soil chemical analysis. QA topics are not discussed but QA information can be found in CCME (1993), FAO (1998), Taylor (1990), IUPAC (1997), and ISO 17025 (2005).

5.2 SOIL CHEMICAL ANALYSIS AND ITS POTENTIAL ERRORS

Determining a property or a concentration of an analyte in a soil sample follows four general steps:

1 Sample collection and handling

2 Sample shipping and transport

3 Sample preparation and analysis

4 Results data entry, handling, and reporting

Each of these steps has the potential to introduce errors into the final estimate of a property or a concentration. The careful use of tested and established protocols at each step, along with careful tracking of the samples, can help minimize, but not eliminate the errors. Table 5.1 outlines field and laboratory sources of error, while Table 5.2 indicates some corrective actions to counteract specific laboratory errors.

5.2.1 Sample Collection and Handling

Bias caused by sampling is often difficult and expensive to measure. Field spikes (samples of analyte-free media such as clean soil or sand fortified or spiked with known amounts of the target analytes) are sometimes used to assess sampling bias. Sampling errors are usually much larger than analytical errors (Jenkins et al. 1997; Ramsey 1998; IAEA 2004).

5.2.2 Contamination

Contamination is a common source of error in soil measurements (Lewis 1988; USEPA 1989). Field blanks (analyte-free media) are the most effective tools for assessing and controlling contamination. In addition, equipment rinsate blanks may also be used. Field blanks are not effective for identifying matrix interferences or for spotting noncontaminant error sources (such as analyte loss due to volatilization or decomposition). Field spikes, however, can be used for noncontaminant sources.

5.2.3 Soil Sample Storage/Preservation

Physical and chemical changes to soil samples can occur between collection and analysis. Physical changes include volatilization, adsorption, diffusion, and precipitation, while chemical changes include photochemical and microbiological degradation (Maskarinic and Moody 1988).

TABLE 5.1 Field and Laboratory Sources of Uncertainty in Chemical Analysis Data and Their Assessment

Source of error		How to assess the error
Field		
Distributional (spatial) heterogeneity	Nonrandom spatial distribution of sample components	Increase the number of individual increments required to build a representative sample. Take replicates from spatially distinct points and take a larger number of samples. Use a less expensive and less precise analytical method
Compositional heterogeneity	Arises from the complexity of the soil (clay, silt, and sand). The error inherent in using a portion to represent the whole	Increase amount of sample taken (sample mass) to represent the matrix
Sample handling	Error caused by sampling, sample handling, and preservation	Make several large composites and split them into replicates. Also, take a larger number of samples
Laboratory		
Measurement	Error from analytical measurements, including sample preparation	Split samples into replicates just before sample preparation. Splits may be sent to another laboratory for confirmatory analysis
Data handling	Faulty data handling or transcription errors	Automate data transfer, perform data verification

The following QC practices are helpful to store and preserve soil samples:

- Seal sample containers to reduce contamination and prevent water loss.
- Minimize sample container headspace to reduce loss of volatiles.
- Refrigerate or freeze samples during storage and transportation to reduce loss of volatiles and minimize biodegradation.
- Carry out extractions and digestions as soon as possible. This keeps the analyte in the resulting extraction phase (e.g., solvent or acid), thereby stabilizing the analyte. As a result, a sample extract can be held for a longer time, up to the maximum limits as specified by the method.
- Analyze samples as soon as possible.

TABLE 5.2 Corrective Action for Laboratory Sources of Error

Source of error	Corrective action
Segregation or stratification of soils on storage	Rehomogenize before subsampling for analysis
Sample or equipment contamination by the laboratory environment	Store samples, reagents, equipment separately
Sample carryover on extraction vessels or apparatus	Rinse with cleaning solution between samples
Samples weighed, processed, or analyzed out of order	Run a known reference sample at a regular interval
Inaccurate concentrations in calibration solutions	Check new standards against old before use
Sample or calibration solution mismatch	Make up standards in extracting solution used for soil samples
Drift in instrument response	Use frequent calibration/QC checks
Poor instrument sensitivity or high detection limits	Optimize all operating parameters
Faulty data handling or human transcription errors	Proofread input, automate data transfer

Source: From Hoskins, B. and Wolf, A.M., in *Recommended Chemical Soil Test Procedures for the North Central Region*, Missouri Agricultural Experiment Station, Columbia, 1998, 65–69. With permission.

5.2.4 Sample Holding Times

Holding time is the storage time between sample collection and sample analysis, in conjunction with designated preservation and storage techniques (ASTM 2004). Usually microbiological and volatiles analyses have short holding times. A holding time study involves storing replicate spiked samples for a period of time and periodically (e.g., once a day) analyzing three replicates for a specific characteristic (e.g., toxicity). The holding time is established as the time when the concentration or characteristic drops below the criterion set by the DQOs (e.g., a 10% drop). For more information, see Chapter 4 and USACE (2005).

Maximum holding times for soil samples depend on the soil type, the analyte or the characteristic being determined, storage conditions, and loss of sample integrity (Maskarinic and Moody 1988).

Results of samples not analyzed within the specific holding time are considered ''compromised'' (see Section 5.5). The actual result (e.g., concentration) is usually assumed to be equal or greater than the result determined after the holding period has expired.

5.2.5 Subsampling the Soil Sample

In most cases, the soil sample that arrives in the laboratory is not analyzed entirely. Usually only a small subsample is analyzed, and the analyte concentration of the subsample is assumed representative of the sample itself (see Figure 5.1). A subsample cannot be perfectly representative of a heterogeneous sample, and improper subsampling may introduce significant bias into the analytical process. Bias that occurs as a result of subsampling may be improved by procedures such as grinding and homogenizing the original samples (Gerlach et al. 2002). One way to detect errors due to subsampling would be to set up an experiment where one subsamples a reference material, or a material that is already well characterized.

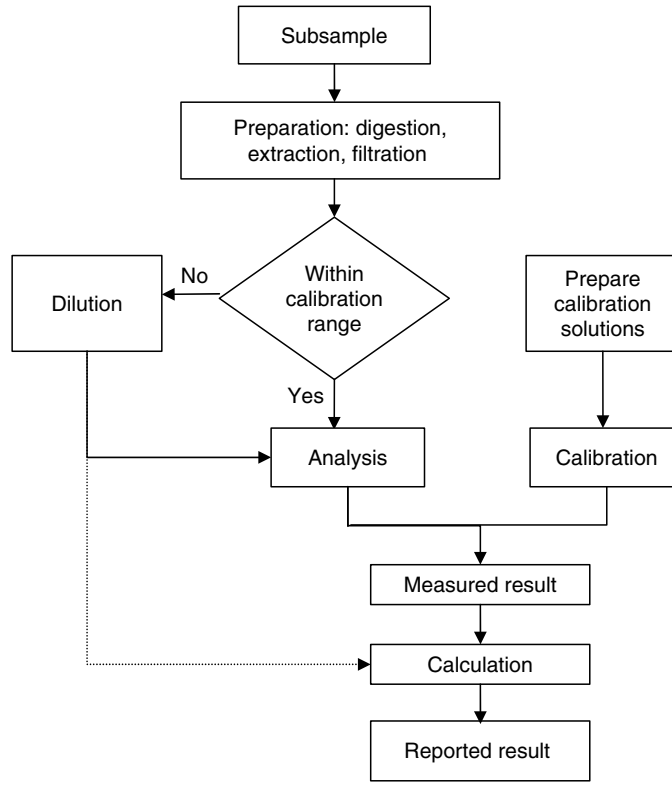

FIGURE 5.1. Laboratory sample process flow.

Once the sample enters the laboratory, it undergoes established procedures from sample preparation to final analysis. After the sample extract is introduced into the analytical instrument, the analyte is sensed by the detector and that information is converted into an electronic signal. The intensities of these electronic signals are converted into concentrations.

5.2.6 Detection Limits

Detection limits are estimates of concentrations where one can be fairly certain that the compound is present. The USEPA in 40 CFR136 (USEPA 1984) defines the method detection level (MDL) as ''the minimum concentration of a substance that can be measured and reported with 99% confidence that the analyte concentration is greater than zero.'' Method detection limits are statistically determined values that define how measurements of an analyte by a specific method can be distinguished from measurements of a blank (''zero'').

The MDL is a widely used precision-based benchmark of laboratory method performance determined during method validation (and periodically reevaluated). As a benchmark it compares the sensitivity and precision of various methods within and between laboratories under optimum conditions (assuming that all the laboratories determine the MDLs consistently), but it says little about the day-to-day performance of a method.

Detection limits are usually determined by analyses of replicate low-level spiked samples or blanks. A detection limit is laboratory specific as it is determined in a particular laboratory with its reagents, equipment, and analysts. Each sample will have its own detection limit,

determined by the matrix of the sample. The more the matrix interferences in the sample, the higher the sample detection limit.

One procedure to determine the MDL for an analyte is by performing seven or eight replicate analyses ($n = 7$ or 8) of the analyte at low concentration. The MDL is defined as $t \times$ sigma, where sigma is the standard deviation and t is the Student's t factor for a 99% probability level ($t = 3$ for $n = 8$). It can be reasoned that at 3 sigma concentration there is only about a 1% chance of a false positive (assuming normal distribution). Still, at the concentration of 3 sigma, there is about a 50% chance of a false negative if data are censored below that level and are treated as nondetections (see Section 5.3.2).

Interpretation of data on trace constituents (e.g., metals, organics, and pesticides) is further complicated by data censoring (not reporting concentrations below a designated limit), nondetections, and variability and bias (less than 100% recovery).

Other benchmarks besides MDL are discussed in the following sections.

Reliable Detection Limit

The reliable detection limit (RDL) is the lowest true concentration in a sample that can be reliably detected (Keith 1991). The most common definition is based on the same statistical principles as the MDL and is often defined as 6 sigma ($2 \times$ MDL), assuming sigma is constant. At this true concentration, the theoretical expected frequency of false negatives is reduced to 1% if measured values were censored at the MDL. Again, the RDL will vary from matrix to matrix and from sample to sample. For a different perspective, consult AOAC (1985), where the limit of reliable measurement is introduced.

Limit of Quantification

The concept of the limit of quantification (LOQ) is that measurements reported at or above this level meet a high standard for quantification, not just detection. Various multiples of sigma have been suggested; the higher the multiple, the greater the confidence in concentrations reported at or above this value. Commonly, the LOQ is defined at 10 sigma or $3.33 \times$ MDL. At 10 sigma, the true concentration is within $\pm 30\%$ of the reported concentration. The LOQ is equivalent to the practical quantitation limit (PQL).

Caution is advised in using method-reporting limits, because many were established using the best estimates of the analytical chemists many years ago and may have little or no statistical basis. Reporting an MDL and a limit of quantitation limit along with low-level data alerts data users of the uncertainties and limitations associated with the data. A better way would be to report $Y \pm U$ at any concentration Y found (i.e., no data censoring), where U is the calculated uncertainty at that concentration.

5.2.7 Reporting Results and Estimates of Uncertainty

A reported value from the laboratory analysis is an estimate of the true concentration in the sample at the time of collection. Thus, this measurement has variability associated with it referred to as measurement uncertainty. This uncertainty in the concentration of an analyte in a soil sample can be categorized into three general types of errors (Taylor 1988; Swyngedouw et al. 2004):

- Random errors that affect the precision of the results
- Systematic errors that affect the bias
- Blunders (mistakes that result in gross errors or lost samples—unpredictable and often yield unknown errors, i.e., the errors cannot be measured)

Although errors due to blunders are mostly controlled through proper education and training, some will always occur. Data verification and validation attempt to detect and reduce these blunders. QC samples may also detect some types of blunders.

Sampling and analytical errors do occur but are independent of each other. Therefore, sampling-related errors cannot be compensated for by the laboratory (AENV 2004). Thus, the limit of uncertainty for data on samples includes both the uncertainty of the sampling and of their measurement (Taylor 1988, 1997; Bevington and Robinson 2003) as indicated by the following equation:

$$S^2_{\text{total}} = S^2_{\text{measurement}} + S^2_{\text{sample}} \tag{5.1}$$

Estimates of uncertainty are obtained by a four-step process (Eurachem 2000):

1. Specification of the analyte
2. Identification of the uncertainty sources
3. Quantification of these uncertainty sources and
4. Calculation of the combined uncertainty

By combining uncertainty sources, only duplicate variance, long-term variance, and uncertainties in bias, calibration, and reference material need to be considered. These sources can be obtained from existing laboratory data, thus they are more easily quantified (Swyngedouw et al. 2004).

An advantage of reporting realistic estimates of uncertainty together with measurements of concentration ($Y \pm U$) is that end users of the analysis can consider the implications of the uncertainty in their use of the data. The traditional deterministic approach is to compare the measured concentration values with an appropriate regulatory threshold value. With this approach, any sampling point that has a reported concentration value below the threshold is classified as ''uncontaminated'' and those above as ''contaminated.'' This approach does not account for uncertainty in the data.

5.3 DATA QUALITY OBJECTIVES

5.3.1 Overview

DQOs specify requirements for analytical data that are clear and unambiguous concerning the intent of an investigation and the data parameters necessary to achieve that intent. These objectives are stated in both qualitative terms concerning the intended end use of the data

as well as in quantitative terms with respect to precision, accuracy, representativeness, comparability, and completeness (USEPA 2000a).

DQOs ensure that the proper methods and procedures (including method modifications) are in place with respect to MDLs, LOQs, or PQLs, applicable requirements, action limits, analyte specificity, analyte selectivity, reproducibility, false positives, and false negatives.

The following issues or stages are important for developing DQOs:

- State the precise problem to be resolved.
- Identify all the decisions needed to resolve the problem.
- Identify all the inputs needed to make the decisions.
- Narrow the boundaries of the project.
- Develop a decision rule.
- Develop uncertainty constraints.
- Optimize the design for obtaining data.

These issues are often termed the ''seven stages of DQO planning.'' Some of these stages can be further expanded as follows. Stage 1 asks ''Are the analyses primarily for characterizing the soil (e.g., pH, organic matter, texture), or for determining contaminant concentrations (e.g., metals, hydrocarbons, salts)?'' or ''Is the purpose of the soil analysis for screening or is it determinative?'' or ''Are average values of the chemicals of concern allowed?'' Chemical analyses are conducted for a purpose; hence, decisions will be made based on the analytical results. Here, one needs to consider the general kind of decisions that will be made (Stage 2). Decisions involving health and safety of the public, impacts of pollutants on the environment, regulatory compliance, and other aspects need to be considered. In Stage 3 one needs to know what analytes need to be analyzed (i.e., what are the chemicals of concern), what the associated action levels are with the decisions of Stage 2, and what detection levels need to be achieved with each analyte.

Since methods are specific for target analytes, a decision is required as to whether a particular method is appropriate or whether it will need to be modified to make it acceptable. Questions that need to be addressed involve the requirements for detection levels, method selectivity, accuracy, precision, and reproducibility (Table 5.3). These questions are addressed in the following sections.

Method Sensitivity (Detection Levels)

Estimating the lowest concentration levels needed to be achieved affects the available methods to choose from, the rates of false positive and false negative data, the ability to composite samples, and the number of samples required to meet the project DQOs.

TABLE 5.3 Recommended Method Selection and Quality Control for Different Situations

QC term	Situation	Assessment	Method selection	Alternative procedure
Sensitivity detection levels	Action level (or desired sensitivity) is close to the detection level	Need to increase the confidence levels by having precision data	Choose a bias-free method with detection levels below the action level	Increase the number of samples and field duplicates
Selectivity	Matrix effects, contamination, and interferences	Blanks for contamination, spikes, or surrogates for matrix effects and interferences	Choose a method with a specific detector that is not influenced by interferences	Run more blanks and spikes
Accuracy	Contamination, procedural losses, need bias-free data	Spikes (spiked samples analyte recovery)	Choose a bias-free method	Run more blanks, laboratory control samples, or standard reference materials
Precision	Need precision data (replicate agreement)	Need to increase confidence or decrease the standard deviations	Select a precise method	Increase replicates
Reproducibility	Multiple operators, laboratories	Interlaboratory studies	Choose an accredited and audited method	Choose another laboratory

Method Selectivity

Method selectivity directly affects the probability of detecting interferences in samples, especially in complex environmental samples. Interferences may cause an increase or decrease in signals of target analytes and thus lead to false positive or false negative conclusions. The tolerance for false positives and/or false negatives in the data is closely related to sample characteristics and method selectivity.

Accuracy

Accuracy is a measure of how close an analytical result is to its true value. It has two components, bias and precision.

Precision

To obtain overall precision (i.e., both sampling and analysis), field replicate samples need to be analyzed. Field replicate samples are two or more portions of a sample collected as close as possible at the same point in time and space to be considered identical. These samples are used to measure imprecision caused by inhomogeneity of the target analytes distributed in the soil. As imprecision increases, the relative standard deviation (RSD) will also increase. It is not unusual for the overall RSD to be larger than those of laboratory values.

Reproducibility

Reproducibility is the precision of measurements for the same sample at different laboratories, or at the same laboratory but determined by a different analyst. Reproducible results are those that can be reproduced within acceptable and known limits of deviation and therefore demonstrate correct and consistent application of standard methodologies.

5.3.2 Decision Errors

As mentioned above, two potential decision errors are identified based on interpreting sampling and analytical data.

False Positives (Decision Error B or False Acceptance)

An important criterion in chemical analytical data is ensuring that a detected parameter is present. Equally important is determining whether the mean concentration in the study area is statistically significantly higher than the action level. In either of these situations, when incorrect conclusions are made, the result is a false positive, i.e., the wrong analytes are concluded to be present. Method blanks are used to demonstrate the absence of false positives. The consequences of decision error B would result in needless expenditure of resources to pursue additional actions and assessments.

False Negatives (Decision Error A or False Rejection)

Correctly concluding from analytical data that analytes are absent from samples is also important. Failing to detect a parameter when it is present is a false negative. Similarly, concluding that a mean analyte concentration in the study area is not statistically significantly higher than the action level, when it actually is, is also a false negative. False negatives are often the result of poor recovery of analytes from soil matrices or are caused

by interferences that mask the analyte response. Method spikes (matrix spikes) are used to demonstrate the absence of false negatives. Minimization of false negatives is important with risk assessment and regulatory agencies. The consequences of decision error A would result in, for example, a health risk going undetected and unaddressed.

Both decision errors need to be examined and a decision made as to which error poses the more severe consequence. As an example, the planning team may decide that the decision error A (false negative) poses more severe consequences, because the true state of soil contamination could go undetected and may cause health risks to neighborhood residents.

Stage 6 of DQO planning sets acceptable limits for precision, accuracy, rates of false positives and/or false negative decision errors and for confidence levels in the sampling, and analytical data that relate to the DQOs. These decision error limits are set relative to the consequences of exceeding them (IAEA 2004). One could initially set the allowable decision errors to be at 1% (i.e., $P = 0.01$). This means that enough samples need to be collected and analyzed so that the chance of making either a false rejection (alpha) or a false acceptance (beta) decision error is only one out of a hundred.

5.4 QC PROCEDURES USED FOR ERROR ASSESSMENT

The type of QC samples to select depends on the DQOs of the site being investigated. Selections should be made depending on the following conditions (see Table 5.4):

- Whether bias-free and/or precision data are required.
- Whether differentiation between laboratory or sampling sources of error is needed.

TABLE 5.4 Types of Quality Control Samples Used in the Field and Laboratory

	Purpose	QC to use
Field	Check representativeness	Field duplicates (precision)
	Check for matrix effects	Surrogates, spikes, duplicates
	Check for contamination	Blanks (field blanks, rinsate blanks)
	Slowdown the chemistry	Holding times, lower temperature, appropriate containers, preservatives
Laboratory	Check representativeness	Laboratory duplicates (from subsamples)
	Check method bias	Laboratory control samples, reference materials
	Check regulations (bias)	Method detection levels (MDL), practical quantitation limits (PQL)
	Check comparability (with other laboratories)	Outside QC samples, e.g., performance test (PT) samples

Source: British Columbia Ministry of the Environment (BCME), 2003.

- Whether the degree of error to be estimated is relatively small (e.g., from typical contamination type sources) or large (e.g., from operator and/or procedural sources).

The methods selected need to be validated on soil matrices typical of those being received for analysis. Such validation does not guarantee that the methods will perform equally well for other soil types. In addition to unanticipated matrix effects, sampling artifacts, equipment malfunctions, and operator errors can also cause inaccuracies. Table 5.2 lists some sources of error that contribute to the uncertainty (variability) in analytical data.

5.4.1 Impact of Bias on Test Results

Bias is defined as the difference between the expected value of a statistic (e.g., sample average) and a population parameter (e.g., population mean). The need to take fewer replicates to reliably determine the mean value is an advantage in terms of cost and time. If no adjustment for bias is made, then for many purposes, the less biased, more variable method is preferable. However, by proper bias adjustment, the more precise method becomes the preferred method. Such adjustment can be based on QC check sample results (USEPA 2000b).

5.4.2 Field Control Samples

Field replicate, background, and rinsate (i.e., analyte-free water) blank samples are the most commonly collected field QA/QC samples for soil analysis. These are described in the following sections and are summarized in Table 5.4.

Field Replicates

Field replicates are field samples obtained from one location, homogenized and divided into separate containers and treated as separate samples throughout the remaining sample handling and analytical processes. These samples are used to assess errors associated with sample heterogeneity, sample methodology, and analytical procedures.

Equipment Rinsate Blanks

A rinsate blank is a sample of analyte-free water run over or through decontaminated field sampling equipment before collection of the next sample. It is used to assess the adequacy of cleaning or decontamination processes in the sampling procedure. The blank is placed in sample containers for handling, shipment, and analysis identical to the field samples.

Field Blanks

A field blank is a sample of analyte-free media, similar to the sample matrix, which is transferred from one vessel to another or exposed to the sampling environment at the sampling site, and shipped to the laboratory with the field samples. It is used to evaluate contamination error associated with field operations and shipping, but may also be used to evaluate contamination error associated with laboratory procedures.

Background Samples

Background samples determine the natural composition of the soil, and are considered ''clean'' samples. Although background samples are not considered QC samples per se, they are best planned for along with the QC samples. They provide a basis for comparison of, for example, contaminant concentration levels with naturally occurring levels of target analytes in the soil samples collected on site. Again, if the objective does not involve whether a site is contaminated or not, then background samples are not needed. If background samples are needed, they are collected first.

Computer expert systems are available that help researchers collect the proper type of QC samples and then calculate how many of each sample type are needed to meet the stated DQOs (Keith 2002; Pulsipher et al. 2003).

5.4.3 Laboratory QA and QC Procedures

Internal QC monitors the laboratory's current performance versus the standards and criteria that have been set, normally at the time of method development or validation.

To ensure that quality data are continuously produced during all analyses and to allow eventual review, systematic checks are performed to show that the test results remain reproducible. Such checks also show if the analytical method is measuring the quantity of target analytes in each sample within acceptable limits for bias (Environment Canada 2002a,b; USEPA 2003; IUPAC 2005). Analytical QC procedures that determine whether the sample handling procedures and laboratory methods are performing as required are presented in Table 5.5.

External laboratory QC involves reference help from other laboratories and participation in national or international interlaboratory sample and data exchange programs such as proficiency testing (PT). Such programs may involve:

- Exchange of samples with another laboratory. These samples would be prepared by a staff member other than the analyst or by the QC department. Similarly, samples prepared by the QC department can be used as internal check samples.

- Participation in interlaboratory sample exchange programs (such as round robins and/or PTs). Often in a PT study, the laboratory is not aware of samples used, in-house, for external performance evaluation.

The necessary components of a complete QA/QC program include internal QC criteria that demonstrate acceptable levels of performance, as determined by a QA review (audit). External review of data and procedures is accomplished by the monitoring activities of accreditation organizations (SCC 2005). This includes laboratory evaluation samples (PT samples, see above) and a periodic (normally every 2 years) on-site assessment of all QA/QC procedures, performed by external assessors from the accrediting organization.

5.5 DATA VERIFICATION AND REVIEW

Data verification occurs after the data analyses are completed. Data verification is a rigorous process whereby QC parameters are evaluated against a set of predetermined criteria or functional guidelines.

TABLE 5.5 Data Verification Checklist and Suggested Procedures

What to check	Why to check	How to check
Holding time (HT)	Holding times must be met for the data to be considered acceptable	Look at the chain of custody (COC) attached to the report, check the sampling date and compare this to the extraction/digestion date (or just the analysis date if no preparation step is performed) given in the report. The number of days must be less than or equal to the required HT
Blanks	Normally, only method blanks and any specific blank submitted with the samples will be reported. No blank should have a reportable concentration of any compound of interest above the reporting limit. Exceptions are the common laboratory contaminants[a]	Look at the blank reports. Any compound that has a concentration reported above the reporting limit in the blank and is present in any sample must be considered estimated or a nondetect at concentrations up to five times the level in the blank (up to 10 times for the common laboratory contaminants[a])
Surrogates	Surrogates only apply to organics at this time. Surrogates are compounds that are spiked (i.e., added at a known concentration) into every organic sample. A surrogate is a compound that is not found in nature and is not a ''normal'' pollutant	Check the report for surrogate recoveries. They should appear at the end of the analytical compounds list for a method. The recoveries should be 30%–150% to be acceptable. If the surrogate recovery is low, then flag positive values reported and reject nondetects. If it is high, then nondetect data are considered acceptable and positive data are flagged as estimated
Matrix spike (MS)/matrix spike duplicates (MSD)/ duplicates (DUP)	Spikes, spike duplicates, and duplicates are used for both organic and inorganic data. Spikes are used to check for accuracy, while duplicates are a check for precision	The MS/MSD/DUP results should appear at the end of the compound list. Verify that the recoveries are reasonable. Some values are: organic analysis (30%–150% recovery); inorganic analysis (80%–120% recovery); and duplicates (<50% relative percent difference[b])
Reporting limits	Reporting limits do not equal the method detection limits (MDLs) Reporting limits are used by laboratories as a level of confidence in reporting a concentration. Sometimes the practical quantitation limit (PQL) is used, which is 2 to 10 times the MDL	Look at the reporting limits. The limits should meet the requirements for the site. The limits for soils vary considerably depending on the method

[a] Common laboratory contaminants often include phthalates, dichloromethane, acetone, 2-butanone, hexanone, zinc, and iron.

[b] Relative percent difference (RPD) $= |X - Y| \times 200/(X + Y)$, where X and Y are the concentrations of each duplicate.

Data quality can be measured in several ways and these form the basis of deciding whether the DQOs have been met:

- Rates (%) of false positive and negatives in the analytical data
- Precision (closeness of values from repeat analyses—expressed as standard deviation)
- Bias (i.e., accuracy)
- Estimation of the uncertainty of the results

This type of information can be used to improve the quality of data interpretation. It is useful to analyze the QC data first and then review the sample data. Typical practices for analyzing QC data are presented in Table 5.5. More information on data verification is available in the literature (e.g., USEPA 1996).

5.5.1 Statistical Control

Besides documenting uncertainty, descriptive statistics from an established QA program can be used to determine if a methodology is in ''statistical control,'' i.e., whether QC criteria are being met over the long term. Check sample statistics are also used as daily decision-making tools during sample analysis to determine if expected results are being generated and if the analytical system is functioning properly (AOAC 1985). As described earlier, QC provides information to determine sample and laboratory data quality using data trend analysis (i.e., statistical process control). Statistical reports that evaluate specific anomalies or disclose trends in many areas are commonly generated (AOAC 1985; Kelly et al. 1992; FAO 1998; Garfield et al. 2000).

These trend analysis techniques are used to monitor the laboratory's performance over time, to detect departures of the laboratory's output from required or desired levels of QC, and to provide an early warning of QA or QC problems that may not be apparent from the results of an individual case.

Trend analyses also provide information needed to establish performance-based criteria for updated analytical protocols, in cases where advisory criteria were previously used (control charts).

5.5.2 Control Charts

Quality assessment statistics can be presented graphically through control charts for ease of interpretation. These charts can be used to present both bias and precision data. Repeated measurements of external or internal reference or QC samples are graphed on a time line. Superimposed on the individual results is the cumulative mean or the known value. Control levels which typically represent ± 2 sigma (upper and lower warning limits, UWL and LWL) and ± 3 sigma (upper and lower control limits, UCL and LCL) from the mean are also included (see Figure 5.2). In a normally distributed sample population, the warning levels represent a 95% confidence interval, while the control limits correspond to a 99% confidence interval. As an example, a single value outside the UCL or LCL is considered unacceptable. If statistical control is considered unacceptable, all routine sample unknowns between the unacceptable check sample(s) and the last check sample that was in control should be rerun.

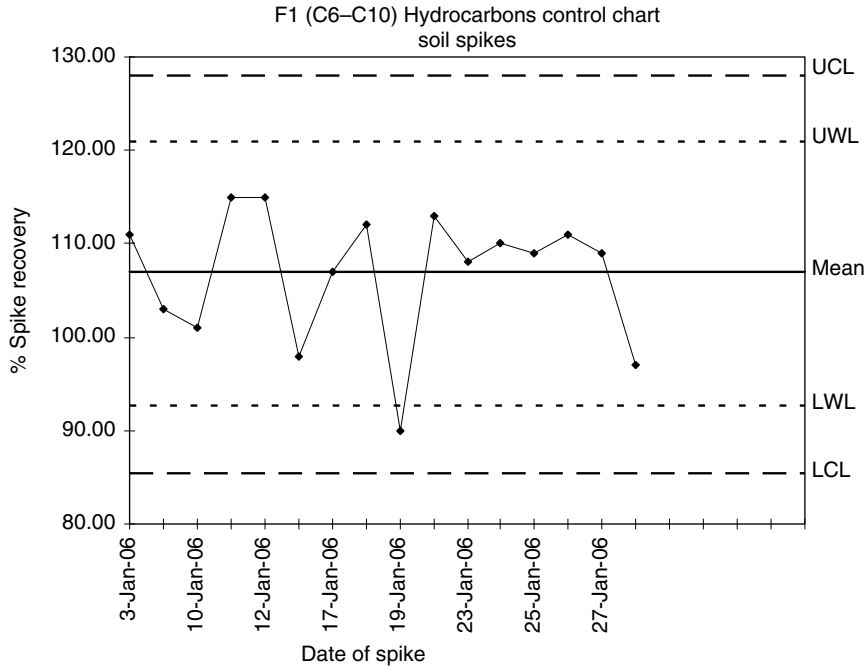

FIGURE 5.2. Example of a control chart. (UCL, upper control level, mean $+3 \times$ standard deviation of values; UWL, upper warning level, mean $+2 \times$ standard deviation of values; mean, average of values; LWL, lower warning level, mean $-2 \times$ standard deviation of values; LCL, lower control level, mean $-3 \times$ standard deviation of values.)

5.5.3 Trace of Test

When data quality is not achieved, a ''trace of test'' is a good verification tool. A systematic approach is applied in this test, starting with a check for calculation and typing errors. Items that are checked include samples, standards, reagents, equipment, glassware, and the analytical instruments and their calibrations. Then the method itself is checked, focusing on method validation factors such as sensitivity (detection limits), precision, recovery, and interferences. Batch control is also checked including laboratory control samples and reference materials used, and inspection of control charts and feedback logs (e.g., complaints).

The order of events in the investigation is the reverse of that given in Figure 5.1 and could be as follows:

1 Confirm that the results were correctly reported and correctly associated to the specific sample.

2 Recheck the results and confirm that they have been calculated correctly.

3 Verify analytical QC associated with the test to ensure the measurement process was in statistical control.

4 Investigate deviations from the routine procedure and the data record.

5 Investigate any nonconformance relating to the sample such as matrix effects and holding times.

6 Determine whether the results make sense: compare the results to other analyses, compare to historical data (if known), and/or communicate with the data user. Computer data checks can be built-in functions of laboratory databases, models, or spreadsheets. Automated QA/QC can be used to facilitate peer review or, in some cases, manual checks.

REFERENCES

Alberta Environment (AENV). 2004. *Alberta Environment Laboratory Data Quality Assurance Policy Procedures and Guidelines*. [Online] Available at: http://www3.gov.ab.ca/env/protenf/publications/Laboratory_Data_Quality_Assurance_Policy_Procedures_2004.pdf (verified March 2005).

American Society for Testing and Materials (ASTM). 2004. D4515-85(2001). *Standard Practice for Estimation of Holding Time for Water Samples Containing Organic Constituents*. ASTM Book of Standards, Vol. 11.02. ASTM International, West Conshohocken, PA.

Association of Official Analytical Chemists (AOAC). 1985. In G.T. Wernimont, Ed. *Use of Statistics to Develop and Evaluate Analytical Methods*. AOAC, Arlington, VA.

Bevington, P. and Robinson, D.K. 2003. *Data Reduction and Error Analysis for the Physical Sciences, 3rd edn*. McGraw-Hill, Toronto.

British Columbia Ministry of the Environment (BCME). Environmental Protection Division, Water, Air and Climate Change Branch 2003. Part A: Quality Control and Quality Assurance. In *BC Field Sampling Manual*: 2003. [Online] Available at: http://www.env.gov.bc.ca/air/wamr/labsys/field_man_03.html#pdf (verified February 2006). See also Section A: Laboratory Quality Assurance/Quality Control. In *BC Environmental Laboratory Manual*: 2005. [Online] Available at: http://www.env.gov.bc.ca/air/wamr/labsys/lab_man_05.html (verified February 2005).

Canadian Association of Environmental Analytical Laboratories (CAEAL). 1999. *Template for the Design and Development of a Quality Manual for Environmental Laboratories [Online] and QC for Environmental Laboratories*. [Online] Available at: http://www.caeal.ca/t_caealpubs.html (verified March 2005).

Canadian Council of Ministers of the Environment (CCME). 1993. Volume I: Main Report. In *Guidance Manual of Sampling, Analysis, and Data Management for Contaminated Sites*. CCME, Winnipeg, Manitoba.

Environment Canada. 2002a. *Contaminated Site Remediation Section Technical Assistance Bulletins*. [Online] Available at: http://www.on.ec.gc.ca/pollution/ecnpd/contaminassist_e.html [verified March 2005]. This Webpage shows a list of Technical Assistance Bulletins. See Section 5: QC samples in Tab#4: Sampling and Analysis of Hydrocarbon Contaminated Soil.

Environment Canada. 2002b. *Guidance Document for the Sampling and Analysis of Metal Mining Effluents*. [Online] Available at: http://www.ec.gc.ca/nopp/docs/rpt/2MM5/en/C7.cfm (verified October 2004).

Eurachem. 2000. *Eurachem Guide: Qualifying Uncertainty in Analytical Measurement, 2nd Edition*. [Online] Available at: http://www.eurachem.ul.pt/guides/QUAM2000-1.pdf (verified February 2007).

Garfield, F.M., Klesta, E., and Hirsch, J. 2000. *Quality Assurance Principles for Analytical Laboratories*, 3rd edn. AOAC International, Gaithersburg, MD.

Gerlach, R., Dobb, D.E., Raab, G.A., and Nocerino, J.M. 2002. Gy Sampling Theory in Environmental Studies. 1. Assessing Soil Splitting Protocols. *J. Chemometr*. 16: 321–328.

Hoskins, B. and Wolf, A.M. 1998. Laboratory quality assurance program. In *Recommended Chemical Soil Test Procedures for the North Central Region*. North Central Regional Research Publication No. 221 (revised), pp. 65–69. Available at: http://muextension.missouri.edu/explorepdf/miscpubs/sb1001.pdf (verified February 2006).

International Atomic Energy Agency (IAEA). 2004. *Soil Sampling for Environmental Contaminants. IAEA-TECDOC-1415*. International Atomic Energy Agency, Vienna. Worked DQOs examples p. 39.

International Organization for Standardization (ISO). 2005. ISO/IEC 17025: 2005 *General Requirements for the Competence of Testing and Calibration Laboratories*. [Online] Available at: http://www.iso.org/iso/en/Catalogue DetailPage.CatalogueDetail?CSNUMBER = 39883&ICS1 = 3&ICS2 = 120&ICS3 = 20 (01 March 2006).

International Union of Pure and Applied Chemistry (IUPAC). 1997. Chapter 18. Quality assurance of analytical processes. In *Compendium of Analytical Nomenclature Definitive Rules 1997*. [Online] Available at: http://www.iupac.org/publications/analytical_compendium/(verified March 2005).

International Union of Pure and Applied Chemistry (IUPAC). 2005. *Terminology in Soil Sampling*. International Union of Pure and Applied Chemistry, Analytical Chemistry Division. *Pure Appl. Chem.* 77(5): 827–841.

Jenkins, T.F., Walsh, M.E., Thorne, P.G., Thiboutot, S., Ampleman, G., Ranney, T.A., and Grant, C.L. 1997. *Assessment of Sampling Error Associated with Collection and Analysis of Soil Samples at a Firing Range Contaminated with HMX*. [Online] Available at: http://www.crrel.usace.army.mil/techpub/CRREL_Reports/reports/ SR97_22.pdf (07 March 2005).

Keith, L.H. 1991. *Environmental Sampling and Analysis—A Practical Guide*. Lewis Publishers, Boca Raton, FL.

Keith, L.H. 2002. *Environmental Monitoring and Measurement Advisor—A New Expert System*. [Online] Available at: http://www.emma-expertsystem.com/EMMA-WTQA.html (verified April 2006).

Kelly, W.D., Ratcliff, T.A., and Nenadic, C. Jr. 1992. *Basic Statistics for Laboratories—A Primer for Laboratory Workers*. John Wiley & Sons, Hoboken, NJ.

Lewis, D.L. 1988. Assessing and controlling sample contamination. In L.H. Keith, Ed. *Principles of Environmental Sampling*. American Chemical Society, Washington, DC, pp. 118–144.

Maskarinic, M.P. and Moody, R.L. 1988. Storage and preservation of environmental sample. In L.H. Keith, Ed. *Principles of Environmental Sampling*. American Chemical Society, Washington, DC, pp. 145–155.

Pulsipher, B., Gilbert, R., and Wilson, J. 2003. *Measurement Uncertainty in Visual Sample Plan*. [Online] Available at: http://dqo.pnl.gov/vsp/PNNLSA38977.pdf (verified February 2006).

Ramsey, M.H. 1998. Sampling as a source of measurement uncertainty: techniques for quantification and comparison with analytical sources. *J. Anal. Atom. Spectrom.* 13: 97–104.

Standards Council of Canada (SCC). 2005. *Programs and Services—Laboratories*. [Online] Available at: http://www.scc.ca/en/programs/laboratory/index.shtml (verified March 2005).

Swyngedouw, C., Chapman, M., Johnston, J., Kubik, S., Montgomery, S., Nam, C., Seveck, M., Shuvell, C.-A., and Lessard, R. 2004. *Laboratory Measurement Uncertainty*. Environmental Informatics Archives 2: 200–212. [Online] Available at: http://www.iseis.org/EIA/pdfstart.asp?no = 04023 (verified May 2006).

Taylor, J.K. 1988. Defining the accuracy, precision, and confidence limits of sample data. In L.H. Keith, Ed. *Principles of Environmental Sampling*. American Chemical Society, Washington, DC, pp. 101–107.

Taylor, J.K. 1990. *Quality Assurance of Chemical Measurements*. Lewis Publishers, Boca Raton, FL.

Taylor, J.K. 1997. *An Introduction to Error Analysis: The Study of Uncertainties in Physical Measurement, 2nd edn*. University Science Books, Sausalito, CA.

United Nations—Food and Agriculture Organization (FAO). 1998. *Guidelines for Quality*

Management in Soil and Plant Laboratories. [Online] Available at: http://www.fao.org/docrep/W7295E/w7295e00.htm (verified March 2005).

U.S. Army Corps of Engineers (USACE). 2005. Chapter 5: *Holding Times and Preservation in Environmental Quality—Guidance for Evaluating Performance-Based Chemical Data.* EM 200-1-10 (June 2005). [Online] Available at: http://www.usace.army.mil/usace-docs/eng-manuals/em200-1-10/(verified February 2006).

U.S. Environmental Protection Agency (USEPA). 1984. *Definition and Procedure for the Determination of the Method Detection Limit*. 40 CFR136.2 Appendix B. [Online] Available at: http://ca.water.usgs.gov/pnsp/rep/interpret/def.html (verified February 2006).

U.S. Environmental Protection Agency (USEPA). 1989. *Soil Sampling Quality Assurance User's Guide*, 2nd edn. [Online] Available at: http://www.epa.gov/nerlesd1/cmb/research/bs122.pdf (verified February 2006).

U.S. Environmental Protection Agency (USEPA). 1996. *Revised Data Validation Guidance* 12/96. [Online] Available at: http://www.epa.gov/ne/oeme (verified March 2005).

U.S Environmental Protection Agency (USEPA). 2000a. *Guidance for the Data Quality Objectives Process (QA/G-4)*. August 2000. [Online] Available at: http://www.epa.gov/quality/qs-docs/g4-final.pdf (verified February 2006).

United States Environmental Protection Agency (USEPA). 2000b. Chapter 5: *Draw Conclusions from the Data, in Practical Methods for Data Analysis, Guidance for Data Quality Assessment*. EPA QA/G-9, QA00 Version (July 2000). [Online] Available at: www.epa.gov/quality/qs-docs/g9-final.pdf (verified February 2006).

U.S. Environmental Protection Agency (USEPA). 2003. Exhibit E Quality Assurance/Quality Control Procedures and Requirements. In *Analytical Methods—Statement of Work for Organic Analysis OLM04.2*. [Online] Available at: http://www.epa.gov/superfund/programs/clp/olm4.htm (verified March 2005).

U.S. Environmental Protection Agency (USEPA). 2004. *Agency-wide Quality System Documents*. [Online] Available at: http://www.epa.gov/quality/qa_docs.html (verified March 2005).

II. DIAGNOSTIC METHODS FOR SOIL AND ENVIRONMENTAL MANAGEMENT

Section Editors: J.J. Schoenau and I.P. O'Halloran

Chapter 6
Nitrate and Exchangeable Ammonium Nitrogen

D.G. Maynard
Natural Resources Canada
Victoria, British Columbia, Canada

Y.P. Kalra and J.A. Crumbaugh
Natural Resources Canada
Edmonton, Alberta, Canada

6.1 INTRODUCTION

Inorganic N in soils is predominantly in the form of nitrate (NO_3) and ammonium (NH_4). Nitrite is seldom present in detectable amounts, and its determination is normally unwarranted except in neutral to alkaline soils receiving NH_4 and NH_4-producing fertilizers (Keeney and Nelson 1982). Soil testing laboratories usually determine NO_3 to estimate available N in agricultural soils, while laboratories analyzing tree nursery and forest soils often determine both NO_3 and NH_4.

There is considerable diversity among laboratories in the extraction and determination of NO_3 and NH_4. In addition, incubation methods (both aerobic and anaerobic) have been used to determine the potentially mineralizable N (see Chapter 46) and nitrogen supply rates using ion exchange resins (see Chapter 13).

Nitrate is water-soluble and a number of solutions including water have been used as extractants. Exchangeable NH_4 is defined as NH_4 that can be extracted at room temperature with a neutral K salt solution. Various molarities have been used, such as 0.05 *M* K_2SO_4, 0.1 *M* KCl, 1.0 *M* KCl, and 2.0 *M* KCl (Keeney and Nelson 1982). The most common extractant for NO_3 and NH_4, however, is 2.0 *M* KCl (e.g., Magill and Aber 2000; Shahandeh et al. 2005).

The methods of determination for NO_3 and NH_4 are even more diverse than the methods of extraction (Keeney and Nelson 1982). These range from specific ion electrode to manual colorimetric techniques, microdiffusion, steam distillation, and continuous flow analysis. Steam distillation is still sometimes employed for ^{15}N; however, for routine

analysis automated colorimetric techniques using continuous flow analyzers are preferred. Segmented flow analysis (SFA) and flow injection analysis (FIA) are continuous flow systems that are rapid, free from most soil interferences, and very sensitive.

The methods for the most commonly used extractant (2.0 *M* KCl) and SFA methods for the determination of NO_3 and NH_4 are presented here. The FIA methods often use the same chemical reactions but with different instruments (e.g., Burt 2004). The steam distillation methods for determination of NO_3 and NH_4 have not been included, since they have not changed much over the last several years. Detailed description of these methods can be found elsewhere (Bremner 1965; Keeney and Nelson 1982).

6.2 EXTRACTION OF NO_3-N AND NH_4-N WITH 2.0 *M* KCl

6.2.1 Principle

Ammonium is held in an exchangeable form in soils in the same manner as exchangeable metallic cations. Fixed or nonexchangeable NH_4 can make up a significant portion of soil N; however, fixed NH_4 is defined as the NH_4 in soil that cannot be replaced by a neutral K salt solution (Keeney and Nelson 1982). Exchangeable NH_4 is extracted by shaking with 2.0 *M* KCl. Nitrate is water-soluble and hence can also be extracted by the same 2.0 *M* KCl extract. Nitrite is seldom present in detectable amounts in soil and therefore is usually not determined.

6.2.2 Materials and Reagents

1 Reciprocating shaker.

2 Dispensing bottle.

3 Erlenmeyer flasks, 125 mL.

4 Nalgene bottles, 60 mL.

5 Filter funnels.

6 Whatman No. 42 filter papers.

7 Aluminum dishes.

8 Potassium chloride (2.0 *M* KCl): dissolve 149 g KCl in approximately 800 mL NH_3-free deionized H_2O in a 1 L volumetric flask and dilute to volume with deionized H_2O.

6.2.3 Procedure

A. Moisture determination

1 Weigh 5.00 g of moist soil in a preweighed aluminum dish.

2 Dry overnight in an oven at 105°C.

3 Cool in a desiccator and weigh.

B. Extraction procedure

1 Weigh (5.0 g) field-moist soil (or moist soil incubated for mineralization experiments) into a 125 mL Erlenmeyer flask. In some instances air-dried soil may also be used (see Comment 1 in Section 6.2.4).

2 Add 50 mL 2.0 *M* KCl solution using the dispensing bottle. (If the sample is limited, it can be reduced to a minimum of 1.0 g and 10 mL to keep 1:10 ratio.)

3 Carry a reagent blank throughout the procedure.

4 Stopper the flasks and shake for 30 min at 160 strokes per minute.

5 Filter through Whatman No. 42 filter paper into 60 mL Nalgene bottles.

6 Analyze for NO_3 and NH_4 within 24 h (see Comment 3 in Section 6.2.4).

6.2.4 Comments

1 Significant changes in the amounts of NO_3 and NH_4 can take place with prolonged storage of air-dried samples at room temperature. A study conducted by the Western Enviro-Agricultural Laboratory Association showed that the NO_3 content of soils decreased significantly after a 3-year storage of air-dried samples at room temperature (unpublished results). Increases in NH_4 content have also been reported by Bremner (1965) and Selmer-Olsen (1971).

2 Filter paper can contain significant amounts of NO_3 and NH_4 that can potentially contaminate extracts (Muneta 1980; Heffernan 1985; Sparrow and Masiak 1987).

3 Ammonium and NO_3 in KCl extracts should be determined within 24 h of extraction (Keeney and Nelson 1982). If the extracts cannot be analyzed immediately they should be frozen. Potassium chloride extracts keep indefinitely when frozen (Heffernan 1985).

4 This method yields highly reproducible results.

6.3 DETERMINATION OF NO_3-N IN 2.0 *M* KCl EXTRACTS BY SEGMENTED FLOW ANALYSIS (CADMIUM REDUCTION PROCEDURE)

6.3.1 Principle

Nitrate is determined by an automated spectrophotometric method. Nitrates are reduced to nitrite by a copper cadmium reductor coil (CRC). The nitrite ion reacts with sulfanilamide

under acidic conditions to form a diazo compound. This couples with *N*-1-naphthyl-ethylenediamine dihydrochloride to form a reddish purple azo dye (Technicon Instrument Corporation 1971).

6.3.2 Materials and Reagents

1 Technicon AutoAnalyzer consisting of sampler, manifold, proportioning pump, CRC, colorimeter, and data acquisition system.

2 CRC—activation of CRC (O.I. Analytical 2001a)—Refer to point 5 in this section for CRC reagent preparation. This procedure must be performed before connecting the CRC to the system. Do not induce air into CRC during the activation process (see Comment 6 in Section 6.3.5 regarding the efficiency of the CRC).

   a. Using a 10 mL Luer-Lok syringe and a 1/4″-28 female Luer-Lok fitting, slowly flush the CRC with 10 mL of deionized H_2O. If any debris is seen exiting the CRC, continue to flush with deionized H_2O until all debris is removed.

   b. Slowly flush the CRC with 10 mL of 0.5 *M* HCl solution. Quickly proceed to the next step as the HCl solution can cause damage to the cadmium surface if left in the CRC for more than a few seconds.

   c. Flush the CRC with 10 mL of deionized H_2O to remove the HCl solution.

   d. Slowly flush the CRC with 10 mL of 2% cupric sulfate solution. Leave this solution in the CRC for approximately 5–10 min.

   e. Forcefully flush the CRC with 10 mL of NH_4Cl reagent solution to remove any loose copper that may have formed within the reactor. Continue to flush until all debris is removed.

   f. The CRC should be stored and filled with deionized H_2O when not in use.

      Note: Solution containing Brij-35 should not be used when flushing or storing the CRC.

      Note: Do not allow any solutions other than deionized H_2O and reagents to flow through the CRC. Some solutions may cause irreversible damage to the reactor.

3 Standards

   a. Stock solution (100 μg NO_3-N mL^{-1}): dissolve 0.7218 g of KNO_3 (dried overnight at 105°C) in a 1 L volumetric flask containing deionized H_2O. Add 1 mL of chloroform to preserve the solution. Dilute to 1 L and mix well.

   b. Working standards: pipet 0.5, 1.0, 1.5, and 2.0 mL of stock solution into a 100 mL volumetric flask and make to volume with 2.0 *M* KCl solution to obtain 0.5, 1.0, 1.5, and 2.0 μg NO_3-N mL^{-1} standard solution, respectively.

4 Reagents

a. Dilute ammonium hydroxide (NH_4OH) solution: add four or five drops of concentrated NH_4OH to approximately 30 mL of deionized H_2O.

b. Ammonium chloride reagent: dissolve 10 g NH_4Cl in a 1 L volumetric flask containing about 750 mL of deionized H_2O. Add dilute NH_4OH to attain a pH of 8.5, add 0.5 mL of Brij-35, dilute to 1 L, and mix well. (*Note*: it takes only two drops of dilute NH_4OH to achieve the desired pH.)

c. Color reagent: to a 1 L volumetric flask containing about 750 mL of deionized H_2O, carefully add 100 mL of concentrated H_3PO_4 (see Comment 2 in Section 6.3.5) and 10 g of sulfanilamide. Dissolve completely. Add 0.5 g of *N*-1-naphthyl-ethylenediamine dihydrochloride (Marshall's reagent), and dissolve. Dilute to 1 L volume with deionized H_2O and mix well. Add 0.5 mL of Brij-35. Store in an amber glass bottle. This reagent is stable for 1 month.

5 Reagents for CRC

a. Cupric sulfate solution (2% w/v): dissolve 20 g of $CuSO_4 \cdot 5H_2O$ in approximately 900 mL of deionized H_2O in a 1 L volumetric flask. Dilute the solution to 1 L with deionized H_2O and mix well.

b. Hydrochloric acid solution (0.5 *M*): carefully add 4.15 mL of concentrated HCl to approximately 70 mL of deionized H_2O in a 100 mL volumetric flask (see Comment 2 in Section 6.3.5). Dilute to 100 mL with deionized H_2O and mix well.

6.3.3 Procedure

1 If refrigerated, bring the soil extracts to room temperature.

2 Shake extracts well.

3 Set up AutoAnalyzer (see Maynard and Kalra 1993; Kalra and Maynard 1991). Allow the colorimeter to warm up for at least 30 min.

4 Place all reagent tubing in deionized H_2O and run for 10 min.

5 Insert tubing in correct reagents and run for 20 min to ensure thorough flushing of the system (feed 2.0 *M* KCl through the wash line).

6 Establish a stable baseline.

7 Place the sample tubing in the high standard for 5 min.

8 Reset the baseline, if necessary.

9 Transfer standard solutions to sample cups and arrange on the tray in descending order.

10 Transfer sample extracts to sample cups and place in the sample tray following the standards.

11 Begin run.

12 After run is complete, rerun the standards to ensure that there has been no drifting. Reestablish baseline.

13 Place tubing in deionized H_2O, rinse and run for 20 min before turning the proportioning pump off.

6.3.4 Calculation

Prepare a standard curve from recorded readings (absorption vs. concentration) of standards and read as μg NO_3-N mL^{-1} in KCl extract. Results are calculated as follows:

$$\text{NO}_3\text{-N in moist soil } (\mu\text{g g}^{-1}) = \frac{\text{NO}_3\text{-N in extract } (\mu\text{g mL}^{-1}) \times \text{volume of extractant (mL)}}{\text{Weight of moist soil (g)}} \tag{6.1}$$

$$\text{Moisture factor} = \frac{\text{Moist soil (g)}}{\text{Oven-dried soil (g)}} \tag{6.2}$$

$$\text{NO}_3\text{-N in oven-dried soil } (\mu\text{g g}^{-1}) = \text{NO}_3\text{-N in moist soil } (\mu\text{g g}^{-1}) \times \text{moisture factor} \tag{6.3}$$

There are data collection software packages associated with the data acquisition systems and these will automatically generate calculated concentration values based on intensities received from the colorimeter and inputs of the appropriate information (e.g., sample weight, extract volumes, and moisture factor).

6.3.5 Comments

1 Use deionized H_2O throughout the procedure.

2 *Warning*: Mixing concentrated acids and water produces a great amount of heat. Take appropriate precautions.

3 All reagent bottles, sample cups, and new pump tubing should be rinsed with approximately 1 *M* HCl.

4 Range: 0.01–2 μg NO_3-N mL^{-1} extract. Extracts with NO_3 concentrations greater than the high standard (2.0 μg NO_3-N mL^{-1}) should be diluted with 2.0 *M* KCl solution and reanalyzed.

5 Prepared CRCs can be purchased from various instrument/parts supplies for SFA systems. Previously, the method called for preparation of a cadmium reductor

column. However, preparation was tedious and time consuming and cadmium granules are no longer readily available.

6 Reduction efficiency of the CRC (O.I. Analytical 2001a).

a. In the CRC, nitrate is reduced to nitrite. However, under some conditions, reduction may proceed further with nitrite being reduced to hydroxylamine and ammonium ion. These reactions are pH-dependent:

$$NO_3 + 2H^+ + 2e \rightarrow NO_2 + H_2O \tag{6.4}$$

$$NO_2 + 6H^+ + 6e \rightarrow H_3NOH + H_2O \tag{6.5}$$

$$NO_2 + 8H^+ + 6e \rightarrow NH_4^+ + 2H_2O \tag{6.6}$$

At the buffered pH of this method, reaction 6.4 predominates. However, if the cadmium surface is overly active, reaction 6.5 and reaction 6.6 will proceed sufficiently to give low results of nitrite.

b. If the cadmium surface is insufficiently active, there will be a low recovery of nitrate as nitrite. This condition is defined as poor reduction efficiency.

c. To determine the reduction efficiency, run a high-level nitrite calibrant followed by a nitrate calibrant of the same nominal concentration. The reduction efficiency is calculated as given below.

$$PR = (N_3/N_2) \times 100 \tag{6.7}$$

where PR is the percent reduction efficiency, N_3 is the nitrate peak height, and N_2 is the nitrite peak height.

d. If the response of the nitrite is as expected but the reduction efficiency is less than 90%, then the CRC may need to be reactivated.

7 The method includes NO_3-N plus NO_2-N; therefore, samples containing significant amounts of NO_2-N will result in the overestimation of NO_3-N.

8 The method given in this section outlines the configuration of the Technicon AutoAnalyzer. However, the cadmium reduction method can be applied to other SFA and FIA systems.

6.3.6 Precision and Accuracy

There are no standard reference samples for accuracy determination. Precision measurements for NO_3-N carried out for soil test quality assurance program of the Alberta Institute of Pedology (Heaney et al. 1988) indicated that NO_3-N was one of the most variable parameters measured. Coefficient of variation ranged from 4.8% to 30.4% for samples with 67.3 $\pm$ 3.2 (SD) and 3.3 $\pm$ 1.0 (SD) μg NO_3-N g^{-1}, respectively.

6.4 DETERMINATION OF NH_4-N IN 2.0 *M* KCl EXTRACTS BY SEGMENTED FLOW AUTOANALYZER INDOPHENOL BLUE PROCEDURE (PHENATE METHOD)

6.4.1 Principle

Ammonium is determined by an automated spectrophotometric method utilizing the Berthelot reaction (Searle 1984). Phenol and NH_4 react to form an intense blue color. The intensity of color is proportional to the NH_4 present. Sodium hypochlorite and sodium nitroprusside solutions are used as oxidant and catalyst, respectively (O.I. Analytical 2001b).

6.4.2 Materials and Reagents

1 Technicon AutoAnalyzer consisting of sampler, manifold, proportioning pump, heating bath, colorimeter, and data acquisition system.

2 Standard solutions:

a. Stock solution #1 (1000 μg NH_4-N mL^{-1}): in a 1 L volumetric flask containing about 800 mL of deionized H_2O dissolve 4.7170 g $(NH_4)_2SO_4$ (dried at 105°C). Dilute to 1 L with deionized H_2O, mix well, and store the solution in a refrigerator.

b. Stock solution #2 (100 μg NH_4-N mL^{-1}): dilute 10 mL of stock solution #1 to 100 mL with 2.0 *M* KCl solution. Store the solution in a refrigerator.

c. Working standards: transfer 0, 1, 2, 5, 7, and 10 mL of stock solution #2 to 100 mL volumetric flasks. Make to volume with 2.0 *M* KCl. This will provide 0, 1, 2, 5, 7, and 10 μg NH_4-N mL^{-1} standard solutions, respectively. Prepare daily.

3 Complexing reagent: in a 1 L flask containing about 950 mL of deionized H_2O, dissolve 33 g of potassium sodium tartrate ($KNaC_4H_4O_6 \cdot H_2O$) and 24 g of sodium citrate ($HOC(COONa)(CH_2COONa)_2 \cdot H_2O$). Adjust to pH 5.0 with concentrated H_2SO_4, add 0.5 mL of Brij-35, dilute to volume with deionized H_2O, and mix well.

4 Alkaline phenol: using a 1 L Erlenmeyer flask, dissolve 83 g of phenol in 50 mL of deionized H_2O. Cautiously add, in small increments with agitation, 180 mL of 20% (5 *M*) NaOH. Dilute to 1 L with deionized H_2O. Store alkaline phenol reagent in an amber bottle. (To make 20% NaOH, dissolve 200 g of NaOH and dilute to 1 L with deionized H_2O.)

5 Sodium hypochlorite (NaOCl): dilute 200 mL of household bleach (5.25% NaOCl) to 1 L using deionized H_2O. This reagent must be prepared daily, immediately before use to obtain optimum results. The NaOCl concentration in this reagent decreases on standing.

6 Sodium nitroprusside: dissolve 0.5 g of sodium nitroprusside ($Na_2Fe(CN)_5NO \cdot 2H_2O$) in 900 mL of deionized H_2O and dilute to 1 L. Store in dark-colored bottle in a refrigerator.

6.4.3 Procedure

Follow the procedure (6.3.3) outlined for NO_3-N (see Kalra and Maynard 1991; Maynard and Kalra 1993).

6.4.4 Calculation

The calculations are the same as given in 6.3.4.

6.4.5 Comments

1 Use NH_4-free deionized H_2O throughout the procedure.

2 All reagent bottles, sample cups, and new pump tubing should be rinsed with approximately 1 *M* HCl.

3 Range: 0.01–10.0 μg NH_4-N mL^{-1} extract. Extracts with NH_4 concentrations greater than the high standard (10.0 μg NH_4-N mL^{-1}) should be diluted with 2.0 *M* KCl solution and reanalyzed.

4 It is critical that the operating temperature is 50°C ± 1°C.

5 The method given in this section outlines the configuration of the Technicon AutoAnalyzer (Technicon Instrument Corporation 1973). However, the phenate method can be applied to other SFA and FIA systems.

6.4.6 Precision and Accuracy

There are no standard reference samples for accuracy determination. Long-term analyses of laboratory samples gave coefficient of variations of 21%–24% for several samples over a wide range of concentrations.

REFERENCES

Bremner, J.M. 1965. Inorganic forms of nitrogen. In C.A. Black, D.D. Evans, J.L. White, E. Ensminger, and F.E. Clark, Eds. *Methods of Soils Analysis. Part 2*. Agronomy No. 9. American Society of Agronomy, Madison, WI, pp. 1179–1237.

Burt, R. (Ed.) 2004. *Soil Survey Laboratory Methods Manual*. Soil Survey Investigations Report No. 42, Version 4.0. United States Department of Agriculture, Natural Resources Conservation Service, Lincoln, NE, 700 pp.

Heaney, D.J., McGill, W.B., and Nguyen, C. 1988. Soil test quality assurance program, Unpublished report. Alberta Institute of Pedology, Edmonton, AB, Canada.

Heffernan, B. 1985. *A Handbook of Methods of Inorganic Chemical Analysis for Forest Soils, Foliage and Water*. Division of Forest Research, CSIRO, Canberra, Australia, 281 pp.

Kalra, Y.P. and Maynard, D.G. 1991. *Methods Manual for Forest Soil and Plant Analysis*. Information Report NOR-X-319. Northern Forestry Centre, Northwest Region, Forestry Canada. Edmonton, AB, Canada, 116 pp. Access online http://warehouse.pfc.forestry.ca/nofc/11845.pdf (July 2006).

Keeney, D.R. and Nelson, D.W. 1982. Nitrogen in organic forms. In A.L. Page, R.H. Miller, and D.R. Keeney, Eds. *Methods of Soil Analysis. Part 2*. Agronomy No. 9, American Society of Agronomy, Madison, WI, pp. 643–698.

Magill, A.H. and Aber, J.D. 2000. Variation in soil net mineralization rates with dissolved organic carbon additions. *Soil Biol. Biochem.* 32: 597–601.

Maynard, D.G. and Kalra, Y.P. 1993. Nitrate and extractable ammonium nitrogen. In M.R. Carter, Ed. *Soil Sampling and Methods of Analysis*. Lewis Publishers, Boca Raton, FL, pp. 25–38.

Muneta, P. 1980. Analytical errors resulting from nitrate contamination of filter paper. *J. Assoc. Off. Anal. Chem.* 63: 937–938.

O.I. Analytical. 2001a. Nitrate plus nitrite nitrogen and nitrite nitrogen in soil and plant extracts by segmented flow analysis (SFA). Publication No. 15300301. College Station, TX, 27 pp.

O.I. Analytical. 2001b. Ammonia in soil and plant extracts by segmented flow analysis (SFA). Publication No. 15330501. College Station, TX, 17 pp.

Searle, P.L. 1984. The Berthelot or indophenol reaction and its use in the analytical chemistry of nitrogen: a review. *Analyst* 109: 549–568.

Selmer-Olsen, A.R. 1971. Determination of ammonium in soil extracts by an automated indophenol method. *Analyst* 96: 565–568.

Shahandeh, H., Wright, A.L., Hons, F.M., and Lascano, R.J. 2005. Spatial and temporal variation in soil nitrogen parameters related to soil texture and corn yield. *Agron. J.* 97: 772–782.

Sparrow, S.D. and Masiak, D.T. 1987. Errors in analysis for ammonium and nitrate caused by contamination from filter papers. *Soil Sci. Soc. Am. J.* 51: 107–110.

Technicon Instrument Corporation 1971. *Nitrate and Nitrite in Water*. Industrial method No. 32–69W. Technicon Instrument Corporation, Tarrytown, New York, NY.

Technicon Instrument Corporation 1973. *Ammonia in Water and Seawater*. Industrial method No. 154–71W. Technicon Instrument Corporation, Tarrytown, New York, NY.

Chapter 7
Mehlich 3-Extractable Elements

N. Ziadi
Agriculture and Agri-Food Canada
Quebec, Quebec, Canada

T. Sen Tran
Institute of Research and Development
in Agroenvironment
Quebec, Quebec, Canada

7.1 INTRODUCTION

During the past few years, numerous techniques and methods have been developed to estimate soil nutrient availability. Among these methods, the Mehlich 3 (M3) is considered an appropriate and economic chemical method since it is suitable for a wide range of soils and can serve as a ''universal'' soil test extractant (Sims 1989; Zbiral 2000a; Bolland et al. 2003). M3 was developed by Mehlich (1984) as multielement soil extraction and is widely used, especially in agronomic studies, to evaluate soil nutrient status and establish fertilizer recommendations mainly for P and K in humid regions. The following elements can be successfully analyzed using M3 extracting solution: P, K, Ca, Mg, Na, Cu, Zn, Mn, B, Al, and Fe. The extracting solution is composed of 0.2 *M* CH_3COOH, 0.25 *M* NH_4NO_3, 0.015 *M* NH_4F, 0.013 *M* HNO_3, and 0.001 *M* ethylene diamine tetraacetic acid (EDTA). M3-extractable phosphorus (M3-P) is obtained by the action of acetic acid and fluoride compounds, while K, Ca, Mg, and Na (M3-K, M3-Ca, M3-Mg, and M3-Na, respectively) are removed by the action of ammonium nitrate and nitric acid. The Cu, Zn, Mn, and Fe (M3-Cu, M-Zn, M3-Mn, and M3-Fe) are extracted by NH_4 and the chelating agent EDTA.

Many studies have compared the M3 method to other chemical and nonchemical methods and reported significant correlations between tested methods (Zbiral and Nemec 2000; Cox 2001; Bolland et al. 2003). Indeed, M3-P is closely related to P extracted by M2, Bray 1, Bray 2, Olsen, strontium chloride–citric acid, and water (Mehlich 1984; Simard et al. 1991; Zbiral and Nemec 2002). In a study conducted in Quebec, Tran et al. (1990) reported that the amount of M3-P is approximately the same as that determined by the Bray 1 method on most noncalcareous soils. Recently, Mallarino (2003) concluded that M3 test is more effective than the Bray test for predicting corn (*Zea mays* L.) response to P across many Iowa soils with pH values ranging from 5.2 to 8.2. A good correlation was also obtained between M3-P and P desorbed by anionic exchange membranes and electroultrafiltration (EUF) techniques

(Tran et al. 1992a,b; Ziadi et al. 2001). Many studies reported a strong correlation between M3-P and plant P uptake or between M3-P and relative plant yield in a wide range of soils (Tran and Giroux 1987; Ziadi et al. 2001; Mallarino 2003). Others, however, have indicated that some alkaline extractants (i.e., $NaHCO_3$) are superior to acidic extractants (M3) when used to evaluate plant P availability (Bates 1990). Depending on the determination method used, the critical level of M3-P for most common crops is about 30 to 60 $\mu g\ g^{-1}$ (Sims 1989; Tran and Giroux 1989; Bolland et al. 2003).

In addition to its value in agronomic studies, M3-P has also been used in environmental studies as an agrienvironmental soil test for P (Sims 1993; Sharpley et al. 1996; Beauchemin et al. 2003). The concept of P saturation degree was developed and successfully used in Europe and North America to indicate the potential desorbability of soil P (Breeuwsma and Reijerink 1992; Beauchemin and Simard 2000). In the mid-Atlantic USA region, Sims et al. (2002) reported that the M3-P/(M3-Al + M3-Fe) can be used to predict runoff and leachate P concentration. In a study conducted in Quebec, Khiari et al. (2000) reported that the environmentally critical (M3-P/M3-Al) percentage was 15%, corresponding to the critical degree of phosphate saturation of 25% proposed in Netherlands using oxalate extraction method (Van der Zee et al. 1987). In Quebec, the ratio of M3-extractable P to Al (M3-P/M3-Al) has been recently introduced in the local recommendation in corn production (CRAAQ 2003). The reader is referred to Chapter 14 for a more complete description of environmental soil P indices.

In addition to P, significant correlations have been obtained between the other nutrients (K, Ca, Mg, Na, Cu, Zn, Mn, Fe, and B) extracted by the M3 solution and other methods currently used in different laboratories (Tran 1989; Cancela et al. 2002; Mylavarapu et al. 2002). Furthermore, Michaelson et al. (1987) reported significant correlation between the amounts of K, Ca, and Mg extracted by M3 and by ammonium acetate. Highly significant correlations have also been reported between M3-extractable amounts of Cu, Zn, Mn, Fe, and B and those obtained by the double acid, diethylene triamine pentaacetic acid-triethanolamine (DTPA-TEA), or 0.1 *M* HCl, Mehlich 1 (Sims 1989; Sims et al. 1991; Zbiral and Nemec 2000).

The use of automated methods to quantify soil nutrients has expanded rapidly since the early 1990s (Munter 1990; Jones 1998). The inductively coupled plasma (ICP) emission spectroscopy is becoming one of the most popular instruments used in routine soil testing laboratories. The ICP instruments (optical emission spectroscopy [OES] or mass spectroscopy [MS]) are advantageous because they are able to quantify many nutrients (P, K, Ca, Mg, and micronutrients) in one analytical process. However, there has been criticism on the adoption of ICP, especially for P, instead of colorimetric methods which have been historically used in soil test calibrations for fertilizer recommendations (Mallarino and Sawyer 2000; Zbiral 2000b; Sikora et al. 2005). Because of observed differences between P values obtained by ICP and by colorimetric methods, some regions in the United States do not recommend the use of ICP to determine P in any soil test extracts (Mallarino and Sawyer 2000). Zbiral (2000b) reported a small, but significant difference (2% to 8%) for K and Mg determined by ICP-OES and flame atomic absorption. In the same experiment, the amount of P determined by ICP-OES was higher by 8% to 14% than that obtained by the spectrophotometric method. Recently, Sikora et al. (2005) confirmed these results when they compared M3-P measured by ICP with that by colorimetric method, and concluded that further research is needed to determine if the higher ICP results are due to higher P bioavailability or analytical interferences. Eckert and Watson (1996) reported that P measured with ICP is sometimes up to 50% higher than P measured with the colorimetric methods. The reason for such differences is

explained by the fact that the spectrophotometry method determines only the orthophosphate forms of P, whereas the ICP determines the total P content (i.e., organic P as well as total inorganic P forms not just orthophosphate) present in the soil extract (Zbiral 2000a; Mallarino 2003). Mallarino (2003) reported a strong relationship between P determined by ICP method and the original colorimetric method ($R^2 = 0.84$) and concluded that M3-P as determined by ICP should be considered as a different test and its interpretation should be based on field calibration rather than conversion of M3-P measured by colorimetric method. Since automated systems are frequently employed to measure the concentration of nutrient ions in the extract and specific operating conditions and procedure for the instrument are outlined in the manufacturer's operating manual, only a manual method is described in this chapter.

7.2 MATERIALS AND REAGENTS

1 Reciprocating shaker

2 Erlenmeyer flasks 125 mL

3 Filter funnels

4 Filter paper (Whatman #42)

5 Disposable plastic vials

6 Instrumentation common in soil chemistry laboratories such as: spectrophotometer for conventional colorimetry or automated colorimetry (e.g., Technicon AutoAnalyzer; Lachat Flow Injection System); flame photometer; or ICP-OES or ICP-MS

7 M3 extracting solution:

   a. Stock solution M3: (1.5 *M* NH_4F + 0.1 *M* EDTA). Dissolve 55.56 g of ammonium fluoride (NH_4F) in 600 mL of deionized water in a 1 L volumetric flask. Add 29.23 g of EDTA to this mixture, dissolve, bring to 1 L volume using deionized water, mix thoroughly, and store in plastic bottle.

   b. In a 10 L plastic carboy containing 8 L of deionized water, dissolve 200.1 g of ammonium nitrate (NH_4NO_3) and add 100 mL of stock solution M3, 115 mL concentrated acetic acid (CH_3COOH), 82 mL of 10% v/v nitric acid (10 mL concentrated HNO_3 in 100 mL of deionized water), bring to 10 L with deionized water and mix thoroughly.

   c. The pH of the extracting solution should be 2.3 $\pm$ 0.2.

8 Solutions for the manual determination of phosphorus:

   a. Solution A: dissolve 12 g of ammonium molybdate ($(NH_4)_6Mo_7O_{24} \cdot 4H_2O$) in 250 mL of deionized water. In a 100 mL flask, dissolve 0.2908 g of potassium antimony tartrate in 80 mL of deionized water. Transfer these two solutions

into a 2 L volumetric flask containing 1000 mL of 2.5 *M* H_2SO_4 (141 mL concentrated H_2SO_4 diluted to 1 L with deionized water), bring to 2 L with deionized water, mix thoroughly, and store in the dark at 4°C.

b. Solution B: dissolve 1.056 g of ascorbic acid in 200 mL of solution A. Solution B should be fresh and prepared daily.

c. Standard solution of P: use certified P standard or prepare a solution of 100 μg mL^{-1} P by dissolving 0.4393 g of KH_2PO_4 in 1 L of deionized water. Prepare standard solutions of 0, 0.5, 1, 2, 5, and 10 μg mL^{-1} P in diluted M3 extractant.

9 Solutions for K, Ca, Mg, and Na determination by atomic absorption:

a. Lanthanum chloride ($LaCl_3$) solution: 10% (w/v).

b. Concentrated solution of cesium chloride (CsCl) and $LaCl_3$: dissolve 3.16 g of CsCl in 100 mL of the 10% $LaCl_3$ solution.

c. Combined K and Na standard solutions: use certified atomic absorption standard and prepare solutions of 0.5, 1.0, 1.5, 2.0 and 0.3, 0.6, 0.9, 1.2 μg mL^{-1} of K and Na, respectively.

d. Combined Ca and Mg standard solutions. Prepare 2, 4, 6, 8, 10 and 0.2, 0.4, 0.6, 0.8, 1.0 μg mL^{-1} of Ca and Mg, respectively.

10 Standard solution for Cu, Zn, and Mn determination by atomic absorption:

a. Combined Cu and Zn standard solution: 0, 0.2, 0.4, 0.8, 1.2 to 2.0 μg mL^{-1} of Cu and of Zn in M3 extractant.

b. Mn standard solutions: prepare 0, 0.4, 0.8, 1.2 to 4 μg mL^{-1} of Mn in diluted M3 extractant.

7.3 PROCEDURE

7.3.1 Extraction

1 Weigh 3 g of dry soil passed through a 2 mm sieve into a 125 mL Erlenmeyer flask.

2 Add 30 mL of the M3 extracting solution (soil:solution ratio 1:10).

3 Shake immediately on reciprocating shaker for 5 min (120 oscillations min^{-1}).

4 Filter through M3-rinsed Whatman #42 filter paper into plastic vials and store at 4°C until analysis.

5 Analyze elements in the filtrate as soon as possible using either an automated or manual method as described below.

7.3.2 Determination of P by Manual Colorimetric Method

1 Pipet 2 mL of the clear filtrate or standard (0 to 10 μg mL^{-1}) P solution into a 25 mL volumetric flask. The sample aliquot cannot contain more than 10 μg of P and dilution of the filtrate with M3 maybe required.

2 Add 15 mL of distilled water and 4 mL of solution B, make to volume with distilled water and mix.

3 Allow 10 min for color development, and measure the absorbance at 845 nm.

7.3.3 Determination of K, Ca, Mg, and Na by Atomic Absorption or by Flame Emission

Precipitation problems can result from the mixture of the CsCl–$LaCl_2$ solution with the M3 extract. It is therefore recommended that the extracts be diluted (at least 1:10 final dilution) as indicated below to avoid this problem.

1 Pipet 1 to 5 mL of filtrate into a 50 mL volumetric flask.

2 Add approximately 40 mL of deionized water and mix.

3 Add 1 mL of the CsCl–$LaCl_3$ solution, bring to volume with deionized water and mix.

4 Determine Ca, Mg by atomic absorption and K, Na by flame emission.

7.3.4 Determination of Cu, Zn, and Mn by Atomic Absorption

The Cu and Zn concentrations in the extract are determined without dilution while the Mn concentration is determined in diluted M3 extract.

7.3.5 Comments

1 Filter paper can be a source of contamination which may affect the end results, especially for Zn, Cu, and Na. Mehlich (1984) proposed to use 0.2% $AlCl_3$ as a rinsing solution for all labware including qualitative filter paper. Based on local tests, we suggest the use of M3 extracting solution as a rinsing solution for filter paper.

2 Because of Zn contamination, Pyrex glassware cannot be used for extraction or storage of the M3 extractant and laboratory standards.

3 Tap water is a major source of Cu and Zn contamination.

7.4 RELATIONSHIPS WITH OTHER EXTRACTANTS

The M3 extractant is widely used as ''universal extractant'' in North America, Europe, and Australia (Zbiral and Nemec 2000; Cox 2001; Bolland et al. 2003). Jones (1998) reported that M3 is becoming the method of choice since many elements can be determined with this

extractant. In Canada, it is used in the soil testing program in the provinces of Quebec and Prince Edward Island (CPVQ 1989; CRAAQ 2003). Many studies have been conducted over the world comparing the M3 method to the commonly used methods (ammonium acetate for K and DTPA for micronutrients) and report in general highly significant relationships between these methods. Some comments on relative amounts of elements extracted are provided below.

1 The amounts of K and Na extracted by M3 are equal to those determined by ammonium acetate (Tran and Giroux 1989).

2 The amounts of Ca and Mg extracted by M3 are about 1.10 times more than those extracted by ammonium acetate method (Tran and Giroux 1989).

3 The amount of Zn extracted by M3 is about one half to three quarters of the amount extracted by DTPA (Lindsay and Norvell 1978).

4 The amount of Cu extracted by M3 is about 1.8 times more than that extracted by DTPA (Makarim and Cox 1983; Tran 1989; Tran et al. 1995).

REFERENCES

Bates, T.E. 1990. Prediction of phosphorus availability from 88 Ontario soils using five phosphorus soil tests. *Commun. Soil Sci. Plant Anal.* 21: 1009–1023.

Beauchemin, S. and Simard, R.R. 2000. Phosphorus status of intensively cropped soils of the St-Lawrence lowlands. *Soil Sci. Soc. Am. J.* 64: 659–670.

Beauchemin, S., Simard, R.R., Bolinder, M.A., Nolin, M.C., and Cluis, D. 2003. Prediction of phosphorus concentration in tile-drainage water from the Montreal lowlands soils. *Can. J. Soil Sci.* 83: 73–87.

Bolland, M.D.A., Allen, D.G., and Walton, K.S. 2003. Soil testing for phosphorus: comparing the Mehlich 3 and Colwell procedures for soils of south-western Australia. *Aust. J. Soil Res.* 41: 1185–1200.

Breeuwsma, A. and Reijerink, J.G.A. 1992. Phosphate saturated soils: a ''new'' environmental issue. In G.R.B. ter Meulen et al., Eds. *Chemical Time Bombs*. Proceedings of the European Conference, Veldhoven, the Netherlands, 2–5 September 1992. Foundation for Ecodevelopment, Hoofddorp, the Netherlands, pp. 79–85.

Cancela, R.C., de Abreu, C.A., and Paz Gonzalez, A. 2002. DTPA and Mehlich-3 micronutrient extractability in natural soils. *Commun. Soil Sci. Plant Anal.* 33: 2879–2893.

Cox, M.S. 2001. The Lancaster soil test method as an alternative to the Mehlich 3 soil test method. *Soil Sci.* 166: 484–489.

CPVQ. 1989. Grille de fertilisation. Conseil des productions végétales du Québec. Ministère de l'Agriculture, des Pêcheries et de l'Alimentation du Québec, Québec, QC, Canada, 128 pp.

CRAAQ. 2003. Guide de référence en fertilisation. 1re édition. Centre de référence en agriculture et agroalimentaire du Québec (CRAAQ). Québec, QC, Canada, 294 pp.

Eckert, D.J. and Watson, M.E. 1996. Integrating the Mehlich-3 extractant into existing soil test interpretation schemes. *Commun. Soil Sci. Plant Anal.* 27: 1237–1249.

Jones, J.B. Jr. 1998. Soil test methods: past, present, and future use of soil extractants. *Commun. Soil Sci. Plant Anal.* 29: 1543–1552.

Khiari, L., Parent, L.E., Pellerin, A., Alimi, A.R.A., Tremblay, C., Simard, R.R., and Fortin, J. 2000. An agri-environmental phosphorus saturation index for acid coarse-textured soils. *J. Environ. Qual.* 29: 1561–1567.

Lindsay, W.L. and Norvell, W.A. 1978. Development of a DTPA soil test for zinc, iron, manganese, and copper. *Soil Sci. Soc. Am. J.* 42: 421–428.

Makarim, A.K. and Cox, F.R. 1983. Evaluation of the need for copper with several soil extractants. *Agron. J.* 75: 493–496.

Mallarino, A. and Sawyer, J.E. 2000. Interpreting Mehlich-3 soil test results, SP126. Iowa State University, University Extension: Ames, IW; www.extension.iastate.edu/Publications/SP126.pdf, Ames Iowa (last verified March 2006).

Mallarino, A.P. 2003. Field calibration for corn of the Mehlich-3 soil phosphorus test with colorimetric and inductively coupled plasma emission spectroscopy determination methods. *Soil Sci. Soc. Am. J.* 67: 1928–1934.

Mehlich, A. 1984. Mehlich-3 soil test extractant: a modification of Mehlich-2 extractant. *Commun. Soil Sci. Plant Anal.* 15: 1409–1416.

Michaelson, G.J., Ping C.L., and Mitchell, C.A. 1987. Correlation of Mehlich-3, Bray 1 and ammonium acetate extractable P, K, Ca, and Mg for Alaska agricultural soils. *Commun. Soil Sci. Plant Anal.* 18: 1003–1015.

Munter, R.C. 1990. Advances in soil testing and plant analysis analytical technology. *Commun. Soil Sci. Plant Anal.* 21: 1831–1841.

Mylavarapu, R.S., Sanchez, J.F., Nguyen, J.H., and Bartos, J.M. 2002. Evaluation of Mehlich-1 and Mehlich-3 extraction procedures for plant nutrients in acid mineral soils of Florida. *Commun. Soil Sci. Plant Anal.* 33: 807–820.

Sharpley, A., Daniel, T.C., Sims, J.T., and Pote, D.H. 1996. Determining environmentally sound soil phosphorus levels. *J. Soil Water Conserv.* 51: 160–166.

Sikora, F.J., Howe, P.S., Hill, L.E., Reid, D.C., and Harover, D.E. 2005. Comparison of colorimetric and ICP determination of phosphorus in Mehlich 3 soil extracts. *Commun. Soil Sci. Plant Anal.* 36: 875–887.

Simard, R.R., Tran, T.S., and Zizka, J. 1991. Strontium chloride–citric acid extraction evaluated as a soil-testing procedure for phosphorus. *Soil Sci. Soc. Am. J.* 55: 414–421.

Sims, J.T. 1989. Comparison of Mehlich-1 and Mehlich-3 extractants for P, K, Ca, Mg, Mn, Cu and Zn in Atlantic Coastal plain soils. *Commun. Soil Sci. Plant Anal.* 20: 1707–1726.

Sims, J.T. 1993. Environmental soil testing for phosphorus. *J. Prod. Agric.* 6: 501–507.

Sims, J.T., Igo, E., and Skeans, Y. 1991. Comparison of routine soil tests and EPA method 3050 as extractants for heavy metals in Delaware soils. *Commun. Soil Sci. Plant Anal.* 22: 1031–1045.

Sims, J.T., Maguire, R.O., Leytem, A.B., Gartley, K.L., and Pautler, M.C. 2002. Evaluation of Mehlich 3 as an agri-environmental soil phosphorus test for the mid-Atlantic United States of America. *Soil Sci. Soc. Am. J.* 66: 2016–2032.

Tran, T.S. 1989. Détermination des minéraux et oligo-éléments par la méthode Mehlich-III. Méthodes d'analyse des sols, des fumiers, et des tissus végétaux. Conseil des productions végétales du Québec. Agdex. 533. Ministère de l'Agriculture, des Pêcheries et de l'Alimentation du Québec, QC, Canada.

Tran, T.S. and Giroux, M. 1987. Disponibilité du phosphore dans les sols neutres et calcaires du Québec en relation avec les propriétés chimiques et physiques. *Can. J. Soil Sci.* 67: 1–16.

Tran. T.S. and Giroux, M. 1989. Evaluation de la méthode Mehlich-III pour déterminer les éléments nutritifs (P, K, Ca, Mg, Na) des sols du Québec. *Agrosol* 2: 27–33.

Tran, T.S., Giroux, M., Audesse, P., and Guilbault, J. 1995. Importance des éléments mineurs en agriculture: symptômes visuels de carence, analyses des végétaux et des sols. *Agrosol* 8: 12–22.

Tran, T.S., Giroux, M., Guilbeault, J., and Audesse, P. 1990. Evaluation of Mehlich-III extractant to estimate the available P in Quebec soils. *Commun. Soil Sci. Plant Anal.* 21: 1–28.

Tran, T.S., Simard, R.R., and Fardeau, J.C. 1992a. A comparison of four resin extractions and ^{32}P isotopic exchange for the assessment of plant-available P. *Can. J. Soil Sci.* 72: 281–294.

Tran, T.S., Simard, R.R., and Tabi, M. 1992b. Evaluation of the electro-ultrafiltration technique (EUF) to determine available P in neutral and

calcareous soils. *Commun. Soil Sci. Plant Anal.* 23: 2261–2281.

Van der Zee, S.E.A.T.M., Fokkink, L.G.J., and van Riemsdijk, W.H. 1987. A new technique for assessment of reversibly adsorbed phosphate. *Soil Sci. Soc. Am. J.* 51: 599–604.

Zbiral, J. 2000a. Determination of phosphorus in calcareous soils by Mehlich 3, Mehlich 2, CAL, and Egner extractants. *Commun. Soil Sci. Plant Anal.* 31: 3037–3048.

Zbiral, J. 2000b. Analysis of Mehlich III soil extracts by ICP-AES. *Rostlinna-Vyroba* 46 (4), 141–146.

Zbiral, J. and Nemec, P. 2000. Integrating of Mehlich 3 extractant into the Czech soil testing scheme. *Commun. Soil Sci. Plant Anal.* 31: 2171–2182.

Zbiral, J. and Nemec, P. 2002. Comparison of Mehlich 2, Mehlich 3, CAL, Egner, Olsen, and 0.01M $CaCl_2$ extractants for determination of phosphorus in soils. *Commun. Soil Sci. Plant Anal.* 33: 3405–3417.

Ziadi, N., Simard, R.R., Tran, T.S., and Allard, A. 2001. Evaluation of soil-available phosphorus for grasses with Electro-Ultrafiltration technique and some chemical extractions. *Can. J. Soil Sci.* 81: 167–174.

Chapter 8
Sodium Bicarbonate-Extractable Phosphorus

J.J. Schoenau
University of Saskatchewan
Saskatoon, Saskatchewan, Canada

I.P. O'Halloran
University of Guelph
Ridgetown, Ontario, Canada

8.1 INTRODUCTION

Sodium bicarbonate ($NaHCO_3$)-extractable phosphorus, commonly termed Olsen-P (Olsen et al. 1954), has a long history of worldwide use as an index of soil-available P on which to base P fertilizer recommendations (Cox 1994). It has been successfully used as a soil test for P in both acid and calcareous soils (Kamprath and Watson 1980). As a soil test, Olsen-P is sensitive to management practices that influence bioavailable soil P levels, such as fertilizer (O'Halloran et al. 1985) or manure (Qian et al. 2004) additions, although it is not suitable for P extraction from soils amended with relatively water-insoluble P materials such as rock phosphate (Mackay et al. 1984; Menon et al. 1989).

As an extractant, $NaHCO_3$ acts through a pH and ion effect to remove solution inorganic P (P_i) plus some labile solid-phase P_i compounds such as phosphate adsorbed to free lime, slightly soluble calcium phosphate precipitates, and phosphate loosely sorbed to iron and aluminum oxides and clay minerals. Sodium bicarbonate also removes labile organic P (Bicarb-P_o) forms (Bowman and Cole 1978; Schoenau et al. 1989) that may be readily hydrolyzed to P_i forms and contribute to plant-available P (Tiessen et al. 1984; O'Halloran et al. 1985; Atia and Mallarino 2002) or be reassimilated by microorganisms (Coleman et al. 1983). Although these labile P_o fractions once mineralized may play an important role in the P nutrition of crops, most regions using the Olsen-P soil test only consider the P_i fraction. A modification of the Olsen-P method is one of the extraction steps used in the sequential extraction procedure for soil P outlined in Chapter 25. In this method, the $NaHCO_3$-extractable P_i (Bicarb-P_i) and Bicarb-P_o are determined after a 16 h extraction. If the researcher is interested in a measure of the impact of treatments or management on these labile P_i and P_o fractions, one can simply follow the $NaHCO_3$ extraction and analysis procedure outlined in Chapter 25, ignoring the initial extraction using exchange resins.

As with many soil tests for P, the Olsen-P test has been used as a surrogate measure of potential P loss through runoff (Pote et al. 1996; Turner et al. 2004) and in regions using the Olsen-P as the recommended soil P test it is often a criterion in soil P indices for assessing risk of P loss and impact on surface waters (Sharpley et al. 1994). The reader is referred to Chapter 14 for a more comprehensive discussion of methods for determining environmental soil P indices. Owing to its widespread use as an extractant for assessing P availability and its utilization in environmental P loading regulations, this chapter covers methodology for measurement of Olsen-P as a soil test.

8.2 SODIUM BICARBONATE-EXTRACTABLE INORGANIC P (OLSEN ET AL. 1954)

In this extraction, a soil sample is shaken with 0.5 *M* $NaHCO_3$ adjusted to a pH of 8.5, and the extract filtered to obtain a clear, particulate-free filtrate. The filtrate is usually a yellowish to dark brown color, depending upon the amount of organic matter removed from the soil. When relatively small amounts of organic matter are removed (pale yellowish-colored filtrates) it is possible to simply correct for its presence by using a blank correction (i.e., measure absorbance of a suitably diluted aliquot without color-developing reagent added). Presence of higher concentrations of organic matter can interfere with the color development in some colorimetric methods, or result in the precipitation of organic materials. Several options exist for the removal of the organic material in the extracts such as the use of charcoal (Olsen et al. 1954) and polyacrylamide (Banderis et al. 1976).

8.2.1 Extraction Reagents

1 Sodium bicarbonate ($NaHCO_3$) extracting solution, 0.5 *M* adjusted to pH 8.5. For each liter of extracting solution desired, dissolve 42 g of $NaHCO_3$ and 0.5 g of NaOH in 1000 mL of deionized water. The $NaHCO_3$ extracting solution should be prepared fresh each month and stored stoppered since changes in pH of solution may occur that can affect the amount of P extracted.

2 If using charcoal to remove organic material from the extracting solution: prepare by mixing 300 g of phosphate-free charcoal with 900 mL of deionized water (see Comment 2 in Section 8.2.3).

3 If using polyacrylamide to remove organic material from the extracting solution: dissolve 0.5 g of polyacrylamide in approximately 600 mL of deionized water in a 1 L volumetric flask. This may require stirring for several hours. When the polymer has dissolved, dilute to volume with distilled water.

8.2.2 Procedure

1 Weigh 2.5 g sample of air-dried (ground to pass through a 2 mm sieve) soil into a 125 mL Erlenmeyer flask. Include blank samples without soil.

2 Add 50 mL of 0.5 *M* $NaHCO_3$ extracting solution at 25°C.

3 If using charcoal to remove dissolved soil organic matter from the extracting solution: add 0.4 mL of the charcoal suspension.

4 If using polyacrylamide to remove dissolved soil organic matter from extracting solution: add 0.25 mL of the polyacrylamide solution.

5 Shake for 30 min on a reciprocating shaker at 120 strokes per minute.

6 Filter the extract into clean sample cups using medium retention filter paper (i.e., VWR 454 or Whatman No. 40). If the filtrate is cloudy, refilter as necessary.

7 See Section 8.3 for the determination of Olsen-P in the filtrates.

8.2.3 Comments

1 The conditions under which the extraction is conducted can influence the amount of P extracted from the soil. Increasing the speed and time of the shaking will usually result in greater amounts of P being extracted (Olsen and Sommers 1982). Limiting extraction times to 30 min have been adopted for most soil testing purposes although a more complete and reproducible extraction may be obtained with a 16 h extraction. Increasing temperature of extraction will also increase the amount of P extracted. Olsen et al. (1954) reported that extracted P_i increased by 0.43 mg P kg^{-1} soil for each 1°C increase in temperature between 20°C and 30°C in soils testing between 5 and 40 mg P kg^{-1} soil. It is therefore important that if the results are to be interpreted in terms of regional management recommendations, the conditions of extraction must be similar to those used for the calibration of the soil test. If the results are for a comparative purpose between samples, then uniformity of extraction conditions between sample extractions is of greater importance than selecting a specific shaking speed, duration, and temperature of extraction.

2 Most commercially available sources of charcoal or carbon black are contaminated with P. It is strongly recommended that the charcoal be washed with 6 *M* HCl to remove the P, followed by repeated washings with deionized water. Analysis of sample blanks of $NaHCO_3$ extracting solution with and without the charcoal solution will indicate if P removal from the charcoal has been successful.

3 The $NaHCO_3$ extracts should be analyzed as soon as possible, as microbial growth can proceed very rapidly, even under refrigeration. One can add one or two drops of toluene to inhibit microbial activity, although this increases the biohazard rating of the filtrates for handling and disposal. Preferably, the filtrates should be stored under refrigeration and analyzed within 5 days if they cannot be analyzed immediately.

8.3 PHOSPHORUS MEASUREMENT IN THE EXTRACT

The amount of orthophosphate in the $NaHCO_3$ extractions is usually determined colorimetrically and various methods, both manual and automated, are available. The manual

method described here is based on one of the most widely used procedures, the ammonium molybdate–antimony potassium tartrate–ascorbic acid method of Murphy and Riley (1962). This method is relatively simple and easy to use and the manual method described is adaptable to automated systems. The addition of antimony potassium tartrate eliminates the need for heating to develop the stable blue color. The phosphoantimonylmolybdenum complex formed has two absorption maxima; one at 880 nm and the other at 710 nm (Going and Eisenreich 1974). Watanabe and Olsen (1965) suggest measuring absorbance at 840 to 880 nm utilizing the greater of the two absorbance maxima, while Chapter 25 suggests using 712 nm to reduce possible interference from traces of organic matter in slightly colored extracts.

8.3.1 Reagents for P Measurement

1 Ammonium molybdate solution: dissolve 40 g of ammonium molybdate ($(NH_4)_6Mo_7O_{24} \cdot 4H_2O$) in 1000 mL of deionized water.

2 Ascorbic acid solution: dissolve 26.4 g of L-ascorbic acid in 500 mL of deionized water. Store under refrigeration at ~2°C. Prepare fresh if solution develops a noticeable color.

3 Antimony potassium tartrate solution: dissolve 1.454 g of antimony potassium tartrate in 500 mL of deionized water.

4 Sulfuric acid (H_2SO_4), 2.5 *M*: slowly add 278 mL concentrated H_2SO_4 to a 2 L volumetric flask containing ~1 L of deionized water. Mix and allow to cool before making to volume with distilled deionized water.

5 Sulfuric acid (H_2SO_4), ~0.25 *M*: slowly add ~14 mL concentrated H_2SO_4 to a 100 mL volumetric flask containing ~75 mL of distilled water. Mix well and make to volume with distilled water.

6 *p*-nitrophenol solution, 0.25% (w/v): dissolve 0.25 g of *p*-nitrophenol in 100 mL of distilled water.

7 Standard P stock solution: prepare 100 mL of a base P standard with concentration of 5 μg P mL^{-1}.

8 Making the Murphy–Riley color-developing solution: using the above reagents, prepare the Murphy–Riley color-developing solution in a 500 mL flask as follows: add 250 mL of 2.5 *M* H_2SO_4, followed by 75 mL of ammonium molybdate solution, 50 mL of ascorbic acid solution, and 25 mL of antimony potassium tartrate solution. Dilute to a total volume of 500 mL by adding 100 mL of deionized water and mix on a magnetic stirrer. The reagents should be added in proper order and the contents of the flask swirled after each addition. Keep the Murphy–Riley solution in an amber bottle in a dark location to protect from light. Fresh Murphy–Riley solution should be prepared daily.

8.3.2 Procedure

1 Pipette 10 mL or a suitable aliquot of the filtered $NaHCO_3$ extract into a 50 mL volumetric flask. Include both distilled water and $NaHCO_3$ blanks. (See Comment 2 in Section 8.3.3).

2 To prepare standards of desired concentration range: 0, 0.1, 0.2, 0.3, 0.4, and 0.8 μg P mL^{-1} in $NaHCO_3$ matrix, add 0, 1, 2, 3, 4, 6, and 8 mL of the base P standard (5 μg P mL^{-1}) to 50 mL volumetric flasks. Then add 10 mL of 0.5 *M* $NaHCO_3$ to each flask.

3 To adjust the pH of the solutions add one to two drops of *p*-nitrophenol to each flask, which should result in a yellow solution. Lower the pH by adding 0.25 *M* H_2SO_4 until the solution just turns colorless.

4 To each flask, add 8 mL of the Murphy and Riley color-developing solution prepared in Section 8.3.1. Make to volume (50 mL) with deionized water, shake and allow 15 min for color development.

5 Measure the absorbance of the standards and samples on a suitably calibrated and warmed-up spectrophotometer set to either 712 or 880 nm. Construct a standard curve using the absorbance values from standards of known P concentration.

8.3.3 Comments

1 The ammonium molybdate, ascorbic acid, and antimony potassium tartrate solutions are generally stable for 2 to 3 months if well stoppered and stored under refrigeration. If quality of the solutions or reagents is suspected, discard and prepare fresh, as deterioration and/or contamination is a common source of error in the analysis.

2 Although several modifications of the Murphy and Riley procedure exist in the literature, when using reagents as originally described by Murphy and Riley (1962) the final concentration of P in the 50 mL volumetric flask should not exceed 0.8 μg P mL^{-1} (Towns 1986) as color development may not be complete. Thus, the suitable aliquot size for color development should contain <40 μg P. See Chapter 24 (Section 24.5) for more discussion on color development using the Murphy and Riley reagents.

8.3.4 Calculation

Using the concentrations of P suggested in Section 8.3.2, the standard curve should be linear. If the standard curve is constructed based on the μg P contained in the 50 mL flask (i.e., 0, 5, 10, 15, 20, 30, and 40 μg P) vs. absorbance, then the sample P content in mg P kg^{-1} soil can be calculated using the following formula:

$$\text{mg P kg}^{-1}\text{ soil} = \mu\text{g P in flask} \times \frac{\text{50 mL (extraction volume)}}{\text{mL aliquot}} \times \frac{1}{\text{g of soil}} \qquad (8.1)$$

REFERENCES

Atia, A.M. and Mallarino, A.P. 2002. Agronomic and environmental soil phosphorus testing in soils receiving liquid swine manure. *Soil Sci. Soc. Am. J.* 66: 1696–1705.

Banderis, A.S., Barter, D.H., and Henderson, K. 1976. The use of polyacrylamide to replace carbon in the determination of Olsen's extractable phosphate in soil. *J. Soil Sci.* 27: 71–74.

Bowman, R.A. and Cole, C.V. 1978. An exploratory method for fractionation of organic phosphorus from grassland soils. *Soil Sci.* 125: 95–101.

Coleman, D.C., Reid, C.P., and Cole, C.V. 1983. Biological strategies of nutrient cycling in soil systems. In A. MacFayden and E.O. Ford, Eds. *Advances in Ecological Research* 13. Academic Press. New York, NY, pp. 1–56.

Cox, F.R. 1994. Current phosphorus availability indices: characteristics and shortcomings. In J.L. Havlin et al., Eds. *Soil Testing: Prospects for Improving Nutrient Recommendations*. Soil Science Society of America Special Publication No. 40. SSSA-ASA, Madison, WI, pp. 101–114.

Going, J.E. and Eisenreich, S.J. 1974. Spectrophotometric studies of reduced molybdoantimonylphosphoric acid. *Anal. Chim. Acta* 70: 95–106.

Kamprath, E.J. and Watson, M.E. 1980. Conventional soil and tissue tests for assessing the phosphorus status of soil. In F.E. Khasawneh, E.C. Sample, and E.J. Kamprath, Eds. *The Role of Phosphorus in Agriculture*. American Society of Agronomy, Madison, WI, pp. 433–469.

Mackay, A.D., Syers, J.K., Gregg, P.E.H., and Tillman, R.W. 1984. A comparison of three soil testing procedures for estimating the plant available phosphorus in soils using either superphosphate or phosphate rock. *N. Z. J. Agric. Res.* 27: 231–245.

Menon, R.G., Hammond, L.L., and Sissingh, H.A. 1989. Determination of plant-available phosphorus by the iron hydroxide-impregnated filter paper (P_i) soil test. *Soil Sci. Soc. Am J.* 53: 110–115.

Murphy, J. and Riley, J.P. 1962. A modified single solution method for the determination of phosphates in natural waters. *Anal. Chem. Acta* 27: 31–36.

O'Halloran, I.P., Kachanoski, R.G., and Stewart, J.W.B. 1985. Spatial variability of soil phosphorus as influenced by soil texture and management. *Can. J. Soil Sci.* 65: 475–487.

Olsen, S.R., Cole, C.V., Watanabe, F.S., and Dean, L.A. 1954. *Estimation of available phosphorus in soils by extraction with sodium bicarbonate*. US Dept. Agric. Circ. 939, Washington, DC.

Olsen, S.R. and Sommers, L.E. 1982. Phosphorus. In A.L. Page, R.H. Miller, and D.R. Keeney, Eds. *Methods of Soil Analysis, 2nd ed. Part 2*. Agronomy No. 9. American Society of Agronomy, Madison, WI, pp. 403–430.

Pote, D.H., Daniel, T.C., Sharpley, A.N., Moore P.A. Jr., Edwards, D.R., and Nichols, D.J. 1996. Relating extractable soil phosphorus to phosphorus losses in runoff. *Soil Sci. Soc. Am. J.* 60: 855–859.

Qian, P., Schoenau, J.J., Wu, T., and Mooleki, P. 2004. Phosphorus amounts and distribution in a Saskatchewan soil after five years of swine and cattle manure application. *Can. J. Soil Sci.* 84: 275–281.

Schoenau, J.J., Stewart, J.W.B., and Bettany, J.R. 1989. Forms and cycling of phosphorus in prairie and boreal forest soils. *Biogeochemistry* 8: 223–237.

Sharpley, A.N., Chapra, S.C., Wedepohl, R., Sims, J.T., Daniel, T.C., and Reddy, K.R. 1994. Managing agricultural phosphorus for protection of surface waters: issues and options. *J. Environ. Qual.* 23: 437–441.

Tiessen, H., Stewart, J.W.B., and Cole, C.V. 1984. Pathways of phosphorus transformations in soils of differing pedogenesis. *Soil Sci. Soc. Am. J.* 48: 853–858.

Towns, T.G. 1986. Determination of aqueous phosphate by ascorbic acid reduction of phosphomolybdic acid. *Anal. Chem.* 58: 223–229.

Turner, B.L., Kay, M.A., and Westermann, D.T. 2004. Phosphorus in surface runoff from calcareous arable soils of the semiarid western United States. *J. Environ. Qual.* 33: 1814–1821.

Watanabe, F.S. and Olsen, S.R. 1965. Test of an ascorbic acid method for determining phosphorus in water and $NaHCO_3$ extracts from soils. *Soil Sci. Soc. Am. Proc.* 29: 677–678.

Chapter 9
Boron, Molybdenum, and Selenium

Ganga M. Hettiarachchi
University of Adelaide
Glen Osmond, South Australia, Australia

Umesh C. Gupta
Agriculture and Agri-Food Canada
Charlottetown, Prince Edward Island, Canada

9.1 INTRODUCTION

Common features of B, Mo, and Se are that all three are nutrient elements that can be mainly found either in anionic or neutral form in soil solution and are relatively mobile in soils. Boron and Mo are essential elements for both plants and animals, while Se is an important element for humans and animals. Both B and Mo are essential micronutrients required for the normal growth of plants, with differences between plant species in the levels required for normal growth of plants. There is a narrow soil solution concentration range defining B or Mo deficiencies and toxicities in plants.

Boron deficiencies can be found most often in humid regions or in sandy soils. Boron is subject to loss by leaching, particularly in sandy soils, and thus responses to B are common for sandy soils as summarized by Gupta (1993). Responses to B have been found on a variety of crops in many countries (Ericksson 1979; Touchton et al. 1980; Sherrell 1983). In contrast, B toxicity can be found mostly in arid and semiarid regions either due to high B in soils or high B containing irrigation water (Keren 1996).

Responses to Mo have been frequently observed in legumes grown on soils that need lime. Elevated levels of Mo in soils and subsequent accumulations of Mo in plants, however, are of more concern than Mo deficiency in soils. High levels of Mo in plants eaten by ruminants can induce molybdenosis, a Mo-induced Cu deficiency (Jarrell et al. 1980).

Yield responses to Se are generally not found. However, it is essential for livestock and is somewhat unique among the essential nutrients provided by plants to animals. In some areas, native vegetation can contain Se levels that are toxic to animals, whereas in other locations,

vegetation can be deficient in Se, also causing animal health problems due to inclusion of low Se forage as part of animal diets (Mikkelsen et al. 1989). The Se concentration in soils in humid regions is generally inadequate to produce crops sufficient in Se to meet the needs of livestock. In acid soils, the ferric-iron selenite complex is formed, which is only slightly available to plants (NAS-NRC 1971). Selenium is generally present in excessive amounts only in semiarid and arid regions in soils derived from cretaceous shales, where it tends to form selenates (Welch et al. 1991). Selenium toxicity problems in the semiarid western United States are generally associated with alkaline soils where Se is present in the selenate form (Jump and Sabey 1989).

9.2 BORON

Boron in soils is primarily in the +3 oxidation state taking the form of the borate anion: $B(OH)_4^-$. The two most common solution species of B are neutral boric acid (H_3BO_3) and borate anion ($B(OH)_4^-$). Boron in soil can either be present in soil solution or adsorbed onto soil minerals such as clays. Below pH 7, H_3BO_3 predominates in soil solution, resulting in only a small amount of B adsorbed onto soil minerals. As the pH increases to about 9, the $B(OH)_4^-$ increases rapidly, increasing B adsorption (Vaughan and Suarez 2003). Only the B in soil solution is important for plants.

A number of extractants such as 0.05 *M* HCl (Ponnamperuma et al. 1981), 0.01 *M* $CaCl_2$ + 0.5 *M* mannitol (Cartwright et al. 1983), hot 0.02 *M* $CaCl_2$ (Parker and Gardner 1981), and 1 *M* ammonium acetate (Gupta and Stewart 1978) have been employed for determining the availability of B in soils. One advantage of using $CaCl_2$ is that it extracts little color from the soil, and predicted error due to this color is found to be low at 0.00–0.07 mg kg^{-1} (Parker and Gardner 1981). Such filtered extracts are also free of colloidal matter.

Oyinlola and Chude (2002) reported that only hot water-soluble B correlated significantly with relative yields in Savannah soils of Nigeria, compared to several other extractants. Likewise Matsi et al. (2000) in northern Greece also noted that hot water-soluble B provided better correlation with yields than ammonium bicarbonate-diethylenetriamine-pentaacetic acid (AB-DTPA). Similar results were reported on some Brazilian soils where hot water-soluble B proved to be superior to HCl and mannitol in predicting the B availability for sunflower (Silva and Ferreyra 1998). Moreover, research work by Chaudhary and Shukla (2004) on acid soils of western India showed that both 0.01 *M* $CaCl_2$ and hot water extractions were suitable for determining the B availability to mustard (*Brassica juncea*).

Contrary to most other findings, Karamanos et al. (2003) concluded that hot water-extractable B was not an effective diagnostic tool for determining the B status of western Canadian soils. They, however, stressed that soil properties, especially organic matter, played an important role in determining the fate of applied B in the soil–plant system. Raza et al. (2002), on the other hand, found hot water-soluble B to be a good estimate of available B in the prairie soils of Saskatchewan. They further stated that soil cation exchange capacity appeared to be an important characteristic in predicting the B availability.

The most commonly used method is still the hot water extraction of soils as originally developed by Berger and Truog (1939) and modified by Gupta (1993). A number of

modified versions of this procedure have since appeared. Offiah and Axley (1988) have used B-spiked hot water extraction for soils. This method is claimed to have an advantage over unspiked hot water extraction in that it removes from consideration a portion of the B fixing capacity of soils that does not relate well to plant uptake. A longer boiling time of 10 min as opposed to the normally used 5 min boiling was found to reduce error for a Typic Hapludult soil by removing enough B to reach the plateau region of the extraction curve (Odom 1980).

Once extracted from the soil, B can be analyzed by the colorimetric methods using reagents such as carmine (Hatcher and Wilcox 1950), azomethine-H (Wolf 1971), and most recently by inductively coupled plasma-atomic emission spectrometry (ICP-AES) (Keren 1996).

9.2.1 Reagents

1 Deionized water

2 Charcoal

9.2.2 Procedure (Gupta 1993)

1 Weigh 25 g air-dried soil, screened through a 2 mm sieve, into a preweighed 250 mL ''acid-washed'' beaker and add about 0.4 g charcoal and 50 mL deionized water and mix. The amount of charcoal added will vary with the organic matter content of the soil and should be in sufficient quantity to produce a colorless extract after 5 min of boiling (see Comments 2 and 3 in Section 9.2.5). A blank containing only deionized water and a similar amount of charcoal as used with the soil samples should also be included.

2 Boil the soil–water–charcoal or water–charcoal mixtures for 5 min on a hotplate.

3 The loss in weight due to boiling should be made up by adding deionized water and the mixture should be filtered while still hot through a Whatman No. 42 or equivalent type of filter paper.

9.2.3 Determination of Boron by the Azomethine-H Method

Reagents

1 Azomethine-H: dissolve 0.5 g azomethine-H in about 10 mL redistilled water with gentle heating in a water bath or under a hot water tap at about 30°C. When dissolved add 1.0 g L-ascorbic acid and mix until dissolved. Make the final volume up to 100 mL with redistilled water. If the solution is not clear, it should be reheated again till it dissolves. Prepare fresh azomethine-H solution for everyday use.

2 Ethylene diamine tetraacetic acid (EDTA) reagent (0.025 *M*): dissolve 9.3 g EDTA in redistilled water and make the volume up to 1 L with redistilled water. Add 1 mL Brij-35 and mix.

3 Buffer solution: dissolve 250 g ammonium acetate in 500 mL redistilled water. Adjust the pH to about 5.5 by slowly adding approximately 100 mL concentrated acetic acid, with constant stirring. Add 0.5 mL Brij-35 and mix.

4 Standard solutions: prepare stock standard A by dissolving 1000 mg B (5.715 g H_3BO_4) in 1 L deionized water and prepare stock standard B by taking 50 mL stock standard A and diluting it to 1 L with 0.4 *M* HCl. Prepare standard solutions from stock standard B by diluting a range of 2.5 to 30 mL stock standard B to 1 L with deionized water to give a range of 0.5 to 6.0 mg B L^{-1} in the final standard solution.

Procedure

1 Take 5 mL of the clear filtrate in a test tube and add 2 mL buffer solution, 2 mL EDTA solution, and 2 mL azomethine-H solution, mixing the contents of the test tube thoroughly after the addition of each solution.

2 Let the solutions stand for 1 h and measure the absorbance at 430 nm on a spectrophotometer.

3 The color thus developed has been found to be stable for up to 3–4 h.

4 The pH of the colored extract should be about 5.0.

9.2.4 Determination of Boron by Inductively Coupled Plasma-Atomic Emission Spectrometry

This technique has been found to be rapid and reliable for determining B in plant digests and soil extracts using the procedure described in Section 9.2.2 by Gupta (1993). An estimated detection limit by ICP-AES at wavelength of 249.77 nm is about 5 μg L^{-1} (APHA 1992) and therefore, it is reasonable to expect method detection limit to be about 100 μg B kg^{-1} soil. Care must be taken to filter samples properly as colloidal-free extracts are recommended for ICP-AES to avoid nebulizer-clogging problems.

9.2.5 Comments

1 All glassware used in plant or soil B analyses must be washed with a 1:1 mixture of boiling HCl acid with deionized water before use. Storage of the filtered extracts before the analysis of B must be in plastic sampling cups.

2 Soils containing higher organic matter may require additional amount of charcoal to obtain a colorless extract, but the addition of excessive amounts of charcoal can reduce the amount of B in the extract.

3 If the filtered solution is not colorless, the extraction may need to be repeated with a higher amount of charcoal.

4 The use of azomethine-H is an improvement over those of carmine (Hatcher and Wilcox 1950), quinalizarin, and curcumin (Johnson and Ulrich 1959), since the

procedure involving this chemical does not require use of a concentrated acid. This method has been found to give comparable results when compared to the carmine method (Gupta 1993).

5 It is difficult to use an autoanalyzer because of its insensitivity at lower B concentrations generally found in the hot water extract of most soils.

9.3 MOLYBDENUM

Molybdenum in soils is primarily in the +6 oxidation state taking the form of the molybdate anion, MoO_4^{2-}. The solution species of Mo, generally in the order of decrease in concentration, are MoO_4^{2-}, $HMoO_4^{-}$, $H_2MoO_4^{0}$, $MoO_2(OH)^{+}$, and MoO_2^{2+}, respectively. The latter two species can be ignored in most soils (Lindsay 1979). Molybdate is adsorbed by oxides, noncrystalline aluminosilicates, and to a lesser extent by layer silicates and adsorption increases with decreasing pH. Therefore, Mo is least soluble in acid soils, especially acid soils containing Fe oxides.

Studies on the extraction of available Mo from soils have been limited. Further, the extremely low amounts of available Mo in soils under deficiency conditions make it difficult to determine Mo accurately. The accumulation of Mo in plants mostly is not related to total concentrations of Mo in soils but rather to available Mo in soils. A variety of extractants have been used in attempts to extract available Mo in soils although no routine soil test for Mo is available. Molybdenum deficiencies are rare and are mostly of concern for leguminous crops. Since excessive Mo in forages can harm animal health, Mo fertilization is usually based on visual deficiency symptoms and/or history of crop rotation.

Many extractants have been employed for the assessment of available Mo in soils. Those extractants are: ammonium oxalate, pH 3.3 (Grigg 1953); water (Gupta and MacKay 1965a); hot water, anion-exchange resin; AB-DTPA (Soltanpour and Workman 1980); ammonium carbonate (Vlek and Lindsay 1977); and Fe oxide strips (Sarkar and O'Connor 2001). However, most of those extractants are used to study the deficiency aspect rather than from consideration of toxic effects (Davies 1980).

Despite its weaknesses, the most commonly used extractant for assessing Mo availability in soils has been ammonium oxalate, buffered at pH 3.3 (Grigg 1953). Examples for the successful use of acid ammonium oxalate in predicting Mo uptake by plants (Wang et al. 1994) and its failures (Mortvedt and Anderson 1982; Liu et al. 1996) can be found in the literature. From studies that failed to predict plant uptake of Mo successfully with acid ammonium oxalate-extractable Mo, it appeared that plant Mo was more closely related to some soil property such as pH other than extractable Mo in soils. Some studies obtained a better regression between acid oxalate-extractable Mo in soil and plant Mo when soil pH was considered as a factor (Mortvedt and Anderson 1982). Sharma and Chatterjee (1997) stated that soil physical properties such as soil pH, organic matter, parent rock, and texture play an important role in determining the Mo availability in alkaline soils. Multiple-regression equations account for the contribution of the individual factors, which would make the critical limits more predictable. Moreover, Liu et al. (1996) found significant correlations ($r^2 = 0.81$) for soil Mo extracted with ammonium oxalate (pH 6.0) in a group of Kentucky soils with Mo uptake by tobacco (*Nicotiana tabacom* L.) growing in

greenhouse. However, ammonium oxalate buffered at pH 3.3 was not statistically well correlated with Mo uptake.

Some methods that have not been widely tested but appear to be promising are anion-exchange resin and AB-DTPA methods. Anion-exchange resins have been used with success to extract plant-available Mo in soils (Ritchie 1988). The AB-DTPA method (Soltanpour and Workman 1980; Soltanpour et al. 1982) has also been used successfully for alkaline and Mo-contaminated soils (Pierzynski and Jacobs 1986, Wang et al. 1994). Moreover, ammonium carbonate (Vlek and Lindsay 1977) also has shown good correlation with plant uptake of Mo, especially for soils that have Mo toxicity problems. This extraction followed by H_2O_2 treatment leaves a decolorized extract that is useful for Mo analysis by colorimetric methods (Wang et al. 1994).

To characterize the available Mo in biosolids-amended soils, Sarkar and O'Connor (2001) compared the potential of Fe-oxide impregnated filter paper with ammonium oxalate extraction method and total soil Mo. Their data showed that the best correlation between plant Mo and soil Mo was obtained using the Fe-oxide strip followed by ammonium oxalate extraction; while total soil Mo was generally not well correlated with plant Mo uptake. Sarkar and O'Connor (2001) further reported that Fe-oxide strips can serve as an analytically satisfactory and practical procedure for assessing available Mo, even in soils amended with biosolids.

Recently, McBride et al. (2003) found that dilute $CaCl_2$ was found to be preferable to Mehlich 3 as a universal extractant for determining Mo and other trace metal availability in clover grown on near neutral soils amended with sewage sludge. Concentration of Mo in alfalfa (*Medicago sativa* L.) on soils treated with sewage sludge was well correlated to readily extractable Mo by 0.01 *M* $CaCl_2$ in the soil. Total Mo and past Mo loading to soil were less reliable predictors of Mo concentration in alfalfa than the soil test for readily extractable Mo (McBride and Hale 2004).

Two methods of extractions are outlined (1) ammonium oxalate, pH 3.0 (modified Grigg 1953) and (2) AB-DTPA (Soltanpour and Schwab 1977).

9.3.1 Extraction of Molybdenum by the Ammonium Oxalate, pH 3.0 Method (Modified Grigg 1953)

Reagents (Gupta and MacKay 1966)

1 Ammonium oxalate, 0.2 *M* buffered to pH 3.0: in a 1 L volumetric flask dissolve 24.9 g of ammonium oxalate and 12.605 g of oxalic acid in approximately 800 mL deionized water. Make to volume with distilled water and mix well.

Procedure

1 Add 15 g air-dried soil, screened through a 2 mm sieve, to a 250 mL beaker or Erlenmeyer flask.

2 Add 150 mL of the buffered (pH 3) 0.2 *M* ammonium oxalate solution and shake for 16 h at room temperature using an orbital shaker at 200 rpm.

3 Filter the extraction through Whatman No. 42 filter paper or equivalent. Centrifuge the filtrate for 20 min.

4 Determine Mo concentration in the clear extract as described in Section 9.3.3. If required, the centrifuged extracts can be acidified to pH < 2 with HNO_3 and stored in 1:1 HNO_3 rinsed plastic or glass containers up to a maximum of 6 months (APHA 1992).

9.3.2 Extraction of Molybdenum by the Ammonium Bicarbonate-Diethylenetriaminepentaacetic Acid Solution Method (Soltanpour and Schwab 1977)

Reagents

1 Ammonium hydroxide (NH_4OH) 1:1 solution.

2 AB-DTPA solution (1 *M* NH_4HCO_3, 0.005 *M* DTPA buffered to pH 7.6): in a 1 L volumetric flask containing approximately 800 mL of distilled-deionized water, add 1.97 g of DTPA and approximately 2 mL of 1:1 NH_4OH solution and mix. (The addition of the 1:1 NH_4OH solution aids in the dissolution of DTPA and helps prevent frothing.) When most of the DTPA is dissolved, add 79.06 g of NH_4HCO_3 and stir until all materials have dissolved. Adjust pH to 7.6 by adding either NH_4OH or HCl and then make to volume using distilled-deionized water.

Procedure

1 Weigh 10 g soil, screened through a 2 mm sieve, into a 125 mL Erlenmeyer flask and add 20 mL of AB-DTPA solution.

2 Shake the mixture in open flasks on a reciprocal shaker at 180 rpm for 15 min and filter the extract using Whatman No. 42 filter paper or its equivalent.

3 Determine Mo as described in Section 9.3.3. The filtered extracts can be preserved until analysis as mentioned under Section 9.3.1 (Reagents (1)).

9.3.3 Determination of Molybdenum

Determine Mo concentration in extracts with graphite furnace atomic absorption spectrometry (GFAAS) or ICP-AES. The standards for GFAAS or ICP must be prepared in the extracting solution matrix.

Since extractable Mo in normal situations is usually in the range of 10 to 50 $\mu g\ L^{-1}$, analytical methods must be sensitive to measure low concentrations. Therefore, most suitable method is GFAAS (Mortvedt and Anderson 1982). It is recommended to use HNO_3 as a matrix modifier (as enhancer); and pyrolytically coated tubes (to minimize problems due to carbide formation) for Mo determination in GFAAS. An estimated detection

limit using pyrolytic graphite tubes is 1 μg L^{-1} (APHA 1992). In situations where one could expect higher concentrations of Mo in the extracting solutions, flame atomic absorption spectrometry or atomic emission spectrometry (either direct or ICP-AES) can be used for Mo analysis (Soltanpour et al. 1996). An estimated detection limit using ICP-AES is 8 μg L^{-1} (APHA 1992) and therefore, it will be safer to assume method detection limits for ICP-AES for Mo to be 80 μg L^{-1} or little lower. For spectrometry determinations standards must be made in AB-DTPA matrix solution. It has also been suggested to treat the extract with concentrated HNO_3 acid before determination of Mo by ICP-AES. After adding 0.5 mL concentrated HNO_3 acid to about 5 mL filtrate, mix it in a beaker on a rotary shaker for about 15 min to eliminate carbonate species.

Determination of Mo in soil extracts can also be done colorimetrically in laboratories that are not equipped with ICP-AES or GFAAS. Refer to Gupta and MacKay (1965b) for details of colorimetric determination of Mo.

9.3.4 Comments

In general, ammonium oxalate shows greater ability to extract Mo from soils and mine spoils compared to AB-DTPA method (Wang et al. 1994).

9.4 SELENIUM

Soil Se forms include very insoluble reduced forms including selenium sulfides, elemental Se (Se^0), and selenides (Se^{-2}) and more soluble selenate (SeO_4^{2-}), and selenite ($HSeO_3^-$, SeO_3^{2-}). Elemental Se, sulfides, and selenides only occur in reducing environments. They are insoluble and not available for plants and living organisms (McNeal and Balistrieri 1989). In alkaline, oxidized soils, selenates are the dominant forms while in slightly acidic, oxidized soils, selenites are dominant. Selenate and selenite precipitates and minerals are highly soluble in aerobic environments and therefore, the solubility of Se is controlled mainly by adsorption and complexation processes. Selenite is proven to be strongly adsorbed to soil surfaces while selenate is weakly adsorbed (Neal et al. 1987).

The parent material has a significant effect upon the Se concentration in plants. For example, field studies conducted on wheat in west central Saskatchewan showed higher Se values in wheat plants grown on lacustrine clay and glacial till, intermediate in plants grown on lacustrine silt, and lowest on aeolian sand (Doyle and Fletcher 1977). A similar trend characterized the C horizon soil, with highest Se values associated with lacustrine clay and lowest with aeolian sand. The findings of Doyle and Fletcher (1977) pointed to the potential usefulness of information on the Se content of soil parent materials when designing sampling programs for investigating regional variations in plant Se content.

Available Se in soils is highly variable. Although there were instances where a direct correlation between soil Se content and the plant grown on those soils existed (Varo et al. 1988), more often the total Se in soil proved to be of little value in predicting plant uptake (Diaz-Alarcon et al. 1996). Selenium uptake by plants depends not only on the form and partitioning of Se species between solution and solid phases but also on the presence of other ions in soil solution (such as SO_4^{-2}) and the species of plants (Bisbjerg and Gissel-Nielsen 1969; Mikkelsen et al. 1989). Therefore, ideally extractants capable of predicting or evaluating plant-available Se should be capable of extracting Se in soil solution as well as Se associated with solid phases that would be potentially released into soil solution. The ability

of an extractant to correlate significantly with plant uptake could vary depending on many factors, some of which are soil type, plant species, season, and location. Uptake of Se by plants and methods that can be used to predict and evaluate plant uptake of Se can be found in the literature (Soltanpour and Workman 1980; Soltanpour et al. 1982; Jump and Sabey 1989; Mikkelsen et al. 1989).

Soltanpour and Workman (1980) found a high degree of correlation between extracted Se by an AB-DTPA extraction procedure developed by Soltanpour and Schwab (1977) and Se uptake by alfalfa for five levels of Se(VI) in a greenhouse study. In addition, they found very high ($r^2 = 0.99$) correlation between AB-DTPA extractable and hot water-extractable Se (Black et al. 1965). The hot water-extractable Se soil test method is developed based on the assumption that soil and soil-like materials that contain appreciable amounts of water-soluble Se (majority as selenates) will give rise to Se-toxic vegetation (Black et al. 1965). Similarly, AB-DTPA should extract water-soluble Se as well as exchangeable selenate and/or selenite into solution due to bicarbonate anion. In addition, Soltanpour et al. (1982) found that the AB-DTPA-extractable Se in soil samples taken from a 0 to 90 cm depth in the autumn before seeding winter wheat (*Triticum aestivum* L.) correlated well with Se in grain samples ($r^2 = 0.82$) that were taken in the following summer.

Selenium in saturated paste extracts could also provide useful information about plant-available Se in soils (U.S. Salinity Laboratory Staff 1954) as mostly the soil:water ratio in these pastes can be related to field soil water content in a predictable manner. Using two Se-accumulating plant species, Jump and Sabey (1989) found that Se in saturated paste water extracts correlated highest with plant Se concentrations from a study that compared Se extracted from 18 different soils and mine-spoil materials by several different extractants (AB-DTPA, DTPA, hot water, saturated paste extract, and Na_2CO_3).

In addition to measuring total extractable Se, determination of Se species in soil solution, saturate paste extract, or any other extraction may also provide insight into potential for plant Se uptake. Mikkelsen et al. (1989) discussed the different mechanisms associated with energy-dependent uptake of Se(VI) and energy-independent uptake of Se(IV). They also discussed the variable uptake of Se by different plant species, which is an additional complication. Davis (1972a,b) demonstrated the variability for absorbing Se among different species within a single plant genus in two greenhouse experiments. All the above suggest that speciation information on Se(VI) and Se(IV) in extractions or soil solutions may also provide useful information on uptake of Se by plants.

Relatively labile forms of Se in soils can be evaluated by using orthophosphate (PO_4) as a soil extractant (Fujii et al. 1988). This is based on the assumptions that PO_4 replaces adsorbed forms of Se and the dominant adsorbed species of Se in these soils is Se(IV). Fujii and Burau (1989) used 0.1 *M* PO_4 solution adjusted to pH 8 and was able to extract 89% to 103% of the sorbed Se(IV) for three surface soils.

Sequential extraction procedures can also be used to identify fractions of Se in soils (Chao and Sanzolone 1989; Lipton 1991) and may be related to plant uptake. The sequential extraction method developed by Chao and Sanzolone (1989) fractionates soil Se into five operationally defined fractions (soluble, exchangeable, oxide bound, sulphide/organic matter bound, and residual or siliceous material associated), whereas the Lipton (1991) method fractionates soil Se into nine operationally defined fractions (soluble, ligand exchangeable, carbonates, oxidizable, easily reducible oxides bound, amorphous oxide bound, crystalline oxide bound, alkali-soluble Al/Si bound, and residual).

9.4.1 Extraction of Selenium in Soils

We will outline five commonly used methods of extractions with appropriate references here.

Five commonly used extractants for Se are given below:

1 AB-DPTA (Soltanpour and Schwab 1977): 10 g of air-dried soil, screened through a 2 mm sieve, is placed in a 125 mL Erlenmeyer flask. Add 20 mL of 1 *M* NH_4HCO_3 + 0.005 *M* DTPA (prepared as described in Section Reagents, p. 101) at pH 7.6. Shake the mixture in an open flask on a reciprocal shaker at 180 rpm for 15 min and filter the extract using Whatman No. 42 filter paper or its equivalent.

2 Hot water (Black et al. 1965): place 10 g of air-dried soil, sieved through a 2 mm sieve, in a 250 mL Erlenmeyer flask. Add 50 mL distilled water, and reflux over a boiling water bath for 30 min. Filter the soil suspension using Whatman No. 42 filter paper or its equivalent.

3 Saturated paste extractants (U.S. Salinity Laboratory Staff 1954): weigh 200 to 400 g of air-dried soil, sieved through a 2 mm sieve into a plastic container with a lid. Weigh the container, and container plus soil. Add distilled water to the soil, while stirring, until soil is nearly saturated. Cover the container and allow the mixture to stand for several hours. Then add more water with stirring to achieve a uniformly saturated soil–water paste. The criteria for saturation should be checked as given here (soil paste glistens as it reflects light, flows slightly when the container is tipped, slides freely and cleanly off a smooth spatula, and consolidates easily by tapping or jarring the container after a trench is formed in the paste with the side of the spatula). Allow the sample to stand for another 2 h, preferably overnight, and then recheck for the sample for saturation criteria. If the paste is too wet, add known amount of dry soil to the paste. Once saturation is attained, weigh the container plus content to get the amount of water added. Transfer the paste to a Büchner funnel fitted with highly retentive filter paper, and apply a vacuum to collect saturation extract in a test tube.

4 0.005 *M* DTPA, 0.01 *M* $CaCl_2$ (2 h DTPA test) (Lindsay and Norvell 1978): 10 g air-dried soil, screened through a 2 mm sieve, is placed in a 50 mL polypropylene centrifuge tube. Add 20 mL of 0.005 *M* DTPA, 0.01 *M* $CaCl_2$ buffered at pH 7.3 with triethanolamine and shake for 2 h on a reciprocating shaker. Centrifuge immediately at 3000 g and filter the supernatant using Whatman No. 42 filter paper or its equivalent.

5 0.5 *M* Na_2CO_3 (Jump and Sabey 1989): 5 g of air-dried soil, screened through a 2 mm sieve, is shaken on a reciprocating shaker in 20 mL of 0.5 *M* Na_2CO_3 solution at pH 11.3 for 30 min. Filter the extract using Whatman No. 42 filter paper or its equivalent.

Procedure

1 The soil:extractant ratio varies from 1:2 to 1:5 and the extraction time from 15 min to 2 h as given in the above-mentioned references or as summarized by Jump and Sabey (1989).

2 The filtered extracts can be analyzed for Se using a hydride-generating system attached to an ICP-AES (Soltanpour et al. 1996). Filtered extracts to be analyzed for Se can be preserved until analysis with either HNO_3 or HCl (pH < 2) to prevent loss of Se from solution (through coprecipitation or methylation of Se followed by volatilization).

All of the above five extractants when tested on soils containing high Se showed high correlation between wheat plant Se and Se extracted from soils (Jump and Sabey 1989). However, Se extracted in saturated soil pastes and expressed as mg Se L^{-1} of extract was found to be the best predictor of Se uptake in Se-accumulating plants. Furthermore, the results suggest that soil or mine-spoil materials that yield more than 0.1 mg Se L^{-1} in saturated extract may produce Se-toxic plants.

In addition, the AB-DTPA extract has been found to predict Se availability better when Se in wheat grain was correlated with Se in the 0–90 cm depth of soil as opposed to the 0–30 cm depth (Soltanpour et al. 1982). This was found to be particularly useful to screen soils and overburden material for potential toxicity of Se.

9.4.2 Determination of Selenium

Selenium in extracting solutions can be accurately determined by hydride generation atomic absorption spectrometry (HGAAS), electrothermal, or GFAAS, ICP-AES as well as combination of chemical methods with colorimetry and fluorometry (APHA 1992). The most common method of choice is the continuous HGAAS. For determination of Se at higher concentration, the ICP-AES coupled with HG may be preferred, in particular when simultaneous determination of other elements such as As is required (Workman and Soltanpour 1980). Matrix matching techniques (for example prepare standards in the same matrix as soil extracts) and extensive QA/QC procedures should be used to assure the quality of determination. For detailed information regarding the HGAAS apparatus and reagents needed for determination of Se, refer to APHA (1992) and Huang and Fujii (1996).

9.4.3 Comments

1 The extractants developed have been found to be suitable for predicting the availability of Se in Se toxic areas only. Because of rather small quantities of available Se in Se-deficient areas, no reliable extractant has yet been developed for such soils. Therefore, plant Se and total soil Se will continue to serve as the best tools available for testing the Se status of Se-deficient soils.

2 The term deficiency or deficient in connection with Se has implications in livestock and human nutrition only and not in plant nutrition since no known yield responses to Se have been found on cultivated crops.

REFERENCES

American Public Health Association (APHA), American Water Works Association, and Water Pollution Control Federation. 1992. *Standard Methods for the Examination of Water and Wastewater*, 18th edn. American Public Health Association, American Water Works Association, and Water Pollution Control Federation, Washington, DC.

Berger, K.C. and Truog, E. 1939. Boron determination in soils and plants using the quinalizarin reaction. *Ind. Eng. Chem.* 11: 540–545.

Bisbjerg, B. and Gissel-Nielsen, G. 1969. The uptake of applied selenium by agricultural plants. I. The influence of soil type and plant species. *Plant Soil* 31: 287–298.

Black, C.A., Evans, D.D., White, J.L., Ensmiger, L.E., and Clark, F.E., Eds. 1965. *Methods of Soil Analysis. Part 2*. Agronomy 9, ASA, Madison, WI, 1122 pp.

Cartwright, B., Tiller, K.G., Zarcinas, B.A., and Spouncer, L.R. 1983. The chemical assessment of the boron status of soils. *Aust. J. Soil Res.* 21: 321–330.

Chao, T.T. and Sanzolone, R.F. 1989. Fractionation of soil selenium by sequential partial dissolution. *Soil Sci. Soc. Am. J.* 53: 385–392.

Chaudhary, D.R. and Shukla, L.M. 2004. Evaluation of extractants for predicting availability of boron to mustard in arid soils of India. *Commun. Soil Sci. Plant Anal.* 35: 267–283.

Davies, B.E. 1980. *Applied Soil Trace Elements*. Wiley-Interscience, Chichester, New York, NY.

Davis, A.M. 1972a. Selenium accumulation in *Astragalus* species. *Agron. J.* 64: 751–754.

Davis, A.M. 1972b. Selenium accumulation in a collection of *Atriplex* species. *Agron. J.* 64: 823–824.

Diaz-Alarcon, J.P., Navarro-Alarcon, M., De la Serrana, H.L., Asensio-Drima, C., and Lopez-Martinez, M.C. 1996. Determination and chemical speciation of selenium in farmlands from southeastern Spain: relation to levels found in sugar cane. *J. Agric. Food Chem.* 44: 2423–2427.

Doyle, P.J. and Fletcher, W.K. 1977. Influence of soil parent material on the selenium content of wheat from west-central Saskatchewan. *Can. J. Plant Sci.* 57: 859–864.

Ericksson, M. 1979. The effect of boron on nectar production and seed setting of red clover (*Trifolium pratense* L.). *Swed. J. Agric. Res.* 9: 37–41.

Fujii, R. and Burau, R.G. 1989. Estimation of adsorbed selenium(IV) in soils, western San Joaquin Valley, California. In *Agronomy Abstracts*. ASA, Madison, WI, p. 200.

Fujii, R., Hatfield, D.B., and Deverel, S.J. 1988. Distribution of selenium in soils of agricultural fields, western San Joaquin Valley, California. *Soil Sci. Soc. Am. J.* 52: 1274–1283.

Grigg, J.L. 1953. Determination of the available molybdenum of soils. *N. Z. J. Sci. Tech. Sect.* A-34: 405–414.

Gupta, S.K. and Stewart, J.W.B. 1978. An automated procedure for determination of boron in soils, plants and irrigation waters. *Schweizerische Landwirtschaftliche Forschung* 17: 51–55.

Gupta, U.C. 1993. Boron, molybdenum, and selenium. In M.R. Carter, Ed. *Soil Sampling and Methods of Analysis*. CRC Press, Boca Raton, FL, pp. 91–99.

Gupta, U.C. and MacKay, D.C. 1965a. Extraction of water-soluble copper and molybdenum from podzol soils. *Soil Sci. Soc. Am. Proc.* 29: 323.

Gupta, U.C. and MacKay, D.C. 1965b. Determination of Mo in plant materials. *Soil Sci.* 99: 414–415.

Gupta, U.C. and MacKay, D.C. 1966. Procedure for the determination of exchangeable copper and molybdenum in podzol soils. *Soil Sci.* 101: 93–97.

Hatcher, J.T. and Wilcox, L.V. 1950. Colorimetric determination of boron using carmine. *Anal. Chem.* 22: 567–569.

Huang, P.M. and Fujii, R. 1996. Selenium and arsenic. In D.L. Sparks et al., Eds. *Methods of Soil Analysis, Part 3—Chemical Methods*. Soil Science Society of America Book Series Number 5. American Society of Agronomy, Madison, WI, pp. 793–831.

Jarrell, W.M., Page, A.L., and Elseewi, A.A. 1980. Molybdenum in the environment. *Residue Rev.* 74: 1–43.

Johnson, C.M. and Ulrich, A. 1959. Analytical methods for use in plant analysis. *Bulletin of the Californian Agricultural Experimental Station No. 766*, Berkeley, CA.

Jump, R.K. and Sabey, B.R. 1989. Soil test extractants for predicting selenium in plants. In L.W. Jacobs, Ed. *Selenium in Agriculture and the Environment*. SSSA Special Publication 23, American Society of Agronomy, Inc., Soil Science Society America, Inc., Madison, WI, pp. 95–105.

Karamanos, R.E., Goh, T.B., and Stonehouse, T.A. 2003. Canola response to boron in Canadian prairie soils. *Can. J. Plant Sci.* 83: 249–259.

Keren, R. 1996. Boron. In D.L. Sparks et al., Eds. *Methods of Soil Analysis, Part 3—Chemical Methods*. Soil Science Society of America Book Series Number 5. American Society of Agronomy, Madison, WI, pp. 603–626.

Lindsay, W.L. 1979. *Chemical Equilibria in Soils*. John Wiley & Sons, New York, NY, 449 pp.

Lindsay, W.L. and Norvell, W.A. 1978. Development of a DTPA soil test for zinc, iron, manganese, and copper. *Soil Sci. Soc. Am. J.* 42: 421–428.

Lipton, D.S. 1991. Association of selenium in inorganic and organic constituents of soils from a semi-arid region. PhD dissertation University of California, Berkeley, CA.

Liu, D., Clark, J.D., Crutchfield, J.D., and Sims, J.L. 1996. Effect of pH of ammonium oxalate extracting solutions on prediction of plant available molybdenum in soil. *Commun. Soil Sci. Plant Anal.* 27: 2511–2541.

Matsi, T., Antoniadis, V., and Barbayiannis, N. 2000. Evaluation of the NH_4HCO_3–DTPA soil test for assessing boron availability to wheat. *Commun. Soil Sci. Plant Anal.* 31: 669–678.

McBride, M.B. and Hale, B. 2004. Molybdenum extractability in soils and uptake by alfalfa 20 years after sewage sludge application. *Soil Sci.* 169: 505–514.

McBride, M.B., Nibarger, E.A., Richards, B.K., and Steenhuis, T. 2003. Trace metal accumulation by red clover grown on sewage sludge-amended soils and correlation to Mehlich 3 and calcium chloride-extractable metals. *Soil Sci.* 168: 29–38.

McNeal, J.M. and Balistrieri, L.S. 1989. Geochemistry and occurrence of selenium: an overview. In L.W. Jacobs, Ed. *Selenium in Agriculture and the Environment*. SSSA Special Publication 23, American Society of Agronomy, Inc. Soil Science Society America, Inc, Madison, WI, pp. 1–13.

Mikkelsen, R.L., Bingham, F.T., and Page, A.L. 1989. Factors affecting selenium accumulation by agricultural crops. In L.W. Jacobs, Ed. *Selenium in Agriculture and the Environment*. SSSA Special Publication 23: ASA and SSSA, Madison, WI, pp. 65–94.

Mortvedt, J.J. and Anderson, O.E. 1982. Forage legumes: diagnosis and correction of molybdenum and manganese problems. *Southern Cooperative Series Bulletin* 278. Georgia Agricultural Experiment Station, Athens, GA.

National Academy of Sciences, National Research Council (NAS-NRC). 1971. *Selenium in Nutrition*. NAS-NRC, Washington, DC.

Neal, R.H., Sposito, G., Holtclaw, K.W., and Traina, S.J. 1987. Selenite adsorption on alluvial soils: I. Soil composition and pH effects. *Soil Sci. Soc. Am. J.* 51: 1161–1165.

Odom, J.W. 1980. Kinetics of the hot-water soluble boron soil test. *Commun. Soil Sci. Plant Anal.* 11: 759–765.

Offiah, O. and Axley, J.H. 1988. Improvement of boron soil test. *Commun. Soil Sci. Plant Anal.* 19: 1527–1542.

Oyinlola, E.Y. and Chude, V.O. 2002. Test methods for available soil boron in some selected soils of northern Nigeria. *Nigerian J. Soil Res.* 3: 78–84.

Parker, D.R. and Gardner, E.H. 1981. The determination of hot-water-soluble boron in some acid Oregon soils using a modified azomethine-H procedure. *Commun. Soil Sci. Plant Anal.* 12: 1311–1322.

Pierzynski, G.M. and Jacobs, L.W. 1986. Molybdenum accumulation by corn and soybeans from a molybdenum rich sewage sludge. *J. Environ. Qual.* 15: 394–398.

Ponnamperuma, F.N., Cayton, M.T., and Lantin, R.S. 1981. Dilute hydrochloric acid as an extractant for available zinc, copper, and boron in rice soils. *Plant Soil* 61: 297–310.

Raza, M., Mermut, A.R., Schoenau, J.J., and Malhi, S.S. 2002. Boron fractionation in some Saskatchewan soils. *Can. J. Soil Sci.* 82: 173–179.

Ritchie, G.S.P. 1988. A preliminary evaluation of resin extractable molybdenum as a soil test. *Commun. Soil Sci. Plant Anal.* 19: 507–516.

Sarkar, D. and O'Connor, G.A. 2001. Estimating available molybdenum in biosolids-amended soil using Fe-oxide impregnated filter paper. *Commun. Soil Sci. Anal.* 32: 2033–2048.

Sharma, P.C. and Chatterjee, C. 1997. Molybdenum mobility in alkaline soils. In U.C. Gupta, Ed. *Molybdenum in Agriculture*. Cambridge University Press, New York, NY, pp. 131–149.

Sherrell, C.G. 1983. Boron deficiency and response in white and red clovers and lucerne. *N. Z. J. Agric. Res.* 26: 197–203.

Silva, F.R. and Ferreyra H.F.F. 1998. Evaluation of boron extractors in soils of Ceará State [Brazil]. *Revista Brasileira De Ciência Do Solo* 22: 471–478.

Soltanpour, P.N., Johnson, G.W., Workman, S.M., Jones, J.B. Jr., and Miller, R.O. 1996. Inductively coupled plasma emission spectrometry and inductively coupled plasma-mass spectrometry. In D.L. Sparks et al., Eds. *Methods of Soil Analysis, Part 3—Chemical Methods*. Soil Science Society of America Book Series Number 5. American Society of Agronomy, Madison, WI, pp. 91–140.

Soltanpour, P.N., Olsen, S.R., and Goos, R.J. 1982. Effect of nitrogen fertilization on dryland wheat on grain selenium concentration. *Soil Sci. Soc. Am. J.* 46: 430–433.

Soltanpour, P.N. and Schwab, A.P. 1977. A new soil test for simultaneous extraction of macro- and micro-nutrients in alkaline soils. *Commun. Soil Sci. Plant Anal.* 8: 195–207.

Soltanpour, P.N. and Workman, S.M. 1980. Use of the NH_4HCO_3–DTPA soil test to assess availability and toxicity of selenium to alfalfa plants. *Commun. Soil Sci. Plant Anal.* 11: 1147–1156.

Touchton, J.T., Boswell, F.C., and Marchant, W.H. 1980. Boron for soybeans grown in Georgia. *Commun. Soil Sci. Plant Anal.* 11: 369–378.

U.S. Salinity Laboratory Staff. 1954. Diagnosis and improvement of saline and alkali soils. *USDA Handbook No.* 60. U.S. Government Printing Office, Washington, DC.

Varo, P., Alfthan, G., Ekholm, P., Aro, A., and Koivistoinen, P. 1988. Selenium intake and serum selenium in Finland: effects of soil fertilization with selenium. *Am. J. Clin. Nutr.* 48: 324–329.

Vaughan, P.J. and Suarez, D.L. 2003. Constant capacitance model prediction of boron speciation for varying soil water content. *Vadose Zone J.* 2: 253–258.

Vlek, P.L.G. and Lindsay, W.L. 1977. Molybdenum contamination in Colorado pasture soils. In W.R. Chappell and K.K. Peterson, Eds. *Molybdenum in the Environment*, Vol. 2. Marcel Dekker, New York, NY, pp. 619–650.

Wang, L., Reddy, K.J., and Munn, L.C. 1994. Comparison of ammonium bicarbonate–DTPA, ammonium carbonate, and ammonium oxalate to assess the availability of molybdenum in mine spoils and soils. *Commun. Soil Sci. Plant Anal.* 25: 523–536.

Welch, R.S., Allaway, W.H., House, W.A., and Kubota, J. 1991. Geographic distribution of trace element problems. In J.J. Mortvedt, C.R. Cox, L.M. Shuman, and R.M. Welch, Eds. *Micronutrients in Agriculture*. SSSA Book Series 4, Soil Science Society America, Inc., Madison, WI, pp. 31–57.

Wolf, B. 1971. The determination of boron in soil extracts, plant materials, composts, manures, water, and nutrient solutions. *Soil Sci. Plant Anal.* 2: 363–374.

Workman, S.M. and Soltanpour, P.N. 1980. Importance of prereducing selenium(VI) to selenium(IV) and decomposing organic matter in soil extracts prior to determination of selenium using hydride generation. *Soil Sci. Soc. Am. J.* 44: 1331–1332.

Chapter 10
Trace Element Assessment

W.H. Hendershot, H. Lalande, and D. Reyes

McGill University

Sainte Anne de Bellevue, Quebec, Canada

J.D. MacDonald

Agriculture and Agri-Food Canada

Quebec, Quebec, Canada

10.1 INTRODUCTION

The current literature contains a wide range of extractants that have been used to evaluate different fractions of metals and metalloids in soils (Tessier et al. 1979; Ross 1994; Ure 1996; Mihaljevic et al. 2003). These techniques fall into two categories: single or sequential extractions. Although sequential extractions have gained considerable popularity, they do have several drawbacks (Beckett 1989; Lo and Yang 1998; Shiowatana et al. 2001). From an analytical point of view, sequential extractions may result in inconsistent results due to reprecipitation of the elements of interest from one extractant to the next and errors caused by adding the different fractions can lead to values that do not agree with analyses of total metals. Perhaps the most important criticism of sequential extractions is that they are not really specific for the intended fraction; examples of extractions that do not remove specific and identifiable chemical forms are abundant in the literature (Beckett 1989; Mihaljevic et al. 2003).

The approach taken here is to select a series of single extractants that range from weak to very strong. Each of the extractants proposed in this chapter selectively dissolves some portion of the total element pool in the soil but no attempt is made to relate this to a specific type of surface or material. For our purposes it is not really important where the trace elements are held on the soil; it is more important that the analysis provides a means of predicting or explaining the interactions of the elements with biota or mobility in the soil system. In some cases, there is extensive literature that can help to relate the results to bioavailability of the elements to specific organisms.

Some of the metals such as Cd, Cu, Ni, Pb, and Zn have received considerable attention over the last 10 years. For these metals there are numerous references that relate the amounts of metals extracted by different chemicals to a biological effect (toxicity or uptake). However, other metals and metalloids are also significant contaminants in soils affected by

anthropogenic activity, but these metals have received much less attention (As, Co, Cr, Mo, Sb, Se, Tl, etc.). In these cases the number of references relating selective chemical extraction results to biological effects is much less abundant but has been growing in recent years (De Gregori et al. 2004). Although in some cases the methods proposed below have not been tested for a wide range of metals and metalloids, by providing a series of standard tests we hope that more studies will be conducted so that a database of response data can be developed. Since the elements forming oxyanions, such as As, Cr, Mo, and Se, behave quite differently in soils compared to the cationic metals, some authors prefer to use extraction procedures developed for phosphate (Van Herreweghe et al. 2003). However, many of the techniques used for the extraction of the metalloid As, for example, were originally developed for cationic metals but yield good results nonetheless (Hall et al. 1996; Mihaljevic et al. 2003).

Four extraction procedures are proposed here and are presented in the order of increasing strength:

1 A column leaching method using water and 80 μM $CaCl_2/CaSO_4$ solution

2 A weak salt solution using 0.01 M $CaCl_2$

3 A strong chelating agent (0.05 M NH_4-ethylenediaminetetraacetic acid [EDTA] partially neutralized with NH_4^+)

4 A strong acid microwave digestion procedure using HNO_3 (USEPA method 3051)

Recent work in our laboratory has led to the development of a column leaching technique that provides a very good simulation of the solubility of trace elements, pH, and ionic strength of solutions collected in the field from forest soils in Ontario and Quebec, Canada (MacDonald et al. 2004a,b). This method consists of an initial washing of the soil with deionized water, followed by an equilibration with very dilute (80 μM) $CaCl_2$ and $CaSO_4$ solution to simulate the ionic strength observed in forest soils. It has been chosen because it provides the extraction procedure best suited to estimate metal mobility under field conditions.

The $CaCl_2$ method is gaining support in Europe and North America as one of the best ways of evaluating bioavailability chemically (Houba et al. 1996; Ure 1996; Peijnenburg et al. 1999; McBride et al. 2003; Walker et al. 2003; Bongers et al. 2004). The method has the advantage of being simple to use in the laboratory and the results between laboratories are less variable than with some other methods (Quevauviller 1998). This is the same solution as is used to measure soil pH in many laboratories. A similar solution but with a slightly higher concentration is also recommended in Chapter 11 for use in estimating bioavailable Al and Mn. Gray et al. (2003) compared several extraction procedures to the ''labile pool'' as measured by isotope dilution; they found that $CaCl_2$ provided the closest comparison to this pool.

It is well known that metal and metalloids added to soils may become strongly bound to the soil particle surfaces (Ross 1994). Whether this is due to specific adsorption or precipitation, the elements that become fixed are mostly found on sites that are in contact with the soil solution. A strong chelating agent should be able to remove trace elements from a wide range of surface adsorption/precipitation sites. Although all of this ''fixed'' metal would not be immediately available, there are studies that show a good correlation between

EDTA-extractable metal and content in biological tissue (Ure 1996; De Gregori et al. 2004). The extraction with 0.05 *M* EDTA is a good choice for estimating this ''potentially available'' fraction (Quevauviller 1998).

The choice of digestion methods is wide and the USEPA alone recommends four different acid mixtures or procedures (Ming and Ma 1998). Total metal content is only obtained when HF is included in the digestion procedure; otherwise silicate minerals are not dissolved. Most laboratories prefer to use a method that does not include HF due to the danger of working with it; HF causes severe burns to skin or eyes. Trace elements found in the silicates are certainly not immediately available and there is a good chance that these trace elements are related to minerals found in the parent material rather than added by anthropogenic activity. For general laboratory purposes the HNO_3 procedure proposed here should provide a very good estimate of trace elements in contaminated soils. Although there are several alternate methods using HNO_3/HCl available (USEPA 1994), an acid mixture without HCl is preferred for inductively coupled plasma-mass spectrometry (ICP-MS) analysis. A preliminary study prepared by Canada's National Water Research Institute shows very good results with this USEPA 3051 method (Alkema and Blum 2001). It is preferred as an appropriate method for numerous elements.

10.2 COLUMN LEACHING WITH ARTIFICIAL SOIL SOLUTION (MACDONALD ET AL. 2004a,b)

Soil samples collected in the field and brought back to the laboratory for extraction yield solutions with significantly higher concentrations than solutions collected by lysimeters in the field from the same soil horizon. To obtain soil solutions that are comparable to those sampled with lysimeters it is necessary to first remove the relatively soluble material that accumulates in a sample following disturbance; this is particularly important here as we are using air-dried soil samples.

The removal of soluble material is done by ''washing'' the column with deionized water until the ionic strength drops to values similar to those found in the field. The column is then equilibrated with an artificial soil solution containing Ca, Cl, and SO_4, the ions most common in the soil solutions we have sampled in eastern Canada.

Initially researchers should monitor changes in pH and electrical conductivity during the washing and equilibrium phases so that they can see whether the concentrations are tending toward relatively constant values. The procedure described below appears to be suitable for a wide range of soils we have tested, but may not work with all soils.

The suction needed to pull the solution through the soil columns can be generated using two very different types of apparatus. The method described below uses a commercially available column extraction apparatus, although it is necessary to replace the original syringes that have a black rubber seal with ones that have an all polyethylene plunger; the leaching can also be done using a multichannel peristaltic pump but it is more difficult to achieve uniform flow rates.

10.2.1 Materials and Reagents

1 80 mL of 80 μM $CaCl_2$–$CaSO_4$ for each column for the four leaching days. This is prepared by dissolving 0.0118 g of $CaCl_2 \cdot 2H_2O$ plus 0.0109 g of $CaSO_4$ in 2 L of ultrapure water.

2 Polyethylene syringes (60 mL) (HNO_3 washed) and high-density polyethylene (HDPE) frits that fit the syringes tightly.

3 Vacuum extractor capable of flow rates of 30 mL h^{-1} and 2–3 mL h^{-1}.

4 10% nitric acid (HNO_3)—trace metal grade: dilute 10 mL of concentrated acid to 100 mL in a volumetric flask.

5 Ultrapure water—usually produced by passing deionized or reverse osmosis water through a special system to produce water with an electrical conductivity less than 18 μS cm^{-1}.

6 0.45 μm membrane filters (nylon or polycarbonate).

10.2.2 Procedure

Pretreatment

1 Extractions should be carried out in an incubator at a temperature between 4°C and 6°C. The apparatus for each soil sample consists of three 60 mL syringes that are connected together vertically; only the syringe barrels are used for the upper two. The upper syringe is used as the reservoir for the solution and is connected to the middle syringe, holding the soil, with a tight-fitting stopper. The lowest syringe is slowly withdrawn by the vacuum extraction device and the solution is sucked out of the upper syringe, through the soil sample and into the bottom syringe. Make sure that there are no leaks in the system or the flow rate will be compromised.

2 Air dry, homogenize, and sieve the soils to 2 mm. Weigh and pack 15 g of mineral soil (5 g of forest floor) into a 60 mL syringe. Encase the soil between two HDPE frits. Insert the upper syringe into the column to hold the solution.

3 Add 30 mL aliquots of ultrapure water. Apply suction at a rate of 30 mL h^{-1}. After all the water has passed through the column wait 2 h before starting the next leaching. Repeat twice more for a total of 90 mL.

4 At the end of step 3, wait 2 h before starting the treatment with $CaCl_2$–$CaSO_4$.

Treatment

1 Leach the columns with 20 mL of 80 μ*M* of $CaCl_2$–$CaSO_4$ at a rate of 2 to 3 mL h^{-1} every 24 h during 4 days. Make sure that air enters the column at the end of each leaching cycle to prevent the columns from becoming anaerobic. Collect the leachates in separate acid-washed bottles.

2 Measure the pH and EC of each of the leachates. Keep the leachates from the last 3 days and mix them together to obtain one sample of about 50 mL. Filter solutions through 0.45 μm membrane filters under vacuum, and collect solutions in polyethylene bottles. Preserve the solution or a subsample of the solution (if part of the solution is being kept for other analyses) after filtration by adding 0.2 mL of 10% HNO_3 per 10 mL of solution, and analyze as soon as possible.

10.2.3 Calculations

The extraction method is not intended as a quantitative analysis of, for example, the water-soluble fraction; however it is appropriate for estimating solid-solution trace element partitioning or to estimate the concentration of trace metals in water leaching from a site.

Partitioning coefficients (K_d) are calculated as the ratio of total metals (determined through hot acid extraction, see Section 10.5) in mg kg^{-1} over metals in solution as mg L^{-1} and have the unit L kg^{-1}:

$$K_d = \frac{\text{Total metal}}{\text{Dissolved metal}} \tag{10.1}$$

10.2.4 Comments

1 Care must be taken to assure that all plasticware in contact with final solutions has been soaked 24 h in 15% HNO_3 and rinsed thoroughly with high-quality deionized water. Blanks should be carried through the entire extraction procedure to assure that solutions are not contaminated by outside sources.

2 Column methods are prone to variability. Great care must be taken to pack columns consistently. We propose adding soil in three steps and compacting the column with 10 light taps of a syringe plunger with the seal removed at each step.

3 Work in duplicate, and include blanks and quality control samples in each batch.

4 This is a fairly time-consuming procedure that takes 5 days to complete. On the first day (usually Monday), the three washing solutions are passed through the columns and collected—3 h each washing (1 h to draw the solution through and 2 h of equilibration); this makes for a 10 h day. The first $CaCl_2$–SO_4 solution is added to the columns when we leave in the evening of the first day, drawn through the columns during the night, and then collected the next morning. This leaching with the $CaCl_2$–SO_4 solution is repeated on the evenings of days 2–4.

10.3 EXTRACTION WITH 0.01 *M* $CaCl_2$ (QUEVAUVILLER 1998)

10.3.1 Materials and Reagents

1 Centrifuge and 50 mL Boston-type polyethylene centrifuge tubes (HNO_3 acid washed).

2 End-over-end shaker (15 rpm).

3 Calcium chloride, 0.01 *M*; in a 1 L polyethylene volumetric flask, dissolve 1.47 g of $CaCl_2 \cdot 2H_2O$ in ultrapure water and make to volume.

4 10% nitric acid (HNO_3)—trace metal grade: dilute 10 mL of concentrated acid to 100 mL in a volumetric flask.

5 0.45 μm membrane filters (nylon or polycarbonate).

10.3.2 Procedure

1 Work at room temperature. Before taking a subsample, make sure your sample is very well homogenized by mixing the sample thoroughly for about a minute. Work in triplicates. Take a subsample of each soil to estimate moisture content. Include two blank solutions (tube and solution without soil) and two quality control samples in each batch of extractions.

2 Weigh about 2.500 g of soil into a 50 mL centrifuge tube and record weight. Add 25 mL of 0.01 *M* $CaCl_2$ to each tube, cap and shake on the end-over-end shaker for 3 h at 15 rpm.

3 Take a subsample to measure pH and discard (one per triplicate). Centrifuge at 5000 *g* for 10 min. Filter, with great care to avoid contamination, through 0.45 μm membrane under low vacuum. Keep the filtrate in a 30 mL polyethylene bottle. Preserve the solution or a subsample of the solution (if part of the solution is being kept for other analyses) after filtration by adding 0.2 mL of 10% HNO_3 per 10 mL of solution, and analyze as soon as possible. If dilutions are required, the amount of HNO_3 should be kept constant.

10.3.3 Calculations

$$\mathrm{M}\ (\mu\mathrm{g\ g^{-1}}) = \mathrm{C}\ (\mu\mathrm{g\ L^{-1}}) \times 0.025\ \mathrm{L}/(\text{wt. soil g} \times (1 - \mathrm{mc})) \qquad (10.2)$$

where M is the metal content, C is the concentration measured, and mc is the moisture content expressed as a 2-decimal fraction (i.e., 5% = 0.05).

10.3.4 Comments

1 Great care must be taken to avoid contamination. Polyethylene should be used to avoid sorption/desorption of metals to or from the walls of the containers. Centrifuge bottles, sample bottles, filtration units must be clean and acid washed followed by an acid soaking in 15% HNO_3 for 24 h and thoroughly rinsed with double-deionized water with a final rinse with ultrapure (or equivalent) water.

2 The version given here is an adaptation from Quevauviller's method; it is a compromise using smaller sample size for routine analysis. The reader is invited to read the original reference cited.

3 Reproducibility is difficult to achieve in this kind of extraction; care should be given to each step of the procedure.

4 As part of the quality control procedure, the analysis of one sample should be repeated in each batch of extractions to evaluate the reproducibly of the whole experiment. When the value of the quality control sample falls outside 2 standard deviations, calculated for all measurements of that sample, the whole batch should be reanalyzed.

10.4 EXTRACTION OF TRACE ELEMENTS WITH 0.05 *M* EDTA

10.4.1 Materials and Reagents

1 Centrifuge and 50 mL Boston-type polyethylene centrifuge tubes (in addition to the acid-washing procedures described in the comments, the labware must be rinsed with EDTA followed by a thorough water rinse before use in this experiment).

2 End-over-end shaker (15 rpm).

3 NH_4-EDTA salt solution 0.05 *M*: EDTA in its ammonium salt form is difficult to obtain in a pure form. The following method offers a means of cleaning common reagent-grade chemicals.

4 Ultrapure water.

5 0.45 μm membrane filters (nylon or polycarbonate).

To purify H_4EDTA

1 Weigh about 100 g H_4EDTA acid and put in a Teflon beaker.

2 Add about 150 mL of 2% HNO_3 trace metal grade.

3 Stir 10 min on magnetic stirrer.

4 Let settle and decant and discard the supernatant.

5 Repeat at least three times with the addition of about 150 mL HNO_3, stir, settle, decant.

6 Rinse with ultrapure water (or equivalent) using the same procedure as above (i.e., add about 150 mL water, stir, settle, decant) at least three times.

7 Dry the prepared chemical in a warm oven (~40°C) overnight (you might have to crush the H_4EDTA before storing).

To prepare pure NH_4OH

Trace metal-grade ammonia can be purchased, but it can also be prepared in the laboratory using reagent-grade ammonia; you need very clean labware and an efficient fumehood.

Under the fumehood, in a very clean desiccator, place a beaker with about 100 mL of concentrated ACS reagent-grade NH_4OH and another Teflon beaker with 100 mL ultrapure water. Replace cover and let stand overnight. The next morning you will have pure 1:1 diluted ammonia in your Teflon beaker.

To prepare purified ammonium EDTA salt

In a 2 L volumetric flask containing about 1.8 L ultrapure water, add 29.2 g purified H_4EDTA. Place on a magnetic stirrer under a fumehood and add about 25 mL of purified 1:1 ammonia prepared as described above. Stir. Continue adding NH_4OH gradually until the H_4EDTA completely dissolves (around pH 6). Adjust to pH 7.0 ($\pm$0.1) and make to volume with ultrapure water. Store in a well stoppered 2 L polyethylene bottle.

10.4.2 Procedure

1 Work at room temperature. Before taking a subsample of soil, make sure your sample is very well homogenized by mixing thoroughly for about a minute. Work in triplicates. Take a subsample of each soil to estimate moisture content. Include two blank solutions (tube and solution without soil) within each batch of extraction. Weigh about 1.000 g of soil in a 50 mL centrifuge tubes and record weight.

2 Add 25 mL of purified 0.05 *M* NH_4-EDTA to each tube, cap and shake on the end-over-end shaker for 1 h at 15 rpm.

3 Centrifuge at 5000 *g* for 10 min, if possible, maintain the temperature of the centrifuge at 20°C, filter through a 0.45 μm membrane, and keep in well-sealed polyethylene bottle at 4°C. Dilute with ultrapure water for analysis. Make sure the standards used for calibration are in the same matrix as the diluted solution.

10.4.3 Calculations

$$\mathrm{M}\ (\mu\mathrm{g\ g^{-1}}) = \mathrm{C}\ (\mu\mathrm{g\ L^{-1}}) \times 0.025\ \mathrm{L}/(\mathrm{wt.\ soil\ g} \times (1 - \mathrm{mc})) \qquad (10.3)$$

where M is the metal content, C is the concentration measured, and mc is the moisture content expressed as a 2-decimal fraction (i.e., 5% = 0.05).

10.4.4 Comments

1 EDTA is a powerful extractant that is capable of extracting significant quantities of trace elements from high affinity sites on the soil surface. Likewise EDTA will extract all elements from the surfaces of plastic and glassware if in contact with the solution. Consequently it is very important to preclean labware with purified 0.5 *M* H_2EDTA followed by a complete water rinse to avoid contamination of the samples.

2 It is also important to use the same matrix for samples and standards. Do not try to acidify the solution before, or while measuring the content of metals as this could cause precipitation of the EDTA.

10.5 HOT ACID-EXTRACTABLE TRACE ELEMENTS (USEPA 1994)

10.5.1 Materials and Reagents

1 Specialized microwave digestion system with Teflon liners

2 Nitric acid (HNO_3)—trace metal grade

3 100 mL polyethylene volumetric flasks

4 Ultrapure water

10.5.2 Procedure

1 Follow the safety directions from the microwave system manufacturers. Work under a fumehood and wear protective clothing and equipment.

2 Weigh up to 0.500 g of soil sample. If sample contains high content of organics or carbonates, decrease the amount weighed. Organic soils and forest floor horizons should be 0.200 g of sample.

3 Add 10 mL HNO_3. If a strong reaction is observed, allow the samples to stand for several hours (or over night) before sealing the containers to decrease the possibility the containers will vent during heating. Close containers and place in the microwave system. Follow the manufacturer's recommendations for a heating program and maintain a temperature of 185°C for at least 10 min.

4 After completion of the digestion, let cool and transfer the whole sample to a 100 mL volumetric flask (final acidity 10% HNO_3). Let settle overnight and decant supernatant into a 30 mL polyethylene bottle.

5 Dilute five times with ultrapure water for analysis on an ICP-MS (final acidity 2%). Standards should be prepared in the same matrix.

10.5.3 Calculations

$$\text{M } (\mu\text{g g}^{-1}) = \text{C } (\mu\text{g L}^{-1}) \times \text{DF} \times 0.100 \text{ L}/(\text{wt. soil g} \times (1 - \text{mc})) \quad (10.4)$$

where M is the metal content, C is the concentration measured, mc is the moisture content expressed as a 2-decimal fraction (i.e., 5% = 0.05), and DF is the dilution factor.

10.5.4 Comments

Refer to the manufacturer's instructions on the proper use of the microwave digestion system. Due to the high pressures that are developed in the reaction vessels, it is important to use a microwave digestion system designed specifically for this purpose. In addition to the danger of having a vessel explode while being heated, it is also very important to properly cool the vessels before trying to open them. Letting them sit for 30 min in an ice bath is recommended.

REFERENCES

Alkema, H. and Blum, J. 2001. *Ecosystem Performance Evaluation QA Program: Trace Elements in Sediments—Study 01*. National Water Research Institute, National Laboratory for Environmental Testing (NLET-TN01-009), Environment Canada, ON, Canada, 62 pp.

Beckett, P.T.H. 1989. The use of extractants in studies on trace metals in soils, sewage sludges and sludge-treated soils. *Adv. Soil Sci*. 9: 144–176.

Bongers, M., Rusch, B., and Van Gestel, C.A.M. 2004. The effect of counterion and percolation on the toxicity of lead for the springtail *Folsomia candida* in soil. *Environ. Toxicol. Chem*. 23: 195–199.

De Gregori, I., Fuentes, E., Olivares, D., and Pinochet, H. 2004. Extractable copper, arsenic and antimony by EDTA solution from agricultural Chilean soils and its transfer to alfalfa plants (*Medicago sativa* L.). *J. Environ. Monit*. 6: 38–47.

Gray, C.W., McLaren, R.G., and Shiowatana, J. 2003. The determination of labile cadmium in some biosolids-amended soils by isotope dilution plasma mass spectrometry. *Aust. J. Soil Res*. 41: 589–597.

Hall, G.E.M., Vaive, J.E., Beer, R., and Hoashi, M. 1996. Selective leaches revisited, with emphasis on the amorphous Fe oxyhydroxide phase extraction. *J. Geochem. Explor*. 56: 59–78.

Houba, V.J.G., Lexmond, T.M., Novozamsky, I., and van der Lee, J.J. 1996. State of the art and future developments in soil analysis for bioavailability assessment. *Sci. Total Environ*. 178: 21–28.

Lo, I.M.C. and Yang, X.Y. 1998. Removal and redistribution of metals from contaminated soils by a sequential extraction method. *Waste Manage*. 18: 1–7.

MacDonald, J.D., Bélanger, N., and Hendershot, W.H. 2004a. Column leaching using dry soil reproduces solid-solution partitioning observed in zero-tension lysimeters: 1. Method development. *Soil Sediment Contam*. 13: 361–374.

MacDonald, J.D., Bélanger, N., and Hendershot, W.H. 2004b. Column leaching using dry soil reproduces solid-solution partitioning observed in zero-tension lysimeters: 2. Trace metals. *Soil Sediment Contam*. 13: 375–390.

McBride, M.B., Mibarger, E.A., Richards, B.K., and Steenhuis, T. 2003. Trace metal accumulation by red clover grown on sewage sludge-amended soils and correlation to Mehlich 3 and calcium chloride-extractable metals. *Soil Sci*. 168: 29–39.

Mihaljevic, M., Ponavic, M., Ettler, V., and Sebek, O. 2003. A comparison of sequential extraction techniques for determining arsenic fractionation in synthetic mineral mixtures. *Anal. Bioanal. Chem*. 377: 723–729.

Ming, C. and Ma, L.Q. 1998. Comparison of four USEPA digestion methods for trace metal analysis using certified and Florida soils. *J. Environ. Qual*. 27: 1294–1300.

Peijnenburg, W.J.M., Posthuma, L., Zweers, P.G.P., Baerselman, R., de Groot, A.C., Van Ween, R.P.M., and Jager, T. 1999. Prediction of metal bioavailability in Dutch field soils for the oligochaete *Enchytraeus crypticus*. *Exotoxicol. Environ. Saf*. 43: 170–186.

Quevauviller, P.H. 1998. Operationally defined extraction procedures for soil and sediment analysis. I. Standardization. *Trends Anal. Chem*. 17: 289–298.

Ross, S.M. 1994. *Toxic Metals in Soil–Plant Systems*. John Wiley & Sons, New York, NY, 469 pp.

Shiowatana, J., McLaren, R.G., Chanmekha, N., and Samphao, A. 2001. Fractionation of arsenic in soil by a continuous-flow sequential extraction method. *J. Environ. Qual*. 30: 1940–1949.

Tessier, A., Campbell, P.G.C., and Bisson, M. 1979. Sequential extraction procedure for the speciation of particulate trace metals. *Anal. Chem*. 51: 844–851.

Ure, A.M. 1996. Single extraction schemes for soil analysis and related applications. *Sci. Total Environ*. 178: 3–10.

U.S. Environmental Protection Agency (USEPA). 1994. Method 3051: Microwave assisted acid digestion of sediments, sludges, soils and oils. (http://www.epa.gov/epaoswer/hazwaste/test/pdfs/3051.pdf); Washington, DC. (Last verified March, 2006)

Van Herreweghe, S., Swennen, R., Vandecasteele, C., and Cappuyns, V. 2003. Solid phase speciation of arsenic by sequential extraction in standard reference materials and industrially contaminated soil samples. *Environ. Pollut*. 122: 323–342.

Walker, D.J., Clemente, R., Roig, A., and Bernal, P. 2003. The effect of soil amendments on heavy metal bioavailability in two contaminated Mediterranean soils. *Environ. Pollut*. 122: 303–312.

Chapter 11
Readily Soluble Aluminum and Manganese in Acid Soils

Y.K. Soon
Agriculture and Agri-Food Canada
Beaverlodge, Alberta, Canada

N. Bélanger
University of Saskatchewan
Saskatoon, Saskatchewan, Canada

W.H. Hendershot
McGill University
Sainte Anne de Bellevue, Quebec, Canada

11.1 INTRODUCTION

Approximately 5% of the 3.95 billion ha of acid soils is used for agricultural production while 67% supports forests and woodlands (von Uexküll and Mutert 1995). Plant growth in acid soils is usually limited by low pH and/or Al toxicity. The solubility of Al and Mn in mineral soils increases rapidly when soil pH drops below a value of 5 so that low pH and high soluble Al and Mn concentrations are interrelated. Although the availability of plant nutrients such as P and Ca can be limiting at low soil pH (Foy 1984; Asp and Berggren 1990), Al toxicity is probably the foremost growth-limiting factor in acid soils (Andersson 1988). Root growth, and consequently water and nutrient uptake, are inhibited when dissolved Al attains toxic levels in soil solutions.

Dissolved Al in acid soil solution is typically comprised of monomeric Al ions (e.g., Al^{3+}, $Al(OH)^{2+}$, and $Al(OH)_2^{+}$) as well as organically complexed and polynuclear forms of Al (e.g., $Al_2(OH)_2^{4+}$ and $Al_{13}O_4(OH)_{24}^{7+}$ (Akitt et al. 1972)). Polynuclear and organically complexed Al species are considered to have little, if any, phytotoxicity (Andersson 1988; Wright 1989) although there is some contrary evidence for polymeric Al (Bartlett and Diego 1972; Hunter and Ross 1991). Ideally, the soil solution in the root zone should be analyzed for phytotoxic Al species concentration. For diagnostic purposes, such procedures

would be too time-consuming. Typically, therefore, the soil is extracted with a dilute neutral salt solution that would perturb the ionic equilibrium as little as possible, and for a time period sufficient only to bring into solution readily soluble Al (i.e., not associated with the solid phase). Included in such extracts would be mainly monomeric and polymeric Al and Al complexed by organic ligands of low-molecular weight.

11.1.1 Aluminum and Manganese Toxicity in Agricultural Soils

Aluminum concentration in plant tissues cannot be used to confirm Al toxicity since it does not accumulate in aboveground plant tissues. Although Mn accumulates in plants somewhat in proportion to plant injury in acid soils, its concentration in plant tissues is not a reliable indicator of its toxicity (Foy 1984). Therefore, Al and Mn toxicity diagnostic criteria, especially Al, have been approached through soil analysis. In a meta-analysis of Al toxicity thresholds for crops and forages, Bélanger et al. (1999) found that the total dissolved Al concentrations associated with negative effects in 10% and 50% of the studies were, respectively, 0.003 and 0.02 m*M*. However, different crops and forages, and even varieties within a species, vary in their sensitivity to dissolved Al.

Soil acidity is usually corrected by liming or adding calcium amendments to the soil. The lime requirement (see Chapter 12), i.e., the amount of $CaCO_3$ or its equivalent that has to be applied to the soil to raise its pH to a certain desired value, usually 6.5, can be determined by equilibrating a soil sample with a buffered salt solution and measuring the pH (Shoemaker et al. 1961; McLean et al. 1978). Kamprath (1970) suggested that liming can also be based on soluble Al extracted from acid soils by a neutral unbuffered salt solution, such as 1 *M* KCl, at least for soil groups such as ultisols and oxisols. In Canada, Hoyt and Nyborg (1971a,b, 1972, 1987) showed that crop response on acid soils was closely related to 0.01 *M* and 0.02 *M* $CaCl_2$-soluble Al and Mn. With the exception of alfalfa, yields of the test crops were more closely correlated with dilute $CaCl_2$-extractable Al than soil pH or exchangeable Al (1 *M* KCl-exchangeable) (Webber et al. 1982; Hoyt and Nyborg 1987). There was little response of barley (*Hordeum vulgare* L.), an Al-sensitive crop, to lime when dilute $CaCl_2$-extractable Al approached 1 mg kg^{-1} (Hoyt et al. 1974). Webber et al. (1977) found that the amount of lime required to lower 0.02 *M* $CaCl_2$-extractable Al to 1 mg kg^{-1} was less than the lime requirement to achieve a pH of 6 as determined by the Shoemaker–McLean–Pratt (SMP) procedure (Shoemaker et al. 1961). Research studies in Australia, New Zealand, and the United States also showed that the Al and Mn extracted by dilute $CaCl_2$ solution are suitable diagnostic criteria for Al and Mn toxicities in acid soils (Wright et al. 1988, 1989; Close and Powell 1989; Conyers et al. 1991).

11.1.2 Aluminum and Manganese Toxicity in Forest Soils

Forest decline since the last 20 years in central Europe and eastern North America has been attributed to several environmental stresses such as gaseous pollutant injury and water stress (Hinrichsen 1986). As with crop species, it was also shown that increased Al activity in the soil solution has adverse effects on tree functions and growth (see review by Cronan and Grigal 1995). Forest soils are typically acidic ($pH < 5$) and thus, the solubility of toxic Al and Mn is generally high. Manganese toxicity to trees was not studied as much. However, as for crop species, foliage Mn status appears to be a better indicator of solution Mn levels compared to Al, but its toxicity is difficult to show due to concomitant high availability of

Al (Hoyle 1972; Kazda and Zvacek 1989). In solution cultures, Hoyle (1972) found that foliage levels of 441 mg Mn kg^{-1} (solution Mn 0.091 m*M*) in yellow birch were optimal for growth but levels above 1328 mg Mn kg^{-1} (solution Mn 0.45 m*M*) were detrimental. In air-polluted European forests, Mn concentrations in soil solutions ranged from 0.018 to 0.36 m*M*, depending on the acid load and parent material type (Kazda and Zvacek 1989).

Joslin and Wolfe (1988) found that dissolved inorganic monomeric Al, total Al, Al^{3+} activity as well as $SrCl_2$-extractable soil Al explained respectively 79%, 74%, 61%, and 61% of the variability in root biomass. The $SrCl_2$-extractable Al and inorganic monomeric Al concentrations at which significant reductions in root branching and fine root biomass was first observed were 10 mg kg^{-1} and 0.1 m*M*, respectively (Joslin and Wolfe 1988, 1989). We used the data from Joslin and Wolfe (1988) to assess how $SrCl_2$-extractable Al and inorganic monomeric Al concentrations are related. Excluding one outlier from the Becket site, 71.2% of the variability in inorganic monomeric Al concentrations (y) can be predicted from $SrCl_2$-extractable Al concentrations (x) using the following power function: $y = 4.70^{0.240x}$. A soil with 10 mg kg^{-1} of $SrCl_2$-extractable Al therefore corresponds to a solution inorganic monomeric Al level of about 0.05 m*M*, which is close to the 0.07 m*M* toxicity threshold obtained from a meta-analysis computed by Bélanger (2000). Finally, Joslin and Wolfe (1989) discussed the unique response of trees at the Becket site (i.e., substantial root growth despite the relatively high foliage Al concentrations and $SrCl_2$-extractable soil Al levels) and suggested that most of the Al absorbed by trees was organically bound. It is known that the complexation of metal cations by organics enhances plant uptake (Arp and Ouimet 1986) but this form is nontoxic to trees (Rost-Siebert 1984). Therefore, the $SrCl_2$ method may not always be a reliable indicator of the potential toxicity of Al in soils where organically bound Al dominates.

11.2 EXTRACTION PROCEDURE FOR AGRICULTURAL SOILS

Hoyt and Nyborg (1972) reported that when Al and Mn in acid soils were extracted with 2.5 to 40 m*M* $CaCl_2$ solutions, generally better correlations with the yield response of three crops were obtained if the extractant was 20 m*M* $CaCl_2$. A subsequent study showed that a 5 min shaking was adequate and gave only slightly lower concentrations of Al than a 1 h shaking and twice the Al concentration as 10 m*M* $CaCl_2$ (Hoyt and Webber 1974). According to Webber et al. (1977), liming is likely not needed for Canadian acid soils when extracted Al is 1 mg kg^{-1} or less. Close and Powell (1989) also used this extraction procedure for New Zealand soils.

11.2.1 Materials and Reagents

1. 0.02 *M* $CaCl_2$: Dissolve 5.88 g of reagent-grade $CaCl_2 \cdot 2H_2O$ in about 250 mL of deionized water and dilute to 2 L.
2. 50 mL centrifuge tubes and rubber stoppers.
3. Whatman No. 42 filter paper or equivalent.
4. Centrifuge, with rotors accepting 50 mL centrifuge tubes.
5. Reciprocal shaker.
6. Liquid dispenser.

11.2.2 Procedure

1 Weigh 10 g of soil (<2mm) into centrifuge tube.

2 Dispense 20 mL of the 0.02 *M* $CaCl_2$ reagent into the centrifuge tube and stopper tightly.

3 Shake 5 min on the shaker (120 oscillations min^{-1}).

4 Remove from shaker and centrifuge at 1250 *g* for 1 min to facilitate rapid filtering.

5 Filter through a fluted filter paper into receptacle for storing the extract.

11.2.3 Comments

A 0.01 *M* $CaCl_2$ solution is closer in ionic strength to the soil solution of agricultural soils than is a 0.02 *M* solution and it is also commonly used to assess other soil chemical properties such as pH and soluble P (Soon 1990). Therefore, it may be advantageous to use 0.01 *M* instead of 0.02 *M* $CaCl_2$ solution when those soil properties are also to be determined. However, a critical level of 0.01 *M* $CaCl_2$-soluble Al has not been proposed. The above procedure has not been tested for soils with organic matter content much higher than 10%.

11.3 EXTRACTION PROCEDURE FOR FOREST SOILS

Since increased Ca availability alleviates toxic effects of Al on trees (i.e., Al toxicity is mostly indirect—it is toxic due to its antagonistic effects on divalent cation uptake (Cronan and Grigal 1995)), the $SrCl_2$ method is advantageous relative to the commonly used $CaCl_2$ procedure in agricultural soils as it allows the quantification of extractable Ca and other cations as well as Ca and Mg to Al ratios. Strontium is slightly more efficient at displacing Al than Ca, but the difference is only about 5% at this ionic strength (0.01 *M*). However, no work has been done on the relative amounts of Al and Mn exchanged with $SrCl_2$, $CaCl_2$, and $BaCl_2$. Such a study would help to clarify the need for using different extractants when the amount of potentially toxic elements was under investigation. The $SrCl_2$ method of Joslin and Wolfe (1989) is described here after some modifications based on the suggestions of Heisey (1995).

11.3.1 Materials and Reagents

1 0.01 *M* $SrCl_2$: Dissolve 5.332 g of reagent-grade $SrCl_2 \cdot 6H_2O$ in about 250 mL of distilled/deionized water and make to volume in a 2 L volumetric flask.

2 50 mL centrifuge tubes and screw caps.

3 Ultracentrifuge accepting 50 mL tubes.

4 End-over-end shaker.

5 Pipette and liquid dispenser.

11.3.2 Procedure

1 Weigh 10 g of soil (dried and <2mm) into centrifuge tube.

2 Add 20 mL of 0.01 *M* $SrCl_2$ to the centrifuge tube.

3 Shake for 60 min at 15 oscillations min^{-1}.

4 Remove from shaker and centrifuge for 30 min at 7000 *g*.

5 Pipette off the supernatant and retain in container for analysis.

11.3.3 Comments

An end-over-end shaker is used here because it is more efficient in wetting and mixing forest soils with a high litter/organic matter content and using a low soil:extractant ratio. The low soil:extractant ratio results in a thick suspension that typically requires a high-speed centrifuge to separate.

11.4 DETERMINATION OF ALUMINUM

Aluminum in the extracts can be measured by atomic absorption (Webber 1974), inductively coupled plasma atomic emission spectroscopy (ICP-AES) (Carr et al. 1991), or by colorimetry (Hoyt and Webber 1974; Carr et al. 1991). Atomic absorption or ICP-AES will give results for total dissolved Al whereas colorimetry should yield results for Al ''reactive'' with the chromogen. What will be included as ''reactive'' Al depends on the equilibration time allowed for color development. Shorter reaction times should yield mainly labile (monomeric) Al whereas longer reaction times would include the determination of polymeric and complexed Al. Grigg and Morrison (1982) showed that the pyrocatechol violet (PCV) method was superior to the Aluminon (aurintricarboxylic acid triammonium salt) method in precision, and automating the procedure resulted in further improvement in its precision. The pyrocatechol method was also recommended by Conyers et al. (1991). The method below is an adaptation of Wilson and Sergeant (1963). The procedure is simple and reliable.

11.4.1 Reagents

1 0.1% (w/v) PCV. Keep in a dark glass bottle.

2 0.1% (w/v) *o*-phenanthroline (OP). Store in a polyethylene bottle.

3 10% (w/v) hydroxylamine hydrochloride (HH). Keep in a polyethylene bottle.

4 10% (w/v) ammonium acetate (buffered at pH 6.2 using acetic acid). Store in a polyethylene bottle.

5 Aluminum working standard solution: from a stock standard solution containing 1 g Al L^{-1}, prepare a working standard containing 100 mg Al L^{-1} in $CaCl_2$

solution of the same molarity as the soil extractant. By further dilution, prepare 5 standards over the range of 0.1 to 2.5 mg Al L^{-1} in $CaCl_2$ solution of the same molarity. For forest soils, standards should be prepared in 0.01 *M* $SrCl_2$.

11.4.2 Procedure

1 Pipette 2 mL of extract or standard solution into 16 mm × 125 mm culture tubes. The tubes should be prewashed with 0.1 *M* HCl. Sample solutions should contain no more than 5 μg Al.

2 Add sequentially 0.5 mL each of PCV, OP, and HH, gently swirling the contents of the tube after each addition. In a batch of samples, each reagent should be added to all samples before adding the next reagent.

3 Add 6 mL of the buffer solution, stopper and invert the tube three times and allow to stand for 1 h.

4 Measure absorbance at 580 nm with a spectrophotometer using 1 cm cuvette. Plot the absorbance values against μg Al. The μg Al value read off the calibration curve gives extracted Al level in mg kg^{-1} soil. If dilution of the extract is required, multiply by the dilution factor.

11.4.3 Comments

The extracts should be analyzed with minimum delay. If delays are inevitable, acidify the samples slightly to prevent polymerization of Al monomers. The PCV powder and the prepared solution should be kept in the dark in tightly sealed containers. Interference by iron is diminished by the OP and HH reagents. Color development is maximal and stable between 1 and 2 h, after which the color gradually declines. Reagent blank values are determined using the soil extractant. It is advisable to use freshly prepared PCV solution. The other reagents are stable for at least 4 weeks when stored at room temperature.

The analysis as described should include monomeric and polymeric Al and weakly complexed Al. Kerven et al. (1989) described a PCV procedure with a reaction time of 60 s to measure only monomeric Al. For forest surface soils, which typically have much higher organic matter content than agricultural soils, the difference between measuring total dissolved Al and monomeric inorganic Al should be more critical. Also much calibration of extractable soil Al with crop response has been done using dissolved total Al (Hoyt and Webber 1974; Hoyt and Nyborg 1987). An autoanalyzer PCV method that uses ion-exchange to separate inorganic monomeric Al from organically complexed Al has been described by McAvoy et al. (1992).

11.5 DETERMINATION OF MANGANESE

Manganese in the soil extract is determined by atomic absorption spectrometry using an oxidizing air–acetylene flame. ICP-AES analysis would also be convenient, especially if Al is to be determined.

REFERENCES

Akitt, J.W., Greenwood, N.N., Khandelwal, B.K., and Lester, G.D. 1972. ^{27}Al nuclear magnetic resonance studies of the hydrolysis and polymerization of the hexa-aquo-aluminium (III) cation. *J. Chem. Soc*., Dalton Trans: 604–610.

Andersson, M. 1988. Toxicity and tolerance of aluminium in vascular plants: a literature review. *Water Air Soil Pollut*. 39: 439–462.

Arp, P. and Ouimet, R. 1986. Uptake of Al, Ca, and P in black spruce seedlings: effect of organic versus inorganic Al in nutrient solutions. *Water Air Soil Pollut*. 31: 367–375.

Asp, H. and Berggren, D. 1990. Phosphate and calcium uptake in beech (*Fagus sylvatica* L.) in the presence of aluminium and natural fulvic acids. *Physiol. Plant* 80: 307–314.

Bartlett, R.J. and Diego, D.C. 1972. Toxicity of hydroxy aluminum in relation to pH and phosphorus. *Soil Sci*. 114: 194–200.

Bélanger, N. 2000. Investigating the long-term influence of atmospheric deposition and forest disturbance on soil chemistry and cation nutrient supplies in a forested ecosystem of southern Quebec, PhD thesis, Department of Natural Resource Science, McGill University, Montreal, QC, Canada, 164 pp.

Bélanger, N., Fyles, H., and Hendershot, W.H. 1999. Chemistry, bioaccumulation and toxicity of aluminum in the terrestrial environment—PSL2 assessment of aluminum salts. A report prepared for the Commercial Chemicals Evaluation Branch, Environment Canada, ON, Canada, 78 pp.

Carr, S.J., Ritchie, G.S.P., and Porter, W.M. 1991. A soil test for aluminium toxicity in acidic subsoils of yellow earths in Western Australia. *Aust. J. Agric. Res*. 42: 875–892.

Close, E.A. and Powell, H.K.J. 1989. Rapidly extracted (0.02 M $CaCl_2$) 'reactive' aluminium as a measure of aluminium toxicity in soils. *Aust. J. Soil. Res*. 27: 663–672.

Conyers, M.K., Poile, G.J., and Cullis, B.R. 1991. Lime responses by barley as related to available soil aluminium and manganese. *Aust. J. Agric. Res*. 42: 379–390.

Cronan, C.S. and Grigal, D.F. 1995. Use of calcium–aluminum ratios as indicators of stress in forest ecosystems. *J. Environ. Qual*. 24: 209–226.

Foy, C.D. 1984. Physiological effects of hydrogen, aluminum and manganese toxicities in acid soil. In F. Adams, Ed. *Soil Acidity and Liming*, 2nd edn. ASA-CSSA-SSSA, Madison, WI, pp. 57–97.

Grigg, J.L. and Morrison, J.D. 1982. An automatic colorimetric determination of aluminium in soil extracts using catechol violet. *Commun. Soil Sci. Plant Anal*. 13: 351–361.

Heisey, R.M. 1995. Growth trends and nutritional status of sugar maple stands on the Appalachian plateau of Pennsylvania, USA. *Water Air Soil Pollut*. 82: 675–693.

Hinrichsen, D. 1986. Multiple pollutants and forest decline. *AMBIO* 15: 258–265.

Hoyle, M.C. 1972. Manganese toxicity in Yellow birch (*Betula alleghaniensis* Butten) seedlings. *Plant Soil* 36: 229–232.

Hoyt, P.B. and Nyborg, M. 1971a. Toxic metals in acid soil. I. Estimation of plant-available aluminum. *Soil Sci. Soc. Am. Proc*. 35: 236–240.

Hoyt, P.B. and Nyborg, M. 1971b. Toxic metals in acid soil. II. Estimation of plant-available manganese. *Soil Sci. Soc. Am. Proc*. 35: 241–244.

Hoyt, P.B. and Nyborg, M. 1972. Use of dilute calcium chloride for the extraction of plant-available aluminum and manganese from acid soil. *Can. J. Soil Sci*. 52: 163–167.

Hoyt, P.B. and Nyborg, M. 1987. Field calibration of liming responses of four crops using soil pH, Al and Mn. *Plant Soil* 102: 21–25.

Hoyt, P.B., Nyborg, M., and Penney, D. 1974. *Farming Acid Soils in Alberta and Northeastern British Columbia*, Publication 1521, Agriculture Canada, Ottawa, ON.

Hoyt, P.B. and Webber, M.D. 1974. Rapid measurement of plant-available aluminum and manganese in acid Canadian soils. *Can. J. Soil Sci*. 54: 53–61.

Hunter, D. and Ross, D.S. 1991. Evidence for a phytotoxic hydroxyl-aluminum polymer in organic soil horizons. *Science* 251: 1056–1058.

Joslin, J.D. and Wolfe, M.H. 1988. Responses of red spruce seedlings to changes in soil aluminum in six amended forest soil horizons. *Can. J. Forest Res.* 18: 1614–1623.

Joslin, J.D. and Wolfe, M.H. 1989. Aluminum effects on northern red oak seedling growth in six forest soil horizons. *Soil Sci. Soc. Am. J.* 53: 274–281.

Kamprath, E.J. 1970. Exchangeable aluminum as a criteria for liming leached mineral soils. *Soil Sci. Soc. Am. Proc.* 35: 252–254.

Kazda, M. and Zvacek, L. 1989. Aluminum and manganese and their relation to calcium in soil solution and needles in three Norway spruce (*Picea abies* L. Karst) stands of Upper Austria. *Plant Soil* 114: 257–267.

Kerven, G.L., Edwards, D.G., Asher, C.J., Hallman, P.S., and Kokot, S. 1989. Aluminium determination in soil solution. II. Short-term colorimetric procedures for the measurement of inorganic monomeric aluminium in the presence of organic acid ligands. *Aust. J. Soil Res.* 27: 91–102.

McAvoy, D.C., Santore, R.C., Shosa, J.D., and Driscoll, C.T. 1992. Comparison between pyrocatechol violet and 8-hydroxquinoline procedures for determining aluminum fractions. *Soil Sci. Soc. Am. J.* 56: 449–455.

McLean, E.O., Eckert, D.J., Reddy, G.Y., and Trieweiler, J.F. 1978. An improved SMP soil lime requirement method for incorporating double buffer and quick-test features. *Commun. Soil Sci. Plant Anal.* 8: 667–675.

Rost-Siebert, K. 1984. Aluminum toxicity in seedlings of Norway spruce (*Picea abies* Karst) and beech (*Fagus sylvatica* L.). In F. Andersson and J.M. Kelly, Eds. *Workshop on Aluminum Toxicity to Trees*. Sveriges Lantbruks Universitet, Uppsala, Sweden.

Shoemaker, H.E., McLean, E.O., and Pratt, P.F. 1961. Buffer method for determining lime requirement of soils with appreciable amounts of extractable aluminum. *Soil Sci. Soc. Am. Proc.* 25: 274–277.

Soon, Y.K. 1990. Comparison of parameters of soil phosphate availability for the northwestern Canadian prairie. *Can. J. Soil Sci.* 70: 227–237.

von Uexküll, H.R. and Mutert, E. 1995. Global extent and economic impact of acid soil. In R.A. Date, et al., Eds. *Plant–Soil Interactions at Low pH: Principles and Management*. Proceedings of the Third International Symposium on Plant–Soil Interactions at Low pH, 12–16 September 1993, Brisbane, Australia. Kluwer Academic Publishers, Dordrecht, the Netherlands, pp. 5–19.

Webber, M.D. 1974. Atomic absorption measurements of Al in plant digests and neutral salt extracts of soils. *Can. J. Soil Sci.* 54: 81–87.

Webber, M.D., Hoyt, P.B., and Corneau, D. 1982. Soluble Al, exchangeable Al, base saturation and pH in relation to barley yield on Canadian acid soils. *Can. J. Soil Sci.* 62: 397–405.

Webber, M.D., Hoyt, P.B., Nyborg, M., and Corneau, D. 1977. A comparison of lime requirement methods for acid Canadian soils. *Can. J. Soil Sci.* 57: 361–370.

Wilson, A.H. and Sergeant, G.A. 1963. The colorimetric determination of aluminium in minerals by pyrocatechol violet. *Analyst* 88: 109–112.

Wright, R.J. 1989. Soil aluminum toxicity and plant growth. *Commun. Soil Sci. Plant Anal.* 20: 1479–1497.

Wright, R.J., Baligar, V.C., and Ahlrichs, J.L. 1989. The influence of extractable and soil solution aluminum on root growth of wheat seedlings. *Soil Sci.* 148: 293–302.

Wright, R.J., Baligar, V.C., and Wright, S.F. 1988. Estimation of plant available manganese in acidic subsoil horizons. *Commun. Soil Sci. Plant Anal.* 19: 643–662.

Chapter 12
Lime Requirement

N. Ziadi
Agriculture and Agri-Food Canada
Quebec, Quebec, Canada

T. Sen Tran
Institute of Research and Development in Agroenvironment
Quebec, Quebec, Canada

12.1 INTRODUCTION

The soil pH indicates the amount of acidity present in the soil solution and is one of the most commonly measured soil properties. It is considered as a standard and routine soil analysis. Soil pH affects the solubility and availability of many elements as well as microbial activity (Curtin et al. 1984; Marschner 1995). An acid soil commonly has concentrations of Al or Mn that are high enough to be toxic to some plants. The target soil pH, which represents the soil pH value associated with optimum plant growth, varies with crop species and can be influenced by soil type. In general, a soil pH of 6.0 to 7.0 is ideal for most agronomic crops such as corn (*Zea mays* L.), soybean (*Glycine max* L. Merr.), and wheat (*Triticum aestivum*). However, a lower target pH may be acceptable for other plants such as potato (*Solanum tuberosum* L.) or blueberry (*Vaccinium* spp.). Liming acid soils to maintain an appropriate pH for plants is, therefore, an essential practice for soil and crop management in many areas.

There are two components of soil acidity that are used in determining lime application: active acidity and exchangeable (reserve) acidity. Active acidity is the concentration of H^+ ions in the soil solution phase and indicates whether or not liming is required to reduce soil acidity. The exchangeable acidity refers to the amounts of H^+ ions present on exchange sites of clay and organic matter fractions of the soils and affects the amount of lime needed to achieve the target soil pH. The greater the exchangeable (reserve) acidity, the more the soil is said to be buffered against change in pH and the greater the lime requirement (LR).

Lime requirement is defined as the amount of agricultural limestone ($CaCO_3$), or any other basic material, required to increase soil pH from acidic conditions to a target level that is optimum for the desired use of the soil. The nature of soil acidity, along with soil physical and chemical properties (mainly soil texture and organic matter content), affects the LR. The test used such as soil–lime incubations, soil–base titrations, or soil–buffer equilibrations can also affect the recommendation for lime (Aitken 1990; Conyers et al. 2000; Alatas et al.

2005). Accurate methods to assess the amount of liming materials are essential, and different LR tests should be used in different geographical areas based both on research and practical experience. The selection of one specific technique to determine LR must also be taken into consideration some practical aspects such as the time available to conduct the test, the required equipment and supplies, the cost, etc. Many techniques and methods have been developed and successfully used worldwide to measure LR and are reported in previous studies (McLean 1982; van Lierop 1990). The majority of these methods are based on the following principles (Sims 1996): (i) the measured LR should reflect the amount of liming material needed to reach the target pH when the lime is applied under field conditions; (ii) LR test should accurately measure all forms of acidity (dissociated and undissociated) present in a soil; (iii) LR test should be calibrated in the geographic area where the test will be used; and (iv) LR test should be calibrated to determine conversion factors between limestone and the other liming materials used.

To estimate the amount of lime required to correct soil acidity and attain a desired soil pH, different procedures can be used through field or laboratory studies. Soil–lime incubations, soil–base titrations, and soil–buffer equilibrations (Viscarra Rossel and McBratney 2003; Machacha 2004; Liu et al. 2005) are the most commonly used methods. Estimation of LR based on field studies, however, remains the most accurate means to determine LR for a soil, and especially to evaluate new liming materials. Although these methods are time consuming and expensive, they are the foundation for the more rapid and inexpensive procedures. In routine soil testing laboratories in North America, the Adam–Evans (A–E) buffer (Adams and Evans 1962) and the Shoemaker–McLean–Pratt (SMP) (Shoemaker et al. 1961) procedures are the most commonly used methods. In Canada for example, Nova Scotia and Newfoundland currently use the A–E procedure while New Brunswick, Prince Edward Island, Ontario, British Columbia, and Quebec use the SMP method. Webber et al. (1977) recommend the SMP method for Canadian acid soils. Tran and van Lierop (1982) and van Lierop (1983) also found the method to be suitable for acid mineral and organic soils in Quebec. Recently, Warman et al. (2000) recommended the replacement of the A–E method with the SMP method in Nova Scotia and Newfoundland. For these reasons, only the SMP method is described in this chapter.

12.2 SHOEMAKER–McLEAN–PRATT SINGLE-BUFFER METHOD

12.2.1 Principles

The SMP method was developed in 1961 from a soil–lime ($CaCO_3$) incubation study using 14 acidic soils from Ohio (Shoemaker et al. 1961). The accuracy of this procedure relies on its calibration of decreasing soil–buffer pH values with increasing LR rates. Originally, this procedure was particularly well adapted for determining the LR of soils needing LR >4.5 Mg ha^{-1}, and with pH values <5.8 and organic matter contents <100 g kg^{-1} (McLean 1982). van Lierop (1990) improved the accuracy of the SMP single-buffer method at low LR values and proposed the amount of lime required to attain target values of 5.5, 6.0, 6.5, and 7.0 (Table 12.1). This improvement is obtained by fitting curvilinear instead of linear equations to the relationships between soil–buffer pH and incubation LR values and is based on a number of LR studies (McLean 1982; Soon and Bates 1986; Tran and van Lierop 1993).

TABLE 12.1 Relationships between Soil SMP-Buffer pH and Lime Requirement Values to Achieve pH 5.5, 6.0, 6.5, and 7.0 of Mineral Soils

	Quantity of liming material (Mg ha^{-1}) required to reach desired pH			
Soil–buffer pH	**5.5**	**6.0**	**6.5**	**7.0**
6.9	0.5	0.6	0.7	0.9
6.8	0.6	1.0	1.2	1.5
6.7	0.7	1.4	1.8	2.2
6.6	0.9	1.8	2.5	2.8
6.5	1.2	2.3	3.3	3.6
6.4	1.6	2.9	4.0	4.4
6.3	2.0	3.5	4.9	5.2
6.2	2.5	4.2	5.7	6.0
6.1	3.1	4.9	6.6	7.0
6.0	3.8	5.6	7.5	8.0
5.9	4.5	6.5	8.5	9.0
5.8	5.3	7.3	9.5	10.0
5.7	6.1	8.2	10.5	11.2
5.6	7.0	9.2	11.6	12.4
5.5	8.0	10.2	12.7	13.6
5.4	9.1	11.3	14.0	14.9
5.3	10.2	12.4	15.0	16.2
5.2	11.4	13.6	16.2	17.6
5.1	12.7	14.8	17.5	19.0
5.0	14.0	16.1	18.8	20.4
4.9	15.5	17.4	20.1	22.0

Source: From van Lierop, W., in R.L. Westerman (Ed.), *Soil Testing and Plant Analysis*, 2nd ed., SSSA, Madison, Wisconsin, 1990, 73–126.

Lime requirement in Mg $CaCO_3$ for a furrow layer of 20 cm depth of soil.

12.2.2 Materials and Reagents

1. pH meter
2. Disposable plastic beakers
3. Automatic pipette
4. Glass stirring rods
5. Mechanical shaker
6. Standard buffers, pH 7.0 and 4.0
7. SMP buffer solution
8. 0.1 *M* HCl, 4.0 *M* NaOH, and 4.0 *M* HCl solutions

The SMP buffer solution can be prepared as follows:

a. Weigh and place in a 10 L bottle the following chemicals:
   - 18 g *p*-nitrophenol ($NO_2C_6H_4OH$);
   - 30 g potassium chromate (K_2CrO_4);
   - 531 g calcium chloride dihydrate ($CaCl_2 \cdot 2H_2O$).

b. Add approximately 5 L of distilled water. Shake vigorously as the water is added, and continue shaking for a few minutes to prevent formation of a crust over the salts.

c. Dissolve 20 g of calcium acetate [$(CH_3COO)_2Ca \cdot H_2O$] in a separate flask containing about 1 L of distilled water.

d. Add solution from step (c) to that from step (b) and continue shaking for about 2 or 3 h.

e. Add 100 mL of dilute triethanolamine (TEA) solution: TEA ($N(CH_2OH)_3$) is very viscous and difficult to pipette accurately. It is recommended that a dilute TEA solution be prepared by diluting 250 mL (or 280.15 g) of TEA to 1 L with distilled water and mix well.

f. Shake the mixture periodically until it is completely dissolved. This takes about 6 to 8 h.

g. Dilute to a final volume of 10 L with distilled water.

h. Adjust pH to 7.5 ± 0.02 by titrating with either 4 *M* NaOH or 4 *M* HCl as required.

i. Filter through fiberglass sheet or cotton mat if necessary.

j. Verify buffer capacity of prepared SMP buffer by titrating 20 mL from pH 7.5 to 5.5 with 0.1 *M* HCl. This should take 0.28 ± 0.005 cmol (+) HCl/pH unit.

The 10 L SMP prepared solution can be used for approximately 500 soil samples.

12.2.3 Procedure

1 Measure 10 mL or weigh 10 g air-dried, screened (<2 mm) soil samples in appropriate beakers.

2 Add 10 mL of distilled water and stir with glass rod and repeat stirring periodically during the next 30 min.

3 Measure the soil pH in the beaker (soil + H_2O) and rinse electrodes with a minimum of distilled water.

4 If the soil pH (H_2O) is less than the desired pH, add 20 mL of SMP buffer to the soil–water mixture (soil–water–buffer ratio is 1:1:2 by volume) and stir with glass rod.

5 Place soil–water–buffer samples on a mechanical shaker for 15 min at about 200 oscillations min^{-1}. Remove samples from shaker and let stand for 15 min. The times of shaking and standing are very important and should be respected. Sims (1996) proposed 30 min of shaking and 30 min of standing.

6 Adjust the pH meter to read 7.5 with SMP buffer.

7 Stir sample thoroughly and read the soil–water–buffer to nearest 0.01 pH unit. Record as soil–buffer pH.

8 Select the amount of lime required to bring the soil to the pH you choose to lime the soil, based on soil–buffer pH relationships used in local recommendations (e.g., CRAAQ 2003; OMAFRA 2003).

9 As the SMP buffer solution can affect the accuracy of the glass electrode after approximately 200 buffer–pH determinations, it is strongly recommended to regenerate the electrodes by appropriate procedure. The combined glass electrode can be regenerated by immersing it into a plastic beaker containing a solution of 10% ammonium hydrogen fluoride ($NH_4F \cdot HF$) for 1 min. Since the $NH_4F \cdot HF$ is a hazardous compound, appropriate protection should be respected according to its Material Safety Data Sheet. After etching, dip electrode into 1:1 H_2O–HCl solution to remove silicate. Rinse the electrode thoroughly with distilled water and immerse in hot 3 *M* KCl solution (50°C) for 5 h. The electrolytes in the electrode (saturated KCl or calomel) must be replaced if necessary.

12.3 COMMENTS

For a LR greater than about 7 Mg limestone ha^{-1}, it is recommended to divide the rate into two or more applications to avoid local overliming (Brunelle and Vanasse 2004). This is important as a liming recommendation assumes that the material is homogeneously incorporated into the plow-layer, a precept that is difficult to achieve in practice. When surface applying liming material, without significant incorporation (i.e., without tillage), the rate should be reduced to about a third. Where some tillage is practiced, but not to the typical plow-layer depth used in the calibration of the test, then the liming rate should be reduced proportionately (van Lierop 1989).

REFERENCES

Adams, F. and Evans, C.E. 1962. A rapid method for measuring lime requirement of Red-Yellow Podzolic soils. *Soil Sci. Soc. Am. Proc.* 26: 355–357.

Aitken, R.L. 1990. Relationship between extractable Al, selected soil properties, pH buffer capacity and lime requirement in some acidic Queensland soils. *Aust. J. Soil Res.* 30: 119–130.

Alatas, J., Tasdilas, C.D., and Sgouras, J. 2005. Comparison of two methods of lime requirement determination. *Commun. Soil Sci. Plant Anal.* 36: 183–190.

Brunelle, A. and Vanasse, A. 2004. Le chaulage des sols. Centre de référence en agriculture et agroalimentaire du Québec, Québec, QC, Canada, 41 pp.

Conyers, M.K., Helyar, K.L., and Poile, G.J. 2000. pH buffering: the chemical response of acidic soils to added alkali. *Soil Sci*. 165: 560–566.

CRAAQ. 2003. Guide de référence en fertilisation, 1re édition. Centre de référence en agriculture et agroalimentaire du Québec (CRAAQ). Québec, QC, Canada, 294 pp.

Curtin, D., Rostad, H.P.W., and Huang, P.M. 1984. Soil acidity in relation to soil properties and lime requirement. *Can. J. Soil Sci*. 64: 645–654.

Liu, M., Kissel, D.E., Cabrera, M.L., and Vendrell, P.F. 2005. Soil lime requirement by direct titration with a single addition of calcium hydroxide. *Soil Sci. Soc. Am. J*. 68: 522–530.

Machacha, S. 2004. Comparison of laboratory pH buffer methods for predicting lime requirement (LR) of acidic soils of Eastern Botswana. *Commun. Soil Sci. Plant Anal*. 35: 2675–2687.

Marschner, H. 1995. Nutrient availability in soils. In *Mineral Nutrition of Higher Plants*, 2nd ed. Academic Press, London, UK, pp. 483–505.

McLean, E.O. 1982. Soil pH and lime requirement. In A.L. Page, R.H. Miller, and D.R. Keeney, Eds. *Methods of Soil Analysis*, *Part 2, Agronomy 9*. SSSA, Madison, WI, pp. 199–224.

OMAFRA. 2003. *Agronomy Guide for Field Crops*. Publication 811. Ministry of Agriculture, Food and Rural Affairs, Toronto, ON, Canada, 348 pp.

Shoemaker, H.E., McLean, E.O., and Pratt, P.F. 1961. Buffer methods for determining lime requirement of soils with appreciable amounts of extractable aluminium. *Soil Sci. Soc. Am. Proc*. 25: 274–277.

Sims, J.T. 1996. Lime requirement. In D.L. Sparks et al., Eds. *Methods of Soils Analysis*, *Part 3*. SSSA, Madison, WI, pp. 491–515.

Soon, Y.K. and Bates, T.E. 1986. Determination of the lime requirement for acid soils in Ontario using the SMP buffer methods. *Can. J. Soil Sci*. 66: 373–376.

Tran, T.S. and van Lierop, W. 1982. Lime requirement determination for attaining pH 5.5 and 6.0 of coarse-textured soils using buffer-pH methods. *Soil Sci. Soc. Am. J*. 46: 1008–1014.

Tran, T.S. and van Lierop, W. 1993. Lime requirement. In M.R. Carter, Ed. *Soil Sampling and Methods of Analysis*. Canadian Society of Soil Science, Lewis Publishers, CRC Press, Boca Raton, FL, pp. 109–113.

van Lierop, W. 1983. Lime requirement determination of acid organic soils using buffer-pH methods. *Can. J. Soil Sci*. 63: 411–423.

van Lierop, W. 1989. Effect of assumptions on accuracy of analytical results and liming recommendations when testing a volume or weight of soil. *Commun. Soil Sci. Plant Anal*. 30: 121–137.

van Lierop, W. 1990. Soil pH and lime requirement. In R.L. Westerman, Ed. *Soil Testing and Plant Analysis*, 2nd edn. SSSA, Madison, WI, pp. 73–126.

Viscarra Rossel, R.A. and McBratney, A.B. 2003. Modelling the kinetics of buffer reactions for rapid field predictions of lime requirements. *Geoderma* 114: 49–63.

Warman, P.R., Walsh, I.Y., and Rodd, A.V. 2000. Field testing a lime requirement test for Atlantic Canada, and effect of soil pH on nutrient uptake. *Commun. Soil Sci. Plant Anal*. 31: 2163–2169.

Webber, M.D., Hoyt, P.B., Nyborg, M., and Corneau, D. 1977. A comparison of lime requirement methods for acid Canadian soils. *Can. J. Soil Sci*. 57: 361–370.

Chapter 13
Ion Supply Rates Using Ion-Exchange Resins

P. Qian and J.J. Schoenau

University of Saskatchewan

Saskatoon, Saskatchewan, Canada

N. Ziadi

Agriculture and Agri-Food Canada

Quebec, Quebec, Canada

13.1 INTRODUCTION

Use of ion-exchange resins to measure nutrient availability in soils was reported as early as 1951 (Pratt 1951) and 1955 (Amer et al. 1955). Since then, many journal articles have been published on the use of ion-exchange resins in agricultural and environmental soil research, mostly focusing on measuring nutrient availability in soil. Anion-exchange resin extraction as a method to assess P availability in soil has been described earlier by Olsen and Sommers (1982) and Kuo (1996). The principle of resin membrane extraction is also briefly described and commented on by Havlin et al. (2005). A review of application of ion-exchange resins in agricultural and environmental research has been provided by Qian and Schoenau (2002a).

Synthetic ion-exchange resins are solid organic polymers with an electrostatic charge that is neutralized by a selected counterion of opposite charge, and hence they function in a manner analogous to charged soil colloids. The strongly acidic cation-exchange (sulfonic acid functional group) resins and strongly basic anion-exchange (tertiary ammonium functional group) resins are chosen for use as a sink to extract nutrient ions in soils and other media. When ion-exchange resins are equilibrated with a solution containing a mixture of ions, proportions adsorbed by resin will not be the same as ionic proportions in the bulk solution, because of preferential selectivity by the resins for various ions. Generally speaking, cations and anions with the lowest affinity to the resin are best for use as counterions. There are two forms of ion-exchange resins that are commercially available. One is bead form and the other is membrane form. The resin beads are normally retained in a sealed nylon bag, while the

resins in membrane form should be cut into the desired size of strips (Qian et al. 1992) before use. Both resin beads and membranes have evolved from initial usage in batch systems where beads or membranes are mixed with a certain amount of soil and water, and then shaken as a suspension for a fixed time period (Amer et al. 1955; Martin and Sparks 1983; Turrion et al. 1999) to diffusion-sensitive systems where ion-exchange resins are placed in direct contact with soil for extended periods (Skogley 1992; Ziadi et al. 1999; Qian and Schoenau 2002b). When ion-exchange resins are used in the diffusion-sensitive systems, it is not easy to place them in the soil *in situ*, especially for resin membrane strips. To overcome the difficulty, resin capsule (made by sealing the resin bead inside a porous shell to form a compact rigid sphere capsule) and PRS probe (made by encapsulating the membrane in a plastic frame to create a probe) are commercially available from UNIBEST (Bozeman, Montana) and Western Ag Innovations (Saskatoon, SK), respectively.

In batch systems, the resins are in aqueous suspension with soil. During extraction, the resins adsorb nutrient ions from soil solution via surface adsorption, and the resins maintain ion concentrations at a low level to facilitate continued nutrient ion desorption from the soil until equilibrium is reached (Sparks 1987). In diffusion-sensitive procedures, resins are placed in direct contact with soil, which provides a measure that includes both the rates of release of ions from different soil surfaces as well as their diffusion rates through bulk soil. The system integrates both chemical and biological transformations as well as diffusion to a sink into the measure of nutrient availability, which accounts for the kinetics of nutrient release and transport (Curtin et al. 1987; Abrams and Jarrel 1992). With its nature of action similar to a plant root in its extraction of nutrient ions in soils, this method is able to account for factors affecting nutrient uptake by plant roots (Qian and Schoenau 1996). The theoretical verification for the procedures has been documented previously (Yang et al. 1991a,b; Yang and Skogley 1992).

With diffusion-sensitive systems, we can easily measure the nutrient supply rate (NSR). The NSR is defined as the amount of nutrient ion adsorbed per unit surface area of resin membrane over the time of duration of direct contact with soil. It can be expressed as μg (or μmol) per cm^2 for the time of direct contact (i.e., 24 h). There is no direct calibration between supply rate data and soil nutrient concentrations determined by conventional extractions as they are different measurements. Using ion-exchange resin membrane in contact with soil to assess nutrient availability is an alternative approach to traditional chemical extractions in that it provides a measure of nutrient ion flux, and is useful in mimicking and tracking the dynamic behavior of ion supply to plant roots in soil (Qian and Schoenau 2002a). It can be considered a unique multiple element assessment that is universal in its application to soils from different regions and of different properties.

Current efforts in assessing nutrient ion supply rate in soil have focused on direct contact of resin with soil either in the laboratory or in the field (Qian and Schoenau 2002a). The embodiment of resin membranes into probes facilitates the use of ion-exchange resins *in situ* in the field or fresh bulk soil samples in the laboratory. A so-called ''sandwich test'' for laboratory testing can be used to measure NSR in soil, which only requires a few grams of soils, and is suitable for soil samples that have been ground and dried in preparation for other types of analysis. The ''sandwich'' test for laboratory testing is described in this chapter.

13.2 LABORATORY MEASUREMENT OF NUTRIENT (ION) SUPPLY RATE—''SANDWICH'' TEST

13.2.1 Principle

The ''sandwich'' test was developed to use a minimum amount of processed (air-dried and ground) soil to achieve a measurement of NSR. The basic principle is to allow the resin membrane to adsorb nutrient ions from soils by directly contacting it with the soil in a moist condition for 24 h.

13.2.2 Materials and Reagents

1. Resin membrane: supplied from Western Ag Innovation Inc. (Saskatoon, SK). Other sources are BDH (Poole, England) and Ionics (Watertown, Massachusetts). The membrane sheets are cut into squares of about 8 cm^2 each to ensure the square is of a size that just fits inside the vial cap.
2. Snapcap vial lids (7 dram).
3. Snapcap vials with lids (7 dram).
4. Parafilm laboratory film.
5. Analytical balance.
6. Shaker.
7. Pipette (1 or 2 mL) and tips (or dropper).
8. 0.5 *M* $NaHCO_3$ solution: dissolve approximately 42 g of $NaHCO_3$ in deionized water and make to volume in a 1 L volumetric flask.
9. 0.5 *M* HCl: mix 42 mL of concentrated HCl with deionized water and make to volume in a 1 L volumetric flask.

13.2.3 Procedure

Preparation/Regeneration

The resin membranes must be cleaned and regenerated before each use. It is very important that used membrane strips are not contaminated with ions of interest before making measurements.

1. Before use, cation-exchange resin membranes must be cleaned/regenerated by soaking in 0.5 *M* HCl twice, for 1 h each time, with 3 mL of HCl per 1 cm^2 of membrane strip. This will put the cation-exchange membrane exchange sites into the proton (H^+) form as the counterion for exchange. The mixture should be stirred or agitated every 15 min or if possible, shaken continuously at slow

speed on a rotary-bench or side-to-side shaker. When the counterions are not protons, the cleaning process should be repeated as many as four times.

2 Clean brand new or regenerate used anion-exchange membranes by soaking in 0.5 *M* $NaHCO_3$ solution four times, for 2 h each time, with 3 mL of $NaHCO_3$ solution per 1 cm^2 of membrane strip. The solution should also be stirred on a regular basis or slowly shaken. This will put the anion-exchange membrane exchange sites into the bicarbonate (HCO_3^-) form.

3 Rinse cleaned or regenerated membrane strips with deionized water, and keep them in deionized water before use.

Extraction

1 Place subsamples of air-dried soil <2 mm into two Snapcap vial lids, filling the lids with soil up to the edges to ensure good contact between the complete surface of the membrane and the soil.

2 Place the Snapcap vial lids with the soil sample on an analytical balance. Add deionized water until the soil in each lid is close to saturated or at field capacity. If adding water just to field capacity, the field capacity of the soil should be estimated in advance to determine how much water is required for the weight of soil used.

3 Place a cation- or anion-exchange membrane strip onto the surface of the soil in one Snapcap vial lid, and then cover with the other Snapcap vial lid, making a ''sandwich,'' with the membrane sandwiched between the two lids containing soil. Normally a cation-exchange membrane sandwich and an anion-exchange membrane sandwich would be made if measurement of all cations and anions is desired.

4 Seal the ''sandwich'' with Parafilm laboratory film to avoid loss of soil moisture during the extraction.

5 Extraction time is normally set at a period of 24 h, similar to the burial time of membranes used in a commercial laboratory.

Elution

1 Add 20 mL of 0.5 *M* HCl to the Snapcap vial (7 dram).

2 Remove the Parafilm from the ''sandwich,'' separate the lids and pick out the membrane strip with plastic tweezers and then wash with deionized water until all soil particles are removed from the membrane surface. It is important that all soil particles are removed to avoid any soil entering into the eluent (HCl).

3 Place the washed membrane strips into the vials with 0.5 *M* HCl. Cap the vials with lids and then shake the vials containing the membranes in a shaker at 200 rpm for 1 h. The cation-exchange membrane and anion-exchange membrane strip from the same sample of soil can both be placed into the same 20 mL of HCl eluent as protons will elute the cations and Cl^- will elute the anions. The eluent should completely cover the membrane strips during shaking to ensure complete elution.

Ion Measurement

Nutrient ion concentrations in HCl can be measured with various instruments commonly used in a soil analytical chemistry laboratory, including manual or automated colorimetry, ion chromatography, atomic absorption-flame emission (AA-FE) spectrometry, or inductively coupled plasma (ICP) spectrometry.

13.2.4 Calculation

NSR can be calculated as

$$\text{NSR} = (C \times V)/S \tag{13.1}$$

where C is the concentration of an adsorbed cation or anion ($\mu g\ mL^{-1}$) in HCl eluent, V is the volume of eluent (mL), and S is the surface area of membrane strip (cm^2).

Example: a ''sandwich'' was prepared with an 8 cm^2 anion-exchange membrane. After 24 h the resin membrane was removed, washed, and placed in 20 mL of 0.5 *M* HCl. The concentration in 0.5 *M* HCl was 10 $\mu g\ NO_3$-N mL^{-1} as measured by colorimetry. The value of NSR is reported as: (10 $\mu g\ mL^{-1} \times 20\ mL)/8\ cm^{-2} = 25\ \mu g\ cm^{-2}$.

13.2.5 Comments

1 Ion-exchange resin membranes are a very sensitive measure of nutrient supply. Thus, maintaining consistent and uniform contact between soil and membrane is an essential condition to achieve reproducible results. If there is incomplete contact between the membrane and the soil, the area of membrane surface that can actually adsorb ions from soil is different than that assumed in the calculation of supply rate.

2 The tests should be under the same moisture and temperature conditions. Moisture and temperature have significant effects on ion diffusion and mineralization/solubilization in soil.

3 The ''sandwich'' test requires only a small amount of air-dried soil (about 4.5 g per 7 dram vial lid or 9 g per ''sandwich''). As such, there is no need to prepare a large amount of sample.

REFERENCES

Abrams, M.M. and Jarrel, W.M. 1992. Bioavailability index for phosphorus using ion exchange resin impregnated membranes. *Soil Sci. Soc. Am. J.* 56: 1532–1537.

Amer, F., Bouldin, D.R., Black, C.A., and Duke, F.R. 1955. Characterization of soil phosphorus by anion exchange resin adsorption and ^{32}P equilibration. *Plant Soil* 6: 391–408.

Curtin, D., Syers, J.K., and Smillie, G.W. 1987. The importance of exchangeable cations and resin-sink characteristics in the release of soil phosphorus. *J. Soil Sci.* 38: 711–716.

Havlin, J.L., Beaton, J.D., Tisdale, S.L., and Nelson, W.L. 2005. Soil fertility evaluation. In *Soil Fertility and Fertilizers: An Introduction to Nutrient Management*, 7th ed. Prentice-Hall, New Jersey, NJ, pp. 298–361.

Kuo, S. 1996. Phosphorus. In Sparks, D.L., Ed. *Methods of Soil Analysis*, *3rd edn. Part 3*. SSSA, Madison, WI, pp. 869–920.

Martin, H.W. and Sparks, D.L. 1983. Kinetics of non-exchangeable potassium release from two Coastal Plain soils. *Soil Sci. Soc. Am. J.* 47: 883–887.

Olsen, S.R. and Sommers, L.E. 1982. Phosphorus. In Page, A.L. et al., Eds. *Methods of Soil Analysis*, *2nd edn. Part 2*. Agronomy Monograph No. 9. ASA and SSSA, Madison, WI, pp. 403–430.

Pratt, P.F. 1951. Potassium removal from Iowa soils by greenhouse and laboratory procedures. *Soil Sci*. 72: 107–118.

Qian, P. and Schoenau, J.J. 1996. Ion exchange resin membrane (IERM): a new approach for in situ measurement of nutrient availability in soil. *Plant Nutr. Fert. Sci*. 2: 322–330.

Qian, P. and Schoenau, J.J. 2002a. Practical applications of ion exchange resins in agricultural and environmental soil research. *Can. J. Soil Sci*. 82: 9–21.

Qian, P. and Schoenau, J.J. 2002b. Availability of nitrogen in solid manure amendments with different C/N ratios. *Can. J. Soil Sci*. 82: 219–225.

Qian, P., Schoenau, J.J., and Huang, W. 1992. Use of ion exchange membranes in routine soil testing. *Commun. Soil Sci. Plant Anal*. 23: 1791–1804.

Skogley, E.O. 1992. The universal bioavailability environment/soil test UNIBEST. *Commun. Soil Sci. Plant Anal*. 23: 2225–2246.

Sparks, D.L. 1987. Potassium dynamics in soils. *Adv. Soil Sci*. 6: 1–63.

Turrion, M.B., Gallardo, J.F., and Gonzales, M.I. 1999. Extraction of soil-available phosphate, nitrate, and sulphate ions using ion exchange membranes and determination by ion exchange chromatography. *Commun. Soil Sci. Plant Anal*. 30: 1137–1152.

Yang, J.E. and Skogley, E.O. 1992. Diffusion kinetics of nutrient accumulation by mix-bed ion-exchange resin. *Soil Sci. Soc. Am. J*. 56: 408–414.

Yang, J.E., Skogley, E.O., Georgitis, S.J., Schaff, B.E., and Ferguson, A.H. 1991a. The phytoavailability soil test: development and verification of theory. *Soil Sci. Soc. Am. J*. 55: 1358–1365.

Yang, J.E., Skogley, E.O., and Schaff, B.E. 1991b. Nutrient flux to mix-bed ion-exchange resin: temperature effects. *Soil Sci. Soc. Am. J*. 55: 762–767.

Ziadi, N., Simard, R.R., Allard, G., and Lafond, J. 1999. Field evaluation of anion exchange membrane as a N soil testing method for grasslands. *Can. J. Soil Sci*. 79: 281–294.

Chapter 14
Environmental Soil Phosphorus Indices

Andrew N. Sharpley
University of Arkansas
Fayetteville, Arkansas, United States

Peter J.A. Kleinman
U.S. Department of Agriculture
University Park, Pennsylvania, United States

Jennifer L. Weld
The Pennsylvania State University
University Park, Pennsylvania, United States

14.1 INTRODUCTION

The loss of phosphorus (P) in agricultural runoff and its input to freshwater bodies is known to accelerate eutrophication (Carpenter et al. 1998; U.S. Geological Survey 1999; Sharpley 2000). As eutrophication of surface water impairs its use for recreation, drinking, and commercial fishing, several strategies have been put in place to minimize impairment by reducing the potential for P loss from agricultural operations (Gibson et al. 2000; U.S. Environmental Protection Agency 2004).

Key components of remedial strategies to decrease P loss from agriculture are the determination of soil P levels that are above those required for optimum crop growth, due to the continual application of P (Sims et al. 1998; Simard et al. 2000; Daverede et al. 2003) and the identification of critical source areas where there is a high risk of P loss due to the coincidence of runoff and erosion with high soil P levels (Sharpley et al. 2001, 2003; Coale et al. 2002). Traditional soil P tests to estimate for crop P availability have been used as surrogate estimates of runoff P enrichment by soil P (Sharpley et al. 1996). Because soil P tests were developed to work on certain soil types (e.g., Mehlich-3 and Bray-1 for acidic soils and Olsen for calcareous, alkaline soils) and do not mimic soil P release to runoff water, efforts have been made to establish environmental soil P tests (Sibbesen and Sharpley 1997; Torbert et al. 2002). The more prominent of these environmental tests include water-extractable soil P and P sorption saturation.

Considerable field-based research has provided data to support the use of water-extractable soil P as an environmental test, which is independent of soil type, to assess the potential for soil to enrich runoff with dissolved P (Pote et al. 1996; McDowell and Sharpley 2001). The extraction of soil with water more closely mimics the interaction between surface soil and rainfall and the subsequent release of P to runoff water than do acidic or basic soil test P extractants. Andraski and Bundy (2003), Andraski et al. (2003), Daverede et al. (2003), Hooda et al. (2000), Pote et al. (1999a,b), and Torbert et al. (2002) all reported water-extractable soil P to be closely related to runoff-dissolved P for both grassed and cropped plots, at a similar or greater level of significance than Bray-1 and Mehlich-3-extractable soil P (Vadas et al. 2005). Increasingly, investigators are using water-extractable P in lieu of runoff data in laboratory studies aimed at comparing environmental and agronomic effects (e.g., Stout et al. 1998).

Estimation of P sorption saturation is based on the premise that the saturation of P sorbing sites for a soil determines P release (intensity factor) as well as the level of soil P (capacity factor) (Breeuwsma and Silva 1992; Kleinman and Sharpley 2002). For example, soils of similar soil test P may have differing capacities to release P to runoff, based on the fact that P would be bound more tightly to clay than sandy soils (Sharpley and Tunney 2000). Phosphorus sorption saturation can also represent the capacity of a soil to sequester further P addition and thereby enrich runoff P (Schoumans et al. 1987; Lookman et al. 1996). For example, the addition of P to a soil with a high P sorption saturation will enrich runoff P more than if P was added to a soil with a low P sorption saturation, independent of soil test P level (Sharpley 1995; Leinweber et al. 1997). Traditional techniques to estimate soil P sorption saturation have relied upon methods that are not commonly performed by soil testing laboratories, such as acid ammonium oxalate extraction in the dark (e.g., Schoumans and Breeuwsma 1997) and P sorption isotherms (e.g., Sharpley 1995). Recent research has shown soil P sorption saturation in acidic soils can be reliably estimated from Mehlich-3-extractable Al and Fe (primary components of P sorption) and P (Beauchemin and Simard 1999; Kleinman and Sharpley 2002; Nair and Graetz 2002).

Soil P sorption has also been used to estimate the potential of a soil to sequester proposed additions of P. In specific cases, a detailed assessment of the P sorption capacity of a soil is a planning requirement of proposed land applications of biosolids, in order to determine the potential for P leaching through a soil profile (U.S. Environmental Protection Agency 1993; Bastian 1995). Traditionally, P sorption isotherms are constructed using batch equilibrations of soil with P added in a supporting solution, usually as KH_2PO_4 in a 0.01 *M* $CaCl_2$ matrix for 24 to 40 h (Syers et al. 1973; Nair et al. 1984). Equations such as the Langmuir, Freundlich, and Tempkin models have been used to describe the relationship between the amount of P sorbed to the P in solution at equilibrium and to calculate P sorption maximum, binding energy, and equilibrium P concentrations for a given soil (Berkheiser et al. 1980; Nair et al. 1984). This chapter will discuss the Langmuir approach only.

While P sorption isotherms can provide a large amount of soil-specific information that is useful to agronomic and environmental characterization of P sorption capacity, they are too time-consuming, complicated, and expensive for routine use by soil testing laboratories (Sharpley et al. 1994). To overcome these limitations, Bache and Williams (1971) suggested a single equilibration using a high concentration of P (single-point isotherm), from which a P sorption index (PSI) was calculated, to rapidly determine soil P sorption capacity. They found that PSI was closely correlated with P sorption maxima determined by the full sorption isotherm for 42 acid and calcareous soils from Scotland ($r = 0.97$; $P > 0.001$) (Bache and Williams 1971). Other researchers have subsequently found PSI to be correlated with

soil P sorption maxima of soils varying widely in chemical and physical properties (Sharpley et al. 1984; Mozaffari and Sims 1994; Simard et al. 1994).

Finally, most states in the United States have now adopted a P indexing approach as part of P-based nutrient management planning requirements, so that areas at greatest risk of P loss can be targeted for remediation or more restrictive management (Sharpley et al. 2003). The P indexing approach is based on the knowledge that most P loss from agricultural watersheds (>75% annually), occurs from small, defined areas of a watershed (<20% land area) (Smith et al. 1991; Schoumans and Breeuwsma 1997; Pionke et al. 2000). The P index ranks these critical source areas by identifying where high P source potential (i.e., soil P and the rate, method, timing, and type of P added as fertilizer or manure) coincides with high transport potential (i.e., surface runoff, leaching, erosion, and proximity to a stream) (Lemunyon and Gilbert 1993). The P index is one of the more successful approaches that addresses P source, management, and transport in a holistic way by attempting to combine important P loss variables into a practical program that assesses specific field's potential for P loss (Gburek et al. 2000; Sharpley et al. 2003). Use of the P index helps farmers, consultants, extension agents, and livestock producers identify (i) agricultural areas or practices that have the greatest potential to accelerate eutrophication and (ii) management options available to land users that will allow them flexibility in developing remedial strategies.

This chapter details the methods used to estimate water-extractable soil P, P sorption saturation, P sorption capacity, and indexing P loss potential for a given site. For all these chemical methods and preparation of reagents used, the use of standard laboratory protective clothing and eye covering is recommended.

14.2 WATER-EXTRACTABLE SOIL P

The extraction of soil P with water provides a rapid and simple means of determining the amount of soil P that can be released from soil to runoff water. The method assumes that extraction with water replicates the reaction between soil and runoff water and is thus, independent of soil type. The following method is a variation of the method described by Olsen and Sommers (1982) for determination of water-soluble P in soils. In summary, P extracted from a soil sample after it has been shaken with water for a specific period of time is measured spectrophotometrically by the colorimetric molybdate–ascorbic acid method (Murphy and Riley 1962). Alternatively, filtrates can be analyzed by inductively coupled plasma-atomic emission spectrometry (ICP-AES), which will measure total dissolved P.

14.2.1 Materials and Reagents

1 Centrifuge tubes (40 mL) with screw caps.

2 End-over-end shaker.

3 Centrifuge.

4 Filtration apparatus (0.45 μm pore diameter membrane filter or Whatman No. 42).

5 Photometer: Spectrophotometer with infrared phototube for use at 880 nm and providing a light path of at least 2.5 cm, preferably a 5 cm path length cell.

For light path lengths of 0.5, 1.0, and 5.0 cm, the P ranges are 0.3–2.0, 0.15–1.30, and 0.01–0.25 mg L^{-1}, respectively.

6 Acid-washed glassware and plastic bottles: Graduated cylinders (5 to 100 mL), volumetric flasks (100, 500, and 1000 mL), storage bottles, pipets, dropper bottles, and test tubes or flasks for reading sample absorbance. The spectrophotometer should be calibrated daily by using factory standard procedures for the laboratory machine.

7 Balances used to weigh reagents and samples are calibrated according to factory specifications and routinely cleaned to ensure proper and accurate working order.

8 Distilled water.

9 A series of P standards (0, 0.25, 0.5, 0.75, and 1.00 mg P L^{-1} as KH_2PO_4) is prepared fresh on the day of analysis.

10 Reagents for ascorbic acid technique for P determination.

a. 2.5 *M* H_2SO_4: Slowly add 70 mL of concentrated H_2SO_4 to approximately 400 mL of distilled water in a 500 mL volumetric flask. After the solution has cooled, dilute to 500 mL with distilled water, mix, and transfer to a plastic bottle for storage. Store in refrigerator until used.

b. Ammonium molybdate solution: Dissolve 20 g of $(NH_4)_6MO_7O_{24} \cdot 4H_2O$ in 500 mL of distilled water. Store in a plastic bottle at 4°C until used.

c. Ascorbic acid, 0.1 *M*: Dissolve 1.76 g of ascorbic acid in 100 mL of distilled water. The solution is stable for about a week if stored in an opaque plastic bottle at 4°C until used.

d. Potassium antimonyl tartrate solution: Using a 500 mL volumetric flask, dissolve 1.3715 g of $K(SbO)C_4H_4O_6 \cdot 1/2H_2O$ in approximately 400 mL of distilled water, and dilute to volume. Store in a dark, glass-stoppered bottle at 4°C until used.

e. Combined reagent: When making the combined reagent, all reagents must be allowed to reach room temperature before they are mixed, and they must be mixed in the following order. To make 100 mL of the combined reagent:

   i. Transfer 50 mL of 2.5 *M* H_2SO_4 to a plastic bottle.
   ii. Add 15 mL of ammonium molybdate solution to the bottle and mix.
   iii. Add 30 mL of ascorbic acid solution to the bottle and mix.
   iv. Add 5 mL of potassium antimonyl tartrate solution to the bottle and mix.

f. If turbidity has formed in the combined reagent, shake and let stand for a few minutes until turbidity disappears before proceeding. Store in an opaque plastic bottle. The combined reagent is stable for less than 8 h, so it must be freshly prepared for each run.

g. Stock phosphate solution: Using a 1000 mL volumetric flask, dissolve 219.5 mg anhydrous KH_2PO_4 in distilled water and dilute to 1000 mL volume; 1 mL contains 50 μg of P.

h. Standard P solutions: Prepare a series of at least six standard P solutions within the desired P range by diluting stock phosphate solution with distilled water.

14.2.2 Procedure

1 Weigh out 2 g of air-dried soil into a 40 mL centrifuge tube. Conduct in duplicate.

2 Add 20 mL of distilled water and shake at 10 rpm end-over-end for 1 h.

3 Centrifuge at about 3000 *g* for 10 min.

4 Filter the solution through a Whatman No. 42 filter paper or 0.45 μm membrane filter if paper filtrates are not clear.

5 Measure P by ICP-AES or by the ascorbic acid technique (see Section 14.2.1).

6 Pipette 20 mL of water extraction filtrate into a 25 mL volumetric flask and add 5 mL of combined Murphy and Riley color reagent.

7 If the P concentration of the extract is greater than the highest standard, a smaller sample aliquot is required. Add revised sample aliquot to volumetric flask, make up to 20 mL with distilled water, and add Murphy and Riley reagent.

8 Measure absorbance (880 nm) and determine concentration from standard curve prepared each day.

14.2.3 Calculations

1 Water-extractable soil P (mg P kg soil^{-1})

$$= [\text{Concentration of P in extract, mg L}^{-1}] \times [\text{volume of extractant, L/mass of soil, kg}] \quad (14.1)$$

2 Minimum detection limit is 0.02 mg kg^{-1}.

3 There is no upper limit of detection, as extracts from soils with large amounts of P can be diluted.

14.2.4 Comments

Air-dried soils can be stored at room temperature in whirl-pack or closed plastic containers, to avoid contamination. Water extracts of soils should be kept at 4°C until P is measured, preferably within 2 days of extraction. A large amount of soil common to the users' area and similar to that being analyzed should be air-dried and archived. The water-extractable soil P concentration of the archived sample is run each day to ensure day-to-day analytical reproducibility. Any deviations form this standard value should be addressed immediately.

14.3 P SORPTION SATURATION

Phosphorus sorption saturation provides insight into a soil's ability to release P to solution as well as its remaining capacity to sorb added P and is defined as follows:

$$P_{sat} = \frac{\text{Sorbed P}}{\text{P sorption capacity}} \tag{14.2}$$

In the method described below, sorbed P is represented by Mehlich-3-extractable soil P and P sorption capacity by Mehlich-3-extractable Al and Fe. Notably, in estimating P sorption saturation from Mehlich data, this study does not include α, the proportion of Mehlich-3 Al and Fe that contribute to P sorption capacity. Use of α in the literature has been primarily associated with P sorption saturation calculated from acid ammonium oxalate data (e.g., van der Zee and van Riemsdijk 1988). Given soil-specific variations in sorption mechanisms affecting P sorption capacity as well as variability in methods used to estimate P sorption, there is little justification for the continued use of this value unless it is measured (Hooda et al. 2000).

14.3.1 Materials and Reagents

1 Centrifuge tubes (40 mL) with screw caps.

2 End-over-end shaker.

3 Centrifuge.

4 Filtration apparatus (0.45 μm pore diameter membrane filter or Whatman No. 42).

5 Mehlich-3 solution as 0.2 *M* CH_3COOH, 0.25 *M* NH_4NO_3, 0.015 *M* NH_4F, 0.013 *M* HNO_3, and 0.001 *M* EDTA (see Chapter 7 for more detail). Store in refrigerator until used.

6 Acid-washed glassware and plastic bottles.

14.3.2 Procedure

1 Weigh out 2.5 g of air-dried soil into a 40 mL centrifuge tube. Conduct in duplicate.

2 Add 25 mL of Mehlich-3 reagent and shake at 10 rpm for 5 min.

3 Filter the solution through a Whatman No. 42 filter paper or 0.45 μm membrane filter if paper filtrates are not clear.

4 Measure P, Al, and Fe by ICP-AES. Represented as P_{M3}, Al_{M3}, and Fe_{M3}, respectively.

14.3.3 Calculations

1 In all cases, molar concentrations of extracted elements (mmol kg^{-1}) were used to determine P_{sat}.

2 For acid soils (pH < 7.0):

$$P_{sat} = \frac{P_{M3}}{Al_{M3} + Fe_{M3}} \tag{14.3}$$

14.3.4 Comments

Soil P sorption saturation is increasingly used as an environmental indicator of soil P availability to runoff and can be easily calculated from data that is readily available through soil testing laboratories and national databases. Several studies show that Mehlich-3 data can be effectively used to estimate P_{sat} for a wide range of acidic and alkaline soils. As most soil testing laboratories currently conducting Mehlich-3 extraction employ ICPs, analytes required to estimate P_{sat} (P_{M3}, Al_{M3}, and Fe_{M3}) are measured simultaneously. However, P estimated by ICP is often greater than by colorimetric methods due to ICP measuring near total (inorganic + organic) dissolved P. Care must be taken in building databases or comparing studies, which have used different methods of determining P in filtrates.

14.4 P SORPTION CAPACITY

Estimates of P sorption vary with soil/solution ratio, ionic strength and cation species of the supporting electrolyte, time of equilibration, range of initial P concentrations, volume of soil suspension to headspace volume in the equilibration tube, rate and type of shaking, and type and extent of solid/solution separation after equilibration (Nair et al. 1984). Even though a similar basic procedure is used to measure P sorption, there is considerable variation in the above parameters, which makes comparison of results among studies difficult. Thus, Nair et al. (1984) proposed a standard P adsorption procedure that would produce consistent results over a wide range of soils. This procedure was evaluated, revised, tested among laboratories, and was eventually proposed as a standardized P adsorption procedure and is detailed below.

14.4.1 Materials and Reagents

1 Centrifuge tubes (40 mL) with screw caps.

2 End-over-end shaker.

3 Centrifuge.

4 Filtration apparatus (0.45 μm pore diameter membrane filter or Whatman No. 42).

5 Photometer: Spectrophotometer with infrared phototube for use at 880 nm and providing a light path of at least 2.5 cm, preferably a 5 cm path length cell. For light path lengths of 0.5, 1.0, and 5.0 cm, the P ranges are 0.3–2.0, 0.15–1.30, and 0.01–0.25 mg L^{-1}, respectively.

6 Acid-washed glassware and plastic bottles: Graduated cylinders (5 to 100 mL), volumetric flasks (100, 500, and 1000 mL), storage bottles, pipets, dropper bottles, and test tubes or flasks for reading sample absorbance. The spectrophotometer should be calibrated daily using factory standard procedures for the laboratory machine.

7 Balances used to weigh reagents and samples are calibrated according to factory specifications and routinely cleaned to ensure proper and accurate working order.

8 Support or equilibrating solution is 0.01 *M* $CaCl_2$. Store in refrigerator until used.

9 Inorganic P solution of 50 mg L^{-1} as KH_2PO_4 in 0.01 *M* $CaCl_2$. Store in refrigerator until used.

14.4.2 Procedure

1 Weigh out 1 g of air-dried soil into a 40 mL centrifuge tube. Conduct in duplicate.

2 Add 0, 1, 2, 5, 10, 15, and 20 mL of stock P solution (50 mg L^{-1}) and make up to a final volume of 25 mL with distilled water and shake at 10 rpm end-over-end for 24 h. This gives equilibrating P concentrations of 0, 50, 100, 250, 500, 750, and 1000 mg P kg $soil^{-1}$ or 0, 2, 4, 10, 20, 30, and 40 mg P L^{-1}, respectively. The range of P concentrations used can be adjusted as needed to ensure the upper concentration represents a distinct curvature of the plotted P sorption isotherm.

3 Centrifuge at 3000 *g* for 10 min.

4 Filter the solution through a Whatman No. 42 filter paper or 0.45 μm membrane filter if paper filtrates are not clear.

5 Measure P by ICP-AES or by the ascorbic acid technique (see Section 14.2.1).

6 Pipette 5 mL of water extraction filtrate into a 25 mL volumetric flask and add 5 mL of combined Murphy and Riley color reagent and make up to 25 mL with distilled water.

7 Adjust sample aliquot as required and make up to a final volume of 25 mL after addition of Murphy and Riley reagent.

8 Measure absorbance (880 nm) and determine concentration from standard curve prepared each day.

14.4.3 Calculation of P Sorption Isotherm

1 The amount of P sorbed by soil (S, mg P kg $soil^{-1}$) is calculated as the difference between added P and P remaining in solution after the 24 h equilibration. Several methods exist for the determination of the amount of P originally sorbed by soil (S_o) such as the least squares fit model, oxalate-extractable P, and anion-membrane exchangeable P (Nair et al. 1998).

2 The Langmuir sorption isotherm is plotted as equilibrium solution P concentration (C, mg P L^{-1}) against P sorbed (S) as shown in Figure 14.1a.

3 Using the Langmuir sorption equation below, P sorption maximum (S_{max}, mg P kg $soil^{-1}$) and binding energy of P to soil (k, L mg P^{-1}) can be calculated.

$$\frac{C}{S} = \frac{1}{kS_{max}} + \frac{C}{S_{max}} \tag{14.4}$$

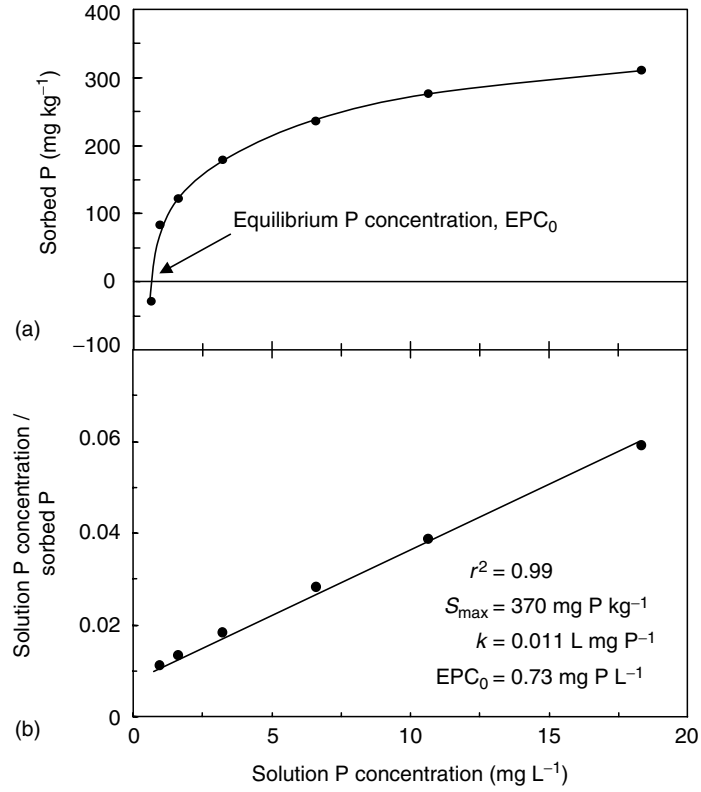

FIGURE 14.1. Representation of Langmuir P sorption isotherm (a) and linear (b) plot from which P sorption maximum, binding energy, and equilibrium P concentration are calculated.

where $S = S' + S_o$, the total amount of P sorbed (mg P kg soil^{-1}); S', P sorbed by soil (mg P kg soil^{-1}); S_o, P originally sorbed (previously sorbed P) (mg P kg soil^{-1}); C, equilibrium solution P concentration after 24 h shaking (mg P L^{-1}); S_{max}, P sorption maximum (mg P kg soil^{-1}); and k, a constant relating the binding energy of P to soil (L mg P^{-1}).

4 P sorption maximum, S_{max}, is calculated as the reciprocal of the slope of the plot C/S vs. C (Figure 14.1a).

5 Binding energy, k, is calculated as the slope/intercept of the same plot (Figure 14.1b).

6 The equilibrium P concentration (EPC_0, mg P L^{-1}), defined as the solution P concentration supported by a soil sample at which no net sorption or desorption occurs, is calculated as the intercept of the isotherm curve on the x-axis (see Figure 14.1).

14.5 P SORPTION INDEX

The procedure to determine PSI using a single-point isotherm approach, described below, is based on Bache and Williams (1971).

14.5.1 Materials and Reagents

1 Centrifuge tubes (40 mL) with screw caps.

2 End-over-end shaker.

3 Centrifuge.

4 Filtration apparatus (0.45 μm pore diameter membrane filter or Whatman No. 42).

5 Photometer: Spectrophotometer with infrared phototube for use at 880 nm and providing a light path of at least 2.5 cm, preferably a 5 cm path length cell. For light path lengths of 0.5, 1.0, and 5.0 cm, the P ranges are 0.3–2.0, 0.15–1.30, and 0.01–0.25 mg L^{-1}, respectively.

6 Acid-washed glassware and plastic bottles: Graduated cylinders (5 to 100 mL), volumetric flasks (100, 500, and 1000 mL), storage bottles, pipets, dropper bottles, and test tubes or flasks for reading sample absorbance. The spectrophotometer should be calibrated daily using factory standard procedures for the laboratory machine.

7 Balances used to weigh reagents and samples are calibrated according to factory specifications and routinely cleaned to ensure proper and accurate working order.

8 Inorganic P solution of 75 mg L^{-1} as KH_2PO_4 in 0.01 *M* $CaCl_2$. Store in refrigerator until used.

14.5.2 Procedure

1 Weigh out 1 g of air-dried soil into a 40 mL centrifuge tube. Conduct in duplicate.

2 Add 20 mL of the 75 mg P L^{-1} sorption solution to the centrifuge tube. This provides a single addition of 1.5 g P kg $soil^{-1}$ and a solution:soil ratio of 20:1.

3 Shake at 10 rpm end-over-end for 18 h.

4 Centrifuge at 3000 *g* for 10 min.

5 Filter the solution through a Whatman No. 42 filter paper or 0.45 μm membrane filter if paper filtrates are not clear.

6 Measure P by ICP-AES or by the ascorbic acid technique (see Section 14.2.1).

7 Pipette 5 mL of water extraction filtrate into a 25 mL volumetric flask and add 5 mL of combined Murphy and Riley color reagent and make up to 25 mL with distilled water.

8 Adjust sample aliquot as required and make up to a final volume of 25 mL after addition of Murphy and Riley reagent.

9 Measure absorbance (880 nm) and determine concentration from standard curve prepared each day.

14.5.3 Calculation of P Sorption Index

1 The PSI is calculated using the quotient $S/\log C$, where S is the amount of P sorbed (mg P kg^{-1}) and C is solution P concentration (mg L^{-1}).

2 Others have shown that expressing PSI directly as the amount of P sorbed (mg P kg^{-1}) is acceptable (Sims 2000).

14.6 P INDEX: SITE RISK ASSESSMENT FOR P LOSS VULNERABILITY

Site vulnerability to P loss in runoff is assessed with the P index by selecting rating values for a variety of source and transport factors. Although procedures and formats of P indices vary regionally, generally the first step in the process is to collect farm information such as farm maps, soil test reports, manure analysis, crop rotations, and manure handling and application information. The second step is to determine erosion rates, runoff class, and distance to receiving water is often needed. A site visit and evaluation is critical to properly evaluate field boundaries, areas of runoff and erosion contributions, and options for improved nutrient management and best management practices. The following procedure outlines the sources of information and calculations for Pennsylvania's P index. English units are most commonly used in P indices, to be consistent with the units used by field practitioners. Factors are given to convert English to metric or SI units.

The screening tool reduces potential time and workload associated with P index evaluations, by identifying fields at greatest risk to P loss using one or more readily available P index factors. In the Pennsylvania P index, the screening tool is Part A of the P index and uses soil test P (Mehlich-3 ppm P) and distance from the bottom edge of a field to a receiving body of water (contributing distance) (Table 14.1).

14.6.1 Procedure

If a soil test P level for a field is either greater than 200 ppm P or if the bottom edge of the field is closer than 150 ft. (50 m) to a receiving body, then the field is determined to have a potentially high risk of P loss. To determine the risk of P loss, additional field factors must be evaluated using Part B of the P index (Table 14.2).

If the soil test P level for the field is less than 200 ppm P and the bottom edge of the field is more than 150 ft. (50 m) from a receiving body, then the field does not have a potentially high risk for P loss and N-based nutrient management recommendations can be followed.

TABLE 14.1 The P Indexing Approach Using a Modified Version of Pennsylvania's Index Version of 8/2002, as an Example Part A—Screening Tool

	Evaluation category	
Soil test P—Mehlich-3 P	>200 ppm ($\mu g\ g^{-1}$)	If yes to either factor
Contributing distance	<150 ft. (50 m)	then proceed to Part B

TABLE 14.2 The Transport Factors Included in Part B of the Pennsylvania P Index Version of 8/2002; Part B—Transport Factors

Characteristics	Risk levels					Risk value
Soil Erosion	Risk value = Annual soil loss = _____ tons/acre/year[a]					
Runoff Potential	Very Low **0**	Low **1**	Medium **2**	High **4**	Very High **8**	
Subsurface Drainage	None **0**		Random **1**		Patterned[b] **2**	
Leaching Potential	Low **0**		Medium **2**	High **4**		
Contributing Distance	>500 ft. (>150 m) **0**	500 to 350 ft. (100 to 150 m) **1**	350 to 250 ft. (75 to 100 m) **2**	150 to 250 ft. (50 to 75 m) **4**	<150 ft. (<50 m) **8**	
Transport Sum = Erosion + Runoff Potential + Subsurface Drainage + Leaching Potential + Contributing Distance						
Modified Connectivity	Riparian buffer *Applies to distances <150 ft. (<50 m)* **0.7**		Grassed waterway or None **1.0**	Direct connection *Applies to distances >150 ft. (>50 m)* **1.1**		
Transport Factor = Transport Sum × Modified Connectivity/22						

The transport value is divided by 22 (i.e. the highest value obtainable) in order to normalize site transport to a value of 1, where full transport potential is realized.

Caution: Many states in the United States have a state-specific P index. Although the principles of most P index tools are similar, individual factors or weightings of those factors vary among states. If available, review your own state's P index. For more specific information on the various indices adopted by states see Sharpley et al. (2003).

[a] 1 ton/acre/year is equivalent to 2.24 Mg ha^{-1} $year^{-1}$.

[b] Or a rapidly permeable soil near a stream.

14.6.2 Warning

Phosphorus indices vary with respect to factors evaluated, coefficients assigned to field conditions and management scenarios, and calculations used to determine P index values. Additionally, P indices are subject to change and modification to reflect current research and policy. In order to ensure the P index is being used and interpreted properly, current regionally approved versions must be obtained and regional training and certification requirements must be met by those specialists using the P index. The information that follows is based on Pennsylvania's P index.

14.6.3 Materials

1 Soil erosion: Soil erosion rate can be calculated using RUSLE 1.06 c (Renard et al. 1997).

2 Runoff potential: Using the predominate soil type in a field (50% or greater of the field area) and county specific tables, which can be provided by USDA-NRCS staff, the index surface runoff class can be determined for each evaluated field. The following describes the USDA-NRCS method for determining index surface runoff class.

3 Subsurface drainage: Using farm information, determine if there is artificial drainage in the field or if the field is near a stream and has rapidly permeable soils. ''Random'' drainage is a single or a few tile lines in a field and ''patterned'' drainage is when most or the entire field is drained with a fill-patterned drainage system. Rapidly permeable soils must occur within 150 ft. (50 m) of a stream and be classified as such by USDA-NRCS.

4 Contributing distance: Determine the contributing distance of each field to be evaluated to receiving water. The distance is measured from the lower edge of the field closest to the receiving water and can be determined using farm maps or by field measurements.

5 Modified connectivity: Accounts for if and where buffers, grassed waterways, ditches, and pipe outlets are present.

- If the field is within 150 ft. (50 m) of water and a riparian buffer is present, select the appropriate modified connectivity factor (i.e., reduces transport value). All buffers must be designed and maintained to meet USDA-NRCS standards.
- If a field is more than 150 ft. (50 m) from water but a direct connection such as a pipe or ditch from field to receiving water is present, select appropriate modified connectivity factor (i.e., increases transport value).
- If a field has a grassed waterway or has no qualifying management practices, then a default coefficient of 1.0 is used (i.e., the transport value is neither increased nor is it decreased).

14.6.4 Calculations

1 Transport sum: Sum the actual soil loss rate (tons/acre/year) with the coefficients for runoff potential, subsurface drainage, and contributing distance. Enter the sum into the transport sum risk value column for each field.

2 Transport factor: Multiply the transport sum by the modified connectivity coefficient and divide the product by 22. Twenty-two is the maximum transport sum value and dividing by this value allows the transport factor to vary generally between 0 and 1. One is the value at which the full (100%) field transport potential is reached. Any other value would represent a relative percentage of the field's full transport potential. The transport factor only exceeds 1 when erosion losses are exceptionally high. Enter the product into the transport factor risk value column for each field.

14.6.5 Materials

1 Soil test P: Current soil test reports.

2 Fertilizer and manure rate: Farm records or a nutrient management plan indicating the amount of P, in pounds of P_2O_5/acre, to be applied to each field.

3 Loss rating for fertilizer and manure application: Farm records or a nutrient management plan indicating the methods and timing used to apply P to each field.

4 Manure P availability: Farm records or a nutrient management plan indicating the manure types, manure groups, or other organic P sources to be applied to each field to be evaluated (Table 14.3).

14.6.6 Calculating the P Index Value

1 Enter all of the transport factors (Part B) and sums of management factors (Part C) into the worksheet below.

2 Multiply Part B by Part C and then the product by 2. The factor of 2 normalizes the final index rating to 100. This is your final P index rating.

3 Look up the associated interpretation and management guidance in Table 14.4.

Field	Part B transport risk	Part C management risk	P Index B × C × 2	Interpretation of the P index
Example	0.55	92	101	Very high

TABLE 14.3 Phosphorus Loss Potential due to Source and Site Management Factors in the P Index; Part C—Source and Site Factors

Contributing Factors	Risk Levels					Risk Value
	Very Low	**Low**	**Medium**	**High**	**Very High**	
Soil test P risk[a]	Risk Value = Soil Test P (ppm as Mehlich-3 P) × 0.20 = _____ ppm × 0.20 = **OR** Risk value = Soil test P (lbs P_2O_5/acre) × 0.05 = _____ lbs P_2O_5/acre × 0.05 =					
Loss rating for P application method and timing	Placed with planter or injected more than 2" (5 cm) deep **0.2**	Incorporated <1 week after application **0.4**	Incorporated >1 week or not incorporated >1 following application in spring-summer **0.6**	Incorporated >1 week or not incorporated following application in autumn-winter **0.8**	Surface applied on frozen or snow covered soil **1.0**	
Fertilizer P risk[a]	Risk Value = Fertilizer P Application Rate × Loss Rating for P Application = Risk Value = _____ lbs P_2O_5/acre × _____ =					
Manure P availability	Organic Phosphorus Source Availability Coefficients					
Manure P risk[a]	Risk Value = Manure P Application Rate × Loss Rating for P Application × P Availability Coefficient = Risk Value = _____ lbs P_2O_5/acre × _____ × _____ =					
Total of Management Risk Factors				**Sum of management factors**	**=**	

Caution: Many states in the United States have a state-specific P index. Although the principles of most P index tools are similar, individual factors or weightings of those factors vary among states. If available, review your own state's P index. For more specific information on the various indices adopted by states see Sharpley et al. (2003).

[a] Conversion factor: 10 lbs P_2O_5/acre is equivalent to 4.89 kg P ha^{-1}.

TABLE 14.4 General Interpretations and Management Guidance for the P Index

P Index value	Rating	General interpretation	Management guidance
<59	Low	If current farming practices are maintained, there is a low risk of adverse impacts on surface waters	N-based applications
60–79	Medium	Chance for adverse impacts on surface waters exists, and some remediation should be taken to minimize P loss	N-based applications
80–100	High	Adverse impact on surface waters. Conservation measures and P management plan are needed to minimize P loss	P application limited to crop removal of P
>100	Very high	Adverse impact on surface waters. All necessary conservation measures and P management plan must be implemented to minimize P loss	No P applied

Caution: Many states in the United States have a state-specific P index. Although the principles of most P index tools are similar, individual factors or weightings of those factors vary among states. If available, review your own region's P index. For more specific information on the various indices adopted by states see Sharpley et al. (2003).

REFERENCES

Andraski, T.W. and Bundy, L.G. 2003. Relationship between phosphorus levels in soil and in runoff from corn production systems. *J. Environ. Qual*. 32: 310–316.

Andraski, T.W., Bundy, L.G., and Kilian, K.C. 2003. Manure history and long-term tillage effects on soil properties and phosphorus losses in runoff. *J. Environ. Qual*. 32: 1782–1789.

Bache, B.W. and Williams, E.G. 1971. A phosphate sorption index for soils. *J. Soil Sci*. 22: 289–301.

Bastian, R.K. 1995. *Biosolids Management Handbook*. EPA 833-R-95-001. USEPA, Office of Water Management, Washington, DC. Available at: http://www.epa.gov/Region8/water/wastewater/biohome/biosolidsdown/handbook/handbook1.pdf (last verified March 1, 2005).

Beauchemin, S. and Simard, R.R. 1999. Soil phosphorus saturation degree: review of some indices and their suitability for P management in Quebec, Canada. *Can. J. Soil Sci*. 79: 615–625.

Berkheiser, V.E., Street, J.J., Rao, P.S.C., and Yuan, T.L. 1980. Partitioning of inorganic orthophosphate in soil–water systems. *CRC Crit. Rev. Environ. Contr*. October 1980, 179–224.

Breeuwsma, A. and Silva, S. 1992. Phosphorus fertilisation and environmental effects in the Netherlands and the Po region (Italy). Report 57, DLO The Winand Staring Centre for Integrated Land, Soil, and Water Research, Wageningen, the Netherlands.

Carpenter, S.R., Caraco, N.F., Correll, D.L., Howarth, R.W., Sharpley, A.N., and Smith, V.H. 1998. Nonpoint pollution of surface waters with phosphorus and nitrogen. *Ecol. Appl*. 8: 559–568.

Coale, F.J., Sims, J.T., and Leytem, A.B. 2002. Accelerated deployment of an agricultural nutrient management tool: the Maryland phosphorus site index. *J. Environ. Qual*. 31: 1471–1476.

Daverede, I.C., Kravchenko, A.N., Hoeft, R.G., Nafziger, E.D., Bullock, D.G., Warren, J.J., and Gonzini, L.C. 2003. Phosphorus runoff: effect of

tillage and soil phosphorus levels. *J. Environ. Qual*. 32: 1436–1444.

Gburek, W.J., Sharpley, A.N., Heathwaite, A.L., and Folmar, G.J. 2000. Phosphorus management at the watershed scale: a modification of the phosphorus index. *J. Environ. Qual*. 29: 130–144.

Gibson, G.R., Carlson, R., Simpson, J., Smeltzer, E., Gerritson, J., Chapra, S., Heiskary, S., Jones, J., and Kennedy, R. 2000. *Nutrient criteria technical guidance manual: lakes and reservoirs* (EPA-822-B00-001). U.S. Environmental Protection Agency, Washington, DC.

Hooda, P.S., Rendell, A.R., Edwards, A.C., Withers, P.J.A., Aitken, M.N., and Truesdale, V.W. 2000. Relating soil phosphorus indices to potential phosphorus release to water. *J. Environ. Qual*. 29: 1166–1171.

Kleinman, P.J.A. and Sharpley, A.N. 2002. Estimating soil phosphorus sorption saturation from Mehlich-3 data. *Commun. Soil Sci. Plant Anal*. 33: 1825–1839.

Leinweber, P., Lunsmann, F., and Eckhardt, K.U. 1997. Phosphorus sorption capacities and saturation of soils in two regions with different livestock densities in northwest Germany. *Soil Use Manage*. 13: 82–89.

Lemunyon, J.L. and Gilbert, R.G. 1993. The concept and need for a phosphorus assessment tool. *J. Prod. Agric*. 6: 483–496.

Lookman, R., Jansen, K., Merckx, R., and Vlassak, K. 1996. Relationship between soil properties and phosphate saturation parameters: a transect study in northern Belgium. *Geoderma* 69: 265–274.

McDowell, R.W. and Sharpley, A.N. 2001. Approximating phosphorus release from soils to surface runoff and subsurface drainage. *J. Environ. Qual*. 30: 508–520.

Mozaffari, P.M. and Sims, J.T. 1994. Phosphorus availability and sorption in an Atlantic Coastal Plain watershed dominated by intensive, animal-based agriculture. *Soil Sci*. 157: 97–107.

Murphy, J. and Riley, J.P. 1962. A modified single solution method for the determination of phosphate in natural waters. *Anal. Chem. Acta* 27: 31–36.

Nair, P.S., Logan, T.J., Sharpley, A.N., Sommers, L.E., Tabatabai, M.A., and Yuan, T.L. 1984. Interlaboratory comparison of a standardized phosphorus adsorption procedure. *J. Environ. Qual*. 13: 591–595.

Nair, V.D. and Graetz, D.A. 2002. Phosphorus saturation in Spodosols impacted by manure. *J. Environ. Qual*. 31: 1279–1285.

Nair, V.D., Graetz, D.A., and Reddy, K.R. 1998. Dairy manure influences on phosphorus retention capacity of Spodosols. *J. Environ. Qual*. 27: 522–527.

Olsen, S.R. and Sommers, L.E. 1982. Phosphorus. In A.L. Page et al., Eds. *Methods of Soil Analysis*. Agronomy 9, 2nd edn. American Society of Agronomy, Inc., Madison, WI, pp. 403–430.

Pionke, H.B., Gburek, W.J., and Sharpley, A.N. 2000. Critical source area controls on water quality in an agricultural watershed located in the Chesapeake Basin. *Ecol. Eng*. 14: 325–335.

Pote, D.H., Daniel, T.C., Nichols, D.J., Moore, P.A., Miller, D.M., and Edwards, D.R. 1999a. Seasonal and soil-drying effects on runoff phosphorus relationships to soil phosphorus. *Soil Sci. Soc. Am. J*. 63: 1006–1012.

Pote, D.H., Daniel, T.C., Nichols, D.J., Sharpley, A.N., Moore, P.A., Miller, D.M., and Edwards, D.R. 1999b. Relationship between phosphorus levels in three ultisols and phosphorus concentrations in runoff. *J. Environ. Qual*. 28: 170–175.

Pote, D.H., Daniel, T.C., Sharpley, A.N., Moore, P.A., Edwards, D.R., and Nichols, D.J. 1996. Relating extractable soil phosphorus to phosphorus losses in runoff. *Soil Sci. Soc. Am. J*. 60: 855–859.

Renard, K.G., Foster, G.R., Weeies, G.A., McCool, D.K., and Yoder, D.C. 1997. Predicting soil erosion by water: a guide to conservation planning with the revised universal soil loss equation (RUSLE). U.S. Department of Agriculture. *Agriculture Handbook 703*. U.S. Government Printing Office, Washington, DC, 384 pp.

Schoumans, O.F. and Breeuwsma, A. 1997. The relation between accumulation and leaching of phosphorus: laboratory, field and modelling results. In H. Tunney et al., Eds. *Phosphorus*

Loss from Soil to Water. CAB International Press, Cambridge, England, pp. 361–363.

Schoumans, O.F., Breeuwsma, A., and de Vries, W. 1987. Use of soil survey information for assessing the phosphate sorption capacity of heavily manured soils. In W. van Duijvenbooden and H.G. van Waegeningh, Eds. *Proceedings of the International Conference on the Vulnerability of Soil and Groundwater to Pollutants*, Noordwijk aan Zee, the Netherlands, pp. 1079–1088.

Sharpley, A.N. 1995. Dependence of runoff phosphorus on extractable soil phosphorus. *J. Environ. Qual*. 24: 920–926.

Sharpley, A.N. (Ed.). 2000. *Agriculture and Phosphorus Management: The Chesapeake Bay*. CRC Press, Boca Raton, FL.

Sharpley, A.N., Daniel, T.C., Sims, J.T., and Pote, D.H. 1996. Determining environmentally sound soil phosphorus levels. *J. Soil Water Conserv*. 51: 160–166.

Sharpley, A.N., Kleinman, P.J.A., McDowell, R.W., and Weld, J.L. 2001. Assessing site vulnerability to phosphorus loss in an agricultural watershed. *J. Environ. Qual*. 30: 2026–2036.

Sharpley, A.N., Sims, J.T., and Pierzynski, G.M. 1994. Innovative soil phosphorus indices: assessing inorganic phosphorus. In J. Havlin et al., Eds. *Soil Testing: Prospects for Improving Nutrient Recommendations*. Soil Science Society America Special Publication 40, Soil Science Society America, Inc., Madison, WI, pp. 403–430.

Sharpley, A.N., Smith, S.J., Stewart, B.A., and Mathers, A.C. 1984. Forms of phosphorus in soils receiving cattle feedlot waste. *J. Environ. Qual*. 13: 211–215.

Sharpley, A.N. and Tunney, H. 2000. Phosphorus research strategies to meet agricultural and environmental challenges of the 21st century. *J. Environ. Qual*. 29: 176–181.

Sharpley, A.N., Weld, J.L., Beegle, D.B., Kleinman, P.J.A., Gburek, W.J., Moore, P.A., and Mullins, G. 2003. Development of phosphorus indices for nutrient management planning strategies in the U.S. *J. Soil Water Conserv*. 58: 137–152.

Sibbesen, E. and Sharpley, A.N. 1997. Setting and justifying upper critical limits for phosphorus in soils. In H. Tunney et al., Eds. *Phosphorus Loss from Soil to Water*. CAB International, Wallingford, England, pp. 151–176.

Simard, R.R., Beauchemin, S., and Haygarth, P.M. 2000. Potential for preferential pathways of phosphorus transport. *J. Environ. Qual*. 29: 97–105.

Simard, R.R., Cluis, D., Gangbazo, G., and Pesant, A. 1994. Phosphorus sorption and desorption indices for soils. *Commun. Soil Sci. Plant Anal*. 25: 1483–1494.

Sims, J.T. 2000. A phosphorus sorption index. In G.M. Pierzynski, Ed. *Methods of Phosphorus Analysis for Soil, Sediments, Residuals, and Waters*. Southern Regional Extension and Research Activity—Information Exchange Group (SERA—IEG) 17. North Carolina State University Press, Raleigh, NC, pp. 22–23.

Sims, J.T., Joern, B.C., and Simard, R.R. 1998. Phosphorus losses in agricultural drainage: historical perspective and current research. *J. Environ. Qual*. 27: 277–293.

Smith, S.J., Sharpley, A.N., Williams, J.R., Berg, W.A., and Coleman, G.A. 1991. Sediment-nutrient transport during severe storms. In S.S. Fan and Y.H. Kuo, Eds. *Fifth Interagency Sedimentation Conference*, March 1991, Las Vegas, NV. Federal Energy Regulatory Commission, Washington, DC, pp. 48–55.

Stout, W.L., Sharpley, A.N., and Pionke, H.B. 1998. Reducing soil phosphorus solubility with coal combustion by-products. *J. Environ. Qual*. 27: 111–118.

Syers, J.K., Harris, R.F., and Armstrong, D.E. 1973. Phosphate chemistry in lake sediments. *J. Environ. Qual*. 2: 1–14.

Torbert, H.A., Daniel, T.C., Lemunyon, J.L., and Jones, R.M. 2002. Relationship of soil test phosphorus and sampling depth to runoff phosphorus in calcareous and noncalcareous soils. *J. Environ. Qual*. 31: 1380–1387.

U.S. Environmental Protection Agency. 1993. *The Standards for the Use or Disposal of Sewage Sludge. Final Rules*. 40 CFR Parts 257, 402, and 503. EPA 822/Z-93/001. Fed. Regist. 58: 9248–9404.

U.S. Environmental Protection Agency. 2004. *Managing Manure Nutrients at Concentrated Animal Feeding Operations*. EPA-821-B-04-006. U.S. Environmental Protection Agency, Office of Water (4303T), Washington, DC. Available online at: http://www.epa.gov/guide/cafo/ (last verified November 10, 2004).

U.S. Geological Survey. 1999. *The Quality of Our Nation's Waters: Nutrients and Pesticides*. U.S. Geological Survey Circular 1225, 82 pp. USGS Information Services, Denver, CO. Available at: http://www.usgs.gov.

Vadas, P.A., Kleinman, P.J.A., and Sharpley, A.N. 2005. Relating soil phosphorus to dissolved phosphorus in runoff: a single extraction coefficient for water quality modeling. *J. Environ. Qual*. 34: 572–580.

van der Zee, S.E.A.T.M. and van Riemsdijk, W.H. 1988. Model for long-term phosphate reactions in soil. *J. Environ. Qual*. 17: 35–41.

Chapter 15
Electrical Conductivity and Soluble Ions

Jim J. Miller
Agriculture and Agri-Food Canada
Lethbridge, Alberta, Canada

Denis Curtin
New Zealand Institute for Crop and Food Research
Christchurch, New Zealand

15.1 INTRODUCTION

Saline soil is defined as one containing sufficient soluble salts to adversely affect the growth of most crop plants (Soil Science Society of America 2001). Soil salinization is a widespread limitation to agricultural production in dryland and irrigated soils throughout the world. Soil salinity reduces crop growth because depression of the osmotic potential of the soil solution limits water uptake by the plant (Corwin and Lesch 2003). Salinity may also cause specific ion toxicity or nutrient imbalances, and soil permeability and tilth may deteriorate if excessive amounts of Na accumulate on the soil's cation-exchange complex.

Soil salinity is generally measured by the electrical conductivity (EC) of a soil extract. A soil is considered saline if the EC of the saturation extract exceeds 4 dS m^{-1} at 25°C (Soil Science Society of America 2001). The main ions comprising soluble salts are cations Na, Ca, Mg; and anions SO_4, and Cl. Minor amounts of K, HCO_3, CO_3, and NO_3 may also be present. Soil sodicity is the accumulation of exchangeable Na, determined by measuring the exchangeable sodium percentage (ESP); or more commonly, estimated from the sodium adsorption ratio (SAR) of a soil–water extract. If the SAR of the saturation extract exceeds 13, the soil is considered sodic (Soil Science Society of America 2001). A more detailed classification scheme for sodic soils based on physical behavior (clay dispersibility), sodium, and salinity levels, has been proposed by Sumner et al. (1998).

Soil salinity or EC may be measured on the bulk soil (EC_a), in the saturation paste extract (EC_e), in water extracts at soil:water ratios of 1:1 to 1:5 ($EC_{1:1}$, $EC_{1:2}$, $EC_{1:5}$), or directly on soil water extracted from the soil in the field (EC_w) (Corwin and Lesch 2003). The EC_a or apparent EC has become one of the most reliable and frequently used measurements to characterize the spatial distribution of soil salinity at field scales. Field methods used to

measure EC_a include Wenner array or four-electrode, electromagnetic (EM) induction, and time domain reflectometry (TDR) (Rhoades and Oster 1986; Rhoades 1990, 1992). The EM induction method is the most popular of these three methods because measurements can be taken quickly over large areas, the large volume of soil measured reduces local-scale variability, and measurements are possible in relatively dry or stony soils because no contact is necessary between the soil and EM sensor (Hendrickx et al. 1992). The EM38 meter, and to a lesser extent, the EM31 meter (Geonics Ltd., Mississauga, Ontario) are most commonly used in soil investigations. The EM38 can measure EC_a to a depth of 1.2 m in the vertical mode and to 0.6 m in the horizontal mode. Mobile systems have been developed in conjunction with global positioning systems (GPS) to allow rapid salinity mapping of large fields (Rhoades 1992; Cannon et al. 1994). The EC_a readings from the EM38 meter are easily converted to EC_e values for different soil temperature, texture, and moisture conditions (Rhoades and Corwin 1981; Corwin and Rhoades 1982; McKenzie et al. 1989).

The EC of aqueous extracts of soil has traditionally been defined in terms of the EC of the saturated soil paste extract (EC_e) (U.S. Salinity Laboratory Staff 1954). Since the EC and concentration of solutes are affected by the soil:water ratio (Reitemeier 1946), this needs to be standardized to allow for consistent universal interpretation across soil texture classes. Exceptions include sandy soils, organic soils, and soils containing gypsum (Robbins and Wiegand 1990). Since it is impractical to routinely extract soil water at typical field-water contents, soil solution extracts must be made at higher than normal water contents. The saturated soil paste approximates the lowest soil:water ratio at which sufficient extract can be routinely removed for analysis of major salinity constituents. The saturated paste method relates more closely to the water holding capacity of the soil than do extracts at a fixed soil:water ratio. The water content of a saturation paste is about twice that at field capacity for most soils (Robbins and Wiegand 1990). Crop tolerance to salinity has traditionally been expressed in terms of EC_e.

Because the saturated paste method requires time and skill, laboratories are increasingly using fixed soil:water ratios (e.g., 1:1, 1:2, 1:5) when measuring soil EC and solute concentrations. However, cation exchange and mineral dissolution as the soil:water ratio widens (Reitemeier 1946) may lead to overestimation of EC and changes in solute composition. This is especially the case in samples containing gypsum, since Ca and SO_4 concentrations remain near-constant over a range of soil:water ratios while the concentration of the other ions decreases with dilution (Robbins and Wiegand 1990). Nevertheless, studies have shown good correlations between EC, Mg, K, and Cl in 1:2 extracts versus saturation paste extracts (Sonneveld and Van den Ende 1971); between EC, Na, Ca + Mg, and Cl in 1:1 and 1:2 extracts versus saturation paste extracts (Hogg and Henry 1984); and between EC, soluble cations (Na, Ca, Mg, K) and anions (SO_4, Cl) in 1:1 extracts versus saturation paste extracts (Pittman et al. 2004). In an analysis of soluble salt data from 87 laboratories in the United States, average residual standard deviation (RSD) was lowest for saturation paste extracts (13.4%), followed by 1:1 extracts (24.2%), and then 1:2 extracts (32.5%) (Wolf et al. 1996). Ninety percent of results for the 1:1 extracts were within ± 2 standard deviations of the mean value (acceptable laboratory performance) compared with 87% of the saturation paste extracts, and 84% of the 1:2 extracts.

Measurement of EC (EC_w) and solutes in the soil water extracted at field-water content is theoretically the best measure of salinity because it indicates the actual salinity level experienced by the plant root (Corwin and Lesch 2003). However, EC_w has not been widely used because it varies as soil–water content changes over time and so it is not a single-valued parameter (Rhoades 1978), and the methods for obtaining soil solutions are too laborious and

costly to be practical (Rhoades et al. 1999). Soil solutions can be obtained from disturbed samples by displacement, compaction, centrifugation, molecular adsorption, and vacuum or pressure extraction methods (Rhoades and Oster 1986). Soil solutions from undisturbed samples can be obtained using various suction-type samplers and salinity sensors (Corwin and Lesch 2003). Kohut and Dudas (1994) reported considerable variation between the properties of saturation paste extracts and immiscibly displaced solutions, with the saturation paste extract having lower EC values, cation concentrations (Na, Mg, K), and anion concentrations.

This chapter will focus mainly on laboratory methods used to measure EC of saturation paste extracts and extracts at fixed soil:water ratios, and on methods available to analyze soluble cations and anions in these extracts.

15.2 EXTRACTION

15.2.1 Saturation Extract (Janzen 1993; Rhoades 1996)

Procedure

1 Determine moisture content or weight of water in air-dry soil samples to be used. Weigh a subsample (30–50 g) of air-dry soil, oven-dry at 105°C, reweigh it, and determine weight of water in air-dry soil.

2 Weigh from 200 to 400 g of air-dry soil with known moisture content into a container with lid. Record the total weight of container and the soil sample. (The weight of soil used will depend on the volume of extract required. In general, approximately one-third of the water added is recovered in the saturation extract.)

3 Add deionized water while mixing to saturate the soil sample. At saturation, the soil paste glistens, flows slightly when the container is tipped, slides cleanly from the spatula, and readily consolidates after a trench is formed upon jarring the container.

4 Allow the sample to stand for at least 4 h and check to ensure saturation criteria are still met. If free water has accumulated on the surface, add a weighed amount of soil and remix. If the soil has stiffened or does not glisten, add distilled water and mix thoroughly.

5 Weigh the container with contents. Record the increase in weight, which corresponds to the amount of water added. (Alternatively, the amount of water added can be determined volumetrically by dispensing water from a burette.) Calculate the saturation percentage (SP) as follows:

$$\text{SP} = \frac{(\text{weight of water added} + \text{weight of water in sample})}{\text{oven-dry weight of soil}} \times 100 \qquad (15.1)$$

6 Allow the paste to stand long enough to establish equilibrium between the soil minerals and the water (at least 4 h, but preferably overnight). If a pH measurement is needed, the samples are then thoroughly mixed and their pH measured with an electrode and pH meter. The pH of the saturation paste is generally more meaningful than the pH of the saturation paste extract (Robbins and Wiegand 1990).

7 Transfer the wet soil to a Buchner funnel fitted with highly retentive filter paper. Apply vacuum and collect extract until air passes through the filter. Turbid filtrates should be refiltered.

8 Store extracts at 4°C until analyzed for EC and soluble cations and anions.

Comments

If possible, organic soils should be extracted without prior drying, which affects the SP. Organic soils may require an overnight saturation period and a second addition of water to achieve a definite saturation endpoint. For fine-textured soils, sufficient water should be added immediately to the soil sample with minimal mixing to bring the sample close to saturation. Do not over-wet coarse-textured soils. Free water on the soil surface after standing indicates oversaturation of coarse-textured soils.

15.2.2 Fixed Ratio Extracts (Janzen 1993; Rhoades 1996)

Procedure

1 Weigh appropriate amount of air-dry soil into a flask, add sufficient deionized water to achieve desired extraction ratio, and shake for 1 h.

2 Filter the suspension using highly retentive filter paper and store filtrate at 4°C before analysis.

Comments

The 1:1 and 1:2 soil:water extraction ratios are preferred over the 1:5 ratio. However, the 1:5 ratio is commonly used in Australian salinity work (Rengasamy et al. 1984; Sumner et al. 1998).

15.3 ANALYSES

15.3.1 Electrical Conductivity (EC_e, $EC_{1:1}$, $EC_{1:2}$, $EC_{1:5}$)

The total solute concentration in the various extracts is normally estimated by measuring EC. Although the relationship between conductivity and salt concentration varies somewhat depending on solution ionic composition, EC provides a rapid and reasonably accurate estimate of solute concentration. The procedure below is for modern EC meters that provide automatic temperature compensation, automatically adjust cell constant internal to the meter, and readout EC directly in μmho cm^{-1} or similar units. For older EC meters that do not have these three features, refer to Rhoades (1996) or American Public Health Association (1998).

Procedure

1 Make up standard 0.010 *M* KCl solution to automatically adjust cell constant internal to the meter. Dissolve 0.7456 g of reagent-grade anhydrous KCl and make up to 1 L using pure water (EC < 0.001 dS m^{-1}). This solution has an EC of 1.413 dS m^{-1} at 25°C and is suitable for most solutions when the cell constant is between 1 and 2. Use stronger or weaker KCl solutions to determine other cell constants.

2 Calibrate conductivity meter using standard KCl solution to automatically adjust cell constant internal to the meter. Rinse probe three times with 0.01 *M* KCl. Adjust temperature of a fourth portion to 25.0°C ± 0.1°C. Adjust temperature compensation dial to 0.0191 C^{-1}. With probe in standard KCl solution, adjust meter to read 1413 μmho cm^{-1} or 1.413 dS m^{-1}.

3 Read conductivity of extracts using EC probe and meter. Report results in SI units of dS m^{-1}.

Comments

Use an EC meter capable of measuring EC with an error not exceeding 1% or 1 μmho cm^{-1} or 0.001 dS m^{-1}. The basic unit of EC is mho cm^{-1}, and is too large for most natural waters (Bohn et al. 1979). A more convenient unit is mmho cm^{-1}. Units in the older literature, or when dealing with low salinity waters, have also been reported as μmho cm^{-1}. The SI unit of conductivity is siemens per meter (S m^{-1}), but results are generally reported as dS m^{-1}. Water with an EC of 0.0002 mho cm^{-1} has an EC of 0.2 mmho cm^{-1}, 200 μmho cm^{-1}, 0.020 S m^{-1}, or 0.2 dS m^{-1}.

15.3.2 Soluble Ion Concentrations—Overview and Comparison of Methods

Various methods are available to analyze soluble cations and anions in soil–water extracts (Table 15.1). Most laboratories have used flame-atomic absorption spectroscopy (FL-AAS) to analyze soluble cations, colorimetric methods on an autoanalyzer to determine Cl and SO_4, and the titrimetric method to analyze HCO_3 and CO_3.

FL-AAS is the preferred instrument for analyzing soluble cations where cost is a major limitation, number of samples will not be large, and extremely low detection limits are not required (Wright and Stuczynski 1996). Ion chromatography (IC) has been mostly used to analyze SO_4 and Cl in aqueous systems (American Public Health Association 1998) and soil extracts (Nieto and Frankenberger 1985a). Although IC can also determine soluble cations in soils (Basta and Tabatabai 1985; Nieto and Frankenberger 1985b), it is seldom used for cation analysis.

TABLE 15.1 Methods That Could Be Used to Measure Concentrations of Soluble Cations and Anions in Saturation Paste and Fixed Ratio Extracts

Method[a]	Na	K	Ca	Mg	Cl	SO_4	HCO_3/CO_3
FL-AAS	X	X	X	X			
IC	X	X	X	X	X	X	
ICP-AES	X	X	X	X	X		
Gravimetric					X	X	
Colorimetric					X	X	
Electrometric					X		X
Turbidimetric						X	
Titrimetric						X	X

[a] FL-AAS, flame-atomic absorption spectroscopy; IC, ion chromatography; ICP-AES, inductively coupled plasma-atomic emission spectroscopy.

Inductively coupled plasma-atomic emission spectroscopy (ICP-AES) has been increasingly used to analyze soluble Na, K, Ca, and Mg in soil extracts (Soltanpour et al. 1996; Wright and Stuczynski 1996) and waters (Vitale et al. 1991). In addition, ICP-AES can be used to determine nonmetals such as S and Cl in aqueous extracts (Richter et al. 1999). The advantages of ICP-AES are the plasma flux is extremely stable compared to conventional flames with FL-AAS, lower detection limits are possible for certain elements, and it has simultaneous multielement capability where 15 to 20 metals in a water sample can be measured in a 2 min period (Vitale et al. 1991). Disadvantages with ICP-AES are high initial cost, high operating costs (gases, power, consumables) (Wright and Stuczynski 1996), and possible severe matrix interferences from high concentrations of total dissolved solids, Na, Ca, Fe, and Al (Vitale et al. 1991).

Soluble Cations

Sodium has been most commonly analyzed using flame emission photometry at 589 nm, and K using flame photometry at 766.5 nm (Robbins and Wiegand 1990; Helmke and Sparks 1996). Pretreatment involves filtering out any solid particles. Calcium has been traditionally analyzed using AAS at 422.7 and 285.2 nm, respectively (Robbins and Wiegand 1990; Suarez 1996). Elements that form stable oxysalts (Al, Be, P, Si, Ti, V, Zr) can interfere with Ca and Mg analyses, but these can be removed by adding 0.1% to 1.0% lanthanum or strontium chloride to the samples.

Soluble Anions

Chloride in soil extracts is most commonly analyzed using potentiometric titration with $AgNO_3$, direct potentiometric analysis using a solid-state selective ion-electrode, automated colorimetric analysis (mercury thiocyanate method) on the autoanalyzer, or by IC (Frankenberger et al. 1996). The mercury thiocyanate method is widely used to determine Cl, but there is a trend toward IC and ICP-AES methods to avoid working with, and disposing of, Hg and cyanate. Gravimetry, turbidimetry, titrimetry, and colorimetry are the most common methods to analyze SO_4 in soil extracts; but the most sensitive and accurate methods for soil extract analyses are the methylene blue (MB) colorimetric and IC methods (Tabatabai 1996). In addition, the automated methylthymol blue method on the autoanalyzer is commonly used to measure SO_4 in aqueous systems (American Public Health Association 1998). This method can directly measure SO_4 in water, unlike the MB colorimetric method, which requires reduction of SO_4 to H_2S. However, similar to Cl, some laboratories are increasingly using IC and ICP-AES to measure SO_4 to avoid working with, and disposing of, thymol. Carbonate and bicarbonate ions are most commonly determined by titrating (titrimetric method) samples to an endpoint of pH 8.4 using phenolphthalein (CO_3) and then to pH 4.7 using methyl orange (HCO_3) (U.S. Salinity Laboratory Staff 1954). Alternatively, a pH probe and meter (electrometric method) can be used to determine the endpoints.

15.4 CALCULATIONS AND INTERPRETATION

15.4.1 Electrical Conductivity

Salt tolerance data for crops have been developed relating crop yield to EC_e. Data have been compiled for 69 herbaceous crops based on controlled tests in the United States and India (Maas 1990) for soils where chloride salts predominate. Salt tolerance data have also been compiled by Ayers and Westcott (1985). Crops grown on gypsiferous soils, such as found in the Canadian Prairies, will tolerate an EC_e of about 2 dS m^{-1} higher than those listed in Maas's table. In Canada, salt tolerance data based on field tests at specific locations have been

TABLE 15.2 Crop Response to Salinity Measured as Electrical Conductivity (EC) of the Saturation Extract

EC (dS m^{-1} at 25°C)	Crop response
0–2	Almost negligible effects
2–4	Yields of very sensitive crops restricted
4–8	Yields of most crops restricted
8–16	Only tolerant crops yield satisfactorily
>16	Only very tolerant crops yield satisfactorily

Source: Adapted from Bernstein, L., *Ann. Rev. Phytopathol.*, 13, 295, 1975.

reported by Holm (1983) and McKenzie (1988). More recently, research at Canada's salt tolerance testing facility (Steppuhn and Wall 1999) reported salt tolerance data for spring-sown wheats (Steppuhn and Wall 1997), as well as for canola, field pea, dry bean, and durum wheat crops (Steppuhn et al. 2001). General salinity effects are presented in Table 15.2.

15.4.2 Expressing Results of Soluble Ion Analyses

Soluble salt data are generally expressed in units such as meq L^{-1} ($mmol_c$ L^{-1}), mg L^{-1}, or mmol L^{-1}. If the results are to be expressed on a mass basis (e.g., mg of Ca per kg of soil), then the mass of air-dry soil, the mass of water added, and water already in the soil need to be known.

15.4.3 Ion Activities and Saturation Index Values

Soil solution data are generally reported as ion concentrations. However, it may sometimes be desirable to express the results as ion activities or thermodynamically effective concentration. The activity of an element, rather than its concentration, may be more closely related to plant response (Adams 1966) and general chemical reactivity (Freeze and Cherry 1979). Ion activity is the product of the ion concentration and the activity coefficient. There is an inverse relationship between the activity coefficient and ionic strength of the soil solution. As salinity or ionic strength of the aqueous solution increases, the activity coefficient decreases, resulting in a lower ion activity that can participate in chemical reactions. Increasing salinity also increases the solubilities of minerals via the ionic strength effect. Ion activities can be estimated from various geochemical models, and some ion activities (e.g., Cl, K) can be directly measured in solution extracts using ion-selective electrodes. Saturation index (SI) values for minerals can also be estimated from geochemical models by dividing the ion activity product of the solution species composing the mineral of interest by the solubility product constant (K_{sp}) of the mineral. SI values <0 indicate undersaturation or dissolution with respect to the mineral, $SI = 0$ indicates saturation or equilibrium between the solution and solid phase, and $SI > 0$ indicates supersaturation or precipitation of the mineral. However, SI values for evaporate minerals from saline soils were found to be poor predictors of minerals formed in evaporated soil solutions (Kohut and Dudas 1994).

15.4.4 Sodium Adsorption Ratio

The SAR, a useful index of the sodicity or relative sodium status of soil solutions, and aqueous extracts, or water in equilibrium with soil, is calculated as follows:

$$SAR = \frac{[Na^+]}{[Ca^{2+} + Mg^{2+}]^{0.5}} \tag{15.2}$$

where cation concentrations are in mmol L^{-1}.

Soils with SAR values greater than 13 are considered to be sodic (Soil Science Society of America 2001), although other critical values have been proposed (Bennett 1988; Sumner et al. 1998). Equation 15.2 is often referred to as the practical SAR (SAR_p), whereas theoretical SAR (SAR_t) values are calculated using the same equation but with free ion activities instead of concentrations (Kohut and Dudas 1994). Since exchangeable cations are difficult to measure in saline soils because of errors arising from anion exclusion or dissolution of slightly soluble minerals, the SAR of soil aqueous extracts has become the principal tool for diagnosing sodic soils (Bohn et al. 1979; Jurinak 1990).

15.4.5 Exchangeable Sodium Percentage

ESP can be estimated from SAR based on the linear equation:

$$\frac{\text{ESP}}{[100 - \text{ESP}]} = K_g\text{SAR} \tag{15.3}$$

where K_g is the Gapon selectivity coefficient. The value of K_g has traditionally been taken as 0.015 $(\text{mmol L}^{-1})^{-0.5}$ (U.S. Salinity Laboratory Staff 1954), though K_g can vary depending on soil organic matter content and pH (Curtin et al. 1995). In general, the affinity of soils for Na decreases as the contribution of organic matter to the cation-exchange capacity increases.

15.4.6 Potassium Adsorption Ratio

The potassium adsorption ratio (PAR) is calculated by substituting K for Na in Equation 15.2. Excessive K concentrations may interfere with crop uptake of other nutrients, decrease soil hydraulic conductivity and permeability, and increase soil erodibility (Hao and Chang 2003). Potassium concentrations are high in livestock manures, and K may become the dominant soluble cation in manured soils (Pratt 1984). Pratt (1984) reported that the long-term hazard of the use of manures on well-leached irrigated lands was more from K than from Na accumulation. Critical PAR values to define soils with excessive K remain to be determined.

15.4.7 Critical Calcium Ratio

A number of studies have shown that crop yield in a salt-affected soil is strongly influenced by the ratio of Ca to that of other cations in the soil solution (Howard and Adams 1965; Carter et al. 1979; Janzen and Chang 1987; Janzen 1993). Yield reductions are typically observed when the ratio of Ca:total cations is below approximately 0.10. This ratio can fall below the critical value in sodic soils (Carter et al. 1979) and in saline, gypsiferous soils where Ca concentrations are low because of the poor solubility of $CaSO_4 \cdot 2H_2O$ (gypsum) (Curtin et al. 1993).

REFERENCES

Adams, F. 1966. Calcium deficiency as a causal agent of ammonium phosphate injury to cotton seedlings. *Soil Sci. Soc. Am. Proc.* 30: 485–488.

American Public Health Association. 1998. In *Standard Methods for the Examination of Water and Wastewater*, 20th edn. APHA, Washington, DC, pp. 1–1207.

Ayers, R.S. and Westcott, D.W. 1985. Water quality for agriculture. FAO Irrigation and Drainage Paper 29 (Rev. 1). FAO, Rome, Italy.

Basta, N.T. and Tabatabai, M. 1985. Determination of exchangeable bases in soils by ion chromatography. *Soil Sci. Soc. Am. J.* 49: 84–89.

Bennett, D.R. 1988. Soil chemical criteria for irrigation suitability classification of Brown Solonetzic soils. *Can. J. Soil Sci.* 68: 703–714.

Bernstein, L. 1975. Effects of salinity and sodicity on plant growth. *Ann. Rev. Phytopathol.* 13: 295–312.

Bohn, H., McNeal, B., and O'Connor, G. 1979. *Soil Chemistry*. John Wiley & Sons, Toronto, ON, Canada.

Cannon, M.E., McKenzie, R.C., and Lachapelle, G. 1994. Soil salinity mapping with electromagnetic induction and satellite-based navigation methods. *Can. J. Soil Sci.* 74: 335–343.

Carter, M.R., Webster, G.R., and Cairns, R.R. 1979. Calcium deficiency in some Solonetzic soils of Alberta. *J. Soil Sci.* 30: 161–174.

Corwin, D.I. and Rhoades, J.D. 1982. An improved technique for determining soil electrical conductivity-depth relations from aboveground electromagnetic measurements. *Soil Sci. Soc. Am. J.* 46: 517–520.

Corwin, D.L. and Lesch, S.M. 2003. Application of soil electrical conductivity to precision agriculture: theory, principles, and guidelines. *Agron. J.* 95: 455–471.

Curtin, D., Selles, F., and Steppuhn, H. 1995. Sodium–calcium exchange selectivity as influenced by soil properties and method of determination. *Soil Sci.* 159: 176–184.

Curtin, D., Steppuhn, H., and Selles, F. 1993. Plant responses to sulfate and chloride salinity: growth and ionic relations. *Soil Sci. Soc. Am. J.* 57: 1304–1310.

Frankenberger, W.T. Jr., Tabatabai, M.A., Adriano, D.C., and Doner, H.E. 1996. Bromine, chlorine, and fluorine. In D.L. Sparks et al., Eds. *Methods of Soil Analysis, Part 3—Chemical Methods*. SSSA Book Series No. 5, SSSA and ASA, Madison, WI, pp. 833–868.

Freeze, R.A. and Cherry, J.A. 1979. *Ground Water*. Prentice-Hall, Englewood Cliffs, NJ.

Hao, X. and Chang, C. 2003. Does long-term heavy manure application increase salinity of a clay loam soil in semi-arid southern Alberta? *Agric. Ecosyst. Environ.* 94: 89–103.

Helmke, P.A. and Sparks, D.L. 1996. Lithium, sodium, potassium, rubidium, and cesium. In D.L. Sparks et al., Eds. *Methods of Soil Analysis, Part 3—Chemical Methods*. SSSA Book Series No. 5, SSSA and ASA, Madison, WI, pp. 551–574.

Hendrickx, J.M.H., Baerends, B., Raza, Z.I., Sadig, M., and Akram, M. 1992. Soil salinity assessment by electromagnetic induction of irrigated land. *Soil Sci. Soc. Am. J.* 56: 1933–1941.

Hogg, T.J. and Henry, J.L. 1984. Comparison of 1:1 and 1:2 suspensions and extracts with the saturation extract in estimating salinity in Saskatchewan soils. *Can. J. Soil Sci.* 64: 699–704.

Holm, H.M. 1983. *Soil Salinity, a Study in Crop Tolerances and Cropping Practices*. Saskatchewan Agriculture Publication No. 25M/3/83. Plant Industry Branch, Regina, SK, Canada.

Howard, D.D. and Adams, F. 1965. Calcium requirement for penetration of subsoils by primary cotton roots. *Soil Sci. Soc. Am. Proc.* 29: 558–562.

Janzen, H.H. 1993. Soluble salts. In M.R. Carter, Ed. *Soil Sampling and Methods of Analysis*. Lewis Publishers, Boca Raton, FL, pp. 161–166.

Janzen, H.H. and Chang, C. 1987. Cation nutrition of barley as influenced by soil solution composition in a saline soil. *Can. J. Soil Sci.* 67: 619–629.

Jurinak, J.J. 1990. The chemistry of salt-affected soils and waters. In K.K. Tanji, Ed. *Agricultural Salinity Assessment and Management*. ASCE, New York, NY, pp. 42–63.

Kohut, C.K. and Dudas, M.J. 1994. Comparison of immiscibly displaced soil solutions and saturated paste extracts from saline soils. *Can. J. Soil Sci.* 74: 409–419.

Maas, E.V. 1990. Crop salt tolerances. In K.K. Tanji, Ed. *Agricultural Salinity Assessment and Management*. ASCE, New York, NY, pp. 262–304.

McKenzie, R.C. 1988. Tolerance of plants to soil salinity. Soil and Water Program, 1987. Pamphlet

88–10. Alberta Special Crops and Horticultural Research Centre, Brooks, AB, Canada.

McKenzie, R.C., Chomistek, W., and Clark, N.F. 1989. Conversion of electromagnetic inductance readings to saturated paste extract values in soil for different temperature, texture, and moisture conditions. *Can. J. Soil Sci.* 69: 25–32.

Nieto, K.F. and Frankenberger, W.T. 1985a. Single ion chromatography. I. Analysis of inorganic anions in soils. *Soil Sci. Soc. Am. J.* 49: 587–592.

Nieto, K.F. and Frankenberger, W.T. 1985b. Single ion chromatography. II. Analysis of ammonium, alkali metals, and alkaline earth cations in soils. *Soil Sci. Soc. Am. J.* 49: 592–596.

Pittman, J.J., Kress, M.W., and Zhang, H. 2004. Comparison of two soil salinity extraction methods. Available at: http://ipec.utulsa.edu/Ipec/Conf2001/Conf/zhang_31.pdf (last verified March, 2006).

Pratt, P.F. 1984. Salinity, sodium, and potassium in an irrigated soil treated with bovine manure. *Soil Sci. Soc. Am. J.* 48: 823–828.

Reitemeier, R.F. 1946. Effect of moisture content on dissolved and exchangeable ions of soils of arid regions. *Soil Sci.* 61: 195–214.

Rengasamy, P., Greene, R.B.S., Ford, G.W., and Mehanni, A.H. 1984. Identification of dispersive behaviour and the management of red-brown Earths. *Aust. J. Soil Res.* 22: 413–431.

Rhoades, J.D. 1978. Monitoring soil salinity: a review of methods. In L.G. Everett and K.D. Schmidt, Eds. *Establishment of Water Quality Monitoring Programs*, Vol. 2. American Water Resource Association, San Francisco, CA, pp. 150–165.

Rhoades, J.D. 1990. Determining soil salinity from measurements of electrical conductivity. *Commun. Soil Sci. Plant Anal.* 21: 1887–1926.

Rhoades, J.D. 1992. Instrumental field methods of salinity appraisal. In G.C. Topp et al., Eds. *Advances in Measurement of Soil Physical Properties: Bringing Theory into Practice*. SSSA Special Publication No. 30. ASA, CSSA, and SSSA, Madison, WI, pp. 231–248.

Rhoades, J.D. 1996. Salinity: electrical conductivity and total dissolved solids. In D.L. Sparks et al., Eds. *Methods of Soil Analysis, Part 3—Chemical Methods*. SSSA Book Series No. 5, SSSA and ASA, Madison, WI, pp. 417–436.

Rhoades, J.D., Chanduvi, F., and Lesch, S. 1999. Soil salinity assessment: methods and interpretation of electrical conductivity measurements. FAO Irrigation and Drainage Paper No. 57. FAO-UN, Rome, Italy.

Rhoades, J.D. and Corwin, D.L. 1981. Determining soil electrical conductivity-depth relations using an inductive electromagnetic soil conductivity meter. *Soil Sci. Soc. Am. J.* 42: 255–260.

Rhoades, J.D. and Oster, J.D. 1986. Solute content. In A. Klute, Ed. *Methods of Soil Analysis*, 2nd ed. Agronomy Monograph 9, ASA and SSSA, Madison, WI, pp. 985–1006.

Richter, U., Krengel-Rothensee, K., and Heitand, P. 1999. In *New Applications for Nonmetals Determination by ICP-AES*. American Laboratory, Shelton, CT, pp. 170–171.

Robbins, C.W. and Wiegand, C.L. 1990. Field and laboratory measurements. In K.K. Tanji, Ed. *Agricultural Salinity Assessment and Management*. ASCE, New York, NY, pp. 201–219.

Soil Science Society of America. 2001. *Glossary of Soil Science Terms*. Soil Science Society of America, Madison, WI.

Soltanpour, P.N., Johnson, G.W., Workman, S.M., Benton Jones, J. Jr., and Miller, R.O. 1996. Inductively coupled plasma emission spectrometry. In D.L. Sparks et al., Eds. *Methods of Soil Analysis, Part 3—Chemical Methods*. SSSA Book Series No. 5, SSSA and ASA, Madison, WI, pp. 417–436.

Sonneveld, C. and Van den Ende, J. 1971. Soil analysis by means of a 1:2 volume extract. *Plant Soil* 35: 505–516.

Steppuhn, H., Volkmar, K.M., and Miller, P.R. 2001. Comparing canola, field pea, dry bean, and durum wheat crops grown in saline media. *Crop Sci.* 41: 1827–1833.

Steppuhn, H. and Wall, K.G. 1997. Grain yields from spring-sown Canadian wheats grown in saline rooting media. *Can. J. Plant Sci.* 77: 63–68.

Steppuhn, H. and Wall, K.G. 1999. Canada's salt tolerance testing laboratory. *Can. Agric. Eng.* 41: 185–189.

Suarez, D.L. 1996. Beryllium, magnesium, calcium, strontium, and barium. In D.L. Sparks et al., Eds. *Methods of Soil Analysis, Part 3—Chemical Methods*. SSSA Book Series No. 5, SSSA and ASA, Madison, WI, pp. 575–602.

Sumner, M.E., Rengasamy, P., and Naidu, R. 1998. Sodic soils: a reappraisal. In M.E. Sumner and R. Naidu, Eds. *Sodic Soils: Distribution, Properties, Management, and Environmental Consequences*. Oxford University Press, New York, NY, pp. 3–17.

Tabatabai, M.A. 1996. Sulfur. In D.L. Sparks et al., Eds. *Methods of Soil Analysis, Part 3—Chemical Methods*. SSSA Book Series No. 5, SSSA and ASA, Madison, WI, pp. 921–960.

U.S. Salinity Laboratory Staff. 1954. *Diagnosis and Improvement of Saline and Alkali Soils*. USDA Handbook No. 60. U.S. Government Printing Office, Washington, DC.

Vitale, R.J., Braids, O., and Schuller, R. 1991. Ground-water sample analysis. In D.M. Nielsen, Ed. *Practical Handbook of Ground-Water Monitoring*. Lewis Publishers, Chelsea, MI, pp. 501–540.

Wolf, A.M., Jones, J.B., and Hood, T. 1996. Proficiency testing for improving analytical performance in soil testing laboratories: a summary of results from the council's soil and plant analysis proficiency testing programs. *Commun. Soil Sci. Plant Anal*. 275: 1611–1622.

Wright, R.J. and Stuczynski, T.I. 1996. Atomic absorption and flame emission spectrometry. In D.L. Sparks et al., Eds. *Methods of Soil Analysis, Part 3—Chemical Methods*. SSSA Book Series No. 5, SSSA and ASA, Madison, WI, pp. 65–90.

III. SOIL CHEMICAL ANALYSES

Section Editors: Y.K. Soon and W.H. Hendershot

Chapter 16
Soil Reaction and Exchangeable Acidity

W.H. Hendershot and H. Lalande

McGill University

Sainte Anne de Bellevue, Quebec, Canada

M. Duquette

SNC-Lavalin

Montreal, Quebec, Canada

16.1 INTRODUCTION

Soil pH is one of the most common and important measurements in standard soil analyses. Many soil chemical and biological reactions are controlled by the pH of the soil solution in equilibrium with the soil particle surfaces.

Soil pH is measured in an aqueous matrix such as water or a dilute salt solution. Soil pH measured in water is the pH closest to the pH of soil solution in the field (this is true for soils with low electrical conductivity and for soils that are not fertilized), but is dependent on the degree of dilution (the soil to solution ratio). Measuring soil pH in a matrix of 0.01 *M* $CaCl_2$, as opposed to water, has certain advantages, but the addition of the salt does lower the pH by about 0.5 pH units compared to soil pH in water (Schofield and Taylor 1955; Courchesne et al. 1995). In soil correlation work, the use of pH in $CaCl_2$ is preferred because the measurement will be less dependent on the recent fertilizer history. Other methods for soil pH measurement, such as pH in 1 *M* KCl, are presented elsewhere (Peech 1965); these methods are not commonly used in Canada for routine analysis and are not included in this chapter.

16.2 SOIL pH IN WATER

When measuring soil pH in water, the main concern is that an increase in the amount of water added will cause an increase in pH; it is therefore important to keep the ratio constant and as low as possible. However, the supernatant solution must be sufficient to immerse the

electrode properly without causing too much stress when inserting the tip of the electrode into the soil and to allow the porous pin on the electrode to remain in the solution above the soil.

16.2.1 Materials and Reagents

1. pH meter: an appropriate instrument provided with two calibration points should be used.
2. Combined electrode: since the volume of soil is generally limited and the soil to solution ratio kept as low as possible, a combination electrode is a valuable asset.
3. 30 mL long form beakers (Pyrex or disposable plastic): beakers that have a narrow shape help to immerse the electrode in the supernatant without introducing the tip into the soil.
4. Stirrers: disposable plastic stirrers or glass rods can be used.

16.2.2 Procedure

1. Weigh 10 g of air-dried mineral soil (<2 mm) into a beaker and add 20 mL of double deionized (d.d.) water. For organic samples, use 2 g of soil in 20 mL of d.d. water. Record the soil to solution ratio used. Include duplicate quality control samples in each batch.
2. Stir the suspension intermittently for 30 min.
3. Let stand for about 1 h.
4. Immerse the electrode into the clear supernatant and record the pH once the reading is constant. Note: Both the glass membrane and the porous salt bridge must be immersed.

16.2.3 Comments

Soil samples containing high amounts of organic matter tend to form a thick dry paste when the ratio is kept the same as for mineral samples; therefore, a decreased ratio of sample to water must be accepted (1:5 or 1:10).

Two pH standards should be used to calibrate the pH meter; they must be chosen in accordance with the pH range expected for the soils analyzed (pH 4.0 and 7.0 or pH 7.0 and 10.0).

A large amount of a soil similar to the samples being analyzed should be kept as an indicator of the variability of pH results over time; duplicate subsamples of this quality control (QC) sample should be run with each batch of samples measured. Failure of the QC to fall within acceptable limits means that the whole batch should be reanalyzed.

16.3 SOIL pH IN 0.01 *M* $CaCl_2$

Standard measurement of soil pH in $CaCl_2$ is probably the most commonly used method to characterize soil pH. As mentioned by Peech (1965), Davey and Conyers (1988), and Conyers and Davey (1988), the use of $CaCl_2$ has some advantages for pH measurement: (1) the pH is not affected within a range of the soil to solution ratios used, (2) the pH is almost independent of the soluble salt concentration for nonsaline soils, (3) this method is a fairly good approximation of the field pH for agricultural soils, (4) because the suspension remains flocculated, errors due to the liquid junction potential are minimized, (5) no significant differences in soil pH determination are observed for moist or air-dried soil, and (6) one year of storage of air-dried soil does not affect the pH.

16.3.1 Material and Reagents

1. pH meter: an appropriate instrument provided with two calibration points should be used.
2. Combined electrode: since the volume of soil is generally limited and the soil to solution ratio kept to a minimum, a combination electrode is a valuable asset.
3. 30 mL long form beakers (Pyrex or disposable plastic): beakers that have a narrow shape help to immerse the electrode in the supernatant without introducing the tip of the electrode in the soil thus avoiding breakage.
4. Stirrers: disposable plastic stirrers or glass rods can be used.
5. Calcium chloride, 0.01 *M*: dissolve 2.940 g of calcium chloride dihydrate ($CaCl_2 \cdot 2H_2O$) with d.d. water in a 2 L volumetric flask. The electrical conductivity of the $CaCl_2$ solution must be between 2.24 and 2.40 mS cm^{-1} at 25°C.

16.3.2 Procedure

1. Weigh 10 g of air-dried mineral soil (<2 mm) or 2 g of organic soil into a 30 mL beaker and add 20 mL of 0.01 *M* $CaCl_2$. Note the soil to solution ratio used. Include duplicate quality control samples in each batch.
2. Stir the suspension intermittently for 30 min.
3. Let stand for about 1 h.
4. Immerse a combination electrode into the clear supernatant and record the pH once the reading is constant. Note: Both the glass membrane and the porous salt bridge must be immersed.

16.3.3 Comments

The pH and electrical conductivity of the $CaCl_2$ should be fairly constant, i.e., pH in the range of 5.5–6.5 and the electrical conductivity around 2.3 mS cm^{-1} at 25°C. If the pH is outside this range, it should be adjusted with HCl or $Ca(OH)_2$ solution. If the electrical conductivity is not within the acceptable range, a new solution must be prepared.

16.4 EXCHANGEABLE ACIDITY (EXPERT PANEL ON SOIL 2003)

In addition to bases (e.g., Ca, Mg, K, Na) there is also an amount of acidity that can be displaced from the exchange complex of a soil. The amount of this acidity is largely a function of soil pH and the exchange capacity. In most soils the exchangeable acidity will be composed of (i) exchangeable H^+, (ii) exchangeable Al as either Al^{3+} or partially neutralized Al-OH compounds such as $AlOH^{2+}$ or $Al(OH)_2^+$, and (iii) weak organic acids.

When a soil is limed, the exchangeable acidity is neutralized as the pH rises. Hence, exchangeable acidity is one measure of the amount of lime that will be needed to correct soil pH.

The method of Thomas (1982) used 1 *M* KCl as the displacing salt solution, whereas the Expert Panel on Soil (2003) proposes 0.1 *M* $BaCl_2$. Since the method proposed in this manual for measuring exchangeable cations uses 0.1 *M* $BaCl_2$, it seems more appropriate to use the same salt solution for measuring exchangeable acidity. Due to the lower concentration of the $BaCl_2$ solution, the amounts of some cations are lower than when the extraction is done with KCl; however, Jonsson et al. (2002) have determined regression equations that could be used to estimate the difference between the two extraction procedures.

16.4.1 Materials and Reagents

1 50 mL centrifuge tubes, a centrifuge capable of generating 5000 *g* and an end-over-end shaker (15 rpm).

2 Replacing solution, barium chloride 0.1 *M*: dissolve 24.43 g of $BaCl_2 \cdot 2H_2O$ with distilled deionized (d.d.) water and make to volume in a 1 L volumetric flask.

3 Aluminum complexing solution, 1 *M* sodium fluoride: dissolve 41.99 g of NaF in about 900 mL of d.d. water in a 1 L beaker and then titrate to the phenolphthalein endpoint with sodium hydroxide (NaOH). Transfer to a 1 L volumetric flask and make to volume.

4 Sodium hydroxide (NaOH), approximately 0.05 *M*, standardized.

5 Phenolphthalein solution: dissolve 1 g of phenolphthalein in 100 mL of ethanol.

16.4.2 Procedures

1 Weigh a 2.5 g sample of mineral soil or 2.0 g of organic soil into a 50 mL centrifuge tube, add 30 ml of 1 *M* $BaCl_2$ solution, and shake for 1 h. Centrifuge at 5000 *g* for 10 min. Transfer supernatant liquid to a 100 mL volumetric flask. Repeat by adding 30 mL aliquots of $BaCl_2$ solution, shaking, centrifuging, and decanting two more times, collecting all the supernatant in the same 100 mL volumetric. Make up to volume with $BaCl_2$ solution and mix. Filter the extract (Whatman No. 42 or equivalent) into a plastic bottle and store in a refrigerator prior to analysis.

2 To obtain exchangeable acidity, pipette 25 mL of the extract into a 100 mL polyethylene beaker, add 4 or 5 drops of phenolphthalein, and titrate with 0.05 *M* NaOH to the first permanent pink endpoint; record the volume of NaOH used as VA. (Note: A deep pink is too far.) Titrate a blank (25 mL of $BaCl_2$ solution) to the endpoint and record the amount VB. Centimoles of $BaCl_2$-extracted acidity per kg of soil (cmol(+) kg^{-1}) are calculated as shown below.

3 To determine exchangeable H^+ acidity, pipette 25 mL of the extract into a 100 mL polyethylene beaker, then add 2.5 mL of 1 *M* NaF, and titrate with 0.05 *M* NaOH to the first permanent pink endpoint (Va). Repeat with a blank sample of $BaCl_2$ (Vb).

16.4.3 Calculation

$$\text{cmol}(+)\ \text{kg}^{-1}\ \text{exchangeable acidity} = \frac{(\text{VA} - \text{VB}) \times \text{M(NaOH)} \times 100 \times \text{V}}{\text{g sample} \times \text{Vs}} \qquad (16.1)$$

cmol(+) kg^{-1} H^+ acidity is calculated using the same equation replacing VA by Va and VB by Vb, where VA or Va are the volumes of titrant used for the determination of exchangeable acidity and H^+, Vs is the volume of extract titrated and V is the total volume of extract collected, M(NaOH) is the concentration of the titrant, and g sample is the mass of soil extracted.

16.4.4 Comments

1 The procedure has been written using a pH indicator solution, which is our preference for manual titrations. However, if an automated titrator is used, the endpoint should be set at pH 7.8.

2 Exchangeable cations and exchangeable acidity (including H^+) can all be determined on the extracts obtained by this multiple washing procedure; this is the procedure recommended by the Expert Panel on Soil (2003). Although this extraction procedure is somewhat more complicated than the 0.1 *M* $BaCl_2$ method proposed in Chapter 18 (Section 18.2), it should give similar results.

REFERENCES

Conyers, M.K. and Davey, B.G. 1988. Observations on some routine methods for soil pH determination. *Soil Sci*. 145: 29–36.

Courchesne, F., Savoie, S., and Dufresne, A. 1995. Effects of air-drying on the measurement of soil pH in acidic forest soils of Quebec, Canada. *Soil Sci*. 160: 56–68.

Davey, B.G. and Conyers, M.K. 1988. Determining the pH of acid soils. *Soil Sci*. 146:141–150.

Expert Panel on Soil 2003. *Manual on Methods and Criteria for Harmonized Sampling, Assessment, Monitoring and Analysis of the Effects of Air Pollution on Forests. Part IIIa. Sampling and Analysis of Soil*. International co-operative

programme on assessment and monitoring of air pollution effects on forests. (www.icp-forests.org/pdf/manual3a.pdf, verified February 9, 2005)

Jonsson, U., Rosengren, U., Nihlgard, B., and Thelin, G. 2002. A comparative study of two methods for determination of pH, exchangeable base cations and aluminium. *Commun. Soil Sci. Plant Anal*. 33: 3809–3824.

Peech, M. 1965. Hydrogen-ion activity. In C.A. Black et al., Eds., *Methods of Soil Analysis. Part 2*. American Society of Agronomy, Madison, WI, pp. 914–926.

Schofield, R.K. and Taylor, A.W. 1955. The measurement of soil pH. *Soil Sci. Soc. Am. Proc*. 19: 164–167.

Thomas, G.W. 1982. Exchangeable cations. In A.L. Page et al., Eds., *Methods of Soil Analysis*. 2nd ed. American Society of Agronomy, Madison, WI, pp. 159–166.

Chapter 17
Collection and Characterization of Soil Solutions

J.D. MacDonald
Agriculture and Agri-Food Canada
Quebec, Quebec, Canada

N. Bélanger
University of Saskatchewan
Saskatoon, Saskatchewan, Canada

S. Sauvé and F. Courchesne
University of Montreal
Montreal, Quebec, Canada

W.H. Hendershot
McGill University
Sainte Anne de Bellevue, Quebec, Canada

17.1 INTRODUCTION

The soil solution plays a dominant role in the uptake of nutrients by plants, has direct impacts on other soil-living organisms, and under certain conditions it is the vector for the migration of dissolved and suspended materials through soils. We are defining the soil solution as the liquid phase of the soil present in the field. This definition precludes all methods in which salt solutions, or water, are added to a soil sample in the laboratory to simulate soil solutions as these procedures may be more accurately defined as soil extractions.

Studies of atmospheric deposition on soils and watersheds often incorporate monitoring of soil solution chemistry. In many cases lysimeters are used to collect soil solution on a regular basis to assess the ability of soils to absorb atmospherically deposited material and to control the release of nutrients and contaminants to ground and surface waters. Studies of macronutrient availability in forest soils may also use lysimeters as a means of measuring available nutrients. Examples of these types of studies are frequently found in the literature (Haines et al. 1982; Beier et al. 1992; Foster et al. 1992; Hendershot et al. 1992; MacDonald et al. 2003; Bélanger et al. 2004).

Field soil solution collectors fall into two main categories: zero-tension lysimeters and tension lysimeters. Both forms of lysimeters consist of an apparatus that is inserted into the soil column and collects water either moving through or held within soil capillaries. Recently, tension lysimetry has been further refined to include microlysimeters that can be used in the study of microenvironments in the soil. The development of microlysimeters shows potential for the study of the heterogeneity of soil solution chemistry at the microscale that is known to occur in soils, yet is poorly understood.

Methods of obtaining soil solution from fresh soil in the laboratory or directly in the field have been developed over the years (Heinrichs et al. 1995; Lawrence and David 1996). These techniques typically result in soil solutions with much higher concentrations of many ions, including dissolved organic matter, than those collected using field lysimeters (Ludwig et al. 1999) and some inconsistencies are observed in results depending on soil moisture content (Jones and Edwards 1993). Nonetheless, laboratory methods for sampling soil solutions from freshly sampled soils, e.g., centrifugation, miscible displacement, and syringe pressure, are useful tools for investigating plant nutrition and worthy of examination (Smethurst 2000).

We include a centrifugation method in this chapter; however, due to concerns raised about the influence of the force of extraction used to extract these solutions, we also propose a simple method developed by Ross and Bartlett (1990) that extracts solutions by applying pressure to moist soils packed in syringes in the field. Like the proposed centrifugation method, the syringe compression method is rapid and simple, and provides an alternative approach in cases where there is concern that centrifugation may overestimate concentrations of certain elements in solutions.

It is not always possible to carry out field studies. To approximate soil solution chemistry in the laboratory using bulk soil samples, we suggest a weak $CaCl_2$ (0.01 *M*) shake and centrifuge extraction (Quevauviller 1998) due to its simplicity and because it is an approach that is easily standardized. We also propose a column leaching extraction method that has been developed for bulk soil samples and has been shown to provide results similar to those obtained from zero-tension lysimeters (MacDonald et al. 2004a,b).

In this chapter, we provide five different procedures to separate the solution phase from the solid phase of soils. For *in situ* studies we propose zero-tension and tension lysimeters, as well as microlysimeters. To acquire solutions from fresh soil samples in the laboratory, we suggest centrifugation and syringe pressure techniques. The preferred methods of laboratory approximations of soil solutions, the column leaching method and weak $CaCl_2$ (0.01 *M*) extraction, can be found in Chapter 10. The applications, advantages, and disadvantages of the different methods of acquiring the soil solution from soils and the solution extractions described in Chapter 10 are summarized in Table 17.1.

17.2 ZERO-TENSION LYSIMETERS

Zero-tension lysimeters collect water moving through the soil profile only when the soil moisture content is greater than the field capacity. Several different designs of zero-tension lysimeters have been proposed. These include simple plates inserted in the soil, models with pierced plates installed in funnels, fiberglass wick-type collectors, and funnels filled with quartz sand. Our preferred design uses a plastic funnel filled with 2 mm quartz sand. Quartz sand is relatively unreactive and when the lysimeter is installed with a good contact between

TABLE 17.1 Advantages, Disadvantages, and Potential Applications of Different Sample Methods and Sampler Types Proposed in the Present Chapter and Chapter 10

Type	Advantages	Disadvantages	Potential applications
Zero-tension lysimeters	Samples can be collected from same soil column over many years Simple system with low maintenance	Does not collect solution except under wet conditions Requires long equilibration (many months to a year) period before samples are representative	Sample solutions that move through the soil with only gravitational potential Long-term solution chemistry monitoring Mobility of elements and fine particles in soils
Tension lysimeters	Samples can be collected from same soil column over many years Low maintenance	Requires long equilibration (many months to a year) period before samples are representative Variable results with soil moisture conditions Not efficient in surface organic horizons	Sample solutions held at potentials greater than gravitational potential Long-term soil solution monitoring Availability of elements in soils
Microlysimeters	Samples can be collected at very precise locations in soils Very high spatial resolution Samples can be repeatedly collected from the same location	High maintenance, fragile devices that are difficult to maintain under field conditions Requires equilibration period Very small (sub mL) solution volumes, hence need adapted analytical procedures and systems	Sample solutions in soil microenvironment, e.g., in the rhizosphere, the outer layer of peds, or in the coatings lining macropores Microscale heterogeneity of soil solutions, nutrient uptake, biogeochemical processes
Centrifugation (low-speed)	Samples can be extracted rapidly from fresh moist soils Reasonable alternative when lysimetry is not available or feasible	Lack of reproducibility of results as solution concentrations are dependent on moisture content of soils and time of sampling Small solution volumes and potential overestimations of certain anions and dissolved organic carbon (DOC)	Provides a single point in time extraction of capillary solutions present in soils Provides estimates of nutrient availability in soils

(continued)

TABLE 17.1 (continued) Advantages, Disadvantages, and Potential Applications of Different Sample Methods and Sampler Types Proposed in the Present Chapter and Chapter 10

Type	Advantages	Disadvantages	Potential applications
Syringe pressure	Samples can be extracted rapidly from fresh, moist soils Minimum disturbance of the soil during solution acquisition Reasonable alternative when lysimetry is not available or feasible	Lack of reproducibility of results as solution concentrations are dependent on moisture content of soils and time of sampling May yield small amounts of solution during dry periods, especially in coarse soil horizons (e.g., sandy loam) with low organic matter content	Provides a single point in time extraction of capillary solutions present in soils Provides estimates of nutrient availability in soils May avoid overestimation of certain elements associated with the force of extraction used in centrifugation
Column leaching	Soil samples can be collected and extracted relatively quickly Solution samples can be replicated from the same bulk soil sample	Estimates of field partitioning, but the method does not reproduce true field conditions Does not provide information on nutrients availability, N, or P	Estimation of field partitioning coefficients of divalent metals Adsorption–desorption studies
0.01 *M* $CaCl_2$ salt extraction, shake, and centrifuge	Solution samples can be replicated from the same bulk soil sample Easily standardized methodology	Solutions are often very different from field solutions collected from the same soil at the same site Cannot measure Ca^{2+} and Cl^-	Information about the chemistry of soil surfaces Adsorption–desorption and bioavailability studies

the quartz sand and the soil column above it, the soil–lysimeter interface has a large contact area. Capillary flow is not as likely to be interrupted and consequently the quartz sand design will tend to collect water under circumstances where the plate lysimeters and pierced plate lysimeters do not. The material is inexpensive relative to commercially available lysimeters. It is better to avoid using the fiberglass wick collectors since the fiberglass is more reactive than the quartz sand, and wick samplers have been suggested to cause modifications to soil solution chemistry (Goyne et al. 2000; Brahy and Delvaux 2001).

17.2.1 Materials

1 180 mm diameter polyethylene or polypropylene funnels

2 2 mm quartz sand

3 75 mm diameter (3″) or 50 mm (2″) acrylonitrile–butadiene–styrene (ABS) drain pipe about 2 m long

4 ABS end cap, and flexible cap for ABS drain pipe

5 19 mm (3/4″) plastic hose pipe fittings, one L-shaped and one straight

6 19 mm (3/4″) clear plastic hose with 3 mm (1/8″) thick wall and about 70 cm long

7 Epoxy two component cement and ABS solvent glue

8 Nylon screening 25 × 50 mm

9 5% (v/v) HCl

17.2.2 Preparation (Figure 17.1)

1 The funnels are prepared by gluing the L pipe fitting into the bottom with epoxy.

2 Cut the ABS drain pipe so that once it is buried it extends above the ground by at least 45 cm (to avoid rain-splash), or in areas of snow, at least the depth of normal snow cover. Attach the hard plastic ABS end cap to one end with either epoxy or ABS glue. Clearly label (paint or engrave) each pipe near the top.

3 Drill a hole in the ABS pipe and insert the straight hose fitting by coating with epoxy and hammering into place. The distance of the hose fitting from the base of the pipe is dependent on the desired volume of the lysimeter reservoir. For 75 mm ABS and a reservoir volume of 1 L, the hose fitting is installed at 23 cm from the bottom, whereas for 2 L, the distance is 45 cm. With 50 mm ABS, the distance for a 1 L reservoir volume is 51 cm. In shallow or rocky soil the 75 mm ABS is easier to install.

4 Acid wash the ABS pipe, the funnel, the clear plastic tube, and enough quartz sand to fill the funnel with 5% HCl. Rinse with deionized water until the electrical conductivity (EC) of wash water is equal or close to that of deionized water.

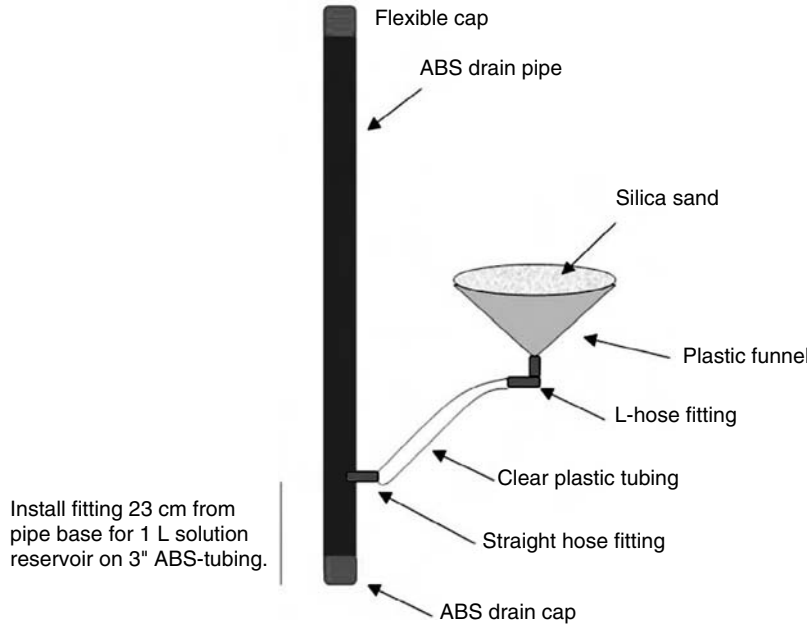

FIGURE 17.1. Schematic of zero-tension lysimeter constructed from ABS-tubing using a silica sand filled funnel as a solution collection device.

5 Place the quartz sand and the funnels with the clear tubing attached into separate plastic bags for transport to the field. The ABS tubes should have plastic taped over the hose fitting and the flexible plastic cap placed on the upper end.

17.2.3 Installation Procedure

1 Cordon off the location of the lysimeter station taking care to avoid walking on the area or contaminating it with soil or other debris.

2 Dig a pit downslope, if the site is not flat, approximately 1 m^2 to a depth greater than that at which the lowest lysimeter is to be installed. Separate the surface layers from the underlying soil so that they can be replaced in such a way that the site is disturbed as little as possible at the end of the installation.

3 Starting with the deepest lysimeter, dig a tunnel into the side of the pit under the delineated area. Use a spare funnel to make sure the tunnel is cut to the correct size to avoid contaminating the acid-washed funnels.

4 Insert the nylon screen into the L fitting, fill the funnel with the quartz sand, and carefully slide it into place making sure that it makes good contact with the soil above it. Press it into place, pack rocks under the L fitting at the bottom, and backfill carefully all around the under surface of the funnel. Ensure that the soil has been well packed around the lysimeter such that contact between the silica sand and the soil column is solidly maintained. Attach the clear tube to the hose fitting in the ABS tube.

5 Several lysimeters at different depths can be installed in the same pit; however, it must be ensured that funnels are placed such that each has an undisturbed cone of soil above it (often requiring a larger pit than anticipated). When all the lysimeters have been installed in the face of the pit, make sure that the clear tube slopes downward from the funnel to the ABS tube. Record the placement of the collectors. Carefully refill the pit.

17.3 TENSION LYSIMETERS

Porous cup tension lysimeters are inserted into the soil such that the porous surface is in contact with the capillaries of the soil column. When a vacuum is applied to the porous cup, solution is drawn out of the capillaries into the lysimeter reservoir. Tension lysimeters extract soil solutions that are maintained within the micropores of the soil and consequently may be immobile. The solutions that they extract have been observed to differ significantly from zero-tension lysimeters (Haines et al. 1982; Hendershot and Courchesne 1991).

Various types of tension lysimeters are available, differing in the type of porous cup that is inserted into the soil. The most commonly used tension lysimeters observed in the literature are the ceramic cup lysimeters that are installed from the surface. Recently, porous poly(tetrafluoroethene) or Teflon® cups have been developed for tension lysimeters to avoid the impact that the exchange capacity of ceramic cups can have on solution chemistry (Swenson 1997; Russell et al. 2004). We have used ceramic cups in the past; and we feel that after adequate stabilization periods in the soil, the ceramic cups are representative of macroelements in soil solution. However, the new Teflon-treated cups appear to be less reactive and are therefore a more reliable method to extract solutions under tension.

17.3.1 Preparation

The lysimeters should be cleaned following the manufacturer's recommendation or using the following procedure. Place the lysimeters in a container with 5% HCl and draw the solution through the porous cup and into the lysimeters using suction. Repeat this procedure three times and ensure that the PVC shaft above the porous cup is also effectively acid washed. Rinse with deionized water until the EC is close or equal to that of deionized water and is constant (may take up to 10 washings). When clean, place the lysimeters in clean plastic bags ready to go into the field.

17.3.2 Installation Procedure

1 Cordon off the location of the lysimeter station and take care to avoid walking on the area or contaminating it with soil or other debris.

2a Surface installation: place a plastic sheet with a hole the same diameter as the lysimeters on the soil surface to trap soil as it is excavated. Using an auger the same size as the lysimeters, dig a hole to the required depth.

i. Install the lysimeters and refill the hole around the lysimeter shaft with soil from the same soil horizon in which the lysimeters are installed. Carefully reconstruct the soil horizons above the lysimeters until the hole is filled.

ii. Ensure that the soil is tightly sealed around the lysimeter shaft so that preferential flow does not occur. In soils where good soil-to-lysimeter contact is difficult to establish, a slurry can be prepared using soil taken from the same depth as that of the lysimeter. A small amount of slurry is poured into the auger hole before installation of the lysimeter.

2b Pit installation: dig a pit approximately 1 m^2 to a depth greater than that at which the lowest lysimeter is to be installed.

i. Separate the surface layers from the underlying soil so that they can be replaced in such a way that the site is disturbed as little as possible at the end of the installation.

ii. Starting with the deepest lysimeter, dig a tunnel into the side of the pit under the delineated area equal in diameter to the porous cup. Carefully insert the porous cup ensuring good contact with the tunnel walls. Repeat for all lysimeter depths.

iii. Connect the vacuum and sample tubes. Record the position of the lysimeters and carefully refill the pit and replace the surface layers.

3 Apply a vacuum of 30–60 kPa to the lysimeter. It is recommended that a constant vacuum be maintained in the lysimeter. Constant vacuum systems will provide cumulative samples over periods between sample collections; however, systems that maintain a constant vacuum between sampling periods are expensive. It is also possible to use discontinuous systems and apply a vacuum for a period of several days before sample collection. It should be noted that discontinuous vacuum systems will provide samples that are representative of the short time period over which the vacuum is maintained.

17.4 SAMPLING SOIL SOLUTIONS FROM LYSIMETERS

Soil solutions can be extracted from lysimeter reservoirs using handheld vacuum pumps or peristaltic pumps ensuring that solutions are not cross-contaminated during collection.

1 Lysimeters should be completely emptied each time they are sampled. Record the total volume of solution removed from the lysimeter.

2 Solutions should be transferred immediately to coolers and maintained at 4°C in the dark for transport to the laboratory.

3 Once solutions are in the laboratory, set aside a small subsample of soil solutions (10–20 mL) and filter the rest of the solution using low vacuum through 0.4 μm polycarbonate filters. Solutions intended for analysis of elements that could be modified through contact with the air (nitrogen species for example) should be sealed in polycarbonate vials immediately after filtration, leaving little to no air space. A subsample for metal analysis should be acidified (0.2% HNO_3 v/v); trace metal-grade acid should be used if trace elements are to be analyzed.

4 Filtration will modify solution pH, therefore take the pH and EC of unfiltered subsamples of solutions immediately at room temperature.

17.4.1 Comments

1 Solutions should be drawn from the lysimeter reservoirs on a regular sampling schedule. Typically, lysimeter monitoring is carried out on a weekly, biweekly, or monthly schedule. Solutions that remain in the reservoir for long time periods may be modified, due to decomposition of dissolved organic carbon or the dissolution of suspended colloidal materials. Furthermore, it should be noted that lysimeter solutions, once separated from the soil, do not preserve *in situ* gas partial pressures and their associated chemistry.

2 The installation of lysimeters causes significant disturbance to the soil. Ensure that the lysimeters have stabilized before beginning a sampling regime. After installation, the pH and EC of lysimeter solutions should be monitored. Solutions cannot be considered representative of the soil chemistry until the pH and EC of the solution have stabilized. Stabilization periods for lysimeters can be long (6 months to 1 year). The pH and EC are good indicators of the stabilization point of soil solutions, but the initial data produced from lysimeters should be examined to ensure that stabilization of all elements of interest has occurred, particularly for nitrogen species.

17.5 MICROLYSIMETERS

The investigation of the microscale heterogeneity of soil materials, in particular the spatial variability in the liquid phase, requires a lysimeter system that is adapted to the characteristic small scale of the soil environment of interest. Göttlein et al. (1996) described a system for microscale lysimetry that allowed the monitoring of soil solution at a high spatial resolution to study gradients in concentrations of elements in the root–soil interface. The lysimeter unit consists of a 1 mm diameter ceramic cell with 1 μm pore size attached to 1.59 mm capillary tubing and connected to a vacuum device to extract the solution from the soil matrix. At a suction of 35 kPa, these cylindrical cups can sample solution in the volume of soil extending to a distance of $\geq$1 cm from their surface (Göttlein et al. 1996) and sample volumes range from 50 to 300 μL collected on a weekly basis at a suction of 40 kPa. Other microlysimeter designs have been proposed, but the cylindrical microlysimeters developed by Göttlein et al. (1996) are presented in this chapter because their design has been the most widely tested.

17.5.1 Materials

1 Ceramic capillaries with porosity of about 48%, 1 mm wide, and a suggested maximum pore size of 1 μm.

2 Polyetheretherketone (PEEK) tubing 1.59 mm (1/16″) wide, 50 mm long with an inside diameter (ID) of 0.75 mm; this tubing, used for high-pressure liquid chromatography (HPLC), is widely available (see Section 17.5.4).

3 Epoxy, two component cement.

4 PEEK tubing with an ID of 0.25 mm.

5 HPLC fitting to couple microlysimeters with 0.25 mm ID tubing.

6 Vacuum pump.

7 Vacuum chamber made of PVC with a Plexiglas cover with a connector to attach the vacuum pump (see Figure 17.2).

8 Sampling vials 2 mL in volume with caps.

9 Vial rack.

10 Plexiglas plate, rigid and about 20 mm thick, or rhizotron made of transparent Plexiglas plates.

11 Stainless steel rod with the same dimensions as the individual microlysimeters (1.59 mm wide × 50 mm long).

17.5.2 Construction and Preparation (Figure 17.2)

1 Cut the ceramic capillary into 12 mm long segments.

2 Seal the tip (exterior end) of the ceramic capillary by melting over a Bunsen burner to obtain a microceramic cup 10 mm long with a glass tip.

3 Cut the 0.75 mm ID PEEK tubing into 50 mm lengths.

4 Insert the 10 mm long ceramic cup 5 mm into the 0.75 mm ID PEEK tube.

5 Glue the ceramic cup to the PEEK tube using a two-part cement to complete assembly of the microlysimeter (Figure 17.2).

6 Clean the microlysimeters by drawing 5% HCl through the porous cup and into the tubing using suction. Repeat three times and then rinse with deionized water until the EC is close or equal to that of deionized water and is constant (may take up to 10 washings).

7 Fix a 0.25 mm ID PEEK tubing of the appropriate length to each of the microlysimeters.

8 Construct a vacuum chamber made of transparent Plexiglas and connected to a vacuum pump, as in Figure 17.2.

9 Install the vial rack and vials with caps in the vacuum chamber. Pierce holes in the caps.

10 Connect the tubing fixed to the microlysimeters to the vial through the hole pierced in the cap to avoid contamination and limit evaporation.

11 When clean, place all equipment in clean plastic bags ready to go into the field.

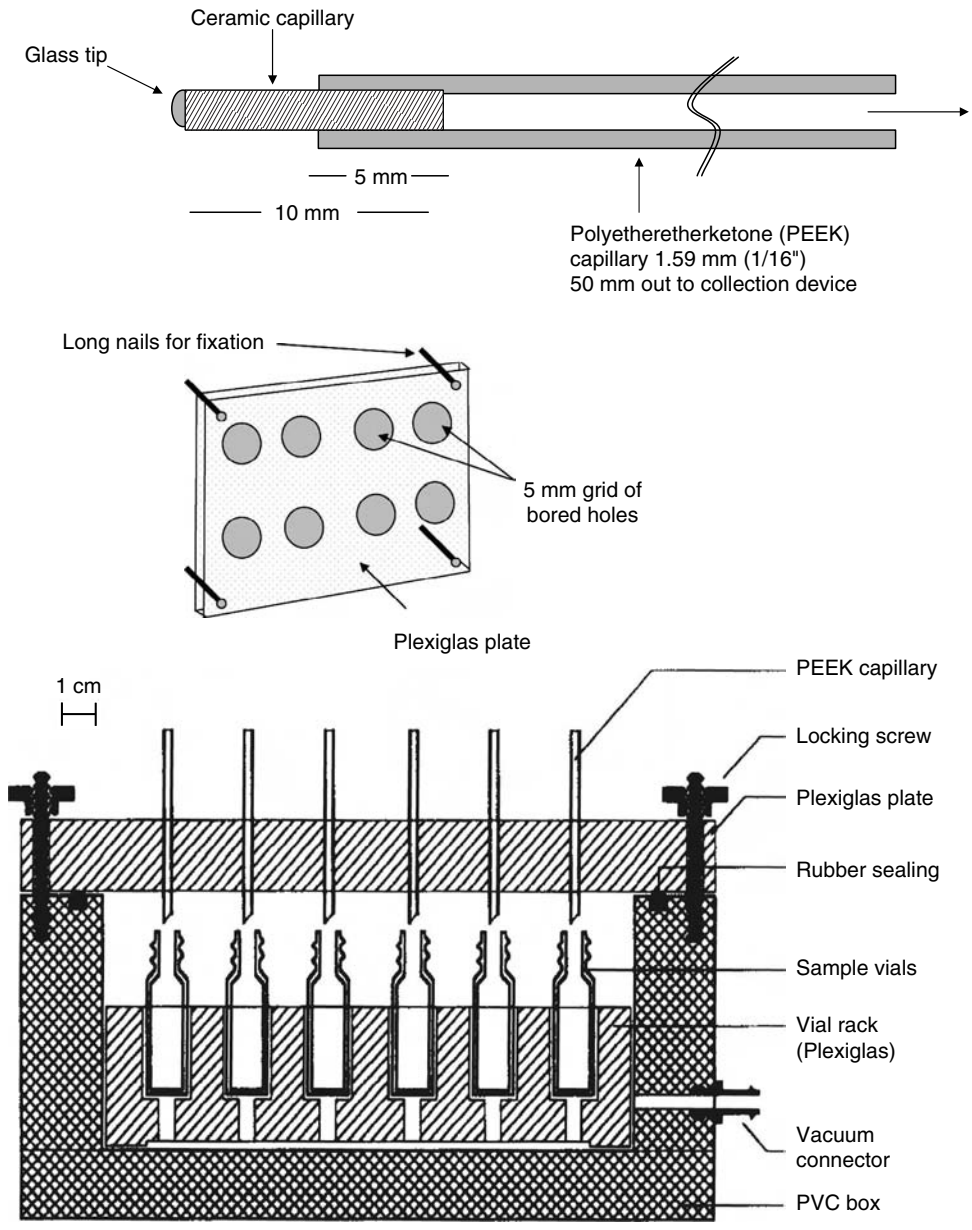

FIGURE 17.2. Schematic of microlysimeter suction device, support plate, and sample collection chamber for solutions from microlysimeters for microlysimeter installation. (From Göttlein, A., Hell, U., and Blasek, R., *Geoderma*, 69, 147, 1996. With permission.)

17.5.3 Installation Procedure (Figure 17.3)

1 Determine the location where the microlysimeters are to be installed in the soil, either on the face of a natural profile or in soil materials contained in a rhizotron.

2 At that point, make a hole in the soil having the dimension of the microlysimeters using the stainless steel rod.

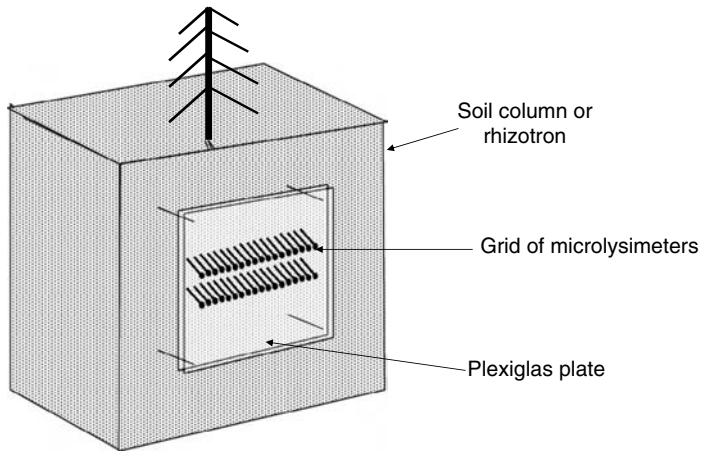

FIGURE 17.3. Installation of microlysimeters. (From Dieffenbach, A., Göttlein, A., and Matzner, E., *Plant Soil*, 192, 57, 1997. With permission.)

3 Remove the rod from the channel and insert the microlysimeter in the soil to the desired depth. Determine the exact position of the tip of the suction cup.

4 Use the Plexiglas plate, with holes the size of the microlysimeters (or one of the faces of the rhizotron), to support individual microlysimeters and to ensure their precise and constant position in the soil (Figure 17.3).

5 Apply a vacuum of 30–40 kPa to the microlysimeter. It is recommended that a constant vacuum be maintained in the lysimeter. It is also possible to use discontinuous systems and apply a vacuum for short time periods.

6 Like any lysimeter, microlysimeters should be allowed to equilibrate with the surrounding soil and the pH and EC of solutions should be monitored. Once pH and EC are stable, data from the microlysimeters can be considered to be representative of soil solution chemistry.

7 Solutions should be transferred immediately to coolers and maintained at 4°C in the dark for transport to the laboratory.

17.5.4 Comments

1 Microlysimeters solution volumes are small and can easily be contaminated, so the selection of tubing and container types is crucial to limit the adsorption of major ions, trace metals, or organic acids to surfaces during sampling and storage. Nylon or Teflon is recommended to reduce the sorption of trace metals whereas glass materials are suggested for dissolved organic substances.

2 The solution volumes collected with microlysimeters are in the range 50–300 μL. Therefore, analytical methods adapted to very small solution volumes are needed; for example, capillary electrophoresis (CE) (Göttlein and Blasek 1996) and other methods based on high-resolution inductively coupled plasma–mass

spectrometry (Puschenreiter et al. 2005) have been used to analyze major anions and cations in very small sample volumes.

17.6 SEPARATION OF SOIL SOLUTION IN THE LABORATORY

A variety of methods to obtain soil solutions in the laboratory from freshly sampled soils have been proposed. These methods include low- and high-speed centrifugation (Gillman 1976; Reynolds 1984) displacement methods with miscible (Adams 1974; Wolt and Graveel 1986) and immiscible liquids (Kinniburgh and Miles 1983) and positive air pressure in sealed cylinders (Lawrence and David 1996). These methods have been compared and generally produce similar results (Adams et al. 1980; Wolt and Graveel 1986; Elkhatib et al. 1987). In all cases, the key to obtaining minimally altered results is the processing of the sample shortly after collection. Centrifugation is recognized as a rapid and simple method. The method that we propose is the classic Davies and Davies (1963) method outlined in the previous edition of this book with the exception that we propose the use of high-density polyethylene (HDPE) frits to contain the soil in the syringe as opposed to glass wool.

Although centrifugation is probably the most commonly used method to separate the soil solution from the solid phase in the laboratory, Ross and Bartlett (1990), when comparing high-speed centrifugation with miscible displacement and syringe compression on forest floor and Bhf horizons, came to the conclusion that high-speed centrifugation should be avoided as it yields high H^+ and F^- concentrations as well as occasionally high Cl^-, SO_4^{2-}, and NO_3^- levels. The miscible displacement method, though it yielded large amounts of solution, was tedious and time-consuming. Since increased processing time inevitably results in increased alteration of soil solutions, we feel that the simple and relatively rapid syringe pressure technique is a good alternative for extracting solutions from moist soils. The syringe technique yielded solutions with similar chemistry to that of the miscible displacement method and the precision of analyses on duplicated samples was as good, or better, than the displacement or centrifugation methods.

17.6.1 Centrifugation (Davies and Davies 1963)

Material and Equipment

1. The centrifuge apparatus is a 60 mL syringe that has been cut to 55 mm and is used to contain the fresh moist soil sample and a solution cup that can be made by cutting the top of a 50 mL HDPE centrifuge tube (see Figure 17.4).
2. Centrifuge with horizontal rotors and 50 mL centrifuge shields or adaptors, preferably with refrigeration.
3. HDPE frits, 27 mm in diameter.
4. Small solution bottles (HDPE).
5. Parafilm.
6. 0.4 μm polycarbonate membrane filters.

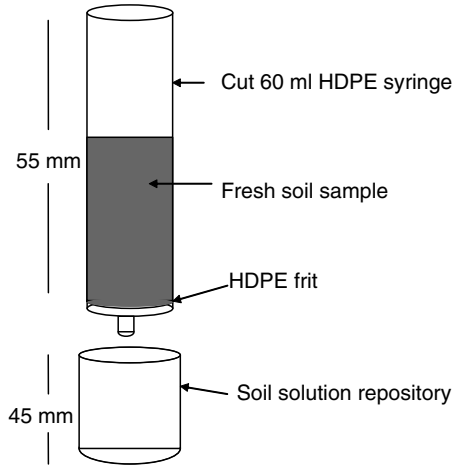

FIGURE 17.4. Schematic of device used to collect soil solutions during separation with a centrifuge. (From Soon, Y.K. and Warren, C.J., in M.R. Carter (Ed.), *Soil Sampling and Methods of Analysis*, Lewis Publishers, CRC Press, Boca Raton, Florida, 1993. With permission.)

Method

1 All plasticware in contact with soil samples and solutions should be acid washed (5% HCl) and rinsed with deionized water until the EC of the rinse water is close or equal to that of deionized water and is constant. If trace elements are of interest, plasticware should be prepared according to procedures outlined in Chapter 10.

2 Insert an HDPE frit into the base of the modified 60 mL syringe.

3 Place about 25 g of moist soil in the soil container (10 g if the soil is organic) and cover with parafilm to avoid evaporation during the centrifugation procedure. A subsample of each soil may be kept to determine the moisture.

4 Place the solution collecting cup under the syringe containing the soil in the centrifuge shield.

5 Centrifuge at a relative centrifugal force (RCF) of 1500 *g* at the bottom of the soil column for 30 min.

6 Set aside a portion of the solutions for analysis of pH and EC. Transfer the rest of the solution to clean storage bottles. Solutions may be further filtered using low vacuum through 0.4 μm polycarbonate filters before storage and analysis. A subsample for metal analysis should be acidified (0.2% HNO_3 v/v); trace metal-grade acid should be used if trace elements are to be analyzed.

7 Replicate all samples and include blanks.

17.6.2 Syringe Pressure Method (Ross and Bartlett 1990)

Materials

1. 60 mL polyethylene syringes
2. HDPE frits, 27 mm in diameter
3. Deionized H_2O
4. Compression apparatus (see Figure 17.5)
5. 0.4 μm polycarbonate membrane filters

Method

1. Wash HDPE frits with deionized H_2O.
2. Fit the HDPE frits into the bottom of the syringes.
3. Pack fresh soil samples (ideally within 12 h of sampling) into the polyethylene syringes.
4. Initiate pressure in the compression apparatus. Discard the first 5–10 drops. Reapply pressure for 15 min and collect remaining solution.
5. Set aside a portion of the solutions for analysis of pH and EC. Transfer the rest of the solution to clean storage bottles. Solutions may be further filtered using low vacuum through 0.4 μm polycarbonate filters before storage and analysis.

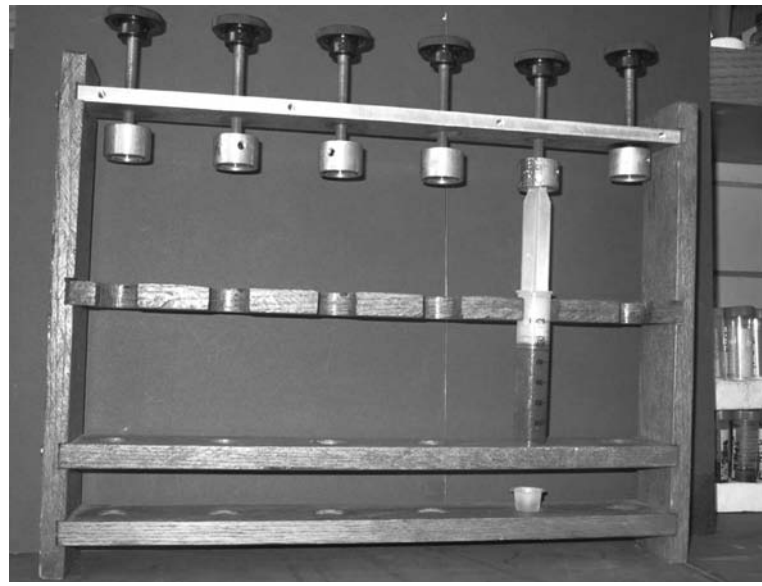

FIGURE 17.5. The compression device for the syringe pressure extraction method (photo courtesy of Don Ross).

A subsample for metal analysis should be acidified (0.2% HNO_3 v/v); trace metal-grade acid should be used if trace elements are to be analyzed.

6 Replicate all samples and include blanks.

17.6.3 Comments

1 In both methods, soil solutions should be separated from the soils as rapidly as possible after sampling. Soil samples should be kept cool (4°C in the dark but not frozen) before solutions are extracted. The time taken to separate the soil solution from the soil solid phase after the disturbance of taking the soil out of its natural environment is important in reducing sampling artifacts (Qian and Wolt 1990; Ross and Bartlett 1990).

2 The force of extraction during centrifugation can be calculated as the RCF:

$$\text{RCF} = \frac{(2\pi n)^2 r}{g} \tag{17.1}$$

where n is the number of revolutions per second, r the distance from the center of rotation in centimeters, and g is 981 cm s^{-2}. The RCF is related to the size of pores (assumed to be capillary pores) drained by the centrifugal force. For example, pores of 1 μm diameter are drained at an RCF of roughly 1000 g (Edmunds and Bath 1976; Soon and Warren 1993). The force of extraction used in the syringe pressure method should also be measured and recorded to ensure comparable and consistent results.

3 Both methods will produce low volumes of solution (1–3 mL) and may require several replicates bulked together to produce enough solution for a range of solution analyses. Bulked solutions should also be replicated to provide a clear idea of the reproducibility of the procedure (i.e., if three extracted solutions are bulked together to produce a 5–10 mL sample; six solutions should be extracted to produce a replicate).

REFERENCES

Adams, F. 1974. Soil solutions. In E.W. Carson, Ed. *The Plant Root and Its Environment*. University Press of Virginia, Charlottesville, VA, pp. 441–482.

Adams, F., Burmester, C., Hue, N.V., and Long, F.L. 1980. A comparison of column displacement and centrifuge methods for obtaining soil solutions. *Soil Sci. Soc. Am. J.* 44: 733–735.

Beier, C., Hansen, K., Gundersen, P., Andersen, B.R., and Rasmussen, L. 1992. Long-term field comparison of ceramic and poly(tetrafluoroethene) porous cup soil water samplers. *Environ. Sci. Technol.* 26: 2005–2011.

Bélanger, N., Coté B., Fyles, J.W., Courchesne, F., and Hendershot, W.H. 2004. Forest regrowth as the controlling factor of soil nutrient availability 75 years after fire in a deciduous forest of Southern Quebec. *Plant Soil* 262: 363–372.

Brahy, V. and Delvaux, B. 2001. Comments on Artifacts caused by collection of soil solution with passive capillary samplers. *Soil Sci. Soc. Am. J.* 65: 1571–1572.

Davies, B.E. and Davies, R.I. 1963. A simple centrifugation method for obtaining small samples of soil solution. *Nature* 198: 216–217.

Dieffenbach, A., Göttlein, A., and Matzner, E. 1997. In-situ soil solution chemistry in an acid forest soil as influenced by growing roots of Norway spruce (*Picea abies* [L.] Karst.). *Plant Soil* 192: 57–61.

Edmunds, W.M. and Bath, A.H. 1976. Centrifuge extraction and chemical analysis of interstitial waters. *Environ. Sci. Technol.* 10: 467–472.

Elkhatib, E.A., Hern, J.L., and Staley, T.E. 1987. A rapid centrifugation method for obtaining soil solution. *Soil Sci. Soc. Am. J.* 51: 578–583.

Foster, N.W., Mitchell, M.J., Morrison, I.K., and Shepard, J.P. 1992. Cycling of acid and base cations in deciduous stands of Huntington Forest, New York, and Turkey Lakes, Ontario. *Can. J. Forest Res.* 22: 167–174.

Gillman, G.P. 1976. A centrifuge method for obtaining soil solution. CSIRO Division of Soils, Report No. 16, Adelaide, Australia.

Göttlein, A. and Blasek, R. 1996. Analysis of small volumes of soil solution by capillary electrophoresis. *Soil Sci.* 161: 705–715.

Göttlein, A., Hell, U., and Blasek, R. 1996. A system for microscale tensiometry and lysimetry. *Geoderma* 69: 147–156.

Goyne, K.W., Day, R.L., and Chorover, C. 2000. Artifacts caused by collection of soil solution with passive capillary samplers. *Soil Sci. Soc. Am. J.* 64: 1330–1336.

Haines, B.L., Waide, J.B., and Todd, R.L. 1982. Soil solution nutrient concentrations sampled with tension and zero-tension lysimeters: report of discrepancies. *Soil Sci. Soc. Am. J.* 46: 547–555.

Heinrichs, H., Bottcher, G., Brumsack, H., and Pohlman, M. 1995. Squeezed soil-pore solutes—a comparison to lysimeter samples and percolation experiments. *Water Air Soil Poll.* 89: 189–204.

Hendershot, W.H. and Courchesne, F. 1991. Comparison of soil solution chemistry in zero tension and ceramic cup tension lysimeters. *J. Soil Sci.* 42: 577–583.

Hendershot, W.H., Mendes, L., Lalande, H., Courchesne, F., and Savoie, S. 1992. Soil and stream water chemistry during spring snowmelt. *Nord. Hydrol.* 23: 13–26.

Jones, D.L. and Edwards, A.C. 1993. Effect of moisture content and preparation technique on the composition of soil solution obtained by centrifugation. *Commun. Soil Sci. Plant Anal.* 24: 171–186.

Kinniburgh, D.G. and Miles, D.L. 1983. Extraction and chemical analysis of interstitial water from soils and rocks. *Environ. Sci. Technol.* 17: 362–368.

Lawrence, G.B. and David, M.B. 1996. Chemical evaluation of soil-solution in acid forest soil. *Soil Sci.* 161: 298–313.

Ludwig, B., Meiwes, K.J., Khanna, P., Gehlen, R., Fortmann, H., and Hildebrand, E.E. 1999. Comparison of different laboratory methods with lysimetry for soil solution composition—experimental and model results. *J. Plant Nutr. Soil Sci.* 162: 343–351.

MacDonald, J.D., Bélanger, N., and Hendershot, W.H. 2004a. Column leaching using dry soil reproduces solid-solution partitioning observed in zero-tension lysimeters. 2. Trace metals. *Soil Sed. Contam.* 13: 361–374.

MacDonald, J.D., Bélanger, N., and Hendershot, W.H. 2004b. Column leaching using dry soil reproduces solid-solution partitioning observed in zero-tension lysimeters. 1. Method Development. *Soil Sed. Contam.* 13: 375–390.

MacDonald, J.D., Johnson, D., Taillon, K., Hale, B., and Hendershot, W.H. 2003. Modeling the effect of trace metals emissions on boreal forest soils. *J. Human Ecol. Risk Assess.* 9: 723–747.

Puschenreiter, M., Wenzel, W.W., Wieshammer, G., Fitz, W.J., Wieczorek, S., Kanitsar, K., and Köllensperger, G. 2005. Novel micro-suction-cup design for sampling soil solution at defined distances from roots. *J. Plant Nutr. Soil Sci.* 168: 386–391.

Qian, P. and Wolt, J.D. 1990. Effects of drying and time of incubation on the composition of displaced soil solution. *Soil Sci.* 149: 367–374.

Quevauviller, P.H. 1998. Operationally defined extraction procedures for soil and sediment analysis. I. Standardization. *Trends Anal. Chem.* 17: 289–298.

Reynolds, B. 1984. A simple method for the extraction of soil solution by high speed centrifugation. *Plant Soil* 78: 437–440.

Ross, D.S. and Bartlett, R.J. 1990. Effects of extraction methods and sample storage on properties of solutions obtained from forested spodosols. *J. Environ. Qual.* 19: 108–113.

Russell, C.A., Kosola, K.R., Paul, E.A., and Robertson, G.P. 2004. Nitrogen cycling in poplar stands defoliated by insects. *Biogeochemistry* 68: 365–381.

Smethurst, P.J. 2000. Soil solution and other soil analyses as indicators of nutrient supply: a review. *Forest Ecol. Manag.* 138: 397–411.

Soon, Y.K. and Warren, C.J. 1993. Soil solution. In M.R. Carter, Ed. *Soil Sampling and Methods of Analysis*. Lewis Publishers, CRC Press, Boca Raton, FL, pp. 201–214.

Swenson, B. 1997. Unsaturated flow in a layered, glacial-contact delta deposit measured by the use of 18 O, Cl^- and Br^- as tracers. *Soil Sci.* 162: 242–253.

Wolt, J. and Graveel, J.G. 1986. A rapid routine method for obtaining soil solution using vacuum displacement. *Soil Sci. Soc. Am. J.* 50: 602–605.

Chapter 18
Ion Exchange and Exchangeable Cations

W.H. Hendershot and H. Lalande

McGill University

Sainte Anne de Bellevue, Quebec, Canada

M. Duquette

SNC-Lavalin

Montreal, Quebec, Canada

18.1 INTRODUCTION

Soils possess electrostatic charge as a result of atomic substitution in the lattices of soil minerals (permanent charge) and because of hydrolysis reactions on broken edges of the lattices and the surfaces of oxides, hydroxides, hydrous oxides, and organic matter (pH-dependent charge). These charges attract counterions (exchangeable ions) and form the exchange complex. The principle of the methods used to measure exchangeable ions is to saturate the exchange complex with some ion that forces the exchangeable ions already present on the charged surfaces into solution (law of mass action). Exchange capacity can then be calculated as the sum of the individual cations displaced from the soil (summation method); or the ion used to saturate the exchange complex, termed the index ion, can be displaced with a concentrated solution of a different salt and the exchange capacity calculated as the amount of the index ion displaced (displacement method).

The cation-exchange capacity (CEC) is a measure of the amount of ions that can be adsorbed, in an exchangeable fashion, on the negative charge sites of the soil (Bache 1976). The results are commonly expressed in centimoles of positive charge per kilogram of soil (cmol(+) kg^{-1}). Anion-exchange capacity (AEC) is expressed in terms of negative charge (cmol(−) kg^{-1}). In most Canadian soils, CEC is much greater than AEC; as a result, in most routine soil analysis, only CEC and exchangeable cations are measured.

The measurement of CEC is complicated by (1) errors due to the dissolution of soluble salts, $CaCO_3$, and gypsum ($CaSO_4 \cdot H_2O$); (2) specific adsorption of K and NH_4 in the interlayer position in vermiculites and micas (including illite or hydrous mica); and (3) the specific adsorption of trivalent cations such as Al^{3+} or Fe^{3+} on the surface of soil particles.

In general, the errors can be reduced by using a method of CEC determination that employs reagents of similar concentration and pH to those of the soil to be analyzed. For this reason a method buffered at pH 7.0 or 8.2 using relatively high concentrations of saturating and extracting solutions will decrease errors due to dissolution of $CaCO_3$ and gypsum in soils from arid regions (Thomas 1982). In acidic soils, solutions buffered at pH 7.0 or 8.2 are less effective in replacing trivalent cations and an unbuffered method will provide a better estimate of the CEC and exchangeable cations.

Methods using a solution at a buffered pH are commonly used with agricultural soils providing a measurement that is independent of recent fertilization and liming practices. For forest soils and other low pH soils, it is often preferable to measure CEC at the pH of the soil (see Section 18.2), thus providing a more accurate measure of exchangeable cations and CEC under field conditions.

Soils containing appreciable amounts of amorphous materials (e.g. podzols, some brunisols, and soils containing volcanic ash) will show order of magnitude changes in CEC and AEC as a result of acidification or liming. The method for measuring pH-dependent CEC and AEC (see Section 18.3) is provided for those who wish to study the variation in charge properties as a function of pH. The method provides more useful information than does the potentiometric titration method. Although both can be used to give an estimate of the point of zero charge (PZC), the pH-dependent CEC and AEC method also provides a measure of the absolute amount of exchange capacity at any pH.

18.2 EXCHANGEABLE CATIONS AND EFFECTIVE CEC BY THE $BaCl_2$ METHOD (HENDERSHOT AND DUQUETTE 1986)

The $BaCl_2$ method provides a rapid means of determining the exchangeable cations and the ''effective'' CEC of a wide range of soil types. In this method CEC is calculated as the sum of exchangeable cations (Ca, Mg, K, Na, Al, Fe, and Mn). The method is particularly applicable in forestry or studies of environmental problems related to soils where information on the CEC at the pH of the soil in the field is of prime importance. In soils with large amounts of pH-dependent cation-exchange sites, the value measured at pH 7 will be considerably higher than that measured by this method. Problems may arise if this method is used with saline soils containing very high levels of SO_4 since $BaSO_4$ will precipitate.

This method has been compared to other methods of determining the CEC at the soil pH and provides comparable results (Hendershot and Duquette 1986; Ngewoh et al. 1989). Barium is a good flocculant and is able to displace trivalent cations. The relatively low ionic strength of the equilibrating solution causes a smaller change in pH than do more concentrated salt solutions. This method is simple and rapid; however, it is recommended that exchangeable iron and manganese be measured since they may be more abundant in some acidic soils than other commonly considered cations such as potassium and sodium.

The Expert Panel on Soil (2003) proposes an alternative method that involves three successive additions of 0.1 *M* $BaCl_2$. The soil:solution ratio of 1:60 and the successive shaking and decanting steps result in higher measured values of exchangeable cation. However, the more complicated procedure is less suitable for routine laboratory analysis. Since the method proposed in this chapter for measuring exchangeable cations uses 0.1 *M* $BaCl_2$, it seems more appropriate to use the same salt solution for measuring exchangeable acidity.

Jonsson et al. (2002) have determined regression equations that could be used to estimate the difference between the two extraction procedures.

The results of this method are dependent on the soil:solution ratio used, with higher values of exchangeable cations obtained with smaller amounts of soil. The suggested weights of soil are a reasonable compromise. We have decreased the maximum amount of soil to be used from 3.0 to 1.5 g compared to the previously published methodology (Hendershot et al. 1993). If results are to be compared over time, or between sites, it is important that standard weights of sample be used.

18.2.1 Materials and Reagents

1 Centrifuge tubes (50 mL) with screw caps and low-speed centrifuge.

2 End-over-end shaker.

3 Barium chloride, 0.1 *M*: dissolve 24.43 g of $BaCl_2 \cdot 2H_2O$ with double deionized (d.d.) water and make to volume in a 1 L volumetric flask.

4 Standards of Ca, Mg, K, Na, Al, Fe, and Mn are prepared using atomic absorption reagent-grade liquid standards of 1000 mg L^{-1}. The matrix in the standards must correspond to the $BaCl_2$ concentration of the analyzed sample (diluted or non-diluted matrix).

5 Lanthanum solution, 100 mg L^{-1}: dissolve 53.5 g of $LaCl_3 \cdot 7H_2O$ in a 200 mL volumetric flask and make to volume (for analysis by atomic absorption spectrophotometry [AAS]).

6 Cesium solution, 100 g L^{-1}: dissolve 25.2 g CsCl in a 200 mL volumetric flask and make to volume (for analysis by AAS).

18.2.2 Procedure

1 Weigh out about 0.5 g of air-dry (<2 mm) organic soil or fine-textured soil to 1.5 g of coarse-textured soil into a 50 mL centrifuge tube. Record the exact weight of soil used to the nearest 0.001 g. Include blanks, duplicates, and quality control samples.

2 Add 30.0 mL of 0.1 *M* $BaCl_2$ to each tube and shake slowly on an end-over-end shaker (15 rpm) for 2 h.

3 Centrifuge (15 min, 700 *g*) and filter the supernatant (SN) with Whatman No. 41 filter paper.

4 Analyze the following cations in the SN solution with an AAS or any other suitable instrument: Ca, Mg, K, Na, Al, Fe, and Mn. Dilution (10- or 100-fold) is usually required for Ca, K, and Mg. The addition of 0.1 mL of La solution and 0.1 mL of Cs solution to a 10 mL aliquot of diluted extract is required for the determination of Ca, Mg, and K by AAS. (For detailed instructions on this and other aspects of analysis refer to the manual for your AAS.) Preservation

of samples by acidifying to 0.2% HNO_3 will prevent the loss of metals, such as Fe and Al.

5 If desired, the pH of the equilibrating solution can be measured on a separate aliquot of the $BaCl_2$ solution before filtering. Leakage of K from the KCl salt bridge of the pH electrode is significant and therefore the same aliquot cannot be used for K analysis and pH measurement.

18.2.3 Calculations

1 Exchangeable cations

$$M^+ \text{ cmol(+) kg}^{-1} = \text{C cmol(+) L}^{-1} \times (0.03 \text{ L/wt.soil g}) \times 1000 \text{ g kg}^{-1} \times \text{DF} \quad (18.1)$$

where M^+ is the concentration of an adsorbed cation, cmol(+) kg^{-1}, C is the concentration of the same cation measured in the $BaCl_2$ extract (cmol(+) L^{-1}), and DF is the dilution factor, if applicable.

2 Effective CEC

$$\text{Effective CEC cmol(+) kg}^{-1} = \Sigma M^+ \text{cmol(+) kg}^{-1} \quad (18.2)$$

3 Percent base saturation

$$\% \text{ BS} = (\Sigma \text{Ca} + \text{Mg} + \text{Na} + \text{K/Effective CEC}) \times 100 \quad (18.3)$$

18.2.4 Comments

1 A large amount of a soil similar to the samples being analyzed should be kept as an indicator of the variability of results over time; duplicate subsamples of this quality control (QC) sample should be run with each batch of samples measured. Failure of the QC to fall within acceptable limits means that the whole batch should be reanalyzed. Analysis of QC samples is also useful to verify that samples analyzed by different people in the same laboratory are comparable, and that results do not change from one year to another or from one batch of chemicals to another.

2 For the sake of simplicity AAS standards are usually made up by diluting 1000 mg L^{-1} concentrate to lower concentration values suitable for the range of the instrument being used. Calibrate the machine using the corresponding cmol(+) L^{-1} value; the conversion values are as follows:

1 mg L^{-1} Ca = 5.00×10^{-3} cmol(+) L^{-1};
1 mg L^{-1} Mg = 8.23×10^{-3} cmol(+) L^{-1};
1 mg L^{-1} K = 2.56×10^{-3} cmol(+) L^{-1};
1 mg L^{-1} Na = 4.35×10^{-3} cmol(+) L^{-1};
1 mg L^{-1} Al = 11.11×10^{-3} cmol(+) L^{-1};
1 mg L^{-1} Fe = 1.79×10^{-3} cmol(+) L^{-1};
1 mg L^{-1}Mn = 3.64×10^{-3} cmol(+) L^{-1}.

18.3 pH-DEPENDENT AEC–CEC (FEY AND LeROUX 1976)

In the literature, the method of Fey and LeRoux (1976) is often cited in research on pH-dependent CEC and AEC. The method is time-consuming because of the multiple saturation and pH adjustment steps. An alternative is to add different amounts of acid or base to the soil suspensions and measure the resulting pH. This method is preferred because there are fewer steps, and therefore it is faster with less chance of errors due to contamination or loss of soil. The only disadvantage with the modified procedure is that it is more difficult to obtain an even distribution of pH values than with the method of Fey and LeRoux, but this can be corrected by rerunning the analysis and adjusting the amounts of HNO_3 or $Ca(OH)_2$ added.

18.3.1 Materials and Reagents

1 Centrifuge tubes (50 mL) with screw caps and low-speed centrifuge.

2 Vortex centrifuge tube mixer and end-over-end shaker.

3 Calcium nitrate, 0.05 *M*: dissolve 23.62 g of calcium nitrate tetrahydrate ($Ca(NO_3)_2 \cdot 4H_2O$) with d.d. water in a 2 L volumetric flask.

4 Nitric acid, 0.1 *M*: dilute 6.3 mL of concentrated nitric acid (HNO_3) with d.d. water in a 1 L volumetric flask.

5 Calcium hydroxide, 0.05 *M*: dissolve 3.70 g of calcium hydroxide ($Ca(OH)_2$) with d.d. water in a 1 L volumetric flask, and filter through a Whatman No. 41 filter (a prefiltration step can be done using a glass microfiber filter [Whatman GF/C]).

6 Calcium nitrate, 0.005 *M*: dilute 200 mL of 0.05 *M* $Ca(NO_3)_2$ solution with d.d. water in a 2 L volumetric flask.

7 Potassium chloride, 1.0 *M*: dissolve 149.12 g of potassium chloride (KCl) with d.d. water in a 2 L volumetric flask.

8 Lanthanum solution, 100 mg L^{-1}: dissolve 53.5 g of $LaCl_3 \cdot 7H_2O$ in a 200 mL volumetric flask and make to volume (for analysis by AAS).

9 Cesium solution, 100 g L^{-1}: dissolve 25.2 g CsCl in a 200 mL volumetric flask and make to volume (for analysis by AAS).

18.3.2 Procedure

1 Weigh 20 empty 50 mL centrifuge tubes to the nearest 0.001 g (one set of 20 tubes for each soil sample to be analyzed).

2 Add 1.0 g subsamples of air-dry <2 mm soil to each tube and record the weight of the tube plus soil to the nearest 0.001 g. The analysis is done in duplicate for each targeted pH and corresponds to one pair of quality control samples per batch. If moist soil is used, start by weighing out four additional samples into small beakers and air-dry to determine the weight of moist soil equivalent to 1 g of air-dried soil.

3 Add 25 mL 0.05 *M* $Ca(NO_3)_2$ solution, cap the tubes, and shake for 1 h using an end-over-end shaker (15 rpm).

4 Centrifuge (10 min, 700 *g*) and discard SN by decantation. Be careful to avoid loss of soil during decantation.

5 Add a new 25 mL aliquot of 0.05 *M* $Ca(NO_3)_2$ solution to each tube. Then add 0, 0.25, 0.5, 1.0, or 2.5 mL of 0.1 *M* HNO_3 to tubes in duplicate, and finally add 0.25, 0.5, 1.0, or 2.5 mL of 0.05 *M* $Ca(OH)_2$ to the remaining tubes in duplicate. Add 1.0 mL of 0.1 *M* HNO_3 or 0.05 *M* $Ca(OH)_2$ to the quality control sample. A vortex mixer is useful to resuspend the soil after addition of the solution.

6 Cap and shake overnight on an end-over-end shaker.

7 Centrifuge (10 min, 700 *g*) and discard SN.

8 Resuspend the soil in 25 mL of 0.005 *M* $Ca(NO_3)_2$, centrifuge (10 min, 700 *g*), and discard SN.

9 Repeat step 8, but measure pH in a separate aliquot of the SN and keep the remaining SN for the analysis of Ca and NO_3 (after 100-fold dilution with d.d. water). Weigh tubes plus the soil and the interstitial soil solution.

10 Add 25 mL of 1.0 *M* KCl, shake for 1 h, and centrifuge (10 min, 700 *g*).

11 Keep this SN for determination of displaced Ca and NO_3. Dilute this KCl extract 10-fold with d.d. water.

12 Measure Ca by AAS in the 10-fold diluted KCl extract (saved in step 11) and in the 0.005 *M* $Ca(NO_3)_2$ equilibration solution (saved in step 9). The addition of 0.1 mL of La solution and 0.1 mL of Cs solution to a 10 mL aliquot of diluted extract is required for the determination of Ca by AAS. (For detailed instructions on this and other aspects of analysis refer to the AAS manual.)

13 Measure NO_3 in the undiluted KCl extract (saved in step 11) and in the diluted 0.005 *M* $Ca(NO_3)_2$ equilibration solution (saved in step 9).

18.3.3 Calculations

1 Residual Ca and NO_3

a. Volume of interstitial solution

Subtract the weight of the empty tube with the soil (step 2) from weight measured in step 9 to calculate weight of residual 0.005 *M* $Ca(NO_3)_2$ solution (Vol_{res}). Assume 1 g equals 1 mL.

b. Residual amount of Ca and NO_3(Ca_{res} and $NO_{3\ res}$):

$$Ca_{res}\ (mol) = Vol_{res}\ (mL) \times Ca_{sol}\ (mM) \times 0.001\ (L\ mL^{-1}) \times DF \qquad (18.4)$$

$$NO_{3\,res}\ (mol) = Vol_{res}\ (mL) \times NO_{3\,sol}\ (mM) \times 0.001\ (L\ mL^{-1}) \times DF \qquad (18.5)$$

where Ca_{sol} and $NO_{3\,sol}$ are the measured concentrations of calcium and nitrate in the 0.005 *M* $Ca(NO_3)_2$ wash solution saved in step 9 (units in m*M*) and DF is the dilution factor if applicable.

2 Total amount of calcium and nitrate ($Ca_tNO_{3\,t}$) in the KCl extract (including the residual):

$$\begin{aligned} Ca_t\ (mmol) &= Ca_{KCl}\ (mM) \times 25\ (mL) \times 0.001\ (L\ mL^{-1}) \times DF \\ NO_{3\,t}\ (mmol) &= NO_{3\,KCl}\ (mM) \times 25\ (mL) \times 0.001\ (L\ mL^{-1}) \times DF \end{aligned} \qquad (18.6)$$

where Ca_{KCl} and $NO_{3\,KCl}$ are the calcium and nitrate concentrations (m*M*) in the KCl extract saved in step 11; and DF is the dilution factor if applicable.

3 Calculation of the CEC and AEC:

$$CEC\ cmol(+)\ kg^{-1} = (Ca_t - Ca_{res})\ (mmol) \times 0.2\ (cmol(+)\ mmol^{-1}) \times 1000\ (g\ kg^{-1})/wt.soil\ (g) \qquad (18.7)$$

$$AEC\ cmol(-)\ kg^{-1} = (NO_{3\,t} - NO_{3\,res})\ (mmol) \times 0.1\ (cmol(-)\ mmol^{-1}) \times 1000\ (g\ kg^{-1})/wt.soil\ (g) \qquad (18.8)$$

4 Plot CEC and AEC as a function of final equilibrium pH measure in step 9 of Section 18.3.2.

18.4 EXCHANGEABLE CATIONS AND TOTAL EXCHANGE CAPACITY BY THE AMMONIUM ACETATE METHOD AT pH 7.0 (LAVKULICH 1981)

The method described here was developed by Lavkulich (1981) for standard analysis of a wide range of soil types. It involves fewer steps than some other similar methods such as that of McKeague (1978). Problems with this approach to measuring exchangeable cations and CEC have been discussed extensively in the literature (Chapman 1965; Bache 1976; Rhoades 1982; Thomas 1982) but we agree with the conclusion of Thomas (1982) that ''there is no evidence at the present time that cations other than NH_4^+ give results that are less arbitrary than those obtained using NH_4^+.''

Errors due to the dissolution of $CaCO_3$ and gypsum will result in an excess of Ca^{2+} being extracted by NH_4^+ and a decrease in the amount of NH_4^+ retained due to competition between Ca^{2+} and NH_4^+ during equilibration in the saturating step. In soils containing these minerals, exchangeable Ca will be too high and total CEC too low. The former problem can not easily be corrected (Thomas 1982); however, more accurate measurement of CEC in this type of soil can be obtained by using the method described by Rhoades (1982).

Fixation of K^+ and NH_4^+ in phyllosilicates can result in either an over- or underestimation of exchangeable K^+ when NH_4^+ is used as an extractant depending on whether the NH_4^+ moves through the interlayer positions replacing the K^+ or whether it causes the collapse of the edges preventing further exchange.

Compared to the other methods presented in this chapter, this method uses a larger sample size, which helps to decrease the sample to sample variability. Another advantage of this procedure is that there are no decantation steps that can cause the loss of sample, particularly in the case of organic soils.

The method described below can be used to measure either exchangeable cations and CEC or just exchangeable cations. In the latter case, the sum of exchangeable cations (including Al) could be used as an estimate of CEC. Due to the high pH of the extracting solution, the amount of Al measured will usually be lower than that displaced by $BaCl_2$ or KCl.

18.4.1 Materials and Reagents

1 Centrifuge tubes: 100 mL centrifuge tubes and stoppers.

2 Reciprocal shaker.

3 Buchner funnels (55 mm diameter) and 500 mL filtering flasks connected to low-pressure vacuum line.

4 Ammonium acetate, 1 *M*: dissolve 77.08 g of NH_4OAc with d.d. water and make to volume in a 1 L volumetric flask. Adjust pH to 7.0 with ammonium hydroxide or acetic acid.

5 Isopropanol.

6 Potassium chloride, 1 *M*: dissolve 74.6 g of KCl with d.d. water and make to volume in a 1 L volumetric flask.

7 Standard ammonium solution, 200 mg L^{-1} N: dissolve 0.238 g of $(NH_4)_2SO_4$ (dried for 3–4 h at 40°C) in about 100 mL of d.d. water and then dilute to volume in a 250 mL volumetric flask. Prepare diluted standards of 10, 20, 40, and 80 mg L^{-1} from the 200 mg L^{-1} stock.

8 Prepare Ca, Mg, K, and Na standards using 1 *M* NH_4OAc as the matrix.

18.4.2 Procedures

For Exchangeable Cations

1 a. For samples low in organic matter: weigh out 10.000 g of soil into a 100 mL centrifuge tube.

b. For samples high in organic matter: weigh out 5.000 or 2.000 g.

c. Prepare a blank and include a quality control sample.

2 Add 40 mL of 1 *M* NH_4OAc to the centrifuge tube. Stopper the tube and shake for 5 min on a reciprocal shaker (115 rpm). Remove tubes from shaker, agitate to rinse down soil adhering to the sides of the tube, and let stand overnight.

3 Shake tube again for 15 min. Prepare Buchner funnels with Whatman No. 42 filter paper and place them above 500 mL filtering flasks.

4 Transfer contents of the tube to the funnel with suction applied. Rinse the tube and the stopper with 1 *M* NH_4OAc from a wash bottle.

5 Wash the soil in the Buchner funnel with four 30 mL portions of 1 *M* NH_4OAc. Let each portion drain completely before adding the next, but do not allow the soil to become dry or cracked.

6 Transfer the leachate to a 250 mL volumetric flask; rinse the filtering flask with 1 *M* NH_4OAc and make up to volume with 1 *M* NH_4OAc. Mix well and save a portion of the extract for analysis of Al, Ca, Mg, K, and Na. Keep samples refrigerated prior to analysis.

For Total-Exchange Capacity (CEC)

1 Replace the funnels containing the ammonium-saturated soil onto the filtering flasks. To remove the residual NH_4OAc from the soil, wash the soil in the Buchner funnel with three 40 mL portions of isopropanol, again letting each portion drain completely before adding the next (turn off the suction after the last washing before the soil dries out). Discard the isopropanol washings and rinse the flask well with tap water followed by d.d. water.

2 Replace the funnels onto the flasks and leach the soil with four 50 mL portions of 1 *M* KCl, again letting each portion drain completely before adding the next. Transfer the leachate to a 250 mL volumetric flask. Rinse the filtering flask into the volumetric flask with d.d. water and make up to volume with d.d. water. Mix well and save a portion of the extract for analysis of NH_4 by auto analyzer.

18.4.3 Calculations

1 Exchangeable cations:

$$M^+ \text{ cmol(+) kg}^{-1} = \text{C cmol(+) L}^{-1} \times (0.25 \text{ L/wt soil g}) \times 1000 \text{ g kg}^{-1} \qquad (18.9)$$

where M^+ is the concentration of adsorbed cation, cmol(+) kg^{-1}; and C is the concentration of cation in the NH_4OAc extract (cmol(+) L^{-1}).

Note: see Section 18.2.4 for conversion of mg L^{-1} to cmol(+) L^{-1}.

2 CEC:

$$\text{CEC cmol(+) kg}^{-1} = (\text{mg L}^{-1}\ \text{N} \times (1 \text{ cmol(+)}/140 \text{ mg})) \times (0.25 \text{ L/wt.soil g}) \times 1000 \text{ g kg}^{-1} \qquad (18.10)$$

REFERENCES

Bache, B.W. 1976. The measurement of cation exchange capacity of soils. *J. Sci. Food Agric*. 27: 273–280.

Chapman, H.D. 1965. Cation exchange capacity. In C.A. Black et al., Eds., *Methods of Soil Analysis*. Agronomy 9, American Society of Agronomy, Madison, WI, pp. 891–901.

Expert Panel on Soil. 2003. *Manual on Methods and Criteria for Harmonized Sampling, Assessment, Monitoring and Analysis of the Effects of Air Pollution on Forests. Part IIIa. Sampling and Analysis of Soil*. International co-operative programme on assessment and monitoring of air pollution effects on forests. (www.icp-forests.org/pdf/manual3a.pdf, verified February 9, 2005)

Fey, M.V. and LeRoux, J. 1976. Electric charges on sesquioxidic soil clays. *Soil Sci. Soc. Am. J*. 40: 359–364.

Hendershot, W.H. and Duquette, M. 1986. A simple barium chloride method for determining cation exchange capacity and exchangeable cations. *Soil Sci. Soc. Am. J*. 50: 605–608.

Hendershot, W.H., Lalande, H., and Duquette, M. 1993. Ion exchange and exchangeable cations. In M.R. Carter, Ed., *Soil Sampling and Methods of Analysis*. Lewis Publishers, Boca Raton, FL, pp. 167–175.

Jonsson, U., Rosengren, U., Nihlgard, B., and Thelin, G. 2002. A comparative study of two methods for determination of pH, exchangeable base cations and aluminium. *Commun. Soil Sci. Plant Anal*. 33: 3809–3824.

Lavkulich, L.M. 1981. *Methods Manual, Pedology Laboratory*. Department of Soil Science, University of British Columbia, Vancouver, British Columbia, Canada.

McKeague, J.A. 1978. *Manual on Soil Sampling and Methods of Analysis*, 2nd ed. Canadian Society of Soil Science, AAFC, Ottawa, Ontario, Canada.

Ngewoh, Z.S., Taylor, R.W., and Shuford, J.W. 1989. Exchangeable cations and CEC determinations of some highly weathered soils. *Commun. Soil Sci. Plant Anal*. 20: 1833–1855.

Rhoades, J.D. 1982. Cation exchange capacity. In A.L. Page et al., Eds., *Methods of Soil Analysis*. Agronomy 9, 2nd ed. American Society of Agronomy, Madison, WI, pp. 149–157.

Thomas, G.W. 1982. Exchangeable cations. In A.L. Page et al., Eds., *Methods of Soil Analysis*. Agronomy 9, 2nd ed. American Society of Agronomy, Madison, WI, pp. 159–165.

Chapter 19
Nonexchangeable Ammonium

Y.K. Soon
Agriculture and Agri-Food Canada
Beaverlodge, Alberta, Canada

B.C. Liang
Environment Canada
Gatineau, Quebec, Canada

19.1 INTRODUCTION

It has been known since the early part of the twentieth century that some types of soils have the ability to bind ammonium (to certain types of clay minerals, predominantly vermiculite and mica types) such that it is not readily recovered by extraction with dilute acid or alkali (McBeth 1917). This form of ammonium is referred to as fixed or nonexchangeable ammonium (NEA). Barshad (1951) proposed that fixed ammonium should be defined as ammonium that is not displaceable with prolonged extraction or leaching of soil with potassium salt solution. The proportion of soil N as NEA usually does not exceed 10% in surface soils, but it can increase with depth of soil to over 50% in some subsoil horizons (Hinman 1964; Bremner 1965). Sources of NEA in the soil include (i) NH_4^+ produced by mineralization of organic matter, and added through ammoniacal-N fertilizer material, and (ii) indigenous or native fixed ammonium found in parent rock materials. There is considerable interest in quantifying the NEA pool because the amount in the soil through the rooting depth can be considerable, and its availability to plants and microorganisms has been demonstrated in many studies (Kudeyarov 1981; Scherer 1993; Green et al. 1994; Scherer and Werner 1996; Soon 1998). Soderland and Svensson (1976) estimated that there is as much fixed NH_4^+-N as there is plant biomass N in the global soil–plant system. The NEA pool in the soil has been found to be a slow-release reservoir of available ammonium when the exchangeable NH_4^+ levels become depleted (Drury and Beauchamp 1991). Ammonium fixation and release must be characterized and quantified especially in soils with a high ammonium fixation capacity (i.e., soils with a high vermiculite or mica content) in order to efficiently manage N use in soils for agronomic and environmental reasons.

Several procedures have been developed for the determination of NEA (Young and Aldag 1982); however, the most widely accepted method is that of Silva and Bremner (1966). Bremner et al. (1967) evaluated several methods and found that all except the Silva and Bremner method have defects: (i) the pretreatments used to eliminate interference by organic

N compounds were either inefficient, or led to gain or loss of NEA, and (ii) the procedures used to release NEA were not quantitative, or led to formation of NH_4-N from organic N compounds. According to Keeney and Nelson (1982), the Silva–Bremner method enjoys widespread use because of its apparent lack of defects; however, they cautioned that ''there is no way of establishing that the KOBr–HF method is accurate . . .''. Bremner et al. (1967) mentioned two possible problems associated with the determination of NEA: intercalated organic materials containing N that are released by the HF treatment and the presence of metal ammonium phosphates that are not soluble in KOBr or KCl but soluble in HF. Although either one will result in an overestimation of NEA, under normal conditions the contribution of either one would be remote or very slight. The Silva–Bremner procedure involves and comprises three basic steps: (i) removal of exchangeable NH_4^+ cations, (ii) oxidation and removal of organic matter including organic N, and (iii) extraction of NEA with HF and HCl, and determination of the released NH_4^+. A slightly and a substantially modified version of the method will be described below.

Zhang and Scherer (1998) proposed a simplified version (method A) of the Silva–Bremner method, which reduced the time involved and the amount of reagents used. A more substantial modification that eliminated entirely the HF extraction step (method B) was proposed by Nieder et al. (1996) and Liang et al. (1999): here, NEA in the soil residue left from the KOBr and KCl extractions is determined directly by dry combustion in an automated N-analyzer. This is a major advancement for the procedure because it eliminates the hazardous HF extraction step and the subsequent disposal of the HF, saving time in the process by reducing the number of steps in the procedure. Nitrogen isotope ratios can also be very conveniently determined when the N-analyzer is connected by a continuous flow linkage to a $^{15}N/^{14}N$ isotope ratio mass spectrometer.

19.2 POTASSIUM HYPOBROMITE–HYDROFLUORIC ACID EXTRACTION

The procedure described below is an adaptation of the Silva and Bremner (1966) method by Zhang and Scherer (1998). In this variation of the method, organic matter in the sample is oxidized in a centrifuge tube immersed in a boiling water bath (instead of a beaker heated with a hot plate) and subsequent extraction steps are carried out without having to transfer the residual soil to a centrifuge tube. Zhang and Scherer (1998) also found that heating in a microwave oven (1150 watt) at 50% of full power for 10 min gave similar NEA values to heating in a boiling water bath. Use of microwave ovens of different power would likely require adjustments by trial and error. The method using a boiling water bath is described.

19.2.1 Materials and Reagents

1 50 mL polypropylene or polyethylene centrifuge tubes with lined screw caps.

2 Potassium hydroxide (KOH) solution, 2 *M*: Dissolve 112.2 g of KOH in approximately 600 mL of distilled deionized water and, after cooling, dilute to 1 L volume.

3 Potassium hypobromite (KOBr) solution, prepared immediately before use: Add 6 mL of Br to 200 mL of 2 *M* KOH solution. Add the Br slowly (approximately 0.5 mL min^{-1}) with constant stirring, keeping the KOH solution cool in an ice-bath during the addition.

4 0.5 *M* Potassium chloride (KCl) solution: Dissolve 149 g of KCl in 600 mL of deionized water and make up to 4 L.

5 Hydrofluoric acid–hydrochloric acid solution (approximately 5 *M* HF–1 *M* HCl): With a 1 L measuring cylinder, transfer 1.5 L of deionized water to a 2 L graduated polypropylene or polyethylene conical flask. Add slowly, with continuous stirring, 167 mL of conc. HCl (specific gravity 1.19) followed by 325 mL of approximately 52% HF (approximately 31 *M*). Dilute with deionized water up to the 2 L mark and mix well.

6 Boiling water bath.

7 Reciprocal shaker.

19.2.2 Extraction Procedure

1 Weigh 0.5 g of finely ground soil (<60 mesh) in a 50 mL centrifuge tube. Record the weight of tube and soil. Add 10 mL of KOBr solution, and screw the cap on. Invert the centrifuge tube several times to mix up the contents, loosen screw cap, and leave it standing for 2 h. In the mean time, heat up the water bath.

2 Place the centrifuge tubes in a rack and then immerse the rack in a boiling water-bath so that the water level in the water bath exceeds the level of the KOBr solution in the centrifuge tube. Once the solution in the centrifuge tubes starts to boil, allow it to continue boiling for 10 min.

3 Remove the tubes and allow the contents to cool and settle. If necessary, centrifuge at 1000 *g* for 5 min.

4 Decant and discard the clear supernatant solution.

5 Add 30 mL of 0.5 *M* KCl, suspend the soil by shaking for 5 min, and centrifuge at 1000 *g* for 5 min. Decant the clear supernatant solution.

6 Repeat step 5 two more times.

7 Weigh the centrifuge tube and soil. The increase over the initial weight (in step 1) is taken to represent the volume of KCl retained by the soil. This liquid volume has to be added to the acid reagent volume added in step 8 when calculating mg kg^{-1} soil of NEA.

8 Add 10 mL of 5 *M* HF–1 *M* HCl working solution and shake for 24 h on a reciprocal shaker at 120 cycles min^{-1}. If the sample contains carbonates, allow the evolved CO_2 to escape before starting the overnight shaking.

9 Centrifuge at 1000 *g* for 5 min. Decant the clear supernatant solution into a plastic vial for subsequent NH_4-N determination.

19.2.3 Determination of Extracted NH_4-N

The original Silva–Bremner method determines nonexchangeable NH_4-N in the acid extractant by steam distillation and subsequent titrimetry. However, colorimetric determination using the development of indophenol has been used by Doram and Evans (1983) and Soon (1998). A manual procedure is outlined below, which is easily adaptable for automated analysis. The autoanalyzer method outlined in Chapter 6 for exchangeable NH_4-N determination or the procedure described by Kempers and Zweers (1986) can be readily adapted for analysis of NEA.

Reagents

Unless specified otherwise, all reagents used must be of analytical grade.

1. Trisodium citrate solution: Dissolve 20.0 g of $Na_3C_6H_8O_7 \cdot 2H_2O$ in 700 mL of deionized water. Dissolve 10.0 g of NaOH in deionized water and dilute to 700 mL. Combine the citrate and NaOH solution (reagent A).

2. Salicylate–nitroprusside reagent: Dissolve 18.0 g of sodium salicylate ($HOC_6H_4CO_2Na$, 2-hydroxybenzoic acid, sodium salt) in 250 mL of water. Dissolve 0.20 g of sodium nitroprusside ($Na_2Fe(CN)_5NO \cdot 2H_2O$) in 250 mL of water. Combine the two reagents and store in a brown bottle (reagent B).

3. Alkaline hypochlorite solution: Dissolve 1.5 g of NaOH in 50 mL of deionized water, add 8 mL of sodium hypochlorite (5%–5.25% NaOCl), and dilute to 100 mL (reagent C). Prepare fresh as needed.

4. Ammonium standard solution: 0, 5, 10, 15, 20, and 25 μg NH_4-N mL^{-1} in 5 *M* HF–1 *M* HCl prepared by dilution of 1000 mg N L^{-1} stock solution.

Procedure

1. Pipette 0.2 mL of the HF–HCl soil extract or ammonium standard solutions (containing up to 5 μg NH_4-N) into a 16 mm × 125 mm culture tube.

2. Add 7 mL of reagent A and mix immediately.

3. Add 2 mL of reagent B and mix immediately.

4. Add 0.5 mL of reagent C and mix immediately.

5. Immediately cover with a dark colored plastic sheet and leave for 60 min for color to develop.

6. Measure absorbance of standard and test solutions at 660 nm using 1 cm cuvette.

7. The concentrations of NH_4-N in the test solutions are read off the calibration curve, either manually or by the processor in the spectrophotometer.

8 Results can be calculated as follows:

$$\text{mg NEA kg}^{-1}\text{soil} = \mu\text{g } NH_4\text{-N per mL extract} \times (10 + \text{increase in weight in step 7 of Section 19.2.2}) \times F/\text{weight of soil} \quad (19.1)$$

where F is the dilution factor if dilution of the extract is required, and weight is measured in grams.

Comments

1 A final solution pH of about 13 will result in maximum color development. The advantages of salicylate as a substitute for phenol are increased sensitivity, lower toxicity, and increased stability (Kempers and Zweers 1986). Sodium citrate was found to be a better complexing agent for removing interfering elements than either EDTA or potassium sodium tartrate (Willis et al. 1993).

2 If the automated procedure is to be used, the following steps should be taken to minimize the slow corrosion of glass elements of the analytical cartridge. An analytical cartridge with dialyzer is used to further dilute the fluoride concentration in the test solution. The wash solution used need not contain hydrofluoric acid, and this does not influence the baseline: its acidity is maintained using 6 *M* HCl.

19.3 POTASSIUM HYPOBROMITE–DRY SOIL COMBUSTION METHOD

This major modification of the Silva and Bremner (1966) method was proposed by Nieder et al. (1996). However, the procedure gained greater prominence only after more extensive testing and validation by Liang et al. (1999). The method follows the Silva–Bremner method from the oxidation and removal of organic materials through the removal of exchangeable NH_4^+ cations. It is assumed that any NH_4^+ not removed from the soil at this stage would be nonexchangeable or fixed. This N fraction is then determined by dry (Dumas) combustion of the sample using an automated N-analyzer. Liang et al. (1999) showed that dry combustion recovered 100% of fixed NH_4^+ and gave results similar to those obtained using the full Silva–Bremner method. The coefficient of variation for 17 soils was 6.4% for the full Silva–Bremner method and 2.0% for the modified version.

19.3.1 Materials and Reagents

1 50 mL polypropylene or polyethylene centrifuge tubes with lined screw caps.

2 Potassium hydroxide (KOH) solution, 2 *M*: Dissolve 112.2 g of KOH in approximately 600 mL of distilled deionized water and, after cooling, dilute to 1 L volume.

3 Potassium hypobromite (KOBr) solution, prepared immediately before use: Add 6 mL of Br to 200 mL of 2 *M* KOH solution. Add the Br slowly (approximately 0.5 mL min^{-1}) with constant stirring, keeping the KOH cool in an ice-bath during the addition.

4 0.5 *M* Potassium chloride (KCl) solution: Dissolve 149 g KCl in 600 mL of deionized water and make up to 4 L.

5 Boiling water bath.

6 Reciprocal shaker.

19.3.2 Procedure

1 Weigh 0.5 g of finely ground soil (100 mesh) into a centrifuge tube. Record the weight of tube and soil. Add 10 mL of KOBr solution and screw the cap on. Invert centrifuge tube several times to mix up contents, loosen screw cap, and allow to stand for 2 h. In the mean time, heat the water bath.

2 Place the centrifuge tubes in a rack and then immerse the rack in a boiling water bath so that the water level in the water bath exceeds the level of the KOBr solution in the centrifuge tube. Once the solution in the centrifuge tubes starts to boil, allow it to continue boiling for 10 min.

3 Remove the tubes and allow the contents to cool and settle. Centrifuge at 1000 *g* for 5 min if necessary.

4 Decant and discard the clear supernatant solution.

5 Add 30 mL of 0.5 *M* KCl, suspend the soil by shaking for 5 min, centrifuge at 1000 *g* for 5 min. Decant the clear supernatant solution.

6 Repeat step 5 two more times.

7 Dry residue overnight in a drying oven at 105°C or freeze-dry the residue.

8 Weigh dry residue. (Let this weight be *Y* g.)

19.3.3 Determination of NEA in the Residue

Follow the procedure for the elemental N-analyzer that is to be used. Samples (normally 50–100 mg) are weighed in tin foil sample cups which are loaded into autosamplers. Combustion of the samples with oxygen at 1030°C converts NEA to N_2 and NO_x gases (with other combustion products). These gases are routed to a reduction furnace containing heated Cu, which removes excess oxygen and converts NO_x to N_2, which is separated by gas chromatography and the concentration of N_2 is measured using a thermal conductivity detector (for more on dry combustion for N determination see Chapter 22). The analyzer is calibrated with certified standards.

Since the determination is done on a sample that is free of organic matter, a correction is needed to convert the analytical result to a whole soil basis. Suppose that (i) the instrument determines NEA to be *Z*% of residue, and (ii) the weight of the dry residue (in grams) as determined in step 8 is *Y*. Multiply *Z*% by 10 to convert percent to milligram per gram or gram per kilogram basis. Since the weight of the original whole soil samples is 0.5 g, the corrected value of NEA in the original soil (in milligram per kilogram) $= Z \times 10 \times Y/0.5$.

19.3.4 Comments

The method has several advantages of the original Silva and Bremner (1966) method. The use of an automated N-analyzer for the determination of NEA in the soil residue (i) eliminates the use and handling of hydrofluoric acid, (ii) increases the precision of the method, and (iii) simplifies and simultaneously allows the determination of N isotopic ratios by linking an isotopic ratio mass spectrometer to the elemental analyzer. It also shortens the time required for analysis.

REFERENCES

Barshad, I. 1951. Cation exchange in soils: I. Ammonium fixation and its relation to potassium fixation and to determination of ammonium exchange capacity. *Soil Sci.* 72: 361–371.

Bremner, J.M. 1965. Inorganic forms of nitrogen. In C.A. Black et al., Eds., *Methods of Soil Analysis, Part 2—Chemical and Microbiological Properties*. American Society of Agronomy, Madison, WI, pp. 1179–1238.

Bremner, J.M., Nelson, D.W., and Silva, J.A. 1967. Comparison and evaluation of methods of determining fixed ammonium in soils. *Soil Sci. Soc. Am. Proc.* 31: 466–472.

Doram, D.R. and Evans, L.J. 1983. Native fixed ammonium and fixation of added ammonium in relation to clay mineralogy in some Ontario soils. *Can. J. Soil Sci.* 63: 631–639.

Drury, C.F. and Beauchamp, E.G. 1991. Ammonium fixation, release, nitrification and immobilization in high and low fixing soils. *Soil Sci. Soc. Am. J.* 55: 125–129.

Green, C.J., Blackmer, A.M., and Yang, N.C. 1994. Release of fixed ammonium during nitrification in soils. *Soil Sci. Soc. Am. J.* 58: 1411–1415.

Hinman, W.C. 1964. Fixed ammonium in some Saskatchewan soils. *Can. J. Soil Sci.* 44: 151–157.

Keeney, D.R. and Nelson, D.W. 1982. Nitrogen—inorganic forms. In A.L. Page et al., Eds., *Methods of Soil Analysis, Part 2—Chemical and Microbiological Properties*, 2nd edn. American Society of Agronomy, Soil Science Society America, Madison, WI, pp. 643–698.

Kempers, A.J. and Zweers, A. 1986. Ammonium determination in soil extracts by the salicylate method. *Commun. Soil Sci. Plant Anal.* 17: 715–723.

Kudeyarov, V.N. 1981. Mobility of fixed ammonium in soil. *Ecol. Bull.* (Stockholm) 33: 281–290.

Liang, B.C., MacKenzie, A.F., and Gregorich, E.G. 1999. Measurement of fixed ammonium and nitrogen isotope ratios using dry combustion. *Soil Sci. Soc. Am. J.* 63: 1667–1669.

McBeth, I.G. 1917. Fixation of ammonia in soils. *J. Agr. Res.* 9: 141–155.

Nieder, R., Neugebauer, E., Willenbockel, A., Kersebaum, K.C., and Richter, J. 1996. Nitrogen transformation in arable soils of north-west Germany during the cereal growing season. *Biol. Fert. Soils*. 22: 179–183.

Scherer, H.W. 1993. Dynamics and availability of the non-exchangeable NH_4-N—a review. *Eur. J. Agron.* 2: 149–160.

Scherer, H.W. and Werner, W. 1996. Significance of soil micro-organisms for the mobilization of non-exchangeable ammonium. *Biol. Fert. Soils.* 22: 248–251.

Silva, J.A. and Bremner, J.M. 1966. Determination and isotope-ratio analysis of different forms of nitrogen in soils. 5. Fixed ammonium. *Soil Sci. Soc. Am. Proc.* 30: 586–594.

Soderland, R. and Svensson, B.H. 1976. The global nitrogen cycle. In B.H. Svensson and R. Soderland, Eds., *Nitrogen, Phosphorus, and Sulphur—Global Cycles.* SCOPE Report 7.

Soon, Y.K. 1998. Nitrogen cycling involving non-exchangeable ammonium in a gray luvisol. *Biol. Fert. Soils*. 27: 425–429.

Willis, R.B., Schwab, G.J., and Gentry, C.E. 1993. Elimination of interferences in the colorimetric analysis of ammonium in water and soil extracts. *Commun. Soil Sci. Plant Anal*. 24: 1009–1019.

Young, J.L. and Aldag, R.W. 1982. Inorganic forms of nitrogen in soil. In F.J. Stevenson, Ed., *Nitrogen in Agricultural Soils*. American Society of Agronomy, Madison, WI, pp. 43–66.

Zhang, Y. and Scherer, H.W. 1998. Simplification of the standard method for the determination of nonexchangeable NH_4-N in soil. *Z. Pflanenernähr. Bodenk*. 161: 101–103.

Chapter 20
Carbonates

Tee Boon Goh
University of Manitoba
Winnipeg, Manitoba, Canada

A.R. Mermut
University of Saskatchewan
Saskatoon, Saskatchewan, Canada

20.1 INTRODUCTION

Inorganic carbon occurs in soils commonly as the carbonate minerals calcite ($CaCO_3$), dolomite ($CaMg(CO_3)_2$), and magnesian calcites ($Ca_{1-x}Mg_xCO_3$). Other less common forms are aragonite ($CaCO_3$) and siderite ($FeCO_3$). Carbonate in soils can be of primary (inherited from parent material) or secondary (pedogenic) origin. Secondary carbonates are usually aggregates of silt- and clay-sized calcite crystals that are easily identified in grain mounts. Larger crystals of calcite or dolomite are of primary origin (Doner and Lynn 1989). Once routinely reported by sedimentologists, the qualitative and quantitative determination, especially of Ca and Mg carbonates, is useful in studies of soil genesis and classification, and micronutrient and phosphorus sorption. Furthermore, soil carbonates affect root and water movement, soil pH (Nelson 1982), and the nature of the exchange complex (St. Arnaud and Herbillon 1973). The variability in topsoil carbonate content due to incorporation of subsoil calcite and dolomite has been used successfully to explain differences in crop yield in eroded landscapes (Papiernik et al. 2005).

A variety of methods can be used for the determination of calcite, dolomite, and magnesian calcite in soils. Chemical determinations of carbonates include the use of empirical standard curves relating pH to known carbonate content as well as the measurement of CO_2 evolved when treated with acid. These permit a measurement of inorganic C from carbonates in soil. Most procedures express the carbonate content as the calcium carbonate equivalent. Further analysis of the Ca and Mg content provides a means of estimating the kind of inorganic carbonate in soil. The largest source of error is in apportioning the cations between the carbonate minerals and the soluble cations from the exchange complex of the soil.

In instances where the carbonates are of primary origin, and hence consist of larger crystals, it may first be useful to separate them by density fractionation techniques (Jackson 1985; Laird and Dowdy 1994) before further attempting to distinguish between calcite and dolomite.

20.2 CARBONATE CONTENT BY USE OF EMPIRICAL STANDARD CURVE (LOEPPERT ET AL. 1984)

The analysis is suitable for rapid and routine analysis of large numbers of samples. A known quantity of acetic acid is consumed by reaction with carbonates, and the final pH following complete dissolution of $CaCO_3$ is recorded for each sample. Calcium carbonate content is determined empirically from a standard curve relating pH to weight of $CaCO_3$ according to the equation

$$\mathrm{pH} = K + n \log [\mathrm{CaCO_3}/(T - \mathrm{CaCO_3})] \tag{20.1}$$

where K and n are constants and T is the total amount of $CaCO_3$ that could be completely neutralized by the quantity of acetic acid used.

20.2.1 Reagents and Equipment

1 Calcite standard: Pure calcite such as Iceland spar calcite ground to <270 mesh in size is suitable.

2 Acetic acid, 0.4 *M*: Dilute 400 mL of 1 *M* CH_3COOH to the mark in a 1 L volumetric flask with deionized distilled water.

3 pH meter: A digital pH meter is recommended.

4 Ultrasonic probe: A suitable model with a probe that can be inserted into a 50 mL centrifuge tube.

20.2.2 Procedure

Standard Curve

1 Weigh accurately, Iceland spar calcite, ranging from 5 to 500 mg into separate 50 mL polypropylene centrifuge tubes.

2 Add 25 mL of 0.4 *M* acetic acid, which is sufficient to exactly neutralize all the $CaCO_3$ in the largest sample of the standard (500 mg $CaCO_3$), according to the reaction:

$$\mathrm{CaCO_3 + 2CH_3COOH \rightarrow Ca^{2+} + 2CH_3COO^- + H_2O + CO_2}$$

3 Shake tubes intermittently for 8 h. At approximately hourly intervals, swirl the contents for a few minutes to allow for adequate mixing and degassing. Allow tubes to stand overnight with caps loosened to allow escape of CO_2.

4 A final degassing is carried out for approximately 30 s using an ultrasonic probe at low setting to prevent excessive splashing.

5 Centrifuge and record pH of the supernatant to two decimal places after 4 min.

6 Plot standard curve of pH versus log $[CaCO_3/(T - CaCO_3)]$. Note: T is the weight of $CaCO_3$ (mg) used to exactly neutralize the volume of acetic acid used and will vary if either the volume or concentration of acetic acid is changed.

Calcium Carbonate Content of Soil Samples

1 Weigh accurately, up to 2 g soil (<100 mesh size) containing up to 400 mg $CaCO_3$. Reduce the soil sample weight if the carbonate content exceeds 20%.

2 Repeat steps (2) through (5) as for the standard curve above.

20.2.3 Calculations

From the pH value recorded, determine the value of log $[CaCO_3/(T - CaCO_3)]$ using the standard curve and calculate the weight of $CaCO_3$ (mg) in the soil sample. The total carbonate content so determined is expressed as percent calcium carbonate equivalent.

$$\%\ CaCO_3\ \text{equivalent} = \frac{\text{mg } CaCO_3}{\text{mg sample}} \times 100 \tag{20.2}$$

20.2.4 Comments

If dolomite is present in the soil sample, increased reaction times may be required for the dissolution to go to completion. The accuracy of results is influenced by (i) proton consumption by soil constituents, (ii) acid-generating hydrolysis reactions during mineral decomposition, (iii) high PCO_2, (iv) volatilization of acetic acid, and (v) errors in pH determination. These can be minimized by standard additions of Ca^{2+}, from a solution of $CaCl_2$, to all samples and standards; grinding of samples to increase reactivity of sand-sized carbonates and reduction of reaction time between acetic acid and other minerals; use of covers to reduce loss of acetic acid; degassing CO_2; and reduction of suspension effects in pH reading (Loeppert et al. 1984).

20.3 APPROXIMATE GRAVIMETRIC METHOD (ALLISON AND MOODIE 1965; RAAD 1978)

A preweighed soil sample containing carbonates is reacted with acid. The resultant loss in weight from CO_2 released is used to calculate the calcium carbonate content. Calcite and dolomite cannot be accurately distinguished, but a fair estimate of the proportion of dolomite in the sample can be obtained by checking the weight loss with time.

20.3.1 Reagents

1 Hydrochloric acid (HCl), 4 *M*.

2 Hydrochloric acid (HCl)–ferrous chloride ($FeCl_2 \cdot 4H_2O$) reagent: Dissolve 3 g of $FeCl_2 \cdot 4H_2O$ per 100 mL of 4 *M* HCl immediately before use.

20.3.2 Procedure

1 Weigh a stoppered, 50 mL Erlenmeyer flask containing 10 mL of the HCl−$FeCl_2$ reagent.

2 Transfer a 1–10 g soil sample containing between 100 and 300 mg of carbonate to the flask gradually to avoid excessive frothing.

3 After effervescence has subsided, replace the stopper loosely and allow the carbonate to decompose further in the mixture for about 30 min with occasional swirling to displace any accumulated CO_2. Replace the stopper and weigh the flask with its contents.

4 Repeat step (3) until the change in weight of the flask and its contents is no more than 2–3 mg. The reaction is usually complete within 2 h.

20.3.3 Calculations

Weight of CO_2 lost from carbonates = difference in initial and final weights of (flask + stopper contents)

$$\%\ CaCO_3\ \text{equivalent} = \frac{\text{g } CO_2 \text{ lost}}{\text{g soil}} \times 227.3 \tag{20.3}$$

20.3.4 Comments

When dolomite is present, it is considerably less reactive to cold HCl. Therefore, if the weight is observed to decrease markedly after 30 min, some dolomite is present. The use of acid containing $FeCl_2$ as an antioxidant eliminates errors caused by oxidizing interferences due to MnO_2 in soil. The accuracy of this method depends upon the accuracy of weighing and the degree to which CO_2 retained in solution is compensated for by loss of water vapor.

20.4 QUANTITATIVE GRAVIMETRIC METHOD (USDA SOIL CONSERVATION SERVICE 1967)

The loss in weight of a soil sample is measured accurately after reaction between carbonates in the soil and acid. In this method, the loss of water vapor evolved with CO_2 is eliminated by a trap containing anhydrone. The addition of a CO_2 trap to the apparatus is an alternative to the method, by measuring the gain rather than the loss in weight, and provides a check against any leaks in the connections to the glassware. With several units in operation, the method is quite rapid and accurate.

20.4.1 Apparatus

The apparatus is assembled as depicted in Figure 20.1 for the weight loss method. A polyethylene drying tube packed with Ascarite II^R to trap CO_2 can also be attached to the end of the gas train after stopcock D in the weight gain method.

20.4.2 Reagents

1 Hydrochloric acid (HCl), 6 *M*.

2 HCl–ferrous chloride ($FeCl_2 \cdot 4H_2O$) reagent: Dissolve 3 g of $FeCl_2 \cdot 4H_2O$ per 100 mL of 6 *M* HCl immediately before use.

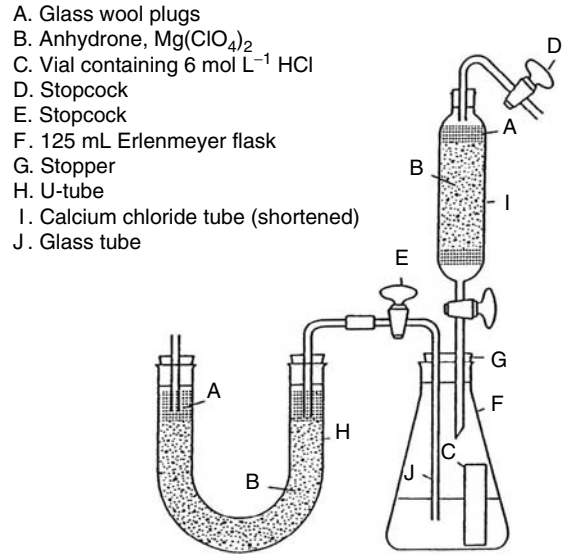

FIGURE 20.1. Apparatus for accurate quantitative determination of calcium carbonate equivalent. (From Raad, A.A., in J.A. McKeague (Ed.), *Manual on Soil Sampling and Methods of Analysis*, 2nd edn. Canadian Society of Soil Science, AAFC, Ottawa, Ontario, Canada, 1978.)

3 Anhydrone ($Mg(ClO_4)_2$), drying agent.

4 Ascarite II^R: 20–30 mesh, optional.

20.4.3 Procedure

Weight Loss Method

1 Weigh a 1–10 g sample of oven-dry soil (<100 mesh) containing <1 g $CaCO_3$ equivalent in a 125 mL Erlenmeyer flask.

2 Wash down the sides of the flask with 10 mL of deionized distilled water.

3 Transfer 7 mL of HCl–$FeCl_2$ reagent into vial C (Figure 20.1), and place the vial upright in the flask without spilling any acid.

4 Moisten stopper G with glycerin, sprinkle it with a small amount of 180 mesh abrasive to overcome slipperiness, and assemble the apparatus as in Figure 20.1 without connecting the U-tube to stopcock E. Close stopcocks D and E.

5 Place the apparatus beside the balance and allow the temperature in the flask to equilibrate with that of the air in the balance.

6 Using tongs, place the apparatus on the weighing pan, open stopcock D, and record weight to the nearest 0.1 mg. Close stopcock D immediately. Weigh again after 10 min to ensure that weight has stabilized.

7 Open stopcock D and shake the flask to upset vial C, thus allowing the acid to react with the soil.

8 After 10 min, attach the U-tube H to the apparatus, open stopcock E, and apply gentle suction at stopcock D at a rate of 5–10 bubbles per second at tube J to sweep out CO_2 with dry air. Shake the flask at 10 min intervals.

9 Stop the suction when the reaction is complete (usually 30 min; 1 h if dolomite is present). Close stopcocks D and E. Disconnect the U-tube H. Wait for 1 h and weigh the apparatus and its contents with stopcock D open. Check the weight after 10 min.

10 Calculate as follows:

$$\%\ CaCO_3\ \text{equivalent} = \frac{(\text{Initial weight, g} - \text{Final weight, g})}{\text{Sample weight, g}} \times 227.3 \qquad (20.4)$$

Weight Gain Method

1 Weigh drying tube containing Ascarite II^R to the nearest 0.1 mg. Attach to the apparatus depicted in Figure 20.1 at stopcock D.

2 Proceed as described in the weight loss method but apply suction at the end of the polyethylene drying tube so that the gas train passes through the CO_2 trap.

3 Disconnect from the CO_2 trap and weigh drying tube and its contents.

4 Calculate as follows:

$$\%\ CaCO_3\ \text{equivalent} = \frac{(\text{Final weight, g} - \text{Initial weight, g})}{\text{Sample weight, g}} \times 227.3 \qquad (20.5)$$

20.4.4 Comments

The results obtained by the two methods should agree within the limits of weighing error. Larger discrepancies may indicate leaks in the connections of the apparatus.

20.5 QUANTIFICATION OF CALCITE AND DOLOMITE (PETERSON ET AL. 1966)

The citrate buffer method described by Raad (1978) is presented here. Calcite and dolomite are selectively dissolved in a citrate buffer solution, Ca and Mg in solution are determined, and the calcite content of the sample is calculated. It is assumed that dolomite has a Ca:Mg molar ratio of 1:1 and the only sources of Ca and Mg in the solution are calcite and dolomite (i.e., no magnesian calcite is present), and exchangeable calcium and magnesium have been removed first or otherwise accounted for (Hesse 1971). The portion of dolomite

dissolved in the citrate buffer is calculated from the Mg in solution; an equivalent amount of Ca is assigned to it; and the remaining Ca determines the calcite content of the sample. The total dolomite content of the sample is obtained by the difference between the total carbonate content previously determined in another subsample and the portion of carbonate from calcite. As a check of accuracy, the dolomite content of the sample can also be calculated from the Mg in solution. The method is useful if clay-sized dolomite is present in the sample.

20.5.1 Reagents

1 Citrate buffer: Dissolve 64 g citric acid ($C_6H_8O_7$) in 1 L of deionized water. Titrate to pH 5.85 with concentrated NH_4OH.

2 Sodium chloride–ethanol: Dissolve 58.5 g NaCl in 30% (v/v) ethanol and bring to 1 L with deionized water.

3 Sodium dithionite.

20.5.2 Procedure

1 Weigh 50–500 mg oven-dry soil ground to pass a 100 mesh sieve into a 50 mL centrifuge tube.

2 Wash twice with NaCl–ethanol solution and discard washing.

3 Add 25 mL of citrate buffer solution, and heat in a water bath at 80°C. Add approximately 0.5 g of sodium dithionite and continue heating with stirring for about 15 min.

4 Centrifuge and collect supernatant in a 250 mL volumetric flask. Wash the residue once with 25 mL of citrate buffer, centrifuge, and collect the supernatant. Make to volume with deionized water.

5 Determine Ca and Mg in solution by atomic absorption spectroscopy using standards made up in the same concentrations of citrate buffer and dithionite. Standards and sample solutions should contain 1 mg La mL^{-1} to minimize interference effects.

6 The total carbonate content is determined in another subsample by other quantitative methods (Section 20.2).

20.5.3 Calculations

The molecular formula of calcite is $CaCO_3$, and the molecular formula of dolomite is $CaMg(CO_3)_2$. If total citrate-soluble Ca $= X$ mmol, and citrate-soluble dolomite Mg $= Y$ mmol, then citrate-soluble dolomite-Ca $= Y$ mmol, and the mmol calcite-Ca $= X - Y$. Since 1 mmol of Ca is contained in 1 mmol of calcite, and since 1 mmol calcite weighs 100 mg, then:

$$\%\ \text{calcite in sample} = \frac{(X - Y)\ \text{mmol}}{\text{mg sample}} \times \frac{100\ \text{mg}}{\text{mmol}} \times 100 \tag{20.6}$$

The dolomite content of the sample can be calculated if total carbonate in sample = Z mmol. Since total carbonate = calcite carbonate + dolomite carbonate, the mmol dolomite-$CO_3 = Z - (X - Y)$, and since 2 mmol of carbonate is contained in 1 mmol of dolomite, then, the mmol dolomite $= \frac{1}{2}$ (mmol dolomite-CO_3) $= \frac{1}{2}[Z - (X - Y)]$, and since 1 mmol dolomite weighs 184 mg, then

$$\%\ \text{dolomite in sample} = \frac{\frac{1}{2}[Z - (X - Y)]\ \text{mmol}}{\text{mg sample}} \times \frac{184\ \text{mg}}{\text{mmol}} \times 100 \tag{20.7}$$

Alternatively, the dolomite content can be calculated by the mmol dolomite-Mg = Y:

$$\%\ \text{dolomite in sample} = \frac{Y\ \text{mmol}}{\text{mg sample}} \times \frac{184\ \text{mg}}{\text{mmol}} \times 100 \tag{20.8}$$

The % $CaCO_3$ equivalent of the dolomite present

$$= \frac{[Z - (X - Y)]\ \text{mmol}}{\text{mg sample}} \times \frac{100\ \text{mg}}{\text{mmol}} \times 100 \tag{20.9}$$

20.5.4 Comments

The dolomite content calculated from dolomite-CO_3 should agree with that calculated from the Mg in solution unless some source of citrate-soluble Mg other than dolomite, or magnesian calcite is present. If magnesian calcite is present, the calcite content of the sample will be underestimated. Therefore, identification and quantification of magnesian calcite (e.g., St. Arnaud et al. 1993) should be conducted for more specialized research.

REFERENCES

Allison, L.E. and Moodie, C.D. 1965. Carbonate. In C.A. Black et al., Eds., *Methods of Soil Analysis, Part 2—Chemical and Microbiological Properties* 1st ed. American Society for Agronomy, Madison, WI, pp. 1379–1396.

Doner, H.E. and Lynn, W.C. 1989. Carbonate, halide, sulfate and sulfide minerals. In J.B. Dixon and S.B. Weed, Eds., *Minerals in Soil Environments*, 2nd ed. Soil Science Society of America, Madison, WI, pp. 279–330.

Hesse, P.R. 1971. *A Textbook of Soil Chemical Analysis*. Chemical Publishing Co., Inc. New York, NY.

Jackson, M.L. 1985. *Soil Chemical Analysis—Advanced Course*, 2nd edn. M.L. Jackson, Madison, WI.

Laird, D.A. and Dowdy, R.H. 1994. Preconcentration techniques in soil mineralogical analyses. In J.E. Amonette and L.W. Zelazny, Eds.,

Quantitative Methods in Soil Mineralogy. Soil Science Society of America, Madison, WI, pp. 236–266.

Loeppert, R.H., Hallmark, C.T., and Koshy, M.M. 1984. Routine procedure for rapid determination of soil carbonates. *Soil Sci. Soc. Am. J.* 48: 1030–1033.

Nelson, R.E. 1982. Carbonate and gypsum. In A.L. Page et al., Eds., *Methods of Soil Analysis, Part 2—Chemical and Microbiological Properties*, 2nd edn. American Society of Agronomy, Madison, WI, pp. 81–197.

Papiernik, S.K., Lindstrom, M.J., Schumacher, J.A., Farenhorst, A., Stephens, K.D., Schumacher, T.E., and Lobb, D.A. 2005. Variations in soil properties and crop yield across an eroded prairie landscape. *J. Soil Water Conserv*. 60: 47–54.

Peterson, G.W., Chesters, G., and Lee, G.B. 1966. Quantitative determination of calcite and dolomite in soils. *J. Soil Sci*. 17: 328–338.

Raad, A.A. 1978. Carbonates. In J.A. McKeague, Ed., *Manual on Soil Sampling and Methods of Analysis*, 2nd ed. Canadian Society of Soil Science, AAFC, Ottawa, ON, Canada, pp. 86–98.

St. Arnaud, R.J. and Herbillon, A.J. 1973. Occurrence and genesis of secondary magnesium-bearing calcites in soils. *Geoderma* 9: 279–298.

St. Arnaud, R.J., Mermut, A.R., and Goh, Tee Boon. 1993. Identification and measurement of carbonate minerals. In M.R. Carter, Ed., *Soil Sampling and Methods of Analysis*. Lewis Publishers, Boca Raton, FL, pp. 737–754.

USDA Soil Conservation Service. 1967. Calcium carbonate. In Soil survey investigations report No. 1. *Soil Survey Laboratory Methods and Procedures for Collecting Soil Samples*. U.S. Government Printing Office, Washington DC, pp. 28–30.

Chapter 21
Total and Organic Carbon

J.O. Skjemstad and J.A. Baldock

Commonwealth Scientific and Industrial Research Organization

Glen Osmond, South Australia, Australia

21.1 INTRODUCTION

Carbon in soils exists in both organic and inorganic forms. Carbonate, in a variety of forms, makes up the inorganic component of total carbon (TC), whereas a range of organic moieties make up the organic carbon (OC) component. The terms OC or organic matter associated with soil have been defined in various ways. Stevenson (1994) and Baldock and Nelson (1998) defined OC as the total of all organic materials existing within and on soil, whereas Oades (1988) excluded charcoal and charred materials and MacCarthy et al. (1990) excluded nondecayed plant and animal tissues, their partial decomposition products, and the living soil biomass. In reality, however, the methods used to determine both TC and OC do not discriminate between the various fractions described above, and consequently, the all encompassing definition of OC used by Stevenson (1994) and Baldock and Nelson (1998) is also used in this chapter.

There are a number of approaches available for the determination of TC and OC in soils. These are broadly based on either the chemical or thermal oxidation of soil OC. Chemical or wet oxidation is followed by the measurement of expelled CO_2 (Snyder and Trofymow 1984) or the consumption of oxidant required to quantitatively oxidize the OC (Walkley and Black 1934). Under acidic conditions, any chemical or wet oxidation methods that measure expelled CO_2 will also include carbonate C and will be a measure of TC. In dry combustion methods, samples are heated to high temperatures, usually exceeding 1000°C in the presence of excess O_2. Under these conditions, all C present in OC and carbonate is quantitatively converted to CO_2. Liberated CO_2 may be determined gravimetrically (Allison et al. 1965), volumetrically (Rayment and Higginson 1992), titrimetrically (Snyder and Trofymow 1984), or spectrometrically (Merry and Spouncer 1988). If thermal oxidation (dry combustion) at temperatures exceeding 1100°C is used, all carbon in the sample including carbonates will be determined (Giovannini et al. 1975). For both chemical and thermal oxidation methods where CO_2 is measured, a correction for carbonate can be made from a separate carbonate measurement or the carbonate may be removed with acid before carbon analysis.

A comparison of several titrimetric and gravimetric methods was made by Kalembasa and Jenkinson (1973) and showed that dry combustion methods were the more precise. Loss on ignition at various temperatures has also been used as a simple predictor of soil organic matter in soil types where clay contents are low (Ball 1964; Lowther et al. 1980) but these methods are not recommended if alternative methods are available.

21.2 DRY COMBUSTION METHODS

Currently, there are a large number of instruments available commercially for the determination of TC. Some instruments will simultaneously determine C and one or more of the following additional elements: N, H, and S. For some instruments, an induction furnace is used to heat the sample rather than the more commonly available resistance furnace. These methods rely on the addition of Fe chips and catalysts to the sample to produce high temperatures of up to 1400°C (Rayment and Higginson 1992) or the use of a quartz enclosed graphite crucible to heat the sample externally (Allison et al. 1965).

For all instruments, combustion is usually carried out at high temperatures (>1000°C) and in a stream of O_2. This is to ensure that all C species are quantitatively converted to CO_2. At lower temperatures, combustion may not be complete, resulting in the generation of some CO or incomplete decomposition of carbonate species. Unless the CO is converted to CO_2, losses will be recorded due to the inability of detectors tuned to CO_2 to detect CO. This can be overcome by mixing a catalyst such as V_2O_5 (Morris and Schnitzer 1967) with the sample, or by the inclusion of a catalytic conversion furnace (usually CuO) in the train prior to detection. For some instruments, samples are loaded into Sn or Al cups and the sample and cup are ignited. The exothermic reaction that takes place as the Sn or Al cups ignite increases the combustion temperature significantly, even though the furnace may operate at 1000°C or less.

Carbonates will be decomposed at elevated temperatures (500°C–1000°C) to also produce CO_2; and so for OC measurements, carbonates must be either removed prior to combustion or a correction must be made. Some authors have suggested using low combustion temperatures to confine the carbon measured to only that contained within organic materials. However, this requires temperatures <720°C, since dolomite starts to decompose above this temperature. At temperatures <720°C, not only is the production of CO an issue, but also a substantial amount of charcoal can be generated and may not fully oxidize if the combustion duration is short.

Carbonate is removed through the addition of acid before analysis. Sulfurous acid (H_2SO_3) is the only suitable acid because its reducing properties minimize the oxidation of OC during the process (Piper 1944). This can be accomplished in two ways: either by destruction of the carbonate within the combustion vessel or before subsampling for OC analysis. The former approach is preferable because it minimizes sample handling, but the combustion vessel needs to be large enough in relation to the sample size to enable the addition of excess acid and the potential effervescence that may result. Three methods are described here; addition of acid directly to the combustion vessels at two different scales and a method for removing carbonate before subsampling.

A range of modern instruments with several levels of automation are commercially available for dry combustion methods. The two most common detection systems are based on infrared or thermal conductivity measurement. All instruments are provided with comprehensive

instructions on the setting up, standardization, and use of the equipment for routine analysis. For the remainder of this section, we will not describe TC and OC analysis based around one or more specific instruments but will discuss the issues that arise at different parts of the carbon analysis train and how these may be dealt with.

21.2.1 Removal of Carbonate—Large Combustion Vessel

This method is directed toward instruments such as those manufactured by Laboratory Equipment Corporation (LECO), which utilize large ceramic combustion boats with a 5–6 mL capacity. These boats are porous and so acid treatment cannot be performed directly within the boat, since some leakage will occur and OC rendered soluble by the treatment will be lost. The sample is therefore weighed into a commercially available Ni liner placed within the combustion boat.

Reagents

6% (w/v) H_2SO_3 solution.

Procedure

1. Weigh 0.1–1.0 g of soil (<0.15 mm) into a Ni liner placed within a ceramic combustion boat, and place on a hot plate. Larger samples are not recommended unless the samples are known to contain only very small concentrations of carbonate and low concentrations of OC.

2. Moisten samples with a little distilled or deionized water and add 1.0 mL of 6% H_2SO_3 to each boat and allow to stand. Meanwhile, turn on the heating plate and set the temperature to ensure that the samples do not exceed 70°C. Because of the insulating properties of the ceramic boat and the generally large loss of heat from the hot plate between samples, the hot plate temperature may need to be set as high as 120°C.

3. When the samples have stopped reacting, add a further 1.0 mL of 6% H_2SO_3. It is important that the samples are not allowed to dry until the treatment is completed, since this will lead to deterioration in the Ni liner and ultimately leakage. Some evaporation will be necessary, however, to allow the addition of sufficient acid to complete the carbonate removal.

4. When addition of acid no longer promotes a reaction, allow the samples to dry.

5. Analyze samples using an OC determinator as described by the manufacturer, but ensure that the initial weight of the sample (prior to 6% H_2SO_3 treatment) is entered into the calculation and not the final weight after treatment.

Comments

14 mL of 6% H_2SO_3 is required to neutralize 1.0 g of $CaCO_3 \cdot H_2SO_3$ solutions will slowly deteriorate with time, losing SO_2; and more acid may be needed depending on the age of the H_2SO_3 solution.

21.2.2 Removal of Carbonate—Small Combustion Vessel

This method is directed toward instruments such as those manufactured by Carlo Erba, which utilize small samples placed in metal combustion cups. For pretreatment for carbonate, Ag cups are recommended instead of the normal Sn or Al cups, since Ag has a much greater resistance to 6% H_2SO_3. The reaction is carried out in a small Al block that has been drilled out to hold the capsules with a reasonably tight fit similar to that described by Verardo et al. (1990).

Reagents

6% (w/v) H_2SO_3 solution.

Procedure

1 Place Ag cups into a small Al block. Weigh up to 20 mg of the sample (<0.02 mm) into the cups and place the small block onto a heating plate.

2 Add 10 μL distilled or deionized water to each sample. This slows the initial reaction when 6% H_2SO_3 is added and minimizes the risk of losing sample due to a strong effervescence. Add 10 μL of 6% H_2SO_3 to each sample and allow to stand. Meanwhile, turn on the heating plate and set temperature to 70°C.

3 When reaction has ceased, add another 10 μL of acid. It is important that the samples are not allowed to dry until the treatment is complete, because this will lead to deterioration in the Ag cups and they may crumble during the balling process. Some evaporation will be necessary, however, to allow the addition of sufficient acid to complete the carbonate removal.

4 When addition of acid no longer promotes a reaction, allow the samples to dry and analyze samples using an OC determinator as described by the manufacturer ensuring that the initial weight of the untreated soil is used in the calculations.

21.2.3 Removal of Carbonate Prior to Subsampling

Reagents

6% (w/v) H_2SO_3 solution.

Procedure

1 Weigh 1.0–2.0 g of sample into a preweighed test tube or beaker and place in a digestion block or on a hot plate.

2 Add 1.0 mL of 6% H_2SO_3 and allow the reaction to subside. Meanwhile, turn on the block/hot plate and set temperature to 70°C.

3 Continue to add 6% H_2SO_3 in 1.0 mL aliquots until further addition no longer yields a reaction and allow samples to dry.

4 When dry, remove samples from block, place in a desiccator or cabinet with silica gel, and allow to cool. Weigh tube or beaker, and quantitatively remove treated sample. Maintain samples in an oven dry state (105°C) under desiccation for OC analysis.

5 Take 10 g of soil and place in a preweighed beaker or silica dish. Dry for 24 h at 105°C in an oven. Cool in a desiccator and reweigh.

Calculations

This pretreatment modifies the sample in two ways. First, because the sample is heated, the water content of the sample is changed; and second, because SO_3^{2-} has more mass than CO_3^{2-}, the mass of the sample will increase. These changes need to be taken into consideration when calculating the OC content of the sample.

1 Oven dry factor (ODF) is calculated as

$$\text{ODF} = (\text{weight air dry soil})/(\text{weight oven dry soil}) \tag{21.1}$$

2 $$\text{Soil OC content (105°C) g kg}^{-1} = (\text{OC content of treated sample g kg}^{-1}) \times (\text{weight of sample post treatment at 105°C})/(\text{weight of sample taken for treatment/ODF}) \tag{21.2}$$

21.2.4 Correction for Carbonate

For analyzers that rely on a continuous flow of exhaust gases for the determination of CO_2, and the temperature of the combustion is high (>1000°C), a correction for carbonate content can be made mathematically. Some analyzers, however, rely on the collection of a given volume of exhaust gases that limits the time over which the sample is heated to high temperature. This is common in instruments that analyze for C and N simultaneously. Under these conditions, carbonates may not be fully decomposed and the TC may be underestimated. This can often be overcome by taking much smaller samples, but such analyzers need to be tested to determine whether a TC measurement in the presence of carbonate is quantitative. If not, then a simple correction is not quantitative and carbonates will need to be removed before analysis as described by one of the procedures given above.

For those analyzers that quantitatively determine TC, the following correction can be made:

$$\text{OC g kg}^{-1} = \text{TC g kg}^{-1} - 0.12 \times \text{CaCO}_3\ \text{g kg}^{-1} \tag{21.3}$$

21.2.5 Standards

Preignition of combustion vessels may be necessary to eliminate contamination. For metal cups, this can be achieved at 550°C and for ceramic boats at 1000°C for 16 h.

A wide range of materials can be used as OC standards for these instruments. These include $CaCO_3$, EDTA, sucrose, glucose, potassium hydrogen phthalate, and urea.

Standard materials of given C content can also be purchased from companies such as LECO. It is recommended, but not essential, that the standards used exhibit similar combustion characteristics to the samples. This becomes an issue when highly organic standards or samples are used. For continuously monitoring instruments, the linear operating range of the detector may be exceeded if the standards or samples ''flash'' and an intense pulse of CO_2 passes through the detector within a short time. This can be overcome by reducing the rate of combustion by covering the sample with a layer of ignited sand. The sand used should be <1 mm and ignited at $>1000°C$ over at least 24 h with frequent stirring of the sand to ensure any C present is totally combusted to CO_2.

The linear operating range of the detector can be determined by analyzing different weights of standards and samples over a range that encompasses expected TC and OC contents.

21.3 DICHROMATE REDOX METHODS

With these methods, dichromate ($Cr_2O_7^{2-}$) solution in combination with sulfuric acid (H_2SO_4) is used to oxidize OC to CO_2. The orange dichromate is reduced to the green Cr^{3+} form according to the following equation:

$$2H_2Cr_2O_7 + 6H_2SO_4 + 3C \rightarrow 2Cr_2(SO_4)_3 + 3CO_2 + 8H_2O \quad (21.4)$$

The oxidation state (Baldock et al. 2004) of the C in the organic matter can influence the consumption of oxidant. Molecules with a high H/C ratio, such as lipids, give higher recoveries than molecules with high O/C ratio (Skjemstad 1992). Because soil organic matter is highly diverse in chemistry, these two effects tend to cancel one another when the whole soil is considered; however, variations in oxidation state of OC with increasing extent of decomposition have been documented (Baldock et al. 2004). This issue, therefore, may be more serious if specific soil OC fractions are being considered.

If consumption of oxidant is to be used, the analysis can be performed with heating (Heanes 1984) or without external heating (Walkley and Black 1934). The consumption of oxidant can be determined either by titration using an indicator or platinum–calomel electrode or colorimetrically. If only the heat of reaction is used with no applied external heating, as in the case of the Walkley and Black (1934) method, then a 75%–80% recovery of carbon is usually obtained and a conversion factor of 1.3 is commonly used to equate the OC value to the thermal oxidation (dry combustion) methods. This factor will vary among soil types and with depth and must be applied with caution.

Any material that can be oxidized by the dichromate will be measured as OC. Chlorides are quantitatively oxidized to free chlorine by chromic acid. Thus, where consumption of dichromate is used to determine OC, the presence of Cl can result in erroneously high OC contents. This methodological error can be corrected when the Cl content of the sample is known. Four Cl ions have the same reducing power as 1 C atom ($4Cl \equiv 2O \equiv 1C$) and hence 11.83 g of Cl is equivalent to 1 g of C. Several workers have suggested that the addition of Ag_2SO_4 can suppress Cl interference (Walkley 1947). Heanes (1984), however, demonstrated that the addition of Ag_2SO_4 either as a solid or in solution with the H_2SO_4 was ineffective. For saline soils therefore, it is recommended that the correction for measured Cl be used rather than additions of Ag_2SO_4.

In this chapter, we detail two methods. One based on the Schollenberger (1945) method uses external heating and titration with an indicator. The alternative method uses external heating and colorimetric determination of Cr^{III} (Heanes 1984). Reduced forms of Fe and Mn may also interfere with these methods. These interferences are rare but can be overcome by the procedures described in Jackson (1958). The use of steel or iron mills should also be avoided since these can act as a source of Fe metal, which is readily oxidized under the conditions of the reaction.

21.3.1 Dichromate Redox Colorimetric Method (Heanes 1984)

The dichromate redox colorimetric method utilizes the formation of the green Cr^{III} species resulting from the reduction of the orange dichromate (Cr^{VI}) species. The amount of dichromate consumed is determined against a set of standards and measured on a spectrometer in the visual range. Carbonates are not determined by this procedure but Cl will interfere. Because the dichromate solution is not used as the primary standard in this method, we describe here the use of the more soluble $Na_2Cr_2O_7$ salt rather than the K salt.

Reagents

1 Na dichromate solution: dissolve 50 g of $Na_2Cr_2O_7$ in distilled or deionized water and dilute to 1 L.

2 Sulfuric acid: 98% conc. H_2SO_4.

3 Standards: dissolve 1.376 g of glucose monohydrate in distilled or deionized water and dilute to 250 mL. A small crystal of $HgCl_2$ can be added to preserve the standard against microbial decomposition. 1.0 mL of this solution = 2.0 mg of OC.

Procedure

1 Prepare standards by adding a range of aliquots of the glucose solution to borosilicate tubes (25 mm OD) marked at 100 mL. A convenient range is 1–12 mL of standard that equates to 2–24 mg of OC. Tubes containing glucose solution and a blank are dried in an oven at a temperature not exceeding 60°C.

2 Weigh 0.1–2.0 g of air-dried soil (<0.15 mm) containing <20 mg of OC into digestion tubes.

3 Add 10.0 mL of $Na_2Cr_2O_7$ solution, and while agitating add 20.0 mL of 98% H_2SO_4 cautiously so that the reaction is confined to the bottom of the tube. Agitate for a further 30 s before inserting into a preheated (135°C) digestion block. Agitate tubes occasionally to ensure all of the soil material is exposed to the chromic acid mixture.

4 After 45 min, remove tubes from the block and allow to cool. Add 50 mL of distilled or deionized water to digest and agitate with a thick-walled glass capillary tube that has a stream of air passing through it so that the samples are thoroughly mixed. After removal from the block, the samples still contain H_2SO_4 at a strong enough concentration to cause heating when water is added.

If the tubes are inverted after the addition of water, enough heat is generated to potentially cause hot chromic acid to be lost. Agitation with the assistance of a stream of air prevents any losses. When cool, make the tubes up to 100 mL with distilled or deionized water and invert to mix using a rubber bung.

5 Decant diluted chromic acid mixture into 15 mL centrifuge tubes and centrifuge at 2000 rpm for 15 min. Measure the absorbance of the centrifuged samples at 600 nm in a 10 mm cell.

Calculations

Construct a standard curve plotting absorbance at 600 nm against mg C present in the standards. Using this curve, estimate the mg C in the unknown samples.

$$\text{g C kg}^{-1}\text{soil} = \text{mg C in digest/weight soil in grams} \tag{21.5}$$

If the mg C content of samples is <2 or >20, analysis should be repeated with more or less weight to bring them within the optimum range of the determination.

Modification for Saline Soils

For saline soils, a separate determination of the chloride content of the soil is required and expressed as g Cl kg^{-1} soil. The OC content of the soil is then corrected for the Cl content:

$$\text{g C kg}^{-1}\text{soil} = \text{apparent g C kg}^{-1}\text{ soil} - (\text{g Cl kg}^{-1}\text{soil}/12) \tag{21.6}$$

21.3.2 Dichromate Redox Titration Method

This procedure is similar to the spectroscopic method but utilizes the unreacted dichromate (Cr^{VI}) that remains following the reaction of OC with acid dichromate. Back titration with Fe^{II} solution is used to determine the remaining dichromate. The procedure described here is based on that described by Schollenberger (1945) with the modification by Jackson (1962) for the *o*-phenanthroline indicator. *N*-phenanthranilic acid (Nelson and Sommers 1982) or diphenylamine (Piper 1944) can be substituted. Carbonates do not interfere but Cl does and a correction must be made if Cl levels are high.

Reagents

1 Digestion mixture: dissolve 39.22 g of $K_2Cr_2O_7$ (dried at 90°C) in 800–900 mL of distilled or deionized water in a large glass beaker. Carefully add 1 L of 98% H_2SO_4. As the acid is added, the mixture will become very hot and will boil. When cool, make to 2 L with distilled or deionized water. This solution is 0.067 *M* (0.4 *N*) in dichromate and 9 *M* in H_2SO_4 and is the primary standard for the OC determination.

2 Ferrous ammonium sulphate: dissolve 157 g of $Fe(NH_4)_2(SO_4)_2 \cdot 6H_2O$ in about 1 L of distilled or deionized water containing 100 mL of 98% H_2SO_4. Make to 2 L to give a ~0.2 *M* (~0.2 *N*) solution. The solution does not store well and must be standardized against the dichromate solution at each use.

3 Phosphoric acid: 85% H_3PO_4.

4 Indicator solution: dissolve 3.00 g of *o*-phenanthroline monohydrate (Ferroin) and 1.40 g of $FeSO_4 \cdot 7H_2O$ in distilled or deionized water and dilute to 200 mL. Alternatively, dissolve 0.1 g of *N*-phenanthranilic acid and 0.1 g of Na_2CO_3 in 100 mL of distilled or deionized water or dissolve 0.5 g of diphenylamine in 100 mL of 98% H_2SO_4 containing 20 mL of distilled or deionized water.

Procedure

1 Weigh samples (<0.15 mm) up to 1.0 g that contain between 1 and 10 mg of OC into 100 mL digestion tubes. Add 15 mL of digestion mixture and place on digestion block preheated to 150°C.

2 After 45 min, remove samples from the block and allow to cool before quantitatively transferring solution and sample to a titration vessel with approximately 50 mL of distilled or deionized water. Add 5 mL of 85% H_3PO_4 and four drops of indicator. The H_3PO_4 eliminates interference from Fe^{III}.

3 Titrate with $Fe(NH_4)_2(SO_4)_2$ solution to a color change from green to reddish brown for the *o*-phenanthroline, dark violet–green to light green for the *N*-phenanthranilic acid, and violet–blue to green for the diphenylamine.

4 Two unheated blanks are also titrated to standardize the $Fe(NH_4)_2(SO_4)_2$ solution.

Calculations

1 Calculate the molarity (normality) of the $Fe(NH_4)_2(SO_4)_2$ solution as

$$\text{Molarity of } Fe(NH_4)_2(SO_4)_2 \text{ solution} = (15 \times 0.4)/T_1 \tag{21.7}$$

where T_1 is the titer of the $Fe(NH_4)_2(SO_4)_2$ solution in mL.

2 Calculate the OC concentration in the sample as

$$\text{g OC kg}^{-1}\text{soil} = (B - T_2) \times M \times 3/W \tag{21.8}$$

where B and T_2 are titers in mL of heated blank and sample, respectively, M is the molarity of the $Fe(NH_4)_2(SO_4)_2$ solution, and W is the weight of sample in grams.

21.4 DICHROMATE OXIDATION CO_2 TRAP METHOD (SNYDER AND TROFYMOW 1984)

With this method, the sample is oxidized with a H_2SO_4–dichromate mixture and the evolved CO_2 is captured in NaOH solution and determined by titration using either an indicator or pH meter. This approach is more complex than the redox approach but most of the interferences encountered with the redox methods are eliminated. A further advantage of this method is that the trapped CO_2 can also be used to determine isotopic composition (Amato 1983). Various vessels have been used to contain the reaction and collect the CO_2. Snyder and

Trofymow (1984) used tubes with screw caps, Amato (1983) used tubes with subaseals, and Dalal (1979) used McCartney bottles.

Because of the acidic conditions under which the reaction progresses, any carbonates present will also be quantitatively converted to CO_2 and determined. If carbonates are present, OC is determined by either first removing the carbonates in the reaction vessel or correcting for their presence. Carbonate content can either be determined using the same reaction vessel or can be determined by another suitable method of analysis.

The method as described by Snyder and Trofymow (1984) can handle solid or liquid samples and uses a temperature of 120°C. If only solid samples are processed, the digestion can be performed at a higher temperature, provided it remains below the boiling point of the acid mixture. If boiling occurs, the vessels may leak or even break. For the determination of OC only in the presence of carbonates, an acid pretreatment is required or the TC can be corrected for carbonate as outlined in Section 21.2.4.

21.4.1 Preparation of Reaction Tubes

Standard culture tubes capped with screw caps containing a conical polyseal are modified with three indentations near the top capable of supporting an inserted glass vial (15 × 45 mm). Alternatively, a glass rod bent at one end can be inserted into the tube so that the bend in the rod supports the vial at an appropriate distance above the reaction mixture (Amato 1983). Amato (1983) also suggests the use of regular digestion tubes sealed with subaseals. Either approach is satisfactory.

21.4.2 Reagents

1. Pretreatment acid mixture (for elimination of carbonates): dilute 57 mL of 98% H_2SO_4 in 600 mL of distilled or deionized water and add 92 g of $FeSO_4 \cdot 7H_2O$. Dissolve and make to 1 L to give approximately 1 *M* H_2SO_4 containing 5% antioxidant.

2. Digestion mixture: these are kept separate and only combined in the reaction tube: (a) $K_2Cr_2O_7$ and (b) a mixture of three parts 98% H_2SO_4 and two parts 85% H_3PO_4.

3. CO_2 absorption solution: dissolve 16.0 g of NaOH and bring to 200 mL with distilled or deionized water to give a ~2 *M* solution. This should be kept in an airtight flask or under a CO_2 trap.

4. Indicator solution: dissolve 0.4 g of thymolphthalein in 100 mL in a mixture of 1:1 ethanol:distilled or deionized water.

5. Barium chloride solution: dissolve 41.66 g of $BaCl_2$ (48.86 g of $BaCl_2 \cdot H_2O$) in distilled or deionized water and make to 200 mL to give a ~1 *M* solution.

6. Titrant: use exactly 1.000 *M* HCl.

The following reagents are for use with the two endpoint titration procedure in combination with a pH meter or autotitrator.

7 Tris standard solution: dissolve 2.8000 g of Tris (hydroxy-methyl)-amino-methane (MW = 121.14) in distilled or deionized water and make to 100 mL.

8 ~0.5 *M* HCl: dilute 100 mL of conc. HCl to 2 L with distilled or deionized water.

21.4.3 Oxidation Procedure

Soil sample (ground to <0.15 mm) weights are limited to 2.0 g. Liquid samples up to 5 mL can be digested without pretreatment; larger samples must be evaporated to <5 mL in the digestion tube at 100°C. When liquid samples are processed, the temperature of the digest must be limited to 120°C.

For samples containing up to 10% carbonates, 3 mL of pretreatment acid is added per gram of soil. The pretreatment is done in the digestion tube by shaking them uncapped for 60 min on a reciprocal or orbital shaker set at slow speed. The water added with the acid limits the digestion temperature to 120°C.

1 Place samples into the bottom of the digestion tubes with a long spatula and then pretreat to remove carbonates.

2 Approximately 1 g of $K_2Cr_2O_7$ is added using a long glass funnel. Add 25 mL of the digestion acid mixture and quickly insert the CO_2 trap (vial containing NaOH).

3 Tightly cap the tubes and place in a digestion block preheated to 150°C (120°C for wet samples) for 2 h.

4 Remove the tubes from the block and after 12 h, remove and titrate contents of the CO_2 trap.

21.4.4 Comments

The amount of NaOH in the trap limits the amount of CO_2 that can be absorbed. Using 1 mL of 2 *M* NaOH in a 6 mL capacity vial allows the titration to be made directly in the vial. 1 mL of 2 *M* NaOH will trap 12 mg of CO_2-C, but absorption efficiency drops before this maximum is approached.

21.4.5 Titration Procedure

Carbonic acid trapped in the NaOH can be titrated by the direct, two endpoint method, or by back titration.

Back Titration Procedure

1 Add 2 mL of 1 *M* $BaCl_2$ solution to the NaOH to precipitate $BaCO_3$.

2 Add approximately five drops of the thymolphthalein indicator solution and titrate the NaOH with 1.000 *M* HCl using a microburette accurate to 0.001 mL. Four blanks per 40 tube digestion batch should be included.

Calculation

The OC content of the soil or plant material is calculated as

$$\text{g OC kg}^{-1}\text{sample} = (\text{mL HCl blank} - \text{mL HCl sample}) \times 6/\text{weight sample} \quad (21.9)$$

since 2 mol of OH^- are equivalent to 1 mol (12 g) of C and molarity of the acid is 1.00.

Two Endpoint Titration Procedure

1 Pipette accurately 20.0 mL of Tris standard into a titration vessel and titrate with ~0.5 *M* acid to pH 4.7. Perform standardization of acid at least three times.

2 Three blanks of the NaOH solution and NaOH traps are then titrated against standardized 0.5 *M* HCl as follows.

3 Titrate each solution slowly using standardized 0.5 *M* HCl to pH 8.3 and note volume (T_1). Continue titration to pH 3.8 and note volume (T_2).

If using an auto burette, the speed of the titrations and endpoints will need to be optimized for the burette and strength of acid to ensure the endpoints at pH 8.3 and 3.8 are not overshot.

Calculation

$$\text{Molarity of HCl}(M_{\text{HCl}}) = 0.23114 \times 20/\text{mean titre HCl} \quad (21.10)$$

$$\text{g C kg}^{-1}\text{sample} = (T_1 - T_2) \times M_{\text{HCl}} \times 6/\text{weight sample} \quad (21.11)$$

REFERENCES

Allison, L.E., Bollen, W.B., and Moodie, C.D. 1965. Total carbon. In C.A. Black et al. Eds., *Methods of Soil Analysis, Part 2—Chemical and Microbiological Properties*. American Society of Agronomy, Madison, WI, pp. 1346–1366.

Amato, M. 1983. Determination of carbon ^{12}C and ^{14}C in plant and soil. *Soil Biol. Biochem.* 15: 611–612.

Baldock, J.A., Masiello, C.A., Gélinas, Y., and Hedges, J.I. 2004. Cycling and composition of organic matter in terrestrial and marine ecosystems. *Mar. Chem.* 92: 39–64.

Baldock, J.A. and Nelson, P.N. 1998. Soil organic matter. In M. Sumner, Ed., *Handbook of Soil Science*. CRC Press, Boca Raton, FL, pp. B25–B84.

Ball, D.F. 1964. Loss-on-ignition as an estimate of organic matter and organic carbon in non-calcareous soils. *J. Soil Sci.* 15: 84–92.

Dalal, R.C. 1979. Simple procedure for the determination of total carbon and its radioactivity in soils and plant materials. *Analyst* 104: 151–154.

Giovannini, G., Poggio, G., and Sequi, P. 1975. Use of an automatic CHN analyser to determine organic and inorganic carbon in soils. *Commun. Soil Sci. Plant Anal.* 6: 39–49.

Heanes, D.L. 1984. Determination of total organic-C in soils by an improved chromic acid digestion and spectrophotometric procedure. *Commun. Soil Sci. Plant Anal.* 15: 1191–1213.

Jackson, M.L. 1958. *Soil Chemical Analysis*. Prentice Hall, Englewood Cliffs, NJ.

Jackson, M.L. 1962. *Soil Chemical Analysis*. Constable & Co. Ltd., London.

Kalembasa, S.J. and Jenkinson, D.S. 1973. A comparative study of titrimetric and gravimetric methods for the determination of organic carbon in soil. *J. Sci. Food Agric*. 24: 1085–1090.

Lowther, J.R., Smethurst, P.J., Carlyle, J.C., and Nambiar, E.K.S. 1980. Methods for determining organic carbon in podsolic sands. *Commun. Soil Sci. Plant Anal*. 21: 457–470.

MacCarthy, P., Malcolm, R.L., Clapp, C.E., and Bloom, P.R. 1990. An introduction to soil humic substances. In P. McCarthy et al. Eds., *Humic Substances in Crop and Soil Science: Selected Readings*. Soil Science Society America, Madison, WI, pp. 1–12.

Merry, R.H. and Spouncer, L.R. 1988. The measurement of carbon in soils using a microprocessor-controlled resistance furnace. *Commun. Soil Sci. Plant Anal*. 19: 707–720.

Morris, G.F. and Schnitzer, M. 1967. Rapid determination of carbon in organic matter by dry-combustion. *Can. J. Soil Sci*. 47: 143–144.

Nelson, D.W. and Sommers, L.E. 1982. Total carbon, organic carbon, and organic matter. In A.L. Page et al. Eds., *Methods of Soil Analysis, Part 2—Chemical and Microbiological Properties*, 2nd edn. American Society of Agronomy, Soil Science Society America, Madison, WI, pp. 539–579.

Oades, J.M. 1988. The retention of organic matter in soils. *Biogeochemistry* 5: 35–70.

Piper, C.S. 1944. *Soil and Plant Analysis*. The University of Adelaide, Adelaide, SA, Australia.

Rayment, G.E. and Higginson, F.R. 1992. *Australian Laboratory Handbook of Soil and Water Chemical Methods*. Inkata Press, Melbourne, Victoria, Australia.

Schollenberger, C.J. 1945. Determination of soil organic matter. *Soil Sci*. 59: 53–56.

Skjemstad, J.O. 1992. Genesis of podzols on coastal dunes in southern Queensland. III. The role of aluminium-organic complexes in profile development. *Aust. J. Soil Res*. 30: 645–665.

Snyder, J.D. and Trofymow, J.A. 1984. A rapid accurate wet oxidation diffusion procedure for determining organic and inorganic carbon in plant and soil samples. *Commun. Soil Sci. Plant Anal*. 15: 587–597.

Stevenson, F.J. 1994. Humus Chemistry. *Genesis, Composition, Reactions*. 2nd edn. John Wiley & Sons, New York, NY.

Verardo, D.J., Froelich, P.N., and McIntyre, A. 1990. Determination of organic carbon and nitrogen in marine sediments using the Carlo Erba NA-1500 analyser. *Deep-Sea Res*. 37: 157–165.

Walkley, A. 1947. A critical examination of a rapid method for determining organic carbon in soils—effect of variations in digestion conditions and of inorganic soil constituents. *Soil Sci*. 63: 251–264.

Walkley, A. and Black, I.A. 1934. An examination of the Degtjareff method for determining soil organic matter, and a proposed modification of the chromic acid titration method. *Soil Sci*. 37: 29–38.

Chapter 22
Total Nitrogen

P.M. Rutherford, W.B. McGill, and J.M. Arocena

University of Northern British Columbia

Prince George, British Columbia, Canada

C.T. Figueiredo

University of Alberta

Edmonton, Alberta, Canada

22.1 INTRODUCTION

Total soil N includes all forms of inorganic and organic soil N. Inorganic N includes soluble forms (e.g., NO_2^- and NO_3^-), exchangeable NH_4^+, and clay-fixed nonexchangeable NH_4^+. Organic N content includes numerous identifiable and nonidentifiable forms (Stevenson 1986) and can be determined by the difference between total soil N and inorganic soil N content. Total N analyses may be divided into two main types: (i) wet digestion (e.g., Kjeldahl method) or (ii) dry combustion (e.g., Dumas method). Wet digestion techniques involve conversion of organic and inorganic N to NH_4^+ in acid and its subsequent measurement. Salts (e.g., K_2SO_4) and catalysts (e.g., Cu) are usually added to increase digestion temperatures and accelerate oxidation of organic matter (Bremner 1996). The dry combustion method normally involves an initial oxidation step followed by passage of the gases through a reduction furnace to reduce NO_x to N_2. The quantity of N_2 is usually determined using a thermal conductivity detector. Near-infrared reflectance spectrometry has recently been used for the determination of total soil N (Chang and Laird 2002), but the method will not be described here.

The Dumas method is becoming increasingly common due to greater availability and simplicity of modern automated instruments, which can determine C, H, N, or S on the same sample, and O with a simple modification. Modern systems are available in various configurations and have improved accuracy and precision for total N determination over earlier models (Bremner 1996). Dry combustion instruments for total N may be connected in-line with an isotope ratio mass spectrometer for simultaneous analyses of ^{15}N (Minagawa et al. 1984; Marshall and Whiteway 1985; Kirsten and Jansson 1986). Bellomonte et al. (1987) concluded that the automated Dumas procedure was comparable to Kjeldahl analysis for heterogeneous substrates. They reported, using a commercial Dumas system for total N analysis, coefficients of variation of 0.79% for cereal flour and 1.08% for meat. Reports since then confirm total N in plant materials, feeds, excreta, carcasses, and other agricultural

materials determined by dry combustion to be comparable to or slightly greater than by Kjeldahl digestion (Matejovic 1995; Etheridge et al. 1998; Schindler and Knighton 1999; Marcó et al. 2002). Results are slightly more variable with soils. While results for total soil N have been reported as comparable for Kjeldahl and dry combustion methods in some studies (Artiola 1990; Yeomans and Bremner 1991), total N determined by dry combustion was found to be slightly lower but proportional to Kjeldahl determination by Kowalenko (2001). Others have found total soil N by dry combustion to be slightly greater than conventional Kjeldahl digestion (McGeehan and Naylor 1988; Vittori Antisari and Sequi 1988). High NO_3^- concentrations in sample materials contribute to lower total N by the Kjeldahl method if pretreatments to include NO_3^- (see below) are not used (Matejovic 1995; Watson and Galliher 2001); however, NO_3^- alone may not account for lower Kjeldahl values (Simonne et al. 1998).

Kjeldahl procedures are still widely used for total N determination. Although some fixed or intercalary NH_4^+ is normally included in Kjeldahl digestion, it may not be quantitatively extracted from soils with a high proportion of their N constituted as fixed NH_4^+. In such cases, an HF–HCl pretreatment, as described by Bremner (1996), may be necessary to free intercalary NH_4^+. Corti et al. (1999) reported a method to measure fixed NH_4^+ using a Kjeldahl digestion followed by distillation, and a digestion of the residue with 5 *M* HF:1 *M* HCl and a second distillation to quantify strongly fixed NH_4^+. Vittori Antisari and Sequi (1988) reported that both dry combustion and microwave digestion with HF–HCl, H_3BO_3, and H_2O_2 followed by micro-Kjeldahl distillation were effective at including fixed NH_4^+ in total N analysis.

Given the time involved in Kjeldahl analyses, efforts have been made to speed up digestions. One such example is the peroxy method, which replaces K_2SO_4 and metal catalyst with peroxymonosulfuric acid (H_2SO_5), and involves carbonizing the sample in H_2SO_4 before adding the peroxy reagent (viz. $H_2SO_4 + H_2O_2$). It is 25 times faster than conventional Kjeldahl procedures and fully recovers the N of a variety of plant materials and one of the most refractory organic compounds, nicotinic acid (Hach et al. 1985). To enhance safety and improve speed, Hach et al. (1987) developed a system using a Vigreux fractionation head to simplify the addition of the peroxy reagent, and to maintain constant residual H_2O_2 in the digestion solution. A procedure for soils described by Christianson and Holt (1989) takes only 38 min; however, N recovery from six soils ranged from 89% to 98% compared to Kjeldahl digestion. Further investigation on soil materials would be warranted. Mason et al. (1999) used microwave heating to accelerate digestion using only H_2SO_4 and $CuSO_4$ for twofold reduction in time for soil samples. Their system can perform six digests simultaneously. Although microwave-assisted digestion has been widely adopted for sample preparation for metal analyses (Smith and Arsenault 1996), it has not received wide application for digestion of soils for total N analysis.

The total time required for Kjeldahl determination of N can be reduced considerably by using automated colorimetric analysis of NH_4^+. The most common method uses the Berthelot or indophenol reaction, which is specific for ammonia, and is well-documented (Searle 1984). The method has similar results and precision as the distillation procedure (Schuman et al. 1973). Mason et al. (1999) used the method following microwave-assisted digestion of soil. A manual version of the Berthelot reaction has been used to quantify NH_4^+ from Kjeldahl digestion of soils (Wang and Oien 1986).

The presence of NO_3^- can be a concern because unmodified Kjeldahl digestion recovers some, but not all, NO_3^-, thereby precluding the addition of NO_3^- from a separate analysis to

the Kjeldahl total N values (Goh 1972; Wikoff and Moraghan 1985; Bremner 1996). Hence, methods were developed to include NO_3^- in Kjeldahl digestions. Pruden et al. (1985) proposed pretreatment of soil with Zn and $CrK(SO_4)_2$ to reduce NO_3^- to NH_4^+ before proceeding with normal Kjeldahl digestion. Dalal et al. (1984) proposed adding sodium thiosulfate to the digestion mixture to reduce NO_3^- or NO_2^-. The method requires no pretreatment and is satisfactory with wet or dry samples. DuPreez and Bate (1989) reported that phenyl acetate added to dry samples resulted in quantitative recovery of NO_3^- or NO_2^-. Phenyl acetate reacts with NO_3^- or NO_2^- under acidic conditions to form nitrophenolic compounds from which N is fully recovered. The procedure requires no additional reductant or pretreatment but is suitable for dry samples only.

Selection of the most suitable combination of variables for the Kjeldahl method must be based on local requirements and facilities. Digestion options include H_2SO_4 with or without H_2O_2, heating mantles or digestion blocks, macro- or semimicro digestion, inclusion or omission of NO_2^- plus NO_3^-. Subsequent measurement of NH_4^+ may use the Berthelot reaction, NH_4^+ electrode, diffusion in digestion tubes or Conway dishes, steam distillation directly from digestion tubes or from standard taper flasks, macro- or semimicro distillation, titration with an indicator or using automated titrators. Several semiautomatic to fully automatic distillation systems are now commercially available and allow for very rapid analysis. Digestion in tubes using block heaters with the temperature controlled electronically is now common. Several modern infrared digestion systems are available and have much faster heat-up and cool-down times than traditional aluminum block systems.

The choice here has been to present details of modern methods that could be widely used, to introduce special purpose methods by way of comments, and to provide citations for older or classical methods. Micro-Kjeldahl digestion procedures are given with and without steps to include NO_2^- and NO_3^-. Usually NO_2^- plus NO_3^- is a negligible component of soil total N, and procedure given in Section 22.2 should be satisfactory. Macro-Kjeldahl procedures are little used nowadays because of the cost and disposal of chemicals used in the digestion, and the high precision of micro-Kjeldahl and Dumas procedures.

22.2 MICRO-KJELDAHL DIGESTION FOLLOWED BY STEAM DISTILLATION: WITHOUT PRETREATMENT TO INCLUDE NO_2^- AND NO_3^- QUANTITATIVELY

This method is appropriate for total N determination on samples of surface soil horizons in which the NO_3^- and NO_2^- contents are negligible. If used with samples containing significant amounts of NO_3^- or NO_2^-, the results will be higher than for the fixed NH_4^+ plus organic N content alone, but lower than for total N including NO_3^- and NO_2^-. This method is not recommended for analysis of total N in soil samples from ^{15}N tracer studies because of the significant influence of highly labeled NO_2^- or NO_3^- on ^{15}N analyses. The method outlined in Section 22.3 is recommended for such samples.

22.2.1 Materials and Reagents: Digestion

1 Heating block with digestion tubes, timer, and temperature controller (see Section 22.2.5). The block must be capable of maintaining a temperature of 360°C for up to 5 h. Blocks holding 40 tubes (20 mm OD × 350 mm long) calibrated to hold 0.1 L are commonly used for micro-Kjeldahl digestions.

2 Air condenser designed to fit over the digestion tubes in the block (see Section 22.2.5).

3 Concentrated (18 *M*) H_2SO_4.

4 Low N content K_2SO_4, $CuSO_4$: mixed in mass ratio of 8.8:1 (K_2SO_4: $CuSO_4 \cdot 5H_2O$). Approximately 3.5 g of mix is required per sample.

5 Hengar granules, both selenized and nonselenized.

22.2.2 Materials and Reagents: Distillation and Titration

1 Micro-Kjeldahl steam distillation apparatus (Figure 22.1). See Section 22.2.5.

2 Steam distillation flasks: 0.5 L round bottom, with 19/38 standard taper ground glass joint.

3 NaOH: 10 *M* and 0.1 *M*, prepared in CO_2-free deionized water.

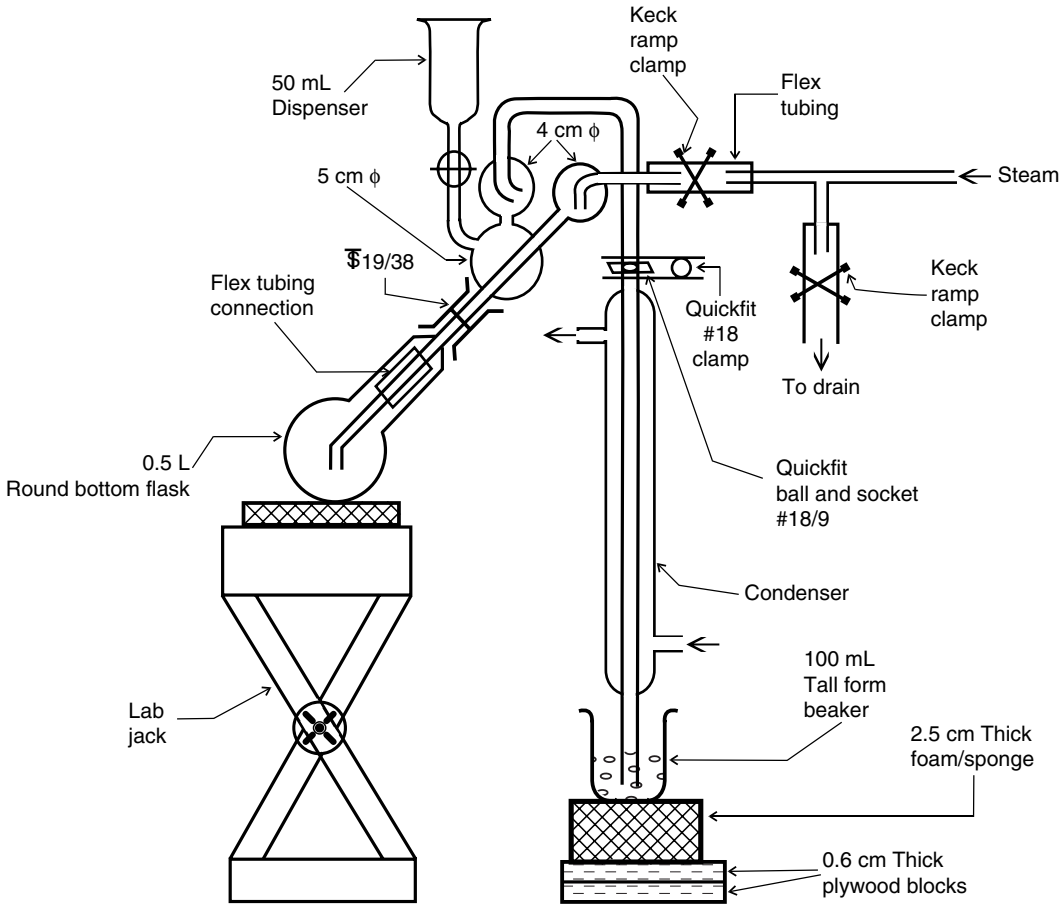

FIGURE 22.1. Steam distillation apparatus.

4 Boric acid (2% w/v) plus indicator: place 80 g of boric acid (H_3BO_3) powder into a 0.25 L beaker. Add ~20–40 mL of H_2O and mix with a glass rod to wet all the H_3BO_3. Pour into ~3 L of H_2O in a 4 L flask and stir with an electric stir rod. Once wet, the H_3BO_3 dissolves readily. Add 80 mL of mixed indicator prepared as follows: 0.099 g bromocresol green and 0.066 g methyl red dissolved in 100 mL ethanol. Add 0.1 *M* NaOH cautiously until the solution turns reddish-purple (pH 4.8–5.0). Make up to 4 L with deionized H_2O and mix thoroughly.

5 Graduated beakers: 100 mL.

6 Burette: 10 mL graduated at 0.02 or 0.01 mL intervals. A magnetic stirrer is desirable.

7 H_2SO_4: 0.01 *M* (standardized).

22.2.3 Procedure: Digestion, Distillation, and Titration

1 Place sample, containing about 1 mg N, in a dry digestion tube. This will usually vary from 0.25 to 2.0 g.

2 Add 2 mL deionized H_2O (3 mL if using 2 g soil) and swirl to wet all the soil.

3 To each tube add 3.5 g of K_2SO_4: $CuSO_4$, mix.

4 Add one selenized and one nonselenized Hengar granule.

5 Add 10 mL concentrated H_2SO_4.

6 Place the digestion tubes into the digestion block.

7 Program the block to raise the temperature to 220°C and maintain it there for 1.5 h. Digestion will start and water will be removed during this time.

8 After 1.5 h of digestion at 220°C, put the air condensers onto the digestion tubes in the block.

9 Program the block to raise the temperature to 360°C and maintain it there for 3.5 h.

10 After digestion is complete, cool the samples overnight in the block or on a fiberglass pad.

11 Remove the air condenser and rinse with water.

12 Slowly and with swirling, add 25 mL deionized water to each cooled digestion tube. Vortex the sample to dissolve salts that may have solidified during cooling. If all the material does not enter into suspension, warm gently until it does. Transfer the sample quantitatively, with three washes of deionized water, to a 0.5 L round-bottom distillation flask.

13 With the condensers on, connect the distillation flask to the steam distillation apparatus; secure with a clamp.

14 Open the steam supply to the distillation head to allow steam into the tubing. Be sure the drain line is already open so that steam can exit to the drain.

15 Place a 100 mL graduated beaker with 5 mL of 2% H_3BO_3 under the condenser so that the tip of the condenser is immersed in the H_3BO_3.

16 Very slowly add an excess (usually 30 mL; see Section 22.2.5) of 10 *M* NaOH through the distillation head. Do not completely empty the NaOH reservoir, otherwise NH_3 may be lost through the stopcock.

17 Close the pinch clamp, or stopcock, going to the steam drain; this directs steam into the distillation flask. The steam generation rate should be such that the distillate is collected at about 6 mL min^{-1}. Collect 40 mL of distillate.

18 Open the pinch clamp to the steam drain and remove the distillation flask then close the pinch clamp to the distillation head. This sequence is important to prevent steam burns and drawback of fluid from the distillation flask into the steam line.

19 Wash the tip of the condenser into the beaker.

20 Titrate the distillate with 0.01 *M* H_2SO_4. The color change at the endpoint is from green to pink (pH $\approx$ 5.4).

22.2.4 Calculations

One mL of 1 *M* H_2SO_4 is equivalent to 28.01 mg of N.

$$\text{Total N, g kg}^{-1} = \frac{(\text{mL sample} - \text{mL blank}) \times M \times 28.01}{\text{oven-dry mass of soil sample (g)}} \tag{22.1}$$

where M is the molarity of standard H_2SO_4, mL sample is the volume of standard H_2SO_4 used during titration of sample, and mL blank is the volume of standard H_2SO_4 used during titration of blank.

The blank is included from the digestion step onward; it contains all materials excluding a soil sample.

22.2.5 Comments

1 Soil samples should be dried (usually air-drying) and ground to pass a 100 mesh (150 μm) sieve.

2 Heating blocks and tubes supplied by Tecator or Technicon have been found satisfactory for Kjeldahl digestions in our laboratory. The air condenser described by Panasiuk and Redshaw (1977) can be constructed by a competent glassblower. Equivalent devices are available from Tecator. A variety of sophisticated digestion systems are also available from VELP, Gernhart, and other manufacturers (e.g., Fisher, VWR, Cole Parmer, or other suppliers). Some of these units use infrared

digestion to greatly decrease heating and cooling times over traditional aluminum block systems.

3 The K_2SO_4: $CuSO_4$ mix can be prepared in the laboratory, obtained as a loose mix or in appropriately sized packages (~3.5 g) from commercial suppliers (e.g., Kjeltabs—trademark of Tecator, Inc.). Bulk mixes should use low N materials and be kept tightly sealed during storage to avoid absorption of moisture and caking.

4 A variety of manual, semiautomatic to fully automatic distillation systems are available from a variety of manufacturers (e.g., Labconco, Gerhardt, VELP). These systems are quite rapid, often reducing distillation times to ~2 min from ~7 to 8 min for the setup shown in Figure 22.1. Distillation systems similar to those in Figure 22.1 are described by Bremner (1996) and Bremner and Breitenbeck (1983). Commercial systems specifically designed for use with digestion tubes are available. We have used two distillation heads, each supplied with steam from a 5 L round-bottom boiling flask heated by a 600 W heating mantle. Several dozen Hengar granules are placed in each flask. Concentrated phosphoric acid (about 2 mL) is added to each boiling flask to absorb NH_3.

5 We have eliminated sample transfer from the digestion tube to a distillation flask by doing digestions in a 0.25 L digestion tube designed for a block that holds 20, rather than 40, tubes. The distillation head was modified by attaching a rubber stopper with a hole through which the standard taper joint of the distillation head fits. The 0.25 L digestion tube is attached to the distillation unit by fitting the end over the rubber stopper. It is held securely in place with a clamp, allowing distillation directly from the digestion tube. The distillation system described by Bremner and Breitenbeck (1983) uses tubes designed for the 40 tube blocks.

6 The NaOH must be added slowly and carefully to avoid violent bubbling that would force the liquid into the condenser and contaminate the distillation head. The amount of NaOH needed varies with the amount of H_2SO_4 consumed during digestion of the sample. Consumption of H_2SO_4 varies with the amount of soil organic matter and reduced minerals present; e.g., 1 g of C consumes 10 mL of H_2SO_4 (Bremner 1996).

7 Distillation can be replaced by autoanalyzer analysis of the digested sample. When we use this approach, the digested sample is diluted to 0.1 L followed by an autoanalyzer method for colorimetric measurement of NH_4^+ (Smith and Scott 1991).

8 Use of an automatic titrator can improve consistency and eliminate the need to mix an indicator into the boric acid solution.

9 The above Kjeldahl digestion method does not quantitatively recover fixed NH_4^+ in most soils. For total N analysis of soils with a high proportion of their N as fixed NH_4^+, an HF–HCl modification as described by Bremner (1996) may be necessary to release fixed NH_4^+.

22.3 MICRO-KJELDAHL DIGESTION FOLLOWED BY STEAM DISTILLATION: NO_2^- AND NO_3^- INCLUDED QUANTITATIVELY

This is the method of choice for total N analysis of samples of surface soil horizons containing an appreciable quantity of N as NO_2^- or NO_3^-. Because of the significant influence of highly labeled NO_2^- or NO_3^- on ^{15}N analyses, this method is recommended for analysis of total N in all soil samples from ^{15}N tracer studies. This method is the same as in Section 22.2, except for the addition of a pretreatment to oxidize NO_2^- to NO_3^- and then to reduce the NO_3^- to NH_4^+.

22.3.1 Materials and Reagents: Pretreatment and Digestion

1 All items from Section 22.2.1, plus the following:

2 Potassium permanganate solution: dissolve 50 g $KMnO_4$ in 1 L deionized H_2O; store in an amber bottle.

3 H_2SO_4, 9 *M*: dilute concentrated H_2SO_4 to twice its volume with deionized H_2O.

4 Fe powder; finer than 100 mesh sieve.

5 *N*-octyl alcohol.

22.3.2 Materials and Reagents: Distillation and Titration

All items from Section 22.2.2.

22.3.3 Procedure: Pretreatment to Reduce NO_2^- and NO_3^- to NH_4^+

1 Place sample, containing about 1 mg N, in a dry digestion tube. Usually this is 0.25–2.0 g of soil.

2 Add 2 mL deionized H_2O (3 mL if using 2 g soil) and swirl to wet all the soil.

3 Add 1 mL $KMnO_4$ and swirl for 30 s.

4 Hold the digestion tube at a 45° angle and very slowly pipette 2 mL dilute H_2SO_4.

5 Allow to stand for 5 min.

6 Add one drop *N*-octyl alcohol (to control frothing).

7 Add 0.5 g reduced Fe using a scoop, through a dry, long-stemmed funnel or thistle funnel tube.

8 Immediately cover the digestion tube with an inverted 25 mL beaker or 50 mL Erlenmeyer flask inverted to prevent loss of water.

9 Swirl to bring the Fe into contact with the acid.

10 Allow to stand (about 15 min) until strong effervescence has ceased.

11 Place digestion tubes into the digestion block and program it to raise the temperature to 100°C and hold it there for 1 h.

12 Cool the tubes before proceeding to digestion.

22.3.4 Procedure: Digestion, Distillation, and Titration

Follow steps 3 to 20 inclusive, of Section 22.2.3.

22.3.5 Calculations

Use Equation 22.1, described in Section 22.2.4.

22.3.6 Comments

1 The $KMnO_4$ oxidizes NO_2^- to NO_3^-, which is reduced to NH_4^+ by reduced Fe.

2 *N*-octyl alcohol is added to reduce frothing.

3 Goh (1972) concluded that it was not necessary to include the permanganate pretreatment when reduced iron is used as a reductant in the procedure to include NO_3^-.

4 See Section 22.2.5 for additional important information.

22.4 DUMAS METHODS

Several automated Dumas systems are available (Kirsten and Jansson 1986; Tabatabai and Bremner 1991; Bremner 1996). Many systems combust the sample in a stream of pure O_2 at high temperatures, producing NO_x and N_2. An aliquot of gas is carried by pure He into a reduction zone where elemental Cu reduces NO_x to N_2, which is subsequently measured by a thermal conductivity detector. Other systems convert total N to N_2 by fusing the sample in a graphite crucible at very high temperatures in a He atmosphere, followed by determination of N_2 by gas chromatography (Bremner 1996). Numerous configurations are available depending on what other elements (e.g., C, H, S, O) are also to be determined. Since Dumas procedures are quite variable and instrument dependent, it is not possible to provide a generic methodology here.

Compared to Kjeldahl, Dumas techniques have the advantage of requiring less laboratory space, provide rapid analysis, require less chemical reactants, do not produce noxious fumes or hazardous chemical wastes, and include all forms of N without lengthy pretreatments (Bellomonte et al. 1987; Vittori Antisari and Sequi 1988). They are suitable for ^{15}N tracer studies when linked by a continuous flow interface from the nitrogen analyzer to an isotope ratio mass spectrometer (Fiedler and Proksch 1975; Minagawa et al. 1984; Marshall and Whiteway 1985). For tracer studies, they avoid digestion, distillation, titration, evaporation, and subsequent oxidation of NH_3 to N_2.

Sample variability is a concern with combustion techniques because of the small sample size required in some instruments (<50 mg). Schepers et al. (1989) recommended that plant and

soil samples should be ball milled before combustion analysis. Arnold and Schepers (2004) reported on a simple roller-mill grinding procedure as an alternative to ball milling plant and soil samples. See Bremner (1996), Kowalenko (2001), Pérez et al. (2001), and Wang et al. (1993) for further information on grinding and sample preparation.

We recommend that soil samples be air-dried and passed through a 2 mm (10 mesh) sieve. Subsamples are then finely ground using a ball-mill such as the Brinkmann, Mixer Mill, model MM2. With the grinder set to its maximum setting, soils take 1.5–2 min to grind to a fine powder (<100 mesh). Ensure grinding capsules and balls are well cleaned before attempting the next sample. If samples are resinous, grind a small scoop of pure silica sand between samples (for ≈30 s) to help clean the resin from the ball and capsules; vacuum and wipe capsules and balls before grinding the next sample. After fine grinding, samples should be dried overnight at 60°C–70°C and cooled in desiccators before weighing for analysis.

REFERENCES

Arnold, S.L. and Schepers, J.S. 2004. A simple roller-mill grinding procedure for plant and soil samples. *Commun. Soil Sci. Plant Anal.* 35: 537–545.

Artiola, J.F. 1990. Determination of carbon, nitrogen and sulfur in soils, sediments and wastes: a comparative study. *Int. J. Environ. Chem.* 41: 159–171.

Bellomonte, G., Costantini, A., and Giammarioli, S. 1987. Comparison of modified automatic Dumas method and the traditional Kjeldahl method for nitrogen determination in infant food. *J. Assoc. Off. Anal. Chem.* 70: 227–229.

Bremner, J.M. 1996. Nitrogen—total. In D.L. Sparks et al., Eds. *Methods of Soil Analysis, Part 3—Chemical Methods*. Soil Science Society of America, American Society of Agronomy, Madison, WI, pp. 1085–1121.

Bremner, J.M. and Breitenbeck, G.A. 1983. A simple method for determination of ammonium in semimicro-Kjeldahl analysis of soils and plant materials using a block digester. *Commun. Soil Sci. Plant Anal.* 14: 905–913.

Chang, C.W. and Laird, D.A. 2002. Near-infrared reflectance spectroscopic analysis of soil C and N. *Soil Sci.* 167: 110–116.

Christianson, C.B. and Holt, L.S. 1989. Rapid digestion procedure for the determination of total N and nitrogen-15 content of soils. *Soil Sci. Soc. Am. J.* 53: 1917–1919.

Corti, G., Agnelli, A., and Ugolini, F.C. 1999. A modified Kjeldahl procedure for determining strongly fixed NH_4^+-N. *Eur. J. Soil Sci.* 50: 523–534.

Dalal, R.C., Sahrawat, K.L., and Myers, R.J.K. 1984. Inclusion of nitrate and nitrite in the Kjeldahl nitrogen determination of soils and plant materials using sodium thiosulphate. *Commun. Soil Sci. Plant Anal.* 15: 1453–1461.

DuPreez, D.R. and Bate, G.C. 1989. A simple method for the quantitative recovery of nitrate-N during Kjeldahl analysis of dry soil and plant samples. *Commun. Soil Sci. Plant Anal.* 20: 345–357.

Etheridge, R.D., Pesti, G.M., and Foster, E.H. 1998. A comparison of nitrogen values obtained utilizing the Kjeldahl nitrogen and Dumas combustion methodologies (Leco CNS 2000) on samples typical of an animal nutrition analytical laboratory. *Anim. Feed Sci. Technol.* 73: 21–28.

Fiedler, R. and Proksch, G. 1975. The determination of nitrogen-15 by emission and mass spectrometry in biochemical analysis: a review. *Anal. Chim. Acta* 78: 1–62.

Goh, K.M. 1972. Comparison and evaluation of methods for including nitrate in the total determination of soils. *J. Sci. Food Agric.* 23: 275–284.

Hach, C.C., Bowden, B.K., Kopelove, A.B., and Brayton, S.V. 1987. More powerful peroxide

Kjeldahl digestion method. *J. Assoc. Off. Anal. Chem.* 70: 783–787.

Hach, C.C., Brayton, S.V., and Kopelove, A.B. 1985. A powerful Kjeldahl nitrogen method using peroxymonosulfuric acid. *J. Agric. Food Chem.* 33: 1117–1123.

Kirsten, W.J. and Jansson, K.H. 1986. Rapid and automatic determination of nitrogen using flash combustion of large samples. *Anal. Chem.* 58: 2109–2112.

Kowalenko, C.G. 2001. Assessment of LECO CNS-2000 analyzer for simultaneously measuring total carbon, nitrogen and sulfur in soil. *Commun. Soil Sci. Plant Anal.* 32: 2065–2078.

Marcó, A., Rubio, R., Compañó, R., and Casals, I. 2002. Comparison of the Kjeldahl method and a combustion method for total nitrogen determination in animal feed. *Talanta* 57: 1019–1026.

Marshall, R.B. and Whiteway, J.N. 1985. Automation of an interface between a nitrogen analyzer and an isotope ratio mass spectrometer. *Analyst* 110: 867–871.

Mason, C.J., Coe, G., Edwards, M., and Riby, P.G. 1999. The use of microwaves in the acceleration of digestion and colour development in the determination of total Kjeldahl nitrogen in soil. *Analyst* 124: 1719–1726.

Matejovic, I. 1995. Total nitrogen in plant-material determined by means of dry combustion—a possible alternative to determination by Kjeldahl digestion. *Commun. Soil Sci. Plant Anal.* 26: 2217–2229.

McGeehan, S.L. and Naylor, D.V. 1988. Automated instrumental analysis of carbon and nitrogen in plant and soil samples. *Commun. Soil Sci. Plant Anal.* 19: 493–505.

Minagawa, M., Winter, D.A., and Kaplan, I.R. 1984. Comparison of Kjeldahl and combustion methods for measurement of nitrogen isotope ratios in organic matter. *Anal. Chem.* 56: 1859–1861.

Panasiuk, R. and Redshaw, E.S. 1977. A simple apparatus used for effective fume control during plant tissue digestion using a heating block. *Commun. Soil Sci. Plant Anal.* 8: 411–416.

Pérez, D.V., de Alcantara, S., Arruda, R.J., and Meneghelli, N.D.A. 2001. Comparing two methods for soil carbon and nitrogen determination using selected Brazilian soils. *Commun. Soil Sci. Plant Anal.* 32: 295–309.

Pruden, G., Kalembasa, S.J., and Jenkinson, D.S. 1985. Reduction of nitrate prior to Kjeldahl digestion. *J. Sci. Food Agric.* 36: 71–73.

Schepers, J.S., Francis, D.D., and Thompson, M.T. 1989. Simultaneous determination of total C, total N and ^{15}N in soil and plant material. *Commun. Soil Sci. Plant Anal.* 20: 949–959.

Schindler, F.V. and Knighton, R.E. 1999. Sample preparation for total nitrogen and N-15 ratio analysis by the automated Dumas combustion method. *Commun. Soil Sci. Plant Anal.* 30: 1315–1324.

Schuman, G.E., Stanley, M.A., and Knudsen, D. 1973. Automated total nitrogen analysis of soil and plant samples. *Soil Sci. Soc. Am. Proc.* 37: 480–481.

Searle, P.L. 1984. The Bertholet or indophenol reaction and its use in the analytical chemistry of nitrogen. *Analyst* 109: 549–568.

Simonne, E.H., Harris, C.E., and Mills, H.A. 1998. Does the nitrate fraction account for differences between Dumas-N and Kjeldahl-N values in vegetable leaves? *J. Plant Nutr.* 21: 2527–2534.

Smith, F.E. and Arsenault, E.A. 1996. Microwave assisted sample preparation in analytical chemistry. *Talanta* 43: 1207–1268.

Smith, K.A. and Scott, A. 1991. Continuous-flow, flow-injection, and discrete analysis. In K.A. Smith, Ed. *Soil Analysis: Modern Instrumental Techniques*, 2nd ed. Marcel Dekker, New York, pp. 183–227.

Stevenson, F.J. 1986. *Cycles of Soil: Carbon, Nitrogen, Phosphorus, Sulfur, Micronutrients*. John Wiley & Sons, New York, NY.

Tabatabai, M.A. and Bremner, J.M. 1991. Automated instruments for determination of total carbon, nitrogen, and sulfur in soils by combustion techniques. In K.A. Smith, Ed. *Soil Analysis: Modern Instrumental Techniques*, 2nd ed. Marcel Dekker, New York, NY, pp. 261–286.

Vittori Antisari, L. and Sequi, P. 1988. Comparison of total nitrogen by four procedures and sequential determination of exchangeable ammonium, organic nitrogen and fixed ammonium in soil. *Soil Sci. Soc. Am. J.* 52: 1020–1023.

Wang, D., Snyder, M.C., and Bormann, F.H. 1993. Potential errors in measuring nitrogen content of soils low in nitrogen. *Soil Sci. Soc. Am. J.* 57: 1533–1536.

Wang, L. and Oien, A. 1986. Determination of Kjeldahl nitrogen and exchangeable ammonium in soil by the indophenol method. *Acta Agric. Scand.* 36: 60–70.

Watson, M.E. and Galliher, T.L. 2001. Comparison of Dumas and Kjeldahl methods with automatic analyzers on agricultural samples under routine rapid analysis conditions. *Commun. Soil Sci. Plant Anal.* 32: 2007–2019.

Wikoff, L. and Moraghan, J.T. 1985. Recovery of soil nitrate by Kjeldahl analysis. *Commun. Soil Sci. Plant Anal.* 16: 923–929.

Yeomans, J.C. and Bremner, J.M. 1991. Carbon and nitrogen analysis of soils by automated combustion techniques. *Commun. Soil Sci. Plant Anal.* 22: 843–850.

Chapter 23
Chemical Characterization of Soil Sulfur

C.G. Kowalenko
Agriculture and Agri-Food Canada
Agassiz, British Columbia, Canada

M. Grimmett
Agriculture and Agri-Food Canada
Charlottetown, Prince Edward Island, Canada

23.1 INTRODUCTION

Sulfur is relatively abundant in the terrestrial environment and assumed to be the 15th most abundant element (Arnhold and Stoeppler 2004). It is present in the soil in a variety of forms, both organic and inorganic, and various valence states (Blanchar 1986), each having different chemical, biological, and environmental significance. Various chemical analyses have been proposed to measure the various forms of sulfur in soils, for different purposes (e.g., soil genesis, plant availability, or environmental assessment). The relative success for measuring different forms, however, is limited by available chemical quantification methods. The most common basic measurements of soil sulfur forms are total, organic, inorganic, and extractable (i.e., plant-available) sulfur.

23.1.1 Total Sulfur

Measurement of total sulfur is an important measurement on its own but it is often also involved in quantifying specific forms by difference calculation (e.g., total organic S = total S minus total inorganic S). Numerous methods have been proposed for determining total sulfur, but none are universally accepted (Tabatabai 1982; Blanchar 1986). Almost all methods for measuring total soil require two steps: (1) conversion of all sulfur to one form and (2) quantification of the resulting form. Methods available for the conversion step include ashing (or dry combustion) and wet digestion (Tabatabai 1982; Blanchar 1986). Dry ashing includes use of ovens, heating elements, open flames (e.g., fusion), enclosed flames (e.g., oxygen flask), or high-temperature combustion using induction or resistance furnaces. Wet digestion may be either alkaline or acidic. Numerous sulfur quantification methods are available for gases and solutions in oxidized or reduced forms. Gases can be

quantified directly by infrared, chemiluminescent, coulometric, flame photometric, and other methods. Solutions (either absorbed/dissolved gases, liquid digests, or solubilized solids) are usually analyzed as sulfide or sulfate by spectrometry (colorimetry, flame emission, atomic absorption, etc.), ion-selective electrode, titration, gravimetry, and chromatography. Both or either of the conversion and the quantification steps can be automated. X-ray fluorescence (Jenkins 1984) measures sulfur in one step.

Comparisons of methods for determining total sulfur in soils have been conducted (e.g., Gerzabek and Schaffer 1986); however, the comparisons have been limited with respect to the scope of soils analyzed and the type of methods compared (Tabatabai and Bremner 1970b; Matrai 1989; Kowalenko 2001). Variable results occurred and no one method could clearly be said to give a true estimate of total sulfur (Hogan and Maynard 1984; Kowalenko 2000). The highest value cannot necessarily be taken as the true value.

Several studies have found that high-temperature combustion has not resulted in particularly satisfactory results for some soil samples, but more recent instrumentation has shown good results (Kowalenko 2001). Many combustion units have relatively high detection limits for analysis of materials, such as coal, that have substantial concentrations of sulfur. X-ray fluorescence requires an adjustment for the organic matter content in the sample (Brown and Kanaris-Sotiriou 1969). The success of low-temperature ashing has been variable (Tabatabai and Bremner 1970a; Killham and Wainwright 1981). Acid digestion should be used with caution, as gaseous losses of sulfur are possible (Randall and Spencer 1980). Dry ashing with sodium bicarbonate and silver oxide followed by ion chromatography (IC) or hydriodic acid reduction has shown variable results (Tabatabai and Bremner 1970b; Tabatabai et al. 1988). A fusion technique proposed for geological samples using sodium peroxide followed by IC was not completely satisfactory (Stallings et al. 1988). Hordijk et al. (1989) found good agreement for total sulfur measurement in freshwater sediments by IC with inductively coupled plasma (ICP) and roentgen fluorescence methods after Na_2CO_3/KNO_3 fusion.

23.1.2 Organic Sulfur

Organic sulfur accounts for most of the sulfur present in the surface horizons of soils (Tabatabai 1982; Blanchar 1986). A number of methods have been attempted to directly determine organic sulfur compounds in soils (Kowalenko 1978), but none have been universally accepted. Measurement of sulfur-containing amino acids such as methionine, cystine, etc., requires special precautions and these compounds do not appear to account for a very large portion of the total sulfur present. There has been some success in determining the sulfur content of lipid extracts (Chae and Lowe 1981; Chae and Tabatabai 1981), but this fraction also accounts for only a small portion of the sulfur in the soil. Sulfur that is present in microorganisms does not constitute a specific organic compound and may include inorganic as well as various organic forms. This fraction comprises only a small portion of the total sulfur (Strick and Nakas 1984; Chapman 1987) but may have considerable biological significance. In order to estimate microbial sulfur, the method requires the measurement of extractable inorganic sulfate.

Lowe and DeLong (1963) proposed the determination of carbon-bonded sulfur using a digestion with Raney nickel in sodium hydroxide. Although this method was shown to be quite specific for carbon-bonded sulfur, and hence most of the organic sulfur in soils, the method is not quantitative due to interference problems in soils and soil extracts (Freney et al. 1970; Scott et al. 1981). The difference between total sulfur and hydriodic acid-reducible sulfur appears to provide a better estimate of carbon-bonded sulfur than direct determination

by Raney nickel digestion. The success of this or other difference approaches to quantifying organic sulfur in soils depends on accurate measurements of all fractions involved in the calculation. Likewise, determining organic sulfur by subtracting inorganic from total sulfur requires accurate measurement of all inorganic forms that are present in the sample.

23.1.3 Inorganic Sulfur

Inorganic sulfur is largely in oxidized (sulfate) form in aerobic soils, and in reduced forms (sulfide, elemental sulfur, etc.) in anaerobic soils (Tabatabai 1982; Blanchar 1986). No single method has been developed to measure total inorganic sulfur that includes reduced and oxidized forms. Highly reduced forms of sulfur are not very soluble; therefore, cannot be readily extracted for quantification. Methods for directly determining reduced inorganic sulfur have been proposed, but not thoroughly evaluated (Barrow 1970; Watkinson et al. 1987) because these forms are limited in agricultural soils. Zinc–hydrochloric acid distillation has been used to measure reduced inorganic sulfur in soils (David et al. 1983; Roberts and Bettany 1985), but would not include all inorganic forms (Aspiras et al. 1972). Digestion of soil with tin and hydrochloric or phosphoric acid has been proposed for measuring sulfide, but this method is not specific to inorganic sulfur (Melville et al. 1971; Pirela and Tabatabai 1988).

Elemental sulfur can occur naturally in some soils such as those that are anaerobic and associated with marine or marsh situations, or from aerial depositions (e.g., industrial pollution) and fertilizer applications. Measurement of elemental sulfur in soils usually requires extraction with an organic solvent (e.g., chloroform, acetone, toluene) followed by colorimetry, liquid or gas chromatography, or ICP (Maynard and Addison 1985; Clark and Lesage 1989; O'Donnell et al. 1992; Zhao et al. 1996).

Inorganic sulfate may be present in water in the soil, bound or adsorbed on soil surfaces, as relatively insoluble compounds such as gypsum (Nelson 1982), or in association with calcium carbonate (Roberts and Bettany 1985). Sulfate is adsorbed on positive charges that occur in acidic soils (Tabatabai 1982), although a recent study has shown that sulfate-binding mechanisms are complex (Kowalenko 2005). Solution and adsorbed inorganic sulfate are assumed to be immediately available for plant uptake. To measure total inorganic sulfate in soils, all of these forms would need to be measured. Although there is a good theoretical basis for solution and adsorbed pools being present in the soil, there are practical limitations in their extraction and subsequent quantification. The choice of the extractant will depend on analytical equipment available, form of sulfate (e.g., solution, sorbed) to be examined, and type of soil to be analyzed. Numerous solutions have been used for extracting combined soluble and adsorbed sulfate including acetates, carbonates, chlorides, phosphates, citrates, and oxalates (Beaton et al. 1968; Jones 1986). Most of these studies have focused on measurement of plant-available rather than total inorganic sulfate. If only soil solution sulfate is to be measured, water would theoretically be sufficient. However, weak calcium chloride is often preferred, since it depresses clay and organic matter during extraction (Tabatabai 1982). Lithium chloride is also used, since lithium would inhibit microbial activity that may mineralize organic sulfur during and after extraction (Tabatabai 1982). Adsorbed sulfate (together with solution sulfate) is usually extracted with sodium, potassium, or preferably, calcium phosphate (Beaton et al. 1968). A concentration of 500 mg P L^{-1} is usually adequate to displace sulfate in most soils; however, for soils that fix considerable phosphate, 2000 mg P L^{-1} may be required. Alkaline solutions theoretically are effective for extracting adsorbed sulfate, since the adsorption mechanism is pH dependent, but would extract additional, highly colored organic materials that cause

problems for some sulfate quantification methods. Acidic extractants may extract portions of gypsum- or carbonate-associated sulfate that may be present in some soils. Buffered extractants may result in more consistent results. Preextraction treatment on the sample such as air drying will also influence the results (Kowalenko and Lowe 1975; Tabatabai 1982). Specialized methods are required to measure insoluble sulfate in gypsiferous (Khan and Webster 1968; Nelson 1982) or acid-sulfate (Begheijn et al. 1978) soils. It is possible that oxidized forms other than sulfate such as thiosulfate, tetrathionate, or sulfite (Nor and Tabatabai 1976; Wainwright and Johnson 1980) may be found in soils, but are probably present only as intermediates during oxidation or reduction of sulfur.

There are a number of methods for quantifying sulfate (Patterson and Pappenhagen 1978; Tabatabai 1982), but not all are compatible with all soil extract solutions. The method should be quantitative, adequately sensitive, free from interferences, and specific for sulfate. Unfortunately, there does not appear to be a specific, direct colorimetric method to determine sulfate. The most frequently used sulfate quantification methods applied to soil extracts include precipitation with barium or sulfide analysis after hydriodic acid reduction. There are numerous variations for barium-precipitation methods, including titrimetric, turbidimetric, gravimetric, and colorimetric methods (Beaton et al. 1968), but all are subject to interferences. The hydriodic acid reduction method is quite sensitive and relatively free from interferences, but the reduction procedure is time consuming, difficult to automate, and the chemicals are costly. The hydriodic acid reagent (Johnson and Nishita 1952; Beaton et al. 1968) reduces both organic and inorganic sulfate to sulfide. This method has been used extensively for soil analyses. It is quite specific for sulfate (Tabatabai 1982), whether organic or inorganic, therefore, is not specific to inorganic sulfate. Various pretreatments have been attempted to make the methods specific to inorganic sulfate, but each has distinct limitations (Kowalenko and Lowe 1975). Pirela and Tabatabai (1988) have shown that the hydriodic reagent will decompose some elemental sulfur, thus, the resulting values should be interpreted accordingly. More recently, IC, ICP, and x-ray fluorescence have been used for sulfur analysis of soil extracts (Gibson and Giltrap 1979; Tabatabai 1982; Maynard et al. 1987). Although IC is specific for inorganic sulfate analysis, it is quite sensitive and not affected significantly by interferences; specialized instrumentation and attention to the choice of the extraction salts (concentration and types) are required. Inductively coupled plasma spectrophotometry and x-ray fluorescence provide fast quantification; however, they include all forms (organic and inorganic) of sulfur.

23.2 DIGESTION FOR TOTAL SULFUR DETERMINATION (TABATABAI AND BREMNER 1970a; KOWALENKO 1985)

Since there is potential for sulfur to be lost by volatilization from hot, acidic solutions, an alkaline solution is preferred for digesting soil samples for total sulfur determination. A method that uses sodium hypobromite for the digestion developed by Tabatabai and Bremner (1970a) is described here. The method is modified from the original by the use of a different custom-built reduction/distillation apparatus (Kowalenko 1985) that allows the measurement of sulfur as sulfide using bismuth to quantify the resulting sulfide rather than methylene blue reaction (Kowalenko and Lowe 1972). The bismuth method combined with the modified glassware apparatus has the advantages of short analysis time, versatility for types of sulfur analyses, and the equipment requirements are small. The digestion and quantification must be done in the same vessel; therefore, an alternate sulfur quantification method (e.g., ICP or IC) should not be substituted for the hydriodic acid method without assessment of effectiveness and making appropriate modifications.

23.2.1 Materials and Reagents

1 Sodium hypobromite digestion reagent: in a fume hood, add slowly with constant stirring 3 mL of bromine to 100 mL 2 *M* sodium hydroxide. This reagent has limited stability, and should be prepared immediately before use or at least daily.

2 Formic acid (90%).

3 Temperature-controlled digestion block: the block heater (commercially available or can be custom-built) must accommodate the sample vessel and be capable of maintaining a temperature of 250°C–260°C.

23.2.2 Apparatus

The recommended apparatus (Kowalenko 1985) for the sample digestion and subsequent sulfur determination by hydriodic acid reduction is custom-built glassware and includes two components, the vessel into which the sample is placed (capable of being heated in a block) and a part that fits onto this vessel to form an airtight unit that includes the ability to dispensing the reducing solution for nitrogen gas flushing (Figure 23.1). The inlet of the gas flush is attached to a steady and controllable source of nitrogen gas, and the outlet should include an arm with a capillary dropper attached by flexible inert tubing such that the exiting gas is bubbled through the sodium hydroxide absorbing solution. The hydriodic acid reduction procedure is described in Section 23.3. The apparatus must be supported to allow it to be lowered to and lifted from a block to heat the sample vessel at 110°C–115°C during the hydriodic acid reduction phase.

23.2.3 Procedure

1 Weigh a finely ground (<100 mesh) soil sample directly into the dry sample vessel. The sample size (an oven-dry basis is recommended) should be adjusted so that the sulfur content is within the range of the calibration standards. For example, digest 0.1–0.4 g of Ah horizon of mineral soil or 0.1 g or less of organic horizon with a 30 mL bismuth sulfide final volume that provides a 0–200 mg S range of analysis.

2 Add 3 mL of the sodium hypobromite digestion reagent and thoroughly wet the soil sample with the reagent by swirling the tube. After letting the sample stand for 5 min, evaporate the mixture to dryness in the digestion block at 250°C–260°C, then continue heating for an additional 30 min. Remove from heat and allow the tube to cool for about 5 min.

3 Resuspend the digested sample in 1 mL of water by swirling and heating briefly. After cooling, add 1 mL of formic acid to eliminate any excess bromine that may be present.

4 Quantify the sulfur content with the hydriodic acid reduction reagent method (as described in Section 23.3).

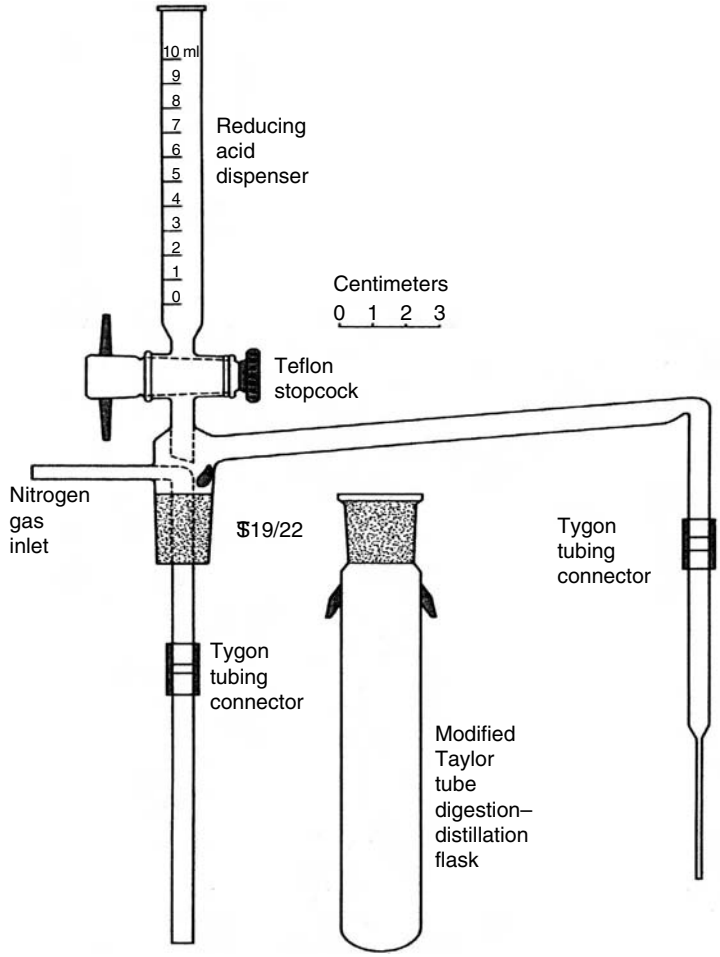

FIGURE 23.1. Simplified digestion–distillation apparatus for total- or sulfate–S analyses. (From Kowalenko, C.G., *Commun. Soil Sci. Plant Anal.*, 16, 289, 1985. With permission.)

23.2.4 Calculations

Calculate the sulfur content (as mg S kg^{-1}) of the sample by taking into consideration the oven-dry weight of the sample and using the standard curve produced by the hydriodic acid determination of sulfur in the sample (see Section 23.3.3).

23.2.5 Comments

1 The sulfur content of soil samples containing a large amount of organic material may be underestimated by this method as described, and sequential digestions, and/or longer heating times may be required (Guthrie and Lowe 1984).

2 This digestion method can also be used to determine total sulfur content in solutions, but the aliquot of the solution should be dried before the digestion is conducted (Kowalenko and Lowe 1972). However, an ICP instrument capable of

sulfur determination could be used as an alternative direct analysis since the instrument operates on liquid samples and measures total sulfur. Ion chromatography which also works with liquids, measures a specific form of sulfur (e.g., sulfate); therefore, would have to be applied to a digested sample to determine total sulfur.

23.3 SULFATE DETERMINATION BY HYDRIODIC ACID REAGENT REDUCTION

The quantification of sulfate in soil studies has been limited by the lack of an accurate, suitable, and direct colorimetric analysis method. As noted earlier, sulfate colorimetric methods that have been used are essentially based on precipitation with barium, and, hence, all are subject to interference and most lack sufficient sensitivity. The other method that has been used widely in soil studies is based on the reduction of sulfate with hydriodic acid reagent and sulfur measured on the resulting hydrogen sulfide. More recently, several new sulfur analytical methods have been developed and used for soil studies with ICP and IC being predominant. Both of these methods require specialized and expensive instrumentation. Since their operation is specific to the instrument and defined by the manufacturer, they will not be described here. Although instruments for these methods are now widely available, there have been few assessments of their effectiveness or comparisons with values using traditional methods in soil studies. It is generally accepted that interference is limited for ICP measurements, but the sulfur measurement includes all forms rather than sulfate specifically. Ion chromatography can be specific for sulfate measurements, but is subject to interference by a wide array of anions and cations including those that are a part of traditional digestion and extraction solutions. These potential interferences must be addressed in each specific case. These influences can be circumvented in a variety of ways and depend on the specific instrument that is used. The hydriodic acid method is, therefore, outlined here because it does not require specialized instrumentation and procedures, and has a long history of application to soils. The method involves hydriodic acid reagent described by Johnson and Nishita (1952) used in a modified apparatus (Kowalenko 1985) and bismuth sulfide (Kowalenko and Lowe 1972) rather than methylene blue quantification of the sulfur evolved as hydrogen sulfide.

23.3.1 Materials and Reagents

1 Custom-built reduction/distillation apparatus and heating block (Kowalenko 1985) as outlined in Section 23.2.2.

2 Nitrogen gas: the gas must be relatively pure and free from sulfides in particular. The gas may be purified by bubbling it through a solution containing 5 to 10 g mercuric chloride in 100 mL of 2% (w/v) potassium permanganate. The flow of the nitrogen gas to the reduction/distillation apparatus should be regulated to approximately 200 mL min^{-1}. This can be done by commercially available flow meters (e.g., Rotometer [Kowalenko 1985]) or forcing the gas through an appropriate length (e.g., 30 cm) of capillary glass tubing (Kowalenko and Lowe 1972).

3 Hydriodic acid reducing reagent: mix 4 volumes (e.g., 400 mL) of hydriodic acid (e.g., 57% with 1%–2.5% hypophosphorus acid preservative), 1 volume (e.g., 100 mL) of hypophosphorus acid (50%), and 2 volumes (e.g., 200 mL) of

formic acid (90%) and, while bubbling purified nitrogen gas through it, heat for 10 min at 115°C–117°C. Continue the nitrogen gas flow through the reagent while cooling. The heating should be done in a well-ventilated hood; refluxing or a special gas-trapping apparatus (Tabatabai 1982) is recommended. Since this reagent is not very stable, only sufficient reagent for several days of sample and standard analyses should be prepared. Storage in a brown bottle and refrigeration will extend its stability.

4 1 *M* sodium hydroxide: for absorbing hydrogen sulfide.

5 Bismuth reagent: dissolve 3.4 g bismuth nitrate pentahydrate in 230 mL glacial acetic acid. Also, dissolve 30 g gelatin in 500 mL water and mix thoroughly. Both solutions will require gentle heating for dissolution. Filter the bismuth solution if it is not clear. The final bismuth reagent is prepared by combining the bismuth and gelatin solutions and diluting to 1 L. This reagent is quite stable at room temperature.

6 Sulfate–S standards: prepare a 1000 mg S L^{-1} stock solution by dissolving 5.435 g dried reagent-grade potassium sulfate and diluting to 1 L. Working standards are made by appropriate dilutions.

7 Spectrophotometer: the instrument should be suitable for measurement at 400 nm and capable of accommodating small (e.g., 7.5 mL) volumes, including provision for rinsing the cuvette or analysis chamber.

23.3.2 Procedure

1 Weigh a portion of dry, whole soil or pipette an appropriate volume (e.g., 2–5 mL) of the filtered extract into the modified Taylor tube for the hydriodic acid reduction/distillation apparatus and evaporate (up to 100°C) the aliquot of the extract solution to dryness. The weight of soil or volume of extract solution should be adjusted in size such that the amount of sulfur in the apparatus will be within the range of calibration standards that is conducted.

2 Assemble the custom-built reduction/distillation apparatus above the small heating block in such a way that the modified Taylor tube can be easily installed on or removed from the dispenser portion. This can be accomplished by either having the heater in a fixed position and the dispenser portion with the Taylor tube easily raised and lowered, or the dispenser plus Taylor tube fixed and the heater on a jack assembly. A tube (50 mL test tube or larger, depending on the range of the standard curve) containing the sodium hydroxide solution for absorbing the hydrogen sulfide should be fixed in a position such that the nitrogen gas from the outlet of the apparatus will bubble through several centimeters of the absorbing solution. The volume of the absorbing solution is adjusted for the concentration range of sulfate to be analyzed. Adjust the nitrogen gas at the appropriate rate and fill the burette with reducing reagent. As each distillation is completed and the Taylor tube is removed, a watch glass should be placed above the heater to intercept any drops of reducing reagent. The entire apparatus should be adequately ventilated.

3 Condition the reduction/distillation apparatus by attaching a modified Taylor tube containing a high (e.g., 200 mg S L^{-1}) sulfate standard to the reduction/distillation

apparatus, place the apparatus in heating position, adjust the nitrogen gas flow, and dispense 4 mL of reducing reagent into the attached Taylor tube. The apparatus requires conditioning at the beginning of each new session with high sulfate–sulfur standard to ensure quantitative initial distillation. Distill until all the sulfate has been reduced and transferred into the absorbing solution. The time required for this process will vary with the flow rate of the nitrogen and the ''dead'' volume within the apparatus. About 8 to 10 min should be adequate, but calibration under specific conditions is recommended (Kowalenko 1985). After distillation of the hydrogen sulfide is complete, remove the tube containing the absorption solution from the apparatus and check that the distillation process is functioning by immediately adding an appropriate volume of bismuth reagent and mix thoroughly. This volume should correspond to the volume of the absorbing solution (2:1 absorbing solution:bismuth reagent) depending on the range of the standard sulfate–sulfur required. For example, 20 mL of absorbing solution is suitable for a 1–200 mg S L^{-1} range and 5 mL for a 1–40 mg S L^{-1} range.

4 After the initial setup and conditioning of the apparatus, digested soil samples, whole soil sample or dried soil extract aliquot, and dried standards are distilled into appropriate volumes of absorption solution, and bismuth reagent is immediately added in preparation for quantitative measurements of the bismuth sulfide produced. Measurements are best conducted in batches and adequate standards included in each batch. Measure absorbance of the sample and standard solutions at 400 nm.

23.3.3 Calculations

For measurements of sulfate in a soil sample placed directly into the sample vessel of the hydriodic acid analysis apparatus, prepare the standard curve for the bismuth colorimetric determination as an appropriate range of a quantity (e.g., mg S) of sulfur distilled in a single analysis. Then the concentration of sulfur in the soil sample is calculated as the quantity of sulfur relative to the standard curve divided by the weight of the soil (oven-dry basis) in the vessel during the analysis. Also, for measurements on solution samples, standardize the apparatus on an appropriate range of a quantity of sulfur in a single analysis, but calculate the concentration of the sulfur on an oven-dry basis taking into account the aliquot size of the analyzed solution that was dried in the apparatus sample vessel and the ratio of the analyzed solution to the weight of the soil.

23.3.4 Comments

1 Filter paper has been found to contain variable amounts of sulfate which will be leached during the filtration. Washing the filter paper with some of the extractant prior to filtration is recommended.

2 Water has been shown to reduce the efficiency of hydriodic acid reagent to reduce sulfate to sulfide (Kowalenko and Lowe 1975); therefore, the standard and sample solution aliquot volumes should either be the same throughout or all the liquid of the aliquot evaporated to dryness. Although evaporating the sample to dryness is time consuming, it does provide an opportunity for altering the sensitivity of the analysis (i.e., evaporate a small volume for soils with a significant sulfate–sulfur content or a large volume for soils with a low sulfate–sulfur content).

3 The methylene blue color reaction is subject to interference; therefore, passing the nitrogen gas through a pyrogallol–sodium phosphate wash just prior to the hydrogen sulfide absorption is recommended (Johnson and Nishita 1952). The bismuth sulfide method is much less sensitive to interference; therefore, the pyrogallol–sodium phosphate wash can be eliminated (Kowalenko and Lowe 1972). Use of a Taylor tube rather than a condenser to provide refluxing can shorten reduction/distillation times from 60 to 10 min (Kowalenko 1985). The apparatus is also simpler to fabricate and is versatile for different types of analyses. Although the sensitivity of the bismuth reaction is considerably lower than the methylene blue reaction, it can be adequately enhanced for most soil studies by decreasing the volume into which the hydrogen sulfide is absorbed and/or by increasing the size of the original sample being analyzed. However, as the volumes of the absorbing solution and bismuth reagent are decreased to increase the sensitivity, increased attention must be given to the precision and reproducibility of absorbing solution and bismuth reagent volume measurements, particularly relative to the standard samples. The spectrophotometer should be capable of accommodating the small sample sizes involved, including appropriate rinsing between samples.

4 The original sulfate determination procedure (Johnson and Nishita 1952) recommended that the nitrogen gas should be purified before use. Currently available sources of nitrogen are more uniform and free from impurities; therefore, purification of the gas may be omitted. The purity of the gas for analysis purposes can be evaluated by examining blanks. There should also be fairly good control of the flow rate of the nitrogen gas with a high enough rate to transfer the hydrogen sulfide produced into the receiver solution quickly, but slow enough that the sulfide gas can be absorbed by the sodium hydroxide.

5 Sources of contamination, such as rubber connectors or lubricants for sealing connections, should be considered, particularly in the reduction/distillation procedure. A small amount of water is adequate to seal the Taylor tube to the rest of the apparatus during the reduction/distillation.

6 Hydriodic acid is available in concentrations ranging from 48% to 66% and with or without preservative. Although these products contain varying quantities of sulfate contamination, the sulfate is removed by heating the mixed reagent. The 57% hydriodic acid with preservative has been found to be acceptable. If other products are used, the proportion of hydriodic acid to the other acids may need adjustment and the final reagent tested for effectiveness. Adequate time should be allowed for acquisition of hydriodic acid, as stocks are often limited.

7 Although the hydriodic acid reduction procedure is not influenced by a wide variety of salts, it is recommended that the standards should be similar to the sample's matrix (e.g., water for whole soil or the solution used for extraction). For the alkaline digested soil, standards should be included through the digestion process. This precaution will also provide a check on sulfate or sulfide contamination that may be present in the extract or digestion solutions.

8 The hydriodic acid method, although relatively specific for sulfate, includes both inorganic and organic forms. This should not be neglected when the results are being interpreted. When this method is used to determine total organic sulfate

(or total carbon-bonded sulfur by difference) the capability of accurately determining total inorganic sulfate or total sulfur must be considered, particularly when unusual samples (e.g., subsurface, anaerobic, organic, etc. samples) are being examined. The difference value will involve the error or variability associated with two analyses rather than one.

REFERENCES

Arnhold, W. and Stoeppler, M. 2004. Sulfur. In E. Marian, M. Anke, M. Ihnat, and M. Stoeppler, Eds. *Elements and Their Compounds in the Environment. Occurrence, Analysis, and Biological Relevance*, 2nd ed. Wiley-VCH Verlag GmbH & Co., Weinheim, Germany, pp. 1297–1319.

Aspiras, R.B., Keeney, D.R., and Chesters, G. 1972. Determination of reduced inorganic sulfur forms as sulfide by zinc-hydrochloric acid distillation. *Anal. Lett.* 5: 425–432.

Barrow, N.J. 1970. Note on incomplete extraction of elemental sulfur from wet soil by chloroform. *J. Sci. Food Agric.* 21: 439–440.

Beaton, J.D., Burns, G.R., and Platou, J. 1968. Determination of sulfur in soils and plant material. Technical Bulletin No. 14. The Sulfur Institute, Washington, DC, 56 pp.

Begheijn, L. Th., van Breeman, N., and Velthorst, E.J. 1978. Analysis of sulfur compounds in acid sulfate soils and other recent marine soils. *Commun. Soil Sci. Plant Anal.* 9: 873–882.

Blanchar, R.W. 1986. Measurement of sulfur in soils and plants. In M.A. Tabatabai, Ed. *Sulfur in Agriculture*. American Society of Agronomy, Madison, WI, pp. 465–490.

Brown, G. and Kanaris-Sotiriou, R. 1969. Determination of sulfur in soils by x-ray fluorescence analysis. *Analyst* 94: 782–786.

Chae, Y.M. and Lowe, L.E. 1981. Fractionation by column chromatography of lipids and lipid sulfur extracted from soils. *Soil Biol. Biochem.* 13: 257–260.

Chae, Y.M. and Tabatabai, M.A. 1981. Sulfolipid and phospholipid in soils and sewage sludges in Iowa. *Soil Sci. Soc. Am. J.* 45: 20–25.

Chapman, S.J. 1987. Microbial sulfur in some Scottish soils. *Soil Biol. Biochem.* 19: 301–305.

Clark, P.D. and Lesage, K.L. 1989. Quantitative determination of elemental sulfur in hydrocarbons, soils, and other materials. *J. Chromatogr. Sci.* 27: 259–261.

David, M.B., Schindler, S.C., Mitchell, M.J., and Strick, J.E. 1983. Importance of organic and inorganic sulfur to mineralization processes in a forest soil. *Soil Biol. Biochem.* 15: 671–677.

Freney, J.R., Melville, G.E., and Williams, C.H. 1970. The determination of carbon bonded sulfur in soil. *Soil Sci.* 109: 310–318.

Gerzabek, Von M.H. and Schaffer, K. 1986. Determination of total sulfur in soil—a comparison of methods. *Die Bodenkultur* 37: 1–6.

Gibson, A.R. and Giltrap, D.J. 1979. Measurement of extractable soil sulfur in the presence of phosphate using ion-exchange resin paper discs and XRF spectrometry. *N.Z. J. Agric. Res.* 22: 439–443.

Guthrie, T.F. and Lowe, L.E. 1984. A comparison of methods for total sulfur analysis of tree foliage. *Can. J. Forest Res.* 14: 470–473.

Hogan, G.D. and Maynard, D.G. 1984. Sulfur analysis of environmental materials by vacuum inductively coupled plasma emission spectrometry (ICP-AES). In *Proceedings of Sulfur-84*. Sulfur Development Institute of Canada (SUDIC), Calgary, AB, Canada, pp. 676–683.

Hordijk, C.A., van Engelen, J.J.M., Jonker, F.A., and Cappenberg, T.E. 1989. Determination of total sulfur in freshwater sediments by ion chromatography. *Water Res.* 23: 853–859.

Jenkins, R. 1984. X-ray fluorescence analysis. *Anal. Chem.* 56: 1099A−1106A.

Johnson, C.M. and Nishita, H. 1952. Microestimation of sulfur in plant materials, soils, and irrigation waters. *Anal. Chem.* 24: 736–742.

Jones, M.B. 1986. Sulfur availability indexes. In M.A. Tabatabai, Ed. *Sulfur in Agriculture*. Agronomy No. 27. American Society of Agronomy, Madison, WI, pp. 549–566.

Khan, S.U. and Webster, G.R. 1968. Determination of gypsum in solonetzic soils by an x-ray technique. *Analyst* 93: 400–402.

Killham, K. and Wainwright, M. 1981. Closed combustion method for the rapid determination of total S in atmospheric polluted soils and vegetation. *Environ. Pollut. (Ser. B)* 2: 81–85.

Kowalenko, C.G. 1978. Organic nitrogen, phosphorus, and sulfur in soils. In M. Schnitzer and S.U. Khan, Eds. *Soil Organic Matter. Developments in Soil Science 8*. Elsevier, New York, pp. 95–136.

Kowalenko, C.G. 1985. A modified apparatus for quick and versatile sulfate–sulfur analysis using hydriodic acid reduction. *Commun. Soil Sci. Plant Anal.* 16: 289–300.

Kowalenko, C.G. 2000. Influence of sulfur and nitrogen fertilizer applications and within season sampling time on measurement of total sulfur in orchardgrass by six different methods. *Commun. Soil Sci. Plant Anal.* 31: 345–354.

Kowalenko, C.G. 2001. Assessment of LECO CNS-2000 analyzer for simultaneously measuring total carbon, nitrogen, and sulfur in soil. *Commun. Soil Sci. Plant Anal.* 32: 2065–2078.

Kowalenko, C.G. 2005. Binding of inorganic sulfate and phosphate in humid-climate soils measured by using column leaching, equilibration, and extraction methods. *Can. J. Soil Sci.* 85: 599–610.

Kowalenko, C.G. and Lowe, L.E. 1972. Observations on the bismuth sulfide colorimetric procedure for sulfate analysis in soil. *Commun. Soil Sci. Plant Anal.* 3: 79–86.

Kowalenko, C.G. and Lowe, L.E. 1975. Evaluation of several extraction methods and of a closed incubation method for sulfur mineralization. *Can. J. Soil Sci.* 55: 1–8.

Lowe, L.E. and DeLong, W.A. 1963. Carbon bonded sulfur in selected Quebec soils. *Can. J. Soil Sci.* 43: 151–155.

Matrai, P.A. 1989. Determination of sulfur in ocean particulates by combustion-fluorescence. *Mar. Chem.* 26: 227–238.

Maynard, D.G. and Addison, P.A. 1985. Extraction and colorimetric determination of elemental sulfur in organic horizons of forest soils. *Can. J. Soil Sci.* 65: 811–813.

Maynard, D.G., Kalra, Y.P., and Radford, F.G. 1987. Extraction and determination of sulfur in organic horizons of forest soils. *Soil Sci. Soc. Am. J.* 51: 801–805.

Melville, G.E., Freney, J.R., and Williams, C.H. 1971. Reaction of organic sulfur compounds in soil with tin and hydrochloric acid. *Soil Sci.* 112: 245–248.

Nelson, R.E. 1982. Carbonate and gypsum. In A.L. Page, R.H. Miller, and D.R. Keeney, Eds. *Methods of Soil Analysis, Part 2—Chemical and Microbiological Properties*, 2nd ed. American Society of Agronomy, Madison, WI, pp. 181–197.

Nor, Y.M. and Tabatabai, M.A. 1976. Extraction and colorimetric determination of thiosulfate and tetrathionate in soils. *Soil Sci.* 122: 171–178.

O'Donnell, A.G., He, Z., and Syers, J.K. 1992. A biphasic extraction procedure for the simultaneous removal of elemental sulfur and sulfate from soils. *J. Sci. Food Agric.* 59: 395–400.

Patterson, G.D., Jr. and Pappenhagen, J.M. 1978. Sulfur. In D.F. Boltz and J.A. Howell, Eds. *Colorimetric Determination of Nonmetals*. John Wiley & Sons, Toronto, ON, Canada, pp. 463–527.

Pirela, H.J. and Tabatabai, M.A. 1988. Reduction of organic sulfur in soils with tin and phosphoric acid. *Soil Sci. Soc. Am. J.* 52: 959–964.

Randall, P.J. and Spencer, K. 1980. Sulfur content of plant material: a comparison of methods of oxidation prior to determination. *Commun. Soil Sci. Plant Anal.* 11: 257–266.

Roberts, T.L. and Bettany, J.R. 1985. The influence of topography on the nature and distribution of soil sulfur across a narrow environmental gradient. *Can. J. Soil Sci.* 65: 419–434.

Scott, N.M., Bick, W., and Anderson, H.A. 1981. The measurement of sulfur-containing amino acids in some Scottish soils. *J. Sci. Food Agric*. 32: 21–24.

Stallings, E.A., Candelaria, L.M., and Gladney, E.S. 1988. Investigation of a fusion technique for the determination of total sulfur in geological samples by ion chromatography. *Anal. Chem.* 60: 1246–1248.

Strick, J.E. and Nakas, J.P. 1984. Calibration of a microbial sulfur technique for use in forest soils. *Soil Biol. Biochem.* 16: 289–291.

Tabatabai, M.A. 1982. Sulfur. In A.L. Page, R.H. Miller, and D.R. Keeney, Eds. *Methods of Soil Analysis, Part 2—Chemical and Microbiological Properties*, 2nd ed. American Society of Agronomy, Madison, WI, pp. 501–538.

Tabatabai, M.A., Basta, N.T., and Pirela, H.J. 1988. Determination of total sulfur in soils and plant materials by ion chromatography. *Commun. Soil Sci. Plant Anal*. 19: 1701–1714.

Tabatabai, M.A. and Bremner, J.M. 1970a. An alkaline oxidation method for determination of total sulfur in soils. *Soil Sci. Soc. Am. Proc*. 34: 62–65.

Tabatabai, M.A. and Bremner, J.M. 1970b. Comparison of some methods for determination of total sulfur in soils. *Soil Sci. Soc. Am. Proc*. 34: 417–420.

Wainwright, M. and Johnson, J. 1980. Determination of sulfite in mineral soils. *Plant Soil* 54: 299–305.

Watkinson, J.L., Lee, A., and Lauren, D.R. 1987. Measurement of elemental sulfur in soil and sediments: field sampling, sample storage, pretreatment, extraction and analysis by high-performance liquid chromatography. *Aust. J. Soil Res.* 25: 167–178.

Zhao, F.J., Loke, S.Y., Crosland, A.R., and McGrath, S.P. 1996. Method to determine elemental sulfur in soils applied to measure sulfur oxidation. *Soil Biol. Biochem.* 28: 1083–1087.

Chapter 24
Total and Organic Phosphorus

I.P. O'Halloran
University of Guelph
Ridgetown, Ontario, Canada

B.J. Cade-Menun
Stanford University
Stanford, California, United States

24.1 INTRODUCTION

This chapter describes several methods used for the determination and characterization of total phosphorus (P_t) and organic phosphorus (P_o) in soils.

Determination of the P_t in soil requires the solubilization of P through the decomposition or destruction of mineral and P_o containing materials in the soil. Historically, the two most widely recognized procedures for the determination of soil P_t are the sodium carbonate (Na_2CO_3) fusion method and the perchloric acid ($HClO_4$) digestion method (Olsen and Sommers 1982). Currently, neither method is widely used in studies involving the determination of soil P_t. Although the Na_2CO_3 fusion method is considered the most reliable procedure for quantitative determination of P_t in soils, it is laborious, tedious, and generally unsuitable for the analyses of large numbers of samples. Digestion with $HClO_4$, although more adaptable as a routine laboratory procedure, requires the use of fume hoods specifically designed for the $HClO_4$ digestion. The potential danger of explosions, due to $HClO_4$ buildup or reaction of $HClO_4$ with organic materials, has led many institutions and laboratories to discontinue the use of $HClO_4$ digestions. Given the greater applicability of the $HClO_4$ digestion method as a routine laboratory procedure for the analysis of a large number of samples, this procedure has been included in the current text. The reader is referred to the previous edition of this text (O'Halloran 1993) or Olsen and Sommers (1982) for details on the Na_2CO_3 fusion method. Three additional methods for the determination of P_t in soil are presented in this chapter. One involves the alkaline oxidation of the sample using sodium hypobromite (NaOBr)/sodium hydroxide (NaOH) (Dick and Tabatabai 1977) and the other two are wet acid digestion procedures using either sulfuric acid (H_2SO_4)/hydrogen peroxide (H_2O_2)/hydrofluoric acid (HF) (Bowman 1988) or H_2SO_4/H_2O_2/lithium sulfate (Li_2SO_4)/selenium (Se) (Parkinson and Allen 1975).

Soil P_o methods can be divided into methods that attempt to measure the total P_o and methods that attempt to characterize both the amount and the forms of P_o in the soil.

The first group consists of extraction (Mehta et al. 1954; Bowman and Moir 1993) or ignition techniques (Saunders and Williams 1955). In each case, total soil P_o is not determined directly, but rather is calculated as the increase in inorganic P (P_i) measured after the digestion of a soil extract or ignition of a soil sample. The ignition technique is less laborious than the extraction techniques, but it is also subject to a greater number of errors.

Characterization of soil P_o forms can be done either by sequential fractionation techniques that provide operationally defined pools of P_o or techniques that identify specific groups or forms of P_o materials in soils. Sequential fractionation techniques, such as the modified procedure of Hedley et al. (1982) that is presented in Chapter 25 of this manual, characterize soil P_o forms by measuring P_t and soluble-reactive P (srP) in each fraction and then assuming that the difference between P_t and srP is P_o. However, caution should be used when interpreting P_o results by sequential fractionation: first, because there is the potential for P_o forms to be altered by previous extractants within any sequential fractionation procedure; and second, because srP measures only orthophosphate (HPO_4^{2-}, $H_2PO_4^-$), the ''P_o'' measured by the difference between P_t and srP in a solution may also include complex P_i forms such as pyrophosphate or polyphosphates.

In the identification of specific P_o compounds, four groups of soil P_o compounds have been detected in soils. Orthophosphate monoesters are esters of phosphoric acid, with one C moiety per P, and include inositol phosphates, sugar phosphates, phosphoproteins, and mononucleotides. Orthophosphate diesters are also esters of phosphoric acid, but have two C moieties per P. These include DNA, RNA, phospholipids, teichoic acid, and aromatic compounds. Phosphonates contain C–P bonds rather than ester linkages, and occur as phosphonic acids and phosphonolipids. The final group of soil P_o compounds is orthophosphate anhydrides. Although most of these are complex P_i compounds such as pyrophosphate and polyphosphate, this grouping also includes important organic orthophosphate anhydrides such as adenosine diphosphate (ADP) and adenosine triphosphate (ATP). More details on soil P_o compounds can be found in Condron et al. (2005).

A range of techniques is available to examine specific soil P_o compounds. Most involve extraction with a reagent specific to the recovery of a particular P compound, followed by analysis using techniques such as ^{31}P nuclear magnetic resonance (NMR) spectroscopy, enzyme hydrolysis, thin-layer chromatography, high-performance liquid chromatography (HPLC), and mass spectroscopy. These methods are often laborious, may require complex and expensive instrumentation, and may be specific to only one P compound or group of P compounds. In addition, the interpretation of results is limited by incomplete extraction or poor detection. Presented in this chapter are two common procedures to characterize P_o compounds in soil extracts: ^{31}P NMR spectroscopy and enzyme hydrolysis. Both allow the determination of the relative proportions of a range of P compounds in soil samples.

24.2 TOTAL PHOSPHORUS

Currently, the most popular approaches to soil P_t determinations involve either alkali or acid oxidation or digestion of the soil samples. Each of the following methods has an advantage over the Na_2CO_3 fusion method in that they are more adaptable for the routine analysis of a greater number of soil samples. As mentioned previously, digestion with $HClO_4$ requires special $HClO_4$ fume hoods, and care must be taken to avoid explosions. It has been reported that the $HClO_4$ digestion method gives relatively low P_t values in highly weathered materials and with samples containing apatite inclusions (Syers et al. 1967, 1968, 1969). Each of the

remaining three methods has been reported to produce similar to slightly greater results to those obtained with the $HClO_4$ digestion procedure (Dick and Tabatabai 1977; Bowman 1988; Rowland and Grimshaw 1985) without the need for a special fume hood to carry out the oxidation or digestion. The $H_2SO_4/H_2O_2/HF$ digestion method is relatively fast and is ideally suited for small numbers of samples. This procedure, however, requires HF-resistant materials, since HF attacks glass. The NaOBr/NaOH and $H_2SO_4/H_2O_2/Li_2SO_4$/Se methods are well suited for the analysis of large numbers of samples.

The reader is also referred to two additional procedures for the determination of soil P_t that may be of interest. The first involves a fusion method using NaOH that melts at a lower temperature than Na_2CO_3 (325°C versus 850°C), and therefore allows the use of nickel rather than platinum crucibles (Smith and Bain 1982). Although this procedure was initially reported to give similar soil P_t values as the Na_2CO_3 fusion method for 10 Scottish soils (Smith and Bain 1982), problems with low recoveries of soil P_t in New Zealand soils with high organic matter content (soils that have >80% weight loss on ignition) have been identified (Taylor 2000). The second method is based on the Thomas et al. (1967) method for plant tissue digestion using H_2SO_4/H_2O_2 to digest a soil sample in an aluminum block digestor. This procedure is presented as the final step (i.e., digestion of soil residue) in the sequential fractionation procedure described in Chapter 25. Agbenin and Tiessen (1994) found for semiarid tropical soils in Brazil that the H_2SO_4/H_2O_2 method gave comparable to slightly higher soil P_t values than the Na_2CO_3 fusion method. Gasparatos and Haidouti (2001) studying 15 soils varying in extractable P levels reported that this method gave soil P_t values that were 95%–105% of those obtained with $HClO_4$ digestion.

Regardless of the procedures selected, it is recommended that finely ground soil, 0.15–0.18 mm (100–80 mesh), be used to allow for efficient recovery or extraction of P from the soil material, and to improve the reproducibility. The moisture content of the soil should be known so as to allow expression of P content on an oven-dried basis. Blank samples containing no soil should also be included to assess the possibility of P contamination and to serve as a suitable reagent blank for the colorimetric determination of P. Inclusion of a reference sample with known P_t and the use of duplicate samples are also encouraged.

24.2.1 Perchloric Acid Digestion (Olsen and Sommers 1982)

As a safety precaution, samples should routinely be predigested in concentrated nitric acid (HNO_3) before proceeding with the $HClO_4$ digestion. This method is suitable for the determination of soil P_t in a large number of samples, although the use of an $HClO_4$ fume hood is essential. The digestion can be carried out using 250 mL Erlenmeyer flasks and a hot plate, or by using an aluminum block digestor with 75, 100, or 250 mL digestion tubes (see comments on p. 268). The $HClO_4$ digestion typically recovers 92%–96% as much P as the Na_2CO_3 fusion method (Sommers and Nelson 1972; Dick and Tabatabai 1977; Bowman 1988), although the pretreatment of soil samples with HF can increase the recovery of P (Kara et al. 1997).

Materials and Reagents

1 $HClO_4$ fume hood

2 Hot plate (with 250 mL Erlenmeyer flasks) or aluminum block digestor (with 250 mL digestion tubes)

3 HNO_3, concentrated

4 $HClO_4$, 60%

5 Color developing solution (see Section 24.5.1)

Procedure

1 Accurately weigh approximately 2.0 g of finely ground soil into a 250 mL volumetric or Erlenmeyer flask.

2 Add 20 mL concentrated HNO_3 to flask and mix well. Heat (approximately 130°C) to oxidize the organic matter in the sample. Organic matter oxidation is complete when the dark color due to the organic matter in the sample disappears.

3 Allow the soil–HNO_3 mixture to cool slightly. In the $HClO_4$ fume hood, add 30 mL of $HClO_4$ and digest the sample at the boiling temperature (approximately 200°C) for 20 min. During this time dense white fumes should appear and the insoluble solid material left in the bottom of the flask or digestion tube should appear like white sand. If necessary, use a little (less than 2 mL) extra $HClO_4$ to wash down any black particles that have stuck to the sides of the flask or digestion tube. Heat for another 10–15 min.

4 Allow the mixture to cool. With distilled/deionized water transfer the mixture to a 250 mL volumetric flask and make to volume with distilled/deionized water. Mix thoroughly.

5 Allow sediment to settle before taking an aliquot for analysis.

6 Determine P concentration in an aliquot of the clear supernatant as indicated in Section 24.5.

Comments

A 40 tube aluminum block digestion system with volumetric 75 or 100 mL digestion tubes can also be used in this procedure by using half the amounts of sample, HNO_3, and $HClO_4$ described above. The digested material is diluted to a final volume of 75 or 100 mL (step 4).

24.2.2 Sodium Hypobromite/Sodium Hydroxide Alkaline Oxidation Method (Dick and Tabatabai 1977)

This method involves boiling to dryness a mixture of soil and NaOBr–NaOH solution using a sand bath or, as modified by Cihacek and Lizotte (1990), an aluminum block digestor. Formic acid is added after completion of the NaOBr–NaOH treatment to destroy residual NaOBr remaining after oxidation of the sample. Soil P_t is then extracted from the sample using 0.5 *M* H_2SO_4. The method permits the digestion of a large number of samples at one time, although more manipulation of the sample is required compared to the $HClO_4$ method. Dick and Tabatabai (1977) using a wide range of soils from the United States and Brazil found that for soil P_t this method removed about 96% as much P as the Na_2CO_3 fusion method, and was comparable (about 1% higher) to the P determined by $HClO_4$ digestion. Cihacek and Lizotte (1990), using soils from the Great Plains region of the United States, found that this procedure

removed significantly (about 3%) more P than the $HClO_4$ digestion. Kara et al. (1997) found this method to recover 93%–100% of the P determined by Na_2CO_3 fusion and 99%–102% of the P determined by $HClO_4$ digestion on soils from Scotland and Turkey.

Materials and Reagents

1 Sand bath for which the temperature of the sand can be regulated at 260°C–280°C or an aluminum block digestor (see Comment 3 on p. 270).

2 Fume hood.

3 Boiling flask (50 mL) with stoppers or digestion tubes for the aluminum block digestor.

4 Centrifuge and 50 mL centrifuge tubes.

5 NaOH, 2 *M*: dissolve 80 g NaOH in a 1 L volumetric flask containing 600 mL of distilled/deionized water. Allow to cool and make to volume with distilled/deionized water.

6 NaOBr/NaOH solution: prepare this solution in a fume hood by adding 3 mL of bromine slowly (0.5 mL min^{-1}) and with constant stirring to 100 mL of 2 *M* NaOH. Prepare the NaOBr–NaOH solution immediately before use.

7 Formic acid (HCOOH), 90%.

8 H_2SO_4, 0.5 *M*: add 28 mL concentrated H_2SO_4 to 600 mL distilled/deionized water in a 1 L volumetric flask. Mix, allow to cool, and make to volume using distilled/deionized water.

9 Color developing solutions (see Section 24.5.1).

Procedure

1 Accurately weigh between 0.10 and 0.20 g of finely ground soil into a dry 50 mL boiling flask.

2 Add 3 mL of NaOBr–NaOH solution to the boiling flask, and swirl the flask for a few seconds to mix the contents. Allow the flask to stand for 5 min, and then swirl the flask again for a few seconds.

3 Place the flask upright in a sand bath (temperature regulated between 260°C and 280°C) situated in a fume hood. Heat the flask for 10–15 min until its contents are evaporated to dryness, and continue heating for an additional 30 min.

4 Remove the flask from the sand bath, cool for about 5 min, add 4 mL of distilled/deionized water and 1 mL of 90% HCOOH. Mix the contents, and then add 25 mL of 0.5 *M* H_2SO_4. Stopper the flask and mix the contents.

5 Transfer the mixture to a 50 mL plastic centrifuge tube and centrifuge at 15,000 *g* for 1 min.

6 Determine P concentration in an aliquot of the clear supernatant as indicated in Section 24.5.

Comments

1 It is very important that the NaOBr–NaOH solution be prepared immediately before use. Dick and Tabatabai (1977) reported that storing the NaOBr–NaOH at 4°C for 24 h reduced P_t values by 2%–4%.

2 Sample sizes up to 0.5 g can be analyzed for most soils. However, samples containing high amounts of Fe show large decreases in the value of P_t when sample sizes are increased above 0.2 g.

3 A sand bath may be prepared by placing 3–4 cm of silica sand on a hot plate; however, even temperature regulation across the sand bath can be difficult to achieve. Cihacek and Lizotte (1990) found that the use of an aluminum block digestor resulted in a more uniform heating of all samples and improved the precision of P_t determination.

24.2.3 Sulfuric Acid/Hydrogen Peroxide/Hydrofluoric Acid Digestion (Bowman 1988)

This method involves the digestion of the soil sample by the sequential additions of concentrated H_2SO_4, H_2O_2, and HF. The precision and accuracy is similar to that of the $HClO_4$ method and gives soil P_t values that are approximately 94% of those obtained with Na_2CO_3 fusion (Bowman 1988). This method is suited for the analysis of a small number of samples at one time. The time required for manual additions of the H_2O_2 and HF is similar to the manipulations required for the NaOBr–NaOH method, which makes the procedure slightly more labor intensive than the $HClO_4$ or $H_2SO_4/H_2O_2/Li_2SO_4$/Se methods.

Materials and Reagents

1 Fluoropolymer beaker (100 mL) of known weight

2 Fume hood

3 Balance or 50 mL volumetric flask

4 Quantitative fine filter paper (e.g., Whatman No. 42)

5 H_2SO_4, concentrated

6 H_2O_2, 30%

7 HF, concentrated (see Comment 1, p. 271)

8 Color developing solutions (see Section 24.5.1)

Procedure

1 Accurately weigh 0.5 g of finely ground soil into a 100 mL fluoropolymer beaker of known weight. Use 0.25 g for soil high in organic matter.

2 In the fume hood add 5 mL (9.2 g) of H_2SO_4 to the soil and gently swirl to suspend solid materials adhering to the bottom of the beaker.

3 In the fume hood, slowly add 0.5 mL of H_2O_2 and mix vigorously to promote the oxidation of organic materials. Repeat this step until 3 mL of H_2O_2 has been added to the beaker. Let the sample sit until the reaction with H_2O_2 has subsided.

4 Add 0.5 mL of HF to the beaker and mix. Repeat this step again so that a total of 1 mL of HF has been added.

5 Place beaker on a preheated hot plate (approximately 150°C) for 10–12 min to eliminate excess H_2O_2.

6 Remove beaker, and while sample is still warm, wash down the sides of the beaker with 10–20 mL of distilled/deionized water. Mix and cool to room temperature.

7 Weigh the beaker and its contents and add sufficient distilled/deionized water to bring the final contents weight to 55 g (equivalent to 50 mL volume). Alternatively, the material in the beaker can be quantitatively transferred to a 50 mL volumetric flask and made to volume using distilled/deionized water.

8 Mix and filter the extract.

9 Determine P concentration in an aliquot of the clear filtrate as indicated in Section 24.5.

Comments

1 HF acid attacks glass and it is very important that HF-resistant materials such as polytetra fluoroethylene (PTFE) are used. An example of such material is Teflon. (The use of this trade name is provided for the benefit of the reader and does not imply endorsement by the CSSS.)

2 Excess H_2O_2 will interfere with the colorimetric determination of P in the digested sample. The formation of a yellow color instead of the blue color normally associated with the reduced molybdophosphate complex indicates the presence of excess H_2O_2.

24.2.4 Sulfuric Acid/Hydrogen Peroxide/Lithium Sulfate/Selenium Digestion (Parkinson and Allen 1975)

This method involves the digestion of the soil sample with H_2SO_4 and H_2O_2. The addition of the salt Li_2SO_4 allows for the use of a higher digestion temperature and Se is added as a catalyst in the oxidation of the organic material present in the sample. Rowland and Grimshaw (1985) studying 103 soils across eight major soil types in Britain found that this procedure has a similar accuracy, and on average removed slightly more P (103%) than the $HClO_4$ digestion. The digestion is usually completed after 2–2.5 h and is therefore somewhat longer than the other procedures. However, using an aluminum block digestor with either 75 or 100 mL tubes enables the analysis of a large number of samples at a time, with a relatively modest amount of sample manipulation. Samples may also be digested using 50 mL boiling flasks, although it is critical that the proper soil:digestion mixture ratio is maintained to ensure proper digestion of the sample.

Materials and Reagents

1 Aluminum digestion block with 100 mL volumetric digestion tubes having a suitable stopper or sealing device (i.e., silicon stopper). A hot plate is required if using 50 mL boiling flasks.

2 Fume hood.

3 Vortex mixer (optional).

4 Silicon stopper (or other device) for sealing digestion tubes.

5 H_2SO_4, concentrated.

6 H_2O_2, 30%.

7 Lithium sulfate monohydrate ($Li_2SO_4 \cdot H_2O$).

8 Selenium (Se) powder.

9 Color developing solutions (see Section 24.5.1).

Procedure

1 Digestion solution: the day before sample digestion, mix 175 mL of H_2O_2 with 0.21 g Se powder and 7 g $Li_2SO_4 \cdot H_2O$ in a suitable container. A plastic, sealable bottle is preferred as some pressure may develop in the container. Store this solution in a refrigerator overnight; the Se powder should be dissolved by the following day. Do not heat the solution to dissolve the Se as this may severely decrease the effectiveness of the H_2O_2. This solution is stable for 2–3 weeks.

2 Accurately weigh 0.2–0.4 g of finely ground soil into a 100 mL digestion tube.

3 To reduce the risk of ''bumping'' an inert boiling stone, glass, or PTFE bead can be added to the digestion tube (see Comment 1, p. 273).

4 In a fume hood add 5 mL of concentrated H_2SO_4 to the digestion tube and swirl (or use vortex mixer) until soil is thoroughly mixed with the acid and turns a dark brown or black color.

5 Carefully and slowly add 1 mL of the digestion mixture to the digestion tube. The sample should react by foaming or spattering and due caution should be exercised. If there is no apparent reaction with the addition of the digestion mixture, gently tap the tube to facilitate the mixing of the digestion solution with the acid–soil mixture. Repeat this step three more times to add a total of 4 mL of digestion mixture.

6 Place the digestion tubes in a cold block digestor and gradually increase the temperature over a 1–1.5 h period until a temperature of 360°C is reached and maintained for 30 min. There should be evidence of H_2SO_4 vapors refluxing in the tubes.

7 Remove tubes from the block digestor and allow to cool (5–10 min). Add 0.5 mL H_2O_2, washing down any soil particles that are stuck to the sides of the digestion tube, mix well and replace on block for 30 min.

8 Repeat step 7 until solution is a clear to milky-white color (usually requires two 0.5 mL additions of H_2O_2) indicating a complete digestion of the soil organic matter (SOM). Note, some samples with relatively high iron contents may have a yellowish tinge, which will not change with further additions of H_2O_2.

9 After the final heating for 30 min, remove the tubes from the block digestor and allow to cool for 30 min. Slowly add 20–30 mL distilled/deionized water and mix (vortex) the sample to ensure the residue is easily suspended in the solution.

10 Add distilled/deionized water until liquid level is slightly below the volumetric mark on the tubes. Allow the solution to cool before making to final volume with distilled/deionized water.

11 Stopper or seal the tube and thoroughly mix the contents by slowly inverting the tubes several times.

12 Allow the contents to settle before decanting into storage containers. Let the samples sit overnight in a refrigerator or filter through quantitative fine filter paper before colorimetric analysis.

13 Determine P concentration in an aliquot of the clear filtrate as indicated in Section 24.5.

Comments

1 Digestions at high temperatures involving soil–acid mixtures can cause bumping resulting in the violent and dangerous ejection of materials from the digestion tube. The risk of bumping can be reduced through the use of inert boiling stones, glass, or PTFE beads that facilitate a consistent, smooth boiling of the acid. This is more likely to be a problem with blanks than with tubes containing the sample.

2 Alternatively, 210 mL of concentrated H_2SO_4 can be added to the digestion solution prepared in step 1, and the addition of concentrated H_2SO_4 directly to the sample (step 3) omitted. A total of 9 mL of the digestion mixture would be required for each sample, and should be added in careful and incremental additions to avoid too vigorous a reaction that may cause loss of material from the tube or flask. This digestion mixture should be refrigerated and is stable for 2–3 weeks.

24.3 TOTAL ORGANIC PHOSPHORUS

Total soil P_o is not measured directly, but rather as the increase in P_i resulting from the ignition of a soil sample or digestion of a soil extract. Differences among techniques or soil types may reflect a change in the efficiency of the procedure, rather than a true change in the amount of P_o in the soil. The extraction techniques (Anderson 1960; Bowman 1989; Bowman and Moir 1993) involve the use of various acid and base treatments with the

subsequent determination of the P_i and P_t in the extractants. The two major problems with these techniques are the incomplete extraction of soil P_o and the possible hydrolysis of P_o by the extractants. In general, these techniques tend to give the lower range of soil P_o values. The ignition techniques use either high (550°C, Saunders and Williams 1955) or low (250°C, Legg and Black 1955) temperatures to oxidize soil P_o to P_i. Matched ignited and unignited samples are then extracted with either weak or strong acids. The difference between P_i (ignited sample) and P_i (unignited sample) is considered P_o. This technique may result in erroneous estimates of P_o due to incomplete oxidation of P_o and changes in the solubilities of P minerals by ignition at either high or low temperatures, while ignition at higher temperatures may also cause volatilization of P. Each technique has its advantages and disadvantages, depending on the situation and the purpose of the study in question. As indicated by Bowman (1989), the extraction techniques are more suited for comparisons of P_o levels across different soil types, whereas ignition techniques are more suitable for comparisons among treatments within a soil type. Due to the errors that may be associated with P_o determinations and since the P_o is determined by difference, little significance can be given to treatments that differ by less than 20 μg P g^{-1} soil (Olsen and Sommers 1982).

As indicated by Condron et al. (1990), several studies have reported good agreement between ignition and extraction techniques with ignition methods tending to give higher soil P_o values, although studies have shown higher soil P_o levels with extraction compared to ignition techniques (Condron et al. 1990; Agbenin et al. 1999). In addition, considerable differences between the two techniques have been noted for certain soil types. Further information regarding comparisons of various methods for the determination of P_o in soils can be obtained by referring to Condron et al. (1990, 2005), Dormaar and Webster (1964), Steward and Oades (1972), and Turner et al. (2005).

For improved accuracy and precision of analysis, it is recommended that the soils used be air-dried and finely ground (0.15–0.18 mm; 100–80 mesh). Duplicate soil samples and blanks containing no sample should be used in each analysis. There are no certified reference materials for total organic P.

24.3.1 Hydrochloric Acid/Sodium Hydroxide Extraction Method (Anderson 1960 as Modified by Condron et al. 1990)

In this method, soils are sequentially extracted with 0.3 *M* NaOH, concentrated HCl (hot and then at room temperature), 0.5 *M* NaOH at room temperature, and 0.5 *M* NaOH at 90°C. The P_i in extracts is determined immediately after extraction and the P_t is determined after the oxidation of the organic matter with persulfate digestion.

Materials and Reagents

1 Heat-resistant polypropylene screw-top centrifuge tubes (50 mL) with caps.

2 Water bath at 90°C.

3 Centrifuge.

4 Vortex mixer (optional).

5 End-over-end shaker.

6 Oven for NaOH extraction of samples at 90°C.

7 Autoclave.

8 Aluminum foil.

9 Volumetric flasks (50 and 100 mL).

10 H_2SO_4, concentrated.

11 H_2SO_4 0.9 *M*: add 50 mL of concentrated H_2SO_4 to a 1 L volumetric flask containing 600 mL of distilled/deionized water. Mix and make to volume using distilled/deionized water.

12 HCl, concentrated.

13 NaOH, 0.3 *M*: dissolve 12 g NaOH in a 1 L volumetric flask containing approximately 700 mL of distilled/deionized water. Make to volume with distilled/deionized water.

14 NaOH, 0.5 *M*: dissolve 20 g NaOH in a 1 L volumetric flask containing approximately 700 mL of distilled/deionized water. Make to volume with distilled/deionized water.

15 Ammonium persulfate: $(NH_4)_2S_2O_8$.

16 Color developing solutions (see Section 24.5.1).

Extraction Procedure

1 Weigh 0.5 g of finely ground soil into a 50 mL polypropylene centrifuge tube.

2 0.3 *M* NaOH extraction: add 30 mL of 0.3 *M* NaOH, cap the tube, and shake on an end-over-end shaker for 16 h at room temperature. After shaking, centrifuge (12,500 *g*) the soil suspension for 10 min and then carefully decant the supernatant into a 100 mL volumetric flask ensuring that the soil residue remains in the tube.

3 Concentrated HCl extraction: to the soil residue in the centrifuge tube add 10 mL of concentrated HCl, mix thoroughly, and then place the tube in an 82°C water bath for 10 min. Remove the tube from the water bath, add 5 mL concentrated HCl, and allow to stand at room temperature for 1 h with regular (approximately every 15 min) vortex shaking. Centrifuge (12,500 *g*) for 10 min, carefully decant the supernatant into a 50 mL volumetric flask, and make to volume using distilled/deionized water.

4 Room temperature 0.5 *M* NaOH extraction: to the soil residue in the centrifuge tube add 20 mL 0.5 *M* NaOH, mix well, and allow to stand for 1 h at room temperature with regular (approximately every 15 min) vortex shaking. Centrifuge (12,500 *g*) the soil suspension for 10 min, and carefully decant the supernatant into the 100 mL volumetric flask containing the previous 0.3 *M* NaOH extract.

5 Hot 0.5 *M* NaOH extraction: to the soil residue in the tube, add 30 mL of 0.5 *M* NaOH, shake to suspend the soil in solution. Loosely cover the tubes with an inverted 50 mL beaker or funnel and place in an 82°C oven for 8 h. Remove tubes from the oven, allow to cool, centrifuge (12,500 *g*), and decant the supernatant into the 100 mL volumetric flask containing the previous two NaOH extracts. Make the contents of the 100 mL volumetric flask to volume using distilled/deionized water.

Determination of P_i and Total P in the Extracts

Determination of P_i

1 To determine P_i in the NaOH extract, pipette a suitable aliquot (usually $\leq$5 mL) into a 50 mL centrifuge tube. Acidify to precipitate organic material by adding 2.0 mL of 0.9 *M* H_2SO_4 and set in a refrigerator for 30 min. Centrifuge at 25,000 *g* for 10 min at 0°C. Decant the supernatant into a 50 mL volumetric flask. Using a little acidified water, rinse the tube carefully so as not to dislodge any of the precipitated organic matter, and add the liquid to the contents of the flask (repeat two or three times). Develop color as described in Section 24.5.2 starting with pH adjustment (step 3).

2 To determine P_i in the HCl extract, pipette a suitable aliquot (usually $\leq$5 mL) into a 50 mL volumetric flask. Develop color as described in Section 24.5.2 starting with pH adjustment (step 3).

Determination of total P

1 To colorimetrically determine total P in the extracts, pipette a suitable aliquot (usually $\leq$2 mL) of solution into a 50 mL volumetric flask.

2 To the NaOH extract add $\approx$0.5 g $(NH_4)_2S_2O_8$ and 10 mL of 0.9 *M* H_2SO_4.

3 To HCl extract add $\approx$0.4 g $(NH_4)_2S_2O_8$ and 10 mL deionized/distilled water.

4 Cover the mouth of the flask with aluminum foil (double layer for HCl extract) and autoclave (60 min for HCl extracts and 90 min for NaOH extracts).

5 Cool, add approximately 10 mL distilled/deionized water. Develop color as described in Section 24.5.2 starting with pH adjustment (step 3).

Calculations

Total P_o in the soil sample is determined as the summation of the total P in the HCl and NaOH extracts minus the summation of the P_i in the HCl and NaOH extracts. After determining the concentration of P in the digests and extracts and converting each to a soil weight basis (e.g., mg P kg^{-1} soil), P_o is calculated as

$$P_o = (\text{HCl-}P_t + \text{NaOH-}P_t) - (\text{HCl-}P_i + \text{NaOH-}P_i) \quad (24.1)$$

Comments

1 P_i should be determined in the extracts as soon as possible to reduce the chance of P hydrolysis resulting in an underestimation of soil P_o.

2 Soils high in humic materials and metals, such as forest soils and wetland soils, may lose P_i through the formation of P–metal–organic matter complexes during the precipitation of organic matter (Darke and Walbridge 2000), resulting in overestimation of P_o concentrations. P_o concentrations for these types of soils should be confirmed with a second method, such as ignition (Section 24.3.3).

3 Instead of acidifying an aliquot of the NaOH extract to precipitate organic matter, P_i can be determined directly, provided a suitable blank is used to correct for absorbance by organic matter in solution. To do this, pipette equal aliquots of the same sample extract into two separate 50 mL volumetric flasks and adjust the pH. To one add 8 mL of the color developing solution as described in Section 24.5. To the other add 8 mL of the color developing solution without ascorbic acid added. Dilute to volume and measure absorbance. The absorbance of the solution without ascorbic acid is subtracted from the absorbance of the solution with ascorbic acid.

4 Total P in the extracts can be determined directly using ICP, although dilution may be required if samples are relatively high in organic matter.

5 Total P in the extracts can also be determined by other digestion techniques such as the procedure of Thomas et al. (1967) using H_2SO_4/H_2O_2, or the potassium persulfate digestion using a hotplate (Bowman 1989).

24.3.2 Basic EDTA Extraction Method (Bowman and Moir 1993)

In this procedure, P_o is extracted from the soil using 0.25 *M* NaOH and 0.05 *M* disodium ethylene diamine tetraacetic acid (Na_2EDTA). This method is simple, faster than either the HCl/NaOH extraction method of Anderson (1960) or the ignition method of Saunders and Williams (1955), and is equally efficient. Excessive amounts of EDTA in solution can interfere with the colorimetric determination of P. Acidification of the extracts to pH $\leq$ 1.5 will precipitate both extracted SOM and EDTA, and this precipitate can then be removed by centrifugation or filtration (Nnadi et al. 1975) allowing for the determination of srP in solution.

Materials and Reagents

1 Heat-resistant polypropylene screw-top centrifuge tubes (50 mL).

2 Centrifuge.

3 Incubator or oven set at 85°C.

4 Quantitative fine filter paper (e.g., Whatman No. 42).

5 NaOH, 0.5 *M*: dissolve 10 g NaOH in a 500 mL volumetric flask containing 300 mL of distilled/deionized water. Make to volume with distilled/deionized water.

6 Na_2EDTA, 0.1 *M*: dissolve 18.6 g Na_2EDTA in a 500 mL volumetric flask containing 300 mL of distilled/deionized water. Make to volume with distilled/deionized water.

7 NaOH–EDTA mixture: combine the 0.5 *M* NaOH and 0.1 *M* Na_2EDTA solutions (final concentration 0.25 *M* NaOH + 0.05 *M* Na_2EDTA).

8 Ammonium persulfate: $(NH_4)_2S_2O_8$.

9 H_2SO_4 5.5 *M*: add 306 mL of concentrated H_2SO_4 to a 1 L volumetric flask containing 500 mL of distilled/deionized water. Mix, cool, and make to volume using distilled/deionized water.

10 H_2SO_4 0.9 *M*: add 50 mL of concentrated H_2SO_4 to a 1 L volumetric flask containing 600 mL of distilled/deionized water. Mix and make to volume using distilled/deionized water.

11 Color developing solutions (see Section 24.5.1).

Extraction Procedure

1 Weigh 0.5 g of finely ground soil into a heat-resistant 50 mL centrifuge tube.

2 Add 25 mL of combined NaOH–EDTA solution to the tube, cap tightly, and shake briefly to mix.

3 Loosen caps. Place in incubator or oven (preheated to 85°C) for 10 min.

4 Cap tightly and incubate for 1 h 50 min (2 h incubation total).

5 Centrifuge at 25,000 *g* for 10 min.

6 Filter supernatant and keep the filtrate for analysis.

Determination of P_i and Total P in the Extract

1 Determination of P_i: pipette $\leq$5 mL of extract into a 50 mL centrifuge tube. Acidify by adding 0.5 mL 0.9 *M* H_2SO_4. Cool in refrigerator for 30 min. Centrifuge at 25,000 *g* for 10 min at 0°C. Decant the supernatant into a 50 mL volumetric flask. Using a little acidified water, rinse the tube carefully so as to not dislodge any of the precipitated organic matter and add the liquid to the contents of the flask (repeat two or three times). Develop color as described in Section 24.5.2 starting with pH adjustment (step 3).

2 Determination of total P: pipette $\leq$5 mL extract into a 25 mL volumetric flask. Add $\approx$0.5 g $(NH_4)_2S_2O_8$ and 10 mL of 0.9 *M* H_2SO_4. Cover the mouth of the flask with aluminum foil and autoclave for 90 min. Cool, add approximately 10 mL distilled/deionized water, and develop color as described in Section 24.5.2 starting with pH adjustment (step 3).

Calculations

After determining the concentration of P in the digests and extracts and converting each to a soil weight basis (e.g., mg P kg^{-1} soil), P_o is calculated as

$$P_o = P_t \text{ (digest or ICP)} - P_i \text{ (extract)} \quad (24.2)$$

Comments

1 The initial 10 min period with loose caps is to minimize gas buildup.

2 The combination of EDTA and NaOH simultaneously eliminates the formation of cationic bridges with SOM and solubilized organic matter (Bowman and Moir 1993). This eliminates the need for acid pretreatment.

3 Extraction at room temperature for 16 h produced similar P_o concentrations as extracting at 85°C for 2 h.

4 As discussed in Comments, pp. 276 and 277, the removal of organic matter by precipitation may produce inaccurate estimations of P_o concentrations in soils high in humic materials and metals.

5 P_i in the NaOH–EDTA extract can also be determined directly following the same procedure as outlined in the third point in Comments, p. 277. If this alternative procedure is used, the aliquot size should not exceed 4 mL, because excessive EDTA will retard color development.

6 Total P in the extract can be determined using an ICP, or by other methods such as the procedure of Thomas et al. (1967) using H_2SO_4/H_2O_2, or potassium persulfate digestion using a hotplate (Bowman 1989).

24.3.3 Ignition Method (Saunders and Williams 1955, as Modified by Walker and Adams 1958)

In this method, P_o is estimated by the difference between 0.5 *M* H_2SO_4-extractable P in a soil sample ignited at 550°C and an unignited sample. The method is suitable for the determination of soil P_o in a large number of samples. Dormaar and Webster (1964) have indicated that significant volatile losses of P may occur at temperatures above 400°C, especially with peat soils.

Materials and Reagents

1 Muffle furnace and porcelain crucibles for igniting soils at 550°C.

2 Polypropylene centrifuge tubes (100 mL) with caps or stoppers.

3 Shaker capable of holding the above tubes.

4 Centrifuge.

5 H_2SO_4, 0.5 *M*: add 28 mL concentrated H_2SO_4 to 600 mL distilled/deionized water in a 1 L volumetric flask. Allow to cool and make to volume using distilled/deionized water.

6 Color developing solutions (see Section 24.5.1).

Procedure

1 Weigh 1.0 g of finely ground soil in a porcelain crucible, and place the crucible in a cool muffle furnace.

2 Slowly raise the temperature of the muffle furnace to 550°C over a period of approximately 2 h. Continue to heat the samples at 550°C for 1 h, then remove the samples and allow them to cool.

3 Transfer the ignited soil to a 100 mL polypropylene centrifuge tube for extraction.

4 To a separate 100 mL polypropylene centrifuge tube, weigh 1.0 g of unignited soil for the extraction of P_i.

5 Add 50 mL of 0.5 *M* H_2SO_4 to both samples, mix well, and allow to sit lightly stoppered for a few minutes to relieve pressure from CO_2 released from any carbonates that may be present in the soil sample. Tightly stopper the tubes and place them on a shaker for 16 h. Blank samples containing only 0.5 *M* H_2SO_4 should also be included.

6 Centrifuge the samples at approximately 1500 *g* for 15 min. If the extract is not clear, filtration using acid-resistant filter paper may be required.

7 Determine P concentration in an aliquot of clear supernatant or filtrate as indicated in Section 24.5.

Calculations

After determining the concentration of P in the extracts and converting each to a soil weight basis (e.g., mg P kg^{-1} soil), P_o is calculated as

$$P_o = P_i \text{ (ignited sample)} - P_i \text{ (unignited sample)} \quad (24.3)$$

Comments

To prevent volatilization of P from the sample, care must be taken to not allow temperatures in the muffle furnace to exceed 550°C when using mineral soils (Sommers et al. 1970; Williams et al. 1970).

24.4 ORGANIC PHOSPHORUS CHARACTERIZATION

There are no direct methods to speciate soil P_o. Although there have been attempts to characterize P_o directly in soil using solid-state ^{31}P NMR spectroscopy, results have generally been poor due to line broadening from the close association of soil P with paramagnetics such as Fe (Cade-Menun 2005). As such, soil P_o must be extracted before speciation. Association with mineral components stabilizes much of the soil P_o, making it difficult to extract, and using strong acid or base extraction introduces the risk of P_o hydrolysis. Thus, the ideal extractant for chemical characterization of soil P_o should maximize recovery while minimizing alteration of chemical structure. Post extraction, the ideal speciation technique should allow the quantitative determination of the relative proportions of a range of P

compounds. Two techniques that best fit these criteria are solution ^{31}P NMR spectroscopy and enzyme hydrolysis.

24.4.1 NaOH–EDTA Extraction for Solution ^{31}P NMR Spectroscopy

From its first use on soil extracts by Newman and Tate (1980), solution ^{31}P NMR spectroscopy has substantially advanced our knowledge of P_o compounds in soil and other environmental samples. Various extractants have been used including 0.5 *M* NaOH alone or combined with either EDTA or the cation-exchange resin Chelex (Bio-Rad Laboratories). (The use of this trade name is provided for the benefit of the reader and does not imply endorsement by the CSSS.) The choice of extractant will influence both the recovery of P_o from soil and the composition of extracted compounds (Cade-Menun and Preston 1996; Cade-Menun et al. 2002). The extractant most commonly used at present is a combination of NaOH–EDTA based on the Bowman and Moir (1993) extraction procedure for total P_o, described in Section 24.3.2.

^{31}P NMR spectroscopy allows the characterization of the relative abundances of both P_o and P_i forms in an extract. Figure 24.1 shows ^{31}P NMR spectra for standard reference materials available from the National Institute of Standards and Testing (NIST) in the United States. The top sample is apple leaf reference, and the bottom is the San Joaquin soil reference. Note the differences in the relative abundances of P_o and P_i compounds.

It is beyond the scope of this chapter to fully describe the workings of a ^{31}P NMR spectrometer, and exact analytical procedures will vary with each spectrometer. Please see Cade-Menun (2005) for important considerations on conducting a successful ^{31}P NMR experiment on soil extracts. Included here is a protocol to extract soil samples for ^{31}P NMR spectroscopy.

Materials and Reagents

1. Polypropylene screw-top 50 mL centrifuge tubes.
2. Mechanical shaker for the centrifuge tubes.
3. Vortex mixer (optional).
4. Centrifuge.
5. Freezer.
6. Freeze dryer.
7. NMR spectrometer with broadband probe. Ideally, a 500 MHz (for proton) spectrometer and a 10 mm probe (see Cade-Menun 2005).
8. NaOH, 10 *M*: dissolve 20 g NaOH in a 50 mL volumetric flask containing 30 mL of distilled/deionized water. Allow to cool and make to volume with distilled/deionized water.
9. NaOH, 0.5 *M*: dissolve 10 g NaOH in a 500 mL volumetric flask containing 300 mL of distilled/deionized water. Allow to cool and make to volume with distilled/deionized water.

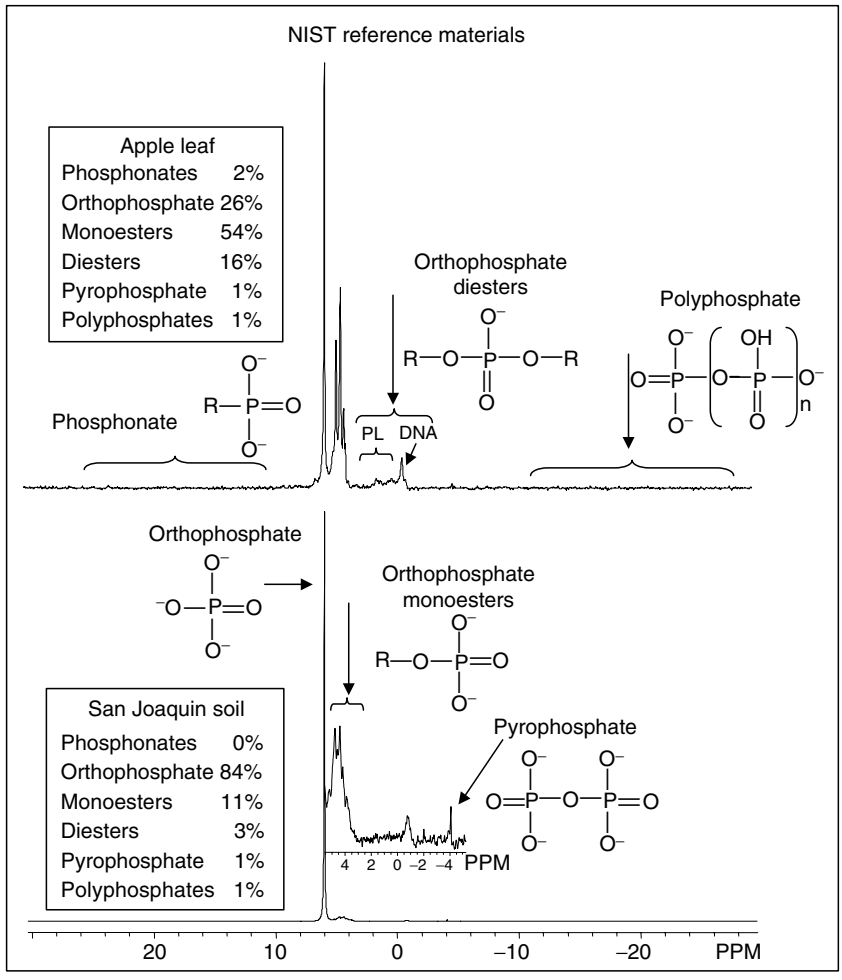

FIGURE 24.1. ^{31}P nuclear magnetic resonance (NMR) spectra of NIST apple leaf reference and NIST San Joaquin reference soil, showing the range of P compounds that can be identified using this technique, and their relative abundance in soil and foliar samples. (PL is phospholipids; DNA is deoxyribonucleic acid.) The inset for the soil spectrum shows the expanded orthophosphate monoester, diester, and pyrophosphate region.

10 Na_2EDTA, 0.1 *M*: dissolve 18.6 g Na_2EDTA in a 500 mL volumetric flask containing 300 mL of distilled/deionized water. Make to volume with distilled/deionized water.

11 NaOH–EDTA mixture: combine the 0.5 *M* NaOH and 0.1 *M* Na_2EDTA solutions (final concentration 0.25 *M* NaOH + 0.05 *M* Na_2EDTA).

12 Deuterium oxide (D_2O) suitable for NMR analyses.

Procedure

1 Weigh 1–2 g of soil into a 50 mL centrifuge tube. Use larger sample if soil is known to be low in P_t. Use smaller sample if high in Fe or organic matter.

2 Add 30 mL of combined NaOH–EDTA solution to the tube and cap tightly.

3 Shake at room temperature for 5–16 h. Longer extractions can increase the recovery of total P, particularly occluded P forms, but may also increase the risk of degradation of P forms such as RNA and phospholipids.

4 Centrifuge at 1500 *g* for 20 min. Decant supernatant into another 50 mL centrifuge tube. If the supernatant contains particulate material, samples should be filtered before decanting into the second centrifuge tube.

5 Remove 1 mL of supernatant. Dilute to 10 mL with distilled/deionized water, and analyze for P, Fe, and Mn.

6 Cap centrifuge tubes containing remainder of supernatant tightly, and freeze for 16–24 h, until completely frozen. Note: freeze tubes on a slant to maximize surface area.

7 Remove caps from tubes and cover loosely with Parafilm (poke small holes in Parafilm to allow air to circulate) or similar material. Place tubes upright in freeze-dryer flasks. Lyophilize for 24–48 h according to freeze-dryer instructions, until completely dry. Remove tubes from freeze-dryer flask. Cap tightly. Store at room temperature.

8 If using a spectrometer with a 10 mm probe, samples can be redissolved directly in the centrifuge tube by adding 1.6 mL of distilled/deionized water, 1 mL of D_2O, and 0.4 mL of 10 *M* NaOH (to adjust the pH to >12, for maximum peak separation). Let stand for 30 min, mixing or vortexing occasionally to dissolve all solids. Centrifuge at 1500 *g* for 20 min. Decant into NMR tube. If using a spectrometer with a 5 mm probe, adjust volumes accordingly.

9 See Cade-Menun (2005) for a discussion of suitable spectrometer parameters to conduct a successful ^{31}P NMR experiment on soil extracts.

24.4.2 Organic Phosphorus Characterization by Enzyme Hydrolysis

Characterization of P_o is based on the principle that substrate-specific phosphatase enzymes will release P_i from specific P forms. Thus, by adding commercially available phosphatase enzymes to soil extracts and colorimetrically analyzing the P_i released, the P forms within the extracts can be grouped into P compound categories. The specific classification of P forms will depend on the enzymes used in the assay. For example, acid phosphatase or alkaline phosphatase will hydrolyze orthophosphate monoesters in general, while phytase will hydrolyze one specific orthophosphate monoester, phytic acid (*myo*-inositol hexakisphosphate).

One aspect of enzyme hydrolysis is that it can be conducted on a number of different soil extracts, including water, sodium bicarbonate ($NaHCO_3$), NaOH, and HCl, and has been used with sequential extraction procedures (e.g., He and Honeycutt 2001). However, solutions should be adjusted to the suitable pH range for each enzyme before characterization with enzyme hydrolysis.

A number of different protocols exist for enzyme hydrolysis, including the universal buffer procedure recently developed by He et al. (2004). The following protocol was adapted from Turner et al. (2002, 2003) and Toor et al. (2003).

Materials and Reagents

1 Polypropylene screw-top 50 mL centrifuge tubes.

2 Shaker capable of holding the above tubes.

3 Calibrated disposable plastic centrifuge tubes (15 mL), 5 for each soil sample to be extracted.

4 Incubator or shaking water bath, set at 37°C.

5 Centrifuge.

6 0.45 μm membrane filter and vacuum filtration apparatus.

7 NaOH, 1 *M*: dissolve 20 g NaOH in a 500 mL volumetric flask containing 300 mL of distilled/deionized water. Allow to cool and make to volume with distilled/deionized water.

8 $NaHCO_3$, 0.5 *M* pH 8.5: dissolve 21 g $NaHCO_3$ and 0.25 g of NaOH in a 500 mL beaker containing 300 mL of distilled/deionized water. Transfer to a 500 mL volumetric flask, and make to volume with distilled/deionized water.

9 Sodium azide (NaN_3), 25 m*M*: dissolve 0.163 g NaN_3 in a 100 mL volumetric flask containing 40 mL of distilled/deionized water. Make to volume with distilled/deionized water.

10 H_2SO_4, 3 *M*: add 83 mL of concentrated H_2SO_4 to 500 mL volumetric flask containing 300 mL of distilled/deionized water. Mix and allow to cool before making to final volume with distilled/deionized water.

11 Tris–HCl buffer, 2 *M*: dissolve 31.5 g Tris–HCl powder (Polysciences, Inc., Warrington, PA) and 0.041 g $MgCl_2 \cdot 6H_2O$ in a 100 mL beaker containing 60 mL of distilled/deionized water. Adjust to pH 8. Transfer to a 100 mL volumetric flask, and make to volume with distilled/deionized water.

12 Glycine–HCl buffer, 2 *M*: dissolve 0.041 g $MgCl_2 \cdot 6H_2O$ in a 100 mL beaker containing 60 mL of distilled/deionized water. Add 20 mL of 1 *M* Glycine–HCl buffer, 10× concentrate (Polysciences, Inc., Warrington, PA). Check pH, which should be 2.5. Transfer to a 100 mL volumetric flask, and make to volume with distilled/deionized water.

13 Enzymes: suitable enzymes can be obtained from a variety of sources. (All the following enzymes are available from Sigma Chemicals, St. Louis, MO: trade names are mentioned only for the benefit of the reader.)

   a. Alkaline phosphatase (EC 3.1.3.2), Type V-IIS, from bovine intestinal mucosa, activity of preparation 1 unit mL^{-1}: add 0.1 mL of alkaline phosphatase (2.2 mg protein per mL, 2420 units activity per mg protein) to 20 mL of 2 *M* Tris–HCl buffer, pH 8.

b. Phospholipase C (EC 3.1.4.3), Type XI, from *Bacillus cereus*, activity of preparation 1 unit mL^{-1}: add 24.94 mg of phospholipase (16.04 units activity mg^{-1} solid) and 0.1 mL of alkaline phosphatase to 20 mL of 2 *M* Tris–HCl buffer, pH 8. See Comment 5, p. 286.

c. Phosphodiesterase (EC 3.1.4.1), Type IV, from *Crotalus atrox* venom, activity of preparation 0.03 units mL^{-1}: add 20 mg of phosphodiesterase (0.02 units activity mg^{-1} solid) and 0.1 mL of alkaline phosphatase to 20 mL of 2 *M* Tris–HCl buffer, pH 8. See Comment 5, p. 286.

d. Phytase (EC 3.1.3.8), Type *myo*-inositol hexakisphosphate 3-phosphohydrolase, from *Aspergillus ficuum*, activity of preparation 1 unit mL^{-1}: add 23 mg of phytase (1.1 units activity mg^{-1} solid) to 80 mL of 2 *M* Glycine–HCl buffer, pH 2.5. Centrifuge for 10 min at 1500 *g*.

14 Magnesium chloride ($MgCl_2$), 2 m*M*: dissolve 0.041 g $MgCl_2 \cdot 6H_2O$ in a 100 mL volumetric flask containing 60 mL of distilled/deionized water. Make to volume with distilled/deionized water.

15 Color developing solution: see Section 24.5.1.

Procedures

1 Weigh 1.5 g of soil into a 50 mL centrifuge tube. Blank samples containing no soil should also be analyzed.

2 Add 30 mL of 0.5 *M* $NaHCO_3$. Shake for 30 min.

3 Centrifuge at approximately 1500 *g* for 15 min. Filter supernatant through 0.45 μm filters.

4 Label five 15 mL centrifuge tubes for each extracted soil sample or blank. Four tubes should be labeled with the names of the enzymes (one per enzyme), while the fifth tube should be labeled ''control.'' Add 1 mL of the $NaHCO_3$ extract to five 15 mL centrifuge tubes for each extracted soil sample. Preacidify by adding 0.1 mL of 3 *M* H_2SO_4 and neutralize by adding 0.12 mL of 1 *M* NaOH (see Comment 2, p. 286.

5 Add 1 mL of 25 m*M* NaN_3 to prevent microbial activity.

6 Add 0.25 mL of each enzyme–buffer mixture to the appropriately labeled tube for each sample or blank. Add 0.25 mL of the $MgCl_2$ solution to the controls. Dilute to 5 mL with distilled/deionized water.

7 Incubate with shaking at 37°C for 16 h (incubator or shaking water bath).

8 Terminate enzyme reaction by adding 1 mL of color developing solution (see Section 24.5). Final volume for samples (and standards) is 6 mL.

9 Measure the absorbance after 12 min at 880 nm. Calculate P_i concentration in solution by comparison to a standard curve. Note that phosphodiesterase and

phytase cause slight interferences with the molybdate blue reaction. Prepare separate calibration curves from orthophosphate standards containing the enzymes.

Comments

1 All buffers contain 2 m*M* $MgCl_2$ because Mg^{2+} ions are natural activators of phosphatase enzymes (Dixon and Webb 1966).

2 The preacidification and neutralization steps are necessary to remove carbonates from bicarbonate extractions, to prevent foaming during subsequent colorimetric analysis.

3 ''Activity of preparation'' refers to the activity in the centrifuge tube with the soil extract and other reagents.

4 Commercial phytase is not purified, and contains other P-hydrolyzing enzymes. For a purification procedure, see Hayes et al. (2000).

5 Alkaline phosphatase was added to the phospholipase and phosphodiesterase preparations because phosphodiesterase and phospholipase hydrolyze only one ester-P bond on the diester molecule. This leaves an orthophosphate monoester, which requires alkaline phosphatase to completely release orthophosphate (Turner et al. 2002).

6 If working with acid extracts, use acid phosphatase (EC 3.1.3.2) rather than alkaline phosphatase.

7 Sodium azide and phosphodiesterase from *Crotalus atrox* venom are both poisons, and should be handled and disposed of accordingly.

Calculations

Functional classes of organic P compounds are calculated as

1 labile monoester P: hydrolyzed by alkaline phosphatase;

2 phospholipids: the difference between the P released by phospholipase + alkaline phosphatase and the P released by alkaline phosphatase alone;

3 nucleic acids: the difference between the P released by phosphodiesterase + alkaline phosphatase and the P released by alkaline phosphatase alone; and

4 inositol hexakisphosphate (phytic acid): the difference between the P released by phytase and all other treatments.

24.5 DETERMINATION OF PHOSPHORUS

The determination of P in solutions is usually conducted by colorimetric methods or by inductively coupled plasma (ICP) spectroscopy. Colorimetric methods for the determination of P in solution require that the desired pool of soil P that is extracted from the soil is

completely converted to orthophosphate, while total P in solution may be analyzed without prior digestion by ICP.

One of the most commonly used methods for the colorimetric determination of orthophosphate concentration in solutions is the method developed by Murphy and Riley (1962). This method uses the blue color developed by a phosphoantimonylmolybdenum complex (Going and Eisenreich 1974; Drummond and Maher 1995) reduced by ascorbic acid to estimate the concentration of orthophosphate in solution. As the procedure was originally developed for seawater, Murphy and Riley (1962) only assessed adherence to Beer's law up to a final solution concentration (i.e., solution in which the color has been developed) of 0.2 mg P L^{-1}. The procedure is suitable for final solution P concentrations of approximately 0.8 mg P L^{-1} (Rodriguez et al. 1994) and subsequent modifications of the strength of the antimony (Sb) and ascorbic acid solutions have extended this to a final solution concentration of 3 mg P L^{-1} (Harwood et al. 1969). This procedure is fairly simple, less susceptible to interferences than procedures using $SnCl_2$ as a reductant, and is capable of being used manually or adapted to automated systems (Drummond and Maher 1995). A manual method as modified by Watanabe and Olsen (1965) is present here, and is suitable for aliquots containing between 1 and 40 μg srP when made to a final volume of 50 mL for color determination.

24.5.1 Reagents

1 Ammonium molybdate solution: dissolve 12 g of ammonium molybdate tetrahydrate ($(NH_4)_6Mo_7O_{24} \cdot 4H_2O$) in 250 mL distilled/deionized water.

2 Potassium antimony tartrate solution: dissolve 0.2908 g of potassium antimony tartrate ($KSbOC_4H_4O_6$) in 100 mL distilled/deionized water.

3 H_2SO_4 2.5 *M*: to a 1 L volumetric flask containing approximately 600 mL of distilled/deionized water slowly add 139 mL of concentrated (18 *M*) H_2SO_4. Mix by swirling the contents of the flask, allow to cool, and make to volume with distilled/deionized water.

4 Reagent A: combine the three solutions above in a 2 L volumetric flask, make to volume with distilled/deionized water and mix thoroughly. Store in a Pyrex glass bottle in a refrigerator.

5 Color developing solution: dissolve 1.056 g of ascorbic acid in 200 mL of reagent A and mix. Prepare this solution daily and do not use if more than 24 h old.

6 *p*-Nitrophenol solution: dissolve approximately 0.25 g of *p*-nitrophenol in 100 mL of distilled/deionized water.

7 NaOH 4 *M*: in a 1 L volumetric flask dissolve 160 g of NaOH in approximately 800 mL of distilled/deionized water. Allow to cool, make to volume using distilled/deionized water, and mix thoroughly.

8 H_2SO_4 0.25 *M*: slowly add 14 mL of concentrated H_2SO_4 to 1 L volumetric flask containing approximately 800 mL of distilled/deionized water, make to volume with distilled/deionized water, and mix thoroughly.

9 Standard P stock solution (100 mg P L^{-1}): dissolve 0.4394 g of potassium dihydrogen phosphate (KH_2PO_4) in 1 L of distilled/deionized water. Prepare a working standard (10 mg P L^{-1}) by dilution with distilled/deionized water.

24.5.2 Procedure

1 Pipette an aliquot containing 1–40 μg of P into a 50 mL volumetric flask containing approximately 15 mL distilled/deionized water.

2 Pipette standard P solutions into a set of volumetric flasks so as to encompass the range of P concentrations anticipated in the extracts. To each flask containing a standard solution, pipette an aliquot of blank solution equal to the aliquot size of the sample.

3 Add 1–2 drops of *p*-nitrophenol and adjust the pH of the solution to ~5. If the sample aliquot has a pH <5, add 4 *M* NaOH drop wise until the solution turns yellow in color and then add 0.25 *M* H_2SO_4 until colorless. If the sample aliquot has a pH >5, add 0.25 *M* H_2SO_4 until colorless.

4 Add 8 mL of the color developing solution, make to volume with distilled/deionized water, and mix thoroughly. After 10 min read absorbance at either 882 or 712 nm (if solution is slightly colored due to the presence of organic matter).

5 Appropriate standards (final solution concentrations of 0–0.8 μg P mL^{-1}, or 0–40 μg P in the 50 mL volumetric flask) should be analyzed in the same manner as samples, and contain similar amounts of extracting or digestion solutions as the samples.

24.5.3 Comments

1 Many versions of the Murphy and Riley (1962) procedure have been published, and the reader is cautioned that deviations from proposed methodologies can lead to erroneous results. The development of a stable blue color that adheres to Beer's law requires the proper adjustment of solution pH, as well as specific ranges of Mo, Sb, and ascorbic acid concentrations relative each other, to the amount of P in the sample, or both (Harwood et al. 1969; Going and Eisenreich 1974; Rodriguez et al. 1994; Drummond and Maher 1995). Any changes to proposed methods should be verified using samples and standards of known P content.

2 The original method described by Watanabe and Olsen (1965) for sodium bicarbonate extracts of soil P used 25 mL volumetric flasks, and therefore only 4 mL of color developing reagent and a sample aliquot containing a maximum of 20 μg P.

3 Arsenate (AsO_4) will also form a blue color with the Murphy and Riley solution. Olsen and Sommers (1982) indicate that in most soils the average As concentration is 6 mg kg^{-1}, and as such would be a negligible amount compared to typical P concentrations in soils. However, if a soil has been contaminated with As, this could lead to substantial overestimation of P in the sample. In soils with high As contents, Olsen and Sommers (1982) recommend reducing AsO_4 to AsO_3 by

adding 5 mL of sodium hydrogen sulfite solution (5.2 g of $NaHSO_3$ dissolved in 100 mL of 0.5 M H_2SO_4) to the sample aliquot and either heating the mixture in a water bath for 30 min (20 min at 95°C) or letting it stand for 4 h before adjusting pH and developing the color.

REFERENCES

Agbenin, J.O., Iwuafor, E.N.O., and Ayuba, B. 1999. A critical assessment of methods for determining organic phosphorus in savanna soils. *Biol. Fert. Soils* 28: 177–181.

Agbenin, J.O. and Tiessen, H. 1994. Phosphorus transformations in a toposequence of Lithosols and Cambisols from semi-arid northeastern Brazil. *Geoderma* 62: 345–362.

Anderson, G. 1960. Factors affecting the estimation of phosphate esters in soil. *J. Sci. Food Agric.* 11: 497–503.

Bowman, R.A. 1988. A rapid method to determine total phosphorus in soils. *Soil Sci. Soc. Am. J.* 52: 1301–1304.

Bowman, R.A. 1989. A sequential extraction procedure with concentrated sulfuric acid and dilute base for soil organic phosphorus. *Soil Sci. Soc. Am. J.* 53: 362–366.

Bowman, R.A. and Moir, J.O. 1993. Basic EDTA as an extractant for soil organic phosphorus. *Soil Sci. Soc. Am. J.* 57: 1516–1518.

Cade-Menun, B.J. 2005. Using phosphorus-31 nuclear magnetic resonance spectroscopy to characterize phosphorus in environmental samples. In B.L. Turner, E. Frossard, and D. Baldwin, Eds. *Organic Phosphorus in the Environment*. CABI Publishing. Wallingford, UK, pp. 21–44.

Cade-Menun, B.J., Liu, C.W., Nunlist, R., and McColl, J.G. 2002. Soil and litter ^{31}P-NMR: Extractants, metals and P relaxation times. *J. Environ. Qual.* 31: 457–465.

Cade-Menun, B.J. and Preston, C.M. 1996. A comparison of soil extraction procedures for ^{31}P NMR spectroscopy. *Soil Sci.* 161: 770–785.

Cihacek, L.J. and Lizotte, D.A. 1990. Evaluation of an aluminum digestion block for routine total soil phosphorus determination by alkaline hypobromite oxidation. *Commun. Soil Sci. Plant Anal.* 21: 2361–2370.

Condron, L.M., Moir, J.O., Tiessen, H., and Stewart, J.W.B. 1990. Critical evaluation of methods for determining total organic phosphorus in tropical soils. *Soil Sci. Soc. Am. J.* 54: 1261–1266.

Condron, L.M., Turner, B.L., and Cade-Menun, B.J. 2005. Chemistry and dynamics of soil organic phosphorus. In J.T. Sims and A.N. Sharpley, Eds. *Phosphorus, Agriculture and the Environment*. Soil Science Society of America. Madison, WI, USA, pp. 87–121.

Darke, A.K. and Walbridge, M.R. 2000. Al and Fe biogeochemistry in a floodplain forest: Implications for P retention. *Biogeochemistry* 51: 1–32.

Dick, W.A. and Tabatabai, M.A. 1977. An alkaline oxidation method for determination of total phosphorus in soils. *Soil Sci. Soc. Am. J.* 41: 511–514.

Dixon, M. and Webb, E.C. 1966. *Enzymes*. Longman Scientific. London, UK.

Dormaar, J.F. and Webster, G.R. 1964. Losses inherent in ignition procedures for determining total organic phosphorus. *Can. J. Soil Sci.* 44: 1–6.

Drummond, L. and Maher, W. 1995. Determination of phosphorus in aqueous solution via formation of the phosphoantimonylmolybdenum blue complex: Re-examination of the optimum conditions for the analysis of phosphate. *Anal. Chim. Acta* 302: 69–74.

Gasparatos, D. and Haidouti, C. 2001. A comparison of wet oxidation methods for determination of total phosphorus in soils. *J. Plant Nutr. Soil Sci.* 164: 435–439.

Going, J.E. and Eisenreich, S.J. 1974. Spectrophotometric studies of reduced molybdoantimonylphosphoric acid. *Anal. Chim. Acta* 70: 96–106.

Harwood, J.E., van Steenderen, R.A., and Kühn, A.L. 1969. A rapid method for orthophosphate analysis at high concentrations in water. *Water Res.* 3: 417–423.

Hayes, J.E., Richardson, A.E., and Simpson, R.J. 2000. Components of organic phosphorus in soil that are hydrolysed by phytase and acid phosphatase. *Biol. Fert. Soils* 32: 279–286.

He, Z., Griffin, T.S., and Honeycutt, C.W. 2004. Enzymatic hydrolysis of organic phosphorus in swine manure and soil. *J. Environ. Qual.* 33: 367–372.

He, Z. and Honeycutt, C.W. 2001. Enzymatic characterization of organic phosphorus in animal manures. *J. Environ. Qual.* 30: 1685–1692.

Hedley, M.J., Stewart, J.W.B., and Chauhan, B.S. 1982. Changes in inorganic and organic soil phosphorus fraction induced by cultivation practices and by laboratory incubations. *Soil Sci. Soc. Am. J.* 46: 970–976.

Kara, D., Özsavasçi, C., and Alkan, M. 1997. Investigation of suitable digestion methods for the determination of total phosphorus in soils. *Talanta* 44: 2027–2032.

Legg, J.O. and Black, C.A. 1955. Determination of organic phosphorus in soils. II. Ignition method. *Soil Sci. Soc. Am. Proc.* 19: 139–143.

Mehta, N.C., Legg, J.O., Goring, C.A.I., and Black, C.A. 1954. Determination of organic phosphorus in soils. I. Extraction method. *Soil Sci. Soc. Am. Proc.* 18: 443–449.

Murphy, J. and Riley, J.P. 1962. A modified single solution method for the determination of phosphate in natural waters. *Anal. Chim. Acta.* 27: 31–36.

Newman, R.H. and Tate, K.R. 1980. Soil phosphorus characterization by ^{31}P nuclear magnetic resonance. *Commun. Soil Sci. Plant Anal.* 11: 835–842.

Nnadi, L.A., Tabatabai, M.A., and Hanaway, J.J. 1975. Determination of phosphate extracted from soils by EDTA and NTA. *Soil Sci.* 119: 203–209.

O'Halloran, I.P. 1993. Total and organic phosphorus. Pages 213–229 *in* M.R. Carter, Ed. *Soil Sampling and Methods of Analysis*. Canadian Society of Soil Science. Lewis Publishers, Boca Raton, FL, USA.

Olsen, S.R. and Sommers, L.E. 1982. Phosphorus. Pages 403–430 *in* A.L. Page, R.H. Miller, and D.R. Keeney, Eds. *Methods of Soil Analysis. Part 2*. 2nd ed. Agronomy No. 9. American Society of Agronomy, Madison, WI, USA.

Parkinson, J.A. and Allen, S.E. 1975. A wet oxidation procedure suitable for the determination of nitrogen and mineral nutrients in biological material. *Commun. Soil Sci. Plant Anal.* 6: 1–11.

Rodriguez, J.B., Self, J.R., and Soltanpour, P.N. 1994. Optimal conditions for phosphorus analysis by the ascorbic acid-molybdenum blue method. *Soil Sci. Soc. Am. J.* 58: 866–870.

Rowland, A.P. and Grimshaw, H.M. 1985. A wet oxidation procedure suitable for total nitrogen and phosphorus in soil. *Commun. Soil Sci. Plant Anal.* 16: 551–560.

Saunders, W.M. and Williams, E.G. 1955. Observations on the determination of organic phosphorus in soils. *J. Soil Sci.* 6: 254–267.

Smith, B.F.L. and Bain, D.C. 1982. A sodium hydroxide fusion method for the determination of total phosphate in soils. *Commun. Soil Sci. Plant Anal.* 13: 185–190.

Sommers, L.E., Harris, R.F., Williams, J.D.H., Armstrong, D.E., and Syers, J.K. 1970. Determination of total organic phosphorus in lake sediments. Limnol. *Oceanogr.* 15: 301–304.

Sommers, L.E. and Nelson, D.W. 1972. Determination of total phosphorus in soils: A rapid perchloric acid digestion procedure. *Soil Sci. Soc. Am. Proc.* 36: 902–904.

Steward, J.H. and Oades, J.M. 1972. The determination of organic phosphorus in soils. *J. Soil Sci.* 23: 38–49.

Syers, J.K., Williams, J.D.H., Campbell, A.S., and Walker, T.W. 1967. The significance of apatite inclusions in soil phosphorus studies. *Soil Sci. Soc. Am. Proc.* 31: 752–756.

Syers, J.K., Williams, J.D.H., Tyner, E.H., and Walker, T.W. 1969. Primary and secondary origin of ''nonextractable'' soil inorganic phosphorus. *Soil Sci. Soc. Am. Proc.* 33: 635–636.

Syers, J.K., Williams, J.D.H., and Walker, T.W. 1968. The determination of total phosphorus in

soils and parent materials. *N. Z. J. Agric. Res.* 11: 757–762.

Taylor, M.D. 2000. Determination of total phosphorus in soil using simple Kjeldahl digestion. *Commun. Soil Sci. Plant Anal.* 31: 2665–2670.

Thomas, R.L., Sheard, R.W., and Moyer, J.R. 1967. Comparison of conventional and automated procedures for nitrogen, phosphorus and potassium analysis of plant material using a single digestion. *Agron. J.* 59: 240–243.

Toor, G.S., Condron, L.M., Di, H.J., Cameron, K.C., and Cade-Menun, B.J. 2003. Characterization of organic phosphorus in leachate from a grassland soil. *Soil Biol. Biochem.* 35: 1319–1325.

Turner, B.L., Cade-Menun, B.J., Condron, L.M., and Newman, S. 2005. Extraction of organic phosphorus from soil and manure. *Talanta* 66: 294–306.

Turner, B.L., Cade-Menun, B.J., and Westermann, D.T. 2003. Organic phosphorus composition and potential bioavailability in semi-arid arable soils of the western United States. *Soil Sci. Soc. Am. J.* 67: 1168–1179.

Turner, B.L., McKelvie, I.D., and Haygarth, P.M. 2002. Characterization of water-extractable soil organic phosphorus by phosphatase hydrolysis. *Soil Biol. Biochem.* 34: 27–35.

Walker, T.W. and Adams, A.F.R. 1958. Studies on soil organic matter. I. Influence of phosphorus content of parent materials on accumulation of carbon, nitrogen, sulfur and organic phosphorus in grassland soils. *Soil Sci.* 85: 307–318.

Watanabe, F.S. and Olsen, S.R. 1965. Test of an ascorbic acid method for determining phosphorus in water and $NaHCO_3$ extracts from soil. *Soil Sci. Soc. Am. Proc.* 29: 677–678.

Williams, J.D.H., Syers, J.K., Walker, T.W., and Rex, R.W. 1970. A comparison of methods for the determination of soil organic phosphorus. *Soil Sci.* 110: 13–18.

Chapter 25
Characterization of Available P by Sequential Extraction

H. Tiessen
Inter-American Institute for Global Change Research
Sao Jose dos Campos, Sao Paulo, Brazil

J.O. Moir
University of Saskatchewan
Saskatoon, Saskatchewan, Canada

25.1 INTRODUCTION

Phosphate availability is a function of chemical equilibrium-controlled solubility and rate-limited processes. Most methods for available P determination attempt to quantify P solubility using different extractants, but few relate this to P supply rates that are relevant to plant uptake.

Soil test methods for P do not measure the quantity of P available to a crop, but extract a portion of soil P that is related to plant-available P. This relationship is usually established over years of agronomic experimentation and testing of fertilizer responses through regression equations. These equations relate plant performance to soil test P levels, or indicate fertilizer requirement for optimum crop production. Results obtained with this approach are not always transferable between crops or soil types, and different equations are established by soil testing services for varying crops and soils. The approach does not work when perennial plants or natural ecosystems are examined, because measurable pools are often small, and P cycling is the major determinant of P availability. Since any ''immediately available'' pool of P is constantly replenished through dissolution or desorption of ''less-available'' P, and through the mineralization of organic P, ''plant-available'' P is strongly time-dependent.

25.2 SOIL TEST METHODS FOR AVAILABLE P

Agronomic tests for available P are designed with several aims; they should:

1 Be simple enough for routine application.

2 Extract sufficient P to be easily measurable.

3 Extract P that represents a significant portion of potential plant uptake, so that plant supply is represented closely by the quantity measured rather than being dependent on P turnover and replenishment of the measured pool.

4 Not extract significant amounts of P that are not plant available over the growing period.

This is achieved with moderately acidic or alkaline solutions which release P associated with the soil mineral phase without solubilizing significant amounts of phosphatic minerals. Alternatively, or in combination with these pH changes, specific anions are introduced that bring P into solution by competing with P sorption sites or by lowering the solubility of cations that bind P in the soil. Based on these principles, numerous extraction methods exist, all of which have some merits and limitations and are used in various parts of the world, where their value relies on long-term correlation studies that establish the relationship between extractable P and crop response. An exhaustive review of extraction methods by a working group in Spain (Anon. 1982) listed 50 different methods and more than 50 publications comparing different extracts.

The most common methods are probably the alkaline bicarbonate method of Olsen et al. (1954) and the acid ammonium fluoride extraction (Bray and Kurtz 1945) with various modifications. An extraction using lactate (Egnér et al. 1960) is popular in Europe. The rationale for the use of bicarbonate or lactate for the extraction of available P is that plant roots produce CO_2 which forms bicarbonate in the soil solution as well as various organic acids similar to lactate that may solubilize soil P. It is proposed that these extractants somehow simulate the solubilizing action of plant roots and, thus, give a more appropriate measure of plant-available P. Chelating extracts (Onken et al. 1980) have been proposed for similar reasons. An advantage of chelating extracts is that the same extract can also be used for cation soil testing (micronutrients and K).

The bicarbonate extractant (Olsen et al. 1954) has been used successfully on a wide range of acid to alkaline soils. Available P is extracted with a solution of sodium bicarbonate of pH 8.5 for 30 min. Interference from organic matter dissolved in the solution has frequently been eliminated by sorbing the organic matter onto activated acid-washed charcoal (carbon black) added to the extract, but it is difficult to obtain P-free charcoal. An alternative was therefore developed which eliminates organic interference with polyacrylamide (Banderis et al. 1976). If organic matter content in the extract is low (as judged by its yellow coloring) a blank correction can be used. When the blue phosphomolybdate complex is measured at a wavelength of 712 nm, color interference from the yellow organic matter is negligible. However, using color correction with blanks will not work at high organic matter concentrations in the extract because the organic matter will precipitate upon acidification during the Murphy and Riley (1962) procedure and interfere with P colorimetry. The extraction time of 30 min has been designed for rapid routine soil testing. A more complete extraction is obtained by extracting for 16 h (Colwell 1963). For all applications that attempt to functionally evaluate the bicarbonate-extractable P pool, and that include organic P determination, the more complete 16 h extract should be used, because at 30 min the extraction is far from complete.

The acid ammonium fluoride extraction (Bray and Kurtz 1945) has been widely used on acid and neutral soils, and a large database exists. This is a purely chemical test that cannot be interpreted in terms of plant function like the bicarbonate or some of the organic acid or chelating extracts. Fluoride has been used to extract Al-associated P, but it is not obvious what the link to plant availability would be. In addition, Ca phosphates which are of low

plant availability in high-pH soils would be extracted by the acid and give excessive values for available P. The relatively low acid strength and importance of acidity for the extraction mechanism make the method unsuitable for calcareous or strongly alkaline soils, which would partially neutralize the acidity and eliminate the standard test conditions. However, buffered variations of this soil test have been reported to correlate well with bicarbonate-extracted P and plant response to P (van Lierop 1988; Soon 1990).

25.3 APPROACHES FOR CHARACTERIZING AVAILABLE P

Since available P is a functional concept rather than a measurable quantity, no simple direct measurements are available. Plant-available P is that P taken up by a plant during a specific period, such as a cropping season, year, or growth cycle. Since the plant obtains P from the soil solution through its roots or root symbionts, available P is composed of solution P plus P that enters the solution during the period used to define availability. Phosphorus may enter the solution by desorption or dissolution of inorganic P (P_i) associated with the soil's solid phase, or by the mineralization of organic P (P_o). In some dystrophic rain forests, P may not even cycle through the soil, but can be taken up directly from plant litter.

It is difficult to resolve whether desorption or dissolution replenishes solution P from P_i forms. In one case the solubility product of the least-soluble P compound, and in the other, the saturation of sorbent surfaces would determine the P supply at equilibrium. Countless publications have fitted theoretical equations to the reverse of these reactions—precipitation and adsorption. Empirical data usually fit either process to some degree (Syers and Curtin 1989). There is an increasing realization, though, that solid-phase P is not static, and that sorption–desorption and precipitation–dissolution equilibria change with time due to secondary processes (Parfitt et al. 1989) such as recrystallization (Barrow 1983) or solid-state diffusion (Willett et al. 1988). A measurement of available P_i therefore needs to consider both the amounts and rates of release of P from the solid phase. Very few appropriate methods have been published. Among the approaches taken are repeated water extracts and sorption–desorption isotherms (Fox and Kamprath 1970; Bache and Williams 1971), possibly at elevated temperatures to substitute for impractically long reaction times (Barrow and Shaw 1975).

A simple and more realistic approach is the use of anion-exchange resin, a sink for solution P_i. The resin offsets the equilibrium between dissolved and soluble P_i, and ''exchangeable'' P_i as well as some of the more soluble precipitated P forms will enter the depleted solution and be absorbed by the resin. The P sorbed by the resin is subsequently measured. Several different methods have been developed and tested, using different anionic forms, ratios of soil:water:resin, times and methods of shaking, and enclosure in bags or mixing through the suspension (Sibbesen 1977, 1978; Barrow and Shaw 1977). By far the simplest method uses polyester- or Teflon-based anion-exchange membranes, which can be cut into strips and used repeatedly and easily (Saggar et al. 1990; Schoenau and Huang 1991). These ion-exchange membranes have also been used *in situ*, inserted or buried in soil where they integrate processes of nutrient release and diffusion (to the membrane) over time (Qian and Schoenau 1997). When choosing resin membranes, it is important that the resin is part of the membrane material, i.e., cannot be abraded by the soil, and that they are resistant to the chemicals used in P extractions, such as dilute HCl or chloroform (if microbial P is to be measured). It also helps if they are stiff enough to be easily handled.

The pool measured by resin extraction is very similar to that assessed with isotopic dilution (Amer et al. 1955). The sorption by a resin is usually complete within 20 h, and only minor

changes are observed thereafter. Isotopic exchange also reaches a relatively constant state within a few hours, and the disappearance of isotope from the solution is used to estimate the size of the labile pool into which the isotope has been diluted. In a variation of the isotopic dilution method, carrier-free ^{32}P is added to a soil suspension, and the initial rapid removal of label is measured. This is followed by a determination of the continuing slow changes (Fardeau and Jappe 1980). These continuing changes represent the activity of less soluble or kinetically slower pools of soil P, which replenish available P at rates varying from days to years. On some soils with low or moderate P sorption, the continuing reduction in radioactivity in the liquid phase of the suspension has been extrapolated to times corresponding to seasons or longer with some success in estimating plant-available P. However, errors of extrapolation over long times can be large (Bühler et al. 2003; Chen et al. 2003). Phosphorus taking part in longer term transformations can be examined with sequential extractions, which first remove labile P, and then the more stable forms.

The sequential extraction method proposed by Chang and Jackson (1957) and modified by Williams et al. (1967) employs, sequentially, NH_4Cl to extract ''labile'' P_i, NH_4F to dissolve Al-associated P_i, NaOH to extract Fe-bound P_i, and dithionite–citrate to dissolve ''occluded'' P_i forms. A subsequent extraction with HCl dissolves Ca-bound P_i and the residue is analyzed by Na_2CO_3 fusion for residual total P. Alternatively, the residue can be analyzed for P_o by ignition plus acid extraction before the Na_2CO_3 fusion (Williams et al. 1967). As in all other methods of P_o determination, the amount of P_o is not measured directly but calculated by difference: acid-extractable P_i is subtracted from the greater amount of P_i rendered acid extractable after ignition of the soil organic matter (Saunders and Williams 1955) (see Chapter 24).

The procedure presented many interpretational problems: P_i can reprecipitate during the fluoride extraction, the separation of Al- and Fe-associated P_i is not reliable, and the reductant soluble or occluded P_i is an ill-defined pool (Williams and Walker 1969). However, the sequence of alkaline followed by acid extraction gives a reliable distinction between Al + Fe and Ca-associated P_i (Kurmies 1972). This distinction reflects the weathering stage of the soil and can be used to monitor the fate of rock phosphate fertilizer in weathered soils that contain little Ca-bound P. The P_o extracted by the procedure has usually been ignored although it was shown to be important in plant nutrition (Kelly et al. 1983).

An alternative P fractionation scheme was developed by Hedley et al. (1982a) building on the experience with previous extractions. This sequential extraction aims at quantifying labile (plant-available) P_i, Ca-associated P_i, Fe + Al-associated P_i, as well as labile and more stable forms of P_o. Labile P_i, i.e., P_i adsorbed on surfaces of sesquioxides or carbonates (Mattingly 1975), is extracted with resin and bicarbonate. Hydroxide-extractable P_i is less plant available (Marks 1977) and is thought to consist of amorphous and some crystalline Al and Fe phosphates. A more precise characterization of these P_i forms is unlikely to be possible since mixed compounds containing Ca, Al, Fe, P, and other ions predominate in soils (Sawhney 1973). Organic P extracted with bicarbonate is easily mineralizable and contributes to plant-available P (Bowman and Cole 1978). More stable forms of P_o are extracted with hydroxide (Batsula and Krivonosova 1973).

Each of the extracts obtained can be assigned some role in the P transformations occurring in soil under incubation (Hedley et al. 1982a) or cultivation (Tiessen et al. 1983), in the rhizosphere (Hedley et al. 1982b), or in soil development (Tiessen et al. 1984; Roberts et al. 1985; Schlesinger et al. 1998; Miller et al. 2001). These empirical assignments can then be used to characterize P status of the soil relative to a conceptual model of P pools and their transformations. Little has changed in the functional assignment or characteristics attributed

to those P extracts since the papers published in the 1980s, although some authors group fractions in ways that reveal interesting concepts on the function of the soil P cycle. Cross and Schlesinger (2001) group P_i and P_o fractions of the different extracts together reporting each extract's total P, and implying that the mode of stabilization is the most important characteristic, not necessarily the distinction between organic and inorganic forms. Soil mineralogy clearly affects the interpretation of P fractions. In semiarid, calcareous soils, Cross and Schlesinger (2001) identified acid-extractable P not only as true calcium phosphates but also as various associations of P with carbonates. To distinguish such fractions more clearly, Samadi and Gilkes (1998) added (among other modifications) an ammonium acetate extract before the acid extraction.

This fractionation approach is currently the only one that can be used with moderate success for the evaluation of available P_o. Cross and Schlesinger (1995) used the ratio of bicarbonate P_o to resin plus bicarbonate total P as an index for the bioavailability of P. This is probably only valid in temperate soils. Due to the reactivity of mineralized P with the soil's mineral phase, determination of a potentially mineralizable P_o pool, analogous to the mineralizable N or S pools measured with incubation and leaching techniques (Ellert and Bettany 1988), is not feasible. The nature of different extractable P_o pools is even less well defined than that of the P_i pools (Stewart and Tiessen 1987). Their turnover and availability frequently depend on the mineralization of C during which P is released as a side product, although solubilized P_o will be rapidly mineralized by soil enzymes. Most progress on understanding soil P_o has come from organic matter studies (Tiessen et al. 1983; Stewart and Tiessen 1987). It is often more appropriate to determine P in physical soil organic matter fractions, than to try and relate a chemically extracted P_o to biological function. Unless one has good reasons to believe that an extracted organic fraction can be biologically defined, it is probably best to group the organic fractions and use the sequential fractionation as a multiple extractant to obtain as much as possible of the soil's P_o.

The original fractionation (Hedley et al. 1982a) left between 20% and 60% of the soil's P unextracted. This residue often contained significant amounts of P_o that sometimes participated in relatively short-term transformations. On relatively young Ca-dominated soils, this residual P_o can be extracted by NaOH after the acid extraction, while on more weathered soils, hot HCl (Mehta et al. 1954) extracts most of the organic and inorganic residual P. The hot HCl method appears to work satisfactorily on most soils, and is presented below as part of an extensive soil P fractionation.

25.4 P FRACTIONATION PROCEDURE

25.4.1 Equipment and Materials

1. 50 mL centrifuge tubes with screw caps and refrigerated high-speed centrifuge
2. Shaker, preferably overhead type so that soils do not clump together in the round bottom of the centrifuge tubes
3. 0.45 μm membrane filter and filtration apparatus
4. Water bath
5. Block digester with 75 or 100 mL digestion tubes

6 Autoclave or household pressure cooker

7 Plastic vials for storing extracts

8 Whatman No. 40 filter paper (or equivalent)

25.4.2 Extracting Solutions

1 0.5 *M* HCl: dilute 88.5 mL conc. HCl to 2 L with deionized H_2O.

2 0.5 *M* $NaHCO_3$ (pH 8.5): dissolve 84 g $NaHCO_3$ + 1 g NaOH in deionized H_2O and make to 2 L.

3 0.1 *M* NaOH: dissolve 4 g NaOH in deionized H_2O and bring final volume to1 L.

4 1 *M* HCl: add 177 mL conc. HCl (11.3 *M*) to about 500 mL of deionized H_2O and bring to final volume of 2 L.

5 H_2O_2: 30% hydrogen peroxide.

6 Concentrated H_2SO_4 (18 *M*).

7 Resin strips: use anion-exchange membrane cut into strips (9 × 62 mm) and convert to bicarbonate form. To regenerate after the adsorbed P has been extracted with HCl, wash resin strips for 3 days with 6 batches of 0.5 *M* HCl, followed by washing a further 3 days with 6 batches of 0.5 *M* $NaHCO_3$ (pH 8.5). Then rinse well with deionized/distilled water.

25.4.3 Extraction Procedure

Day 1: Weigh 0.5 g soil into a 50 mL centrifuge tube, add 2 resin strips + 30 mL deionized water, and shake overnight (16 h, and 30 rpm if using overhead shaker). See comments below of fineness of grinding of soil samples.

Day 2: Remove resin strips and wash soil back into tube using deionized water. Place resin strip in a clean 50 mL tube, add 20 mL 0.5 *M* HCl. Set aside for 1 h to allow gas to escape, cap and shake overnight. Determine P using Murphy and Riley method (see section at top of p. 301). Centrifuge soil suspension at 25,000 *g* for 10 min at 0°C. Decant water through a 0.45 μm membrane filter. Discard water and wash any soil off filter back into the tube with a little 0.5 *M* $NaHCO_3$ (pH 8.5) solution. Add more $NaHCO_3$ solution to bring solution volume to 30 mL (by weighing) and shake suspension overnight (16 h). Cap the tubes and resuspend soil by handshaking before putting on mechanical shaker.

Day 3: Centrifuge soil suspension at 25,000 *g* for 10 min at 0°C. Decant $NaHCO_3$ extract through a membrane filter into a clean vial. Determine inorganic and total P on bicarbonate extract. Wash any soil off filter back into the tube using a little 0.1 *M* NaOH. Make volume of NaOH solution to 30 mL and shake suspension overnight (16 h).

Day 4: Centrifuge suspension at 25,000 *g* for 10 min at 0°C. Decant NaOH extract through a membrane filter into a clean vial. Determine inorganic and total P on NaOH extract. Wash any soil off filter back into the tube using a little 1 *M* HCl. Make volume of HCl to 30 mL and shake suspension overnight.

Day 5:

1 Centrifuge soil suspension at 25,000 *g* for 10 min at 0°C. Decant HCl extract through a membrane filter into a clean vial. Determine P in extract. (In this step, any residue that right be on the filter paper is not washed back into the tube; decant gently so as to not lose any soil.)

2 Soil residue heated with 10 mL conc. HCl in a waterbath at 80°C for 10 min. (Vortex to mix soil and HCl well and loosen caps before putting into the hot bath. The mixture will take about 10 min to come to temperature—check with a thermometer in a tube containing HCl only—i.e., the tubes will be in the hot water for a total of 20 min.) Remove and add a further 5 mL conc. HCl, vortex and allow to stand at room temperature for 1 h (vortex every 15 min). Tighten caps, centrifuge at 25,000 *g* for 10 min at 0°C, and decant supernatant into a 50 mL volumetric flask. Wash soil twice with 10 mL H_2O, centrifuge, and add supernatant solution to contents in the flask. Make to volume, and if necessary filter through a Whatman No. 40 paper (or equivalent), and determine inorganic and total P in HCl solution.

3 Add 10 mL deionized water to soil residue and disperse soil. Transfer suspension into 75 mL digestion tubes using the minimum amount of water possible to transfer all soil residues, add 5 mL conc. H_2SO_4 + one boiling chip (Hengar Granules, Hengar Co., Philadelphia, Cat. No. 136C), vortex and put on a cold digestion block. Raise the temperature very slowly to evaporate water and when 360°C is reached start treating with H_2O_2 in the following way: remove tubes from heat and let cool to hand-warm; add 0.5 mL of H_2O_2; reheat for 30 min, during which H_2O_2 is used up. Repeat H_2O_2 addition until liquid is clear (usually about 10 times). Make sure there is adequate heating after the final H_2O_2 addition, since residual H_2O_2 interferes with the P determination. Cool, make to volume, shake, and transfer to vials (either filter or allow residue to settle out overnight). Determine P in solution (see Section at top of p. 300). (This digestion is based on Thomas et al. 1967.)

25.4.4 Comments

1 The intensity of soil grinding greatly affects the amount of P extractable, particularly for the resin extraction which removes P from accessible surfaces. Interlaboratory testing has shown differences of an order of magnitude attributable to grinding between 2 mm screened and 60 mesh ground samples. The decision on how fine to grind should be based on a trade-off between sample homogeneity (important in a sample size of only 0.5 g) and preservation of the ''natural'' extractability of resin P. We have generally opted for moderate crushing of samples to 20 mesh.

2 Sequential extraction is a lengthy procedure. A batch of samples will take a week (including the weekend) to process. It is therefore important to reconcile the aim of the study with what this fractionation can produce. If geological transformations are the target, one can probably do without the resin and bicarbonate extracts; if labile pools are the target, the more resistant fractions may not be

important, and it would be more useful to include microbial P or organic matter separations. In many highly weathered soils, cold acid-soluble P is so little that it is probably a ''contaminant'' from the previous extract.

25.4.5 Analysis of P in Extracts

Reagents for P Determination

1 Ammonium molybdate: dissolve 40.0 g ammonium molybdate in deionized H_2O and bring to a final volume of 1 L.

2 Ascorbic acid: dissolve 26.4 g L-ascorbic acid in deionized H_2O and bring to a final volume of 0.5 L.

3 Antimony potassium tartrate: dissolve 1.454 g antimony potassium tartrate in deionized H_2O and bring to a final volume of 0.5 L.

4 2.5 *M* H_2SO_4: slowly add 278 mL conc. H_2SO_4 to 1 L of deionized H_2O and bring to a final volume of 2 L.

5 Color developing reagent: to 250 mL 2.5 *M* H_2SO_4, add 75 mL ammonium molybdate solution, then 50 mL ascorbate solution and finally 25 mL of antimony potassium tartrate solution. Swirl contents of flask after each addition. Dilute to a total volume of 500 mL with deionized H_2O and mix.

6 For organic matter precipitation and pH adjustment make up:

0.9 *M* H_2SO_4: bring 100 mL conc. H_2SO_4 to 2 L with H_2O.

0.25 *M* H_2SO_4: bring 100 mL 2.5 *M* H_2SO_4 to 1 L with H_2O.

4 *M* NaOH: dissolve 160 g NaOH and dilute to 1 L with H_2O.

7 *p*-nitrophenol, 10% (w/v), aqueous solution.

8 Ammonium persulfate, $(NH_4)_2S_2O_8$.

Determination of P Recovered from the Resin Strip and of P_i in HCl Extracts

This method (Murphy and Riley 1962) is used directly for the P recovered from the resin strip and for P_i determination in the two HCl extracts:

1 Pipette a suitable aliquot into a 50 mL volumetric flask. The calibration curve is linear for up to a concentration of about 1 mg of P L^{-1}. Use two drops of *p*-nitrophenol as an indicator. If the extract is acid, first adjust pH with 4 *M* NaOH to yellow and then with ~0.25 *M* H_2SO_4 until the indicator turns clear. For alkaline extracts, just acidify until solution is clear. Note that most analytical problems are related to the solution being adjusted too acid.

2 Add 8 mL of color developing solution, make to volume, shake and read on spectrophotometer at 712 nm after 10 min (color is stable for several hours).

Determination of Inorganic P in 0.5 *M* $NaHCO_3$ and 0.1 *M* NaOH Extracts

1 Pipette 10 mL solution into a 50 mL centrifuge tube.

2 Acidify to pH 1.5 and set in fridge for 30 min:

(a) to acidify 0.5 *M* $NaHCO_3$ extract use: 6 mL of 0.9 *M* H_2SO_4;

(b) to acidify 0.1 *M* NaOH extract use: 1.6 mL of 0.9 *M* H_2SO_4.

3 Centrifuge at 25,000 *g* for 10 min at 0°C.

4 Decant supernatant into a 50 mL volumetric flask.

5 Rinse tube carefully so as not to disturb the organic matter with a little acidified water and add to the solution in the flask (2 or 3 times).

6 Adjust pH and measure P by the Murphy and Riley method (see section at bottom of p. 300).

Determination of Total P in 0.5 *M* $NaHCO_3$, 0.1 *M* NaOH, and Conc. HCl Extracts (EPA 1971)

Dissolved organic matter is oxidized with ammonium persulfate before P analysis:

1 Pipette 5 mL solution into a 50 mL volumetric flask.

2 To 0.5 *M* $NaHCO_3$ extract: add ~0.5 g ammonium persulfate + 10 mL 0.9 *M* H_2SO_4.

(a) To 0.1 *M* NaOH extract: add ~0.6 g ammonium persulfate + 10 ml 0.9 *M* H_2SO_4.

(b) To conc. HCl extract: add ~0.4 g ammonium persulfate + 10 mL deionized water.

The persulfate may be added by volume using a spatula with a spoon at one end rather than weighing every time.

3 Cover with tinfoil (double layer for conc. HCl) and autoclave:

$NaHCO_3$ and HCl extracts for 60 min, NaOH extract for 90 min. (Instead of an autoclave, a household pressure cooker can also be used.)

4 Adjust pH and measure P by the Murphy and Riley method (see section at top of p. 300).

25.4.6 Comments

1 The aliquot size of extract for the Murphy and Riley procedure may vary from 1 mL for high P concentration acid extracts up to 40 mL in the case of very low P resin extracts.

2 Most times when things go wrong, it is due to interferences in the Murphy and Riley colorimetry. Insufficient pH control before color development is the most common problem with color development. Residual oxidant from one of the digestion steps will of course interfere with the reduction step of the color development. In some soils, we have seen interference from soluble silica in the reacidified NaOH extract, resulting in a positive drift (i.e., increase) in absorbance. This interference is difficult to manage if it occurs. Very consistent absorbance reading at exactly 10 min helps but results will remain doubtful.

25.5 INTERPRETATION AND LIMITATIONS

The interpretation of data obtained from this sequential fractionation is based on an understanding of the action of the individual extractants, their sequence (Figure 25.1), and their relationship to the chemical and biological properties of the soil. It must be remembered that, while the fractionation is an attempt to separate P pools according to their lability, any chemical fractionation can at best only approximate biological functions. Resin P is reasonably well defined as freely exchangeable P_i, since the resin extract does not chemically modify the soil solution. Bicarbonate extracts a P_i fraction, which is likely to be plant available, since the chemical changes introduced are minor and somewhat representative of root action (respiration). This fraction is not comparable to the widely used fertility test

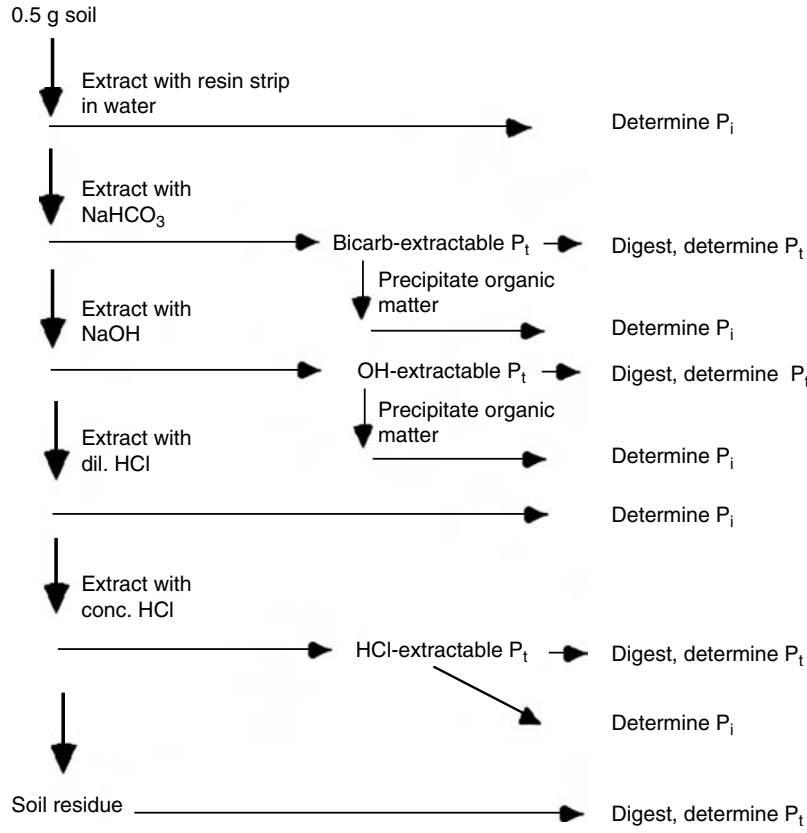

FIGURE 25.1. Flow chart of the sequential P extraction.

(Olsen et al. 1954) because the resin-extractable pool has already been removed at this point and because Olsen P is extracted over only 30 min.

Bicarbonate-P_i and OH-P_i are not really completely separate pools, particularly in acid soils, but represent a continuum of Fe- and Al-associated P extractable with increasing pH (the soils original pH to 8.5 to 13). The P_o extracted with these two extractants is also likely to represent similar pools. Since P_o is determined by difference between total P (P_t) and P_i in each extract, there is a source of error. The P_t determination is quite reliable, but P_i is determined in the supernatant after precipitation of organic matter with acid. Any nonprecipitated P_o (fulvic acid P) will not significantly react with the Murphy and Riley reagent, so that P_i is rarely overestimated. Any P_i, though, that precipitates along with the organic matter upon acidification would be erroneously determined as P_o ($P_t - P_i$). This may happen with P_i associated with Fe or Al hydroxides, which are soluble at high pH but insoluble at low pH. It has so far been impossible to quantify the P_o overestimation. In soils with low-extractable organic matter contents (low enough not to cause precipitation in the acid Murphy and Riley reagent), it is possible to determine P_i in the extract without prior acid precipitation using a blank correction for the extracts' color.

The dilute HCl P_i is clearly defined as Ca-associated P, since Fe- or Al-associated P that might remain unextracted after the NaOH extraction is insoluble in acid. There is rarely any P_o in this extract. Dilute acid is well known to be inefficient in extracting organic carbon from soils, and therefore, does not extract much P_o.

The hot concentrated HCl extract does not present the same problems as the other P_o extracts, since P_i is determined directly. This extract is useful for distinguishing P_i and P_o in very stable residual pools. However, at the same time, P_o extracted at this step may simply come from particulate organic matter that is not alkali extractable but may be easily bioavailable. Any P protected by cellulosic structure would be biologically available as a byproduct of cellulose breakdown, but would only become extractable in the hot concentrated acid step. The residue left after the hot concentrated HCl extraction is unlikely to contain anything but highly recalcitrant P_i.

It is important to remember that this sequential extraction does not provide direct measures of biologically or geochemically important P pools. It provides circumstantial evidence that is more valuable if it can be corroborated by other methods such as isotope or organic matter studies. Particularly, for a reliable interpretation of P_o transformations, it is advisable to supplement the fractionation with a suitable characterization of soil organic matter, so that characteristics can be inferred from the combined results of different techniques.

REFERENCES

Amer, F., Bouldin, D.R., Black, C.A., and Duke, F.R. 1955. Characterization of soil phosphorus by anion exchange resin adsorption and ^{32}P equilibration. *Plant Soil* 6: 391–408.

Anon. 1982. Groupo de trabajo de normalisacion de metodos analiticos. Revision bibliografica de metodos de extraction de phosphoro assimilable en suelos 1957–1980. *Anales de Edafologia y Agrobiologia* 41: 1085–1112.

Bache, B.W. and Williams, E.G. 1971. A phosphate sorption index for soils. *J. Soil Sci.* 22: 289–301.

Banderis, A.S., Barter, D.H., and Henderson, K. 1976. The use of polyacrylamide to replace

carbon in the determination of Olsen's extractable phosphate in soil. *J. Soil Sci.* 27: 71–74.

Barrow, N.J. 1983. On the reversibility of phosphate sorption by soils. *J. Soil Sci.* 34: 751–758.

Barrow, N.J. and Shaw, T.C. 1975. The slow reactions between soil and anions. 2. Effect of time and temperature on the decrease in phosphate concentration in the soil solution. *Soil Sci.* 119: 167–177.

Barrow, N.J. and Shaw, T.C. 1977. Factors affecting the amount of phosphate extracted from soil by anion exchange resin. *Geoderma* 18: 309–323.

Batsula, A.A. and Krivonosova, G.M. 1973. Phosphorus in the humic and fulvic acids of some Ukrainian soils. *Soviet Soil Sci.* 5: 347–350.

Bowman, R.A. and Cole, C.V. 1978. Transformations of organic phosphorus substances in soils as evaluated by $NaHCO_3$ extraction. *Soil Sci.* 125: 49–54.

Bray, R.H. and Kurtz, L.T. 1945. Determination of total, organic and available forms of phosphorus in soils. *Soil Sci.* 59: 39–45.

Bühler, S., Oberson, A., Sinaj, S., Friesen, D.K., and Frossard, E. 2003. Isotope methods for assessing plant-available phosphorus in acid tropical soils. *Eur. J. Soil Sci.* 54: 605–616.

Chang, S.C. and Jackson, M.L. 1957. Fractionation of soil phosphorus. *Soil Sci.* 84: 133–144.

Chen, C.R., Sinaj, S., Condron, L.M., Frossard, E., Sherlock, R.R., and Davis, M.R. 2003. Characterization of phosphorus availability in selected New Zealand grassland soils. *Nutr. Cycl. Agroecosys.* 65: 89–100.

Colwell, J.D. 1963. The estimation of the phosphorus fertilizer requirement of wheat in southern New South Wales by soil analysis. A*ust. J. Exp. Agric. Anim. Husb.* 3: 190–197.

Cross, A.F. and Schlesinger, W.H. 1995. A literature review and evaluation of the Hedley fractionation: applications to the biogeochemical cycle of soil phosphorus in natural ecosystems. *Geoderma* 64: 197–214.

Cross, A.F. and Schlesinger, W.H. 2001. Biological and geochemical controls on phosphorus fractions in semiarid soils. *Biogeochemistry* 52: 155–172.

Egnér, H., Riehm, H., and Domingo, W.R. 1960. Untersuchungen über die chemische Bodenanalyse als Grundlage für die Beurteilung des Nährstoffzustandes der Böden. 2. Chemische Extraktionsmethoden zur Phosphor- und Kaliumbestimmung. Kungl. *Landbrukshögskolans Annaler, Uppsala, Sweden* 26: 199–215.

Ellert, B.H. and Bettany, J.R. 1988. Comparisons of kinetic models for describing net sulfur and nitrogen mineralization. *Soil Sci. Soc. Am. J.* 52: 1692–1702.

EPA 1971. *Methods of Chemical Analysis for Water and Wastes*. Environmental Protection Agency, Cincinnati, OH.

Fardeau, J.C. and Jappe, J. 1980. Choix de la fertilisation phosphorique des sols tropicaux: emploi du phosphore 32. *Agron. Trop.* 35: 225–231.

Fox, R.L. and Kamprath, E.J. 1970. Phosphate sorption isotherms for evaluating the phosphate requirements of soils. *Soil Sci. Soc. Am. Proc.* 34: 902–907.

Hedley, M.J., Stewart, J.W.B., and Chauhan, B.S. 1982a. Changes in inorganic and organic soil phosphorus fractions induced by cultivation practices and by laboratory incubations. *Soil Sci. Soc. Am. J.* 46: 970–976.

Hedley, M.J., White, R.E., and Nye, P.H. 1982b. Plant-induced changes in the rhizosphere of rape seedlings. III. Changes in L-value, soil phosphate fractions and phosphatase activity. *New Phytol.* 91: 45–56.

Kelly, J., Lambert, M.J., and Turner, J. 1983. Available phosphorus forms in forest soils and their possible ecological significance. *Commun. Soil Sci. Plant Anal.* 14: 1217–1234.

Kurmies, B. 1972. Zur Fraktionierung der Bodenphosphate. *Die Phosphorsäure* 29: 118–151.

Marks, G. 1977. Beitrag zur präzisierten Charakterisierung von pflanzen-verfügbarem Phosphat in Ackerböden. *Arch. Acker Pflanzenbau Bodenkd.* 21: 447–456.

Mattingly, G.E.G. 1975. Labile phosphate in soils. *Soil Sci.* 119: 369–375.

Mehta, N.C., Legg, J.O., Goring, C.A.I., and Black, C.A. 1954. Determination of organic phosphorus

in soils: I. Extraction method. *Soil Sci. Soc. Am. Proc*. 18: 443–449.

Miller, A.J., Schuur, E.A.G., and Chadwick, O.A. 2001. Redox control of phosphorus pools in Hawaiian montane forest soils. *Geoderma* 102: 219–237.

Murphy, J. and Riley, J.P. 1962. A modified single solution method for the determination of phosphate in natural waters. *Anal. Chim. Acta* 27: 31–36.

Olsen, S.R., Cole, C.V., Watanabe, F.S., and Dean, L.A. 1954. *Estimation of available phosphorus in soils by extraction with sodium bicarbonate*. U.S. Department of Agriculture Circular 939, USDA, Washington, DC.

Onken, A.B., Matheson, R., and Williams, E.J. 1980. Evaluation of EDTA-extractable P as a soil test procedure. *Soil Sci. Soc. Am. J*. 44: 783–786.

Parfitt, R.L., Hume, L.J., and Sparling, G.P. 1989. Loss of availability of phosphate in New Zealand soils. *J. Soil Sci*. 40: 371–382.

Qian, P. and Schoenau, J.J. 1997. Recent developments in use of ion exchange membranes in agricultural and environmental research. *Recent Res. Devel. Soil Sci*. 1: 43–54.

Roberts, T.L., Stewart, J.W.B., and Bettany, J.R. 1985. The influence of topography on the distribution of organic and inorganic soil phosphorus across a narrow environmental gradient. *Can. J. Soil Sci*. 65: 651–665.

Saggar, S., Hedley, M.J., and White, R.E. 1990. A simplified resin membrane technique for extracting phosphorus from soils. *Fert. Res*. 24: 173–180.

Samadi, A. and Gilkes, R.J. 1998. Forms of phosphorus in virgin and fertilized calcareous soils of Western Australia. *Aust. J. Soil Res*. 36: 585–601.

Saunders, W.M.H. and Williams, E.G. 1955. Observations on the determination of total organic phosphorus in soils. *J. Soil Sci*. 6: 254–267.

Sawhney, B.L. 1973. Electron microprobe analysis of phosphates in soils and sediments. *Soil Sci. Soc. Am. Proc*. 37: 658–660.

Schlesinger, W.H., Bruijnzeel, L.A., Bush, M.B., Klein, E.M., Mace, K.A., Raikes, J.A., and Whittaker, R.J. 1998. The biogeochemistry of phosphorus after the first century of soil development on Rakata Island, Krakatau, Indonesia. *Biogeochemistry* 40: 37–55.

Schoenau, J.J. and Huang, W.Z. 1991. Anion-exchange membrane, water, and sodium bicarbonate extractions as soil tests for phosphorus. *Commun. Soil Sci. Plant Anal*. 22: 465–492.

Sibbesen, E. 1977. An investigation of the anion exchange resin method for soil phosphate extraction. *Plant Soil* 46: 665–669.

Sibbesen, E. 1978. A simple ion exchange resin procedure for extracting plant available elements from soil. *Plant Soil* 50: 305–321.

Soon, Y.K. 1990. Comparison of parameters of soil phosphate availability for the northwestern Canadian prairie. *Can. J. Soil Sci*. 70: 222–237.

Stewart, J.W.B. and Tiessen, H. 1987. Dynamics of soil organic phosphorus. *Biogeochemistry* 4: 41–60.

Syers, J.K. and Curtin, D. 1989. Inorganic reactions controlling phosphorus cycling. In H. Tiessen, Ed. *P Cycles in Terrestrial and Aquatic Ecosystems. Regional Workshop 1*. Proceedings of a Workshop by the Scientific Committee on Problems of Environment (SCOPE). University of Saskatchewan, Saskatoon, SK, Canada, pp. 17–29.

Thomas, R.L., Sheard, R.W., and Moyer, J.R. 1967. Comparison of conventional and automated procedures for nitrogen, phosphorus, and potassium analysis of plant material using a single digestion. *Agron. J*. 59: 240–243.

Tiessen, H., Stewart, J.W.B., and Cole, C.V. 1984. Pathways of phosphorus transformations in soils of differing pedogenesis. *Soil Sci. Soc. Am. J*. 48: 853–858.

Tiessen, H., Stewart, J.W.B., and Moir, J.O. 1983. Changes in organic and inorganic phosphorus composition of two grassland soils and their particle size fractions during 60–70 years of cultivation. *J. Soil Sci*. 34: 815–823.

van Lierop, W. 1988. Determination of available phosphorus in acid and calcareous soils with the Kelowna multiple-element extractant. *Soil Sci*. 146: 284–291.

Willett, I.R., Chartres, C.J., and Nguyen, T.T. 1988. Migration of phosphate into aggregated particles of ferrihydrite. *J. Soil Sci*. 39: 275–282.

Williams, J.D.H., Syers, J.K., and Walker, T.W. 1967. Fractionation of soil inorganic phosphate by a modification of Chang and Jackson's procedure. *Soil Sci. Soc. Am. Proc*. 31: 736–739.

Williams, J.D.H. and Walker, T.W. 1969. Fractionation of phosphate in a maturity sequence of New Zealand basaltic soil profiles. *Soil Sci*. 107: 22–30.

Chapter 26
Extractable Al, Fe, Mn, and Si

F. Courchesne and M.-C. Turmel
University of Montreal
Montreal, Quebec, Canada

26.1 INTRODUCTION

The dissolution methods for extracting Al, Fe, Mn, and Si are valuable tools to help determine the chemical forms of these elements in soils. The results are useful in studies of soil classification, soil genesis, soil reactivity, and metal mobility or bioavailability in soils. For example, the nature and amounts of extractable organic and inorganic Al and Fe may reflect the pathway of soil genesis. Also, extractable soil constituents are generally fine grained with large specific surface area and therefore, have a marked effect on physical and chemical soil properties and behavior. For these reasons, extraction data, notably for Al and Fe, are commonly used as chemical criteria for soil classification. Moreover, extractions are often performed to establish the mechanisms of metal retention and fractionation in contaminated soils. A variety of chemical extractants are used to approximate the amounts and forms of Al, Fe, Mn, and Si in soils. Five of the most commonly used extractions are discussed here and four methods are presented.

Dithionite–citrate removes organically complexed Al, Fe, and Mn, amorphous inorganic Al, Fe, and Mn compounds, noncrystalline aluminosilicates as well as finely divided hematite, goethite, lepidocrocite, and ferrihydrite (Mehra and Jackson 1960; Guest et al. 2002). It is much less effective in removing crystalline oxides and hydroxides of Al. The method extracts virtually no Al, Fe, Mn, or Si from most crystalline silicate minerals or opal, and thus, provides an estimate of ''free'' (nonsilicate) Fe in soils. The procedure may have to be repeated to dissolve silt- and sand-size goethite and hematite completely (Kodama and Ross 1991). Magnetite is not dissolved. Ross and Wang (1993) indicated that coefficients of variation at Fe levels of 1.4% and Al levels of 0.45% are 6.3% and 7.8%, respectively.

Acid ammonium oxalate removes organically complexed and amorphous inorganic forms of Al, Fe and, to a lesser extent, Mn and noncrystalline aluminosilicates from soils (McKeague 1967). It also dissolves poorly ordered phases like allophane and imogolite to some extent and their amount in soils can be estimated from oxalate-extractable Al and Si concentrations, taking into account that oxalate also extracts organically complexed Al (Parfitt and Henmi 1982). Oxalate only slightly attacks crystalline Al and Fe oxides, most crystalline silicate minerals, opal, goethite, hematite, and lepidocrocite, but it dissolves considerable amounts of

magnetite (Baril and Bitton 1967) and of finely divided, easily weathered silicates, such as olivine. Ross and Wang (1993) indicated that coefficients of variation at Fe levels of 0.67% and Al levels of 0.67% are 7.2% and 4.1%, respectively.

Hydroxylamine is closely similar to oxalate in its extraction capacity (Chao and Zhou 1983). It is also commonly used to extract soil Mn. Unlike ammonium oxalate, however, hydroxylamine does not dissolve magnetite and can therefore be used as an alternative to ammonium oxalate for soils containing magnetite (Ross et al. 1985). Ross and Wang (1993) indicated that the coefficients of variation at Fe levels of 0.63% and Al levels of 0.62% are 4.5% and 3.0%, respectively.

Tiron, 4,5-dihydroxy-1,3-benzene-disulfonic acid (disodium salt), does not dissolve magnetite either and its use has been suggested instead of oxalate (Kodama and Ross 1991). Furthermore, Tiron dissolves pedogenic opaline silica (Kendrick and Graham 2004), whereas, neither oxalate nor hydroxylamine dissolves this soil component effectively. Tiron is currently used mainly to remove coatings on clays (Ross and Wang 1993). However, it should also be suitable for soils ground to pass a 0.15 mm (100-mesh) sieve.

Sodium pyrophosphate extracts organically complexed Al and Fe from soils. Manganese compounds are also dissolved. It only slightly dissolves noncrystalline inorganic forms, and it does not significantly attack silicate minerals and crystalline Al and Fe oxides or hydroxides (McKeague et al. 1971). The pyrophosphate solution does not dissolve opal and is a poor extractant for allophane or imogolite (Wada 1989). Ross and Wang (1993) indicated that the coefficients of variation at Fe levels of 0.64% and Al levels of 0.69% are 5.9% and 6.0%, respectively. The specificity of the method for organic complexes of Al and Fe has been challenged because amorphous and poorly ordered inorganic Al and Fe solid phases were found to be significantly removed by the pyrophosphate extract (Kaiser and Zech 1996).

From the results of these methods, the following quantities can be estimated:

A. Finely divided crystalline Fe solid phases like goethite, hematite, and lepidocrocite: dithionite Fe–oxalate Fe or dithionite Fe–hydroxylamine Fe or dithionite Fe–Tiron Fe

B. Noncrystalline inorganic forms of Fe including ferrihydrite: oxalate Fe–pyrophosphate Fe or hydroxylamine Fe–pyrophosphate Fe or Tiron Fe–pyrophosphate Fe

C. Organic complexed Fe: pyrophosphate Fe

Relationships B and C also hold approximately for Al; this is not the case for relationship A. In the case of Mn, both dithionite and oxalate attack crystalline oxide forms to some extent and differences between extracts are not easy to interpret. The noncrystalline forms of Si, such as opaline silica, are completely extracted only by Tiron (Kodama and Ross 1991). They are not extracted by oxalate and only partly by dithionite and hydroxylamine. Poorly crystalline and noncrystalline aluminosilicates, including allophane and imogolite, are extracted by oxalate, hydroxylamine, and Tiron. Dithionite and pyrophosphate are much less effective in extracting these compounds.

A survey of the literature on the extraction of Al, Fe, Mn, and Si from soils clearly shows that the laboratory procedures employed vary considerably among extractions and between

studies. Yet, results from different extractions are frequently compared in studies on soil genesis and metal fractionation. Moreover, the effects of the grinding of soil samples and of the filtration of extracts on the amounts of Al, Fe, Mn, or Si extracted are documented (Loveland and Digby 1984; Neary and Barnes 1993). The reduction of particle size by grinding is nonetheless necessary when weighing out small subsamples because it increases the homogeneity between subsamples and, thus, the repeatability of the extraction. In this context, and because of the operational character of the extraction schemes, investigators are strongly encouraged to report the procedures they used, notably, with respect to the preparation of soil samples (sieving, grinding) and to the centrifugation (*g* force) or the filtration of extracts (type of membrane, pore size). In the methods proposed here, all the samples are ground to 0.15 mm.

26.2 DITHIONITE–CITRATE METHOD (SOIL CONSERVATION SERVICE, U.S. DEPARTMENT OF AGRICULTURE 1972)

The dithionite–citrate method consists of shaking soils overnight in the presence of a reducing and complexing solution. Dithionite creates a reducing environment and dissolves metallic oxides whereas the Na-citrate chelates the dissolved metals and buffers the pH to near 7 to avoid the precipitation of FeS compounds. This treatment is particularly useful for dissolving the ''free'' Fe in soils. Caution must however be exercised when interpreting extracted Al. The overnight shaking procedure is simpler than the dithionite–citrate–bicarbonate method of Mehra and Jackson (1960), and it gives closely similar results (Sheldrick and McKeague 1975). This extractant is used in the Canadian System of Soil Classification (Soil Classification Working Group 1998) for describing Fe accumulation in Gleysols.

26.2.1 Reagents

1 Sodium hydrosulfite (dithionite), $Na_2S_2O_4$

2 Sodium citrate ($Na_3C_6H_5O_7 \cdot 2H_2O$), 0.68 *M* (200 g L^{-1})

3 Certified atomic absorption standards, ±1%

26.2.2 Procedure

1 Weigh 0.500 g of <2 mm air-dry soil, ground to pass a 0.15 mm (100 mesh) sieve, into a 50 mL screw-cap plastic centrifuge tube (use 0.2 g for clays and 1 g for coarse soils).

2 Add 25 mL of the sodium citrate solution.

3 Add about 0.4 g of dithionite (a calibrated scoop may be used).

4 Stopper tightly and shake overnight (16 h) in an end-over-end shaker. A horizontal shaker can also be used although interparticle abrasion can be increased.

5 Remove stoppers and centrifuge for 20 min at 510 *g* (centrifuge at higher speed for samples rich in clay particles). Filter extracts containing suspended materials.

6 For determining Al, Fe, Mn, and Si by atomic absorption spectroscopy (AAS), prepare standard solutions of these elements containing the same concentration of extracting solution, here Na-citrate with dithionite, as the extracting solution. Gently heat the solution to dissolve dithionite. Note that at high concentration, the precipitation of dithionite can rapidly block the AAS burner. The amount of dithionite added to standard solutions can be lowered to reduce this effect.

7 An air–acetylene flame is suitable for the determination of Fe and Mn, and a nitrous oxide–acetylene flame is used for Al and Si.

8 If it is necessary to dilute the extracts, either dilute them with the extracting solution or prepare standards containing the same concentration of extracting solution as the diluted extracts.

26.2.3 Calculations

1 $$\%\ \text{Fe, Al, Mn, Si} = \frac{\mu\text{g mL}^{-1}\ \text{in final solution} \times \text{extractant (mL)} \times \text{dilution}}{\text{sample weight (g)} \times 10{,}000} \qquad (26.1)$$

2 For example, for 0.500 g of sample, 25 mL of extractant, 5 times dilution, and a 48 μg Fe mL^{-1} concentration:

$$\%\ \text{Fe in sample} = \frac{48 \times 25 \times 5}{0.500 \times 10{,}000} = 1.2 \qquad (26.2)$$

26.3 ACID AMMONIUM OXALATE METHOD (IN THE DARK) (MCKEAGUE AND DAY 1966)

The acid NH_4-oxalate method was developed in 1922 by Tamm to remove the sesquioxide weathering products from soils. It was revised by Schwertmann (1959), who showed that it could estimate noncrystalline and poorly ordered Al and Fe forms in soils. It extracts the amorphous Al and Fe accumulated in podzolic B horizons (McKeague and Day 1966) and is thus useful to identify podzolic B horizons. Oxalate also dissolves allophane and imogolite (Wada 1989). In the soil taxonomy, amounts of Al and Fe extracted with oxalate are criteria for andic soil properties (Soil Survey Staff 1990). The extraction must be conducted in the dark to prevent photodecomposition of the oxalate solution.

26.3.1 Reagents

1 Solution A: Ammonium oxalate solution $(NH_4)_2C_2O_4 \cdot H_2O$, 0.2 *M* (28.3 g L^{-1}).

2 Solution B: Oxalic acid solution $H_2C_2O_4 \cdot 2H_2O$, 0.2 *M* (25.2 g L^{-1}).

3 Mix 700 mL of A and 535 mL of B, check pH, and adjust to 3.0 by adding A or B.

4 Certified atomic absorption standards, ±1%.

26.3.2 Procedure

1 Weigh 0.250 g of <2 mm air-dry soil, ground to pass a 0.15 mm (100 mesh) sieve, into a 15 mL screw-cap plastic centrifuge tube (weigh 0.125 g for samples with >2% extractable Fe or Al).

2 Add 10 mL of the acid ammonium oxalate solution and stopper the tube tightly.

3 Place the tubes in an end-over-end shaker and shake for 4 h in the dark. A horizontal shaker can also be used although interparticle abrasion can be increased.

4 Centrifuge the tubes for 20 min at 510 *g* (centrifuge at higher speed for samples rich in clay particles), decant the clear supernatant into a suitable container, and analyze within a few days. Extracts should be stored in the dark to avoid the photoinduced degradation of oxalate and the subsequent precipitation of dissolved metals.

5 For determining Al, Fe, Mn, and Si by atomic absorption, follow standard atomic absorption procedures. Consider the points mentioned in Section 26.2.2.

26.3.3 Calculations

1 $$\%\ \text{Fe, Al, Mn, Si} = \frac{\mu\text{g mL}^{-1}\ \text{in final solution} \times \text{extractant (mL)} \times \text{dilution}}{\text{sample weight (g)} \times 10{,}000} \qquad (26.3)$$

2 For example, for 0.250 g of sample, 10 mL of extractant, 5 times dilution, and a 12 μg Fe mL^{-1} concentration:

$$\%\ \text{Fe in sample} = \frac{12 \times 10 \times 5}{0.250 \times 10{,}000} = 0.24 \qquad (26.4)$$

26.4 ACID HYDROXYLAMINE METHOD (ROSS ET AL. 1985; WANG ET AL. 1987)

The acid hydroxylamine extraction is used in geochemical studies for removing noncrystalline material, notably hydrous Mn oxides, from crystalline Fe oxides with minimal dissolution of associated Fe oxides like magnetite (Chao and Zhou 1983). Ross et al. (1985) and Wang et al. (1987) modified this procedure and tested it on soil samples. For Al and Fe, the results were similar to those obtained by oxalate extraction with the advantage that hydroxylamine did not dissolve magnetite. There was less agreement between the Si results obtained by the two methods. The suitability of hydroxylamine as an extractant for Mn in soils has not been fully tested yet. Hydroxylamine solutions are also more easily analyzed than oxalate solutions by AAS because the latter tend to clog the burner.

26.4.1 Reagents

1 Prepare a hydroxylamine hydrochloride–hydrochloric acid (0.25 *M* $NH_2OH \cdot HCl$, 0.25 *M* HCl) solution by adding 21.5 mL of concentrated HCl and 17.37 g of $NH_2OH \cdot HCl$ to a 1 L volumetric flask and making to volume with deionized water.

2 Certified atomic absorption standards, ±1%.

26.4.2 Procedure

1 Weigh 0.100 g of <2 mm air-dry soil, ground to pass a 0.15 mm (100 mesh) sieve, into a 50 mL screw-cap plastic centrifuge tube.

2 Add 25 mL of the hydroxylamine solution and stopper the tube tightly.

3 Place the tubes in an end-over-end shaker and shake overnight (16 h). A horizontal shaker can also be used although interparticle abrasion can be increased.

4 Centrifuge the tubes for 20 min at 510 *g* (centrifuge at higher speed for samples rich in clay particles), decant the clear supernatant into a suitable container, and analyze within a few days.

5 For determining Al, Fe, Mn, and Si by atomic absorption, follow standard atomic absorption procedures. Consider the points mentioned in Section 26.2.2.

26.4.3 Calculations

1 $$\%\ \text{Fe, Al, Mn, Si} = \frac{\mu\text{g mL}^{-1}\ \text{in final solution} \times \text{extractant (mL)} \times \text{dilution}}{\text{sample weight (g)} \times 10{,}000} \qquad (26.5)$$

2 For example, for 0.100 g of sample, 25 mL of extractant, 5 times dilution, and a 6 μg Fe mL^{-1} concentration:

$$\%\ \text{Fe in sample} = \frac{6 \times 25 \times 5}{0.100 \times 10{,}000} = 0.75 \qquad (26.6)$$

26.5 SODIUM PYROPHOSPHATE METHOD (MCKEAGUE 1967)

Sodium pyrophosphate is a common extractant for Al, Fe, and Mn associated with soil organic matter. It does not extract opal or crystalline silicates. The method is used in the Canadian System of Soil Classification as chemical criteria for identifying podzolic B horizons, in the soil taxonomy for spodic horizons and by the FAO for classifying podzolic soils (Soil Survey Staff 1990; FAO 1990; Soil Classification Working Group 1998). The pyrophosphate extraction is strongly dependent on the centrifugation and filtration procedures because, in some cases, finely divided colloidal silicates and oxides remain dispersed after low-speed centrifugation. High-speed centrifugation or ultrafiltration is then necessary to clear the extracts (McKeague and Schuppli 1982; Schuppli et al. 1983).

26.5.1 Reagents

1 Sodium pyrophosphate solution ($Na_4P_2O_7 \cdot 10H_2O$), 0.1 *M* (44.6 g L^{-1}).

2 Superfloc (N-100) 0.1% (1.0 g L^{-1}). Available from Cytec Canada Inc., 7900 Taschereau Bld, A-106 Suite, Brossard, Que., J4X 1C2.

3 Certified atomic absorption standards, ±1%.

26.5.2 Procedure

1 Weigh 0.300 g of <2 mm air-dry soil, ground to pass a 0.15 mm (100 mesh) sieve, into a 50 mL screw-cap plastic centrifuge tube (use 1 g for samples low in extractable Fe and Al).

2 Add 30 mL of sodium pyrophosphate solution and stopper the tube tightly.

3 Shake overnight (16 h) in an end-over-end shaker. A horizontal shaker can also be used although interparticle abrasion can be increased.

4 Centrifuge at 20,000 *g* for 10 min or, alternatively, add 0.5 mL of 0.1% superfloc solution and centrifuge at 510 *g* for 10 min. Note the following points:

   a. Concentrations of Fe and Al in sodium pyrophosphate extracts of some samples may decrease progressively by centrifugation for longer times or at higher speeds.

   b. Ultrafiltration through a 0.025 μm Millipore filter is recommended for tropical soils and for samples giving questionable results by the centrifugation methods.

5 Decant a portion of the clear supernatant into a suitable container and analyze within a few days. Extracts containing suspended materials should be filtered.

6 For determining Al, Fe, and Mn by atomic absorption, follow standard atomic absorption procedures. Consider the points mentioned in Section 26.2.2.

26.5.3 Calculations

1 $$\%\ \text{Fe, Al, Mn} = \frac{\mu\text{g mL}^{-1}\ \text{in final solution} \times \text{extractant (mL)}}{\text{sample weight (g)} \times 10{,}000} \tag{26.7}$$

2 For example, for 0.300 g of sample, 30 mL of extractant, and a 75 μg Fe mL^{-1} concentration:

$$\%\ \text{Fe in sample} = \frac{75 \times 30}{0.300 \times 10{,}000} = 0.75 \tag{26.8}$$

REFERENCES

Baril, R. and Bitton, G. 1967. Anomalous values of free iron in some Quebec soils containing magnetite. *Can. J. Soil Sci.* 47: 261.

Chao, T.T. and Zhou, L. 1983. Extraction techniques for selective dissolution of amorphous iron oxides from soils and sediments. *Soil Sci. Soc. Am. J.* 47: 225–232.

FAO (Food and Agriculture Organization of the United Nations). 1990. *Soil Map of the World: Revised Legend.* Rome.

Guest, C.A., Schulze, D.G., Thompson, I.A., and Huber, D.M. 2002. Correlating manganese x-ray absorption near-edge structure spectra with extractable soil manganese. *Soil Sci. Soc. Am. J.* 66: 1172–1181.

Kaiser, K. and Zech, W. 1996. Defects in estimation of aluminum in humus complexes of podzolic soils by pyrophosphate extraction. *Soil Sci.* 161: 452–458.

Kendrick, K.J. and Graham, R.C. 2004. Pedogenic silica accumulation in chronosequence soils, Southern California. *Soil Sci. Soc. Am. J.* 68: 1295–1303.

Kodama, H. and Ross, G.J. 1991. Tiron dissolution method used to remove and characterize inorganic compounds in soils. *Soil Sci. Soc. Am. J.* 55: 1180–1187.

Loveland, P.J. and Digby, P. 1984. The extraction of Fe and Al by 0.1 *M* pyrophosphate solutions: a comparison of some techniques. *J. Soil Sci.* 35: 243–250.

McKeague, J.A. 1967. An evaluation of 0.1 *M* pyrophosphate and pyrophosphate–dithionite in comparison with oxalate as extractants of the accumulation products in Podzols and some other soils. *Can. J. Soil Sci.* 47: 95–99.

McKeague, J.A., Brydon, J.E., and Miles, N.M. 1971. Differentiation of forms of extractable iron and aluminum in soils. *Soil Sci. Soc. Am. Proc.* 35: 33–38.

McKeague, J.A. and Day, J.H. 1966. Dithionite and oxalate-extractable Fe and Al as aids in differentiating various classes of soils. *Can. J. Soil Sci.* 46: 13–22.

McKeague, J.A. and Schuppli, P.A. 1982. Changes in concentration of Fe and Al in pyrophosphate extracts of soil, and composition of sediment resulting from ultra centrifugation in relation to spodic horizons. *Soil Sci.* 134: 265–270.

Mehra, O.P. and Jackson, M.L. 1960. Iron oxide removal from soils and clays by a dithionite–citrate system buffered with sodium bicarbonate. *Clays Clay Miner.* 7: 317–327.

Neary, A.J. and Barnes, S.R. 1993. The effect of sample grinding on extractable iron and aluminum in soils. *Can. J. Soil Sci.* 73: 73–80.

Parfitt, R.L. and Henmi, T. 1982. Comparison of an oxalate-extraction method and an infrared spectroscopic method for determining allophane in soil clays. *Soil Sci. Plant Nutr.* 28: 183–190.

Ross, G.J. and Wang, C. 1993. Extractable Al, Fe, Mn, and Si. In M.R. Carter, Ed. *Soil Sampling and Methods of Analysis*. Lewis Publishers, Boca Raton, FL, pp. 239–246.

Ross, G.J., Wang, C., and Schuppli, P.A. 1985. Hydroxylamine and ammonium oxalate solutions as extractants for Fe and Al from soil. *Soil Sci. Soc. Am. J.* 49: 783–785.

Schuppli, P.A., Ross, G.J., and McKeague, J.A. 1983. The effective removal of suspended materials from pyrophosphate extracts of soils from tropical and temperate regions. *Soil Sci. Soc. Am. J.* 47: 1026–1032.

Schwertmann, U. 1959. Die frectionierte Extraction der freien Eisenoxide in Böden, ihre mineralogischen Formen und ihre Entstehungsweisen. *Z. Pflanzenernaehr. Dueng. Bodenkund* 84: 194–204.

Sheldrick, B.H. and McKeague, J.A. 1975. A comparison of extractable Fe and Al data using methods followed in the USA and Canada. *Can. J. Soil Sci.* 55: 77–78.

Soil Classification Working Group. 1998. *The Canadian System of Soil Classification*. Agriculture and Agri-food Canada, Ottawa, Canada.

Soil Conservation Service, U.S. Department of Agriculture. 1972. Soil survey laboratory methods and procedures for collecting soil samples. Soil Survey Investigations Report No. 1 (revised), U.S. Government Printing Office, Washington, DC.

Soil Survey Staff. 1990. *Keys to Soil Taxonomy*, 4th ed. SMSS Technical Monograph No. 6. Blacksburg, VA.

Wada, K. 1989. Allophane and imogolite. In J.B. Dixon and S.B. Weed, Eds. *Minerals in Soil Environments*. Soil Science Society of America, Madison, WI, pp. 1051–1087.

Wang, C., Schuppli, P.A., and Ross, G.J. 1987. A comparison of hydroxylamine and ammonium oxalate solutions as extractants for Al, Fe, and Si from Spodosols and Spodosol-like soils in Canada. *Geoderma* 40: 345–355.

Chapter 27
Determining Nutrient Availability in Forest Soils

N. Bélanger
University of Sasketchewan
Saskatoon, Saskatchewan, Canada

D. Paré
Natural Resources Canada
Quebec, Quebec, Canada

W.H. Hendershot
McGill University
Sainte Anne de Bellevue, Quebec, Canada

27.1 INTRODUCTION

Nitrogen (N) is the major nutrient determining tree growth, and this has been demonstrated abundantly in the Boreal Shield with fertilization trials or net N mineralization studies (e.g., Attiwil and Adams 1993; Reich et al. 1997). However, Ingestad (1979a,b) also showed that any other nutrient (but particularly phosphorus (P) and potassium (K)) could be limiting if supplied at a rate lower than tree demand, even if N was in excess. For example, fertilization trials with N alone or in combination with P, K, or both stimulated the growth of black spruce (*Picea mariana* (Mill.) BSP) (e.g., Wells 1994; Paquin et al. 1998) and jack pine (*Pinus banksiana* Lamb.) (e.g., Morrison and Foster 1995; Weetman et al. 1995). A much lower number of studies have showed the benefits of increased calcium (Ca) and magnesium (Mg) availability on tree nutrition and yields in Canadian forests (Hamilton and Krause 1985; Bernier and Brazeau 1988; Thiffault et al. 2006). A review by Binkley and Högberg (1997) suggested that fertilization trials with Ca and Mg have only occasionally favored the growth of northern tree species. The benefits of Ca and Mg fertilization may actually be related to an indirect effect of liming on N availability (Nohrstedt 2001; Sikström 2002). The lack of scientific evidence about the role of soil nutrients (other than N) on improved tree nutrition and growth may be due to the fact that permanent site variables such as climate, drainage, and soil physical properties have a stronger influence on trees (Post and Curtis 1970).

The forest floor has been the focus of many nutrition studies because it has a large fraction of the fine roots (Steele et al. 1997), it can be used for linking N and P turnover to tree productivity and nutrition (e.g., Paré and Bernier 1989; Reich et al. 1997), and it generally represents a large fraction of the total soil nutrient pools (Bélanger et al. 2003). However, K, Ca, and Mg in trees are believed to be derived primarily from mineral weathering and recent studies suggest that parent material elemental composition and estimates of mineral weathering can be better indicators of their availability (van Breemen et al. 2000; Bailey et al. 2004; Thiffault et al. 2006). As for P, its availability is not only constrained by the decay process and biological sinks (plant and microbial uptake) but also by geochemical sinks.

Forest soils share many characteristics with agricultural soils, but the way they are used and managed requires a different approach in many situations. The objective of this chapter is to suggest what we believe are the most acceptable analyses for determining N, K, Ca, and Mg availability in forest ecosystems and establishing a link with tree nutrition, growth, and mortality. We focus on (1) mineralizable N; (2) pH, effective cation exchange capacity (ECEC), and exchangeable cations; and (3) elemental Ca, Mg, and K composition and their release from mineral weathering. Indices of available P are mostly limited to the extraction of labile P and the reader should refer to Chapter 24 and Chapter 25 for more details. Methods for determining soil organic carbon, pH in water or $CaCl_2$ solution, electrical conductivity and soluble salts, carbonates (calcite and dolomite), total and fractions of sulfur, and pyrophosphate-extractable Fe and Al can either be found in other chapters (mostly in Section III) or in Kalra and Maynard (1991). These methods are not specific to agricultural soils and consequently can be used for forest soils. Moreover, issues related to sampling of forest soils and expressing data on a concentration or mass basis are discussed in Chapter 2.

27.2 MEASURING AVAILABLE NITROGEN IN FOREST SOILS

Several techniques have been used to estimate net N mineralization in the field. Each method has its own limitations and there is no consensus on a best method (see Binkley and Hart 1989). These methods could be divided into field incubation, laboratory incubation, chemical extraction, and measurements of gross N fluxes using ^{15}N (to better understand the microbial dynamics of N transformations). Binkley and Hart (1989) provided a comprehensive review of the components of N availability assessments in forest soils. In recent years, the view of the N cycle in forested ecosystem has substantially changed. The following findings may have a large impact on the measurement techniques that are considered most appropriate for forest soils as well as on the interpretation of the results:

1. Ericoid and ectomycorrhizal fungi have the capacity to scavenge organic sources of N and P and to participate in the decomposition process (Read et al. 2004). Therefore, incubations that exclude active plant roots may underestimate fluxes, especially in boreal or coniferous forests.

2. Organic N is the dominant form of N in soil solutions (Qualls et al. 2000) and some plants and associated mycorrhizal fungi can absorb dissolved organic N (Näsholm et al. 1998).

3. Studies reporting gross N fluxes have indicated substantial rates of gross mineralization and nitrification even in systems where little mineral N accumulates during mineralization assays.

Given this information, net N mineralization measured with incubation techniques cannot be viewed as a direct measure of plant-available N but rather as an index of this process (see Schimel and Bennett 2004). We provide here the description of two incubation techniques that would likely be correlated with field N fluxes even though the soils are not in contact with living roots. The methodologies described consider periods of incubations that are long enough to avoid the immobilization phase typical of forest soils with high C:N ratios and therefore allow part of the more labile fractions of soil N to be mineralized and measured. The first technique is a long-term laboratory incubation that assesses the potentially mineralizable N fraction of the soil. The second method is a field incubation that is sensitive to field microclimatic conditions. These two techniques have been compared in Brais et al. (2002).

27.2.1 Long-Term Laboratory Incubation

The fraction of potentially mineralizable N (N_0) and its mineralization constant (k) can be assessed with long-term laboratory incubations (Stanford and Smith 1972); some related methods for measuring mineralizable N in agricultural soils are given in Chapter 46. The long-term laboratory incubation technique given here can be used to measure production of dissolved organic N, C, and P (Smith et al. 1998), and CO_2 (Côté et al. 2000). The effect of temperature on mineralization rates can be assessed with this technique to give insight on the reactivity of soil organic matter to changes in temperature regime (Paré et al. 2006). Soil disturbance during sampling and sample preparation (e.g., drying, grinding, or sieving; and refrigerating or freezing) can have an impact on microbial activity and this is of importance for obtaining indices of N turnover and availability (e.g., Van Miegroet 1995; Ross and Hales 2003). The field logistics and the study's objectives will determine the methodology used and the interpretation of the data must be done accordingly. For the sake of simplicity, however, these effects and the different methods used are not further considered in this chapter. Rather, we describe a technique using fresh moist samples that we believe yields reliable estimates of the potential of the soil for N and C release under standard conditions.

Materials and Reagents

1. Plastic filtration units are used (Falcon Filter units, Becton Dickinson, Model 7102) but the original nitrocellulose filter of the microlysimeter has to be replaced by a glass–fiber filter (Nadelhoffer 1990).
2. Glass wool.
3. 1 *M* HCl.
4. 0.005 *M* K_2SO_4.
5. Vacuum pump (60 mm Hg).
6. Buchner funnels.
7. Whatman No. 42 filter paper.
8. Acid washed 1 mm (18 mesh) silica sand.

Procedure

1 Volumetric soil samples are collected; fresh, moist samples are sieved through 6 and 4 mm screens for organic humus layers (FH) and mineral horizons, respectively, to remove coarse fragments and roots. The samples are then weighed. To maintain the soil structure of the moist samples as much as possible, the large mesh sizes are used while homogenizing the material.

2 The soil material is weighed to obtain samples of 25 g of the fresh organic humus layer (about 9 g of dry FH material on average) and 100 g of fresh mineral soil (about 73 g of dry mineral soil on average), and inserted into the top part of the filtration units above a layer of prewashed (1.0 *M* HCl and deionized water) glass wool. The soil material is then packed slightly to obtain a total volume of soil of 70 and 100 cm^3 for the organic layer and the mineral layer, respectively. Fine-textured mineral soils can be mixed with acid-washed silica sand (50% soil volume). Silica sand is washed with 1 *M* HCl and rinsed until the conductivity falls to that of demineralized water.

3 Soil samples are incubated in growth chambers at 22°C. The relative humidity level is maintained around 85% to keep the soil moist. The microcosm remains open to air exchange inside the growth chamber unless a respiration measurement is taken over for short periods (24–48 h). Water content is verified by weighing and adjusted to 85% of field capacity weekly.

4 Soils are flushed monthly with 100 mL 0.005 *M* K_2SO_4. Solution is gently added to the soil with a burette (2×50 mL) to limit disturbance to the soil structure. Soils are allowed to drain freely; the excess solution is removed by applying vacuum. If the solution contains soil particles, it can be refiltered using a Buchner funnel and filter paper. Samples are transferred to the refrigerator at 4°C and should be analyzed for ammonium, nitrate, and total N within 2 weeks.

Calculations

Cumulative mineralized N through time (N_t) is fitted to the following simple negative exponential model (Stanford and Smith 1972):

$$N_t = N_0(1 - e^{-kt}) \tag{27.1}$$

where N_0 is potential mineralizable N, and k is mineralization rate and is unitless. N_0 can be expressed on a total N basis to estimate organic matter quality or on an area basis to give the reserve of potentially mineralizable N for a given soil depth. See Chapter 46 for more details.

Comments

Higher temperatures of incubation are often used (e.g., 35°C). These high temperatures often provide a better fit and convergence of first-order models. However, Equation 27.1 parameters (N_0 and k) are sensitive to temperature (MacDonald et al. 1995; Paré et al. 2006) and we recommend using a soil temperature that is high (e.g., 22°C), but not outside the range of temperatures observed in surface soils under a closed forest canopy.

27.2.2 Field Incubation

Field incubation techniques include incubating a soil sample in the field with the least possible disturbance and estimating the net amounts of ammonium and nitrate that accumulated in the sample. The incubation period varies from a week to a year. These techniques originate from *in situ* buried bags (Eno 1960) where samples are incubated in a polyethylene bag. The main drawback of this method is the disturbance to the soil sample, which can increase mineralization rates from 2- to 10-fold according to Raison et al. (1987). The latter authors have described the use of *in situ* incubations in closed-top tubes perforated on the sides and open at the bottom. This technique limits disturbance of the soil samples while allowing the use of the samples to a greater depth (40 cm). In addition, Di Stefano and Gholz (1986) have proposed the use of a resin core above and below the incubated core. The resin core above is discarded at the end of the measurement period. Its only use is to prevent contamination with atmospheric N inputs. Nitrogen mineralization is estimated as the net amount of N mineralized in the soil core in addition to the N captured by the bottom resin core. This technique may provide conditions that more closely mimic those in intact soils because it allows water movement in the soil core as well as the removal of the products of mineralization. A simpler alternative is the use of closed-top cores; since there is no water flux into the top of the cores, it is assumed that there is no leaching loss from the bottom. We describe here closed-top field incubations.

Materials and Reagents

1. ABS cores, 30 cm long, 4.5 cm in diameter, capped
2. 2 *M* KCl solution
3. Whatman No. 42 filter paper
4. Reciprocating shaker
5. Erlenmeyer flasks (250 mL)
6. Funnels

Procedure

1. Two tubes are brought to the field. The first one is used to collect a soil sample for initial determination of mineral N content. The second one is inserted in the soil to the required depth near the first tube and is left in the field for the incubation period (i.e., 1 week to 1 year; 6 weeks incubations gave reproducible results on a rich soil in the boreal mixedwood although it was too short to measure net mineralization in black spruce sites).
2. Tubes collected from the field are kept in a cooler and should be extracted within 48 h.
3. The soil samples are separated into forest floor and mineral soil samples. They are sieved through 6 and 4 mm screens for organic humus layers and mineral horizons, respectively. The total wet weight of the soil that is kept is weighed.

4 A subsample is dried at 65°C for organic horizons and at 105°C for mineral soil horizons to estimate water content, and these subsamples are also used for determination of total N and total C preferably on a CN analyzer (see Chapter 21 and Chapter 22).

5 An amount of fresh soil that corresponds to 10 g dry weight (about half for strongly organic samples) is placed into a 250 mL Erlenmeyer flask. Then add 100 mL of KCl solution. Flasks are capped and shaken for 1 h and then filtered through a Whatman No. 42 filter. Solutions are analyzed for NH_4-N and NO_3-N (see Chapter 6).

Calculations

The difference between final and initial concentrations is used to express net N mineralization, net nitrification, net ammonium production, or all the above. Production rates are expressed in N weight, on time, and on either soil dry weight, total N or C basis to express the quality of the soil organic matter, or on an area basis to get an estimate of nutrient fluxes.

Comments

1 We would advise the use of long incubation periods or the use of laboratory incubations in soil with high C:N, high organic matter content, low N turnover, little net nitrification, little nitrate in soil solution, or presence of ericoid and ectomycorrhizal fungi. On the other hand, short-term incubations would be suitable for forests with thin or nonexistent organic layers that undergo net nitrification (such as sugar maple [*Acer saccharum* Marsh.] forests).

2 We often found very low and negative rates of net mineralization (net immobilization) in boreal black spruce forests with thick organic layers (D. Paré, unpublished data). Such results are frequent and not often published. In all cases, it is advisable to compare results with the nutrient budget.

3 Estimates of N in litterfall and immobilization in biomass provide estimates of N mineralization that are totally independent of incubation estimations and that should match them. Although it is not always possible to obtain such an estimate, the comparison of incubation results with budget estimates should be done on a few plots within the forest and soil types investigated.

27.3 SOIL pH, EFFECTIVE CATION EXCHANGE CAPACITY, AND EXCHANGEABLE CATIONS

27.3.1 Soil pH

Because of the variations in ionic strength of agricultural soils, the most common method of measuring their pH in Canada is the 0.01 *M* $CaCl_2$ method. By measuring the pH in an electrolyte of known concentration, the effects of variable ionic strength of the soil solutions are largely eliminated. Forest soils, on the other hand, tend to have close to the same ionic strength throughout the year, except as influenced by variations in water content. For this reason, many researchers choose to use pH measured in water. Since the ionic strength of the measurement solution is lower, the pH obtained will be closer to that observed by plants

growing in the field. Researchers should be aware that the disturbance caused by sampling and drying soils does have an effect on the measured pH (Courchesne et al. 1995). A discussion on the choice of pH methods can be found in Chapter 16 along with a detailed description of the methods themselves.

27.3.2 Effective Cation Exchange Capacity and Exchangeable Cations

The use of an unbuffered $BaCl_2$ solution is now generally preferred for determination of ECEC. The $BaCl_2$-compulsive exchange procedure (Gillman and Sumpter 1986) is recommended for determining CEC on all soils (except soils containing salts, carbonates, or zeolites) (Sumner and Miller 1996). Similarly, Chapter 18 suggests the use of a simplified $BaCl_2$ extraction. The $BaCl_2$ extraction has the ability to displace trivalent cations at lower ionic strength without being preferentially adsorbed compared to the NH_4Cl or KCl extractions. Although the extraction can modify pH because the ionic strength of 0.3 mol L^{-1} (for 0.1 *M* $BaCl_2$) of the solution is still about three orders of magnitude higher than the soil solution of a sandy Podzol, it causes smaller changes in pH than the more concentrated solutions (e.g., 1 mol L^{-1} for 1 *M* KCl or NH_4Cl). In this method, ECEC is calculated by summing exchangeable cations (Ca, Mg, K, Na, Al, Fe, and Mn).

The method of Chapter 18 is strongly recommended for acid forest soils such as Podzols as well as Sombric and Dystric Brunisols (or Dystric Cambisols according to the Food and Agriculture Organization of the United Nations (1974)). For boreal plain forests with higher soil pH values (above pH 5.5–6.0) and low levels of exchangeable aluminum and manganese (e.g., Melanic and Eutric Brunisols [or Eutric Cambisols], Gray Luvisols [or Albic Luvisols], and Chernozems), the unbuffered NH_4Cl extraction is also acceptable and is commonly used (Kalra and Maynard 1991). However, although most agronomists are interested in determining the amount of exchange sites for management or control of soil pH, usually by liming, forest soil scientists are also interested in knowing the cation species (base vs. acid) held on these exchange surfaces. The method proposed here is therefore a one-step extraction that uses an unbuffered NH_4Cl solution and that allows the measurement of ECEC as well as the individual contribution of Ca, Mg, K, and Na to ECEC (and Al, Fe, and Mn if needed).

Materials and Reagents

1 Centrifuge tubes (50 mL) with screw caps.

2 Ultracentrifuge accepting 50 mL tubes.

3 End-over-end shaker.

4 Ammonium chloride, 1 *M*: dissolve 53.5 g of NH_4Cl with double deionized (d.d.) water and make to volume in a 1000 mL volumetric flask.

5 Standards of Ca, Mg, K, Na, Al, Fe, and Mn are prepared using atomic absorption reagent-grade standards of 1000 mg L^{-1}. The matrix in the standards must correspond to the NH_4Cl concentration of the analyzed sample (diluted or nondiluted matrix).

6 Lanthanum solution, 100 mg L^{-1}: dissolve 53.5 g of $LaCl_3 \cdot 7H_2O$ in a 200 mL volumetric flask and make to volume (for analysis by atomic absorption spectroscopy [AAS]).

7 Cesium solution, 100 g L^{-1}: dissolve 25.2 g CsCl in a 200 mL volumetric flask and make to volume (for analysis by AAS).

8 Whatman No. 41 filter paper.

Procedure

1 Weigh out about 2.5 g of dry organic soil (FH samples) or fine-textured mineral soil and about 12.5 g of dry (<2 mm) coarse-textured mineral soil into a 50 mL centrifuge tube. Record the exact weight of soil used to the nearest 0.001 g. Include blanks, duplicates, and quality control samples.

2 Add 25.0 mL of 1 *M* NH_4Cl to each tube and shake slowly on an end-over-end shaker (15 rpm) for 2 h.

3 Ultracentrifuge (15 min, 7000 *g*) and filter the supernatant with Whatman No. 41 filter paper.

4 Analyze Ca, Mg, K, Na, Al, Fe, and Mn in the supernatant solution with AAS or other suitable instrument. Dilution (10- or 100-fold) will likely be required for Ca, K, Mg, and Na. The addition of 0.1 mL of La solution and 0.1 mL of Cs solution to a 10 mL aliquot of diluted extract is required for the determination of Ca, Mg, and K by AAS (for detailed instructions on this and other aspects of analysis refer to the manual for your AAS). If needed, preservation of samples by acidifying to 0.2% HNO_3 will prevent the loss of Fe and Al.

Calculations

1 Exchangeable cations:

$$M^+ \text{ cmol}_c \text{ kg}^{-1} = C \text{ cmol}_c \text{ L}^{-1} \times (0.025 \text{ L/wt. soil g}) \times 1000 \text{ g kg}^{-1} \times \text{ DF} \quad (27.2)$$

where M^+ is the concentration of an adsorbed cation ($\text{cmol}_c \text{ kg}^{-1}$); C is the concentration of the same cation measured in the NH_4Cl extract ($\text{cmol}_c \text{ L}^{-1}$); and DF is the dilution factor (if applicable).

2 Effective CEC:

$$\text{Effective CEC cmol}_c \text{ kg}^{-1} = \Sigma \text{ cmol}_c \text{ Ca, Mg, K, Na, Fe, Al, Mn kg}^{-1} \quad (27.3)$$

See Section 18.2.4 in Chapter 18 for details on quality controls, standards, and the effects of different soil:solution ratios on results.

27.3.3 Contribution of Exchangeable H^+ to Effective Cation Exchange Capacity

It is difficult to account for the amount of H^+ coming from the exchange reaction and its contribution to ECEC from NH_4Cl or $BaCl_2$ extractions because some H^+ in the extract may come from sources other than exchangeable H^+ (e.g., dissociation of organic acids) or be

produced or consumed in reactions involving Al–OH complexes or hydrolysis of free Al^{3+} (Thomas and Hargrove 1984). The salt solution, ionic strength, and the soil: solution ratios have an influence on the amount of exchangeable H^+ displaced from exchange sites. Therefore, the contribution of exchangeable H^+ to ECEC or base saturation is operationally defined from titration of a 1 *M* KCl extract as suggested by Thomas (1982) (see Chapter 18 for details on methodology). Exchangeable H^+ is relatively abundant in acidic organic horizons (e.g., forest floor material), but acidic mineral soils such as Bhf and Bf horizons also have high enough amounts to draw our attention (Ross et al. 1996; Bélanger et al. 2006). Bélanger et al. (2006) noted that ''fundamentally, any valid measure of ECEC must therefore include some estimate of exchangeable H^+ concentration or a demonstration that it is negligible''. Unfortunately, the direct measurement of exchangeable H^+ is time-consuming and not practical for routine analysis. Therefore, Bélanger et al. (2006) have used soil pH in water (as proposed in Chapter 16) and ECEC (using $BaCl_2$ as described in Chapter 18) to estimate exchangeable H^+ concentrations in FH and podzolic (spodic) B samples of acidic forest soils developed from granitic bedrock or parent material. Although Equation 27.4 provides good estimates of the proportion of exchangeable H^+ on the exchange complex of organic and podzolic B horizons from all types of forests, we recommend the readers build specific relationships using their own samples if greater predicting power is required:

$$\log(\text{exch. } H^+)/\text{ECEC} = 0.682 - (0.308 \times \text{soil pH in water}); \quad R^2 = 0.691 \qquad (27.4)$$

27.4 ELEMENTAL P, K, Ca, AND Mg COMPOSITION AND RELEASE BY MINERAL WEATHERING

It has long been recognized that Ca and Mg in trees are derived primarily from Ca and Mg released into the soil solution from mineral weathering (van Breemen et al. 2000; Blum et al. 2002), and additional studies suggest that parent material elemental composition can be a reliable indicator of tree Ca and Mg nutrition. For example, Thiffault et al. (2006) examined soil and foliar nutrient status of black spruce and balsam fir (*Abies balsamea* (L.) Mill.) stands in Quebec subject to whole-tree and stem-only harvesting and found that total mineral parent C elemental content was more indicative of nutrient limitations than surface soil-available nutrient concentrations: the signal of this low Ca and Mg availability was very weak in the upper soil layers, including the forest floor, probably because the chemistry of these layers is largely controlled by litter material with relatively well-balanced nutrient ratios (Knecht and Göransson 2004). Additional studies suggest that parent material elemental composition may be an important predictor of tree mortality as well as Ca and Mg nutrition. For example, van Breemen et al. (1997) showed that sugar maple mortality in the northeastern United States increased with decreasing elemental Ca in the parent C material. Sugar maple foliar Ca and Mg status and mortality were also more strongly linked to B horizons compared to forest floor Ca and Mg chemistry (Bailey et al. 2004).

Bailey et al. (2004) further suggested that a model that calculates release of Ca and Mg from soil mineral weathering of the parent C material would likely be successful in predicting stand nutrition and productivity. Many indices of soil mineral weathering have been developed in the past (Birkeland 1999), but one of the preferred approaches compares the concentration of elements in the various soil horizons to the concentration of elements on the presumably unaltered parent material in the C horizon (Kirkwood and Nesbitt 1991; Bain et al. 1994; Hodson 2002). Adjustments are made to consider additions of organic matter and the leaching of elements that are not of interest in the study because both will affect the concentration of the elements studied. Therefore, an equation using an element resistant to

weathering (most often zirconium and titanium) is used to normalize the data for mobile elements. Assuming the age of the soil is known, the release rate of a mobile element in a particular horizon can be calculated using the following equations (Hodson 2002):

$$R = (E_{PM} - E_i^*) \times \rho \times Z/t \tag{27.5}$$

and

$$E_i^* = E_i \times C_{PM}/C_i \tag{27.6}$$

where R is the element release rate ($\mu g\ m^{-2}\ year^{-1}$), E_{PM} is the concentration of element E in the parent material ($\mu g\ g^{-1}$), E_i^* is the adjusted concentration of element E in horizon i ($\mu g\ g^{-1}$), E_i is the concentration of element E in the horizon i ($\mu g\ g^{-1}$), ρ is the horizon density ($g\ m^{-3}$), Z is the horizon thickness (m), t is the soil age (years), C_{PM} is the concentration of immobile element C in the parent material ($\mu g\ g^{-1}$), and C_i is the concentration of immobile element C in horizon i ($\mu g\ g^{-1}$).

In forest soils, the concentration of immobile elements tends to decrease with depth; there is a concentration effect from bottom to top because of the loss of mobile elements and accumulation of organic matter in upper soil horizons (Melkerud et al. 2000; Courchesne et al. 2002; Hodson 2002). Research has shown that some of the elements that are resistant to weathering can nonetheless be eluviated and we recommend that anyone applying this technique study the results of authors such as those mentioned above.

Weathering rates in the >50 μm fraction are sometimes assumed to be negligible because of the relatively low surface area and lack of easily weatherable minerals in that fraction (Kolka et al. 1996). Therefore, the method is sometimes employed on the silt fraction (2–50 μm) alone after wet sieving to remove sand and by multiple centrifugations to remove clay. In this case, the expression ($E_{PM} - E_i^*$) is multiplied by the silt mass in that horizon, which can be measured after determination of soil bulk density, particle size distribution, and horizon thickness.

Wavelength dispersive x-ray fluorescence spectroscopy on fused beads is generally the preferred approach to determine the elemental composition of soil samples (e.g., van Breemen et al. 1997; Melkerud et al. 2000), but this can also be determined by inductively coupled plasma (ICP) or AAS on samples digested using hydrofluoric acid.

REFERENCES

Attiwil, P. and Adams, M.A. 1993. Nutrient cycling in forests. *New Phytol*. 124: 561–582.

Bailey, S.W., Horsley, S.B., Long, R.P., and Hallett, R.A. 2004. Influence of edaphic factors on sugar maple nutrition and health on the Allegheny Plateau. *Soil Sci. Soc. Am. J*. 68: 243–252.

Bain, D.C., Mellor, A., Wilson, M.J., and Duthie, D.M.L. 1994. Chemical and mineralogical weathering rates and processes in an upland granitic till catchment in Scotland. *Water Air Soil Poll*. 73: 11–27.

Bélanger, N., MacDonald, J.D., Paré, D., Thiffault, E., Claveau, Y., and Hendershot, W.H. 2006. The assessment of exchangeable hydrogen ions in Boreal Shield soils of Quebec. *Can. J. Soil Sci*. 86: 513–521.

Bélanger, N., Paré, D., and Yamasaki, S.H., 2003. The soil acid–base status of boreal black spruce

stands after whole-tree and stem-only harvesting. *Can. J. Forest Res.* 33: 1874–1879.

Bernier, B. and Brazeau, M. 1988. Magnesium deficiency symptoms associated with sugar maple dieback in a Lower Laurentians site in southeastern Quebec. *Can. J. Forest Res.* 18: 1265–1269.

Binkley, D. and Hart, S.C. 1989. The components of nitrogen availability assessments in forest soils. *Adv. Soil Sci.* 10: 57–112.

Binkley, D. and Högberg, P. 1997. Does atmospheric deposition of nitrogen threaten Swedish forests? *Forest Ecol. Manag.* 92: 119–152.

Birkeland, P.W. 1999. *Soils and Geomorphology*, 3rd ed. Oxford University Press, New York, 430 pp.

Blum, J.D., Klaue, A., Nezat, C.A., Driscoll, C.T., Johnson, C.E., Siccama, T.G., Eagar, C., Fahey, T.J., and Likens, G.E. 2002. Mycorrhizal weathering of apatite as an important calcium source in base-poor forest ecosystems. *Nature* 417: 729–731.

Brais, S., Paré, D., Camiré, C., Rochon, P., and Vasseur, C. 2002. Nitrogen net mineralization and dynamics following whole-tree harvesting and winter windrowing on clayey sites of northwestern Quebec. *Forest Ecol. Manag.* 157: 119–130.

Côté, L., Brown, S., Paré, D., Fyles, J., and Bauhus, J. 2000. Dynamics of carbon and nitrogen mineralization in relation to stand type, stand age and soil texture in the boreal mixedwood. *Soil Biol. Biochem.* 32: 1079–1090.

Courchesne, F., Hallé, J.-P., and Turmel, M.-C. 2002. Bilans élémentaires holocènes et altération des minéraux dans trois sols forestiers du Québec méridional. *Géogr. Phys. Quatern.* 56: 5–17.

Courchesne, F., Savoie, S., and Dufresne, A. 1995. Effects of air-drying on the measurement of soil pH in acidic forest soils of Quebec, Canada. *Soil Sci.* 160: 56–68.

Di Stefano, J. and Gholz, H.L. 1986. A proposed use of ion exchange resin to measure nitrogen mineralization and nitrification in intact soil cores. *Commun. Soil Sci. Plant Anal.* 17: 989–998.

Eno, C. 1960. Nitrate production in the field by incubating the soil in polyethylene bags. *Soil Sci. Soc. Am. Proc.* 24: 277–279.

Food and Agriculture Organization of the United Nations. 1974. *FAO-UNESCO Soil Map of the World*, Vol. 1, Legend. UNESCO, Paris, France, 59 pp.

Gillman, G.P. and Sumpter, E.A. 1986. Modification to the compulsive exchange method to for measuring exchange characteristics of soils. *Aust. J. Soil Res.* 24: 61–66.

Hamilton, W.N. and Krause, H.H. 1985. Relationship between jack pine growth and site variables in New Brunswick plantations. *Can. J. Forest Res.* 15: 922–926.

Hodson, M.E. 2002. Experimental evidence for mobility of Zr and other trace elements in soils. *Geochim. Cosmochim. Acta* 66: 819–828.

Ingestad, T. 1979a. Nitrogen stress in birch seedlings. II. N, P, Ca, and Mg nutrition. *Physiol. Plant.* 45: 149–159.

Ingestad, T. 1979b. Mineral nutrient requirement of *Pinus silvestris* and *Picea abies* seedlings. *Physiol. Plant.* 45: 373–380.

Kalra, Y.P. and Maynard, D.G. 1991. *Methods Manual for Forest Soil and Plant Analysis*. Information Report NOR-X-319. Forestry Canada, Northwest Region, Northern Forestry Centre, Edmonton, Alberta, Canada.

Kirkwood, D.E. and Nesbitt, H.W. 1991. Formation and evolution of soils from an acidified watershed: Plastic Lake, Ontario, Canada. *Geochim. Cosmochim. Acta* 55: 1295–1308.

Knecht, M.F. and Göransson, A. 2004. Terrestrial plants require nutrients in similar proportions. *Tree Physiol.* 24: 447–460.

Kolka, R.K., Grigal, D.F., and Nater, E.A., 1996. Forest soil mineral weathering rates: use of multiple approaches. *Geoderma* 73: 1–21.

MacDonald, N.W., Zak, D.R., and Pregitzer, K.S. 1995. Temperature effects on kinetics of microbial respiration and net nitrogen and sulphur mineralization. *Soil Sci. Soc. Am. J.* 59: 233–240.

Melkerud, P.A., Bain, D.C., Jongmans, A.G., and Tarvainen, T. 2000. Chemical, mineralogical and morphological characterization of three podzols developed on glacial deposits in Northern Europe. *Geoderma* 94: 125–148.

Morrison, I.K. and Foster, N.W. 1995. Effect of nitrogen, phosphorus and magnesium fertilizers on growth of a semimature jack pine stand, northwestern Ontario. *For. Chron.* 71: 422–425.

Nadelhoffer, K.J. 1990. Microlysimeter for measuring nitrogen mineralization and microbial respiration in aerobic soil incubations. *Soil Sci. Soc. Am. J.* 54: 411–415.

Näsholm, T., Ekblad, A., Nordin. A., Giesler, R., Högberg, M., and Högberg, P. 1998. Boreal forest plants take up organic nitrogen. *Nature* 392: 914–916.

Nohrstedt, H.-Ö. 2001. Effects of liming and fertilization (N, P, K) on chemistry and N turnover in acidic forest soils in SW Sweden. *Water Air Soil Pollut.* 139: 343–354.

Paquin, R., Margolis, H.A., and Doucet, R. 1998. Nutrient status and growth of black spruce layers and planted seedlings in response to nutrient addition in the boreal forest of Quebec. *Can. J. Forest Res.* 28: 729–736.

Paré, D. and Bernier, B. 1989. Origin of the phosphorus deficiency observed in declining sugar maple stands in the Quebec Appalachians. *Can. J. Forest Res.* 19: 24–34.

Paré, D., Boutin, R., Larocque, G., and Raulier, F. 2006. Effect of temperature on soil organic matter decomposition in three forest biomes of eastern Canada. *Can. J. Soil Sci.* 86: 247–256.

Post, B.W. and Curtis, R.O. 1970. Estimation of northern hardwood site index from soils and topography in the Green Mountains of Vermont. *Vermont Agr. Exp. Station Bull.* 664: 1–17.

Qualls, R.G., Haines, B.L., Swank, W.T., and Tyler, S.W. 2000. Soluble organic and inorganic nutrient fluxes in clearcut and mature deciduous forests. *Soil Sci. Soc. Am. J.* 64: 1068–1077.

Raison, R.J., Connell, M.J., and Khanna, P.K. 1987. Methodology for studying fluxes of soil mineral-N in situ. *Soil Biol. Biochem.* 19: 521–530.

Read, D., Leake, J.R., and Perez-Moreno, J. 2004. Mycorrhizal fungi as drivers of ecosystem processes in heathland and boreal forest biomes. *Can. J. Bot.* 82: 1243–1263.

Reich, P.B., Grigal, D.F., Aber, J.A., and Gower, S.T. 1997. Nitrogen mineralization and productivity in 50 hardwood and conifer stands on diverse soils. *Ecology* 78: 335–347.

Ross, D.S., David, M.B., Lawrence, G.B., and Bartlett, R.J. 1996. Exchangeable hydrogen explains the pH of spodosol Oa horizons. *Soil Sci. Soc. Am. J.* 60: 1926–1932.

Ross, D.S. and Hales, H.C. 2003. Sampling-induced increases in net nitrification in the Brush Brook (Vermont) watershed. *Soil Sci. Soc. Am. J.* 67: 318–326.

Schimel, J.P. and Bennett, J. 2004. Nitrogen mineralization: challenges of a changing paradigm. *Ecology* 85: 591–602.

Sikström, U. 2002. Effects of liming and fertilization (N, PK) on stem growth, crown transparency and needle element concentrations of *Picea abies* stands in southwestern Sweden. *Can. J. Forest Res.* 32: 1717–1727.

Smith, C.K., Munson, A.D., and Coyea, M.R. 1998. Nitrogen and phosphorus release from humus and mineral soil under black spruce forests in central Quebec. *Soil Biol. Biochem.* 30: 1491–1550.

Stanford, G. and Smith, S.J. 1972. Nitrogen mineralization potentials of soils. *Soil Sci. Soc. Am. Proc.* 36: 465–472.

Steele, S.J., Gower, S.T., Vogel, J.G., and Norman, J.M. 1997. Root mass, net primary production and turnover in aspen, jack pine and black spruce forests in Saskatchewan and Manitoba, Canada. *Tree Physiol.* 17: 577–587.

Sumner, M.E. and Miller, W.P. 1996. Cation exchange capacity and exchange coefficients. In D.L. Sparks et al., Eds. *Methods of Soil Analysis, Part 3—Chemical Methods*, 3rd ed. Soil Science Society of America and American Society of Agronomy, Madison, WI, pp. 1201–1229.

Thiffault, E., Paré, D., Bélanger, N., Munson, A.D., and Marquis, F. 2006. Harvesting intensity in the boreal forest: impacts on soil nutrient availability and tree nutrition. *Soil Sci. Soc. Am. J.* 70: 691–701.

Thomas, G.W. 1982. Exchangeable cations. In A.L. Page, A.H. Miller, and D.R. Keeney, Eds. *Methods of Soil Analysis, Part 2—Chemical and Microbiological Properties*, 2nd ed. American Society of Agronomy and Soil Science Society of America, Madison, WI, pp. 159–165.

Thomas, G.W. and Hargrove, W.L. 1984. The chemistry of soil acidity. In F. Adams, Ed. *Soil Acidity and Liming*, 2nd ed. American Society of Agronomy, Madison, WI, pp. 3–56.

van Breemen, N., Finzi, A.C., and Canham, C.D. 1997. Canopy tree–soil interactions within temperate forests: effects of soil elemental composition and texture on species distributions. *Can. J. Forest Res.* 27: 1110–1116.

van Breemen, N., Lundström, U.S., and Jongmans, A.G. 2000. Do plants drive podzolization via rock-eating mycorrhizal fungi. *Geoderma* 94: 163–171.

Van Miegroet, H. 1995. Inorganic nitrogen determined by laboratory and field extractions of two forest soils. *Soil Sci. Soc. Am. J.* 59: 549–553.

Weetman, G.F., Dallaire, L.C., and Fournier, R. 1995. Long term effects of repeated N fertilization and straw application in a Jack pine forest. 1. Twenty-two-year growth response. *Can. J. Forest Res.* 25: 1978–1983.

Wells, E.D. 1994. Effects of planting, spacing and refertilization on growth and nutrition of black spruce (*Picea mariana*) planted on a minerotrophic peatland in Newfoundland, Canada. *Can. J. Forest Res.* 24: 1302–1311.

Chapter 28
Chemical Properties of Organic Soils

A. Karam
Laval University
Quebec, Quebec, Canada

28.1 INTRODUCTION

Organic soils are rich in fresh plant material or organic materials at various stages of decomposition, namely fibric, hemic, and sapric materials (Soil Survey Staff 2003). These soils usually form under conditions of water saturation. Organic soils include muck and peat soils or histosols (Canada and United States of America), the tundras, the Irish peat bogs, the moor peats (Australia), les sols hydromorphes organiques (France), and earthy peat soils in Great Britain (Okruszko and Ilnicki 2003). Common organic soil parent materials may include mosses (such as sphagnum), gyttja, dy, marl, volcanic ash, cattails, reeds, sedges, pondweed, grasses, and various ''water-loving'' deciduous and coniferous shrubs and trees. Organic soils can contain silicate minerals from trace to appreciable amounts. The characteristics of organic soils depend mainly on the nature of the vegetation that was deposited in the water and the degree of decomposition (Mokma 2005).

Although the chemical properties of organic soils are different from those of their mineral counterparts, the chemical methods given for mineral soils are also applicable to organic soils; therefore, these analytical procedures are not repeated here. The analyst may choose an appropriate method from other chapters.

28.2 SAMPLE PREPARATION (ASTM 1988)

28.2.1 Introduction

Soil testing is complicated by the larger range of volume percentage of the solid phase, computed as the ratio of bulk density to particle density, and water contents in samples of organic soils compared with mineral soils, and with a greater influence of organic soil drying on soil chemical properties (Parent and Khiari 2003). According to Watson and Isaac (1990), quantitative analysis of soil samples can be broken down into six steps: (i) handling and

preparation of the samples, (ii) weighing samples, (iii) dissolution of samples/extraction of elements, (iv) pretreatment or removal of interferences, if needed, (v) measuring a property of the sample, and (vi) calculating and reporting of concentration of analyte. Handling and preparation of organic soils before soil analysis are critical. Chemical analyses may be conducted on fresh samples (field moisture content) or on air-dried samples. It should be noted that drying organic soils increases dry bulk density, volume of the solid phase (Ilnicki and Zeitz 2003), and mineralization of organic P (Daughtrey et al. 1973), decreases pH measured in water, 0.01 *M* $CaCl_2$, and 1 *M* KCl compared with the field-moist condition (van Lierop and Mackenzie 1977), and may lead to higher soil test levels of certain nutrients, such as available P and K (Daughtrey et al. 1973; Anderson and Beverly 1985). These latter authors postulate that screened organic soils are more easily compacted upon drying, and conversely expand upon rehydration. Parent and Khiari (2003) noted that air-dried pristine peat contained more P in available form than fresh peat. Anderson and Beverly (1985) recommend that organic soils be sampled on a volume basis in order to ensure uniformity of results. Harrison (1979) suggested that where soils vary in bulk density, soil data should be expressed in terms of soil volume.

28.2.2 Materials

1 Analytical balance

2 Blender, high speed

3 Large flat pan or equivalent

4 Spoon or spatula

28.2.3 Procedure

1 Mix organic soil sample thoroughly and weigh a 100 to 300 g representative sample. Determine the mass of the sample and spread evenly on a large flat pan, square rubber sheet, or paper. Crush soft lumps with a spoon or spatula and let the sample come to moisture equilibrium with room air, not less than 24 h.

2 Stir occasionally to maintain maximum air exposure of the entire sample.

3 When the mass of the sample reaches a constant value, calculate the moisture removed during air drying as a percentage of the as-received mass.

4 Grind a representative portion of the air-dried sample 1 to 2 min in a high-speed blender. Determine the amount, in grams, of air-dried sample equivalent to 50 g of as-received sample as follows:

$$\text{Equivalent sample mass, g} = 50.0 - [(50 \times M)/100] \tag{28.1}$$

where *M* is the percent of moisture removed in air drying.

5 Place the sample in a moisture-proof container.

28.3 MOISTURE AND ASH CONTENT (ASTM 1988)

28.3.1 Introduction

The simplest method for the direct determination of moisture content is the gravimetric method, which involves the measurement of water lost by weighing a soil sample (as-received) before and after it is dried at 105°C–110°C in an oven. The moisture content is expressed either as a percent of the oven dry mass or of the as-received mass. This method may not be suitable when a dried soil sample is used to assess nitrogen, pH, cation exchange, and other soil chemical properties. An alternative method that removes the total moisture and provides a more stable sample, the air-dried sample, has been suggested by the ASTM Committee (ASTM 1997). This method includes two steps: (1) evaporation of moisture in air at room temperature (air-drying) and (2) the subsequent oven drying of the air-dried sample at 105°C.

There are basically two procedures involved in the determination of the ash (inorganic fraction) of a peat or organic sample: dry-ashing methods and wet-ashing methods.

The dry-ashing method involves the removal of organic matter by combustion of the sample at medium temperature (375°C to 800°C) in a temperature-regulated muffle furnace. The principal errors in dry-ashing arise through incomplete combustion when the temperature or time allowed for combustion is insufficient, and through losses resulting from the use of too high a temperature (Allen 1989).

If necessary, samples are dried (105°C–110°C) before ashing. The substance remaining after ignition is the ash and includes mineral impurities such as sand. The weight lost on ignition is calculated and considered as an approximate measure of the organic content of acid organic soils and noncalcareous peatlands. Vessels suggested for ashing are porcelain, quartz, or platinum dishes. Sample weights used vary from 0.25 to 2.00 g. The ash may be further dissolved in an acid solution for elemental analysis.

28.3.2 Materials

1. Muffle furnace—controlled to ±5°C for ashing at 600°C
2. High-form porcelain, 30 mL crucible
3. Porcelain crucible cover or aluminum foil, heavy duty
4. Desiccator cabinet or nonvacuum, desiccator with desiccant
5. Analytical balance and spoons
6. Electric drying oven: regulated to a constant temperature of 105°C

28.3.3 Procedure

1. Weigh a 2 g sample of 2 mm oven-dried soil (105°C) into a tared high-form porcelain, 30 mL crucible with 0.1 mg accuracy. Determine the mass of the covered high-form porcelain crucible. Remove the cover and place the crucible in a muffle furnace.

2 Gradually bring the temperature in the furnace to 370°C and maintain it for 1 h and then ash the sample either at 550°C for 16–20 h (Andrejko et al. 1983) or at 600°C for 6 h (Goldin 1987).

3 Remove the crucible from the furnace, cover, place it in a desiccator, allow to cool, and weigh with 0.1 mg accuracy. Save the crucible and its contents for metal ion determination.

28.3.4 Calculation

Calculate the ash content as follows:

$$\text{Ash, g/100 g} = [(a - c)/(b - c)] \times 100 \tag{28.2}$$

where a is the final weight (g) of crucible and ash; b is the weight (g) of crucible and sample; and c is the weight (g) of empty crucible.

The procedure described above can be used to determine the amount of organic matter as follows:

$$\%\ \text{Organic matter} = 100 - \%\ \text{mineral content (ash)} \tag{28.3}$$

28.3.5 Comments

1 Using the above procedure for determining ash content it has been shown by Andrejko et al. (1983) that a temperature setting of 550°C is satisfactory for most purposes. The standard method approved by the ASTM Committee (ASTM 1997) proposes a temperature setting of 440°C and heating until the sample is completely ashed (no change of mass occurs after a further period of heating).

2 Dry ashing may overestimate the amount of organic matter in the soil. Positive errors are dependent on soil properties, such as the amount of carbonates and the amount and type of clay present in the mineral fraction of the soil (Goldin 1987).

3 The procedure outlined above measures the mass percentage of ash and organic matter in organic soil, including moss, humus, and reed–sedge types (Day et al. 1979).

4 Samples should be placed in the muffle furnace cold and the temperature allowed to rise slowly to avoid volatilization losses, which are aggravated by violent deflagration.

5 Use high-form porcelain crucibles with covers or equivalent if ashes are retained for elemental analysis. These crucibles eliminate possible contamination of the ash by boron, which may volatilize from the furnace walls (Williams and Vlamis 1961).

6 Values derived from loss-on-ignition results should only be considered as approximate (Allen 1989).

28.4 TOTAL ELEMENT ANALYSIS (ELEMENTS OTHER THAN NITROGEN, CARBON, OXYGEN, AND HYDROGEN)

28.4.1 Introduction

Most methods that have been developed for the determination of total elements in organic soils involve a two-step procedure, namely: (i) the complete destruction of both organic and inorganic fractions of the soil matrix by various digestion/oxidation procedures in order to liberate all elements in solution and (ii) the determination of soluble elements by various techniques. The chemical procedure involved in the destruction of organic materials (peat, plants, sediments, soils) falls basically into two groups: (a) dry-ashing methods and (b) wet-ashing (or digestion) methods.

In the dry-ashing procedure, the organic material is ignited in an electrically controlled temperature muffle furnace with fume disposal at low (400°C) or medium temperature (550°C–660°C) to oxidize organic matter and the ions are extracted from the ash with an acid solution: 1.5 *M* HCl (Ali et al. 1988), 6 *M* HCl (Kreshtapova et al. 2003), or 2 *M* HNO_3 (Day et al. 1979). Dry-ashed sample may be heated on a hot plate with dilute HCl to dissolve the residues and then with concentrated hydrofluoric (HF) acid to destroy any silicates present (Papp and Harms 1985).

Wet digestion involves complete dissolution of the organic material to convert elements to soluble forms by heating with concentrated acids in either open or closed vessels. This phase is then followed by determination of the liberated ions. Dissolution technique can be performed by hot plate, hot block digestion, or pressured digestion systems. Open or closed vessels can be used in microwave systems while open vessels are usually used in block digestion. Disadvantages of open vessel digestion systems include the greater risk of loss of volatile elements. Microwave digestion is a commonly used practice in many laboratories. Important variables in a microwave digestion procedure are the microwave energy power profiles (power, time, and pressure), the volume and combination of acids used, and the acid-to-sample ratio.

Recently, a new wet digestion procedure for the determination of As in biomasses, coal, and organic-rich sediment samples using hydride generation–atomic fluorescence spectrometry (HG–AFS) has been developed (Chen et al. 2005). This method involves digestion of 200 mg sample aliquots with 3 mL HNO_3 (65%) + 0.1 mL HBF_4 (~50%), heating in a microwave autoclave up to a temperature of 240°C. After digestion, no evaporation of HNO_3 to remove acid from the digests is needed before arsine generation can be carried out.

The following microwave acid digestion procedure is a modification and synthesis from methods proposed by Papp and Harms (1985), Weiss et al. (1999), and Morrell et al. (2003). It employs microwave heating of the sample, first in $HNO_3 + H_2O_2$ to oxidize organic matter and then in HNO_3 + HF to decompose any remaining organic material and complete dissolution of the inorganic fractions of the peat or organic soil. The first gentle phase of the digestion program, the organic, carbon-rich matrix components are slowly converted to CO_2 to avoid foaming (Krachler et al. 2002).

28.4.2 Materials

1 Microwave oven-assisted sample digestion system, with closed vessels

2 Nitric acid (HNO_3), concentrated (trace metal grade), 65%

3 Hydrogen peroxide (H_2O_2), 30%

4 Hydrofluoric acid (HF), 40% or 48%, as recommended by the instrument manufacturer

5 Polyfluoroethylene (PTFE) Teflon vessels

6 Polypropylene volumetric flask, 50 mL

7 Screw-capped polypropylene bottles, 60 mL

28.4.3 Procedure

1 Weigh a 250 mg of air-dried and finely ground soil (100 mesh) of known moisture content in a 60 mL Teflon digestion tube with a cap.

2 Add 4 mL of trace metal-grade concentrated HNO_3 and 1 mL of H_2O_2.

3 Place the vessel in the microwave and digest the soil for 30 min at 296 W.

4 Seal the vessel with the cap and digest for 15 min at 296 W.

5 Cool for approximately 35 min well below the boiling point of the acid at atmospheric pressure, and then open the reaction chamber.

6 Add 4 mL concentrated HNO_3 + 1 mL concentrated HF. Seal the vessel with the cap and digest as follows: 4 min at 250 W, 8 min at 565 W, 4 min at 450 W, 4 min at 350 W, 5 min at 250 W, and vent for 35 min. Other operating power and temperature parameters can be set as specified by the instrument manufacturer.

7 After cooling, loosen the vessel cap in order to expel the interior gas into a fume hood. Remove the cap and allow the vessel to stand for ca. 2 min to remove any further gas.

8 Transfer the tube contents into a 50 mL polypropylene volumetric flask. Wash the inside of the tube and cap, and adjust the volume to 50 mL with distilled/deionized water. A colorless digestion solution is an indication of efficient destruction of the organic matter.

9 Store the sample solutions in 60 mL screw-capped polypropylene bottles before analysis for metals and other elements of interest.

10 Perform a blank containing all reagents used in the sample digestion.

28.4.4 Comments

1 This procedure does not purport to address all of the safety problems associated with its use. It is the responsibility of the user of this procedure to establish appropriate safety and health practices and determine the applicability of regulatory limitations before use. The analyst should read carefully all warnings

and follow all hints and instructions provided with the instruction manual issued by the instrument manufacturer to ensure correct and safe operation of the instrument.

2 Peat samples containing mixtures of fine-grained matter and plant or fibrous material should be dried in an oven at 50°C and then mixed thoroughly in a low-speed blender to preserve all parts of the sample. To achieve the proper homogeneity with the use of small amounts of samples, dried soil or peat samples have to be ground to pass through 100 mesh sieve. The portion left on the sieve should be ground again for a short period, sieved, and so on until the complete sample could pass through the sieve.

3 All vessels have to be checked for metals and other elements contamination before use. Avoid using commercial detergents containing phosphate or other elements. The reagents and filter paper selected should be as free of metals and P as possible. It is essential to use reagents and distilled water of suitably low metal content, taking into consideration that the concentrated mineral acids are generally used in amounts several times that of the sample.

4 Low sample amounts may result in a good decomposition result, but may impair the analytical accuracy. Excessive sample amounts may lead to a poor decomposition result.

5 Add the nitric acid slowly, with swirling, to the sample. More HNO_3 may be needed to achieve the complete oxidation of organic matter. Nitric acid may react violently with some samples containing high organic material. Hydrogen peroxide has a high oxidization potential and can produce very strong reactions.

6 Addition of acids and sample digestion must be conducted in a fume hood with adequate ventilation.

7 Hydrofluoric acid is normally used in the acid mixture to dissolve silicates, which are present in the samples and more HF will be required for the decomposition of peat or organic soils high in silicate minerals. However, HF can give rise to problems in glassware and torch damage of some spectrometers, in particular inductively coupled plasma–mass spectrometry (ICP–MS) (Melaku et al. 2005). This problem can be avoided by using an HF-resistant nebulizing system and plasma torch (Swami et al. 2001). Special safety instructions must be observed when handling HF. Avoid the use of Pyrex glass materials or quartz vessels.

8 In the HNO_3/HF treatment, some elements such as Ca, Mg, Al, and rare earth elements may form insoluble fluorides that easily precipitate (Krachler et al. 2002; Wang et al. 2004); H_3BO_3 solution is often added to digestion mixtures to dissolve slightly soluble fluorides. In such cases, proceed as follows: add 10 mL of H_3BO_3 solution (5%, m/v) per 1 mL of HF (Swami et al. 2001) to the decomposed sample (step 7), seal the vessel again and subject it to a second decomposition run at high temperature or power rating for 10–15 min. After cooling, loosen the vessel cap in order to expel the interior gas into a fume hood. Remove the cap and allow the vessel to stand for ca. 2 min to remove any further gas. In cases of incomplete dissolution, continue to microwave until the sample is dissolved. Transfer the sample to a polypropylene volumetric flask and dilute with distilled/deionized

water to a fixed volume of 50 mL. This dissolution method is not suited for the determination of B in the soil digest.

9 Selection of the most suitable digestion method must be based on local requirements and facilities. Digestion mixture options include: $HNO_3 + HClO_4 + HF$ (Papp and Harms 1985), $HNO_3 + H_2O_2 + HF$ and $HNO_3 + H_2O_2 + HClO_4 + HF$ (Weiss et al. 1999), $HNO_3 + HBF_4$ (Krachler et al. 2002), $HNO_3 + HCl$ and $HNO_3 + HCl + HF$ (Burt et al. 2003), $HNO_3 + HClO_4$; hot plate, microwave or block digestion, open or closed vessel. An $HNO_3 + HClO_4$ treatment of peat or soil samples is not always complete and a residue (siliceous materials) might remain. Filtration using Whatman No. 42 filter paper is desirable to keep the solution free of solid particles that cause clogging of the capillary tip of spectrometers. Acid digestion procedure using $HClO_4$ requires a $HClO_4$ fume hood. Perchloric acid is a very strong oxidizing agent that bears many risks and should not be used alone, but only in combination with other acids. As a safety precaution, it is recommended that organic samples be digested in HNO_3 before proceeding with $HNO_3/HClO_4$ digestion. Only use $HClO_4$ in microwave oven for processes that have been approved by the manufacturer. Perchloric acid can react with explosive force if the digestion mix approaches dryness. In general, perchlorates are easily soluble and the use of $HClO_4$ can considerably reduce the amount of HNO_3 required and complete the oxidation in a shorter time.

10 The analyst may use a suitable dilution factor depending on the detection limit of the instrument and the concentration of the element.

11 Metals in the digestion solution may be determined by atomic absorption spectroscopy (AAS) and La is added to the extracting solution (Ca and Mg determinations) as a suppressant. Sodium and potassium are commonly determined on a flame emission spectrophotometer. Low content at ppb level of some elements may be determined by using graphite furnace atomic absorption spectroscopy (GFAAS). The majority of elements may be determined by inductively coupled plasma–atomic emission spectrometry and –mass spectrometry (ICP–AES and ICP–MS). Selenium can be determined by using a hydride-generating system attached to an ICP emission spectrometer. If B is one of the elements of interest, it should be determined in H_3BO_3-free digestion solution. Phosphorus, sulfur, and boron may be determined by spectrophotometric methods.

REFERENCES

Ali, M.W., Zoltai, S.C., and Radford, F.G. 1988. A comparison of dry and wet ashing methods for the elemental analysis of peat. *Can. J. Soil Sci.* 68: 443–447.

Allen, S.E. 1989. *Chemical Analysis of Ecological Materials*, 2nd edn. Blackwell Scientific Publications, Oxford, UK.

Anderson, D.L. and Beverly, R.B. 1985. The effects of drying upon extractable phosphorus, potassium and bulk density of organic and mineral soils of the Everglades. *Soil Sci. Soc. Am. J.* 49: 362–366.

Andrejko, M.J., Fiene, F., and Cohen, A.D. 1983. Comparison of ashing techniques for determination of inorganic content of peats. In P.M. Jarret, Ed. *Testing of Peats and Organic Soils*. ASTM STP 820. American Society for Testing and Materials, Philadelphia, PA, pp. 5–20.

ASTM (American Society for Testing and Materials). 1988 (02974). *Annual Book of ATM Standards*, Volume 04.08. ASTM, Philadelphia, PA.

ASTM (American Society for Testing and Materials). 1997. *Annual Book of ATM Standards*, Volume 11.05. ASTM, Philadelphia, PA.

Burt, R., Wilson, M.A., Mays, M.D., and Lee, C.W. 2003. Major and trace elements of selected pedons in the USA. *J. Environ. Qual.* 32: 2109–2121.

Chen, B., Krachler, M., Gonzalez, Z.I., and Shotyk, W. 2005. Improved determination of arsenic in environmental and geological specimens using HG–AFS. *J. Anal. At. Spectrom.* 20: 95–102.

Daughtrey, Z.W., Gilliam, J.W., and Kamprath, E.J. 1973. Soil test parameters for assessing plant-available P of acid organic soils. *Soil Sci.* 115: 438–446.

Day, J.H., Rennie, P.J., Stanek, W., and Raymond, G.P. 1979. Peat testing manual. Associate committee on geotechnical research. National Research Council of Canada. Technical Memorandum No. 125, Ottawa, Canada.

Goldin, A. 1987. Reassessing the use of loss-on-ignition for estimating organic matter content in noncalcareous soils. *Commun. Soil Sci. Plant Anal.* 18: 1111–1116.

Harrison, A.F. 1979. Variation of four phosphorus properties in woodland soils. *Soil Biol. Biochem.* 11: 393–403.

Ilnicki, P. and Zeitz, J. 2003. Irreversible loss of organic soil functions after reclamation. In L.-E. Parent and P. Ilnicki, Eds. *Organic Soils and Peat Materials for Sustainable Agriculture*. CRC Press, Boca Raton, FL, pp. 15–32.

Krachler, M., Mohl, C., Emons, H., and Shotyk, W. 2002. Analytical procedures for the determination of selected trace elements in peat and plant samples by inductively coupled plasma mass spectrometry. *Spectrochim. Acta*, Part B, 57: 1277–1289.

Kreshtapova, V.N., Krupnov, R.A., and Uspenskaya, O.N. 2003. Quality of organic soils for agricultural use of cutover peatlands in Russia. In L.-E. Parent and P. Ilnicki, Eds. *Organic Soils and Peat Materials for Sustainable Agriculture*. CRC Press, Boca Raton, FL, pp. 175–186.

Melaku, S., Dams, R., and Moens, L. 2005. Determination of trace elements in agricultural soil samples by inductively coupled plasma–mass spectrometry: microwave acid digestion versus aqua regia extraction. *Anal. Chim. Acta* 543: 117–123.

Mokma, D.L. 2005. Organic soils. In D. Hillel, J.L. Hatfield, D.S. Powlson, C. Rosenzweig, K.M. Scow, M.J. Singer, and D.L. Sparks, Eds. *Encyclopedia of Soils in the Environment*, Vol. 3. Elsevier Academic Press, Amsterdam, pp. 118–129.

Morrell, J.J., Keefe, D., and Baileys, R.T. 2003. Copper, zinc, and arsenic in soil surrounding Douglas-Fir poles treated with ammoniacal copper zinc arsenate (ACZA). *J. Environ. Qual.* 32: 2095–2099.

Okruszko, H. and Ilnicki, P. 2003. The moorsh horizons as quality indicators of reclaimed organic soils. In L.-E. Parent and P. Ilnicki, Eds. *Organic Soils and Peat Materials for Sustainable Agriculture*. CRC Press, Boca Raton, FL, pp. 1–14.

Papp, C.S.E. and Harms, T.F. 1985. Comparison of digestion methods for total elemental analysis of peat and separation of its organic and inorganic components. *Analyst* 110: 237–242.

Parent, L.E. and Khiari, L. 2003. Nitrogen and phosphorus balance indicators in organic soils. In L.-E. Parent and P. Ilnicki, Eds. *Organic Soils and Peat Materials for Sustainable Agriculture*. CRC Press, Boca Raton, FL, pp. 105–136.

Soil Survey Staff. 2003. *Keys to Soil Taxonomy*, 9th edn. USDA. Natural Resources Conservation Service, Washington, DC.

Swami, K., Judd, C.D., Orsini, J., Yang, K.X., and Husain, L. 2001. Microwave assisted digestion of atmospheric aerosol samples followed by inductively coupled plasma mass spectrometry determination of trace elements. *Fresen. J. Anal. Chem.* 369: 63–70.

van Lierop, W. and Mackenzie, A.F. 1977. Soil pH and its application to organic soils. *Can. J. Soil Sci.* 57: 55–64.

Wang, J., Nakazato, T., Sakanishi, K., Yamada, O, Tao, H., and Saito, I. 2004. Microwave digestion with HNO_3/H_2O_2 mixture at high temperatures for determination of trace elements in coal by ICP–OES and ICP–MS. *Anal. Chim. Acta* 514: 115–124.

Watson, M.E. and Isaac, R.A. 1990. Analytical instruments for soil and plant analysis. In R.L. Westerman, Ed. *Soil Testing and Plant Analysis*, 3rd edn. Soil Science Society of America, Madison, WI, pp. 691–740.

Weiss, D., Shotyk, W., Schäfer, H., Loyall, U., Grollimund, E., and Gloor, M. 1999. Microwave digestion of ancient peat and determination of Pb by voltammetry. *Fresen. J. Anal. Chem.* 363: 300–305.

Williams, D.E. and Vlamis, J. 1961. Boron contamination in furnace dry ashing of plant material. *Anal. Chem.* 33: 967–968.

IV. SOIL BIOLOGICAL ANALYSES

Section Editors: E. Topp and C.A. Fox

Chapter 29
Cultural Methods for Soil and Root-Associated Microorganisms

J.J. Germida and J.R. de Freitas
University of Saskatchewan
Saskatoon, Saskatchewan, Canada

29.1 INTRODUCTION

Soil is an ecosystem that contains a variety of microbial populations whose members represent many physiological types. For example, some microorganisms, such as fungi, are aerobic chemoorganotrophs (heterotrophs) and use organic compounds as a source of carbon and energy. Others, such as nitrifying bacteria, are aerobic chemolithotrophs (autotrophs) using CO_2 as a carbon source and oxidizing reduced inorganic N compounds to obtain energy. Some microorganisms require special growth factors, a specific environmental pH, low O_2 levels, or the absence of O_2 (i.e., anaerobes) for optimum growth. The chemical, physical, and biological characteristics of a particular soil, as well as the presence of growing plants, will influence the numbers and activities of its various microbial components. Furthermore, because of the heterogeneous nature of soil, many different physiological types of organisms will be found in close proximity to one another. The microbial community in soil is important because of its relationship to soil fertility and the biogeochemical cycling of elements, and the potential use of specific members for industrial applications. Thus, there is a need to enumerate and isolate major and minor members of the microbial community in soils.

The nonselective enumeration and isolation of soil microorganisms is relatively straightforward, but the final result is not necessarily meaningful (Parkinson et al. 1971; Wollum 1994). On the other hand, selective enumeration and isolation of specific physiological types of microorganisms can provide useful and meaningful data (e.g., Lawrence and Germida 1988; Germida 1993; Koedam et al. 1994). Methods to enumerate and isolate soil microorganisms are constantly changing as our knowledge of the types of microorganisms present in soil expands (Vincent 1970; Woomer 1994; Pepper and Gerba 2005). This chapter provides basic principles and references on enumeration procedures and culture media for representative types of soil microorganisms.

29.2 PRINCIPLES

Enumeration of viable soil microorganisms may be accomplished by the plate count technique or most probable number (MPN) technique. The underlying principles are (i) dispersing of a sample in a suitable diluent, (ii) distributing an aliquot to an appropriate growth medium, (iii) incubating inoculated plates under suitable conditions, and (iv) counting the developed colonies or MPN tubes. These procedures are fairly standard and may be used to enumerate populations in bulk (Germida 1993) and rhizosphere (Goodfellow et al. 1968; Kucey 1983) soils along with root-associated and endophytic populations (Germida et al. 1998).

The composition of the growth medium used to enumerate microbial populations is important as it will affect the final result. Growth media may be selective or nonselective, although no medium is truly nonselective (James 1958). Selective media contain components, which allow or favor the growth of a desired group of organisms. Nonselective media should encourage growth of as many diverse groups of organisms as possible. To enumerate a specific physiological type of microorganism it is usually possible to design a growth medium which, when incubated under appropriate conditions of atmosphere and temperature, reduces interference from nondesired populations. For example, chitin-degrading actinomycetes may be enumerated on medium containing chitin as the sole source of carbon and nitrogen (Lingappa and Lockwood 1962; Hsu and Lockwood 1975), and inclusion of specific antibiotics prevents growth of undesired organisms (Williams and Davies 1965). Similar selective media are available for many different soil microorganisms, e.g., phosphate-solubilizing bacteria (Kucey 1983), siderophore-producing microorganisms (Koedam et al. 1994), free-living nitrogen-fixing bacteria (Rennie 1981; Knowles and Barraquio 1994), nitrifying bacteria (Schmidt and Belser 1994), or sulfur-oxidizing organisms (Postgate 1966; Germida 1985; Lawrence and Germida 1988).

Although the plate count and MPN techniques are simple to perform, their usefulness will be limited by a number of key factors (Germida 1993; Wollum 1994; Woomer 1994). Many times choice of media, problems with dispersion, and even adsorption of microbes to pipette walls can interfere with standardization of these procedures. It should be pointed out that consistency and adequate use of replicate samples will help to minimize some of these problems. Investigators must realize that microorganisms are not uniformly dispersed within the soil environment, and that numbers of any particular microorganism are not synonymous with its importance.

29.3 SPREAD PLATE-COUNTING METHOD

Enumeration of microbial populations by the spread plate method is a simple and rapid method to count viable microbial cells in soil. However, counts obtained are generally 10- to 100-fold less than those determined by microscopic counts of soil smears (Skinner et al. 1952). Reasons for this discrepancy include measurement of viable and nonviable counts in soil smears, and the inability to provide adequate or appropriate nutrients in the growth media for spread plate counts (Germida 1993). Basically, this method consists of preparing a serial dilution (e.g., 1:10 dilutions) of a soil sample in an appropriate diluent, spreading an aliquot of a dilution on the surface of an agar medium, and incubating the agar plate under appropriate environmental conditions. These spread plates may be used not only for counting microbial populations but also as a starting source for isolation of organisms. In this latter case, an isolated colony is picked and repeatedly streaked on a suitable growth medium to check for purity. After several such transfers it may be cultured and preserved for future

study and identification. Selective or nonselective media may be used, depending on the nature of the desired microorganisms. Soil extract agar (James 1958) is commonly used as a nonselective medium for enumerating soil bacteria. Recently proposed alternatives to soil extract agar include a defined ''soil solution equivalent medium'' (Angle et al. 1991), ''trypticase soy agar and/or R2A medium''—two commercially available complex media (Martin 1975; Reasoner and Geldreich 1985).

29.3.1 Materials

1 Petri plates containing ca. 20 mL of an appropriate agar medium, e.g., soil extract agar

2 Dilution bottles (e.g., 50×160 mm; 200 mL capacity) and (or) test tubes (e.g., 18×150 mm) containing appropriate diluent such as sterile tap water

3 Sterile 1 and 10 mL pipettes

4 Glass spreader (i.e., glass rod shaped like a hockey stick)

5 Glass beaker containing 95% ethanol (ETOH)

29.3.2 Preparation of Agar Petri Plates

1 Agar media may be prepared from commercially available dehydrated components or from recipes found in the literature. The American Type Culture Collection (2005) and Atlas (1995) are an excellent source of media recipes and relevant references. Prepare media according to directions, sterilize in the autoclave at 1.05 kg cm^{-2} and 121°C for 20 min, cool to a pouring temperature of ca. 48°C. Some components of a medium may be heat labile and must be filter-sterilized and then added to the autoclaved agar medium (cooled to ca. 48°C–49°C) just before pouring plates.

2 Distribute ca. 20 mL of media into sterile glass or disposable, presterilized plastic Petri plates and allow the agar to solidify. The plates should be allowed to sit at room temperature for 24–48 h, allowing excess surface moisture to be absorbed into the agar; this helps prevent microbial colonies from spreading over the agar surface. Poured plates not used immediately may be stored under refrigeration (2°C–5°C) for up to 2 weeks in plastic bags. These stored plates should be removed and allowed to warm to room temperature before use.

29.3.3 Preparation of Soil Dilutions

1 Samples should be collected, handled, and stored with due consideration to their ultimate use, and the effects these steps will have on microbial populations.

2 Pass representative soil samples through a 2 mm mesh sieve and mix thoroughly.

3 Weigh out a 10.0 g portion of the soil into a dilution bottle containing 95 mL of a diluent. Glass beads (ca. 25×2 mm beads) may be added to this dilution blank to facilitate mixing. Cap the bottle, place on a mechanical shaker, and shake for

10 min. Alternatively, shake by hand moving the bottle through specified arc a number of times (e.g., a 45° arc at least 50–100 times). This first dilution represents a 1:10 or a 10^{-1} dilution.

4 After removing the bottle from the shaker, shake vigorously before removing aliquots. To prepare a serial 1:10 dilution series of the soil sample, transfer a 10 mL sample to a 90 mL dilution blank cap and shake the dilution bottle (alternatively it is possible to transfer 1 mL samples to 9 mL dilution blanks [prepared in 18 × 150 mm test tubes]). Continue this sequence until a dilution of 10^{-7} is reached. Subsequent spread plating of a 0.1 mL aliquot of this dilution will allow enumeration of up to 3×10^{10} colony-forming units (cfu) per g soil. Experience will indicate the appropriate range of dilutions for samples being analyzed.

29.3.4 Preparation of Dilutions from Root-Associated Bacteria

For bacteria isolation from the root interior (endophytic), root material is collected from soil and maintained at ca. 5°C until processed in the laboratory (Foster and Rovira 1976). Approximately 10.0 g of fresh root material is shaken to eliminate adhering soil and then washed in sterile tap water. Subsequently, roots are placed in a 250 mL Erlenmeyer containing 100 mL of 1.05% sodium hypochlorite (NaClO) and shaken (200 rpm) for 10 min. Roots are washed (4×) in sterile tap water and aseptically blended in a sterile Waring blender containing 90 mL sterile phosphate buffered saline (PBS)—see recipe below. This will result in 1/10 dilution, i.e., 10.0 g roots and 90 mL sterile water. The root suspension is serially diluted in PBS and aliquots of appropriate dilutions spread plated onto selective and/or nonselective nutrient media depending on the nature of the study.

29.3.5 Preparation of Agar Spread Plates

1 Select a range of four dilutions that will adequately characterize the microorganisms in the sample. Transfer 0.1 mL aliquots to a separate plate from the highest dilution. Note that a 0.1 mL aliquot from a 10^{-7} dilution corresponds to an actual dilution of 10^{-8} on the plate. Repeat the process, transferring 0.1 mL aliquots from each of the next three successive and lower dilutions onto each of triplicate plates for each dilution.

2 Spread the suspension on the agar surface using a sterile glass spreader for each plate. The glass spreader is kept submerged in a beaker of ETOH and excess ETOH burned off before use. In the spreading step start with the highest dilution and progress to the next lower dilution, continuing the sequence until all the plates have been spread. Alcohol flame the glass spreader between each plate. Invert the plates and place in an incubator at an appropriate temperature.

3 Incubation conditions will depend on the facilities and the purpose of the study. When possible, one should try to mimic environmental conditions. Generally, spread plates samples are incubated in the dark, in an aerobic environment at a temperature between 24°C and 28°C. Incubation periods and conditions will vary depending on the nature of the organisms being enumerated.

4 After a suitable incubation interval, plates are removed from the incubator and those containing 30 to 300 colonies are counted. Plates with spreading or

swarming organisms should be excluded from the final count. The colonies can be counted manually or by an automated laser colony counter.

29.3.6 Calculations

Average the number of colonies per plate for the dilution giving between 30 and 300 colonies. Determine the number of cfu g^{-1} of dry soil (DW) as follows:

$$\text{Number of cfu g}^{-1}\ \text{soil}_{\text{DW}} = \frac{\text{(mean plate count)} \times \text{(dilution factor)}}{\text{dry weight soil, initial dilution}} \tag{29.1}$$

where

$$\text{Dry weight soil} = \text{(weight moist soil, initial dilution)} \times \left(1 - \frac{\%\ \text{moisture, soil sample}}{100}\right) \tag{29.2}$$

29.3.7 Comments

Because bacteria may exist in soil as groups or clumps of cells, it is often desirable to disperse these cells so that colonies on spread plates arise from one cell. This may be accomplished by shaking on a mechanical shaker or by hand, through application of a high shearing force as with Waring blender, by sonic vibration (Stevenson 1959), mechanical vibration (Thornton 1922), and through the use of deflocculating agents.

29.3.8 Type of Dilutions

A number of diluents may be used. In most cases, tap or distilled water is adequate. Other diluents routinely used include:

1. Physiological saline: NaCl, 8.5 g; distilled water, 1 L.
2. PBS: NaCl, 8.0 g; KH_2PO_4, 0.34 g; K_2HPO_4, 1.21 g; distilled water, 1 L. Adjust pH to 7.3 with 0.1 *M* NaOH or HCl.
3. Peptone water: Peptone, 1.0 g; distilled water, 1 L.

29.3.9 Types of Media

The choice of medium depends on the type of organism desired. Media may be made selective by omitting or altering a component, or by incubation conditions. For enumeration of total heterotrophic populations in soil, a general nonselective medium is usually employed. The following are examples of growth media commonly used to enumerate total soil bacteria, root-associated bacteria, actinomycetes, and fungi. Additional examples of specific media are described in Section 29.5.

Media for Total Heterotrophic Bacteria

1. Soil extract agar (James 1958): One kg of soil is autoclaved with 1 L of water for 20 min at 1.05 kg cm^{-2}. The liquid is strained and restored to 1 L in volume. If it is

cloudy, a little $CaSO_4$ is added and after being allowed to stand, it is filtered through Whatman paper No. 5. The extract may be sterilized and solidified with agar (1.5%) as it is, or after the addition of other nutrients, e.g., 0.025% K_2HPO_4 or 0.1% glucose, 0.5% yeast extract, and 0.02% K_2HPO_4.

2 Tryptic soy agar (Martin 1975): Add 3.0 g of tryptic soy broth and 15.0 g of agar to 1 L distilled water. Sterilize the medium by autoclaving.

3 R2A (Reasoner and Geldreich 1985): Yeast extract, 0.5 g; Proteose Peptone No. 3, 0.5 g; casamino acids, 0.5 g; glucose, 0.5 g; soluble starch, 0.5 g; K_2HPO_4, 0.3 g; $MgSO_4 \cdot 7H_2O$, 0.05 g; sodium pyruvate, 0.3 g; agar, 15.0 g; distilled water, 1 L. Adjust the pH to 7.2 with crystalline K_2HPO_4 or KH_2PO_4 and sterilize the medium by autoclaving.

Media for Actinomycetes

Starch–casein agar (Küster and Williams 1966): Starch, 10.0 g; casein (vitamin free), 0.3 g; KNO_3, 2.0 g; NaCl, 2.0 g; K_2HPO_4, 2.0 g; $MgSO_4 \cdot 7H_2O$, 0.05 g; $CaCO_3$, 0.02 g; $FeSO_4 \cdot 7H_2O$, 0.01 g; agar, 15.0 g; distilled water, 1 L; pH, 7.2. Sterilize in autoclave as described above. Media can be improved by addition of fungistatic agents (Williams and Davies 1965).

Media for Fungi

1 Czapek-Dox agar: Solution I: Sucrose, 30.0 g; $NaNO_3$, 2.0 g; K_2HPO_4, 0.1 g; KCl, 0.5 g; $MgSO_4 \cdot 7H_2O$, 0.5 g; $FeSO_4$, trace; distilled water, 500 mL; pH, 3.5 using 10% lactic acid. Solution II: Agar, 15.0 g; distilled water, 500 mL. If desired, 0.5 g of yeast extract may be added (Gray and Parkinson 1968). Sterilize solutions I and II by autoclaving separately. Cool both solutions to pouring temperature, pour solution I aseptically into solution II and use immediately.

2 Streptomycin–rose bengal agar (Martin 1950): Glucose, 10.0 g; peptone, 5.0 g; KH_2PO_4, 1.0 g; $MgSO_4 \cdot 7H_2O$, 0.5 g; rose bengal, 0.03 g; agar, 20.0 g; tap water, 1 L. Autoclave, cool medium to about 48°C and add 1 mL of a solution of streptomycin (0.3 g 10 mL^{-1} sterile water). The final concentration of streptomycin in medium should be about 30 $\mu g\ mL^{-1}$.

29.4 MOST PROBABLE NUMBER METHOD

This method employs the concept of dilution to extinction in order to estimate the number of microorganisms in a given sample (Taylor 1962; Woomer 1994). It is based on the presence or absence of microorganisms in replicate samples in each of several consecutive dilutions of soil. For example, if a series of test tubes containing broth medium are inoculated with aliquots representing a dilution series from 10^{-4} through 10^{-7}, and the highest dilution exhibiting growth is 10^{-5}, then the number of cells present may be estimated to be between 10^4 and 10^5. The key is that the desired organism must possess a unique characteristic or metabolic trait, which can be detected. Thus, this technique can be used to count microorganisms based on growth (i.e., turbidity), metabolic activity such as substrate disappearance and product formation. Other uses for the MPN technique include enumeration of infective vesicular–arbuscular mycorrhizae (VAM) propagules in soil (see Chapter 30) or nodule-forming rhizobia in soil (see Chapter 31).

To estimate total heterotrophic counts of a soil sample the MPN procedure is similar to the spread plate count method, except that aliquots of dilutions are inoculated into test tubes of liquid medium. Alternatively, multiwell microtiter plates (e.g., 24 wells per plate) may be used in place of test tubes; this allows a savings of materials, reagents, incubator space, and allows for increased replication.

29.4.1 Materials

1 Twenty five test tubes containing appropriate culture medium or 1 disposable sterile microtiter plates—24 or 96 wells per plate

2 Water dilution blanks (see Section 29.3.1)

3 Sterile 1 and 10 mL pipettes (see Section 29.3.1)

29.4.2 Procedures

1 Prepare medium appropriate for the desired organism.

2 Dispense aliquots of medium in test tubes and sterilize or dispense aliquots of sterile medium into presterile microtiter plates.

3 Prepare a serial 1:10 dilution sequence of the soil sample (see Section 29.3.2).

4 Select a range of dilutions that will adequately characterize the organisms in the sample. Transfer 0.1 mL aliquots to each separate well in five replicate microtiter plate wells, starting with the highest dilution. Repeat the procedure, transferring 0.1 mL aliquots from each of the next successive and lower dilutions into each of the five replicate wells for each dilution.

5 Incubate MPN assay tubes and/or plates under appropriate conditions.

6 After suitable incubation, score wells positive for growth or physiological reaction.

29.4.3 Calculations

The MPN of organisms in the original sample is calculated by reference to an MPN table (e.g., Cochran 1950). Designate as p_1 the number of positive tubes in the least concentrated dilution in which all tubes are positive or in which the greatest number of tubes is positive. Let p_2 and p_3 represent the numbers of positive tubes in the next two higher dilutions. Refer to Table 29.1 and find the row of numbers in which p_1 and p_2 correspond to the values observed experimentally. Follow that row of numbers across the table to the column headed by the observed value of p_3. The figure at the point of intersection is the MPN of organisms in the quantity of the original sample represented in the inoculum added in the second dilution. This figure is multiplied by the appropriate dilution factor to obtain the MPN value for the original sample.

As an example, consider the instance in which a 10-fold dilution with 5 tubes at each dilution yielded the following numbers of positive tubes after incubation: 5 at 10^{-4}, 5 at 10^{-5}, 4 at 10^{-6}, 2 at 10^{-7}, and 0 at 10^{-8}. In this series, $p_1 = 5$, $p_2 = 4$, and $p_3 = 2$. For this

TABLE 29.1 Table of Most Probable Numbers for Use with 10-Fold Dilutions and 5 Tubes per Dilution

		Most probable number for indicated values of p_3					
p_1	p_2	0	1	2	3	4	5
0	0	—	0.018	0.036	0.054	0.072	0.090
0	1	0.018	0.036	0.055	0.073	0.091	0.11
0	2	0.037	0.055	0.074	0.092	0.11	0.13
0	3	0.056	0.074	0.093	0.11	0.13	0.15
0	4	0.075	0.094	0.11	0.13	0.15	0.17
0	5	0.094	0.11	0.13	0.15	0.17	0.19
1	0	0.020	0.040	0.060	0.080	0.10	0.12
1	1	0.040	0.061	0.081	0.10	0.12	0.14
1	2	0.061	0.082	0.10	0.12	0.15	0.17
1	3	0.083	0.10	0.13	0.15	0.17	0.19
1	4	0.11	0.13	0.15	0.17	0.19	0.22
1	5	0.13	0.15	0.17	0.19	0.22	0.24
2	0	0.045	0.068	0.091	0.12	0.14	0.16
2	1	0.068	0.092	0.12	0.14	0.17	0.19
2	2	0.093	0.12	0.14	0.17	0.19	0.22
2	3	0.12	0.14	0.17	0.20	0.22	0.25
2	4	0.15	0.17	0.20	0.23	0.25	0.28
2	5	0.17	0.20	0.23	0.26	0.29	0.32
3	0	0.078	0.11	0.13	0.16	0.20	0.23
3	1	0.11	0.14	0.17	0.20	0.23	0.27
3	2	0.14	0.17	0.20	0.24	0.27	0.31
3	3	0.17	0.21	0.24	0.28	0.31	0.35
3	4	0.21	0.24	0.28	0.32	0.36	0.40
3	5	0.25	0.29	0.32	0.37	0.41	0.45
4	0	0.13	0.17	0.21	0.25	0.30	0.36
4	1	0.17	0.21	0.26	0.31	0.36	0.42
4	2	0.22	0.26	0.32	0.38	0.44	0.50
4	3	0.27	0.33	0.39	0.45	0.52	0.59
4	4	0.34	0.40	0.47	0.54	0.62	0.69
4	5	0.41	0.48	0.56	0.64	0.72	0.81
5	0	0.23	0.31	0.43	0.58	0.76	0.95
5	1	0.33	0.46	0.64	0.84	1.1	1.3
5	2	0.49	0.70	0.95	1.2	1.5	1.8
5	3	0.79	1.1	1.4	1.8	2.1	2.5
5	4	1.3	1.7	2.2	2.8	3.5	4.3
5	5	2.4	3.5	5.4	9.2	16	—

Source: From Cochran, W.G., *Biometrics*, 5, 105, 1950. With permission.

combination of p_1, p_2, and p_3, Table 29.1 gives 2.2 as the MPN of organisms in the quantity of inoculum applied in the 10^{-6} dilution. Multiplying this MPN by the dilution factor 10^6 gives 2.2 million as the MPN value for the original sample.

As a second example, consider the same situation as above except that the most concentrated dilution is 10^{-6}. Under these circumstances, $p_1 = 4$, $p_2 = 2$, and $p_3 = 0$. For this combination of p_1, p_2, and p_3, Table 29.1 gives 0.22 as the MPN of organisms in the quantity of inoculum applied in the 10^{-7} dilution. Multiplying 0.22 by 10^7 yields 2.2 million organisms as the MPN value for the original sample, as before.

TABLE 29.2 Factors for Calculating the Confidence Limits for the Most Probable Number Count

Number of tubes per dilution (*n*)	Factor for 95% confidence limits with indicated dilution ratios			
	2	**4**	**5**	**10**
1	4.00	7.14	8.32	14.45
2	2.67	4.00	4.47	6.61
3	2.23	3.10	3.39	4.68
4	2.00	2.68	2.88	3.80
5	1.86	2.41	2.58	3.30
6	1.76	2.23	2.38	2.98
7	1.69	2.10	2.23	2.74
8	1.64	2.00	2.12	2.57
9	1.58	1.92	2.02	2.43
10	1.55	1.86	1.95	2.32

Source: From Cochran, W.G., *Biometrics*, 5, 105, 1950. With permission.

The 95% confidence limits for MPN values can be calculated from prepared tables. A compilation of factors keyed to rate of dilution and to number of tubes per dilution is shown in Table 29.2. To find the upper confidence limit at the 95% level, multiply the MPN value by the appropriate factor from the table. To find the lower limit, divide the MPN value by the factor. In the first example above, the factor is 3.30, and the confidence limits are

$$(2.2)(3.30) = 7.26$$

and

$$(2.2)/(3.30) = 0.66.$$

29.4.4 Comments

The MPN method is usually employed to enumerate and isolate organisms that will not readily grow on solid agar medium, or those that cannot be readily identified from the background community. For example, autotrophic-nitrifying bacteria (Schmidt and Belser 1994) and sulfur-oxidizing bacteria (Postgate 1966; Germida 1985; Lawrence and Germida 1988) are routinely enumerated using the MPN assay. The medium employed may be used to measure total growth, and hence optical density is satisfactory measurement. Alternatively, a physiological reaction may be monitored. For example, oxidation of sulfur to an acidic end product will alter pH and the difference may be recorded by using an appropriate pH indicator. The procedure may be used to provide a relative estimate of the numbers of many diverse physiological groups of organisms in soils. Choice of media and incubation conditions is limited only by our knowledge of specific physiological groups.

29.5 MEDIA FOR THE ENUMERATION AND ISOLATION OF SOIL MICROORGANISMS (GRAY AND PARKINSON 1968)

29.5.1 Media for Isolation Heterotrophic Bacteria

1 Peptone yeast extract agar (Goodfellow et al. 1968): Peptone, 5.0 g; yeast extract, 1.0 g; $FePO_4$, 0.01 g; agar, 15.0 g; distilled water, 1 L; pH, 7.2.

2 Nutrient agar: Yeast extract, 1.0 g; beef extract, 3.0 g; peptone, 5.0 g; sodium chloride, 5.0 g; agar, 15.0 g; distilled water, 1 L; pH, 7.3.

3 Fluorescent pseudomonads (Sands and Rovira 1970; Simon et al. 1973): Proteose Peptone, 20.0 g; agar, 12.0 g; glycerol, 10.0 g; K_2SO_4, 1.5 g; $MgSO_4 \cdot 7H_2O$, 1.5 g; distilled water, 940 mL. Adjust pH to 7.2 with 0.1 *M* NaOH before autoclaving. Sterilize by autoclaving. Add 150,000 units of penicillin G, 45 mg of novobiocin, 75 mg of cycloheximide, and 5 mg of chloramphenicol to 3 mL of 95% ethanol. Dilute to 60 mL with sterile distilled water, and add (filter-sterilized using a sterile 0.45 μm Millipore filter) to the cooled (48°C) medium before pouring. Prepared plates should be dried overnight before using and may be stored in the refrigerator for several weeks before use.

29.5.2 Media for Isolation of Specific Physiological Groups of Organisms

Microorganisms Involved in Carbon Transformations

1 Cellulose agar (Eggins and Pugh 1961): $NaNO_3$, 0.5 g; K_2HPO_4, 1.0 g; $MgSO_4 \cdot 7H_2O$, 0.5 g; $FeSO_4 \cdot 7H_2O$, 0.01 g; cellulose (ball-milled), 12.0 g; agar, 15.0 g; distilled water, 1 L.

2 Chitin agar: Ball-milled, purified chitin, 10.0 g; $MgSO_4 \cdot 7H_2O$, 1.0 g; K_2HPO_4, 1.0 g; agar, 15.0 g; distilled water, 1 L.

3 Starch agar: 0.2% soluble starch may be added to any suitable growth medium as an alternative or additional carbohydrate. Starch hydrolysis is shown by flooding incubated plates with an iodine solution and then noting clear zones.

Microorganisms Involved in Nitrogen Transformations

1 Combined carbon medium—Free-living putative nitrogen-fixing bacteria (Rennie 1981): Solution I: K_2HPO_4, 0.8 g; KH_2PO_4, 0.2 g; $Na_2FeEDTA$, 28.0 mg; $Na_2MoO_4 \cdot 2H_2O$, 25.0 mg; NaCl, 0.1 g; yeast extract, 0.1 g; mannitol, 5.0 g; sucrose, 5.0 g; Na-lactate (60% v/v), 0.5 mL; distilled water, 900 mL; agar, 15.0 g. Solution II: $MgSO_4 \cdot 7H_2O$, 0.2 g; $CaCl_2$, 0.06 g; distilled water, 100 mL. Solution III: Biotin, 5.0 μg mL^{-1}; *p*-aminobenzoic acid (PABA), 10.0 μg mL^{-1}. Autoclave solutions I and II, cool to 48°C and mix thoroughly, then add (filter-sterilized using a sterile 0.45 μm filter) 1 mL L^{-1} of solution III.

2 *Azotobacter* enrichment broth: $MgSO_4 \cdot 7H_2O$, 0.2 g; K_2HPO_4, 1.0 g; $FeSO_4 \cdot 7H_2O$, 0.02 g; $CaCl_2$, 0.02 g; $MnCl_2 \cdot 7H_2O$, 0.002 g; $NaMoO_4 \cdot 2H_2O$, 0.001 g; distilled water, 1 L; pH, 7.0; ethyl alcohol (95%), 4.0 mL (add to autoclaved and cooled media).

3 *Azotobacter chroococcum* and *A. agilis* (Ashby's medium): These two *Azotobacter* species utilize mannitol as their only carbon source. $MgSO_4 \cdot 7H_2O$, 0.2 g; K_2HPO_4, 0.2 g; NaCl, 0.2 g; $CaSO_4 \cdot 7H_2O$, 0.1 g; $CaCO_3$, 3.0 g; $Na_2MoO_4 \cdot 2H_2O$, 25.0 mg; mannitol, 10.0 g; agar, 15.0 g; distilled water, 1 L. For isolation of *A. indicus*, substitute mannitol by glucose (5.0 g L^{-1}).

4 Yeast extract mannitol medium (Allen 1957): Mannitol, 10.0 g; K_2HPO_4, 0.5 g; NaCl, 0.1 g; $MgSO_4 \cdot 7H_2O$, 0.2 g; $CaCO_3$, 3.0 g; yeast extract, 0.4 g; agar, 15.0 g; distilled water, 1 L.

5 Nitrifying bacteria (Lewis and Pramer 1958): Na_2HPO_4, 13.5 g; KH_2PO_4, 0.7 g; $MgSO_4 \cdot 7H_2O$, 0.1 g; $NaHCO_3$, 0.5 g; $(NH_4)_2SO_4$, 2.5 g; $FeCl_3 \cdot 6H_2O$, 14.4 mg; $CaCl_2 \cdot 7H_2O$, 18.4 mg; distilled water, 1 L; pH, 8.0.

Microorganisms Involved in Sulfur Transformations

1 *Thiobacillus thiooxidans* or *T. thioparus* (Postgate 1966): $(NH_4)_2SO_4$, 0.4 g; KH_2PO_4, 4.0 g; $MgSO_4 \cdot 7H_2O$, 0.5 g; $CaCl_2$, 0.25 g; $FeSO_4$, 0.01 g; powdered sulfur, 10.0 g or $Na_2S_2O_7$, 5.0 g; distilled water, 1 L; pH, 7.0. This medium can be made selective for *T. thiooxidans*-like bacteria by using S° as the sulfur source and adjusting the initial pH to <3.5.

2 *T. denitrificans* (Postgate 1966): KNO_3, 1.0 g; Na_2HPO_4, 0.1 g; $Na_2S_2O_7$, 2.0 g; $NaHCO_3$, 0.1 g; $MgCl_2$, 0.1 g; distilled water, 1 L; pH, 7.0. This medium may be used for agar plates, or dispensed into test tubes containing small Durham fermentation tubes to capture gas. Incubate under anaerobic conditions.

REFERENCES

Allen, O.N. 1957. *Experiments in Soil Bacteriology*, 3rd ed. Burgess Publishing Company, Minneapolis, MN.

American Type Culture Collection 2005. Microbial media formulations, web page address: http://www.atcc.org/common/catalog/media/mediaIndex.cfm (last verified April 2006), Rockville, MD.

Angle, J.S., McGrath, S.P., and Chaney, R.L. 1991. New culture medium containing ionic concentrations of nutrients similar to concentrations found in soil solutions. *Appl. Environ. Microbiol.* 57: 3674–3676.

Atlas, R.M. 1995. *Handbook of Media for Environmental Microbiology*. CRC Press, Boca Raton, FL, 544 pp.

Cochran, W.G. 1950. Estimation of bacterial densities by means of the ''most probable number''. *Biometrics* 5: 105–116.

Eggins, H.O.W. and Pugh, G.J.F. 1961. Isolation of cellulose-decomposing fungi from soil. *Nature* (London) 193: 94–95.

Foster, R.C. and Rovira, A.D. 1976. Ultrastructure of wheat rhizosphere. *New Phytol.* 76: 343–352.

Germida, J.J. 1985. Modified sulfur containing media for studying sulfur oxidizing microorganisms. In D.E. Caldwell, J.A. Brierley, and C.L. Brierly, Eds. *Planetary Ecology*. Van Nostrand Reinhold, New York, NY, pp. 333–344.

Germida, J.J. 1993. Cultural methods for soil microorganisms. In M.R. Carter, Ed. *Soil Sampling and Methods of Analysis*. A Special Publication of the Canadian Society of Soil Science. Lewis Publishers, Boca Raton, FL, pp. 263–275.

Germida, J.J., Siciliano, S., de Freitas, J.R., and Seib, A.M. 1998. Diversity of root-associated bacteria associated with field-grown canola (*Brassica napus* L.) and wheat (*Triticum aestivum* L.). *FEMS Microbiol. Ecol.* 26: 43–50.

Goodfellow, M., Hill, I.R., and Gay, T.R.G. 1968. Bacteria in a pine forest soil. In T.R.G. Gray and D. Parkinson, Eds. *The Ecology of Soil Bacteria*. University of Toronto Press, Toronto, ON, Canada, pp. 500–515.

Gray, T.R.G. and Parkinson, D., eds. 1968. *The Ecology of Soil Bacteria*. An International Symposium. University of Toronto Press, Toronto, ON, Canada.

Hsu, S.C. and Lockwood, J.L. 1975. Powdered chitin as a selective medium for enumeration of actinomycetes in water and soil. *Appl. Microbiol.* 29: 422–426.

James, N. 1958. Soil extract in soil microbiology. *Can. J. Microbiol.* 4: 363–370.

Knowles, R. and Barraquio, W.L. 1994. Free-living dinitrogen-fixing bacteria. In R.W. Weaver et al., Eds. *Methods of Soil Analysis, Part 2—Microbiological and Biochemical Properties*. Soil Science Society of America, Madison, WI, pp. 180–197.

Koedam, N., Wittouck, E., Gaballa, A., Gillis, A., Höfte, M., and Cornelis, P. 1994. Detection and differentiation of microbial siderophores by isoelectric focusing and chrome azurol S overlay. *Biometals* 7: 287–291.

Kucey, R.M.N. 1983. Phosphate-solubilizing bacteria and fungi in various cultivated and virgin Alberta soils. *Can. J. Soil Sci.* 63: 671–678.

Küster, E. and Williams, S.T. 1966. Selection of media for isolation of streptomycetes. *Nature* (London) 202: 928–929.

Lawrence, J.R. and Germida, J.J. 1988. Most-probable number procedure to enumerate S°-oxidizing, thiosulfate producing heterotrophics in soil. *Soil Biol. Biochem.* 20: 577–578.

Lewis, R.F. and Pramer, D. 1958. Isolation of Nitrosomonas in pure culture. *J. Bacteriol.* 76: 524–528.

Lingappa, Y. and Lockwood, J.L. 1962. Chitin media for selective isolation and culture of actinomycetes. *Phytopathology* 52: 317–323.

Martin, J.K. 1975. Comparison of agar media for counts of viable soil bacteria. *Soil Biol. Biochem.* 7: 401–402.

Martin, J.P. 1950. Use of acid, rose bengal and streptomycin in the plate method for estimating soil fungi. *Soil Sci.* 69: 215–232.

Parkinson, D., Gray, T.R.G., and Williams, S.T. 1971. *Methods for Studying the Ecology of Soil Microorganisms*. IBP Handbook No. 19. Blackwell Scientific Publications, Oxford, UK.

Pepper, I.L. and Gerba, C.P. 2005. *Environmental Microbiology: A Laboratory Manual*, 2nd ed. Elsevier, Amsterdam, the Netherlands, 209 pp.

Postgate, J.R. 1966. Media for sulphur bacteria. *Lab. Pract.* 15: 1239–1244.

Reasoner, D.G. and Geldreich, E.E. 1985. A new medium for the enumeration and subculture of bacteria from potable water. *Appl. Environ. Microbiol.* 49: 1–7.

Rennie, R.J. 1981. A single medium for the isolation of acetylene-reducing (dinitrogen-fixing) bacteria from soils. *Can. J. Microbiol.* 27: 8–14.

Sands, D.C. and Rovira, A.D. 1970. Isolation of fluorescent pseudomonads with a selective medium. *Appl. Microbiol.* 20: 513–514.

Schmidt, E.L. and Belser, L.W. 1994. Autotrophic nitrifying bacteria. In R.W. Weaver et al., Eds. *Methods of Soil Analysis, Part 2—Microbiological and Biochemical Properties*. Soil Science Society of America, Madison, WI, pp. 159–179.

Simon, A., Rovira, A.D., and Sands, D.C. 1973. An improved selective medium for the isolation of fluorescent pseudomonads. *J. Appl. Bacteriol.* 36: 141–145.

Skinner, F.A., Jones, P.C.T., and Mollison, J.E. 1952. A comparison of a direct- and a plating-counting technique for the quantitative estimation of soil microorganisms. *J. Gen. Microbiol.* 6: 261–271.

Stevenson, I.L. 1959. The effect of sonic vibration on the bacterial plate count of soil. *Plant Soil* 10: 1–8.

Taylor, J. 1962. The estimation of numbers of bacteria by ten-fold dilution series. *J. Appl. Bacteriol.* 25: 54–61.

Thornton, H.G. 1922. On the development of a standardized agar medium for counting soil bacteria with special regard to the repression of spreading colonies. *Ann. Appl. Biol.* 9: 241–274.

Vincent, J.M. 1970. *A Manual for the Practical Study of the Root-Nodule Bacteria*. IBP Handbook No. 15. Blackwell Scientific Publications, Oxford, UK.

Williams, S.T. and Davies, F.L. 1965. Use of antibiotics for selective isolation and enumeration of actinomycetes in soil. *J. Gen. Microbiol*. 38: 251–261.

Wollum, A.G. II. 1994. Soil sampling for microbiological analysis. In R.W. Weaver et al., Eds. *Methods of Soil Analysis*, *Part 2—Microbiological and Biochemical Properties*. Soil Science Society of America, Madison, WI, pp. 1–14.

Woomer, P.L. 1994. Most probable number counts. In R.W. Weaver et al., Eds. *Methods of Soil Analysis*, *Part 2—Microbiological and Biochemical Properties*. Soil Science Society of America, Madison, WI, pp. 59–79.

Chapter 30
Arbuscular Mycorrhizae

Y. Dalpé
Agriculture and Agri-Food Canada
Ottawa, Ontario, Canada

C. Hamel
Agriculture and Agri-Food Canada
Swift Current, Saskatchewan, Canada

30.1 INTRODUCTION

Most plant species live in a symbiotic association with mycorrhizal fungi whose establishment in roots increases the water supply and mineral nutrition. These soil-borne fungi colonize the root cortex and develop external filaments, making connecting bridges between roots and soil. They are recognized as improving plant fitness and soil quality. Widely distributed under all ecosystems, they are the most common type of symbionts involved in agricultural systems, influencing both plant production and plant protection.

The mycorrhizal fungi can be subdivided into three major categories: (1) the arbuscular mycorrhizal (AM) fungi, obligate symbionts, which belong to the Glomeromycota associated with the majority of herbaceous and cultivated plants and with some deciduous trees, (2) the ectomycorrhizal (EM) fungi taxonomically associated with Basidiomycetes and Ascomycetes found in symbiosis mostly with trees, and (3) the ericoid mycorrhizal (ERM) fungi, a symbiosis between mainly Ascomycetes and plants from the Ericaceae family (e.g., blueberry, rhododendron, and heather-type plants).

30.2 SAMPLING STRATEGY

Several procedures used in mycorrhizal research are time consuming. Thus, sampling plans will often have to be a compromise between a desire for precision and limited resources. More intensive or targeted sampling protocols are required in heterogeneous sites to allow for the accurate measurement of variables. Therefore, knowledge of the conditions causing variation in the distribution of AM structures in soil may help develop efficient sampling plans.

Sampling strategies must be planned carefully according to the experimental goal, the conditions of the study area, and knowledge on how these conditions may influence AM fungi distribution in soil. The AM fungi occurrence in soil is largely driven by the plant

distribution. Some plant species do not host AM fungi. These non-host species are found particularly in the families Polygonaceae, Juncaceae, Brassicaceae, Caryophyllaceae, Chenopodiaceae, Amaranthaceae, Cistaceae, Pinaceae, Fagaceae, Ericaceae, and Ranunculaceae. Furthermore, different plant species may selectively augment different AM species in their surroundings, and in some plant communities, AM fungi species distribution may follow plant species distribution (Gollotte et al. 2004).

AM spore abundance generally decreases with soil depth and spores are generally absent below the root zone. Approximately 75% of the AM spores and hyphae found in tilled and no-tilled fields in eastern Canada are found in the top 15 cm of the soil, but these structures are still present at 20–25 cm depth (Kabir et al. 1998b). Very few propagules are found below 40–50 cm (Jakobsen and Nielsen 1983). AM populations at depth are not only thinner, but their composition may also differ from that of the top soil populations. These populations may be more stable than those in the top soil layer, which is influenced by crop management (Oehl et al. 2005). AM fungi tend to follow plant root distribution and, in row crops, they are more abundant under the row than in between rows (Kabir et al. 1998a). AM root colonization development is a three-phase process including a lag phase, an exponential phase, and a plateau (McGonigle 2001). The length of the lag phase depends on the mycorrhizal potential of the soil and the mycorrhizal dependency of the host plant and may be increased by lower soil temperature. For example, root colonization peaks at flowering in maize and decreases thereafter up to host senescence (Kabir et al. 1998a).

Sampling strategy must be adapted to the requirements of the problems studied. The evaluation of AM biodiversity under mixed plant populations would require that samples be taken in the vicinity of all plant species. The evaluation of the abundance of AM fungi in a given area would require a more random sampling plan. For example, a stratified random sampling plan would be the most efficient strategy to generate a soil sample representative of an experimental monocultured plot at a given point in time. This procedure is given below.

30.2.1 Materials and Reagents

1 Labeled plastic bags

2 Graduated bulb planter or soil probe

3 Bucket

30.2.2 Procedure

1 Take an equal number of soil cores at random in each of the following predetermined zones: (a) directly on the row and (b) in between rows. In crops with wide interrows, one may decide to sample (a) on the row, (b) between rows, and (c) midpoint between the row and midrow. The number of separate sampling sets will depend on plot size and homogeneity.

2 Place cores in a bucket as you go, up to completion of the plot sampling exercise.

3 Pour the content of the bucket into an appropriately labeled plastic bag. The soil cores can be conveniently pooled to produce a single representative sample for a plot, which can be sieved, mixed, and subsampled for different analyses.

4 Avoid leaving plastic bags with their contents under the sun as they may heat up quickly. The use of coolers is recommended.

30.2.3 Comments

Soils are commonly sampled to 15 cm depth, but the selection of a sampling depth may be based on specific considerations. For example, one may like to sample the plow layer, i.e., the top 20, 15, or 7.5 cm, depending on the tillage system used, or up to a known rooting depth. The number of cores required depends on the core size—the larger the core the smaller the number of samples—and site uniformity. Heterogeneous sites require more intensive sampling. In an apparently homogeneous field plot, it is advisable to take at least three core sets if a large core is used (e.g., a bulb planter). Using a soil probe, 10–12 cores can rapidly be taken from a plot and mixed in a bucket.

30.3 DETERMINATION OF ROOT COLONIZATION BY STAINING

Root clearing and staining reveal the intraradical phase of AM fungi and allow the evaluation of the extent of AM root colonization. Clearing is usually done by boiling root samples in a solution of KOH on a hot plate or in the autoclave, to remove alkali-soluble tannins. Tender roots like those of cucumber, corn, or onion may require only 5–10 min, whereas clearing some tree roots may require more than 1 h in a boiling 10% KOH solution. Roots can be cleared at room temperature as well. This method produces high quality root material, but requires several hours or days of soaking in the KOH solution. Further soaking in 30% H_2O_2 (Phillips and Hayman 1970) or in 3% NaOCl acidified with a few drops of 5 *M* HCl (Bevege 1968) solutions has also been used to remove some residual tannins in roots that are difficult to clear.

Staining solutions have evolved along a decreasing toxicity gradient from being lactophenol-based (Phillips and Hayman 1970) to lactoglycerol-based (Brundrett et al. 1994) and household vinegar-based (Vierheilig et al. 1998) or mild acids such as dilute hydrochloric acid (HCl) or even tonic water (Walker 2005). At last, ordinary permanent ink has been proposed as a replacement for possibly carcinogenic stains, such as chlorazol black E, trypan blue, and acid fuchsin (Vierheilig et al. 1998). The ink and vinegar staining technique is given here, as it is a safe and inexpensive method. Staining with trypan blue is given as an alternative. The performance of different stains varies with the quality of the AM root material under evaluation and with the plant species. Information on other commonly used stains can be found in an article by Brundrett et al. (1984) who compared the performance of chlorazol black E, trypan blue, acid fuchsin, and aniline blue.

30.3.1 Materials and Reagents

1 Aqueous solution of 10% (w/v) KOH.

2 Black Shaeffer ink solution: 5% black Shaeffer ink (Ft. Madison, Iowa) in household vinegar (5% acetic acid); or trypan blue solution: 0.5 g trypan blue in 500 mL glycerol, 450 mL H_2O, and 50 mL 1% HCl with a destaining solution: 500 mL glycerol, 450 mL H_2O, and 50 mL 1% HCl.

3 Water acidified with vinegar or 1% HCl.

4 Sample staining cassettes (Omnisette Embedding Cassettes, Fisher Scientific, Nepean, Ontario). In absence of cassettes, vials, beakers, or Erlenmeyer flasks can be used as recipients for roots.

5 Lead pencil.

6 1 L beaker.

7 Hot plate.

30.3.2 Procedure

1 Cut roots into 1 cm fragments and take a representative sample that is small enough to lay somewhat loosely in the sample staining cassettes in such a way as to permit the circulation of liquids around the roots being processed. A representative sample can be achieved by mixing the root pieces in a volume of water. Ensure that no soil adheres to the root pieces to be stained. For a representative evaluation of root colonization level, a minimum of 50 and an optimum of 100 mounted root segments are required.

2 Place the root samples in the sample staining cassettes labeled with a lead pencil (ink will vanish with KOH). In the absence of sample staining cassettes, the whole procedure can be performed using vials, beakers, or Erlenmeyer flasks. Root segments are introduced into the containers, soaked in the prescribed solutions, and recovered manually or by filtration to a 50 μm mesh nylon sheet.

3 Place sample staining cassettes in a 1 L beaker. The beaker should not be more than half full.

4 Cover with the KOH solution.

5 Place the beaker with its contents on a hot plate and boil for the time it takes to clear the roots. It usually takes 10–30 min, but it can also take hours, depending on the plant species and the quality of the root material.

6 Discard the KOH solution and rinse the cassettes several times with tap water.

7 It is then advisable to rinse in acidified water if Shaeffer ink is used for staining or in 1% HCl, in the case of trypan blue.

8 Boil gently in the ink–vinegar stain for 3 min or in the trypan blue solution for 15–60 min.

9 Discard the ink–vinegar solution and rinse the cassettes in tap water acidified with a few drops of vinegar. Trypan blue stained roots are placed in a destaining solution: 500 mL glycerol, 450 mL H_2O, and 50 mL 1% HCl over night. The trypan blue staining solution can be carefully filtered to remove root debris and reused for subsequent root staining. Store the stained root cassettes or the vials containing roots in acidified tap water or in destaining solutions at 4°C.

30.3.3 Comments

Very small root fragments can be secured in between two pieces of nylon screen or filter paper before being placed in the sample staining cassette to prevent loss of material. In this case, care must be taken to ensure proper rinsing between the clearing and staining solutions. Toth et al. (1991) proposed a way to calculate AM fungal biomass from colonized root length and root radius.

30.4 DETERMINATION OF ROOT COLONIZATION USING GRID-LINE INTERSECT

Stained roots are most often scored for colonization using the grid-line intersect method (Giovannetti and Mosse 1980). McGonigle et al. (1990) modified this method into the ''magnified intersection method'' in which roots are examined at 200× magnification. This method involves the inspection of intersections between the microscope eyepiece crosshair and roots. Closer examination allows for accurate recognition and recording of arbuscular, hyphal, and vesicular colonization. Hyphal and vesicular colonization should be interpreted with caution as they can be produced by nonmycorrhizal fungi. This warning also holds for the grid-line intersect method. With the slide method (Giovannetti and Mosse 1980), 50 to 100 1 cm root sections are mounted on slides in polyvinyl lactoglycerol (PVLG) mounting media (Omar et al. 1979) (166 g polyvinylalcohol high viscosity—24–32 cP—dissolved in 10 mL H_2O is added to 10 mL lactic acid and 1 mL glycerol). The length of colonized root tissue is measured and compared to the total length of root observed. Results are expressed as a percent.

Biochemical methods have also been used to determine AM fungal colonization of roots. These sometimes present the advantage of discriminating between AM fungi and other root endophytes in addition to allowing the evaluation of lignified or large roots, which cannot be cleared. Chitin (Hepper 1977), 24-methyl/methylene sterols (Fontaine et al. 2004), and phospholipid fatty acid (PLFA) C16:1ω5 (van Aarle and Olsson 2003) were proposed as indicators of AM colonization. Biochemical methods of measurements of intraradical AM colonization have some limitations. Chitin is not specific to AM fungi; it is present in the cell wall of zygomycetous fungi. The relative abundance of sterols and fatty acid indicators is not consistent among AM fungal species. Thus, use of biochemical indicators of AM colonization is not recommended for the evaluation of field-grown plant roots as colonization, in this case, is likely the result of a mixed fungal population.

The grid-line intersect method is simple, relatively rapid, and appropriate for most routine determinations of the mycorrhizal colonization of roots. This method is described below.

30.4.1 Materials and Reagents

1. A plastic Petri dish on the underside of which lines were lightly etched with a sharp scalpel blade. Lines can be random or arranged in a grid pattern. Gridded dishes can also be directly purchased.
2. Wash bottle containing water acidified with a few drops of vinegar or HCl.
3. Tweezers and needle to disperse the roots.

4 Dissecting microscope.

5 Two-key desktop counter for keeping track of point counts.

6 Cleared and stained roots.

30.4.2 Procedure

1 A stained root sample is placed in the etched Petri dish and dispersed using a jet of acidified water from the wash bottle, tweezers, and needle.

2 Scanning the grid-lines under the dissecting microscope, the total number of points where a root intersects a line is recorded using the key-counter. In parallel, the number of these intersects bearing AM colonization is also recorded. For example, if AM colonization is found in 42 out of a total of 100 intersects, AM root colonization would equal 42%.

30.4.3 Comments

Root length can easily be assessed concurrently with root scoring, using the relationship of Newman (1966):

$$R = An/2H \tag{30.1}$$

where R is the root length, A the area of the Petri dish, n the total number of root $\times$ grid-line intersects, and H the sum of all etched lines' lengths.

When root measurement is sought, care must be taken not to lose roots in the processes of staining, clearing, washing, and extracting roots from a known amount of soil. Colonized and total root length densities are best expressed as lengths of total or colonized roots per volume of soil.

30.5 DETERMINATION OF THE SOIL MYCORRHIZAL POTENTIAL

There are four methods for assessing the mycorrhizal potential of the soil:

1 The most probable number (MPN) method was applied to estimate AM fungal propagules in soil by Porter (1979). The method involves repeated serial dilutions with pasteurized volumes of the soil to be tested, and growth of a trap plant. Trap plant roots are examined for presence or absence of AM colonization, and values of MPN are derived from published statistical tables (Fisher and Yates 1963; Woomer 1994). The MPN method is laborious and yields only imprecise estimates of propagule numbers. Furthermore, the intense mixing of the soil under study dictated by the method disrupts AM hyphal networks that may also be involved in soil infectivity. Thus this method considers the MPN of infective spores and vesicles, underestimating soil infectivity.

2 An improved method for mycorrhizal soil infectivity (MSI) determination was proposed by Plenchette et al. (1989) as an alternative to the MPN method.

With the MSI, soil dilution series are made similarly to the MPN method, but population of 10 plants, rather than single plants, are grown. The relationship between the percentage of mycorrhizal plants and the minimum amount of nonsterile soil in a dilution allows for a calculation of the amount of soil required to induce mycorrhizal infection in 50% of the plants, which is one unit of MSI. This method is more precise than the MPN but involves growing a plant population rather than single plants as with the MPN, and thus requires the examination of hundreds and thousands of root systems.

3 Franson and Bethlenfalvay (1989) have proposed to count infection units formed on a trap plant root system directly extracted from the substrate as the expression of the mycorrhizal infectivity of a soil. This requires great skill and precision because infection points rapidly become sources of additional infections in addition to being hard to distinguish. It is unlikely that all AM fungal propagules in a soil sample will be synchronized in initiating root infection and, thus, this method will likely underestimate the number of propagules in a soil.

4 A simple infectivity assay can be more conveniently conducted. Trap plants are grown in the soil under examination for 2–4 weeks, a period of time long enough for colonization to occur but short enough to avoid mycorrhizal development to reach its full potential, a point at which plants may become uniformly colonized (see McGonigle 2001). Brundrett et al. (1994) proposed to grow trap plants in undisturbed cores to maintain an intact AM mycelium in the soil under evaluation. In contrast to the MPN and MSI methods, the intact core method accurately evaluates soil infectivity. The limitation of this method is that its end result is not a convenient number of propagules, but the percentage of colonization of a trap plant after a number of days. This method is appropriate to compare the mycorrhizal potential of soils or plots within the framework of an experiment. Furthermore, AM fungi are filamentous, a type of growth that makes it impossible to determine where a propagule starts and ends. Thus, rate of colonization expresses soil AM infectivity more realistically than a number of propagules. This method is reported below.

30.5.1 Materials and Reagents

1 Appropriately labeled steel cylinders with a tapered and sharpened lower end, which sends the pressure outward and preserves the soil core when it is pushed into the soil. These cylinders serve as growth containers. As many cylinders as there are plots multiplied by the number of desired subsamples per plot are needed.

2 Small wooden board to cover and push cylinders in the soil.

3 Trowel to lift the cylinders.

4 Knife to level off the lower end of the soil core.

5 Nylon mesh and high-gauge rubber bands to close the lower end of the cylinder while allowing drainage.

6 Growth chamber to control temperature, humidity, and lighting conditions to allow repetition of the assay at other times.

7 Perforated plastic trays with corrugated bottom that will allow cores to drain excess water while maintaining the soil in place upon watering.

8 Germinated seeds or seedlings of the desired species of trap plant. Note that more than one species can be grown simultaneously in each core. The number of plants of each species should be kept constant among growth cylinders. Clover seedlings inoculated with *Rhizobium* (Brundrett et al. 1994) have been used, but any mycotrophic plant species may be used.

9 Polyester wool may be used to cover the surface of cores, particularly in the case of soil rich in clay, in order to protect the soil surface structure from water damage during watering events.

30.5.2 Procedure

1 Cover the cylinders with the wooden board and push it in the soil until filled.

2 Carefully dig the cylinders out of the soil.

3 Invert the cylinders holding the surface with your palm or on the wooden board, level off the lower surface of the core, cover it with the nylon mesh, and secure this mesh with a high-gauge rubber band. Avoid exposing the cores to excessive heat during the collection process.

4 Carefully carry the cores to a clean greenhouse work bench.

5 Insert germinated seeds or plantlets in the center of the cores. Seeds can be placed in pairs and thinned to one per pair after a few days.

6 Cover the soil surface with polyester wool to protect the soil structure.

7 Place in corrugated trays in growth chamber at required preset settings.

8 Water very gently to field capacity when required, to avoid soil structure degradation.

9 Grow the trap plants for about 2–4 weeks (see Section 30.5.3).

10 Clear, stain, and assess the roots, as per the methods given in Section 30.3, for their percentage of mycorrhizal colonization using the grid-line intersect method (see Section 30.4), and determine simultaneously total root length.

30.5.3 Comment

It is worthwhile having extra cores available to assess periodically the status of root colonization before harvest and ensure that trap plants have adequate amount of mycorrhizal development.

30.6 EVALUATION OF THE EXTRARADICAL PHASE OF AM FUNGI

Several methods have been used to quantify the extraradical mycelium of AM fungi. Soil chitin measurement has been used to estimate AM fungal biomass in soil (Bethlenfalvay and Ames 1987). Chitin measurement does not give an estimate of the active AM extraradical hyphal biomass. Chitin is also abundant in invertebrates, exoskeletons, and zygomycetous fungi.

The spread of AM fungi extraradical hyphae in soil was studied using root exclusion chambers. Sequential sampling in compartmentalized growth containers allowed the comparison of the spread of AM fungal species from a root barrier into a hyphal compartment (Schuepp et al. 1987; Jakobsen et al. 1992). A rotating wire system was proposed to facilitate the task of extracting extraradical hyphae from mineral soil samples with low clay content (Vilarino et al. 1993; Boddington et al. 1999). The method of root exclusion chambers has been the most popular way to evaluate the size of the extraradical AM hyphae in soil, even though there are some limitations to direct measurement of hyphae extracted from soil. AM fungal hyphae are generally nonseptate and some researchers found morphological features typical of AM mycelia such as hyphal size (Ames et al. 1983), angle of branching, and wall characteristics. But considering the different morphologies found among AM genera, the range of possible AM extraradical hyphae size (from <1 μm in the fine endophytes to 18 μm in *Glomus manihotis* (Dodd et al. 2000)) and, on the other hand, the diversity of other soil fungi, one must conclude that the identity of coenocytic hyphae extracted from a soil sample is at best uncertain, especially in hyphal pieces bearing no branching. Also, much of the AM hyphae extracted from soil are neither viable nor functional and vital staining techniques must be applied if the amount of active hyphae is sought.

Inserted membrane techniques in which a membrane of a material resilient to decomposition is inserted in the soil to trap the hyphae that will cross it were proposed by Wright and Upadhyaya (1999) and Balaz and Vosatka (2001). These methods are simple and rapid. They give a measure of total hyphae cross-section plates. This method can be used with immunodetection of the AM fungi-specific protein glomalin (Wright and Upadhyaya 1999; Wright 2000) to assess the proportion of AM and saprophytic fungi. Inserted membrane techniques should be considered where data on hyphal density are not necessary.

Fatty acids are often specific to taxonomic groups. The phosphate group of phospholipids, the lipids making up membranes, is rapidly cleaved in soil, and PLFA measurement reflects the occurrence of living or recently dead organisms. The measurement of AM fungi PLFA indicator thus provides information on the functionality of the organisms. The PLFA 16:1ω5 is the preferred indicator of AM fungal biomass (Balser et al. 2005). The fatty acids 16:1ω5, 18:1ω7, 20:4, and 20:5 were proposed as indicative of AM fungi (Olsson et al. 1995; Olsson 1999). AM fungi do not have completely specific fatty acids; 20:4 and 20:5 are present in algae and protozoa but are rare in non-AM fungi and bacteria, and 16:1ω5 and 18:1ω7 occur in some bacterial genera but are not normally found in other fungi. Background level of the PLFA 16:1ω5 ranging from 30% to 60% was attributed to the presence of bacteria in soil. The fatty acid 16:1ω5 is dominant in many AM fungal species although it was absent from several *Glomus* species and from most *Gigaspora* species (Graham et al. 1995). Whole-cell fatty acid (WCFA) 16:1ω5, which is a more specific indicator of AM fungi than PLFA 16:1ω5, was correlated with hyphal length but the relationship varied seasonally (Gryndler et al. 2006). A nonmycorrhizal control can be used to correct for background levels of the fatty acid 16:1ω5. PLFA data on bacterial biomass, which can be generated simultaneously,

can be used to interpret changes in the abundance of the fatty acid 16:1ω5. Neutral lipid fatty acid (NLFA) 16:1ω5 should also be monitored because it highly dominates reserve fatty acids of all AM fungi tested, and because bacteria produce very little neutral lipids. The measurement of NLFA 16:1ω5 can be used to support observation on the variation in fatty acid 16:1ω5 from the PLFA fraction.

A method for lipid extraction from soil and measurement of PLFA and NLFA 16:1ω5 (J.M. Clapperton, personal communication, Agriculture & Agri-Food Canada, Lethbridge, Alberta) is given below.

30.6.1 Materials and Reagents

Extraction

1. Weighing boats
2. 35 mL glass centrifuge tubes
3. Dichloromethane (DMC)
4. Methanol (MeOH)
5. Citrate buffer
6. Saturated NaCl solution
7. 7 mL glass vials
8. Pipette
9. Nutating shaker
10. Centrifuge
11. N_2-gas flow drying manifold (we use a Reacti-Vap III)
12. Hot plate at 37°C (we use a Reacti-Therm III)

Lipid-Class Separation

1. Clamp-holder construction with 10 clamps (to hold columns)
2. Pasteur pipettes filled with silica gel up to 2 cm from the top (columns)
3. Pasteur pipettes fitted with pipetting bulb
4. 4 mL glass vials
5. DCM
6. Acetone

7 MeOH

8 N_2-gas flow drying manifold (we use a Reacti-Vap III)

9 Hot plate at 37°C (we use a Reacti-Therm III)

Transmethyl Esterization

1 N_2-gas flow drying manifold (we use a Reacti-Vap III)

2 Hot plate at 37°C (we use a Reacti-Therm III)

3 Pasteur pipettes fitted with pipetting bulb

4 Micropipette with tips

5 MeOH

6 H_2SO_4 (concentrated)

7 Water bath

8 Hexane

9 Vortex mixer

10 Ultrapure water

11 Methyl nonadecanoate (19:0; Sigma, Aldrich)

12 200 μL glass syringe with needle

13 100 μL tapered glass inserts and gas chromatograph (GC) vials

Gas Chromatography Measurement of Fatty Acids

1 16:1ω5 standard fatty acid (from MJS Biolynx #MT1208).

2 Gas chromatograph with flame ionization detector (FID). We use a Varian 3900 GC equipped with a CP-8400 autosampler, helium as carrier gas (30 mL min^{-1}), and a 50 m Varian Capillary Select FAME #cp7420 column.

30.6.2 Procedure

Extraction

1 To extract total soil lipids, shake 4 g (dry weight equivalent) of frozen or fresh soil in 9.5 mL DMC:MeOH:citrate buffer (1:2:0.8 v/v) for 2 h in glass centrifugation tubes.

2 Add 2.5 mL of DMC and 10 mL of a saturated NaCl solution to each tube and shake for five more minutes.

3 Centrifuge tubes at 1500 *g* for 10 min.

4 Pipet the organic fraction into clean vials.

5 Add 5 mL of DCM:MeOH (1:1 v/v) to the tubes.

6 Shake for 15 min.

7 Centrifuge for 10 min at 1000 *g*.

8 Combine the organic fractions in the corresponding vials and dry under a flow of N_2 at 37°C in the fume hood.

9 Dissolve samples in 2 mL of DCM.

10 Samples can be stored at −20°C for a short time, if necessary.

Lipid-Class Separation

Lipid-class separation is conducted in silica gel columns made with Pasteur pipettes.

1 Using a pipette, load samples onto columns washing the vials twice with a small amount of DCM and adding the wash to the columns. Care must be taken to keep solvent level above the silica gel at all times.

2 Elute the neutral lipid fraction first by leaching columns with approximately 2 mL of DCM, collecting the eluent in 4 mL vials.

3 Elute the glycolipid fraction by leaching columns with approximately 2 mL of acetone, collecting the eluent in other 4 mL vials.

4 Elute the phospholipid fractions by leaching columns with approximately 2 mL of MeOH, collecting also the eluent in 4 mL vials.

5 Discard the glycolipid fraction.

6 Dry the neutral and phospholipid fractions under a flow of N_2 at 37°C in the fume hood.

7 Dissolve the dried fractions in a few mL of MeOH for PLFA or DCM for NLFA and store at −20°C.

Transmethyl Esterization

Fatty acid methyl esters are created through mild acid methanolysis as follows:

1 Dry neutral and phospholipids fractions under a flow of N_2 at 37°C in the fume hood.

2 Add half a Pasteur pipette full of MeOH/H_2SO_4 (25:1 v/v) to the vials.

3 Place vials in an 80°C water bath for 10 min.

4 Cool to room temperature.

5 Add 1 Pasteur pipette of hexane, vortex vials for 30 s, and leave to settle for 5 min.

6 Discard the lower fraction.

7 Add 1 mL of ultrapure water, vortex vials for 30 s, let stand for 5 min.

8 Discard the aqueous fraction entirely.

9 Add 10 μL of methyl nonadecanoate, the internal standard.

10 Dry samples under a flow of N_2 at 37°C in the fume hood.

11 Wash vials with 50 μL of hexane using a glass syringe.

12 Transfer the samples into 100 μL tapered glass inserts, and place inside a GC vial.

Gas Chromatography Measurement of Fatty Acids

1 Sample (2 μL) injection is in 5:1 split mode.

2 In our program, for example, the injector is held at 250°C and the FID at 300°C. The initial oven temperature, 140°C, is held for 5 min, raised to 210°C at a rate of 2° C min^{-1}, then raised from 210°C to 250°C at a rate of 5° C min^{-1}, and finally held for 12 min.

Peak Identification

Identification of peaks is based on comparison of retention times to a known 16:1ω5 standard. Amounts are derived from the relative area under specific peaks, as compared to the 19:0 peak value, which is calibrated according to a standard curve made from a range of concentrations of the 19:0 FAME standard dissolved in hexane. The abundance of individual PLFAs is expressed as micrograms PLFA per gram dry soil.

The amount of fatty acid is calculated with the following formula:

$$16{:}\,1\omega5 = (A_{16:1\omega5}/A_{\text{istrd}})C_{\text{istd}}D \tag{30.2}$$

where 16:1ω5 is the calculated concentration of the AM fungal indicator (moles or weight per unit volume), $A_{16:1\omega5}$ is the GC area of the AM fungal indicator, A_{istrd} is the GC area of the internal injection standard as determined by the GC data system (unitless), C_{istd} is the concentration of the internal injection standard given, and D is the appropriate dilution factor.

30.6.3 Comments

Solvents used throughout the procedure are HPLC grade, and tubes and vials are made of glass and their screw-top caps lined with Teflon. Organic solvents are toxic and must be

handled in the fume hood. The use of parafilm is prohibited. Care must be taken to avoid contamination with extraneous lipids. For example, the use of gloves is recommended. A bacterial and fungal saprobe fatty acid indicators mix (Supelco Bacterial Acid Methyl Esters #47080-U) can be used in conjunction with the AM fungal indicator 16:1ω5 to simultaneously obtain information on the whole soil microbial community.

30.7 METHOD TO EVALUATE AM EXTRARADICAL MYCELIUM

A number of methods have been used to study the extraradical mycelium of AM fungi. The cultivation of AM fungi on transformed root cultures has generated considerable knowledge on the physiology of AM fungi. This body of work was reviewed by Fortin et al. (2002). This system, in which the plant component of the AM symbiosis is reduced to a root often transformed by the *Agrobacterium rhizogenes* plasmid, is artificial. Giovannetti and her group successfully used a membrane sandwich method from which much knowledge on the extraradical phase of AM fungi was also gained (Giovannetti et al. 1993, 2001). This method is closer to reality as whole plants are used, although the environment of the symbioses formed is artificial and bidimensional. In this method clean AM spores are germinated in between two Millipore7 membranes (0.45 μm diameter pores) placed on moist sterile quartz grit in 14 cm diameter Petri dishes. Clean plantlets are added to the sandwich. Sandwiches are harvested at intervals to monitor mycorrhizal development. Rillig and Steinberg (2002) have used glass beads of different sizes to simulate different hyphal growing space conditions to show the large influence of the environment on hyphae length and glomalin production. Friese and Allen (1991) have used root observation chambers to describe runner hyphae, hyphal bridges, absorptive hyphal networks, germ tubes, and infection networks produced in soil by spores and root fragments. Although a root observation chamber allows the study of the morphology of arbuscular mycorrhizae formed in soil, this system may not be representative of the field situation. The film method in which a soil-molten agar suspension was poured into films was proposed by Jones et al. (1948). These agar films can be dried and stained to facilitate the enumeration of entrapped organisms under the microscope. A modification of this method was used to document AM hyphal links formed between the roots of different plant species. This method can be useful for examining interactions between roots, AM hyphae, and soil microorganisms in the field; it is described below.

30.7.1 Materials and Reagents

1. Warm 1.5% water agar
2. Microscope slides
3. Tray
4. Thin plastic film (Saran wrap)
5. Colored plastic flags to facilitate slides recovery in the field
6. A staining solution made of 15 mL phenol (5% aqueous), 1 mL of aniline blue W.S. (1% aqueous), and 4 mL of glacial acetic acid (use fume hood, gloves, and eye protection)

7 Euparal mounting medium (Bioquip, Gardena, California)

8 95% Ethanol

30.7.2 Procedure

1 Place the microscope slides side-by-side in a tray.

2 Pour the water agar on the slides to produce a thin agar coat on the slides.

3 When cold and solidified, free and remove the agar-coated slides from the tray using a scalpel. Store the fresh agar-coated slides wrapped in plastic film at 4°C. In the field, remove the plastic wrap from the slides. Bury the slides vertically in the rhizosphere at a chosen distance from the plant roots.

4 Mark the location of each buried slide with a plastic flag.

5 After a period of time, carefully dig out the buried slides cutting off the soil around the slide with a scalpel and any fine roots that might have grown in the agar coat. Agar-coated slides can remain buried for a few months.

6 In the laboratory, delicately wash the bulk of adhering soil off in a water bath.

7 Dry the agar films at 60°C for 15–20 min.

8 Under the fume hood, immerse the dried films for 1 h in the staining solution.

9 Wash and dehydrate in 95% ethanol and permanent mount in Euparal.

30.7.3 Comments

Phenol and phenol-containing solutions should be handled under the fume hood using gloves and eye protection. Good results are also obtained with fuchsin acid staining.

30.8 EXTRACTION OF AM FUNGI

Soil sampling strategies may generate the need to analyze in detail the composition of harvested soil samples for their AM spore population, spore abundance, and spore species diversity. Moreover, the extracted spores may provide starting inoculum in the form of isolated spores that may be used to obtain mixed or purified species inoculum.

According to the type of soil worked on, different approaches may be taken to facilitate the bulk isolation of spores from a soil substrate. The density gradient centrifugation method for spore extraction together with spore sieving and decanting is probably the most common method for AM spore extraction, especially for biodiversity and taxonomical studies (Khan 1999). However, it is very time consuming and less appropriate for most basic AM soil species and soil population investigations; the spore extraction method proposed below is the result of an adaptation of combined methodologies of soil sieving, decanting, sucrose

centrifugation, and filtrating. Literature provides descriptions and evaluated methodologies that may help in refining the techniques when special requirements are needed. These requirements mainly concern diverse gradient methods (Ohms 1957; Allen et al. 1979; Furlan et al. 1980; Kucey and McCready 1982) and wet-sieving approaches (Gerdemann and Nicolson 1963; Daniels and Skipper 1982; Singh and Tiwari 2001). Book chapters and review articles have also been dedicated to the evaluation and description of procedures (Tommerup 1992; Brundrett et al. 1996; Clapp et al. 1996; Jarstfer and Sylvia 1997; Johnson et al. 1999; Khan 1999).

Once spores are extracted from soil material, they can be used directly as starting inoculum or classified by morphotypes as done for population studies (Smilauer 2001; Brundrett 2004). Spores may then be separated according to their size, their color, and their subtending hyphae morphology before being mounted on microscopic slides for AM fungi diversity assessment. When extracted spores are expected to serve as starting inoculum for the propagation of AM fungal strains, a preliminary spore vitality test is highly recommended. This can be done by a time-consuming evaluation of the germination potential of isolated spores. Moreover, dehydrogenase-activated stains such as tetrazolium bromide stain (3-(4,5-dimethylthiazol-yl) 2–5-diphenyl-2H-tetrazolium bromide (MTT)) and tetrazolium chloride stain (2-(*p*-iodophenyl)-3-(*p*-nitrophenyl)-5-phenyl-2H-tetrazolium chloride (INT)) have been frequently tested and used for the evaluation of AM spore vitality (An and Hendrix 1988; Meier and Charvat 1993; Walley and Germida 1995). Even though the interpretation of such staining approaches may be confusing, sometimes they remain the easiest and least time-consuming methods to estimate the spore vitality of a population. Procedures for spore extraction and viable staining of spores are given below.

Because of the laborious process associated with AM fungi spore extraction from soil samples, the limited species-specific spore morphological characters, and the incapacity to identify AM fungi from colonized roots, molecular-based techniques have been developed to study AM fungal communities. Several polymerase chain reaction (PCR)-based methods have been developed and applied to the detection of AM fungi and to the study of genetic diversity either directly from soil samples or from colonized root segments (Claassen et al. 1996; Vandenkoornhuyse et al. 2002). The nested PCRs (two steps amplification) allow a rapid and efficient method for the study of soil and root AM fungal communities (van Tuinen et al. 1998; Jacquot et al. 2000; Jansa et al. 2003; de Souza et al. 2004). Polymerase chain reaction–denaturing gradient gel electrophoresis (PCR–DGGE) can also be used for direct analysis of amplified DNA from soil and root samples. It allows the separation of DNA products of the same length and the distinction of single-base substitution between different nucleotide sequences, does not require a cloning process (Ma et al. 2005; Sato et al. 2005), and can discriminate between species (Kowalchuk et al. 2002; de Souza et al. 2004).

Finally, quantitative real-time PCR based on the detection of a fluorescent signal produced proportionally to amplification of a PCR product allows not only detection but also quantification of genomic DNA (Filion et al. 2003; Isayenkov et al. 2004).

General discussion on the comparative value and applications of PCR-based method for the study of soil fungi communities and investigations with AM fungal diversity can be consulted respectively in Anderson and Cairney (2004) and Clapp et al. (2002).

30.8.1 Extraction of AM Spores from Soil by Sieving and Sucrose Techniques

Materials and Reagents

1. Scale
2. Flasks (1 L)
3. Sieves set (suggested mesh size: 1000 μm to intercept gravel, soil debris; 500, 150, and 50 μm to recover sporocarps and spores of different sizes)
4. Centrifuge tubes: round bottom 100 mL
5. Centrifuge
6. Vacuum filter apparatus (vacuum source, Buchner funnel and side-arm flask (2 L))
7. Filter paper (Whatman No. 1 (40 μm))
8. Plastic Petri dishes
9. Sucrose 50% (w/v)
10. Tween 80 (optional)

Procedure

1. Weigh 50 g of soil and pour in a 1 L flask with 200–300 mL of water.
2. Shake vigorously and then allow the soil to soak for 30 min to 1 h.
3. Pour the water and soil mix through the sieves piled in a decreasing order of mesh size (largest mesh on the top to retain debris), ensure recovery of the entire soil mix by carefully rinsing the flask. This allows the recovery of all soil material for spore extraction.
4. Wash the soil with running water, manually breaking soil aggregates if required, being careful not to clog the small mesh sieve. At this step, root pieces can also be recovered for either root colonization evaluation or inoculum material.
5. Recover the entire soil from each sieve, distribute the soil material in centrifuge tubes (max 10 mL of soil volume), fill the tube with a 50% (w/v) sucrose solution, thoroughly mix the tube content with a glass or metal rod, and centrifuge at 800 *g* for 4 min. (Optional step, see next section.)
6. Recover supernatants on a 40 μm paper filter and wash carefully to dilute sucrose concentration as it affects the spore wall morphology for the subsequent identification process.

7 Pour spores in water into a plastic Petri dish, or vacuum filter the spores on filter paper for examination under a dissecting microscope.

Comments

When an evaluation of the spore abundance is required, it is necessary to measure soil moisture content in order to express spore abundance as the number of spores recovered by weight in grams of dry soil weight. For steps 2–4, a drop of dispersant such as Tween 80 can be added to water to facilitate the separation of spores from soil debris. The dispersant does not seem to affect either spore morphology for further species identification, or spore germination potential. Depending on the soil texture, sucrose extraction and centrifugation (step 5) can be skipped especially when working with sandy soils because spores are easily separated from silica particles by a vigorous shaking of the soil–water–Tween mix. In this case, vacuum filtration is recommended and should be performed 2–3 times in order to recover a maximum number of spores. On the other hand, AM spore extraction from organic soil containing an abundance of partially decomposed plant debris requires the combination of sieving and sucrose extraction processes with, in some cases, the repetition of the extraction step 5 at least twice. The newly proposed use of low concentration of HCl or hydrofluoric acid for cleaning and separating spores from their surrounding organic material (Garampalli and Reddy 2002) yielded cleaner spores suitable for microscopic observations and *in vitro* culture propagation. However, extreme care should be taken in the use of such chemicals and the extraction should be performed under a fume hood to avoid inhalation. For hydrofluoric acid special fume hoods are needed.

30.8.2 Extraction of Vesicles through Enzymatic Digestion of Roots

Vesicles are excellent AM fungal propagules. Strullu and Plenchette (1991) proposed their use in alginate beads as high quality root inoculum. Monoxenic culture of spores can also provide high quality inoculum, but only a few species can be grown *in vitro*. Vesicle extraction from root is another way to produce clean inoculum of the AM species that cannot be cultivated *in vitro*. Another application for extracted vesicles is the initiation of root organ cultures because intraradical vesicles are devoid of attached organic debris and cleaner than soil extracted spores.

Materials and Reagents

1 Scalpel

2 Enzyme solution made of 0.2 g L^{-1} of macerozyme, 0.5 g L^{-1} of driselase, and 1.0 g L^{-1} of cellulase

3 250 mL beaker

4 Blender

5 50 μm sieve

Procedure

1 Cut 10 g of roots in 3–10 mm segments.

2 Place root pieces in 100 mL of the enzyme solution.

3 Incubate overnight at room temperature.

4 Wash digested tissues with demineralized water.

5 Homogenize in a blender.

6 Filter the homogenized sample on a 50 μm sieve and recover clusters of vesicles attached to hyphae under the dissecting microscope.

Comments

Jabaji-Hare et al. (1984) used mortar and pestle, a homogenizer, filtration, and density centrifugation to quantify and recover vesicles for biochemical analysis.

REFERENCES

Allen, M.F., Moore, T.S., and Christensen, M. 1979. Growth of vesicular–arbuscular mycorrhizal and non-mycorrhizal *Bouteloua gracilis* in defined medium. *Mycologia* 71: 666–669.

Ames, R.N., Reid, C.P.P., Porter, L.K., and Cambardella, C. 1983. Hyphal uptake and transport of nitrogen from two ^{15}N-labelled sources by *Glomus mosseae* a vesicular–arbuscular mycorrhizal fungus. *New Phytol*. 95: 381–396.

An, A.Q. and Hendrix, J.W. 1988. Determining viability of endogonaceous spores with a vital stain. *Mycologia* 80: 259–261.

Anderson, I.C. and Cairney, J.W.G. 2004. Diversity and ecology of soil fungal communities increased understanding through the application of molecular techniques. *Environ. Microbiol*. 6: 769–779.

Balaz, M. and Vosatka, M. 2001. A novel inserted membrane technique for studies of mycorrhizal extraradical mycelium. *Mycorrhiza* 11: 291–296.

Balser, T.C., Treseder, K.K., and Ekenler, M. 2005. Using lipid analysis and hyphal length to quantify AM and saprotrophic fungal abundance along a soil chronosequence. *Soil Biol. Biochem.* 37: 601–604.

Bethlenfalvay, G.J. and Ames, R.N. 1987. Comparison of two methods for quantifying extraradical mycelium of vesicular–arbuscular mycorrhizal fungi. *Soil Sci. Soc. Am. J*. 51: 834–837.

Bevege, D.I. 1968. A rapid technique for clearing tannins and staining intact roots for detection of mycorrhizas caused by *Endogone* spp., and some records of infection in Australasian plants. *T. Brit. Mycol. Soc*. 51: 808–810.

Boddington, C.L., Bassett, E.E., Jakobsen, I., and Dodd, J.C. 1999. Comparison of techniques for the extraction and quantification of extra-radical mycelium of arbuscular mycorrhizal fungi in soils. *Soil Biol. Biochem.* 31: 479–482.

Brundrett, J. 2004. Diversity and classification of mycorrhizal associations. *Biol. Rev*. 79: 473–495.

Brundrett, M.C., Bougher, N., Grove, T., and Malajczuk, N. 1996. *Working with Mycorrhizas in Forestry and Agriculture*. ACIAR Monograph Series No. 32.

Brundrett, M.C., Melville, L., and Peterson, L. 1994. *Practical Methods in Mycorrhiza Research*. Mycologue Publications, Sydney, British Columbia, Canada.

Brundrett, M.C., Piché, Y., and Peterson, R.L. 1984. A new method for observing the morphology of vesicular–arbuscular mycorrhizae. *Can. J. Bot*. 62: 2128–2134.

Claassen, V.P., Zasoski, R.J., and Tyler B.M. 1996. A method for direct soil extraction and PCR amplification of endomycorrhizal fungal DNA. *Mycorrhiza* 6: 447–450.

Clapp, J.P., Fitter, A.H., Merryweather, J.W., and Hall, G.S. 1996. Arbuscular mycorrhizas. In G.S. Hall, Ed. *Methods for the Examination of Organismal Diversity in Soils and Sediments*. CAB International, Wallingford, Oxon, UK, pp. 145–161.

Clapp, J.P., Helgason, T., Daniell, T.J., and Young, J.P.W. 2002. Genetic studies of the structure and diversity of arbuscular mycorrhizal fungal communities. In M.G.A. van der Heijden and I. Sanders, Eds. *Mycorrhizal Ecology*. Springer-Verlag, Berlin, Germany, pp. 201–224.

Daniels, B.A. and Skipper, H.D. 1982. Methods of the recovery and quantitative estimation of propagules from soil. In N.C. Schenck, Ed. *Methods and Principles of Mycorrhizal Research*. American Phytopathological Society, St. Paul, MN, pp. 29–35.

de Souza, F.A., Kowalchuk, G.A., Leeflang, P., van Veen, J.A., and Smit, E. 2004. PCR-denaturing gradient gel electrophoresis profiling of inter-and intraspecies 18S rRNA gene sequence heterogeneity is an accurate and sensitive method to assess species diversity of arbuscular mycorrhizal fungi of the genus *Gigaspora*. *Appl. Environ. Microbiol*. 70: 1413–1424.

Dodd, J.C., Boddington, C.L., Rodriguez, A., Gonzalez-Chavez, C., and Mansur, I. 2000. Mycelium of arbuscular mycorrhizal fungi (AMF) from different genera: form, function and detection. *Plant Soil* 226: 131–151.

Filion, M., St-Arnaud, M., and Jabaji-Hare, S.H. 2003. Direct quantification of fungal DNA from soil substrate using real-time PCR. *J. Microbiol. Meth*. 53: 67–76.

Fisher, R.A. and Yates, F. 1963. *Statistical Tables for Biological, Agricultural and Medical Research*, 6th ed. Oliver and Boyd, Edinburgh, Scotland, UK.

Fontaine, J., Grandmougin-Ferjani, A., Glorian, V., and Durand, R. 2004. 24-Methyl/methylene sterols increase in monoxenic roots after colonization by arbuscular mycorrhizal fungi. *New Phytol*. 163: 159–167.

Fortin, J.A., Bécard, G., Declerck, S., Dalpé, Y., St-Arnaud, M., Coughlan, A.P., and Piché, Y. 2002. Arbuscular mycorrhiza on root-organ cultures. *Can. J. Bot*. 80: 1–20.

Franson, R.L. and Bethlenfalvay, G.J. 1989. Infection unit method of vesicular–arbuscular mycorrhizal propagule determination. *Soil Sci. Soc. Am. J*. 53: 754–756.

Friese, C.F. and Allen, M.F. 1991. The spread of VA mycorrhizal fungal hyphae in the soil: inoculum types and external hyphal architecture. *Mycologia* 83: 409–418.

Furlan, V., Bartschi, H., and Fortin, J.A. 1980. Media for density gradient extraction of endomycorrhizal spores. *T. Brit. Mycol. Soc*. 75: 336–338.

Garampalli, R.H. and Reddy, C.N. 2002. A simple technique for clearing adherent debris of VAM fungal spores for identification. *Mycorrhiza News* 14: 14–15.

Gerdemann, J.W. and Nicolson, T.H. 1963. Spores of mycorrhizal *Endogone* species extracted from soil by wet sieving and decanting. *T. Brit. Mycol. Soc*. 46: 235–244.

Giovannetti, M., Fortuna, P., Citernesi, A.S., Morini, S., and Nuti, M.P. 2001. The occurrence of anastomosis formation and nuclear exchange in intact arbuscular mycorrhizal networks. *New Phytol*. 151: 717–724.

Giovannetti, M. and Mosse, B. 1980. An evaluation of techniques for measuring vesicular–arbuscular mycorrhizal infection in roots. *New Phytol*. 84: 489–500.

Giovannetti, M., Sbrana, C., Avio, L., Citernesi, A.S., and Logi, C. 1993. Differential hyphal morphogenesis in arbuscular mycorrhizal fungi during pre-infection stages. *New Phytol*. 125: 587–593.

Gollotte, A., van Tuinen, D., and Atkinson, D. 2004. Diversity of arbuscular mycorrhizal fungi colonising roots of the grass species *Agrostis capillaris* and *Lolium perenne* in a field experiment. *Mycorrhiza* 14: 111–117.

Graham, J.H., Hodge, N.C., and Morton, J.B. 1995. Fatty acid methyl ester profiles for characterization of glomalean fungi and their endomycorrhizae. *Appl. Environ. Microbiol*. 61: 58–64.

Gryndler, M., Larsen, J., Hrselova, H., Rezacova, V., Gryndlerova, H., and Kubat, J. 2006. Organic and mineral fertilization, respectively, increase and decrease the development of external mycelium of arbuscular mycorrhizal fungi in a long-term field experiment. *Mycorrhiza* 16: 159–166.

Hepper, C.M. 1977. A colorimetric method for estimating vesicular–arbuscular mycorrhizal infection in roots. *Soil Biol. Biochem.* 9: 15–18.

Isayenkov, S., Fester, T., and Hause, B. 2004. Rapid determination of fungal colonization and arbuscule formation in roots of *Medicago truncatula* using real-time (RT) PCR. *J. Plant Physiol.* 161: 1379–1383.

Jabaji-Hare, S., Sridhara, S.I., and Kendrick, B. 1984. A technique for the isolation of intramatrical vesicles from vesicular–arbuscular mycorrhizae. *Can. J. Bot.* 62: 1466–1468.

Jacquot, E., van Tuinen, D., Gianinazzi, S., and Gianinazzi-Pearson, V. 2000. Monitoring species of arbuscular mycorrhizal fungi in planta and in soil by nested PCR: application to the study of the impact of sewage sludge. *Plant Soil* 226: 179–188.

Jakobsen, I., Abbott, L.K., and Robson, A.D. 1992. External hyphae of vesicular–arbuscular mycorrhizal fungi associated with *Trifolium subterraneum* L. *New Phytol.* 120: 371–379.

Jakobsen, I. and Nielsen, N.E. 1983. Vesicular–arbuscular mycorrhiza in field-grown crops. I. Mycorrhizal infection in cereals and peas at various times and soil depths. *New Phytol.* 93: 401–413.

Jansa, J., Mozafar, A., Kuhn, G., Anken, T., Ruh, R., Sanders, R., and Frossard, E. 2003. Soil tillage affects the community structure of mycorrhizal fungi in maize roots. *Ecol. Appl.* 13: 1164–1176.

Jarstfer, A.G. and Sylvia, D. 1997. Isolation, culture, and detection of arbuscular mycorrhizal fungi. In C.J. Hurst, G.R. Knudsen, M.J. McInerney, L.D. Stetzenbach, and M.V. Walter, Eds. *Manual of Environmental-Microbiology*. American Society for Microbiology, Washington, DC, pp. 406–412.

Johnson, N.C., O'Dell, T.E., and Bledsoe, C.S. 1999. Methods for ecological studies of mycorrhizae. In G.P. Robertson, D.C. Coleman, C.S. Bledsoe, and P. Sollins, Eds. *Standard Soil Methods for Long Term Ecological Research*. Oxford University Press, Oxford, UK, pp. 378–412.

Jones, P.C.T., Mollison, J.E., and Quenouille, M.H. 1948. A technique for the quantitative estimation of soil micro-organisms. *J. Gen. Microbiol.* 2: 54–69.

Kabir, Z., O'Halloran, I.P., Fyles, J.W., and Hamel, C. 1998a. Dynamics of the mycorrhizal symbiosis of corn (*Zea mays* L.): effects of host physiology, tillage practice and fertilization on spatial distribution of extra-radical mycorrhizal hyphae in the field. *Agric. Ecosyst. Environ.* 68: 151–163.

Kabir, Z., O'Halloran, I.P., Widden, P., and Hamel, C. 1998b. Vertical distribution of arbuscular mycorrhizal fungi under corn (*Zea mays* L.) in no-till and conventional tillage systems. *Mycorrhiza* 8: 53–55.

Khan, Q.Z. 1999. Evaluation of techniques for isolation of vesicular–arbuscular mycorrhizal fungi. *Ann. Plant Prot. Sci.* 7: 239–241.

Kowalchuk, G.A., de Souza, F.A., and van Veen J.A. 2002. Community analysis of arbuscular mycorrhizal fungi associated with *Ammophila arenaria* in Dutch coastal sand dunes. *Mol. Ecol.* 11: 571–581.

Kucey, R.M.N. and McCready, R.G.L. 1982. Isolation of vesicular–arbuscular mycorrhizal spores: a rapid method for the removal of organic detritus from wet-sieved soil samples. *Can. J. Microbiol.* 28: 363–365.

Ma, W.K., Siciliano, S.D., and Germida, J.J. 2005. A PCR–DGGE method for detecting arbuscular mycorrhizal fungi in cultivated soils. *Soil Biol. Biochem.* 37: 1589–1597.

McGonigle, T.P. 2001. On the use of non-linear regression with the logistic equation for changes with time of percentage root length colonized by arbuscular mycorrhizal fungi. *Mycorrhiza* 10: 249–254.

McGonigle, T.P., Miller, M.H., Evans, D.G., Fairchild, G.L., and Swan, J.A. 1990. A new method which gives an objective measure of colonization of roots by vesicular–arbuscular mycorrhizal fungi. *New Phytol.* 115: 495–501.

Meier, R. and Charvat, I. 1993. Reassessment of tetrazolium bromide as a viability stain for spores of vesicular–arbuscular mycorrhizal fungi. *Am. J. Bot.* 80: 1007–1015.

Newman, E.I. 1966. A method for estimating total length of root in a sample. *J. Appl. Ecol.* 3: 139–145.

Oehl, F., Sieverding, E., Ineichen, K., Ris, E.-A., Boller, T., and Wiemken, A. 2005. Community structure of arbuscular mycorrhizal fungi at different soil depths in extensively and intensively managed agroecosystems. *New Phytol.* 165: 273–283.

Ohms, R.E. 1957. A flotation method for collecting spores of a Phycomycetous mycorrhizal parasite from soil. *Phytopathology* 47: 751–752.

Olsson, P.A. 1999. Signature fatty acids provide tools for determination of the distribution and interactions of mycorrhizal fungi in soil. *FEMS Microbiol. Ecol.* 29: 303–310.

Olsson, P.A., Bååth, E., Jakobsen, I., and Söderström, B. 1995. The use of phospholipid and neutral lipid fatty acids to estimate biomass of arbuscular mycorrhizal fungi in soil. *Mycol. Res.* 99: 623–629.

Omar, M.B., Bolland, L., and Heather, W.A. 1979. A permanent mounting medium for fungi. *Bull. Br. Mycol. Soc.* 13: 31–32.

Phillips, J.M. and Hayman, D.S. 1970. Improved procedures for clearing roots and staining parasitic and vesicular–arbuscular mycorrhizal fungi for rapid assessment of infection. *T. Brit. Mycol. Soc.* 55: 158–161.

Plenchette, C., Perrin, R., and Duvert, P. 1989. The concept of soil infectivity and a method for its determination as applied to endomycorrhizas. *Can. J. Bot.* 67: 112–115.

Porter, W.M. 1979. The ''Most Probable Number'' for enumerating infective propagules of vesicular–arbuscular mycorrhizal fungi. *Aust. J. Soil Res.* 17: 515–519.

Rillig, M.C. and Steinberg, P.D. 2002. Glomalin production by an arbuscular mycorrhizal fungus: a mechanism of habitat modification? *Soil Biol. Biochem.* 34: 1371–1374.

Sato, K., Suyama, Y., Saito, M., and Sugawara, K. 2005. A new primer for discrimination of arbuscular mycorrhizal fungi with polymerase chain reaction–denature gradient gel electrophoresis. *Grassland Sci.* 51: 179–181.

Schuepp, H., Miller, D.D., and Bodmer, M. 1987. A new technique for monitoring hyphal growth of vesicular–arbuscular mycorrhizal fungi through soil. *T. Brit. Mycol. Soc.* 89: 429–436.

Singh, S.S. and Tiwari, S.C. 2001. Modified wet sieving and decanting technique for enhanced recovery of vesicular–arbuscular mycorrhizal fungi from forest soils. *Mycorrhiza News* 12: 12–13.

Smilauer, P. 2001. Communities of arbuscular mycorrhizal fungi in grassland: seasonal variability and effects on environment and host plants. *Folia Geobot.* 36: 243–263.

Strullu, D.G. and Plenchette, C. 1991. The entrapment of *Glomus* sp. in alginate beads and their use as root inoculum. *Mycol. Res.* 95: 1194–1196.

Tommerup, I.C. 1992. Methods for the study of the population biology of vesicular–arbuscular mycorrhizal fungi. In J.R. Norris, D.J. Read, and A.K. Varma, Eds. *Methods in Microbiology. Vol. 24. Techniques for the Study of Mycorrhiza*. Academic Press, Amsterdam, the Netherlands, pp. 23–51.

Toth, R., Miller, R.M., Jarstfer, A.G., Alexander, T., and Bennett, E.L. 1991. The calculation of intraradical fungal biomass from percent colonization in vesicular–arbuscular mycorrhizae. *Mycologia* 83: 553–558.

van Aarle, I.M. and Olsson, P.A. 2003. Fungal lipid accumulation and development of mycelial structures by two arbuscular mycorrhizal fungi. *Appl. Environ. Microbiol.* 69: 6762–6767.

van Tuinen, D., Jacquot, E., Zhao, B., Gollotte, A., and Gianninazzi-Pearson, V. 1998. Characterization of root colonization profiles by a microcosm community of arbuscular mycorrhizal fungi using 25SrDNA-targeted nested PCR. *Mol. Ecol.* 7: 879–887.

Vandenkoornhuyse, P., Husband, R., Daniell, T.J., Watson, J., Duck, J.M., Fitter, A.H., and Young, J.P.W. 2002. Arbuscular mycorrhizal community composition associated with two plant species in a grassland ecosystem. *Mol. Ecol.* 11: 1555–1564.

Vierheilig, H., Coughlan, A.P., Wyss, U., and Piché, Y. 1998. Ink and vinegar, a simple staining technique for arbuscular-mycorrhizal fungi. *Appl. Environ. Microbiol.* 64: 5004–5007.

Vilarino, A., Arines, J., and Schuepp, H. 1993. Extraction of vesicular–arbuscular mycorrhizal mycelium from sand samples. *Soil Biol. Biochem.* 25: 99–100.

Walker, C. 2005. A simple blue staining technique for arbuscular mycorrhizal and other root-inhabiting fungi. *Inoculum* 45: 69–69.

Walley, F.L. and Germida, J.J. 1995. Estimating the viability of vesicular–arbuscular mycorrhizae fungal spores using tetrazolium salts as vital stains. *Mycologia* 87: 273–279.

Woomer, P.L. 1994. Most probable number counts. In R.W. Weaver et al., Eds. *Methods of Soil Analysis*, *Part 2—Microbiological and biochemical properties*. Soil Science Society of America, Madison, WI, pp. 59–80.

Wright, S.F. 2000. A fluorescent antibody assay for hyphae and glomalin from arbuscular mycorrhizal fungi. *Plant Soil* 226: 171–177.

Wright, S.F. and Upadhyaya, A. 1999. Quantification of arbuscular mycorrhizal fungi activity by the glomalin concentration on hyphal traps. *Mycorrhiza* 8: 283–285.

Chapter 31
Root Nodule Bacteria and Symbiotic Nitrogen Fixation

D. Prévost
Agriculture and Agri-Food Canada
Quebec, Quebec, Canada

H. Antoun
Laval University
Quebec, Quebec, Canada

31.1 INTRODUCTION

Symbiotic nitrogen fixation in plants occurs in root nodules of legumes and nonlegumes. The bacterium rhizobium is one of the most studied symbiotic nitrogen-fixing bacteria because it nodulates legumes, which are environmentally significant in soil N fertility management of cultivated lands. The majority of nonleguminous nodules belong to the *Alnus*-type symbiosis, in which the actinomycete *Frankia* is the microsymbiont. The cyanobacteria *Nostoc* or *Anabaena* nodulate the Cycadales, while the bacterium rhizobium forms *Parasponia*-type symbioses.

This chapter focuses on the methodology developed to study the rhizobium–legume symbiosis. The global success of legume production is due to the development of inoculation technologies and cropping systems by multidisciplinary teams. Microbiologists, soil scientists, plant physiologists, plant breeders, and agronomists contributed to this breakthrough. Increased knowledge in rhizobial ecology is mainly due to the development of molecular techniques. Moreover, the taxonomy of the microsymbiont rhizobium has considerably changed since the last edition of this chapter (Rice and Olsen 1993). The use of genotypic and phenotypic approaches, applied to isolates obtained from a large number of legume species and from different regions, resulted in reclassification of known rhizobial species and in an increased number of new species.

Symbiotic rhizobia belong to the α-subclass of Proteobacteria (α-rhizobia). However, some tropical legumes are nodulated by strains of *Burkholderia* and *Ralstonia* species belonging to the β-subclass of Proteobacteria. These strains evolved from diazotrophs through multiple lateral *nod* gene transfers, and this phenomenon seems to be widespread in nature (Chen et al. 2003). The current taxonomy of rhizobia (Rhizobia_Taxonomy 2006) includes the genera *Rhizobium*

(14 species), *Mesorhizobium* (10 species), *Azorhizobium* (1 specie), *Sinorhizobium*, which could be renamed as *Ensifer* (11 species), *Bradyrhizobium* (5 species), and six other genera (*Methylbacterium*, *Burkholderia*, *Ralstonia*, *Devosia*, *Blastobacter*, and *Ochrobacterium*).

In this chapter, the general term ''rhizobia'' will be used for the designation of bacteria that form nodules on legumes root and stem. Table 31.1 shows the rhizobial species associated to some indigenous and cultivated legumes. Recent classification of rhizobia isolated from legumes in tropic regions is not included.

TABLE 31.1 Some Indigenous and Cultivated Legumes in Canada and Their Nodulating Rhizobial Species

Legume species		
Latin name	**Common name**	**Rhizobial species**
Arachis hypogae	Peanut	*Bradyrhizobium* sp.[a]
Astragalus cicer	Cicer milkvetch	*Mesrohizobium* sp.[a]
Astragalus sinicus		*Mesorhizobium huakuii*
Astragalus adsurgens		*M. septentrionale, M. temperatum*
Cicer arietinum	Chickpea	*Mesorhizobium ciceri* *Mesorhizobium mediterraneum*
Galega	Goat's rue	*Rhizobium galegae*
Glycine max	Soybean	*Bradyrhizobium japonicum* *B. elkanii, B. liaoningense,* *Sinorhizobium fredii,* *S. xinjiangense*
Lathyrus spp.	Flat pea, tangier pea beach pea	*Rhizobium leguminosarum* bv. viceae
Lathyrus sativus	Chickling vetch, grass pea	*Rhizobium leguminosarum* bv. viceae
Lathyrus pratensis	Yellow vetchling	*Rhizobium leguminosarum* bv. viceae
Lens culinaris	Lentil	*Rhizobium leguminosarum* bv. viceae
Lotus corniculatus	Birsfoot trefoil	*Mesorhizobium loti*
Lupinus spp.	Lupine (white, blue, yellow)	*Bradyrhizobium* sp.
Medicago spp.	Alfalfa	*Sinorhizobium meliloti, S. medicae*
Melilotus spp.	Sweetclover (white, yellow)	*Sinorhizobium meliloti, S. medicae*
Onobrychis vivifolia	Sainfoin	*Rhizobium* sp.[a]
Oxytropis sp.		*Mesorhizobium* sp.[a]
Phaseolus vulgaris	Common beans	*Rhizobium leguminosarum* bv. phaseoli *R. gallicum, R. giardinii, R. etli*
Pisum sativum	Field, garden pea	*Rhizobium leguminosarum* bv. viceae
Securigera varia	Crownvetch	*Rhizobium* sp.[a]
Trifolium spp.	Clover	*Rhizobium leguminosarum* bv. trifolii
Vicia sativa	Common vetch	*Rhizobium leguminosarum* bv. viceae
Vicia villosa	Hairy vetch	*Rhizobium leguminosarum* bv. viceae
Vicia faba	Faba bean, broadbean	*Rhizobium leguminosarum* bv. viceae

Source: Adapted from Sahgal, M. and Johri, N., *Curr. Sci.*, 84, 43, 2003. Updated from http://www.rhizobia.co.nz/Rhizobia_Taxonomy.html.

[a] Species designation is still unknown for these legumes.

Methods commonly used for the isolation and estimation of rhizobial populations in soils and for the evaluation of symbiotic nitrogen fixation will be described to enable a scientist with little experience obtain reliable results. Examples of methodologies using genetic tools to directly isolate and estimate the size of rhizobial populations in soils will be briefly presented; references will be given for more complete information.

31.2 ISOLATION OF RHIZOBIA

Symbiotic rhizobia are common colonizers of the rhizosphere of both legume and nonlegume plants and in addition to legumes they are also endophytes of several nonlegumes like rice and maize (Sessitsch et al. 2002). However, nonsymbiotic rhizobia can also be present in soil (Sullivan et al. 1996) and therefore, the methodology described here is aimed at the isolation of nodule-forming rhizobia in legumes. Rhizobia can be isolated either by collecting nodules from field grown legumes or by inducing nodule formation by inoculating surface disinfected legume seeds with soil suspensions under aseptic laboratory conditions (see Section 35.3). Guidelines for collecting nodules and preserving them during a collecting trip have been described and discussed by Date and Halliday (1987) and by Somasegaran and Hoben (1994).

The procedure given here is a general description of the basic steps to be followed in obtaining a culture of rhizobia inhabiting the nodules of selected plant (Rice and Olsen 1993).

31.2.1 Material

1. Tools for excavating plants and removing roots—spade, garden trowel, knife, etc.
2. Plastic sampling bags.
3. Cooler and dry ice.
4. Collection vessel: (a) glass vial with screw cap (10 to 20 mL capacity) containing a desiccant (anhydrous calcium chloride or silica gel) occupying one-fourth the volume of the container, held in place by a cotton wool plug or (b) glass or plastic vial with screw cap containing 50% glycerol.
5. 95% (w/v) ethanol.
6. Disinfectant solution: 8% (w/v) sodium or calcium hypochlorite solution or 3% (v/v) hydrogen peroxide solution.
7. Sterile water, test tubes, and glass rods.
8. Petri dishes containing 20 mL yeast-extract mannitol agar (YMA):
   Composition (g L^{-1}): mannitol, 10.0; K_2HPO_4, 0.5; $MgSO_4 \cdot 7H_2O$, 0.2; NaCl, 0.1; yeast extract, 1.0; agar, 15.0. Adjust pH to 7.0 with 1 *M* NaOH or HCl before autoclaving at 121°C for 15 min.
9. Screw cap tubes with slants of YMA; sterile mineral oil.
10. Cryovials-containing YMB (YMA without agar) with 25% glycerol.

31.2.2 Procedure

1 With a spade, cut around the selected plant a block of soil with approximately 15 cm in diameter to a depth of at least 20 cm.

2 Pull the block, and carefully remove soil from roots. Avoid detaching secondary roots from the plant. This step can be greatly facilitated by immersion of the soil block in water and allowing soil to fall away. Using a sieve of an appropriate mesh, depending on nodule size, is useful to catch nodules that may become detached from the root.

3 If isolation can be performed within 24 h, put the roots with nodules in the sampling bag and transport them to the laboratory in the cooler. Fresh root nodules can be kept in the refrigerator overnight, and processed as indicated in step 6.

4 For a longer storage period, place the nodules in the collection vessel. Nodules preserved this way can last 6–12 months. However, as rhizobial recovery may vary depending on legume species and storage temperature, nodules should be processed within 3 weeks. Place dry nodules in water for 60 min to allow them to fully imbibe. Nodules stored for more than 3 weeks should be kept in the refrigerator overnight to imbibe.

5 Alternatively, in our laboratory, we observed that nodules can be preserved for more than 1 year at −20°C in vials containing about 50% glycerol. Moreover, if there is no time to take out nodules from roots at the sampling time, nodulated roots from pots or field can be preserved, wrapped in a paper towel imbibed in 50% glycerol, placed in a plastic bag, and stored at −20°C.

6 Immerse nodules for 5–10 s in 95% ethanol, and then in disinfectant for 3–4 min.

7 Remove disinfectant and rinse at least five times in sterile water.

8 Check the surface sterility of nodules by passing them on the surface of YMA plates. Discard isolates originating from a surface-contaminated nodule.

9 Crush each nodule with a sterile glass rod in a test tube. Add sterile water to make a turbid suspension and transfer a drop to YMA plates.

10 Streak the drop of suspension onto the agar surface so that suspension is progressively diluted.

11 Incubate the plates in an inverted position at the optimum temperature for the targeted rhizobial species (25°C–30°C). Make daily observation for the appearance of colonies typical of *Rhizobium* or *Bradyrhizobium* (Somasegaran and Hoben 1994).

12 Pick off and restreak well-isolated single colonies on fresh plates to obtain pure cultures. If more than one typical colony appears on a plate, each of these types should be taken to pure culture.

13 For short-term storage, transfer pure culture isolates to screw cap YMA agar-slant tubes. Incubate and completely cover rhizobial growth with cold sterile mineral oil. Keep in the refrigerator for up to 1 year. For longer storage period, suspend rhizobial cells in a cryovial-containing YMB with 25% glycerol and keep at −80°C.

14 Authenticate each pure culture isolate by confirming nodule-forming ability on test host plants grown under axenic conditions in growth pouches (see Section 31.3) or in Leonard jar assemblies (Vincent 1970; Gibson 1980).

31.2.3 Comments

1 Senescent nodules may contain fungi that can cause heavy overgrowth on agar plate. This problem can be reduced by adding 20 μg mL^{-1} cycloheximide to YMA. Prepare a fungicide stock solution by dissolving 0.5 g of cycloheximide in 25 mL of 95% (v/v) ethanol. Add 1.2 mL of fungicide stock solution to 1 L of YMA cooled to 50°C–55°C. Cycloheximide is very toxic if swallowed, inhaled, or absorbed through the skin.

2 Bacterial contaminants and β-rhizobia can be distinguished from α-rhizobia by incorporating Congo Red in YMA at a concentration of 25 μg mL^{-1} (to each L of YMA add 10 mL of a stock solution of 250 mg Congo Red in 100 mL of water). When incubated in the dark, α-rhizobia show little or no Congo Red absorption, they form colonies that are white, opaque, or occasionally pink, while other bacteria absorb the red dye, and their colonies are dark red. There are, however, exceptions, some strains of *Sinorhizobium meliloti* can absorb the dye strongly and α-rhizobia will absorb the dye if plates are exposed to light for an hour or more (Somasegaran and Hoben 1994).

3 Frequently, more than one colony type, with all morphological characteristics of rhizobia, will appear on one plate from one nodule. In some cases, these colony types will form nodules on the host, and in other cases, one or more types may be incapable of forming nodules. These types of contaminants are often ''latent'' in that they appear to be carried along in subsequent transfers without detection and will suddenly appear, particularly if the culture is grown under nutritional and physical stress. It is therefore extremely important that new isolates and cultures undergoing frequent transfer be thoroughly checked onto test plants and reisolation from fresh nodules.

31.3 ENUMERATION OF RHIZOBIA BY THE MOST PROBABLE NUMBER PLANT-INFECTION TECHNIQUE

The most probable number (MPN) plant-infection technique has been used for many years for the enumeration of rhizobia in soils. It has also been adapted for the enumeration of rhizobia in inoculants by the Canadian Food Inspection Agency (CFIA) for the legume inoculant testing program.

The MPN procedure relies upon the pattern of positive or negative nodulation responses of host plants inoculated with consecutive series of dilutions of sample (soil, inoculants,

preinoculated seeds) containing rhizobia. The method is based on the following major assumptions: (1) a single viable rhizobium cell inoculated onto its specific host in a nitrogen-free medium will cause nodule formation, (2) nodulation is the proof of infective rhizobia, (3) the validity of the test is demonstrated by the absence of nodules on uninoculated plants, and (4) absence of nodules on inoculated plants is proof of the absence of infective rhizobia. The procedure described below is adapted from the official ''Methods for testing legume inoculants and preinoculated seed products'' by CFIA (Anonymous 2005).

31.3.1 Materials

1 Disposable seed germination pouches (Mega International, St. Paul. Minneapolis): they are designed to observe root development and so, they can be advantageously used to replace pots and glassware. The pouch (16 × 20 cm) is made of a strong and transparent polyester film capable of withstanding steam sterilization at 100 kPa (15 lb $in.^{-2}$) for up to 20 min. Inserted in the pouch is a sleeve-like paper germination towel that is folded along the top edge into a trough and perforated to permit roots to escape from the seeding area. In practice, sterilization is not required, since the pouches are free of rhizobia. This type of pouch can be divided into two parts that permit two tests in the same pouch: the paper germination towel is cut into two and the polyester pouch is split by hermetically sealing the pouch itself. It is recommended to sterilize modified pouches.

2 Undamaged seeds of the appropriate legume species: they are surface disinfected by immersion in 95% ethanol for 30 s followed by either: (1) 10 min in 3%–5% hydrogen peroxide (H_2O_2) solution or (2) 10 min in 5% sodium hypochlorite (NaClO) solution, or (3) by immersion in conc. H_2SO_4 for 10 min. The seeds are then washed or rinsed thoroughly with at least five changes of sterile, distilled water.

3 Nitrogen-free plant nutrient solution: $CoCl_2 \cdot 6H_20$, 0.004 mg; H_3BO_3, 2.86 mg; $MnCl_2 \cdot 4H_2O$, 1.81 mg; $ZnSO_4 \cdot 7H_2O$, 0.22 mg; $CuSO_4 \cdot 5H_2O$, 0.08 mg; $H_2MoO_4 \cdot H_2O$, 0.09 mg; $MgSO_4 \cdot 7H_20$, 492.96 mg; K_2HPO_4, 174.18 mg; KH_2PO_4, 136.09 mg; $CaCl_2$, 110.99 mg; $FeC_6H_5O_7 \cdot H_2O$, 5.00 mg; distilled water, 1 L. Use HCl or NaOH 1.0 *M* solution to bring to pH 6.8 ± 0.1. Sterilize by autoclaving at 100 kPa for 20 min.

4 Sterile buffer diluent solution: peptone, 1.0 g; KH_2PO_4, 0.34 g; K_2HPO_4, 1.21 g; distilled water, 1 L. pH = 7.0 ± 0.1.

5 Stomacher (a paddle blender) and Stomacher bags, or professional Waring Blender. Basic models are adequate for regular cell dispersion. These can be purchased from various sources.

6 Growth chamber or room providing 16,000 lux, 22°C during 16 h light period and 18°C during the dark period, and relative humidity at 65%–70%.

31.3.2 Procedure

1 Add 30 mL of sterile plant nutrient solution to each pouch and place pouches in rack.

2 Place aseptically 20 small (e.g., alfalfa, clover) or 15 intermediate (e.g., sainfoin) surface disinfected seeds directly in the trough of each pouch and incubate in darkness at 20°C (for about 2 days) until the radicles have elongated to 0.5–1.0 cm. In the case of large seeds (e.g., pea, soybean), pregerminate surface disinfected seeds either on three layers of Kimpak germination paper or in sterile humid vermiculate and incubate at 20°C (for about 2 days) until the radicles have elongated to 0.5–1.0 cm; then, place five seedlings carefully in the trough of the pouch, by introducing each radicle into a perforation. Growth units are ready for inoculation. For convenience, they can be kept in a fridge (4°C) for up to 1 week, before their inoculation.

3 A 10-fold dilution (w/v) of the soil sample is prepared as follows: Place 10 g of soil into 90 mL of sterile buffer diluent in a Waring Blender and disperse for 2 min at 12,600 rpm or in a Stomacher bag and disperse for 1 min. Transfer a 10 mL aliquot of the soil suspension to a bottle containing 90 mL of diluent and shake for 5 min. Tenfold serial dilutions (v/v) using a minimum 1 mL buffer-inoculant suspension in buffer diluent, are made as required, depending on the expected number of rhizobia in the soil sample. Soils in which legumes have been grown may contain about 10^4 rhizobia per gram of dry soil, and therefore, the 10-fold dilution series should be carried out to the 10^{-1} or 10^{-2} level before starting the fivefold dilution series.

4 Fivefold dilution series are prepared by mixing 1.0 mL of the final 10-fold dilution and 4.0 mL of sterile phosphate-peptone buffer. Six or seven consecutive fivefold dilutions are made and 4 mL of each dilution level is used to inoculate four growth pouches (1 mL per pouch), except for the last dilution where five pouches are inoculated. Practically, fivefold dilutions and inoculation can be done simultaneously in the following convenient way: take 4 mL of the first fivefold dilution (which has 5 mL) and inoculate four growth pouches with 1 mL in each applied to the root zone of the plantlets. Add 4 mL of diluent to the remaining 1 mL in the dilution tube, mix and take 4 mL of this new dilution for inoculation of other pouches as just described. Repeat these steps until the last fivefold dilution, and use all the last 5 mL to inoculate five pouches. Leave an uninoculated control pouch between each set of four or five inoculated pouches.

5 Place rack of pouches in the growth chamber, and water aseptically with sterile distilled water as required. Examine after 3 weeks for the presence of nodules; legume species that show slow development (e.g., soybean) are examined after 4 weeks. Controls must be free of nodules for the test to be meaningful. Record results as ''+'' for a growth unit (pouch) showing nodulated plants or ''−'' for a growth unit showing no nodules.

31.3.3 Calculation of the MPN of Rhizobia

1 Record the number of positive growth units (pouches) at each dilution level, from the least to the most dilute. This will yield to a six-digit code: a typical result could be: 4,4,4,1,1,0. Locate this series of number on the MPN table (Table 31.2) and read the corresponding number of rhizobia. A computer software program, Most Probable Number Enumeration System (MPNES), is also available and useful in assigning population estimates to codes which are

TABLE 31.2 Most Probable Number (MPN) of Nodule Bacteria Calculated from the Distribution of Positive (Nodulated) Growth Units in a Plant-Infection Test Based on a Fivefold Dilution Series

Number of positive (nodulated) growth units							
Fivefold dilution series						MPN of nodule bacteria	
1:5	1:25	1:125	1:625	1:3,125	1:15,625[a]	Estimate	Confidence limits (95%)
0	1	0	0	0	0	1.0	0.1–7.7
0	2	0	0	0	0	2.1	0.5–9.2
0	3	0	0	0	0	3.0	0.9–10.6
1	0	0	0	0	0	1.1	0.2–7.9
1	1	0	0	0	0	2.3	0.6–9.6
1	2	0	0	0	0	3.5	1.1–11.9
1	3	0	0	0	0	4.9	1.6–14.6
2	0	0	0	0	0	2.6	0.6–10.1
2	1	0	0	0	0	4.0	1.2–12.8
2	2	0	0	0	0	5.5	1.9–16.0
2	3	0	0	0	0	7.2	2.7–19.6
3	0	0	0	0	0	4.6	1.5–14.1
3	1	0	0	0	0	6.5	2.3–18.0
3	2	0	0	0	0	8.7	3.3–23.0
3	3	0	0	0	0	11.3	4.4–29.2
4	0	0	0	0	0	8.0	3.0–21.5
4	1	0	0	0	0	11.4	4.4–29.5
4	2	0	0	0	0	16.2	6.2–42.4
4	3	0	0	0	0	24.2	9.0–64.9
4	4	0	0	0	0	40.4	15.3–106.6
4	0	1	0	0	0	10.8	4.2–28.1
4	1	1	0	0	0	15.1	5.8–39.2
4	2	1	0	0	0	21.5	8.1–57.4
4	3	1	0	0	0	32.8	12.2–87.9
4	0	2	0	0	0	14.1	5.4–36.6
4	1	2	0	0	0	19.6	7.4–51.9
4	2	2	0	0	0	28.3	10.5–76.1
4	3	2	0	0	0	43.6	16.6–114.2
4	0	3	0	0	0	18.1	6.9–47.7
4	1	3	0	0	0	25.2	9.4–67.6
4	2	3	0	0	0	36.4	13.7–96.8
4	3	3	0	0	0	56.5	21.9–146.0
4	4	1	0	0	0	5.7×10	$2.2–14.7 \times 10$
4	4	2	0	0	0	8.1×10	$3.1–21.2 \times 10$
4	4	3	0	0	0	12.1×10	$4.5–32.4 \times 10$
4	4	4	0	0	0	20.2×10	$7.6–53.3 \times 10$
4	4	0	1	0	0	5.4×10	$2.1–14.0 \times 10$
4	4	1	1	0	0	7.5×10	$2.9–19.6 \times 10$
4	4	2	1	0	0	10.8×10	$4.0–28.7 \times 10$
4	4	3	1	0	0	16.4×10	$6.1–43.9 \times 10$
4	4	0	2	0	0	7.1×10	$2.7–18.3 \times 10$
4	4	1	2	0	0	9.8×10	$3.7–26.0 \times 10$
4	4	2	2	0	0	14.1×10	$5.3–38.1 \times 10$
4	4	3	2	0	0	21.8×10	$8.3–57.1 \times 10$
4	4	0	3	0	0	9.1×10	$3.4–23.8 \times 10$

(continued)

TABLE 31.2 (continued) Most Probable Number (MPN) of Nodule Bacteria Calculated from the Distribution of Positive (Nodulated) Growth Units in a Plant-Infection Test Based on a Fivefold Dilution Series

Number of positive (nodulated) growth units							
Fivefold dilution series						MPN of nodule bacteria	
1:5	1:25	1:125	1:625	1:3,125	1:15,625[a]	Estimate	Confidence limits (95%)
4	4	1	3	0	0	12.6×10	$4.7–33.8 \times 10$
4	4	2	3	0	0	18.2×10	$6.9–48.4 \times 10$
4	4	3	3	0	0	28.2×10	$10.9–73.0 \times 10$
4	4	4	1	0	0	2.9×10^2	$1.1–7.3 \times 10^2$
4	4	4	2	0	0	4.1×10^2	$1.6–10.6 \times 10^2$
4	4	4	3	0	0	6.0×10^2	$2.3–16.2 \times 10^2$
4	4	4	4	0	0	10.1×10^2	$3.8–26.6 \times 10^2$
4	4	4	0	1	0	2.7×10^2	$1.0–7.0 \times 10^2$
4	4	4	1	1	0	3.8×10^2	$1.5–9.8 \times 10^2$
4	4	4	2	1	0	5.4×10^2	$2.0–14.4 \times 10^2$
4	4	4	3	1	0	8.2×10^2	$3.1–22.0 \times 10^2$
4	4	4	0	2	0	3.5×10^2	$1.4–9.2 \times 10^2$
4	4	4	1	2	0	4.9×10^2	$1.8–13.0 \times 10^2$
4	4	4	2	2	0	7.1×10^2	$2.6–19.0 \times 10^2$
4	4	4	3	2	0	10.9×10^2	$4.2–28.6 \times 10^2$
4	4	4	0	3	0	4.5×10^2	$7.7–11.9 \times 10^2$
4	4	4	1	3	0	6.3×10^2	$2.3–16.9 \times 10^2$
4	4	4	2	3	0	9.1×10^2	$3.4–24.2 \times 10^2$
4	4	4	3	3	0	14.1×10^2	$5.4–36.7 \times 10^2$
4	4	4	4	1	0	14.3×10^2	$5.5–36.9 \times 10^2$
4	4	4	4	2	0	20.3×10^2	$7.8–53.0 \times 10^2$
4	4	4	4	3	0	30.2×10^2	$11.2–81.3 \times 10^2$
4	4	4	4	4	0	50.5×10^2	$19.0–133.8 \times 10^2$
4	4	4	4	0	1	13.5×10^2	$5.2–35.3 \times 10^2$
4	4	4	4	1	1	18.8×10^2	$7.2–49.0 \times 10^2$
4	4	4	4	2	1	26.9×10^2	$10.1–71.8 \times 10^2$
4	4	4	4	3	1	41.0×10^2	$15.3–110.2 \times 10^2$
4	4	4	4	0	2	17.7×10^2	$6.8–45.9 \times 10^2$
4	4	4	4	1	2	24.5×10^2	$9.2–65.0 \times 10^2$
4	4	4	4	2	2	35.3×10^2	$13.1–95.4 \times 10^2$
4	4	4	4	3	2	54.4×10^2	$20.6–143.8 \times 10^2$
4	4	4	4	0	3	22.6×10^2	$8.6–59.7 \times 10^2$
4	4	4	4	1	3	31.4×10^2	$11.7–84.7 \times 10^2$
4	4	4	4	2	3	45.5×10^2	$17.0–121.4 \times 10^2$
4	4	4	4	3	3	70.6×10^2	$27.1–184.2 \times 10^2$
4	4	4	4	4	1	7.1×10^3	$2.7–18.6 \times 10^3$
4	4	4	4	4	2	10.1×10^3	$3.8–27.0 \times 10^3$
4	4	4	4	4	3	15.1×10^3	$5.4–42.6 \times 10^3$
4	4	4	4	4	4	25.2×10^3	$8.6–74.0 \times 10^3$
4	4	4	4	4	5	$>35.5 \times 10^3$	

[a] Five growth units inoculated with 1 mL aliquots from this dilution level.

not included in published MPN tables (Woomer et al. 1990). It is available from University of Hawaii, NifTAL Project, 1000 Holomua Avenue, Paia, HI 96779, USA.

2 MPN estimate refers to the number of rhizobia present in 1 mL of the 10-fold dilution used to make the fivefold dilution for plant inoculation and it is assumed that the inoculation volume is 1.0 mL. To determine the number of viable rhizobia per gram of soil/inoculant, multiply the MPN estimate by the reciprocal of the level of the 10-fold dilution (before inoculation) that was used to start the fivefold dilutions. This number can be adjusted with soil humidity when results are expressed per gram of dry soil.

31.3.4 Comments

1 It is important to manipulate aseptically seeds and growth units with sterile devices during all steps to avoid contamination by rhizobia. Moreover, special care should be taken when watering pouches during test. Plastic drinking straws placed at a corner inside the pouch facilitate watering and provide rigidity to the pouch.

2 When this method is used to estimate number of rhizobia in liquid or solid legume inoculant products, the level of the 10-fold dilution required to start the fivefold dilution should be about 10^5–10^6. For preinoculated seeds, the starting dilution is made by placing 100 seeds in 100 mL diluent (1:1), 10-fold dilutions can be done depending on the expected number of rhizobia; the MPN number found is per seed.

31.4 DIRECT ISOLATION AND ENUMERATION OF RHIZOBIA FROM SOILS

The use of host plant for the isolation of rhizobia is an indirect procedure that has the disadvantage to recover only strains that have the ability to compete for nodulating the host plant. For ecological study of natural populations, the direct recovery of rhizobia on a semiselective medium has been shown to be satisfactory in studies with *S. meliloti*, *Rhizobium leguminosarum*, and *Bradyrhizobium japonicum*. The semiselective media have been developed to limit the growth of soil microorganisms and favor the growth of rhizobial species. In the case of *S. meliloti* and *R. leguminosarum,* colonies are usually identified by hybridization with a rhizobium species-specific DNA probe.

For scientists not familiar with molecular biology techniques, it is recommended to obtain training from colleagues using these techniques. Thus, detailed molecular biology techniques will not be described here; they can be found in manufacturer's instructions, in bench-top guides (Caetano-Anollés and Gresshoff 1997), and more advanced molecular biology books (Sambrook et al. 1989; Sambrook and Russell 2001).

The basis of colony hybridization is to transfer or replicate bacterial colonies to membranes (nitrocellulose filters, nylon or Whatman No. 541 filter papers). The membranes are lyzed to immobilize DNA, and they are hybridized with a specific DNA-labeled probe (radioactive or nonradioactive). Colonies that are bound to the probe are detected by autoradiography (for radioactive probe) or with IgG conjugated to a reporter molecule (for nonradioactive probe).

31.4.1 Isolation and Enumeration of *S. meliloti*

Medium AS (Nutrient-Poor Agar Medium) (Bromfield et al. 1994)

Composition (g L^{-1}): yeast extract, 0.1; tryptone, 0.4; $CaCl_2$, 0.1; NaCl, 5.0; cycloheximide, 0.15; Congo Red, 0.025; agar, 10.0. Congo Red is prepared as a stock solution and added to the medium before autoclaving at 121°C, 15 min. Cycloheximide is prepared as a stock solution sterilized by membrane filtration and added to the autoclaved molten media.

Soil dilution for inoculation: 10-fold dilutions are made in sterile water, the initial 10-fold dilution being mixed for 15 min on a wrist action shaker. Appropriate dilutions levels (1:1000 and 1:100) are then made, depending on the expected soil bacterial and rhizobial populations and 0.1 mL is used to inoculate AS agar plates. Good results are obtained when about 100–300 cfu (colony-forming units) are growing per plate. About 7 to 100 rhizobial colonies per plate can be easily detected by hybridization. When using 1:100 and lower soil dilutions, the medium AS can be supplemented with 0.05% sodium deoxycholate and 12.5 m*M* Tris–HCl, pH 8.0 (Barran et al. 1997) to reduce the total number of soil bacterial colonies.

Colony Blot Hybridization for *S. meliloti*

A replica of the arrangement of colonies on the agar plate is made by pressing a membrane (Whatman filter paper or nitrocellulose filter) on the surface of the plate to lift the colonies. This replica is treated with alkali to lyze the cells, and the paper is then hybridized to a labeled probe (^{32}P). Those colonies that have bound to the probe are identified by autoradiography. Two probes have been used successfully for the detection of *S. meliloti*. The probe pRWRm61 derived from the insertion element IS*Rm*5 hybridizes strongly to total genomic DNA of the majority of *S. meliloti* strains, except few strains from Australia or from eastern Mediterranean (Wheatcroft et al. 1993; Barran et al. 1997). The probe pSW95 derived from the *nodH* gene of *S. meliloti* strain RCR2011 (SU47) (Debelle and Sharma 1986) is highly species-specific and has been used for the detection of Canadian *S. meliloti* isolates (Bromfield et al. 1994).

31.4.2 Isolation of *R. leguminosarum*

Medium MNBP (Louvier et al. 1995) and LB (Miller 1972)

The medium MNBP reduces colony counts of total soil bacteria by 88%–95%. LB medium (on which *R. leguminosarum* is unable to grow) is used as counter selection step. Colonies growing only on MNBP are identified by colony blot hybridization. This technique is very long, suitable for the isolation of *R. leguminosarum*, but not practical for their enumeration. This procedure offers the advantage of reducing the number of ''putative'' rhizobium colonies to be tested as compared to a nonselective medium.

MNBP composition (g L^{-1}): $Na_2HPO_4 \cdot 12H_2O$, 0.045; $MgSO_4 \cdot 7H_2O$, 0.10; $FeCl_3$, 0.02; $CaCl_2$, 0.04; mannitol, 1.00; NH_4NO_3, 0.005; biotin, 0.0005; thiamine, 0.0005; Ca pantothenate, 0.0005; bacitracin, 0.025; penicillin G, 0.003; cycloheximide, 0.10; benomyl, 0.005; pentachloronitrobenzene, 0.0035; agar, 15.0. Adjust pH to 6.8 and autoclave at 121°C, 15 min. Vitamins and antimicrobial substances are prepared in stock solutions in deionized water and sterilized by membrane filtration. They are added to sterile and molten agar.

LB composition (g L^{-1}): Tryptone, 10.0; yeast extract, 5.0; NaCl, 10.0; agar, 15.0. Adjust pH to 7.2 and autoclave at 121°C, 15 min.

TY composition (g L^{-1}): Tryptone, 5.0; yeast extract, 3.0; $CaCl_2 \cdot H_2O$, 0.87; agar, 12.0. Adjust pH to 6.8–7.2 with 1 *M* NaOH. A precipitate forms after autoclaving at 121°C, 15 min.

Soil dilutions for inoculation: 0.1 mL of soil dilutions (10^{-3}) is plated on medium MNBP (25 plates). After 2–3 days growth, mucous-spreading colonies are excised (about 30% of the agar plate surface) to prevent overgrowth. The remaining colonies in each plate are transferred by velveting replication to LB and MNBP plates. The colonies growing only on MNBP plates (about 300 per plate) are transferred to TY agar slopes for further identification by hybridization. With the soils tested during method development, about 20 colonies per plate showed strong homology. The use of this approach reduces the number of colonies to be tested as compared to a nonselective media.

Colony Blot Hybridization for *R. leguminosarum*

Colonies obtained from MNBP plates and kept on TY agar are grown 48 h in 200 μL of TY liquid medium in microplates. From each microplate well, 25 μL of these cultures (OD 650: 0.2–0.3) is spotted on nylon filters. After lysis, the nylon filters are hybridized with one of the *nod* gene probes: pIJ1246, specific for *R. leguminosarum* bv. viciae; pIJ1098, specific for *R. leguminosarum* bv. phaseoli; pRt587, specific for *R. leguminosarum* bv. trifolii (Laguerre et al. 1993). The probes are labeled with digoxigenin-dUT, hybridized, and detected using a kit according to the manufacturer's instructions.

31.4.3 Isolation and Quantification of *Bradyrhizobium* Species

Medium BJMS (Tong and Sadowsky 1994)

This medium allows the isolation of *B. japonicum* and *B. elkanii* from soils, on the basis of their resistance to more than 40 ug of the metal ions Zn^{2+} and Co^{2+} per mL. There is no need to identify colonies by hybridization, the medium is selective for *Bradyrhizobium* and does not allow the growth of *Rhizobium* sp.

Composition (g L^{-1}): HM salts medium (Na_2HPO_4, 0.125; Na_2SO_4, 0.25; NH_4Cl, 0.32; $MgSO_4 \cdot 7H_2O$, 0.18; $FeCl_3$, 0.004; $CaCl_2 \cdot 2H_2O$, 0.013; *N*-2-hydroxyethylpiperazine-*N*′-2-ethane sulfonic acid, 1.3; 2-(*N*-morpholino)ethane sulfonic acid, 1.10); the pH is adjusted to 6.6 with 5 *M* NaOH (Cole and Elkan 1973). This solution is supplemented with: yeast extract, 10.0; L-arabinose, 10.0; Na-gluconate, 10.0; BG (brilliant green), 0.001; pentachloronitrobenzene (PCNB), 0.5; $ZnCl_2$, 0.83; $CoCl_2$, 0.88. The BG and heavy metals are prepared in stock solutions sterilized by filtration. PCNB is prepared as a 10% solution in acetone, then, it can be added to autoclaved 0.05% Triton X-100 to aid in the suspension. These substances are added to the sterile and molten medium.

Soil dilutions for inoculation: Before making serial dilutions, rhizobia are extracted from soils in the following way: 10 g of soil are placed in 95 mL of gelatin–ammonium phosphate solution (1% gelatin in water, adjusted to pH 10.3 and hydrolyzed by autoclaving, 10 min; Kingsley and Bohlool 1981), containing 0.5 mL of Tween 80 and 0.1 mL of silicone antifoam AF72 (General Electric Co., Waterford, New Jersey). Suspensions are shaken on a wrist action shaker for 30 min, and settled for an additional 30 min. The upper aqueous

phase is transferred to a sterile tube from which serial 10-fold dilutions are made for agar plate inoculation.

Comments: The number of contaminants is low (2–5 colonies per plate at the 10^{-1} soil dilution). *Bradyrhizobium* forms small and whitish colonies. However, some *Bradyrhizobium* of serocluster 123 (e.g., strain USDA123) are inhibited at these concentrations; if this serotype is expected, the media can be modified by lowering concentrations of BG (0.0005 g L^{-1}) and PCNB (0.25 g L^{-1}) or by substituting PCNB by cycloheximide (0.1 to 0.2 g L^{-1}).

Isolation of *B. japonicum* and Other Slow-Growing Rhizobia (Gault and Schwinghamer 1993)

Selective media containing various combinations of antibiotics and heavy metal compounds that are toxic to most soil bacteria including *Rhizobium* species are proposed; the effectiveness of combinations may vary according to the soil type. The basic medium SG used for growth of *B. japonicum* is supplemented with antibiotics and fungicides.

SG agar medium composition (g L^{-1}): KH_2PO_4, 0.35; K_2HPO_4, 0.25; $MgSO_4 \cdot 7H_2O$, 0.15; NaCl, 0.10; $CaCl_2 \cdot 2H_2O$, 0.08; biotin, 0.05; thiamin, 0.0003; Na-gluconate, 3.0; Difco yeast extract, 1.70; $(NH_4)_2SO_4$, 1.0. An effective combination of inhibitors to add is (mg L^{-1}): tetracycline, 10–15; rifampicin, 4–10; chloramphenicol, 15–25; cycloheximide, 50–60; pimafucin, 40. The addition of $ZnSO_4 \cdot 7H_2O$, 80–130, or $NiSO_4 \cdot 6H_2O$, 40–80, may add selectivity in some soils. Stock solutions of antibiotics and chemicals are prepared in water and sterilized by membrane filtration.

Soil dilutions: 2 g of soil sample is added to 10 mL of sterile water, thoroughly agitated and allowed to sediment for 3 h before drawing off the supernatant suspension. This suspension is serially diluted and 0.5 mL is surface-spread on the agar medium. Soil dilution can be made according to each laboratory procedure.

Comments: Although it is not proposed as a counting method, there is generally good agreement between this method and MPN plant-infection technique.

31.5 DIRECT DETECTION OF RHIZOBIA

Culture-independent methods involving polymerase chain reaction (PCR)-based approaches have potential for specific detection of rhizobia in the environment (soils, nodules, roots, inoculants) without the step of cultivation. Depending on the discrimination level (species or strain detection), it is possible to identify specific DNA (oligonucleotoides from total DNA, chromosomal, or symbiotic genes) which can be used in PCR-based protocols or in hybridization methods, as seen in Section 31.4.

The variations in rhizobial genome were initially studied to determine the diversity and to type and identify rhizobia from culture collections. Genes coding for 16S rRNA are used to identify rhizobia at the species and higher levels, while intergenic spacer (IS;16S–23S rDNA IGS) genes allow the differentiation of strains within a same species. DNA fingerprints obtained by using repetitive extragenic palindromic (REP) and enterobacterial repetitive intergeneric consensus (ERIC) primers have been used to identify and classify members of several rhizobial species (Laguerre et al. 1996). Symbiotic genes are useful to type and

classify rhizobia, as shown by the use of *nod* probes (from nodulation genes) in hybridization protocols in Section 31.4.1 and Section 31.4.2. Insertion sequences (IS) or repeated DNA sequences (RS) are used for strain identification and for evaluating the genetic structure of populations (Hartmann et al. 1992).

PCR-based protocols require firstly the extraction of microbial DNA from environment samples. In soils, this step may be more difficult than anticipated, as soils have complex composition. Compounds in the DNA extracts may inhibit subsequent PCR amplification and different DNA extraction methods affect the abundance and composition of bacterial community (Martin-Laurent et al. 2001). In nodules, DNA extraction is not necessary, as PCR can been preformed directly from crushed nodules (Tas et al. 1996). However, DNA extracted from nodules was used in a microarray assay (Bontemps et al. 2005). Recent advances on isolation of DNA and detection of DNA sequences in environmental samples have been recently published (Kowalchuk et al. 2004).

Although PCR is recognized as the most sensitive qualitative method for the detection of specific DNA in environmental samples, its quantification has become restricted to the clinical area (Jansson and Leser 2004). Until now, there is no standardized and robust screening tool for the direct detection and counting of rhizobia in soils. Only few protocols have been developed to trace specific strains, such as in competition studies for nodulation (Tas et al. 1996) or in root colonization (Tan et al. 2001).

31.6 SYMBIOTIC NITROGEN-FIXING EFFICIENCY OF RHIZOBIA

An efficient *Rhizobium* is a strain that is able to compete in the field with other indigenous rhizobia for the colonization of the rhizosphere of its homologous legume partner, under various soil physical and chemical conditions. This efficient strain will form many large nitrogen-fixing nodules on the roots of the plant host that will supply, for most legumes, from 70% to 90% of the plant need in nitrogen. Thus, the best way to estimate the symbiotic efficiency of rhizobial isolates is to do plant inoculation trials in field plots. However, as only about 10% of field-isolated strains are very efficient, if we aim at developing inoculant strains, the symbiotic efficiency of a large number of isolates has to be tested. Because of that, a first screening is performed under artificial axenic conditions in tubes, growth pouches, Leonard jars, or pots filled with sand or vermiculite or a mixture of both. These laboratory methods allow the identification of strains with high N_2-fixing ability, but they do not reflect the competitive ability of the strains. This can be alleviated by performing assays in potted field soils (Somasegaran and Hoben 1994). However, the real symbiotic efficiency of a strain cannot be determined without field plot inoculation trials. All legume inoculation experiments require prior elaboration of a proper experimental design. For information concerning the methodology and experimental designs for screening for effective strains, field site selection and preparation, we refer the readers to the book of Somasegaran and Hoben (1994). Usually treatments in addition to selected rhizobial strains include uninoculated and nitrogen fertilized controls (Vincent 1970). As commercially available legume inoculants include very efficient strains of rhizobia intensively tested under field conditions, if available for your area such an inoculant will be a proper control.

Although rhizobia have several plant growth promoting mechanisms of action (Antoun and Prévost 2005), symbiotic N_2 fixation is the most important mechanism in legumes. The different methods used for measuring symbiotic N_2 fixation in legumes were appraised by Azam and Farooq (2003).

31.6.1 Dry Matter Yield

As biological N_2 fixation is a major source of nitrogen for legumes, this biological activity is directly linked to dry matter yields in several legumes. This simple and inexpensive method is ideal in particular for field-based studies where other methods like the acetylene reduction technique are very variable. Harvested fresh matter (shoots, roots, or pods) are dried in an oven at 70°C until it reaches a constant weight (approximately 48 h). With forage legumes like alfalfa (*Medicago sativa*) it is necessary to take the shoots dry matter yield of a second cut, since it gives most information required to evaluate correctly the symbiotic efficiency of a *Sinorhizobium meliloti* isolate (Bordeleau et al. 1977).

31.6.2 Nodule Index

Since nodules are the site of N_2 fixation, a rapid visual nodule index based on nodule number ranging from 0 (absence of nodules) to 5 (the highest observed number of nodules) was frequently used to evaluate the efficiency of the symbiotic N_2 fixation of rhizobial isolates. However, as inefficient strains also can form numerous nodules, the following nodule index taking into account nodule number, size, and color is a more accurate evaluation (Ben Rebah et al. 2002):

$$\text{Nodulation index} = A \times B \times C \leq 18$$

Nodule size	Value *A*
Small	1
Medium	2
Large	3

Nodule color	Value *B*
White	1
Pink	2

Nodule number	Value *C*
Few	1
Several	2
Many	3

Nodules harboring efficient rhizobia are usually large and they contain leghemoglobin and are colored pink to red. Nodules formed by inefficient rhizobia are small and white. A legume inoculated with a very efficient strain of rhizobia will have a nodule index ranging from 12 to 18, while an inefficient strain will produce a nodule index of 6 or less. This nodule index will be very useful in screening isolates in Leonard jars, growth pouches, or pot experiments. This index will not be practical to use with field trials, because recuperation of roots with all nodules requires time consuming archaeological methodology.

31.6.3 Total-N Difference (Rice and Olsen 1993)

This is a relatively simple procedure, commonly used when only total-N analysis is available. The amount of N fixed by legumes is estimated from the difference in N yield between legume and a nonfixing (reference) plant grown in the same soil under the same conditions as the legume. The most suitable reference plant is an unnodulated plant of the legume being tested (Bremer et al. 1990). This can be achieved only when the soil in which the experiment

is being conducted contains no rhizobia which form effective nodules on the legume. The use of a nonnodulating isoline of the legume provides a suitable reference plant that gives reliable results (Smith and Hume 1987), but nonlegume plants have also been used successfully (Bell and Nutman 1971; Rennie 1984). The major assumption with this method is that the legume and the reference plant assimilate the same amount of soil N. However, differences in soil N uptake because of differences in root morphologies may result in erroneous estimates of N_2 fixation.

The procedure is simple in that all that is required is the inclusion of the reference crop treatment in the design of the field experiment. Care must be used in sampling to ensure that as much of the above-ground portion of the plants as possible is harvested without contaminating the plant material with soil. The plant samples are then processed and analyzed for total-N by the Kjeldahl method. Calculate the total yield from the percent total-N in the plant material and the dry matter yield, and obtain the difference in total-N yield between the legume and the reference crop, which will give the estimate of N_2 fixation.

31.6.4 Acetylene Reduction Assay

In nodules, bacteroids are the *Rhizobium* cells producing nitrogenase, the enzyme responsible for the reduction of N_2 to NH_3. Several other compounds are also reduced by nitrogenase, including acetylene (C_2H_2) reduced to ethylene (C_2H_4). The acetylene reduction assay (ARA) involves the enclosure of excised nodules, detached root systems, or whole plants in a closed container containing 10% C_2H_2. The size of the container will vary according to the plant material under study (glass tubes to mason jars). After specific incubation periods the C_2H_4 produced is quantified in the container by using a gas chromatograph equipped with hydrogen flame ionization detector, which can detect very low concentrations of C_2H_4. Nitrogenase activity is usually expressed as μmol C_2H_4 $plant^{-1}$ h^{-1} or μmol C_2H_4 g^{-1} nodule fresh or dry weight h^{-1}. Standard procedure and calculation for the ARA test were previously described (Turner and Gibson 1980; Somasegaran and Hoben 1994; Weaver and Danso 1994). This method is very sensitive, and is greatly affected by plant disturbance (Singh and Wright 2003). The ARA does not measure total nitrogenase activity because the assay conditions themselves cause decline in nitrogenase activity, and thus ARA cannot be used to calculate the exact amount of N_2 fixed. However, ARA is a valuable tool to assess relative differences in nitrogenase activity in the *Rhizobium*/legume symbioses (Vessey 1994), in pot-grown legumes but not in field-based studies (Minchin et al. 1994). ARA is a nondestructive method that can be very useful when selecting plants for N_2 fixation traits, since it allows later production of seeds from the same plant (Hardarson 2001). The ARA assay is about 1000 times more sensitive than the $^{15}N_2$, and furthermore, it is cheap and simple in its application (Knowles and Barraquio 1994).

31.6.5 Methods Involving ^{15}N

The ^{15}N isotope dilution method involves the growth of N_2 fixing and nonfixing reference plants in soil labeled with ^{15}N labeled inorganic or organic fertilizers. A nitrogen-fixing plant will have lower ^{15}N enrichment as compared to a nonfixing plant due to assimilation of unlabeled N_2 from the air (Hardarson 1994). The amount of N_2 accumulated during a growing season can be calculated using this methodology.

Calculation of the %N derived from the atmosphere (%Ndfa) can be made using the following equation:

$$\%\text{Ndfa} = (1 - \%\text{Ndff}_F/\%\text{Ndff}_{NF}) \quad (31.1)$$

Where $\%Ndff_F$ and $\%Ndff_{NF}$ are %N derived from fertilizer or tracer by fixing (F) and nonfixing (NF) plants receiving the same amount and enrichment of ^{15}N (Hardarson 1994).

The ^{15}N natural abundance method is based on the same principle as the isotope dilution method, but no ^{15}N-enriched material is added to soil (Weaver and Danso 1994). During N turnover reactions in soil, ^{14}N is preferentially lost into the atmosphere which results in a slightly higher $^{15}N/^{14}N$ ratio in soil than atmospheric N_2. Thus nitrogen-fixing plants have lower ^{15}N enrichment than nonfixing plants and this has been used to measure biological nitrogen fixation.

Detailed methodology on the use of ^{15}N isotope dilution method and ^{15}N natural abundance is described by Hardarson (2001) and Weaver and Danso (1994).

REFERENCES

Anonymous 2005. Methods for testing legume inoculant and preinoculated seed products. Fertilizers Act, Section 23, Regulations, Canadian Food Inspection Agency, Canada.

Antoun, H. and Prévost, D. 2005. Ecology of plant growth promoting rhizobacteria. In Siddiqui, Z.A., Ed. *PGPR: Biocontrol and Biofertilization*. Springer, New York, NY, pp. 1–38.

Azam, F. and Farooq, S. 2003. An appraisal of methods for measuring symbiotic nitrogen fixation in legumes. *Pak. J. Biol. Sci*. 18:1631–1640.

Barran, L.R., Bromfield, E.S.P., and Whitwill, S.T. 1997. Improved medium for isolation of *Rhizobium meliloti* from soil. *Soil Biol. Biochem*. 29: 1591–1593.

Bell, F. and Nutman, P.S. 1971. Experiments on nitrogen fixation by nodulated Lucerne. *Plant Soil Special Vol*.: 231–234.

Ben Rebah, F., Prévost, D., and Tyagi, R.D. 2002. Growth of alfalfa in sludge-amended soils and inoculated with rhizobia produced in sludge. *J. Environ. Qual*. 31: 1339–1348.

Bontemps, C., Golfier, G., Gris-Liebe, C., Carrere, S., Talini, L., and Boivin-Masson, C. 2005. Microarray-based detection and typing of the rhizobium nodulation gene *nodC*: Potential of DNA arrays to diagnose biological functions of interest. *Appl. Environ. Microbiol*. 71: 8042–8048.

Bordeleau, L.M., Antoun, H., and Lachance, R.A. 1977. Effets des souches de *Rhizobium meliloti* et des coupes successives de la luzerne (*Medicago sativa*) sur la fixation symbiotique d'azote. *Can. J. Plant Sci*. 57: 433–439.

Bremer, E., Van Kessel, C., Nelson, L., Rennie, R.J., and Rennie, D.A. 1990. Selection of *Rhizobium leguminosarum* strains for lentil (*Lens culinaris*) under growth room and field conditions. *Plant Soil* 121: 47–56.

Bromfield, E.S.P., Wheatcroft, R., and Barran, L.R. 1994. Medium for direct isolation of *Rhizobium meliloti* from soils. *Soil Biol. Biochem*. 26: 423–428.

Caetano-Anollés, G. and Gresshoff, P.M. 1997. *DNA Markers: Protocols, Applications, and Overviews*. Wiley-Liss Inc., New York, NY, 364 pp.

Chen, W-M., Moulin, L., Bontemps, C., Vandamme, P., Béna, G., and Boivin-Masson, C. 2003. Legume symbiotic nitrogen fixation by β-proteobacteria is widespread in nature. *J. Bacteriol*. 185: 7266–7272.

Cole, M.A. and Elkan, G.H. 1973. Transmissible resistance to penicillin G, neomycin, and chloramphenicol in *Rhizobium japonicum*. *Antimicrob. Agents Chemother*. 4: 248–253.

Date, R.A. and Halliday, J. 1987. Collection, isolation, cultivation and maintenance of rhizobia.

In Elkan, G.H., Ed. *Symbiotic Nitrogen Fixation Technology*. Marcel Dekker, New York, NY, pp. 1–27.

Debelle, F. and Sharma, S.B. 1986. Nucleotide sequence of *Rhizobium meliloti* RCR2011 genes involved in host specifity of nodulation. *Nucl. Acid Res*. 14: 7453–7472.

Gault, R.R. and Schwinghamer, E.A. 1993. Direct isolation of *Bradyrhizobium japonicum* from soil. *Soil Biol. Biochem*. 25: 1161–1166.

Gibson, A.H. 1980. Methods for legumes in glasshouse and controlled environment cabinets. In Bergersen, F.J., Ed. *Methods for Evaluating Biological Nitrogen Fixation*. John Wiley & Sons, New York, NY, pp. 139–184.

Hardarson, G. 1994. International FAO/IAEA programmes on biological nitrogen fixation. In Graham, P.H., Sadowsky, M.J., and Vance, C.P., Eds. *Symbiotic Nitrogen Fixation*. Kluwer Academic Publishers, Dordrecht, the Netherlands, pp. 189–202.

Hardarson, G. 2001. Use of ^{15}N to quantify biological nitrogen fixation in legumes. In *IAEA-TCS-14. Use of Isotope and Radiation Methods in Soil and Water Management and Crop Nutrition*. International Atomic Energy Agency, Vienna, Austria, pp. 58–70.

Hartmann, A., Gatroux, G., and Amarger, N. 1992. *Bradyrhizobium japonicum* strain identification by RFLP analysis using the repeated sequence RSα. *Lett. Appl. Microbiol*. 15: 15–19.

Jansson, J.K. and Leser, T. 2004. Quantitative PCR of environmental samples. In Kowalchuk, G.A., de Bruijn, F.J., Head, I.M., Akkermans, A.D.L., and van Elsas, J.D., Eds. *Molecular Microbial Ecology Manual*, 2nd Ed., Vol. 1. Kluwer Academic Publishers, Dordrecht, the Netherlands, pp. 445–463.

Kingsley, M.T. and Bohlool, B.B. 1981. Release of *Rhizobium* spp. from tropical soils and recovery for immunofluorescence enumeration. *Appl. Environ. Microbiol*. 42: 241–248.

Knowles, R. and Barraquio, W.L. 1994. Free-living dinitrogen-fixing bacteria. In Weaver, R.W., Angle, S., and Bottomley, P., Eds. *Method of Soil Analysis, Part 2—Microbiological and Biochemical Properties*. Soil Science Society of America, Madison, WI, pp. 179–197.

Kowalchuk, G.A., de Bruijn, F.J., Head, I.M., Akkermans, A.D.L., and van Elsas, J.D. 2004. *Molecular Microbial Ecology Manual*, 2nd Ed., Vol. 1. Kluwer Academic Publishers, Dordrecht, the Netherlands. 849 pp.

Laguerre, G., Bardin, M., and Amarger, N. 1993. Isolation from soil of symbiotic and nonsymbiotic *Rhizobium leguminosarum* by DNA hybridization. *Can. J. Microbiol*. 39: 1142–1149.

Laguerre, G., Mavingui, P., Allard, M.-H., Charnay, M.-P., Louvrier, P., Mazurier, S.-I., Rigottier-Gopis, L., and Amarger, N. 1996. Typing of rhizobia by PCR DNA fingerprinting and PCR-restriction fragment length polymorphism analysis of chromosomal and symbiotic gene regions: Application to *Rhizobium leguminosarum* and its different biovars. *Appl. Environ. Microbiol*. 62: 2029–2036.

Louvier, P., Laguerre, G., and Amarger, N. 1995. Semiselective medium for isolation of *Rhizobium leguminosarum* from soils. *Soil Biol. Biochem*. 27: 919–924.

Martin-Laurent, F., Philippot, L., Hallet, S., Chaussod, R., Germon, J.C., Soulas, G., and Catroux, G. 2001. DNA extraction from soils: Old bias for new microbial diversity analysis methods. *Appl. Environ. Microbiol*. 67: 2354–2359.

Miller, J.H. 1972. *Experiments in Molecular Genetics*. Cold Spring Harbor Laboratory, Cold Spring Harbor, NY, 466 pp.

Minchin, F.R., Witty, J.F., and Mytton, L.R. 1994. Reply to 'Measurement of nitrogenase activity in legume root nodules: In defense of the acetylene reduction assay' by J.K. Vessey. *Plant Soil* 158: 163–167.

Rennie, R.J. 1984. Comparison of N balance and ^{15}N isotope dilution to quantify N_2 fixation in field grown legumes. *Agron. J*. 76: 785–790.

Rhizobia_Taxonomy 2006. [Online] Available htpp://www.rhizobia.co.nz/Rhizobia Taxonomy.html [March 2006]

Rice, W.A. and Olsen, P.E. 1993. Root nodule bacteria and nitrogen fixation. In Carter, M.R., Ed. *Soil Sampling and Methods of Analysis*.

Canadian Society of Soil Science, Lewis Publishers, Boca Raton, FL, pp. 303–317.

Sahgal, M. and Johri, N. 2003. The changing face of rhizobial systemics. *Curr. Sci*. 84: 43–48.

Sambrook, J., Fritsch, E.F., and Maniatis, T. 1989. *Molecular Cloning: A Laboratory Manual*. Cold Spring Harbor Laboratory Press, Woodbury, NY.

Sambrook, J. and Russell, T.W. 2001. *Molecular Cloning: A Laboratory Manual*, 3rd Ed., Cold Spring Harbor Laboratory Press. Woodbury, NY. Paperback edition or online. Available http://www.MolecularCloning.com [March 2006]

Sessitsch, A., Howieson, J.G., Perret, X., Antoun, H., and Martínez-Romero, E. 2002. Advances in *Rhizobium* research. *Crit. Rev. Plant Sci*. 21: 323–378.

Singh, G. and Wright, D. 2003. Faults in determining nitrogenase activity. *J. Agron. Crop Sci*. 189: 162–168.

Smith, D.L. and Hume, D.J. 1987. Comparison of assay methods for nitrogen fixation utilizing white bean and soybean. *Can. J. Plant Sci*. 67: 11–20.

Somasegaran, P. and Hoben, H.J. 1994. *Handbook of Rhizobia. Methods in Legume-Rhizobium Technology*. Springer-Verlag, New York, NY, 450 pp.

Sullivan, J.T., Eardly, B.D., Van Berkum, P., and Ronson, C.W. 1996. Four unnamed species of nonsymbiotic rhizobia isolated from the rhizosphere of *Lotus corniculatus*. *Appl. Environ. Microbiol*. 62: 2818–2825.

Tan, Z., Hurek, T., Vinuesa, P., Müller, P., Ladha, J.K., and Reinhold-Hurek, B. 2001. Specific detection of *Bradyrhizobium* and *Rhizobium* strains colonizing rice (*Oryza sativa*) roots by 16S–23S ribosomal DNA intergenic spacer targeted-PCR. *Appl. Environ. Microbiol*. 67: 3655–3664.

Tas, E., Leinonen, P., Saano, A.S., Räsänen, L.A., Kaijalainen, S., Piippola, S., Hakola, S., and Lindström, K. 1996. Assessment and competitiveness of rhizobia infecting *Galega orientalis* on the basis of plant yield, nodulation, and strain identification by antibiotic resistance and PCR. *Appl. Environ. Microbiol*. 62: 529–535.

Tong, Z. and Sadowsky, M.J. 1994. A selective medium for the isolation and quantification of *Bradyrhizobium japonicum* and *Bradyrhizobium elkanii* strains from soils and inoculants. *Appl. Environ. Microbiol*. 60 (2): 581–586.

Turner, G.L. and Gibson, A.H. 1980. Measurement of nitrogen fixation by indirect means. In Bergersen, F.J., Ed. *Methods for Evaluating Biological Nitrogen Fixation*. John Wiley & Sons, New York, NY, pp. 111–138.

Vessey, J.K. 1994. Measurement of nitrogenase activity in legume root nodules: In the defense of the acetylene reduction assay. *Plant Soil* 158: 151–162.

Vincent, J.M. 1970. *A Manual for the Practical Study of Root-Nodule Bacteria*. Blackwell Scientific, Oxford, UK.

Weaver, R.W. and Danso, S.K.A. 1994. Dinitrogen Fixation. In Weaver, R.W., Angle, S., and Bottomley, P., Eds. *Method of Soil Analysis, Part 2—Microbiological and Biochemical Properties*. Soil Science Society of America, Inc., Madison, WI, USA, pp. 1019–1045.

Wheatcroft, R., Bromfield, E.S.P., Laberge, S., and Barran, L.R. 1993. Species specific DNA probe and colony hybridization of *Rhizobium meliloti*. In Palacios, R., Mora, J., and Newton, W.E., Eds. *New Horizons in Nitrogen Fixation*. Kluwer, Boston, MA, USA, p. 661.

Woomer, P., Bennett, J., and Yost, R. 1990. Overcoming the inflexibility of most-probable number procedures. *Agron. J*. 82: 349–353.

Chapter 32
Microarthropods

J.P. Winter
Nova Scotia Agricultural College
Truro, Nova Scotia, Canada

V.M. Behan-Pelletier
Agriculture and Agri-Food Canada
Ottawa, Ontario, Canada

32.1 INTRODUCTION

In most soils, 90% of the microarthropod population is composed of Collembola (springtails) and Acari (mites), while the remainder includes Protura, Diplura, Pauropoda, and Symphyla (Wallwork 1976). While our understanding of microarthropod ecology is still in its infancy, we know that they can play a significant role in accelerating plant residue decomposition through their interactions with the microflora (Seastedt 1984; Moore and Walter 1988; Coleman et al. 2004). They are ''litter transformers'' fragmenting decomposing litter and improving its availability to microbes (Wardle 2002). Fecal pellets of the particle-feeding microarthropods, Collembola and the acarine suborder Oribatida (also called Cryptostigmata), have a greater surface-to-volume ratio than the original leaf litter and can lead to greater decomposition per unit time (Coleman et al. 2004). The flow of energy and nutrients through the soil also may be accelerated by microarthropods grazing on microflora, causing increased rates of microbial biomass turnover. The importance of microarthropods to litter breakdown rates varies with litter quality and is higher on litter of high C:N ratio (low quality) (Coleman et al. 2004). Collembola and Oribatida (which include Astigmata (Norton 1998)) are predominantly saprophages and mycophages, but some Oribatida show opportunistic predation on nematodes and other microfauna, and scavenging on small dead arthropods. The acarine suborders Prostigmata and Mesostigmata are mainly predatory, but some Prostigmata and Mesostigmata (Uropodina) are mycophages (Wallwork 1976; Norton 1985a).

Within a climatic region, the main factors determining the abundance of soil microarthropods include: (1) the type and quantity of decomposing organic residues and their effects on the microfloral population, (2) the stability of soil structure, especially pore space, and (3) the soil water regime (Wallwork 1976). They are especially abundant in the litter of boreal forest floors (e.g., 300,000 individuals m^{-2}), but are much less numerous in cultivated soils (50,000 individuals m^{-2}) (Petersen and Luxton 1982).

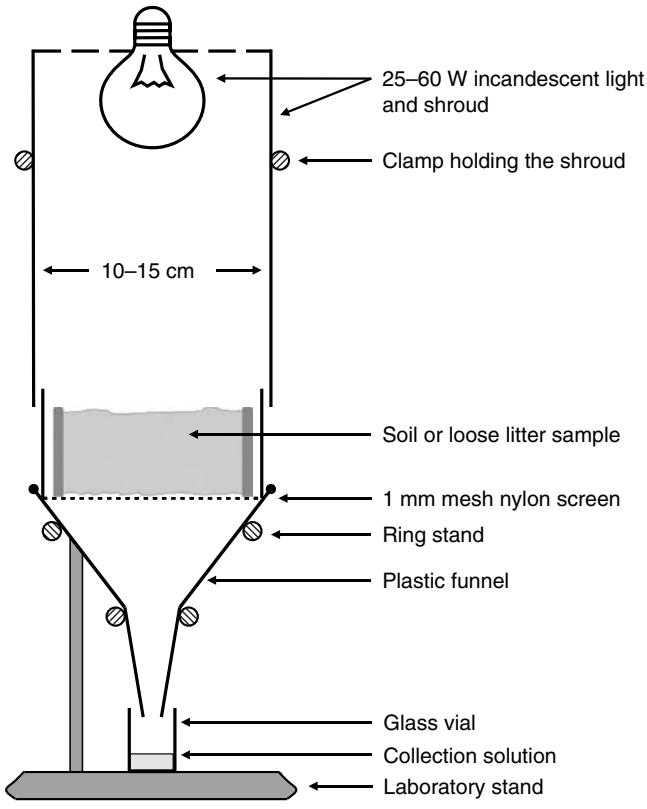

FIGURE 32.1. A simple bench-top Berlese–Tullgren dynamic extractor that can be operated at room temperature or in a room cooled to 4°C. The light source could be an incandescent desk lamp. This style of extractor is available commercially. (From Burkard Scientific 2006. *Tullgren Funnels*. Uxbridge, Middlesex, UK. Available at: http://www.burkardscientific.co.uk (last verified, June 2006).)

Methods for extracting microarthropods from plant litter and soil have been reviewed by Evans et al. (1961), Macfadyen (1962), Murphy (1962a,b), Edwards and Fletcher (1971), Edwards (1991), and Coleman et al. (2004). Essentially, the methods fall into two categories:

1 Dynamic (or active) methods require the participation of the animals to move through the sample medium, away from repellent stimuli toward attractant stimuli. A basic dymanic extractor is illustrated in Figure 32.1. Typically, a sample of soil or litter is placed upon a sieve, and then the top of the sample is warmed and dried while maintaining the bottom cool and moist. As the sample dries from top down, fauna move downward to escape desiccation, and finally drop from the lower surface to be collected in a container below. Fauna will fall from the bottom of the sample throughout the duration of extraction but the greatest exodus occurs as the lower surface of the sample dries to −1500 kPa, and the temperature rises to above 30°C (Petersen 1978; Takeda 1979). Fauna fall into a collecting jar containing a preservative solution.

2 Mechanical separation uses the physical and chemical properties of the animals, such as body size, density, and hydrophobicity, to mechanically extract them.

Common procedures suspend soil by stirring it in a saline solution or in an oil–water mixture. When stirring is stopped, microarthropods float to the liquid surface. In the case of oil–water suspensions, when stirring stops, oil floats to the surface carrying within it lipophilic microarthropods but little hydrophilic plant residue.

Two methods for extracting soil microarthropods are described in this chapter: Dynamic extraction using a high (temperature and moisture) gradient extractor, and mechanical separation in a water–heptane mixture. The heptane method is more expensive to operate, but can be used to validate the high-gradient extractor. This chapter provides suggestions for soil sampling, and gives a recommended example of both the active and the mechanical extraction methods. Techniques for handling and storing microarthropods are briefly described.

32.2 SAMPLING

When using dynamic methods for extraction, it is essential that the fauna are viable, and that every effort is made to facilitate their escape from the sample. Soft-bodied animals, such as Collembola, Prostigmata, and immatures of Oribatida and Mesostigmata, are very easily damaged by rough handling. It is essential that the soil samples are not compacted during collection so that the animals can successfully escape through the pore space and be counted.

Soil samples for dynamic extractors may be taken by pressing a metal cylinder or ''corer'' into the soil. The bottom edge of the cylinder should be beveled to facilitate cutting into the soil. When sampling a series of depths down a column of soil, a sampling tool such as illustrated in Figure 32.2 may be used. The soil is retained within metal- or heat-resistant plastic rings. To reduce sample compaction, the internal diameter of these rings is 1 mm wider

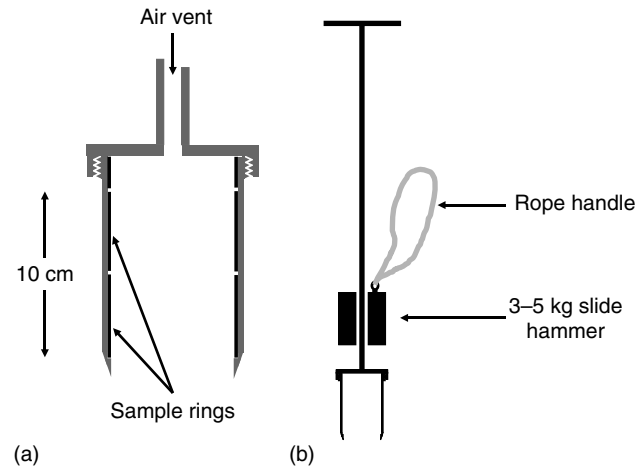

FIGURE 32.2. Cross-section of a hammer-driven coring tool for sampling soil while minimizing compaction. (a) Expanded view of the sampling bit containing sampling-holding rings. The cutting edge diameter should be 1 mm narrower than the internal holding-ring diameter to reduce friction on the holding-ring walls. A hollow handle shaft allows air to escape as the soil enters the corer. (b) The whole sampler showing the metal hammer that drops onto the sampling bit forcing it into the soil. A rubber disk cut from the side of an autotire will dampen hammer impact.

diameter than the cutting edge of the sampler. Plant litter may be sampled by cutting around the exterior of a corer with a sharp knife while exerting downward pressure on the corer.

32.2.1 Comments

1 Leading edge of the soil corer should be kept sharp so as to minimize compaction of the sample while the corer is being pressed into the soil.

2 Use a core at least 5 cm diameter to avoid sample compaction.

3 Height of the soil core has an important effect on the ability of fauna to escape. A height of 2.5–5 cm is satisfactory for most well-structured soils. Extraction of fauna from soils with low macroporosity may be best from cores 2.5 cm in height.

4 Compaction of the soil during sampling may occur even if a sampling tool is used (Figure 32.2). To avoid compaction, the height of the corer should be similar to its diameter. When sampling deeper than 10 cm, layers of soil may have to be sampled separately.

5 If using a sampling tool such as in Figure 32.2, try separating the series of cylinders with fine needles. Slicing apart the cores with a knife may be necessary in soils containing roots, but the knife can smear the soil and block the pores.

6 Place soil cores into plastic bags, and label bags indicating the top of core. Transport in a chest preferably cooled to 5°C–10°C. Protect cores from vibrations during travel.

7 It is best to extract samples as soon as possible after collection from the field. Lakly and Crossley (2000) observed that numbers extracted decreased linearly over several days when stored at 6°C. Storage conditions may cause changes in the microarthropod population structure due to predation, breeding, moulting, or mortality (Murphy 1962a).

32.3 EXTRACTION METHODS

32.3.1 High-Gradient Dynamic Extraction

Drying soil to drive out microarthropods was pioneered by Berlese in 1905 and Tullgren in 1918 (Murphy 1962a). Macfadyen (1955) greatly improved the method by developing the first high-gradient extractor. The extractor described here (Figure 32.3) is for intact soil cores or loose litter samples. It is similar to that of Crossley and Blair (1991) and was chosen for its simple construction and because it incorporates most of the refinements (Merchant and Crossley, 1970; Norton, 1985b) made to the earlier Macfadyen (1955) design. This extractor is best operated in a ventilated room, with good air circulation, refrigerated to about 4°C. We describe a single-extractor module. It has a light bulb heat source that dries soil or litter from above, causing fauna to fall into a collecting cup below. Several of these modules are operated in an array separated from each other by at least 3–4 cm. Our modular design is intended as an example, and building your own extractor can be adapted to locally available materials.

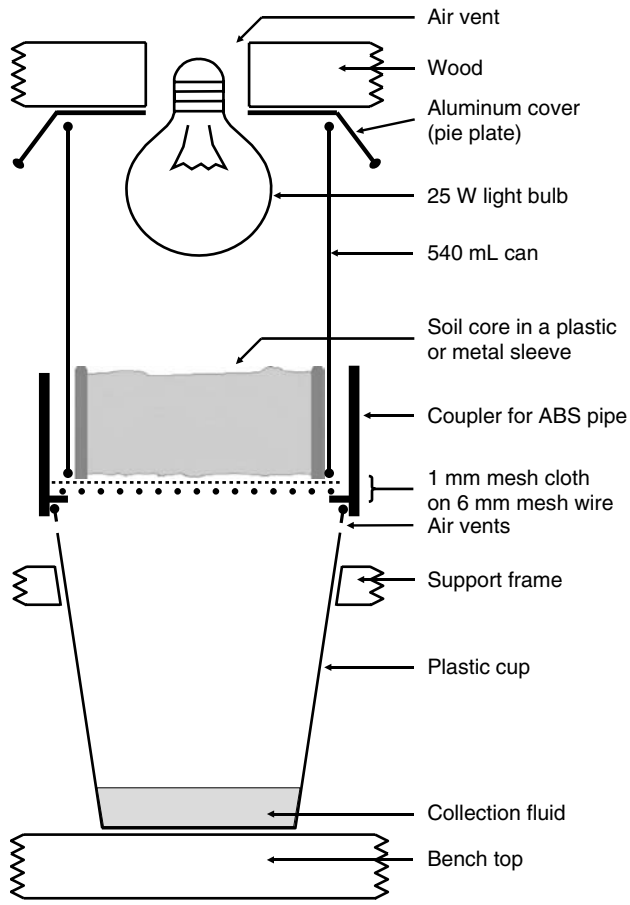

FIGURE 32.3. Cross-section of a high-gradient extractor module.

Materials and Methods

The main body of an extractor module is made from a cylindrical coupling (90 mm internal diameter, 80 mm tall) normally used to join ''3-inch'' acrylonitrile butadiene styrene (ABS) black plastic pipe. The bottom 30 mm of the coupling is not needed and can be cut off making it 50 mm tall (Figure 32.3). A flange inside the coupling supports a disk of 6 mm wire mesh (hardware cloth), painted to prevent rusting. On top of this mesh is placed a disk of finer mesh made from plastic window fly screen or a couple of layers of cheese cloth. The fine mesh prevents contamination of the collected fauna with soil, but holes must be at least 1 mm wide to allow microarthropods to pass through. On top of the finer mesh is placed the soil or litter sample. Soil samples are taken with metal cylinders or a coring device (Figure 32.2), and are contained within a ring of plastic or metal (50–75 mm internal diameter). The height of the soil core is usually 30–50 mm. Around and above the soil core is a metal cylinder made from a 540 mL food can (83 mm internal diameter). The can supports a light source above the soil, and encloses the space between the soil and light so as to retain heat.

The source of heat is a 25 W incandescent light bulb with a diffused-white glass globe. The bulb is held in a chandelier socket, around which is a reflector made from an aluminum pie plate. The air space above the soil sample vents out around the chandelier socket.

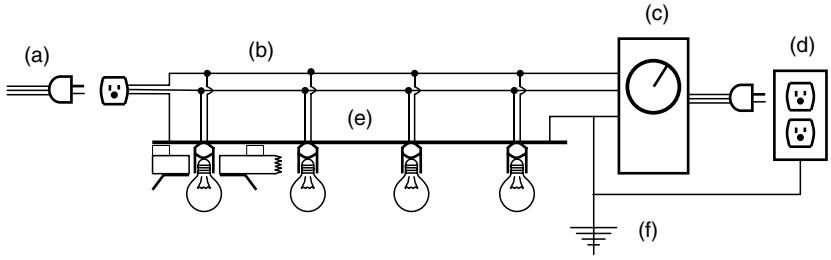

FIGURE 32.4. A row of lights for four high-gradient extractor modules: (a) connection to the next row of lights, (b) wires connecting chandelier sockets in parallel, (c) rheostat to control light intensity, (d) wall socket, (e) metal bar with attached sockets, and (f) the metal bar and rheostat are grounded through the wall socket. A row of lights is gently placed on top of a row of extraction modules.

Below the wire mesh supporting the soil sample is a cup into which microarthropods are collected. We use a plastic beverage cup that has 90 mm external diameter at the upper lip. This allows the cup to fit snugly within the ABS pipe coupling, and press up against the flange which supports the wire mesh and soil. The snug fit of the cup prevents fauna from escaping the apparatus (more durable cups can be made by cutting the tops off polypropylene histology sample jars). At the bottom of the cup is placed 20 mL of collecting solution (below). The cup is placed in a hole of a support frame of plywood or plexiglass that prevents the apparatus from being accidently knocked over.

The ideal collecting solution should kill and preserve fauna without producing repellent or noxious vapors. A 50% solution of propylene glycol can be used. Some people prefer to collect into water, and rinse the cup down with 95%, nondenatured, ethyl alcohol at the end of collecting to kill the fauna. For molecular studies of fauna, they are collected into 95% ethyl alcohol, but the cups must be perforated for ventilation (see comments below).

The above describes a single module of a high-gradient extractor. In practice, many modules are used simultaneously in rows of 4 to 6, with more rows connected as needed (Figure 32.4).

In each row, the chandelier sockets are screwed onto a metal bar, and wired together in parallel with 14 standard wire gauge (SWG) extension chord wire. The brightness of the bulbs (i.e., heat emitted) is controlled by a rheostat or light-dimmer switch. The maximum number of modules depends on the power supply and the rheostat. For safe operation, you should aim not to exceed 80% of the rated output of your power supply. If the wall socket supplies 15 A (at 120 V) then the extractor should not draw more than 12 A (or fifty-seven 25 W bulbs: recall that power (W) = current (A) · potential difference (V)). Moreover, the number of bulbs should not exceed the capacity of the rheostat or it will overheat. For example, a 600 W rheostat has a capacity for twenty-four 25 W bulbs. The metal bar holding the chandelier sockets and the rheostat are all grounded through the wall socket.

Procedure

1 Place a disk of 1 mm window screen, or cheese cloth onto the wire mesh of an extractor module.

2 For a soil core, push the core within its sampling ring into the can, and then place it onto the module screens. Soil samples should be oriented so that the end of the core

that was uppermost in the field faces downward in the extractor (see Comment 3, below). For loose litter samples, place the can onto the module screens, then load litter in through the top of the can. Litter should not be more than 50 mm deep.

3 Place 20 mL of collecting solution into a collecting cup. Gently attach the cup onto the bottom of the module. Avoid vibrations that cause soil debris to fall into the solution and make sorting microarthropods more difficult. (Misting the sample surface with tap water before loading may reduce the amount of soil contaminating the collection solution.)

4 Once a row of 4–6 modules have been loaded, gently place the light source on top. Continue until all samples are loaded.

5 Turn on the lights, and adjust the rheostat to give an initial temperature at the top of the samples of 15°C–20°C. (An access hole for a thermometer can be made beside one of the lights.) The objective is to gradually dry samples from the top down to the bottom over the course of 3 to 4 days. Most microarthropods will have exited the sample by the time the bottom of the sample dries. If the bottom of a sample is damp, then the extraction is not complete. For a sample from a well-structured surface soil, the rheostat is adjusted to increase the temperature at the sample surface to 20°C–25°C on day 2, 25°C–30°C on day 3, 30°C–35°C on day 4, and 40°C on day 5. Soil samples high in organic matter may take longer to extract. Soil samples with low macroporosity, such as poorly structured clay soils, may have to be dried gradually owing to slower downward migration of fauna. Less heat energy is required for litter samples so as not to dry them too rapidly. Operate the extractor in a vibration-free environment.

6 Periodically check to see that the extraction solution has not evaporated, but usually, water from the soil condenses in the collection cup.

7 At the end of an extraction, turn off the lights and with minimum vibration, remove the collection cup. Pour the contents of the cup into storage vials, and carefully rinse down the cups with additional collection fluid to remove any attached fauna. Remove and clean sample holders and screens (see Section 32.5).

8 If reporting microarthropod abundance as number per mass of dry soil, or estimating soil bulk density, dry soil samples at 105°C for 3 days. Do not dry the soil at 105°C if you are going to extract it with heptane (below).

9 *Caution*: Propolyne glycol is moderately toxic and slightly flammable; ethyl alcohol is toxic and very flammable. Avoid inhalation of fumes and skin contact. Handle the chemicals in a well-ventilated room and with gloves, laboratory coat, and eye protection. The refrigerated room containing the extractor must be ventilated and have air circulated to prevent a build-up of alcohol fumes, which could be ignited by a spark.

Comments

1 Advantages of this extractor are that it minimizes cross contamination of samples by fauna, the bottoms of samples do not dry prematurely, and the environment in different extractor modules is relatively uniform.

2 In general, incandescent light bulbs serve as a source of drying heat, not light. Light may repel microarthropods, but it has been regarded as somewhat of a neutral stimulus (Murphy 1962a) and may in some cases be an attractant. Merchant and Crossley (1970) observed that light emitted from bulbs painted white were more efficient for extracting microarthropods than clear bulbs, or those of various colors. Chemical repellents have been used, but they are not as effective as light bulbs (Murphy 1962a).

3 It is best to operate the extractor in a room cooled to around 4°C, because this helps create the temperature gradient in the soil core. The extractor can be operated at room temperature, but it will be less efficient at expelling fauna than at 4°C.

4 Inverting soil cores when placing them in a high-gradient extractor is recommended since escape through soil pores is facilitated. For cores taken at the soil surface, fauna are often most abundant at the top of the core, and soil voids tend to increase in size toward the top. Inverting surface cores reduces the volume of soil through which most fauna must pass.

5 Higher numbers of fauna are usually recovered from intact soil cores rather than cores that have been removed from corers and crumbled over the extractor screen (Macfadyen 1961). No one has provided a clear explanation for this, but disrupting the soil may injure delicate fauna, or reduce the extraction efficiency by altering the rate of soil drying.

6 Seventy-five percent, nondenatured, ethyl alcohol is a common collection fluid (Coleman et al. 2004), and for specimens that will be used for molecular studies 95% ethyl alcohol is recommended. Five percent glycerol can be added, in case the alcohol evaporates during extraction. While this fluid was successful for collecting fauna through a funnel into a vial, the efficiency for collecting into a cup could be seriously reduced, especially for Collembola (Seastedt and Crossley 1978). For this reason, a low-volatile, 50% solution of propylene glycol (technical grade) is recommended. A 10%–50% solution of picric acid is preferred by some authors (e.g., Meyer 1996) instead of alcohol, but can explode if it dries out. Leaving a small (0.5 cm) space between the jar cap and jar will minimize the effects of collecting solution fumes. The extractor design of Crossley and Blair (1991) is open below the sample, minimizing effects of collecting solution fumes. Similarly, the Rothamsted-modified Macfadyen high-gradient funnel has a space below the sample minimizing the effects of collecting solution fumes (Bater 1996, see Figure 13.2). If one needs to extract into ethyl alcohol, the extractor illustrated in Figure 32.1 has sufficient ventilation and is recommended for this solution rather than the extractor in Figure 32.3. The extractor in Figure 32.3 can be ventilated by perforating the top of the collection cup below the rim with a hot glass rod to make 0.5 cm holes, although a few animals may escape through these holes.

7 Little information exists on the effects of sample water content on the rate and efficiency of fauna extraction. Greater uniformity in moisture content across soil cores may produce more uniform extraction efficiency. However, finding a method to rapidly and uniformly wet all cores without affecting fauna is difficult. Most researchers do not adjust cores for moisture content. Field moisture content

at the time of sampling should be measured, to explain vertical migrations of microarthropods in response to rainfall.

9 Contaminating the collection fluid with soil particles and plant debris can greatly increase the difficulty of sorting and counting specimens. Physical barriers have been described that prevent plant or soil from falling (Murphy 1962a; Woolley 1982), but unfortunately, they usually decrease the extraction efficiency. If necessary, microarthropods in a dirty collecting solution may be floated off using a concentrated salt solution (see Section 32.3.2).

10 Efficiency of a high-gradient extractor is affected by its construction, operation, and the nature of the samples (André et al. 2002). Many observations of their efficiency report values greater than 75% for Acari and Collembola (Lussenhop 1971; Marshall 1972; Petersen 1978). However, when extracting microarthropods from semiarid soils, Walter et al. (1987) found efficiencies ranging from 26% to 66%. Takeda (1979) found the extraction efficiency for Collembola to vary from 28% in the summer to 88% in the winter. Therefore, precise ecological research requires calibration of the high-gradient extractor. For this purpose, one may select a subset of samples from a range of habitats, and follow high-gradient extraction with the heptane extraction method described below.

32.3.2 Mechanical Extraction: Heptane Flotation

Introduction

The simplest flotation method uses a saturated solution of sodium chloride or magnesium sulfate. The soil sample is disrupted and stirred in the solution (specific gravity of 1.2 Mg m^{-3}), and the less dense fauna (1.0–1.1 Mg m^{-3}) float to the surface. After leaving the solution to stand for 15 min, the fauna are decanted off the surface of the solution and stored in 70% ethyl alcohol solution. This technique has proven successful for Acari and Collembola, but not for large oribatid mites, especially those with adhering soil, and some larger insects (Murphy 1962b). This technique is unsuitable for samples containing large amounts of organic matter and a high-gradient extractor would be more effective (Edwards and Fletcher 1971).

Better extraction of fauna may be achieved by stirring the sample in a mixture of oil and water. When left undisturbed, oil droplets rise to the surface. Microarthropods enter the oil phase since their cuticles are lipophilic. The surface of plant residues tends to be hydrophilic and is not coated in oil. Both plant residues and microarthropods float to the surface, leaving the mineral components to settle. Plant residues reside at the top of the aqueous phase, while microarthropods reside in the oil above, at the oil–water interface. The oil phase containing microarthropods and a little of the aqueous phase are decanted off. Plant fragments can be found in the oil if small droplets of oil adhere to their surfaces, or if they contain substantial amounts of entrapped air. Adding the sample to water and subjecting it to a partial vacuum before stirring it with oil can help to force out entrapped air.

A method of oil–water extraction of soil microarthropods is described below. It is an adaptation by Walter et al. (1987) of the standard flotation procedure of the Association of Official Analytical Chemists (Williams 1984). Recently, simplifications to this procedure have been proposed (Geurs et al. 1991), and it has been adapted for processing large (18 L) volumes of soil (Kethley 1991).

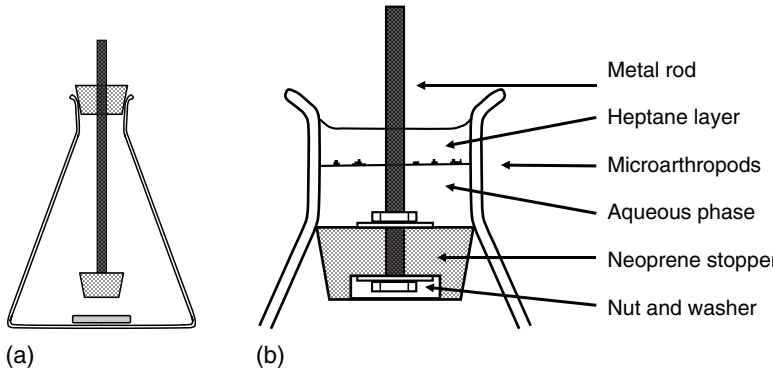

FIGURE 32.5. Equipment for heptane flotation of microarthropods. (a) Erlenmeyer flask with stopper in the lowered position and (b) enlarged view with the stopper raised to the neck of the flask.

Materials and Reagents

1 A magnetic stirrer and a 50 mm Teflon-coated stirring bar, or a variable speed rotary shaker.

2 A stainless steel sieve, finer than 50 μm.

3 A Wildman trap flask (Figure 32.5) consisting of a 1–2 L wide-mouthed Erlenmeyer flask into which is inserted a close-fitting neoprene stopper supported on a metal rod 5 mm in diameter and about 10 cm longer than the height of the flask. The rod is threaded at the lower end and furnished with a nut and washers to hold the stopper in place.

4 95%–100% ethyl alcohol, not denatured. Dilutions are made with distilled water on a percent volume basis.

5 *n*-Heptane containing <8% toluene.

Procedure (Walter et al. 1987)

1 Stage I is the immersion of the soil sample in ethyl alcohol to kill the microarthropods and fix the populations at the time of sampling. The entire soil core (ca. 100 g dry mass) is placed in a 2 L beaker and 500 mL of 95% ethyl alcohol is added. Parafilm is placed over the beaker to prevent evaporation. Samples may be stored in this condition for at least a few weeks with no obvious decrease in extraction efficiency. Samples are allowed to sit for at least 24 h before flotation to help free microarthropods from soil aggregates.

2 Stage II involves the clearing of organic material from the sample, the establishment of an aqueous phase, and the division of the soil sample into volumes of material that may be efficiently extracted in 2 L Erlenmeyer flasks. The mixture is placed in a vacuum chamber to eliminate air from the plant debris (time required, 2–10 min, varies with amount of plant material). The bulk of the alcohol is decanted through a fine mesh, stainless steel sieve (finer than 50 μm).

Care must be taken to rinse oils and floating surface debris from the beaker. The material in the sieve is briefly rinsed sequentially with 95% (or 100%) ethyl alcohol, 70% ethyl alcohol, and finally with distilled water, before back-rinsing the contents of the sieve into a beaker with distilled water. Distilled (or degassed) water is added to the beaker to bring the total volume to approximately 800 mL. The sample is allowed to stand for 3–5 min, then the surface debris and most of the water is decanted through the sieve, before rinsing the sieve with distilled water and finally back-rinsing the sieve with distilled water into the beaker. The soil sample, now in an aqueous phase, is divided between two wide-mouth 2 L Erlenmeyer flasks (if smaller soil cores are used, a single flask is adequate), and each is placed on a magnetic stirring plate and provided with a magnetic stirring bar and a metal rod with a neoprene stopper or wafer at one end (Figure 32.5).

3 Stage III is the movement of the microarthropods from the soil sample (aqueous phase) into the heptane layer, and the isolation of the heptane layer from the aqueous phase. The neoprene stopper is placed below the water surface and approximately 25 mL of heptane is slowly poured down the rod. The rod holding the neoprene stopper is clamped to hold the neoprene stopper above the level of the magnet, but below the water–heptane interface. A notched square of parafilm placed over the flask mouth reduces evaporation of the heptane. (Alternatively, the rod can be slid through a tight fitting hole in a second neoprene stopper which fits the mouth of the flask. In this way, the flask can be sealed and the lower neoprene stopper held off the flask bottom (Figure 32.5a).) The mixture is stirred at the lowest speed that effectively suspends the sample with heptane for 10–15 min (to ensure that the microarthropods in the sample have time to be trapped by the heptane layer). The mixture can also be stirred on a variable speed rotary shaker at the lowest speed necessary. The sample is then allowed to stand for about 5 min to allow soil particles to settle. Distilled water is slowly poured along the rod to raise the heptane layer into the neck of the flask, and then allowed to stand for 2–3 min. The neoprene stopper is gently rotated to dislodge soil debris, and then slowly raised into the neck of the flask, isolating the heptane layer and a small volume of water (Figure 32.5b) from the bulk of the mixture volume. The trapped volume (Figure 32.5b) is then rinsed into the sieve with 100% ethyl alcohol to cut the heptane. Material in the sieve is further rinsed with 95% ethyl alcohol and finally back-rinsed with 95% ethyl alcohol before rinsing into a suitable container with 70% ethyl alcohol.

4 *Caution*: Both heptane and ethyl alcohol are toxic and very flammable. Work in a fume hood and wear gloves, laboratory coat, and splash protection for body and eyes.

Comments

1 It is often useful to repeat the flotation process when microarthropods are abundant. The neoprene stopper is gently lowered to the bottom of the flask. The bulk of the aqueous phase is decanted through the sieve. The walls of the flask are rinsed with 100% ethyl alcohol to dissolve the film of heptane, and approximately 100 mL of distilled water is added to the flask. This new volume of water is decanted through the sieve. Material in the sieve is rinsed with 100% and then 95% ethyl alcohol before a final back-rinsing with distilled water into the flask. Distilled water is added to the flask to bring the volume to approximately 400 mL and the flotation procedure is repeated as above.

2 Not all mechanical methods are more efficient than using a high-gradient extractor (Edwards and Fletcher 1971). However, Walter et al. (1987) found the heptane flotation method extracted four times as many individuals and twice as many species as a high-gradient extractor. Microarthropods from laboratory cultures were added to dry-sieved soil, then using a single flotation cycle, the extraction efficiency of heptane flotation was estimated: for the acarine suborders; Prostigmata (39%), Mesostigmata (69%), Oribatida (without Astigmata) (84%) and Astigmata (95%); and Collembola (89%). A second flotation cycle increased overall extraction efficiency from 78% to 88%.

3 One problem with mechanical methods is that both living and dead specimens are extracted. In the case of some hard-bodied mites, the presence of anal or genital shields, and the absence of fungal mycelia within a body shell, may be helpful in identifying mites that were viable at the time of sample collection. With other categories of fauna, this may not be possible, and an overestimation of the active animal population can result.

4 Use of organic solvents for extraction may be prohibited in some areas. A flotation method using a saturated sugar solution, developed by Snider and Snider (1997), yielded higher captures of microarthropods than did high-gradient extractions in hardwood forest soils, but is very labor intensive.

32.4 COMPARING HIGH-GRADIENT AND HEPTANE EXTRACTION METHODS

The high-gradient extractor has the following advantages and disadvantages when compared to heptane extraction.

1 Advantages:

a. Less costly to operate and less labor intensive.

b. Animals are extracted in better condition for identification. Mechanical methods damage many specimens.

c. More effective than mechanical methods in separating microarthropods from plant litter.

2 Disadvantages:

a. Different species may not respond equally to the applied stimuli. For example, light may be an attractant for some and a repellent for others. In response to desiccation, some species may become quiescent, or attach themselves to large fauna expecting to be carried to a more favorable environment (phoretic behavior).

b. Different stages in the life cycle of the species respond differently to applied stimuli (Tamura 1976; Takeda 1979). For example, nonactive stages, such as moulting stages, eggs, phoretic stages, quiescent stages, cannot be extracted. This is a serious consideration for Oribatida as 30% of the life cycle may be

spent in moulting (Luxton 1982). Small-sized juveniles are usually less easily extracted than more mobile adults (Søvik and Leinaas 2002).

c. Extractability of different taxa may vary with time of year (Leinaas 1978; Takeda 1979), weather events, and climate. High-gradient extractors may be less effective for hot arid climates (Walter et al. 1987).

d. Extractability of different taxa may vary with soil depth and between different soils. Soil properties such as organic matter and texture can affect soil porosity and continuity of pore space, and thereby, affect extraction efficiency.

e. During extraction eggs can hatch and mortality can occur.

f. Efficiency is affected by apparatus construction and operation.

It is prudent to use both dynamic and mechanical methods to account for differences in extraction efficiency between species, species in different soils, and environmental change at the experimental site. A useful technique is to select a subset of samples from the high-gradient extractor, and then extract the same samples with the heptane (Walter et al. 1987). Other methods for calibrating high-gradient extractors have been critically reviewed by Petersen (1978).

32.5 HANDLING AND IDENTIFICATION

32.5.1 Introduction

It is not extremely difficult to identify soil microarthropods at a low level of taxonomy such as the acarine suborders or Collembolan families. A good general key and a relatively short consultation with a specialist in soil fauna may be all that is required to acquaint a novice with the basic level of classification. On the other hand, detailed classification to the genus and species level requires a high level of skill. Taking a course in classification (e.g., Ohio State University 2006) is recommended. A basic key to soil fauna has been published by Dindal (1990). Dindal (1990) and Behan-Pelletier (2003) supply major bibliographies on the biology and taxonomy of microarthropods.

For basic information on handling and storing specimens, and for making slide mounts for examination under a light microscope, refer to Evans et al. (1961, 1985), Krantz (1978), and Woolley (1982). Preparation of specimens by serial sectioning and for electron microscopy is discussed by Krantz (1978). Methodology for laboratory culturing of microarthropods is given by Evans et al. (1961) and Krantz (1978). An outline of the time required for the different steps in extraction, sorting, and identification of microarthropods is given in Marshall et al. (1994).

32.5.2 Storage Solutions

Microarthropods collected in propylene glycol can be stored in that solution for a few months; however, it has not been proven for prolonged storage. A 70% ethyl alcohol solution is commonly used to preserve a collection of fauna. To guard personal health, the ethyl alcohol should be free of denaturing additives. Adding 5% glycerol to the alcohol is

recommended to prevent desiccation of the specimens where the alcohol could evaporate. Concentrations of ethyl alcohol greater than 80% are not recommended, unless specimens will be used for molecular studies, since shrinkage of specimens can occur, and they may become brittle. Some fauna, such as Collembola, may have a waxy cuticle and be difficult to wet with storage solution. Collembola can be dewaxed by heating in 70% alcohol at 60°C for 1 h. This should cause them to be thoroughly wetted by the preservative solution and sink.

Specimens can be stored in the ethyl alcohol solution in small (2 mL), glass shell vials. Enclosing small vials in larger vials of ethyl alcohol solution is recommended when archiving a collection. If specimens are to be sent to a taxonomist for identification, they should be shipped in ethyl alcohol solution rather than mounted on slides, unless requested otherwise.

32.5.3 Preliminary Sorting and Clearing

Handling of microarthropods is carried out in liquid—usually the collecting or storage solutions—in a Syracuse watch glass or Perspex dish, or in lactic acid on a cavity slide. The animals can be manipulated by an assortment of wire loops, minute spatulas, Pasteur pipettes, or tungsten wire microneedles (Norton and Sanders 1985). Sorting at low levels of taxonomic resolution can be done at $>60\times$ magnification under a stereomicroscope, with occasional reference to higher magnification under a compound microscope. For higher magnification, specimens can be temporarily mounted in lactic acid on cavity microscope slides.

32.6 BRIEF STATISTICAL CONSIDERATIONS

Microarthropods often exhibit a ''nugget'' distribution in soil with high numbers associated with plant residue and low numbers a few centimeters away. Observations are usually quite variable and may show a skewed frequency distribution. If so, the raw data may need to be normalized by $\log(x+1)$ transformation before analysis of variance. Sampling should pay attention to ecosystem details such as the spatial arrangements of plants, plant litter, and bare soil. Many samples may be necessary when comparing agricultural practices, since these soils are often not as radically different in faunal numbers compared to soils from more diverse ecosystems.

REFERENCES

André, H.M., Ducarme, X., and Lebrun, P. 2002. Soil biodiversity: myth, reality, or conning? *Oikos* 96: 3–24.

Bater, J.E. 1996. Micro- and macro-arthropods. In G.S. Hall, Ed. *Methods for the Examination of Organismal Diversity in Soils and Sediments*. CAB International, Oxford, UK, pp. 163–174.

Behan-Pelletier, V.M. 2003. Acari and Collembola biodiversity in Canadian agricultural soils. *Can. J. Soil Sci*. 83: 279–288.

Burkard Scientific 2006. *Tullgren Funnels*. Burkard Scientific, PO Box 55, Uxbridge, Middx, UB8 2RT, UK. Available at: http://www.burkardscientific.co.uk (last verified, June 2006).

Coleman, D.C., Crossley, D.A. Jr., and Hendrix, P.F. 2004. *Fundamentals of Soil Ecology*. Elsevier, Amsterdam, the Netherlands, 386 pp.

Crossley, D.A. Jr. and Blair, J.M. 1991. A high-efficiency, ''low-technology'' Tullgren-type extractor for soil microarthropods. *Agric. Ecosyst. Environ*. 34: 187–192.

Dindal, D.L. 1990. *Soil Biology Guide*. John Wiley & Sons, New York, NY, 1349 pp.

Edwards, C.A. 1991. The assessment of populations of soil-inhabiting invertebrates. *Agric. Ecosyst. Environ*. 34: 145–176.

Edwards, C.A. and Fletcher, K.E. 1971. A comparison of extraction methods for terrestrial arthropods. In J. Phillipson, Ed. *Methods of Study in Quantitative Soil Ecology: Population, Production, and Energy Flow*. IPB Handbook No. 18. Blackwood Scientific, London, UK, pp. 150–185.

Evans, G.O., Griffiths, D.A., Macfarlane, D., Murphy, P.W., and Till, W.M. 1985. *The Acari: A Practical Manual. Vol. 1. Morphology and Classification*. University of Notingham School of Agriculture, University of Notingham, School of Agriculture, Sutton Bonington, Loughborough, Leics, UK.

Evans, G.O., Sheals, J.G., and Macfarlane, D. 1961. *The Terrestrial Acari of the British Isles. Vol. 1. Introduction and Biology*. British Museum (Natural History), London, UK, 219 pp.

Geurs, M., Bongers, J., and Brussaard, L. 1991. Improvements to the heptane flotation method for collecting microarthropods from silt loam soil. *Agric. Ecosyst. Environ*. 34: 213–221.

Kethley, J. 1991. A procedure for extraction of microarthropods from bulk soil samples with emphasis on inactive stages. *Agric. Ecosyst. Environ*. 34: 193–200.

Krantz, G.W. 1978. *A Manual of Acarology*. Oregon State University Press, Corvallis, OR, 509 pp.

Lakly, M.B. and Crossley, D.A. 2000. Tullgren extraction of soil mites (Acarina): effect of refrigeration time on extraction efficiency. *Exp. Appl. Acar*. 24: 135–140.

Leinaas, H.P. 1978. Seasonal variation in sampling efficiency of Collembola and Protura. *Oikos* 31: 307–312.

Lussenhop, J. 1971. A simplified canister-type soil arthropod extractor. *Pedobiologia* 11: 40–45.

Luxton, M. 1982. The biology of mites from beech woodland. *Pedobiologia* 23: 1–8.

Macfadyen, A. 1955. A comparison of methods for extracting soil arthropods. In D.K. McE. Kevan, Ed. *Soil Zoology*. Butterworth, London, UK, pp. 315–332.

Macfadyen, A. 1961. Improved funnel-type extractors for soil arthropods. *J. Anim. Ecol*. 30: 171–184.

Macfadyen, A. 1962. Soil arthropod sampling. In *Advanced Ecology*. Research, Academic Press, London, UK, pp. 1–34.

Marshall, S.A., Anderson, R.S., Roughley, R.E., Behan-Pelletier, V., and Danks, H.V. 1994. Terrestrial arthropod biodiversity: planning a study and recommended sampling techniques. A brief prepared by the Biological Survey of Canada (Terrestrial Arthropods). Published by the Entomological Society of Canada Supplement to the Bulletin, Vol. 26 (1). Available at: http://www.biology.ualberta.ca/bsc/briefs/brterrestrial.htm, March 1994.

Marshall, V.G. 1972. Comparison of two methods of estimating efficiency of funnel extractors for soil microarthropods. *Soil Biol. Biochem.* 4: 417–426.

Merchant, V.A. and Crossley, D.A. Jr. 1970. An inexpensive high-efficiency Tullgren extractor for soil microarthropods. *J. Georgia Entomol. Soc*. 5: 83–87.

Meyer, E. 1996. Mesofauna. In F. Schinner, R. Öhlinger, E. Kandeler, and R. Margesin, Eds. *Methods in Soil Biology*. Springer-Verlag, Berlin, Germany, pp. 338–345.

Moore, J.C. and Walter, D.E. 1988. Arthropod regulation of micro- and mesobiota in belowground detrital food webs. *Ann. Rev. Entomol*. 33: 419–439.

Murphy, P.W. 1962a. Extraction methods for soil animals. I. Dynamic methods with particular reference to funnel processes. In P.W. Murphy, Ed. *Progress in Soil Zoology*. Butterworths, London, UK, pp. 75–114.

Murphy, P.W. 1962b. Extraction methods for soil animals. II. Mechanical methods. In P.W. Murphy, Ed. *Progress in Soil Zoology*. Butterworths, London, UK, pp. 115–155.

Norton, R.A. 1985a. Aspects of the biology of soil arachnids, particularly saprophagous and mycophagous mites. *Quaest. Entomol*. 21: 523–541.

Norton, R.A. 1985b. A variation of the Merchant–Crossley soil microarthropod extractor. *Quaest. Entomol*. 21: 669–671.

Norton, R.A. 1998. Morphological evidence for the evolutionary origin of Astigmata (Acari: Acariformes). *Exp. Appl. Acar*. 22: 559–594.

Norton, R.A. and Sanders, F. 1985. Superior microneedles for manipulating and dissecting soil invertebrates. *Quaest. Entomol*. 21: 673–674.

Ohio State University 2006. Acarology Summer Program, The Ohio State University, Columbus, OH. Available at: http://www.biosci.ohio-state.edu/~acarolog/sum2k1.htm (last verified, June 2006).

Petersen, H. 1978. Some properties of two high gradient extractors for social microarthropods and an attempt to evaluate their extraction efficiency. *Natura Jutlandica* 20: 95–122.

Petersen, H. and Luxton, M. 1982. A comparative analysis of soil fauna populations and their role in decomposition processes. *Oikos* 39: 287–388.

Seastedt, T.R. 1984. The role of microarthropods in decomposition and mineralization processes. *Ann. Rev. Entomol*. 29: 25–46.

Seastedt, T.R. and Crossley, D.A. Jr. 1978. Further investigations of microarthropod populations using the Merchant–Crossley high-gradient extractor. *J. Georgia Entomol. Soc*. 13: 333–338.

Snider, R.M. and Snider, R.J. 1997. Efficiency of arthropod extraction from soil cores. *Ent. News* 108: 203–208.

Søvik, G. and Leinaas, H.P. 2002. Variation in extraction efficiency between juvenile and adult oribatid mites: *Ameronothrus lineatus* (Oribatida, Acari) in a Macfadyen high-gradient canister extractor. *Pedobiologia* 46: 34–41.

Takeda, H. 1979. On the extraction process and efficiency of MacFadyen's high-gradient extractor. *Pedobiologia* 19: 106–112.

Tamura, H. 1976. Biases in extracting Collembola through Tullgren funnel. *Rev. Ecol. Biol. Sol*. 13: 21–34.

Wallwork, J.A. 1976. *The Distribution and Diversity of Soil Fauna*. Academic Press, London, UK, 355 pp.

Walter, D.E., Kethley, J., and Moore, J.C. 1987. A heptane flotation method for recovering microarthropods from semiarid soils, with comparison to the Merchant–Crossley high-gradient extraction method and estimates of microarthropod biomass. *Pedobiologia* 30: 221–232.

Wardle, D.A. 2002. *Communities and Ecosystems: Linking the Aboveground and Belowground Components*. Princeton University Press, Princeton, NJ.

Williams, S., Ed. 1984. In *Official Methods of Analysis of the Association of Official Analytical Chemists*, XIV edition, pp. 887–890.

Woolley, T.A. 1982. Mites and other soil microarthropods. In A.L. Page et al., Eds. *Methods of Soil Analysis, Part 2—Chemical and Microbiological Properties*. Soil Science Society of America, Madison, WI, pp. 1131–1142.

Chapter 33
Nematodes

T.A. Forge
Agriculture and Agri-Food Canada
Agassiz, British Columbia, Canada

J. Kimpinski
Agriculture and Agri-Food Canada
Charlottetown, Prince Edward Island, Canada

33.1 INTRODUCTION

This chapter addresses the extraction of nematodes from soil. All life stages of migratory endoparasites (e.g., *Pratylenchus* spp.) can be found in soil or roots at any given point of time (Vrain et al. 1997), and proper population quantification depends on analyses of both root and soil subpopulations. The most common methods for extraction of migratory endoparasites from roots and other plant tissues include the shaker method (Bird 1971; Barker 1985a; Ingham 1994) and the mist chamber extraction method (Barker 1985a; Hooper 1986b; Hooper and Evans 1993; Ingham 1994). Eggs and second-stage (infective) juveniles of the sedentary endoparasites (e.g., *Meloidogyne* spp., *Heterodera* spp., and *Globodera* spp.) are usually extracted from soil, and counts require interpretation with knowledge of the life cycles of species in the region. The intermediate and adult stages of sedentary endoparasites are not easily extracted from roots, but root tissue can be cleared and stained to facilitate observation (and quantification) of the intermediate and adult stages of sedentary endoparasites (Hooper 1986c; Hooper and Evans 1993; Baker and Gowen 1996).

Methods for extraction of nematodes from soil may be divided into two general categories: (1) those based on nematode motility and (2) those based on nematode physical characteristics such as size and specific density (Verschoor and De Goede 2000). Most methods based on motility are modifications of the Baermann funnel technique (Baermann 1917). The Baermann funnel was developed initially to recover nematodes from animal feces, and it was adapted and modified by plant nematologists to recover nematodes from soil or plant tissue (Hooper 1986a,b). Specific extraction techniques derived from the Baermann funnel depend on nematode activity. Therefore, extraction efficiency is influenced by the inherent differences in motility among nematode species, sample handling, and soil texture (Kimpinski and Welch 1971; Viglierchio and Schmitt 1983; Barker 1985b). Sieving centrifugal-flotation

is the most widely used method based on nematode size and density. Efficiency of the centrifugation–flotation method is affected primarily by nematode size, as small nematodes are more easily lost through one of the sieving steps (Barker 1985a).

Extraction efficiency is critical in estimating populations as accurately as possible in order to properly characterize nematode populations (Ferris 1987). An extraction method can be chosen to optimize recovery efficiency of the target species. For example, members of the Criconematidae are relatively inactive and known to be more efficiently extracted via centrifugal-flotation than Baermann funnel (Barker 1985a). In recent years, more research has been directed at analyses of entire communities of free-living (microbivorous, omnivorous, and predacious) nematodes as indicators of status of the soil food web. The influences of extraction methods on nematode community analyses have only recently begun to be addressed. McSorley and Frederick (2004) reported that Baermann funnel extraction was relatively more efficient at recovering omnivores and predators whereas centrifugal-flotation was relatively more efficient at recovering herbivores. More research is needed on the optimization and standardization of extraction methods when analysis of the entire soil nematode community is the primary objective.

33.2 SAMPLE PRETREATMENT

Nematode spatiotemporal variation and statistical considerations for sampling have been reviewed and described in detail elsewhere (Barker 1985b; Ingham 1994). Soil samples should be kept in polyethylene bags to prevent drying, and refrigerated (but not frozen) as soon as possible after field sampling. Samples should not be left in direct sunlight, particularly during summer. The initial step in sample processing involves removing coarse fragments and root pieces, usually by passing the sample through a sieve. Unless the objectives are to specifically target some of the smaller species (e.g., *Pratylenchus* spp., *Meloidogyne* spp. juveniles, or *Heterodera* spp. juveniles) it is suggested that the soil be passed through a sieve of >5 mm opening or not sieved at all; for example, some of the larger dorylaimid nematodes (e.g., *Xiphinema* spp.) appear to be damaged when soil is passed through 2 mm or smaller sieves.

33.3 BAERMANN FUNNEL TECHNIQUE (BAERMANN 1917)

The basic method is to wrap the sample in cloth or paper tissue and partly submerge it in a funnel filled with water. As nematodes move about in the saturated material, they settle out of the material and sink to the bottom of the neck of the funnel where they can be recovered.

33.3.1 Materials and Reagents

1. 10 cm diameter glass narrow-stem funnels, with 5 cm sections of rubber tubing attached to the end of each funnel
2. Spring-type tubing clamps
3. Basket-like screen inserts made from nylon screen (100 to 250 μm opening) glued onto PVC rings (2 cm wide) cut from 7.5 cm diameter PVC pipe

4 Three-ply facial tissue cut into 10 cm diameter circles

5 Racks to hold the funnels

33.3.2 Procedure

1 Mix soil thoroughly but gently, so as not to injure nematodes.

2 Place facial tissue on the screen.

3 Spread 25 g soil evenly over the tissue. If tissue has not been cut into a circle, fold corners over the soil sample.

4 Use clamp to close rubber tubing at the bottom of the funnel.

5 Pour water in the top of the funnel until it is about 1 cm above the level of the bottom of the screen when it is in place. Tap the stem of the funnel or drain a quantity of the water to remove bubbles from the stem.

6 Gently place the screen insert in the funnel, allowing the soil to wet up from the bottom.

7 Adjust water volume using a squirt bottle (squirt around the edges of the basket, not directly onto the soil). Soil should be completely saturated but not completely immersed.

8 Cover the screen/funnel with the lid of a Petri dish or a piece of plastic wrap, and incubate at room temperature for 7 days.

9 Release clamp and drain >20 mL of water from the funnel into a scintillation vial or large test tube (e.g., 50 mL polyethylene centrifuge tube).

10 Allow >1 h for nematodes to settle to the bottom of the test tubes or vials.

11 Siphon off all but bottom 5 to 10 mL (depending on size of counting dish), pour contents into a counting dish, allow a few minutes for nematodes to settle, and examine with a stereomicroscope or inverted microscope at 10 to 70× magnification.

33.3.3 Comments

1 Advantages of the Baermann funnel technique in its original or modified form are that the equipment is simple and easy to set up, and the method can be used to process many samples. Many nematology laboratories modify bookshelves to function as batteries of large numbers of funnel supports.

2 A disadvantage of the Baermann funnel technique is the lack of oxygen, especially in the base of the funnel where the nematodes collect. To overcome this, Stoller

(1957) attached a thin polyethylene tube and bubbled oxygen or fresh air into the water. Another disadvantage is that the small area of screen limits the volume of soil that can be extracted effectively, as extraction efficiency decreases with increasing thickness of the soil layer (Bell and Watson 2001).

3 The use of a pan or tray in place of the funnel allows oxygen to diffuse more rapidly into the shallow water and thin soil layer (Whitehead and Hemming 1965). Such adaptations of Baermann's approach are known as Whitehead and Hemming trays, Baermann trays, or Baermann pans. Baermann pans are generally larger and more amenable to extraction of larger volumes of soil.

33.4 BAERMANN PAN TECHNIQUE

The equipment and procedures outlined below are similar to the Townshend (1963) method.

33.4.1 Materials and Reagents

1 Teflon-coated aluminum cake pans, approximately 20 cm diameter and 5 cm deep. Alternatively, the plastic trays used under plant pots can be used.

2 Saran or nylon screens (18 cm diameter) glued with neoprene cement to acrylic or PVC rings (15 mm high and 4 mm thick). Rings can be made by cutting sections off, of 18 cm diameter acrylic or PVC pipe. Three acrylic legs are cemented to the outside of each ring and a small piece of acrylic is glued to the center of each screen, to hold the screen about 4 mm from the bottom of the cake pan. Metal screens should not be used since metallic ions can be toxic to nematodes (Pitcher and Flegg 1968).

3 Three-ply facial tissue, preferably cut in circles 20 cm in diameter.

4 Large test tubes (with racks).

33.4.2 Procedure

1 Mix soil thoroughly but gently, so as not to injure nematodes.

2 Place 20 cm diameter three-ply paper tissue on each screen.

3 Spread 50 g soil in a thin layer over the paper tissue. If tissue has not been cut into a circle, fold corners over soil sample.

4 Place the screen with soil in each cake pan. Each cake pan should contain enough water to saturate the soil sample, but not completely immerse it.

5 Stack pans and cover with a plastic hood or place in a large plastic bag to reduce evaporation. Add water to pans every few days if needed (around edges, do not pour water directly onto sample).

6 Incubate samples at room temperature for several days.

7 Lift the screen and allow water to drain from the soil into the pan for 10 to 15 s. Rinse the bottom of the screen into the pan with a wash bottle.

8 Swirl water in the pan and pour the contents into a large test tube. Rinse pan with a bit more water and add to test tube.

9 Allow >1 h for nematodes to settle at the bottom of test tubes.

10 Siphon down to 5 to 10 mL (depending on size of counting dish) and pour contents carefully into a counting dish, allow a few minutes for nematodes to settle, and examine with a stereomicroscope at 10 to 70×.

11 (Alternative to step 10) Contents of the pan can be poured over a 500 mesh sieve (26 μm opening) held at a 45° angle until the volume remaining on the screen is reduced to about 15 mL and then rinsed via a funnel into a 20 mL scintillation vial or test tube of similar size with a squirt bottle.

33.4.3 Comments

Barker (1985a) indicates that 3- to 14-day incubations are necessary for maximum nematode recovery. We have found that about 90% of extractable *Pratylenchus penetrans* are recovered after 7 days with the Baermann pan method. Bell and Watson (2001) found that extraction efficiency of some species decreased with an increase in the volume of soil placed in Baermann pans.

33.5 SIEVING–BAERMANN FUNNEL TECHNIQUE

Decanting and sieving can be used to first extract nematodes from most of the soil solids, followed by Baermann funnel to complete extraction of remaining nematodes from the residue left on the screen.

33.5.1 Materials and Reagents

1 Baermann funnels with screen inserts (as described above) and racks

2 Two 1 L pitchers

3 Large slotted spoon

4 Sieves (20 cm diameter) with 500, 250, 180, 38, and 26 μm openings (respectively, 35, 60, 80, 400, and 500 mesh)

5 50 mL centrifuge tubes and racks

33.5.2 Procedure

1 Place 100 g soil in the pitcher. Add about 250 mL water and using fingers gently break up any clods.

2 Bring water volume to 1 L and using slotted spoon, stir vigorously for 20 s.

3 Let suspension settle for 30 s (sand drops out of suspension) and pour supernatant through 35 mesh sieve into a second pitcher and rinse the 35 mesh sieve.

4 (Optional) If recovery of cysts is an objective, place an 80 mesh sieve between the 35 mesh sieve and the pitcher (a cyst is the body of a dead female of the family Heteroderidae, and is a spherical, moisture-resistant structure that may contain several hundred eggs). Cysts will be retained on the 80 mesh sieve.

5 Immediately pour contents of the second pitcher over the 400 mesh screen while holding the screen at 45° angle, taking care not to allow the suspension to overflow the sieve. Gentle tapping of the screen will help water pass through the residue of silt, organic matter, and nematodes.

6 When the remaining nematode-containing residue has been reduced to about 25 mL, use a squirt bottle to rinse the residue into a 50 mL centrifuge tube; place a short-stem funnel in the centrifuge tube to assist rinsing the sample into the tube.

7 Fill Baermann funnel with water as described above and place screen with tissue into funnel (allowing the tissue to become wet).

8 Allow contents of centrifuge tube to settle for >1 h and gently siphon off all but bottom 15 mL. Swirl and pour evenly over tissue. Rinse centrifuge tube with small volume of water and pour onto tissue.

9 Cover, incubate for 48 h, and collect sample as described for direct Baermann funnel technique.

33.5.3 Comments

1 While some nematodes may be lost during the decanting and sieving, for some species, this approach may be more efficient than Baermann funnel extraction directly from soil because there is less material for the nematodes to move through.

2 This approach is easily adapted to processing larger soil samples (e.g., 250 g soil), which is desirable when the target species are not abundant or economic threshold population densities are low. For example, population densities of *Xiphinema* and *Longidorus* species are often less than 10 nematodes per 100 g soil, and extraction from 250 g soil or more can yield less variable population estimates.

3 While this approach is faster than either direct Baermann funnel or Baermann pan, it also requires more labor for each sample.

33.6 CENTRIFUGAL-FLOTATION METHOD (CAVENESS AND JENSEN 1955; JENKINS 1964)

This is a quick and easy method for extracting nematodes from soil. Specimens can be obtained in a few minutes and recovery of inactive species and nematode eggs is greater than from most other methods of extraction. The details outlined below are primarily from a modified version described by Barker (1985a).

33.6.1 Materials and Reagents

1 Centrifuge with swinging bucket head that will hold 50 mL or larger tubes and can operate to 420 *g*.

2 50 mL centrifuge tubes and racks.

3 Sieves (20 cm diameter) with 500, 38, and 26 μm openings (respectively, 35, 400, and 500 mesh).

4 Beakers, 600 mL size.

5 Sucrose solution with a specific gravity of 1.18 (454 g of sugar in water to make 1 L of solution), though a specific gravity range of 1.10 to 1.18 is satisfactory for most soil-inhabiting nematodes (Thistlethwayte and Riedel 1969).

6 Vibratory or vortex-style test tube mixer.

33.6.2 Procedure

1 Perform steps 1–6 described for the sieving–Baermann funnel technique above.

2 Place centrifuge tubes in centrifuge. Be sure to balance the tubes.

3 Centrifuge at 420 *g* for 5 min.

4 Gently pour off supernatant from each tube (nematodes are in soil at bottom of tubes).

5 Fill centrifuge tubes with sugar solution and mix.

6 Centrifuge for 60 s at 420 *g*. Nematodes should remain suspended in the sugar solution. Do not use the brake to stop the centrifuge, as this may dislodge the soil from the bottom of the tubes.

7 Pour sucrose solution from each tube into a 600 mL beaker containing about 500 mL of water to reduce the high osmotic concentration.

8 Pour contents of each 600 mL beaker slowly onto a 500 mesh sieve held at 45° angle.

9 Gently rinse the nematodes on the 500 mesh sieve into a 20 mL scintillation vial or test tube of similar size.

10 Allow >1 h for nematodes to settle to the bottom of the test tube.

11 Siphon down to 5 to 10 mL (depending on size of counting dish), pour carefully into a counting dish, allow a few minutes for nematodes to settle, and examine with a stereomicroscope at 10 to 70×.

33.6.3 Comments

1 Centrifugal-flotation usually recovers a higher percentage of inactive specimens, particularly the Criconematidae, than the Baermann funnel (Kimpinski and Welch 1971; Viglierchio and Schmitt 1983). However, this technique may not be convenient for large numbers of samples, since each soil aliquot requires a fair degree of handling and manipulation.

2 The high osmotic concentration of the sugar solution sometimes damages or distorts specimens (Viglierchio and Yamashita 1983), and extraction efficiency of the method may be less than 50% of the nematodes in a sample (Viglierchio and Schmitt 1983; Barker 1985a).

33.7 FENWICK CAN (FENWICK 1940)

This relatively inexpensive apparatus is widely used for extracting cysts from soil samples weighing several hundred grams. The basic principle is that cysts contain air and will float to the surface. Details outlined below are taken from Ayoub (1980) and Shepherd (1986).

33.7.1 Materials and Reagents

1 A 30 cm high can, usually made of brass, tapered toward the top and having a sloped base. A drain hole (2.5 cm diameter) closed with a rubber stopper is located in the side of the can at the low end of the slope. Just below the top of the can is a sloping collar with a rim 6 cm high that tapers toward a 4 cm wide outlet.

2 Large brass funnel 20.5 cm diameter, with a 20.5 cm long stem.

3 Sieves (20 cm diameter) with 1000, 850, and 250 μm openings (respectively, 18, 20, and 60 mesh), and one 60 mesh sieve about 8 cm in diameter.

4 Beaker, 600 mL in size.

33.7.2 Procedure

1 Mix soil thoroughly, remove large stones and very coarse materials, and air dry for several hours.

2 Fit large brass funnel containing 18 mesh sieve into top of can.

3 Fit 20 mesh sieve over 60 mesh sieve and place under collar outlet of can to collect overflow of water.

4 Fill can with water and wet 20 and 60 mesh sieves.

5 Place soil sample on 18 mesh sieve and wash through into can with a jet of water. This will cause organic material, some soil, and many of the cysts in the soil to overflow into the collar and pass down onto 20 and 60 mesh sieves.

6 Rinse debris on the 20 mesh sieve to facilitate movement of cysts through openings down to the 60 mesh sieve.

7 Discard coarse material on 20 mesh sieve.

8 Wash material on 60 mesh sieve into a 600 mL beaker.

9 Pour floating material from 600 mL beaker through the 8 cm diameter, 60 mesh sieve. Rotate beaker to remove material adhering to sides and discard sediment on bottom.

10 Using a small laboratory scoop or spoon, transfer material from sieve onto one or more counting dishes.

11 Add enough water to counting dishes to float material and examine with a stereomicroscope.

12 Transfer cysts or suspected cysts using a dissecting needle to sample vial containing a few milliliter of water.

33.7.3 Comments

1 This technique is quite efficient, and Shepherd (1986) claims that 70% of cysts in a soil sample are floated up and captured on the sieves.

2 The equipment is inexpensive and easy to set up, and the extraction takes little time. However, special equipment may be necessary when large numbers of samples are being processed (Ayoub 1980).

3 An alternate procedure (after step 9) is to flush the material from the 60 mesh sieve with a wash bottle onto rapid flow filter paper in a funnel, let drain, and examine the filter paper surface for cysts.

4 While the Fenwick can is a widely used method, other methods such as the Schuiling centrifuge may have comparable extraction efficiencies and be more convenient (Kimpinski et al. 1993).

REFERENCES

Ayoub, S.M. 1980. *Plant Nematology, an Agricultural Training Aid*. NemaAid Publications, Sacramento, CA. 195 pp.

Baermann, G. 1917. Eine einfache Methode zur Auffindung von *Anchylostomum* (Nematoden) Larven in Erdproben. *Geneesk Tijdschr. Ned. Ind*. 57: 131–137.

Baker, T.J. and Gowen, S.R. 1996. Staining nematodes and arbuscular mycorrhizae in the same root sample. *Fundam. Appl. Nematol*. 19: 607–608.

Barker, K.R. 1985a. Nematode extraction and bioassays. In K.R. Barker, C.C. Carter, and J.N. Sasser, Eds. *An Advanced Treatise on Meloidogyne*,

Volume II Methodology. USAID, North Carolina State University Graphics, Raleigh, NC, USA, pp. 19–35.

Barker, K.R. 1985b. Sampling nematode communities. In K.R. Barker, C.C. Carter, and J.N. Sasser, Eds. *An Advanced Treatise on Meloidogyne*, Volume II Methodology. USAID, North Carolina State University Graphics, Raleigh, NC, USA, pp. 3–17.

Bell, N.L. and Watson, R.N. 2001. Optimizing the Whitehead and Hemming tray method to extract plant parasitic and other nematodes from two soils under pasture. *Nematology* 3: 179–185.

Bird, G.W. 1971. Influence of incubation solution on the rate of recovery of *Pratylenchus brachyurus* from cotton roots. *J. Nematol.* 3: 378–385.

Caveness, F.E. and Jensen, H.J. 1955. Modification of the centrifugal-flotation technique for the isolation and concentration of nematodes and their eggs from soil and plant tissue. *Proc. Helminth. Soc. Wash.* 22: 87–89.

Fenwick, D.W. 1940. Methods for the recovery and counting of cysts of *Heterodera schachtii* from *Soil. J. Helminthol.* 18: 155–172.

Ferris, H. 1987. Extraction efficiencies and population estimation. In J.A. Veech and D.W. Dickson, Eds. *Vistas on Nematology*. Society of Nematologists, Hyattsville, MD, USA, pp. 63–69.

Hooper, D.J. 1986a. Extraction of free-living stages from soil. In J.F. Southey, Ed. *Laboratory Methods for Work with Plant and Soil Nematodes*. Ministry of Agriculture, Fisheries and Food, Reference Book 402, Her Majesty's Stationery Office, London, UK, pp. 5–30.

Hooper, D.J. 1986b. Extraction of nematodes from plant material. In J.F. Southey, Ed. *Laboratory Methods for Work with Plant and Soil Nematodes*. Ministry of Agriculture, Fisheries and Food, Reference Book 402, Her Majesty's Stationery Office, London, UK, pp. 51–58.

Hooper, D.J. 1986c. Preserving and staining nematodes in plant tissues. In J.F. Southey, Ed. *Laboratory Methods for Work with Plant and Soil Nematodes*. Ministry of Agriculture, Fisheries and Food, Reference Book 402, Her Majesty's Stationery Office, London, UK, pp. 81–85.

Hooper, D.J. and Evans, K. 1993. Extraction, identification and control of plant-parasitic nematodes. In K. Evans, D.L. Trudgill and J.M. Webster, Eds. *Plant Parasitic Nematodes in Temperate Agriculture*. CAB International, Wallingford, UK, pp. 1–59.

Ingham, R. 1994. Nematodes. In R.W. Weaver et al., Eds. *Methods of Soil Analysis, Part 2—Microbiological and Biochemical Properities*. Soil Science Society of America, Madison, WI, pp. 459–490.

Jenkins, W.R. 1964. A rapid centrifugal-flotation technique for separating nematodes from soil. *Plant Dis. Rep.* 48: 692.

Kimpinski, J., Plumas, G., and MacDonald, M.C. 1993. Occurrence of the clover cyst nematode, *Heterodera trifolii*, in Prince Edward Island soils. *J. Nematol.* 25(4S): 876–879.

Kimpinski, J. and Welch, H.E. 1971. Comparison of Baermann funnel and sugar flotation extraction from compacted and non-compacted soils. *Nematologica* 17: 319–320.

McSorley, R. and Frederick, J.J. 2004. Effect of extraction method on perceived composition of the soil nematode community. *Appl. Soil Ecol.* 27: 55–63.

Pitcher, R.S. and Flegg, J.J.M. 1968. An improved final separation sieve for the extraction of plant-parasitic nematodes from soil debris. *Nematologica* 14: 123–127.

Shepherd, A.M. 1986. Extraction and estimation of cyst nematodes. In J.F. Southey, Ed. *Laboratory Methods for Work with Plant and Soil Nematodes*. Ministry of Agriculture, Fisheries and Food, Reference Book 402, Her Majesty's Stationery Office, London, UK, pp. 31–49.

Stoller, B.B. 1957. An improved test for nematodes in soil. *Plant Dis. Rep.* 41: 531–532.

Thistlethwayte, B. and Riedel, R.M. 1969. Expressing sucrose concentration in solutions used for extracting nematodes. *J. Nematol.* 1: 387–388.

Townshend, J.L. 1963. A modification and evaluation of the apparatus for the Oostenbrink direct cotton wool filter extraction method. *Nematologica* 9: 106–110.

Verschoor, B.C. and De Goede, R.G.M. 2000. The nematode extraction efficiency of the Oostenbrink elutriator-cottonwool filter method with special reference to Nematode Body Size and Life Strategy. *Nematology* 2: 325–342.

Viglierchio, D.R. and Schmitt, R.V. 1983. On the methodology of nematode extraction from field samples: Comparison of methods for soil extraction. *J. Nematol*. 15: 450–454.

Viglierchio, D.R. and Yamashita, T.T. 1983. On the methodology of nematode extraction from field samples: Density flotation techniques. *J. Nematol*. 15: 444–449.

Vrain, T.C., Forge, T.A., and De Young, R. 1997. Population dynamics of *Pratylenchus penetrans* parasitizing raspberry. *Fundam. Appl. Nematol*. 20: 29–36.

Whitehead, A.G. and Hemming, J.R. 1965. A comparison of some quantitative methods of extracting small vermiform nematodes from soil. *Ann. Appl. Biol*. 55: 25–38.

Chapter 34
Earthworms

M.J. Clapperton
Agriculture and Agri-Food Canada
Lethbridge, Alberta, Canada

G.H. Baker
Commonwealth Scientific and Industrial
Research Organization
Glen Osmond, South Australia, Australia

C.A. Fox
Agriculture and Agri-Food Canada
Harrow, Ontario, Canada

34.1 INTRODUCTION

Earthworms are regularly referred to as "ecosystem engineers" because of the dramatic changes they impose on the structural, chemical, and biological properties of the soil. As such, there has been increasing interest in using earthworms as ecological indicators of soil quality, beneficial land management, and industrial remediation. However, there are instances where earthworms that were accidentally or intentionally (to increase soil productivity) introduced have become invasive (Gundale et al. 2005). Regardless, earthworms are relatively easy to find, recognize, and sample, and with limited instruction, can be identified into specific taxonomic groups, making the ideal starting point for studying soil biology or ecology.

The abundance and distribution of earthworms are very food-resource restricted or patchy, with populations being distributed at different depths according to species and life stage, and varying seasonally and diurnally within a population or earthworm community. This can make decisions on when to sample, how many samples to take, where to sample, and what sampling method to use more difficult. So before beginning a project, it is important to understand basic earthworm life history, feeding, and behavior.

There are three major ecological groupings defined by feeding, behavior, and burrowing patterns (Lee 1959, 1985; Bouché 1977) with some overlap depending on the soil type, moisture content, and temperature. Earthworms that live in the litter layer feeding primarily on coarse particulate organic matter are epigeic species. These species tend to be short lived with high metabolism and reproductive rates. Endogeic species live throughout the mineral

soil horizons feeding on soil and organic matter, leaving their temporary burrows filled with castings as they move horizontally and vertically through the soil. Depending on soil conditions, endogeic earthworms will feed and cast on the soil surface, thoroughly mixing mineral and organic soil horizons: they are the "earth worker" earthworm species. Anecic earthworm species like *Lumbricus terrestris* L. form deep vertical (mostly permanent) burrows with typically one or two surface entrances. They feed primarily on surface litter that is pulled into the burrow or gathered and mixed with castings into a midden that surrounds the opening to the burrow. These broad ecological categories (epigeic, endogeic, anecic) indicate the need to use different sampling strategies to obtain more accurate earthworm population estimates.

Field sampling methods can be classified into the following categories: physical (earthworms are sorted and removed from the litter, soil, and other habitats by hand), behavioral (stimulated to move out of the habitat where they are being collected), and indirect (populations are estimated by trapping, baiting, or counting casts or middens). There is no single method that will be most effective for all sites and circumstances, a combination of methods will most often yield the most accurate estimates. For example, populations of deep vertical burrowing species (anecic earthworms) are best sampled using behavioral methods such as chemical repellents in combination with midden or casting counts, whereas, endogeic and some epigeic species are easily sampled by hand-sorting methods.

The spatial distribution of earthworm populations and changes in species diversity with time are not well understood, making it critical that sampling strategies are appropriate to yield best estimates of population and diversity. Sampling designs can include following a grid pattern with specific intervals, using a series of transects at randomly selected coordinates, or points with radiating transects. Sampling at regular intervals throughout the year will give an estimate of when earthworm populations are greatest or most diverse.

Preserving the integrity of specimens is critical for taxonomic and molecular genetic studies. There are occasions when dissecting earthworms is necessary and decaying specimens can make this delicate task and future comparisons using molecular genetic techniques impossible. Well-maintained reference or synoptic collections are invaluable for tracking species composition changes over time.

This chapter describes the most commonly used and recommended field sampling methods for earthworms. The notes and hints included with the methods are based on field and laboratory experiences and the comments will help to optimize field effectiveness and efficiency. The methods for sampling, handling, and transporting are relevant to a broad range of soil research interests including ecotoxicology.

34.2 SAMPLING DESIGN

In all the methods, it is important that samples are taken at stratified random coordinates within a sampling plot and be sufficient in number and size to yield accurate estimates (Southwood 1978). Data from controlled experiments can provide a good basis for investigated cause and effect relationships between different management practices and earthworm population density, biomass and species composition (Blair et al. 1996). However, the required number and sizes of samples will vary from one study to another, and different numbers of samples may be required to adequately measure the abundances of different species.

Earthworm populations are mostly distributed in patches, which can be related to vegetation, as well as the physical, chemical and biological properties of the soil, making the number, size, and distribution of the sampling units difficult to determine. Studies have shown that by decreasing the field sampling area, the total variance of data increased (Rossi and Nuutinen 2004) and Whelan (2004) determined that at a forest or agricultural landscape scale, at least forty 1 m^2 sampling units per hectare were required to make an unbiased estimate of earthworm numbers and biomass.

34.3 PHYSICAL METHODS

34.3.1 Hand Sorting

Hand sorting is the most commonly used procedure for earthworm sampling. This method leads to high soil disturbance, is very labor intensive, but more importantly works in all soil types. A volume of soil of a prescribed dimension is removed either by spade, corer, or collar and the earthworms are sorted from the collected soil by hand. Sampling efficiency varies with sample size and shape of the sampling unit. In many studies, square shapes are used that range in size from 25×25 cm to 45×45 cm, with sampling depth ranging from 10 to 125 cm. Sampling depth will need to be varied according to the depth at which the earthworms are active. For agricultural fields, Dickey and Kladivko (1989) determined that the most efficient size/shape sampling unit for earthworms was 10 cm along the crop row and 45 cm across the row (i.e., 10×45 cm). However, for cocoons, the most efficient size/shape was a 30×30 cm square. Consider sampling the soil in layers to determine the appropriate depth. Preliminary experiments to determine sample size, shape, and species diversity are warranted when beginning a new project. In one study, Clapperton (1999) found that cocoons were mostly deposited below the 20 cm depth.

Materials and Reagents

1 Equipment for removing a prescribed volume of soil can include the following:

a. Templates made from wood or metal for maintaining the consistency of sample unit size and shape. Instructions for constructing various size/shape sampling templates are given on the Wormwatch (2002) Web site.

b. Garden spade or shovel (square ended spades are best for maintaining sample unit dimensions). Depth measurements marked in increments of 5 or 10 cm on the blade of the spade with spray paint are essential.

c. Metal corers (driven into the soil by hand or with a tamping machine). *Note*: Corers will not work well in dry, loosely aggregated, or sandy soils.

d. Plastic collars (i.e., PVC pipe 20 cm length with 30 cm inside diameter) can be pressed into the soil and left for a period of time, so that the soil can settle, and then the collar with the soil inside pried-out with a pry bar or spade, giving a clean fracture across the inside diameter of the collar (Conner et al. 2000): these same plastic collars can also be used as cages for doing more controlled field experiments with earthworms (Baker et al. 1996).

2 Materials for sorting earthworms from soil:

   a. Light-colored trays or shallow plastic containers or tubs with lids and large thick plastic or heavy-duty garbage bags.

   b. Gloves (plastic or cloth) for hand protection.

   c. Portable tables and chairs are optional.

3 Soil temperature electronic probe or soil thermometer (15 cm length).

Procedure

1 Select the site and sampling strategy: use transects for pasture and more natural sites, and grid sampling designs for repeated sampling over a season. Record the soil temperature at each sampling location. Place the template on the soil surface and dig around the template with a spade to the desired depth or depths. If you are hand sorting more than one depth or layer of soil, hand sort one layer before you sample the next. Soil cores can be extracted immediately next to the earthworm sampling site for measuring soil moisture content and other soil properties that might be appropriate (i.e., pH, soil carbon) (see other chapters for methodology details).

2 There are two choices for hand sorting in the field: the soil is sorted in the field and then replaced in the hole, or removed from the field in a thick plastic or garbage bag, kept cool, and sorted away from the field, out of the weather. It may be necessary to remove samples for sorting from the field when time is limited or weather conditions are poor. If the samples cannot be sorted immediately, they should be stored in a cool room (as close as possible to the soil temperature in the field or 15°C–20°C) and sorting should take place within 1 week from the time of sampling (see Comment 1 below).

3 Place the soil directly onto a light-colored tray, plastic sheet, or large shallow storage container. Begin hand sorting by systematically breaking-up clods and gently massaging the soil through fingers. Deposit the examined soil in a shallow container or onto a plastic sheet so that the unexamined soil remains separate. Periodically take the time to search through the recently examined soil for any earthworms or cocoons that may have been missed (see Comment 2 below).

4 Place the sorted earthworms and cocoons into separately labeled containers. Follow the procedures described later in this chapter for handling and preserving earthworms (see Section 34.8).

Comments

1 After the soil is sorted, for some projects to maintain the integrity of the field site, the soil may need to be returned to the field and each soil sample returned to the exact location, and, in some cases, in the appropriate order, i.e., top layer last.

2 Earthworms are often cut into pieces when digging with the spade to remove the soil. During hand sorting, it may be possible to match halves, but if not, count

only the heads. All body parts in the sample should be included as total biomass, but only the fragments with the head or only the anterior fragments (but not both) are included in tallying the total number of earthworms in a sample.

3 Hand sorting is not practical when most of the earthworms in the sampling area are deep vertical burrowing anecic species. Chemical repellents (see Section 34.4) applied in the hole after the soil sample has been removed can be used to retrieve the anecics that escaped further down into the soil during digging.

4 Alternatively, if the soil is particularly hard or sticky making it difficult to massage by hand, you can use a watering hose to gently wash away the soil or pass the soil through sieves or screens to expose and recover earthworms, cocoons, and hatchlings.

Hand sorting requires a limited amount of equipment and is a reasonably reliable method for determining earthworm numbers (aestivating or dormant earthworms are also recovered), biomass, and cocoons. Hand sorting can also be adapted for sampling litter- and soil surface-dwelling earthworms (Wormwatch 2002). The main disadvantage of hand sorting is that it is a very laborious, time-intensive, and tedious method. It is also important to note that earthworms can sense vibrations caused by the soil disturbance associated with the sampling, so after you insert the spade or shovel check for escaping earthworms. However, validated time-limited soil sorting is a useful alternative for repetitive sampling over an extended time (Schmidt 2001a).

34.3.2 Washing and Sieving

Sieving by hand is very laborious and usually not worth the extra effort compared with hand sorting for population studies (Raw 1960). A mechanical procedure was developed and used by Bouché (1972) and Bouché and Beugnot (1972). There are portable washing machines: soil is placed on top of a series of different mesh-size sieves, washed through the sieves by sprinklers mounted above and below the sieves on a free-standing frame, and earthworms and cocoons collected on the various-sized sieves. The water is supplied from a truck-mounted tank and an air compressor is used to pressurize the water lines. Washing machines are fast and efficient as long as there is not too much clay in the soil.

34.4 BEHAVIORAL METHODS

The use of chemical repellents (e.g., hot mustard, formalin) to expel earthworms is the most commonly used method of the behavioral methods. These methods tend to be nondestructive thereby maintaining the integrity of the field site. Heat extraction is very useful for undisturbed soil cores and turf samples. Earthworms can also be expelled from the soil with electricity and vibration, both of which are less commonly used in research.

Chemical repellents irritate the mucus tissue layer of the earthworm, which causes the earthworm to move onto the soil surface, where it can be easily collected. Edwards and Bohlen (1996) described the historical records for the different chemicals (mercuric chloride, potassium permanganate, formalin, etc.) that have been used to extract earthworms, many of which are extremely hazardous and toxic for handling. The most widely used and accepted of the chemical repellents by the research community has been formalin, a technique first proposed by Raw (1959). However, the use of formalin has become more restricted because of toxicity and environmental concerns. Thus, the use of alternative less-toxic chemical

repellents such as hot mustard has been investigated (Gunn 1992; Lawrence and Bowers 2002; Kukkonen et al. 2004), and gained favor. The use of dishwashing liquid soap is an inexpensive nontoxic alternative, recommended for exploratory purposes only (East and Knight 1998).

Chemical repellents applied to the soil can bring earthworms to the surface, where they can be more easily collected by hand (St. Remy and Daynard 1982). Chemical repellents do not work well in all soil types because of soil porosity and chemical characteristics, which can prevent adequate chemical dispersal. The efficiency of extraction also varies with the soil temperature and moisture, which limit the activity of earthworms. In temperate climates, spring soil temperatures of 10°C–20°C with good moisture conditions represent the time when most species are active, giving the best representative population sample (Clapperton et al. 1997).

Chemical repellents work best in field situations when the earthworms are active and close to the surface. Sampling for earthworms when soil conditions are saturated or close to saturation means the repellent will not infiltrate the soil, instead pooling on the surface, and in dry soil, the repellent solution will either not penetrate the soil or disappear down large cracks. The use of chemical repellents has been most effective for sampling *Lumbricus terrestris* and other anecic or deep-burrowing species, and completely ineffective on aestivating earthworms (Raw 1959; Lee 1985; Chan and Munro 2001). In habitats where horizontal burrowers (endogeics) coexist with anecics, chemical repellents are more quantitatively effective for sampling endogeics (Bouché 1976). The deep vertical burrows of anecic species transport the chemical irritant more effectively into the soil where it can reach the other earth-working or endogeic species. Where there is no evidence of anecic earthworm activity, the use of chemical repellents is of limited value (Clapperton et al. 1997; Chan and Munro 2001). Chemical repellents can be combined with hand sorting (see Section 34.3); the repellent is poured onto the soil at the bottom of the hole (after the soil sample for hand sorting has been removed) and anecic species are expelled (Barnes and Ellis 1979).

Regardless of the situation, it should be recognized that chemical repellents alone do not extract all earthworm species from the soil. The primary advantage of this technique over hand sorting is the speed of the procedure, especially for studies where multiple replicates are required to determine the spatial distribution pattern of earthworm populations.

34.4.1 Hot Mustard

Materials and Reagents

1 Hot dry mustard powder (finely ground hot mustard seeds are available in bulk from various food stores, i.e., 2.27 kg boxes provide for about 40 sampling points; smaller tins of approximately 115 g available in food stores are costly for more than exploratory field experiments).

2 Sturdy wide-mouth plastic containers with lids, spatulas, small and large whisks, teaspoons, and long-handled spoons for mixing hot mustard.

3 Plastic gloves, laboratory coat, and dust mask for personal protection. Access to fume hood or vented laboratory bench area.

4 Sampling containers should be wide-mouthed 500 mL glass jars with metal lids and jar rings or wide-mouthed plastic containers with lids. Also, paper towels,

boxes, or plastic containers to hold the jars in the upright position and keep them from breaking, and a large chest cooler (with ice packs) are needed.

5 Sampling frames 0.6 m × 0.6 m: constructed of approximately 10 cm high wood or metal sheets with hinged corners to lay flat when not in use. Depending on the study requirements, other sample sizes can be used (i.e., 0.25 m^2). The bottom edge of the frame can be bevelled or sharpened to facilitate setting into the soil more easily. If planning a large sampling event with several field crew members, it is advisable to have 10–15 frames available for time efficiency. Then more than one person can be working at the same time.

6 Spade, field flags (90 cm wire flags); lawn leaf rake to remove any loose surface litter or crop residues from the soil surface; hedge cutters, shears, or gas-powered edge trimmer to trim grassed sampling sites (i.e., sod) to enable the chemical repellent to infiltrate into the soil more easily.

7 Household plastic bucket/pail (10 L or more capacity) graduated in liters.

8 Plastic garden watering can with sprinkler attachment (7 L capacity or more). Large plastic funnel to fit into watering-can opening. If planning a large field monitoring activity, have at least 5–10 cans available to allow for mixing suspensions at the same time while sampling is taking place. *Note*: The holes in the sprinkler attachment need to be large enough to allow for the ground mustard seed residues to pass easily through without plugging.

9 Water tank (i.e., plastic tank 150–200 L capacity) or several 20 L plastic containers.

10 Soil thermometer (15 cm long) or electronic temperature probe.

11 70% Ethanol (add 30 mL distilled water to 70 mL 95% ethanol).

Procedure

1 Preparation for field sampling:

a. Weigh 53 g of hot mustard powder into a plastic container with leakproof lid. *Caution*: Wear protective plastic gloves, laboratory coat, and dust mask. The active ingredients that provide the "hotness" in hot mustard are related to allyl-isothiocyanate compounds, which can cause respiratory irritation and watering of eyes. A fume hood or vented bench area should be used.

b. One day or a minimum 3 h before leaving for sampling site: in a fume hood or vented bench area, open the plastic container containing the 53 g of dry hot mustard powder. Slowly add aliquots of 50 mL water, to a total of 150 mL, stirring constantly using a spoon, spatula, or whisk until you have a smooth thick paste that can be easily poured. Replace the lid and let the mixture stand for at least 3 h for the "hotness" to develop.

c. Prepare either glass jars or plastic containers using the appropriate method based on whether you will be retrieving and transporting the earthworms from the field to laboratory. Prepare sampling labels with site information in pencil

or computer-printed labels (laser-printed labels will remain readable with solvent spills, while ink jet-printed labels will not).

d. If you will be preserving the earthworms for identification in the laboratory, use 500 mL glass jars. Add 125–150 mL 70% alcohol. If you are anticipating a large number of earthworms at the sampling points, add 200–250 mL 70% alcohol to the jar, so that all the earthworms are immersed in the 70% ethanol to maintain the integrity of the sample. Place in original boxes or plastic tubs for transport to field.

e. If you are returning the earthworms to the field, do not use the glass jars or alcohol. Prepare each wide-mouthed plastic container placing a water saturated paper towel in the bottom and cover with lid (preferably perforated to allow for build-up of ammonia from earthworm excretions to escape; holes should be small enough not to allow worms to escape). Place in chest cooler for transport to field.

2 Preparing the field site:

a. Select a suitable sampling area according to experimental design or requirements of study and identify the sampling locations in field with numbered field flags.

b. Lightly rake the surface residues from selected sampling area. If sampling in thick sod, cut the grass to soil level with hedge trimmers or gas-powered edge trimmer. This is to allow for better observation of the earthworms as they emerge.

c. At each prepared sampling area, place the wooden or metal frame in the open position on the surface of the soil, and with a shovel, where possible, pack soil around the base of frame to prevent the mustard suspension from leaking underneath the frame when it is poured onto the soil. Place one sampling container for retrieving the earthworms at each location. *Note*: For some sampling locations, it may not be possible to bank up soil along the frame as the integrity of the soil must remain undisturbed or sod conditions prevent doing so. The extent of water leakage under the frame can be controlled by applying small amounts of the mustard mixture at a time and waiting for it to infiltrate into the soil before pouring on additional amounts.

d. Record field site information, sample number on earthworm container, and sampling flag number. If needed for some treatment plot studies, record field location of sampling area on field treatment design or sketch map.

e. Insert soil thermometer or electronic probe and record the soil temperature.

3 Applying hot mustard in the field:

a. In the household plastic pail, add about 3 L water from the plastic water tank/containers. Wearing plastic gloves, immerse the entire container of mustard paste into the bucket and swirl it around to rinse the container. Use a spatula or brush to remove any remaining mustard paste from

the plastic container. With a large whisk, long-handled spoon, or cordless drill with a paint stirrer attached, stir the mustard/water mixture in the pail making sure that there are no large lumps. Add additional water to the pail to bring the water level up to 7 L mark stirring the suspension vigorously.

b. Insert plastic funnel into sprinkling can and slowly pour the mustard mixture from the pail stopping periodically to remix the contents.

c. Always stir the mustard mixture in the bucket immediately before transferring the contents to the sprinkling can. If mustard grains remain in the bucket, do not add more water to rinse remnants into the watering can. This procedure is based on 7 L being poured on each of the sampling areas, and further addition of water will dilute the effectiveness as well as compromise the ability to compare data between sampling points.

d. Place sampling container for holding earthworms next to the sampling frame. For Mason jars containing 70% ethanol, do not leave the lid off the jar as the ethanol will rapidly vaporize; this will change the concentration of the ethanol. Balance the lid loosely on the jar and lift when adding worms to the jar and replace the lid immediately.

e. Apply the mustard mixture slowly and evenly over the soil area within the boundaries defined by the frame, so that it has time to infiltrate the soil. Earthworms should appear within 1 to 2 min.

4 Collecting earthworms from the sampling area:

If earthworms are to be kept, then use gloves to gently pick up emerging worms with long-nosed or broad tweezers and drop the earthworm into the glass jar. It is important to pick the earthworms as they emerge, do not wait until the earthworm is stopped and anchored, because it will separate in half when you pull. Only pick up the earthworms that emerge within the confines of the frame and wait until the entire earthworm is out of its burrow so you do not miss or damage an earthworm. It usually takes about 15 to 25 min before the earthworm activity ends. If soil temperatures are low (approximately 5°C–8°C), the earthworms will be slower to emerge (a time limit of between 20 and 25 min is appropriate for each sampling point). However, the time limit for retrieving earthworms should be adjusted to field conditions at the time of sampling. Place the boxes or tubs of glass jars in the chest cooler, particularly if air temperatures are very warm. Upon return from the field, place samples in a cold room (10°C) or in the refrigerator until processing can take place. If processing is delayed for longer than 2 weeks, replace the ethanol in each jar to preserve the earthworms better.

Comments

1 Consistency is one of the most important concepts when performing experiments or using a method: use the same brand of mustard for the entire experiment if possible.

2 Zaborski (2003) suggested using the chemical allyl isothiocyanate (the most active ingredient in hot mustard) to expel earthworms and concluded that there was no difference in the numbers of earthworms extracted using allyl isothiocyanate compared to formalin, but cautioned at the extreme care needed in handling the chemical.

3 In a study that examined the efficiency and effectiveness of using the hot mustard method described above to extract earthworms, Lawrence and Bowers (2002) found that hot mustard extracted 61.4% (4.2% SE) of the earthworms, 62.3% (4.3% SE) of the biomass, and 84.5% (4.4% SE) of the species from 40 sampling sites. When resampling the site with hand sorting to examine the efficiency of mustard repellent, they found that 100% *Dendrobaena octaedra*, approximately 70% *L. terrestris, Aporrectodea rosea,* and *Aporrectodea caliginosa* approximately 50% *Allolobophora chlorotica* and 45% *Octolasion tyrtaeum* had been expelled by the hot mustard repellent.

34.4.2 Formalin Extraction

Materials and Reagents

1 37% Formalin (formaldehyde) *Caution*: Formalin needs to be handled with extreme care as it is acutely toxic following inhalation or skin contact causing serious injury or mortality, and is a potential carcinogen. Do not use formalin if study will be located near drains or water courses or would infiltrate the soil to the groundwater. Use appropriate safety procedures as recommended on material safety data sheets (MSDS). Dilute formalin solution 0.5% (v/v) is prepared directly in field in relation to the quantity of water that is applied with watering can.

2 Dispensing pipette or graduated cylinder, gloves, personal safety protection as identified in the MSDS for exposure to vapors and handling under field conditions.

3 Field materials are the same as for hot mustard (see Section Materials and Reagents, p. 432).

Procedure

1 Prepare the dilute formalin solution of 0.5% (v/v) with water (add 50 mL formalin to 8 L water). Using a dispensing pipette on the formalin bottle adds to the efficiency of the procedure of preparing formalin solution under field conditions. Alternatively, before going to the field, add 50 mL formalin to leakproof glass bottle that can be tightly sealed. In the field, pour the 50 mL formalin into 8 L sprinkling can and mix thoroughly. *Note*: If the sprinkling can's capacity is less than 8 L, the amount of formalin used should be adjusted. *Caution*: Follow all transport regulations with respect to transporting hazardous and toxic materials in motor vehicles.

2 Sprinkle 8 L formalin solution evenly onto frame area. Pick up earthworms with tweezers until all activity stops (about 15–25 min) as described above for hot mustard procedure (steps 2–4). *Caution*: Care must be taken to avoid inhaling formalin vapors (see MSDS for advice on personal protective gear). Place earthworms into glass jars with 70% alcohol. It is unlikely that earthworms exposed to formalin will survive, so please do not return them to the field site.

3 Field cleanup: Before leaving the field, rinse all watering cans with any left over water and transport all samples and materials in contact with formalin in a trailer or secured in the back of a pickup truck. Dispose and clean materials as per MSDS requirements.

4 Place the glass jars in a cold room at 4°C–10°C until the earthworms can be processed (i.e., identified and weighed for biomass).

34.4.3 Heat Extraction

This method is used less frequently than others, but has its place for extracting earthworms from intact soil cores or sods (Satchell 1969; Lee 1985; McLean and Parkinson 1997; Tisdall and McKenzie 1999). This method is not appropriate for extracting anecic species like *Lumbricus terrestris*, unless combined with a chemical repellent method (see introduction to Section 34.4).

34.4.4 Electrical Extraction

This method is successful for qualitative but not quantitative studies of some species (Lee 1985; Petersen 2000). It is particularly useful under conditions where the soil is not too wet and the species present are susceptible to alternating electrical current (Satchell 1955). The electrical octet method in an agricultural field study was shown to be a reliable and a useful alternative for using a chemical repellent, but not hand sorting (Schmidt 2001b).

34.4.5 Mechanical Vibration

Earthworms can be induced to the soil surface by vibrating the soil (Reynolds 1973), a technique called grunt'n is used extensively by fishing-bait collectors in the southern USA.

34.5 INDIRECT SAMPLING ESTIMATES

34.5.1 Trapping and Baiting

Pitfall traps can be used to sample earthworms that are active on the soil surface (Boyd 1957; Bouché 1972, 1976). This method assumes that the target animals will not actively avoid falling into the trap, which makes this method best regarded as qualitative and semiquantitative. This method has been used successfully for surface-active earthworms and for comparing the incidence of surface activity of species on a diurnal or seasonal basis, or in relation to weather patterns (Bouché 1972). Bait-lamina strips are an alternate method having been used to measure the activity of earthworms within a sampling unit (Gestel et al. 2003).

34.5.2 Counting Middens and Castings

The number of casts produced within a prescribed area may give an indirect measure of the presence of certain species (not all species cast on the surface and some only cast on the surface at specific times of the season), but the data have to be treated with caution. The numbers of casts reflect not only abundance, but also activity, and casts can accumulate and disintegrate in dry weather and wet weather, respectively. Taking these cautions into account, Hauser and Asawalam (1998) proposed a continuous cast sampling technique that produced valid data without disturbing the soil. The number of middens in a particular sample area is a nondestructive method that has been used to successfully quantify the

earthworm *Lumbricus terrestris*; however, the sample unit size does need to account for the spatial patterns of middens (Rossi and Nuutinen 2004).

34.5.3 Mark and Recapture

Most of the conventional marking techniques used for invertebrates are inappropriate for earthworms, principally because earthworms lack hard exoskeletons. Nevertheless, a number of techniques have been tried: staining with nontoxic dyes (Meinhart 1976; Mazaud and Bouché 1980), radioactive isotopes (Joyner and Harmon 1961; Gerard 1963), and freeze-banding (Lee 1985). Espinosa et al. (1997) injected a phosphorescent dye into earthworms in a mark and recapture study in Puerto Rico, USA, the dye lasted at least 4 months.

34.5.4 Acoustic Estimates

The use of sound is a new and perhaps promising technique that would allow for undisturbed field sampling of earthworms and other larger soil invertebrates; and when combined with geostatistical analysis, can be used for soil mapping of the populations (Brandhorst-Hubbard et al. 2001).

34.6 RETRIEVING EARTHWORM COCOONS

Cocoons contain the eggs of earthworms. The number of eggs per cocoon varies between earthworm species, being generally greater for epigeic than endogeic and anecic species (i.e., r- versus K-selected species). Climatic and edaphic factors are thought to affect reproductive rates of earthworms although there is limited information (Wever et al. 2001) regarding this. Knowing when, where, and under what climatic conditions, soil and plant community cocoons are deposited can prove useful for predicting populations, and for understanding more about reproductive physiology. Cocoons can be sampled by hand sorting and flotation methods, the same methods as applied to earthworms. However, these methods when applied to cocoons suffer the same core problems as they do with earthworms (inefficient, especially for smallest cocoons, laborious). Some authors (e.g., Baker et al. 1992) have noted the presence of cocoons in the soil when hand sorting and some others have quantified their abundance (Clapperton 1999). This approach can at least demonstrate seasonality. Some cocoons remain viable in the soil during hot, dry periods, although in a shriveled and difficult state to easily see, and hatch later when moist conditions prevail, e.g., the epigeic *Microscolex dubius* (Doube and Auhl 1998). Other cocoons perish when exposed to hot, dry conditions. Holmstrup (1999) described and verified (Holmstrup 2000) a method to study the reproductive rate of earthworms in the field. Identifying cocoons directly to species can be quite difficult and cannot be considered quantitative, but pictorial keys do exist for some of the common European species, which have become cosmopolitan (Edwards and Lofty 1972; Sims and Gerard 1985). Of course, cocoons can be reared to identify the earthworms that hatch from them, but this may take many months of rearing to obtain an identifiable earthworm. Cocoons can be reared simply in moist soil in the laboratory, but the rearing temperature can have a marked influence on the rate of development (Baker and Whitby 2003).

34.7 INTERPRETATION AND ANALYSIS OF EARTHWORM DATA

Data regarding earthworm populations are usually expressed as the total number or biomass per unit area, and more generally as number or grams per square meter. It is appropriate to express data from hand sorting on a volume basis, although this means that to compare results from repellent methods, the reader needs to convert from cubic meters to square meters.

Data can be represented as total earthworms for the community, or categorized into species within the community, functional groups such as anecic, endogeic or epigeic, or maturity classes such as adults and juveniles (nonclitellate individuals). Species can also be represented as a percentage of the total number of earthworms. If you are hand sorting and sampling at more than one depth, it may be useful to represent the percentage of each species at each sampling depth (Clapperton 1999). All body parts in the sample should be included as total biomass, but only head or anterior fragments are included in the total number of earthworms in a sample.

34.7.1 Earthworm Biomass

Earthworm biomass (i.e., weight) is often recorded in combination with earthworm numbers. Biomass may more accurately indicate the level of a particular soil function than population numbers. Conclusions concerning the relative influences of different-sized species of earthworms on soil properties and plant production can vary according to whether population numbers or biomass is used as the basis for equating the presence of the species (Baker et al. 1999).

There are several sources of error in the measurement of biomass once the earthworms have been collected (e.g., state of hydration of the specimens, presence of soil in the gut in relation to recent feeding, loss of weight following preservation). For example, Piearce (1972) found that earthworms preserved in 5% formalin lost 3–5% of their body weight after 1 week. It is usual to express earthworm biomass in terms of dry weight or weight at a standard level of hydration/period of preservation. Several authors (e.g., Martin, 1986; Springett and Gray 1992; Dalby et al. 1996) describe methods for voiding gut contents from earthworms to eliminate this source of error, particularly when setting up experiments in which subsequent growth is to be measured. Blair et al. (1996) argued that ash-free dry mass gave a more accurate comparison of data from different times and studies. The method of Dalby et al. (1996) is summarized here.

34.7.2 Procedure for Voiding Earthworm Gut Contents for Biomass Assessment

1 Earthworms are collected from the field or culture box and placed on water-saturated filter paper or moist paper towels, either in plastic Petri dishes (held together with tape or rubber bands so the earthworms cannot escape) or sealed pots for 24 h, during which time the vast majority of their gut contents are voided.

2 Earthworms should be maintained at a temperature suitable for them (e.g., 15°C for most Lumbricidae seems appropriate). Earthworms should be gently washed in water (leaving them to "swim" in a jar of water for a minute or so serves this purpose), before dabbing dry on toweling and weighing. Earthworm tissue dry weight can be measured after drying at 60°C for 24 h. Horse hair or soft bristle paint brushes of various sizes are useful for removing excess soil from earthworm bodies; they are also more gentle than forceps for handling earthworms.

Note: The procedure should be followed at both the beginning and end of an experiment involving growth measurements.

34.7.3 Comments

1 Not all the gut contents can be voided, some contents inevitably adhere within the invaginations of the gut lining. After washing the earthworm under a gentle stream of water, with the thumb and forefinger gently, but firmly, milk the gut contents

beginning from two-thirds of the way from the head to the anus. Confining earthworms with water, moist filter paper, or plain paper toweling also serves to equilibrate water content across earthworms within and between collection times (see Dalby et al. 1996 for further details). Allowing earthworms to be confined for longer than 24 h will further reduce gut content (by a small amount), but may cause the body of the worm to begin deteriorating.

2 Some sampling methods may be quite accurate in estimating earthworm biomass because they extract the largest individuals in the population efficiently, yet inaccurate in estimating population numbers because many small individuals are missed. For example, Raw (1960) obtained 52% of the earthworm numbers and 84% of the earthworm biomass by hand sorting a wet grassland soil in which the animals were mostly confined to a thick turf mat. Small species and immature specimens of larger species were most commonly missed by the hand sorting. In contrast, Raw (1960) obtained 89% of the numbers and 95% of the biomass by hand sorting a pasture soil with no root mat, and 59% of the numbers and 90% of the biomass from a poorly structured clay soil in an old, arable field.

34.8 PREPARING EARTHWORMS FOR REFERENCE COLLECTIONS

Earthworms collected for population or biomass estimates, and molecular genetic studies may be stored in 70% ethanol (v/v). However, representative specimens for identification and long-term storage in synoptic collections need to be handled and stored differently so they do not decompose or become unsuitably brittle for dissection.

34.8.1 Procedure for Preservation and Storage

1 Earthworms required for future taxonomic purposes need to be first anesthetized in 15%–20% v/v ethanol for approximately 15 min or until they no longer respond to gentle prodding. It is also useful to gently massage the earthworms into a straight position with a soft-bristled paint brush.

2 In a fume hood, transfer the earthworms into a small amount of 4% v/v formaldehyde in a shallow flat-bottomed dish, cover with and saturate another piece of paper towel with formaldehyde, and leave it overnight or for 2–3 h (in the fume hood) to be fixed or preserved. *Note*: If the earthworms cannot be immediately preserved, transfer them into 70% ethanol, replace the discolored ethanol regularly, and store in a cool place until they can be preserved.

3 Following preservation, store earthworms for the longer term in 90% ethanol in limited volume glass containers with Teflon-lined screw-top lids. The ethanol should be replaced periodically once it becomes yellow colored. Paper labels written in pencil should be placed on the inside and outside of the container. Store the synoptic earthworm collection in a dark, cool place.

34.8.2 Taxonomic Identification of Earthworms

Many of the common earthworm species can be identified from external characteristics with a good hand-lens or low-power binocular dissecting scope, without dissection. However, only adult earthworms (with a clitellum) can be accurately identified in this manner.

A number of general earthworm taxonomic references are available including Sims and Gerard (1985), Schwert (1990), Reynolds (1977), Ljungström (1970), and online sources such as Wormwatch (2002).

34.9 TRANSPORTING EARTHWORMS

34.9.1 Field to Laboratory

Earthworms can be identified and counted in the field, or transported back to the laboratory to determine biomass, and confirm identifications. They can be kept alive on moist paper towels in plastic containers that have adequate aeration, or in screw-top containers with water. In this way, earthworms will void some gut contents before being weighed and preserved in ethanol. Live earthworms should be stored overnight in a cold room or in a refrigerator at 4°C–8°C. Earthworms can also be directly collected into formalin or ethanol in a leakproof screw-top container; we recommend using 70% ethanol (v/v).

REFERENCES

Baker, G.H., Barrett, V.J., Carter, P.J., and Woods, J.P. 1996. Method for caging earthworms for use in field experiments. *Soil Biol. Biochem.* 28: 331–339.

Baker, G.H., Barrett, V.J., Grey-Gardner, R., and Buckerfield, J.C. 1992. The life history and abundance of the introduced earthworms *Aporrectodea trapezoides* and *A. caliginosa* (Annelida: Lumbricidae) in pasture soils in the Mount Lofty Ranges, South Australia. *Aust. J. Ecol.* 17: 177–188.

Baker, G.H., Carter, P.J., and Barrett, V.J. 1999. Influence of earthworms, *Aporrectodea* spp. (Lumbricidae), on pasture production in south-eastern Australia. *Aust. J. Agr. Res.* 50: 1247–1257.

Baker, G.H. and Whitby, W.A. 2003. Soil pH preferences and the influences of soil type and temperature on the survival and growth of *Aporrectodea longa* (Lumbricidae). *Pedobiologia* 47: 745–753.

Barnes, B.T. and Ellis, F.B. 1979. Effects of different methods of cultivation and direct drilling and disposal of straw residues, on populations of earthworms. *J. Soil Sci.* 30: 669–679.

Blair, J.M., Bohlen, P.J., and Freckman, D.W. 1996. Soil invertebrates as indicators of soil quality. In J.W. Doran and A.J. Jones, Eds. *Methods for Assessing Soil Quality*. Soil Science Society of America, Madison, WI, pp. 273–291.

Bouché, M.B. 1972. Lombriciens de France. Ecologie et Systématique. INRA Publications 72-2. Institut National des Recherches Agriculturelles, Paris, France.

Bouché, M.B. 1976. Etude de l'actvité des invertébrés épigés parairiaux. I. Résultats généraux et géodrilogiques (Lumbricidae: Oligochaeta). *Rev. Ecol. Biol. Sol.* 13: 261–281.

Bouché, M.B. 1977. Stratégies lombriciennes. In U. Lohm and T. Persson, Eds. Soil Organisms as Components of Ecosystems. *Biol. Bull.* (Stockholm) 25: 122–132.

Bouché, M.B. and Beugnot, M. 1972. Contribution à l'approche méthodologique de l'étude des biocénoses. II. L'extraction des macroéléments du sol par lavage-tamisage. *Ann. Zool. Ecol. Amin.* 4: 537–544.

Boyd, J.M. 1957. Comparative aspects of the ecology of Lumbricidae on grazed and ungrazed natural maritime grasslands. *Oikos* 8: 107–121.

Brandhorst-Hubbard, J.L., Flanders, K.L., Mankin, R.W., Guertal, E.A., and Crocker, R.L. 2001. Mapping of soil insect infestations sampled by excavation and acoustic methods. *J. Econ. Entomol.* 94: 1452–1458.

Chan, K.Y. and Munro, K. 2001. Evaluating mustard extracts for earthworm sampling. *Pedobiologia* 45: 272–278.

Clapperton, M.J. 1999. Tillage practices, and temperature and moisture interactions affect earthworm populations and species composition. *Pedobiologia* 43: 1–8.

Clapperton, M.J., Miller, J.J., Larney, F.J., and Lindwall, C.W. 1997. Earthworm populations as affected by long-term tillage practices in southern Alberta, Canada. *Soil Biol. Biochem.* 29: 631–633.

Conner, R.L., Clapperton, M.J., and Kuzyk, A.D. 2000. Control of take-all in soft white spring wheat with seed and soil treatments. *Can. J. Plant Pathol.* 22: 91–98.

Dalby, P.R., Baker, G.H., and Smith, S.E. 1996. "Filter paper method" to remove soil from earthworm intestines and standardise the water content of earthworm tissue. *Soil Biol. Biochem.* 28: 685–687.

Dalby, P.R., Baker, G.H., and Smith, S.E. 1996. "Filter paper method" to remove soil from earthworm intestines and to standardise the water content of earthworm tissue. *Soil Biol. Biochem.* 28: 685–687.

Dickey, J.B. and Kladivko, E.J. 1989. Sample unit sizes and shapes for quantitative sampling of earthworm populations in crop lands. *Soil Biol. Biochem.* 21: 105–111.

Doube, B.M. and Auhl, L. 1998. Over-summering of cocoons of the earthworm, *Microscolex dubius* (Megascolecidae) in a hot dry Mediterranean environment. *Pedobiologia* 42: 71–77.

East, D. and Knight, D. 1998. Sampling soil earthworm populations using household detergent and mustard. *J. Biol. Educ.* 32: 201–206.

Edwards, C.A. and Bohlen, P.J. 1996. *Biology and Ecology of Earthworms.* 3rd ed. Chapman and Hall, London.

Edwards, C.A. and Lofty, J.R. 1972. *Biology of Earthworms.* Chapman & Hall, London.

Espinosa, E., Liu, Z., and Zou, X. 1997. Estimating earthworm birth and death rates using a mark and recature technique. Abstracts of the 6th International Symposium on Earthworm Ecology. Vigo, Spain, p. 185.

Gerard, B.M. 1963. The activities of some species of Lumbricidae in pasture land. In J. Doeksen and J. van der Drift, Eds. *Soil Organisms.* North Holland, Amsterdam, The Netherlands, pp. 49–54.

Gestal, C.A.M., Kruidenier, M., and Berg, M.P. 2003. Suitability of wheat straw decomposition, cotton strip degradation and bait-lamina feeding tests to determine soil invertebrate activity. *Biol. Fert. Soils* 37: 115–123.

Gundale, M.J., Jolly, W.M., and Deluca, T.H. 2005. Susceptibility of a northern hardwood forest to exotic earthworm invasion. *Conserv. Biol.* 19: 1075–1083.

Gunn, A. 1992. The use of mustard to estimate earthworm populations. *Pedobiologia* 36: 65–67.

Hauser, S. and Asawalam, D.O. 1998. A continuous sampling technique to estimate surface cast production of the tropical earthworm *Hyperiodrilus africanus*. *Appl. Soil Ecol.* 10: 179–182.

Holmstup, M. 1999. Cocoon production of *Aporrectodea longa* Ude and *Aporrectodea rosea* Savigny (Oligochaeta; Lumbricidae) in a Danish grass field. *Soil Biol. Biochem.* 31: 957–964.

Holmstrup, M. 2000. Field assessment of toxic effects on reproduction in the earthworms *Aporrectodea longa* and *Aporrectodea rosea*. *Environ. Toxicol. Chem.* 19: 1781–1787.

Joyner, J.W. and Harmon, N.P. 1961. Burrows and oscillative behaviour therein of *Lumbricus terrestris*. *Proc. Indiana Acad. Sci.* 71: 378–384.

Kukkonen, S., Palojarvi, A., Rakkolainen, M., and Vestberg, M. 2004. Peat amendment and production of different crop plants affect earthworm populations in field soil. *Soil Biol. Biochem.* 36: 415–423.

Lawrence, A.P. and Bowers, M.A. 2002. A test of the "hot" mustard extraction method of sampling earthworms. *Soil Biol. Biochem.* 34: 549–552.

Lee, K.E. 1959. The earthworm fauna of New Zealand. New Zealand Department of Science and Industrial Research Bulletin 130. Wellington, New Zealand.

Lee, K.E. 1985. *Earthworms. Their Ecology and Relationships with Soils and Land Use*. Academic Press, Sydney, NSW, Australia.

Ljungström, P.-O. 1970. Introduction to the study of earthworm taxonomy. *Pedobiologia* 10: 265–285.

Martin, N.A. 1986. Earthworm biomass: influence of gut content and formaldehyde preservation on live-to-dry weight ratios of three common species of pasture Lumbricidae. *Soil Biol. Biochem.* 18: 245–250.

Mazaud, D. and Bouché, M.B. 1980. Introductions en surpopulation et migrations de lombriciens marques. In D.L. Dindal, Ed. *Soil Biology as Related to Land Use Practices*. Proceedings of the 7th International Soil Zoology Colloquium, Syracuse, New York, 1979. U.S. Environmental Protection Agency, Washington, DC, pp. 687–701.

McLean, M.A. and Parkinson, D. 1997. Changes in the structure, organic matter and microbial activity of pine forest following the introduction of *Dendrobaena octaedra* (Oligochaeta, Lumbricidae). *Soil Biol. Biochem.* 29: 537–540.

Meinhart, 1976. Dauerhafte Markierung von Regenwurmen durch ihre lebendfarbung. Nachrichtenbl. *Dtsch. Pflanzenschutzdienstes* (Braunschweig) 28: 84–86.

Petersen, H. 2000. Collembola populations in an organic crop rotation: population dynamics and metabolism after conversion from clover-grass ley to spring barley. *Pedobiologia* 44: 502–515.

Piearce, T.G. 1972. Acid intolerant and ubiquitous Lumbricidae in selected habitats in north Wales. *J. Anim. Ecol.* 41: 397–410.

Raw, F. 1959. Estimating earthworm populations by using formalin. *Nature* (London) 184: 1661–1662.

Raw, F. 1960. Earthworm population studies: a comparison of sampling methods. *Nature* (London) 187: 257.

Reynolds, J.W. 1973. Earthworm (Annelida: Oligochaeta) ecology and systematics. In D.L. Dindal, Ed. *Proceedings of 1st Soil Microcommunities Conference, Syracuse, NY*. US Atomic Energy Commission, Office of Information Services Centre, Washington, DC, pp. 95–120.

Reynolds, J.W. 1977. *The Earthworms (Lumbricidae and Sparganophilidae of Ontario)*. Royal Ontario Museum, Life Sciences, Miscellaneous Publications, Toronto, ON, Canada.

Rossi, J.P. and Nuutinen, V. 2004. The effect of sampling unit size on the perception on the spatial pattern of earthworm (*Lumbricus terrestris* L.) middens. *Appl. Soil Ecol.* 27: 189–196.

Satchell, J.E. 1955. An electrical method of sampling earthworm populations. In D.K.McE. Kevan, Ed. *Soil Zoology*. Butterworths, London, UK, pp. 356–364.

Satchell, J.E. 1969. Methods of sampling earthworm populations. *Pedobiologia* 9: 20–25.

Schmidt, O. 2001a. Time-limited soil sorting for long-term monitoring of earthworm populations. *Pedobiologia* 45: 69–85.

Schmidt, O. 2001b. Appraisal of the electrical octet method for estimating earthworm populations in arable land. *Ann. Appl. Biol.* 138: 231–241.

Schwert, D.P. 1990. Oligochaeta: Lumbricidae. In D.L. Dindal, Ed. *Soil Biology Guide*. John Wiley and Sons, New York, 341–356.

Sims, R.W. and Gerard, B.M. 1985. *Earthworms. Synopses of the British Fauna*, No. 31. Linnaean Society of London, London, UK.

Southwood, T.R.E. 1978. *Ecological Methods*. Chapman and Hall, London, UK.

Springett, J.A. and Gray, R.A.J. 1992. Effect of repeated low doses of biocides on the earthworm *Aporrectodea caliginosa* in laboratory culture. *Soil Biol. Biochem.* 24: 1739–1744.

St. Remy, E.A. de and Daynard, T.B. 1982. Effects of tillage methods on earthworm populations in monoculture corn. *Can. J. Soil Sci.* 62: 699–703.

Tisdall, J.M. and McKenzie, B.M. 1999. A method of extracting earthworms from cores of soil with minimum damage to the soil. *Biol. Fert. Soils* 30: 96–99.

Wever, L.A., Lysyk, T.J., and Clapperton, M.J. 2001. The influence of soil moisture and temperature on the survival, aestivation, growth and development of juvenile *Aporrectodea tuberculata* (Eisen) (Lumbricidae). *Pedobiologia* 45: 121–133.

Whelan, J.K. 2004. Spatial and temporal distribution of earthworm patches in corn field, hayfield and forest systems of southwestern Québec, Canada. *Appl. Soil Ecol.* 27: 143–151.

Wormwatch, 2002. www.wormwatch.ca Agriculture and Agri-Food Canada and Environment Canada, Environmental Monitoring and Assessment Network, Ottawa, ON, Canada.

Zaborski, E.R. 2003. Allyl isothiocyanate: an alternative chemical expellant for sampling earthworms. *Appl. Soil Ecol.* 22: 87–95.

Chapter 35
Enchytraeids

S.M. Adl
Dalhousie University
Halifax, Nova Scotia, Canada

35.1 INTRODUCTION

The enchytraeids, sometimes referred to as ''potworms,'' are distributed globally and are common in most soils. Enchytraeids are a family of earthworms (Oligochaeta: Annelida: Clitellata: Enchytraeidae) where species lengths range from several hundred micrometers to 6 cm. Their internal anatomy is similar to earthworms and easily described from live specimens viewed at the microscope because the epidermis and cuticle are usually transparent, although tissues are lightly pigmented in some forms.

At least 600 species are described from aquatic and terrestrial habitats mostly in Europe (Dash 1990). However, most species remain to be described yet as many regions are still unsampled. For identification, the monographs of Nielsen and Christensen (1959, 1961, 1963) describe many European species. Since then, many new species of Enchytraeids have been described in the literature. An identification key to genera, as well as a list of many North American species, can be found in Dash (1990). The genus *Fridericia* was reviewed recently (Schmelz 2003). The biology (Dash 1983) and ecology of enchytraeids can be found in reviews (Lagerloef et al. 1989; Didden 1993; van Vliet 2000).

Enchytraeids are important to the food web and to organic matter decomposition in most soils. They can even be found under snow and glacier ice. They are common in the sub-Arctic where larger species occur, and more abundant in soils rich in organic matter as well as in the forest floor. Their abundances range between 10^3 and 10^5 m^{-2} in the organic horizons. Their food preferences include macrodetritus and microdetritus, especially if it has been partly digested and softened by fungal activity (Dosza-Farkas 1982; Kasprzak 1982; Toutain et al. 1982). They can burrow into and out of decomposing roots and litter. At least some species have difficulty, or, are not capable of, digesting cellulose. Protists, hyphae, and bacteria ingested with litter must be considered an important part of the diet. Some mineral particles may be ingested during feeding. Development of eggs in cocoons requires 2–4 months depending on species and temperature. Fragmentation, parthenogenesis, and self-fertilization occur.

35.2 SAMPLING AND EXTRACTION

Soil samples are removed with a soil probe and then extracted in a cool room by a modified Baermann funnel method that is used for nematodes. Extraction efficiency is variable and with some species and soils can be poor. Enchytraeids will be found throughout the rooted zone of the soil. The protocol below is suited for sampling field sites to recover a representative number of individuals. The number of cores required will depend on the aims and objectives of the study. The number of funnel set-ups required (Section 35.2.1) equals the number of soil cores obtained. A second procedure (Section 35.2.2) based on a silica gel extraction can be more efficient and faster, but it is more costly.

35.2.1 Wet Extraction Method

The principle of the method is to disintegrate the soil structure by adding water. The enchytraeids sink with gravity as they move. A heat source, such as a light bulb, can be used to increase the movement of the enchytraeids and it can enhance the numbers collected. The soil particles are held back by a mesh. The extraction aims at collecting a maximum of individuals, with as little soil particles as possible.

Materials and Reagents

1 Soil probe 5–8 cm diameter

2 Zipper-type resealable plastic bag to hold each core

3 Marker pen

4 Glass funnel 10 cm diameter

5 Flexible rubber hose to fit funnel stem

6 Clip for rubber hose

7 Cheesecloth or plastic 1 mm mesh

8 Distilled water

9 40 W tungsten light bulb with rheostat adjustment

10 Dissecting microscope

11 Inverted microscope

12 Petri dish

Procedure

1 Remove a soil core to 3 cm depth from the selected field site.

2 Place soil core in a zipper-type resealable plastic bag, seal without disturbing the core, and label appropriately.

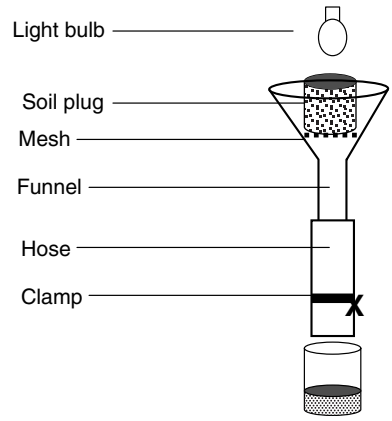

FIGURE 35.1. A modified Baermann funnel method used for extracting nematodes.

3 Keep samples undisturbed in a cool place (walk in cooler or refrigerator) until ready for extraction.

4 Place the soil core on a layer of cheesecloth or plastic mesh in the funnel (Figure 35.1).

5 Clip tight the hose with a clamp to prevent water draining.

6 Fill the funnel with distilled water to reach 1/4 up the core height. Pour the water along the side of the funnel, not over the soil.

7 Remove any accumulated air bubbles in the glass stem of the funnel by letting some water drain. Replenish with water if necessary.

8 Turn on the light bulb to low intensity, and allow the surface of the soil core to warm gently for 3 h.

9 Adjust the light intensity to warm the soil surface further to 40°C and let stand from half a day to a day.

10 On the second day, drain the water in the funnel to collect enchytraeids, and repeat daily for several days until enchytraeids are no longer extracted. Keep this extract in a Petri dish for microscopy. Refill funnel each time with fresh oxygenated water by pouring water in the funnel, not on the soil core.

11 Enumerate the enchytraeids in a Petri dish under a dissecting microscope.

12 Examine with an inverted microscope (or compound microscope) at 40–400× magnification to identify species.

Comments

1 A split core soil sampler that allows recovery of intact soil cores is preferable.

2 For soil samples greater than 3 cm depth, it is best to obtain successive cores labelled 0–3 cm and 3–6 cm, etc. These cores are then extracted separately.

3 Sampled soil can be kept cool in a cold room (or refrigerator) for a few days prior to extraction, below 10°C. It is best to begin the extraction within a day or two.

4 Some prefer to carry out this extraction without a light bulb, over a longer period. Others prefer to carry out the extraction in a cold room, with a light bulb.

5 A useful conversion of length to biomass is 1 mm = 0.88 mg fresh weight.

35.2.2 Silica Gel Extraction

This procedure is more efficient than the wet extraction protocol (Phillips et al. 1999). Soil mineral particles are denser and sink in the solution, while organisms and some organic matter float in the colloid. The enchytraeids float to the top in the colloidal silica with gentle mixing. The protocol extracts include other invertebrates such as tardigrades, nematodes, microarthropods. Testate amoeba are also separated from the soil and float in the gel.

Materials and Reagents

1 Fresh soil sample

2 Glass beaker, 250 mL

3 Glass rod or spatula for mixing

4 Ludox CL 30% colloidal silica (Sigma-Aldrich)

5 Petri dish, 10 cm diameter

Procedure

1 Place the soil in the beaker without disturbing or breaking apart the soil too much.

2 Pour the silica gel onto the soil to cover the soil by more than 1 cm.

3 With a glass rod or a spatula, gently mix together the silica gel and soil, and let stand 30 min.

4 Pour out the surface 1 cm thick of silica gel into a Petri dish for microscopy.

5 Top up the colloidal silica in the soil to 1 cm above the surface. Stir again, let stand 30 min, and pour into a Petri dish for a second observation.

Comments

1 The protocol by Phillips et al. (1999) used Ludox AM30. We find that Ludox CL provides intact immobilized specimen that can be photographed and described with ease. The specimens die shortly after contact with the colloidal suspension.

2 Ludox dries if spilled and the crystals are harmful. Avoid breathing in and any contact with skin. The soil and the suspension will require adequate safe disposal, according to local and federal regulations.

3 Organic material will also float in the suspension and the specimens must be sorted for through the debris.

35.3 FIXATION AND STAINING

The description and identification of species must be carried out using live specimens and supported with drawings and photographs if possible. Monographs and keys detail the necessary observations for identification. Prior to fixation, it is best to let the enchytraeids clear their gut in water in a Petri dish for a few hours in a cool place. Fixed specimens are required for reference only. The procedures here are based on that of Anneke Beylich (Institut für Angewandte Bodenbiologie, Hamburg), but see also Protocol 35.2.2 above.

35.3.1 Materials and Reagents

1 Saturated picric acid (*Caution*: See comments below)

2 Formaldehyde (~35%)

3 Glacial acetic acid

4 Ethanol 70% v/v

5 Boraxcarmine or paracarmine stain solution

6 Acid ethanol (5 drops hydrochloric acid in 100 mL of 70% ethanol)

7 Ethanol 95%

8 Ethanol 100% or 100% isopropanol

9 Xylene

10 Permount

11 Microscope slide

12 Cover slide

13 Pasteur pipette (1.5 mL) and pipette rubber bulb

14 Glass test tube (10 mL)

35.3.2 Procedure

1 Mix picric acid, formaldehyde, and acetic acid in ratio 15:5:1. This is Bouin's fixative. *Caution*: Handle all solutions with gloves in fume hood. Crystalline picric acid is explosive. Avoid spills and keep cap clean. See comments below.

2 Warm 1 mL Bouin fixative placed in a test tube in a water bath, to 60°C–80°C.

3 Place specimen for fixation in the hot Bouin's fixative in the test tube. Remove test tube from water bath to cool and keep the specimen in this fixative 2–6 h.

4 Remove the fixative with a Pasteur pipette. Do not disturb the enchytraeids as they are brittle and fragile at this stage.

5 Add 1 mL 70% ethanol and let stand 15 min.

6 Remove as much ethanol as possible with a pipette and repeat ethanol wash several times until the specimen is whitish.

7 Remove last wash of ethanol and add 1 mL of stain solution. Let stand 10–30 min.

8 Remove stain with a new Pasteur pipette.

9 Destain by adding 1 mL acid ethanol. Let stand until enchytraeids are pale red, with dark septal glands. This will take 2–3 h in thin specimen up to 2 days in thicker specimen.

10 Remove acid ethanol with a new Pasteur pipette.

11 Dehydrate the specimen by adding 1 mL 95% ethanol for 30 min.

12 Replace 95% ethanol with 1 mL 100% ethanol for 15 min.

13 Replace 100% ethanol with another 1 mL 100% ethanol, and let stand 30 min.

14 Add 1 mL xylene, and let stand 15 min.

15 Remove most of the ethanol and xylene with a clean Pasteur pipette, and dispose of safely.

16 Add 1 mL xylene, and let stand 30 min.

17 With a Pasteur pipette (or wide bore pipette) gently remove specimen and place on a microscope slide, with a little xylene carry over. Work quickly to avoid evaporation.

18 Add one or two drops Permount to cover specimen.

19 Place cover slide and let dry overnight.

35.3.3 Comments

1 Fixation and staining can also be carried out in a watch glass in the fume hood. *Caution*: Hot and cold Bouin solution, and the ingredients, should be handled with care in a fume hood, with gloves. Consult Material Safety Data Sheets for hazards and safety precautions. Consult your safety officer for handling and disposal of the fixative, and for a spill clean-up protocol.

2 100% ethanol can be replaced with 100% isopropanol.

3 Xylene can be substituted with less toxic clearing agents, such as CitriSolv (Fisher Scientific). Ask your local supplier.

4 Observation is easier with an inverted microscope with long working distance objectives.

5 Certain species may not fix rapidly enough to preserve the relaxed (not contracted) shape. In these situations a variety of anesthetics can be employed prior to fixation. These include carbonated water or 20% ethanol. The anesthetic is added drop by drop to the extracted living specimen while monitoring relaxation at the microscope.

6 As an alternative to this protocol, Ludox CL colloidal silica 30% suspension (Sigma-Aldrich) immobilizes the specimen, and permits description and photography without contraction or deformation of specimen (see Section 35.2.2).

35.4 CULTIVATION

There are no standard procedures for cultivation on artificial media that are effective with all enchytraeids. Certain genera are easy to cultivate (*Cognettia*, *Enchytraeus*, *Lumbricillus*), but most do not reproduce satisfactorily in the laboratory. Natural soil based approaches are more satisfactory and promising with environmental samples. You should be prepared to engage in some trial and error experimentation to determine what works best for different species.

35.4.1 Materials and Reagents

1 Forest soil organic horizon (see comments below)

2 Container to hold the soil

3 Autoclave

35.4.2 Procedure

1 Sift through the soil to remove earthworms and macroinvertebrates.

2 For maintaining stock species, soil should be autoclaved 10 min to destroy existing invertebrates. This step can be omitted if the soil is not for a monoculture, but if a variety of local enchytraeid species are to be maintained.

3 Place the soil in a suitable container (see comments below) with a loose fitting lid that permits aeration.

4 The soil should not be excessively compacted in order to maintain aeration. Gentle pressing by hand is sufficient. The soil should be watered regularly to maintain the soil damp.

5 Optional: An inoculum of natural fauna including microarthropods and protists should be returned to this soil to maintain the decomposition food web. This is easily achieved by separately extracting for these organisms, as described in Chapter 32 and Chapter 36.

6 The enchytraeids are selected from the soil extraction protocol and placed in this soil.

7 Optional: For long term cultivation of enchytraeids, new air dried crumbed leaf litter should be added every several months. This can be supplemented with flakes of oatmeal.

35.4.3 Comments

1 Suitable containers vary with the amount of soil and the number of enchytraeids required. We have used 125 mL to 500 mL plastic containers for maintaining single species, or 20 L aquarium for maintaining a mixture of species.

2 Some species prefer wetter habitats, whereas other will do well in drier soil. The amount of wetness in the container should mimic the natural habitat of the species.

3 Some species prefer soils with less organic matter. In this case, sand and potting soil can be mixed together, or mineral soil from an agricultural field (without fertilizer or pesticides) can be used instead of the forest soil.

4 The sterilization time by autoclaving is kept short to permit survival of some of the fungal and bacteria species. They are required to decompose the soil organic matter, to facilitate digestion, and assimilation by the enchytraeids. Soils with an inoculum of soil fungi, protists and microinvertebrates returned may be more stable in the long term.

REFERENCES

Dash, M.C. 1983. *The Biology of Enchytraeidae*. International Book Distributors, Dehradum, India, p. 171.

Dash, M.C. 1990. Enchytraeidae. In D.L. Dindal, Ed. *Soil Biology Guide*. John Wiley and Sons, New York, NY, pp. 311–340.

Didden, W.A.M. 1993. Ecology of Enchytraeidae. *Pedobiologia* 37: 2–29.

Dosza-Farkas, K. 1982. Konsum verschiedener Laubarten durch Enchytraeiden (Oligochaeta). *Pedobiologia* 23: 251–255.

Kasprzak, K. 1982. Review of Enchytraeids (Oligochaeta, Enchytraeidae) community structure and function in agricultural ecosystems. *Pedobiologia* 23: 217–232.

Lagerloef, J., Andren, O., and Paustian, K. 1989. Dynamics and contribution to carbon flows of Enchytraeidae (Oligochaeta) under four cropping systems. *J. Appl. Ecol.* 26: 183–199.

Nielsen, C.O. and Christensen, B. 1959. The Enchytraeidae. Critical revision and taxonomy of European species. Studies on Enchytraeidae VII. *Nat. Jutl.* 8–9: 1–160.

Nielsen, C.O. and Christensen, B. 1961. Studies on Enchytraeidae VII. Critical revision and taxonomy of European species. Supplement 1. *Nat. Jutl.* 10: 1–23.

Nielsen, C.O. and Christensen, B. 1963. Studies on Enchytraeidae VII. Critical revision and taxonomy of European species. Supplement 2. *Nat. Jutl.* 10: 1–19.

Phillips, C.T., Kuperman, R.G., and Checkai, R.T. 1999. A rapid and highly efficient method for extracting enchytraeids from soil. *Pedobiologia* 43: 523–527.

Schmelz, R.M. 2003. Taxonomy of Fridericia (Oligochaeta, Enchytraeidae). Revision of species with morphological and biochemical methods. *Abh. Naturwiss. Ver. Hamb. (NF)* 38, 450 pp.

Toutain, F., Vilemin, G., Albrecht, A., and Reisinger, O. 1982. Etude ultrastructurale des processus de biodégradation. II. Modèles Enchytraeids-litières de Feuillus. *Pedobiologia* 23: 145–156.

van Vliet, P.C.J. 2000. Enchytraeids. In M. Sumner, Ed. *The Handbook of Soil Science*. CRC Press, Boca Raton, Fl, pp. C-70–C-75.

Chapter 36
Protozoa

S.M. Adl
Dalhousie University
Halifax, Nova Scotia, Canada

D. Acosta-Mercado
University of Puerto Rico
Mayaguez, Puerto Rico

D.H. Lynn
University of Guelph
Guelph, Ontario, Canada

36.1 INTRODUCTION

Among the microbial groups, protozoa are involved in pivotal processes in both aquatic and terrestrial ecosystems. In soil ecosystems, protozoa are conspicuous (Berthold and Palzenberger 1995), serving as consumers and prey for other soil microorganisms (Clarholm 1981), influencing the development and metabolic activities of bacterial communities (Pussard et al. 1994; Griffiths et al. 1999), and concomitantly increasing plant biomass (Kuikman et al. 1990; Alphei et al. 1996). The role and diversity of protozoa in the soil has been the subject of recent reviews (Adl 2003; Adl and Gupta 2006). An extensive literature was synthesized in two earlier reviews (Foissner 1987; Darbyshire 1994), and Bonkowski (2004) reviewed the interactions of protozoa with plant roots.

Protozoa are defined as heterotrophic, nonfilamentous protists. The major role of protozoa in decomposition food webs is usually assumed to be as bacterivores. Although this is primarily correct, protozoa consumers are more diverse, influencing the rest of the food web by feeding on each other, fungal components, and even on some soil metazoans. Ingestion of prey through a cytostome in smaller protozoa, like nanoflagellates, is usually one bacterium or protist at a time. In larger species with a cytostome, particularly larger ciliates, ingestion of hundreds of bacteria or several protists occurs at the same time in one food vacuole. A few amoeboid genera, a couple of ciliate genera, and some testate amoebae can ingest fungal hyphae or the cytoplasm of hyphae and spores. These genera are fungivorous and cultured or baited on spores or hyphae. The Eumycetozoa (slime moulds) are primary saprotrophs that digest woody or cellulosic substrates, such as bark, leaf litter, wood, or dung.

Some protozoa, such as testate amoebae and histophagous ciliates, are consumers on invertebrates or dying microinvertebrates like nematodes. They can be seen to aggregate around weak individuals. In general, most species have some prey preference and not all bacterial or protist prey species are nutritionally equivalent. Dispersal cells of chytrids and Peronosporomycetes taxa should not be confused with bacterivorous flagellates. These dispersal stages of saprotrophic or predatory species on invertebrates are usually seeking an adequate substrate to settle on.

In general, the highest diversity of species and abundances of individuals are encountered in the litter and organic horizons, decreasing with depth into the mineral soil. Some enrichment occurs along the rhizosphere, which is especially noticeable in desert environments or along rows of crops in agro-ecosystems. Diurnal and seasonal variation in environmental conditions such as temperature and moisture can greatly affect abundances of active protozoa. Some soil protozoan species are only active seasonally or during certain soil moisture and temperature combinations. The magnitude of changes in abundance can fluctuate by 100× over 24 h following rain, warming, or cooling of the soil (Adl and Coleman 2005). Abundances of active cells can be as low as a few hundred cells per gram dry soil under arid conditions or in nutrient poor or eroded soils. In forest soils, abundances of active cells can be as high as 10^7 cells per gram dry soil or litter under favorable conditions.

Methods for measuring the abundance of protozoa have been classified as direct and indirect. These terms usually refer to enumeration without culturing or with culturing, respectively. Enumeration of active cells without culturing is the only approach to provide reliable estimates of in situ abundance of active (i.e., noncyst) protozoa. These methods have the following advantages: there is a minimum of preparative steps; they do not rely on numerous untested assumptions; and they are not as time-consuming as culture-based methods. Disadvantages, however, include low taxonomic resolution, and the problem that samples must be inspected within a day or two after collection.

Estimates of active cells that employ the most probable number (MPN) approach involve the preparation of replicate dilution series in a culture medium and counting on successive days. These methods (e.g., Rønn et al. 1995; Anderson 2000; Fredslund et al. 2001) are essentially modifications of the ring method (Singh 1955). Culture-based estimations are necessary to determine species frequency and biodiversity, but cannot be used to determine the abundance of active species in soil. Berthold and Palzenberger (1995) and Foissner (1987) discussed the potential sources of error for culture-based methods. Culture-based methods have been notorious for favoring r-selected strategist species at the expense of slower growing species, and those that do not feed on bacteria (Coûteaux and Palka 1988; Adl 2003). Moreover, abundances estimated using MPN methods vary depending on the MPN equation used, storage duration and conditions, soil processing, and culture protocol. In agreement with Adl and Coleman (2005), Berthold and Palzenberger (1995), Foissner (1987) and others, we do not recommend that MPN methods be applied.

This chapter will provide an introduction to methods for enumerating soil protozoa. Identification of protozoan species, and assessment of diversity or community structure, is outside the scope of this chapter. Readers interested in species identification and classification can begin by consulting ''The Illustrated Guide to the Protozoa'' (Lee et al. 2000), which uses an older system of classification but has useful keys, descriptions of various taxa, and references, and Adl et al. (2005) for the nomenclature and taxonomy of protists. An efficient method for the extraction and identification of ciliates was described by Acosta-Mercado and Lynn (2003). Testate amoebae can be extracted and identified using a slide smear

technique (Korganova and Geltser 1977), or on membranes (Lousier and Parkinson 1981). Mycophagous amoebae can be identified using fungal spores as bait (Duczek 1983). A more extensive list of methods for soil protozoa can be obtained on the Internet (Dalhousie University Soil Ecology Portal 2006).

36.2 MICROSCOPES

The inverted microscope is the principal instrument for observation and enumeration of protozoa in soil samples. Phase contrast objectives with long working distances are required for most procedures. Magnifications necessary for observing protozoa are 100× to 400×. The quality of the objectives should be plan apochromat or equivalent.

A dissecting microscope is useful for sorting through samples flooded with water. A high-resolution plan apochromat objective (1×) is recommended with illumination from below, and tilting mirror in the base to provide oblique transmitted illumination. With 10× eye-pieces and zoom, a magnification of at least 80× can be reached. The tilting mirror is essential, especially with smaller species. Larger flagellates and the smaller species of ciliates and testate amoebae can be visualized with these microscopes. Lower resolution models are suitable for most ciliates and testate amoebae, but the smaller species will be missed. Amoebae should not be counted with dissecting microscopes.

36.3 STANDARD SOLUTIONS

The following are useful for the preparation of soil suspensions and dilutions, general culture of cells, or preparation of fixed slide preparations. A more extensive list is available on the Internet (Dalhousie University Soil Ecology Portal 2006).

36.3.1 Phosphate Buffers

Phosphate buffers are used to adjust a medium to the same pH as the soil samples. They are also a component of culture media. Potassium- or sodium-based buffers are made by mixing together different volumes of a basic solution with an acidic solution. Prepare phosphate buffers as outlined in Table 36.1.

36.3.2 Phosphate Buffered Soil Saline

The solution below can be used to hold cells in suspension or for washing cells. It is less damaging to cells than using distilled water or deionized water. Na_2HPO_4 and KH_2PO_4 can be replaced with a phosphate buffered solution of known pH according to Table 36.1.

Reagents

1 8 g NaCl

2 0.2 g KCl

3 1.44 g Na_2HPO_4

TABLE 36.1 Quantities of Solutions Required to Prepare (a) Potassium or (b) Sodium-Based Buffers

(a) Preparation of 0.1 M Potassium Phosphate 10× Buffer at 25°C[a]		
pH	**1 M K_2HPO_4 (mL)**	**1 M KH_2PO_4 (mL)**
5.8	8.5	91.5
6.0	13.2	86.8
6.2	19.2	80.8
6.4	27.8	72.2
6.6	38.1	61.9
6.8	49.7	50.3
7.0	61.5	38.5
7.2	71.7	28.3
7.4	80.2	19.8
7.6	86.6	13.4
7.8	90.8	9.2
8.0	94.0	6.0
(b) Preparation of 0.1 M Sodium Phosphate 10× Buffer at 25°C[a]		
pH	**1 M Na_2HPO_4 (mL)**	**1 M NaH_2PO_4 (mL)**
5.8	7.9	92.1
6.0	12.0	88.0
6.2	17.8	82.2
6.4	25.5	74.5
6.6	35.2	64.8
6.8	46.3	53.7
7.0	57.7	42.3
7.2	68.4	31.6
7.4	77.4	22.6
7.6	84.5	15.5
7.8	89.6	10.4
8.0	93.2	6.8

[a] To obtain 0.1 M buffer solution dilute ten times.

4 0.24 g KH_2PO_4

5 0.0476 g $MgCl_2$

6 0.147 g $CaCl_2$

7 800 mL distilled water

8 1 M HCl

Add the weighed salts in sequence to the water in a flask while stirring. Adjust pH with HCl to that of the soil under study (or from which the cells were obtained). Top up to 1.0 L with distilled water. Final salt concentrations should be 137 mM NaCl, 2.7 mM KCl, 10 mM Na_2HPO_4, 2 mM KH_2PO_4, 0.5 mM $MgCl_2$, and 1 mM $CaCl_2$. Cell suspensions can be kept in this buffer for a few hours. For maintaining cells longer, the standard soil extract (SSE) or standard soil solution (SSS) below should be used.

36.3.3 Agar (1.5%)

Add 1.5 g agar to 100 mL of distilled or deionized water in an Erlenmeyer flask and autoclave for 20 min. The agar can also be prepared by substituting the water with SSE (see Section 36.3.4), SSS (see Section 36.3.5), or wheat grass medium (see Section 36.3.7).

36.3.4 Standard Soil Extract

A standard soil extract provides a solution that contains dissolved nutrients from a soil sample. It cannot be used as a growth medium on its own, but is often used as a supplement to growth media. The exact composition of the solution varies with the soil used and with each preparation. It is useful for providing a solution with ions similar to the soil used. Prepare SSE using 300 g soil from A horizon and 1.0 L distilled or deionized water:

1. Add the soil to the water in a large beaker and stir for 1 h.
2. Let settle for 30 min and filter through several layers of cheesecloth into an Erlenmeyer flask.
3. Dispense into screw cap bottles and autoclave 30 min.

36.3.5 Standard Soil Solution

A standard soil solution contains known amounts and concentrations of ions. It is useful when the composition of the solution needs to be standardized and can be used to replace water when a precise solution composition is required. Prepare SSS as outlined in Table 36.2. Weigh salts in sequence and dissolve one at a time into the water in a large flask with continuous stirring. Adjust pH of solution to desired level with phosphate buffers (see Section 36.3.1). It is important to add the phosphate buffer, along with the KH_2PO_4, as they are the main sources of phosphate for the medium. The final pH (pH $\pm$ 0.3) should be close to that of the soil under study, or from which the cells were obtained. Adjust volume to 1.0 L and dispense into screw cap bottles. Autoclave 20 min and store at 4°C. Stock solutions can be prepared at 100× and refrigerated.

36.3.6 Wheat Grass Medium 0.1% (w/v)

This is a general medium that can be used to culture many protozoan species. Combine wheat grass powder (1.0 g) and water (1.0 L distilled or deionized water) in a 2 L Erlenmeyer flask.

TABLE 36.2 Preparation of Standard Soil Solution with Molarity of Components in the Final Solution

Weight	Final molarity
6.8×10^{-4} g L^{-1} KH_2PO_4	5×10^{-6}
1.116 g L^{-1} $FeCl_3$	6.88×10^{-3}
0.241 g L^{-1} $MgSO_4$	2.00×10^{-3}
0.544 g L^{-1} $CaSO_4$	4.00×10^{-3}
0.133 g L^{-1} NH_4Cl	2.48×10^{-3}
0.253 g L^{-1} KNO_3	2.50×10^{-3}
0.14 g L^{-1} NaCl	2.4×10^{-3}
900 mL distilled water	—

Bring to a boil and let infuse at a gentle rolling boil for 2 min. Let settle and cool for 1 h. Filter through several layers of cheesecloth into a new flask and discard grass residue. Adjust pH to desired level with a phosphate buffer (see Section 36.3.1 above). The pH should be close (pH $\pm$ 0.3) to that of the soil under study. Dispense the medium into screw cap bottles and autoclave for 20 min.

The wheat grass medium can also be prepared with SSS or SSE instead of distilled or deionized water. The medium can be diluted further to 1/10 or 1/100 strength to reduce bacterial growth. Many species will only be observed if bacterial growth is low.

36.4 SOIL SAMPLING AND SAMPLE STORAGE

Planning the sampling approach has probably not received as much attention in the literature as it is due. Some important questions to ask are—are diversity and abundance spatially correlated? Will aggregating samples influence the strength of the inferences to be drawn? What is the scale of interest? The approach to sampling the soil will depend ultimately upon the objectives of the study. Soil is typically collected using a shovel, soil core sampler of varying diameter, large diameter cork borer, spoon, or curved spatula (scoopula). To prevent cross-contamination between samples, it is necessary to clean sampling tools with a volatile alcohol that disrupts cell membranes (such as >5% ethanol).

36.4.1 Materials

1 Scoopula or auger

2 15 mL screw cap plastic tubes (e.g., Falcon tubes) and plastic bags

3 Water and alcohol proof marking pen

4 Squeeze bottle of 5% ethanol and clean paper towels

5 Hand-held thermometer probe (optional)

6 Field note book and pencil

7 Styrofoam cooler box with ice packs for transport

36.4.2 Procedure

1 Select a quadrat (75 $\times$ 75 cm).

2 Subsample the quadrat to 10 cm depth with the scoopula by removing a more or less intact soil plug of about 1 cm diameter to fit in a tube.

3 Place the core in a tube without forcing or crushing the soil, since this would affect soil porosity, gas exchange, and moisture content. Label the tube appropriately.

4 Rinse the scoopula with ethanol to wash off soil and wipe dry with a clean paper towel.

5 Subsample the quadrat two more times as above.

6 Obtain temperature readings at 2 and 10 cm depth.

7 Place labeled sample tubes in a plastic bag.

8 Repeat with more quadrats as necessary, depending on the nature of the study and size of the field under study.

9 Place plastic bags with samples in the cooler for transport. Cover ice packs with a sweater or blanket. Do not place samples directly on ice, or in contact with the cold.

36.4.3 Comments

1 For direct counts of active species, samples must be processed within a day or two. Species composition will change as temperature or moisture in the sample changes. Typically, bacteria and therefore the bacterivore community will change, and this will also affect overall protozoan species composition and relative abundances.

2 If samples are to be stored for a long time (weeks or months), it is recommended to let the soil air dry slowly over several days. This is accomplished by opening the bags, or removing the caps from the tubes, and letting the soil dry over several days in the refrigerator at 10°C to 15°C. This allows time for cells to encyst in their own time. When sufficiently dry, containers can be sealed and transferred to 4°C. However, it is important to explore empirically how these storage conditions influence abundance and diversity before beginning a study. For example, tropical and subtropical species may not be adapted to survive storage at cold temperatures or under very dry conditions (Acosta-Mercado and Lynn 2003).

36.5 ABUNDANCE OF ACTIVE NAKED AMOEBAE

Although most procedures underestimate the abundances of naked amoebae, the following procedure works well with most soils and litter samples. It has the advantage of not damaging the amoebae, and allows them to crawl out on their own in search of food. Naked amoebae can be assigned to the gymnamoebae, Mastigamoebidae, Eumycetozoa, Heterolobosea, Cercozo, and Gromia. Conversion factors for biomass calculations (Table 36.3) should be used for purposes of standardization and cross-comparisons between data sets.

36.5.1 Materials

1 Petri dishes of 5 cm in diameter

2 1.5% water agar

3 Parafilm

TABLE 36.3 Conversion Factors for Estimating Biomass of Soil Protozoa[a]

Parameter	Convert to	Conversion factor
Biovolume	Wet weight	1 $\mu m^3 = 1$ pg
Biovolume	Dry weight	1 $\mu m^3 = 0.15$ pg
Biovolume	Organic carbon	1 $\mu m^3 = 0.11$ pg
Wet weight	Dry weight	15% of wet weight
Dry weight	Ash-free dry weight	10% of dry weight
Dry weight	Organic carbon	50% of dry weight
Dry weight	Nitrogen	4%–7% of dry weight
Ash-free dry weight	Joule (J)	1 mg = 17–20 J
Organic carbon	Joule (J)	1 mg = 46 J

[a] Proposed by Foissner et al. (1992), these represent average values and need to be applied with the understanding that they may either under or overestimate the ''true'' biomass of any particular species.

4 20 or 200 μL pipettor with tips (cut-off tips to wider diameter with scissors or razor blade)

5 Small spatula

6 Aluminum foil

7 Precision balance

8 Fresh soil sample

9 Inverted microscope

36.5.2 Procedure

1 Melt the agar in a water bath or microwave when ready to use.

2 Pour the agar in 5 cm Petri dishes, to an even thickness of 1.5–2.5 mm, and let cool. Plates must be prepared fresh each time as the agar surface desiccates with storage. The agar must be thin enough for the long distance objectives to focus on the surface of the agar.

3 Subsample a soil core with a spatula to obtain a composite of about 1 g that represents the entire core. In cores that are not friable, the side of the spatula is used to cut slices through the core profile.

4 Transfer about 1 g fresh soil (representing the sample) to a test tube with just enough deionized water to obtain a mud that can be pipetted.

5 Take up 20 μL and place the end of the pipette tip onto the agar surface of one Petri dish. Do not expel the volume of mud, but rather deliver enough soil to produce a spot of mud on the surface. With most soils this occurs without depressing the pipettor. Repeat to obtain six spots in a row.

6 Release the volume of soil suspension in the pipettor back into the soil-water suspension. Take up a new subsample.

7 Repeat the subsampling and spotting to obtain 18–24 spots, arranged in rows and columns.

8 Seal the plates with Parafilm, turn agar-side up, label, and incubate the dishes overnight in the dark at about the temperature of the soil when sampled.

9 Repeat the spotting procedure with the soil suspension and the same pipette tip onto a small strip of aluminum foil of known weight. Obtain ten spots and allow to air dry. Weigh the foil again. Use the weight difference to calculate a mean weight for the soil droplets. This is the mean dry weight of each soil droplet.

10 Observe plates with the inverted microscope at 200× magnification with phase contrast. Amoebae appear at the edge of the soil droplets, and begin to migrate across the agar with time. Enumeration is by counting the number of cells at the edge of each droplet. When they are too numerous, a square grid in the ocular eyepiece can be used to count representative areas at the edge of droplets.

36.5.3 Comments

1 With sandy soils or samples that are friable, it will be difficult to spot rows of soil. An alternative procedure is to spread the soil-water suspension as a thin layer across the entire plate. The soil is spread thinly enough so as not to obscure observations. It is then critical to know what weight of soil was spread.

2 There are typically 10^4–10^6 active amoebae per gram dry soil. Therefore, there can be 10–1000 cells in 1 mg of dry soil spotted. Samples with abundant amoebae will require more dilution in a thinner suspension.

3 To avoid desiccation and cell lysis, it is necessary to use moist soil samples and handle them promptly.

4 Observation of samples the next day may include taxa that excysted with the addition of water and reproduced during the overnight incubation.

36.6 ABUNDANCE OF ACTIVE FLAGELLATES

This is a very efficient procedure that provides statistically reliable and repeatable results. Flagellates are represented in the Mastigamoebidae, dispersal stages of Eumycetozoa, Chytridiomycetes, Euglenida, Kinetoplastea, Heterolobosea, Cercozoa, and Peronosporomycetes. Conversion factors for biomass calculations (Table 36.3) should be used for purposes of standardization and cross-comparisons between data sets.

36.6.1 Materials

1 Fresh soil sample

2 Precision balance and spatula

3 Distilled or deionized water

4 20 μL pipettor with disposable tips (cut-off tips to wider diameter with scissors or razor blade)

5 Petri dishes, 5 cm diameter

6 Hemocytometer for phase contrast microscopy

7 Inverted microscope

36.6.2 Procedure

1 Place 1 g fresh soil in a Petri dish with 5 mL of water.

2 Gently separate the soil and mix the suspension evenly. Let the heavy particles settle for 30 s.

3 Pipette 15 μL of suspension to hemocytometer chamber and cover.

4 Scan the counting chamber with 200× and 400× under phase contrast. Choose an appropriate grid size to obtain counts of 5 to 50 cells. Use the volume of the grid size selected to calculate protozoan abundance.

5 Repeat the procedure three to five times until a stable mean abundance value is obtained.

6 The final calculation of abundance must take into account the initial dilution of soil into the Petri dish suspension (e.g., 1 g into 5 mL).

36.6.3 Comments

1 This is a rapid and highly reproducible method for enumerating and identifying flagellates. The microscopist may choose to classify the flagellates into a number of taxonomic groups or functional groups according to their expertise.

2 Typically, there are 10^5–10^7 flagellates per gram of dry soil. It may be necessary to dilute the soil suspension further for the counting chamber. In soils with a high proportion of clay, it may be necessary to dilute the soil to obtain a clear suspension to visualize the cells.

36.7 ABUNDANCE OF ACTIVE CILIATES AND TESTATE AMOEBAE

Active ciliates are usually found during moist periods when bacterial abundances are elevated. Their abundances decline to zero as soils dry, or bacterial populations decrease in abundance and activity.

Testate amoebae are common in surface soil and in the litter, and they can be found burrowed inside decomposing plant tissue fragments. They are valuable as bioindicators in agro-ecosystems and sites under remediation. Their numbers fluctuate seasonally in

temperate regions. When they are found active, their abundances can exceed 10^6 g^{-1} soil or litter. Conversion factors for biomass calculations (Table 36.3) should be used for purposes of standardization and cross-comparisons between data sets.

36.7.1 Materials

1 Fresh soil sample

2 Petri dishes, 5 cm in diameter

3 Distilled or deionized water

4 Precision balance and spatula

36.7.2 Procedure

1 Place 5 mL of water in a Petri dish and add 0.5 g of fresh soil. Gently suspend the soil in the plate.

2 Observe the plate with a dissection microscope, scanning for ciliates or testate amoebae.

3 Tally the number of ciliates swimming, or of testate amoebae at the bottom. Ciliates will be in the water column as well as on the bottom in the sediment. If a good dissection microscope is not available, an inverted microscope with phase contrast setting can be used at 50× magnification. However, this increases the possibility of double counting or missing some.

4 Discard the suspension, and using the same Petri dish, repeat the procedure at least three times to obtain a mean.

5 Abundances are expressed as number of cells per gram of dry soil.

36.7.3 Comments

1 If too much solution is used, the volume to be scanned will not be entirely in focus and satisfactory counts will be difficult to obtain. If there are too many active individuals, a 1 cm square grid can be drawn under the plate, or plates with premarked grids can be purchased. If the soil texture interferes with observations, reduce the amount of soil used.

2 Testate amoebae will be at the bottom of the plate in the sediment. The active species will be moving or exploring substrates with pseudopodia. Better estimates are obtained by scanning transects through the plate using the inverted microscope at 200× or 400× with phase contrast. For calculations, the number of individuals encountered per transect must be multiplied by the fraction of the plate scanned, or the fraction of the soil weight it represents. See Krebs (1999) for transect methods. Many testate amoebae will stop feeding, or moving during the extraction and enumeration process. Empty tests should be distinguished from living specimens.

3 The membrane filter method (Louisier and Parkinson 1981) and the slide smear method (Korganova and Geltser 1977) provide good estimates. Both the membranes and the slide smears can be prepared and scored at a later time.

4 The adaptation of a membrane filter method for ciliates was also described (Acosta-Mercado and Lynn 2003). The staining protocol is complicated, but it permits species identification.

36.8 LEAF LITTER PROTOZOA

The forest floor and surface litter of other soils, such as grasslands and no-till agricultural fields, are rich in protists that bury into the litter and cover the surfaces of decomposing plant tissues. These can be extracted, enumerated, and identified. Activity of some groups, such as testate amoebae, is seasonal, while the activity of others varies with moisture in the litter layers. Cysts of inactive species remain viable in the litter and are reactivated cyclically with changes in moisture and temperature in the litter.

36.8.1 Materials

1 24-well plates (e.g., Falcon multiwell flat bottom plates)

2 Glass Pasteur pipettes, two pairs of fine-tip forceps, one pair of small scissors

3 95% ethanol, alcohol burner

4 100 mL beaker with distilled or deionized water

5 Leaf litter samples

6 Precision balance

7 Aluminum foil

8 1000 μL pipettor with tips

9 Hot plate

36.8.2 Procedure

1 Fill each well of a 24-well plate with 300 μL of distilled or deionized water.

2 Holding the leaf litter between forceps, with the scissors cut off fragments of leaf litter (about 0.3 g) onto a preweighed square of aluminum foil. Record the weight of fragments transferred to each well. Do not damage leaf surfaces that carry the cysts, spores, and active cells. The aim is to subsample a representative sample of the surfaces.

3 Transfer the fragments into the first well, forcing below the surface of the water. Fragments should be cut small enough to fit easily into each well bottom.

4 Pass instruments through ethanol and flame with alcohol burner between samples. Make sure that instruments are cool before handling a new sample. They can be passed through a beaker of sterile deionized water after flaming to cool.

5 Repeat with other forest floor or litter bag samples.

6 Incubate the plates at 15°C or at the field temperature overnight.

7 In the morning, prepare a replicate plate with water. Starting with the first well, lift leaf fragments from bottom with forceps, and rinse surfaces with the water in the same well, using a Pasteur pipette. The aim is to release cells from the surfaces back into the well. Place the rinsed fragments into the new replicate plate in a fresh well.

8 Flame the metal instruments between each well, and rinse the Pasteur pipette in hot water (using a beaker with water on a hot plate set at about 80°C). Proceed in this way with each well. Incubate the new replicate plate for 1–2 days, and proceed to the microscope with the first plate.

9 Observe the first plate without the leaves at the inverted microscope with phase contrast. Each well bottom should be scanned at 200× and 400× magnifications for amoebae, testate amoebae, flagellates, and ciliates. If abundances are too high, a transect method should be used for the statistical estimate (Krebs 1999). Also scan the water column for ciliates and flagellates. If flagellate abundances are too high to count, proceed to estimate active flagellates using a hemocytometer.

10 Observe the replicate plate after 1–2 days of incubation, by repeating the procedure, this time transferring the litter fragments back into the first plate. The operation can be repeated several times over a couple of weeks. Most of the useful data will be obtained during the first 5–10 days.

11 Abundance estimates from the first overnight incubation can be expressed as g^{-1} litter. This sample will include cells that were active when the leaves were processed, as well as cysts that were excysted early on (these will tend to be r-selected species). Samples from subsequent observations represent cultured individuals, and later excysting species, and are not useful for abundance calculations. The subsequent observations are used for tallying species diversity, as different species excyst with time.

36.8.3 Comments

Invertebrates will also be seen, especially rotifers and nematodes, and occasionally tardigrades, ostracods, and enchytraeids. However, their numbers are generally too small to quantify, or to provide detailed lists of invertebrate species. The procedure can be adapted to work with invertebrates if larger litter subsamples are used in 5 or 10 cm diameter Petri dishes.

REFERENCES

Acosta-Mercado, D. and Lynn, D.H. 2003. The edaphic quantitative protargol stain: A sampling protocol for assessing soil ciliate abundance and diversity. *J. Microbiol. Meth.* 53: 365–375.

Adl, M.S. 2003. *The Ecology of Soil Decomposition*. CABI, Wallingford, UK.

Adl, M.S. and Coleman, D.C. 2005. Dynamics of soil protozoa using a direct count method. *Biol. Fert. Soil* 42: 168–171.

Adl, M.S. and Gupta, V.V.S.R. 2006. Protists in soil ecology and forest nutrient cycling. *Can. J. Forest Res.* 36: 1805–1817.

Adl, M.S., Simpson, A.G.B., Farmer, M.A., Andersen, R.A., Anderson, O.R., Barta, J., Bowser, S., Brugerolle, G., Fensome, R., Fredericq, S., James, T.Y., Karpov, S., Kugrens, P., Krug, J., Lane, C., Lewis, L.A., Lodge, J., Lynn, D.H., Mann, D., McCourt, R.M., Mendoza, L., Moestrup, Ø., Mozley-Standridge, S.E., Nerad, T.A., Shearer, C., Smirnov, A.V., Spiegel, F., and Taylor, F.J.R. 2005. The new higher level classification of eukaryotes with emphasis on the taxonomy of protists. *J. Eukaryot. Microbiol.* 52: 399–451.

Alphei, J., Bonowski, M., and Scheu, S. 1996. Protozoa, Nematoda and Lumbricidae in the rhizosphere of *Hordelymus europaeus* (Poaceae): Faunal interactions, response of microorganisms and effects on plant growth. *Oecologia* 106: 111–116.

Anderson, O.R. 2000. Abundance of terrestrial gymnamoebae at a Northeastern U.S. site: A four year study, including El Niño Winter of 1997–1998. *J. Eukaryot. Microbiol.* 47: 148–155.

Berthold, A. and Palzenberger, M. 1995. Comparison between direct counts of active soil ciliates (Protozoa) and most probable number estimates obtained by Singh's dilution culture method. *Biol. Fert. Soils* 19: 348–356.

Bonkowski, M. 2004. Protozoa and plant growth: The microbial loop in soil revisited. *New Phytol.* 162: 617–631.

Clarholm, M. 1981. Protozoan grazing of bacteria in soil-impact and importance. *Microb. Ecol.* 7: 343–350.

Côuteaux, M.M. and Palka, L. 1988. A direct counting method for soil ciliates. *Soil Biol. Biochem.* 20: 7–10.

Dalhousie University Soil Ecology Portal. 2006. http://soilecology.biology.dal.ca/index.htm (accessed 27th June 2006).

Darbyshire, J.F. 1994. *Soil Protozoa*. CABI, Wallingford, UK.

Duczek, L.J. 1983. Populations of mycophagous amoebae in Saskatchewan soils. *Plant Disease* 67: 606–608.

Foissner, W. 1987. Soil protozoa: Fundamental problems, ecological significance, adaptations in ciliates and testacean, bioindicators and guide to the literature. In J.O. Corliss and D.J. Patterson, Eds. *Progress in Protistolology*. Vol. 2. Biopress, Bristol, UK, pp. 69–212.

Foissner, W., Berger, H., and Kohmann, F. 1992. Taxonomische und ökologische Revision der Ciliaten des Saprobiensystems—Band II: Peritrichia, Heterotrichida, Odontostomitida. Informationsberichte des Bayerischen Landesamtes für Wasserwirtschaft, Heft 5/92.

Fredslund, L., Ekelund, F., Jacobsen, C.S., and Johnsen, K. 2001. Development and application of a most probable number-PCR assay to quantify flagellate populations in soil samples. *Appl. Environ. Microbiol* 67: 1613–1618.

Griffiths, B.S., Bonkowski, M., Dobson, G., and Caul, S. 1999. Changes in soil microbial community structure in the presence of microbial-feeding nematodes and protozoa. *Pedobiologia* 43: 297–304.

Korganova, G.A. and Geltser, J.G. 1977. Stained smears for the study of soil Testacida (Testacea, Rhizopoda). *Pedobiologia* 17: 222–225.

Krebs, C.J. 1999. *Ecological Methodology*. 2nd edn. Benjamin Cummings, New York, NY, USA.

Kuikman, P.J., Jansen, A.G., Van Veen, J.A., and Zehnder, A.J.B. 1990. Protozoan predation and the turnover of soil organic carbon and nitrogen in the presence of plants. *Biol. Fert. Soils* 10: 22–28.

Lee, J.J., Leedale, G.F., and Bradbury, P. (eds.) 2002. *An Illustrated Guide to the Protozoa*. 2nd ed. Society of Protozoologists, Lawrence, KS (Year 2000).

Lousier, J.D. and Parkinson, D. 1981. Evaluation of a membrane filter technique to count soil and litter Testacea. *Soil Biol. Biochem.* 13: 209–213.

Pussard, M., Alabouvette, C., and Levrat, P. 1994. Protozoan interactions with the soil microflora and possibilities for biocontrol of plant pathogens. In J.F. Darbyshire, Ed. *Soil Protozoa*. CAB International, Oxford, UK, pp. 123–146.

Rønn, R., Ekelund, F., and Christensen, S. 1995. Optimizing soil extract and broth media for MPN-enumeration of naked amoebae and heterotrophic flagellates in soil. *Pedobiologia* 39: 10–19.

Singh, B.N. 1955. Culturing soil protozoa and estimating their numbers in soil. In D.K. Kevan, Ed. *Soil Zoology*. Butterworths, London, UK, pp. 104–111.

Chapter 37
Denitrification Techniques for Soils

C.F. Drury
Agriculture and Agri-Food Canada
Harrow, Ontario, Canada

D.D. Myrold
Oregon State University
Corvallis, Oregon, United States

E.G. Beauchamp
University of Guelph
Guelph, Ontario, Canada

W.D. Reynolds
Agriculture and Agri-Food Canada
Harrow, Ontario, Canada

37.1 INTRODUCTION

Denitrification is the biological reduction of nitrate (NO_3^-) and nitrite (NO_2^-) ions into gaseous nitrogen (N) in the form of nitric oxide (NO), nitrous oxide (N_2O), and dinitrogen (N_2) gases. In agricultural soils, inorganic N is an essential nutrient taken up by crop roots, whereas gaseous N is largely lost from the root zone via off-gassing.

The main denitrification processes in soils include biological denitrification and chemodenitrification. Biological denitrification is a microbially mediated reduction process that occurs under partially to completely anaerobic soil conditions, whereas chemodenitrification occurs primarily in acidic soils ($pH < 5.0$) that also contain NO_2^- (Nelson 1982; Tiedje 1994). Extensive reviews of soil-based denitrification processes appear in Tiedje (1988), Firestone and Davidson (1989), Conrad (1995), and McKenney and Drury (1997).

It is important to measure denitrification in agricultural and forest soils, as the gases produced (especially NO and N_2O) are potent greenhouse gases that contribute to global warming; and the loss of inorganic N from the root zone reduces both crop productivity and

the efficacy of expensive N fertilizers. Knowledge of soil denitrification is also essential for determining soil N budgets on plot, field, regional, and national scales so that best/beneficial management practices can be developed, which both maximize the efficacy of N amendments including fertilizers and manure and minimize the off-gassing of N-based greenhouse gasses.

This chapter will focus on methods for measuring biological denitrification, because the pH of most agricultural soils exceeds 5.0, thus greatly reducing the importance of chemodenitrification. We will also restrict ourselves to laboratory incubation methods, with the exception of the ^{15}N technique that is applicable to field, greenhouse, and laboratory environments.

The approaches commonly used to measure denitrification losses from a soil system involve using (1) acetylene (C_2H_2) to block the conversion of N_2O to N_2 in a closed system and measuring the accumulation of N_2O over time; (2) ^{15}N-labeled NO_3^- as a tracer in a closed system and determining the accumulation of ^{15}N-labeled N_2O or N_2; or (3) a flow through system in which an inert gas scrubs the intermediate products NO and N_2O before N_2O has time to be converted to N_2. The advantages and limitations of each technique will be discussed. Analytical methods involving N_2O emissions from field sites using chambers will be discussed in Chapter 65. Micrometerological techniques to measure N_2O emissions have been described by Wagner-Riddle et al. (1996, 1997) and for NO emissions by Taylor et al. (1999). Readers should also be aware that field techniques that utilize N_2O concentration gradients at varying depths in the soil profile are also available for measuring N_2O flux from soils (Burton and Beauchamp 1994; Burton et al. 1997).

The most widely used technique to determine denitrification losses from the soil system is the acetylene inhibition technique that was initially developed by Yoshinari et al. (1977). This technique utilizes the ability of acetylene to inhibit the conversion of N_2O to N_2 and it thereby enables the investigator to obtain the potential amount of N_2O evolved from the soil system. The advantages of this technique are that it is relatively easy to use and it is easy to measure increases in N_2O concentrations following the addition of acetylene as the atmospheric concentrations of N_2O are comparatively low (319 ppb in 2005). However, there are many limitations to the use of acetylene, because the inhibition could be reversed when residues containing high sulfide contents such as alfalfa are present (de Catanzaro et al. 1987) or when incubations are carried out for too long (Yeomans and Beauchamp 1978). In addition, when oxygen concentrations greater than 400 $\mu L\ O_2\ L^{-1}$ are present in the soil, NO, C_2H_2, and O_2 can interact and form NO_2, which is an artifact of the method as C_2H_2 is not normally present in soils (Bollmann and Conrad 1997; McKenney et al. 1997). Since this reaction occurs at very low O_2 concentrations, it would be expected to occur in all incubations except those that are under completely anaerobic conditions. Since NO_2 is not routinely measured, this reaction would lead to an underestimation of the total amount of NO_3^- denitrified.

Three methods that use the acetylene inhibition technique will be described. The first of the acetylene inhibition methods involves the determination of the basal denitrification rate of soil (i.e., the denitrification rate of soils incubated anaerobically without any additional amendments). The second is the potential denitrification rate, which is a short-term incubation under anaerobic conditions and the soils are supplied with NO_3^- and an available carbon source. The third method is the soil core technique, which involves a short-term incubation of an undisturbed soil core under aerobic headspace conditions and no added amendments. This technique focuses on the impact of inherent architecture (soil structure and the presence of anaerobic microsites) on the denitrification process.

In the three acetylene inhibition methods, we recommend that at least four gas samples be taken and a linear regression used to determine the denitrification rate. Nonlinear rates occur when new enzymes are produced, such as when carbon and N substrates are supplied (i.e., the denitrification potential method). By restricting the incubation to 5 h in the denitrification potential assay, the problem associated with the synthesis of new enzymes is minimized. Although the basal denitrification rate and the soil core methods do not normally involve additional carbon or NO_3^-, they both utilize short incubation times (6 h) and significant new enzyme synthesis would be unlikely.

Two techniques for measuring denitrification are also described, which do not use acetylene and avoid the inherent problems associated with acetylene. The ^{15}N tracer technique has many advantages including the ability to separate the contribution of applied N from native N to denitrification gas emissions. If the objective of the study is to examine soil processes, mechanisms, and reaction rates, then the ^{15}N tracer technique would be the method of choice; however, this method is more labor- and cost-intensive. The continuous flow method is used when the researcher wishes to quantify both the NO and N_2O emissions from soils. This technique involves a humidified inert gas that is passed through a column of soil and NO and N_2O concentrations in the gas stream are measured. There are however, a limited number of samples that could be evaluated at any instance with the continuous gas flow method.

37.2 PREPARING EVACUATED CONTAINERS FOR COLLECTING EVOLVED GASES

Gas samples are collected and analyzed for either NO, N_2O, or N_2 as described in all of the denitrification methods. With autosamplers connected to gas chromatographs and isotope ratio mass spectrometers, errors associated with the manual injection of a gas sample into the gas chromatograph have been eliminated. These errors are associated with the accuracy in the injection volume, the premature leakage of the septum in the injector of the gas chromatograph when undue force is applied during injection and frequent breakage of injector needles. Since the robotic arm of the sample injector injects the sample with a constant pressure straight into the septum, it is now possible to run several hundred gas samples using the same septum. Further, the slow uniform injection with the autosampler enables injection of thousands of samples into the gas chromatograph without having the needle bend or break.

Because autosamplers require storage of the gas sample before injection, it is important to ensure that the sample container used to collect the gas sample is evacuated efficiently. We have found that sample containers with the black screw-top lids, which hold a rubber septum (such as the Exetainer, Labco Limited, Buckinghamshire, UK), can be evacuated more efficiently and hold a vacuum for a greater period of time compared to other storage containers, such as Vacutainers (Becton Dickinson, Franklin Lakes, NJ).

37.2.1 Analyzers and Materials to Evacuate Exetainers

1. High-vacuum rotary pump.
2. Gas manifold attached to the rotary pump with a diffusion valve (Figure 37.1). Plug valves that are attached to syringes and needles.
3. Digital vacuum gauge (0.01–20 torr).
4. Exetainers, 5.9 mL (Labco, UK).

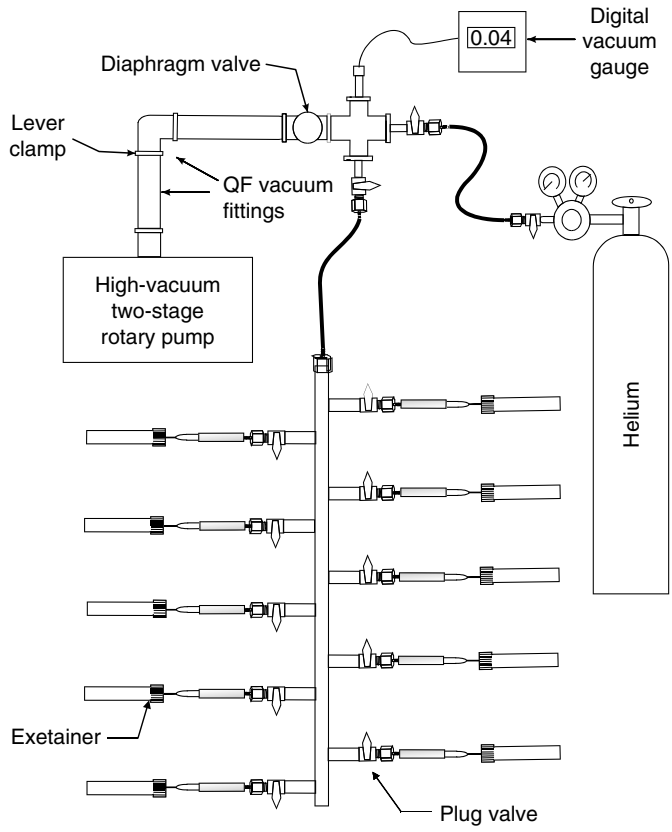

FIGURE 37.1. A schematic diaphragm of the manifold that can be used for both the evacuation of gas sample vials and for the flushing of incubation flasks with an inert gas. Quick flange (QF) fittings are used to connect the pump to the vacuum tubing. The digital vacuum gauge is capable of measuring a vacuum between 0.01 and 20 torr. To evacuate the sample vials, the diaphragm valve is opened and the plug valve attached to the inert gas cylinder is closed, the syringe plug valves are opened and then the vacuum pump is started. To flush the incubation flasks, the diaphragm valve is closed and the plug valves attached to the inert gas cylinder and syringes are opened, and the vacuum pump is stopped.

37.2.2 Procedure

1 Insert a needle that is attached to a vacuum manifold (Figure 37.1) into each Exetainer (5.9 mL).

2 Open the diaphragm valve, ensure that the plug valve attached to the gas cylinder is closed, and the syringe plug valves are open, and then start the high-vacuum rotary pump. It is convenient to evacuate 10 Exetainers at a time.

3 Evacuate the containers to <0.05 torr vacuum for 4 min and then close the plug valve attached to each needle. Remove the Exetainers from each needle immediately.

4 It is advisable to sacrifice one of the Exetainers during each evacuation to ensure that the system is leak free. This is done by inserting a needle into the lid while the Exetainer is immersed upside down in a beaker of water (Rochette and Bertrand 2003). The Exetainer should fill with water and the air bubble that remains in the Exetainer should be at most the size of a pea. This method of evacuation ensures that there would be minimal contamination resulting from the injection of gas samples into the evacuated containers.

5 During the assay, it is recommended that a volume greater than 5.9 mL be injected into each Exetainer so that the pressure inside each container exceeds atmospheric pressure. This restricts any external gas from leaking into the Exetainer. Standards should also be collected and stored in the Exetainers using the same method as for collecting the samples. It should also be noted that when gas chromatographs are fitted with valves that contain vented sample loops (i.e., 0.25 mL), the sample and standard gas pressure is equilibrated to ~101 kPa within the sample loop after injection and prior to switching the valve to direct the sample through the columns.

37.2.3 Comments

1 When Exetainers are evacuated using the procedure described above, they maintained 96% of the total vacuum after 35 days and 89% after 136 days (Rochette and Bertrand 2003). Most of the leakage from the Exetainers occurs within seconds of removing the needle from the Exetainer. This leakage could be further reduced by adding a second Teflon septum to the Exetainer (Rochette and Bertrand 2003). With the two septa, 98% of the vacuum was present after 136 days of storage. In some laboratories, silicone sealant (Silicone I or II) is used in place of the second septum to reduce gas leakage from the Exetainers. The only caution is that the silicone may clog the injector of the gas chromatograph unless a dead-volume filter-frit is used.

2 There are other gas containers besides the Exetainer that could be used to collect and store samples for gas analysis. These containers should be used with care to ensure that trace quantities of N_2O are purged prior to collecting the gas sample. Alternatively, gas-tight syringes could be used for the collection and storage of gas samples; however, these would have to be manually injected into the gas chromatograph instead of using an autosampler.

3 When repetitive gas samples are taken from a flask with a comparatively low volume such that $\geq$5% of the headspace volume is removed, then this volume of gas is not able to absorb additional molecules of N_2O being produced during the denitrification process. For this reason, a correction factor is required to account for the sequential gas sampling (see Section 37.5.2).

37.3 CREATING AN ANAEROBIC ENVIRONMENT

The basal denitrification method and the potential denitrification method require the displacement of the atmosphere in the soil pores and incubation container with an inert gas such as helium or argon. The manifold described previously may be used to accomplish this task (Figure 37.1).

37.3.1 Procedure

1 Close the diaphragm valve attached to the vacuum pump and open the plug valve attached to the inert gas cylinder.

2 Place the flask containing moist soil and fitted with a Suba Seal (William Freeman Limited, Barnsley, England) into a rigid container to ensure that the flask is not tipped over when the air is displaced with an inert gas. Insert two needles into the Suba Seal and attach one needle to a manifold connected to an inert gas cylinder (helium or argon); the second needle is attached to a vacuum tube, which is inserted into a 400 mL beaker of water. The beaker should also be held in the rigid container to ensure that it is not tipped over during the flushing process.

3 Slowly turn on the regulator of the inert gas cylinder until a steady stream of bubbles is released through the water and flush the flasks for 15 min. After 15 min, close the regulator on the gas cylinder, remove the needle attached to the manifold, and when there are no more bubbles being emitted, remove the second needle from the Suba Seal. This ensures that the flasks will be equilibrated to atmospheric pressure (101 kPa). Oxygen analysis of the headspace gas could also be used to verify that the soils are incubated under anaerobic conditions.

37.4 PREPARATION OF SOIL SAMPLES FOR DENITRIFICATION ASSAYS

With the exception of the soil core methods, soil samples are collected from the field or laboratory, mixed, and weighed at the start of the soil incubation. There are however several sample preparation aspects that must be considered in collecting and preparing the soil sample. In several studies, it has been shown that N_2O emissions have been enhanced when aggregated soils have been crushed (Seech and Beauchamp 1988; Drury et al. 2004). This is primarily due to the increased exposure of protected carbon to the denitrifier population. Therefore, minimal amount of aggregate disruption is recommended unless it is the expressed purpose of the study to focus on particular aggregate size fractions or the protection of carbon within the aggregates. When soil samples contain stones or large pieces of undecomposed plant material, these could be removed using sieving techniques (4 mm sieve). The removal of stones and undecomposed plant residue would ensure consistency when comparing results both within and between studies.

Fresh soil samples are always preferable to those that have been stored. If soil storage is required, then the soils should be stored moist at 4°C. When soil storage at cold temperatures is required, then it would be preferable to preincubate the soils for a minimum of 24 h at the same temperature that will be used during the assay to enable the microbes in the soils to acclimate to the higher incubation temperature.

37.5 BASAL DENITRIFICATION RATE (DRURY ET AL. 1991; BEAUCHAMP AND BERGSTROM 1993)

Basal denitrification rate provides an estimate of the indigenous denitrifier activity that is controlled by both the available carbon and nitrate content of the soil. When soils are prepared for this assay, they are traditionally broken up and sieved. This mixing and sieving

can result in a more homogeneous sample; however, any aggregates present in the soil would be disrupted.

37.5.1 Analyzers and Materials

1 Gas chromatograph fitted with an electron capture detector. It would be preferable to have an autosampler attached to the gas chromatograph.

2 Exetainers (5.9 mL) may be used to store the gas samples if an autosampler is used.

3 A manifold for evacuating sample containers (Exetainers) would be required (see Section 37.2 and Figure 37.1).

4 Acetylene passed through a concentrated sulfuric acid solution and then a distilled-water wash will remove organic impurities such as acetone that may serve as a carbon substrate for denitrifiers (Hyman and Arp 1987). When there is a color change in the sulfuric acid, it should be replaced. Alternatively, acetone-free acetylene could be produced from calcium carbide, which would eliminate the requirement for further purification (Hyman and Arp 1987).

5 Inert gas source (helium or argon) connected to a manifold (Figure 37.1).

6 Erlenmeyer flasks (250 mL) with rubber septum stoppers (Suba Seal, William Freeman, Limited, Barnsley, UK). Silicone should be applied to the outside of the serum stoppers to reduce leakage when taking gas samples.

37.5.2 Procedure

1 Sieve field-moist soil through a 4 mm sieve to remove stones and undecomposed plant residue.

2 Add a sufficient weight of field-moist soil into a 250 mL Erlenmeyer flask to obtain an oven-dry soil weight of 20 g. Add distilled water (if necessary) to bring the soil up to its field-capacity water content (soil water potential of -33 kPa) on a gravimetric basis (i.e., mass of water per unit mass of dry soil). Insert a Suba Seal into the top of each flask. Note that the gravimetric water content of the field-moist soil and the soil at field capacity must be determined beforehand in order to determine how much field-moist soil to add to the flask, and how much water to add to obtain the field-capacity water content.

3 Flush the headspace in each flask with an inert gas such as helium or argon as described previously. Using a syringe, remove a mass of gas from each flask by collecting a gas sample equivalent to 10% of the headspace volume, then use another syringe to replace the sampled volume with acetone-free acetylene.

Because the flask is sealed (closed system), sample removal by syringe will cause a pressure drop that must be taken into account in order to collect the desired headspace volume from the flask. This pressure change is due to the increased volume which occurs when the syringe is inserted into the flask and the headspace gas is extracted (i.e. just before the needle is withdrawn from the flask).

Using the ideal gas law and constant temperature, the sample volume that must be collected by the syringe is given by

$$V_S = \frac{C}{(100 - C)} V_F; \quad C < 100 \tag{37.1}$$

where V_S (mL) is the required syringe sample volume, C (%) is the desired percentage of flask headspace volume to be collected, and V_F (mL) is the headspace volume of the flask. Hence, if the flask has a headspace volume $V_F = 240.5$ mL, and the desired removal is $C = 10\%$, then the required syringe sample volume is $V_S = [10/(100 - 10)] \times 240.5$ mL $= 26.72$ mL.

As mentioned above, once the sample is removed, sufficient acetylene is injected back into the flask to return the flask to its original pressure. Since the flask is a closed system, the volume of acetylene injected, V_a, is given by

$$V_a = \frac{C}{100} V_F \tag{37.2}$$

Hence, if $C = 10\%$ and $V_F = 240.5$ mL, then $V_a = 24.05$ mL.

4 Incubate the soil at 20°C for 24 h. After 1, 2, 4, and 6 h, remove a 9 mL gas sample from each flask and store it in a 5.9 mL Exetainer.

5 Analyze the gas samples and standards on a gas chromatograph equipped with an electron capture detector. The gas samples and standards are initially injected with an autosampler into a vented 0.25 mL sampling loop connected to a 10 port valve so that the sample injected into the gas chromatograph will be at a 101 kPa pressure (i.e., atmospheric pressure). Gas samples in the loop will be initially injected into a precolumn and the N_2O will then enter the main column. The precolumn will then be backflushed to vent so as to remove water vapor that may be present in the gas sample. Nitrous oxide will be separated in the main column using a 5.0 m long Porapak Q chromatography column with Ar (95%) and CH_4 (5%) carrier-gas flowing at a rate of 30 mL min^{-1} at 70°C. Nitrous oxide concentrations will then be determined using an electron capture detector at 350°C.

6 Calculate the headspace volume in the incubation flask. The headspace of the Erlenmeyer flask must be determined to know how much helium or argon to remove and how much acetylene to add to obtain a 10% volume of acetylene. In addition, the volume of headspace is required when calculating the N_2O flux from the soil. The headspace volume (V_h) is the total volume of the incubation flask (V_{total}) minus the volumes of soil (V_{soil}) and water (V_{water}) in the flask, i.e.,

$$V_h = V_{total} - (V_{soil} + V_{water}) \tag{37.3}$$

V_{total} can be determined by subtracting the weight of the empty Erlenmeyer flask and Suba Seal from the weight when the flask is completely filled with distilled water and the Suba Seal inserted. A needle inserted in the Suba Seal helps remove the trapped air when the Suba Seal is placed in the water-filled Erlenmeyer flask. Standard 250 mL Erlenmeyer flasks have a total volume of 254 mL when the Suba

Seal is inserted (i.e., the volume of headspace above the 250 mL line marked on the flask is included in the calculation).

V_{soil} is based on the average particle density of mineral agricultural soils (2.65 g cm^{-3}). Hence, if 25 g of field-moist soil contains 20 g of oven-dry soil (all water removed), then the soil would occupy 7.55 mL.

V_{water} is based on the amount of water in the soil during the incubation; i.e., if the soil was adjusted to 30% gravimetric water content for the incubation, then there would be (0.3) × (20 g dry soil) = 6.00 mL of water present assuming a water density of 1 g mL^{-1}. Hence,

$$V_h = 254 \text{ mL} - (7.55 \text{ mL} + 6.00 \text{ mL}) = 240.45 \text{ mL}$$

7 Calculate the volume of N_2O evolved over the 24 h incubation period (Equation 37.4). The N_2O volume must be adjusted to account for dissolved N_2O in soil solution via the Bunsen absorption coefficient ($\alpha = 0.632$ mL N_2O mL^{-1} water at 20°C; Tiedje 1982). A correction factor is also required to account for the sequential removal of gas samples from the flask (Equation 37.5 and Equation 37.6). The N_2O concentration evolved from the soil at time t is calculated using the ideal gas law ($PV = nRT$) and the mass of 1 mole of N_2O gas (28.0134 g N_2O-N mol^{-1}) as described in Equation 37.7. The volume of evolved N_2O gas is consequently calculated using

$$V_{N_2O_t} = \frac{C_t[V_h + (V_{water}\,\alpha)]}{CF_n} \times \frac{1\text{L}}{1000 \text{ mL}} \tag{37.4}$$

where $V_{N_2O_t}$ (μL) is the volume of N_2O emitted from the soil at time t, C_t (μL N_2O L^{-1}) is the N_2O gas concentration in the gas phase at time t, V_h (mL) is the volume of the headspace, V_{water} (mL) is the volume of water in the soil during the incubation, and α (mL N_2O mL^{-1} water) is the Bunsen absorption coefficient. The CF_n value is a dimensionless correction factor that accounts for the fact that the removed sample volumes of headspace gas are not available to absorb the subsequent production of N_2O molecules, thus making the measured N_2O concentrations (C_t) greater than if no sample removal had occurred. The correction factor has the form (Drury and Reynolds, unpublished data)

$$CF_n = \left[\sum_{i=1}^{n-1}\left(\frac{V_h + V_s}{V_h}\right)^i\left(\frac{t_{i+1} - t_i}{t_n}\right)\right] + \frac{t_1}{t_n}; \quad n = 2, 3, 4, \ldots. \tag{37.5}$$

where CF_n (dimensionless) is the correction factor for sample n, V_h (mL) is the headspace volume in the incubation flask, V_s (mL) is the syringe sample volume, t_i (h) are the cumulative sampling times since start of incubation where $t_0 = 0$, t_1 (h) is the cumulative time corresponding to sample 1, and t_n (h) is the cumulative time corresponding to sample n. Assumptions built into Equation 37.5 include constant V_h and V_s, and a constant rate of gas production. Note also that the correction factor does not apply to the first sample ($n = 1$), as all of the original headspace volume is still present when the first sample is collected. Hence,

$$CF_1 = 1 \tag{37.6}$$

for sample 1 collected at t_1.

The concentration of N_2O nitrogen is then calculated using the ideal gas law:

$$N_2O\text{-}N_t = \frac{V_{N_2O_t} \times P \times \left(28.0134 \text{ g } N_2O\text{-N mol}^{-1}\right)}{R \times T \times M_s} \quad (37.7)$$

where $N_2O\text{-}N_t$ (μg N_2O-N g^{-1}) is the concentration of N_2O-N at time t, $V_{N_2O_t}$ (μL) is the volume of N_2O in the flask (Equation 37.4), P is the pressure in kPa, R is the universal gas constant (8.31451 L kPa mol^{-1} K^{-1}), T is temperature in K, and M_s is the oven-dry mass of soil (g).

Hence, for an incubation system where

headspace volume, $V_h = 240.5$ mL
sample (syringe) volume, $V_s = 9.0$ mL
water volume in soil, $V_{water} = 6.0$ mL
standard atmospheric pressure, $P = 101.325$ kPa
incubation temperature, $T = 293.15$ K (20°C)
mass oven-dry soil, $M_s = 20.0$ g

then, for a measured N_2O gas concentration of $C_t = 25$ μL N_2O L^{-1} collected at $t_1 = 1$ h ($n = 1$, $CF_1 = 1$), Equation 37.7 produces $N_2O\text{-}N_{(t=1\text{ h})} = 0.3556$ μg N_2O-N g^{-1}. Similarly, a measured N_2O gas concentration of $C_t = 104$ μL N_2O L^{-1} collected at $t_3 = 4$ h ($n = 3$, $CF_3 = 1.04748$, Equation 37.7) produces $N_2O\text{-}N_{(t=4\text{ h})} = 1.4123$ μg N_2O-N g^{-1}.

8 At the end of the incubation add 100 mL 2 *M* KCl to the soil, shake for 1 h, and filter the extract to determine the amount of NO_3^- remaining in the soil. See Chapter 6 for additional details concerning NO_3^- extraction and analysis. When NO_3^- is limiting, the amount of N_2O evolved will be reduced.

37.5.3 Comments

1 Basal denitrification rates are measured as the soils are not amended with either NO_3^- or carbon. Denitrification rates may be low if either NO_3^- or available carbon are limiting. Further, slow diffusion of the carbon and NO_3^- to the denitrifier sites may also reduce the amount of N_2O evolved with this basal denitrification method. If the desire is to measure denitrification under non-limiting conditions (i.e., without carbon or NO_3^- limitation or a diffusional limitation) then the potential denitrification method (Section 37.6) could be used.

2 Although this method provides an estimate of the denitrification rate based on the indigenous soil chemical and biological properties, the physical disruption of the soil resulting from the sampling, sieving, and mixing procedures homogenizes the soil samples and alters the soil structure. The replacement of the soil atmosphere with an inert gas to create anaerobic conditions and the addition of water to bring the soils to field capacity enable the investigator to compare differences in soils and treatments under anaerobic conditions. However, these

sample preparation steps do not enable the investigator to estimate *in situ* denitrification rates.

3 Samples containing high amounts of sulfide (e.g. soils with high alfalfa residues) should be evaluated using a different technique as acetylene inhibition of N_2O reduction to N_2 is reversed in the presence of high sulfide (deCatanzaro et al. 1987). Also, highly reducing conditions or high concentrations of fermentable carbon compounds cause NO_3^- to be converted to NH_4^+ through dissimilatory nitrate reduction (deCatanzaro et al. 1987).

4 The use of acetylene at 10% of the headspace volume also inhibits nitrification. Hence, the NO_3^- substrate production would be affected, and as a result, it is preferable to limit the incubation time.

5 There is a possibility that either NO_3^- or carbon substrate becomes limiting for the denitrifiers during the 6 h incubation. Nitrate limitation could be confirmed by extracting the soil and measuring the amount of available NO_3^- at the end of the incubation. Further, if an examination of the data over the 6 h period reveals a curvilinear pattern, then either the incubation time could be reduced or the data could be fitted using a curvilinear equation (Pell et al. 1996).

6 The inert gases, helium and argon are recommended for replacement of the soil atmosphere as they do not inhibit the denitrification process.

37.6 DENITRIFICATION POTENTIAL (SMITH AND TIEDJE 1979; MARTIN ET AL. 1988; LUO ET AL. 1996; PELL ET AL. 1996)

Denitrification potential or potential denitrification activity provides an estimate of the amount of NO_3^- that can be denitrified when carbon and NO_3^- are not limiting and the soil atmosphere is anaerobic (i.e., O_2 is not inhibiting the process). This measurement is intended to provide an estimate of the indigenous denitrifier population and associated enzyme activity. However, when NO_3^- (a terminal electron acceptor) and an available carbon source (energy) are added to soils, the microbial population may be induced to produce additional enzymes, which would create an artifact with this assay. Therefore, methods should be employed to ensure that additional enzyme production is negligible. One such technique involves the addition of chloramphenicol to the soil to inhibit the synthesis of new enzymes. However, there is some evidence in the literature suggesting that chloramphenicol may also inhibit the existing enzymes and thereby result in an underestimation of the denitrification potential (Pell et al. 1996). Therefore, we do not recommend that chloramphenicol be used in this assay. Instead, since the production of new enzymes takes time, this problem can be avoided by reducing the incubation time to, at most, 5 h. This should then allow the investigator to measure the potential denitrification under ''ideal'' conditions.

37.6.1 Analyzers and Materials

1 Gas chromatograph fitted with an electron capture detector. It would be preferable to have an autosampler attached to the gas chromatograph.

2 Exetainers (5.9 mL) could be used to store the gas samples if an autosampler is used.

3 A manifold for evacuating sampling containers (Exetainers) would be required (see above and Figure 37.1).

4 Acetylene purified by passing through concentrated sulfuric acid and then a distilled water wash to remove organic impurities that may serve as a carbon substrate for denitrifiers (Hyman and Arp 1987). When there is a color change in the sulfuric acid, it should be replaced. Alternatively, acetone-free acetylene could be produced from calcium carbide, which would eliminate the requirement for further purification (Hyman and Arp 1987).

5 Inert gas source (helium or argon) connected to a manifold (Figure 37.1).

6 Erlenmeyer flasks (250 mL) fitted with a rubber septum (Suba Seal, Barnsley, England). Silicone should be applied to the outside of the septum to reduce leakage when taking gas samples.

37.6.2 Procedure

1 Sieve field-moist soil through a 4 mm sieve to remove stones and undecomposed plant residue.

2 Weigh 25 g field-moist soil (to obtain an oven-dry mass of about 20 g) into a 250 mL Erlenmeyer flask. Add 25 mL of a solution that will provide 300 μg glucose-C g^{-1} soil and 50 μg NO_3^--N g^{-1} soil. Nitrate concentrations ≥100 μg NO_3^--N g^{-1} soil have been found to inhibit denitrification activity (Luo et al. 1996).

3 Flush the atmosphere in each flask with an inert gas such as helium as described previously. Remove a headspace gas sample from each flask equivalent to 10% of the headspace volume (see Section 37.5.2 for equations and an example calculation). Add acetone-free acetylene to the flask equivalent to 10% of the headspace volume.

4 Shake the soil slurries on a rotary shaker at 225 rev min^{-1} (Pell et al. 1996). The incubation temperature should be adjusted to 20°C. Gas samples (9 mL) could be taken with a syringe after 1, 2, 3, and 5 h and these samples could be injected and stored in evacuated Exetainers (5.9 mL).

5 Analyze the gas samples and standards on a gas chromatograph equipped with an electron capture detector. The analysis of the gas samples and setup of the gas chromatograph are described in Section 37.5.2.

6 Calculate the amount of N_2O at each time interval (see Section 37.5.2 for calculation methods). The factor that differs between this method and the method in Section 37.5 is the total volume of solution in the flask (i.e., the amount of water in the soil as well as the 25 mL solution added). This additional volume of water affects both the calculation of headspace volume (Equation 37.3) as well as the amount of dissolved N_2O in the solution using the Bunsen absorption coefficient (Equation 37.4).

37.6.3 Comments

1. Pell et al. (1996) observed that the potential denitrification assay is a continuous process involving both existing and newly synthesized enzymes without a discrete linear growth phase and nonlinear growth phase. They found that the product formation equation provided a good fit to their data and enabled them to determine both the activity of the existing enzymes as well as the growth rate of the organisms.

2. Soils should be analyzed within 5 days of sampling as potential denitrification activity has been found to decrease if soils are stored for longer time periods (Luo et al. 1996).

3. There is some disagreement in the literature concerning whether the flasks are shaken or not. The advantage of shaking the flasks is that this will ensure that diffusion of the substrates is not a limiting factor when measuring the potential denitrification rate.

37.7 DENITRIFICATION USING UNDISTURBED SOIL CORES

The availability of NO_3^- and carbon substrate to the resident denitrifier population and the degree of oxygen diffusion to the site impact the extent of denitrification losses from a soil. Hence, the architecture of the soil including the extent of aggregation, compaction, and physical processes that influence gas and water movement and the presence of anaerobic microsites impact the amount of NO_3^- lost through denitrification. For these reasons, intact soil cores can be used to evaluate the impact of the soil architecture on the denitrification process. There are however some limitations with the collection and use of these samples in a denitrification assay. Firstly, when sampling, it is critical that the soil core is collected without compacting the soil. Even if compaction is minimized, there is likely some disturbance of the soil close to the soil sample surface, especially the soil touching the core wall. Secondly, gaseous diffusion of acetylene into the core or denitrification gases out of the core may be restricted when the core is incubated in a closed system. This assay is designed to evaluate the impact of the soil environment on the amount of NO_3^- lost to denitrification. Soil texture, structure, and their ability to support a denitrifier population that produces denitrifier enzymes affect the extent of denitrification losses measured by this assay.

37.7.1 Analyzers and Materials

1. Gas chromatograph fitted with an electron capture detector. It would be preferable to have an autosampler attached to the gas chromatograph.

2. If an autosampler is used, Exetainers (5.9 mL) could be used to store the gas samples.

3. A manifold for evacuating sampling containers (Exetainers) would be required (see above and Figure 37.1).

4. Acetylene passed through a concentrated sulfuric acid solution and then a distilled water wash to remove organic impurities such as acetone that may serve as

carbon substrate for denitrifiers (Hyman and Arp 1987). When there is a color change in the sulfuric acid, it should be replaced. Alternatively, acetone-free acetylene could be produced from calcium carbide, which would eliminate the requirement for further purification (Hyman and Arp 1987).

5 Aluminum cylinders (5 cm diameter and 5 cm length) with an outside beveled cutting edge.

6 Sealed jars (e.g., 500 mL wide-mouth mason jars) with lids fitted with Suba Seal serum stoppers. The serum stoppers should be coated with silicone to reduce gas leakage into or out of the jar.

37.7.2 Procedure

1 Collect soil cores in the field using either a hydraulic probe or by hand using a mallet and board to carefully and evenly tap the core into the soil (beveled cutting edge down). Caution must be exercised to ensure that the soil is not appreciably compacted when taking the sample. A grab sample should also be collected to determine the gravimetric soil moisture content. When the soil surface is rough, the core could be inserted just below the soil surface (~1 cm). If the core is taken manually, then this could be accomplished by placing a second core on top of the core that is inserted into the soil and gently tapping the top of the second core. This would place the pressure on the cylinder wall and minimize the pressure exerted on the soil surface.

2 Place a cap on either end of the core to prevent any soil from falling out of the core and then place the core in a plastic bag to reduce water loss and return the core to the laboratory. It is preferable to start the incubation as soon as the core is brought to the laboratory. If this is not possible, store the core at 4°C to reduce microbial activity. Weigh the cylinder containing the soil and place it in the mason jar. Close the lid of the jar. Remove 10% of the headspace gas and add acetone-free acetylene to achieve a 10% concentration of acetylene in the jar (see Section 37.5.2 for calculating the headspace volume and Equation 37.1 and Equation 37.2 to determine the volume of headspace to remove and the volume of acetylene to add to the incubation jar).

3 Incubate the soils at 20°C for 6 h. Remove at least four headspace gas samples over a 6 h period (9 mL each) using a gastight syringe (i.e., at 1, 2, 4, and 6 h). This allows enough time for the acetylene to diffuse into the cores while ensuring that NO_3^- does not become limiting. Calculate the N_2O-N_t concentration at each time interval using the equations described in Section 37.5.2. Determine the rate of N_2O production by using linear regression of N_2O concentration versus sampling time.

37.7.3 Comments

1 The headspace of the jar must be determined to know how much air to remove and acid-scrubbed acetylene to add to the jar to obtain a 10% volume of acetylene in the jar. In addition, the volume of headspace (V_h) is required when calculating the N_2O flux from the soil. Equation 37.3 could be used to calculate

the headspace volume. The one additional factor that would have to be taken into consideration is the volume of the aluminum cylinder. With the soil core technique, the V_{total} could be determined by weighing a mason jar containing the empty aluminum cylinder (before the soil core is collected) with the lid and Suba Seal and then reweighing the jar containing the aluminum cylinder once it is filled with water and with the lid and Suba Seal attached. The mass of water would be the difference between these two measurements and the total volume could then be calculated based on the mass and density of water (i.e., V_{total} = mass of water/water density).

2 The diffusion of the acetylene into the intact soil cores can be improved by removing intact cores from cylinders or by using perforated cylinders. If the cylinder is removed or perforated (e.g. by drilling holes), then both C_2H_2 and the oxygen in the headspace would have increased access to the interior of the soil core. In this case, it may be preferable to flush the flask with an inert gas such as helium before C_2H_2 is added to avoid oxygen inhibition of denitrification. When acetylene is added to the jar, pumping the headspace gas containing the acetylene with a large syringe can also increase the amount or rapidity with which acetylene enters the soil pores.

3 High spatial and temporal variability of denitrification rates in field soils require a careful consideration and sampling strategy. The influence of sample size on denitrification has been discussed by Parkin et al. (1987). It should be noted that denitrification rates frequently show a lognormal distribution and statistical methods would have to be adjusted accordingly.

4 A gas flow method has also been used to determine the denitrification rate from intact soil cores (Parkin et al. 1984). In this method, acetylene is added to the recirculating gas stream, which flows through the soil core at 300 mL min^{-1}. The primary advantages of this method are that the measurements are rapid and the analytical variability is low (Parkin et al. 1984). The potential disadvantage with this method is that the aeration status of the microsites may differ from the microsites in cores that are incubated under static conditions (Parkin et al. 1984).

37.8 ^{15}N TRACER TECHNIQUES (HAUCK ET AL. 1958; MULVANEY AND VANDEN HEUVEL 1988; ARAH 1992)

The theory for measuring denitrification by measuring the isotopic composition of N_2 produced from a soil that had been labeled with $^{15}NO_3^-$ was developed almost 50 years ago (Hauck et al. 1958), but it was not applied for nearly 25 years, primarily because advances in isotope ratio mass spectrometry were required. This method was initially called ''isotope distribution'' (Hauck et al. 1958; Hauck and Bouldin 1961), because it is based on distinguishing the binomial distribution of N_2 molecular species formed during the reduction of ^{15}N-labeled NO_3^- from the background binomial distribution of the N_2 molecular species of the atmosphere. This approach has also been termed the ''Hauck technique'' (Mosier and Schimel 1993; Mosier and Klemedtsson 1994) and ''nonequilibrium technique'' (Bergsma et al. 2001).

Through the years, the equations developed by Hauck et al. (1958) have been modified and refined for modern equipment (Siegel et al. 1982; Mulvaney 1984; Arah 1992; Bergsma et al. 1999).

An alternative calculation approach, known as ''isotope pairing,'' was developed by Nielsen (1992) for measuring denitrification in sediments (Steingruber et al. 2001). All calculation approaches yield the same result (Hart and Myrold 1996). The procedure described here will use the terminology and equations presented by Arah (1992), which seem to be used most widely.

It should be noted that variations of the isotope distribution method have been used for measuring N_2O flux (Mulvaney and Kurtz 1982; Mulvaney and Boast 1986; Stevens et al. 1993) and partitioning the contributions of nitrification and denitrification to N_2O flux (Arah 1997; Stevens et al. 1997; Bergsma et al. 2001). Some groups have also equilibrated the N_2 molecular species prior to isotope ratio mass spectrometry using a variety of off- and online methods (Craswell et al. 1985; Kjeldby et al. 1987; Well et al. 1993), which may provide increased sensitivity with some instruments (Well et al. 1998).

A procedure for measuring denitrification in the field using the isotope distribution approach is given below. It can be easily modified for laboratory measurements of soils incubated in gastight containers as described in Section 37.8.3.

37.8.1 Analyzers and Materials

1 Gas collection chambers. Various sizes and materials are used, but a chamber of 15–30 cm diameter made of polyvinyl chloride pipe that is sealed with a polyvinyl chloride cap fitted with a rubber septum is common. The total volume of the chamber is usually kept small to maximize sensitivity.

2 Syringes and needles to remove gas samples.

3 Evacuated vials such as Exetainers (5.9 mL or 12 mL) to store gas samples. Often these vials are matched to the autosampler system of the isotope ratio mass spectrometer used for analysis.

4 Solution of a ^{15}N-labeled NO_3^- salt, typically 99 atom% ^{15}N to allow enrichment of the soil NO_3^- pool to about 50 atom% ^{15}N.

5 Isotope ratio mass spectrometer (or access to a service laboratory with the capacity to measure gas samples).

37.8.2 Procedure

1 Soil microplots are established at a size consistent with the gas collection chamber that will be used. The gas collection chamber can be pressed into the surface to a depth of a few centimeters of soil, or a permanent base that is implanted to a deeper depth can be used. The gas collection chamber is then attached to this base when measurements are being made.

2 The microplot is labeled with NO_3^- enriched to 50 atom% ^{15}N or greater. Because of the high enrichment, only a small amount of label must be added, perhaps double or triple the native NO_3^- pool size. It is important, however, to add this label as evenly as possible. Thus the NO_3^- is usually dissolved in water and injected according to a grid pattern.

TABLE 37.1 Example Calculations for Denitrification Using the Principle of Isotope Distribution[a]

	Ion current		Molecular fraction		Atom fraction ^{15}N
Time (h)	r''	r'''	^{29}x	^{30}x	^{15}a
0	0.007353	0.00001352	0.007299	0.00001342 (x_a)	0.003663 (a_a)
24	0.007420	0.00002927	0.007365	0.00002905 (x_m)	0.003712 (a_m)

Source: From Arah, J.R.M., *Soil Sci. Soc. Am. J.*, 56, 795–800. 1992.

[a] Definitions:
$r'' = {}^{29}N_2{}^+/{}^{28}N_2{}^+$
$r''' = {}^{30}N_2{}^+/{}^{28}N_2{}^+$
$^{29}x = r''/(1 + r'' + r''')$
$^{30}x = r'''/(1 + r'' + r''')$
$^{15}a = [^{29}x + (2)(^{30}x)]/2$
d = fraction of N_2 from denitrification
a_p = atom fraction of $^{15}NO_3{}^-$ pool

Calculations:
$d = (a_m - a_a)^2/(x_m + a_a{}^2 - 2a_a a_m) = 0.0001545$
$a_p = a_a + (x_m + a_a{}^2 - 2a_a a_m)/(a_m - a_a) = 0.3182$

3 The gas collection chamber is set over the labeled soil and gas samples are taken periodically during the incubation period, which might be a few hours. Samples taken from a chamber over a nonlabeled plot also are taken to determine the background labeling of N_2 in the atmosphere. Gas samples are most conveniently stored in evacuated tubes such as Exetainers for later mass spectroscopic analysis. A longer incubation time can be used to increase sensitivity; however, care must be taken that an extended emplacement of the gas collection chamber does not disturb the system by decreasing aeration, increasing temperatures, or affecting plant processes.

4 An isotope ratio mass spectrometer is used to measure $^{29}N_2/^{28}N_2$ and $^{30}N_2/^{28}N_2$ ratios. These data are then used in rather complex calculations (Table 37.1) that give both the atom% ^{15}N of the $NO_3{}^-$ pool that underwent denitrification (a_p) and the fraction of the headspace gas that came from denitrification (d). The denitrification flux is calculated by multiplying the fraction from denitrification by the total amount of N_2 gas in the chamber and dividing by the soil surface area and time. This flux is a function of both production (the denitrification rate) and transport; thus, further calculations are needed to calculate the denitrification rate (Hutchinson and Mosier 1981). Note that only d, and not a_p, is required to calculate the denitrification rate.

37.8.3 Comments

1 The ^{15}N gas emission method suffers from similar gas diffusion problems as the acetylene block methods. Consequently, it is not surprising that the two methods have agreed quite well when comparisons have been made (Myrold 1990; Malone et al. 1998). In theory, it can be shown that denitrification may be under- or overestimated if the $NO_3{}^-$ pool is not uniformly labeled; however, empirical evidence has not shown this to be a major problem.

2 Measurements of denitrification when soils are at or near saturation can be biased by entrapped gas bubbles and lead to an underestimation of denitrification rates and fluxes (Lindau et al. 1988; Well and Myrold 1999).

3 Nonuniform distribution of $^{15}NO_3^-$ has been shown from theoretical and empirical studies to result in an overestimation of the ^{15}N enrichment of the soil NO_3^- pool and an underestimation of the true denitrification rate (Mulvaney and Vanden Heuvel 1988; Vanden Heuvel et al. 1988; Arah 1992; Bersgma et al. 1999).

4 The detection limits for measuring denitrification by isotope distribution are a function of mass spectrometer sensitivity, incubation volume, and incubation time; but in general, rates as low as 2.5–16 g N ha^{-1} day^{-1} can be measured (Siegel et al. 1982; Mosier and Klemedtsson 1994; Russow et al. 1996; Well et al. 1998; Stevens and Laughlin 2001). Although lengthening the incubation time can increase sensitivity, this must be balanced against potential disturbances associated with having the gas collection chamber in place too long, such as decreased aeration, increasing temperature, or altered plant processes.

5 This procedure can be adapted to laboratory measurements by using the approaches presented in Section 37.5 for sieved soils and Section 37.7 for intact cores. The primary difference is that the soils are labeled with a solution of a ^{15}N-labeled NO_3^- salt and acetylene is not added. Gas samples are taken as described above and the fraction of the gas coming from denitrification is calculated as shown in Table 37.1. The denitrification flux is calculated by multiplying the fraction from denitrification by the total amount of N_2 gas in the chamber and dividing by the soil dry weight and time.

37.9 CONTINUOUS FLOW METHODS (MCKENNEY ET AL. 1996)

A gas-flow system is used with a constant flow of humidified inert gas (N_2 or He) sparging NO and N_2O from anaerobic soil columns. The main advantage with this technique is that it allows for measurement of both NO and N_2O flux from soil. In addition, C_2H_2 is not required in this assay as the high flow rate minimizes the conversion of N_2O to N_2. The disadvantage with this technique is that only a limited number of soils can be evaluated in one run.

37.9.1 Analyzers and Materials

1 Analyzers: chemiluminescent NO analyzer, gas chromatograph with an electron capture detector

2 Controlled temperature bath

3 Vacuum manifold with needle valves attached to a humidified distilled water column (Figure 37.2) and a column containing the sample (e.g. soil and any amendments under investigation)

4 Mass flow controlled for measuring gas flow rates from each sample column

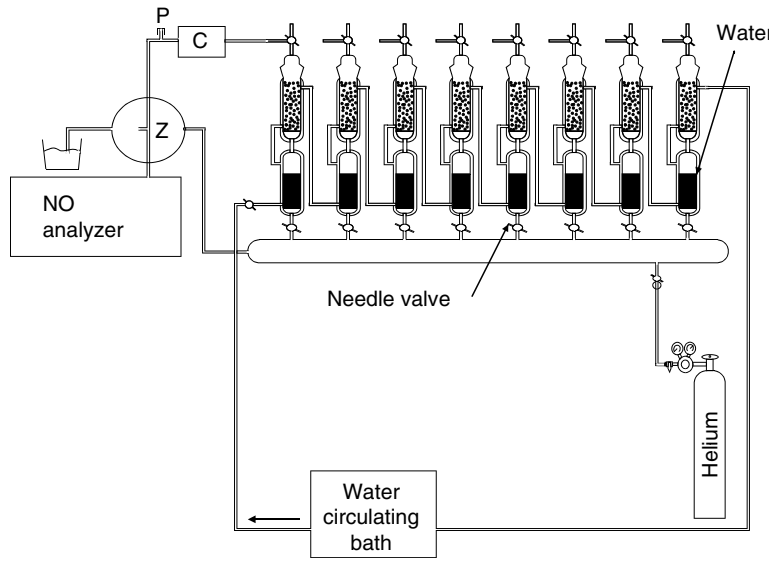

FIGURE 37.2. A schematic diagram of a continuous flow system for measuring NO and N_2O flux from soil (modified from McKenney et al. 1996). Each soil column (stippled area) is preceded by a water column to control humidity. The outer chambers of the humidifier and soil columns are filled with water and connected to a controlled temperature water circulating bath. Gas flows from an inert gas cylinder through the needle valves to the water column and then through the soil column. After the soil column, a subsample of the gas flows through a flow controller into a zero volume flask (Z) and a subsample is analyzed for NO. A port (P) is inserted between the flow controller and the zero volume flask to allow manual collection of gas samples for N_2O analysis.

37.9.2 Procedure

1 Connect an inert gas cylinder to a manifold with a separate needle valve for each sample column (Figure 37.2).

2 Adjust the flow rate of the inert gas to 370 mL min^{-1} using a mass flow controller. The inert gas is initially passed through a humidifier column of distilled deionized water (Pyrex tubes 2.5 cm i.d. and 25 cm length) and then into a second Pyrex column (2.5 cm i.d. and 35 cm length) that contains 100 g (dry weight basis) soil sample in which the desired amount of water is added. In some studies, the soils are maintained at field capacity (−33 kPa). Both the humidifier column and the soil column have an outer jacket in which water is circulated at a constant temperature using a constant temperature bath. This ensures that the soils and sparging gas are also kept at constant temperature during the incubation.

3 The gas evolved from the soil is analyzed for NO based on the chemiluminescent reaction of NO with O_3 using a $NO/NO_2/NO_x$ analyzer. This will be accomplished by flowing the gas stream from the soil columns through a ''zero gas'' (N_2) constant pressure flask directly into the instrument.

4 The N_2O gas samples are collected at various time periods over a 48 h period (e.g., 0.25, 1, 2, 4, 8, 24, 32, and 48 h) using preevacuated (<0.05 torr) 5.9 mL Exetainers. Standards from a calibrated reference gas cylinder are collected in Exetainers in a similar manner to the samples, and both samples and standards are injected (2.5 mL) into a gas chromatograph fitted with an automatic sampling system.

5 The gas samples and standards are analyzed using a gas chromatograph attached to an autosampler. (See Section 37.5.2 for information concerning the operating parameters of the gas chromatograph.)

6 The net production rates of NO and N_2O were calculated using the equations:

$$q_{NO} = \frac{[NO] \times Q}{M_S} \tag{37.8}$$

$$q_{N_2O} = \frac{[N_2O] \times Q}{M_S} \tag{37.9}$$

where q_{NO} and q_{N_2O} are the fluxes of NO and N_2O, [NO] and [N_2O] are the concentrations of NO and N_2O in the effluent gas, Q is the measured total flow rate of the effluent gas through the column, and M_s is the mass of dry soil. The total amount of evolved NO and N_2O (i.e., total mass of NO or N_2O produced during the incubation per unit mass of dry soil) can then be calculated by integrating the area under the individual flux curves.

37.9.3 Comments

1 Nitric oxide standards must be stored in a gas cylinder that uses a stainless steel regulator to prevent corrosion.

2 Note that Paul et al. (1994) studied NO production under static lab conditions. However, NO is so reactive that the measurements may have been compromised.

3 The temperature can also be adjusted by incubating the soils in a temperature-controlled room.

REFERENCES

Arah, J.R.M. 1992. New formulae for mass spectrometric analysis of nitrous oxide and dinitrogen emissions. *Soil Sci. Soc. Am. J.* 56: 795–800.

Arah, J.R.M. 1997. Apportioning nitrous oxide fluxes between nitrification and denitrification using gas-phase mass spectrometry. *Soil Biol. Biochem.* 29: 1295–1299.

Beauchamp, E.G. and Bergstrom, D.W. 1993. Denitrification. In M.R. Carter, Ed. *Soil Sampling and Methods of Analysis*. Lewis Publishers, Boca Raton, FL, pp. 351–357.

Bergsma, T.T., Bergsma, Q.C., Ostrom, N.E., and Robertson, G.P. 1999. A heuristic model for calculation of dinitrogen and nitrous oxide flux from nitrogen-15-labeled soil. *Soil Sci. Soc. Am. J.* 63: 1709–1716.

Bergsma, T.T., Ostrom, N.E., Emmons M., and Robertson, G.P. 2001. Measuring simultaneous

fluxes from soil of N_2O and N_2 in the field using the ^{15}N-gas ''nonequilibrium'' technique. *Environ. Sci. Technol.* 35: 4307–4312.

Bollmann, A. and Conrad, R. 1997. Acetylene blockage technique leads to underestimation of denitrification rates in oxic soils due to scavenging of intermediate nitric oxide. *Soil Biol. Biochem.* 29: 1067–1077.

Burton, D.L. and Beauchamp, E.G. 1994. Profile nitrous oxide and carbon dioxide concentrations in a soil subject to freezing. *Soil Sci. Soc. Am. J.* 58: 115–122.

Burton, D.L., Bergstrom, D.W., Covert, J.A., Wagner-Riddle, C., and Beauchamp, E.G. 1997. Three methods to estimate N_2O fluxes as impacted by agricultural management. *Can. J. Soil Sci.* 77: 125–134.

Conrad, R. 1995. Soil microbial processes involved in production and consumption of atmospheric trace gases. *Adv. Microb. Ecol.* 14: 207–250.

Craswell, E.T., Byrnes, B.H., Holt, L.S., Austin, E.R., Fillery, I.R.P., and Strong, W.M. 1985. Nitrogen-15 determination of nonrandomly distributed dinitrogen in air. *Soil Sci. Soc. Am. J.* 49: 664–668.

deCatanzaro, J.B., Beauchamp, E.G., and Drury, C.F. 1987. Denitrification vs. dissimilatory nitrate reduction in soil with alfalfa, straw, glucose and sulfide treatments. *Soil Biol. Biochem.* 19: 583–587.

Drury, C.F., McKenney, D.J., and Findlay, W.I. 1991. Relationships between denitrification, microbial biomass and indigenous soil properties. *Soil Biol. Biochem.* 23: 751–755.

Drury, C.F., Yang, X.M., Reynolds, W.D., and Tan, C.S. 2004. Influence of crop rotation and aggregate size on carbon dioxide and nitrous oxide emissions. *Soil Till. Res.* 79: 87–100.

Firestone, M.K. and Davidson, E.A. 1989. Microbial basis of NO and N_2O production and consumption in soil. In M.O. Andrea and D.S. Schimel, Eds. *Exchanger of Trace Gases between Terrestrial Ecosystems and the Atmosphere*. John Wiley & Sons, New York, NY, pp. 7–21.

Hart, S.C. and Myrold, D.D. 1996. ^{15}N tracer studies of soil nitrogen transformations. In T.W. Boutton and S.I. Yamasaki, Eds. *Mass Spectrometry of Soils*. Marcel Dekker, Inc., New York, NY, pp. 225–245.

Hauck, R.D. and Bouldin, D.R. 1961. Distribution of isotopic nitrogen in nitrogen gas during denitrification. *Nature* (London) 191: 871–872.

Hauck, R.D., Melsted, S.W., and Yankwich, P.E. 1958. Use of N-isotope distribution in nitrogen gas in the study of denitrification. *Soil Sci.* 86: 287–291.

Hutchinson, G.L. and Mosier, A.R. 1981. Improved soil cover method for field measurement of nitrous oxide flux. *Soil Sci. Soc. Am. J.* 45: 311–316.

Hyman, M.R. and Arp, D.J. 1987. Quantification and removal of some contaminating gases from acetylene used to study gas-utilizing enzymes and microorganisms. *Appl. Environ. Microbiol.* 53: 298–303.

Kjeldby M., Erikson A.B., and Holtan-Hartwig, L. 1987. Direct measurement of dinitrogen evolution from soil using nitrogen-15 emission spectrometry. *Soil Sci. Soc. Am. J.* 51: 1180–1183.

Lindau, C.W., Patrick, W.H., de Laune, R.D., Reddy, K.R., and Bollich, P.K. 1988. Entrapment of $^{15}N_2$ during soil denitrification. *Soil Sci. Soc. Am. J.* 52: 538–540.

Luo, J., White, R.E., Ball, P.R., and Tillman, R.W. 1996. Measuring denitrification activity in soils under pasture: optimizing conditions for the short-term denitrification enzyme assay and effects of soil storage on denitrification activity. *Soil Biol. Biochem.* 28: 409–417.

Malone, J.P., Stevens, R.J., and Laughlin, R.J. 1998. Combining the ^{15}N and acetylene inhibition techniques to examine the effect of acetylene on denitrification. *Soil Biol. Biochem.* 30: 31–37.

Martin, K., Parsons, L.L., Murray, R.E., and Smith, M.S. 1988. Dynamics of soil denitrifier populations: relationships between enzyme activity, most probable numbers counts, and actual N gas loss. *Appl. Environ. Microbiol.* 54: 2711–2716.

McKenney, D.J. and Drury, C.F. 1997. Nitric oxide production in agricultural soils. *Glob. Change Biol.* 3: 317–326.

McKenney, D.J., Drury, C.F., and Wang, S.W. 1996. Effect of acetylene on nitric oxide production

in soil under denitrifying conditions. *Soil Sci. Soc. Am. J.* 60: 811–820.

McKenney, D.J., Drury, C.F., and Wang, S.W. 1997. Reaction of NO with C_2H_2 and O_2: implications for denitrification assays. *Soil Sci. Soc. Am. J.* 61: 1370–1375.

Mosier, A.R. and Klemedtsson, L. 1994. Measuring denitrification in the field. In R.W. Weaver, J.S. Angle, and P.J. Bottomley, Eds. *Methods of Soil Analysis, Part 2—Microbiological and Biochemical Properties*. Soil Science Society of America, Madison, WI, pp. 1047–1066.

Mosier, A.R. and Schimel, D.S. 1993. Nitrification and denitrification. In R. Knowles and T.H. Blackburn, Eds. *Nitrogen Isotope Techniques*. Academic Press, San Diego, CA, pp. 181–208.

Mulvaney, R.L. 1984. Determination of ^{15}N-labeled dinitrogen and nitrous oxide with triple collector mass spectrometers. *Soil Sci. Soc. Am. J.* 48: 690–692.

Mulvaney, R.L. and Boast, C.W. 1986. Equations for determination of nitrogen-15 labeled dinitrogen and nitrous oxide by mass spectrometry. *Soil Sci. Soc. Am. J.* 50: 360–363.

Mulvaney, R.L. and Kurtz, L.T. 1982. A new method for determination of ^{15}N-labeled nitrous oxide. *Soil Sci. Soc. Am. J.* 46: 1178–1184.

Mulvaney, R.L. and Vanden Heuvel, R.M. 1988. Evaluation of nitrogen-15 tracer techniques for direct measurement of denitrification in soil: IV. Field studies. *Soil Sci. Soc. Am. J.* 52: 1332–1337.

Myrold, D.D. 1990. Measuring denitrification in soils using ^{15}N techniques. In N.P. Revsbech and J. Sørensen, Eds. *Denitrification in Soils and Sediments*. Plenum Press, New York, NY, pp. 181–198.

Nelson, D.W. 1982. Gaseous losses of nitrogen other than through denitrification. In F.J. Stevenson, Ed. *Nitrogen in Agricultural Soils*. American Society of Agronomy, Madison, WI, pp. 327–363.

Nielsen, L.P. 1992. Denitrification in sediment determined from nitrogen isotope pairing. *FEMS Microbiol. Ecol.* 86: 357–362.

Parkin, T.B., Kaspar, H.F., and Sexstone, A.J. 1984. A gas-flow soil core method to measure field denitrification rates. *Soil Biol. Biochem.* 16: 323–330.

Parkin, T.B., Starr, J.L., and Meisinger, J.J. 1987. Influence of sample size measurements on soil denitrification. *Soil Sci. Soc. Am. J.* 51: 1492–1501.

Paul, J.W., Beauchamp, E.G., and Zhang, X. 1994. Nitrous and nitric oxide emissions during nitrification and denitrification from manure-amended soil in the laboratory. *Can. J. Soil Sci.* 73: 529–553.

Pell, M., Stenberg, B., Stennström, J., and Torstensson, L. 1996. Potential denitrification activity assay in soil—with or without chloramphenicol. *Soil Biol. Biochem.* 28: 393–398.

Rochette, P. and Bertrand, N. 2003. Soil air sample storage and handling using polypropylene syringes and glass vials. *Can. J. Soil Sci.* 83: 631–637.

Russow, R., Stevens, R.J., and Laughlin, R.J. 1996. Accuracy and precision for measurement of the mass ratio 30/28 in dinitrogen from air samples and its application to the investigation of N losses from soil by denitrification. *Isotopes Environ. Health Stud.* 32: 289–297.

Seech, A.G. and Beauchamp, E.G. 1988. Denitrification in soil aggregates of different sizes. *Soil Sci. Soc. Am. J.* 52: 1616–1621.

Siegel, R.S., Hauck, R.D., and Kurtz, L.T. 1982. Determination of $^{30}N_2$ and application to measurement of N_2 evolution during denitrification. *Soil Sci. Soc. Am. J.* 46: 68–74.

Smith, M.S. and Tiedje, J.M. 1979. Phases of denitrification following oxygen depletion in soil. *Soil Biol. Biochem.* 11: 261–267.

Steingruber, S.M., Friedrich, J., Gächter, R., and Wehrli, B. 2001. Measurement of denitrification in sediments with the ^{15}N isotope pairing technique. *Appl. Environ. Microbiol.* 67: 3771–3778.

Stevens, R.J. and Laughlin, R.J. 2001. Lowering the detection limit for dinitrogen using the enrichment of nitrous oxide. *Soil Biol. Biochem.* 33: 1287–1289.

Stevens, R.J., Laughlin, R.J., Atkins, G.J., and Prosser, S.J. 1993. Automated determination of nitrogen-15-labeled dinitrogen and nitrous oxide

by mass spectrometry. *Soil Sci. Soc. Am. J.* 57: 981–988.

Stevens, R.J., Laughlin, R.J., Burns, L.C., and Arah, J.R.M. 1997. Measuring the contributions of nitrification and denitrification to the flux of nitrous oxide from soil. *Soil Biol. Biochem.* 29: 139–151.

Taylor, N.M., Wagner-Riddle, C., Thurtell, G.W., and Beauchamp, E.G. 1999. Nitric oxide fluxes from an agricultural soil using a flux-gradient method. *J. Geophys. Res.* 104: 12213–12220.

Tiedje, J.M. 1982. Denitrification. In A.L. Page et al., Eds. *Methods of Soil Analysis*, *Part 2*. American Society of Agronomy, Madison, WI, pp. 1011–1026.

Tiedje, J.M. 1988. Ecology of denitrification and dissimilatory nitrate reduction to ammonium. In A.J.B. Zehnder, Ed. *Biology of Anaerobic Microorganisms*. John Wiley & Sons, New York, NY, pp. 179–244.

Tiedje, J.M. 1994. Denitrifiers. In R.W. Weaver, J.S. Angle, and P.S. Bottomley, Eds. *Methods of Soil Analysis, Part 2—Microbiological and Biochemical Properties*. Soil Science Society of America, Madison, WI, pp. 245–267.

Vanden Heuvel, R.M., Mulvaney, R.L., and Hoeft, R.G. 1988. Evaluation of nitrogen-15 tracer techniques for direct measurement of denitrification in soil: II. Simulation studies. *Soil Sci. Soc. Am. J.* 52: 1322–1326.

Wagner-Riddle, C., Thurtell, G.W., Kidd, G.E., Beauchamp, E.G., and Sweetman, R. 1997. Estimates of nitrous oxide emissions from agricultural fields over 28 months. *Can. J. Soil Sci.* 77: 135–144.

Wagner-Riddle, C., Thurtell, G.W., King, K.M., Kidd, G.E., and Beauchamp, E.G. 1996. Nitrous oxide and carbon dioxide fluxes from a bare soil using a micrometeorological approach. *J. Environ. Qual.* 25: 898–907.

Well, R., Becker, K.-W., Langel, R., Meyer, B., and Reineking, A. 1998. Continuous flow equilibration for mass spectrometric analysis of dinitrogen emissions. *Soil Sci. Soc. Am. J.* 62: 906–910.

Well, R., Becker, K.-W., and Meyer, B. 1993. Equilibrating of ^{15}N gases by electrodeless discharge: a method of indirect mass spectrometric analysis of $^{30}N_2$ for denitrification studies in soils. *Isotopenpraxis* 29: 175–180.

Well, R. and Myrold, D.D. 1999. Laboratory evaluation of a new method for *in situ* measurement of denitrification in water-saturated soils. *Soil Biol. Biochem.* 31: 1109–1119.

Yeomans, J.C. and Beauchamp, E.G. 1978. Limited inhibition of nitrous oxide reduction in soil in the presence of acetylene. *Soil Biol. Biochem.* 10: 517–519.

Yoshinari, T., Hynes, R., and Knowles, R. 1977. Acetylene inhibition of nitrous oxide reduction and measurement of denitrification and nitrogen fixation in soil. *Soil Biol. Biochem.* 9: 177–183.

Chapter 38
Nitrification Techniques for Soils

C.F. Drury
Agriculture and Agri-Food Canada
Harrow, Ontario, Canada

S.C. Hart
Northern Arizona University
Flagstaff, Arizona, United States

X.M. Yang
Agriculture and Agri-Food Canada
Harrow, Ontario, Canada

38.1 INTRODUCTION

Nitrification is the aerobic conversion of ammonium (NH_4^+) into nitrite (NO_2^-) and nitrate (NO_3^-) by nitrifying bacteria. There are several chemoautotrophic bacteria such as *Nitrosomonas*, *Nitrosospira*, *Nitrosococcus*, and *Nitrosovibrio* involved in the first step of the process whereby ammonium is oxidized to nitrite (Schmidt 1982; Paul and Clark 1996). In soil systems, *Nitrobacter* and *Nitrosospira*-like bacteria are involved in the second step whereby nitrite is converted to nitrate (Schmidt 1982; Bartosch et al. 2002). The ammonia-oxidizing bacteria and the nitrite-oxidizing bacteria are usually found together, and as a result, nitrite rarely accumulates in soil (Paul and Clark 1996).

There are several reasons why it is important to know the nitrification rate in soils. The conversion of NH_4^+ to NO_3^- increases the mobility of nitrogen (N) in soil (because of the dominance of negatively charged surfaces on soil colloids), potentially increasing N availability to plants, but also potentially increasing N loss via leaching. Furthermore, the formation of NO_3^- from NH_4^+ via nitrification also increases the potential for gaseous loss of N from the soil via the process of denitrification (see Chapter 37). The nitrification process has a net acidifying effect on the soil and the resulting drop in soil pH may alter the availabilities of other plant nutrients (Paul and Clark 1996). In addition, standard methods to measure nitrification are required when various nitrification inhibitors or fertilizer formulations (e.g., polymer coated N fertilizer, super granules, etc.) are evaluated.

Considerable information is available in the literature concerning the key variables (temperature, moisture, pH, NH_4^+, and oxygen) that affect the nitrification process in soils

(Schmidt 1982; Paul and Clark 1996; Stark and Firestone 1996). Three laboratory techniques and one field assay for estimating the nitrification rate are described in this chapter. In addition, the advantages and disadvantages of each method and key factors that should be considered in conducting these assays are discussed. Guidelines for the collection, preparation, and storage of the soils and their subsequent extraction are also provided.

The three laboratory incubation techniques include measurements of net nitrification rate (the net change in the soil NO_3^- pool size after NH_4^+ is added to soil and the soil incubated under constant temperature and moisture conditions), potential nitrification rate (nitrification of an NH_4^+ and phosphate amended soil in which diffusional constraints are reduced and aeration optimized by using a soil slurry with flasks shaken on an orbital shaker), and gross nitrification rate (measurement of the actual rate of NO_3^- production using $^{15}NO_3^-$ pool dilution). Gross nitrification is the method of choice when high rates of immobilization or denitrification are anticipated, or when a more ''realized'' rather than ''potential'' measurement is desired. Nitrification assays that only measure the net change in the NO_3^- pool size (i.e., net nitrification assays) may underestimate the actual nitrification rate as some of the NO_3^- formed may be immobilized by soil microbes or consumed by other processes during the incubation (e.g., denitrification and dissimilatory NO_3^- reduction to ammonium; deCatanzaro et al. 1987; Stark and Hart 1997; Silver et al. 2001).

The *in situ* technique involves collecting soil cores from field sites, destructively sampling one of the cores to determine the initial NO_3^- concentrations and replacing the remaining cores (or soils in polyethylene bags) in the field and measuring the NO_3^- accumulated after a specified time period. This technique enables nitrification to occur under field conditions, which include diurnal temperature fluctuations (see the description of Section 38.6 for additional discussion concerning various ways of handling moisture fluctuations with soil cores). Ammonium is the substrate for autotrophic (and some heterotrophic) nitrification reactions (Paul and Clark 1996), and it is typically added to soils through fertilizer addition (urea, NH_4^+, or anhydrous ammonia), manure addition, atmospheric deposition, or from the mineralization of plant or soil organic N. Once NH_4^+ is present, it could then be (1) immobilized by the soil microbes, especially if an available carbon (C) source is present, such as fresh plant residues (Schimel 1986; Compton and Boone 2002); (2) assimilated by plants; (3) volatilized if the soil is alkaline (Vega-Jarquin et al. 2003); (4) fixed by clay minerals (Drury et al. 1989; Kowalenko and Yu 1996); or (5) nitrified to NO_2^- and then to NO_3^- (Drury and Beauchamp 1991). Hence, decreases in NH_4^+ concentration over time cannot be solely attributed to nitrification because of the occurrence of other competing chemical or microbial processes in the soil. Instead, incubating soil and measuring the net increase in pool sizes of NO_2^- and NO_3^- would be a more useful indicator of the nitrification rate in soil.

The N mineralization and nitrification rate of soils could be used by producers or foresters to predict the amount of available N to crops or trees. For managed systems, this information could be used to adjust N application rates and timing and thereby match plant demand and minimize environmental impacts. Although most plants can readily absorb and utilize both NH_4^+ and NO_3^-, NO_3^- is more readily transported to roots. Nitrate is, however, susceptible to leaching losses, especially in humid regions, and to denitrification losses when the soil is under anaerobic conditions and when a C source is available to the denitrifiers (Parkin and Meisinger 1989; Bergstrom et al. 1994; Drury et al. 1996). In addition to regulating the N inputs to soil, nitrification can also be regulated with nitrification inhibitors such as nitrapyrin or dicyandiamide, or by applying smaller amounts of urea- or NH_4^+-based fertilizers several times during the growing season.

38.2 SOIL PREPARATION, ANALYSIS, AND STORAGE

Soils used in these assays should be collected and stored (at 4°C) as intact cores if possible, and processed within 4 days of sampling. Ross and Hales (2003) have recently found in some ''sensitive'' forest soils that even relatively minor disturbances, such as the equivalent of footsteps in the field, can induce significant increases in extractable NO_3^-. Storing soils for periods longer than 4 days results in increased NO_3^- levels (T.O. Oloya, C.F. Drury, and K. Reid, unpublished data). Further, freezing and thawing soil samples or drying soil samples have also been found to increase soil NH_4^+ levels, which could affect nitrification rate estimates. These storage considerations apply to both the preparation of soils for use in these assays as well as the analysis of the soil samples after they are incubated.

One of the potential pitfalls with filtration of soil extracts is the possibility of NH_4^+ and NO_3^- contamination in the filter papers (Sparrow and Masiak 1987). Not only has there been a wide variation in NH_4^+ and NO_3^- contamination between different grades (qualitative vs. quantitative) and types of filter papers (cellulose vs. glass fiber), but a wide variation in contamination has also been reported between lots and within packages (Sparrow and Masiak 1987). To reduce this error, a prewashing with 2 *M* potassium chloride (KCl) or deionized water has been recommended followed by a small amount of the soil extract before collecting the extract for analysis (Kowalenko and Yu 1996).

When soils are extracted for NH_4^+ and NO_3^- concentration, moist samples are weighed into flasks and 2 *M* KCl solution added, followed by shaking for 1 h on an orbital or reciprocating shaker, and then filtering or centrifuging the extract. The extracts are then analyzed on an autoanalyzer for NH_4^+ using the Berthelot reaction and for NO_3^- using the cadmium reduction method (Tel and Heseltine 1990). Cadmium reduces NO_3^- to NO_2^-, and NO_2^- is colorimetrically analyzed in this method. Hence, the cadmium reduction method provides estimates of the sum of NO_2^- and NO_3^-; however, most soils have very little NO_2^- present. If the investigator wishes to determine the concentration of NO_2^- alone, then the cadmium column could be removed from the manifold and the extract reanalyzed. The difference between the analysis with the cadmium column ($NO_2^- + NO_3^-$) and without the column (NO_2^-) would then provide the NO_3^- concentration of the soil extract.

38.3 NET NITRIFICATION RATE (DRURY AND BEAUCHAMP 1991; HART ET AL. 1997)

In this method, net nitrification rate is determined from the net amount of NO_3^- produced in soils incubated at field capacity and at 20°C (or field-relevant temperatures) over a 28-day period. This assay is applied differently for fertilized soils (i.e., agricultural soils) or non-fertilized soils (many forest soils or soils from unimproved pastures). Agricultural soils typically receive N fertilizer when nonleguminous crops are grown (e.g., maize [*Zea mays* L.] and cereal crops). In humid regions where overwinter NO_3^- losses through leaching or denitrification are prevalent (Drury et al. 1993; Drury et al. 1996), N is applied in spring or as a side-dress application in early summer. To manage and model this applied N, it is important to know how quickly NH_4^+ is nitrified to NO_2^- and NO_3^-. In contrast, N is not routinely applied to forested soils and the nitrification rate is controlled by the ambient NH_4^+ concentration for autotrophic nitrifiers and by the organic N and NH_4^+ concentrations for heterotrophic nitrifiers. Therefore, exogenous NH_4^+ additions would be included in this assay for fertilized agricultural soils, but NH_4^+ additions may not be used if unfertilized forest or unfertilized agricultural soils are evaluated.

This net nitrification assay will typically provide lower estimates of nitrification than the potential nitrification assay (Section 38.4). In the potential nitrification assay, the high speed of the orbital shaker ensures that the soil is always well aerated and diffusional constraints are minimized by the constant mixing of the soil slurry. Whereas in the net nitrification assay, the presence of anaerobic microsites especially in fine-textured soil may reduce the nitrification rate similar to what happens under field conditions. Some diffusional constraints may be overcome by incubating the soil at field capacity (−33 kPa), but certainly not to the same extent as would occur with the shaken soil-slurry method (potential nitrification rate). Additionally, some microbial immobilization of NO_3^- may also occur with the net nitrification assay because of the presence of diffusional constraints (Chen and Stark 2000). The net nitrification assay does, however, provide a laboratory-based estimate (constant temperature and moisture using disturbed soils) of nitrification that may be representative of the rate occurring under comparable temperature and moisture conditions in the field. The alternative is to use an *in situ* core method (Section 38.6). However, the core method is much more labor-intensive, thus reducing the number of replicate analyses that can be made with a given effort.

The nitrification process involves both autotrophic and heterotrophic microbes. Autotrophic nitrification has been found to be inhibited by acetylene, chlorate, and nitrapyrin (Bundy and Bremner 1973; Hynes and Knowles 1980; Hart et al. 1997). However, heterotrophic nitrification is not affected by these chemicals. Hence, nitrification assays conducted in the presence of inhibitors such as acetylene can provide an estimate of heterotrophic nitrification. The difference between nitrification assays without and with acetylene would therefore provide an estimate of autotrophic nitrification.

This laboratory assay also allows for the measurement of evolved carbon dioxide (CO_2) if the flasks are fitted with rubber septa to allow for periodic gas sampling (see Chapter 37 for a description of gas collection in Exetainers [Labco Limited, Buckinghamshire, UK] and the subsequent analysis on a gas chromatograph). This information is used to estimate the microbial respiration rate that can be used to gauge the potential for immobilization of N. The ratio of evolved CO_2 to net mineralization rate can be used to estimate the NH_4^+ availability to nitrifiers (Schimel 1986). Soluble C is never added to the soils in these assays as the addition of C substrates to soils often enhances NH_4^+ and NO_3^- immobilization, resulting in lower rates of net nitrification (Kaye et al. 2002).

38.3.1 Materials and Reagents

1 250 mL Erlenmeyer flasks or centrifuge tubes

2 Parafilm to cover the Erlenmeyer flasks

3 A filtration system with funnels and prerinsed Whatman No. 40 filter papers

4 An incubator set to 20°C (or to the temperature that corresponds to field conditions. For agricultural soils, the temperature may correspond to soil temperatures which are observed when fertilizer is applied to soil).

5 An orbital shaker that can hold 250 mL Erlenmeyer flasks or centrifuge tubes

6 An autoanalyzer that can be used to colorimetrically determine NH_4^+ and NO_3^- in 2 *M* KCl extracts

38.3.2 Procedure

1 Sieve the soil through a 4 mm sieve to remove stones and large plant residues.

2 Mix the sieved soil and then determine the gravimetric water content by weighing a subsample of field-moist soil into a weighed aluminum container, drying the container in an oven set at 105°C for 48 h and reweighing the soil sample and container. The gravimetric water content is calculated as follows:

$$\text{Gravimetric water content } (\%) = 100 \times (M_{swc} - M_{sc})/(M_{sc} - M_c) \qquad (38.1)$$

where M_{swc} is the mass of the moist soil and container, M_{sc} is the mass of the dry soil and container, and M_c is the mass of the empty container.

3 Weigh seven subsamples (20 g moist soil each) of soil for each treatment and replicate into 250 mL Erlenmeyer flasks.

4 Determine the initial NH_4^+ and NO_3^- concentrations for the first subsample from each soil treatment by adding 100 mL of 2 *M* KCl to the soil; shake the flask for 1 h on a rotary shaker and filter the soil through a prewashed Whatman No. 40 filter paper or by centrifuging the extract using a refrigerated centrifuge. Analyze the extract for NH_4^+ using the Berthelot reaction, and for NO_3^- using the cadmium reduction method (Tel and Heseltine 1990).

5 For fertilized soils, add a $(NH_4)_2SO_4$ solution to provide 75 mg N kg^{-1} to each of the remaining six subsamples. Adjust the volume of the solution such that the final moisture content of amended soil is brought up to field capacity (−33 kPa). For unfertilized soils (e.g., many forest soils), it would be preferable to not add NH_4^+; however, the soil water content would still have to be brought up to field capacity.

6 Incubate the six subsamples of soil at 20°C (or the field-based temperature, especially for spring applied N) and extract one of the samples at each time period (1, 3, 7, 14, 21, and 28 days) as described previously.

7 The net nitrification rate can be calculated as the increase in NO_3^- concentration over time using linear regression.

38.3.3 Comments

1 In unfertilized soils such as many forest soils, N fertilizer is not applied and the net nitrification rate is based on the net amount of native soil NH_4^+ that is nitrified over the 28-day period, or the net amount of organic N nitrified by heterotrophic nitrifiers. In soils with extremely high N-status (e.g., soils under N-fixing trees like red alder; Hart et al. 1997), the background NH_4^+ (or organic N) level is high enough that NH_4^+ availability does not severely limit autotrophic nitrification during the assay. However, in many unfertilized forest soils, virtually all of the initial NH_4^+ present in the soil is nitrified prior to the end of the 28-day period; under these conditions, the nitrification rate is largely controlled by the soil N mineralization rate (i.e., supply of the substrate). In these situations, it may be preferable to add NH_4^+ in order to ensure that NH_4^+ does not become limiting during the assay or only use data from the linear phase of the incubation.

2 For soils with a high nitrification rate and thus having low NH_4^+ levels at the end of the incubation, it is recommended that the data from the linear phase of the incubation is used to calculate the net nitrification rate or the assay could be repeated using a higher NH_4^+ addition rate.

3 Temperature of the incubation could be adjusted to correspond to the soil temperatures measured in the field. For agricultural soils, this may be the average soil temperature that occurs in the top 15 cm of soil over the 28-day period following fertilizer application. When differences in soil temperature during the day are fairly small, the average daily temperature from field sites may be used in the laboratory incubation (Sierra 2002). If, however, large diurnal fluctuations are observed, then it may be preferable to account for the nonlinear response of nitrification to soil temperature (Sierra 2002).

4 Nitrification inhibitors such as 1% (v/v) acetylene in the incubation flask headspace selectively inhibit autotrophic nitrification. Pennington and Ellis (1993) compared two autotrophic nitrification inhibitors (acetylene (1%) vs. chlorate (745 mg kg^{-1})) and found acetylene to be the more effective inhibitor. If it is desirable to separate autotrophic nitrification from heterotrophic nitrification, then two separate incubations could be conducted. The flasks would have to be fitted with rubber septa, which allow for the addition of acetylene. In one set of flasks, 1% of the headspace would be removed and the equivalent volume of C_2H_2 added. For calculations of the amount of headspace to remove and acetylene to add, the reader is referred to Chapter 37 (Equation 37.1 and Equation 37.2). Nitrification in the presence of acetylene would represent heterotrophic nitrification, whereas autotrophic nitrification would be the difference between the soils incubated without acetylene and those incubated with acetylene.

5 The analytical method should be adapted for the range in NO_3^- concentrations found in the particular soil extracts, as well as account for any differences in the extraction matrix that may affect the colorimetric analyses.

38.4 POTENTIAL NITRIFICATION RATE (BELSER AND MAYS 1980; HART ET AL. 1994b)

The potential nitrification rate is the nitrification rate that occurs under ideal conditions (Belser and Mays 1980) in which ample NH_4^+ is present, the soil is well aerated, and NH_4^+ diffusion is not restricted. In this assay, the nitrification rate is controlled primarily by the size of the nitrifier population and the incubation temperature (20°C). Several laboratory incubation techniques have been used to determine the nitrification potential, including incubations of soil slurry shaken in flasks (Belser and Mays 1980), aerobic incubation of soil in beakers (Robertson and Vitousek 1981), incubations involving periodic leaching of soil in microlysimeters (Robertson 1982), and incubations of soil in perfusion columns (Killham 1987). Of these approaches, the shaken soil-slurry method for nitrification potential determination is generally the most reproducible and the easiest to interpret (Verchot et al. 2001). In this method, soil slurries are shaken for 24 h and subsamples are obtained at various intervals over this time period and analyzed for NO_3^-.

38.4.1 Materials and Reagents

1 250 mL Erlenmeyer flasks.

2 Orbital shaker that holds 250 mL Erlenmeyer flasks.

3 Autoanalyzer system for determining NH_4^+ and NO_3^- concentrations in soil extracts.

4 Filtration racks, funnels, and prerinsed Whatman No. 40 filter papers. Alternatively, a refrigerated centrifuge could be used.

5 A 10 mL automatic pipette with tips that have been cut to increase the size of the opening and thereby prevent clogging when pipetting the soil slurries.

6 Storage vials for the filtered soil extracts.

7 Stock and working solutions:

a. Potassium monobasic phosphate (KH_2PO_4) stock solution, 0.2 *M*. Dissolve 27.22 g of KH_2PO_4 in 1 L of water.

b. Potassium dibasic phosphate (K_2HPO_4) stock solution, 0.2 *M*. Dissolve 34.84 g of K_2HPO_4 in 1 L of water.

c. Ammonium sulfate ($(NH_4)_2SO_4$) stock solution, 50 m*M*. Dissolve 6.607 g $(NH_4)_2SO_4$ in 1 L of water.

d. Combine 1.5 mL KH_2PO_4 stock solution, 3.5 mL K_2HPO_4 stock solution, and 15 mL $(NH_4)_2SO_4$ stock solution in a 1 L volumetric flask and then bring up to volume. Adjust to pH 7.2 by adding dilute H_2SO_4 or NaOH solutions while the combined (working) solution is stirred.

38.4.2 Procedure

1 Pass the soil sample through a 4 mm sieve to remove large plant debris and stones and mix the sieved soil sample.

2 Weigh a 15 g field-moist soil sample into a 250 mL Erlenmeyer flask. Cover with Parafilm that has been pierced several times to enable gas diffusion into and out of the flask.

3 Determine the gravimetric water content of a second subsample of the soil as described previously.

4 Add 100 mL of the working solution containing 1.5 m*M* NH_4^+ and 1 m*M* PO_4^{3-}.

5 Shake the soil slurry at 180 rpm using an orbital shaker. This high speed helps to maintain aerobic conditions. Incubate the soil slurry at 20°C.

6 Remove 10 mL samples at 2, 6, 20, and 24 h using an automatic pipette fitted with the modified pipette tips (i.e., wide bore). Ensure that the flasks are shaken immediately before sampling in order to maintain the same soil:solution ratio as the remaining slurry.

7 Filter the slurry through a prerinsed Whatman No. 40 filter paper. Alternatively, the slurry could be centrifuged and the extract decanted to remove any particles that would interfere with the subsequent colorimetric analysis.

8 Analyze the filtrate on an autoanalyzer for NH_4^+ using the Berthelot reaction and NO_3^- using the cadmium reduction method (Tel and Heseltine 1990).

9 Perform a linear regression on the NO_3^- concentration data over time to determine the slope. The nitrification rate (NR) can then be determined as follows:

$$\text{NR (mg N kg}^{-1}\text{ day}^{-1}) = \frac{\text{slope (mg N L}^{-1}\text{ h}^{-1}) \times (100\text{ mL} + V_w) \times 24\text{ h day}^{-1} \times 1\text{ L } 1000\text{ mL}^{-1} \times 1000\text{ g kg}^{-1}}{M_s} \quad (38.2)$$

where M_s is the dry mass (g) of soil ($M_s = 15$ g)/(1 + (gwc/100%)); gwc is the percent gravimetric water content (see Equation 38.1); and V_w is the volume of water (mL) contained in the 15 g of moist soil ($V_w = M_w/D_w$). The density of water (D_w) at 20°C is 0.9982 g mL^{-1}. $M_w = M_s \times$ (gwc/100%).

38.4.3 Comments

1 It is critical to ensure that a representative subsample containing soil and solution is obtained to maintain the soil:solution ratio of the original slurry. Any settling of the slurry will cause errors in analysis.

2 Shaker speed must be at least 180 rpm to ensure that aerobic conditions are obtained. No significant difference was found when the shaker speed was increased from 180 to 200 rpm. Shaker speeds less than 155 rpm result in anaerobic conditions that lead to NO_3^- losses through denitrification (Stark 1996).

3 It is advisable to analyze the filtered soil samples for NH_4^+ to ensure that NH_4^+ does not become limiting during the soil incubation. Soils with minerals that have a high NH_4^+ fixation capacity or microbial N immobilization may require additional NH_4^+ if low NH_4^+ levels are observed.

4 In soils with high C availability, NO_3^- loss in the slurry via denitrification may occur due to a high rate of heterotrophic activity during the incubation. Increasing shaker speed may alleviate this problem if it occurs.

5 If the soil has a high initial NO_3^- concentration or has very low nitrification rates, addition of sodium chlorate (1.1 g of $NaClO_3$ L^{-1}) can increase the sensitivity of the assay, because NO_2^- rather than NO_3^- becomes the end-product of nitrification (Belser and Mays 1980).

6 The method can be modified to accommodate organic horizons or soils by reducing the mass of material used (by about a factor of 10), and by cutting the

organic material to pieces smaller than 4 mm in size. Furthermore, the pipetted solutions will have to be filtered rather than centrifuged.

7 Soil slurries should be filtered immediately after collection to prevent further nitrification. The extracts should be stored at 4°C and analyzed as soon as possible. If long delays in analysis are anticipated, it is recommended that the extracts are stored frozen. Make sure that the samples are shaken vigorously after they are thawed and before analysis.

8 Although other time intervals besides 2, 6, 20, and 24 h can be used, the best estimation of the slope is by concentrating points at either end of the line (the so-called ''leverage points'').

38.5 GROSS NITRIFICATION RATE (HART ET AL. 1994b, 1997; CHEN AND STARK 2000)

The soil gross, or actual, nitrification rate is the rate of production of NO_3^- in the soil. It is similar to the other methods described above in that it is determined in the absence of plant uptake and leaching losses of NO_3^-. However, it differs from these other methods in that it does not simply assess the net change in the soil NO_3^- pool over time, which is subject to changes from both productive (i.e., nitrification) and consumptive (i.e., microbial immobilization of NO_3^-, denitrification, dissimilatory NO_3^- reduction) processes of NO_3^-. Instead, the principles of isotopic dilution are used to estimate the nitrification rate separately from these consumptive processes of soil NO_3^-. Under conditions when the soil is well mixed and aerated and high NH_4^+ concentrations are maintained (like in the shaken soil-slurry method described above), little NO_3^- consumption is likely to take place, so the net change in the NO_3^- pool over time approximates the gross nitrification rate (Stark and Firestone 1995). However, in all other assays of nitrification, these conditions are not all met and gross rates of nitrification can greatly exceed net rates, even in soils that exhibit small NO_3^- pools (Stark and Hart 1997).

The gross nitrification rate is determined by adding $^{15}NO_3^-$ to the soil, enriching the ambient soil NO_3^- pool in ^{15}N. The NO_3^- pool ''dilutes'' isotopically (i.e., a decrease in the abundance of $^{15}NO_3^-$ relative to the total NO_3^- pool) and changes in size over time as autotrophic nitrifiers convert predominately $^{14}NH_4^+$ to $^{14}NO_3^-$, or as heterotrophic nitrifiers convert predominately organic ^{14}N or $^{14}NH_4^+$ to $^{14}NO_3^-$. However, NO_3^- consumptive processes change the size of the NO_3^- pool but not the isotopic composition significantly. Hence, under the assumptions of constant transformation rates during the incubation period, the absence of recycling of the transformed N, and uniform mixing of the labeled and unlabeled NO_3^- pools, the rate of nitrification and NO_3^- consumption can be calculated analytically (Hart et al. 1994b).

The method described below is for mixed (disturbed) mineral soils and can be applied both in the laboratory and the field. In many soils, soil disturbance can affect gross nitrification rates (Booth et al. 2006). If the measurement of the gross nitrification rate in undisturbed soil samples is desired, see Hart et al. (1994b).

38.5.1 Materials and Reagents

1 A 5 mL syringe and fine-gauge needle

2 A $K^{15}NO_3$ solution (40 mg N L^{-1}) at 99% ^{15}N enrichment

3 Vials appropriate for holding 4 mL of the $K^{15}NO_3$ solution

4 A 2 *M* KCl solution; dissolve 1.49 kg of reagent grade KCl in 10 L of deionized water

5 Polyethylene 120 mL specimen containers with tight fitting lids

6 An orbital or reciprocating shaker for agitating the KCl–soil suspensions

7 Filtration rack, funnels, and Whatman No. 40 filter papers preleached with KCl or deionized water

8 An incubator set to the desired incubation temperature

9 An autoanalyzer that can be used to colorimetrically determine ammonium and nitrate in 2 *M* KCl extracts

10 Other reagents as required for NH_4^+ and NO_3^- analyses of KCl extracts of soil

11 Other materials and reagents required to prepare KCl extracts of soil for ^{15}N-analyses of NO_3^- (see Stark and Hart 1996)

12 An isotope-ratio mass spectrometer (IRMS) for measuring the $^{15}N/^{14}N$ ratios of samples enriched in ^{15}N relative to natural abundance values and of relatively low N mass (typically <100 μg N)

38.5.2 Procedure

1 Collect enough soil from the field at the desired depth to provide >120 g oven-dry equivalent (ODE) of soil per replicate. Pass the field-moist soil sample through a 4 mm sieve to remove large plant debris and stones, and mix the sieved soil sample.

2 Weigh approximately 120 g ODE of sieved, field-moist soil into a 30×30 cm polyethylene bag (e.g., ''freezer storage bag'' that is 4 mil or >100 μm thick). This thickness is necessary to reduce the likelihood that the bag will be punctured during vigorous mixing and addition of the ^{15}N label with the needle (see below). Mix well and remove one 20 g ODE subsample and extract immediately with 2 *M* KCl in a 120 mL specimen cup. This subsample will be used to determine the initial soil NO_3^- (and NH_4^+) pool sizes of the replicate. Filter and store the KCl extract as described previously. Remove a second 20 g ODE subsample and determine the gravimetric water content of the unamended soil as described previously.

3 Mix the soil again and spread out evenly along one side of the bag interior, with the bag on a flat surface.

4 Using a fine-gauge needle and a 5 mL syringe, add 4 mL of a $K^{15}NO_3$ (40 mg N L^{-1}) solution at a 99% ^{15}N enrichment dropwise to the soil. Prior to the start of the assay, it is useful to have all of the 4 mL aliquots of ^{15}N solution already dispensed into separate 5 mL vials. It is best to add about 1 mL of solution

evenly across the soil surface as possible, remix, and again spread out the soil in the bag, repeating the procedure another three times.

5 After the final addition, mix the soil well and remove two 20 g ODE subsamples. One of these subsamples goes into a metal weighing boat for gravimetric water content determination as described above. The second subsample is extracted with 100 mL of 2 *M* KCl in a 120 mL specimen cup, and serves as the time-0 extract for the estimates of the NO_3^- pool size and the ^{15}N enrichment of the NO_3^- pool. Filter and store the KCl extract as described previously, taking care to collect as much of the extract solution as possible.

6 Close the polyethylene bag filled with ambient air (to keep the soil aerobic) and incubate in the dark at laboratory temperature (or some other desired temperature) for 1–2 days. The ideal length of incubation (i.e., where the rate of ^{15}N isotope dilution is maximized) depends on the gross nitrification rate and the NO_3^- pool size: for higher gross nitrification rates and smaller NO_3^- pool sizes use the shorter incubation period; whereas for lower gross nitrification rates and larger NO_3^- pool sizes, use the longer incubation period.

7 After the incubation period, mix the soil and remove a final ODE subsample of ~20 g and extract with 100 mL of 2 *M* KCl in a 120 mL specimen cup. This subsample serves as the time-*t* extract for the estimates of the NO_3^- pool size and the ^{15}N enrichment of the NO_3^- pool. Filter and store the KCl extract as described previously, taking care to collect as much of the extract solution as possible.

8 Calculate the gross nitrification rate (GNR) and the NO_3^- consumption (c_N) with the following equations:

$$\mathrm{GNR} = (([\mathrm{NO_3^-}]_0 - [\mathrm{NO_3^-}]_t)/t) \times (\log(\mathrm{APE}_0/\mathrm{APE}_t)/\log([\mathrm{NO_3^-}]_0/[\mathrm{NO_3^-}]_t)) \tag{38.3}$$

$$c_N = \mathrm{GNR} - (([\mathrm{NO_3^-}]_t - [\mathrm{NO_3^-}]_0)/t) \tag{38.4}$$

where

GNR = gross nitrification rate (mg of N kg^{-1} soil day^{-1}).

c_N = NO_3^- consumption rate (mg of N kg^{-1} soil day^{-1}).

t = time (days).

APE = the atom% ^{15}N enrichment of a N pool enriched with ^{15}N minus the atom% ^{15}N enrichment of that pool prior to ^{15}N addition.

APE_0 = atom% ^{15}N excess of NO_3^- pool at time 0.

APE_t = atom% ^{15}N excess of NO_3^- pool at time *t*.

$[NO_3^-]_0$ = total NO_3^- concentration (mg N kg^{-1}) at time 0; $[NO_3^-]_t$ = total NO_3^- concentration (mg N kg^{-1}) at time *t*.

t = 1–2 days as suggested here.

38.5.3 Comments

1 Background or "natural" ^{15}N abundance (prior to ^{15}N addition) can be assumed to be 0.3663 atom% ^{15}N; for more precise work, this value can be measured in the KCl extracts of soil taken before ^{15}N addition (see above).

2 Equations 38.3 and 38.4 are valid only for cases when n is not equal to c_N. Kirkham and Bartholomew (1954) provide another equation for the condition when $n = c_N$, which is seldom encountered.

3 Atom% ^{15}N enrichment of the NO_3^- pools from the time-0 and time-t KCl extracts is determined on an IRMS. The NH_4^+ in the extract is first removed (by increasing the pH to ≈10) and then the NO_3^- is converted to NH_3 (with the addition of Devarda's alloy) and collected on acidified filter disks in a closed system by the process of gaseous diffusion. The filtered disks are then dried (over concentrated acid), placed in a tin capsule, and then analyzed on an IRMS connected to an elemental analyzer (see Stark and Hart 1996 for details). The total NO_3^- concentrations are determined by colorimetric analysis of the KCl extracts as described above. Extraction volumes are adjusted to include water in the soil for calculating NO_3^- concentrations (e.g., see Equation 38.2). The gravimetric water content of the amended soil can be compared to that of the unamended sample to provide a check on the amount of labeled solution added to the soil.

4 Initial (before ^{15}N addition) soil sample extract can be analyzed for both NH_4^+ and NO_3^- to provide information regarding the size of these pools prior to the gross nitrification measurement. This information may be useful for interpreting the gross nitrification and NO_3^- consumption data. For instance, the NH_4^+ pool size provides some idea of NH_4^+ availability to autotrophic nitrifiers. Furthermore, the amount of increase in the NO_3^- pool size that occurs with the $^{15}NO_3^-$ addition can also be determined by comparing this initial NO_3^- value with the amount of $^{15}NO_3^-$ added (i.e., 2 mg NO_3^--N kg^{-1} oven-dry soil). This information may be useful in interpreting c_N, as NO_3^- consumption depends, in part, on the NO_3^- pool size; relatively small increases in the NO_3^- pool following ^{15}N addition (<50% increase) are not likely to alter c_N substantially (Hart et al. 1994a,b).

5 Time-zero extraction is the appropriate correction for abiotic consumptive processes of the added ^{15}N that occur immediately after addition of the ^{15}N label. However, if some of the added ^{15}N is converted to a nonextractable form at time-0 and then released back into the soil solution during the incubation period, the actual rate of isotopic dilution will be underestimated, resulting in an underestimate of the gross nitrification rate. Conversely, if the added $^{15}NO_3^-$ displaces $^{14}NO_3^-$ present on soil colloids continuously over the entire incubation period rather than instantaneously after ^{15}N addition, gross nitrification rates will be overestimated. Using sterilized soils, Davidson et al. (1991) found that abiotic fixation of added $^{15}NO_3^-$ was completed prior to the time-0 extraction, so the time-0 extraction was the appropriate method for correcting isotope dilution estimates. We have verified that this assumption holds on a wide range of wildland soils (S.C. Hart, E.B. Smith, and J.M. Stark, unpublished data). However, other soil types may behave differently, so we recommend testing the dynamics of

abiotic $^{15}NO_3^-$ consumption in each soil to which the isotope dilution method is to be applied (see Davidson et al. 1991).

6 Incubation time, amount of ^{15}N injected, and the ^{15}N enrichment of the solution can be varied. The advantages and disadvantages of these choices are discussed by Davidson et al. (1991). Addition of 4 mL of ^{15}N solution to an 80 g ODE soil sample causes an increase in soil water content of approximately 0.05 kg kg^{-1}. This wet-up may stimulate microbial activity and increase N transformation rates, especially if the soil is very dry. A smaller volume of a more concentrated ^{15}N solution can be injected reducing the wet-up effect; however, this may result in a less uniform distribution of the label. A simulation model developed by Stark (1991) suggests that this amount of water addition should only significantly alter gross nitrification and NO_3^- consumption rates at soil water potentials less than −0.35 MPa prior to label addition (Hart et al. 1994a). Attempts to use the addition of ^{15}N-labeled gases (e.g., ^{15}NO) to enrich the soil NO_3^- pool in ^{15}N, as has been tried for the soil NH_4^+ pool (Murphy et al. 2003), show some promise (Stark and Firestone 1995). The development of such a method would allow uniform labeling of a soil without any increase in the ambient soil water content; however, we know of no studies that have evaluated this method sufficiently for it to be applied routinely.

7 This method has been applied *in situ*, where all soil labeling and extraction takes place at the field site (see Hart et al. 1994a). The bags containing the labeled soil are buried at the depth chosen for the field study for the duration of the incubation period. Make sure the plastic bags containing the soil sample are completely covered to avoid direct insolation that would result in excessive heating of the soil within the bag, and that they remain aerated by closing the polyethylene bag filled with ambient air. This approach provides gross nitrification rates that have more field relevance than selecting a constant and arbitrary laboratory temperature.

8 Soil may be wetted up to near field capacity prior to label addition if the investigator desires a more maximal rate that is not limited by water availability (Stark and Firestone 1996). However, if a potential rate is desired, we suggest using the shaken soil-slurry method because of its ease and reproducibility compared to this isotope dilution method. Combining a field-based measurement of gross nitrification and the shaken soil-slurry method can be a powerful approach for evaluating the limitations to nitrification under field conditions (see Davidson et al. 1990).

9 It is imperative that the soils remain aerobic during the incubation period because autotrophic nitrification is an aerobic process. Also, under aerobic conditions where denitrification is minimal, c_N will be essentially equivalent to the rate of microbial immobilization of NO_3^-, making the assessment of controls on processes less ambiguous.

10 Heterotrophic nitrification can be separated from total (heterotrophic plus autotrophic) nitrification using a slight modification of the procedure described here (employing autotrophic nitrification inhibitors; see Hart et al. 1997).

11 This method can be modified for organic soils and horizons by chopping the material into small pieces (<1 cm in length) and reducing the mass of ODE used

per subsample by a factor of about 10 (i.e., add 4 mL of solution to 10 g ODE of organic matter, etc.; Hart et al. 1994b).

12 Gross nitrification method requires the use of relatively expensive ^{15}N-labeled salts. Furthermore, isotope preparation and analysis can be time consuming as well as costly, and the investigator must have access to an IRMS either in their laboratory or through a service laboratory. The time and cost required for the gross nitrification method is considerably greater than the other techniques described in this chapter. However, this technique is the method of choice when the investigator wishes to measure nitrification independent of the other N transformations such as denitrification and immobilization.

38.6 *IN SITU* METHODS FOR DETERMINING NET NITRIFICATION (ENO 1960; ADAMS AND ATTIWILL 1986)

The original method developed by Eno (1960) used disturbed soil samples that were sieved, mixed, and incubated in the field by burying samples in thin-walled polyethylene bags (the so-called buried bag method). The net increase in the amount of NO_3^- produced during the field incubation provides an estimate of the net nitrification rate. One of the advantages to this technique is that the temperature of the soils in these bags fluctuated to a similar extent as the surrounding soil, while allowing sufficient gas exchange through the polyethylene bag to maintain aerobic conditions. Additionally, by containing the soil in a polyethylene bag, NO_3^- losses via leaching and plant uptake are prevented; hence, net changes in the soil NO_3^- pool within the bag over the incubation period are equivalent to the net nitrification rate. However, the buried bag method does not allow for changing soil moisture contents during the incubation. Further, using disturbed soil samples (resulting in reduced diffusional limitations to the nitrification process) may significantly increase net N nitrification rates (Binkley and Hart 1989). However, Burns and Murdoch (2005) found that the net nitrification rates were not significantly different between mixed soil contained in buried bags and intact soil contained in capped PVC tubes (see below).

Another *in situ* method for measuring net nitrification rates was proposed by Adams and Attiwell by incubating intact soil cores that have been minimally disturbed. They found that net nitrification rates between these two methods were not significantly different. Soil cores are loosely covered to minimize leaching losses of N, while plant uptake of NO_3^- is prevented (Adams and Attiwill 1986). Knoepp and Swank (1995) found that capped PVC cores (only the top was capped) were preferable over buried bags as the soil moisture content in the soil cores varied qualitatively with the surrounding bulk soil, whereas the soil moisture content was kept relatively constant in the buried bags. Apparently, water was able to move into and out of the bottom of the soil core through capillary action. For both capped PVC cores and buried bags, however, soil moisture content in the incubating soil does not track changes in bulk soil moisture very closely because the contained soil has less evapotranspirational losses compared to bulk soils, and new precipitation inputs are prevented. Hence, incubation periods should be selected where bulk soil moisture dynamics during the incubation period are minimal. The use of relatively undisturbed soil cores helps to overcome some of the disadvantages associated with the use of disturbed soil (Cabrera and Kissel 1988; Sierra 1992), but nitrate losses can still occur as a result of denitrification.

Nitrate leaching losses can be accounted for if the soil core includes an ion exchange resin (IER) bag at the bottom of the core to trap any NO_3^- leaching from the soil (resin-core

method; Binkley and Hart 1989). Like the other *in situ* methods, the incubation temperature of the soil core is the same temperature as the surrounding soil. Additionally, if the top of the core is open, then the soil is also susceptible to drying conditions that result from evaporation, as well as wetting conditions that result from precipitation inputs. However, because of the absence of plant roots within the core and the hydraulic discontinuity created between the resin bag and the soil, the changes in the soil moisture content in the core may differ from the surrounding soil (Hart and Firestone 1989).

38.6.1 Materials and Reagents

1 Thin-walled, PVC cylinders (inner diameter could vary from 5 to 10 cm and length could vary from 10 to 30 cm), with the lower end sharpened to facilitate insertion with minimal compaction of the contained soil

2 Filtration rack, funnels, and Whatman No. 40 filter papers preleached with KCl or deionized water

3 A 2 *M* KCl solution; dissolve 1.49 kg of reagent grade KCl in 10 L of deionized water

4 Other reagents as required for NH_4^+ and NO_3^- analyses of KCl extracts of soil (see Chapter 6)

38.6.2 Procedure

1 Generally, sampling locations are selected at random within the study site, collecting two, paired soil cores (an initial and incubated core) at each of at least six different locations within the site to be characterized. Stratified-random sampling designs can be used where net nitrification rates are known to covary with different strata (e.g., plant cover types; see Kaye and Hart 1998).

2 Determine the bulk density, soil moisture content, and initial NH_4^+ and NO_3^- contents on one of the cores.

3 Determine the initial NH_4^+ and NO_3^- concentration of the sample by extracting 20 g of the field-moist soil sample with 100 mL of 2 *M* KCl as described previously. Filter and analyze the extracts on an autoanalyzer for NH_4^+ using the Berthelot reaction and for NO_3^- using the cadmium reduction method (Tel and Heseltine 1990), and express the results on a dry weight basis.

4 Place a nylon mesh screen (53 μm) over the bottom of each core to be incubated, and fasten it to the side of the core using a durable elastic band. The nylon mesh screen minimizes soil loss while allowing water and gas exchange. This step can be skipped if soil loss from the bottom of the core is minimal during the incubation.

5 Return the soil core to the hole from which it originated. The connection between the bulk soil and soil core would likely be aided if some of the bulk soil was granulated and placed in the bottom of the hole before the core was inserted.

6 Place a cap that has four to five holes (approximately 1–2 mm diameter) drilled in the side of the cap to allow for gas exchange on top of each core.

7 After approximately 28 days (longer incubation periods of up to 4 months may be used over the winter), remove the incubated cores, mix the soil and weigh 20 g of moist soil from each core into a 250 mL Erlenmeyer flask, extract with 2 *M* KCl, and analyze for NH_4^+ and NO_3^- as described previously. A separate subsample from each core is analyzed for soil moisture content.

38.6.3 Comments

1 One of the main advantages of this field technique is that it enables the investigator to evaluate various treatments on the nitrification process where the soil experiences the variations in temperature and moisture that normally occur in the field. The typically low night-time temperatures (in temperate and boreal environments) and potentially high day-time temperatures may limit microbial activity, resulting in nitrification rates that are often lower than the rates obtained using either the laboratory net nitrification rate method or the shaken soil-slurry method (potential nitrification rate) described previously (Jefts et al. 2004).

2 Desorption curve studies suggest that a nylon cloth with 53 μm pore size works well, provided that there is an adequate hydraulic connection between the soil in the core and the bulk soil (see Chapter 72). Establishing and maintaining hydraulic connection requires that the bottom of the cloth-covered core be pressed firmly against the bulk soil.

3 Many studies are now using intact soil cores that are placed within buried polyethylene bags (15–30 μm thick) to determine the *in situ* net nitrification rate (Binkley and Hart 1989). These do not use the nylon mesh screen or the cap. With this technique, the soil moisture within the core does not fluctuate with the surrounding soil. However, one of the advantages of this method is that no NO_3^- losses by mass flow or diffusion can occur from the soil contained within the polyethylene bag; diffusional losses of NO_3^- from capped soil cores are possible.

4 Alternatively, open cores could be used and leaching allowed to occur if a mixed-bed, IER bag is placed below the soil core to trap leached NO_3^- (e.g., Binkley and Hart 1989; Hart and Firestone 1989). The IER bag traps any NO_3^- (and NH_4^+) leaching from the incubated soil core, while allowing water to pass freely out of the core. The IER bag is removed and extracted with KCl after the core is incubated in the field, and the amount of NO_3^- that has leached from the soil core into the resin is determined. The net nitrification rate is the sum of the amount of NO_3^- collected on the IER bag and the net change in the soil NO_3^- pool within the soil core.

5 It is advisable to use PVC cores instead of metal cores. Soil temperature was elevated within metal cylinders used for soil incubation, particularly when assays of surface soils are conducted during the summer months (Raison et al. 1987; Edmonds and McColl 1989), or in agricultural fields at the beginning of the season when shading by the crop canopy is negligible.

6 In some studies, perforated cores were used to further enable the soils to undergo moisture fluctuations similar to the changes experienced in the surrounding environment. Adams et al. (1989) found that soil moisture levels within cores were within 5% of those in bulk soils when perforated cores were used.

However, any water loss or gain from these cores would also affect the NO_3^- concentration within the soil core, resulting in error in the net nitrification rate estimate.

7 In some situations, such as when shallow surface soils are investigated, when numerous stones are present, or the soil lacks structure, it may be preferable to use the original method of burying a disturbed, mixed soil in a polyethylene bag instead of using an intact soil core (Eno 1960; Adams et al. 1989; Pajuste and Frey 2003). If buried bags are used and the soil is very wet or very dry when it is first sampled, then the investigator may wish to either compare soil incubations at varying moisture contents or adjust the soil moisture of the mixed samples to a standard level such as field capacity (−33 kPa). If mixed samples are used, weigh a 100 g, field-moist sample and seal in the polyethylene bag (15–30 μm thick; Gordon et al. 1987). Rebury the soil bags in their original holes and remove bags after 28 days. Process the soil as described previously.

REFERENCES

Adams, M.A. and Attiwill, M.P. 1986. Nutrient cycling and nitrogen mineralization in eucalypt forests of south-eastern Australia. *Plant Soil* 92: 341–362.

Adams, M.A., Polglase, P.J., Attiwill, M.P., and Weston, C.J. 1989. *In situ* studies on nitrogen mineralization and uptake in forest soils: some comments on methodology. *Soil Biol. Biochem.* 21: 423–429.

Bartosch, S., Hartwig, C., Spieck, E., and Bock, E. 2002. Immunological detection of *Nitrospira*-like bacteria in various soils. *Microb. Ecol.* 43: 26–33.

Belser, L.W. and Mays, E.L. 1980. Specific incubation of nitrite oxidation by chlorate and its use in assessing nitrification in soils and sediments. *Appl. Environ. Microbiol.* 39: 505–510.

Bergstrom, D.W., Tenuta, M., and Beauchamp, E.G. 1994. Increase in nitrous oxide production in soil induced by ammonium and organic carbon. *Biol. Fert. Soils* 18: 1–6.

Binkley, D. and Hart, S.C. 1989. The components of nitrogen availability assessments in forest soils. *Adv. Soil Sci.* 10: 57–112.

Booth, M.S., Stark, J.M., and Hart, S.C. 2006. Soil-mixing effects on inorganic nitrogen production and consumption in forest and shrubland soils. *Plant Soil* 289: 5–15.

Bundy, L.G. and Bremner, J.M. 1973. Inhibition of nitrification in soils. *Soil Sci. Soc. Am. Proc.* 37: 396–398.

Burns, D.A. and Murdoch, P.S. 2005. Effects of clearcut on the net rates of nitrification and N mineralization in a northern hardwood forest, Catskill Mountains, New York, USA. *Biogeochemistry* 72: 123–146.

Cabrera, M.L. and Kissel, D.E. 1988. Potentially mineralizable nitrogen in disturbed and undisturbed soil samples. *Soil Sci. Soc. Am. J.* 52: 1010–1015.

Chen, J. and Stark, J.M. 2000. Plant species effects and carbon and nitrogen cycling in a sagebrush-crested wheatgrass soil. *Soil Biol. Biochem.* 32: 47–57.

Compton, J.E. and Boone, R.D. 2002. Soil nitrogen transformations and the role of light fraction organic matter in forest soils. *Soil Biol. Biochem.* 34: 933–943.

Davidson, E.A., Hart, S.C., Shanks, C.A., and Firestone, M.K. 1991. Measuring gross N mineralization, immobilization, and nitrification by ^{15}N isotopic pool dilution in intact soil cores. *J. Soil Sci.* 42: 335–349.

Davidson, E.A., Stark, J.M., and Firestone, M.K. 1990. Microbial production and consumption of nitrate in an annual grassland. *Ecology* 71: 1968–1975.

deCatanzaro, J.B., Beauchamp, E.G., and Drury, C.F. 1987. Denitrification vs. dissimilatory nitrate reduction in soil with alfalfa, straw, glucose and sulfide treatments. *Soil Biol. Biochem.* 19: 583–587.

Drury, C.F. and Beauchamp, E.G. 1991. Ammonium fixation, release, nitrification, and immobilization in high- and low-fixing soils. *Soil Sci. Soc. Am. J.* 55: 125–129.

Drury, C.F., Beauchamp, E.G., and Evans, L.J. 1989. Fixation and immobilization of recently added $^{15}NH_4^+$ in selected Ontario and Quebec soils. *Can. J. Soil Sci.* 69: 391–400.

Drury, C.F., McKenney, D.J., Findlay, W.I., and Gaynor, J.D. 1993. Influence of tillage on nitrate loss in surface runoff and tile drainage. *Soil Sci. Soc. Am. J.* 57: 797–802.

Drury, C.F., Tan, C.S., Gaynor, J.D., Oloya, T.O., and Welacky, T.W. 1996. Influence of controlled drainage subirrigation on surface and tile drainage nitrate loss. *J. Environ. Qual.* 25: 317–324.

Edmonds, R.L. and McColl, J.G. 1989. Effects of forest management on soil nitrogen in *Pinus radiata* stands in the Australian Capital Territory. *Forest Ecol. Manag.* 29: 199–212.

Eno, C.F. 1960. Nitrate production in the field by incubation of soil in polyethylene bags. *Soil Sci. Soc. Am. Proc.* 24: 277–279.

Gordon, A.M., Tallas, M., and Van Cleve, K. 1987. Soil incubations in polyethylene bags: effect of bag thickness and temperature on nitrogen transformations and CO_2 permeability. *Can. J. Soil Sci.* 67: 65–75.

Hart, S.C., Binkley, D., and Perry, D.A. 1997. Influence of red alder on soil nitrogen transformations in two conifer forests of contrasting productivity. *Soil Biol. Biochem.* 29: 1111–1123.

Hart, S.C. and Firestone, M.K. 1989. Evaluation of three *in situ* soil nitrogen availability assays. *Can. J. Forest Res.* 19: 185–191.

Hart, S.C., Nason, G.E., Myrold, D.D., and Perry, D.A. 1994a. Dynamics of gross nitrogen transformations in an old forest: the carbon connection. *Ecology* 75: 880–891.

Hart, S.C., Stark, J.M., Davidson, E.A., and Firestone, M.K. 1994b. Nitrogen mineralization, immobilization, and nitrification. In R.W. Weaver, S. Angle, P. Bottomed, D. Bezdicek, S. Smith, A. Tabatabai, and A. Wollum, Eds. *Methods of Soil Analysis, Part 2—Microbiological and Biochemical Properties.* Soil Science Society of America, Madison, WI, pp. 985–1018.

Hynes, R.K. and Knowles, R. 1980. Denitrification, nitrogen fixation and nitrification in continuous flow laboratory soil columns. *Can. J. Soil Sci.* 60: 355–363.

Jefts, S.S., Fernandez, I.J., Rustad, L.E., and Dail, D.B. 2004. Comparing methods for assessing forest soil net nitrogen mineralization and net nitrification. *Commun. Soil Sci. Plant Anal.* 19: 2875–2890.

Kaye, J.P., Binkley, D., Zou, X., and Parrotta, J.A. 2002. Non-labile soil 15-nitrogen retention beneath three tree species in a tropical plantation. *Soil Sci. Soc. Am. J.* 66: 612–619.

Kaye, J.P. and Hart, S.C. 1998. Ecological restoration alters nitrogen transformations in a ponderosa pine-bunchgrass ecosystem. *Ecol. Appl.* 8: 1052–1060.

Killham, K. 1987. A new perfusion system for the measurement of potential rates of soil nitrification. *Plant Soil* 97: 267–272.

Kirkham, D. and Bartholomew, W.V. 1954. Equations for following nutrient transformation in soil utilizing tracer data. *Soil Sci. Soc. Am. Proc.* 18: 33–34.

Knoepp, J.D. and Swank, W.T. 1995. Comparison of available soil nitrogen assays in control and burned forested sites. *Soil Sci. Soc. Am. J.* 59: 1750–1754.

Kowalenko, C.G. and Yu, S. 1996. Assessment of nitrate adsorption in soils by extraction equilibration and column-leaching methods. *Can. J. Soil Sci.* 76: 49–57.

Murphy, D.V., Recous, S., Stockdalem, E.A., Fillery, I.R.P., Jensen, L.S., Hatch, D.J., and Goulding, K.W.T. 2003. Gross nitrogen fluxes in soil: theory, measurement and application of ^{15}N pool dilution techniques. *Adv. Agron.* 79: 69–118.

Pajuste, K. and Frey, J. 2003. Nitrogen mineralization in podzol soils under boreal Scots pine and Norway spruce stands. *Plant Soil* 257: 237–247.

Parkin, T.B. and Meisinger, J. 1989. Denitrification below the crop rooting zone as influenced by surface tillage. *J. Environ. Qual.* 18: 12–16.

Paul, E.A. and Clark, F.E. 1996. *Soil Microbiology and Biochemistry*, 2nd ed. Academic Press Inc., San Diego, CA, 188 pp.

Pennington, P.I. and Ellis, R.C. 1993. Autotrophic and heterotrophic nitrification in acidic forest and native grassland soils. *Soil Biol. Biochem.* 25: 1399–1408.

Raison, R., Connell, M., and Khanna, P. 1987. Methodology for studying fluxes of soil mineral-N *in situ*. *Soil Biol. Biochem.* 19: 521–530.

Robertson, G.P. 1982. Factors regulating nitrification in primary and secondary succession. *Ecology* 63: 1561–1573.

Robertson, G.P. and Vitousek, P.M. 1981. Nitrification potentials in primary and secondary succession. *Ecology* 62: 376–386.

Ross, D.S. and Hales, H.C. 2003. Sampling-induced increases in net nitrification in the Brush Brook (Vermont) watershed. *Soil Sci. Soc. Am. J.* 67: 318–326.

Schimel, D.S. 1986. Carbon and nitrogen turnover in adjacent grassland and cropland ecosystems. *Biogeochemistry* 2: 345–357.

Schmidt, E.L. 1982. Nitrification in soil. In F.J. Stevenson, Ed. *Nitrogen in Agricultural Soils*. American Society of Agronomy, Madison, WI, pp. 252–283.

Sierra, J. 1992. Relationship between mineral N content and N mineralization rate in disturbed soil samples incubated under field and laboratory conditions. *Aust. J. Soil Res.* 30: 477–492.

Sierra, J. 2002. Nitrogen mineralization and nitrification in tropical soil: effects of fluctuating temperature conditions. *Soil Biol. Biochem.* 34: 1219–1226.

Silver, W.L., Herman, D.J., and Firestone, M.K. 2001. Dissimilatory nitrate reduction to ammonium in upland tropical forest soils. *Ecology* 82: 2410–2416.

Sparrow, S.D. and Masiak, D.T. 1987. Errors in analyses for ammonium and nitrate caused by contamination from filter papers. *Biol. Fert. Soils* 6: 33–38.

Stark, J.M. 1991. Environmental factors versus ammonium-oxidizer population characteristics as dominant controllers of nitrification in a California oak woodland-annual grassland soil. Ph.D. Diss., Univ. of California, Berkeley, CA.

Stark, J.M. 1996. Shaker speeds for aerobic soil slurry incubations. *Commun. Soil Sci. Plant Anal.* 27: 2625–2631.

Stark, J.M. and Firestone, M.K. 1995. Isotopic labeling of soil nitrate pools using nitrogen-15-nitric oxide gas. *Soil Sci. Soc. Am. J.* 59: 844–847.

Stark, J.M. and Firestone, M.K. 1996. Kinetic characteristics of ammonium-oxidizer communities in a California oak woodland-annual grassland. *Soil Biol. Biochem.* 28: 1307–1317.

Stark, J.M. and Hart, S.C. 1996. Evaluation of a diffusion technique for preparing salt solutions, Kjeldahl digests, and persulfate digests for nitrogen-15 analysis. *Soil Sci. Soc. Am. J.* 60: 1846–1855.

Stark, J.M. and Hart, S.C. 1997. High rates of nitrification and nitrate turnover in undisturbed coniferous forests. *Nature* 385: 61–74.

Tel, D.A. and Heseltine, C. 1990. The analysis of KCl soil extracts for nitrate, nitrite and ammonium using a TRAACS 800 autoanalyzer. *Commun. Soil Sci. Plant Anal.* 21: 1681–1688.

Vega-Jarquin, C., Garcia-Mendoza, M., Jablonowski, N., Luna-Guido, M., and Dendooven, L. 2003. Rapid immobilization of applied nitrogen in saline-alkaline soils. *Plant Soil* 256: 379–388.

Verchot, L.V., Holmes, Z., Mulon, L., Groffman, P.M., and Lovett, G.M. 2001. Gross vs. net rates of N mineralization and nitrification as indicators of functional differences between forest types. *Soil Biol. Biochem.* 33: 1889–1901.

Chapter 39
Substrate-Induced Respiration and Selective Inhibition as Measures of Microbial Biomass in Soils

V.L. Bailey and H. Bolton, Jr.
Pacific Northwest National Laboratory
Richland, Washington, United States

J.L. Smith
U.S. Department of Agriculture
Washington State University
Pullman, Washington, United States

39.1 INTRODUCTION

The determination of soil microbial biomass can be extremely valuable for process studies because of the time dependence of microbially mediated reactions. The mineralization of elements such as carbon and nitrogen and the degradation of many (organic) chemicals have kinetics that depend upon the concentration of substrate and the physicochemical soil environment, and require microbial biomass as a reactive agent. If rapid methods for biomass determinations were reliable and were not influenced by changing soil conditions, the effect of microbial biomass on the kinetics of mineralization, chemical degradation, and nutrient uptake could be determined.

The substrate-induced respiration (SIR) method is a simple, rapid, and economical method to determine microbial biomass C in soils and residues. The theory behind this method is that the initial rate of microbial CO_2 production in response to a soluble energy-yielding substrate would be proportional to the mass of organisms. This method, which was initially developed to distinguish bacterial and fungal biomass, has been calibrated to the chloroform fumigation incubation method (CFIM) for measuring soil microbial biomass (see Chapter 49). Two requirements of the method are (a) the soil must be saturated, with respect to the response, with substrate and (b) the response to the addition of substrate must be measured before any increase in organism biomass. Thus preliminary experiments are required to develop a glucose saturation curve and a microbial growth curve for lag time determination (Smith et al. 1985).

This method has been used to evaluate the effects of tillage on soil processes and microbial biomass (Lynch and Panting 1980; Ross 1980; Adams and Laughlin 1981) and the effects of pesticides (Anderson et al. 1981), metals (Brookes and McGrath 1984), and forest clear-cutting (Ayanaba et al. 1976) on the microbial biomass. The measurement of microbial biomass is also critical in studying nutrient and energy flows in soil systems (Paul and Voroney 1980; van Veen et al. 1985; Smith and Paul 1990).

The selective inhibition method uses fungicides and bactericides to measure the ratio of fungal activity to bacterial activity (Anderson and Domsch 1973). This approach predates the calibration of SIR as a measure of microbial biomass (Anderson and Domsch 1978), but is essentially a variation of that method. The ratio of fungal-to-bacterial activity (F:B) estimated by the selective inhibition compares the activities of these two communities, rather than their relative abundances within the total soil microbial biomass (i.e., F:B from phospholipid fatty acid analyses). Some researchers have reported a relationship between ratios for activities and the ratios for the biomass (Bailey et al. 2002; Bååth and Anderson 2003).

39.2 SUBSTRATE-INDUCED RESPIRATION

The SIR method has been given significant attention since its development in the late 1970s (Anderson and Domsch 1978) and it continues to be used, tested, and modified into the twenty-first century. The SIR method is useful for potential biomass estimations (preincubated soils) and incubation studies, where microbial biomass is estimated at different time periods and for *in situ* analysis of microbial biomass. The method has been criticized for its reliance on glucose utilizing organisms to determine the entire broad spectrum and amount of soil microbial biomass. Smith et al. (1985) pointed out the concern of the changing nutrient status of soil during long-term incubations and suggested using a balanced nutrient substrate such as glucose + nutrient broth when determining respiration response. Others have investigated optimizing soil water content as well as substrate additions (West and Sparling 1986) and the effect of soil texture and organic matter (Kaiser et al. 1992; Lin and Brookes 1999). Another adaptation made the method useful for determining microbial biomass on plant residues (Beare et al. 1990). The SIR method is widely used and perhaps overly used with respect to using the original Anderson and Domsch (1978) equation for converting CO_2 evolved to microbial biomass C. For researchers who use similar soils in numerous experiments over years of research, we would suggest developing a specific correlation between the CFIM and the SIR method. Once established, this relationship should be consistent for long periods of time. The same should be true of the glucose saturation curve to develop optimal concentrations of substrate and the microbial growth curve that determines the time after substrate addition that microbial growth occurs.

39.2.1 Materials and Reagents

1 Any suitable soil incubation vessel. If the respired CO_2 is to be determined by gas chromatography (GC), the incubation vessel should be equipped with a gas-tight rubber septum. Larger incubation vessels will be needed to conduct the method if the respired CO_2 will be determined by titration of a base trap (see Section 39.2.4). The typical GC method would use 40 mL flat-bottom glass vials with screw cap septa or 50 mL Erlenmeyer flasks with sleeve type rubber stoppers.

2 Reagent grade dextrose (glucose) FW 180.16.

3 Dispensing pipette.

4 Small spatula.

5 Gas chromatograph (GC) with TCD detector.

6 CO_2 standard gases.

39.2.2 Procedure

Basic SIR Procedure

1 Weigh out 10 g (oven-dry weight; ODW) replicate soil samples and place into 40 mL incubation vials. The soil must be dry enough to accept a measurable amount of liquid without becoming waterlogged.

2 Add the appropriate amount of glucose solution as determined by a glucose saturation curve (see next section). Briefly mix the soil, flush with hydrated air, and cap with a septum. Record the time and prepare the next vial.

3 After 1 h, sample the headspace of the vial with a syringe and inject the appropriate amount of gas into the GC. Repeat for each vial at the appropriate time. We have used a Hewlett Packard 5890 Series II gas chromatograph equipped with a Carboxen-1000 column with 60/80 mesh, 4.5 m by 0.3175 cm (Supelco) to measure the concentration of CO_2 in 1 mL of headspace gas. The injection temperature was 150°C, and the detector temperature was 300°C. The initial oven temperature was 150°C, and ramped up to 210°C in the first 2 min. The total run time (R_t) was 4.5 min, and CO_2 elution had an R_t of 3.9 min.

4 Calculate the percent CO_2 in the headspace by comparing to a standard CO_2 curve or as calculated in step 1 (Section 39.2.3). Determine the CO_2 respiration rate and the conversion to microbial biomass C from Equation 39.2 through Equation 39.4.

Glucose Saturation Curve

1 Weigh out 10 g (ODW) replicate soil samples and place into 40 mL incubation vials. Prepare enough replicate vials to accommodate 4–6 concentrations of glucose. Suggested concentrations of glucose are 0, 200, 400, 600, and 800 μg glucose g^{-1} soil, corresponding to 0, 80, 160, 240, and 320 μg C g^{-1} soil. Glucose solution concentrations should be adjusted such that the added solution brings the soil to near field capacity (−0.033 MPa).

2 Prepare one vial at a time, adding the appropriate amount of glucose solution, or in the case of the control vial, the same volume of water. Briefly mix the soil, flush with hydrated air, and cap with a septum. Record the time and prepare the next vial.

3 After 1 h, sample the headspace of the vial with a syringe and inject the appropriate amount of gas into the GC. Repeat for each vial at the appropriate time.

4 For the saturation curve, plot the 1 h response versus glucose addition. The plot should reach a maximum value, where higher concentrations of glucose do not provide a greater response. The optimal glucose concentration used for SIR analysis should be at the high end of the constant response curve, to be sure that under changing conditions the soil will still be saturated with respect to glucose.

Microbial Growth Curve

1 Weigh out 10 g (ODW) replicate soil samples and place into 40 mL incubation vials.

2 Add the appropriate amount of glucose solution to provide the soil glucose concentration determined from the glucose saturation curve. Briefly mix the soil, flush with hydrated air, and cap with a septum. Record the time and prepare the next vial.

3 After 1 h, sample the headspace of the vial with a syringe and inject the appropriate amount of gas into the GC. Flush the vial with hydrated air and reseal. For 6–8 h, repeat sampling every hour.

4 Calculate the CO_2 respiration rate from Equation 39.2. Plot the hourly CO_2 respiration rate versus time. Determine when the CO_2 respiration rate increases (any time period before the respiration rate increases can be used for sampling the SIR).

Soil Pretreatment and Preparation

1 For measuring microbial biomass on fresh sampled soil, sample the soil when the water content is less than field capacity (−0.033 MPa). Sieve (2–6 mm) and homogenize the soil. Weigh out two subsamples for moisture determination at 105°C. Weigh out 3–10 g subsamples and place each into a 40 mL glass vial. Follow the basic SIR procedure above.

2 For measuring the potential soil microbial biomass concentration, follow step 1 above, then cover the opening of the vials with parafilm and incubate the vials for 5–7 days in the dark. Aerate the vials with hydrated air at least once during the preincubation. After the preincubation, follow the basic SIR procedure above.

3 For microbial biomass analysis during soil incubation, it is best to prepare a number of vials at the start of the incubation and destructively sample the vials as the incubation progresses. Thus prepare the soil as described in step 1, using three subsamples for each time period. At each required time, remove three vials from the incubation chamber and follow the basic SIR procedure above.

4 For the *in situ* determination of microbial biomass, use a 7×5 cm (height $\times$ diameter) cylinder of plastic or metal. Press the cylinder 5 cm into the soil, remove the core, place a 5 cm diameter thin rubber sheet into the hole, and replace the core. Other replicate cores need to be taken to determine the water content of the soil. Predetermine or estimate the mass of dry soil in the cylinder. Prepare numerous injections of glucose solution to reach the proper glucose concentration per gram of soil and the optimum water content. Cover the cylinder

with an air-tight plastic cap capable of being penetrated with a needle. After 1 h, sample the headspace of the cylinder and proceed as in the basic SIR procedure.

39.2.3 Calculations

1 % CO_2 in the vial headspace is calculated from

$$\%\ CO_{2(\text{headspace})} = \frac{(\text{peak height}_{\text{sample}} - \text{peak height}_{\text{air}})}{\text{peak height}_{\text{standard}}} \times \%\ CO_{2(\text{standard})} \qquad (39.1)$$

2 If the CO_2 is measured by GC, the quantity of CO_2 evolved from the soil must be determined from the concentration of CO_2 in the headspace. This is not necessary if a hydroxide trap is used. When 10 g of soil (ODW) is used, a CO_2 respiration rate per gram of soil (ODW) is calculated from

$$CO_2\ (\text{mL}\ h^{-1}\ g^{-1}\ \text{soil}) = \frac{\left(\frac{\%\ CO_{2(\text{headspace})}}{100}\right) \times [\text{total vial headspace (mL)}]}{1\ \text{h} \times 10\ \text{g soil}} \qquad (39.2)$$

3 Microbial biomass C calculated with the equation of Anderson and Domsch (1978) valid at 22°C ± 0.5°C is

$$\text{mL}\ CO_2\ h^{-1}\ 100\ g^{-1}\ \text{soil} = \text{respiration rate} \times 100 \qquad (39.3)$$

$$\text{mg biomass C}\ 100\ g^{-1}\ \text{soil} = 40.04 \times (\text{mL}\ CO_2\ h^{-1} 100\ g^{-1}\ \text{soil}) + 0.37 \qquad (39.4)$$

39.2.4 Comments

1 SIR procedure can be conducted using NaOH traps to absorb CO_2 from the induced respiration. Since the measurement is generally on an hour basis, the amount of soil will generally need to be increased to two- or threefold, due to the low sensitivity of the titration method of quantifying CO_2. It would also be acceptable to trap the CO_2 for 3 h and use in Equation 39.2 (this is valid only if the CO_2 rate is constant over this period as shown by the microbial growth curve). High-pH soils (>7) may not be suited to these static trapping methods; as pH increases, an increasing amount of CO_2 can dissolve in the soil solution as HCO_3^-. A continuous flow system is required to accurately measure CO_2 evolution rates (Martens 1987).

2 Incubation time period after substrate addition can vary if the lag period is maintained. Variations include measuring after 1 h (or parafilm the vials for 2 h and then measure the CO_2 produced in the third hour). These variations are usually for convenience if large numbers of samples are being processed.

3 Some general commonalities do exist for this method. Many soils have a glucose saturation of between 600 and 1000 μg glucose g^{-1} soil. Saturation levels generally increase with organic C levels, but texture does not seem to influence the saturation level. Soils with significant amounts of native litter, i.e., forest soils, can have very high saturation levels.

4 Presence of pollutants in the soil or severe oligotrophic conditions (e.g., subsoils) may contribute to modify the C respired/C assimilated ratio would severely skew the results such that Equation 39.3 would be no longer valid. This equation was derived for soils that are under ''average'' conditions, in which living cells from all different physiological stages were present (Anderson and Domsch 1978). Soils that differ from this assumption would be best suited to alternate measures of soil microbial biomass, such as chloroform fumigation-extraction (see Chapter 49). To ensure that soils meet the conditions of the equation, a 1 week preincubation of the soil after sieving or storage is recommended (Anderson and Domsch 1978).

5 Precision of the SIR method is very good and many reports in the literature show a replicate variability of 1% to 6% coefficient of variability (CV). Our field data (unpublished) show that in a 0.5 ha field with $n = 220$ samples, the spatial CV of microbial biomass by SIR was 31% and triplicate subsample variability was 3%. Over larger scales (60 km^2) with $n = 161$, the spatial CV was 53%, and the replicate CV only 5%. Thus the method is far more precise than our ability to interpret the variability of microbial biomass in nature.

6 Equation 39.1 through Equation 39.4 in Section 39.2.3 can be changed to suit the investigator such that if the vials are flushed with CO_2-free air, an air peak need not be subtracted. In addition, many GC programs compare peak height or area to a standard curve and provide % CO_2 as a direct output. Likewise, microbial biomass is usually reported as μg biomass C g^{-1} soil, rather than mg biomass C 100 g^{-1} soil.

39.3 SELECTIVE INHIBITION (ANDERSON AND DOMSCH 1975; BAILEY ET AL. 2003)

The use of antibiotics to selectively inhibit microbial activities in soils was first proposed by Anderson and Domsch (1973). This approach uses a fungicide to selectively suppress fungal activities and a bactericide to suppress bacterial activities, permitting the calculation of F:B. Soil respiration is stimulated by the addition of a small amount of glucose and is measured as CO_2 evolved from the separate and combined additions of the antibiotics. Typically, the fungicides of choice have been cycloheximide (Badalucco et al. 1994) or captan (Beare et al. 1990). The bactericides have traditionally been streptomycin (Badalucco et al. 1994) or oxytetracycline (Beare et al. 1990), though recently bronopol (Bailey et al. 2003) and chloramphenicol (Nakamoto and Wakahara 2004) have been successfully used in this procedure. Our research indicates that it may be useful to survey these different antibiotics to determine which pair is most effective for a particular soil (Bailey et al. 2003; Nakamoto and Wakahara 2004). It is always necessary to optimize the method by creating a respiration inhibition curve for the fungicide and bactericide in order to determine the optimum concentrations of these chemicals. The glucose concentration used should correspond to the maximum respiration response, as described above for a glucose saturation curve.

Typically, F:B ratios reported in the literature range from 0.54 to 3.04 for agricultural soils (Beare et al. 1992). However, values as high as 13.5 for a restored prairie soil (Bailey et al. 2002) and 18.2 for an acidic beech soil (Blagodatskaya and Anderson 1998) have also been reported. These results are often confounded by the ''inhibitor additivity ratio'' (IAR), which is a measure of the effectiveness of the antibiotics against the soil microorganisms.

The IAR indicates nontarget inhibition. An IAR that significantly exceeds 1.0 indicates that the separate additions of the fungicide and bactericide are inhibiting a greater proportion of the respiration than when added together, because their activities are overlapping. This overlap may cause a misrepresentation of the F:B, as the overlapping activities cannot be assumed to be evenly ascribed to both the fungicide and bactericide. In soils with low IARs but high F:B ratios, even a small overlap can exert a large influence on the smaller of the two microbial groups (Bailey et al. 2002). Others have proposed that an IAR >1.0 could be due to the combined addition of the antibiotics being less efficient than the separate addition. We agree with Beare et al. (1990) and Velvis (1997) in recommending that this ratio be optimized at 1.0, since nontarget inhibition is most likely the source of the apparent overlap. Therefore, it is important that the optimization of the procedure includes trials of the combined antibiotic additions to focus the outcome to an IAR as close to 1.0 as possible. One way of doing this is to decrease the concentrations of antibiotics; Velvis (1997) noted that as the quantity of cycloheximide that was added to soil increased, it began to inhibit the bacterial population as well as the target fungal population. In spite of these concerns, IARs as high as 3.12 have been reported (Imberger and Chiu 2001). Such large IAR values introduce large uncertainties to the calculated ratios.

No fungicide–bactericide pairing will completely inhibit soil respiration over the 6 h incubation period (Wardle and Parkinson 1990; Bailey et al. 2002). Respiration observed in the presence of both a bactericide and a fungicide may be due to several reasons:

- Only synthesis of new biomass is susceptible to the antibiotics used (Anderson and Domsch 1973).
- Constitutive enzymes likely are present and active during the experiment (Heilmann et al. 1995).
- Degradation of these constitutive enzymes may be slow during the incubation, while new enzymes are not synthesized, due to the antibiotics (Heilmann et al. 1995).
- Antibiotic-resistant strains of fungi and bacteria may contribute to soil respiration (Heilmann et al. 1995).
- Antibiotics themselves may serve as substrates for nontarget organisms (Badalucco et al. 1994; Alphei et al. 1995).
- Some of the antibiotics may sorb to soil components or be otherwise modified such that they are not fully effective for the entire 6 h (Alphei et al. 1995).
- Little is known about unculturable soil microorganisms, and their sensitivities to antibiotics. These organisms may continue their normal metabolism in the presence of these antibiotics.

Some may argue that the F:B-distribution in the growing, antibiotic-susceptible fraction of the biomass may be assumed to be directly proportional to the F:B-distribution in the unaffected, already existing biomass defined by ''D'' (Equation 39.6) (Anderson and Domsch 1975). We advise caution in doing so, as there is no evidence that this is the case. The insensitive fraction may be differentially composed of suites of organisms that are not culturable by current approaches and whose responses to antibiotics cannot therefore be verified in isolation.

We have found that it is necessary to add the glucose approximately 1 h after adding the antibiotics; adding glucose with the antibiotics appears to stimulate respiration prior to the antibiotic inhibition, causing misleadingly high respiration values.

The respiration of CO_2 from the soil may be measured by either GC (Bailey et al. 2003) or hydroxide trapping (Anderson 1982). The method presented here uses a GC and is subject to the same concerns regarding high-pH soils as were discussed under substrate-induced respiration.

We base the method below on 1 g samples of soil (ODW); the method can be scaled to 5 or 10 g of soil, depending on the amount of CO_2 that can be measured. It may be difficult to distribute the antibiotics through larger soil samples.

39.3.1 Materials and Reagents

Refer to Section 39.2.1 with the addition of

1 Fungicide (cycloheximide or captan)

2 Bactericide (oxytetracycline-HCl, streptomycin sulfate, or bronopol)

3 Analytical balance (to four decimal places) for accurately weighing the antibiotics

4 Small weigh boats

5 Spatulas for mixing antibiotic with soil

39.3.2 Procedure

Antibiotic Inhibition Curves

The following procedure must be done for each antibiotic and soil combination. It is recommended that each treatment has three replicates:

1 Preweigh a range of quantities of one of your antibiotics. Such a range may be 250–8000 $\mu g\ g^{-1}$ soil. Weigh out an additional quantity of talc to bring the total quantity of material to 0.02 g g^{-1} soil. Also weigh out 0.02 g talc g^{-1} of soil as a zero antibiotic treatment.

2 Weigh 1 g (ODW) moist soil into a weigh boat and sprinkle with the antibiotic–talc mixture. Use a stainless steel spatula to mix the insoluble material thoroughly with the soil, taking care to break up aggregates and distribute the antibiotic–talc evenly throughout the sample. Add the soil–antibiotic–talc mixture to a tube. Seal the tube with a foam plug or other permeable seal to prevent contamination of the tube.

3 Add glucose 1 h later to the soil–antibiotic–talc mixture and immediately seal the tube with a sealable sampling cap. Let the sealed tubes incubate in the dark for exactly 6 h.

4 Measure the amount of CO_2 in the headspace of each tube after the 6 h of incubation. The GC method described for SIR may be used.

5 Plot a graph of CO_2-formation versus antibiotic concentration. To minimize the risk of inhibiting nontarget organisms when selecting the concentration of antibiotic for the procedure, optimal concentrations are often slightly lower than the concentration causing maximal inhibition.

Selective Inhibition

1 Preweigh the optimum quantities of antibiotic and talc as described for the optimization curve, above. For each antibiotic, a minimum of three replicates for each treatment should be prepared. The treatments are as follows:

   a. No antibiotics—just 0.02 g talc g^{-1} soil

   b. Fungicide—the predetermined optimal amount of fungicide in 0.02 g talc g^{-1} soil

   c. Bactericide—the predetermined optimal amount of bactericide in 0.02 g talc g^{-1} soil

   d. Fungicide + bactericide—the predetermined optimal amounts of both antibiotics in a total of 0.02 g talc g^{-1} soil

2 Weigh 1 g (ODW) moist soil into a weigh boat and sprinkle with the antibiotic–talc mixture. Blend the talc or antibiotic–talc mixture into the soil, add mixture to tube, and plug the tube with a foam stopper as described in Antibiotic Inhibition Curves, p. 523 (step 2).

3 Add glucose 1 h later after the addition of the talc or antibiotic–talc mixture. Then seal the tube with a Mininert valve or Subaseal, and incubate in the dark for 6 h.

4 Measure the concentration of CO_2 in the headspace of each tube and convert this to the total amount of CO_2 evolved.

39.3.3 Calculations

1 Fungal-to-bacterial activity ratio:

$$\text{F:B} = \frac{A - B}{A - C} \tag{39.5}$$

where A is the respiration rate measured (μg CO_2 h^{-1} g^{-1} soil) in the absence of inhibitors; B is the respiration rate in the presence of the fungicide; and C is the respiration rate in the presence of the bactericide.

2 Inhibitor additivity ratio:

$$\text{IAR} = \frac{(A - B) + (A - C)}{A - D} \tag{39.6}$$

where D is the respiration rate measured in the presence of both antibiotics together.

39.3.4 Comments

1 Because the series of incubations needed to optimize, this procedure can be time-consuming; we have found that it is useful to condition soils by preincubating them at their −0.033 MPa moisture content, in the dark at room temperature, for several days prior to adding the antibiotics and glucose. This allows the multiple incubations (glucose, fungicide, bactericide, and IAR optimization) to be conducted on the soil at relatively consistent metabolic states. This may also be done to optimize the procedure; a fresh sample of the same soil may then be incubated according to the parameters determined on the stored and conditioned soil samples.

2 Antibiotics vary in their solubility. Good results may be obtained by adding water-soluble antibiotics as aqueous solutions; however, the water must be added to all treatments, just as with the talc. If using aqueous additions, check the solubility of each antibiotic in water, as some of the higher concentrations may exceed the solubility limit of the chemical. Also, some forms of antibiotics are less soluble than others (e.g., oxytetracycline hydrochloride is much more soluble than oxytetracycline dihydrate). Using talc as a carrier is particularly important when small quantities of antibiotic are applied to the soils; mixing the antibiotic with the talc allows for a more uniform distribution of the antibiotic through the soil.

3 There is some concern that using glucose to stimulate respiration skews the microbial community, causing the measurement of the F:B ratio to reflect only the glucose-responsive population. However, the levels of respiration (particularly in the inhibited treatments) may be below accurate detection limits without some stimulation of the biomass.

4 Another concern that has been raised regarding the selective inhibition procedure is that the antibiotics cause the death of a significant fraction of susceptible microbes, which may serve as substrate for surviving organisms and this metabolism may partly invalidate the selective inhibition procedure. Anderson and Domsch (1975), in their original presentation of the method, stipulate that the short incubation (6–8 h) reduces the likelihood that CO_2 production may come from the degradation of the inhibitors; the short incubation would similarly reduce the likelihood that CO_2 production from the dead biomass would significantly alter the CO_2 respired from the glucose.

5 We have provided suggestions as to the range of concentrations that may be effective. Soils with particularly high organic matter contents may require even more antibiotic to inhibit respiration, as some of the antibiotics may be sorbed by organic matter or other soil components (Alphei et al. 1995).

REFERENCES

Adams, T.M. and Laughlin, R.J. 1981. The effects of agronomy on the carbon and nitrogen contained in the soil biomass. *J. Agric. Sci.* 97: 319–327.

Alphei, J., Bonkowski, M., and Scheu, S. 1995. Application of the selective inhibition method to determine bacterial:fungal ratios in three beechwood soils rich in carbon—optimization of inhibitor concentrations. *Biol. Fert. Soils.* 19: 173–176.

Anderson, J.P.E. 1982. Soil respiration. In A.L. Page, R.H. Miller, and D.R. Keeney, Eds.

Methods of Soil Analysis, Part 2—Chemical and Microbiological Properties, 2nd ed. ASA–SSSA, Madison, WI, pp. 831–871.

Anderson, J.P.E., Armstrong, R.A., and Smith, S.N. 1981. Methods to evaluate pesticide damage to the biomass of the soil microflora. *Soil Biol. Biochem.* 13: 149–153.

Anderson, J.P.E. and Domsch, K.H. 1973. Quantification of bacterial and fungal contributions to soil respiration. *Arch. für Mikrobiol.* 93: 113–127.

Anderson, J.P.E. and Domsch, K.H. 1975. Measurement of bacterial and fungal contributions to respiration of selected agricultural and forest soils. *Can. J. Microbiol.* 21: 314–322.

Anderson, J.P.E. and Domsch, K.H. 1978. A physiological method for the quantitative measurement of microbial biomass in soils. *Soil Biol. Biochem.* 10: 215–221.

Ayanaba, A.A., Tuckwell, S.B., and Jenkinson, D.S. 1976. The effects of clearing and cropping on the organic reserves and biomass of tropical forest soils. *Soil Biol. Biochem.* 8: 519–525.

Bååth, E. and Anderson, T.H. 2003. Comparison of soil fungal/bacterial ratios in a pH gradient using physiological and PLFA-based techniques. *Soil Biol. Biochem.* 35: 955–963.

Badalucco, L., Pomaré, F., Grego, S., Landi, L., and Nannipieri, P. 1994. Activity and degradation of streptomycin and cycloheximide in soil. *Biol. Fert. Soils.* 18: 334–340.

Bailey, V.L., Smith, J.L., and Bolton, H., Jr. 2002. Fungal-to-bacterial ratios in soils investigated for enhanced carbon sequestration. *Soil Biol. Biochem.* 34: 1385–1389.

Bailey, V.L., Smith, J.L., and Bolton, H., Jr. 2003. Novel antibiotics as inhibitors for the selective respiratory inhibition method of measuring fungal:bacterial ratios in soil. *Biol. Fert. Soils.* 38: 154–160.

Beare, M.H., Neely, C.L., Coleman, D.C., and Hargrove, W.L. 1990. A substrate-induced respiration (SIR) method for measurement of fungal and bacterial biomass on plant residues. *Soil Biol. Biochem.* 22: 585–594.

Beare, M.H., Parmelee, R.W., Hendrix, P.F., Cheng, W., Coleman, D.C., and Crossley, D.A., Jr. 1992. Microbial and faunal interactions and effects on litter nitrogen and decomposition in agroecosystems. *Ecol. Monogr.* 62: 569–591.

Blagodatskaya, E.V. and Anderson, T.-H. 1998. Interactive effects of pH and substrate quality on the fungal-to-bacterial ratio and QCO_2 of microbial communities in forest soils. *Soil Biol. Biochem.* 30: 1269–1274.

Brookes, P.C. and McGrath, S.P. 1984. Effects of metal toxicity on the size of the soil microbial biomass. *J. Soil Sci.* 35: 341–346.

Heilmann, B., Lebuhn, M., and Beese, F. 1995. Methods for the investigation of metabolic activities and shifts in the microbial community in a soil treated with a fungicide. *Biol. Fert. Soils.* 19: 186–192.

Imberger, K.T. and Chiu, C.-Y. 2001. Spatial changes of soil fungal and bacterial biomass from a sub-alpine coniferous forest to grassland in a humid, sub-tropical region. *Biol. Fert. Soils.* 33: 105–110.

Kaiser, E.-A., Müeller, T., Joergensen, R.G., Insam, H., and Heinemeyer, O. 1992. Evaluation of methods to estimate the soil microbial biomass and the relationship with soil texture and organic matter. *Soil Biol. Biochem.* 24: 675–683.

Lin, Q. and Brookes, P.C. 1999. An evaluation of the substrate-induced respiration method. *Soil Biol. Biochem.* 31: 1969–1983.

Lynch, J.M. and Panting, L.M. 1980. Cultivation and the soil biomass. *Soil Biol. Biochem.* 12: 29–33.

Martens, R. 1987. Estimation of microbial biomass in soil by the respiration method: importance of soil pH and flushing methods for the measurement of respired CO_2. *Soil Biol. Biochem.* 19: 77–81.

Nakamoto, T. and Wakahara, S. 2004. Development of substrate induced respiration (SIR) method combined with selective inhibition for estimating fungal and bacterial biomass in humic andosols. *Plant Prod. Sci.* 7: 70–76.

Paul, E.A. and Voroney, R.P. 1980. Nutrient and energy flows through soil microbial biomass. In D.C. Ellwood, J.N. Hedger, M.J. Latham, J.M. Lynch, and J.H. Slater, Eds. *Contemporary Microbial Ecology*, Academic Press, London, New York, NY, pp. 215–237.

Ross, D.J. 1980. Evaluation of a physiological method for measuring microbial biomass in soils from grasslands and maize fields. *NZ J. Sci*. 23: 229–236.

Smith, J.L., McNeal, B.L., and Cheng, H.H. 1985. Estimation of soil microbial biomass: an analysis of the respiratory response of soils. *Soil Biol. Biochem*. 17: 11–16.

Smith, J.L. and Paul, E.A. 1990. The significance of soil biomass estimations. In J.M. Bollag and G. Stotzky, Eds. *Soil Biochemistry*, Marcel Dekker, New York, NY, pp. 357–396.

van Veen, J.A., Ladd, J.N., and Amato, M. 1985. Turnover of carbon and nitrogen through the microbial biomass in a sandy loam and a clay soil incubated with (^{14}C(U))glucose and $^{15}N(NH_4)2SO_4$ under different moisture regimes. *Soil Biol. Biochem*. 17: 747–756.

Velvis, H. 1997. Evaluation of the selective respiratory inhibition method for measuring the ratio of fungal:bacterial activity in acid agricultural soils. *Biol. Fert. Soils*. 25: 354–360.

Wardle, D.A. and Parkinson, D. 1990. Response of the soil microbial biomass to glucose, and selective inhibitors, across a soil moisture gradient. *Soil Biol. Biochem*. 22: 825–834.

West, A.W. and Sparling, G.P. 1986. Modifications to the substrate-induced respiration method to permit measurement of microbial biomass in soils of differing water contents. *J. Microbiol. Meth*. 5: 177–189.

Chapter 40
Assessment of Soil Biological Activity

R.P. Beyaert
Agriculture and Agri-Food Canada
London, Ontario, Canada

C.A. Fox
Agriculture and Agri-Food Canada
Harrow, Ontario, Canada

40.1 INTRODUCTION

Methods are available for characterizing the diversity of soil organisms to quantify their numbers and biomass, and to identify these populations at a given time (Phillipson 1971). Soil biota populations are never static with respect to diversity, population abundance, and biomass. Soil biota can be influenced positively and negatively by land management and land use thereby affecting both the extent of their activity in the soil and their dynamic contributions to soil processes (Curry et al. 1998; Fox et al. 2003).

Increased knowledge that soil organisms are actively involved in crop residue decomposition and organic matter formation and turnover has emphasized the need to quantify and identify the soil biomass, as well as understand the functional dynamics of this soil population. The rate of decomposition or breakdown of organic matter over time provides a measure of the overall soil biological activity by allowing a measure of the change in an organic substrate that integrates the numerous physical, chemical, and biological activities within soil.

This chapter describes two different methods for determining biological activity in soil. Both of these methods have been identified as useful tools for this assessment in a recent review that used ecological relevance, ease of use, and standardization as criteria (Knacker et al. 2003). The first, the litterbag technique, estimates the rate of decomposition of an organic substrate by determining its mass loss over time. The second, the bait-lamina method, estimates the soil biological activity by measuring the feeding activity of soil organisms under field conditions over a designated time period.

40.2 LITTERBAG ASSESSMENT OF BIOLOGICAL ACTIVITY

The litterbag method, originally developed by Bocock and Gilbert (1957), is a commonly used direct measure of plant residue decomposition as a result of biological activity. The litterbag technique has been used to assess the effects of various environmental factors, such as temperature (Christensen 1985a; Moore 1986; Henriksen and Breland 1999); moisture (Moore 1986; Andrén et al. 1992) and seasonal fluctuations (Quested et al. 2005); the decomposer species involved in decomposition (Vreeken-Buijs and Brussaard 1996; Curry and Byrne 1997); resource quality (Christensen 1986; Robinson et al. 1994); soil type (Christensen 1985b); various management practices such as tillage (Burgess et al. 2002, 2003), residue incorporation, and removal (Curtin and Fraser 2003); time of residue incorporation (Beare et al. 2002); and weed-management strategies (Wardle et al. 1993, 1994; Yadvinder-Singh et al. 2004) on the breakdown of organic material.

The technique is based on the loss in mass of a known quantity of organic material with time and, therefore, provides an assessment of the activity of soil organisms. The organic material is contained within sealed bags made of nondegradable mesh material and is either left exposed on the soil surface or buried in the soil for various periods. Once retrieved, the amount of residue remaining or the loss in mass after various time periods is determined and then used as a measure of the amount of decomposition that has occurred.

The method provides a simple, affordable means of estimating the biological activity involved in the decomposition process. Its advantages include the following: mass loss measurements requiring common, simple instrumentation, confinement of residues within a material that allows access to the crop residues by soil organisms, easy retrieval of the residues, and exposure of the litterbag contents to the environment by allowing penetration by rain, sun, and wind through the mesh material. While studies investigating sources of contamination with mineral (Herrick 1995; Potthoff and Loftfield 1998; Idol et al. 2002) or organic debris (Rustad 1994; Cortez and Bouché 1998) and others comparing the litterbag method with other measurements of residue decomposition (Cogle et al. 1987; Knacker et al. 2003; Kurz-Besson et al. 2005) have outlined some of the limitations of the litterbag method, the benefits of the procedure outweigh its drawbacks and the method provides a reliable index for comparing biological activity in different environments and under different management practices.

40.2.1 Materials and Reagents

1 Rotating drum mixer

2 Nylon or fiberglass mesh with suitable sized openings (see Comments 1 and 2 in Section 40.2.7)

3 Brush or mist sprayer

4 Aluminum cans for moisture determination

5 Drying oven

6 Muffle furnace

7 Ceramic crucibles

8 2.5 *M* HCl; dilute 208 mL of concentrated HCl to 1 L

9 Desiccator

10 Metal or plastic tags and thin wire

11 Metal tethering stakes for surface applied residues

12 ''Zipper-type'' resealable polyethylene bags

40.2.2 Residue Collection and Processing

1 Collect crop residues by randomly sampling the portion above and below the ground of the crop from a known area in the field and removing the harvestable portion of the crop.

2 Weigh the fresh crop residues and store in a cool, dry area until just before determining dry matter and ash content of the residues.

3 Oven-dry aluminum moisture cans, cool in a desiccator, and weigh to the nearest 0.1 mg.

4 Weigh a 5 g subsample of fresh residues into a preweighed aluminum moisture can.

5 Dry the uncovered can in a drying oven at 65°C until weight loss ceases.

6 Cool the aluminum can and dried residues in a desiccator until constant weight and calculate the percent of dry matter.

7 Grind the dried sample used in the dry matter determination to pass through a 1 mm sieve.

8 Thoroughly wash and rinse the ceramic crucibles with 2.5 *M* HCl with deionized water, respectively.

9 Oven-dry the crucibles, cool in a desiccator, and weigh to the nearest 0.1 mg.

10 Weigh 5–10 g of the ground crop residue into a preweighed crucible, oven-dry the residues with crucible at 100°C until they weigh constant, cool in desiccator, and weigh to the nearest 0.1 mg.

11 Place the crucible containing the dried residues in a muffle furnace at 500°C for 4 h.

12 Cool the crucible containing ash in desiccator, weigh to nearest 0.1 mg, and calculate the ash content of the residue.

13 Determine the amount of residue addition per unit area by calculating the dry, ash-free residue weight of residues per area sampled.

14 Cut the residues to approximately 5 cm lengths and mix thoroughly by tumbling in a rotating drum mixer such as a cement mixer.

15 Preprocess the mixed residues by passing them over a screen with a slightly larger mesh opening than the mesh material used to construct the litterbags to remove residue particles smaller than the mesh openings. This procedure minimizes the losses of material during loading, transportation, and installation of the litterbags.

16 Determine the amount of fresh residue required to equal the amount approximating the residue inputs per area of the various treatments calculated from the harvesting procedure above. The amount of fresh residues added to each litterbag can be estimated by calculating the appropriate residue addition per litterbag area when the litterbag is installed horizontally. The weight of residue is corrected to provide the residue additions on an ash-free, dry residue basis.

40.2.3 Litterbag Construction

1 Cut strips of the mesh material to the required length and width. The number of strips required will be twice that of the number of bags required for the study. Alternatively, strips can be cut to twice the width and folded in half to reduce the number of sides to be sealed. The number of bags required can be calculated by determining the number of retrieval times by the number of treatments times the number of replicates in the study.

2 Construct the required number of litterbags by sealing three of the four sides of mesh strips together by heat sealing, stapling, or sewing with nylon thread. Additional ''traveler'' litterbags are constructed to allow a determination of the litter loss during transport and handling during the installation procedure as outlined by Harmon et al. (1999).

3 Calculate the required amount of fresh crop residues required per litterbag.

4 Weigh the calculated amount of fresh crop residues to the nearest 0.01 g and place the residues into the open side of each litterbag including traveler litterbags. Seal the opening to completely enclose the residue within the bag. Attach an aluminum or plastic tag with the appropriate identification codes to the bag with thin wire. Identification codes should outline the site, treatment, and replication and removal time for each litterbag.

40.2.4 Litterbag Installation

1 Carefully transport all litterbags to the field site. Traveler litterbags should also be transported to the site and handled in the same fashion as the other bags.

2 Install the litterbags into the field plots. For plots that are managed under conventional and minimum tillage, the litterbags should be buried horizontally within the tillage layer. Soil should be removed from the tillage layer to the depth of burial and the litterbag is placed in the void as flat as possible to ensure contact with the soil and covered with the soil originally removed. The wire attaching the tag to the bag should be of sufficient length so that the tag remains at the soil surface when

the bags are buried to allow easy identification. For surface placed residues, such as in no-tillage management, the litterbag should be placed flat on the soil surface, with tags visible and tethered to the soil by metal stakes to ensure contact with the soil surface. The bags located within the same plot but retrieved at different times should be placed in a random order and far enough apart to reduce the effects of spatial autocorrelation.

3 Traveler litterbags should be retrieved immediately after placement in the field and the residues processed and reweighed to the nearest 0.01 g. The initial ash-free, dry weight of the residue in the litterbags is corrected for the determined loss due to transport and handling.

40.2.5 Litterbag Retrieval and Processing

1 At various times from the initial litterbag placement, the bags should be retrieved from the field. Since loss in mass occurs at a faster rate during the initial phase of the decomposition, retrieval times can be spaced more closely initially and spaced further apart during the latter stages of the study to allow detection of the large changes occurring during the initial decomposition phase. It is important to handle the litterbags with care during retrieval to ensure that the decomposing residues do not fragment and fall out of the bags before processing. Any fragmentation or loss of material should be recovered as best as possible and recorded. The retrieved bags are placed into a labeled, polyethylene resealable bag, and sealed in the field and carefully returned to the laboratory.

2 Remove the litterbag from the polyethylene bag and carefully remove any soil and living plant material adhering to the surface of the bag before further processing. The contents of each retrieved bag are then removed and cleaned by brushing or washing under a mist sprayer to remove loosely adhering soil particles.

3 Uncorrected dry weight of the residue contained in each of the retrieved bags is determined by oven-drying at 65°C until weight loss has ceased and weighing the dried residue contained in a bag to the nearest 0.01 g.

4 Grind the residues in a Wiley mill to pass through a 1.0 mm sieve.

5 Determine the ash content of the retrieved residue by dry ashing a ground subsample of the retrieved litter in a muffle furnace at 500°C for 4 h as described in Section 40.2.2.

6 Correct the dry weight of the litterbag contents to an ash-free, dry weight basis to account for the effects of soil contamination in the litterbags by subtracting the gain in ash content from the dry weight of the litterbag contents.

40.2.6 Calculations

Determination of Dry Matter Weight of Fresh Residues

Calculate the percent dry matter of the residues as

$$\mathrm{DM}_{\%} = (1 - \{[(X_\mathrm{i} - X_\mathrm{c}) - (X_\mathrm{d} - X_\mathrm{c})]/(X_\mathrm{i} - X_\mathrm{c})\}) \times 100 \qquad (40.1)$$

where $DM_{\%}$ is the percent dry matter weight of the residues, X_i is the initial wet weight of the residues plus the aluminum can, X_c is the dry weight of the aluminum can plus lid, and X_d is the dry weight of the residues plus the aluminum can.

Calculate the dry weight of the residues as

$$DM_R = X_T \times \left(\frac{DM_{\%}}{100}\right) \tag{40.2}$$

where DM_R is the dry matter weight of the collected residues, X_T is the total fresh weight of the collected residues, and $DM_{\%}$ is the percent dry matter weight of the residues.

Correction for Ash Content of Residues

Calculate the percent ash content of the residues as

$$A_{Ri} = \left[\frac{(X_{apc} - X_{pc})}{(X_{dpc} - X_{pc})}\right] \times 100 \tag{40.3}$$

where A_{Ri} is the percent ash content of the residues, X_{apc} is the dry weight of the ash and ceramic crucible, X_{pc} is the weight of the dry ceramic crucible, and X_{dpc} is the dry weight of the residue and ceramic crucible.

Correct the dry mass weight of the residues for ash content as

$$DM_{AFR} = \{DM_R - [DM_R \times (A_{Ri}/100)]\} \tag{40.4}$$

where DM_{AFR} is the ash-free, dry weight of the residues collected, DM_R is the dry matter weight of the collected residues, and A_{Ri} is the percent ash content of the residues.

Determination of Ash-Free, Dry Weight of Residues per Unit Area

Calculate the ash-free residue weight per square meter as

$$DM_{AFRM} = DM_{AFR}/A_m \tag{40.5}$$

where DM_{AFRM} is the ash-free, dry weight of residue per square meter, DM_{AFR} is the ash-free, dry weight of the residues collected, and A_m is the area over which the sample was obtained in square meters.

Determination of the Amount of Fresh Residue to Add to Litterbag

The area represented by the litterbag can be calculated as

$$A_L = L \times W \tag{40.6}$$

where A_L is the area of the litterbag in square meters, L is the length of the litterbag in meters, and W is the width of the litterbag in meters.

Calculate the dry, ash-free weight of residue to add to each litterbag as

$$\mathrm{DM_{AFLi}} = \mathrm{DM_{AFRM}} \times A_{\mathrm{L}} \tag{40.7}$$

where $\mathrm{DM_{AFLi}}$ is the ash-free, dry weight of residue per litterbag, $\mathrm{DM_{AFRM}}$ is the ash-free, dry weight of residue per unit area, and A_{L} is the area of the litterbag in square meters.

Calculate the weight of fresh residues to add to each litterbag as

$$R_{\mathrm{FL}} = \{\mathrm{DM_{AFLi}} + [\mathrm{DM_{AFLi}} \times (A_{\%}/100)]\} \times (1/\mathrm{DM_{\%}}) \tag{40.8}$$

where R_{FL} is the weight of fresh residues to add to the litterbag, $\mathrm{DM_{AFLi}}$ is the ash-free, dry weight of residue per litterbag, $\mathrm{A_{\%}}$ is the percent ash content of the residues, and $\mathrm{DM_{\%}}$ is the percent dry matter weight of the residues.

Correction for Loss due to Transport and Handling

Calculate the final ash-free, dry weight of residue contained in the litterbags after transport and handling as

$$\mathrm{DM_{RAFLic}} = \sum \mathrm{DM_{AFT}}/n \tag{40.9}$$

where $\mathrm{DM_{RAFLic}}$ is the ash-free, dry matter weight of the residues contained in the installed litterbags, $\mathrm{DM_{AFT}}$ is the ash-free, dry weight of the residues contained in the collected traveler litterbags, and n is the number of traveler litterbags used to determine the losses due to transport and handling.

Correction for Ash Content in Retrieved Litterbag Material

Calculate the percent ash content of the contents of the retrieved litterbag as

$$A_{\mathrm{Lt}} = [(X_{\mathrm{apct}} - X_{\mathrm{pct}})/(X_{\mathrm{dpct}} - X_{\mathrm{pct}})] \times 100 \tag{40.10}$$

where A_{Lt} is the percent ash content of the retrieved litterbag material, X_{apct} is the dry weight of the ash plus ceramic crucible, X_{pct} is the weight of the dry ceramic crucible, and X_{dpct} is the dry weight of the retrieved litterbag material and ceramic crucible.

Calculate the ash-free, dry weight of the retrieved litterbag material as

$$\mathrm{DM_{AFLt}} = \mathrm{DM_{Lt}} - [\mathrm{DM_{Lt}} \times (A_{\mathrm{Lt}}/100)] \tag{40.11}$$

where $\mathrm{DM_{AFLt}}$ is the ash-free, dry weight of the retrieved litterbag material, $\mathrm{DM_{Lt}}$ is the dry weight of the retrieved litterbag material, and A_{Lt} is the percent ash content of the retrieved litterbag material.

Calculation of Mass Loss and Percent Residue Remaining

The proportion of mass loss can be calculated with the following calculation:

$$\%\ M_t = [(\mathrm{DM_{AFLic}} - \mathrm{DM_{AFL}}t)/\mathrm{DM_{AFLic}}] \times 100 \tag{40.12}$$

where $\%\ M_t$ is the percent mass loss at retrieval time t, DM_{AFLt} is the ash-tree, dry weight of residue remaining at retrieval time t, and DM_{AFLic} is the corrected initial ash-free, dry weight of residue contained in the litterbag. Conversely, the percent dry weight remaining at each retrieval time is calculated with the following calculation:

$$\%\ R_t = (DM_{AFLt}/DM_{AFLic}) \times 100 \tag{40.13}$$

where $\%\ R_t$ is the percent weight remaining at retrieval time t, DM_{AFLt} is the ash-free, dry weight of residue remaining at retrieval time t, and DM_{AFLic} is the corrected initial ash-free, dry weight of residue contained in the litterbag.

40.2.7 Comments

1 Measurement of the decomposition of crop residues in the field with the litterbag technique presents a number of problems that are related to the underlying assumption that weight loss due to decomposition occurs at the same rate in the artificial environment of the litterbag created as that occurring without the litterbag. The construction of the litterbags will influence both the abiotic and biotic factors that affect the decomposition of crop litter. The size of the litterbags will affect the spatial variability of the factors influencing decomposition, such as microclimate or the occurrence of soil fauna and flora. Most studies have used litterbags ranging in size from 15 to 600 cm^2 (Knacker et al. 2003). However, larger litterbags with sides up to 30–46 cm in length and a size of 1300 cm^2 have been used (Baker III et al. 2001). To minimize the effects of poor soil–residue contact with this technique, the length and width of the final litterbag should ensure that the thickness of the residues is minimized and should be similar to that which would occur without the mesh bag. For litterbags that are buried within a tillage layer, the amount of residues contained in the litterbag may be corrected for the volume rather than surface area occupied by the litterbag.

2 Increasing the mesh size of the litterbag material increases the access to the residues by soil fauna, reduces the artificial effects of microclimate, and increases the potential loss of fragmented material. Therefore, the mesh size of litterbags is usually selected to minimize the undesired loss of residue and the maintenance of natural conditions within the litterbags. The 2.0 mm mesh size indicated above is small enough to allow free entry of soil fauna yet is sufficiently small to minimize losses of the decomposing residues. In some cases, litterbags with smaller mesh sizes on the bottom surface and larger mesh sizes on the top surface have been used to minimize these adverse affects (Baker III et al. 2001). In some studies, litterbags of varying mesh sizes have been used to exclude soil organisms by size and have allowed a comparison of the contributions of soil organisms of varying sizes to the decomposition process (Vreeken-Buijs and Brussaard 1996; Curry and Byrne 1997; Cortez and Bouché 1998). Others have used an additional set of litterbags treated with naphthalene to inhibit the activity of microarthropods and determined the rate of litter decomposition with and without microarthropod activity (Heneghan et al. 1998).

3 Material placed into the litterbag should as closely as possible resemble the material that is returned to the field to allow an estimate of the decomposition rate under field conditions. Therefore, the crop residues should be collected at harvest and processed in such a way that the material has a similar architecture

and quality as those in the field. In many litterbag studies, the residues have been cut into fragments of 2–5 cm in length to retain their structural integrity and allow uniform mixing of the various plant parts yet minimize the adverse affects on the microclimate within the litterbags. Such crop residues include very different plant materials, which have different palatabilities and thus, decomposition rates. If the material is not similar in each of the litterbags, there is an increasing variability in the amount of material remaining among the litterbags. Therefore, when dividing the material into portions for each litterbag, it may be advisable to weigh the appropriate amount of each plant component (i.e., leaves, stem, pods) for each litterbag rather than mixing the plant parts and weighing the appropriate amount of combined plant residues for each litterbag. Depending on the aim of the study, the decomposition for each plant part can be followed by placing each plant part into its own litterbag to alleviate the variability associated with mixing plant parts.

4 Processing the residues before its addition to the field should be minimized to reduce the adverse affects on residue quality. Air-dried forest-leaf litter has been shown to have significantly slower rates of decomposition than fresh-leaf litter and resulted in gross underestimates of the rate of mass loss when air-dried leaves were used in litterbag studies (Taylor 1998). Cold-water extraction has resulted in a substantial loss in water-soluble constituents from barley straw and lead to a ''lag phase'' during the initial stages of decomposition and slower overall decomposition rates compared to untreated straw (Christensen 1985a). Therefore, it is recommended that the residues added to the litterbags not be dried or washed before installation into the field. The initial dry matter weight should be corrected for moisture and ash content as described above.

5 Residues in the retrieved litterbags may be contaminated with external material leading to an underestimation of the actual decomposition of the litterbag material. Various cleanup procedures such as hand removal, and brushing and washing with water have been used to remove foreign material from the retrieved residues during decomposition studies using the litterbag procedure (Andrén et al. 1992; Wardle et al. 1993; Cortez and Bouché 1998). While hand picking and brushing lead to incomplete removal of organic and mineral contaminants, washing procedures undoubtedly remove water-soluble materials from the residues. Cold-water extraction following an incubation period resulted in removal of substantial amounts of nutrients and increased mass loss compared to untreated straw (Christensen 1985a). For this reason, cleaning the retrieved residues by washing with water should be kept to a minimum to reduce losses in mass due to leaching of nutrients and the resulting overestimates of decomposition rates.

6 It has been assumed that correcting the dry weight of the litterbag material for ash content has corrected for contamination by mineral material in most litterbag studies. However, some researchers have argued that contamination with mineral and organic material in litterbags can be significant and that other adjustments for contamination should be made (Christensen 1985b; Blair 1988; Idol et al. 2002). Blair (1988) and Christensen (1985b) have provided equations to correct for contamination by adjusting for the ash content of the soil outside the litterbag assuming that the composition of the soil inside and outside the litterbag is similar. This correction procedure would slightly underestimate the residue mass loss if smaller soil particles preferentially enter the litterbags (Christensen 1985b), but

was preferable to simply calculating residue mass loss as the percent of ash-free, dry matter remaining (Blair 1988). Idol et al. (2002) described a procedure in which a correction for mineral and organic contamination was determined by subtracting the gain in weight of field-incubated litterbags containing a non-decomposable control material at each retrieval time. This method resulted in significantly higher decomposition rates than those determined using uncorrected or ash-free, dry weight corrected weights.

7 Assessment of the biological activity can be made by examining differences in either the proportion of mass loss or the proportion of residue remaining at various times among the treatments means. The most common statistical method of examining this type of data is with an analysis of variance. In these comparisons, values at $t = 0$ are not included since the mean percent remaining at $t = 0$ is 100 for all treatments. In addition to statistical comparisons involving an analysis of variance, the treatment trends can be compared by fitting the decomposition data to mathematical models to estimate decay constants that describe the loss in mass over time. Model selection has been based on both the mathematical properties of the model and the relationships between the models and the biology involved in residue decomposition. In some cases, these models have been modified to include the effects of temperature and moisture (Andrén et al. 1992) or the data corrected for the effects of moisture and temperature before fitting the data to the model (Moore 1986) to allow for the influence of these driving variables on the decomposition process. A comprehensive review of the merits, disadvantages, and potential interpretation problems associated with the use of analysis of variance and the use of mathematical models to describe the data can be found in Wieder and Lang (1982).

8 Assessment of results from litterbag studies can clearly be improved when the study site is well characterized. Such a characterization would include a description of soil and site properties (e.g., pH, texture, water-holding capacity, vegetation, climate), usage of the site, as well as biological data (e.g., on the abundance of earthworms or the microbial biomass). This is especially important when measuring the impact of anthropogenic stress like pesticides on decomposition processes, since the fate of chemicals in soil is influenced by the soil organism community (Singer et al. 2001). The influence of predators on litter decomposition by feeding on saprophagous animals of the meso- and macrofauna is usually indirect, but there is evidence showing that exclusion of top predators might affect the activity of the soil microflora with concomitant changes in the decomposition rate of organic matter (Lawrence and Wise 2000). The relative importance of microorganisms compared to soil animals varies with environmental conditions. In general, the influence of soil animals on decomposition increases with harsh environmental conditions such as drought or low temperatures (Tian et al. 1997).

40.3 BAIT-LAMINA PROCEDURE

Bait-lamina strips are used to monitor the overall feeding activity of soil organisms for accessing a carbon source introduced into the soil. Originally designed by von Törne (1990) and applied by others (Larink 1993; Kratz 1998), the bait-lamina strip consists of a thin strip of plastic (approximately 6 mm wide by 15 cm long) with a total of 16 drilled 2 mm diameter

holes, each at 0.5 cm interval for a total monitoring length of 8 cm. An organic-based material attractive to soil organisms is prepared and pressed into the holes. Generally, 16 strips are inserted into the soil for a specific time period (usually for 14 days) to allow for feeding by the soil organisms. When each set is removed from the soil, the percentage of emptied holes in comparison with the total number of holes represents the feeding activity of soil biota at each depth interval for accessing a carbon-based source.

40.3.1 Materials

1. Cellulose paper (acid washed, ashless, for column chromatography) (from J.T. Baker Chemical Co. 1-5225). An alternative Sigma Chemical Co. Cellulose Microgranular EC No 232-674-9 [9004-34-6] C-6413. Purchase 1 kg size.

2. Bentonite clay. Available from American Colloid Company. VOLCLAYHPM-20. http://www.colloid.com/AGP/Tech/Volclay%20HPM-20.pdf

3. Agar-agar (gum agar). No. A-7002. Available from Sigma Chemical Co. May be other sources for agar-agar.

4. Wheat bran (Quaker oats). Available from grocery store. Must be ground as fine as possible to pass through a 0.5 mm sieve. Grind bran in a plant tissue grinder until it has the particle size range as the other ingredients.

5. Bait-lamina strips. Available only from following: terra protecta GmbH, Himbeersteig 18, D-14129 Berlin, Germany (http://www.terra-protecta.de).

6. Distilled water, wide-mouthed plastic or glass container (250–500 mL size) with lid, small spatula, spoon, plastic or latex gloves, flexible putty knives, thick plastic sheet, saran wrap, plastic trays, boxes or plastic bags for holding completed sets of bait-lamina strips.

7. Light box or light table.

8. Steel probe with sturdy wooden handle for making pilot hole in soil. The steel probe should be thin and slightly wider than the width of strips and its length should be at least 15 cm; the steel probe should be thick enough not to bend under pressure of pushing; a 908 gm (2 lb) sledge hammer may be needed for inserting the probe into medium-to-strongly compacted soils, where pushing the probe by hand is difficult.

9. Template (6.4 mm) plywood with 16 holes drilled the width of steel probe: Drill four rows of four holes with 10 cm spacing in a 4×4 pattern. Other configurations of board length and number of drilled holes can be used as needed. The use of a template is optional depending on nature of project and the strips may be placed randomly into the soil.

10. Soil corer, soil thermometer (15 cm length), aluminum cans for soil-moisture sample or time-domain reflectometry (TDR) moisture meter, field flags (76–92 cm length).

40.3.2 Preparation of Bait-Lamina Strips

Before starting, wash the strips thoroughly with soap and water to remove any residual material from both new and previously used strips and rinse with distilled water. Some research protocols may require rinsing the bait-lamina strip in a hypochlorite or 70% ethanol to sterilize the strips before using.

Ingredients for bait mixture are as follows:

1 Cellulose paper 6.5 g

2 Agar-agar 1.5 g

3 Bentonite clay 1.0 g

4 Wheat bran 1.0 g

5 Distilled water

40.3.3 Preparation of Bait-Lamina Strips for Insertion in Field

1 With permanent marker, place a line at the 0 cm point across both sides of the strip.

2 Weigh all dry ingredients outlined in Section 40.3.2 into a plastic or glass container. *Caution*: Ingredients (1 to 4) are fine-powder ingredients and will disperse readily. Wear appropriate breathing mask and clothing as recommended in material safety data sheets.

3 Wear latex/plastic gloves during preparation of bait strips. Add small quantities (5–10 mL at a time) of distilled water to the dry ingredients and thoroughly mix the materials with a spatula until a damp (not saturated) fine-to-medium granular paste with a consistency similar to cookie dough is attained. Complete the mixing of the parts with the spatula or by hand to achieve a smooth consistency of the bait material. Do not let the paste become wet and soggy as it will not adhere to the holes.

4 Procedure for filling the strips:

   i) By hand: Place a plastic sheet on the bench (easier to cleanup). Wear gloves to protect hands. Take a small quantity of paste from the container and with thumb and index finger squeeze the bait material along the series of holes using a downward movement to push as much bait as possible into the holes, with pressure on the fingers, smooth the bait across the hole opening such that the level of bait is even with the plastic strip, do not overfill the holes; do not reverse the direction of application as this will tend to pull applied material out of the holes.

   ii) By knife: If numerous strips are needed, inserting the bait by hand can be extremely tiring. A flexible putty knife or a similar implement can be used to push the paste into the holes. Place the plastic sheet on laboratory bench, and

then lay several strips down on the plastic sheet and with the putty knife push and squeeze as much paste into the holes as possible on one side then flip the strips over and repeat application of bait.

5 When the paste fills the holes in the strip, set to dry by placing the strip at an angle on the rim of the tray (dries completely in 1–2 h). Following the first application of paste, it will be normal that the bait in most of the holes will have shrunk resulting in partially filled holes, or holes with shrinkage cracks. A second (or even third) application of paste will be necessary to achieve complete filling. Repeat step 4 to apply a second coating of bait material.

6 After the second application, place the dried strip onto the light table or light box, to determine if light is visible through any of the holes. If light is visible or some holes are still partially filled, a third coating will be necessary.

7 When the strips are dry, carefully clean away any excess bait remaining on the strip around the holes with a dissecting needle or metal spatula. Make a final check that there is no light transmission through the holes. The strips are now ready for packaging for field insertion.

8 Count individual sets of 16 strips and place the set of strips in a plastic bag or box used as a carrying container in the field. A set of 16 strips is the literature standard for field assessment that is most often used for monitoring soil biological activity, but, if needed, other combination of reduced number of strips can be used. But it should also be noted that this can affect the variability of results.

40.3.4 Field Placement of Bait Lamina

1 Locate sampling area in field. Position the template board on soil surface. Near the template board, insert soil thermometer and let equilibrate (approximately 1 min before recording). Remove the set of strips from the carrying container or plastic bag.

2 Holding onto the template board, make a pilot hole into the soil by inserting the steel probe through one of the holes in the template. Push the probe by hand (or if needed use a hammer) into the soil far enough to account for both the 8 cm length of strip plus the space under the template board as it rests on the soil surface. Remove the steel probe and insert one strip into the pilot hole. Work with one hole at a time. When all 16 strips are inserted through the holes in the template, carefully lift the template board off the soil surface and set aside. Adjust the level of each strip in the pilot hole so that the marked 0 cm line on the strip is even with the soil surface then using thumb and index finger pinch the soil tight about the 0 cm line to firmly set the strip into the soil.

3 Record the soil temperature.

4 Take core sample of soil to measure gravimetric soil moisture. In close proximity to the inserted set of strips, with the soil core sampler, remove a 10 cm core of soil for measuring field moisture content at the time of insertion of the strips. Place the soil sample into the moisture can. Alternatively, if available, a TDR moisture meter (see Chapter 70) can be used to record site soil-moisture at each

sampling point. Soil-moisture and temperature data are needed to account for soil conditions at the time of monitoring, that is, at time of insertion of strips and at time of removal.

5 Place field-marking flags around the sampling area approximately 30 cm away from each of the four corners of the strips to quickly locate the strips on returning to the field, to identify the sample site location, and to alert others not to walk or drive over this area in the field.

40.3.5 Field Removal of Bait Strips

1 Remove the field flags. Insert the soil thermometer near the sample set to equilibrate.

2 Pull each strip slowly from the soil and place it carefully into plastic bag labeled with field identification, count all strips before leaving sampling site (this is very important to ensure that all of the strips have been removed). If the soil is very moist, often there will be a visible film of water on the strip. Set the strip aside to dry off somewhat before placing in the plastic bag or using a soft tissue paper, carefully pat off the excess water before placing in the plastic bag.

3 Take 10 cm soil core sample and place in soil-moisture can for determining gravimetric water content; or, use electronic TDR moisture probe. Record soil temperature.

4 Place sets of strips in refrigerator until able to assess. Prior to assessing strips if material in the holes is still moist, place the set of 16 strips out in a flat dish or container to dry completely (about 1–2 h). Having the material completely dry in the strips is essential for proper assessment of the holes.

40.3.6 Recording Bait-Lamina Data

1 Use a recording sheet to manually assess each individual strip for completely empty holes (see Figure 40.1). For half-eaten holes, one must examine the individual holes on both sides of the strip. For half-eaten holes, it will be very obvious that the bait has been completely removed from one side of the strip but still remains full on the opposite side of the strip. Only record those holes as half-eaten where the bait is completely missing on one side. Do not record holes with only a small portion of bait missing; these missing areas are likely artifacts from the insertion of the bait and not the result of feeding activity. If there are shrinkage cracks present in the bait material, which are obvious on the edges of the holes, do not record the holes.

2 A digital scanner can be used to keep a permanent record of each set. The scanned image of the set of strips can be used as a quality check for manual reading and for presentations.

3 When recording is complete, the strips can be cleaned and prepared for reuse. Soak the strips in water overnight. Use a toothbrush or a small brush to clean remnants from the holes, let strips dry then refill with bait for reuse.

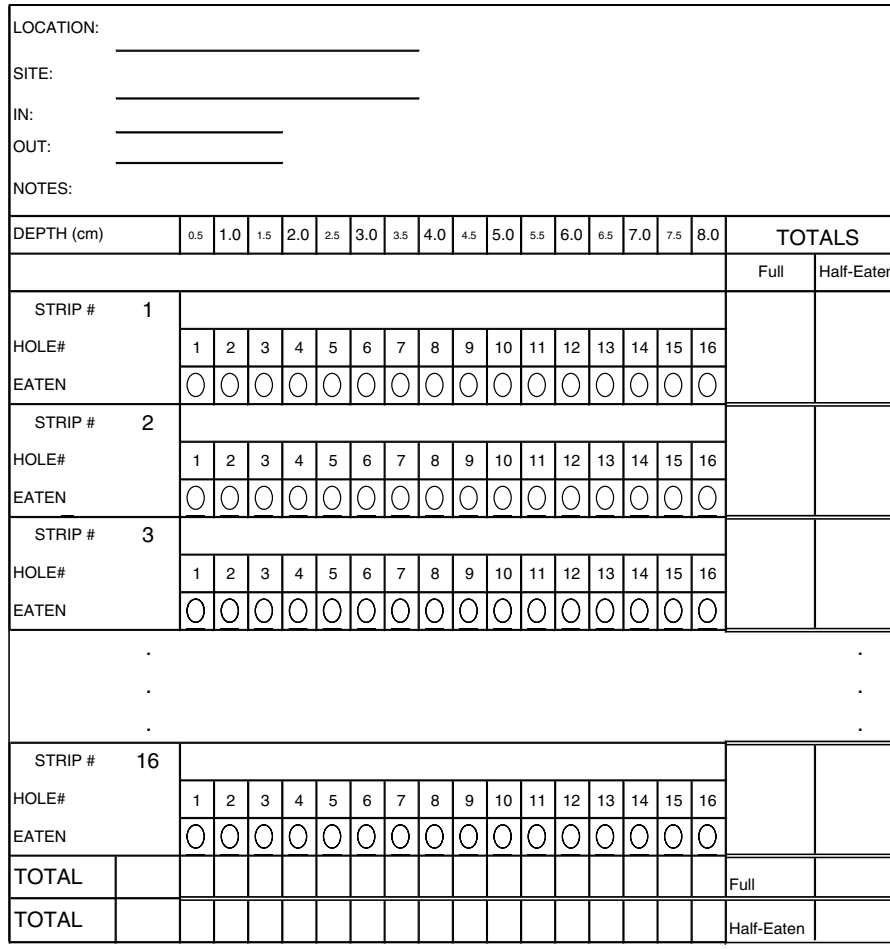

FIGURE 40.1. Data-recording sheet for bait-lamina strip assessment of biological activity. Completely empty (fully eaten) holes are recorded by coloring in the circle; half-eaten holes are marked with a diagonal through the circle. The numbers of fully eaten and half-eaten holes are tallied for each strip along the right-hand side and for each depth interval at the bottom of the sheet. (Designed by J. Miller, AAFC, London, Ontario.)

4 Data on the number of empty and half-eaten holes are tabulated and analyzed to determine the percent of biological or feeding activity with each 0.5 cm interval with 8 cm depth.

40.3.7 Comments

1 Recipe for the bait mixture is based on protocols for the standardization of the bait-lamina assay that were recommended at a workshop in Braunschweig, Germany (Larink and Kratz 1994; Helling et al. 1998). Other bait mixtures can be designed to assess specific components of soil biological activity that could include toxicological studies or research related to the remediation of soils.

2 When working with the bait mixture, the paste will dry out. Add a few drops of water to return the paste to working consistency. Cover any unused paste with saran wrap or container lid to reduce drying. If large portions of the paste remain, store it overnight in a refrigerator, otherwise discard it. Do not keep bait material longer than 1 day to prevent mould and bacteria build-up. Always use freshly mixed paste for best results.

3 It is extremely important that no light is visible through any of the holes in the strip as this is the crucial baseline starting point. The test for determining the extent of biological activity is based on an accounting of the holes from where the bait has been removed by soil organism feeding. Consequently, every hole in the series must be completely filled and without shrinkage cracks. Once dried, the bait material will be quite stable in the strip; the bait should not pop out of the hole even if the strips are slightly bent.

4 When inserting the strips into soil that is quite moist and friable to a depth 10 cm or more, the strips can be individually pushed into soil by hand but most times the probe will be needed to make a pilot hole. *Caution*: If soil is compacted, the steel probe must be sturdy enough not to bend or break when pounded into the soil with the small sledge hammer (908 g). It is best to wait until sampling conditions are such that sufficient soil moisture is present to be able to push the probe into soil for the most part by hand.

5 Above-described procedure for field placement is based on inserting the strips into the soil surface layer, which is the most common use. Alternative insertion protocols may involve inserting the strips horizontally at selected depths or use in greenhouse pot studies.

6 Strips are usually left in the soil for 2 weeks (suggested literature time) and then removed. The objective is to achieve a balance between having enough holes emptied such that comparisons between treatments are robust, but the strips are not left in the soil for such a lengthy time period that nearly every hole in each strip is emptied making comparisons of any treatment effect impossible. Longer or shorter time periods can be used to account for soil conditions and project requirements. Best soil monitoring conditions tend to occur when the soil temperature in the 15 cm surface is between 10°C and 20°C and soil-moisture conditions range from slightly moist to field capacity. Usually, in Canada, these soil-moisture and temperature conditions are optimum during spring and fall. If the same site is being monitored several times during the year or over a period of years, in order to obtain consistent comparisons, it is recommended for all future sampling events to adhere as close as possible to the same time interval for each sampling interval. Over time, the different sampling periods will provide a mean range of biological activity accounting for different temperature and moisture conditions. A good strategy at a new site in the first year of monitoring is to undertake more than one sampling event (of set time period) to determine the potential range of activity under different temperature and moisture conditions. For example, spring and fall results may be different and early fall (or spring) may vary from late fall (or spring).

7 When monitoring a new site, additional sets of strips can be placed at the site and their progress checked periodically. A set of test strips can be removed at the end of the 2 weeks time period for assessment of quantity of empty holes. If biological

activity is suspected to be very high at the new site and optimum moisture and temperature conditions prevail, the test strips should be checked earlier (i.e., after the first week). If more than 40% of the holes are empty on more than 10 of the strips, the sets may need to be removed earlier than the 2 week time period. If there are only a few empty holes (<20%) in the complete set of 16 strips, it may be beneficial to leave the strips in for an additional week, particularly if one has reason to believe from other data on soil biota population abundance that the potential for activity may be high at the site.

8 Low activity, that is, finding very few empty holes, in spite of evidence for high populations can often be attributed to current soil-moisture or temperature conditions being less than optimum in the upper 10 cm during the initial 2 week monitoring period, especially if conditions were hot and droughty, or either very wet or very dry moisture conditions combined with prevailing cold temperatures. In addition, some soil types such as coarse sands with very low organic matter content may be naturally low in soil biota diversity and abundance.

9 The strategy for field monitoring is to place out, at a minimum, three replicate sets of strips in order to be able to apply statistical analyses to the data to determine, for instance, means, standard deviation, and standard errors. For example, placing three or more replicates in a field treatment, or alternatively using the field experimental block design to account for replicate samples having as a minimum one set in each treatment per block. It is possible to use less than 16 strips in a set, but care must be taken to assess whether the reduction in number of strips placed out in a set has a significant influence on the resulting data.

REFERENCES

Andrén, O., Steen, E., and Rajkai, K. 1992. Modelling the effect of moisture on barley straw and root decomposition in the field. *Soil Biol. Biochem.* 24: 727–736.

Baker III, T.T., Lockaby, B.G., Conner, W.H., Meier, C.E., Stanturf, J.A., and Burke, M.K. 2001. Leaf litter decomposition and nutrient dynamics in four southern forested floodplain communities. *Soil Sci. Soc. Am. J.* 65: 1334–1347.

Beare, M.H., Wilson, P.E., Fraser, P.M., and Butler, R.C. 2002. Management effects on barley straw decomposition, nitrogen release, and crop production. *Soil Sci. Soc. Am. J.* 66: 848–856.

Blair, J.M. 1988. Nitrogen, sulphur and phosphorus dynamics in decomposing deciduous leaf litter in the southern Appalachians. *Soil Biol. Biochem.* 20: 693–701.

Bocock, K.L. and Gilbert, O.J.W. 1957. The disappearance of leaf litter under different woodland conditions. *Plant Soil* 9: 179–185.

Burgess, M.S., Mehuys, G.R., and Madramootoo, C.A. 2002. Decomposition of grain-corn residues (*Zea mays L.*): A litterbag study under three tillage systems. *Can. J. Soil Sci.* 82: 127–138.

Burgess, M.S., Mehuys, G.R., and Madramootoo, C.A. 2003. Nitrogen dynamics of decomposing corn residue components under three tillage systems. *Soil Sci. Soc. Am. J.* 66: 1350–1358.

Christensen, B.T. 1985a. Decomposability of barley straw: Effect of cold-water extraction on dry weight and nutrient content. *Soil Biol. Biochem.* 17: 93–97.

Christensen, B.T. 1985b. Wheat and barley straw decomposition under field conditions: Effect of soil type and plant cover on weight loss, nitrogen, and potassium content. *Soil Biol. Biochem.* 17: 691–697.

Christensen, B.T. 1986. Barley straw decomposition under field conditions: Effect of placement and initial nitrogen content on weight loss

and nitrogen dynamics. *Soil Biol. Biochem.* 18: 523–529.

Cogle, A.L., Saffigna, P.G., Strong, W.M., Ladd, J.N., and Amato, M. 1987. Wheat straw decomposition in subtropical Australia. I. A comparison of ^{14}C labelling and two weight-loss methods for measuring decomposition. *Aust. J. Soil Res.* 25: 473–479.

Cortez, J. and Bouché, M.B. 1998. Field decomposition of leaf litters: earthworm–microorganism interactions—the ploughing effect. *Soil Biol. Biochem.* 30: 795–804.

Curry, J.P., Bolger, T., and Purvis, G. (Eds.) 1998. Special Issue XII International Colloquium on Soil Zoology: Soil Organisms and Soil Resource Management. Dublin, 22–26 July, 1996. *Appl. Soil Ecol.* 9: 1–543.

Curry, J.P. and Byrne, D. 1997. Role of earthworms in straw decomposition in a winter cereal field. *Soil Biol. Biochem.* 29: 555–558.

Curtin, D. and Fraser, P.M. 2003. Soil organic matter as influenced by straw management practices and inclusion of grass and clover seed crops in cereal rotations. *Aust. J. Soil Res.* 41: 95–106.

Fox, C.A., Topp, E., Mermut, A., and Simard, R. (Eds.) 2003. Soil biodiversity in Canadian agroecosystems. *Can. J. Soil Sci.* 83 (Special Issue): 227–336.

Harmon, M.E., Nadelhoffer, K.J., and Blair, J.M. 1999. Measuring decomposition, nutrient turnover, and stores in plant litter. In G.P. Robertson, D.C. Coleman, C.S. Beldsoe, and P. Sollins, Eds., *Standard Soil Methods for Long-term Ecological Research*. Oxford University Press, New York, pp. 202–240.

Helling, B., Pfeiff, G., and Larink, O. 1998. A comparison of feeding activity of collembolan and enchytraeid in laboratory studies using the bait lamina test. *Appl. Soil Ecol.* 7: 207–212.

Heneghan, L., Coleman, D.C., Zou, X., Crossley, D.A., Jr., and Haines, B.L. 1998. Soil microarthropod community structure and litter decomposition dynamics: A study of tropical and temperate sites. *Appl. Soil Ecol.* 9: 33–38.

Henriksen, T.M. and Breland, T.A. 1999. Decomposition of crop residues in the field: evaluation of a simulation model developed from microcosm studies. *Soil Biol. Biochem.* 31: 1423–1434.

Herrick, J.E. 1995. Simple method for the determination of mass loss rates for soil-contaminated samples in decomposition studies. *Pedobiologia* 69: 74–77.

Idol, T.W., Holzbaur, K.A., Pope, P.E., and Poder, F., Jr. 2002. Control-bag correction for forest floor litterbag contamination. *Soil Sci. Soc. Am. J.* 66: 620–623.

Knacker, T., Förster, B., Römbke, J., and Frampton, G.K. 2003. Assessing the effects of plant production products on organic matter breakdown in arable fields—litter decomposition test systems. *Soil Biol. Biochem.* 35: 1269–1287.

Kratz, W. 1998. The bait-lamina test. *Environ. Sci. Pollut. Res.* 5: 94–96.

Kurz-Besson, C., Coûteaux, M.-M., Thiéry, J.M., Berg, B., and Remacle, J. 2005. A comparison of litterbag and direct observation methods of Scots pine needle decomposition measurement. *Soil Biol. Biochem.* 37: 2315–2318.

Larink, O. 1993. Bait lamina as a tool for testing feeding activity of animals in contaminated soils. In M.H. Donker, H. Eijsackers, and F. Heimbach, Eds. *Ecotoxicology of Soil Organisms*. Lewis Publishers, Boca Raton, FL, pp. 339–345.

Larink, O. and Kratz, W. 1994. Köderstreifen-Workshop in Braunschweig—ein Resümee. *Braunschw. Naturkundl. Schr.* 4: 647–651.

Lawrence, K.L. and Wise, D.H. 2000. Spider predation on forest-floor Collembola and evidence for indirect effects on decomposition. *Pedobiologia* 44: 33–39.

Moore, A.M. 1986. Temperature and moisture dependence of decomposition rates of hardwood and coniferous leaf litter. *Soil Biol. Biochem.* 18: 427–435.

Phillipson, J. 1971. Methods of study in quantitative soil ecology: population, production and energy flow. In *IBP Handbook No. 18*. Blackwell Scientific Publications, Oxford, UK, 297 pp.

Potthoff, M. and Loftfield, N. 1998. How to quantify contamination of organic litter bag material with soil? *Pedobiologia* 42: 147–153.

Quested, H.M., Callaghan, T.V., Cornelissen, J.H.C., and Press, M.C. 2005. The impact of hemiparasitic plant litter on decomposition: direct, seasonal and litter mixing effects. *J. Ecol.* 93: 87–98.

Robinson, C.H., Dighton, J., Frankland, J.C., and Roberst, J.D. 1994. Fungal communities on decaying wheat straw of different resource qualities. *Soil Biol. Biochem.* 26: 1053–1058.

Rustad, L.E. 1994. Element dynamics along a decay continuum in a red spruce ecosystem in Maine, USA. *Ecology* 75: 867–879.

Singer, A.C., Jury, W., Luepromchai, E., Yahng, C.-S., and Crowley, D.E. 2001. Contribution of earthworms to PCB remediation. *Soil Biol. Biochem.* 33: 765–776.

Taylor, B.R. 1998. Air-drying depresses rates of leaf litter decomposition. *Soil Biol. Biochem.* 30: 403–412.

Tian, G., Brussard, L., Kang, B.T., and Swift, M.J. 1997. Soil fauna-mediated decomposition of plant residues under constrained environmental and residue quality conditions. In G. Cadisch and K.E. Giller, Eds. *Driven by Nature. Plant Litter Quality and Decomposition*. CAB International, Wallingford, UK, pp. 125–134.

von Törne, E. 1990. Assessing feeding activities of soil living animals: 1. Bait-lamina tests. *Pedobiologia* 34: 89–101.

Vreeken-Buijs, M.J. and Brussaard, L. 1996. Soil mesofauna dynamics, wheat residue decomposition and nitrogen mineralization in buried litterbags. *Biol. Fert. Soils* 23: 374–381.

Wardle, D.A., Nicholson, K.S., and Rahman, A. 1994. Influence of herbicide applications on the decomposition, microbial biomass, and microbial activity of pasture shoot and root litter. *N.Z. J. Agric. Res.* 37: 29–39.

Wardle, D.A., Yeates, G.W., Watson, R.N., and Nicholson, K.S. 1993. Response of soil microbial biomass and plant litter decomposition to weed management strategies in maize and asparagus cropping systems. *Soil Biol. Biochem.* 25: 857–868.

Wieder, R.K. and Lang, G.E. 1982. A critique of the analytical methods used in examining decomposition data obtained from litterbags. *Ecology* 63: 1636–1642.

Yadvinder-Singh, Bijay-Singh, Ladha, J.K., Khind, C.S., Khera, T.S., and Bueno, C.S. 2004. Effects of residue decomposition on productivity and soil fertility in rice–wheat rotation. *Soil Sci. Soc. Am. J.* 68: 854–864.

Chapter 41
Soil ATP

R.P. Voroney
University of Guelph
Guelph, Ontario, Canada

G. Wen
Lemington, Ontario, Canada

R.P. Beyaert
Agriculture and Agri-Food Canada
London, Ontario, Canada

41.1 INTRODUCTION

Adenosine 5′-triphosphate (ATP) levels determined by the firefly luciferin–luciferase bioluminescence technique have long been used as a measure of microbial biomass in soils and sediments (Karl and LaRock 1975; Jenkinson et al. 1979; Verstraete et al. 1983; Maire 1984). Early studies showed that the amount of soil ATP was highly correlated with soil microbial biomass C, as determined using the chloroform fumigation–incubation or fumigation–extraction methods (see Chapter 49) (Tate and Jenkinson 1982; Jenkinson 1988). Research has confirmed a rather constant ratio of soil biomass C:ATP between 150 and 200 (De Nobili et al. 1996). Recent studies have reported soil biomass C:ATP ratios of 208–217 for 14 agricultural soils (Martens 2001) and soil biomass ATP concentrations of 11 μM ATP g^{-1} biomass C (Contin et al. 2002) and 11.4 μM ATP g^{-1} biomass C (Dyckmans et al. 2003), which are comparable to 11.7 μM ATP g^{-1} biomass C reported by Jenkinson (1988). These values are equivalent to ~6.1 mg ATP g^{-1} biomass C or a soil biomass C:ATP ratio of 164 (assuming the anhydrous di-Mg salt of adenosine triphosphate has a formula weight of 553.8).

Beyond measurements of soil microbial biomass, researchers have applied ATP and ATP-related measurements to monitor the impact of varied soil environments on microbiological and biochemical processes (Dilly and Nannipieri 2001; Wen et al. 2001; Joergensen and Raubuch 2002; Raubuch et al. 2002; Shannon et al. 2002; Joergensen and Raubuch 2003). Also, ATP measurements have been used to study effects of multiyear applications of metal-containing sewage sludges and wastes from mining and manufacturing (Chander et al. 2001; Renella et al. 2003). In a review, Nannipieri et al. (1990) suggest that soil ATP content could also be used as an index of microbiological activity because ATP measurements respond to

imposed environmental variables within minutes, allowing detection of subtle changes better than other methods.

ATP is an extremely labile constituent of living cells that is rapidly hydrolyzed ($t_{1/2} < 1$ h) when released from dead cells (Webster et al. 1984). Potential problems that can occur in the determination of soil ATP are: (1) incomplete inactivation of enzymes involved in both ATP synthesis and degradation, (2) solubilization of the ATP, ensuring maximum release from living cells, (3) hydrolysis of released ATP by organic and inorganic soil constituents, (4) adsorption of released ATP onto soil colloids, (5) coprecipitation of released ATP, (6) complexation of the ATP with soluble material in the extract that prevents its detection in the assay, and (7) presence of substances that inhibit luciferase or alter characteristics of the light production (Eiland 1983; Webster et al. 1984; Wen et al. 2001).

Webster et al. (1984) proposed an extraction procedure for measuring soil ATP, referred to as the phosphoric acid (PA) method, which successfully overcame many of the difficulties previously associated with soil ATP measurements and resulted in high ATP recovery rates (Vaden et al. 1987). Comparison studies have since shown that the amounts of soil ATP extracted with PA are identical to those extracted with TCA-phosphate-paraquat (Ciardi and Nannipieri 1990). Given this good agreement between extraction methods and the need for using chemicals that are easily obtainable and also less toxic, carcinogenic, or mutagenic to minimize exposure and environmental risks, we propose the PA extraction procedure as the preferred technique for estimating the ATP content in soil. The soil ATP extraction we describe here is essentially the method of Webster et al. (1984), incorporating improvements proposed by Vaden et al. (1987) and Wen et al. (2005). ATP in the soil extract is assayed using the classic luciferin–luciferase system.

41.2 SOIL ATP METHOD

41.2.1 Soil Sampling and Preparation

Samples of fresh field moist soils are gently crushed and passed through a 2 mm sieve to remove coarse mineral particles and plant debris, and to obtain a homogenous sample; plant roots and residues are removed by hand picking. Soils can be analyzed in their field moist state; alternatively, soil moisture content can be adjusted with deionized water (Type 1) to ~50% of its water holding capacity (soil moisture content at −60 kPa water potential). Since disturbance of the soil during sampling and sieving affects microbial biomass and activity, the soil should be incubated in the laboratory for a short period (5–7 days) at the ambient soil temperature (Tate and Jenkinson 1982; Nannipieri et al. 1990) prior to ATP extraction.

41.2.2 Reagents

1 Basic Tris buffer (pH 10.66, 0.1 *M*) is prepared by dissolving 12.11 g Tris (hydroxymethyl) aminomethane in water and bringing the volume to 1 L.

2 HEPES (4-(2-hydroxyethyl)piperazine-1-ethanesulfonic acid) buffer (pH 7.75, 25 m*M*) is prepared by dissolving 5.96 g HEPES in ~900 mL water; titrate to pH 7.75 with 1 *M* NaOH and bring the final volume to 1 L.

3 ATP assay mix dilution buffer is prepared by reconstituting the ATP assay mix dilution buffer (Sigma-Aldrich) in 50 mL of water. Given that 100 μL of ATP assay

mix dilution buffer is used for each reading, 10 mL is sufficient for 100 readings. ATP assay mix dilution buffer is used also for preparation of the ATP standard calibration curve.

4 Luciferin–luciferase enzyme solution is prepared by reconstituting the ATP assay mix (Sigma-Aldrich) in 5 mL of ice-cold water (use a 30–50 mL glass vial). Allow the enzyme solution to stand for 10 min and then add the ATP assay mix to 20 mL of ice-cold ATP assay mix dilution buffer. Allow the enzyme solution to stand on ice for 1 h before use.

5 PA extractant (1 L) is prepared by mixing the reagents in the following order: 340 mL of Lubrol (polyethylene glycolmonocetylether) (MP Biomedicals, Inc.) solution prepared by dissolving 5 g Lubrol in 340 mL water and heated to 45°C to 50°C, 200 mL of 3.33 *M* PA, 200 mL of 10 *M* urea (heating and stirring to dissolve), 200 mL of dimethyl sulfoxide (DMSO), 40 mL of adenosine solution containing 5 mg adenosine mL^{-1}) (Sigma-Aldrich). Heat mixture to 35°C and add 20 mL of 1 *M* EDTA. The extractant should be kept warm (>25°C) and used soon after preparation, otherwise precipitation of EDTA may occur.

The 1 *M* EDTA solution is prepared as follows: 18.612 g of disodium, dihydrate EDTA, and 2.248 g of solid NaOH is dissolved in water to which is added ~7 mL of 1 *M* NaOH solution to adjust the pH to 7.8–8.0, and the total volume is brought to 50 mL. The EDTA solution should be prepared just prior to addition to the heated extractant mixture. The temperature of the Lubrol solution is kept >35°C until used (Vaden et al. 1987).

6 ATP standard stock solution is prepared by reconstituting a vial containing ~1 mg (2 μ*M*) of ATP disodium hydrate (formula weight 551.1) (Sigma-Aldrich) in 10 mL of cold water, giving a solution that is ~0.2 m*M* ATP (see label on vial for actual amount). This standard stock solution can be divided into 0.5 mL portions (contained in 4 mL plastic vials with lids) and, if not immediately used, kept frozen (−15°C) for later use.

7 The ATP standard calibration curve relating ATP concentrations to light intensity expressed in relative light units (RLU) is prepared in ATP assay mix dilution buffer. Typically, it should span an ATP assay concentration range from 0 to 0.60 p*M* ATP $assay^{-1}$ when added as a component to the reaction mixture. Prepare an ATP working standard for establishing the standard curve by taking a 0.1 mL aliquot of the ATP standard stock solution and bring up to 10 mL with cold water. Take a 0.1 mL aliquot of this solution and bring to 10 mL with ATP assay mix dilution buffer. This ATP working standard, containing 20 p*M* ATP mL^{-1}, is thoroughly mixed, and kept on ice. Prepare 1 mL of each of the ATP standards using the ATP working standard solution and the ATP assay mix dilution buffer as shown in Table 41.1. These standards are substituted for the pure ATP assay mix dilution buffer (100 μL) addition in the reaction mixture. A plot of the logarithm of RLU generated by the luciferin–luciferase reaction vs. the logarithm of the ATP standard concentration gives a linear relationship.

8 The ATP spiking solution for measurement of the recovery efficiency is prepared by taking a 0.3 mL aliquot of the ATP standard stock solution and adding, while mixing, to 0.3 mL with HEPES buffer. This ATP spiking solution contains 0.10 μ*M* ATP mL^{-1} HEPES and is kept on ice.

TABLE 41.1 Construction of the ATP Standard Calibration Curve

ATP standard concentration (p*M* ATP assay^{-1})	ATP working standard (μL)	ATP assay mix dilution buffer (μL)
0	0	1000
0.1	50	950
0.2	100	900
0.3	150	850
0.4	200	800
0.5	250	750
0.6	300	700

9 An autoclaved soil extract for preparing the ATP standard calibration curve is prepared by weighing 5 g soil (oven-dry weight) into a 100 mL glass centrifuge tube and immediately autoclaving it at 121°C for 20 min. After cooling, the tube is capped and kept frozen until used. After thawing, the soil is extracted as described below for fresh soil.

41.2.3 Extraction Procedure

1 Triplicate 5 g (dry weight) portions of fresh soil are weighed into 100 mL glass centrifuge tubes (equipped with screw caps) to which is added 50 mL of extractant, while gently shaking, and placed in an ice bath.

2 ATP recovery efficiency is measured by adding 50 μL of the ATP spiking solution (containing 5 n*M* ATP) to a tube containing 5 g soil + 50 mL extractant (also gently shaking and kept in an ice bath). A soil control is prepared by adding 50 μL HEPES buffer alone to a tube containing 5 g soil + 50 mL extractant.

3 The soil plus extractant is homogenized and sonicated for 1 min at a setting of 7 using a Brinkmann Polytron Homogenizer equipped with a stainless steel tip (PTA 20S, Kinematica), or for 2 min at full power using a 20 kHz 140 W Branson Sonifier (Model 200) equipped with a 12.5 mm diameter probe. During sonication, the centrifuge tube is kept cooled in an ice bath and covered with parafilm to prevent losses by splashing. (Between soil samples, the tip is carefully washed with water, with the machine turned on for a brief period, and dried.) The centrifuge tubes are capped and shaken on a wrist-action shaker (180 strokes min^{-1}) for 30 min, after which the tubes are centrifuged for 20 min at 31,000 *g* and 4°C.

4 Duplicate 0.2 mL aliquots of the supernatant from the soil sample extract are transferred to 4 mL glass sample cups and neutralized by addition of 3.2 mL Tris buffer.

5 The same procedure is repeated for neutralization of the autoclaved soil extract (or the extractant alone) for use in analysis of ATP standards.

6 The neutralized extracts should be either kept at 4°C and analyzed immediately or immediately frozen and stored at −15°C until ATP determinations can be

carried out. Frozen extracts are thawed immediately before measurement and kept at 4°C.

41.2.4 Assay Procedure

1 The final reaction mixture for the assay (325 μL in total) is prepared by adding to a cuvette the following, in order:

(i) 100 μL of water;

(ii) 100 μL of pure ATP assay mix dilution buffer;

(iii) 25 μL of neutralized soil extract;

(iv) 100 μL of luciferin–luciferase solution; the cuvette is immediately placed in the instrument for counting.

2 For construction of the ATP standard calibration curve, the final reaction mixture for the assay (325 μL in total) is prepared by adding to a cuvette the following, in order:

(i) 100 μL of water;

(ii) 100 μL ATP assay mix dilution buffer containing the ATP standards;

(iii) 25 μL of neutralized extract of autoclaved soil (preferable) or neutralized extractant;

(iv) 100 μL of luciferin–luciferase solution; the cuvette is immediately placed in the instrument for counting.

3 The most reliable method of determining ATP concentrations is with light detecting instruments, such as a commercially available photometer or a liquid scintillation counter (operated in noncoincident mode) set to an integral counting mode. If a luminometer (Lumac Model 1070, Lumac Systems Inc. P.O. Box 2805, Titusville, FL 32780, USA) is used, it should be turned on for 30 min prior to measurements to allow the electronics to stabilize. The delay time is set to 5 s to avoid an error reading of the immediate light flash, produced during mixing of luciferin–luciferase with ATP. The counting time integration setting is 10 s. Determinations of ATP in each extract are carried out in duplicate. Periodic standardization should be performed during the day to check for instrument stability. If the grid electrical supply is highly variable, it is advisable to install a UPS power filter to ensure greater instrument stability.

41.3 CALCULATION OF SOIL ATP CONTENT

41.3.1 Assay ATP Concentration

ATP content in each assay is obtained using the equation of the standard calibration curve relating the logarithm of the assay RLU vs. the logarithm of the ATP standard concentrations (expressed in pM ATP assay^{-1}).

41.3.2 Soil ATP Recovery Efficiency

A measure of the soil ATP recovery efficiency is made from the measurement of the spike ATP recovered in the assay using the following two equations:

$$\text{Recovery efficiency (RE)} = \frac{\text{Spike ATP measured in assay}}{\text{ATP added in spiked sample assay}} \tag{41.1}$$

where

$$\text{Spike ATP measured in assay} = (\text{ATP in soil} + \text{spike assay}) - \text{ATP in soil assay} \tag{41.2}$$

$$\text{ATP added in spike assay} = 0.1469\ \text{p}M\ \text{ATP}.$$

41.3.3 Soil ATP Content in the Assay

The soil ATP content in the assay is determined from the measured assay ATP content and the recovery efficiency using the following equation:

$$\text{Soil ATP in the assay (p}M\ \text{assay}^{-1}) = \frac{\text{Measured assay ATP content}}{\text{RE}} \tag{41.3}$$

41.3.4 Soil ATP Content

Soil ATP content is calculated from the soil ATP in the assay, the volume of neutralized extract (NE) assayed (25 μL), the quantity of neutralized extract (3.4 mL), the quantity of soil extract (SE) neutralized (0.2 mL), the quantity of soil extract (50 mL extractant + soil water content), and the quantity of soil extracted (5 g) using the following equation:

$$\text{Soil ATP (p}M\ \text{g}^{-1}\text{soil}) = \frac{\text{Soil ATP (p}M)}{0.025\ \text{mL NE assay}} \times \frac{3.4\ \text{mL NE}}{0.2\ \text{mL SE}} \times \frac{(50 + \text{SW})\ \text{mL SE}}{5\ \text{g soil}} \tag{41.4}$$

where SW is the water in the soil sample calculated using the following equation:

$$\text{Soil water (SW) (mL)} = 5\ \text{g (oven-dry soil)} \times \text{gravimetric soil water content (\%)} \tag{41.5}$$

Results are typically expressed as nM g^{-1} soil:

$$\text{Soil ATP (n}M\ \text{g}^{-1}\ \text{soil}) = \frac{\text{Soil ATP (p}M\ \text{g}^{-1}\ \text{soil})}{1000} \tag{41.6}$$

41.4 COMMENTS

1 Most of the reagents used, except where noted, are readily obtainable and are certified analytical grade. Deionized water (Type 1) should be used throughout for preparation of the reagent solutions.

2 Luciferase activity and the wavelength of light emitted are pH sensitive, therefore, neutralization of the soil extract and adjustment of the reaction

mixture to an optimal pH are critical for maximizing assay sensitivity (Wen et al. 2005).

3 An autoclaved soil extract should be used for preparing the ATP standard calibration curve to ensure a similar chemistry in the ATP standards as that of the soil extract.

4 The composition of the reaction mixture gives precise control of the reaction mixture pH (pH should be ~7.75) while diluting components in the extract that may affect enzyme activity.

5 It is critical that all glassware be very clean and that new gloves be worn to avoid contamination of the samples with foreign ATP. Undiluted, these reagents are able to detect concentrations as low as 0.002 p*M* ATP mL^{-1}.

6 Soil ATP measurements using this method are relatively precise; three replicate determinations on the same soil sample should be able to detect differences in ATP content of 5%–10% at a 0.05% level of probability.

41.5 ATP AND MICROBIAL BIOMASS

The soil ATP method is an extremely sensitive method for studying soil microbial biomass and its activity. Because the method can be carried out quickly, it has potential for use in studying soils under rapidly changing environmental conditions (e.g., wetting and drying, freezing, and thawing). It can also be used for samples derived from select soil microhabitats such as aggregate surfaces and intra-aggregate spaces within the soil matrix or from the rhizosphere (Nannipieri et al. 1990).

Further information about the average physiological state of the soil microbial biomass can be obtained by measurements of the adenylate energy charge (AEC) (Brookes et al. 1987; Vaden et al. 1987; Raubuch et al. 2002; Joergensen and Raubuch 2003; Raubuch et al. 2006). The AEC is a relation between the concentrations of the adenine nucleotides, according to the following equation:

$$\text{Adenylate energy charge (AEC)} = \frac{[\text{ATP}] + 0.5\ [\text{ADP}]}{[\text{ATP}] + [\text{ADP}] + [\text{AMP}]} \tag{41.7}$$

where ATP, ADP, and AMP are the soil concentrations (in $\mu M\ g^{-1}$ soil) of adenosine triphosphate, adenosine diphosphate, and adenosine monophosphate, respectively. AEC values of 0.7–0.95 have been reported for fresh soils and 0.4–0.5 for air-dried soils.

Further efficiencies in analysis can be gained by measuring the content of all three adenylates in one step using ion-paired reverse-phase high-performance liquid chromatography (HPLC) techniques (Dyckmans and Raubuch 1997).

REFERENCES

Brookes, P.C., Newcombe, A.D., and Jenkinson, D.S. 1987. Adenylate energy charge measurements in soil. *Soil Biol. Biochem.* 19: 211–217.

Chander, K.C., Dyckmans, J., Joergensen, R.G., Meyer, B., and Raubuch, M. 2001. Different sources of heavy metals and their long-term

effects on soil microbial properties. *Biol. Fert. Soils* 34: 241–247.

Ciardi, C. and Nannipieri, P. 1990. A comparison of methods for measuring ATP in soil. *Soil Biol. Biochem.* 22: 725–727.

Contin, M., Jenkinson, D.S., and Brookes, P.C. 2002. Measurement of ATP in soil: correcting for incomplete recovery. *Soil Biol. Biochem.* 34: 1381–1383.

De Nobili, M., Diaz-Raviña, M., Brookes, P.C., and Jenkinson, D.S. 1996. Adensoine 5′-triphosphate measurements in soils containing recently added glucose. *Soil Biol. Biochem.* 28: 1099–1104.

Dilly, O. and Nannipieri, P. 2001. Response of ATP content, respiration rate, and enzyme activities in an arable and a forest soil to nutrient additions. *Biol. Fert. Soils* 34: 64–72.

Dyckmans, J., Chander, K., Joergensen, R.G., Priess, J., Raubuch, M., and Sehy, U. 2003. Adenylates as an estimate of microbial biomass C in different soil groups. *Soil Biol. Biochem.* 35: 1485–1491.

Dyckmans, J. and Raubuch, M. 1997. A modification of a method to determine adenosine nucleotides in forest organic layers and mineral soils by ion-paired reverse-phase high performance liquid chromatography. *J. Microbiol. Methods* 30: 13–20.

Eiland, F. 1983. A simple method for quantitative determination of ATP in soil. *Soil Biol. Biochem.* 15: 665–670.

Jenkinson, D.S. 1988. Determination of microbial biomass carbon and nitrogen in soil. In J.R. Wilson, Ed. *Advances in Nitrogen Cycling in Agricultural Ecosystems*. CAB International, Wallingford, UK, pp. 368–386.

Jenkinson, D.S., Davidson, S.A., and Powlson, D.S. 1979. Adenosine triphosphate and microbial biomass in soil. *Soil Biol. Biochem.* 11: 521–527.

Joergensen, R.G. and Raubuch, M. 2002. Adenylate energy charge of a glucose-treated soil without adding a nitrogen source. *Soil Biol. Biochem.* 34: 1317–1324.

Joergensen, R.G. and Raubuch, M. 2003. Adenylate energy charge and ATP-to-biomass C ratio in soils differing in the intensity of disturbance. *Soil Biol. Biochem.* 35: 1161–1164.

Karl, D.M. and LaRock, P.A. 1975. Adenosine triphosphate measurements in soil and marine sediments. *J. Fish. Res. Board Can.* 5: 599–607.

Maire, N. 1984. Extraction de l'adenosine triphosphate dans les sols: une nouvelle methode de calcul des pertes en ATP. *Soil Biol. Biochem.* 16: 361–366.

Martens, R. 2001. Estimation of ATP in soil: extraction methods and calculation of extraction efficiency. *Soil Biol. Biochem.* 33: 973–982.

Nannipieri, P., Grego, S., and Ceccanti, B. 1990. Ecological significance of the biological activity in soil. In J.M. Bollag and G. Stotzky, Eds. *Soil Biochemistry*, Vol. 6. Marcel Dekker, New York, NY, pp. 293–355.

Raubuch, M., Campos, A., and Joergensen, G.R. 2006. Impact of cycloheximide addition on adenylates in soil. *Soil Biol. Biochem.* 38: 222–228.

Raubuch, M., Dyckmans, J., Joergensen, R.G., and Kreutzfeldt, M. 2002. Relation between respiration, ATP content, and adenylate energy charge (AEC) after incubation at different temperatures and after drying and rewetting. *J. Plant Nutr. Soil Sci.* 165: 435–440.

Renella, G., Reyes Ortigoza, A.L., Landi, L., and Nannipieri, P. 2003. Additive effects of copper and zinc on cadmium toxicity to phosphatase activities and ATP content of soil as estimated by the ecological dose (ED_{50}). *Soil Biol. Biochem.* 35: 1203–1210.

Shannon, D., Sen, A.M., and Johnson, D.B. 2002. A comparative study of the microbiology of soils managed under organic and conventional regimes. *Soil Use Manage.* 18: 274–283.

Tate, K.R. and Jenkinson, D.S. 1982. Adenosine triphosphate (ATP) and microbial biomass in soil: effects of storage at different temperature and different moisture levels. *Commun. Soil Sci. Plant Anal.* 13: 899–908.

Vaden, V.R., Webster, J.J., Hampton, G.J., Hall, M.S., and Leach, F.R. 1987. Comparison of methods for extraction of ATP from soil. *J. Microbiol. Methods* 7: 211–217.

Verstraete,W., Van de Werf, H., Kucnerowicz, F., Ilaiwi, M., Verstraeten, L.M.J., and Vlassak, K. 1983. Specific measurement of soil microbial ATP. *Soil Biol. Biochem.* 15: 391–396.

Webster, J.J., Hampton, G.J., and Leach, F.R. 1984. ATP in soil: a new extractant and extraction procedure. *Soil Biol. Biochem.* 16: 335–342.

Wen, G., Voroney, R.P., Curtin, D., Schoenau, J.J., Qian, P.Y., and Inanaga, S. 2005. Modification and application of a soil ATP determination method. *Soil Biol. Biochem.* 37: 1999–2006.

Wen, G., Voroney, R.P., Schoenau, J.J., Yamamoto, T., and Chikushi, J. 2001. Assessment of ionic quenching on soil ATP bioluminescence reaction. *Soil Biol. Biochem.* 33: 1–7.

Chapter 42
Lipid-Based Community Analysis

K.E. Dunfield
University of Guelph
Guelph, Ontario, Canada

42.1 INTRODUCTION

Soil microbial communities are incredibly complex, with estimates of more than 4000 bacterial genomes in a single soil sample (Torsvik et al. 1990; Amann et al. 1995). However, evidence has shown that less than 1% of soil bacteria are cultivable using common laboratory media under standard conditions (Torsvik et al. 1990; Ovreas and Torsvik 1998). Therefore, it is important to choose a method of community analysis that does not rely on isolation and cultivation techniques. Methods that extract cellular components that are representative of most bacterial species directly from soils have become popular. These methods are based on the characterization of bacterial cell constituents such as lipids and nucleic acids that can be directly extracted from a soil sample without the need for isolating bacterial cells (Drenovsky et al. 2004). This chapter will focus on lipid-based community analysis, while nucleic acid based methods are described in Chapter 43.

Bacterial lipids are key energy storage and cellular membrane compounds that include free fatty acids, hydrocarbons, fatty alcohols, and membrane bound fatty acids such as phospholipids and glycolipids (Kennedy 1994). Bacterial taxa often have unique fatty acid profiles that can be identified and used as indicators of microbial community structure (White et al. 1979; Sasser 1990). Lipid analysis of soil microbial communities consists of recovering lipids by extraction in organic solvents followed by analysis with high-resolution fused-silica capillary gas chromatography (Kennedy 1994). Fatty acids are identified with the aid of computer programs such as the Sherlock Microbial Identification System (MIDI, Inc., Newark, DE), by comparison of their retention times in a column against the retention times of bacterial fatty acid standards. Two protocols for extracting lipids from soil are commonly used. Fatty acid methyl ester (FAME) analysis targets all soil fatty acids, and phospholipid fatty acid (PLFA) analysis specifically targets the phospholipid fatty acids found in viable microbial cells.

Fatty acid methyl ester analysis uses a one day, 4-step chemical extraction protocol to saponify and methylate all lipids in a soil sample, extract the FAMEs and analyse them

through gas chromatography, resulting in a fatty acid profile of the soil. Soil FAME profiles can be compared in order to monitor shifts in the overall community structure and are highly reproducible when obtained from communities under similar environmental conditions (Haack et al. 1994). MIDI-FAME analysis has been used successfully to compare the microbial communities in two or more soils, or in a soil under different management practices or cropping regimes (Klug and Tiedje 1993; Cavigelli et al. 1995; Dunfield and Germida 2001, 2003). This method extracts all lipids in living or dead cells, including animal and plant biomass in various stages of decomposition (Ibekwe and Kennedy 1999). A variety of approaches can be taken during the statistical analysis to minimize interference from plant and animal sources, such as ignoring known plant fatty acids, or fatty acids with chain lengths exceeding 20 carbons, which are more characteristic of eukaryotes than prokaryotes (Buyer and Drinkwater 1997; Fang et al. 2001). However, due to the existence of common fatty acids in plants, animals, and microbes, this method cannot reliably be used for taxonomic characterization of the microbial community by lipid biomarker analysis.

Phospholipid fatty acid analysis is a more intensive six day protocol that extracts all fatty acids, isolates phospholipids from other soil lipids using solid-phase extraction, converts them into FAMEs and analyzes them through gas chromatography (Bligh and Dyer 1959; Bobbie and White 1980; Bossio and Scow 1998). This method has the advantage that phospholipids are found only in live bacterial cell membranes, and are degraded upon cell death; therefore, a PLFA profile is indicative of the live microbial community in the soil (White et al. 1979; Zelles et al. 1992). Several studies have used PLFA to monitor shifts in the overall soil microbial community structure (Bååth et al. 1992; Bossio and Scow 1998; Feng et al. 2003). In addition, given that PLFA profiles are derived from viable microbial biomass, specific biomarker fatty acids can be used as indicators of a particular group of bacteria, providing a taxonomic representation of the soil microbial community (Pankhurst et al. 2001). For example, hydroxyl fatty acids are derived primarily from Gram-negative bacteria, especially *Pseudomonas* spp., whereas, cyclopropane fatty acids are indicators of other groups of Gram-negative bacteria, such as *Chromatium*, *Legionella*, *Rhodospirillum*, and *Campylobacter* (Harwood and Russell 1984; Wollenweber and Rietschel 1990; Cavigelli et al. 1995). Branched fatty acids, such as *a* 15:0, are commonly thought to be markers for Gram-positive bacteria such as *Clostridium* and *Bacillus* (Ratledge and Wilkinson 1988; Ibekwe and Kennedy 1999), and 18:3 ω6, 9, 12c, is a fatty acid primarily found in lower fungi (Harwood and Russell 1984). A detailed survey of biomarker fatty acids used as taxonomic indicators has been published in a review by Zelles (1999).

The MIDI-FAME (42.2) and PLFA (42.3) protocols are presented in this chapter. Detailed comparisons of the two methods can be found in recent literature (Pankhurst et al. 2001; Petersen et al. 2002; Drenovsky et al. 2004). In general, PLFA represents a functionally more well-defined fraction of soil lipids than MIDI-FAME, specifically analyzes microbial community composition, and provides more consistent fatty acid profiles among sample replicates. However, the MIDI-FAME extraction is not as time consuming, and requires a smaller sample mass to recover a reliable community fingerprint (Petersen et al. 2002; Drenovsky et al. 2004). Researchers should decide which method to use by taking into consideration the above comparisons of the methods, specifically whether taxonomic analysis of the community through biomarker analysis is necessary or whether time and sample size are limiting.

42.2 FATTY ACID METHYL ESTER ANALYSIS (SASSER 1990; MODIFIED FOR SOIL BY CAVIGELLI ET AL. 1995)

42.2.1 Materials and Reagents

1 25 mL test tubes with Teflon lined caps.

2 Reagent 1 (saponification reagent). 4 *M* NaOH in 50% methanol. 45 g sodium hydroxide, 150 mL methanol, and 150 mL distilled water.

3 Vortex.

4 Water bath (100°C).

5 Reagent 2 (methylation reagent). 6.0 *M* HCl in 50% methanol. 325 mL certified 6.0 *M* HCl, and 275 mL methanol.

6 Water bath (80 $\pm$ 1°C).

7 Cold water bath.

8 Reagent 3 (extraction reagent). 1:1 (v/v) hexane:methyl tert-butyl ether (MTBE). 200 mL hexane, and 200 mL MTBE.

9 Rotary shaker.

10 Centrifuge.

11 Pasteur pipettes, tips flamed to remove contaminants.

12 15 mL test tubes with Teflon lined caps.

13 Reagent 4 (wash reagent). 0.3 *M* NaOH. 10.8 g NaOH dissolved in 900 mL distilled water.

14 Gas chromatograph (GC) vials.

15 GC equipped with a 25 m (5% phenyl)-methylpolysiloxane column, programable 170°C to 260°C at 2°C min^{-1} equipped with flame ionization detector and integrator.

16 Hydrogen gas (99.999% pure).

17 Nitrogen gas (99.999% pure).

18 Air, industrial grade, dry.

19 Computer containing MIDI-Sherlock peak identification software (Microbial ID Inc., Newark, DE).

42.2.2 Procedure

1 Place 5 g dry weight of soil into a 25 mL test tube with Teflon lined cap.

2 Saponify fatty acids by adding 5 mL of Reagent 1. Vortex for 10 s. Incubate at 100°C for 5 min. Vortex for 10 s. Incubate at 100°C for 25 min. Allow to cool to room temperature.

3 Add 10 mL Reagent 2. This drops the pH of the solution below 1.5 and causes methylation of the fatty acid. Vortex for 10 s. Incubate at 80°C for 10 min. Cool rapidly in cold water bath.

4 Add 1.5 mL Reagent 3. This extracts the FAMEs into the organic phase for use with the GC. Shake on rotary shaker for 10 min. Centrifuge at 121 *g* for 5 min. Transfer top phase to a 15 mL test tube.

5 Add 3.0 mL Reagent 4. To wash samples and reduce contamination of the injection port liner, the column, and the detector. Shake on a rotary shaker for 5 min. Centrifuge at 129 *g* for 3 min. Transfer top phase to a GC vial.

6 Separate FAMEs by gas chromatography. GC conditions are controlled by the MIDI Sherlock program (MIDI, Inc., Newark, DE). Basically, a 2 μL injection of the samples is analyzed with a GC at an initial temperature of 170°C, ramped to 260°C at 2°C min^{-1} using hydrogen as the carrier gas, N_2 as the make up gas, and air to support the flame. Peaks are identified using bacterial fatty acid standards and MIDI-Sherlock peak identification software.

42.2.3 Comments

1 All reagents should be of high-performance liquid chromatography grade.

2 Caution should be taken in Step 2. Tube contents may boil up and leak out the test tube, which could cause fatty acids to volatilize and escape (Schutter and Dick 2000).

3 All glassware should be washed and then fired in a muffle furnace at 450°C for a minimum of 4 h to remove traces of lipids.

42.3 PHOSPHOLIPID FATTY ACID ANALYSIS (BLIGH AND DYER 1959; MODIFIED BY BOSSIO AND SCOW 1998; SMITHWICK ET AL. 2005)

42.3.1 Fatty Acid Extraction

Materials and Reagents

1 Teflon centrifuge tubes.

2 One-phase extraction mixture, 1:2:0.8 (v/v/v) chloroform:methanol:phosphate buffer.

3 Phosphate buffer (1 *M*). 39 mL 1 *M* K_2HPO_4, 61 mL KH_2PO_4, fill to 1 L, adjust to pH 7.0.

4 Shaker.

5 Centrifuge.

6 Separatory funnel.

7 Chloroform ($CHCl_3$).

8 Glass tubes.

9 Fume hood.

10 Vacuum aspirator.

11 Compressed nitrogen gas cylinder.

Procedure

1 Place 8 g dry weight of freeze-dried soil into a Teflon centrifuge tube.

2 Add 23 mL of one-phase extraction mixture. Shake for 2 h in dark. Centrifuge for 10 min at 756 *g*. Decant supernatant to a separatory funnel.

3 Re-extract soil by adding 23 mL of one-phase extraction mixture and shaking for 30 min. Centrifuge for 10 min at 756 *g*. Decant supernatant and combine with supernatant from Step 2.

4 Add 12 mL phosphate buffer and 12 mL $CHCl_3$ to combined supernatants. Vortex for 1 min, vent periodically. Let stand in dark overnight to allow phases to separate.

5 In a fume hood, remove upper aqueous phase with a vacuum aspirator. Decant the bottom $CHCl_3$ layer containing the lipids into a clean glass tube, and dry under N_2 gas at 32°C.

6 Add 0.5 mL $CHCl_3$ to wash lipids. Swirl to dissolve the fatty acid residue, and transfer to a clean glass tube. Repeat four times (2 mL total). Dry down samples.

Comments

1 Glassware should be cleaned, then fired in a muffle furnace at 450°C for a minimum of 4 h to remove traces of lipids. Rinse items that will not tolerate heat with hexane.

2 Cloudiness of sample in Step 6 indicates the presence of water in the sample. This is problematic because the water will attack the double bonds in the fatty acids. Therefore, add methanol with a dropper until the solution clears and continue with Step 6 (Balser 2005).

42.3.2 Solid-Phase Extraction of Phospholipids (Zelles and Bai 1993)

Materials and Reagents

1 Solid-phase extraction columns packed with 0.5 g silica.

2 Chloroform ($CHCl_3$).

3 Acetone.

4 Methanol.

5 Glass tubes.

6 Compressed N_2 gas cylinder.

Procedure

1 Set up solid-phase extraction columns packed with 0.50 g Silica. Condition column with 3 mL $CHCl_3$.

2 Add 250 μL $CHCl_3$ to glass tube containing dried lipids. Transfer to the column. Repeat four times (1 mL total).

3 Add 5 mL $CHCl_3$ to the column, and allow draining by gravity. This fraction contains the neutral lipids, discard or save for further analysis.

4 Add 5 mL acetone to the column, and allow draining by gravity. Repeat one time (10 mL total). This fraction contains the glycolipids, discard or save for further analysis.

5 Add 5 mL methanol to the column, and allow draining by gravity. This fraction contains phospholipids, save and dry under N_2 at 32°C.

Comments

Researchers are sometimes interested in analyzing other lipids. The neutral lipid fraction in Step 3 can be saved if interested in analyzing sterols for estimates of fungal biomass, and the glycolipid fraction can be saved if interested in analyzing polyhydroxyalkanoates (PHAs) (White and Ringelberg 1998).

42.3.3 Conversion to Fatty Acid Methyl Esters by Mild Alkaline Methanolysis

Materials and Reagents

1 1:1 (v/v) Methanol:toluene. 100 mL methanol and 100 mL toluene to hexane rinsed bottle.

2 0.2 *M* methanolic KOH, freshly prepared. Dissolve 0.28 g KOH in 25 mL methanol.

3 Vortex.

4 Ultrapure water.

5 1 *M* acetic acid. Add 58 mL glacial acetic acid to water for a total volume of 1 L.

6 Hexane.

7 Centrifuge.

8 Amber GC vial.

9 Compressed N_2 gas cylinder.

10 19:0 methyl ester in hexane (25 ng mL^{-1}).

11 GC vial with glass insert.

Procedure

1 Redissolve dried phospholipids in 1 mL of 1:1 methanol:toluene and 1 mL 0.2 *M* methanolic KOH. Vortex briefly. Incubate at 37°C for 15 min. Allow sample to cool to room temperature.

2 Extract FAMEs by adding 2 mL water, 0.3 mL 1 *M* acetic acid, and 2 mL hexane. Shake tube then vortex for 30 s. Separate phases by centrifugation for 5 min at 484 *g*. Remove hexane (upper) layer, and transfer to an amber GC vial.

3 Wash aqueous phase from Step 2, and remove remaining FAMEs by adding 2 mL hexane to the bottom layer. Shake tube then vortex for 30 s. Separate phases by centrifugation for 5 min at 480 *g*. Remove hexane (upper) layer, and transfer to GC vial containing FAMEs from Step 2. Dry sample under N_2 at room temperature. Store sample at −20°C in the dark.

4 Suspend samples in 150 μL hexane containing 19:0 methyl ester (25 ng mL^{-1}) as an internal standard, and transfer to a GC vial containing a glass insert.

42.3.4 Gas Chromatographic Analysis

Phospholipid fatty acid samples can be analysed by gas chromatography as described in the procedure for MIDI-FAME analysis (Step 6 of Section 42.2.2).

42.4 CHARACTERIZING FATTY ACID DATA

42.4.1 Fatty Acid Identification

After GC analysis FAMEs are identified by their equivalent chain length (ECL) values using programs such as the Sherlock Microbial Identification System (MIDI Inc., Newark, DE). Straight-chain saturated fatty acids are assigned an ECL value corresponding to the number of carbons in the FAME chain (e.g., 11:0 = ECL 11.000). Because ECLs are a constant

property of a specific FAME, published ECLs in a library of FAMEs can be used for identification (White and Ringelberg 1998).

42.4.2 Nomenclature

Terminology to describe fatty acids is described by A:B ωC, where A indicates the total number of carbon atoms, B the number of double bonds, and ωC indicates the position of the double bond from the methyl end of the molecule. The prefixes *i* and *a* refer to iso and anteiso methyl branching. The suffixes c for *cis* and t for *trans* refer to geometric isomers. Hydroxy groups are indicated by OH. Cyclopropyl groups are denoted by '*cy*.' 10 ME refers to a methyl group on the tenth carbon from the carboxylic end of the fatty acid (White and Ringelberg 1998; Smithwick et al. 2005).

42.4.3 Statistical Analyses

Multivariate analysis such as principal components analysis (PCA) is often used to compare fatty acid profiles of soil microbial communities. PCA is used to summarize data in which multiple variables have been measured for each sample (Cavigelli et al. 1995). This is particularly useful for lipid-based community analysis where more than 40 fatty acids are commonly found in the profile of a single soil. An analysis of variance comparing the average peak area or percent of total of each fatty acid for each treatment is possible, but time-consuming, and ecologically meaningless. Principal components analysis linearly transforms an original set of variables (fatty acids) into a substantially smaller set of uncorrelated variables (principal components) that represent most of the information in the original data set (Dunteman 1989). Principal component (PC) are ordered with respect to their variation so that the first few account for most of the variation present in the data. A visual representation of the variation in the data can be presented in a PC plot, where the score of the first two or three PC are plotted in a two- or three-dimensional graph. PC plots are commonly presented in literature to compare the diversity of a soil microbial community based on FAME or PLFA data (Fang et al. 2001; Dunfield and Germida 2001, 2003; Feng et al. 2003). Further information is obtained by examining the eigenvalue loadings associated with each PC. This value reflects the contribution of each original variable to the variation in the PC, and can be used to identify the fatty acids that contribute the most to variation in the communities. These fatty acids can then be selected to undergo further analysis.

REFERENCES

Amann, R., Ludwig, W., and Schleifer, K.H. 1995. Phylogenetic identification and *in situ* detection of individual microbial cells without cultivation. *Microbiol. Rev.* 59: 143–169.

Bååth, E., Frostegård, Å., and Fritze, H. 1992. Soil bacterial biomass, activity, phospholipids fatty acid pattern, and pH tolerance in an area polluted with alkaline dust deposition. *Appl. Environ. Microbiol.* 58: 4026–4031.

Balser, T. 2005. Phospholipid-fatty acid analysis. (Online). Available at http://www.cnr.berkeley.edu/soilmicro/methods/BalserPLFA.pdf. Verified March 2006.

Bligh, E.G. and Dyer, W.J. 1959. A rapid method of total lipid extraction and purification. *Can. J. Biochem. Physiol.* 37: 911–917.

Bobbie, R.J. and White, D.C. 1980. Characterzation of benthic microbial community structure by

high-resolution gas chromatography of fatty acid methyl esters. *Appl. Environ. Microbiol.* 39: 1212–1222.

Bossio, D.A. and Scow, K.M. 1998. Impacts of carbon and flooding on soil microbial communities: phospholipids fatty acid profiles and substrate utilization patterns. *Microb. Ecol.* 35: 265–278.

Buyer, J.S. and Drinkwater, L.E. 1997. Comparison of substrate utilization assay and fatty acid analysis of soil microbial communities. *J. Microbiol. Methods* 30: 3–11.

Cavigelli, M.A., Roberson, G.P., and Klug, M.J. 1995. Fatty acid methyl ester (FAME) profiles as measures of soil microbial community structure. *Plant Soil* 170: 99–113.

Drenovsky, R.E., Elliott, G.N., Graham, K.J., and Scow, K.M. 2004. Comparison of phospholipids fatty acid (PLFA) and total soil fatty acid methyl esters (TSFAME) for characterizing soil microbial communities. *Appl. Environ. Microbiol.* 36: 1793–1800.

Dunfield, K.E. and Germida, J.J. 2001. Diversity of bacterial communities in the rhizosphere and root-interior of field-grown genetically modified *Brassica napus*. *FEMS Microbiol. Ecol.* 38: 1–9.

Dunfield, K.E. and Germida, J.J. 2003. Seasonal changes in the rhizosphere of microbial communities associated with field-grown genetically modified canola (*Brassica napus*). *Appl. Environ. Microbiol.* 69: 7310–7318.

Dunteman, G.H. 1989. Principal Components Analysis No. 69. In Lewis-Beck, M.S., ed. *Quantitative Applications in the Social Sciences*. Sage Publications, Newbury Park.

Fang, C., Radosevich, M., and Fuhrmann, J.J. 2001. Characterization of rhizosphere microbial community structure in five similar grass species using FAME and BIOLOG analyses. *Soil Biol. Biochem.* 33: 679–682.

Feng, Y., Motta, A.C., Reeves, D.W., Burmester, C.H., van Stanten, E., and Osborne, J.A. 2003. Soil microbial communities under conventional-till and no-till continuous cotton systems. *Soil Biol. Biochem.* 35: 1693–1703.

Haack, S.K., Garchow, H., Odelson, D.A., Forney, L.J., and Klug, M.J. 1994. Accuracy, reproducibility, and interpretation of fatty acid profiles of model bacterial communities. *Appl. Environ. Microbiol.* 60: 2483–2493.

Harwood, J.L. and Russell, N.J. 1984. *Lipids in Plants and Microbes*. George Allen and Unwin Ltd., Herts, U.K.

Ibekwe, A.M. and Kennedy, A.C. 1999. Fatty acid methyl ester (FAME) profiles as a tool to investigate community structure of two agricultural soils. *Plant Soil* 206: 151–161.

Kennedy, A.C. 1994. Carbon utilization and fatty acid profiles for characterization of bacteria. In R.W. Weaver et al., Eds. *Methods of Soil Analysis, Part 2—Microbiological and Biochemical Properties*. Soil Science Society of America, Madison, WI, USA, pp. 543–556.

Klug, M.J. and Tiedje, J.M. 1993. Response of microbial communities to changing environmental conditions: chemical and physiological approaches. In Guerrero, R. and Pedros-Alio, C., Eds. *Trends in Microbial Ecology*. Spanish Society for Microbiology, Barcelona, Spain, pp. 371–374.

Ovreas, L. and Torsvik, V. 1998. Microbial diversity and community structure in two different agricultural soil communities. *Microb. Ecol.* 36: 303–315.

Pankhurst, C.E., Yu, S., Hawke, B.G., and Harch, B.D. 2001. Capacity of fatty acid profiles and substrate utilization patterns to describe differences in soil microbial communities associated with increased salinity or alkalinity at three locations in South Australia. *Biol. Fert. Soils* 33: 204–217.

Petersen, S.O., Frohne, P.S., and Kennedy, A.C. 2002. Dynamics of a soil microbial community under spring wheat. *Soil Sci. Soc. Am. J.* 66: 826–833.

Ratledge, C. and Wilkinson, S.G. 1988. *Microbial Lipids*. Academic Press, Inc., New York, NY.

Sasser, M. 1990. Identification of bacteria by gas chromatography of cellular fatty acids. Tech. Note #101. Microbial ID, Newark, DE.

Schutter, M.E. and Dick, R.P. 2000. Comparison of fatty acid methyl ester (FAME) methods for

characterizing microbial communities. *Soil Sci. Soc. Am. J.* 64: 1659–1668.

Smithwick, E.A.H., Turner, M.G., Metzger, K.L., and Balser, T.C. 2005. Variation in NH_4^+ mineralization and microbial communities with stand age in lodgepole pine (*Pinus contorta*) forests, Yellowstone National Park (USA). *Soil Biol. Biochem.* 37: 1546–1559.

Torsvik, V., Goksoyr, J., and Daae, F.L. 1990. High diversity in DNA of soil bacteria. *Appl. Environ. Microbiol.* 56: 782–787.

White, D.C., Davis, W.M., Nickels, J.S., King, J.D., and Bobbie, R.J. 1979. Determination of the sedimentary microbial biomass by extractable lipid phosphate. *Oecologia* 40: 51–62.

White, D.C. and Ringelberg, D.B. 1998. Signature lipid biomarker analysis. In Burlage, R.S., Atlas, R., Stahl, D., Geesey, G., and Sayler, G., Eds. *Techniques in Microbial Ecology*. Oxford University Press, New York, NY, pp. 255–272.

Wollenweber, H.W. and Rietschel, E.T. 1990. Analysis of lipopolysaccharide (lipid A) fatty acids. *J. Microbiol. Methods* 11: 195–211.

Zelles, L. 1999. Fatty acid patterns of phospholipids and lipopolysaccharides in the characterization of microbial communities in soil: a review. *Biol. Fert. Soils* 29: 111–129.

Zelles, L. and Bai, Q.Y. 1993. Fractionation of fatty acids derived from soil lipids by solid phase extraction and their quantitative analysis by GC–MS. *Soil Biol. Biochem.* 25: 495–507.

Zelles, L., Bai, Q.Y., Beck, T., and Beese, F. 1992. Signature fatty acids in phospholipids and lipopolysaccharides as indicators of microbial biomass and community structure in agricultural soils. *Soil Biol. Biochem.* 24: 317–323.

Chapter 43
Bacterial Community Analyses by Denaturing Gradient Gel Electrophoresis

E. Topp and Y.-C. Tien
Agriculture and Agri-Food Canada
London, Ontario, Canada

A. Hartmann
National Institute of Agronomic Research
Dijon, France

43.1 INTRODUCTION

In ''traditional'' microbiology, soil bacteria are quantified by methods that detect viable cells, by plate counting or most probable number (MPN) enumeration, for example. The major weakness of this approach is that only those organisms that are viable and able to grow in the chosen media at the specified incubation conditions (e.g., temperature) will be detected. Microbiologists have long suspected that the bacteria that are amenable to culturing using conventional methods represent only a tiny fraction of those in soil. Most likely, because these have fastidious requirements that have foiled the development of suitable cultivation techniques, or because they are in obligate association with other organisms such as protozoa. The reannealing behavior of DNA isolated from soil suggests that a single gram of soil may contain up to 10,000 bacterial types (Torsvik et al. 1996). A gram of agricultural soil typically contains a billion or more bacteria. There are estimated to be about 5×10^{30} prokaryotic individuals on Earth, of which 49×10^{27} are in the top meter of cultivated land on the Earth's surface (Whitman et al. 1998). The exploration of this hitherto unseen microbial world is now feasible using methods that can elucidate the abundance, identity, and activity of bacteria without relying on culturing. Methods that exploit the sequence of bacterial nucleic acids extracted directly from soil are particularly powerful in this regard.

There are three types of nucleic acids that are informative in soil microbial ecology: DNA, ribosomal RNA (rRNA), and messenger RNA (mRNA). A fundamental dogma in biology is that each organism carries its own genetic ''blueprint,'' or genome, composed of DNA (some viruses being the exception to the rule). Through the processes of transcription and

translation, the genes encoded in the DNA control the synthesis and specify the amino acid composition of each and every protein that can be made by the organism. Each protein is encoded by a unique DNA sequence, which is transcribed to an mRNA molecule that directs the order of amino acid assembly by the protein synthesis machinery. The critical component of the protein synthesis machinery is the ribosome, which is built of protein and three different types of rRNA molecules. One of the ribosomal RNA genes, which encodes the 16S rRNA molecule, is a tool of choice in bacterial taxonomy. Portions of the gene sequence are highly conserved among different bacterial groups, and can be used to identify bacteria, and establish their evolutionary relatedness.

Overall, the presence of specific rDNA sequences is informative with respect to specific types of bacteria, and the quantity of these molecules informative with respect to the abundance in soil of their bacterial owners.

Denaturing gradient gel electrophoresis–polymerase chain reaction (DGGE–PCR) analysis is a relatively tractable and powerful culture-independent approach that can be used to characterize bacterial community composition (Muyzer and Smalla 1998; Muyzer 1999). The method yields a community ''fingerprint'' that can be responsive to soil treatments. For example, 16S rDNA from soil extract is PCR amplified using primers that are universal for bacteria that will hybridize to conserved sequences and amplify a fragment of this gene from most bacteria in the soil. The composition of the PCR product mixture, with respect to the number of products and their DNA sequences, will vary according to the diversity and identity of the bacteria in the soil. The base sequence of the DNA bands resolved in the gel can be elucidated and compared to known sequences to gain insights into the identity of the bacteria. This is accomplished by excising individual gel bands, eluting the DNA into a buffer, cloning the fragment into a suitable vector, sequencing the cloned DNA, and comparing the sequence with archived sequences (e.g., using the basic local alignment search tool [BLAST] program to match with sequences in the National Center for Biotechnology Information [NCBI] database [McGinnis and Madden 2004]).

43.2 OBTAINING DNA FROM SOILS (MARTIN-LAURENT ET AL. 2001)

43.2.1 Considerations and Principles

The objective is to extract and purify DNA from the soil microbial community such that it is suitable for amplification by PCR. The PCR will not work if humic materials and other inhibitory substances are not removed from the extract. Two types of methods for obtaining DNA are generally used. The first method consists of extracting DNA from soil microorganisms isolated directly from the soil matrix. This method is tedious since density gradient centrifugation is used to isolate microorganisms, and a strong bias in the community structure can be introduced since the efficiency of the recovery varies from 5% to 20% depending on the soil. The second and more generally used method consists of extracting DNA directly from bulk soil. The operational challenge with this approach is to extensively purify the DNA, removing humic materials that will otherwise interfere with the PCR. Here, we describe a method based on combined mechanical and chemical lysis of microbes from bulk soil and subsequent purification of DNA. This method has proven to be efficient on a wide range of soils and is rather simple to set up and operate.

There are a number of commercial kits now available for extracting DNA from soil, and different options for optimizing yield and quality of the extracted DNA. The method described here is based on the method described by Martin-Laurent et al. (2001) with some modifications. Genomic DNA is extracted from bulk soil by a mechanical lysis of microbial cells, which is achieved by bead beating and by a chemical lysis achieved by sodium dodecyl sulfate (SDS), anionic detergent. Soil is then eliminated by centrifugation and DNA precipitated by isopropanol in the presence of potassium acetate. DNA is first purified on a poly(vinylpolypyrrolidone) (PVPP) column and then on a glass milk cartridge (Geneclean Turbo Kit, Bio 101 Systems, Qbiogene).

43.2.2 Materials and Reagents

1 Ice bucket, ice

2 Screw cap tubes (2 mL, sterile) and snap cap microtubes (2 mL, 1.5 mL, sterile)

3 Glass beads 0.1 and 2 mm in diameter (sterile)

4 Bead beater (Mikrodismembrator S, B. Braun Biotech International)

5 Water bath or dry heating block for 2 mL tubes adjustable to 70°C

6 Freezer (−20°C)

7 Microbiospin chromatography columns (Biorad, #732-6204)

8 Refrigerated benchtop centrifuge fitted with a 1.5 mL microtube rotor, capable of 14,000 *g*

9 Horizontal agarose gel electrophoresis equipment and power supply (capable of at least 300 V)

10 Gel image capture equipment (e.g., Alphalmager, Alpha Innotech Corporation)

11 Micropipettors and sterile tips

12 Lysis buffer: Tris–HCl pH 8, 100 m*M*; Na_2 EDTA pH 8, 100 m*M*; NaCl, 100 m*M*; SDS, 2% (w/v)

13 Potassium acetate (CH_3COOK) pH 5.5, 3 *M*

14 Poly(vinylpolypyrrolidone) (PVPP; Sigma–Aldrich Chemical Co.)

15 Isopropanol and ethanol

16 Calf thymus DNA

17 Geneclean Turbo Kit (Bio 101 Systems, Qbiogene)

18 Agarose and TBE buffer: per liter of 5 × stock, 54 g Tris base, 27.5 g boric acid, 20 mL 0.5 *M* EDTA, pH 8.0

19 Ethidium bromide staining solution (0.4 mg L^{-1})

43.2.3 Procedure

1 DNA extraction from soil should be performed on freshly collected moist (not dried) soil. Alternatively fresh soil samples could be stored in plastic microtubes at −80°C after rapid freezing in liquid nitrogen. Air drying the soil will change its microbial composition and is to be avoided.

2 Moist soil (equivalent to 250 mg dry weight) is dispensed into a 2 mL screw cap tube. In each tube, 0.5 g of 0.1 mm diameter glass beads and two 2 mm diameter glass beads are added. One mL of lysis buffer is added. The tubes are shaken in a bead beater for 30 s at 1600 rpm. Then tubes are incubated at 70°C for 20 min in the dry heating block or water bath. Tubes are centrifuged at 14,000 *g* for 1 min and the supernatant transferred into a new sterile 2 mL tube. The supernatant volume is measured and one-tenth of the volume of 3 *M* potassium acetate pH 5.5 is added. The tube is incubated on ice for 10 min and centrifuged at 14,000 *g* for 5 min. The supernatant volume is transferred into a new 2 mL tube. To precipitate the DNA, one volume of cold (−20°C) isopropanol is added and tubes are incubated for 30 min at −20°C, then centrifuged at 14,000 *g* for 30 min and the supernatant carefully discarded. The DNA pellet is washed in 200 μL of cold 70% ethanol and air dried for 30 min at room temperature. DNA is finally resuspended in 100 μL of sterile water.

3 DNA is cleaned up by passage through PVPP columns, prepared just prior to use by the following procedure: Microbiospin columns are placed in 2 mL microtubes and filled with 92 mg of PVPP powder; 400 μL of sterile water is added, and then the assembly is centrifuged at 1000 *g* for 2 min (10°C). Add a second portion of 400 μL of sterile water and centrifuge again. Place the column in a new 2 mL tube and carefully load the DNA extracted in the previous step onto the top of the column. Columns are incubated for 5 min on ice and then centrifuged for 4 min at 1000 *g* (10°C). The volume of eluted DNA solution should be 80–90 μL.

4 DNA eluted from PVPP columns is further purified using the Geneclean Turbo Kit according to the manufacturer recommendations (protocol 5.1 rapid isolation of DNA from PCR reactions and other enzymatic solutions). DNA is finally recovered in a volume of 30–50 μL of water.

5 Purified DNA is quantified by visualizing the band following agarose gel electrophoresis (1% agarose gel in TBE buffer). Known amounts of calf thymus DNA (e.g., 10, 50, 100, and 200 ng per well) are loaded besides the purified soil DNA samples.

6 After electrophoresis, gels are stained with ethidium bromide and photographed under UV light illumination. After image analysis, soil DNA quantities are computed from the regression curve obtained from the calf thymus DNA standards.

43.3 AMPLIFYING DNA FROM SOIL BY PCR (DIEFFENBACH AND DVEKSLER 2003)

43.3.1 Considerations and Principles

The PCR selectively and exponentially replicates specific DNA sequences, corresponding to the oligonucleotide primers used in the reaction. For studies of soil microbial ecology, the PCR is extremely useful in a number of ways. It can be used to generate large amounts of DNA needed for establishing community composition and identity using various electrophoretic fingerprinting or hybridization approaches. The PCR can be primed using specific oligonucleotides that amplify genes of interest only, a positive reaction indicating the presence of those sequences. Finally, target sequences in the soil DNA can be quantified if a thermocycler capable of doing real-time quantitative PCR is available (e.g., a LightCycler PCR System, Roche Applied Science). Primers amplifying specific gene sequences of interest can be obtained from the literature, or readily derived using software packages designed for this purpose (e.g., PrimerSelect, DNAStar Inc.). For any given primers used, the various temperature and time steps used to program the thermocycler, repeatedly denaturing the DNA template, annealing the primers, and extending the new strand of DNA, can be obtained from the literature or optimized in preliminary experiments.

43.3.2 Materials and Reagents

1. Ice bucket and ice
2. Micropipettors (dedicated to PCR only) suitable for delivering various volumes (1–1000 μL capacity), and sterile aero seal tips
3. Plastic PCR tubes suitable for running 25 or 100 μL reactions
4. Thermocycler, preferably with heated lid
5. PCR preparation hood with UV lamp for destroying ambient DNA contaminants (recommended)
6. Reagents for PCR master mix; Taq polymerase (5 units μL^{-1}) and 10× reaction buffer (provided by the Taq supplier), dNTPs, and 25 m*M* $MgCl_2$
7. Oligonucleotide primers. We use universal Bacterial 16S rDNA primers one of which is GC clamped according to Santegoeds et al. (1998)
8. Purified soil DNA template for the PCR

43.3.3 Procedure

1. A series of autoclaved 0.5 mL PCR tubes are labeled and set on ice. A PCR master mix containing all components except the soil DNA template is prepared and dispensed into the PCR tubes. The total volume of the master mix is calculated and adjusted on the basis of the number of reactions to be undertaken. The final mixture volume for each reaction is 100 μL with the following composition: 10 μL of 10× PCR reaction buffer; 0.5 μ*M* of each of the primers; 0.2 m*M* of

each dNTP; three units of Taq polymerase, sufficient autoclaved Milli-Q water to bring the volume to 96 μL.

2 While still on ice, template DNA (generally 4 μL of 1:10 dilution of soil DNA, containing about 40 ng of DNA) is added, the solution is mixed by repeatedly pipetting up and down, and placed into the thermocycler. The DNA is amplified by ''touchdown'' PCR, which has been optimized for the universal bacterial primers used in the experiments. The thermocycler is programed as follows: 5 min at 94°C, three cycles of 1 min at 94°C, 1 min at 65°C, 2 min at 72°C; three cycles of 1 min at 94°C, 1 min at 63°C, 2 min at 72°C; three cycles of 1 min at 94°C, 1 min at 61°C, 2 min at 72°C; three cycles of 1 min at 94°C, 1 min at 59°C, 2 min at 72°C; three cycles of 1 min at 94°C, 1 min at 58°C, 2 min at 72°C; three cycles of 1 min at 94°C, 1 min at 57°C, 2 min at 72°C; three cycles of 1 min at 94°C, 1 min at 56°C, 2 min at 72°C; 14 cycles of 1 min at 94°C, 1 min at 55°C, 2 min at 72°C; and final extension of 5 min at 72°C. PCR tubes are removed and stored at −20°C.

3 Yield and PCR fragment size are evaluated by electrophoresis through 1% agarose as specified in Section 43.2.3.

43.4 REVEALING COMMUNITY COMPOSITION BY DGGE (MUYZER AND SMALLA 1998)

43.4.1 Considerations and Principles

The PCR products produced from a mixed soil DNA template will be of near identical size, reflecting the generally uniform size of DNA between the conserved PCR priming sites. The mixture cannot, therefore, be resolved using standard agarose gel electrophoresis on the basis of size separation. Using DGGE, PCR products are separated on the basis of their melting behavior, determined by the DNA composition, in a gel that contains a vertical gradient of denaturant consisting of increasing concentrations of urea and formamide. The PCR is done with one of the two oligonucleotide DNA primers having a so-called GC-clamp added. This is a GC-rich segment of DNA that does not readily denature or melt. The double-stranded GC-clamped PCR products migrate through the DGGE gel to the point where the lowest temperature melting domain is sufficiently unstable that the double-stranded DNA unravels into the single-stranded forms. The partially denatured molecule stops migrating in the gel when held together by the still double-stranded GC-clamp. Thus, a PCR mixture that contains many molecules varying in their melting behavior will yield a mixture of bands that have migrated to different locations in a DGGE gel. The distribution of bands represents a community fingerprint whose characteristics will vary with the number and identity of the bacteria. DGGE is quite flexible in its application. Targets chosen for analysis may be 16S rDNA or functional genes encoding enzymes of interest. The primers can be chosen to reveal very broad or more distinct groups of bacteria. The gel composition (i.e., concentration of denaturants) and running conditions can be varied to optimize band resolution according to the melting properties of the PCR products.

43.4.2 Materials and Reagents

1 DGGE apparatus: These can most easily be purchased commercially. We use the BioRad DCode Universal Mutation Detection System. It includes a temperature

control module and a ''sandwich'' core upon which two 16 cm gels can be electrophoresed simultaneously. It also comes with a kit for gel casting consisting of two sets of plates, two sets of clamps and 1 mm spacers, two single-well 1 mm prep combs, and comb gaskets.

2 Gradient gel-casting apparatus: We use a simple acrylic two-chamber linear gradient maker. The solutions are delivered by gravity into the gel-casting sandwich by means of a narrow 25 cm long plastic tube connected to a 20-gauge syringe needle via a luer-lock fitting.

3 Electrophoresis power supply: A direct current (DC) voltage power supply, which has a maximum voltage limit of 500 V DC and a maximum power limit of 50 W.

4 Pipettors for loading samples: A capacity of 100 μL fitted with long pipet tips used for loading polyacrylamide DNA sequencing gels.

5 Trays for staining and destaining gels, a UV transilluminator for revealing stained bands, and a conventional or digital camera for capturing gel images.

6 Software for digitizing, archiving, and analyzing images is very useful.

7 Stock solutions for casting polyacrylamide gel: The concentration of denaturant to be used is adjusted according to the desired gradient range, in the example here from 35% to 65% denaturant, where 100% is defined as 7 *M* urea (H_2NCONH_2; 420.4 g L^{-1} water) and 40% v/v formamide (CH_3NO).

Caution: Acrylamide monomer is teratogenic (can potentially cause cancer, birth defects) and is a neurotoxin. It must be handled with extreme care and in a fume hood only. Once the gel polymerization has taken place, it is safe to handle with gloves.

8 50 × Tris-acetate-EDTA (TAE) buffer: Add the following to 900 mL distilled water. 242 g Tris base, 57.1 mL glacial acetic acid, and 18.6 g EDTA. Adjust volume to 1 L with additional distilled water.

Caution: Glacial acetic acid is extremely volatile and corrosive and must be manipulated in a fume hood. In a complete TAE buffer (pH of 8.3), the acetate is no longer volatile.

Stock solutions for the low and the high denaturant concentrations have the following composition:

	Low (35%)	**High (65%)**
40% Acrylamide/Bis (37.5:1)	25 mL	25 mL
50 × TAE	2 mL	2 mL
Formamide (deionized)	14 mL	26 mL
Urea	14.7 gm	27.3 gm
Total volume	100 mL	100 mL

9 Reagents for catalyzing acrylamide polymerization: A freshly prepared solution of 10% (w/v) ammonium persulfate ($(NH_4)_2S_2O_8$) in water and *N,N,N′,N′*-tetramethylethylenediamine (TEMED).

Caution: $(NH_4)_2S_2O_8$ is an extremely powerful oxidizing agent, and TEMED is extremely volatile, flammable, corrosive, and fatal if inhaled. These materials must be manipulated in a fume hood.

10 Gel loading dye: The 6 × loading buffer contains 0.25% bromophenol blue, 0.25% xylene cyanol FF, and 70% glycerol in distilled water.

11 Staining solution: 1 × TAE buffer containing 1 × SYBR Green I.

12 1 × TAE running buffer for gel electrophoresis is made by diluting 50 × TAE (see 8 above) concentrated stock solution 50-fold.

43.4.3 Procedure

1 At least 1 μg of GC-clamped DNA from each sample is obtained by PCR. The quantity and quality of the DNA is evaluated and adjusted. It is important to optimize the PCR reaction to minimize unwanted products that may interfere with gel analysis. The PCR products should be evaluated for purity by agarose gel electrophoresis before being loaded onto the DGGE gel. A clear, bright PCR fragment with limited primer dimer signal is expected for DGGE gel running. In order to obtain sufficient DNA for the DGGE analysis, it may be necessary to combine the products of several PCR reactions, and concentrate them by ethanol precipitation to an ideal concentration of about 150 ng μL^{-1}. DNA can be quantified accurately in a fluorometer in a standard 2 mL assay. Adjust the volume of DNA in each sample to 20 μL with water; add 5 μL of loading dye and mix by vortexing briefly.

2 Fifteen mL of the high and 15 mL of the low concentration denaturant are added into the gradient maker. The high concentration is always added into the chamber that will empty first, the low concentration solution to the chamber that will empty last. Acrylamide polymerization is initiated immediately prior to gel casting by adding to each chamber 150 μL of 10% $(NH_4)_2S_2O_8$ and 15 μL of TEMED. The solutions are allowed to drain into the gel-casting sandwich by gravity, and the comb is set into the still-liquid solution. The gel is allowed to polymerize for at least 1 h at room temperature (about 20°C).

3 Buffer reservoir is filled with 1 × TAE, and the gel sandwich placed into the reservoir. The temperature setting is adjusted to 60°C, and the apparatus is allowed to warm to the set point. The 25 μL DNA samples are carefully added into the bottom of each well using a sequencing gel pipet tip. The gel apparatus is then run for 16 h at a constant voltage of 100 V.

4 Carefully disassemble the gel sandwich and remove the gel from the glass plates. Place the gel into a tray containing 150 mL of 1 × TAE buffer and 15 μL of 10,000 × SYBR Green I. Stain for 40 min, then carefully transfer the gel into a tray containing 250 mL of 1 × TAE buffer, and destain for 5–20 min. Place the gel on a UV transilluminator and photograph for DNA capture.

43.4.4 Analysis

Information can be extracted both from the DGGE fingerprint patterns and the DNA sequences of specific bands. Gel images can be visually compared to readily detect significant differences or consistent features in the community fingerprint pattern, and how these vary according to soil treatment or conditions. Examples of studies that have employed this approach include evaluating the impact of cropping with transgenic potatoes on rhizospheric communities, the effect of temperature on the community structure of ammonia-oxidizing bacteria in soil, the impact of soil management and plant species on nitrogen-transforming bacteria, and the effect of long-term contamination with organic and heavy metal pollutants on global bacterial community structure (Heuer et al. 2002; Avrahami and Conrad 2003; Becker et al. 2006; Patra et al. 2006). Various statistical analyses are available to establish treatment effects (Fromin et al. 2002; Kropf et al. 2004). The identity of the bacteria from which specific bands in the profile originate can be established by excision, elution, cloning, DNA sequencing, and comparison with published databases. Examples of studies that have employed this approach include establishing the identity of bacteria associated with the decomposition of rice straw in anoxic soils, the elucidation of soil bacteria associated with cysts of the soybean cyst nematode (*Heterodera glycines*), and the identification of antibiotic-producing rhizospheric pseudomonads that suppress soilborne plant pathogens (Weber et al. 2001; Nour et al. 2003; Bergstra-Vlami et al. 2005). Overall, these studies provide examples of various analytical strategies that can be chosen by the investigator based on the specific research question, the detail of answer required, and the resources available.

REFERENCES

Avrahami, S. and Conrad, R. 2003. Patterns of community change among ammonia oxidizers in meadow soils upon long-term incubation at different temperatures. *Appl. Environ. Microbiol*. 69: 6152–6164.

Becker, J.M., Parkin, T., Nakatsu, C.H., Wilbur, J.D., and Konopka, A. 2006. Bacterial activity, community structure, and centimeter-scale spatial heterogeneity in contaminated soil. *Microb. Ecol*. 51: 220–231.

Bergsma-Vlami, M., Prins, M.E., Staats, M., and Raaijmakers, J.M. 2005. Assessment of genotypic diversity of antibiotic-producing pseudomonas species in the rhizosphere by denaturing gradient gel electrophoresis. *Appl. Environ. Microbiol*. 71: 993–1003.

Dieffenbach, C.W. and Dveksler G.S., Eds. 2003. *PCR Primer: A Laboratory Manual*, 2nd ed. Cold Spring Harbor Laboratory Press. Plainview, NY, USA.

Fromin, N., Hamelin, J., Tarnawski, S., Roesti, D., Jourdain-Miserez, K., Forestier, N., Teyssier-Cuvelle, S., Gillet, F., Aragno, M., and Rossi, P. 2002. Statistical analysis of denaturing gel electrophoresis (DGE) fingerprinting patterns. *Environ. Microbiol*. 4: 634–643.

Heuer, H., Kroppenstedt, R.M., Lottmann, J., Berg, G., and Smalla, K. 2002. Effects of T4 lysozyme release from transgenic potato roots on bacterial rhizosphere communities are negligible relative to natural factors. *Appl. Environ. Microbiol*. 68: 1325–1335.

Kropf, S., Heuer, H., Gruning, M., and Smalla, K. 2004. Significance test for comparing complex microbial community fingerprints using pairwise similarity measures. *J. Microbiol. Methods* 57: 187–195.

Martin-Laurent, F., Philippot, L., Hallet, S., Chaussod, R., Germon, J.-C., Soulas, G., and Catroux, G. 2001. DNA extraction from soils: Old bias for new microbial diversity analysis methods. *Appl. Environ. Microbiol*. 67: 2354–2359.

McGinnis, S. and Madden, T.L. 2004. BLAST: At the core of a powerful and diverse set of

sequence analysis tools. *Nucleic Acids Res*. 32: W20–W25.

Muyzer, G. 1999. DGGE/TGGE: A method for identifying genes from natural ecosystems. *Curr. Opin. Microbiol*. 2: 317–322.

Muyzer, G. and Smalla, K. 1998. Application of denaturing gradient gel electrophoresis (DGGE) and temperature gradient gel electrophoresis (TGGE) in microbial ecology. *Ant. van Leeuw*. 73: 127–141.

Nour, S.M., Lawrence, J.R., Zhu, H., Swerhome, G.D.W., Welsh, M., Welacky, T.W., and Topp, E. 2003. Bacteria associated with cysts of the soybean cyst nematode (*Heterodera glycines*). *Appl. Environ. Microbiol*. 36: 607–615.

Patra, A.K., Abbadie, L., Clays-Josserand, A., Degrange, V., Grayston, S.J. Guillaumaud, N., Loiseau, P., Louault, F., Mahmood, S., Nazaret, S., Philipot, L., Poly, F., Prosser, J.I., and Le Roux, I. 2006. Effects of management regime and plant species on the enzyme activity and genetic structure of N-fixing, denitrifying, and nitrifying bacterial communities in grassland soils. *Environ. Microbiol*. 8: 1005–1016.

Santegoeds, C.M., Ferdelman, T.G., Muyzer, G., and de Beer, D. 1998. Structural and functional dynamics of sulfate-reducing populations in bacterial biofilms. *Appl. Environ. Microbiol*. 64: 3731–3739.

Torsvik, V., Sorheim, R., and Goksoyr, J. 1996. Total bacterial diversity in soil and sediment communities—a review. *J. Ind. Microbiol. Biotechnol*. 17: 170–178.

Weber, S., Stubner, S., and Conrad, R. 2001. Bacterial populations colonizing and degrading rice straw in anoxic paddy soil. *Appl. Environ. Microbiol*. 67: 1318–1327.

Whitman, W.B., Coleman, D.C., and Wiebe, W.J. 1998. Prokaryotes: The unseen majority. *Proc. Nat. Acad. Sci. USA* 95: 6578–6583.

Chapter 44
Indicators of Soil Food Web Properties

T.A. Forge
Agriculture and Agri-Food Canada
Agassiz, British Columbia, Canada

M. Tenuta
University of Manitoba
Winnipeg, Manitoba, Canada

44.1 INTRODUCTION

The soil food web is a conceptual simplification of the soil biota, in which the microflora and microfauna are aggregated into general trophic groups that describe major flows of energy (organic C) and nutrients (primarily N and P) (Figure 44.1). Analyses of soil food web structure can provide insight into how soil management practices influence microbial immobilization, and turnover of energy and nutrients (Wardle 2002). Roots, plant residues, agrochemicals, and animal manures are the primary inputs of energy and nutrients to cropped soil. Bacteria and some fungi are the initial decomposers of such organic inputs, and soil food webs can be compartmentalized into bacterial and fungal channels representing very different storage efficiencies and turnover rates (Edwards 2000; Wardle 2002). Thus, separation of bacterial and fungal biomass is a fundamental component of soil food web analyses. Soil protozoa, nematodes, and microarthropods are the principal consumers of the microbial biomass (Figure 44.1). Through their grazing, they regulate microbial community structure and enhance mineralization of nutrients. The protozoa are primarily bacterivorous. The soil nematode community includes bacterivores, fungivores, omnivores, predators (which consume other microfauna), and root-grazers, in addition to the true plant parasites, which are covered in Chapter 33 (Edwards 2000; Wardle 2002). The soil microarthropod community is dominated by Collembola and Acarina (mites), and includes fungivore, bacterivore, omnivore, and predator trophic groups (Edwards 2000; Wardle 2002). Methods for extraction of microarthropods, nematodes, protozoa, and total microbial biomass are described in Chapters 32, 33, 36, and 49, respectively.

It is important to note that resource preferences of many taxonomic groups of soil fauna are not directly known, rather, they are inferred from morphological similarity with species of

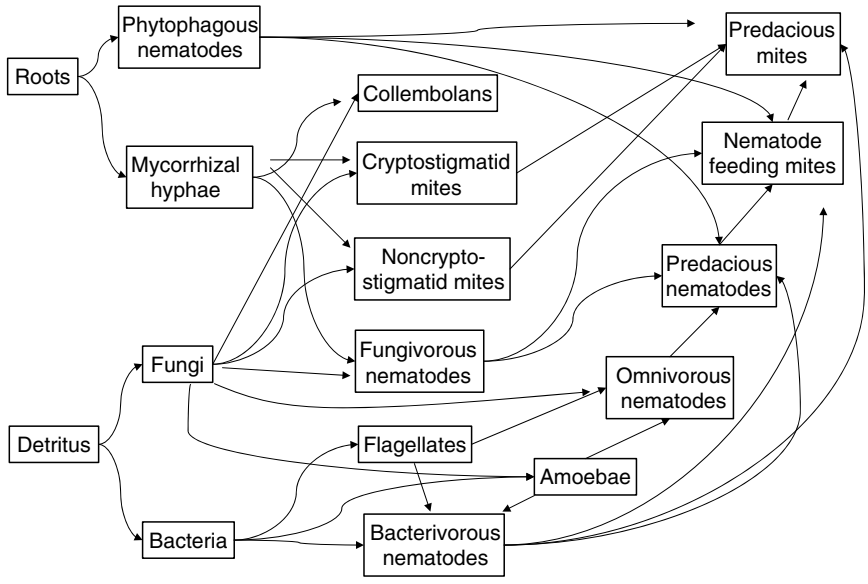

FIGURE 44.1. A soil food web. (Adapted from Hunt, H.W., Coleman, D.C., Ingham, E.R., Ingham, R.E., Elliot, E.T., Moore, J.C., Rose, S.L., Reid, C.P.P., and Morley, C.R., *Biol. Fert. Soils*, 3, 57, 1987.)

known feeding habits. Consequently, the categorization of soil fauna into broad trophic groups, such as in Figure 44.1, is a gross simplification of the complex interactions that occur in real soil food webs. Microarthropod feeding habits have been assessed on the basis of gut enzymes in addition to mouthpart morphology (Behan-Pelletier 1999). New approaches involving stable isotope and fatty acid analyses are making it possible to confirm food resources for various groups of soil fauna, and measure actual fluxes of C through components of the food web (Fitter et al. 2005; Ruess et al. 2005). In the future, these approaches may become powerful tools for assessing the relative strengths of different pathways within the soil food web without the need for detailed microscopic observation and identification.

One approach for describing soil food webs involves obtaining data on biomass of the major trophic groups, and then using the food web model originally described by Hunt et al. (1987) (see Figure 44.1) to estimate flows of C, N, and P through the trophic groups. This model has been tested against actual measurements, of soil C and N mineralization (e.g., De Ruiter et al. 1993; Hassink et al. 1994; Berg et al. 2001), and fluxes of ^{13}C through some components of the food web (Leake et al. 2006). A truncated version of the model, utilizing only data on bacteria, fungi, protozoa, and nematodes, captures the trophic interactions that make the greatest direct contributions to N mineralization (Hassink et al. 1994; Forge et al. 2005). Introductory information on the conversion of bacterial, fungal, nematode, and protozoan abundance data to biomass, for use in soil food web model analyses, is included in this chapter. Actual construction of soil food web models is beyond the scope of this chapter, and readers are referred to Irvine et al. (2006), De Ruiter et al. (1993), and Hunt et al. (1987) for more details.

Another approach for describing soil food webs involves focusing on one or a few organism groups, and using information on changes in community structure within those groups as indicators of changes in properties of the broader soil food web.

For example, the ratio of fungal biomass to total microbial biomass provides information on the relative extent to which C, N, and P are channeled through fungus–fungivore pathways of the soil food web, which is of functional importance because it influences nutrient turnover rates and storage efficiencies. Similarly, some specific descriptors of nematode community structure are becoming popular as indicators of changes in soil food web properties, and will be described in more detail in this chapter. Microarthropod community data can be used in a similar way (e.g., Behan-Pelletier 1999; Parisi et al. 2005), but specific indices of microarthropod community structure have not been adopted as widely as nematode indices for routine assessment of soil food web properties.

This chapter will describe methods for distinguishing bacterial and fungal biomass, obtaining data on nematode community structure, and calculating nematode community indices that provide information on the properties of soil food webs.

44.2 DIFFERENTIATING FUNGAL AND BACTERIAL BIOMASS

Bacterial and fungal biomass can be differentiated via biochemical, physiological, and microscopic approaches. Guggenberger et al. (1999) used glucosamine and muramic acid as markers of fungal and bacterial contributions to microbial-derived soil organic matter, respectively. Other researchers have inferred bacterial biomass from the difference between total biomass, determined via chloroform fumigation–extraction (Chapter 49), and fungal biomass, determined via measurement of ergosterol (Montgomery et al. 2000). Phospholipid fatty acid (PLFA) profiles of bacteria and fungi differ, and specific PLFA compounds have been used as biomarkers of bacterial and fungal biomass in soil (Chapter 49; Frostegard and Bååth 1996; Bossio et al. 1998). The substrate-induced respiration (SIR) method for measuring total biomass has been adapted for separate measurement of fungal and bacterial biomass (Chapter 39; Beare et al. 1990; Lin and Brookes 1999). SIR of soil samples amended with cycloheximide (fungal inhibitor) and streptomycin (bacterial inhibitor) gives estimates of respiration activity of bacterial and fungal biomass, respectively. This procedure assesses only metabolically active components of the respective groups, and is therefore an indicator of biomass, not a direct measure of total biovolume or biomass per se. Fierer et al. (2005) designed general bacterial and fungal primers, allowing for the estimation of bacterial and/or fungal DNA in soil by quantitative polymerase chain reaction; such DNA-based techniques may provide a rapid and reproducible indication of bacterial and fungal biomass in soil.

Measurement of microbial biovolumes via microscopy is the most direct method for measuring the biomass of bacteria and fungi, but it is also the most labor-intensive. Recent advances in digital image analysis and confocal laser scanning microscopy have great potential to drastically reduce the labor associated with direct microscopic assessment of microbial biovolumes (Bloem et al. 1995; Bölter et al. 2002).

Since the agar film method was first described by Jones and Mollison (1948), numerous variations have been developed (Bottomley 1994). Membrane filter techniques have become popular for fungal biovolume measurement, but they may not necessarily be more effective than the agar film technique (Bååth and Söderström 1980). Modifications of agar film and membrane filter techniques involving the use of fluorescein diacetate (FDA) or tetrazolium chloride make it possible to discriminate empty or dead hyphae and bacteria, respectively, from metabolically active hyphae and bacterial cells (Bottomley 1994). The following procedure is an adaptation of the agar film technique. It is particularly convenient because

it allows for estimation of total (but not metabolically active) fungal and bacterial biomass on the same agar film slides.

44.2.1 Materials and Reagents

1 Waring blender

2 Fluorescent immunology slides with 15 mm diameter rings (e.g., VWR cat. No. 48349-057); rinsed in 70% ethanol and air-dried before use

3 Nonfluorescent immersion oil (Cargille type A) and #1 cover slips

4 Staining jars

5 Epifluorescence microscope with ocular micrometer and/or grid micrometer

6 Formalin solution (37%–40% (v/v) formaldehyde)

7 Purified agar solution (0.15%): 1.5 g purified agar in 1000 mL distilled water, bring to boil, and then keep molten in 50°C water bath

8 Acridine orange stock solution: 1 g in 500 mL distilled water

44.2.2 Procedure

1 Place 5.0 g fresh soil into a Waring blender with 500 mL distilled water. Blend on highest setting for 1 min. Allow sand to settle for 10 s.

2 Transfer 1 mL to a test tube with 3.5 mL 0.15% agar solution (50°C) and 0.5 mL formalin (final conc. 3.7% formaldehyde), resulting in a 1:500 soil suspension in 0.1% agar.

3 Vortex and immediately deliver 0.1 mL onto each of the two 15 mm diameter circular areas on an immunology slide. Using a needle, ensure that the suspension spreads to the edge of each circular area. Place in warm, dust-free area to air-dry (about 4 h).

4 Immerse slides in acridine orange staining solution (5 mL stock solution + 95 mL water) for 30 min. Remove and gently rinse by dunking in a beaker of distilled water, and allow to air-dry.

5 Place a drop of nonfluorescent immersion oil (e.g., Cargille type A) or glycerol on each smear, and cover with a #1 cover slip.

6 Observe 20 randomly chosen fields-of-view from two perpendicular transects through the diameter of each smear (10 fields-of-view/transect) at 400× to 600× under phase contrast. Using an ocular grid, estimate the length of hyphae in each field-of-view via the gridline intersect method (Newman 1966). Alternatively, use an ocular micrometer to estimate the length of each hyphal fragment encountered in each transect.

7 Observe under oil immersion at 1000× using epi-illumination and a filter set appropriate for acridine orange (excitation 490 nm, emission 520 nm). Bacterial cells will appear green to yellow against a dark background. Count the cells in each of 20 randomly chosen fields-of-view within each agar film, and categorize into the following five size/shape categories (values in μm): (i) <0.5× <0.5, (ii) 0.5× (0.5−1.0), (iii) 0.5× (1.0−2.0), (iv) >0.5× >2.0, and (v) >1.0× >1.0 as described by Lundgren (1984). Nominal volumes for these size classes are 0.03, 0.22, 0.34, 0.75, and 1.77 μm^3, respectively (Lundgren 1984). Calculate the average number of cells of each size class per field-of-view.

44.2.3 Calculations

Using a stage micrometer, determine the area covered by each field-of-view for your microscope using the 40× and 100× objectives, A_{v40} and A_{v100}, respectively. Calculate the total area of each smear, A_s (177 mm^2 for 15 mm diameter smears); then calculate biomass for each size class:

$$\text{Bacterial biomass} - \text{C/g moist soil } (B_b) = [N_{ave}(A_s/A_{v100})/0.1 \text{ mL} \times D \times V_b \times C_v] \quad (44.1)$$

where N_{ave} is the average number of cells (for the size class) per field-of-view, A_s is the total area of the smear, A_v is the area of the field-of-view, D is the dilution factor (500 for the above example), V_b is average biovolume for the size class (μm^3), and C is the specific carbon content of bacteria (fg C/μm^3). Bloem et al. (1995) reported C to be 196 fg/μm^3:

$$\text{Fungal biomass} - \text{C/g moist soil } (B_f) = (\pi r^2 L_{ave}) \times (A_s/A_{v40})/0.1 \text{ mL} \times D \times (b/v) \times C_m \quad (44.2)$$

where L_{ave} is the average hyphal length (μm) per field-of-view and (b/v) is the ratio of biomass/biovolume for fungi. Values ranging from 200 to 330 fg/μm^3 have been used (Bottomley 1994). C_m is the C content as a fraction of total mass; a value of 0.5 has been used (Van Veen and Paul 1979).

44.2.4 Comments

1 Above example starts with a 1:500 soil suspension. Depending on the soil, it may be necessary to use more or less dilute suspensions. Ideally, bacterial counts should average 15 to 30 cells per field-of-view. Larger cell densities tend to lead to counting fatigue and error. The occurrence of cell clusters is problematic for counting, as they can result in underestimation and large variability. Many researchers have used dispersants such as 0.1% sodium pyrophosphate or Calgon, but Bloem et al. (1995) performed a systematic comparison and found that dispersants did not significantly improve bacterial counts.

2 Sodium dithionate solution (3.5 g in 100 mL distilled water) apparently helps reduce photobleaching during epifluorescence viewing, and can be used as a mounting medium.

3 In the absence of an epifluorescence microscope, phenolic aniline blue, acetic aniline blue, or tryptophan aniline blue can be used. Bacterial cells will appear

dark blue against a bright background. Fungal hyphae take up aniline blue stains to varying degree, but phase contrast is generally the most reliable method for observing fungal hyphae.

44.3 NEMATODE FEEDING GROUPS AND INDICATORS OF FOOD WEB STRUCTURE

Several specific indices of nematode community structure are particularly useful for assessing changes in structure of the soil food web as a whole. In this chapter we use the term ''structure'' to refer to the presence and relative dominance of major trophic groups (Figure 44.1) as well as the degree to which the trophic groups are composed of a diversity of functional groups or guilds. Bongers (1990; 1999) ranked nematode families on a scale of 1 to 5 on the basis of their positions in the colonizer-persister continuum (c-p ranking). The maturity index (MI), a weighted mean representing the c-p ranking of the community, is a general indicator of community response to disturbance, environmental stress, and addition of easily decomposed, high-N organic materials. Ferris et al. (2001) expanded on the MI concept and differentiated changes in nematode communities into enrichment and structure trajectories, and applied weightings to reflect the differential importance of certain nematode families to either food web enrichment or development of structure (Table 44.1).

Organic matter inputs, tillage, and other changes that result in increased microbial production/turnover also result in increased abundance of enrichment opportunist nematodes, represented primarily by bacterivores in the families Rhabditidae, Diplogasteridae, and Panagrolaimidae, and fungivores in the families Aphelenchidae and Aphelenchoididae (Table 44.1). Ferris et al. (2001) described an enrichment index (EI) that measures the increased abundance of bacterivore and fungivore enrichment opportunists. The channel index (CI) is a measure of the extent to which the biomass of decomposers is dominated by bacteria or fungi; high values of the CI reflect fungal-dominated decomposition pathways. The EI and overall abundance of bacterivorous nematodes have both been positively correlated with N mineralization (Hassink et al. 1993; Forge and Simard 2001; Ferris and Matute 2003; Parfitt et al. 2005).

A few families of bacterivores and fungivores, and all omnivores and carnivores, indicate more structured food webs (i.e., being higher trophic feeders and indicative of greater functional diversity within broad trophic groups); these taxa have been assigned greater enrichment-structure (E-S) weightings (Table 44.1). The structure index (SI) is a measure of the extent to which the nematode community is dominated by these taxa. While the SI is not a measure of taxonomic diversity per se, taxonomic diversity increases with the addition of taxa with high c-p and structure weightings (Ferris et al. 2001). The significance of this relationship is that the SI, based on family-level nematode identification rather than species-level identification, may be used for assessment of changes in faunal biodiversity, and perhaps overall soil biodiversity.

This section will describe how to assess nematode community structure, assuming the ability to identify nematodes at the level of family (preferably genus). Instruction on basic nematode identification is outside the scope of this chapter. Freckman and Baldwin (1990) is a good primer on soil nematode identification. Some nematology laboratories provide intensive workshops on nematode identification.

TABLE 44.1 Feeding Groups, Colonizer-Persister Rankings (c-p) and Enrichment-Structure (E-S) Weightings for Common Families of Terrestrial Nematodes

Family	Feeding group	c-p ranking	E-S weighting
Tylenchidae	F-Rh	3	1.8 (s)
Aphelenchidae	F	2	0.8 (b,e)
Aphelenchoididae	F	2	0.8 (b,e)
Neotylenchidae	F	2	0.8 (b,e)
Anguinidae	F	2	0.8 (b,e)
Iotonchiidae	F	2	0.8 (b,e)
Rhabditidae	B	1	3.2 (e)
Bunonematidae	B	1	3.2 (e)
Diplogasteridae	B	1	3.2 (e)
Tylopharingidae	B	1	3.2 (e)
Panagrolaimidae	B	1	3.2 (e)
Cephalobidae	B	2	0.8 (b)
Teratocephalidae	B	3	1.8 (s)
Monhysteridae	B	2	0.8 (b)
Plectidae	B	2	0.8 (b)
Achromadoridae	B	3	1.8 (s)
Desmodoridae	B	3	1.8 (s)
Odontolaimidae	B	3	1.8 (s)
Basianiidae	B	3	1.8 (s)
Prismatolaimidae	B	3	1.8 (s)
Ironidae	B	4	3.2 (s)
Tripylidae	B	3	1.8 (s)
Alaimidae	B	4	3.2 (s)
Mononchidae	C	4	3.2 (s)
Anatonchidae	C	4	3.2 (s)
Nygolaimidae	C	5	5.0 (s)
Dorylaimidae	O	4	3.2 (s)
Chrysonematidae	O	5	5.0 (s)
Thornenematidae	O	5	5.0 (s)
Nordiidae	O	4	3.2 (s)
Qudsianematidae	O	4	3.2 (s)
Aporcelaimidae	O–C	5	5.0 (s)
Belondiridae	O	5	5.0 (s)
Actinolaimidae	C	5	5.0 (s)
Discolaimidae	C	5	5.0 (s)
Leptonchidae	F	4	3.2 (s)
Diphtherophoridae	F	3	1.8 (s)

Source: Data extracted from Bongers, T., *Plant Soil*, 212, 13, 1999 and Ferris, H., Bongers, T., and de Goede, R.G.M., *Appl. Soil Ecol.*, 18, 13, 2001, with the exception of the Tylenchidae, which were classified as root feeders in the original scheme of Bongers (1990, 1999).

F-Rh, fungivore-root-hair feeders; F, fungivore; B, bacterivore; O, omnivore; C, carnivore. Values in parentheses designate the summation groups in which the family is included: b, basal; e, enrichment; s, structure.

44.3.1 Materials and Reagents

1 Inverted microscope with mechanical stage or compound, and stereomicroscope

2 Gridded counting dish capable of holding >4 mL suspension to fit inverted microscope or stereomicroscope

3 Conical-bottom 15 mL centrifuge tubes

4 Microscope slides, #1 cover slips, fingernail polish

5 Pasteur pipettes

6 Extracted nematodes (Chapter 33)

44.3.2 Counting

1 Pour nematode sample onto counting dish, observe with dissecting stereomicroscope, and determine total nematodes as described in Chapter 33.

2 Rinse sample into a 15 mL conical-bottom centrifuge tube, and allow nematodes to settle for >2 h or, alternatively, centrifuge at 420 *g* for 5 min. Using a Pasteur pipette or pipette attached to vacuum, remove all but the bottom 0.5 mL of suspension. Immerse tube in 60°C water bath for 1 min to heat-kill nematodes.

3 Suspend nematodes by shaking and remove 0.25 mL using Pasteur pipette, and transfer one drop to each of the two positions on a microscope slide. Cover each drop with a #1 coverslip and seal with fingernail polish. These temporary mounts will generally last through a single workday but often dry out over longer periods. It is best to keep slides cool by placing in a refrigerator if observation is to occur hours after slide preparation.

4 Observe with compound microscope at 400×. Make regularly spaced transects through each coverslip, identifying each nematode encountered according to genus, family, or trophic group until 100 nematodes have been identified.

5 Alternatively, a high-quality inverted microscope with 4× and 40× objectives can be used, which allows nematodes to be counted (40×), and then identified (400×) in one counting dish. When utilizing this approach, it is helpful to first use the compound microscope (400× to 1000×) to observe a large number of nematodes (i.e., 500) from the experimental site, identify the dominant taxa present, and learn to recognize the major genera or families during routine counting or categorizing with the inverted microscope at 40× to 400×.

44.3.3 Calculations

Calculate the relative abundance (p_i) of each family listed in Table 44.1 from the identification of 100 nematodes: $p_i = n_i/100$. Multiply total nematode abundance by relative abundance of each family to get the absolute abundance (P_i) of each family.

Apply C-P rankings to the families as tabulated by Bongers (1990, 1999; Table 44.1), and E-S weightings according to the scheme of Ferris et al. (2001; Table 44.1). Relevant weighted abundances are calculated as follows, with summation across relevant families:

$$\text{Weighted abundance of basal taxa } (b) = \sum (v_b \times n_b) \tag{44.3}$$

where n_b is the abundance of each family representing basal characteristics of the food web and v_b is the weighting associated with each of those families (0.8):

$$\text{Weighted abundance of enrichment opportunists } (e) = \sum (v_e \times n_e) \tag{44.4}$$

where n_e is the abundance of each family representing enrichment characteristics of the food web and v_e is the weighting associated with each of those families (1.8 or 3.2):

$$\text{Weighted abundance of fungivore enrichment opportunists } (f_e) = \sum (v_{f_e} \times n_{f_e}) \tag{44.5}$$

where n_{f_e} is the abundance of each fungivorous family representing enrichment characteristics of the food web and v_{f_e} is the weighting associated with each of those families (0.8):

$$\text{Weighted abundance of structure taxa } (s) = \sum (v_s \times n_s) \tag{44.6}$$

where n_s is the abundance of each family representing structural characteristics of the food web and v_s is the weighting associated with each of those families (0.8 to 5):

$$\text{Enrichment index} = e/(b + e) \times 100 \tag{44.7}$$

$$\text{Structure index} = s/(b + s) \times 100 \tag{44.8}$$

$$\text{Channel index} = f_e/e \times 100 \tag{44.9}$$

44.3.4 Comments

Obtaining total counts is best accomplished with live nematodes, as movement aids detection in the counting dish at 40×. If the identification step cannot be accomplished promptly, the samples can be reduced to 0.9 mL, heat-killed as described before, and then 0.1 mL of 16% formaldehyde (40% formalin solution) added as a preservative.

44.4 CALCULATION OF MICROFAUNAL BIOMASS FOR FOOD WEB MODELING

If the nematode data will be used in a food web model for calculating nutrient fluxes or simulating food web dynamics, it is necessary to convert numbers of organisms in each trophic group to biomass. Nematode lengths and widths can be determined during the identification step with a compound microscope, and converted to biovolume according to Andrassy (1956). Alternatively, biomass can be inferred from published measurements of each taxon (Forge et al. 2005). After extraction and quantification of protozoa (Chapter 36), protozoan biovolume can be estimated from measurements of mean cell diameter, assuming a spherical shape. Forge et al. (2003) obtained an average diameter of 10 μm for a flagellate-dominated protozoan assemblage. Protozoan biovolume can then be converted to biomass-C using a conversion factor of 0.212 pg C μm^{-3} (Griffiths and Ritz 1988).

REFERENCES

Andrassy, I. 1956. The determination of volume and weight of nematodes. *Acta Zool. (Hungarian Acad. Sci.)* 2: 1–15.

Bååth, E. and Söderström, B. 1980. Comparisons of the agar-film and membrane-filter methods for the estimation of hyphal lengths in soil, with particular reference to the effect of magnification. *Soil. Biol. Biochem.* 12: 385–387.

Beare, M.H., Neely, C.L., Coleman, D.C., and Hargrove, W.L. 1990. A substrate-induced respiration (SIR) method for measurement of fungal and bacterial biomass on plant residues. *Soil Biol. Biochem.* 22: 585–594.

Behan-Pelletier, V.M. 1999. Oribatid mite biodiversity in agroecosystems: Role for bioindication. *Agric. Ecosyst. Environ.* 74: 411–423.

Berg, M., DeRuiter, P., Didden, W., Jansen, M., Schouten, T., and Verhoef, H. 2001. Community food web, decomposition and nitrogen mineralization in a stratified Scots pine forest soil. *Oikos* 94: 130–142.

Bloem, J., Veninga, M., and Shepherd, J. 1995. Fully automatic determination of soil bacterium numbers, cell volumes, and frequencies of dividing cells by confocal laser scanning microscopy and image analysis. *Appl. Environ. Microbiol.* 61: 926–936.

Bölter, M., Bloem, J., Meiners, K., and Moller, R. 2002. Enumeration and biovolume determination of microbial cells—A methodological review and recommendations for applications in ecological research. *Biol. Fert. Soils* 36: 249–259.

Bongers, T. 1990. The maturity index: An ecological measure of environmental disturbance based on nematode species composition. *Oecologia* 83: 14–19.

Bongers, T. 1999. The Maturity Index, the evolution of nematode life history traits, adaptive radiation and cp-scaling. *Plant Soil* 212: 13–22.

Bossio, D.A., Scow, K.M., Gunapala, N., and Graham, K.J. 1998. Determinants of soil microbial communities: effects of agricultural management, season, and soil type on phospholipid fatty acid profiles. *Microb. Ecol.* 36: 1–12.

Bottomley, P. 1994. Light microscopic methods for studying soil microorganisms. In R.W. Weaver et al., Eds. *Methods of Soil Analysis, Part 2—Microbiological and Biochemical Properties*. Soil Science Society of America, Madison, WI, pp. 81–106.

De Ruiter, P.C., Van Veen, J.A., Moore, J.C., Brussaard, L., and Hunt, H.W. 1993. Calculation of nitrogen mineralization in soil food webs. *Plant Soil* 157: 263–273.

Edwards, C.A. 2000. Soil invertebrate controls and microbial interactions in nutrient and organic matter dynamics in natural and agroecosystems. In D.C. Coleman and P.F. Hendrix, Eds. *Invertebrates as Webmasters in Ecosystems*. CABI Publishing, Wallingford, UK, pp. 141–159.

Ferris, H., Bongers, T., and de Goede, R.G.M. 2001. A framework for soil food web diagnostics: Extension of the nematode faunal analysis concept. *Appl. Soil Ecol.* 18: 13–29.

Ferris, H. and Matute, M.M. 2003. Structural and functional succession in the nematode fauna of a soil food web. *Appl. Soil Ecol.* 23: 93–110.

Fierer, N., Jackson, J.A., Vilgalys, R., and Jackson, R.B. 2005. Assessment of soil microbial community structure by use of taxon-specific quantitative PCR assays. *Appl. Environ. Microbiol.* 71: 4117–4120.

Fitter, A.H., Gilligan, C.A., Hollingworth, K., Kleczkowski, A., Twyman, R.M., Pitchford, J.W., and Members of the NERC Soil Biodiversity Programme. 2005. Biodiversity and ecosystem function in soil. *Funct. Ecol.* 19: 369–377.

Forge, T.A., Bittman, S., and Kowalenko, C.G. 2005. Responses of grassland soil nematodes and protozoa to multi-year and single-year applications of dairy manure slurry and fertilizer. *Soil Biol. Biochem.* 37: 1751–1762.

Forge, T.A., Hogue, E., Neilsen, G., and Neilsen, D. 2003. Effects of organic mulches on soil microfauna in the root zone of apple: implications for nutrient fluxes and functional diversity of the soil food web. *Appl. Soil Ecol.* 22: 39–54.

Forge, T.A. and Simard, S.W. 2001. Structure of nematode communities in forest soils of southern British Columbia: Relationships to nitrogen mineralization and effects of clearcut harvesting and fertilization. *Biol. Fert. Soils* 34: 170–178.

Freckman, D.W. and Baldwin, J.G. 1990. Nematoda. In D.L. Dindal, Ed. *Soil Biology Guide*. John Wiley and Sons, New York, NY, pp. 155–200.

Frostegard, A. and Bååth, E. 1996. The use of phospholipid fatty acid analysis to estimate bacterial and fungal biomass in soil. *Biol. Fert. Soils* 22: 59–65.

Griffiths, B.S. and Ritz, K. 1988. A technique to extract, enumerate and measure protozoa from mineral soils. *Soil Biol. Biochem.* 20: 163–173.

Guggenberger, G., Frey, S.D., Six, J., Paustian, K., and Elliott, E.T. 1999. Bacterial and fungal cell-wall residues in conventional and no-tillage agroecosystems. *Soil Sci. Soc. Am. J.* 63: 1188–1198.

Hassink, J., Bouwman, L.A., Zwart, K.B., and Brussaard, L. 1993. Relationships between habitable pore space, soil biota and mineralization rates in grassland soils. *Soil Biol. Biochem.* 25: 47–55.

Hassink, J., Neutel, A.M., and De Ruiter, P.C. 1994. C and N mineralization in sandy and loamy grassland soils: The role of microbes and microfauna. *Soil Biol. Biochem.* 11: 1565–1571.

Hunt, H.W., Coleman, D.C., Ingham, E.R., Ingham, R.E., Elliott, E.T., Moore, J.C., Rose, S.L., Reid, C.P.P., and Morley, C.R. 1987. The detrital food web in a shortgrass prairie. *Biol. Fert. Soils* 3: 57–68.

Irvine, L., Kleczkowski, A., Lane, A.M.J., Pitchford, J.W., Caffrey, D., and Chamberlain, P.M. 2006. An integrated data resource for modelling the soil ecosystem. *Appl. Soil Ecol.* 33: 208–219.

Jones, P.C.T. and Mollison, J.E. 1948. A technique for the quantitative estimation of soil microorganisms. *J. Gen. Microbiol.* 2: 54–69.

Leake, J.R., Ostle, N.J., Rangel-Castro, J.I., and Johnson, D. 2006. Carbon fluxes from plants through soil organisms determined by field $^{13}CO_2$ pulse-labelling in an upland grassland. *Appl. Soil Ecol.* 33: 152–175.

Lin, Q. and Brookes, P.C. 1999. Comparison of substrate induced respiration, selective inhibition and biovolume measurements of microbial biomass and its community structure in unamended, ryegrass-amended, fumigated and pesticide-treated soils. *Soil Biol. Biochem.* 31: 1999–2014.

Lundgren, B. 1984. Size classification of soil bacteria: Effects on microscopically estimated biovolumes. *Soil Biol. Biochem.* 16: 283–284.

Montgomery, H.J., Monreal, C.M., Young, J.C., and Seifert, K.A. 2000. Determination of soil fungal biomass from soil ergosterol analyses. *Soil Biol. Biochem.* 32: 1207–1217.

Newman, E.I. 1966. A method for estimating the total length of root in a sample. *J. Appl. Ecol.* 3: 139–145.

Parfitt, R.L., Yeates, G.W., Ross, D.J., Mackay, A.D., and Budding, P.J. 2005. Relationships between soil biota, nitrogen and phosphorus availability, and pasture growth under organic and conventional management. *App. Soil Ecol.* 28: 1–13.

Parisi, V., Menta, C., Gardi, C., Jacomini, C., and Mozzanica, E. 2005. Microarthropod communities as a tool to assess soil quality and biodiversity: A new approach in Italy. *Agric. Ecosyst. Environ.* 105: 323–333.

Ruess, L., Schütz, K., Haubert, D., Häggblom, M.M., Kandeler, E., and Scheu, S. 2005. Application of lipid analysis to understand trophic interactions in soil. *Ecology* 86: 2075–2082.

Van Veen, J.A. and Paul, E.A. 1979. Conversion of biovolume measurements of soil organisms, grown under various moisture tensions, to biomass and their nutrient content. *Appl. Environ. Microbiol.* 37: 686–692.

Wardle, D.A. 2002. *Communities and Ecosystems: Linking the Aboveground and Belowground Components*. Princeton University Press, Princeton, NJ, USA.

V. SOIL ORGANIC MATTER ANALYSES

Section Editors: E.G. Gregorich and M.H. Beare

Chapter 45
Carbon Mineralization

D.W. Hopkins
Scottish Crop Research Institute
Dundee, Scotland, United Kingdom

45.1 INTRODUCTION

Organic matter in soils is the complex mixture of organic compounds derived from the dead and decaying remains of plants, animals, and microorganisms, and their corpses and metabolic wastes at different stages of decomposition. Mineralization of organic carbon (C) is the conversion from the organic form to inorganic compounds as a result of decomposition reactions carried out by decomposer organisms, the vast majority of which are microorganisms (bacteria and fungi) (Gregorich et al. 2001). In the process of utilizing soil organic matter, heterotrophic soil organisms release CO_2 during respiration. The release of CO_2 as a metabolic by-product of organic matter decomposition is referred to as C mineralization. Because soil organic matter is a complex mixture of organic compounds of different biological origins and at different stages of decay, C mineralization is the result of a complex set of biochemical processes conducted by a wide range of organisms. Despite the fact that it is a simplification of the actual process, C mineralization measurements are commonly used in investigations of soils and the data have a wide range of applications in agriculture, forestry, ecology, and the environmental sciences. One reason for this is the relative ease with which CO_2 can be measured in the laboratory. There are a wide range of methods for measuring CO_2 production in the field and at the landscape scale, but this chapter is concerned with measuring C mineralization under controlled laboratory conditions and only limited reference is made to field methods to illustrate some principles.

Data on mineralization of soil C may be used in two ways. The rate of C mineralization measured over periods from a few days to a few weeks is commonly used as an indicator of general biological activity because it is an integrated measure of the combined respiration rate of all the organisms active in the soil under specific conditions. However, with time and without inputs of fresh organic matter, the rate of C mineralization declines as the most readily available soil organic matter is depleted. The total CO_2-C released when the rate of production subsides is an index of the readily mineralizable fraction of organic C in soil. Given enough time, however, all, or virtually all, soil organic matter will be mineralized and therefore the total mineralizable C fraction is equivalent, or close, to the total organic C content of the soil. It is important to distinguish between the total amount of C that will be mineralized eventually and the fraction readily mineralized during the initial period of rapid

decomposition when the most easily utilized and accessible components are decomposed. This chapter focuses on the readily mineralizable fraction of the soil organic matter, which is believed to be a biologically meaningful, albeit operationally defined, fraction of the soil organic matter. However, defining biologically meaningful fractions is fraught with difficulties (Hopkins and Gregorich 2005). Because the readily mineralizable C is one such operationally defined fraction, the conditions under which it is measured need to be carefully specified. It should also be recognized that there is no inherent linkage between the size of the readily mineralizable C fraction and the rate of C mineralization measured over the short-term. Two soils may contain the same amount of readily mineralizable C, but because of more favorable conditions for decomposition, one may have a much faster initial rate of C mineralization than the other.

45.2 SOIL PREPARATION AND INCUBATION CONDITIONS

Before the start of the mineralization assay, some degree of sample preparation is inevitable, but in general, this should be kept to a minimum consistent with being able to prepare a representative and suitable sample. Soil is usually sieved (<2 mm) in the field moist state to enable representative sampling and to remove stones and large pieces of plant material. Drying and grinding the soil should be avoided because these lead to substantial increases in mineralization, commonly referred to as a ''flush'' of respiration. The flush is caused by the mineralization of nonbiomass released from physical protection and the C from organisms killed by drying and rapid rehydration (Powlson 1980; Wu and Brookes 2005). Even sample collection and preparation without harsh treatments such as drying and grinding lead to a short-lived (3–4 days) flush of respiration. It is recommended that soil be preincubated under the same temperature and moisture conditions to be used in the C mineralization assay for a period of 7–10 days to allow equilibration before the start of the assay.

Incubation temperatures in the range 20°C–25°C are frequently used (e.g., Hopkins et al. 1988; Šimek et al. 2004), but the actual temperature used can be set to match the objectives of the particular study. If the aim of the investigation is specifically to determine the effect of temperature on mineralization, the incubation temperature is of paramount importance. Recent papers have drawn attention to the possibility that mineralization of different fractions of the soil organic matter may (or may not) respond differently to incubation temperature (Bol et al. 2003; Fang et al. 2005; Fierer et al. 2005), with obvious implications for predicting the effects of climate change on soil organic C reservoir. If a stable temperature is required throughout an incubation, as is often the case, then it is necessary to use a temperature-controlled room or incubator. Similar to temperature, the moisture content of the soil during incubation needs careful consideration. Moisture contents between 50% and 60% water holding capacity (e.g., Rey et al. 2005; Wu and Brookes 2005) are commonly used because the optimum moisture content for mineralization usually falls in this range. However, alternative moisture contents are used when the aim of the investigation is to determine the effect of moisture or wet–dry cycles on mineralization (e.g., Rey et al. 2005; Chow et al. 2006; Hopkins et al. 2006).

45.3 INCUBATION AND DETECTION METHODS

Three incubation approaches to measure C mineralization in soils in the laboratory are described. In two of them, the soil is enclosed in a sealed vessel and the CO_2 produced is either allowed to accumulate in the headspace and then determined, or the CO_2 is trapped

TABLE 45.1 Some Advantages and Disadvantages of Different Approaches to Determining C Mineralization in Soils under Laboratory Conditions

Approach	Advantages	Disadvantages
Closed chamber incubation with CO_2 accumulation in the headspace	Inexpensive Common equipment requirements Easily replicated IRGA of CO_2 can be very rapid	Composition of the atmosphere changes because of O_2 depletion and CO_2 enrichment, therefore unsuitable for long-term incubations (i.e., >5–10 days) unless the headspace is flushed Not suitable for soils with pH above neutrality because some CO_2 is absorbed in the soil solution Usually only suitable for short-term incubations
Closed chamber incubation with CO_2 trapping	Can be inexpensive Can have simple equipment requirements Usually easily replicated Usually suitable for both short- and long-term incubations	Composition of the atmosphere changes because of O_2 and CO_2 depletion, therefore may unsuitable for long-term incubations if there is a large O_2 demand Automated, multichannel respirometers are expensive Manual titration of alkali traps can be time consuming and produce toxic waste products that require disposal
Open chamber incubation with continuous flushing and CO_2 trapping	Suitable for both long- and short-term incubations	More expensive More complex equipment Less easily replicated

as it is produced (usually in alkali solution) and then determined. In the third, the soil is incubated in a flow-through system in which the headspace is replaced by a stream of CO_2-free air and the CO_2 released from the soil is trapped or measured continuously as the air flows out of the chamber. The particular choice of approach will depend on the equipment and other resources (e.g., financial) available to the investigator and a consideration of the advantages and disadvantages of the different methods (Table 45.1).

The method of CO_2 analysis is determined by a combination of the incubation approach adopted and the instrumentation available. Four methods commonly used to determine CO_2 produced from soil are outlined below.

45.3.1 Acid–Base Titrations

Carbon dioxide can be trapped in alkali (typically KOH or NaOH) and then determined by backtitration of the excess alkali with a dilute acid (Hopkins et al. 1988; Schinner et al. 1996). In its simplest form, this can be done by a manual titration using a burette with a pH indicator. Automatic titrators that measure pH with an electrode and deliver acid from a mechanized burette can increase the precision, although rarely the sample throughput.

45.3.2 Infrared Gas Analysis

Carbon dioxide absorbs radiation in the infrared region and detection of this absorbance is at the heart of infrared gas analyzers (IRGAs) used to determine CO_2 in both closed and open chamber incubation systems (e.g., Bekku et al. 1995; Schinner et al. 1996; Rochette et al. 1997; King and Harrison 2002). There are a range of IRGAs commercially available, and many of those used for measuring CO_2 from soil are modifications of systems used for photosynthesis measurements.

45.3.3 Conductiometry

Carbon dioxide trapped in alkali can be determined conductiometrically on the principle that the impedance of the alkali solution declines as CO_2 is absorbed. Although stand-alone conductiometric systems can be assembled (Chapman 1971; Anderson and Ineson 1982), this method of CO_2 detection is usually an integral part of multichannel respirometers (Nordgren 1988) which are expensive, but permit a high degree of replication and near-continuous measurements.

45.3.4 Gas Chromatography

Gas chromatography (GC) provides very precise analysis, but is suitable only for incubation approaches in which CO_2 accumulates. There is wide variety of GCs available for CO_2 determination and a review of the different types is beyond the scope of this chapter. However, the commonest GC methods involve separation on packed columns and detection using either a thermal conductivity (i.e., hot-wire) detector (e.g., Hopkins and Shiel 1996; Schinner et al. 1996). One advantage of GC is that the instruments are very versatile and can be modified for use in many types of analyses other than CO_2 determination by reconfiguring the injector, column, and detector.

45.4 CLOSED CHAMBER INCUBATION WITH ALKALI CO_2 TRAPS

45.4.1 Materials and Reagents

1 Incubation jars with gastight lids (Mason or Kilner types; Figure 45.1)

2 Glass vials (20–50 mL) for the alkali solution and water

3 *M* NaOH solution

4 0.5 *M* HCl solution

5 Phenolphthalein solution

6 1 *M* $BaCl_2$

7 Pipettes

8 Burette or automatic titrator

9 Magnetic stirrer (optional)

10 Incubator or controlled environment room (optional)

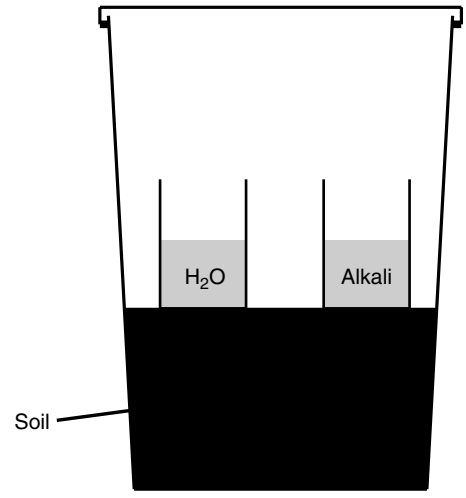

FIGURE 45.1. Closed incubation vessel with NaOH traps for CO_2.

45.4.2 Procedure

Weigh 100–150 g (dry weight equivalent) into jars and record the weight of each jar plus soil without its lid. Place one vial containing 10 mL of 1 *M* NaOH and one vial containing water into each jar and seal them with the lids (Figure 45.1). Incubate the jars in the dark and at the desired temperature. The CO_2 can be assayed at intervals of 3–10 days typically. For each mole of CO_2 trapped in the NaOH, 2 moles of NaOH will be converted to Na_2CO_3 (Equation 45.1). Therefore, the total CO_2 produced is twice the depletion of NaOH in the trap. Remove the vials of water and NaOH and then backtitrate the excess NaOH with HCl (Equation 45.2) using phenolphthalein as an indicator after having removed dissolved CO_2 and carbonates by precipitation with the addition of 2 mL of $BaCl_2$.

$$2NaOH + CO_2 \rightarrow Na_2CO_3 + H_2O \tag{45.1}$$

$$NaOH + HCl \rightarrow NaCl + H_2O \tag{45.2}$$

For example, if 5 mL of 0.5 *M* HCl was required to backtitrate the excess NaOH in an alkali trap that originally contained 10 mL of 1.0 *M* NaOH after precipitating the carbonates with $BaCl_2$, then the CO_2 content of the traps would be calculated as

$$CO_2 \text{ in trap} = 0.5 \times (((V_{NaOH} \times C_{NaOH})/1000) - ((V_{HCl} \times C_{HCl})/1000)) \tag{45.3}$$

where V_{NaOH} is the initial volume of NaOH (mL), C_{NaOH} is the initial molar concentration of NaOH, V_{HCl} is the volume of HCl used in the titration (mL), and C_{HCl} is the molar concentration of HCl used in the titration.

$$\begin{aligned}\text{So, } CO_2 \text{ in the trap} &= 0.5 \times [((10 \times 1.0)/1000) - ((5 \times 0.5)/1000)] \\ &= 0.00375 \text{ mol C}\end{aligned}$$

Where the incubation involved 100 g of dry weight equivalent soil and an incubation time of 48 h, the C mineralization rate would be calculated as

$$\begin{aligned}\text{C mineralization rate} &= \text{CO}_2 \text{ in the trap}/(\text{soil mass in g} \times \text{incubation time in h}) \\ &= 0.00375/(100 \times 48) \\ &= 0.00000078 \text{ mol C g}^{-1} \text{ soil h}^{-1} \text{ or } 0.78 \text{ μmol C g}^{-1} \text{ soil h}^{-1}\end{aligned} \quad (45.4)$$

If the incubation is to be continued, wipe any condensation from the inside of the jar and the lid, weigh the jars, and correct for any weight loss by addition of water. Then put fresh NaOH and water vials in the jars, reseal them, and continue the incubation.

45.4.3 Comments

The method given here is very general and may be adapted to address a wide range of specific research questions. Among other factors, the amount of soil, the temperature and moisture conditions, the concentration and amount of NaOH, and the incubation time can all be adjusted to suit particular applications. It is, however, important to be sure that the headspace in the jars is large enough to avoid the risk of anaerobiosis during long-term incubations. Typically, 100–150 g soil in a 1000 mL vessel is suitable for 3–4 days incubation intervals. It is also important to ensure that the amount of NaOH is adequate to trap all the CO_2 produced. If the amount of CO_2 produced is small, reducing the NaOH concentration will increase the sensitivity of the assay. Carbonic anhydrase can be added to the analyte to catalyze the dissolution of CO_2 in water and allow titration between two pH endpoints, 8.3 to 3.7 (Underwood 1961). An automatic titrator and a magnetic stirrer can be used to help improve the precision of the titration. However, these are not essential as the assays can be carried out satisfactorily using manual equipment provided the operator is careful and skilful.

Commonly used protocols that employ closed chamber incubations to measure soil biological activity and to quantify the amount of readily mineralizable C in soil are given below. Closed chamber techniques involving alkali traps for measuring CO_2 production in the field have also been described by Anderson (1982) and Zibilske (1994).

45.5 CLOSED CHAMBER INCUBATION WITH CO_2 ACCUMULATION

45.5.1 Materials and Reagents

1 Miniaturized incubation vessels (Figure 45.2a and Figure 45.2b)

2 1% CO_2 gas standard mixture

3 Gas chromatograph

4 Incubator (optional)

45.5.2 Procedure

This procedure is based on that of Heilmann and Beese (1992) as modified by Hopkins and Shiel (1996). Weigh 10–15 g (dry weight equivalent) soil into glass vials, put them into the

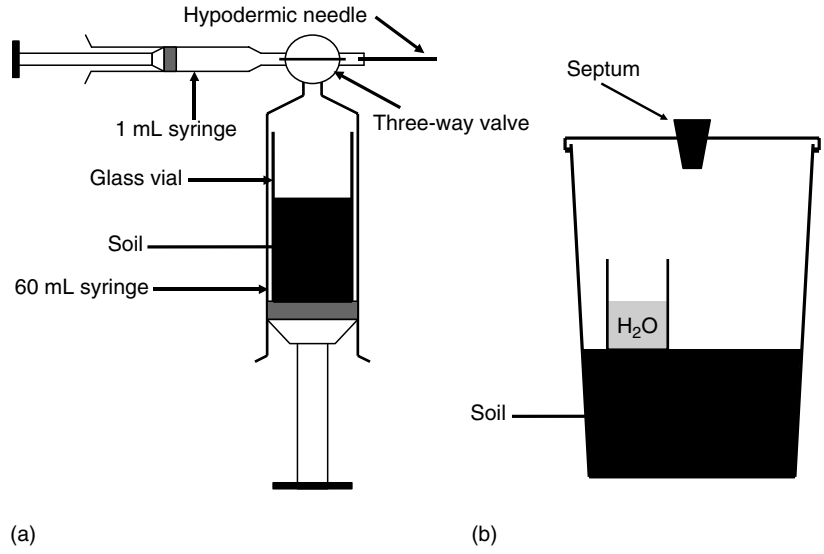

FIGURE 45.2. Two different (a and b) closed incubation vessels in which CO_2 can accumulate.

incubation chambers, and set the volume of the incubation chamber by adjusting the plunger before closing the three-way tap (Figure 45.2a). After 2–3 days, remove a sample of the headspace gas using the smaller sampling syringe, flushing it several times to ensure mixing. Analyze the gas sample by GC. Many GC configurations can be used. In the method of Hopkins and Shiel (1996), a GC fitted with a 1.32 m long × 3 mm internal diameter stainless steel column packed with 80/100 mesh Poropak Q and a thermal conductivity detector was used. After sampling the gas from the headspace, the air in the incubation chambers should be replenished before they are resealed and the incubation continued. The incubation chamber shown in Figure 45.2b is an adaptation of the chamber used in Figure 45.1, which can be used for CO_2 accumulation.

45.5.3 Comments

Soils may contain CO_2 sinks, such as alkaline soil solution in which bicarbonate may accumulate (Martens 1987) and chemoautotrophic bacteria which reduce CO_2 (Zibilske 1994). The importance of these sinks is often overlooked, but in alkaline soils, where the capacity for CO_2 dissolution is large or where the respiratory CO_2 flux is small they may lead to underestimates of C mineralization, methods in which CO_2 is trapped may be preferable.

The incubation chambers can be assembled from easily available materials; however, because some grades of plastic are permeable to CO_2 and the joints between components may leak, it is advisable either to check plastic materials before starting or to use glass equipment. If plastic syringes are used, care should be taken to ensure that the insides of the syringe barrels and the plungers do not get scored by soil particles as this will cause them to leak. Because the headspace volume is relatively small, prolonged incubation without replenishing the headspace is not advisable as this will increase the chance of anaerobiosis and will also increase the risk of leakage.

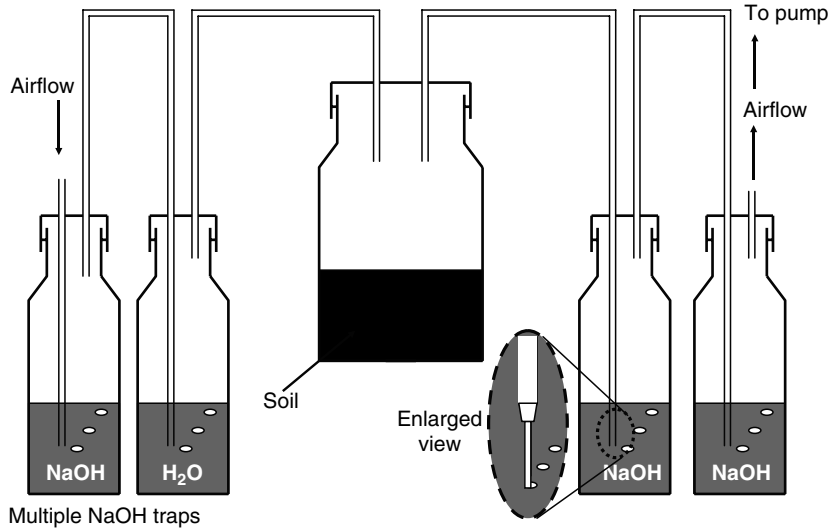

FIGURE 45.3. Open incubation vessel in which CO_2 released into a CO_2-free air stream is trapped in NaOH traps. (Adapted from Zibilske, L.M., in R.W. Weaver, S. Angle, P. Bottomly, D. Bezdieck, S. Smith, A. Tabatabai, and A. Wollum (Eds), *Methods of Soil Analysis, Part 2—Microbiological and Biochemical Processes*, Soil Science Society of America, Madison, Wisconsin, 1994.)

45.6 OPEN CHAMBER INCUBATION

The system outlined in Figure 45.3 is suitable for collecting CO_2 in an open chamber incubation in which the airflow is maintained either by a suction pump or vacuum line to draw air through the apparatus, or by air pumps (such as a diaphragm aquarium pump) or compressed gas cylinders to force air through the apparatus. Depending on the source of the air, it is necessary to consider the purity of the gas and if necessary use supplementary concentrated H_2SO_4 scrubbers to remove organic contaminants from the compressed gas cylinder or carried over from the pumps. The CO_2 bubble traps on the upstream side of the soil can be replaced with soda lime traps. After the incubation, the contents of the NaOH traps are quantitatively transferred to a beaker and the CO_2 produced is determined by titration as described in Section 45.4.2. The main advantages of this approach are that there is no risk of anaerobiosis or leakage of accumulated CO_2, and soil drying is reduced by the air flowing through the water bottle immediately upstream of the incubation chamber. The equipment can be assembled from easily available laboratory glassware. However, for replicated measurements multiple systems will be required and this will increase the amount of laboratory space required.

45.7 CONDUCTIOMETRIC RESPIROMETERS

There is a range of dedicated multichannel respirometers, which can be used to measure CO_2 production (and in some cases other gases) in soils, sediments, composts, animals, and cell cultures (including microorganisms). A systematic account of the operation of these instruments is beyond the scope of this chapter. The instrument which appears to be most widely used in soil research is the Respicond instrument (Nordgren 1988). This instrument comprises up to 96 chambers (Figure 45.4) in which CO_2 is trapped in KOH. Absorbed CO_2 leads to a fall in the conductance of the trap as the KOH concentration falls. This change in

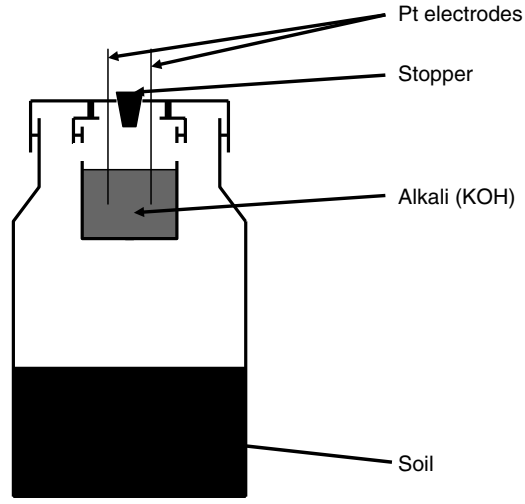

FIGURE 45.4. Closed incubation vessel using within the Respicond respirometer. (Adapted from Nordgren, A., *Soil Biol. Biochem.*, 20, 955, 1988.)

conductance can be measured as frequently as every 30–45 min and the instrument can run for many months with only minimal interruptions. The conductance measurement is very sensitive to temperature fluctuations and variations in the electrical supply to the instrument. Although the instrument has integral temperature control, best results are obtained when it is located in a temperature-controlled room with an isolated electricity supply.

REFERENCES

Anderson, J.M. and Ineson, P. 1982. A soil microcosm system and its application to measurements of respiration and nutrient leaching. *Soil Biol. Biochem.* 14: 415–416.

Anderson, J.P.E. 1982. Soil respiration. In A.L. Page et al., Eds. *Methods of Soil Analysis, Part 2—Chemical and Biological Properties*, 2nd ed. Agronomy Society of America, Madison, WI, pp. 831–871.

Bekku, Y., Koizumi, H., and Iwaki, H. 1995. Measurement of soil respiration using closed-chamber method—an IRGA technique. *Ecol. Res.* 10: 369–373.

Bol, R., Bolger, T., Cully, R., and Little, D. 2003. Recalcitrant soil organic materials mineralize more efficiently at higher temperatures. *Z. Pflanzen. Boden.* 166: 300–307.

Chapman, S.B. 1971. Simple conductiometric soil respirometer for field use. *Oikos* 22: 348.

Chow, A.T., Tanji, K.K., Gao, S.D., and Dahlgren, R.A. 2006. Temperature, water content and wet–dry cycle effects on DOC and carbon mineralization in agricultural peat soils. *Soil Biol. Biochem.* 38: 477–488.

Fang, C.M., Smith, P., Moncrieff, J.B., and Smith, J.U. 2005. Similar responses of labile and resistant soil organic matter pools to changes in temperature. *Nature* 433: 57–59.

Fierer, N., Craine, J.M., McLauchlan, K., and Schimel, J.P. 2005. Litter quality and the temperature sensitivity of decomposition. *Ecology* 82: 320–326.

Gregorich, E.G., Turchenek, L.W., Carter, M.R., and Angers, D.A. 2001. *Soil and Environmental Sciences Dictionary*. CRC Press, Boca Raton, FL.

Heilmann, B. and Beese, F. 1992. Miniaturized method to measure carbon dioxide production and

biomass of soil microorganisms. *Soil Sci. Soc. Am. J.* 56: 596–598.

Hopkins, D.W. and Gregorich, E.G. 2005. Carbon as a substrate for soil organisms. In R.D. Bardgett, M.B. Usher, and D.W. Hopkins, Eds. *Biodiversity and Function in Soils*, British Ecological Society Ecological Reviews. Cambridge University Press, Cambridge, pp. 57–79.

Hopkins, D.W. and Shiel, R.S. 1996. Size and activity of soil microbial communities in long-term experimental grassland plots treated with manure and inorganic fertilizers. *Biol. Fert. Soils* 22: 66–70.

Hopkins, D.W., Shiel, R.S., and O'Donnell, A.G. 1988. The influence of sward species composition on the rate of organic matter decomposition in grassland soil. *J. Soil Sci.* 39: 385–392.

Hopkins, D.W., Sparrow, A.D., Elberling, B., Gregorich, E.G., Novis, P., Greenfield, L.G., and Tilston, E.L. 2006. Carbon, nitrogen and temperature controls on microbial activity in soils from an Antarctic dry valley. *Soil Biol. Biochem* 38: 3130–3140.

King, J.A. and Harrison, R. 2002. Measuring soil respiration in the field: an automated closed chamber system compared with portable IRGA and alkali adsorption methods. *Commun. Soil Sci. Plant Anal.* 33: 403–423.

Martens, R. 1987. Estimation of microbial biomass in soil by the respiration methods: importance of soil pH and flushing methods for respired CO_2. *Soil Biol. Biochem.* 19: 77–81.

Nordgren, A. 1988. Apparatus for the continuous, long-term monitoring of soil respiration rate in large numbers of samples. *Soil Biol. Biochem.* 20: 955–957.

Powlson, D.S. 1980. The effects of grinding on microbial and non-microbial organic matter in soil. *J. Soil Sci.* 31: 77–85.

Rey, A., Petsikos, C., Jarvis, P.G., and Grace, J. 2005. Effect of temperature and moisture on rates of carbon mineralization in a Mediterranean oak forest soil under controlled and field conditions. *Eur. J. Soil Sci.* 56: 589–599.

Rochette, P., Ellert, B., Gregorich, E.G., Desjardins, R.L., Pattey, E.L., Lessard, R., and Johnson, B.G. 1997. Description of a dynamic closed chamber for measuring soil respiration and its comparison with other techniques. *Can. J. Soil Sci.* 77: 195–203.

Schinner, F., Öhlinger, R., Kandeler, E., and Margesin, R. 1996. *Methods in Soil Biology*. Springer-Verlag, Berlin, Germany.

Šimek, M., Elhottová, D., Klimeš, F., and Hopkins, D.W. 2004. Emissions of N_2O and CO_2, denitrification measurements and soil properties in red clover and ryegrass stands. *Soil Biol. Biochem.* 36: 9–21.

Underwood, A.L. 1961. Carbonic anhydrase in the titration of carbon dioxide solutions. *Anal. Chem.* 33: 955–956.

Wu, J. and Brookes, P.C. 2005. The proportional mineralization of microbial biomass and organic matter caused by air-drying and rewetting of a grassland soil. *Soil Biol. Biochem.* 37: 507–515.

Zibilske, L.M. 1994. Carbon mineralization. In R.W. Weaver, S. Angle, P. Bottomly, D. Bezdieck, S. Smith, A. Tabatabai, and A. Wollum, Eds. *Methods of Soil Analysis, Part 2—Microbiological and Biochemical Processes*, SSSA Book Series No. 5. Soil Science Society of America, Madison, WI, pp. 835–863.

Chapter 46
Mineralizable Nitrogen

Denis Curtin
New Zealand Institute for Crop and Food Research
Christchurch, New Zealand

C.A. Campbell
Agriculture and Agri-Food Canada
Ottawa, Ontario, Canada

46.1 INTRODUCTION

Nitrogen (N) is generally the most common growth-limiting nutrient in agricultural production systems. The N taken up by crops is derived from a number of sources, particularly from fertilizer, biological N fixation and mineralization of N from soil organic matter, crop residues, and manures (Keeney 1982). The contribution of mineralization to crop N supply may range from <20 to >200 kg N ha^{-1} (Goh 1983; Cabrera et al. 1994) depending on the quantity of mineralizable organic N in the soil and environmental conditions (soil temperature and moisture) that control the rate of mineralization. Large amounts of mineralizable N can accumulate under grassland with the result that crops grown immediately after cultivation of long-term grass may derive much of their N from mineralization. In contrast, soils that have been intensively cropped often mineralize little N, leaving crops heavily dependent on fertilizer N.

Potentially mineralizable N is a measure of the active fraction of soil organic N, which is chiefly responsible for the release of mineral N through microbial action. Mineralizable N is composed of a heterogeneous array of organic substrates including microbial biomass, residues of recent crops, and humus. Despite a continuing research effort (Jalil et al. 1996; Picone et al. 2002), chemical tests that are selective for the mineralizable portion of soil N are not available and incubation assays remain the preferred way of estimating mineralizable N.

Stanford and Smith (1972) proposed a method to estimate potentially mineralizable N based on the mineral N released during a 30 week aerobic incubation of a soil:sand mixture under optimum temperature and moisture conditions. Although this procedure is regarded as the standard reference method, its main application is as a research tool because it is too time-consuming for routine use. Shortened versions of the aerobic incubation method have been found useful in evaluating soil N supplying power (Paul et al. 2002; Curtin and

McCallum 2004), but these assays still take several weeks to complete and require considerable technical expertise.

An anaerobic incubation method for estimating mineralizable N was proposed by Keeney and Bremner (1966). This anaerobic (i.e., waterlogged soil) technique has significant practical and operational advantages over aerobic techniques in that the incubation period is relatively short (7 days) and the need for careful adjustment of soil water content is avoided. This assay is occasionally used for routine soil fertility testing by commercial laboratories. Although Keeney and Bremner (1966) reported good correlations between anaerobically mineralizable N (AMN) and plant N uptake under greenhouse conditions, subsequent work with field-grown crops has given mixed results (Thicke et al. 1993; Christensen et al. 1999).

46.2 POTENTIALLY MINERALIZABLE N

46.2.1 Theory

In theory, potentially mineralizable N is the amount of N that will mineralize in infinite time at optimum temperature and moisture. It is estimated by incubating soil under optimal conditions and measuring N mineralized as a function of time by periodically leaching mineral N from the soil. Potentially mineralizable N is calculated using a first-order kinetic model:

$$N_{\min} = N_0(1-\mathrm{e}^{-kt}) \tag{46.1}$$

where $N_{\min}$ is cumulative N mineralized in time t, N_0 is potentially mineralizable N, and k is the mineralization rate constant. This equation has two unknowns (N_0 and k), which are usually estimated by least-squares iteration using appropriate statistics software.

46.2.2 Materials

1 Incubator capable of maintaining temperatures of up to 40°C (and humidity near 100% so that soils do not dry out during incubation).

2 Vacuum pump to extract leachate at ~ -80 kPa.

3 Leaching units to hold incubating soils. These can be purpose-made leaching tubes (Campbell et al. 1993), commercially available filter units (e.g., 150 mL membrane filter units; MacKay and Carefoot 1981), or Buchner funnels (Ellert and Bettany 1988; Benedetti and Sebastiani 1996).

4 Glass wool to make a pad ~6 mm thick at the bottom and 3 mm on top of the incubating sample.

5 Acid-washed, 20 mesh quartz sand.

6 0.01 *M* $CaCl_2$ leaching solution (made from a stock solution of $CaCl_2$).

7 N-free nutrient solution containing 0.002 *M* $CaSO_4$, 0.002 *M* $MgSO_4$, 0.005 *M* $Ca(H_2PO_4)_2$, and 0.0025 *M* K_2SO_4 to replace nutrients removed from the soil during leaching.

46.2.3 Procedure

1 Soils are usually air-dried and sieved before incubation, but field-moist soil may also be used. The N mineralization rate can be quite sensitive to sample pretreatment, particularly in the early phase of incubation (see Section 46.2.5).

2 Mix 15–50 g of soil with sand at a soil:sand ratio of 1:1 for medium-textured soils and 1:2 for fine-textured soils. It may be helpful to apply a light mist of water to prevent particle/aggregate size segregation during transfer to the leaching tubes.

3 Sand–soil mixture is supported in the leaching tube on a glass wool pad or by a sandwich of glass wool/Whatman glass microfiber filter/glass wool. A thin pad of glass wool is placed on top of the soil–sand mixture to prevent aggregate disruption when leaching solution is applied.

4 Native mineral N is leached using 100 mL of 0.01 *M* $CaCl_2$, applied in small increments (~10 mL) followed by 25 mL of N-free nutrient solution. The soil–sand mixture is initially allowed to drain naturally, then a vacuum (−80 kPa) is applied to remove excess water. Discard the first leachate.

5 Tubes are stoppered at both ends and placed in an incubator at 35°C. A hypodermic needle (38 mm, 16–18 gauge) is inserted in the bottom to facilitate aeration. Twice per week the top stopper is briefly removed to facilitate aeration.

6 Step 4 (leaching) is repeated every 2 weeks for the first 8–10 weeks of incubation and every 4 weeks thereafter. The collected leachate is filtered through a prewashed Whatman No. 42 filter paper and analyzed for NO_3- and NH_4-N.

7 Incubation can be terminated when cumulative N mineralized approaches a plateau. This usually occurs after about 20 weeks (see Section 46.2.5).

46.2.4 Calculations

Nonlinear least-square regression is the preferred statistical technique to estimate N_0 and k in the first-order kinetic model (Campbell et al. 1993; Benedetti and Sebastiani 1996). Rough estimates of N_0 and k are needed to initiate the calculation. We suggest an initial estimate of $k \sim 0.10$ per week (values normally between 0.05 and 0.20 per week) and N_0 can be assumed to be about 50% greater than cumulative mineralized N at the end of the incubation period (Campbell et al. 1993).

46.2.5 Comments

1 The most appropriate way of handling samples before incubation has not been established. Both air-dry soil and field-moist samples have been used. Where moist samples are to be used, they should be refrigerated (about 4°C) in the period between sampling and incubation. Campbell et al. (1993) recommend air-drying after collection, which may be appropriate in regions where soils become air-dry in the field. Air-drying can kill off part of the microbial biomass and rapid mineralization of this microbial-N will occur upon rewetting.

The single-exponential model (Equation 46.1) may not adequately describe the initial flush of mineralization that occurs after rewetting (Cabrera 1993) and data for the first 2 weeks have sometimes been excluded when estimating N_0 (Stanford and Smith 1972). The degree of sample disturbance (e.g., fineness of sieving) may also influence the results. However, Stenger et al. (2002) found little difference in N mineralization (6 month incubation) between intact and sieved (<2 mm) soils.

2 An assumption implicit in Equation 46.1 is that there is only one pool of mineralizable N. This assumption is dubious as there is clear evidence for the existence of several forms of ''active'' N. There have been attempts to improve data fit by assuming two or three pools of mineralizable N (Deans et al. 1986). While a two pool (i.e., double exponential) model usually fits laboratory N mineralization data more precisely than a single-exponential model (Curtin et al. 1998), many workers consider the improvement insufficient to warrant its use for general purposes (Campbell et al. 1988).

3 Values of N_0 and k obtained by data fit to Equation 46.1 can vary depending on temperature, moisture content, and duration of incubation (Wang et al. 2003). The optimum temperature for N mineralization is often considered to be 35°C. Campbell et al. (1993) suggested that incubation at a lower temperature (e.g., 28°C) may result in a lag phase in N mineralization during the first 2 weeks of incubation. A lag phase may be exhibited by soils containing C-rich substrates (e.g., forest soils) where net N mineralization may initially be low because N immobilization predominates (Scott et al. 1998). Optimum soil moisture content is about field capacity (−5 to −10 kPa). The incubation time should, ideally, be at least 25 weeks (Ellert 1990). Values of N_0 tend to increase and k to decrease as incubation time is extended (Paustian and Bonde 1987; Wang et al. 2003). Cumulative N mineralized (N_{min}) typically increases asymptotically to reach a plateau after about 16–20 weeks of incubation (Campbell et al. 1993).

4 A problem inherent in fitting the first-order model to mineralization data is that there tends to be an inverse relationship between N_0 and k. It has been argued that to obtain values of N_0 that are truly indicative of the amount of mineralizable in the soil, k should be set to a standard value (e.g., 0.054 per week) (Wang et al. 2003). This approach minimizes the effect of incubation time on N_0 (values not affected by changes in incubation duration from 20 to 40 weeks; Wang et al. 2003).

46.3 SHORT-TERM AEROBIC INCUBATION

Short-term aerobic incubation techniques have the obvious advantage that a more timely estimate of mineralizable N can be obtained, and, since periodic leaching is not required, the labor requirement is reduced. Based on analysis of two data sets, Campbell et al. (1994) showed that N mineralized in the first 2 weeks of incubation was reasonably well related to N_0 in North American soils. However, this may not always be the case. Certain soils (e.g., forest soils with high C:N ratio; Scott et al. 1998) can immobilize substantial N during short incubation and net N mineralized in the short-term may not be closely related to N_0. Various short-term incubation assays have been proposed; they differ in incubation duration and temperature. Parfitt et al. (2005) reported that N mineralized in a 56 day aerobic incubation (25°C) was closely correlated with N uptake by legume-based pastures in New Zealand.

Nitrogen mineralized in a 28 day aerobic incubation (20°C) was closely related to N uptake by a greenhouse-grown oat (*Avena sativa* L.) crop from 30 soils representing a range of management histories and parent materials (Curtin and McCallum 2004). Longer (56 vs. 28 days) incubations may give results that more accurately reflect N supply over a growing season, but may not be attractive where timeliness of results is an important consideration. Field rates of mineralization may be estimated by adjusting the basal value (i.e., the value determined by incubation under defined temperature and moisture conditions) using soil temperature and moisture adjustment factors (Paul et al. 2002).

The following procedure is based on the method used by Scott et al. (1998) and Parfitt et al. (2005).

46.3.1 Procedure

1 Weigh sieved (<4 or 5 mm), field-moist soil (equivalent to about 5 g of dry soil) into 125 mL polypropylene containers (use of field-moist soil is recommended to avoid the flush of mineralization that occurs when air-dry soil is rewetted; however, air-dry samples may be appropriate for semiarid soils).

2 Add water to adjust the soil water content so that it is equivalent to −10 kPa. Soil water content at −10 kPa is normally determined from tension table measurements on a separate sample.

3 Cover containers with polyethylene (30 μm) held in place with rubber bands and place in plastic trays containing water, enclosed in large polyethylene bags (to maintain high humidity).

4 Incubate at the desired temperature (20°C to 30°C) for the required time period (e.g., 28 or 56 days).

5 Measure mineral N (NO_3- plus NH_4-N) at the end of incubation by extraction with 2 *M* KCl. Mineral N in the soil before incubation is determined by extracting a separate sample with KCl.

6 Mineralized N is calculated by subtracting initial mineral N from that determined at the end of the incubation.

46.4 ANAEROBIC INCUBATION

This technique offers important operational and practical advantages that make it more suitable for routine use than aerobic incubation. The incubation period is relatively short (7 days); the same volume of water is added to all soils regardless of water holding capacity; and NH_4-N only needs to be measured because NO_3-N is not produced under anaerobic conditions.

46.4.1 Procedure

1 Weigh 5 g of sieved (<4 or 5 mm) soil into a 50 mL plastic, screw-cap centrifuge tube. Add 10 mL of distilled water to submerge the soil, stopper the tube, and place in a constant temperature (40°C) cabinet/incubator for 7 days.

2 Remove tube from incubator and add 40 mL of 2.5 *M* KCl (after dilution with water in the sample, final KCl concentration is 2 *M*). Mix contents of tube, centrifuge at 1900 *g*, and filter the supernatant (prewashed Whatman No. 42).

3 Determine NH_4-N in the supernatant. Measure the amount of NH_4-N in the soils before incubation by extracting a separate sample with KCl. Mineralized N is estimated by deducting this preincubation NH_4-N value from the amount measured in the incubated sample.

46.4.2 Comments

1 Since most arable soils do not contain appreciable NH_4-N, it may be possible to dispense with the initial NH_4-N measurement; however, preliminary checks should be carried out to verify that native NH_4-N is negligible (Keeney 1982).

2 Sample preparation has not been standardized; air-dry and field-moist soils are commonly used to measure AMN. Larsen (1999) suggests that pretreatment (air-drying, freezing) can have a strong effect on AMN and he recommends the use of fresh, field-moist soil.

3 Although AMN is correlated with the N mineralized in an aerobic incubation, the relationship is often not very close (Curtin and McCallum 2004).

4 To be useful as part of a fertilizer N recommendation system, an empirical calibration of AMN against crop performance under local field conditions is recommended (Christensen et al. 1999).

46.5 CHEMICAL INDICES OF NITROGEN MINERALIZATION CAPACITY

Because of the time requirement of the biological assays described above, chemical tests have been evaluated as possible surrogates. Chemical procedures have the advantage that they can be more rapid and precise than biological (incubation) assays but, to date, no extractant has been capable of simulating the microbially mediated release of mineral N that occurs in incubated soil. Most chemical tests are relatively simple in their mode of action, i.e., they selectively extract a particular form or forms of N. On the other hand, mineralization is a complex microbial process comprised of subprocesses that release (gross mineralization) and consume (immobilization) mineral N. Net N mineralization, as measured in incubation assays, is the balance between the processes of gross N mineralization and N immobilization. Chemical tests that select for labile fractions of soil N have potential in estimating gross N mineralization (Wang et al. 2001). However, predicting net N mineralization based on a chemical extraction test is more problematic because such tests cannot account for N immobilization.

Although many chemical tests for N availability have been proposed (listed by Keeney 1982), none of them has been adopted for general or routine use in soil fertility evaluation. Perhaps the chemical test that has attracted most attention in the past decade is hot 2 *M* KCl extraction, which causes hydrolysis of some organic N to NH_4 (Gianello and Bremner 1986). Despite some encouraging observations (Gianello and Bremner 1986; Jalil et al. 1996; Beauchamp et al. 2004), the performance of the test has not been consistent overall

(Wang et al. 2001; Curtin and McCallum 2004). Work on chemical test development and evaluation is continuing (e.g., Mulvaney et al. 2001; Picone et al. 2002). However, there is presently no agreement among researchers on which of the available soil N tests has the most potential to serve as a predictor of soil N supplying power and, until scientific consensus emerges, it would be unwise to recommend any test for general use.

REFERENCES

Beauchamp, E.G., Kay, B.D., and Pararajasingham, R. 2004. Soil tests for predicting the N requirement of corn. *Can. J. Soil Sci.* 84: 103–113.

Benedetti, A. and Sebastiani, G. 1996. Determination of potentially mineralizable nitrogen in agricultural soil. *Biol. Fert. Soils* 21: 114–120.

Cabrera, M.L. 1993. Modeling the flush of nitrogen mineralization caused by drying and rewetting soils. *Soil Sci. Soc. Am. J.* 57: 63–66.

Cabrera, M.L., Kissel, D.E., and Vigil, M.F. 1994. Potential nitrogen mineralization: laboratory and field evaluation. In J.L. Havlin and J.S. Jacobsen, eds. *Soil Testing: Prospects for Improving Nutrient Recommendations*. Soil Science Society of America Special Publication No. 40. SSSA and ASA, Madison, WI, pp. 15–30.

Campbell, C.A., Ellert, B.H., and Jame, Y.W. 1993. Nitrogen mineralization potential in soils. In M.R. Carter, ed. *Soil Sampling and Methods of Analysis*. Lewis Publishers, Boca Raton, FL, pp. 341–349.

Campbell, C.A., Jame, Y.W., Akinremi, O.O., and Beckie, H.J. 1994. Evaluating potential nitrogen mineralization for predicting fertilizer nitrogen requirements of long-term field experiments. In J.L. Havlin and J.S. Jacobsen, eds. *Soil Testing: Prospects for Improving Nutrient Recommendations*. Soil Science Society of America Special Publication No. 40. SSSA and ASA, Madison, WI, pp. 81–100.

Campbell, C.A., Jame, Y.W., and de Jong, R. 1988. Predicting net nitrogen mineralization over a growing season: model verification. *Can. J. Soil Sci.* 68: 537–552.

Christensen, N.W., Qureshi, M.H., Baloch, D.M., and Karow, R.S. 1999. Assessing nitrogen mineralization in a moist xeric environment. *Proceedings, Western Nutrient Management Conference*, Vol. 3, March 4–5, 1999. Salt Lake City, UT. Potash & Phosphate Institute, Norcross, GA, pp. 83–90.

Curtin, D., Campbell, C.A., and Jalil, A. 1998. Effects of acidity on mineralization: pH-dependence of organic matter mineralization in weakly acidic soils. *Soil Biol. Biochem.* 30: 57–64.

Curtin, D. and McCallum, F.M. 2004. Biological and chemical assays to estimate nitrogen supplying power of soils with contrasting management histories. *Aust. J. Soil Res.* 42: 737–746.

Deans, J.R., Molina, J.A.E., and Clapp, C.E. 1986. Models for predicting potentially mineralizable nitrogen and decomposition rate constants. *Soil Sci. Soc. Am. J.* 50: 323–326.

Ellert, B.H. 1990. Kinetics of nitrogen and sulfur cycling in Gray Luvisol soils. Ph.D. thesis, University of Saskavtchewan, Saskatoon. SK, Canada, 397 pp.

Ellert, B.H. and Bettany, J.R. 1988. Comparison of kinetic models for describing net sulfur and nitrogen mineralization. *Soil Sci. Soc. Am. J.* 52: 1692–1702.

Gianello, C. and Bremner, J.M. 1986. Comparison of chemical methods of assessing potentially available organic nitrogen in soil. *Commun. Soil Sci. Plant Anal.* 17: 215–236.

Goh, K.M. 1983. Predicting nitrogen requirements for arable farming: a critical review and appraisal. *Proc. Agron. Soc. New Zealand* 13: 1–14.

Jalil, A., Campbell, C.A., Schoenau, J., Henry, J.L., Jame, Y.W., and Lafond, G.P. 1996. Assessment of two chemical extraction methods as indices of available nitrogen. *Soil Sci. Soc. Am. J.* 60: 1954–1960.

Keeney, D.R. 1982. Nitrogen—availability indices. In A.L. Page et al., Eds. *Methods of Soil Analysis. Part 2, 2nd ed. Chemical and Microbiological Properties,* Agronomy 9. SSSA and ASA, Madison, WI, pp. 711–733.

Keeney, D.R. and Bremner, J.M. 1966. Comparison and evaluation of laboratory methods of obtaining an index of soil nitrogen availability. *Agron. J.* 58: 498–503.

Larsen, J.J.R. 1999. How to estimate potentially plant available soil nitrogen in sandy soils using anaerobic incubation. M.S. thesis, Department of Agricultural Sciences, The Royal Veterinary and Agricultural University, Copenhagen, Denmark.

MacKay, D.C. and Carefoot, J.M. 1981. Control of water content in laboratory determination of mineralizable nitrogen in soils. *Soil Sci. Soc. Am. J.* 45: 444–446.

Mulvaney, R.L., Khan, S.A., Hoeft, R.G., and Brown, H.M. 2001. A soil organic nitrogen fraction that reduces the need for nitrogen fertilization. *Soil Sci. Soc. Am. J.* 65: 1164–1172.

Parfitt, R.L., Yeates, G.W., Ross, D.J., Mackay, A.D., and Budding, P.J. 2005. Relationships between soil biota, nitrogen and phosphorus availability, and pasture growth under organic and conventional management. *Appl. Soil Ecol.* 28: 1–13.

Paul, K.I., Polglase, P.J., O'Connell, A.M., Carlyle, J.C., Smethurst, J.C., and Khanna, P.K. 2002. Soil nitrogen availability predictor (SNAP): a simple model for predicting mineralisation of nitrogen in forest soils. *Aust. J. Soil Res.* 40: 1011–1026.

Paustian, K. and Bonde, T.A. 1987. Interpreting incubation data on nitrogen mineralization from soil organic matter. In J.H. Cooley, Ed. *Soil Organic Matter Dynamics and Soil Productivity.* Proceedings of INTECOL Workshop, INTECOL Bulletin 15. International Association for Ecology, Athens, GA, pp. 101–112.

Picone, L.I., Cabrera, M.L., and Franzluebbers, A.J. 2002. A rapid method to estimate potentially mineralizable nitrogen in soil. *Soil Sci. Soc. Am. J.* 66: 1843–1847.

Scott, N.A., Parfitt, R.L., Ross, D.J., and Salt, G.J. 1998. Carbon and nitrogen transformations in New Zealand plantation forest soils from sites with different N status. *Can. J. Forest Res.* 28: 967–976.

Stanford, G. and Smith, S.J. 1972. Nitrogen mineralization potentials of soils. *Soil Sci. Soc. Am. Proc.* 36: 465–472.

Stenger, R., Barkle, G.F., and Burgess, C.P. 2002. Mineralisation of organic matter in intact versus sieved/refilled soil cores. *Aust. J. Soil Res.* 40: 149–160.

Thicke, F.E., Russelle, M.P., Hesterman, O.B., and Sheaffer, C.C. 1993. Soil nitrogen mineralization indexes and corn response in crop rotations. *Soil Sci.* 156: 322–335.

Wang, W.J., Smith, C.J., Chalk, P.M., and Chen, D. 2001. Evaluating chemical and physical indices of nitrogen mineralization capacity with an unequivocal reference. *Soil Sci. Soc. Am. J.* 65: 368–376.

Wang, W.J., Smith, C.J., and Chen, D. 2003. Towards a standardised procedure for determining the potentially mineralisable nitrogen of soil. *Biol. Fert. Soils* 37: 362–374.

Chapter 47
Physically Uncomplexed Organic Matter

E.G. Gregorich
Agriculture and Agri-Food Canada
Ottawa, Ontario, Canada

M.H. Beare
New Zealand Institute for Crop and Food Research
Christchurch, New Zealand

47.1 INTRODUCTION

Physically uncomplexed organic matter is composed of particles of organic matter (OM) that are not bound to soil mineral particles and can be isolated from soil by density (using heavy liquids) or size (using sieving) fractionation. It is separated from soil on the premise that the association of organic matter with primary soil (mineral) particles alters its function, turnover, and dynamics in the soil environment. Uncomplexed organic matter has been isolated to study the form and function of soil organic constituents and to assess the impacts of land use, management, and vegetation type on carbon (C) and nitrogen (N) turnover and storage (Gregorich and Janzen 1996; Gregorich et al. 2006, and references therein). It has been separated and evaluated in studies pertaining to nutrient availability (Campbell et al. 2001), decomposition of plant residues (Magid and Kjærgaard 2001), physical protection of soil organic matter (Beare et al. 1994), and aggregation processes (Golchin et al. 1994).

Physically uncomplexed organic matter is a mixture of plant, animal, and microorganism parts at different stages of decomposition, and includes pollen, spores, seeds, invertebrate exoskeletons, phytoliths, and charcoal (Spycher et al. 1983; Baisden et al. 2002). Light fraction (LF) organic matter and particulate organic matter (POM) are the most commonly isolated forms of physically uncomplexed organic matter, though they differ in amount and their chemical characteristics. In this chapter, LF is defined as the organic matter recovered when soil is suspended in a heavy solution (i.e., heavier than water) of a known specific gravity, most often in the range of 1.6–2.0 (Sollins et al. 1999). In contrast, POM is defined as the organic matter recovered after passing dispersed soil through a sieve with openings of a defined size, normally between 250 and 53 μm in diameter. The POM has been isolated by size alone (e.g., >53 μm), or by a combination of size and density fractionation procedures (see Cambardella and Elliott 1992).

The proportion of total soil C and N accounted for in physically uncomplexed organic matter can be substantial. Based on a review of more than 65 published papers, Gregorich et al. (2006) showed that for agricultural mineral soils, the amount of soil C and N accounted for in POM is usually much greater than that in the LF. On average, POM (50–2000 μm diameter) accounted for 22% of soil organic C and 18% of total soil N. In contrast, LF organic matter (specific gravity <1.9) accounted for 8% of soil organic C and 5% of total soil N. Limited work has been done on the phosphorus (P) or sulfur (S) content of LF organic matter, but research has shown that less than 5% of soil organic P resides within LF (Curtin et al. 2003; Salas et al. 2003).

The C:N ratio of physically uncomplexed OM is usually wider than that of whole soil, but narrower than that of plant residue. The C:N ratios of LF organic matter tend to narrow as specific gravity increases, ranging from 17 to 22 for specific gravities of 1.0–1.8 and from 10 to 17 for specific gravities of 1.8–2.2 (Gregorich et al. 2006). The relatively wide C:N ratio of LF extracted at low specific gravity (<1.8) reflects the dominant influence of plant constituents (e.g., lignin), whereas at a higher specific gravity the isolated material contains more mineral particles with adsorbed OM. Gregorich et al. (2006) also showed that there is a positive log–linear relationship between the mean size of POM fractions and their C:N ratio. In general, the variation in C:N ratios of larger size fractions is considerably greater than the variation in C:N ratios of smaller size fractions, which is consistent with the findings of Magid and Kjærgaard (2001).

The LF is usually isolated using liquids of a defined specific gravity, most often in the range of 1.6–2.0 (Sollins et al. 1999). POM has been isolated by size alone, or by a combination of size and density fractionation procedures (see Cambardella and Elliott 1992). We present two methods of separating uncomplexed organic matter in this chapter: (1) wet sieving of soil dispersed in a solution of sodium hexametaphosphate to isolate sand-sized (>53 μm) POM and (2) suspension of dispersed soil in a solution of sodium iodide (NaI) at a specific gravity of 1.7 to isolate the LF organic matter. A size of >53 μm is recommended for separating POM because, as a cutoff for the sand fraction in particle size analysis, it has been routinely used in POM studies (Gregorich et al. 2006). The 1.7 specific gravity recommended for isolating LF is in accord with early studies that indicated that this density separated most organomineral and mineral particles from decaying plant residues (Ladd et al. 1977; Scheffer 1977; Ladd and Amato 1980; Spycher et al. 1983).

47.2 PARTICULATE ORGANIC MATTER

Uncomplexed organic matter isolated by size is usually referred to as ''particulate organic matter'' (Cambardella and Elliott 1992) but has also been referred to as ''sand-size organic matter'' or ''macroorganic matter'' (Gregorich and Ellert 1993; Wander 2004). It is isolated by dispersing the soil and collecting the sand-sized fraction on a sieve. Where soils are first passed through a 2 mm sieve, the POM recovered on a 53 μm sieve can be defined as ranging in size from 53 to 2000 μm in diameter and as such represents a quantifiable component of the whole soil organic matter.

47.2.1 Materials and Reagents

1 A sieve with 2 mm openings.

2 Reciprocating or end-over-end shaker and 200–250 mL bottles or flasks with leakproof lids.

3 Sodium hexametaphosphate solution, 5 g L^{-1} $(NaPO_3)_6$.

4 Sieves with 53 μm openings, 10 cm diameter (or larger), placed on top of the polypropylene funnel (larger diameter than sieve) supported by a ring clamp on a laboratory stand.

5 Tall-form beakers of 1 L capacity may be useful to collect the non-POM, silt + clay suspension that is washed through the sieve.

6 A large bottle of distilled water and a spatula or rubber policeman to ensure that the entire silt + clay fraction passes through the sieve.

7 Drying oven.

47.2.2 Procedure

1 Pass field-moist soil through a sieve with 2 mm openings and discard any residues retained on the sieve. Air-dry the soil.

2 Determine the soil water content by oven drying a subsample (5 g) of the soil at 105°C.

3 Weigh 25 g of air-dried soil into each bottle, dispense 100 mL of the sodium hexametaphosphate solution into each bottle, cap the bottles, and shake overnight (e.g., 16 h).

4 Pour the suspension onto the 53 μm sieve using small aliquots of water to rinse the soil from the bottle.

5 Wash the silt + clay-sized fraction, which includes mineral and fine organic matter through the sieve using a fine jet of water from the wash bottle and gently crushing any aggregates with a rubber policeman. The POM (i.e., sand + large particles of organic matter) is retained on the sieve.

6 Rapid drying can be achieved by first oven drying (≈1 h at 40°C) the POM directly on the 53 μm sieves before transferring the POM to a beaker or similar container for final oven drying at 60°C overnight. *Note*: Place a small tray under the sieve to catch any POM that may fall through the openings. Use a spatula or paintbrush to carefully remove the POM from the sieve, taking care to recover all of the sieve contents; record the dry weight of this material.

7 Use a mortar and pestle to grind and homogenize the oven-dry POM to pass through a sieve with 250 μm openings. Determine the concentrations of C, N, and other elements of interest.

47.2.3 Comments

1 Soils are usually air-dried before dispersion to remove the effects of variations in water content. Excessive abrasion of the soil during sample preparation or dispersion can result in fragmentation of the larger particles of organic matter and

thereby lower the recovery of POM. Agents other than sodium hexametaphosphate have been used to disperse the soil before wet sieving (e.g., sonication, shaking with glass beads). In all cases, care should be taken to ensure that the amount of energy used to disperse the soil does not affect the quantity of POM recovered (Oorts et al. 2005).

2 POM may also be recovered by washing the sand-sized material from the sieve into preweighed drying tins using a wash bottle, evaporating overnight, and then oven drying at 60°C. If this is done, care should be taken to ensure that exposure of POM to water at high temperatures (during drying) for extended periods does not alter its chemical composition (e.g., through dissolution of C or nutrients).

3 It is generally assumed that any organic matter bound to the sand contributes relatively little to the carbon and nutrient concentrations measured in the material. However, where it is important to determine the dry weight of sand-free POM or to isolate POM from sand for other analyses, the sand-sized organic matter may be resuspended in a heavy solution to complete a further density separation of the organic matter (e.g., Cambardella and Elliott 1992). If this is done, care should be taken to ensure that the heavy liquid can be washed free from the POM before further analyses are undertaken.

4 Magid and Kjærgaard (2001) advocated the fractionation of POM in studies of residue decomposition. In these cases, it is sometimes useful to isolate different size classes of POM by placing a nest of sieves (e.g., 1000 and 250 μm) on top of the 53 μm sieve (Oorts et al. 2005).

47.3 LIGHT FRACTION ORGANIC MATTER

Light fraction organic matter can be isolated from much of the mineral soil by suspending the soil in a dense liquid and allowing the heavy fraction to settle while the LF floats to the surface. Density fractionation is based on the premise that the lighter soil particles, comprising mainly of freshly added, partially decomposed, and less humified organic matter, are more labile and reactive than heavier particles, which have variable amounts of adsorbed humified organic matter. The LF organic matter is separated by shaking the soil in a solution of NaI (specific gravity = 1.7) and allowing the soil mineral particles to settle for 48 h before recovering the suspended LF organic matter.

47.3.1 Materials and Reagents

1 A sieve with 2 mm openings.

2 Reciprocating or end-over-end shaker, plastic or glass bottles with lids and tall, narrow beakers (at least 250 mL capacity) with rubber stoppers. The shaker action and speed (revolutions or cycles per minute) and the flask orientation and geometry should be recorded, as these variables may influence the degree of soil dispersion.

3 Sodium iodide solution with a specific gravity of 1.7. Slowly add 1200 g of NaI to 1 L of water in a large beaker, while stirring and heating the solution on a

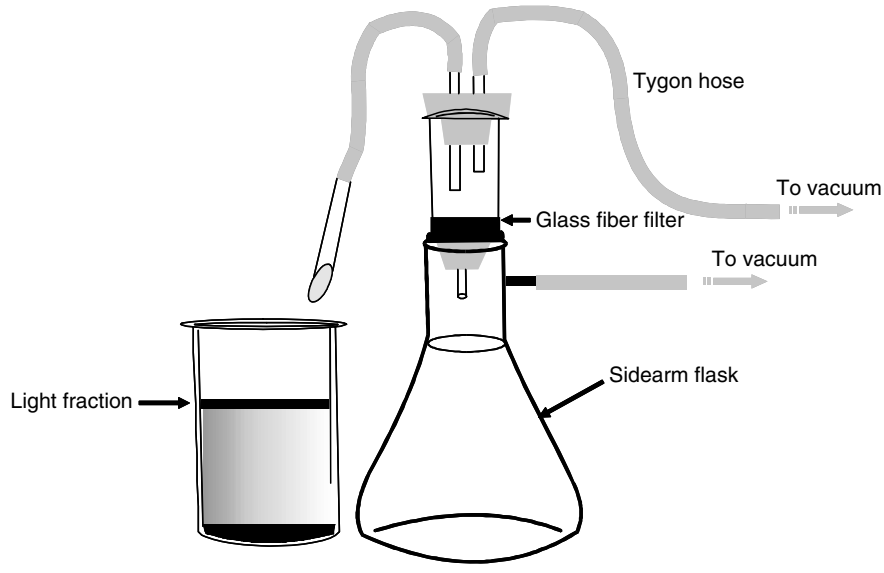

FIGURE 47.1. Vacuum filtration unit with a sidearm flask used to isolate light fraction organic matter.

magnetic mixer. After NaI is dissolved, cool the solution to room temperature and, with a hydrometer, adjust the specific gravity of the solution to 1.7. About 90 mL of solution, containing about 84 g of NaI, is required to separate the LF from each 25 g soil sample.

4 Aspiration unit (see Figure 47.1) consisting of a vacuum hose with a disposable pipette tip cut at a 45° angle to aspirate the LF; a fritted glass filter support; a detachable funnel; a clamp to attach the funnel to the top of the flask and two large (1 L) sidearm flasks, one to collect the dense solution for reuse and the other to collect water washings for discard. Membrane filters (e.g., 0.45 μm Millipore filters) made of nylon or ''quantitative'' filters designed for easy recovery of the LF on the filter may be used without contaminating the LF with filter-derived C.

5 Three wash bottles, one containing the NaI solution (specific gravity = 1.7), one containing 0.01 *M* $CaCl_2$, and one containing distilled water.

47.3.2 Procedure

1 Pass field-moist soil through a sieve with 2 mm openings and discard any residues retained on the sieve. Air-dry the soil.

2 Determine the soil water content by oven drying a subsample (5 g) of the soil at 105°C.

3 Weigh 25 g of soil into each bottle; dispense 50 mL of the NaI solution into each bottle; cap the bottle and shake on a reciprocating shaker for 60 min. Longer shaking times may be required when less vigorous shaking is used.

4 Remove the lids from each bottle; pour the contents of each bottle into a 200 mL beaker using the wash bottle containing NaI to wash the soil from the lids and bottles into the beakers.

5 Allow the beakers to stand on the laboratory bench at room temperature for 48 h.

6 Aspirate the LF organic matter from the surface of each beaker (about the top 25 mL) into the filter unit, apply a suction, and collect the filtrate (specific gravity = 1.7) for reuse. Remove enough of the dense liquid to wash the LF organic matter from the vacuum hose.

7 Without disturbing the clamp or filter, transfer the filter unit from the sidearm flask containing dense solution filtrate (for reuse) to the sidearm flask that will be used to collect the washings. Use the wash bottle containing the $CaCl_2$ to wash any LF from the walls of the vacuum flask and funnel to the filter paper. Use about 75 mL of $CaCl_2$ solution followed by 75 mL of distilled water (at least 150 mL in all) to wash the NaI from the LF organic matter. ($CaCl_2$ will help prevent the clogging of the filter.) Discard the wash water (filtrate), but keep the NaI from the first flask for reuse.

8 Remove the filter and wash the LF into preweighed drying tins. Place tins in the oven at 60°C to obtain the dry weight of the LF.

9 If the soil contains large amounts of plant residue (e.g., forest soils), it may be necessary to repeat the procedure. If so, repeat the LF separation using the NaI solution remaining in step 6 above. First add enough fresh (or filtered) NaI solution (specific gravity of 1.7) to bring the volume to about 50 mL, resuspend the soil, and repeat steps 4–8 described above.

10 Combine the dried LF organic matter recovered from the two separations and use a mortar and pestle to grind this fraction to pass through a sieve with 250 μm openings. Determine the concentrations of C and N (or other elements of interest) in the LF using standard methods.

47.3.3 Comments

1 Various compounds have been used to produce dense solutions to isolate LF organic matter (see Gregorich and Ellert 1993). We recommend the use of NaI as it is less expensive and less toxic than most alternative media, is widely available, and can be used to make solutions with densities up to 1.9 g cm^{-3} at 25°C. Organic solvents have been used to fractionate soils on the basis of density, but these are not recommended because of problems with toxicity, C contamination, and coagulation of suspended particles (Gregorich and Ellert 1993; Sollins et al. 1999). Sodium metatungstate ($Na_6(H_2\ W_{12}\ O_{40})$, Aldrich Chemical Co., Milwaukee, Wisconsin) has been used to prepare solutions with specific gravities up to 3.1 at 25°C (Plewinsky and Kamps 1984). It is considered to be unreactive and solubilizes relatively small amounts of C (Sollins et al. 1999). Colloidal silica (Ludox TM40) has been used to make solutions with densities up to 1.37 g cm^{-3}, but they have a high pH (e.g., ~pH 9) and so may extract substantial amounts of humic materials.

2 In addition to density, several solution properties (e.g., viscosity, surface tension, dielectric constant) may influence the results of density fractionations. For example, the apparent density of LF organic matter will depend on the extent to which the dense solution occupies the cavities in the particles, which in turn depends on the surface tension of the solution.

3 The density of soil particles reflects the ratio of organic materials to mineral particles (Sollins et al. 1999), and small variations in the specific gravity of the heavy liquid can result in large differences in the quantity of C (Richter et al. 1975) and C:N ratio (Gregorich et al. 2006) of the organic matter recovered. Our recommended density of 1.7 g cm^{-3} is within the range used by most researchers (Gregorich et al. 2006). To determine the most appropriate density to use in specific cases, Sollins et al. (1999) recommended undertaking sequential LF separations using solution densities ranging from 1.2 to 1.9 g cm^{-3} and analyzing the fractions obtained for ash content, C content, and C:N ratio. They contend that the optimum density for separating a biologically relevant LF is that above which the ash content of the LF increases substantially or the C:N ratio decreases markedly. It is often helpful to examine the LF under a stereomicroscope to determine the extent of any mineral soil contamination and identify biological constituents of the fractions.

4 The mass of solute required to attain a predetermined specific gravity can be computed from a measure of the solute concentration at a specific temperature. Concentration is expressed as mass fraction, because the mass, rather than volume, of solution components is additive:

$$F = S/(S + L) \tag{47.1}$$

$$S = FL/(1 - F) \tag{47.2}$$

$$S = F\ SG_{sol'n}V_{sol'n} \tag{47.3}$$

where F is the mass fraction, (i.e. mass of solute [Nal] expressed as proportion of mass of solute plus mass of solvent [water]), S the solute mass (g), L the solvent mass (g), $SG_{sol'n}$ the specific gravity of solution, and $V_{sol'n}$ the volume of solution (cm^{-3}). The mass fractions (F) for specific gravities of 1.6, 1.7, 1.8, and 1.9 are 0.51, 0.55, 0.60, and 0.64, respectively. For example, to achieve a Nal solution with a specific gravity of 1.8, where $F = 0.60$, then according to Equation, 47.2, 950 g of water requires 1425 g of Nal (final solution volume ~$(950 + 1425)/1.8$ or 1319 cm^3). Alternatively, Equation 47.3 indicates that 1425 g of Nal is required to prepare 1319 mL of a solution at a specific gravity of 1.8.

5 Centrifugal force (e.g., 1000 *g*) can be used to quickly separate the light and heavy fractions in the above procedure instead of leaving the beakers to stand on the laboratory bench (at 1 *g*) and will allow for more rapid processing of the samples. Use of centrifuge tubes also allows greater vertical separation of the light and heavy fractions and for narrower solution/soil ratios compared to those in the method described above; if the solution/soil ratio is decreased further than 2:1, some of the uncomplexed organic matter could get entrapped within the heavy

fraction during the fractionation procedure. Therefore, if centrifugation is used, it is recommended that the heavy fraction be resuspended and the separation procedures (see step 9 in Section 47.3.2) repeated at least two or three times.

6 It is often useful to determine the C and nutrient content (e.g., N) of the whole soil so that the LF-C or -N can be expressed as a percentage of the whole soil C or N.

47.4 IMPORTANT CONSIDERATIONS

47.4.1 Calculation of Results

The mass of LF organic matter can be expressed as a percentage of the whole soil on a dry weight basis; however, it should be noted that the LF may contain a small amount of mineral soil contaminants that may result in an overestimation of the LF mass. To calculate the proportion of whole soil C in the POM or LF:

$$\text{fraction C/whole soil C} = [\text{fraction}_{dw} \times (\text{POM C or LF C})]/\text{whole soil C} \qquad (47.4)$$

where fraction C/whole soil C is the proportion of whole soil C in the POM or LF, fraction_{dw} is the dry weight of sand-sized or LF organic matter (g fraction/g whole soil), POM C or LF C is the C concentration in the POM or LF sample (g C/g fraction_{dw}), and whole soil C is the C content of the whole soil (i.e., g whole soil C/g whole soil).

Corrections for ash in LFs may help to account for the presence of light minerals or phytoliths. The ash content of the LF can be determined by weighing subsamples in a muffle furnace for 4 h at 550°C before and after ignition.

47.4.2 Losses during Fractionation

When first applying these procedures, it may be useful to determine the recovery efficiency and identify where losses may occur in the fractionation procedure. However, if care is taken with these procedures, it is probably not necessary to determine the recovery efficiency on a regular basis. The mass or organic C content of the whole soil can be compared with the sums of mass or C content in the various fractions to ensure that losses during the fractionation do not introduce appreciable bias. To calculate a mass balance, it is necessary to recover the silt + clay fraction in the sieving method or the heavy fraction in the flotation method. Calcium chloride (e.g., 20 mL of 3 *M* $CaCl_2$) or another flocculating agent can be added to the suspension passing the 53 μm sieve to recover the silt + clay associated organic matter. After the supernatant is siphoned off, the slurry left in the bottom of the beaker can be transferred to containers that are suitable for freeze drying. In the density separation method, the heavy fraction can be recovered by siphoning off the dense solution, and repeated resuspension in wash water followed by centrifugation and aspiration of the supernatant. When the heavy fraction fails to form a stable pellet (usually after two to three washings), it can be frozen in the centrifuge tubes and freeze dried.

47.4.3 Bioassay of the Light Fraction

The type of heavy solution used in separating the LF from whole soil may have deleterious effects on the viability of certain microbial populations and their activities, alter the decomposibility of LF organic matter, or cause complexation with the LF organic matter.

Magid et al. (1996) observed that C mineralization from LF was enhanced when isolated with silica suspension and retarded when separated using sodium polytungstate. We recommend that any studies involving bioassays of the LF also include a thorough evaluation of possible contamination by the media and any resulting effects on decomposition.

47.4.4 Contamination of Uncomplexed Organic Matter with Charcoal or Mineral Soil

Physically uncomplexed organic matter can contain charcoal and its presence could substantially affect the chemistry and turnover of this organic matter. Charcoal has been detected using microscopic techniques in the LF and POM fractions in many soils (Spycher et al. 1983; Baisden et al. 2002). Where investigators are interested in LF or POM as a measure of ''young'' or actively cycling organic matter, removal of charcoal may be important to accurately estimate the size, nutrient content, and turnover of this fraction. However, there are no known standard procedures for correcting for the charcoal content of uncomplexed organic matter.

Given its operational definition, the POM (>53 μm) fraction of soil often contains a high proportion of sand that should be removed by density separation if a measure of the POM mass is required. Depending on the method of separation used, LF organic matter may also contain a small amount of mineral soil contaminants that may contribute some older and probably less labile, mineral-associated organic matter to what is measured in the LF.

REFERENCES

Baisden, W., Amundson, R., Cook, A.C., and Brenner, D.L. 2002. Turnover and storage of C and N in five density fractions from California annual grassland surface soils. *Glob. Biochem. Cycl.* 16: 1117.

Beare, M.H., Hendrix, P.F., and Coleman, D.C. 1994. Water-stable aggregates and organic matter fractions in conventional and no-tillage soils. *Soil Sci. Soc. Am. J.* 58: 777–786.

Cambardella, C.A. and Elliott, E.T. 1992. Particulate soil organic-matter changes across a grassland cultivation sequence. *Soil Sci. Soc. Am. J.* 56: 777–782.

Campbell, C.A., Selles, F., Lafond, G.P., Biederbeck, V.O., and Zentner, R.P. 2001. Tillage–fertilizer changes: effect on some soil quality attributes under long-term crop rotations in a thin black chernozem. *Can. J. Soil Sci.* 81: 157–165.

Curtin, D., McCallum, F.M., and Williams, P.H. 2003. Phosphorus in light fraction organic matter separated from soils receiving long-term applications of superphosphate. *Biol. Fert. Soil.* 37: 280–287.

Golchin, A., Oades, J.M., Skjemstad, J.O., and Clarke, P. 1994. Soil structure and carbon cycling. *Aust. J. Soil Res.* 32: 1043–1068.

Gregorich, E.G., Beare, M.H., McKim, U.F., and Skjemstad, J.O. 2006. Chemical and biological characteristics of physically uncomplexed organic matter. *Soil Sci. Soc. Am. J.* 70: 975–985.

Gregorich, E.G. and Ellert, B.H. 1993. Light fraction and macroorganic matter in mineral soils. In M.R. Carter, Ed., *Soil Sampling and Methods of Analysis*. Canadian Society of Soil Science. Lewis Publishers, Boca Raton, FL, pp. 397–407.

Gregorich, E.G. and Janzen, H.H. 1996. Storage of soil carbon in the light fraction and macroorganic matter. In M.R. Carter and B.A. Stewart, Eds., *Structure and Organic Matter Storage in*

Agricultural Soils. Lewis Publishers, CRC Press, Boca Raton, FL, pp. 167–190.

Ladd, J.N. and Amato, M. 1980. Mineralization in calcareous soils: IV. Changes in the organic nitrogen of light and heavy subfractions of silt- and fine clay-size particles during nitrogen turnover. *Soil Biol. Biochem.* 12: 185–189.

Ladd, J.N., Parsons, J.W., and Amato, M. 1977. Studies of nitrogen immobilization and mineralization in calcareous soils—II. Mineralization of immobilized nitrogen from soil fractions of different particle size and density. *Soil Biol. Biochem.* 9: 319–325.

Magid, J., Gorissen, A., and Giller, K.E. 1996. In search of the elusive ''active'' fraction of soil organic matter: three size-density fractionation methods for tracing the fate of homogeneously ^{14}C-labelled plant materials. *Soil Biol. Biochem.* 28: 89–99.

Magid, J. and Kjærgaard, C. 2001. Recovering decomposing plant residues from the particulate soil organic matter fraction: size versus density separation. *Biol. Fert. Soil*. 33: 252–257.

Oorts, K., Vanlauwe, B., Recous, S., and Merckx, R. 2005. Redistribution of particulate organic matter during ultrasonic dispersion of highly weathered soils. *Eur. J. Soil. Sci.* 56: 77–91.

Plewinsky, B. and Kamps, R. 1984. Sodium metatungstate: a new medium for binary and ternary density gradient centrifugation. *Die Makromolecular Chemie* 185: 1429–1439.

Richter, M., Mizuno, I., Aranguez, S., and Uriarte, S. 1975. Densimetric fractionation of soil organo-mineral complexes. *J. Soil Sci*. 26: 112–123.

Salas, A.M., Elliott, E.T., Westfall, D.G., Cole, C.V., and Six, J. 2003. The role of particulate organic matter in phosphorus cycling. *Soil Sci. Soc. Am. J*. 67: 181–189.

Scheffer, B. 1977. Stabilization of organic matter in sand mixed cultures. In *Soil Organic Matter Studies*, Vol. 2. International Atomic Energy Agency, Vienna, Austria, pp. 359–363.

Sollins, P., Glassman, C., Paul, E.A., Swanston, C., Lajtha, K., Heil, J.W., and Elliott, E.T. 1999. Soil carbon and nitrogen: Pools and fractions. In G.P. Robertson, D.C. Coleman, C.S. Bledsoe, and P. Sollins, Eds., *Standard Soil Methods for Long-Term Ecological Research*. Oxford University Press, Oxford, UK, pp. 89–105.

Spycher, G., Sollins, P., and Rose, S. 1983. Carbon and nitrogen in the light fraction of a forest soil: vertical distribution and seasonal patterns. *Soil Sci*. 135: 79–87.

Wander, M. 2004. Soil organic matter fractions and their relevance to soil function. In F. Magdoff and R.R. Weil, Eds., *Soil Organic Matter in Sustainable Agriculture*. CRC Press, Boca Raton, FL, pp. 67–102.

Chapter 48
Extraction and Characterization of Dissolved Organic Matter

Martin H. Chantigny and Denis A. Angers
Agriculture and Agri-Food Canada
Quebec, Quebec, Canada

Klaus Kaiser
Martin Luther University
Halle-Wittenberg, Halle, Germany

Karsten Kalbitz
University of Bayreuth
Bayreuth, Germany

48.1 INTRODUCTION

Dissolved organic matter (DOM) represents a relatively small fraction of the total organic matter in soil (0.04%–0.2%; Zsolnay 1996). However, because of its mobility and presumed labile nature, DOM is often perceived as the most active fraction of soil organic matter. Research in the past 20 years has shown that DOM can play an important role in a number of key soil processes including the transport of nutrients (Murphy et al. 2000; Michalzik et al. 2001), organic contaminants and metals in the soil profile (Herbert and Bertsch 1995; Zsolnay 1996), replenishment of C at depth (Michalzik et al. 2001; Guggenberger and Kaiser 2003), and as a substrate for microbial activity (Burford and Bremner 1975; McGill et al. 1986; Chantigny et al. 1999; Marschner and Kalbitz 2003).

Dissolved organic matter is operationally defined as the organic matter present in solution that can pass through a 0.45 μm filter (Thurman 1985), though other pore sizes have sometimes been used for specific purposes (Herbert and Bertsch 1995). Various approaches have been used to obtain soil solution samples and these have different implications for the amount and composition of the DOM collected (Zsolnay 1996, 2003; Hagedorn et al. 2002, 2004). Much of the research on soil DOM has focused on temperate forest ecosystems (Zsolnay 1996; Kalbitz et al. 2000), where DOM is most often measured from soil solution samples

collected *in situ* with zero-tension lysimeters. Other techniques involving tension lysimeters, suction cups, and centrifugation have also been used (Herbert and Bertsch 1995; Titus and Mahendrappa 1996). In grasslands and arable soils extraction of DOM with aqueous solutions is more common than the collection of soil solution *in situ* (Zsolnay 1996; Chantigny 2003) partly due to the frequent disturbances caused by management practices in agricultural soils which may interfere with lysimeter equipment. The ''soluble'' soil organic matter extracted with low-ionic strength aqueous solutions is often called water-extractable organic matter (WEOM), and is considered an acceptable surrogate to soil solution DOM collected *in situ* (Herbert and Bertsch 1995; Zsolnay 2003). Soil organic matter can also be extracted with high-ionic strength aqueous solutions. This procedure extracts both soil DOM and some additional organic matter desorbed during the extraction process; it therefore cannot be used as a surrogate to soil solution DOM collected *in situ*. However, soil organic matter extracted with high-ionic strength aqueous solution appears to be enriched in easily biodegradable compounds (Guggenberger et al. 1989; Novak and Bertsch 1991; Hagedorn et al. 2004), which could explain why it is considered to influence soil microbial biomass (e.g., McGill et al. 1986; Liang et al. 1998) and microbial processes such as denitrification (e.g., Burford and Bremner 1975; Lemke et al. 1998), soil respiration/C mineralization (e.g., Gregorich et al. 1998; Chantigny et al. 1999), and N mineralization (e.g., Appel and Mengel 1993; Murphy et al. 2000).

Dissolved organic matter is an expression borrowed from aquatic sciences (Thurman 1985; Zsolnay 2003). In soil science, the term dissolved may refer to organic matter present in any solution, including soil extracts. This might explain the confusion perceived in the scientific literature pertaining to the definition of soil DOM. A clear definition and distinction among the various procedures used to ''dissolve'' soil organic matter would be useful to soil researchers. For convenience, DOM is used in this chapter as a general term, and the most commonly used procedures to obtain soil DOM are classified into three distinct categories: soil solution, water-extractable, and salt-extractable organic matter. General procedures for collection and analysis of each category of soil DOM are presented. Selected procedures for analyzing C and N concentration, key spectroscopic and chemical properties, and biodegradability are also given.

48.2 COLLECTION OF SOIL DISSOLVED ORGANIC MATTER

48.2.1 Soil Solution Organic Matter

Careful selection of procedures to collect soil solution organic matter (SSOM) is needed to ensure that they are most appropriate to the research questions being addressed. Several approaches and devices have been proposed to collect soil solution; the most common involves the *in situ* use of lysimeters or suction cups (Heinrichs et al. 1996; Titus and Mahendrappa 1996; Ludwig et al. 1999), or the centrifugation of field-moist soil samples (reviewed by Zsolnay 1996). The selection of a procedure must be carefully made because different approaches may collect different fractions of the soil solution (Raber et al. 1998; Zsolnay 2003). For instance, zero-tension lysimeters collect freely draining soil solution, whereas tension lysimeters (e.g., suction cups) and centrifugation can collect solution located in smaller soil pores. The possible interferences of lysimeter surfaces with soil solution DOM have been addressed by Guggenberger and Zech (1992), Jones and Edwards (1993), Marques et al. (1996), Wessel-Bothe et al. (2000), and Siemens and Kaupenjohann (2003).

Further details on the collection of soil solution are given in Chapter 17. In any case, soil solution samples must be filtered at 0.45 μm prior to analysis.

48.2.2 Water-Extractable Organic Matter (Adapted from Zsolnay 1996; Kalbitz et al. 2003)

Water-extractable organic matter has been proposed and used as a surrogate to soil solution collected *in situ* (Herbert and Bertsch 1995; Zsolnay 1996). The procedure was developed to minimize or avoid the release of OM through physical disruption of the soil structure and its desorption from exchange sites (Zsolnay 2003).

Materials and Reagents

1. Polypropylene centrifuge tubes (50 mL) or centrifuge bottles (250 mL)
2. Glass rod
3. Pure deionized water or 5 m*M* $CaCl_2$ solution
4. Centrifuge (optional)
5. Glass vacuum filter unit or stainless steel pressure filter unit
6. 0.4 μm polycarbonate filter that fits the filter unit
7. 125 mL Erlenmeyer flasks to support the filter unit (with sidearm if a vacuum filter unit is used)
8. Vacuum pump or other vacuum/pressure system
9. Storage vials of the required volume capacity (glass vials should be preferred; if freezing is necessary then plastic vials should be used)

Procedures

1. Place 5 g of mineral soil (dry mass basis) into a 50 mL centrifuge tube, or 5 g of organic soil (dry mass basis) into a 250 mL centrifuge bottle. Mineral soil samples should be thoroughly mixed or sieved at <6 mm to provide a representative subsample. Extraction procedures should be performed on field-moist soils and started as soon as possible after sampling as WEOM concentration and/or composition may change when field-moist soils are stored at cool temperatures for several days (Chapman et al. 1997b; Kaiser et al. 2001).
2. Add 10 mL of 5 m*M* $CaCl_2$ solution to the mineral soil, or 50 mL of deionized water to the organic soil. Gently stir with a glass rod to make a homogeneous slurry; stir for about 1 min for mineral soil extraction; for organic soil, let stand at 4°C for 24 h and occasionally stir (3–4 times) the slurries with the glass rod. Stirring must be as gentle as possible to avoid significant desorption of soluble materials.

3 Centrifuge at 12,000 *g* for 10 min. This step is optional and is aimed at reducing clogging problems of filters caused by colloidal particles.

4 Filter the slurry (not centrifuged) or supernatant (centrifuged) through the vacuum or pressure filter unit equipped with a 0.4 μm polycarbonate filter.

5 Transfer the filtrate into a glass vial and store at 4°C if analyzed within 2 days; store the filtrate in a plastic vial at −20°C for longer periods.

Comments

1 A 1:2 soil:solution ratio for mineral soils and 1:10 ratio for organic soils are recommended as wider ratios may increase WEOM content by favoring organic matter desorption (Chapman et al. 1997a; Zsolnay 2003).

2 Proposed extraction times (1 min for mineral soil; 24 h for organic soil) have been tested by Zsolnay (1996) and Kalbitz et al. (2003), respectively. However, extraction times of 1 to 5 min were found to have a minimal influence on extraction efficiency of WEOM from mineral soils (Zsolnay 1996). Therefore, it is important to clearly indicate the extraction time used and to be consistent within each study.

3 If filtration is performed under vacuum (negative pressure), care must be taken that vacuum is not too high to avoid cavitation in the filtrate, which might modify the amount and nature of DOM; more details about this and other possible artifacts during DOM collection/extraction are reviewed by Zsolnay (2003).

4 Air-drying soil prior to extraction can increase the concentration of WEOM (Zsolnay et al. 1999; Kaiser et al. 2001), owing to microbial cell lysis and release of soluble components, or swelling of clays.

5 Use of deionized water is not recommended for extraction of mineral soils since it has a dispersive effect on soil aggregates and may favor organic matter desorption from mineral surfaces during extraction (Zsolnay 1996; Kaiser et al. 2001).

6 WEOM obtained with vigorous shaking (e.g., agitation on a reciprocal shaker) should not be considered an acceptable surrogate to soil solution collected *in situ* because the agitation may cause extraction of additional organic materials (Herbert and Bertsch 1995; Zsolnay 1996) of different nature (Zsolnay 2003; Hagedorn et al. 2004), likely due to aggregate disruption and/or abrasion of microbial cells. It then has more similarities with soluble organic materials obtained with the procedures given in the next section.

48.2.3 Salt-Extractable Organic Matter

The organic matter recovered from salt-solution extracts is also often referred to as ''soluble organic matter'' or ''water-soluble organic matter'' in the literature. Salt-extractable organic matter (SEOM) includes both SSOM and additional organic matter desorbed and/or dissolved

during the extraction process (Zsolnay 1996, 2003; Hagedorn et al. 2004). For example, in a literature review Zsolnay (1996) reported SEOM (extraction with 0.5 *M* K_2SO_4 solution) values ranging from 29 to 127 μg g^{-1} dry soil in arable soils as compared to 8 to 13 μg g^{-1} dry soil for WEOM (extraction with either 4 m*M* $CaSO_4$ or 10 m*M* $CaCl_2$). Moreover, the additional material extracted appears to be more biodegradable than SSOM (Guggenberger et al. 1989; Novak and Bertsch 1991; Hagedorn et al. 2004). Therefore, SEOM should not be used as a surrogate to SSOM. Nevertheless, SEOM is often used as an estimate of organic matter readily available to soil heterotrophs (e.g., Burford and Bremner 1975; McGill et al. 1986; Murphy et al. 2000). The procedure given here is similar to that used for soil mineral N extraction (see Chapter 6).

Materials and Reagents

1 Polypropylene centrifuge bottles (250 mL)

2 Reciprocal shaker

3 1 *M* KCl solution

4 Centrifuge (optional)

5 Glass vacuum filter unit or stainless steel pressure filter unit

6 0.4 μm polycarbonate filter that fits the filter unit

7 125 mL Erlenmeyer flask to support the vacuum filter unit (with sidearm if a vacuum filter unit is used)

8 Vacuum pump or other vacuum/pressure system

9 Storage vials of the required volume capacity (glass vials should be preferred; if freezing is necessary then plastic vials should be used)

Procedures

1 Place 20 g of soil (dry mass basis) in a centrifuge bottle. Mineral soil samples should be thoroughly mixed or sieved at <6 mm to provide a representative subsample. Soil samples should be extracted as soon as possible after soil sampling for the same reasons as given in Procedures, p. 619.

2 Add 100 mL of 1 *M* KCl solution. Agitate for 30 min on a reciprocal shaker (about 160 strokes per minute).

3 Centrifuge at 3,000 *g* for 10 min. This step is optional and is aimed at reducing clogging problems of filters caused by an excess of colloidal particles.

4 Filter the slurry (not centrifuged) or supernatant (centrifuged) through the vacuum or pressure filter unit equipped with a 0.4 μm polycarbonate filter.

5 Transfer the filtrate into a glass vial and store at 4°C if analyzed within 2 days; store the filtrate in a plastic vial at −20°C for longer periods.

Comments

1 Extraction and measurement of SEOM in KCl extracts is proposed since this extraction procedure is routinely used to measure soil mineral N content. However, SEOM is also often measured in 0.5 *M* K_2SO_4 extracts, such as those taken from unfumigated soils used in measuring soil microbial biomass based on direct extraction procedures (Vance et al. 1987; see Chapter 49). Hot-water or hot KCl extractions are sometimes used and should not be considered equivalent to SSOM since heating of the soil-water slurry may dissolve more organic material than extraction at room temperature.

2 Air-drying of the soil prior to extraction can increase the amount of SEOM and may change its biodegradability if the additional extracted organic matter has different chemical characteristics. See the reviews by Zsolnay (1996; 2003) and Murphy et al. (2000) for more details about the various approaches used to obtain soil SEOM.

48.3 METHODS FOR CHARACTERIZING DISSOLVED ORGANIC MATTER

It is now widely accepted that DOM has a complex chemical composition and may contribute to a wide range of soil processes. In this section, we present details of relatively inexpensive and simple analytical methods for characterizing the chemical composition and assessing the biodegradability of DOM in soil solution (SSOM) and in soil extracts (WEOM and SEOM). Procedures for quantifying the total C, total N, specific UV absorbance, phenol, hexose, pentose, and amino acid content, and to assess DOM biodegradability are given below.

48.3.1 Carbon Concentration

Carbon is an important constituent of soil DOM. The C concentration in filtered soil solutions or extracts can be measured using wet chemical or automated combustion procedures. Quantification of C may be determined by UV-catalyzed wet oxidation followed by measurement of the evolved CO_2 using an infrared detector. However, C quantification by dry combustion at 700°C–800°C is now preferred since it can readily and more accurately measure inorganic and organic forms of dissolved C.

48.3.2 Nitrogen Concentration (after Cabrera and Beare 1993)

Researchers are often interested in determining the amount of nutrients present in organic forms in the soil solution or aqueous extracts. The organic N present in DOM can be measured by oxidation with potassium persulfate. At high temperature persulfate oxidizes organic N to NO_3^-, which can be measured by standard colorimetric methods (e.g., Cd reduction of NO_3^- to NO_2^-).

Materials and Reagents

1 Certified low-N potassium persulfate ($K_2S_2O_8$; EM Science, EM Industries, Inc. Gibbstown, NJ, USA).

2 Boric acid (H_3BO_4).

3 Nanopure water (specific resistance of 17.8 megohm cm^{-1} or higher).

4 3.75 *M* NaOH solution: dissolve 150 g of NaOH pellets in 900 mL of nanopure water. Let the solution cool down to room temperature. Complete to 1 L with nanopure water.

5 Oxidative solution: dissolve 100 g of $K_2S_2O_8$ and 60 g of H_3BO_4 in 200 mL of 3.75 *M* NaOH solution. Complete to 2 L with nanopure water.

6 50 mL glass tubes equipped with Teflon-lined screw caps.

Oxidation Procedure

1 Measure mineral N (NO_2^--N + NO_3^--N + NH_4^+-N) concentration in the DOM sample using a standard procedure as proposed in Chapter 6.

2 Transfer/pipette 15 mL of DOM sample into a 50 mL glass tube and add 15 mL of the oxidative solution. Immediately close the tube with screw cap, agitate on a vortex for a few seconds, and weigh each tube.

3 Autoclave the loosely capped tubes for 30 min (121°C; 135 kPa).

4 Let cool down at room temperature and then tightly close the tubes. Weigh each tube: water loss during the autoclaving period is generally less than 3% of the initial volume and is used to correct for NO_3^- concentration measured in the oxidized solution.

5 Measure NO_3^- concentration in the oxidized solution using a standard procedure (see Chapter 6).

6 Organic N concentration is calculated as the difference between NO_3^--N concentration in the oxidized sample (Step 5) and the initial mineral N concentration in the nonoxidized sample (Step 1).

Comments

1 Mineral N concentration can be measured in both oxidized and nonoxidized samples with automated flow injection analysis (FIA) systems. Some FIA systems now offer the possibility for online UV-catalyzed persulfate oxidation of organic N, with simultaneous quantification of both the mineral and total dissolved N. The oxidation performance of those automated systems appears as good as the manual procedure presented here.

2 It should be noted that the method may oxidize some N_2, thus the volume of air in the test tubes should be as small as possible (Hagedorn and Schleppi 2000).

48.3.3 Specific UV Absorbance

The specific UV absorbance is an estimate of the concentration of aromatic compounds (Traina et al. 1990; Novak et al. 1992; Chin et al. 1994; Korshin et al. 1997) present in

DOM sample. It has been shown to be positively correlated to the amount of XAD-8 adsorbable dissolved organic C (DOC) (Dilling and Kaiser 2002; Kalbitz et al. 2003) and phenol concentration as measured in the following section. In DOM samples from forest floor horizons, peat samples and A horizons, specific UV absorbance has been shown to be negatively correlated with DOM biodegradability, indicating that aromatic compounds are part of recalcitrant DOM (Kalbitz et al. 2003).

Materials and Reagents

1 1-cm path length quartz glass cuvettes

2 Spectrophotometer

Procedure and Calculations

1 Pour a sufficient amount of DOM sample into the quartz cuvette.

2 Read absorbance at 254–285 nm against blank.

3 Calculate specific UV absorbance by dividing the measured absorbance (in cm^{-1}) by the concentration of DOC (in mg L^{-1}) of the sample. The units of specific UV absorbance are thus given as L mg^{-1} C cm^{-1}.

4 Always report the wavelength used.

Comments

1 To avoid acidification and sparging of sample, specific UV absorbance should be carried out at ambient pH. Quartz glass cuvettes are to be used for this measurement as optical glass or plastic cuvettes may absorb some UV light. Make sure that the sample absorbance does not exceed the linear range of the instrument. If this is the case, dilute the sample with nanopure water.

2 Interferences may be caused by Fe^{2+}, NO_3^-, NO_2^-, and Br^-. However, the interference with NO_3^- can be minimized by performing the determination at 280 nm, and concentrations of NO_2^- and Br^- are generally too small to cause interference.

48.3.4 Phenols

Dissolved phenols, either monomers or oligomers, mainly derive from degradation of polyphenolic plant metabolites, such as tannins and lignin (Guggenberger et al. 1989). They are important metal-complexing agents, can bind proteins, interfere with the sorption of inorganic anions such as phosphate, and may exert allelopathic effects on microorganisms and plants (Herbert and Bertsch 1995; Zsolnay 2003).

Materials and Reagents

1 1.5 mL Eppendorf tubes.

2 Spectrophotometer.

3 1-cm path length quartz or optical glass cuvettes.

4 Microcentrifuge.

5 Folin–Ciocalteu's phenol reagent (available from SIGMA); store in the dark.

6 Saturated Na_2CO_3 solution: dissolve 216 g in 1 L of deionized water.

7 Stock standard solution: 2-hydroxybenzoic acid (analytical grade, 100 mg L^{-1}) deionized water.

8 Working standards: prepare solutions of 2.5, 5, 10, 20, 30, and 40 mg L^{-1} 2-hydroxybenzoic acid by dilution of the stock solution.

Procedure and Calculations

1 Add 0.7 mL of DOM sample, standard, or blank into a 1.5 mL Eppendorf tube.

2 Add 50 μL of Folin–Ciocalteu's reagent.

3 Mix and let stand for 3 min at room temperature.

4 Add 100 μL of the saturated Na_2CO_3 solution.

5 Add 150 μL of deionized water, mix well, and let stand for 10 to 20 min at room temperature.

6 Blue color should develop if phenols are present; blanks should go colorless. If a precipitate is formed, centrifuge for 2 to 3 min (2,000 *g*) and read absorbance immediately.

7 Transfer a sufficient amount of the sample or standard to a glass cuvette and read absorbance at 725 nm against blank.

8 Prepare calibration curve and calculate phenol concentration in mg L^{-1} 2-hydroxybenzoic acid equivalent.

Comments

1 This method can be used for all kinds of aqueous soil extracts, including alkaline soil extracts (Morita, 1980).

2 The method precisely detects phenol concentrations as small as 1 mg L^{-1} 2-hydroxybenzoic acid equivalent.

3 Folin–Ciocalteu's reagent reacts with various phenol monomers and polyphenolic substances. The reaction products vary in their color yields and adsorption maxima. Thus, the method does not accurately measure the total phenol concentration but allows for qualitative comparison of samples. The limitation of the proposed method in estimating phenol concentration has been discussed in detail

by Box (1983) and Ohno and Paul (1998). Rough estimates of monomeric and polymeric phenols can be achieved by precipitating polyphenols with casein and analyzing the supernatant for monomeric phenol concentration. Polyphenol concentration is estimated as the difference between total phenol concentration and monomeric phenol concentration in the precipitated sample (Kuiters and Denneman 1987). Phenols other than 2-hydroxybenzoic acid (e.g., tannins, vanillic acid, gallic acid) can be used as standards. High concentrations of Fe^{2+}, Mn^{2+}, or S^{2-} in samples interfere with the method, likely resulting in overestimation of phenol concentration.

48.3.5 Hexoses

Hexoses in soil DOM are an energy source to soil microbes and therefore may be used as an indicator of DOM biodegradability (DeLuca and Keeney 1993). Apart from glucose, most hexoses in soil are of microbial origin (see Chapter 50).

Materials and Reagents

1 10 mL glass test tubes.

2 Vortex mixer.

3 Spectrophotometer.

4 1-cm path length cuvettes (optical glass or plastic is acceptable).

5 Anthrone–sulfuric acid reagent: dissolve 0.2 g of anthrone (analytical grade) in 100 mL of concentrated (96%–98% v/v) H_2SO_4 (analytical grade), prepare always fresh for the day but let it stand for ca. 1 h at room temperature before use.

6 Stock standard: glucose (analytical grade), 100 mg L^{-1}, in deionized water.

7 Working standards: prepare solutions of 2.5, 5, 10, 20, 30, and 50 mg L^{-1} glucose by dilution from stock standard.

Procedure and Calculations

1 Add 1 mL of DOM sample, standard, or blank to a test tube.

2 Add 2 mL of anthrone–sulfuric acid reagent (beware, the solution heats up).

3 Vortex and let stand for 15 min at room temperature.

4 Transfer a sufficient amount of the anthrone-treated sample or standard to a cuvette and read absorbance at 625 nm against the blank.

5 Prepare calibration curve and calculate hexose concentration in mg L^{-1} glucose equivalent.

Comments

1 This method is a variant of a procedure originally proposed for measurement of carbohydrates in soil hydrolysates (Brink et al. 1960).

2 Typically, the sulfuric acid added with the anthrone reagent is sufficient to hydrolyze the dissolved polysaccharides.

3 The method seems to be robust against interferences from Fe^{2+}, Mn^{2+}, NO_3^-, and Cl^- ions. However careful control, such as a spike-recovery experiment, along with meticulous analytical procedures seem important in obtaining reliable results (Grandy et al. 2000).

4 Glass test tubes should be carefully rinsed with ultrapure water before use to avoid contamination with hexoses. As with all tests using a single compound for calibration, the method tends to overestimate the hexose concentration. For a more detailed analysis of soil hexoses, chromatographic procedures are described in Chapter 50.

48.3.6 Pentoses

Pentoses are an energy source to soil microbes and measuring pentoses along with hexoses provides a measure of the total abundance of carbohydrates in DOM. Pentoses in soil are mainly of plant origin (see Chapter 50). Therefore, the ratio of pentoses-to-hexoses may provide information about the relative abundance of plant-derived carbohydrates in DOM.

Materials and Reagents

1 10 mL glass tubes equipped with Teflon-lined screw caps.

2 Water bath: operating at 95°C.

3 Spectrophotometer.

4 1-cm path length cuvettes (optical glass or plastic is acceptable).

5 Iron chloride reagent: dissolve 0.1 g of $FeCl_3$ (analytical grade) in 100 mL of concentrated (32% v/v) HCl (analytical grade).

6 95% ethanol (analytical grade).

7 Orcinol reagent: dissolve 1 g of orcinol ($CH_3C_6H_3$-1,3-$(OH)_2$; 3,5-dihydroxy-toluene) in 100 mL of 95% ethanol (analytical grade).

8 Stock standard: ribose (analytical grade), 100 mg L^{-1}, in deionized water.

9 Working standards: prepare solutions of 2.5, 5, 10, 20, 30, and 50 mg L^{-1} ribose by dilution from stock standard.

Procedure and Calculations

1 Add 1 mL of DOM sample, standard, or blank into a test tube.

2 Add 1 mL of iron chloride reagent and 1 mL of orcinol reagent, cap the tubes.

3 Keep in the water bath at 95°C for 20 min.

4 Cool on ice for 5 min.

5 Add 2 mL of 95% ethanol, mix.

6 Transfer a sufficient amount of the treated sample or standard to a cuvette and read absorbance at 660 nm against blank.

7 Prepare calibration curve and calculate pentose concentration in mg L^{-1} ribose equivalent.

Comments

1 This method is adapted from a procedure developed for pentoses released from biogenic tissues (Mejbaum 1939). Recently it has been applied to aqueous samples and proved to give reasonable and reliable estimates of total pentose content in DOM (Kawahigashi et al. 2003).

2 As with all tests using a single compound for calibration, the method tends to overestimate the pentose concentration. Test tubes should be rinsed thoroughly with ultrapure water before use to avoid contamination with pentoses. For a more detailed analysis of soil pentoses, chromatographic procedures are described in Chapter 50.

48.3.7 Amino Acids

Free amino acids are found at low concentrations in DOM and thought to be a significant source of N to plants in natural ecosystems and to soil microbes (Jones and Kjelland 2002).

Materials and Reagents

1 10 mL glass tubes equipped with Teflon-lined screw caps.

2 Water bath: operating at 95°C.

3 Water bath: at room temperature.

4 Spectrophotometer.

5 1-cm path length cuvettes (optical glass or plastic is acceptable).

6 Acetate buffer (pH 5.5): dissolve 54 g of Na acetate trihydrate (analytical grade) in 40 mL of deionized water, add 10 mL of glacial acetic acid, adjust pH to 5.5 with NaOH.

7 Ninhydrin reagent: dissolve 2 g of ninhydrin (analytical grade) and 0.3 g of hidrindantin in 75 mL of 2-hydroxy ethanol (analytical grade), purge the solution with N_2 for 30 min, then add 25 mL of acetate buffer (pH 5.5). Prepare solution always fresh and avoid contact with air as much as possible.

8 Dilutant: mix equal amounts of 95% ethanol (analytical grade) and deionized water.

9 Stock standard: leucine (analytical grade), 1000 μmol L^{-1}, in deionized water.

10 Working standards: prepare solutions of 20, 40, 60, 80, and 100 μmol L^{-1} leucine by dilution from stock standard.

Procedure and Calculations

1 Add 2 mL of DOM sample, standard, or blank into a test tube.

2 Slowly add 1.25 mL of the ninhydrin reagent, cap the tubes.

3 Keep in the water bath at 95°C for 25 min.

4 Cool to room temperature in another water bath.

5 Add 4.5 mL of dilutant, mix.

6 Transfer a sufficient amount of the treated sample or standard to a cuvette and read absorbance at 570 nm against blank.

7 Prepare calibration curve and calculate amino acids concentration in μmol L^{-1} leucine equivalent.

Comments

1 This procedure is a variant of the original method by Moore and Stein (1948).

2 The most critical point in the analytical procedure is to keep the ninhydrin reagent from reacting with oxygen. An alternative spectrofluorometric method for the sensitive determination of amino acids was recently proposed by Jones et al. (2002) and relies on the reaction of free amino acids with *o*-phthaldialdehyde and beta-mercaptoethanol.

48.3.8 Proteins

Proteins may be important contributors to dissolved organic N and the source for replenishment of the free amino acids pool in DOM. They therefore have a potential influence on microbial growth in soil.

Materials and Reagents

1 Spectrophotometer.

2 1-cm path length cuvettes (optical glass or plastic is acceptable).

3 Bradford protein reagent (available from SIGMA), store refrigerated.

4 Stock standard: bovine serum albumin (BSA), dissolve 100 mg BSA L^{-1} deionized water. Prepare fresh as it does not preserve well even when frozen.

5 Working standards: prepare solutions of 2.5, 5, 10, 15, 20, and 25 mg L^{-1} BSA by dilution from stock standard.

Procedure and Calculations

1 Add 0.5 mL of Bradford protein reagent into a spectrophotometer cuvette.

2 Add 0.5 mL of DOM sample, standard, or blank.

3 Mix well and let stand for 5 min at room temperature.

4 Read absorbance at 620 nm against blank.

5 Prepare calibration curve and calculate protein concentration in mg L^{-1} BSA equivalent.

Comments

Determination of proteins in aqueous samples is recommended only when samples are fresh. Upon storage, protein concentration seems to decrease rapidly. The method allows for detection of protein concentrations as small as 1 mg L^{-1} BSA equivalent.

48.3.9 Assessment of Biodegradability

Dissolved organic matter represents a potential source of energy and nutrients (especially N and P) to the soil microflora. Microbial consumption of DOM can regulate the production of greenhouse gases such as CH_4 and N_2O both by reducing the O_2 content of soils and by providing the electrons required for methanogenesis and denitrification (Yavitt 1997; Zsolnay 1997; Lu et al. 2000). Furthermore, knowledge about the biodegradability of DOM is also crucial to assessing its contribution to soil organic matter buildup (Kalbitz et al. 2003). The biodegradation of DOM is defined by the metabolic breakdown of these organic compounds by soil microorganisms; it is assessed either by the disappearance rate of DOM, the consumption rate of O_2, or the evolution rate of CO_2 during incubation assays (Marschner and Kalbitz 2003).

Materials and Reagents

1 Teflon, glass, or polypropylene flasks (50 mL) for the incubation

2 Soil inoculum (obtained by shaking a fresh soil sample with 5 m*M* $CaCl_2$ solution for 30 min in a 50 mL polypropylene tube, and filtering at 5 μm)

3 1 g L^{-1} NH_4NO_3 and 1 g L^{-1} K_2HPO_4 aqueous solutions

4 DOM samples

5 Glass vacuum filter holder or stainless steel pressure filtration unit

6 0.4 μm polycarbonate filter that fits the filter holder

7 5 μm polycarbonate filter that fits the filter holder to filter the inoculum

8 125 mL Erlenmeyer flask to support the filter holder (with sidearm if a vacuum filter unit is used)

9 Vacuum pump or other vacuum/pressure system

Procedures and Calculations

1 Transfer/pipette 15 mL of DOM sample (diluted to a C concentration of 10 to 30 mg C L^{-1}) in a Teflon, glass, or polypropylene flask and add 3 mL of each of the NH_4NO_3 and K_2HPO_4 solutions. Prepare all tested DOM samples at least in triplicates.

2 Prepare the microbial inoculum and filter through a 5 μm filter to remove large particles and grazers.

3 Add 150 μL of the inoculum and incubate the capped flasks in the dark at room temperature for 7 days.

4 Two different controls should be prepared: ultrapure water with nutrients and the inoculum can be used to quantify the DOC coming from the inoculum. A second control using a glucose solution instead of the DOM sample is useful to verify the functioning of the inoculum; in this test more than 50% of the glucose-C should be degraded within 7 days.

5 Determine the organic C concentration (see Section 48.3.1) of the filtered (0.4 μm) samples before and after the 7-day incubation. The difference represents the amount of biodegradable DOC.

Comments

1 Since the purpose of this method is to assess readily biodegradable DOM, longer incubation periods will result in larger net removal of organic C from solution (or greater mineralization) and thus give higher estimates of biodegradability (McDowell et al. 2006).

2 Addition of nutrients is recommended because nutrient deficiency may limit the degradation of DOM and result in underestimation of its true biodegradability (McDowell et al. 2006).

3 Comparison of different methods suggests that adding soil inoculum derived from the same soil where DOM samples are obtained is not necessary (McDowell et al. 2006).

4 Size of the incubation vessel should be chosen to avoid oxygen deficiency; the ratio of liquid to headspace volume during the incubation trial should be about 1 or lower.

5 In addition to short-term batch incubations for measurement of biodegradable DOC, McDowell et al. (2006) suggested 42-day incubations with regular monitoring of headspace CO_2 concentrations, conducted at room temperature with an inoculum and nutrients added. Regular monitoring of headspace CO_2 concentration offers additional information by providing biodegradability estimates of both the labile and refractory portions of DOC, which is useful for modeling the fate of DOC in soils.

REFERENCES

Appel, T. and Mengel, K. 1993. Nitrogen fractions in sandy soils in relation to plant nitrogen uptake and organic matter incorporation. *Soil Biol. Biochem.* 25: 685–691.

Box, J.D. 1983. Investigation of Folin–Ciocalteu phenol reagent for the determination of polyphenolic substances in natural waters. *Water Res.* 17: 511–525.

Brink, Jr. R.H., Dubach, P., and Lynch, D.L. 1960. Measurement of carbohydrates in soil hydrolyzates with anthrone. *Soil Sci.* 89: 157–166.

Burford, J.R. and Bremner, J.M. 1975. Relationships between denitrification capacities of soils and total water soluble and readily decomposable soil organic matter. *Soil Biol. Biochem.* 7: 389–394.

Cabrera, M.L. and Beare, M.H. 1993. Alkaline persulfate oxidation for determining total nitrogen in microbial biomass extracts. *Soil Sci. Soc. Am. J.* 57: 1007–1012.

Chantigny, M.H. 2003. Dissolved and water-extractable organic matter in soils: a review on the influence of land use and management practices. *Geoderma* 113: 357–380.

Chantigny, M.H., Angers, D.A., Prévost, D., Simard, R.R., and Chalifour, F.-P. 1999. Dynamics of soluble organic C and C mineralization in cultivated soils with varying N fertilization. *Soil Biol. Biochem.* 31: 543–550.

Chapman, P.J., Edwards, A.C., and Shand, C.A. 1997a. The phosphorus composition of soil solutions and soil leachates: influence of soil:solution ratio. *Eur. J. Soil Sci.* 48: 703–710.

Chapman, P.J., Shand, C.A., Edwards, A.C., and Smith, S. 1997b. Effect of storage and sieving on the phosphorus composition of soil solution. *Soil Sci. Soc. Am. J.* 61: 315–321.

Chin, Y.-P., Aiken, G., and O'Loughlin, E. 1994. Molecular weight, polydispersity, and spectroscopic properties of aquatic humic substances. *Environ. Sci. Technol.* 28: 1853–1858.

DeLuca, T.H. and Keeney, D.R. 1993. Soluble anthrone-reactive carbon in soils: effect of carbon and nitrogen amendments. *Soil Sci. Soc. Am. J.* 57: 1296–1300.

Dilling, J. and Kaiser, K. 2002. A rapid method for the estimation of fractions of dissolved organic matter in water samples using UV photometry. *Water Res.* 36: 5037–5044.

Grandy, A.S., Erich, M.S., and Porter, G.A. 2000. Suitability of the anthrone–sulfuric acid reagent for determining water soluble carbohydrates in soil water extracts. *Soil Biol. Biochem.* 32: 725–727.

Gregorich, E.G., Rochette, P., McGuire, S., Liang, B.C., and Lessard, R. 1998. Soluble organic carbon and carbon dioxide fluxes in maize fields receiving spring-applied manure. *J. Environ. Qual.* 27: 209–214.

Guggenberger, G. and Kaiser, K. 2003. Dissolved organic matter in soil: challenging the paradigm of sorptive preservation. *Geoderma* 113: 293–310.

Guggenberger, G., Kögel-Knabner, I., Haumaier, L., and Zech, W. 1989. Gel permeation chromatography of water-soluble organic matter with deionized water as eluent. II. Spectroscopic and chemical characterization of fractions obtained from an aqueous litter extract. *Sci. Tot. Environ.* 81–82: 447–457.

Guggenberger, G. and Zech, W. 1992. Sorption of dissolved organic carbon by ceramic P-80 suction cups. *J. Plant Nutr. Soil Sci.* 155: 151–155.

Hagedorn, F., Blaser, P., and Siegwolf, R. 2002. Elevated atmospheric CO_2 and increased N deposition effects on dissolved organic carbon–clues from delta C-13 signature. *Soil Biol. Biochem.* 34: 355–366.

Hagedorn, F., Saurer, M., and Blaser, P. 2004. A C-13 tracer study to identify the origin of dissolved organic carbon in forested mineral soils. *Eur. J. Soil Sci.* 55: 91–100.

Hagedorn, F. and Schleppi, P. 2000. Determination of total dissolved nitrogen by persulfate oxidation. *J. Plant Nutr. Soil Sci.* 163: 81–82.

Heinrichs, H., Böttcher, G., Brumsack, H.-J., and Pohlmann, M. 1996. Squeezed soil-pore solutes—a comparison to lysimeter samples and percolation experiments. *Water Air Soil Poll.* 89: 189–204.

Herbert, B.E. and Bertsch, P.M. 1995. Characterization of dissolved and colloidal organic matter in soil solution: a review. In W.W. McFee and J.M. Kelly, Eds. *Carbon Forms and Functions in Forest Soils*. Soil Science Society of America, Madison, WI, pp. 63–88.

Jones, D.L. and Edwards, A.C. 1993. Evaluation of polysulfon hollow fibres and ceramic suction samplers as devices for the *in situ* extraction of soil solution. *Plant Soil* 150: 157–165.

Jones, D.L. and Kjelland, K. 2002. Soil amino acid turnover dominates the nitrogen flux in permafrost-dominated taiga forest soils. *Soil Biol. Biochem.* 34: 209–219.

Jones, D.L., Owen, A.G., and Farrar, J.F. 2002. Simple method to enable the high resolution determination of total free amino acids in soil solutions and soil extracts. *Soil Biol. Biochem.* 34: 1893–1902.

Kaiser, K., Kaupenjohann, M., and Zech, W. 2001. Sorption of dissolved organic carbon in soils: effects of soil sample storage, soil-to-solution ratio, and temperature. *Geoderma* 99: 317–328.

Kalbitz, K., Schmerwitz, J., Schwesig, D., and Matzner, E. 2003. Biodegradation of soil-derived dissolved organic matter as related to its properties. *Geoderma* 113: 273–291.

Kalbitz, K., Solinger, S., Park, J.-H., Michalzik, B., and Matzner, E. 2000. Controls on the dynamics of dissolved organic matter in soils: a review. *Soil Sci.* 165: 277–304.

Kawahigashi, M., Sumida, H., and Yamamoto, K. 2003. Seasonal changes in organic compounds in soil solutions obtained from volcanic ash soils under different land uses. *Geoderma* 113: 381–396.

Korshin, G.V., Li, C.-W., and Benjamin, M.M. 1997. Monitoring the properties of natural organic matter through UV spectroscopy: a consistent theory. *Water Res.* 31: 1787–1795.

Kuiters, A.T. and Denneman, C.A.J. 1987. Water-soluble phenolic substances in soils under several coniferous and deciduous tree species. *Soil Biol. Biochem.* 19: 765–769.

Lemke, R.L., Izaurralde, R.C., and Nyborg, M. 1998. Seasonal distribution of nitrous oxide emissions from soils in the Parkland region. *Soil Sci. Soc. Am. J.* 62: 1320–1326.

Liang, B.C., MacKenzie, A.F., Schnitzer, M., Monreal, C.M., Voroney, P.R., and Beyaert, R.P. 1998. Management-induced change in labile soil organic matter under continuous corn in eastern Canadian soils. *Biol. Fert. Soils* 26: 88–94.

Lu, Y.H., Wassmann, R., Neue, H.U., and Huang, C.Y. 2000. Dynamics of dissolved organic carbon and methane emissions in a flooded rice soil. *Soil Sci. Soc. Am. J.* 64: 2011–2017.

Ludwig, B., Meiwes, K.J., Khanna, P., Gehlen, R., Fortmann, H., and Hildebrand, E.E. 1999. Comparison of different laboratory methods with lysimetry for soil solution composition—experimental and model results. *J. Plant Nutr. Soil Sci.* 162: 343–351.

Marques, R., Ranger, J., Gelhaye, D., Pollier, B., Ponette, Q., and Goedert, O. 1996. Comparison of chemical composition of soil solutions collected by zero-tension plate lysimeters with those from ceramic-cup lysimeters in a forest soil. *Eur. J. Soil Sci*. 47: 407–417.

Marschner, B. and Kalbitz, K. 2003. Controls on bioavailability and biodegradability of dissolved organic matter in soils. *Geoderma* 113: 211–235.

McDowell, W.H., Zsolnay, A., Aitkenhead-Peterson, J.A., Gregorich, E.G., Jones, D.L., Jödemann, D., Kalbitz, K., Marschner, B., and Schwesig, D. 2006. A comparison of methods to determine the biodegradable dissolved organic matter (DOM) from different terrestrial sources. *Soil Biol. Biochem*. 38: 1933–1942.

McGill, W.B., Cannon, K.R., Robertson, J.A., and Cook, F.D. 1986. Dynamics of soil microbial biomass and water-soluble organic C in Breton L after 50 years of cropping to rotations. *Can. J. Soil Sci*. 66: 1–19.

Mejbaum, W. 1939. Über die Bestimmung kleiner Pentosemengen, insbesondere.in Derivaten der Adenylsäure. *Zeitschrift für Physiologische Chemie* 258: 117–120.

Michalzik, B., Kalbitz, K., Park, J.-H., Solinger, S., and Matzner, E. 2001. Fluxes and concentrations of dissolved organic carbon and nitrogen—a synthesis for temperate forests. *Biogeochemistry* 52: 173–205.

Moore, S. and Stein, W.H. 1948. Photometric ninhydrin method for use in the chromatography of amino acids. *J. Biol. Chem*. 176: 367–388.

Morita, M. 1980. Total phenolic content in the pyrophosphate extracts of two peat soil profiles. *Can. J. Soil Sci*. 60: 291–297.

Murphy, D.V., Macdonald, A.J., Stockdale, E.A., Goulding, K.W.T., Fortune, S., Gaunt, J.L., Poulton, P.R., Wakefield, J.A., Webster, C.P., and Wilmer, W.S. 2000. Soluble organic nitrogen in agricultural soils. *Biol. Fert. Soils* 30: 374–387.

Novak, J.M. and Bertsch, P.M. 1991. The influence of topography on the nature of humic substances in soil organic matter at a site in the Atlantic Coastal Plain of South Carolina. *Biogeochemistry* 15: 111–126.

Novak, J.M., Mills, G.L., and Bertsch, P.M. 1992. Estimating the percent aromatic carbon in soil and aquatic humic substances using ultraviolet absorbance spectrometry. *J. Environ. Qual*. 21: 144–147.

Ohno, T. and Paul, R. 1998. Assessment of the Folin and Ciocalteu method for determining soil phenolic carbon. *J. Environ. Qual*. 27: 776–782.

Raber, B., Kögel-Knabner, I., Stein, C., and Klem, D. 1998. Partitioning of polycyclic aromatic hydrocarbons to dissolved organic matter from different soils. *Chemosphere* 36: 79–97.

Siemens, J. and Kaupenjohann, M. 2003. Dissolved organic carbon is released from sealings and glues of pore-water samplers. *Soil Sci. Soc. Am. J*. 67: 795–797.

Thurman, E.M. 1985. *Organic Geochemistry of Natural Waters*. Nijhoff/Junk Publishers, Dordrecht, The Netherlands, 497 pp.

Titus, B.D. and Mahendrappa, M.K. 1996. Lysimeter system designs used in soil research: a review. *Natural Resources Canada and Canadian Forest Service, Newfoundland and Labrador Region*. Information Report N-X-301. Ottawa, ON, Canada, 113 pp.

Traina, S., Novak, J., and Smeck, N.E. 1990. An ultraviolet absorbance method of estimating the percent aromatic carbon content of humic acids. *J. Environ. Qual*. 19: 151–153.

Vance, E.D., Brookes, P.C., and Jenkinson, D.S. 1987. An extraction method for measuring soil microbial biomass C. *Soil Biol. Biochem*. 19: 703–707.

Wessel-Bothe, S., Patzold, S., Klein, C., Behre, G., and Welp, G. 2000. Sorption of pesticides and DOC on glass and ceramic suction cups. *J. Plant Nutr. Soil Sci*. 163: 53–56.

Yavitt, J.B. 1997. Methane and carbon dioxide dynamics in *Typha latifolia* (L.) wetlands in central New York State. *Wetlands* 17: 394–406.

Zsolnay, A. 1996. Dissolved humus in soil waters. In A. Piccolo, Ed. *Humic Substances in Terrestrial Ecosystems*. Elsevier, Amsterdam, The Netherlands, pp. 171–123.

Zsolnay, A. 1997. The complexity of the flux of natural substrates in soils: A freeze-thaw can increase the formation of ischemic and anaerobic microsites. In H. Insam and A. Rangger, Eds. *Microbial Communities*. Springer, Heidelberg, pp. 236–241.

Zsolnay, A. 2003. Dissolved organic matter: artefacts, definitions, and functions. *Geoderma* 113: 187–209.

Zsolnay, A., Baigar, E., Jimenez, M., Steinweg, B., and Saccomandi, F. 1999. Differentiating with fluorescence spectroscopy the sources of dissolved organic matter in soils subjected to drying. *Chemosphere* 38: 45–50.

Chapter 49
Soil Microbial Biomass C, N, P, and S

R.P. Voroney
University of Guelph
Guelph, Ontario, Canada

P.C. Brookes
Rothamsted Research
Harpenden, Hertfordshire, United Kingdom

R.P. Beyaert
Agriculture and Agri-Food Canada
London, Ontario, Canada

49.1 INTRODUCTION

Soil microbial biomass measurements have been used in studies of soil organic matter dynamics and nutrient cycling in a variety of terrestrial ecosystems. They provide a measure of the quantity of living microbial biomass present in the soil, and in arable soils account for ~1%–5% of the total soil organic matter (Jenkinson 1988; Smith and Paul 1990). Measurements of the carbon (C), nitrogen (N), phosphorus (P), and sulfur (S) contained in the soil microbial biomass provide a basis for studies of the formation and turnover of soil organic matter, as the microbial biomass is one of the key definable fractions (Brookes et al. 1990). The data can be used for assessing changes in soil organic matter caused by soil management (Powlson et al. 1987) and tillage practices (Spedding et al. 2004), for assessing the impact of management on soil strength and porosity, soil structure and aggregate stability (Hernández-Hernández and López-Hernández 2002), and for assessing soil N fertility status (Elliot et al. 1996).

Because it is such a sensitive indicator of changing soil conditions, the soil microbial biomass serves as an ''early warning'' of effects of stresses on the soil ecosystem, long before they are detectable by other measurements (Barajas Aceves et al. 1999). Soil microbial biomass measurements have been used for determining the effects of environmental contaminants like heavy metals (Renella at al. 2004; Barajas Aceves 2005), pesticides (Harden et al. 1993), and antibiotics (Castro et al. 2002) on the soil ecosystem, and to

monitor bioremediation of oil-contaminated soils (Plante and Voroney 1998). Linked measurements such as the CO_2 evolved per unit soil microbial biomass, i.e., biomass specific respiration rate, and the microbial biomass as a percentage of soil organic C are useful practical indicators (Barajas Aceves et al. 1999).

Jenkinson (1988) and Smith and Paul (1990), and more recently Carter et al. (1999), have reviewed the significance of soil microbial biomass measurements. There have been several reviews of methods for measurement of the microbial biomass (Horwath and Paul 1994; Joergensen and Brookes 2005).

A wide range of techniques has been used to, directly or indirectly, quantify the size of the microbial biomass in soil. These include direct microscopic counts of soil organisms and conversion to biomass from estimates of organism biovolume, density, solids content, and carbon content (van Veen and Paul 1979); conversion of soil adenosine 5′-triphosphate (ATP) concentrations to microbial biomass (Contin et al. 2001; Dyckmans et al. 2003); arginine mineralization (Lin and Brookes 1999); anthrone reactive C (Badalucco et al. 1992); ninhydrin-reactive N (Amato and Ladd 1988; Mondini et al. 2002); and the substrate-induced respiratory response (Anderson and Domsch 1978; Graham and Haynes 2005). Microbial biomass determinations were first based on measuring the CO_2 produced as a result of chloroform ($CHCl_3$) fumigation during a subsequent 10-day incubation (Jenkinson 1966). Exposing the soil to $CHCl_3$ vapors kills all of the soil organisms by solubilizing the lipids in the cell membrane, releasing the cellular constituents into the soil. Removal of the fumigant and incubation of the fumigated soil results in a ''flush'' of decomposition by the recolonizing population, compared with an unfumigated soil, due to mineralization of these cellular constituents. This flush of CO_2 was shown to be directly proportional to the amount of microbial biomass C. The original fumigation–incubation method to measure soil biomass C (Jenkinson and Powlson 1976) and N (Voroney and Paul 1984) is considered the reference procedure against which other methods are calibrated (Ross 1990). However, it has largely been replaced by the fumigation–extraction method, where the biomass constituents released by $CHCl_3$ fumigation are extracted and analyzed directly to reduce the time required to complete the technique. In this chapter, the fumigation–extraction methods for measurements of soil microbial biomass C, N, P, and S are described.

49.2 CHLOROFORM FUMIGATION–EXTRACTION METHOD

Estimation of soil microbial C, N, P, and S by fumigation–extraction methods has several advantages over the fumigation–incubation method. Besides being rapid, the fumigation–extraction method is applicable to soils of low pH (Couteaux and Henkinet 1990), and to those with recent additions of organic substrates (Vance et al. 1987). Also it avoids the requirement for microbial mineralization of the fumigant-killed biomass during a 10-day incubation period under controlled conditions (Vance et al. 1987; Amato and Ladd 1988; Gallardo and Schlesinger 1990). Therefore, the method can be applied to soils of low initial water content, provided the soils are wetted to between -5 and -10 kPa moisture potential during the fumigation stage (Sparling et al. 1990), and to waterlogged soils or paddy soils (Inubushi et al. 1991). Diaz-Raviña et al. (1992) have used the method in soils heated to 600°C. However, the main advantage is that fumigation–extraction permits microbial biomass measurements in soils with recently added and freshly decomposing substrates (Ocio and Brookes 1990a), and it is ideal for use in conjunction with isotopically labeled substrates (Wu and Brookes 2005).

49.3 MICROBIAL BIOMASS C AND N

Microbial biomass C and N are calculated from the difference between the amount of total C and N extracted from fresh soil fumigated with $CHCl_3$ and the amount extracted from the unfumigated control soil. The total C and N released by $CHCl_3$ fumigation and present in the unfumigated soil are extracted with 0.5 *M* K_2SO_4 and subsequently analyzed (Sparling and West 1988a). The microbial biomass C and N are calculated using an equation relating the increased release of C and N as a result of $CHCl_3$ fumigation and a factor representing the fraction of biomass C and N extracted by K_2SO_4.

49.3.1 Materials and Reagents

Most of the reagents used, except where noted, are readily obtainable and are certified analytical grade. Deionized water (Type 1) should be used throughout for the preparation of the reagent solutions.

1 Ethanol-free $CHCl_3$. See Comment 1 in Section 49.6 for details outlining the purification of reagent grade $CHCl_3$.

2 Large desiccator. The desiccator should be inert to $CHCl_3$ vapor, be of a dry-seal type, and be able to withstand a high vacuum without implosion; a thick-walled glass vacuum desiccator is suitable. A large desiccator may hold about 25 samples simultaneously.

3 0.5 *M* K_2SO_4 extraction solution. To prepare 10 L of extractant, slowly add 871.3 g K_2SO_4 (reagent grade) to about 9.5 L water. Stir the solution on a magnetic stirrer until the K_2SO_4 has dissolved completely (~2 h); adjust the final volume to 10 L with water after the solution has reached room temperature.

4 Miscellaneous materials and reagents:

   a. Fumehood

   b. Boiling chips

   c. 100 mL glass containers with lids

   d. Aluminum-weighing containers for the determination of soil water content

   e. Glass fiber filter papers (Whatman® GF 934-AH)

   f. 50 mL vials per assay for filtrate

49.3.2 Soil Preparation

1 For the standard method, measurements are usually made on sieved soil (<2 mm) that has been preincubated, at 25°C and 40%–50% water holding capacity for several days, to permit soil metabolism and moisture to stabilize

(e.g., Vance et al. 1987). If this is not practical, the soil may be divided into small (<1 cm) pieces and mixed thoroughly prior to fumigation (Ocio and Brookes 1990b), however, it is necessary to use larger soil weights (ca 250 g) than in the standard method. In soils containing large amounts of fresh plant residues and living roots, these must be removed by hand picking or sieving (Mueller et al. 1992).

2 Weigh out three portions of the moist soil, ~15 g, into a weighing container for soil water content determination. Dry soil in the weighing container in an oven at 105°C for at least 24 h or until a constant oven-dry weight is achieved. Cool in a desiccator, reweigh, and determine the water content of the soil sample. All microbial biomass results should be expressed on an oven-dry weight basis.

3 Weigh out six portions of moist soil, 25–50 g each (standard method), into 100 mL glass bottles. This provides (i) three replicates of the soil to be fumigated with $CHCl_3$ vapor for 24 h and then extracted and (ii) three replicates of the unfumigated soil that are extracted immediately.

49.3.3 Fumigation Treatment

Caution: Procedures releasing $CHCl_3$ fumes should be conducted in a fumehood

1 Desiccators should be lined with freshly moistened paper towels. For the fumigation treatment, place the glass sample bottles containing the soil into a desiccator together with a 100 mL beaker containing 50 mL $CHCl_3$ and a few boiling chips. Seal and evacuate the desiccator, taking care to vent the fumes released by the vacuum pump until the $CHCl_3$ boils vigorously and continue evacuating for 1–2 min. Seal the desiccator under vacuum and place it in the dark at room temperature (20°C–25°C) for 24 h.

2 After the 24 h fumigation, release the vacuum, open the desiccator, and remove the beaker of $CHCl_3$ and moistened paper towels. (The waste $CHCl_3$ should be kept in a sealed bottle and disposed as a hazardous waste; the paper towels should be placed in sealed bags and disposed in the regular waste stream.)

3 Remove residual $CHCl_3$ vapor from the soil samples by repeated evacuations, usually three to six times for ~5 min using a water aspirator pump, followed by a two-stage rotary oil pump capable of drawing a vacuum of 10^{-5} kPa, 15–20 min evacuation.

49.3.4 Extraction of Microbial Biomass C and N

1 Add 0.5 *M* K_2SO_4 to the bottles containing the unfumigated control and fumigated samples using the equivalent oven-dry soil weight (g):extractant volume (mL) ratio of 1:2 to 1:5 (Joergensen and Olfs 1998).

2 Cap the jars and place on a shaker (oscillating or rotary) for 1 h. After shaking, filter the soil suspension through Whatman GF 934-AH filter paper. Measurements of organic C and total N can require from 5 to 20 mL of extract depending on the methods of analysis used. Cap and store the filtrate at 4°C for not more than 2 to 3 days, otherwise, freeze until ready for analysis. Upon thawing of frozen K_2SO_4

soil extracts, a white precipitate of $CaSO_4$ occurs in near-neutral or alkaline soils. However, this causes no analytical problems in either method and may be safely ignored (Joergensen and Olfs 1998).

49.3.5 Determination of Extracted C and N

1 Organic C dissolved in the soil extracts can be measured using automated combustion or wet oxidation procedures. However, the preferred method to quantify C in the extracts utilizes high-temperature total C analyzers. These oxidize C in the extracts to CO_2 after removing inorganic C from the sample and determine the concentration of CO_2 generated with an infrared detector. Quantification of C in the extracts can also be determined by UV-catalyzed wet oxidation followed by detection of the CO_2 generated with an infrared detector. Alternatively, C in the extracts can be determined colorimetrically. The determination involves a pretreatment to remove inorganic C by entraining the acidified sample with a high velocity stream of N- or C-free air to purge carbonate-derived CO_2. The sample is then mixed with 0.5 *M* H_2SO_4 and 4% (w/v) potassium persulfate and subjected to UV radiation. The resultant CO_2 generated from the organic C present in the sample is then dialyzed through a silicone rubber membrane and reacted with a weakly buffered phenolphthalein indicator. The decrease in the intensity of the color of the indicator measured at 550 nm is proportional to the organic C content. Standard solutions ranging in concentration from 0 to 150 μg C mL^{-1} are prepared by dilution of a stock potassium biphthalate solution containing 1000 mg C.

2 Organic N in the soil extracts can be determined with the method outlined by Cabrera and Beare (1993). In this procedure, dissolved organic N and NH_4^+ are oxidized to NO_3^- by persulfate. The oxidation can be conveniently run in an autoclave with screw-cap tubes and yields a nontoxic salt solution in which the NO_3^- concentration can be determined using a colorimetric technique involving the Griess–Ilosvay reaction after Cd reduction. Details of the oxidation procedure are provided in Chapter 48 (Section 48.3.2), and details of the measurement of the NO_3^- and NO_2^- concentrations in the extract are provided in Chapter 6.

49.3.6 Calculation of Microbial Biomass C and N

1 Soil water content, expressed on an oven-dry basis (WS):

$$\text{WS (\%)} = [[\text{soil wet weight (g)} - \text{soil dry weight (g)}]/\text{soil dry weight (g)}] \times 100 \quad (49.1)$$

2 Weight of soil sample (oven-dry weight equivalent) taken for microbial biomass measurements (MS):

$$\text{MS (g)} = \text{soil wet weight (g)} \times 100/(100 + \text{WS (\%)}) \quad (49.2)$$

3 Total volume of solution in the extracted soil (VS):

$$\text{VS (mL)} = [(\text{soil wet weight (g)} - \text{soil dry weight (g)})/1\text{g mL}^{-1}] + \text{extractant volume (mL)} \quad (49.3)$$

4 Total weight of extractable C in the fumigated (C_F) and unfumigated (C_{UF}) soil samples:

$$C_F,\ C_{UF}\ (\mu g\ g^{-1}\ soil) = \text{organic C}\ (\mu g/mL) \times [VS\ (mL)/MS\ (g)] \quad (49.4)$$

5 Total weight of extractable N in the fumigated (N_F) and unfumigated (N_{UF}) soil samples:

$$N_F,\ N_{UF}\ (\mu g\ g^{-1} soil) = \text{total N}\ (\mu g/mL) \times [VS\ (mL)/MS\ (g)] \quad (49.5)$$

6 Microbial biomass C in the soil (MB-C):

$$\text{MB-C}\ (\mu g\ g^{-1}\ soil) = (C_F - C_{UF})/k_{EC} \quad (49.6)$$

where $k_{EC} = 0.35$ and represents the efficiency of extraction of microbial biomass C. Values for k_{EC} range from 0.25 to 0.45 (Wu et al. 1990; Joergensen 1996).

7 Microbial biomass N in the soil (MB-N):

$$\text{MB-N}\ (\mu g\ g^{-1}\ soil) = (N_F - N_{UF})/k_{EN} \quad (49.7)$$

where $k_{EN} = 0.5$ and represents the efficiency of extraction of microbial biomass N. Values for k_{EN} range from 0.18 to 0.54 (Joergensen and Mueller 1996).

49.4 MICROBIAL BIOMASS P

Microbial biomass P is calculated from the difference between amounts of inorganic P (P_i) extracted from fresh soil fumigated with $CHCl_3$ and the amount extracted from unfumigated soil (Brookes et al. 1982; Hedley and Stewart 1982). Most of the P released is inorganic (i.e., orthophosphate-P_i). The extractant is 0.5 *M* $NaHCO_3$ (pH 8.5). For acidic soils, Wu et al. (2000) recommended the use of Bray-1 reagent (0.03 *M* NH_4F–0.025 *M* HCl), while Kouno et al. (1995) demonstrated that an anion exchange membrane technique could be used for biomass P measurements in acidic soils and soils of high P retention capacity. Some of the P_i released following fumigation is sorbed to soil colloids, so it is necessary to determine the recovery efficiency for each soil. Recovery efficiency is obtained by spiking a known quantity of P_i to the soil during extraction and measurement of the P_i recovered. The microbial biomass P is calculated by an equation relating the increased release of P_i as a result of $CHCl_3$ fumigation and the fraction of killed biomass P_i extracted by $NaHCO_3$, corrected for the recovery efficiency of the procedure.

49.4.1 Materials and Reagents

1 Ethanol-free $CHCl_3$. See Comment 1 in Section 49.6 for details outlining the purification of reagent grade $CHCl_3$.

2 Large desiccator. The desiccator should be inert to $CHCl_3$ vapor, be of a dry-seal type, and be able to withstand a high vacuum without implosion; a thick-walled glass vacuum desiccator is suitable. A large desiccator may hold about 25 samples simultaneously.

3 0.5 *M* $NaHCO_3$ at pH 8.5 extraction solution (Olsen et al. 1954). To prepare 10 L of the extractant, weigh 420 g $NaHCO_3$ into about 9 L water, add 7.2 g NaOH pellets, adjust the pH to 8.5 with 10 *M* NaOH (or conc. H_2SO_4) if necessary, and then adjust to 10 L with water. Extreme accuracy of reagent concentrations is not required, however, the precise pH of the extractant is critical.

4 250 μg P_i mL^{-1} spiking solution. To prepare 1 L of the spiking solution, dissolve 1.098 g KH_2PO_4 in 900 mL water in a 1 L volumetric flask and bring to volume.

5 Miscellaneous materials and reagents:

a. Fumehood

b. Boiling chips

c. 250 mL glass conical flasks with stoppers or caps

d. Aluminum-weighing containers for determination of soil water content

e. Whatman 42 filter paper

f. 50 mL vials per assay for filtrate

49.4.2 Soil Preparation

1 Sieve and mix soil as described in Section 49.3.2.

2 Weigh and dry soil to determine soil moisture content as described in Section 49.3.2.

3 Weigh out nine portions of moist soil, each containing ~10 g soil (oven-dry basis), into 250 mL conical flasks. This provides (i) three replicates of the soil to be fumigated with $CHCl_3$ vapor for 24 h and then extracted, (ii) three replicates of the unfumigated soil to be kept for 24 h in a sealed desiccator containing water and soda-lime and then extracted, and (iii) three replicates of the unfumigated soil to be kept for 24 h in a sealed desiccator containing water and soda-lime and then extracted with the extractant spiked with P_i.

49.4.3 Fumigation Treatment

1 Fumigation procedures are described in Section 49.3.3.

49.4.4 Extraction of Microbial Biomass P

1 Add 200 mL of the extractant +1 mL water to each of the flasks containing the unfumigated control and fumigated samples, using the equivalent oven-dry soil weight (g):extractant volume (mL) ratio of 1:2 to 1:5.

2 Add 200 mL of the extractant +1 mL of spiking solution to each of the three replicate flasks containing the unfumigated samples to be extracted with spiked extractant using the same soil:extractant ratio as described above.

3 Set of three extractant blanks is included for each full run. The mixtures are shaken at 20°C for 30 min on an orbital shaker (150 rev min^{-1}), then filtered through Whatman 42 filter paper into acid-washed plastic bottles.

49.4.5 Determination of Extracted P

The increase in P_i due to $CHCl_3$ fumigation is used to estimate microbial biomass P. Determination of the P_i present in the soil extracts is measured by the method of Murphy and Riley (1962). Briefly, ammonium molybdate and antimony potassium tartrate react in an acidic environment with phosphate to form an antimony-phospho-molybdate complex. Ascorbic acid is then used to reduce this complex to an intensely blue-colored complex. The absorbance determined at a wavelength of 712 nm is proportional to the phosphate concentration present in the sample over a defined range. A detailed description of the procedure is provided in Chapter 25 (Section 25.4.5).

49.4.6 Calculation of Microbial Biomass P

1 Soil water content (WS) is determined by Equation 49.1.

2 Mass of dry soil (MS) is determined by Equation 49.2.

3 Total volume of solution in the extracted soil (VS):

$$\begin{aligned}\text{VS (mL)} = {} & [\text{soil wet weight (g)} - \text{soil dry weight (g)}/1\ \text{g mL}^{-1}] \\ & + \text{extractant volume (mL)} + 1\ \text{mL (either water or } P_i \text{ spike)}\end{aligned} \tag{49.8}$$

4 Total weight of extractable P_i in the fumigated (F) and unfumigated (UF) soil samples:

$$P_F,\ P_{UF}\ (\mu g\ g^{-1}\ \text{soil}) = P_i\ (\mu g/mL) \times [\text{VS (mL)}/\text{MS (g)}] \tag{49.9}$$

5 Total weight of extractable P_i in the P_i spiked soil samples:

$$P_i\ \text{spiked soil}\ (\mu g\ g^{-1}\ \text{soil}) = P_i\ \text{spiked soil}\ (\mu g/mL) \times [\text{VS (mL)}/\text{MS (g)}] \tag{49.10}$$

6
$$\text{MB-P}\ (\mu g\ g^{-1}\ \text{soil}) = [(P_F - P_{UF})/k_{EP}] \times (100/R) \tag{49.11}$$

where $k_{EP} = 0.40$ and represents the efficiency of extraction of microbial biomass P, and $R = 100\ [(P_i\ \text{spiked soil} - \text{soil}\ P_{UF})/P_i\ \text{spike}]$, and is the percent recovery of the P_i spike, and $P_i\ \text{spike} = 250\ \mu g\ P_i$.

49.5 MICROBIAL BIOMASS S

Microbial biomass S is calculated from the difference between the amount of total S extracted from fresh soil fumigated with $CHCl_3$ and the amount extracted from unfumigated soil (Sagger et al. 1981). Both organic and inorganic forms of S are extracted with $CaCl_2$

during the procedure and analysis requires that organic S is converted to inorganic S to determine the total S extracted. The microbial biomass S is calculated by an equation relating the increased release of S as a result of $CHCl_3$ fumigation and the fraction of killed biomass S extracted by $CaCl_2$.

49.5.1 Materials and Reagents

1 Ethanol-free $CHCl_3$. See Comment 1 in Section 49.6 for details outlining the purification of reagent grade $CHCl_3$.

2 Large desiccator. The desiccator should be inert to $CHCl_3$ vapor, be of a dry-seal type, and be able to withstand a high vacuum without implosion; a thick-walled glass vacuum desiccator is suitable. A large desiccator may hold about 25 samples simultaneously.

3 0.10 *M* $CaCl_2$ extraction solution (Saggar et al. 1981). To prepare 10 L of extracting solution, add 14.7 g $CaCl_2 \cdot 2H_2O$ to about 9.5 L water. Place the solution container on a magnetic stirrer and stir until the $CaCl_2 \cdot 2H_2O$ has dissolved completely and then adjust the final volume to 10 L with water.

4 Miscellaneous materials and reagents:

a. Fumehood

b. Boiling chips

c. 100 mL glass bottles with lids

d. Aluminum-weighing containers for determination of soil water content

e. 0.45 μm Millipore filter (Millipore Corp., Bedford, MA)

f. 50 mL vials per assay for filtrate

49.5.2 Soil Preparation

1 Sieve and mix soil as described in Section 49.3.2.

2 Weigh and dry soil to determine soil moisture content as described in Section 49.3.2.

3 Weigh out six portions of moist soil, 15–50 g each, into 100 mL glass bottles. This provides (i) three replicates of the soil to be fumigated with $CHCl_3$ vapor for 24 h and then extracted and (ii) three replicates of the unfumigated soil to be extracted immediately.

49.5.3 Fumigation Treatment

1 Fumigation procedures are described in Section 49.3.3.

49.5.4 Extraction of Microbial Biomass S

1 Add 0.01 *M* $CaCl_2$ to the bottles containing the unfumigated control and fumigated samples, using the equivalent oven-dry soil weight (g):extractant volume (mL) ratio of 1:2 to 1:5 (Wu et al. 1994).

2 Cap the jars and place on a shaker (oscillating or rotary) for 1 h. After shaking, pass the soil suspension through 0.45 μm Millipore filters. Cap and store the filtrate at 4°C for not more than 2 to 3 days, otherwise freeze until ready for analysis.

49.5.5 Determination of Extracted S

The increase in total S due to $CHCl_3$ fumigation is used to estimate microbial biomass S. Determination of the total S present in the soil extracts involves two steps: (i) conversion of the various S compounds in the extract to one form and (ii) determination of the concentration of the S present. The recommended procedure is an alkaline digestion of the organic S to sulfate followed by reduction to sulfide with HI (Tabatabai and Bremner 1970). The determination of sulfide is then completed colorimetrically. Detailed descriptions of the procedures to convert organic S to sulfate and for the determination of sulfate by reduction to sulfide are given in Chapter 23.

49.5.6 Calculation of Microbial Biomass S

1 Soil water content (WS) is determined by Equation 49.1.

2 The mass of dry soil (MS) is determined by Equation 49.2.

3 Total volume of solution in the extracted soil (VS) is determined by Equation 49.3.

4 Total weight of extractable S in the fumigated (F) and unfumigated (UF) soil samples:

$$S_F,\ S_{UF}\ (\mu g\ g^{-1}\text{soil}) = \text{Total S}\ (\mu g/mL) \times [\text{VS}\ (mL)/\text{MS}\ (g)] \tag{49.12}$$

5 Microbial biomass S in the soil (MB-S):

$$\text{MB-S}\ (\mu g\ g^{-1}\text{soil}) = (S_F - S_{UF})/k_{ES} \tag{49.13}$$

where $k_{ES} = 0.35$ and represents the efficiency of extraction of microbial biomass S. Values for k_{ES} range from 0.30 to 0.35 (Wu et al. 1994).

49.6 COMMENTS

1 Reagent grade $CHCl_3$ is normally stabilized with ethanol (~1% v/v). Ethanol-free $CHCl_3$ must be used to measure microbial biomass C because ethanol cannot be completely removed from the soil after fumigation. Ethanol-stabilized $CHCl_3$ can be used if only microbial biomass N is measured (DeLuca and Keeney 1993). The purification procedure consists of double distillation of $CHCl_3$ at 55°C, followed by washing three times with 18 *M* H_2SO_4 and then five times with deionized

water (Jenkinson and Powlson 1976). Purified $CHCl_3$ is kept in a brown bottle containing anhydrous K_2CO_3 and redistilled. The purified $CHCl_3$ can be stored over anhydrous K_2CO_3 in the dark for up to 3 weeks. Though two to three times more costly, the use of amylene (2-methyl 2-butene) stabilized $CHCl_3$ (HPLC grade) simplifies the procedure, greatly reducing exposure to hazardous $CHCl_3$ fumes (Jenkinson and Powlson 1976), and gives identical results to freshly distilled $CHCl_3$ (Mueller et al. 1992).

2 Weight of soil analyzed for microbial biomass C and N can range from 200 mg (Daniel and Anderson 1992) to 200 g (Ocio and Brookes 1990b). However, to minimize sampling error and increase the precision of the determinations, it is recommended that determinations be completed on a minimum sample size equivalent to 25 g of oven-dried soil.

3 Soils, which do not readily disperse in the extracting solution, should be homogenized before shaking (Winter et al. 1994). Soil samples can be homogenized using a Brinkmann PT 10–35 tissue homogenizer equipped with a saw-tooth PT 20ST probe generator, machine power level set to 4 and homogenized for about 5–10 s.

4 Measurements of microbial biomass should be done on fresh soil samples as quickly as possible (within hours) after sampling, without subjecting the samples to changes in temperature or moisture content. If it is not possible to complete the sample analysis immediately, soil samples should be quickly frozen and kept frozen (−18°C), and then thawed just prior to analysis. However, freezing soil samples may cause changes to the microbial biomass and to the extractability of nonbiomass organic matter (Winter et al. 1994). Ross (1991) has stored soil samples at 4°C with minimal change in microbial biomass.

5 Fumigation–extraction method is relatively precise; three replicate determinations on the same soil sample should be able to detect differences in microbial biomass of 5%–10% at a 0.05% level of probability.

6 Biomass P fumigation–extraction method is extremely sensitive to changes in operating conditions and unless care is taken, reproducible results will not be obtained. It is critical that the extractions be done at the same temperature, shaking speeds, and on the same shaker each time if results are to be compared between soils. It is also important to adopt a standard method of filtration. The one we recommend is to swirl the flask briskly to bring soil particles into suspension, and then to quickly pour the soil extract onto the filter paper. If a ''top up'' of the extract is required, proceed in exactly the same way. Avoid excessive evaporation during the filtration procedure.

7 Microbial biomass C and N assays can be made even more rapidly by substitution of the 24 h $CHCl_3$ fumigation procedure with the addition of liquid $CHCl_3$ to the extracting solution. The liquid $CHCl_3$, 1–2 mL, is added to suspensions of soil in extracting solution just prior to shaking. The use of liquid $CHCl_3$ is preferred for analysis of microbial biomass in substrates containing more than 20% organic matter, e.g., manures and composts. After filtration, $CHCl_3$ is expelled by bubbling CO_2-free air through the filtrate for 1–2 min. While this method greatly simplifies the method, substantially reduces assay time, and is as accurate as the

fumigation direct-extraction method, less microbial biomass is recovered in the extract ($k_{EC} = 0.18$) (Gregorich et al. 1990). This may be an important factor if microbial biomass levels are low.

8 Soil microbial biomass has an average C:N:P:S ratio of ~100:12:2:1 (Smith and Paul 1990).

We have included values of k_{EC}, k_{EN}, k_{EP}, and k_{ES} for the calculation of microbial biomass C, N, P, and S based on the increase in these elements due to $CHCl_3$ fumigation. While we are reasonably confident in the values of microbial biomass extraction efficiency proposed, it is important to appreciate that there is substantial variation in the literature for different soil organisms and across soil types. Most of the values reported in the literature have been obtained using a limited number of laboratory-grown microbial cultures (mostly bacteria) (Saggar et al. 1981; Brookes et al. 1982; Wu et al. 1994) and with *in situ* calibration techniques (Voroney and Paul 1984; Sparling and West 1988b; Bremer and van Kessel 1990). The method has also been calibrated against alternative methods to estimate microbial biomass (Joergensen 1996; Joergensen and Mueller 1996). However, until more research is done to determine extraction efficiencies for a broad range of soil microorganisms, we recommend that the k_{EC}, k_{EN}, k_{EP}, and k_{ES} values used in the microbial biomass calculations be reported in the methodology.

REFERENCES

Amato, M. and Ladd, J.N. 1988. Assay for microbial biomass based on ninhydrin reactive nitrogen in extracts of fumigated soils. *Soil Biol. Biochem.* 20: 107–114.

Anderson, J.P.E. and Domsch, K.H. 1978. A physiological method for the quantitative measurement of microbial biomass in soils. *Soil Biol. Biochem.* 10: 215–221.

Badalucco, L., Gelsomino, A., Dell 'Orco, S., Grego, S., and Nannipieri, P. 1992. Biochemical characterization of soil organic compounds extracted by 0.5 *M* K_2SO_4 before and after chloroform fumigation. *Soil Biol. Biochem.* 24: 569–578.

Barajas Aceves, M. 2005. Comparison of different microbial biomass and activity measurement methods in metal-contaminated soils. *Bioresour. Technol.* 96: 1405–1414.

Barajas Aceves, M., Grace, C., Ansorena, J., Dendooven, L., and Brookes, P.C. 1999. Soil microbial biomass and organic C in a gradient of zinc concentrations around a spoil tip mine. *Soil Biol. Biochem.* 31: 867–876.

Bremer, E. and van Kessel, C. 1990. Extractability of microbial ^{14}C and ^{15}N following addition of variable rates of labelled glucose and $(NH_4)_2SO_4$ to soil. *Soil Biol. Biochem.* 22: 707–713.

Brookes, P.C., Ocio, J.A., and Wu, J. 1990. The soil microbial biomass: its measurement, properties and role in soil nitrogen and carbon dynamics following substrate incorporation. *Soil Microorganisms* 35: 39–51.

Brookes, P.C., Powlson, D.S., and Jenkinson, D.S. 1982. Measurement of microbial biomass phosphorus in soil. *Soil Biol. Biochem.* 14: 319–329.

Cabrera, M.L. and Beare, M.H. 1993. Alkaline persulphate oxidation for determining total nitrogen in microbial biomass extracts. *Soil Sci. Soc. Am. J.* 57: 1007–1012.

Carter, M.R., Gregorich, E.G., Angers, D.A., Beare, M.H., Sparling, G.P., Wardle, D.A., and Voroney, R.P. 1999. Interpretation of microbial biomass measurements for soil quality assessment in humid temperate regions. *Can. J. Soil Sci.* 79: 507–520.

Castro, J., Sanchez-Brunete, C., Rodriguez, J.A., and Tadeo, J.L. 2002. Persistence of chlorpyrifos and endosulfan in soil. *Fres. Environ. Bull.* 11: 578–582.

Contin, M., Todd, A., and Brookes, P.C. 2001. The ATP concentration in the soil microbial biomass. *Soil Biol. Biochem.* 33: 701–704.

Couteaux, M.M. and Henkinet, R. 1990. Anomalies in microbial biomass measurements in acid organic soils using extractable carbon following chloroform fumigation. *Soil Biol. Biochem.* 22: 955–957.

Daniel, O. and Anderson, J.M. 1992. Microbial biomass and activity in contrasting soil materials after passage through the gut of the earthworm *Lumbricus rubellus* Hoffmeister. *Soil Biol. Biochem.* 24: 465–470.

DeLuca, T.H. and Keeney, D.R. 1993. Ethanol-stabilized chloroform as fumigant for estimating microbial biomass by reaction with ninhydrin. *Soil Biol. Biochem.* 25: 1297–1298.

Diaz-Raviña, M., Prueto, A., Acea, M.J., and Carballas, T. 1992. Fumigation–extraction method to estimate microbial biomass in heated soils. *Soil Biol. Biochem.* 24: 259–264.

Dyckmans, J., Chander, K., Joergensen, R.G., Priess, J., Raubuch, M., and Sehy, U. 2003. Adenylates as an estimate of microbial biomass C in different groups. *Soil Biol. Biochem.* 35: 1485–1491.

Elliot, L.F., Lynch, J.M., and Papendick, R.I. 1996. The microbial component of soil quality. In G. Stotsky and J.M.Bollag, Eds. *Soil Biochemistry*, Vol. 9. Marcel Dekker, New York, NY, pp. 1–20.

Gallardo, A. and Schlesinger, W.H. 1990. Estimating microbial biomass nitrogen using the fumigation–incubation and fumigation–extraction methods in a warm-temperate forest soil. *Soil Biol. Biochem.* 22: 927–932.

Graham, M.H. and Haynes, R.J. 2005. Catabolic diversity of soil microbial communities under sugarcane and other land uses estimated by Biolog and substrate-induced respiration methods. *Soil Biol. Biochem.* 29: 155–164.

Gregorich, E.G., Wen, G., Voroney, R.P., and Kachanoski, R.G. 1990. Calibration of a rapid chloroform extraction method for measuring soil microbial biomass C. *Soil Biol. Biochem.* 22: 1009–1011.

Harden, T., Joergensen, R.G., Meyer, B., and Wolters, V. 1993. Mineralization of straw and formation of soil microbial biomass in a soil treated with simazine and dinoterb. *Soil Biol. Biochem.* 25: 1273–1276.

Hedley, M.J. and Stewart, J.W.B. 1982. Method to measure microbial phosphate in soils. *Soil Biol. Biochem.* 14: 377–385.

Hernández-Hernández, R.M. and López-Hernández, D. 2002. Microbial biomass, mineral nitrogen and carbon content in savanna soil aggregates under conventional and no-tillage. *Soil Biol. Biochem.* 34: 1563–1570.

Horwath, W.R. and Paul, E.A. 1994. Microbial biomass. In R.W. Weaver et al., Eds. *Methods of Soil Analysis, Part 2—Microbial and Biochemical Properties*. Soil Science Society of America, Madison, WI, pp. 753–773.

Inubushi, K., Brookes, P.C., and Jenkinson, D.S. 1991. Soil microbial biomass C, N and ninhydrin-N in aerobic and anaerobic soils measured by the fumigation–extraction method. *Soil Biol. Biochem.* 23: 737–741.

Jenkinson, D.S. 1966. Studies on the decomposition of plant material in soil. II. Partial sterilization of soil and the soil biomass. *J. Soil Sci.* 17: 280–302.

Jenkinson, D.S. 1988. Determination of microbial biomass carbon and nitrogen in soil. In J.R. Wilson, Ed. *Advances in Nitrogen Cycling in Agricultural Ecosystems*. CAB International, Wallingford, UK, pp. 368–386.

Jenkinson, D.S. and Powlson, D.S. 1976. The effects of biocidal treatments on metabolism in soil—V. A method for measuring soil biomass. *Soil Biol. Biochem.* 8: 167–177.

Joergensen, R.G. 1996. The fumigation–extraction method to estimate soil microbial biomass: calibration of the k_{EC} value. *Soil Biol. Biochem.* 28: 25–31.

Joergensen, R.G. and Brookes, P.C. 2005. Quantification of soil microbial biomass by fumigation extraction. In R. Margesin and F. Shinner, Eds. *Manual of Soil Analysis*. Springer, Berlin, pp. 281–296.

Joergensen, R.G. and Mueller, T. 1996. The fumigation–extraction method to estimate soil microbial biomass: calibration of the k_{EN} value. *Soil Biol. Biochem.* 28: 33–37.

Joergensen, R.G. and Olfs, H.W. 1998. The variability between different analytical procedures and laboratories for measuring soil microbial biomass C and biomass N by the fumigation extraction method. *Z. Pflanzenernähr Bodenk.* 161: 51–58.

Kouno, K., Tuchiya, Y., and Ando, T. 1995. Measurement of soil microbial biomass phosphorus by an anion exchange membrane method. *Soil Biol. Biochem.* 27: 1353–1357.

Lin, Q. and Brookes, P.C. 1999. Arginine ammonification as a method to estimate soil microbial biomass and microbial community structure. *Soil Biol. Biochem.* 31: 1985–1997.

Mondini, C., Contin, M., Leita, L., and De Nobili, M. 2002. Response of microbial biomass to air-drying and rewetting in soils and compost. *Geoderma* 105: 111–124.

Mueller, T., Joergensen, R.G., and Meyer, B. 1992. Estimation of soil microbial biomass C in the presence of living roots by fumigation–extraction. *Soil Biol. Biochem.* 24: 179–181.

Murphy, J. and Riley, J.P. 1962. A modified single solution method for determination of phosphate in natural waters. *Anal. Chim. Acta* 27: 31–36.

Ocio, J.A. and Brookes, P.C. 1990a. An evaluation of methods for measuring the microbial biomass in soils following recent additions of wheat straw and the characterization of the biomass that develops. *Soil Biol. Biochem.* 22: 685–694.

Ocio, J.A. and Brookes, P.C. 1990b. Soil microbial biomass measurements in sieved and unsieved soil. *Soil Biol. Biochem.* 22: 999–1000.

Olsen, S.R., Cole, C.V., Watanabe, F.S., and Dean, L.A. 1954. Estimation of available phosphorus in soils by extraction with sodium bicarbonate. Circular 935, United States Department of Agriculture, Washington DC.

Plante, A.F. and Voroney, R.P. 1998. Decomposition of land applied oily food waste and associated changes in soil aggregate stability. *J. Environ. Qual.* 27: 395–402.

Powlson, D.S., Brookes, P.C., and Christensen, B.T. 1987. Measurement of soil microbial biomass provides an early indication of changes in total soil organic matter due to straw incorporation. *Soil Biol. Biochem.* 19: 159–164.

Renella, G., Mench, M., van der Lelie, D., Pietramellara, G., Ascher, J., Ceccherini, M.T., Landi, L., and Nannipieri, P. 2004. Hydrolase activity, microbial biomass and community structure in long-term Cd-contaminated soils. *Soil Biol. Biochem.* 36: 443–451.

Ross, D.J. 1990. Estimation of soil microbial C by a fumigation–extraction method: influence of seasons, soils and calibration with the fumigation–incubation procedure. *Soil Biol. Biochem.* 22: 295–300.

Ross, D.J. 1991. Microbial biomass in a stored soil: a comparison of different estimation procedures. *Soil Biol. Biochem.* 23: 1005–1007.

Saggar, S., Bettany, J.R., and Stewart, J.W.B. 1981. Measurement of microbial sulphur in soil. *Soil Biol. Biochem.* 13: 493–498.

Smith, J.L. and Paul, E.A. 1990. The significance of soil microbial biomass estimations. In J.-M. Bollag and G. Stotzky, Eds. *Soil Biochemistry*, Vol. 6. Marcel Dekker, New York, NY, pp. 357–396.

Sparling, G.P., Felthan, C.W., Reynolds, J., West, A.W., and Singleton, P. 1990. Estimation of soil microbial C by a fumigation–extraction method: use on soils of high organic matter content, and reassessment of the k_{EC}-factor. *Soil Biol. Biochem.* 22: 301–307.

Sparling, G.P. and West, A.W. 1988a. Modifications to the fumigation–extraction technique to permit simultaneous extraction and estimation of soil microbial biomass C and N. *Commun. Soil Sci. Plant Anal.* 19: 327–344.

Sparling, G.P. and West, A.W. 1988b. A direct extraction method to estimate soil microbial C: calibration *in situ* using microbial respiration and ^{14}C-labelled cells. *Soil Biol. Biochem.* 20: 337–343.

Spedding, T.A., Hamel, C., Mehuys, G.R., and Madramootoo, C.A. 2004. Soil microbial dynamics in maize-growing soil under different tillage

and residue management systems. *Soil Biol. Biochem.* 36: 499–512.

Tabatabai, M.A. and Bremner, J.M. 1970. An alkaline method for determining total sulfur in soils. *Proc. Soil Sci. Soc. Am.* 34: 62–65.

Vance, E.D., Brookes, P.C., and Jenkinson, D.S. 1987. An extraction method for measuring soil microbial biomass C. *Soil Biol. Biochem.* 19: 703–707.

van Veen, J.A. and Paul, E.A. 1979. Conversion of biovolume measurements of soil organisms grown under various moisture tensions to biomass and their nutrient content. *Appl. Environ. Microbiol.* 37: 686–692.

Voroney, R.P. and Paul, E.A. 1984. Determination of k_C and k_N *in situ* for calibration of the chloroform fumigation incubation method. *Soil Biol. Biochem.* 16: 9–14.

Winter, J.P., Zhang, Z., Tenuta, M., and Voroney, R.P. 1994. Measurement of microbial biomass by fumigation extraction in soil stored frozen. *Soil Sci. Soc. Am. J.* 58: 1645–1651.

Wu, J. and Brookes, P.C. 2005. The proportional mineralization of microbial biomass and organic matter caused by air-drying and rewetting of a grassland soil. *Soil Biol. Biochem.* 37: 507–515.

Wu, J., He, Z.L., Wei, W.X., O'Donnell, A.G., and Syers J.K. 2000. Quantifying microbial biomass phosphorus in acid soils. *Biol. Fert. Soils.* 32: 500–507.

Wu, J., Joergensen, R.G., Pommerening, B., Chaussod, R., and Brookes, P.C. 1990. Measurement of soil microbial biomass C by fumigation–extraction—an automated procedure. *Soil Biol. Biochem.* 22: 1167–1169.

Wu, J., O'Donnell, A.G., He, Z.L., and Syers, J.K. 1994. Fumigation–extraction method for the measurement of soil microbial biomass-S. *Soil Biol. Biochem.* 26: 117–125.

Chapter 50
Carbohydrates

Martin H. Chantigny and Denis A. Angers
Agriculture and Agri-Food Canada
Quebec, Quebec, Canada

50.1 INTRODUCTION

Carbohydrates represent about 10%–15% of total soil organic carbon (Cheshire 1979) and 5%–10% of organic nitrogen (Greenfield 2001). Most carbohydrates are present in soil as complex polysaccharides composed of monomers of either plant or microbial origin (e.g., cellulose, hemicellulose, peptidoglycan, chitin) (Oades and Wagner 1971; Parsons 1981). Carbohydrates can be used by soil microflora as energy and nutrient sources (Alexander 1977; Cheshire 1979), and have been shown to play a key role in the formation and stabilization of soil aggregates (Cheshire 1979; Tisdall and Oades 1982).

Acid hydrolysis is commonly used to extract polysaccharides from soil (e.g., Ivarson and Sowden 1962; Cheshire and Mundie 1966). This procedure breaks down polysaccharides into monosaccharides, which can be quantified using colorimetric methods that include reactions with anthrone (Brink et al. 1960), alkaline-ferricyanide (Cheshire 1979), phenol–sulfuric acid (Lowe 1993), or Ehrlich's reagent (Stevenson 1982a). Acid hydrolysis of the whole soil yields monosaccharides of different structures, but does not distinguish their source compounds. Chromatographic determination of individual neutral sugars has been used to evaluate the relative contribution of plant and microbes to soil carbohydrates (Oades and Wagner 1971; Puget et al. 1999; Chantigny et al. 2000).

Amino sugars are mostly derived from soil microbes (Parsons 1981; Stevenson 1982b), and their chromatographic quantification has been proposed to evaluate the relative abundance of bacteria and fungi in soils (Zelles 1988) with the knowledge that they are present in both the living and necrotic biomasses (Parsons 1981; Amelung 2001). The most common amino sugars occurring in soils are glucosamine, galactosamine, mannosamine, and muramic acid. Muramic acid is exclusively of bacterial origin, whereas chitin produced by fungi is a dominant source of glucosamine in soil (Parsons 1981; Amelung 2001). Therefore, glucosamine and muramic acid have been used as indicators of the relative contributions of fungi and bacteria to soil organic matter accumulation, and aggregate formation and stabilization (Chantigny et al. 1997; Guggenberger et al. 1999; Six et al. 2001).

Individual monosaccharides can be quantified by gas chromatography (Oades et al. 1970; Benzing-Purdie 1981; Zhang and Amelung 1996). Although highly sensitive and specific, gas chromatography is time-consuming and requires complex derivatization procedures to transform the hydrolyzed monomers into volatile components. High-performance liquid chromatography (HPLC) can also be used to quantify monosaccharides and is less time-consuming (Angers et al. 1988; Zelles 1988). Recent developments have improved the sensitivity and specificity of HPLC methods (Martens and Frankenberger 1991; Appuhn et al. 2004). In this chapter, acid hydrolysis procedures to extract soil carbohydrates and two chromatographic methods to quantify individual neutral and amino sugars are presented.

50.2 EXTRACTION OF NEUTRAL SUGARS

Sulfuric acid has been widely used to hydrolyze soil polysaccharides (e.g., Ivarson and Sowden 1962; Cheshire and Mundie 1966). Sugars are found in a variety of polymers which differ in their resistance to acid hydrolysis (Oades et al. 1970; Chantigny et al. 2000). Hot water (Haynes and Francis 1993; Puget et al. 1999) and 0.5 *M* H_2SO_4 (Lowe 1993; Puget et al. 1999) have been proposed to extract the most labile fractions of soil polysaccharides. The use of 2.5 *M* H_2SO_4 has been suggested to hydrolyze most of the noncellulosic polysaccharides (Oades et al. 1970), whereas presoaking in 12 *M* H_2SO_4 followed by hot hydrolysis in 0.5 *M* H_2SO_4 has been used to hydrolyze cellulosic materials (Ivarson and Sowden 1962; Lowe 1993; Puget et al. 1999). A proximate polysaccharide fractionation based on acid resistance can thus be achieved using a series of acid hydrolysis of increasing strength (Chantigny et al. 2000).

50.2.1 Materials and Reagents

1. 12 *M* H_2SO_4. This solution is prepared by slowly adding 667 mL of concentrated H_2SO_4 (96% w/w, reagent grade) to 300 mL of deionized water in a 1 L volumetric flask. Let the solution cool to room temperature and bring to 1 L with deionized water.

2. 2.5 *M* H_2SO_4. This solution is prepared by slowly adding 139 mL of concentrated H_2SO_4 to 850 mL of deionized water in a 1 L volumetric flask. Let the solution cool to room temperature and bring to 1 L with deionized water.

3. 0.5 *M* H_2SO_4. This solution is prepared by diluting 28 mL of concentrated H_2SO_4 in 950 mL of deionized water in a 1 L volumetric flask. Let the solution cool to room temperature and then dilute to 1 L with deionized water.

4. Deionized water.

5. Oven, vortex, centrifuge, glass rod.

6. 50 mL polypropylene centrifuge tubes, with screw caps.

7. 250 mL polypropylene centrifuge bottles, with screw caps.

8. Plastic vials of the appropriate volume for sample storage.

50.2.2 Procedures

Hot-Water Extractable Carbohydrates

1 Weigh 2 g of air-dried, finely ground (<0.15 mm) soil in a polypropylene tube. Air-drying and grinding of the soil before hydrolysis optimize carbohydrate recovery from the soil.

2 Gently add 30 mL of deionized water. Mix on a vortex.

3 Seal tubes with screw caps; incubate for 24 h in an oven set at 85°C.

4 Thoroughly mix the tubes with a vortex and then cool to room temperature.

5 Centrifuge at 16,000 *g* for 10 min.

6 In a second polypropylene tube, transfer 35 parts of the hydrolysate and add one part of concentrated H_2SO_4 (96% w/w, reagent grade).

7 Mix on a vortex and incubate again at 85°C for 24 h. Acidification (step 6) and a second incubation are required for the complete hydrolysis of di-, tri- and oligosaccharides and subsequent determination of individual monomers.

8 Repeat steps 4 and 5.

9 Transfer about 15 mL of the hydrolysate into a plastic vial and store at −20°C until analysis.

Mild-Acid Extractable Carbohydrates

Dilute acid solutions are also used to hydrolyze carbohydrates and are thought to solubilize labile polysaccharides such as microbial materials and hemicellulose. The most often used solutions are 0.5 *M* (e.g., Lowe 1993) and 2.5 *M* H_2SO_4 (e.g., Oades et al. 1970).

1 Proceed as for hot-water extractable carbohydrates, but use 30 mL of either 0.5 *M* or 2.5 *M* H_2SO_4 solution in step 2.

2 Omit steps 6 to 8 as the hydrolysis conditions are already acid.

Strong-Acid Extractable Carbohydrates (Modified from Cheshire and Mundie 1966; Oades et al. 1970)

This extraction procedure includes an initial soaking period, which is aimed at ''softening'' the crystalline forms of polysaccharides, such as cellulose and lignocellulose:

1 Weigh 2 g of air-dried, finely ground (<0.15 mm) soil into a 50 mL centrifuge tube.

2 Add 8 mL of 12 *M* H_2SO_4 and gently mix the soil and acid with a glass rod to ensure that all the soil is moistened with the acid.

3 Loosely cap the tubes and let stand on the bench for 2 h.

4 Transfer the slurry into a 250 mL polypropylene bottle by washing the tube with 184 mL of deionized water to bring the solution to 0.5 *M* H_2SO_4.

5 Seal bottles and incubate for 24 h in an oven set at 85°C.

6 Thoroughly mix the bottles on the vortex and let cool at room temperature.

7 Centrifuge at 16,000 *g* for 10 min. Transfer about 15 mL in a plastic vial and store at –20°C until analysis.

50.2.3 Comments

1 Acid hydrolysis of neutral sugars has been traditionally performed under reflux (100°C–120°C). However, several investigations have been conducted with sealed tubes. Although some authors have reported lower carbohydrate recovery with sealed tubes relative to reflux (Oades et al. 1970), a detailed direct comparison has not been made. The advantages of using sealed tubes, as compared to reflux, are that sealed tubes are easier to use and more samples can be processed.

2 Performing weak acid (0.5 *M* H_2SO_4) instead of hot-water extraction will yield more neutral sugars (Puget et al. 1999; Chantigny et al. 2000). In general, hot-water extracts have been found to be enriched in microbial sugars (mannose, galactose), originating from exopolysaccharides, which may be involved in soil aggregate stabilization (Feller et al. 1991; Haynes and Francis 1993).

3 Mild- and strong-acid extractable carbohydrates are sometimes termed ''noncellulosic'' and ''cellulosic'' carbohydrates, respectively. However, this terminology is an oversimplification, because once plant residues are incorporated into soil they are rapidly colonized and decomposed by microbes, and therefore both microbial- and plant-derived sugars appear in the extracts (Puget et al. 1999; Chantigny et al. 2000).

4 Sugars are present in soils as a complex mixture of polysaccharides with glycosidic linkages having different degrees of resistance to acid hydrolysis. Prolonged hydrolysis can result in the degradation of some carbohydrates (Martens and Loeffelmann 2002). Any acid hydrolysis procedure is a compromise between maximum release of sugars and minimal decomposition (Greenfield 2001). Where possible, sequential hydrolysis of increasing strength may be the best approach for a thorough characterization and accounting of neutral sugars. However, performing only one of the proposed procedures should prove useful in assessing changes in amounts or composition of sugars over time, or for comparative studies.

50.3 EXTRACTION OF AMINO SUGARS (MODIFIED FROM ZELLES 1988)

50.3.1 Materials and Reagents

1 Glass test tubes (25×100 mm) with Teflon-lined screw caps.

2 Multi-port bubbling system with tubing and needles to insert into the glass tubes.

3 N_2 gas to supply in the bubbling system.

4 6 *M* HCl. Prepare this solution by diluting 500 mL of concentrated HCl in 475 mL of deionized water in a 1 L volumetric flask. Allow the solution to cool to room temperature and bring to 1 L with deionized water.

5 Oven, vortex, centrifuge.

6 Plastic vials of the appropriate volume for hydrolysate storage.

50.3.2 Procedures

1 Weigh 1 g of air-dried, finely ground (<0.15 mm) soil in a glass tube. Air-drying and grinding of the soil before hydrolysis optimize the amino sugar recovery from the soil.

2 Add 20 mL of 6 *M* HCl. Thoroughly mix on a vortex.

3 Bubble the mixture with N_2 gas for 1 min to remove O_2 from the solution. Bubbling intensity must be carefully adjusted to control foaming and avoid the loss of solution.

4 Seal tubes with screw caps.

5 Incubate the tubes for 6 h in an oven set at 105°C; cool the tubes on ice to room temperature.

6 Carefully decant 10–15 mL of the hydrolysate into a plastic vial. Alternatively, the hydrolysate may be filtered through a glass fiber filter (e.g., Whatman GF/A) if suspended material is present. Store vials at −20°C until analysis.

50.3.3 Comments

Amino sugar extraction has most often been performed using 6 *M* HCl. However, as mentioned for neutral sugars, hydrolysis conditions must be aimed at maximizing amino sugar yields, while minimizing their decomposition. Though this can be performed under reflux (Greenfield 2001), hydrolysis in sealed tubes for 6 h at 105°C has been commonly used as a simple and efficient method for processing large number of samples (Amelung 2001; Appuhn et al. 2004). Bubbling N_2 through the tubes prior to heating is necessary to remove O_2 and avoid possible oxidation of amino sugars during hydrolysis (Zelles 1988).

50.4 ANALYTICAL PROCEDURES—NEUTRAL SUGARS (MODIFIED FROM MARTENS AND FRANKENBERGER 1991)

50.4.1 Materials and Reagents—Purification of Extracts

1 Strong-anion solid phase exchange (SAX) resin (3 mL Supleclean LC-SAX columns are available from Supelco, Inc., Bellefonte, PA).

2 Strong-cation solid phase exchange (SCX) resin (3 mL Supelclean LC-SCX columns are available from Supelco, Inc., Bellefonte, PA).

3 Solution of 0.5 *M* NaOH, prepared by dissolving 2 g of NaOH in 90 mL of deionized water in a 100 mL volumetric flask. Then, dilute to volume.

4 50 mL glass beakers.

5 Filter papers (Whatman #42).

6 Plastic vials of appropriate volume for storage.

7 1.5 mL Eppendorf centrifuge tubes.

50.4.2 Purification Procedures

1 Transfer 5 mL of any hydrolysate obtained in Section 50.2 in a 50 mL beaker.

2 Slowly add 0.5 *M* NaOH solution to neutralize to pH 6.5–7.0. Record the volume of NaOH solution added to correct for dilution of the hydrolysate and sugar content calculations.

3 Filter the solution (Whatman #934-AH) and collect filtrate in a plastic vial. The neutralized filtrate can be stored at −20°C until analysis.

4 Pass a sufficient volume (generally about 4 mL are sufficient for analytical purposes) of the neutralized filtrate through the SAX resin and collect the cation-purified solution in a beaker.

5 Pass the cation-purified solution through the SCX resin and collect the purified solution in a 1.5 mL Eppendorf tube; store the tubes at −20°C until analysis.

50.4.3 Comments

1 In all cases, soil hydrolysates must be purified prior to chromatographic analysis of neutral sugars to remove any interfering ionic compounds. This purification is the most time-consuming part of the process to measure soil neutral sugars. Using SCX and SAX resins to purify hydrolysates requires conditioning and cleaning of the resins between samples. The conditioning and cleaning procedures are supplied by the resin manufacturer and must be strictly followed to ensure that the columns function correctly. We found that purifying hydrolysate through SAX before SCX extended the life of the resins. When appropriately conditioned and cleaned, the LC-SAX and LC-SCX columns supplied by Supelco can be used to purify three to five samples before being discarded; purification efficiency of these columns is optimized if the hydrolysate flow rate is less than 5 mL per min.

2 Including blank samples during the extraction and purification process is advisable especially when cellulose-based filter papers are used. These filter papers may release some arabinose, xylose, and glucose, which can then be corrected for with blank samples.

50.4.4 Materials and Reagents—Analytical Procedures

1. High-performance anion exchange chromatograph with pulsed amperometry detector (HPAEC-PAD) (Model DX-500, available from Dionex, Sunnyvale, CA). This system must be equipped with a gradient pump, an electrochemical detector, and an autosampler.

2. Detector cell with disposable gold electrode.

3. CarboPac-PA10 precolumn (4×50 mm) in series with an analytical column (4 × 250 mm).

4. 10 to 50 μL injection loops. The volume of the loop to be used is reduced as sugar content increases in the samples.

5. Two eluent organizers and two 2 L eluent containers to store and deliver eluents to the system.

6. 0.5 mL PolyVials with filter caps (available from Dionex) to prepare samples for injection through the autosampler.

7. NaOH solution (50% w/w, available from Fisher Scientific).

8. Nanopure water (specific resistance of 18 MΩ). Prior to use, nanopure water is degassed by filtering (0.45 μm) under vacuum.

50.4.5 Chromatographic Conditions

1. Eluent A: 21 m*M* NaOH: Pour degassed nanopure water in a 2 L volumetric flask. Add 2.1 mL of 50% NaOH solution and dilute to volume. Immediately transfer into a 2 L eluent container and seal the container. Keep the headspace under He atmosphere to avoid carbonate formation.

2. Eluent B: 500 m*M* NaOH: Pour degassed, nanopure water in a 2 L volumetric flask. Add 52.8 mL of 50% NaOH solution and dilute to volume. Immediately transfer into a 2 L eluent container and seal the container. Keep the headspace under He atmosphere to avoid carbonate formation.

3. Set the electrochemical detector mode to ''pulsed amperometry.''

4. Set working pulse potentials (E) and durations (t) to: $E_1 = 0.1$ V, $t_1 = 300$ ms; $E_2 = 0.6$ V, $t_2 = 120$ ms; $E_3 = -0.6$ V, $t_3 = 60$ ms.

5. Transfer about 0.7 mL of the purified sample obtained in step 5 of Section 50.4.2 to a 0.5 mL PolyVial (a PolyVial has a total volume of 1 mL). After inserting the filter cap, only 0.5 mL of sample remains, and the excess sample volume (about 0.2 mL) passes through the filter cap and is wiped off before entering the vial in the autosampler.

TABLE 50.1 System Schedule for Determination of Neutral Sugars in Soil Extracts by High-Performance Anion Exchange Chromatography with Pulsed Amperometry Detection (HPAEC-PAD)

Run time (min)	Step description	Total flow rate (mL min^{-1})	% Eluent A	% Eluent B
0.0	Conditioning	1.0	0	100
13.1	Equilibration	1.0	100	0
22.0	AutoSampler ON	0.8	100	0
23.1	Sample injection	0.8	100	0
43.1	End of run	0.8	100	0

Eluent A: 21 m*M* NaOH solution; Eluent B: 500 m*M* NaOH solution. Solutions must be kept under He atmosphere to prevent carbonate formation.

6 Chromatographic schedule (isocratic analytical condition) is set as shown in Table 50.1.

Under these chromatographic conditions, seven neutral sugars can usually be identified (Figure 50.1).

50.4.6 Comments

1 High-performance liquid chromatography has been proposed to quantify neutral sugars in soil hydrolysates (Angers et al. 1988). However, HPAEC with PAD (HPAEC-PAD) has proven more sensitive and specific for several neutral sugars (Martens and Frankenberger 1991).

2 CarboPac-PA10 column is highly sensitive to the presence of carbonates and other soil contaminants, which decrease sugar retention time, especially for sugars

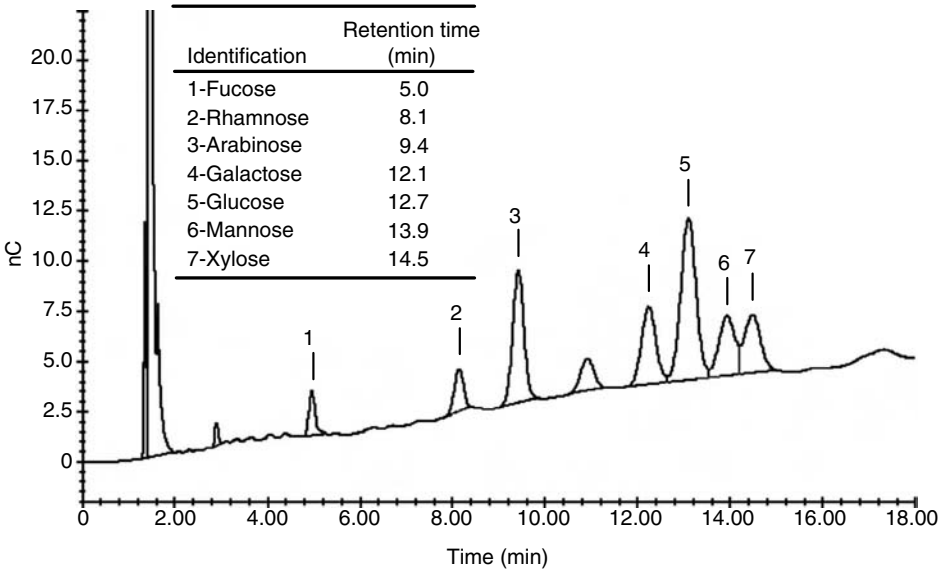

FIGURE 50.1. Typical chromatogram for neutral sugars in a soil extract measured with HPAEC-PAD.

eluting later on the chromatogram. Even though hydrolysates are purified prior to analysis, the sugar retention times will gradually decrease as the number of consecutive injections increases. To avoid identification problems, we recommend that a standard sample be injected every 5 to 10 injections. Alternatively, increasing the duration of the conditioning step (Table 50.1) will also help clean the column and maintain retention times. Renewal of eluents once a week is also advisable to avoid carbonate accumulation in the eluent containers.

50.5 ANALYTICAL PROCEDURES—AMINO SUGARS (MODIFIED FROM ZELLES 1988)

50.5.1 Materials and Reagents

1 High-performance liquid chromatograph equipped with a gradient pump, column-heating device, fluorescence detector, and a manual injection port (in our laboratory we use a HPLC manufactured by Waters Limited, Milford, MA operated under the Millenium system).

2 Analytical column: NOVA-PACK C18, 4 μ, 8 × 100 mm (Waters column #8 NVC18, 4 μ).

3 Guard column: NOVA-PACK C18 4 μ.

4 Rotary vacuum evaporator with heated water bath, and 25 mL boiling flasks.

5 Microcentrifuge to fit 1.5 mL Eppendorf centrifuge tubes.

6 0.5 *M* potassium tetraborate solution: Dissolve 30.55 g of potassium tetraborate in 200 mL of deionized water. Adjust at pH 10.0, if required, with 1 *M* NaOH. Store at room temperature in a sealed glass bottle.

7 *O*-Phthaldialdehyde (OPA) solution: Dissolve 250 mg of 99% pure OPA (available from Sigma) in 50 mL of 0.5 *M* potassium tetraborate. Store the solution at 4°C.

8 2-Mercaptoethanol.

9 Eluent A: Sodium citrate/acetate–methanol–THF. This eluent is prepared by dissolving 25.59 g of sodium citrate in 870 mL of nanopure water (specific resistance of 18 MΩ). In another beaker, dissolve 11.84 g of sodium acetate in 870 mL of nanopure water. Then mix both solutions together and adjust pH to 5.3 with glacial acetic acid. Finally, add 164 mL of methanol and 96 mL of tetrahydrofuran (THF). Mix the solution well and vacuum filter (0.45 μm) to degas the eluent. Store in amber glass bottle.

10 Eluent B: 65% methanol. Measure separately 650 mL of methanol (HPLC grade) and 350 mL of nanopure water. Vacuum filter (0.45 μm) each solution separately, then mix and store in a glass bottle.

11 Column cleaning solution: 100% methanol. Vacuum filter (0.45 μm) HPLC grade methanol and store in a glass bottle.

50.5.2 Sample Preparation and Derivatization

1 In a 25 mL boiling flask, transfer a 1 mL aliquot of the hydrolysate obtained in step 6 of Section 50.3.2, and evaporate to dryness with the rotary vacuum evaporator.

2 Add 980 μL of OPA solution and 20 μL of 2-mercaptoethanol to the flask and mix on a vortex. The derivatization period starts when mercaptoethanol is added.

3 Transfer as much material as possible in a 1.5 mL Eppendorf tube, and centrifuge at ca. 20,000 *g* for 2–3 min.

4 Collect 25 μL of supernatant with the appropriate injection syringe. Inject the sample into the HPLC when the derivatization period reaches 5 min (±15 s) and start the HPLC run. Discard the unused derivatized sample.

50.5.3 Chromatographic Conditions

1 Analytical column temperature: 40°C.

2 Detection: Fluorescence-OPA with emission wavelength set at 425 nm and excitation wavelength set at 338 nm.

3 Detector lamp type: Xenon.

4 Injection volume: 25 μL.

5 Chromatographic schedule (gradient type) (see Table 50.2).

Under these chromatographic conditions, four amino sugars can usually be identified (Figure 50.2).

Important note: The analytical column must be cleaned once a day using the following schedule:

1 Total eluting flow rate is set to 1.5 mL min^{-1}. Gradually (approximately over 2 min) increase the proportion of Eluent B from 15% to 100%. Let stand for at least 5 min.

TABLE 50.2 System Schedule for Determination of Amino Sugars in Soil Extracts by High-Performance Liquid Chromatography (HPLC)

Run time (min)	Step description	Total flow rate (mL min^{-1})	% Eluent A[a]	% Eluent B
0.0	Injection[b]	1.5	85	15
2.5	Gradient phase	1.5	85	15
17.5	Gradient phase	1.5	70	30
20.0	End of gradient	1.5	85	15
25.0	Conditioning	1.5	85	15

[a] Eluent A: sodium citrate/acetate–methanol–THF solution; Eluent B: 65% methanol in water.
[b] At 5 min ±15 s after start of the derivatization period (starts when adding 2-mercaptoethanol to the sample).

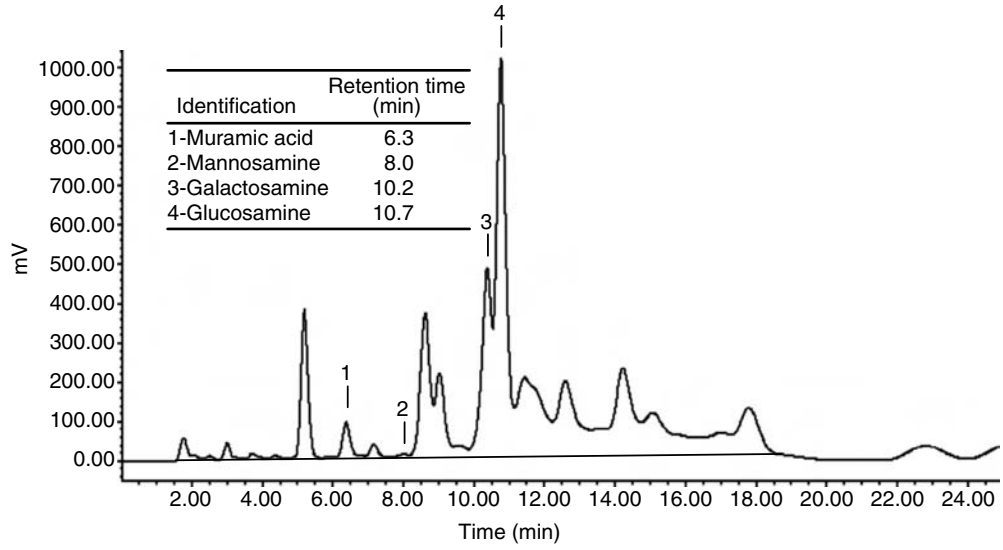

FIGURE 50.2. Typical chromatogram for amino sugars in a soil extract measured with HPLC.

2 Switch from Eluent B to the cleaning solution (100% methanol). Let stand for at least 10 min.

3 Switch back to Eluent B. Let the column equilibrate for 10 min. Gradually (approximately 2 min) increase the proportion of Eluent A back to analytical conditions. Let stand for 15 min before injecting a new sample.

50.5.4 Comments

1 Colorimetric determination of total amino sugars in soil is possible using Ehrlich's reagent (Stevenson 1982a). However, chromatographic analysis is required to determine the abundance of individual amino sugars. The analytical method proposed here was modified from the original HPLC method of Zelles (1988) and is similar to that of Appuhn et al. (2004). However, the chromatographic run of the method we propose is much shorter, does not require a thermostatic regulated autosampler, and the derivatization and injection of the sample into the chromatograph can be done manually.

2 Fluorescent complex formed between amino groups and OPA in the presence of mercaptoethanol is transient (Amelung 2001) and therefore must be the same for all samples. Appuhn et al. (2004) proposed to use an automated derivatization-injection system. However, manual injection is also acceptable provided that the time elapsed between adding the 2-mercaptoethanol to the sample and injecting the sample into chromatograph is kept constant. In our laboratory, a period of 5 min ($\pm$15 s) has been found to be suitable for obtaining a maximum and consistent fluorescence response from amino sugars.

3 Fluorescence emission varies among amino sugars with the strongest values (lowest detection limits) for muramic acid followed in decreasing order by glucosamine, galactosamine, and mannosamine (Appuhn et al. 2004).

REFERENCES

Alexander, M. 1977. *Introduction to Soil Microbiology*, 2nd ed. John Wiley & Sons, Inc., New York, NY, 467 pp.

Amelung, W. 2001. Methods using amino sugars as markers for microbial residues in soil. In R. Lal, J.M. Kimble, R.F. Follett, and B.A. Stewart, Eds. *Assessment Methods for Soil Carbon*. Lewis Publishers, Boca Raton, FL, pp. 233–272.

Angers, D.A., Nadeau, P., and Mehuys, G.R. 1988. Determination of carbohydrate composition of soil hydrolysates by high-performance liquid chromatography. *J. Chromatogr*. 45: 444–449.

Appuhn, A., Joergensen, R.G., Raubuch, M., Scheller, E., and Wilke, B. 2004. The automated determination of glucosamine, galactosamine, muramic acid, and mannosamine in soil and root hydrolysates by HPLC. *J. Plant Nutr. Soil Sci*. 167: 17–21.

Benzing-Purdie, L. 1981. Glucosamine and galactosamine distribution in a soil as determined by gas liquid chromatography in soil hydrolysates: Effect of acid strength and cations. *Soil Sci. Soc. Am. J*. 45: 66–70.

Brink, Jr. R.H., Dubach, P., and Lynch, D.L. 1960. Measurement of carbohydrates in soil hydrolysates with anthrone. *Soil Sci*. 89: 157–166.

Chantigny, M.H., Angers, D.A., and Beauchamp, C.J. 2000. Decomposition of de-inking paper sludge in agricultural soils as characterized by carbohydrate analysis. *Soil Biol. Biochem*. 32: 1561–1570.

Chantigny, M.H., Angers, D.A., Prévost, D., Vézina, L.-P., and Chalifour, F.-P. 1997. Soil aggregation and fungal and bacterial biomass under annual and perennial cropping systems. *Soil Sci. Soc. Am. J*. 61: 262–267.

Cheshire, M.V. 1979. *Nature and Origin of Carbohydrates in Soils*. Academic Press, London, 216 pp.

Cheshire, M.V. and Mundie, C.M. 1966. The hydrolytic extraction of carbohydrates from soil by sulphuric acid. *J. Soil Sci*. 17: 372–381.

Feller, C., François, C., Villemin, G., Portal, J. M., Toutain, F., and Morel, J.L. 1991. Nature des matières organiques associées aux fractions argileuses d'un sol ferrallitique. *C.R. Acad. Sci. Paris Sér*. II 312: 1491–1497.

Greenfield, L.G. 2001. The origin and nature of organic nitrogen in soil as assessed by acidic and alkaline hydrolysis. *Eur. J. Soil Sci*. 52: 575–583.

Guggenberger, G., Frey, S.D., Six, J., Paustian, K., and Elliott, E.T. 1999. Bacterial and fungal cell-wall residues in conventional and no-tillage agroecosystems. *Soil Sci. Soc. Am. J*. 63: 1188–1198.

Haynes, R.J. and Francis, G.S. 1993. Changes in microbial biomass C, soil carbohydrate composition and aggregate stability induced by growth of selected crop and forage species under field conditions. *J. Soil Sci*. 44: 665–675.

Ivarson, K.C. and Sowden, F.J. 1962. Methods for the analysis of carbohydrate material in soil: I. Colorimetric determination of uronic acids, hexoses, and pentoses. *Soil Sci*. 94: 245–250.

Lowe, L.E. 1993. Total and labile polysaccharide analysis of soils. In M.R. Carter, Ed. *Soil Sampling and Methods of Analysis*. Canadian Society of Soil Science. Lewis Publishers, CRC Press, Boca Raton, FL, pp. 373–376.

Martens, D.A. and Frankenberger, Jr., W.T. 1991. Determination of saccharides in biological materials by high-performance anion-exchange chromatography with pulsed amperometric detection. *J. Chromatogr*. 546: 297–309.

Martens, D.A. and Loeffelmann, K.L. 2002. Improved accounting of carbohydrate carbon from plants and soils. *Soil Biol. Biochem*. 34: 1393–1399.

Oades, J.M., Kirkman, M.A., and Wagner, G.H. 1970. The use of gas–liquid chromatography for the determination of sugars extracted from soils by sulfuric acid. *Soil Sci. Soc. Am. Proc*. 34: 230–235.

Oades, J.M. and Wagner, G.H. 1971. Biosynthesis of sugars in soils incubated with

^{14}C glucose and ^{14}C dextran. *Soil Sci. Soc. Am. Proc.* 35: 914–917.

Parsons, J.W. 1981. Chemistry and distribution of amino sugars in soils and soil organisms. In E.A. Paul and J. N. Ladd, Eds. *Soil Biochemistry*, vol. 5. Marcel Dekker, New York, NY, pp. 197–227.

Puget, P., Angers, D.A., and Chenu, C. 1999. Nature of carbohydrates associated with water-stable aggregates of two cultivated soils. *Soil Biol. Biochem.* 31: 55–63.

Six, J., Guggenberger, G., Paustian, K., Haumaier, L., Elliott, E.T., and Zech, W. 2001. Sources and composition of soil organic matter fractions between and within soil aggregates. *Eur. J. Soil Sci.* 52: 607–618.

Stevenson, F.J. 1982a. Nitrogen—Organic forms. In A.L. Page et al., Eds. *Methods of Soil Analysis, Part 2, 2nd ed.* American Society of Agronomy, Madison, WI, pp. 625–641.

Stevenson, F.J. 1982b. Humus Chemistry. John Wiley and Sons, New York, NY, 443 pp.

Tisdall, J.M. and Oades, J.M. 1982. Organic matter and water stable aggregates in soils. *J. Soil Sci.* 33: 141–163.

Zelles, L. 1988. The simultaneous determination of muramic acid and glucosamine in soil by high-performance liquid chromatography with precolumn fluorescence derivatization. *Biol. Fert. Soils* 6: 125–130.

Zhang, X. and Amelung, W. 1996. Gas chromatographic determination of muramic acid, glucosamine, mannosamine, and galactosamine in soils. *Soil Biol. Biochem.* 28: 1201–1206.

Chapter 51
Organic Forms of Nitrogen

D.C. Olk
U.S. Department of Agriculture
Ames, Iowa, United States

51.1 INTRODUCTION

Determination of the chemical forms of soil organic nitrogen (N) has most commonly involved a two-step procedure. First the soil is hydrolyzed by hot mineral acid (usually hydrochloric acid [HCl]), and second the hydrolysate is either distilled to isolate operationally defined N fractions or it is chromatographically separated for identification of common amino acids (Bremner 1965; Stevenson 1994). Normally this approach identifies at most half of the total soil N. This poor recovery may be explained by several factors: HCl hydrolysis does not solubilize a considerable proportion (~20%–35%) of total soil N, a comparable proportion is hydrolyzed from various N forms into NH_4^+, which obscures the original forms, and ~10%–20% of total soil N is hydrolyzable but not identifiable as any of the commonly measured amino acids (Stevenson 1994, 1996).

The acid-insoluble N and the hydrolyzable unknown N are often assumed to consist of organic N compounds more recalcitrant than amino acids, such as heterocyclic N, leading to speculation that the general recalcitrance of soil organic N is due to an abundance of aromatic structures (Flaig et al. 1975; Schulten and Schnitzer 1998). Clear evidence supporting this speculation, though, has not yet been found, and the chemical forms of acid-insoluble N and hydrolyzable unknown N remain uncertain. Much of the acid-insoluble N may be secondary amide N—polypeptides, amino acids, amino sugars, and their residues—that is resistant to acid hydrolysis (Knicker and Hatcher 1997; Nguyen and Harvey 1998).

Newly developed spectroscopic techniques are enabling greater insights into the various forms of soil organic N. Involving advanced instrumentation, these analyses are demonstrating that the bulk of soil organic N is amide, i.e., aliphatic, and that aromatic N is indeed present, but it constitutes at most a modest proportion of soil N. Most evidence has been gained through ^{15}N nuclear magnetic resonance (NMR) spectroscopy using cross-polarization magic-angle spinning (CP/MAS), which in nearly all studies found negligible signals for all N forms other than amide N (Preston 1996; Knicker et al. 1997). Questions remain as to whether the large amide N signal gained by CP/MAS ^{15}N NMR obscures smaller signals for heterocyclic N and whether many forms of heterocyclic N compounds exist in the soil but at

levels too low for clear detection by CP/MAS ^{15}N NMR (Schulten and Schnitzer 1998; Thorn and Mikita 2000).

Other new techniques performed on limited numbers of samples detected modest levels of heterocyclic N compounds, ranging from <10% to ~30% of total N in soil, humic fractions, or decomposing plant litter. These techniques include pyrolysis (Schulten et al. 1995; Bracewell et al. 1980; Olk et al. 2002), nitrogen x-ray absorption near-edge structure (Vairavamurthy and Wang 2002; Jokic et al. 2004), x-ray photoelectron spectroscopy (Abe and Watanabe 2004; Abe et al. 2005), and ^{15}N NMR (Skene et al. 1997; Knicker and Skjemstad 2000; Mahieu et al. 2000). The identified heterocycles included pyridine, pyrrole, and indole.

Despite considerable effort, only very recently has evidence been obtained for the presence in soil organic matter of anilide-like N compounds, which readily form under laboratory conditions through covalent binding of organic N with phenolic compounds. Saturation-pulse-induced dipolar exchange with recoupling (SPIDER) is an advanced NMR technique to selectively observe carbon (C) forms that are bonded to N (Schmidt-Rohr and Mao 2002). Using SPIDER on one soil, Schmidt-Rohr et al. (2004) identified ~20% of soil organic C as being aromatic and bound to N, including <8% as anilides. For a phenol-enriched humic fraction that was extracted from this soil, 25% of the humic N was anilide N and 18% was heterocyclic N. Analysis by ^{15}N NMR of N forms in this humic sample found predominantly secondary amide (Mahieu et al. 2000). Hence the anilide N observed by SPIDER was detected by ^{15}N NMR as amide N, placing in question the capacity of ^{15}N NMR to quantitatively detect anilide N and perhaps also heterocyclic N. The SPIDER analysis is not yet widely available and requires NMR spectrometers with triple resonance.

Amino sugars are thought to account for up to 10+% of total soil N, based on the traditional acid hydrolysis and steam distillation techniques (Parsons 1981; Stevenson 1994) and newer procedures that use gas chromatography, high-performance liquid chromatography (HPLC), or amino acid analyzers with pre- or postcolumn derivatization (Amelung 2001). A recommended procedure for determining amino sugar concentrations is provided in Chapter 50.

Martens and Loeffelmann (2003) and Martens et al. (2006) introduced an analysis for amino acids that simultaneously measures the amino sugars glucosamine and galactosamine and does not require chemical derivatization. With this procedure the soil is hydrolyzed with methanesulfonic acid (MSA) instead of HCl, which avoids the HCl-induced oxidation of S-containing amino acids and degradation of serine and threonine. Also, MSA is nonvolatile and thermally stable at elevated temperatures. Nitrogen forms were detected by anion chromatography and pulsed amperometry, which measures the electrical current produced upon oxidation of each amino compound. This approach identified 51% of total N in several parts of United States Midwestern soils (Martens and Loeffelmann, 2003; Martens et al. 2006), mostly as amino acids with smaller amounts of amino sugars. Another 35% of total soil N was recovered in the hydrolysate as NH_4^+. By comparison, HCl hydrolysis of 12 of these soils followed by anion chromatographic detection identified 47% of total soil N (Martens and Loeffelmann 2003). To date few published studies have used anion chromatography and pulsed amperometry to measure soil N forms.

As discussed above, none of the currently available techniques for quantifying organic N forms in soils achieves a very high recovery or a complete characterization of the organic N forms. Nevertheless, relatively standard techniques for characterizing organic N have been defined and are in regular use. In this chapter, we focus on describing chromatographic

techniques and steam distillation for analysis of organic N forms in hot HCl hydrolysates of soils. A brief description is also given for amino acid and amino sugar analysis by anion chromatography and pulsed amperometry following MSA hydrolysis of soil.

51.2 ANALYSIS FOR NITROGEN FORMS BY HCl HYDROLYSIS FOLLOWED BY STEAM DISTILLATION OR CHROMATOGRAPHY

51.2.1 Preparation of Soil Hydrolysates (Bremner 1965)

Hydrolysis is conducted under reflux with HCl for about 12 h, using 3 mL of 6 *M* HCl/g soil, and the soil hydrolysate is neutralized without prior removal of excess acid.

Materials and Reagents

1 Micro-Kjeldahl digestion unit.

2 Liebig condensers with 24/40 ground-glass joint.

3 Round-bottom flasks fitted with a standard-taper (24/40) ground-glass joint as for the Liebig condenser.

4 Electric heating mantle.

5 Hydrochloric acid, approximately 6 *M*: add 513 mL of concentrated HCl (specific gravity 1.19) to about 500 mL of water, cool, and dilute to 1 L in a volumetric flask.

6 *N*-Octyl alcohol.

7 Sodium hydroxide, approximately 10 *M*: place 3.2 kg of reagent-grade NaOH in a heavy-walled 10 L Pyrex bottle marked to indicate a volume of 8 L. Add 4 L of CO_2-free water and swirl the bottle until the alkali is dissolved. Cool the solution while the neck of the bottle is closed with a rubber stopper, and then dilute it to 8 L by the addition of CO_2-free water. Swirl the bottle vigorously to mix the contents and fit the neck with some arrangement that permits the alkali to be stored and dispensed with protection from atmospheric CO_2.

8 Sodium hydroxide, approximately 5 *M*: dilute 500 mL of 10 *M* NaOH to 1 L and store in a stoppered bottle.

9 Sodium hydroxide, approximately 0.5 *M*: dilute 50 mL of 10 *M* NaOH to 1 L and store in a stoppered bottle.

Procedures

1 Place a sample of finely ground (<100 mesh) soil containing about 10 mg of N in a round-bottom flask fitted with a standard-taper (24/40) ground-glass joint.

2 Add two drops of octyl alcohol and 20 mL of 6 *M* HCl, then swirl the flask to thoroughly mix the acid with the soil.

3 Place the flask in an electric heating mantle and connect it to a Liebig condenser fitted with a 24/40 ground-glass joint.

4 Heat the soil–acid mixture so that it gently boils under reflux for 12 h.

5 Wash the condenser with a small quantity of distilled water and allow the flask to cool, and then remove the flask from the condenser.

6 Filter the hydrolysis mixture through a Buchner funnel fitted with Whatman No. 50 filter paper, using a suction filtration apparatus that allows collection of the filtrate in a 200 mL beaker.

7 Wash the residue with distilled water until the filtrate reaches the 60 mL mark on the beaker.

8 Place the bottom half of the beaker in crushed ice.

9 Neutralize to pH 6.5 $\pm$ 0.1 by slow addition of NaOH with constant stirring to ensure that the hydrolysate does not become alkaline at any stage of the neutralization process. Use 5 *M* NaOH to bring the pH to about 5, and then complete the neutralization using 0.5 *M* NaOH. The hydrolysate can also be cooled in a freezer and cold NaOH used for neutralization.

10 Transfer the neutralized hydrolysate into a 100 mL volumetric flask.

11 Adjust the volume to the mark with the washings obtained by rinsing the beaker, electrodes, and stirring device several times with small quantities of distilled water.

12 Stopper the flask and invert several times to mix the contents.

51.2.2 Measurement of N Compounds in the Acid Hydrolysate

Nitrogen Fractionation Based on Steam Distillation

Nitrogen fractions in the acid hydrolysate have often been distinguished through steam distillation, as described by Stevenson (1996). Nitrogen fractions include total hydrolyzable N, acid-insoluble N, amino acid-N, ammonia-N, amino sugar-N, and hydrolyzable unknown N (Table 51.1). Further use of this fractionation scheme should be questioned as its fractions appear largely irrelevant to N cycling under field conditions (Stevenson 1982), it may have methodological errors (Mulvaney and Khan 2001), and it does not distinguish individual amino compounds.

Analysis for Amino Acids and Amino Sugars by Chromatographic Separation

Several chromatographic methods are available for determining the concentrations of individual amino acids and amino sugars in HCl hydrolysates. To measure the amino acids in hydrolysates of pure proteins, biochemists often combine reverse-phase HPLC with precolumn derivatization and fluorescence detection (Cooper et al. 2001). This approach enables

TABLE 51.1 Steam Distillation Methods for Determining the Various Forms of N in a Soil Hydrolysate

Form of N	Method[a]
Total hydrolyzable N	Steam distillation with NaOH after Kjeldahl digestion with H_2SO_4 and a K_2SO_4-catalyst mixture
Amino acid N	Steam distillation with phosphate–borate buffer after treatment with NaOH at 100°C to remove amino sugars plus NH_4^+ and with ninhydrin (pH 2.5, 100°C) to convert α-amino N to NH_4^+
Amino sugar N	Steam distillation with phosphate–borate buffer at pH 11.2; correction for NH_3-N
Ammonia N	Steam distillation with MgO
Acid-insoluble N	Obtained by difference (total N – hydrolyzable N)
Hydrolyzable unknown N	Obtained from the difference between total hydrolyzable N and the N accounted for as (NH_3 + amino acid + amino sugar)-N

Source: From Stevenson, F.J. in D.L. Sparks et al. (Eds.), *Methods of Soil Analysis, Part 3—Chemical Methods*. Soil Science Society of America, Madison, Wisconsin, 1996, 1185–1200. With permission.

[a] In each method, the NH_3 liberated by steam distillation is collected in a H_3BO_3-indicator solution and determined by titration with standard (0.0025 *M*) H_2SO_4.

sensitive detection of amino acids, but it is not directly applicable to soil due to interference by soil components. Warman and Bishop (1985) adapted reverse-phase HPLC to soil analysis by first dissolving silicate soil minerals with HF and then removing soil metal cations by adsorption onto cation-exchange resin. Jones et al. (2005) used reverse-phase HPLC to measure amino acids in the soil solution. Amelung and Zhang (2001) measured concentrations of each soil amino acid after separation into its two enantiomers, whose molecular structures are mirror-image and nonsuperimposable. Acid hydrolysates were purified of interfering organic compounds by adsorbing the amino acids onto a cation-exchange resin, followed by an oxalic acid wash to remove soil cations. Amino acid enantiomers were then eluted from the resin with NH_4OH, derivatized to form *N*-pentafluoropropionyl-amino acid *iso*-propyl esters, and analyzed by gas chromatography. Amelung and Zhang (2001) reviewed other gas chromatography analyses for soil amino acids. Amelung (2001) described analyses for amino sugars that involved either reverse-phase HPLC or gas chromatography.

By far the most common approach for routine analysis of soil amino acids has been ion-exchange chromatography with post-column derivatization by ninhydrin (triketohydrindane hydrate) (Moore and Stein 1948; Moore et al. 1958). The acid hydrolysate is injected into a liquid chromatograph equipped with a strong cation-exchange column, onto which the amino acids will adsorb, given their positive charge in the acid solution. After other soil components have passed through the column, amino acids are then sequentially eluted from the column by using solution gradients that vary the mobile-phase pH, salt concentration, and temperature. Typically the pH is controlled by varying the level of Na citrate, and salt concentration is controlled by varying the level of NaCl. The eluted amino acids are derivatized with ninhydrin, which binds highly selectively with the α-NH_2 groups of amino acids, peptides, primary amines, and NH_3. The resulting complexes are quantified by measuring their light absorption at both 440 (proline and hydroxyproline) and 570 nm (all other compounds). This method requires a longer run time and is much less sensitive

than fluorescence detection to amino compounds, but it is not vulnerable to interference by other soil components, some of which can also fluoresce when derivatized.

Ion-exchange amino acid analyzers are available from multiple sources, and specific steps in the chromatographic analysis can differ slightly by manufacturer. Manufacturer's specifications should be followed when developing analytical steps, including the selection of reagents and their gradients. Stevenson (1965) described one procedure for ion-exchange chromatography, but significant advances in the capabilities of chromatography columns (Zumwalt and Gehrke 1988) have made this procedure obsolete.

51.2.3 Comments

1 Acid hydrolysis and steam distillation can be performed with relatively affordable equipment. Chromatographic separation requires more advanced instrumentation, which is often available at major research institutes in specialized units such as protein structure laboratories.

2 As previously described, any procedure that involves HCl hydrolysis of the soil will result in a moderate recovery (~50%) of soil N as identifiable amino acids, because of incomplete solubilization of N compounds, cleavage of some amine groups to form free ammonium, and extensive destruction of specific amino acids.

51.3 ANALYSIS FOR INDIVIDUAL AMINO ACIDS AND AMINO SUGARS BY METHANESULFONIC ACID HYDROLYSIS AND ANION CHROMATOGRAPHY–PULSED AMPEROMETRY

As described above, Martens and Loeffelmann (2003) identified amino acids and amino sugars simultaneously by (i) hydrolyzing soil with MSA instead of HCl and (ii) measuring amino compounds by anion chromatography and pulsed amperometry. Use of MSA allowed preservation of some labile amino acids.

The soil is extracted with MSA during autoclaving, and subsequently the supernatant is neutralized to an alkaline pH, making the amino compounds negatively charged. The supernatant is passed through an anion-exchange column that has quaternary NH_4 groups, enabling highly specific adsorption of amino compounds. The amino compounds are eluted with a tertiary gradient of water, NaOH, and Na acetate. This method requires no derivatization, due to the highly specific binding of amino compounds by the column.

This approach has been used for analysis of model amino compounds (Clarke et al. 1999), proteins (Jandik et al. 2001), and soil amino compounds (Martens and Loeffelmann 2003; Martens et al. 2006). Results from this limited number of studies have shown that the optimal autoclaving duration for maximum extraction of amino compounds must be determined for each soil. The optimal duration can differ by soil type (including clay mineral type and clay quantity) and land use practices such as tillage and animal manure amendment. Martens and Loeffelmann (2003) and Martens et al. (2006) used short autoclaving times (30 to 90 min), but at a temperature of 136°C. Unfortunately, many autoclaves cannot achieve temperatures >121°C. Atmospheric oxygen is not excluded during the extraction, creating the potential for partial degradation of amino sugars (Amelung 2001).

REFERENCES

Abe, T., Maie, N., and Watanabe, A. 2005. Investigation of humic acid N with X-ray photoelectron spectroscopy: effect of acid hydrolysis and comparison with ^{15}N cross polarization/magic angle spinning nuclear magnetic resonance spectroscopy. *Org. Geochem.* 36: 1490–1497.

Abe, T. and Watanabe, A. 2004. X-ray photoelectron spectroscopy of nitrogen functional groups in soil humic acids. *Soil Sci.* 169: 35–43.

Amelung, W. 2001. Methods using amino sugars as markers for microbial residues in soil. In R. Lal, J.M. Kimble, R.F. Follett, and B.A. Stewart, Eds. *Assessment Methods for Soil Carbon*. Lewis Publishers, Boca Raton, FL, pp. 233–272.

Amelung, W. and Zhang, X. 2001. Determination of amino acid enantiomers in soils. *Soil Biol. Biochem.* 33: 553–562.

Bracewell, J.M., Robertson, G.W., and Williams, B.L. 1980. Pyrolysis-mass spectrometry studies of humification in a peat and a peaty podzol. *J. Anal. Appl. Pyrol.* 2: 53–62.

Bremner, J.M. 1965. Organic forms of nitrogen. In C.A. Black et al. Eds. *Methods of Soil Analysis*. American Society of Agronomy, Madison, WI, pp. 1148–1178.

Clarke, A.P., Jandik, P., Rocklin, R.D., Liu, Y., and Avdalovic, N. 1999. An integrated amperometry waveform for the direct, sensitive detection of amino acids and amino sugars following anion-exchange chromatography. *Anal. Chem.* 71: 2774–2781.

Cooper, C., Packer, N., and Williams, K., eds. 2001. Amino Acid Analysis Protocols. *Methods in Molecular Biology*, Vol. 159. Humana Press, Totowa, NJ.

Flaig, W., Beutelspacher, H., and Rietz, E. 1975. Chemical composition and physical properties of humic substances. In J.E. Gieseking, Ed. *Soil Components, Vol. 1. Organic Components*. Springer-Verlag, New York, NY, pp. 1–211.

Jandik, P., Pohl, C., Barreto, V., and Avdalovic, N. 2001. Anion exchange chromatography and integrated amperometric detection of amino acids. In C. Cooper, N. Packer, and K. Williams, Eds. Amino Acid Analysis Protocols. *Methods in Molecular Biology*, Vol. 159. Humana Press, Totowa, NJ, pp. 63–85.

Jokic, A., Cutler, J.N., Anderson, D.W., and Walley, F.L. 2004. Detection of heterocyclic N compounds in whole soils using N-XANES spectroscopy. *Can. J. Soil Sci.* 84: 291–293.

Jones, D.L., Shannon, D., Junvee-Fortune, T., and Farrar, J.F. 2005. Plant capture of free amino acids is maximized under high soil amino acid concentrations. *Soil Biol. Biochem.* 37: 179–181.

Knicker, H., Fründ, R., and Lüdemann, H.-D. 1997. Characterization of nitrogen in plant composts and native humic material by natural-abundance ^{15}N CPMAS and solution NMR spectra. In M.A. Nanny, R.A. Minear, and J.A. Leenheer, Eds. *Nuclear Magnetic Resonance Spectroscopy in Environmental Chemistry*. Oxford University Press, New York, NY, pp. 272–294.

Knicker, H. and Hatcher, P.G. 1997. Survival of protein in an organic-rich sediment: possible protection by encapsulation in organic matter. *Naturwissenschaften* 84: 231–234.

Knicker, H. and Skjemstad, J.O. 2000. Nature of organic carbon and nitrogen in physically protected organic matter of some Australian soils as revealed by solid-state ^{13}C and ^{15}N NMR spectroscopy. *Aust. J. Soil Res.* 38: 113–127.

Mahieu, N., Olk, D.C., and Randall, E.W. 2000. Accumulation of heterocyclic nitrogen in humified organic matter: a ^{15}N-NMR study of lowland rice soils. *Eur. J. Soil Sci.* 51: 379–389.

Martens, D.A., Jaynes, D.B., Colvin, T.S., Kaspar, T.C., and Karlen, D.L. 2006. Soil organic nitrogen enrichment following soybean in an Iowa corn–soybean rotation. *Soil Sci. Soc. Am. J.* 70: 382–392.

Martens, D.A. and Loeffelmann, K.L. 2003. Soil amino acid composition quantified by acid hydrolysis and anion chromatography-pulsed amperometry. *J. Agric. Food Chem.* 51: 6521–6529.

Moore, S., Spackman, D.H., and Stein, W.H. 1958. Chromatography of amino acids on sulfonated polystyrene resins: an improved system. *Anal. Chem.* 30: 1185–1190.

Moore, S. and Stein, W.H. 1948. Photometric ninhydrin method for use in the chromatography of amino acids. *J. Biol. Chem.* 176: 367–388.

Mulvaney, R.L. and Khan, S.A. 2001. Diffusion methods to determine different forms of nitrogen in soil hydrolysates. *Soil Sci. Soc. Am. J.* 65: 1284–1292.

Nguyen, R.T. and Harvey, H.R. 1998. Protein preservation during early diagenesis in marine waters and sediments. In B.A. Stankiewicz and P.F. van Bergen, Eds. *Nitrogen-Containing Macromolecules in the Bio- and Geosphere*. ACS Symposium Series 707. American Chemical Society, Washington, DC, pp. 88–112.

Olk, D.C., Dancel, M.C., Moscoso, E., Jimenez, R.R., and Dayrit, F.M. 2002. Accumulation of lignin residues in organic matter fractions of lowland rice soils: a pyrolysis-GC–MS study. *Soil Sci.* 167: 590–606.

Parsons, J.W. 1981. Chemistry and distribution of amino sugars in soils and soil organisms. In E.A. Paul and J.N. Ladd, Eds. *Chemistry and Distribution of Amino Sugars in Soils and Soil Organisms*. Marcel Dekker, New York, NY, pp. 197–227.

Preston, C.M. 1996. Applications of NMR to soil organic matter analysis: history and prospects. *Soil Sci.* 161: 144–166.

Schmidt-Rohr, K. and Mao, J.-D. 2002. Selective observation of nitrogen-bonded carbons in solid-state NMR by saturation-pulse induced dipolar exchange with recoupling. *Chem. Phys. Lett.* 359: 403–411.

Schmidt-Rohr, K., Mao, J.-D., and Olk, D.C. 2004. Nitrogen-bonded aromatics in soil organic matter and their implications for a yield decline in intensive rice cropping. *Proc. Natl. Acad. Sci. USA* 101: 6351–6354.

Schulten, H.-R. and Schnitzer, M. 1998. The chemistry of soil organic nitrogen: a review. *Biol. Fert. Soils* 26: 1–15.

Schulten, H.-R., Sorge, C., and Schnitzer, M. 1995. Structural studies on soil nitrogen by Curie-point pyrolysis—gas chromatography/mass spectrometry with nitrogen-selective detection. *Biol. Fert. Soils* 20: 174–184.

Skene, T.M., Clarke, P., Skjemstad, J.O., and Oades, J.M. 1997. Browning reactions between *Eucalyptus* litter and different nitrogen sources. *Aust. J. Soil Res.* 35: 1085–1091.

Stevenson, F.J. 1965. Amino acids. In C.A. Black et al., Eds. *Methods of Soil Analysis, Part 2—Chemical and Microbiological Properties*. American Society of Agronomy, Madison, WI, pp. 1437–1451.

Stevenson, F.J. 1982. Organic forms of soil nitrogen. In F.J. Stevenson, Ed. *Nitrogen in Agricultural Soils*. ASA-CSSA-SSSA, Madison, WI, pp. 67–122.

Stevenson, F.J. 1994. *Humus Chemistry*, 2nd ed. John Wiley & Sons, New York, NY, 496 pp.

Stevenson, F.J. 1996. Nitrogen–organic forms. In D.L. Sparks et al. Eds. *Methods of Soil Analysis, Part 3—Chemical Methods*. Soil Science Society of America, Madison, WI, pp. 1185–1200.

Thorn, K.A. and Mikita, M.A. 2000. Nitrite fixation by humic substances: nitrogen-15 nuclear magnetic resonance evidence for potential intermediates in chemodenitrification. *Soil Sci. Soc. Am. J.* 64: 568–582.

Vairavamurthy, A. and Wang, S. 2002. Organic nitrogen in geomacromolecules: insights on speciation and transformation with K-edge XANES spectroscopy. *Environ. Sci. Technol.* 36: 3050–3056.

Warman, P.R. and Bishop, C. 1985. The use of reverse-phase HPLC for soil amino-N analysis. *J. Liq. Chromatogr.* 8: 2595–2606.

Zumwalt, R.W. and Gehrke, C.W. 1988. Amino acid analysis: a survey of current techniques. In J.P. Cherry and R.A. Barford, Eds. *Methods for Protein Analysis*. American Oil Chemists' Society, Champaign, IL, pp. 13–35.

Chapter 52
Soil Humus Fractions

D.W. Anderson and J.J. Schoenau
University of Saskatchewan
Saskatoon, Saskatchewan, Canada

52.1 INTRODUCTION

Soil organic matter may be differentiated into humic and nonhumic components. Humic components or humus are the highly transformed, dark brown to black materials that are closely associated with the mineral fraction. Nonhumic material includes both particulate matter (e.g., dead roots) and simple soluble components that are part of the soil solution. Although the definition is straightforward, the consistent separation of humic and nonhumic components is problematic. It is a challenge to develop experimental methods that consistently and definitively separate humic and nonhumic fractions.

MacCarthy (2001) postulated that humic substances are unique in nature and have qualities unlike any other natural substances. The first principle postulates that humic substances represent a supermixture of an extremely wide array of chemical structures. In all likelihood the probability of finding two identical structures is exceedingly remote. By understanding humic substances in this way, it is evident that classical approaches based on isolation, purification, and finally identification of discrete chemical compounds and structures do not apply. This is not to say that extractions should not be used, but that they should be used within the context of this new understanding of the limitations of the classical methods.

Despite concerns about the efficiency of extractions (generally less than one-half of the humus is extracted) and the creation of artifacts during the extraction, extraction and fractionation remain important steps in many studies. Extraction separates the humic materials from the complicating presence of the mineral fraction, removes other inorganic interferences, increases concentration, and renders the organic matter soluble (Swift 1996).

The extraction of organic matter with alkali, the subsequent separation of the extract from the remaining soil, and the acidification of the extract results in three operationally defined fractions: humic acids (HA), fulvic acids (FA), and humin. The FA is the generally yellowish-colored fraction that remains in solution after acidification of the alkaline extract, the HA is the dark brown to black precipitate resulting from the acidification of the extract, and the humin is the material not extracted. About 30% to 60% of the soil humus is removed with alkali extractants.

Humin, the fraction insoluble in aqueous extracts at any pH or the nonextractable humus, is understandably the least studied and, therefore, the least understood part of the organic matter (Rice 2001) despite its being more than 50% of the organic carbon (C) in most soils. In essence, humin is a small amount of organic matter associated with a considerable mass of soil. Humin, compared to HA, is more aliphatic and has significant aromatic and carbohydrate components. About one-third to one-half of the C remaining with the soil residue following alkali extraction can be isolated by simply adding water, dispersing the dilute suspension with ultrasound, and centrifuging to settle out all but the very fine clay (Anderson et al. 1974). Acidification of the centrifugate results in a dark, humic material, thought to be clay-associated. These humic materials (normally part of the humin) are less aromatic, more susceptible to acid hydrolysis, richer in N, and of higher molecular weight than the humic materials extracted in the first step with strong alkali. After isolation of this second HA fraction, the humin remaining with the soil residue is mainly particulate bits of plant root, fungal remains, and charcoal. A method for isolating humin fractions by partitioning between an aqueous phase of varying pH and methylisobutylketone is recommended to those interested in the humin fraction (Rice 2001).

There are a great number of extraction methods involving many different extractants. The extraction method outlined below uses an alkali extractant and is suitable for research involving comparisons of related groups of soils. The extraction and fractionation described are recommended for use, but with a precautionary principle that recognizes their limitations.

52.2 SAMPLING AND SAMPLE PREPARATION

A first concern in sampling is the separation of humic and nonhumic materials. Recognizable plant residues should be removed from the soil surface before coring. Using a core sampler of known volume is recommended (see Chapter 3), in order to calculate bulk density for use in later data analysis. Because of soil variability, and the laborious nature of extractions, taking several cores and then mixing thoroughly to obtain a composite sample may be a good strategy. Sampling the depth of cultivation (Ap horizon) is recommended, although subhorizons (e.g., 0 to 5 cm and 5 to about 15 cm) will help in evaluating differences due to agronomic treatments. Sampling pedologically defined horizons is recommended although different depths of sampling introduce an additional challenge for statistical analyses (see Chapter 1).

Air-drying samples in a dust-free space is recommended. Air-dry samples should be ground lightly using a rolling pin or similar device, and passed through a 2 mm sieve. During this step, in contrast to methods estimating total organic C contents (see Chapter 3), visible roots and other plant residues should be removed. A representative subsample should be finely ground in preparation for analyses such as organic C or nitrogen (N) determination, thereby reducing variability. Extractions may be done on the larger, <2 mm sample.

52.3 ALKALI EXTRACTION

An alkali extraction is used to remove a portion of the soil organic matter. Alkali extractants which are commonly used include 0.1 *M* NaOH, 0.5 *M* NaOH, and 0.1 *M* NaOH–0.1 *M* $Na_4P_2O_7$. The method below describes the use of 0.5 *M* NaOH.

52.3.1 Reagents

1 0.5 *M* HCl: Prepare the reagent by carefully adding 40 mL of concentrated HCl to deionized water and bring the total volume to 1000 mL, working in a fume hood.

This reagent is used as a pretreatment to remove floating plant debris and inorganic forms of C, N, phosphorus (P), and sulfur (S) before extraction with NaOH.

2 0.5 *M* NaOH: dissolve 20.0 g of NaOH in 1000 mL of deionized water. The pH of the solution should be around 13.5. The NaOH solution must be prepared fresh daily and kept tightly covered, as it will absorb carbon dioxide from the atmosphere.

52.3.2 Procedure

1 Place 15 g of air-dried soil (ground to <2 mm) into a 250 mL plastic centrifuge bottle that withstands high-speed refrigerated centrifugation.

2 Add 150 mL of 0.5 *M* HCl. Set aside for 1 h, stirring occasionally. Centrifuge for 15 min at 9000 *g* and pour off the supernatant.

3 To wash the soil free of any remaining HCl, add 150 mL of deionized water to the centrifuge bottle, mix, then centrifuge at 9000 *g* for 15 min, and discard the supernatant.

4 Add 150 mL of fresh 0.5 *M* NaOH to the centrifuge bottle. Flush the headspace of the bottle with oxygen-free N_2 gas, and then quickly tighten the cap.

5 Place the bottle on an end-over-end shaker (60 turns per min) for 18 h.

6 Following the shaking, centrifuge at 9000 *g* for 15 min to separate the NaOH extract from the soil residue. Carefully decant the supernatant into a clean centrifuge bottle and retain for separation into HA and FA fractions. The residue of the extraction (humin) may be discarded or retained for analysis (see Section 52.4).

52.3.3 Comments

1 Pretreatment step removes a small amount of organic matter and the dissolved organic carbon (DOC). The International Humic Substances Society (IHSS) method (Swift 1996) includes the DOC with the FA. The pretreatment should be performed if organic nutrients are to be analyzed with minimal interference.

2 Soils containing calcium carbonate will react violently with the 0.5 *M* HCl.

3 Retention of N_2 headspace during extraction is important in reducing oxidation and CO_2 absorption. For this reason, centrifuge bottles should be selected with a good seal between cap and bottle. A wrist-action shaker may be substituted if an end-over-end shaker is not available.

52.4 SEPARATION INTO HUMIC FRACTIONS

The NaOH extract is fractionated into conventional HA and FA fractions by acidification. The residue of the alkali extraction, sometimes referred to as humin, is largely composed of organic material tightly bound to the mineral fraction. The humin may be discarded, retained

for analysis, or sonified and fractionated into clay-associated HA (HA-B) and FA (FA-B) fractions (Anderson et al. 1974; Bettany et al. 1979).

52.4.1 Reagents

1 6 *M* HCl: Prepare the reagent by carefully adding 50 mL of concentrated HCl to 50 mL of deionized water, working in a fume hood.

2 0.1 *M* NaOH: dissolve 4.0 g of NaOH in 1000 mL of deionized water. This solution is used to redissolve the HA after separation by acidification.

52.4.2 Procedure

1 Using a burette, add 6 *M* HCl to the NaOH extract in the centrifuge bottle until a pH of 1.5 is attained, checking with a pH meter while stirring. The acidification causes precipitation of a portion of the organic matter, that is dark brown to black in color and is termed conventional HA (HA-A), while that which remains in solution after acidification (yellowish in color) is termed conventional FA (FA-A).

2 Centrifuge at 9000 *g* for 15 min to separate the HA and FA.

3 After centrifugation, the supernatant (FA) is removed and retained in vials for analysis. Then 50 mL of 0.1 *M* NaOH is added to the centrifuge bottle to redissolve the precipitate (HA). The HA may then be transferred to a vial for storage and analysis.

4 If desired, the residue of the NaOH extraction (humin) may be fractionated into HA (HA-B) and FA (FA-B) fractions. Mix the residue with 150 mL of deionized water, sonicate for 10 min with an ultrasonifier at 125 W, and then refrigerate and allow the suspension to stand for 48 h.

5 Centrifuge at 9000 *g* for 15 min and remove the supernatant.

6 Acidify the supernatant to pH 1.5 as described above.

7 Remove the precipitate (HA-B) by centrifugation and retain the supernatant (FA-B).

8 Redissolve the HA-B in 100 mL of 0.1 *M* NaOH. Retain the solution for analysis.

52.4.3 Comments

1 HA may be de-ashed by treatment with a hydrofluoric acid–HCl solution as described in the standard IHSS method (Swift 1996). However, such treatments may cause losses of nitrogenous and carbohydrate components (Schnitzer and Schuppli 1989).

2 Samples may be freeze-dried to provide dry humic materials for analysis. A variety of analyses may be performed on the dissolved humic constituents, including elemental analysis by digestion or automated combustion.

3 The carbon content of dissolved humic fractions is commonly measured using a soluble carbon analyzer (see Chapter 48).

4 The ratio of E4:E6, which gives an indication of the molecular weight of the humic substances, may be determined by dissolving an aliquot of HA or FA (a C concentration of 34 $\mu g\ g^{-1}$ works well) in 0.05 *M* $NaHCO_3$ and measuring the ratio of the absorbances at 465 and 665 nm (Kononova 1966; Anderson et al. 1974). The IR and ^{13}C NMR spectra of the humic substances can provide important information on the chemical structure (Schnitzer and Schuppli 1989). Similarly, the FA may be passed through a column of XAD-8 resin to reduce ash content, as described in the standard IHSS method (Swift 1996).

5 Hydrolysis reactions during alkali extractions may be of concern in the study of organic S in humus. The presence of inorganic sulfate in FA extracts has led to the suggestion that organic sulfate groups are hydrolyzed to inorganic sulfate in the NaOH (Schoenau and Bettany 1987). The occurrence of such artifacts emphasizes the need for caution when interpreting the results of organic matter fractionation.

52.5 HUMUS CHARACTERIZATION OF WHOLE SOILS

Several methods are suitable for *in situ* analysis of organic matter in soils and include solid-state ^{13}C NMR spectroscopy (see Chapter 53) and pyrolysis-field ionization mass spectroscopy (Py-FIMS) (Leinweber and Schulten 1999). Hatcher et al. (2001) discusses modern analytical methods that include Py-FIMS and several others developed mainly in the biochemistry field and applicable to the study of complex biomolecules such as humic substances.

Jokic et al. (2003) studied the chemical structures of humus and the organic sulfur species present using a combination of ^{13}C NMR and a synchroton-based method, x-ray absorption near-edge structures (XANES). The method, more specifically K-edge carbon XANES, yielded information on the relative proportions of aliphatic, aromatic, and carbohydrate structures in the organic fraction of whole soils. Work with N-XANES that examined N compounds and identified both amino and heterocyclic forms of N indicates the promise of synchroton spectroscopy in studies of humus (Jokic et al. 2004).

REFERENCES

Anderson, D.W., Paul, E.A., and St. Arnaud, R.J. 1974. Extraction and characterization of humus with reference to clay-associated humus. *Can. J. Soil Sci*. 54: 317–323.

Bettany, J.R., Stewart, J.W.B., and Saggar, S. 1979. The nature and forms of sulfur in organic matter fractions of soils selected along an environmental gradient. *Soil Sci. Soc. Am. J*. 43: 481–485.

Hatcher, P.G., Dria, K.J., Kim, S., and Frazier, S.W. 2001. Modern analytical studies of humic substances. *Soil Sci*. 166: 770–794.

Jokic, A., Cutler, J.N., Anderson, D.W., and Walley, F. 2004. Detection of heterocyclic N compounds in whole soils using N-XANES spectroscopy. *Can. J. Soil Sci*. 84: 291–293.

Jokic, A., Cutler, J.N., Ponomarenko, E., van der Kamp, G., and Anderson, D.W. 2003. Organic carbon and sulfur compounds in wetland soils: insights on structure and transformation processes using K-edge XANES and NMR spectroscopy. *Geochim. Cosmochim. Acta* 67: 2585–2597.

Kononova, M.M. 1966. *Soil Organic Matter*, 2nd ed. Pergamon Press, London, UK, 544 pp.

Leinweber, P. and Schulten, H.R. 1999. Advances in the analytical pyrolysis of soil organic matter. *J. Anal. Appl. Pyrol.* 49: 358–383.

MacCarthy, P. 2001. The principles of humic substances. *Soil Sci.* 166: 738–751.

Rice, J.A. 2001. *Humin. Soil Sci.* 166: 848–857.

Schnitzer, M. and Schuppli, P. 1989. The extraction of organic matter from selected soils and particle size fractions with 0.5 *M* NaOH and 0.1 *M* $Na_4P_2O_7$ solutions. *Can. J. Soil Sci.* 69: 253–262.

Schoenau, J.J. and Bettany, J.R. 1987. Organic matter leaching as a component of carbon, nitrogen, phosphorus, and sulfur cycles in a forest, grassland and gleyed soil. *Soil Sci. Soc. Am. J.* 51: 646–651.

Swift, R.S. 1996. Organic matter characterization. In D.L. Sparks et al., Eds. *Methods of Soil Analysis, Part 3—Chemical Methods.* SSSA Book Series, No. 5. SSSA, American Society of Agronomy, Madison, WI, pp. 1011–1029.

Chapter 53
Soil Organic Matter Analysis by Solid-State ^{13}C Nuclear Magnetic Resonance Spectroscopy

Myrna J. Simpson
University of Toronto
Toronto, Ontario, Canada

Caroline Preston
Natural Resources Canada
Victoria, British Columbia, Canada

53.1 INTRODUCTION

The use of solid-state ^{13}C nuclear magnetic resonance (NMR) spectroscopy to examine the nature of soil organic matter (SOM) has gained popularity over the past two decades because it provides information regarding the chemical nature and relative quantities of carbon (C) structures (Preston 1996; Kögel-Knabner 2000; Preston 2001). The knowledge gained from solid-state ^{13}C NMR has expanded our understanding of SOM structure and is unparalleled in comparison to other techniques because it enables the nondestructive analysis of whole soil samples. Analysis of SOM by solid-state ^{13}C NMR provides information regarding the relative quantities of unsubstituted and substituted aliphatic, aromatic, phenolic, carboxylic, and carbonyl C. In addition, only small quantities of sample are needed (100–500 mg of sample depending on the type of NMR probe) to perform the analysis.

The most commonly applied solid-state ^{13}C NMR method is cross polarization with magic angle spinning (CP/MAS). The CP technique transfers the polarization from abundant ^{1}H nuclei to the less-abundant ^{13}C nuclei and enhances the ^{13}C signal by a factor of up to 4 with actual enhancement factors varying between 1 and 3. The other advantage of the CP method is that it relies on the relaxation time of ^{1}H nuclei which is considerably shorter than that of ^{13}C nuclei, reducing the time required between pulses. Therefore, CP is much faster than direct ^{13}C polarization methods (such as Bloch decay, BD) and allows one to obtain semiquantitative information about the chemistry of C in a soil within a reasonable amount of time (12–24 h). In solid-state ^{13}C NMR, samples are spun at the magic angle of 54.7° to reduce broadening due to chemical shift anisotropy (CSA), which arises from different orientations of molecules in the

solid phase (without MAS, it is possible to observe all the signals from different molecular orientations). In addition, high-power decoupling eliminates the broadening due to dipolar interactions between ^{13}C and ^{1}H.

As NMR technology advances, low-field (100 and 200 MHz) instruments are generally being replaced with higher field (300 MHz and higher) spectrometers. Techniques differ depending on the magnetic field strength (Preston 2001; Dria et al. 2002; Smernik 2005). For example, at higher field strengths, one must use faster spinning rates to remove spinning sidebands (SSBs) that arise from CSA from the spectral window. However, CP efficiency decreases at higher spinning speeds (although BD efficiency is unaffected), and high-speed rotors have lower sample volumes. At higher spinning rates, ramped amplitude (RAMP-CP) pulse programs are often applied to compensate for CP inefficiency, although this capability may not be available on older instruments. If a higher speed probe is not available (i.e., 10–13 kHz at 300 MHz), CP/MAS with total suppression of sideband (TOSS) can be employed. However, it should be noted that the TOSS method may result in distortion of peak areas and lower signal to noise ratio (S/N) that in turn increases the experimental time.

Samples low in organic C and/or samples that are rich in iron oxides should be treated with hydrofluoric (HF) acid before ^{13}C NMR analysis (Preston et al. 1989; Skjemstad et al. 1994; Schmidt et al. 1997; Gélinas et al. 2001; Smernik and Oades 2002; Gonçalves et al. 2003; Schilling and Cooper 2004). Concentration of the organic C content through demineralization of iron-bearing paramagnetic minerals enhances the S/N and often reduces the duration of the experiment. Samples rich in carbonates should be pretreated with hydrochloric (HCl) acid to increase the relative concentration of organic C in the sample. Different concentrations of HF and HCl have been used in the past to reduce the iron content and increase the amount of organic C in a sample. Schmidt et al. (1997) did not detect a change in the organic C distribution after samples were treated with 10% (v/v) HF. Gonçalves et al. (2003) reported C losses in B horizons when using 10% (v/v) HF but did not observe any change in the distribution of C functional groups. Simpson and Hatcher (2004) used lower concentrations (0.1 *M* HCl/0.3 *M* HF) to de-ash samples to prevent any losses of organic C in the sample.

This chapter is to be used as a practical guide to accompany published works. Several review articles have summarized various aspects of methodology and theory of NMR techniques and it is highly recommended to consult related literature for a detailed account of NMR analysis of SOM. Preston (2001) reviewed NMR techniques for SOM, Dria et al. (2002) provide a brief summary of NMR theory and more detailed information on solid-state NMR can be found in Bryce et al. (2001). This chapter will describe practical aspects of preparing samples, acquiring, and processing NMR data. Pretreatment of soil samples with HF acid and HCl acid (for samples rich in carbonates) is highly recommended. This pretreatment concentrates the organic matter, which enhances the S/N of the resulting NMR spectra and removes paramagnetic minerals, such as iron, which can interfere with the acquisition of data.

53.2 SAMPLE PRETREATMENT

53.2.1 Materials

1 Analytical balance.

2 0.1 *M* HCl/0.3 *M* HF solution. *Note*: HF is highly toxic and should only be used in a fume hood. HF will also dissolve glass so only plastic or stainless steel laboratory

ware should be used when handling HF. Gloves should be worn at all times. As a safety measure, calcium gluconate cream (HF antidote cream) should be kept on hand in the event of contact with skin.

3 250 mL, high-density plastic centrifuge tubes with leakproof lids.

4 Horizontal shaker.

5 High-speed centrifuge (capable of 4000 *g*).

6 Deionized water.

7 Freeze drier.

53.2.2 Procedure for Sample Pretreatment

1 Weigh approximately 5–10 g of air-dry sample into a 250 mL plastic centrifuge tube. *Note*: Soil samples should be first passed through a 2 mm sieve and then finely ground (<200 μm in size).

2 Add 200 mL of 0.1 *M* HCl/0.3 *M* HF solution or 0.3 *M* HF solution for samples that are carbonate-free.

3 Shake samples for 18–24 h.

4 Centrifuge samples at 4000 *g* for 20–25 min.

5 Carefully decant the supernatant and replace with fresh 200 mL of 0.1 *M* HCl/0.3 *M* HF solution or 0.3 *M* HF solution and repeat until the organic C content of the sample reaches at least 25%. *Note*: This procedure may need to be repeated a number of times for samples that are low in SOM. HF/HCl solutions should be sent for waste disposal and should not be poured down the sink.

6 Remove excess HCl/HF from the sample by rinsing the sample with deionized water. After removing the last HCl/HF solution, add deionized water, shake the sample for 4–6 h, and then centrifuge at 4000 *g* for 20–25 min. Repeat at least three times to remove excess salts. *Note*: The presence of HF/HCl can cause damage to instruments such as elemental analyzers.

7 Freeze-dry the sample and store in a sealed container for ^{13}C NMR analysis.

53.3 PROCEDURE FOR ^{13}C NMR ANALYSIS

53.3.1 Safety Procedures

A superconducting magnet is always on—do not approach the magnet (this includes from the floors above and below) if you have a pacemaker or similar device installed. Remove metal objects (e.g., keys, paper clips, tools, and penknives), wallets with magnetic strip cards, watches, computer disks, and electronic devices before approaching the magnet. The latter can be damaged, and especially with larger magnets, metal objects can turn into

missiles, causing injury or catastrophic magnet damage (more than $100 K). Be careful not to step on any of the connecting cables.

53.3.2 Sample Preparation

Samples should be added to the rotor in small increments and packed down firmly using the packing tool provided with the instrument. Where sample quantity is less than rotor volume, either packing or leaving the sample loose may be recommended. Balanced spacers may also be used when sample size is limited (especially when spinning at high speeds). Rotor components must be firmly and completely assembled. Poor sample preparation and rotor assembly may result in difficulties with achieving stable spinning or even result in catastrophic rotor or probe failure.

53.3.3 Acquisition Parameters for CP/MAS

CP/MAS is the most common experiment used for analyzing SOM because it is faster than the direct methods discussed below. CP transfers magnetization from abundant ^{1}H nuclei to the less-abundant ^{13}C nuclei and also takes advantage of the relatively fast relaxation of protons and thus allowing the user to acquire signal intensity more quickly than with direct methods.

The following are only general guidelines for setting acquisition conditions; details of spectrometer operation vary widely, therefore consultation with the NMR spectroscopist is highly recommended. The main acquisition parameters are relaxation delay (time required for the nuclei to reequilibrate), proton 90° pulse length, CP contact time (the length of time during which magnetization is transferred from ^{1}H to ^{13}C nuclei), sweep width (SW) (range of frequencies covered in a signal pulse), and acquisition time (the length of time a given free induction decay [FID] is monitored). The recycle time (time between consecutive scans) is the sum of the acquisition time and relaxation delay.

1 *Relaxation delay*: The relaxation delay must be long enough to achieve complete spin–lattice relaxation of the protons (five times the proton spin–lattice relaxation time, T_1H note: spin–lattice relaxation occurs in the longitudinal direction (z-axis) corresponding to the magnetic field). This delay is approximately 4 s for glycine, 1–2 s for SOM samples high in C, such as litter and forest floor, and is often reduced to 0.4 or 0.5 s for low-C mineral soil samples. If proton spin–lattice relaxation is not complete, the S/N ratio is reduced. The other constraint is that very rapid pulsing may cause sample heating or excessive load on the high-power components, so that operators may recommend a longer relaxation time than required by the T_1H constraint.

2 *Proton 90° pulse length*: The proton 90° pulse length is typically 3–4 μs, and should be previously determined on a standard such as glycine. It is usually not determined directly, but by looking at the change in the ^{13}C CP signal as the proton pulse length is varied. The NMR signal is a null at 180° and 360° and negative at 270°. At the start of the CP pulse sequence, the proton magnetization is rotated 90° into the x–y plane, and remains locked there during CP when the ^{13}C and ^{1}H fields are matched in the rotating reference frame.

3 *Cross polarization contact time*: The CP contact time (t_c) is the time during which magnetization is transferred from protons to C. The CP process is most

efficient for C in rigid structures with attached protons, and weakened for C remote from protons, and in structures with motion in the solid state. Therefore, CP is typically very efficient for *O*- and di-*O*-alkyl C in cellulose, and much slower for highly condensed aromatic structures, such as those produced by biomass burning. CP is also less efficient for long alkyl chains that have rotational motion and for methyl and methoxyl groups that can rotate (Alemany et al. 1983). In general, the highest overall intensity is typically found with t_c around 1 ms, but it is sometimes increased to 1.5 or 2 ms to improve the representation of aromatic C, such as those in charcoal. Simply increasing t_c will not continue to increase signal, because of the decay of the proton magnetization in the rotating frame (with a time constant of $T_{1\rho}H$ which is the spin–lattice relaxation time of protons in the rotating frame and is indicative of the rate of proton magnetization decay during contact time). The presence of paramagnetic species such as iron oxides or copper (Cu^{2+}) also reduces CP signal intensity because they reduce the $T_{1\rho}H$ of nearby protons, thus shortening the time that they can transfer magnetization. During simple CP, the proton and C power levels are constant, but with RAMP, either C or proton power may be varied to enhance CP efficiency. This largely compensates for the loss of CP efficiency with high-speed spinning.

After CP, the proton power is left on at sufficient levels to decouple the protons, and the FID signal is acquired. This is the superposition of all the frequencies in the spectrum decaying in time. It may last <5 ms for mineral soil samples, up to 20 ms for fresh litter, and several hundred milliseconds for pure compounds. Observing the FID on the screen gives an idea of the quality to be expected. A fast buildup of signal is expected from a high-C sample, while very broad signals, such as C close to paramagnetic centers and from probe background give a very short-lasting spike. The acquisition time (AQ) should be long enough to capture the FID faithfully, as cutting it off causes artifacts around the baseline and loss of resolution. Alternatively, there is no need to go beyond about twice the length of the FID, as this would simply acquire noise and add to the duty cycle of the instrument. The raw data are stored as the FID, allowing multiple processing.

4 *Sweep width*: For SOM with a chemical shift range of around 200 ppm, the SW should be at least 300 ppm, even up to 400 ppm for samples expected to give broad and weak signals. At 75 MHz for ^{13}C, this means 22,500 to 30,000 Hz. The minimum sampling rate is twice the frequency (called the Nyquist frequency), so for example, with 25,000 SW, the sampling rate is 50,000 Hz, or 20 μs/point (this is called the dwell time). For a 1 K spectrum with 1024 data points, this makes the acquisition time 20.48 ms. This gives a digital resolution of 24.4 Hz/point (sufficient for most SOM samples).

5 *Acquisition time*: For a low-C sample, the acquisition time may even be reduced to 512 points (10.24 ms), but with the sampling rate still corresponding to 1024 points. To increase digital resolution the spectrum size can be increased to 2 K or 4 K, but again, the acquisition time can be shortened if appropriate. These conditions are quite different than for solution (or even solid state) NMR of pure compounds, where the SW is minimized, and data size and acquisition time are typically much larger to optimize resolution.

53.3.4 Direct Polarization or Bloch Decay Parameters

Direct observation experiments are sometimes preferred to analyze SOM. BD is also referred to as direct polarization (DP) or single-pulse excitation (SPE) and is a simple acquisition using a 90° ^{13}C pulse, without intensity enhancement. This technique is employed because in CP, ^{13}C nuclei are observed indirectly through magnetization transfer from nearby ^{1}H nuclei. This may underestimate C that are not in the vicinity of protons, broadened by proximity to paramagnetic species, or have some molecular mobility, and thus, direct observation provides more quantitative intensity distribution. The maximum theoretical CP enhancement is a factor of 4 (corresponding to the $^{1}H/^{13}C$ frequency ratio); although with many SOM samples it is nearer to 1.5–2.5 (Dria et al. 2002). With BD, the relaxation delay is controlled by the spin–lattice relaxation time of ^{13}C, so that delays ($5\times{}^{13}C$ T_1) are typically 100 s. The longer relaxation time for C results in less number of scans and much longer experiment times to acquire spectra with S/N ratios comparable to that obtained by CP. In addition, BD spectra generally have much lower S/N for a given number of scans, and often lower resolution. It may not even be possible to acquire a usable BD spectrum; rather than suggesting a limiting amount of C, one predictor of success is a reasonable CP spectrum after 500 scans. A typical BD acquisition is 1000 scans, requiring at least 24 h, which can be compared with a 1000 scan CP. However, the value of BD spectra lies in their quantitative reliability.

53.3.5 Dipolar Dephasing Parameters

Another very informative experiment is dipolar dephasing (DD). The delay employed in the DD experiment allows signals from protonated C to decay before data acquisition. This results in a spectrum that contains only signals from nonprotonated C and C with molecular mobility (namely, methyl group rotation and vibration (wiggling) of long-chain CH_2 groups). In the DD experiment, decoupling is turned off during a short delay, typically 45–60 μs, between CP and acquisition. With decoupling turned off, the dipolar interactions between the ^{13}C and ^{1}H nuclei cause loss of the ^{13}C signal. Just as for CP, these interactions are weaker for C that are far from protons, or have some motion in the solid state. Therefore, DD spectra have the strongest intensity for C without attached C (typically carboxyl > phenolic > aromatic) and reduced intensity for mobile C, such as methyl, methoxyl, and long-chain CH_2 groups. While DD can be used quantitatively (Hatcher 1987; Smernik and Oades 2001a) it is usually used to obtain qualitative structural information. The dephasing time should be adjusted to null the *O*-alkyl signal around 73 ppm. It should not vary much for similar samples.

53.3.6 Total Suppression of Sideband Parameters

With instruments of 300 MHz and higher, where higher spinning speeds are not available, or not suitable (e.g., a large sample volume is needed to acquire signal), TOSS can be used to eliminate SSBs. This distorts the relative areas, not only by the loss of the intensity in SSBs, but also by the intensity losses (possibly nonselective) during the complex TOSS sequence. These have not been well-studied for SOM. The SSBs appear at multiples of the spinning speed (Figure 53.1), and their severity generally increases with chemical shift, as the bonding asymmetry increases. For example, at 300 MHz and 4500 Hz MAS, TOSS is hardly needed if the aromatic and carboxyl peaks are small. However, at 400 MHz (100 MHz for ^{13}C) with 5 kHz MAS, a spectrum with high aromaticity is hardly useful without TOSS. It is particularly useful to combine TOSS with DD, where intensity is concentrated in high SSB regions, and the results are used qualitatively.

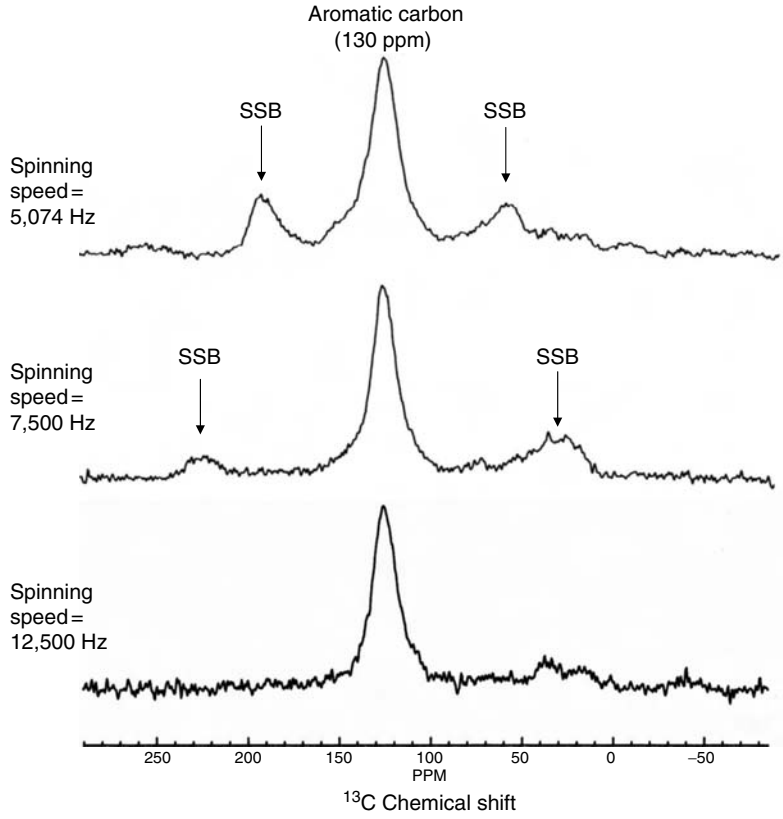

FIGURE 53.1. CP/MAS ^{13}C NMR spectra of charred biomass acquired at 75 MHz (300 MHz instrument) at different spinning speeds illustrating the presence of spinning sidebands (SSBs) at low-spinning speeds. SSBs are spun outside of the spectral window (SW) at higher spinning speeds (12,500 Hz).

53.3.7 Background Signal Considerations

The background signal from rotor and probe components is usually a problem for BD spectra, and CP spectra of samples low in C (Preston 2001; Smernik and Oades 2001b). This is usually seen as a very broad signal with a maximum of around 110–115 ppm, so that it may be interpreted as high aromaticity. Background varies with the type of probe and rotor, and may also be more severe for samples low in C and high in paramagnetic species as the latter seem to induce initial spikes in the FID. The usual approach is to run an empty rotor, and subtract the FIDs. It is not usually necessary to run a background for each sample, or to use the same rotor, although backgrounds must be run for each type of experiment. Smernik and Oades (2000a) found that a 10 s delay gave the same result as longer delays for the BD background signal, but this should be checked for the particular combination of spectrometer and probe. It may not be necessary to have the same number of scans (depending on the software used), as one of the FIDs can be scaled. However, if one wishes to compare the absolute intensity, e.g., of CP vs. BD, the same number of scans should be used for the sample and background. When running a background, it is useful to save the data at several different numbers of scans.

53.3.8 Other Experiments and Considerations

Readers may be interested in other, more sophisticated experiments, such as spin counting to measure ^{13}C observability (Smernik and Oades 2000a,b), specific effects of paramagnetics (Preston et al. 1989; Skjemstad et al. 1994; Schmidt et al. 1997; Gélinas et al. 2001; Smernik and Oades 2002; Gonçalves et al. 2003; Schilling and Cooper 2004), proton spin relaxation editing (PSRE; Preston and Newman 1995), restoration of spectra via TCH and $T_{1\rho}H$ editing (RESTORE, Smernik et al. 2004), more detailed investigations of quantitation (Mao et al. 2000) and molecular mobility (Hu et al. 2000), and two-dimensional NMR techniques (Mao et al. 2001).

53.4 DATA PROCESSING

Several stages are required for data processing, and make a great difference to the final spectrum. It should also be noted that even if researchers cannot acquire their own data, it is very informative and useful for users to process and plot their own data, which is often done at a separate workstation. Fourier transformation converts the time–domain FID into a frequency–domain spectrum. Before this, the FID is usually modified to increase the S/N. The most common manipulation is line broadening (LB), in which the FID is multiplied by a decaying exponential, to enhance the initial portion where the S/N is higher. As a general guide, the LB (in Hz) is typically at least as large as the digital resolution (e.g., 30 Hz). The LB can be increased until it starts to cause loss of resolution or distortion in the spectrum. Sometimes, spectra may be plotted with different LB values, to enhance broader vs. sharper features as displayed in Figure 53.2. LB can be combined with other manipulations. If the AQ

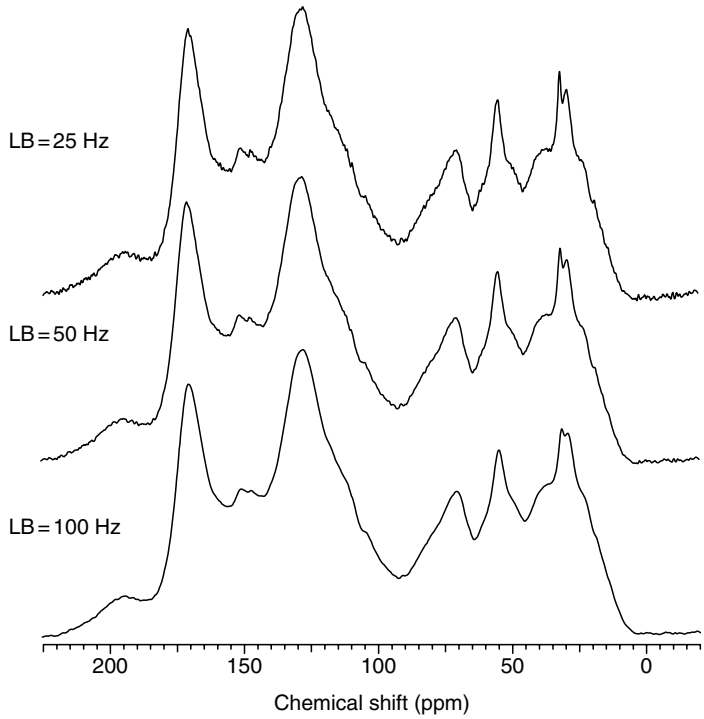

FIGURE 53.2. CP/MAS ^{13}C NMR spectra of HF/HCl-treated peat humic acid processed with different values of line broadening (LB). A loss of resolution is noticeable in the methylene C region (30–34 ppm). Data were acquired at 75 MHz (300 MHz instrument) using RAMP-CP and a MAS rate of 13 kHz.

is much longer than the obvious FID, the last half of the FID may be set to zero. Resolution may be increased by zero-filling—doubling the data size, which interpolates points. The effect of initial spikes can be modified by setting the first two or four points to zero or removing them by left-shifting. A variety of other apodization functions are available, for which a NMR textbook should be consulted.

The purpose of phasing is to produce a pure absorption-mode spectrum, which can be difficult to do with broad features and rolling baselines. Several iterations may be required. An example of a poorly phased and a well-phased spectrum is illustrated in Figure 53.3. Often SOM spectra have a minimum around 110 ppm, and the depth of this valley can be greatly affected by phasing. After phasing, baseline correction may be needed before the spectrum can be integrated. Many NMR data analysis programs have built in automatic and manual baseline correction functions that can be employed to correct baseline irregularities before peak area integration. Integration of a ^{13}C NMR spectrum can be accomplished by using general regions, i.e., alkyl C (0–45 ppm), *O*-alkyl (45–110 ppm), aromatic and substituted aromatic (110–160 ppm), and carboxylic and carbonyl C (160–220 ppm). This approach is commonly used and area regions are typically expressed as the percentage of the total signal (as illustrated in Figure 53.4). Furthermore, chemical shifts can be used to identify specific groups of compounds typically found in SOM, such as those listed in Table 53.1. It should be noted that some NMR methods are not fully quantitative and the data should be considered as semiquantitative estimates. However, solid-state ^{13}C NMR is valuable when comparing soil samples and for understanding SOM degradation and transformation processes and in most instances can be used to make relative comparisons between samples, which are analyzed using the same NMR instrument and acquisition parameters. In addition to using general integration regions, more specific regions can be integrated that

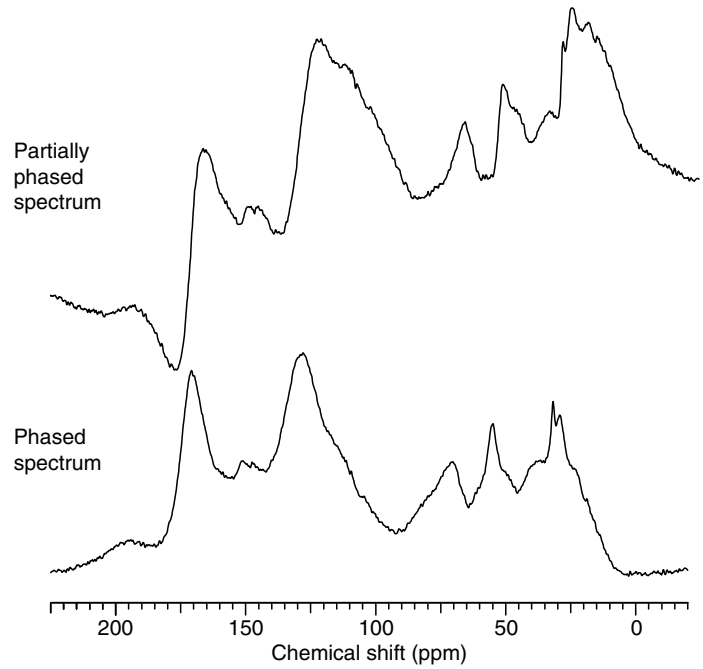

FIGURE 53.3. CP/MAS ^{13}C NMR spectra of HF/HCl-treated peat humic acid. The top spectrum has not been completely phased. When the spectrum is completely phased, both sides of the baseline will be equivalent. Data were acquired at 75 MHz (300 MHz instrument) using RAMP-CP and a MAS rate of 13 kHz.

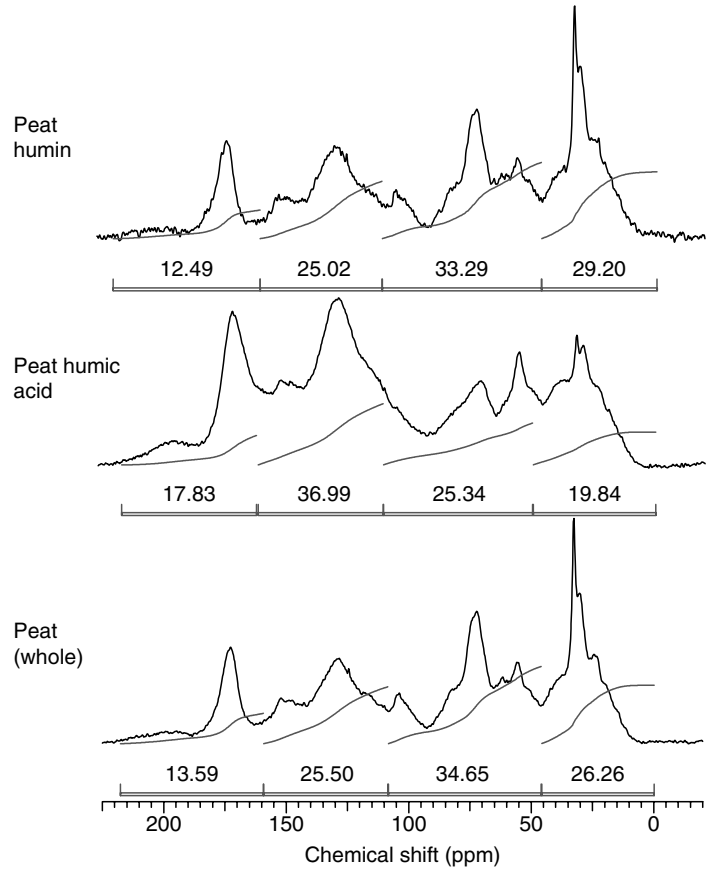

FIGURE 53.4. CP/MAS ^{13}C NMR spectra of HCl/HF-treated peat (whole), peat humic acid, and peat humin. Integrals and relative signal intensities (in percent) are displayed to demonstrate how CP/MAS ^{13}C NMR can be used to compare the relative abundance of structural groups in SOM. Data were acquired at 75 MHz (300 MHz instrument) using RAMP-CP, a MAS rate of 13 kHz and processed with a line broadening of 25 Hz.

TABLE 53.1 Typical Chemical Shift Ranges for Constituents Found in SOM

Chemical shift range (ppm)	C Structure characteristics
0–45	Unsubstituted alkyl C: Includes straight-chain methylene C (30–34 ppm) and terminal methyl groups (15 ppm). Branched methylene C is found more downfield (35–45 ppm)
45–65	Substituted alkyl C such as that found in amines (45–46 ppm) and methoxyl groups (56 ppm)
65–95	Oxygen-substituted C, ring C in carbohydrates, and C in ethers
95–110	Dioxygen-substituted aliphatic C and anomeric C in carbohydrates (105 ppm)
110–145	Aromatic C
145–160	Phenolic C
160–190	Carboxylic, amide, and ester C
190–220	Carbonyl C

Source: Adapted from Malcolm, R.L. in M.H.B. Hayes, P. MacCarthy, R.L. Malcolm, and R.S. Swift (Eds.), *Humic Substances II*, Wiley, New York, 1989, 339–372; Baldock, J.A. and Skjemstad, J.O., *Org. Geochem.*, 31, 697, 2000.

pertain to a specific component (see Table 53.1 for examples of specific regions) or integrate from peak valley to valley.

Data interpretation can go beyond estimates of signal regions. Specific structural components of SOM can be identified based on their chemical shift. Users should keep in mind when identifying SOM structures that many structural entities will have more than one signal in addition to specific chemical shift values. For example, lignin will have both methoxy (56 ppm) and phenolic signals (140–160 ppm).

53.5 COMMENTS

Solid-state NMR methods can be extremely powerful for studying SOM structure and biogeochemistry. This technique is advantageous because it enables the nondestructive analysis of small quantities of whole soils. Samples do not need to be soluble for analysis and the analysis of whole samples reduces the formation of artifacts through extraction. The relative proportion of alkyl, *O*-alkyl, aromatic, phenolic, carboxylic, and carbonyl C can be ascertained. However, NMR instrument access may be limited thus preventing the analysis of large quantities of samples (i.e., NMR may not be used for routine analysis). Samples low in C cannot be analyzed without pretreatment due to both the low natural abundance and low inherent sensitivity of ^{13}C and consequently there are limitations to the quantitative reliability of intensity distributions especially for CP spectra (Mao et al. 2000). However, external spin counting techniques can be used to define what fraction of sample C was actually observed. Finally, the multitude of structures found in SOM may result in broad resonances, which may restrict the detail to which structural assignments can be made. However, solid-state ^{13}C NMR provides information that is complementary to other SOM methods and provides an excellent starting point for more structure-specific approaches such as multidimensional solution-state NMR spectroscopy, mass spectrometry-based analyses, and wet-chemical analysis of specific compounds.

REFERENCES

Alemany, L.B., Grant, D.M., Alger, T.D., and Pugmire, R.J. 1983. Cross polarization and magic angle sample spinning NMR spectra of model organic compounds. 3. Effect of the $^{13}C—^{1}H$ dipolar interaction on cross polarization and carbon–proton dephasing. *J. Am. Chem. Soc.* 105: 6697–6704.

Baldock, J.A. and Skjemstad, J.O. 2000. Role of the soil matrix and minerals in protecting natural organic materials against biological attack. *Org. Geochem.* 31: 697–710.

Bryce, D.L., Bernard, G.N., Gee, M., Lumsden, M.D., Eichele, K., and Wasylishen, R.E. 2001. Practical aspects of modern routine solid-state multinuclear magnetic resonance spectroscopy: one-dimensional experiments. *Can. J. Anal. Sci. Spect.* 46: 46–82.

Dria, K.J., Sachleben, J.R., and Hatcher, P.G. 2002. Solid-state carbon-13 nuclear magnetic resonance of humic acids at high magnetic field strengths. *J. Environ. Qual.* 31: 393–401.

Gélinas, Y., Baldock, J.A., and Hedges, J.I. 2001. Demineralization of marine and freshwater sediments for CP/MAS ^{13}C NMR analysis. *Org. Geochem.* 32: 677–693.

Gonçalves, C.N., Dalmolin, R.S.D., Dick, D.P., Knicker, H., Klamt, E., and Kögel-Knabner, I. 2003. The effect of 10% HF treatment on the resolution of CPMAS ^{13}C NMR spectra and on the quality of organic matter in Ferralsols. *Geoderma* 116: 373–392.

Hatcher, P.G. 1987. Chemical structural studies of natural lignin by dipolar dephasing solid-state

^{13}C nuclear magnetic resonance. *Org. Geochem.* 11: 31–39.

Hu, W.-G., Mao, J., Xing, B., and Schmidt-Rohr, K. 2000. Poly(methylene) crystallites in humic substances detected by nuclear magnetic resonance. *Environ. Sci. Technol.* 34: 530–534.

Kögel-Knabner, I. 2000. Analytical approaches for characterizing soil organic matter. *Org. Geochem.* 31: 609–625.

Malcolm, R.L. 1989. Applications of solid-state ^{13}C NMR spectroscopy to geochemical studies of humic substances. In M.H.B. Hayes, P. MacCarthy, R.L. Malcolm, and R.S. Swift, Eds. *Humic Substances II*. Wiley, New York, pp. 339–372.

Mao, J.-D., Hu, W.-G., Schmidt-Rohr, K., Davies, G., Gabhour, E.A., and Xing, B. 2000. Quantitative characterization of humic substances by solid-state carbon-13 nuclear magnetic resonance. *Soil Sci. Soc. Am. J.* 64: 873–884.

Mao, J.-D., Xing, B., and Schmidt-Rohr, K. 2001. New structural information on a humic acid from two-dimensional ^{1}H–^{13}C correlation solid-state nuclear magnetic resonance. *Environ. Sci. Technol.* 35: 1928–1934.

Preston, C.M. 1996. Applications of NMR to soil organic matter analysis: history and prospects. *Soil Sci.* 161: 144–166.

Preston, C.M. 2001. Carbon-13 solid-state NMR of soil organic matter—using the technique effectively. *Can. J. Soil Sci.* 81: 255–270.

Preston, C.M. and Newman, R.H. 1995. A long-term effect of N fertilization on the ^{13}C CPMAS NMR of de-ashed humin in a second-growth Douglas-fir stand of coastal British Columbia. *Geoderma* 68: 229– 241.

Preston, C.M., Schnitzer, M., and Ripmeester, J.A. 1989. A spectroscopic and chemical investigation on the de-ashing of a humin. *Soil Sci. Soc. Am. J.* 53: 1442–1447.

Schilling, M. and Cooper, W.T. 2004. Identification of copper binding sites in soil organic matter through chemical modifications and ^{13}C CP-MAS NMR spectroscopy. *Environ. Sci. Technol.* 38: 5059–5063.

Schmidt, M.W.I., Knicker, H., Hatcher, P.G., and Kögel-Knabner, I. 1997. Improvement of ^{13}C and ^{15}N CPMAS NMR spectra of bulk soils, particle size fractions and organic material by treatment with 10% hydrofluoric acid. *Eur. J. Soil Sci.* 48: 319–328.

Simpson, M.J. and Hatcher, P.G. 2004. Determination of black carbon in natural organic matter by chemical oxidation and solid-state ^{13}C nuclear magnetic resonance spectroscopy. *Org. Geochem.* 35: 923–935.

Skjemstad, J.O., Clarke, P., Taylor, J.P., Oades, J.M., and Newman, R.J. 1994. The removal of magnetic materials from surface soils. A solid-state ^{13}C CP/MAS NMR study. *Aust. J. Soil Res.* 32: 1215–1229.

Smernik, R.A. 2005. Solid-state ^{13}C NMR spectroscopic studies of soil organic matter at two magnetic field strengths. *Geoderma* 125: 249–271.

Smernik, R.J. and Oades, J.M. 2000a. The use of spin counting for determining quantitation in solid state ^{13}C NMR spectra of natural organic matter. 1. Model systems and the effects of paramagnetic impurities. *Geoderma* 96: 101–129.

Smernik, R.J. and Oades, J.M. 2000b. The use of spin counting for determining quantitation in solid state ^{13}C NMR spectra of natural organic matter. 2. HF-treated soil fractions. *Geoderma* 96: 159–171.

Smernik, R.J. and Oades, J.M. 2001a. ^{13}C-NMR dipolar dephasing experiments for quantifying protonated and non-protonated carbon in soil organic matter and model systems. *Eur. J. Soil Sci.* 52: 103–120.

Smernik, R.J. and Oades, J.M. 2001b. Background signal in solid-state ^{13}C NMR of soil organic matter (SOM)—quantification and minimization. *Solid State Nucl. Mag. Res.* 20: 74–84.

Smernik, R.J. and Oades, J.M. 2002. Paramagnetic effects on solid state carbon-13 nuclear magnetic resonance spectra of soil organic matter. *J. Environ. Qual.* 31: 414–420.

Smernik, R.J., Olk, D.C., and Mahieu, N. 2004. Quantitative solid-state ^{13}C NMR spectroscopy of organic matter fractions in lowland rice soils. *Eur. J. Soil Sci.* 55: 367–379.

Chapter 54
Stable Isotopes in Soil and Environmental Research

B.H. Ellert and L. Rock
Agriculture and Agri-Food Canada
Lethbridge, Alberta, Canada

54.1 INTRODUCTION

Isotopes refer to elements with nuclei having the same number of protons, but differing numbers of neutrons, so that the masses of contrasting isotopes differ by one to a few neutrons. Isotopes of a specific element have the same chemical properties because they have the same number of electrons. Owing to their mass differences, however, isotopes of an element undergo chemical, biological, and physical reactions at slightly and consistently different rates, leading to isotopic fractionation whenever reactants are not exhausted. As a result, natural variations in isotopic abundance provide powerful insight into element dynamics, but fractionation by intertwined transformations can also complicate interpretations.

Isotopes of an element may be stable or radioactive. Radioactive isotopes emit radiation as they undergo radioactive decay and are transformed to new elements. One stable isotope accounts for a majority of those in most elements, and at natural abundance radioactive isotopes are far less plentiful than even the rare stable isotopes. Special reagents containing elements that are artificially enriched in one or more radioactive or stable isotopes are used in manipulative tracer studies. The distinctive isotopic composition of tracers (usually enriched in the normally rare isotope) enables element transfers and transformations to be followed in systems where otherwise it would be difficult or impossible.

Isotopic techniques to study element transfer and transformation in plants and soils were among the earliest peaceful uses of nuclear technology after 1945. These early applications typically involved adding artificially enriched radioactive (e.g., ^{32}P, ^{14}C) or stable isotopes (^{15}N), and subsequently analyzing plant tissues and soil fractions to determine the fate of the added nuclides (Noggle 1951; FAO/IAEA 1966). Similar approaches remain very useful (e.g., Frossard and Sinai 1997; Di et al. 2000; IAEA 2001). Among the earliest and most widely used stable isotopes in agroecosystems is artificially enriched ^{15}N to trace the availability and fate of fertilizer N (Norman and Werkman 1943; Hauck and Bremner 1976). Although stable isotopes tend to be more expensive to obtain and analyze than

radioactive ones, the lack of radioactive N with a sufficiently long half-life ensured early use of ^{15}N in soil and environmental research.

In this chapter we focus on using stable isotopes, at both natural abundance and artificially enriched levels, to investigate biogeochemical cycling in soil and environmental research. We focus on stable isotopes, because (i) they include elements (e.g., ^{2}H, ^{13}C, ^{15}N, ^{18}O, ^{34}S) used to study the productivity and environmental impacts of agriculture, (ii) they have provided insight into the biogeochemical cycling of elements at both natural and artificially enriched levels, (iii) they are not subject to the safety and regulatory concerns of radioactive isotopes when applied at artificially enriched levels, and (iv) recent advances in stable isotope ratio mass spectrometry (IRMS) have improved analytical accessibility and precision. Our main emphasis will be on routine C and N isotopic analysis of common soil constituents.

54.2 NOMENCLATURE, NOTATION, STANDARDS, AND CONVERSIONS

The light elements (<40 u) with stable isotopes most widely used in soil and environmental research include H, C, N, O, and S (Table 54.1), although others have also been used (e.g., Li, B, Si, Cl, He, Ne, Ar). The abundances of the most common isotopes of each element range from 95 to 99 atom%, or more (Table 54.1). Stable isotope studies are based on measured changes in the abundance of the rarer isotopes. Larger shifts are encountered in artificial tracer studies, when reagents highly enriched in the rarer isotope (e.g., urea with 10 to 90 atom% ^{15}N) are added to the system being investigated (ranging from laboratory microcosms to field plots). These studies involve deliberate manipulation of isotopic abundance, are more amenable to carefully focused hypotheses, and target transfers and transformations over smaller temporal and spatial scales. The relatively small shifts associated with natural isotopic fractionation are usually used to study integrated effects of biogeochemical processes over large scales. Robinson (2001) compared the main features of enriched versus natural abundance ^{15}N techniques, and distinguished between using natural ^{15}N as a tracer or an integrator of N cycling processes.

TABLE 54.1 Stable Isotopes Widely Used in Soil and Environmental Research, with Corresponding Atomic Masses (u, g mol^{-1}), Abundances (Atom%)

Element	Isotope	Atomic mass (u)	Nominal abundance (atom%)
Hydrogen	^{1}H	1.007825032	99.984426
	^{2}H or D	2.014101778	0.015574
Carbon	^{12}C	12.000000000	98.894400
	^{13}C	13.003354838	1.105600
Nitrogen	^{14}N	14.003074007	99.633700
	^{15}N	15.000108970	0.366300
Oxygen	^{16}O	15.994914622	99.762060
	^{17}O	16.999131500	0.037900
	^{18}O	17.999160400	0.200400
Sulfur	^{32}S	31.972070730	95.039570
	^{33}S	32.971458540	0.748650
	^{34}S	33.967866870	4.197190
	^{36}S	35.967080809	0.014590

Source: Data after Coplen et al., Water Resources Investigations Report 01-4222, US Department of the Interior, US Geological Survey, Reston, Virginia, 2002 and references therein.

By convention, isotope abundances are expressed as molar fractions or ratios. In artificially enriched tracer studies, abundance typically is expressed as an atom%, which is the atom fraction, F, multiplied by 100:

$$F = {}^{\text{rare}}E/{}^{\text{total}}E \approx {}^{\text{rare}}E/\left({}^{\text{abundant}}E + {}^{\text{rare}}E\right); \quad \text{for example, } {}^{13}\text{C}/\left({}^{12}\text{C} + {}^{13}\text{C}\right) \tag{54.1}$$

where ${}^{\text{rare}}E$ is the moles of the rare isotope of element E and ${}^{\text{abundant}}E$ is the moles of the most abundant isotope of the same element. Atom percent enrichment or atom percent excess (APE) is defined as the difference between sample atom% after dosing with artificially enriched tracer and the baseline or background atom%:

$$\text{APE} = \left(F_{\text{postdose}} - F_{\text{baseline}}\right) \times 100 \tag{54.2}$$

The fractional molar abundance, F, differs from the mass fraction according to differences in isotope masses (Table 54.1). The molar isotope ratio, R, is defined as follows:

$$R = {}^{\text{rare}}E/{}^{\text{abundant}}E; \quad \text{for example, } {}^{13}\text{C}/{}^{12}\text{C} \tag{54.3}$$

Thus F and R are interrelated (to close approximation; for example, contributions of radioactive ^{11}C and ^{14}C usually are negligible relative to ^{12}C and ^{13}C) as follows:

$$R = F/(1 - F) \quad \text{and} \quad F = R/(R + 1) \tag{54.4}$$

In natural abundance studies we are interested in very small variations of R, so abundances in samples of interest are expressed as differences relative to the abundance in an internationally defined standard. This method of expression is called the delta (δ) notation, and is defined as follows:

$$\delta_{\text{sample}}() = \left\{\left(R_{\text{sample}}/R_{\text{standard}}\right) - 1\right\} \times 1000 \tag{54.5}$$

with R_{sample} being the molar isotope ratio in the sample and R_{standard} being that in an international standard (Table 54.2). Thus δ values refer to isotope ratio differences, in parts per thousand, relative to a known standard. The δ value of each standard, and any sample with an identical R, is by definition 0‰. Samples that are enriched in the rare isotope relative to the standard have positive δ values, whereas samples that are depleted in the rare isotope relative to the standard have negative δ values. The absolute R of the international standards (Table 54.2) may be used to convert δ values of a sample back to the molar ratios or fractions of isotopes in the element analyzed using Equation 54.4 and Equation 54.5. To convert a δ value into atom%, the following equation may be used:

$$\text{atom}\% = 100 \times [R_{\text{standard}} \times (1 + (\delta/1000))]/[1 + R_{\text{standard}} + (R_{\text{standard}} \times \delta/1000)] \tag{54.6}$$

More information on units of measurement and their relationships can be found in Boutton (1991) and Scrimgeour and Robinson (2004).

54.3 INSTRUMENTATION

Most often, stable isotope ratios are measured using a gas source IRMS with electron impact ionization. The constituent of interest (e.g., N in whole soil, plant tissue, solute, environmental gas) must first be isolated and converted into a gas (Table 54.2) suitable for IRMS

TABLE 54.2 Gases and Corresponding Masses Analyzed in IRMS for Stable Isotope Analysis of Light Elements, Gas Species with Interfering Masses, and Relevant International Standards with Absolute Isotope Ratios. Isotopes in Bold Refer to the Element of Interest

Element	Gas analyzed	Masses measured	Interfering masses	International standard[a]
Hydrogen	H_2	2: $^{\mathbf{1}}\mathbf{H}^{1}H$	3: $^{1}H^{1}H^{1}H$	V-SMOW
		3: $^{\mathbf{2}}\mathbf{H}^{1}H$		$2R_{\text{V-SMOW}} = 0.00015576$
Carbon	CO_2	44: $^{\mathbf{12}}\mathbf{C}^{16}O^{16}O$	45: $^{12}C^{17}O^{16}O$	V-PDB
		45: $^{\mathbf{13}}\mathbf{C}^{16}O^{16}O$		$13R_{\text{V-PDB}} = 0.0112372$
Nitrogen	N_2	28: $^{\mathbf{14}}\mathbf{N}^{14}N$		
		29: $^{\mathbf{15}}\mathbf{N}^{14}N$		Atmospheric N_2
		30: $^{\mathbf{15}}\mathbf{N}^{\mathbf{15}}\mathbf{N}$		$15R_{\text{atmN2}} = 0.0036765$
	N_2O	44: $^{\mathbf{14}}\mathbf{N}^{14}N^{16}O$	45: $^{14}N^{14}N^{17}O$	
		45: $^{\mathbf{15}}\mathbf{N}^{14}N^{16}O$		
Oxygen	CO_2	44: $^{12}C^{\mathbf{16}}\mathbf{O}^{16}O$	46: $^{13}C^{17}O^{16}O$;	V-SMOW
		46: $^{12}C^{\mathbf{18}}\mathbf{O}^{16}O$	46: $^{12}C^{17}O^{17}O$	$18R_{\text{V-SMOW}} = 0.00200520$
	CO	28: $^{12}C^{\mathbf{16}}\mathbf{O}$	30: $^{13}C^{17}O$	or
		30: $^{12}C^{\mathbf{18}}\mathbf{O}$		V-PDB
	N_2O	44: $^{14}N^{14}N^{\mathbf{16}}\mathbf{O}$	46: $^{15}N^{15}N^{16}O$;	$18R_{\text{V-PDB}} = 0.0020671$
		46: $^{14}N^{14}N^{\mathbf{18}}\mathbf{O}$	46: $^{15}N^{14}N^{17}O$	
Sulfur	SO_2	64: $^{\mathbf{32}}\mathbf{S}^{16}O^{16}O$	66: $^{32}S^{18}O^{16}O$;	V-CDT
		66: $^{\mathbf{34}}\mathbf{S}^{16}O^{16}O$	66: $^{33}S^{17}O^{16}O$;	$34R_{\text{V-CDT}} = 0.0450045$
			66: $^{32}S^{17}O^{17}O$	

[a] V-SMOW, Vienna Standard Mean Ocean Water; V-PDB, Vienna Peedee belemnite; V-CDT, Vienna Cañon Diablo troilite; *R*, molar ratio of the rare to the most abundant isotope of each element (i.e., $2R = {}^{2}H/{}^{1}H$, $13R = {}^{13}C/{}^{12}C$, $15R = {}^{15}N/{}^{14}N$, $18R = {}^{18}O/{}^{16}O$, $34R = {}^{34}S/{}^{32}S$).

analyses. For instance, to determine the isotopic composition of total soil C ($\delta^{13}C$ total C), all carbonaceous constituents (e.g., carbonates, plant residues, aromatic compounds, aliphatic compounds, and charcoal) are first oxidized to CO_2 gas. The masses analyzed by the IRMS are not 12 and 13, but 44 and 45, which represent molecules such as $^{12}C^{16}O^{16}O$ and $^{13}C^{16}O^{16}O$ (Table 54.2).

The software for most IRMS systems converts raw data (ion currents corresponding to the masses of each molecular ion) to δ values for rare isotopes of the element(s) of interest (e.g., $\delta^{13}C$), and corrects for interference by molecules with the same mass (e.g., for mass 45, $^{12}C^{17}O^{16}O$ and $^{13}C^{16}O^{16}O$ differ only in isotopic composition). For details on correcting $\delta^{13}C$ values, refer to Craig (1957), Santrock et al. (1985), or Werner and Brand (2001). Depending on the IRMS software, user intervention may be required to perform similar corrections for other gases, such as N_2O.

An IRMS comprises the following: a vacuum system, an inlet for introducing the sample gas, an ion source for ionizing the sample gas, an acceleration chamber, a magnet for separating the molecular ions (e.g., $^{12}C^{16}O^{16}O^{+}$, $^{13}C^{16}O^{16}O^{+}$, $^{12}C^{18}O^{16}O^{+}$), collectors (Faraday cups) to count the number of molecules, and a computer for instrument control, data acquisition, data storage, and data processing (converting raw counts to δ values, and sometimes computing element concentrations). The components and configuration of IRMS systems have been reviewed elsewhere (Brenna et al. 1997; de Groot 2004).

The stable isotope ratio of an element in a sample, such as finely ground plant tissue or a vial of soil air, may be determined by continuous flow-IRMS or by dual inlet-IRMS. Although various other techniques (e.g., optical emission spectroscopy, infrared spectroscopy, quadrupole MS) have been used, here we focus on CF-IRMS. With dual inlet-IRMS, off-line procedures are used to convert sample constituents to the appropriate gas, and subsequent isotopic analysis is independent from sample preparation and conversion. With CF-IRMS, various front-end preparation devices separate, purify, and convert the samples to the appropriate gas, which is transferred (usually in a stream of He carrier gas) to the IRMS in a continuous flow. The main components that may be included in a CF-IRMS system are shown schematically in Figure 54.1.

Preparation devices are used both to convert solid or liquid samples into gases via combustion (high-temperature oxidation) or pyrolysis (thermal degradation) and to separate, purify, and concentrate gaseous or liquid samples. Elemental analyzers are used to determine the isotope ratios of C, N, and S, while pyrolysis furnaces are used for isotopes of O and H (Gehre and Strauch 2003). Trace gases, such as nitrous oxide, may be preconcentrated to increase signal strength in the IRMS. This is achieved by using an off-line technique or an online peripheral device, such as that described by Brand (1995). Gas chromatography (GC) is used to separate and analyze mixtures of gases. Depending on the compounds to be

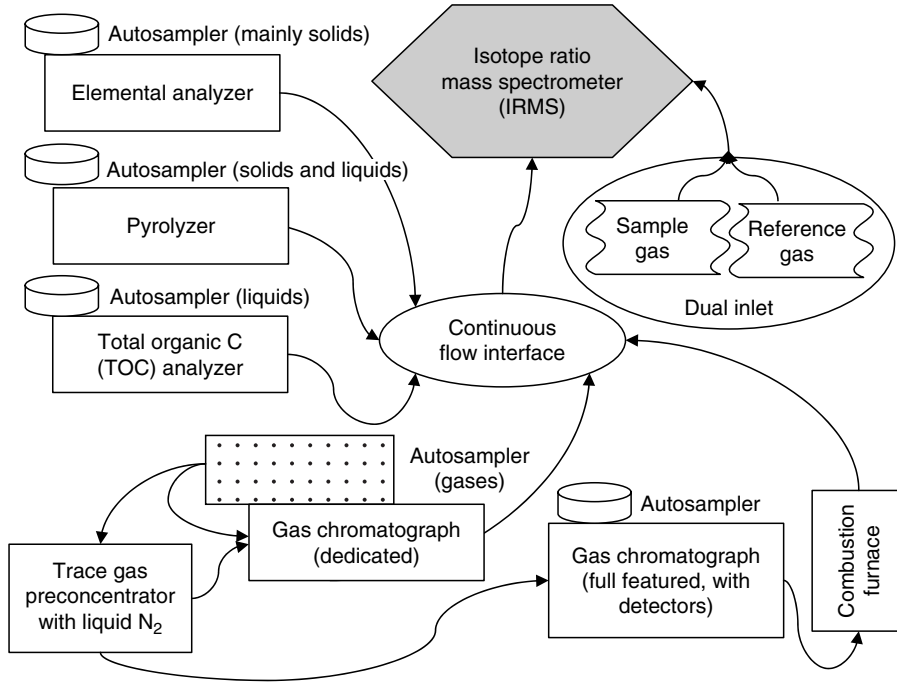

FIGURE 54.1. Schematic diagram of some common instrument configurations for analyzing stable isotopes in environmental samples by CF-IRMS using various front-end preparation devices or a dual inlet. A basic gas chromatograph (GC) to separate inorganic gases, such as CO_2, may be dedicated to CF-IRMS, whereas a full-featured GC with various detectors often is used to separate organic constituents which are oxidized to CO_2 for compound-specific ^{13}C analysis. Most CF-IRMS systems rarely include more than three preparation devices (sometimes including a dual inlet).

analyzed, a combustion furnace may be placed after the GC column, as in compound-specific isotope analysis (CSIA) of organic samples. Detailed information on the use of GC in IRMS can be found in Hayes et al. (1989), Brand et al. (1994), Meier-Augenstein (1999a,b), Whiticar and Snowdon (1999), or Glaser (2005). For determining $\delta^{13}C$ in dissolved C species (organic and inorganic), a total organic C (TOC) analyzer for liquids may be linked via continuous flow to an IRMS (St-Jean 2003).

54.4 SAMPLE PREPARATION AND ANALYSIS

Here we focus on the isotopes of C, N, and O in soils, including solid soil samples, liquid extracts from soils, and soil gases. Teece and Fogel (2004) recently reviewed methods for collecting and storing biological materials for isotopic analyses to address ecological questions. Sample preparation for and analysis of S isotopes are described by Mayer and Krouse (2004). Methods for the isotopic composition of water in soil–plant systems are discussed by Scrimgeour (1995). Practical information on various isotope techniques and their use in soil and environmental research can be found in a recent International Atomic Energy Agency manual (IAEA 2001).

Essential to all isotope analyses is that during sample preparation all isotopes of the element in the sample are completely converted to the gas required for IRMS, and that element contamination is avoided. Incomplete conversion or contamination will likely alter the isotopic composition and compromise the results, especially in natural abundance studies (Robinson 2001).

The final isotopic composition of the sample is expressed relative to a primary international standard, such as V-PDB for $\delta^{13}C$ (see Table 54.2). CF-IRMS systems often include provisions for introducing a sample of reference gas from a pressurized cylinder. In this way, sample gases produced by various preparation devices (e.g., elemental analyzer) may be compared with a uniform aliquot of reference gas, and IRMS performance may be assessed independently. Reference materials with known δ values are also included in an analytical run to verify preparation and overall analytical quality (Coplen et al. 2002). Additional information on referencing techniques and strategies in IRMS can be found in Werner and Brand (2001).

Primary reference materials consist of well-defined minerals or chemicals (e.g., carbonate, nitrate, sucrose), and are prepared and certified by various agencies (e.g., IAEA 2004). Secondary standards, such as soil or plant material that has been calibrated against an internationally certified standard, are often used to verify routine analyses. Ideally, these secondary standards would have a similar background matrix and chemical composition as the samples (Jardine and Cunjak 2005). To this end, IRMS laboratories working with soils and plants are encouraged to develop calibrations for widely distributed soil and plant materials that have some sort of certification for total C and N contents (e.g., see http://chemsrv0.pph.univie.ac.at/wwa/homepage_ww_neu/nist.htm [validated April, 2006]). Isotope values for C and N in natural matrix materials may be available from commercial suppliers (e.g., Elemental Microanalysis Ltd., Okehampton, Devon, UK).

To analyze $\delta^{15}N$ or $\delta^{13}C$ in soils and plants by CF-IRMS, we adjust sample and standard weights so that every capsule contains a similar amount of N or C. This means that much smaller weights of pure chemical standards with high C and N contents may be intermingled with plant and soil samples. Although uncertainty in sample weight should not appreciably

influence isotope measurements, they can influence measured N and C contents. Analytical conditions are more uniform when each capsule contains similar amounts of the element being analyzed and the background sample matrix is comparable.

54.4.1 Determination of the $\delta^{13}C$ Value for Soil Organic Matter

Inorganic C must be eliminated to analyze ^{13}C in soil organic matter, because many soils contain carbonates with greater $\delta^{13}C$ values ($\approx 0‰$ for primary carbonate) than those of organic matter. Small-scale acidification in silver capsules is useful to eliminate inorganic C after weighing and before combusting in an elemental analyzer coupled to an IRMS. This approach is widely used for marine sediments (Nieuwenhuize et al. 1994; Ryba and Burgess 2002), and may be extended to soil organic ^{13}C analysis. Since the organic C concentration is based on the preacidified sample weight, any weight change associated with acidification is immaterial. The C remaining after acidification consists of organic as well as charcoal-like materials, including those in soluble and fine particulate fractions.

Typically, between 10 and 70 mg soil is weighed into silver capsules, depending on the expected amount of soil organic C and instrument sensitivity. Greater sample weights are used when the C or N contents are low, so similar amounts of C or N per capsule are introduced to the elemental analyzer. With prior information on total C and N contents, the amount of inorganic C to be removed by acidification may be estimated as total C minus total N $\times$ 10, assuming an organic C/N ratio of $\approx$10. For example, a 50 mg soil sample containing 0.10% total N and 3.00% total C would have an expected inorganic C content of $\approx$2% (and contain 1 mg). Further assuming this 1 mg is present as $CaCO_3$, at least 28 μL 6 *M* HCl would be required to liberate the carbonate as $CO_{2(g)}$ (at least 167 μL 6 *M* HCl would be required for 50 mg pure $CaCO_3$).

A micropipette is used to dispense 50 to 80 μL of 6 *M* HCl into each capsule. The HCl is added in aliquots of 5 to 10 μL (smaller aliquots for more reactive samples) to every capsule in a tray holding 50, before adding successive aliquots. Others prefer unattended acidification whereby HCl vapor is allowed to diffuse, over several hours in an enclosed desiccator, to samples that have been weighed into capsules and moistened (Harris et al. 2001). Small-scale acidification is hampered when effervescence during the reaction of HCl with soil inorganic C causes capsules to overflow. We prefer direct addition of aqueous HCl, because the addition rate may be adjusted to contain effervescence, and samples are under close observation so that overflowing capsules are easily identified. In such rare instances, the problem sample is discarded and a new sample reacidified. To better contain samples and minimize overflowing, we use silver capsules with 8 mm diameters (wall height 11 mm), and secure 50 capsules in an acrylic holder (custom-built) for acidification and drying.

The total volume of HCl added is sufficient to react with at least 2 times the expected amount of inorganic C in the sample. So long as excess acid is added, it is more important that the entire sample is thoroughly wetted by and reacted with the HCl. For capsules containing >0.5 mg inorganic C (e.g., carbonate-rich subsoils), an intermediate drying period is used to drive off excess liquid after about 80 μL HCl has been added, and then further 10 μL aliquots are added to ensure thorough acidification (rarely more than 240 μL in all). Before the capsules are crimped closed, they are placed in a vacuum oven (approximately 16 h at 65°C and 20 kPa) to remove water and unreacted HCl. After drying, the capsules should be crimped closed and analyzed without delay or kept in a desiccator. If this is not done, calcareous samples will take up atmospheric water, because the reaction of HCl with soil carbonate produces $CaCl_2$ which is hygroscopic.

With silver capsules, the elemental analyzer must be configured properly (adequate temperature, proper O_2 dosing) to ensure complete combustion without the exothermic reaction obtained when tin capsules are combusted (these are corroded by HCl and fail to contain acidified samples). Since the silver capsules do not fully disintegrate in the combustion tube, the ash tends to build up faster and must be removed more frequently to ensure thorough combustion. To avoid inadvertent carbonate losses, the nonacidified samples used to calibrate elemental analyses are kept separate from the acidified samples until the autosampler carousel is loaded.

54.4.2 Determination of Total Soil $\delta^{13}C$ and $\delta^{15}N$ Values

Analysis of total $\delta^{13}C$ and $\delta^{15}N$ values for whole soil is straightforward: finely ground samples (typically 5 to 50 mg) are weighed into tin capsules, and then combusted in an elemental analyzer coupled to an IRMS. Sometimes the isotopes of both elements are determined in a single run (via peak jumping whereby the IRMS is temporarily retuned from masses 28, 29, and 30 to 44, 45, and 46). But this usually involves automated dilution with He at the elemental analyzer–IRMS interface to lower effluent [CO_2] to a measurable range with other parameters optimized for N_2. Isotope ratios of C and N are often determined in separate analytical runs, but the thermal conductivity detector of the elemental analyzer can measure the concentrations of both elements in a single run. Thus the isotope ratio of one element and the concentrations of both C and N may be analyzed in a singe run without dilution or peak jumping. Total soil N concentrations (and $\delta^{15}N$), however, are best determined on nonacidified soil, because acidification may degrade analytical accuracy and precision for N (Harris et al. 2001; Ryba and Burgess 2002). When the main focus is soil organic ^{13}C, we analyze nonacidified samples for total C and N using an independent elemental analyzer, and then analyze acidified samples to determine the organic C content and the $\delta^{13}C$ value by CF-IRMS.

Baccanti et al. (1993) reviewed the main requirements to successfully implement automated flash combustion of C and N. These include proper O_2 dosing to ensure complete oxidation without excessive consumption of reduced Cu, which is used to convert any NO, NO_2, and N_2O to N_2 (essential to recover total sample N and to prevent isobaric interference by N_2O during CO_2 analyses), maintaining a leak-free autosampler to exclude atmospheric N_2 and other extraneous gases, removing ash to maintain combustion in the hot zone, and maintaining unobstructed carrier gas flow through the entire system (especially the $MgClO_4$ moisture trap). Sometimes we use smaller sample weights and/or larger O_2 doses for analyzing C and N in plant tissues (5 to 10 mg and 15 mL at 200 kPa) compared to soils (25 to 75 mg and 10 mL at 200 kPa).

Since the thermal stability of many carbonate minerals is greater than that of most organic constituents, the elemental analyzer must be configured to attain complete conversion to $CO_{2(g)}$ where carbonates are present. To analyze $\delta^{15}N$ in carbonate-rich subsoils with low N contents (i.e., total $C/N > 20$), sometimes we use soda lime to remove CO_2 from the combustion effluent, otherwise CO_2 fragmentation in the IRMS ion source produces CO ions that may interfere with determination of masses 28, 29, and 30 (Table 54.2). At narrower C/N ratios (≤ 20), N_2 and CO_2 peaks are clearly separated, and any CO produced in the source may not be problematic.

54.4.3 Determining $\delta^{15}N$ Value of Ammonium, and $\delta^{15}N$ and $\delta^{18}O$ Values of Nitrate

Various techniques have been used to determine the $\delta^{15}N$ values of ammonium (NH_4^+) and nitrate (NO_3^-). Often nitrate plus nitrite are separated and chemically reduced to NH_4^+,

and then the procedures are the same as when NH_4^+ is the starting point. These include steam distillation, diffusion techniques, and sorption on cation-exchange resin. Diffusion techniques have been widely used in soil and environmental research, including hydrology. By increasing sample pH, aqueous NH_4^+ is converted to NH_3 gas, which diffuses to an acidic trap where it precipitates (e.g., as $(NH_4)_2SO_4$ when trapped by H_2SO_4) after drying. The precipitate is enclosed in a tin capsule, so the $\delta^{15}N$ value may be determined by CF-IRMS using an elemental analyzer. Sebilo et al. (2004) describe an ammonium diffusion technique for determining the $\delta^{15}N$ values of NH_4^+ and NO_3^-. Diffusion techniques, however, do not enable determination of the $\delta^{18}O$ value in nitrate.

Kohl et al. (1971) were among the first to test whether N isotopes can be used to identify the origin of aqueous N in surface water. Their paper sparked insightful discussions on the pros and cons of using natural ^{15}N abundance to study agricultural N dynamics. Taken alone, however, $\delta^{15}N$ values fail to distinguish among various nitrate sources, because the $\delta^{15}N$ values overlap and isotopic fractionation by various N transformations may further obscure the original source signature(s) (e.g., Kendall 1998). Clearer differentiation among nitrate sources became possible, however, after a new technique for measuring $\delta^{18}O$ values in nitrate was introduced by Amberger and Schmidt (1987). $\delta^{18}O$ values in conjunction with $\delta^{15}N$ values of nitrate have been used to assess nitrate sources and transformations in hydrological studies (e.g., Aravena et al. 1993; Durka et al. 1994; Wassenaar 1995; Chang et al. 2002; Rock and Mayer 2002, 2004), although rarely in soil–plant studies. Soil nitrate may originate from several sources, including soil organic N mineralization, inorganic fertilizers, organic amendments, and atmospheric deposition. Hence, the combined use of $\delta^{15}N$ and $\delta^{18}O$ values may provide a powerful tool to elucidate soil N sources and transformations (Högberg 1997). For instance, Mengis et al. (2001) used the dual isotope approach to trace nitrate derived from fertilizer applied to an agricultural soil in the winter when immobilization and remineralization were minimal.

Currently, the most widely used method to determine the $\delta^{18}O$ value of nitrate ($\delta^{18}O_{nitrate}$) is based on extracting aqueous NO_3^- using an anion-exchange resin, and then reacting with Ag_2O to form $AgNO_3$. Precipitated $AgNO_3$ is enclosed in silver capsules for pyrolytic conversion to CO to determine $\delta^{18}O_{nitrate}$, and in tin capsules for Dumas conversion to N_2 to determine $\delta^{15}N_{nitrate}$ via CF-IRMS with a pyrolyzer or an elemental analyzer (Silva et al. 2000). This method is not directly applicable to highly saline solutions, such as 2 *M* KCl extracts from soils, as they interfere with the ion-exchange processes. The method developed for seawater by Casciotti et al. (2002), however, can be used to determine the $\delta^{18}O$ (and $\delta^{15}N$) value of nitrate extracted from soils (Rock and Ellert 2007). The method is based on bacterial reduction of NO_3^- to nitrous oxide (N_2O) via a bacterium that lacks nitrous oxide reductase, so further reduction to N_2 does not occur. This enables determination of both the $\delta^{15}N$ and $\delta^{18}O$ values for the NO_3^- based on the measured N and O isotopic compositions of the N_2O.

54.4.4 Determination of the $\delta^{15}N$ and $\delta^{18}O$ Values of Nitrous Oxide

Trace gases, such as nitrous oxide (N_2O) and methane (CH_4), are at small concentrations (<10 ppmv) in most environmental air samples, so extraneous species must be eliminated and concentrations increased before isotopic analysis by CF-IRMS. To determine the $\delta^{15}N$ and $\delta^{18}O$ values of N_2O collected from soil gas samplers and aboveground air, we use a cryogenic preconcentrator (PreCon; Brand 1995) coupled to a capillary GC and an IRMS. The masses measured with the IRMS are 44, 45, and 46 (Table 54.2). Appropriate corrections must be applied to the raw δ values to account for mass interferences (e.g., Inoue and Mook 1994; Brand 1995).

Various methods have been used to collect *in situ* soil gas and aboveground air for isotopic analysis of N_2O (e.g., Van Groenigen et al. 2005). We used horizontal soil gas sampling tubes extending into otherwise undisturbed soil to collect gas samples while avoiding mass flow along vertical samplers. Soil gas samples were collected during 2 h by connecting evacuated flasks (230 mL, stainless steel) to the gas samplers using capillaries (0.254 mm i.d. by 100 mm long). The volumes used for IRMS ranged from 230 mL when $[N_2O] \leq 4$ ppmv to 10 mL when $[N_2O] \geq 24$ ppmv (dependent upon CF-IRMS sensitivity).

In addition to analyzing the $\delta^{15}N$ and $\delta^{18}O$ values of N_2O, various spectroscopic techniques may be used to determine $\delta^{15}N$ values for specific isotopomers of N_2O ($\delta^{15}N^{\beta}$ for $^{15}N^{14}N^{16}O$ and $\delta^{15}N^{\alpha}$ for $^{14}N^{15}N^{16}O$), as the N_2O molecule has an asymmetric linear structure (Brenninkmeijer and Röckmann 1999; Toyoda and Yoshida 1999). Isotopomers (a contraction of isotope isomer) refer to molecular structures with the same numbers of each isotopic atom but differing in their positions. Beyond bulk $\delta^{15}N$ and $\delta^{18}O$ values, isotopomer determinations may help to further elucidate the relative contribution of nitrification and denitrification to soil N_2O production (e.g., Pérez 2005), although they may not provide unambiguous proof of N_2O origin (Schmidt et al. 2004). Elucidating N_2O sources is crucial if we are to effectively manage soils to reduce N_2O emissions, which often account for a majority of greenhouse gas emissions from primary agriculture.

54.5 LIGHT ISOTOPE APPLICATIONS AND CALCULATIONS

For many years the main application of stable isotope techniques in soil and environmental research centered on ^{15}N-enriched fertilizers to assess the fate of applied N, and later this was extended to probe other N transformations, including biological N fixation, denitrification, and mineralization–immobilization turnover (e.g., Högberg 1997). More recently, stable isotope applications have expanded to include a wider range of elements with isotopes at both artificially enriched and natural levels. For natural abundance studies it must be recognized that some transformations (e.g., NH_3 volatilization, denitrification) may cause significant isotope fractionation, whereas others (e.g., N fixation, leaching) cause almost none. Enrichment or fractionation factors for various N cycling processes can be found in Robinson (2001) and Bedard-Haughn et al. (2003). Another trend has been greater recognition of soil as an ecosystem component, so that in addition to transformations within soils, stable isotope techniques have been used to investigate transfers to other ecosystem components (plants, animals, water, and air). Several books covering basic principles and a range of applications are available (Coleman and Fry 1991; Lajtha and Michener 1994; Sala et al. 2000; Unkovich et al. 2001; de Groot 2004; Fry 2006; Sharp 2007). Here we focus on only three common applications.

54.5.1 Vegetation-Induced Shifts in $\delta^{13}C$ Values of Soil Organic Matter

Among the most common uses of natural ^{13}C abundance in soil research is estimating the proportion of soil organic matter derived from isotopically distinct inputs (Balesdent and Mariotti 1996). As a first approximation, ^{13}C fractionation during decomposition is assumed negligible, so the $\delta^{13}C$ values of soil C inputs and the soil organic matter that accumulates are assumed to be the same (i.e., isotopic equilibrium between inputs and the organic matter pool). If ^{13}C abundance within the inputs changes, the extent to which the inputs are retained as soil organic matter or decomposed back to CO_2 may be inferred from changes in ^{13}C abundance within the organic matter pool.

The most common cause of a change in ^{13}C abundance is a shift in the proportional contributions to soil C inputs by plants using the C3 or C4 photosynthetic pathways. Owing largely to differences in the affinity of the initial carboxylating enzyme for CO_2 (rubisco for the C3 pathway and PEP carboxylase for the C4 pathway), C3 plants discriminate more strongly against atmospheric $^{13}CO_2$ than do C4 plants. Consequently, the $\delta^{13}C$ values of C3 plants typically range from $-30‰$ to $-25‰$, whereas those of C4 plants typically range from $-13‰$ to $-15‰$.

Vegetation-induced shifts in plant ^{13}C inputs occur when native vegetation (C3 forest, C3 prairie, C4 prairie or savanna) is cleared and the land is cropped under vegetation with the contrasting photosynthetic pathway. In such cases, elementary isotope mixing models are used to estimate the proportions of soil organic C derived from each type of vegetation (i.e., that persisting from the original vegetation, and that from the more recent, isotopically distinct vegetation; Figure 54.2). With the approximation that δ values are linearly related to F (i.e., atom fraction), the slope of the mixing line is $1/(\delta_{C4} - \delta_{C3})$ and the intercept is $\delta_{C3}/(\delta_{C4} - \delta_{C3})$, where δ_{C3} is the delta value for C3 vegetation (e.g., $-28‰$) and δ_{C4} is that for C4 vegetation (e.g., $-14‰$). From the slope of the mixing line (Figure 54.2), it is often assumed that each $1‰$ increase in the $\delta^{13}C$ value of soil organic matter roughly represents a 7% increase in amount derived from C4 vegetation.

Isotopic partitioning of soil organic matter between that derived from isotopically distinct soil C inputs (p_{C4}; Figure 54.2, y-axis) and that originally present $(1 - p_{C4})$ provides useful information on C cycling. Changes in p_{C4} through time indicate the kinetics of recent C accumulation and original C persistence (Balesdent and Mariotti 1996). From the quantities of soil organic C (expressed as Mg C ha^{-1} to a specified soil depth or mass after bulk density corrections—see Chapter 3) and their $\delta^{13}C$ values, the quantities of original soil organic C persisting at various times after the shift in plant ^{13}C inputs are calculated as the product of measured soil organic C and $(1 - p_{C4})$. In the simplest instance, a first-order decay model may be fitted to original C persisting at successive times ($C_t = C_0 e^{-kt}$, where C_t is the quantity of original C at time t, C_0 is that just before the ^{13}C shift occurred, and k is the first-order decay coefficient). In turn, k, the half-life $(\ln 2/k)$, and/or the turnover time $(1/k)$ of

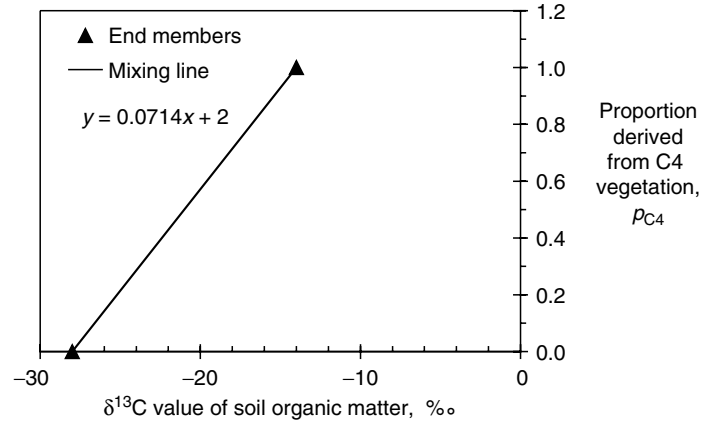

FIGURE 54.2. Elementary isotope mixing model with two end members used to estimate the proportions of soil organic matter derived from C3 and from C4 vegetation.

the original soil organic matter may be estimated as $k = (\ln C_0 - \ln C_t)/t$. Amundson and Baisden (2000) discuss more detailed models for isotopes of soil organic matter.

Variations on the isotopic partitioning approach described above have been used in a wide range of settings. Comparisons have been based on soil samples collected at a single time from carefully paired sites including an unchanged reference site and one or more sites where the shift in ^{13}C inputs had occurred in previous years (i.e., temporal series replaced by relevant comparisons in space). Often the isotopic shift is smaller than the roughly 14‰ difference between C3 and C4 vegetation, and there is a corresponding decline in the resolution of soil organic matter sources. This approach is based on many assumptions including homogeneity of plant ^{13}C inputs, uniformity of ^{13}C abundance in organic matter among contrasting soil layers and fractions, and changes associated with decomposition. For example, $\delta^{13}C$ values of plant C (especially C3 plants) often vary among seasons, water availability, salinity, and N fertilization (Jenkinson et al. 1995; Shaheen and Hood-Nowotny 2005). Fractionation during biosynthesis also culminates in nonuniform ^{13}C distribution among various chemical constituents (Hayes 2001). Lignins and lipids often are depleted by 3‰ to 6‰ compared to carbohydrates, and these decay at different rates. Balesdent and Mariotti (1996) proposed that over the short term (2 to 10 y) there may be minimal fractionation during decay, because increases in residual ^{13}C remaining after detrital respiration are offset by the slower decay of ^{13}C-depleted lignin. In the long term, however, the effect of detrital recycling dominates, and decomposition tends to increase the $\delta^{13}C$ value of remaining organic matter. Thus $\delta^{13}C$ values of organic matter within a soil profile typically increase (by ≈1‰ to 3‰) from surface soils dominated by more recent plant C inputs to subsurface layers containing highly decomposed and persistent materials (Boutton 1991; Accoe et al. 2002).

In theory, the proportional contributions of $n + 1$ distinct sources may be calculated from the use of n different isotopic tracers (e.g., $\delta^{13}C$, $\delta^{15}N$, $\delta^{18}O$, $\delta^{34}S$). In practice, however, the isotopic compositions of the sources are uncertain and the number of potential sources may exceed by more than one the number of usable isotopic tracers. Often it is assumed that variations in the isotopic compositions of the sources (e.g., C3 and C4 vegetation) are negligible relative to those of the pool (e.g., soil organic C) to be partitioned. Phillips and coworkers (Phillips and Gregg 2001, 2003; Phillips et al. 2005) discuss uncertainties in source partitioning, and for systems with too many sources ($>n+1$) they evaluate the influence of source aggregation and present algorithms to calculate the distribution of feasible solutions (IsoError and IsoSource software were available, at the time of writing, from http://www.epa.gov/wed/pages/models.htm).

54.5.2 Fate of ^{15}N-Enriched Fertilizer

Many comprehensive reviews consider the use of field-applied ^{15}N to investigate N cycling in terrestrial ecosystems (e.g., Hauck and Bremner 1976; Di et al. 2000; Bedard-Haughn et al. 2003). The fundamental approach to partition some N pool (e.g., plant N, soil organic N, soil inorganic *N*, volatilized N) between natural N present originally and added ^{15}N-enriched fertilizer is analogous to partitioning soil organic matter between C3 and C4 vegetation (see Section 54.5.1). In enriched experiments, δ values are replaced by APE, and since APE of natural N is zero, the mixing line describing the proportion derived from the enriched source ($p_{\text{enriched\_source}}$) extends from the origin and the slope is the inverse of the APE for the enriched source (i.e., $p_{\text{enriched\_source}} = \text{APE}_{\text{sample}} \times 1/\text{APE}_{\text{enriched\_source}}$). The proportion of the enriched source found in plant dry matter produced during the growing season commonly is used to estimate fertilizer use efficiency (IAEA 2001). First, total plant N yield per unit

area is estimated by harvesting and tissue analysis, then the product of this and $p_{\text{enriched\_source}}$ estimates the plant N derived from fertilizer per unit area. Finally, that number is divided by the fertilizer application rate to estimate the N fertilizer use efficiency.

A wide range of more sophisticated approaches to investigate N cycling using ^{15}N-enriched fertilizers have been developed. Stark (2000) classifies these into tracer techniques, isotope dilution techniques, and isotope models solved numerically. Estimating fertilizer use efficiency as described in the previous paragraph would fall under tracer techniques where the goal is to assess element transfer from one pool (e.g., applied fertilizer N) to another (plant N), and the advantages, assumptions, and pitfalls have been reviewed (e.g., Hauck and Bremner 1976; Stark 2000). In particular, interpretations may be confounded by N pool substitution when the N in various soil pools is replaced by the applied ^{15}N-enriched fertilizer during immobilization–mineralization turnover (Jansson and Persson 1982; Jenkinson et al. 1985). The ^{15}N-enriched fertilizer is immobilized in place of unlabeled N, so that soil inorganic N (immediately available for plant uptake) contains less ^{15}N than there would have been without N pool substitution. Since ^{15}N-enriched reagents are expensive, only small amounts are applied in most studies, and often lateral dispersion is restricted by some form of microplot to help attain uniform isotope distribution and representative sampling (e.g., Follett 2001).

Isotope dilution usually refers to techniques based on labeling a pool with known amount of isotope, and then measuring the size and isotopic abundance of the pool after a predetermined equilibration period. The extent to which the isotope becomes diluted reflects the size of the entire pool accessible to the tracer during the equilibration period (Di et al. 2000). Since isotope mass is conserved, isotope dilution measures the entire equilibrating pool without separating it from the soil. Kirkham and Bartholomew (1954, 1955) developed a series of equations to describe the exchange and subsequent transformations of enriched ^{15}N added to soil, and these equations form the basis for much recent work on deciphering gross rates of N mineralization and immobilization.

54.5.3 Estimating the δ^{15}N Value of an Unknown Source

In some instances, natural isotopic abundance may be used to identify an unknown source and its contribution to a particular biogeochemical pool. Again, users must be aware of the potential for isotopic fractionation during transfers and transformations (especially of soil N), which may complicate the interpretations (Shearer and Kohl 1993).

Consider plant foliage in which the δ^{15}N value of total N ($\delta^{15}N_{\text{foliage}}$) decreases while the concentration ([foliage N]) increases with decreasing distance from an intensive livestock operation (Figure 54.3). The foliage is from standardized plants uniformly grown in the same potting soil, and the source N responsible for increasing [foliage N] is hypothesized to be ammonia emitted from an intensive livestock operation. Changes in the δ^{15}N value of foliage with increasing N content suggest that the source N is isotopically distinct, and that its δ^{15}N value might be estimated. A plot of the measured $\delta^{15}N_{\text{foliage}}$ values versus the inverse of [foliage N] could possibly yield a straight line (Figure 54.3) with an equation in the form of:

$$\delta^{15}N_{\text{foliage}} = \text{slope} \times (1/[\text{foliage N}]) + \text{intercept} \tag{54.7}$$

The intercept of this line would estimate the δ^{15}N value of the unknown source. If the δ values represent simple mixing, a straight line will be observed between the δ values and the

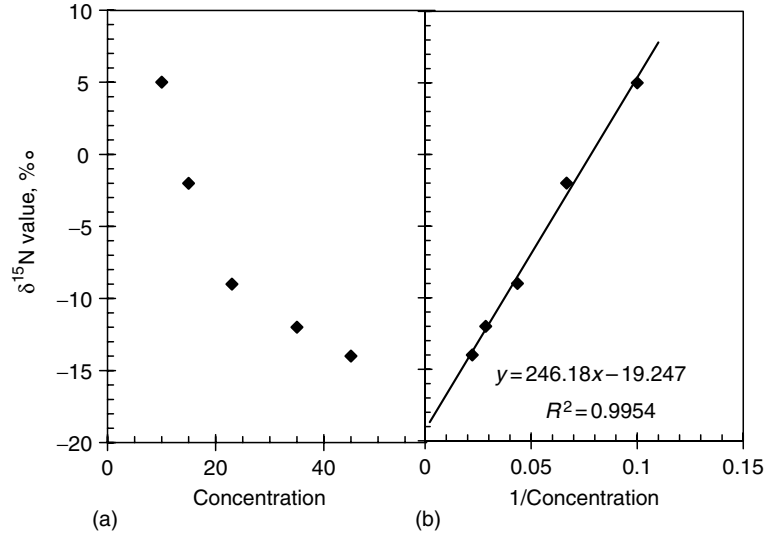

FIGURE 54.3. Hypothetical change in the $\delta^{15}N$ value of potted plant foliage versus (a) total N concentration (arbitrary units) and (b) the reciprocal of total N concentration. The *y*-intercept in panel (b) estimates the $\delta^{15}N$ value of the N source responsible for increasing the total N concentrations and concomitantly decreasing the $\delta^{15}N$ values of the foliage.

inverse of concentration. If, however, isotope fractionation occurs as element concentration increases, the line will curve (Kendall and Caldwell 1998). In turn, knowing the $\delta^{15}N$ values of the N source and of total plant foliage N without inputs from the N source, one can estimate the relative contributions of source N over distance from the livestock operation, as described for partitioning in Section 54.5.1. Similarly, Shearer and Kohl (1993) suggested: $\%N_{df\_unknown} = (\delta^{15}N_{known} - \delta^{15}N_{measured})/(\delta^{15}N_{known} - \delta^{15}N_{unknown})$ where $\%N_{df\_unknown}$ is the percentage N derived from an unknown source with a delta value of $\delta^{15}N_{unknown}$ (e.g., ammonia emitted from livestock operations), $\delta^{15}N_{known}$ is the delta value for the known source (e.g., background soil N), and $\delta^{15}N_{measured}$ is the measured delta value (e.g., for a plant or soil impacted by unknown N inputs).

Similar approaches are widely used in studies of ecosystem respiration. In these studies, the $\delta^{13}C$ values for soil-respired CO_2 may be estimated from plots of the δ values versus the reciprocal of $[CO_2]$ for a series of air samples collected when concentrations are increasing (Keeling 1958, 1961; Flanagan and Ehleringer 1998). Corrections for isotopic fractionation during CO_2 diffusion from the soil may be required.

54.6 COMMENTS ON THE USE OF STABLE ISOTOPES IN ENVIRONMENTAL RESEARCH

Advances in CF-IRMS instrumentation for light elements have improved the accessibility of stable isotope analyses to researchers. Automation has greatly increased analytical throughput, and proper implementation of CF-IRMS has decreased errors associated with sample preparation. For much soil work, field and sampling variability in isotope composition likely exceeds analytical variability. Data are easily misinterpreted if influential sources, transformations, and isotope fractionations are neglected. Consequently, investigators are

encouraged to consider the zeroth rule of O'Leary et al. (1992): ''be sceptical of effects smaller than 1‰.'' While some differences smaller than this may be real and significant, the inherent variability of soils and the heterogeneous nature of soil organic matter may obscure small isotope effects.

Many creative techniques are available for applying isotope analyses to probe biogeochemical cycling of light elements (e.g., N, C, S) and soil ecological processes with greater clarity and specificity (e.g., Staddon 2004). The techniques are best applied, however, to well-designed studies (e.g., Pennock 2004) that are fully characterized using the best available, nonisotopic methods. Stable isotope techniques are most powerful when established on a solid foundation of more conventional analyses (e.g., robust concentration data to estimate biogeochemical fluxes and pools). Thus investigators are encouraged to heed what Kendall and Caldwell (1998) refer to as Fretwell's law: ''Warning! Stable isotope data may cause severe and contagious stomach upset if taken alone. To prevent upsetting reviewers' stomachs and your own, take stable isotope data with a healthy dose of other hydrologic, geologic, and geochemical information. Then, you will find stable isotope data very beneficial.''

REFERENCES

Accoe, F., Boeckx, P., van Cleemput, O., Hofman, G., Zhang, Y., hua Li, R., and Guanxiong, C. 2002. Evolution of the $\delta^{13}C$ signature related to total carbon contents and carbon decomposition rate constants in a soil profile under grassland. *Rapid Commun. Mass Spectrom.* 16: 2184–2189.

Amberger, A. and Schmidt, H.L. 1987. Natürliche Isotopen Gehalte von Nitrat als Indikatoren für dessen Herkunft. *Geochim. Cosmochim. Acta* 51: 2699–2705.

Amundson, R. and Baisden, W.T. 2000. Stable isotope tracers and mathematical models in soil organic matter studies. In O.E. Sala, R.B. Jackson, H.A. Mooney, and R.W. Howarth, Eds. *Methods in Ecosystem Science*. Springer, New York, NY, pp. 117–137.

Aravena, R., Evans, M.L., and Cherry, J.A. 1993. Stable isotopes of oxygen and nitrogen in source identification of nitrate from septic systems. *Ground Water* 31: 180–186.

Baccanti, M., Magni, P., Oakes, W., Lake, J., and Szakas, T. 1993. Application of an organic elemental analyzer for the analysis of nitrogen, carbon, and sulfur in soils. *Am. Environ. Lab.* 5: 16–17.

Balesdent, J. and Mariotti, A. 1996. Measurement of soil organic matter turnover using ^{13}C natural abundance. In T.W. Boutton and S. Yamasaki, Eds. *Mass Spectrometry of Soils*. Marcel Dekker, New York, NY, pp. 83–111.

Bedard-Haughn, A., van Groenigen, J.W., and van Kessel, C. 2003. Tracing ^{15}N through landscapes: potential uses and precautions. *J. Hydrol.* 272: 175–190.

Boutton, T.W. 1991. Stable carbon isotope ratios of natural materials. I. Sample preparation and mass spectrometric analysis. In D.C. Coleman and B. Fry, Eds. *Carbon Isotope Techniques*. Academic Press, New York, NY, pp. 155–171.

Brand, W. 1995. PreCon: a fully automated interface for the pre-GC concentration of trace gases in air for isotopic analysis. *Isotopes Environ. Health Stud.* 31: 277–284.

Brand, W.A., Tegtmeyer, A.R., and Hilkert, A. 1994. Compound-specific isotope analysis: extending toward 15N/14N and 18O/16O. *Org. Geochem.* 21: 585–594.

Brenna, J.T., Corso, T.N., Tobias, H.J., and Caimi, R.J. 1997. High-precision continuous-flow isotope ratio mass spectrometry. *Mass Spectrom. Rev.* 16: 227–258.

Brenninkmeijer, C.A.M. and Röckmann, T. 1999. Mass spectrometry of the intramolecular nitrogen

isotope distribution of environmental nitrous oxide using fragment-ion analysis. *Rapid Commun. Mass Spectrom.* 13: 2028–2033.

Casciotti, K.L., Sigman, D.M., Galanter Hastings, M., Böhlke, J.K., and Hilkert, A. 2002. Measurement of the oxygen isotopic composition of nitrate in seawater and freshwater using the denitrifier method. *Anal. Chem.* 74: 4905–4912.

Chang, C.C.Y., Kendall, C., Silva, S.R., Battaglin, W.A., and Campbell, D.H. 2002. Nitrate stable isotopes: tools for determining nitrate sources among different land uses in the Mississippi River Basin. *Can. J. Fish. Aquat. Sci.* 59: 1874–1885.

Coleman, D.C. and Fry, B., Eds. 1991. *Carbon Isotope Techniques*. Academic Press, San Diego, CA, 274 pp.

Coplen, T.B., Hopple, J.A., Böhlke, J.K., Peiser, H.S., Rieder, S.E., Krouse, H.R., Rosman, K.J.R., Ding, T., Vocke, R.D. Jr., Révész, K.M., Lamberty, A., Taylor, P.D.P., and De Bièvre, P. 2002. Compilation of minimum and maximum isotope ratios of selected elements in naturally occurring terrestrial materials and reagents. Water Resources Investigations Report 01-4222, US Department of the Interior, US Geological Survey, Reston, VA, 98 pp.

Craig, H. 1957. Isotopic standards for carbon and oxygen and correction factors for mass-spectrometric analysis of carbon dioxide. *Geochim. Cosmochim. Acta* 12: 133–149.

de Groot, P.A., ed. 2004. *Handbook of Stable Isotope Analytical Techniques*, Vol. 1. Elsevier, Amsterdam, the Netherlands, 1234 pp.

Di, H.J., Cameron, K.C., and MacLaren, R.G. 2000. Isotopic dilution methods to determine the gross transformation rates of nitrogen, phosphorus, and sulfur in soil: a review of the theory, methodologies, and limitations. *Aust. J. Soil Res.* 38: 213–230.

Durka, W., Schulze, E.D., and Gebauer, G. 1994. Effects of forest decline on uptake and leaching of deposited nitrate determined from N-15 and O-18 measurements. *Nature* 372: 765–767.

FAO/IAEA (Food and Agriculture Organization of the United Nations and the International Atomic Energy Agency). 1966. *The Use of Isotopes in Soil Organic Matter Studies* (Proceedings of the Technical Meeting, Brunswick-Völkenrode, Germany, 1963; Supplement to Journal of Applied Radiation and Isotopes). Pergamon Press, New York, NY, 505 pp.

Flanagan, L.B. and Ehleringer, J.R. 1998. Ecosystem–atmosphere CO_2 exchange: interpreting signals of change using stable isotope ratios. *Trends Ecol. Evol.* 13: 10–14.

Follett, R.F. 2001. Innovative ^{15}N microplot research techniques to study nitrogen use efficiency under different ecosystems. *Commun. Soil Sci. Plant Anal.* 32: 951–979.

Frossard, E. and Sinai, S. 1997. The isotope exchange kinetic technique: a method to describe the availability of inorganic nutrients. Applications to K, P, S, and Zn. *Isotopes Environ. Health Stud.* 33: 61–77.

Fry, B. 2006. *Stable Isotope Ecology*. Springer, New York, NY, 308 pp, plus CD-ROM.

Gehre, M. and Strauch, G. 2003. High-temperature elemental analysis and pyrolysis techniques for stable isotope analysis. *Rapid Commun. Mass Spectrom.* 17: 1497–1503.

Glaser, B. 2005. Compound-specific stable-isotope ($\delta^{13}C$) analysis in soil science. *J. Plant Nutr. Soil Sci.* 168: 633–648.

Harris, D., Horwath, W.R., and van Kessel, C. 2001. Acid fumigation of soils to remove carbonates prior to total organic carbon or carbon-13 isotopic analysis. *Soil Sci. Soc. Am. J.* 65: 1853–1856.

Hauck, R.D. and Bremner, J.M. 1976. Use of tracers for soil and fertilizer nitrogen research. *Adv. Agron.* 28: 219–266.

Hayes, J.M. 2001. Fractionation of the isotopes of carbon and hydrogen in biosynthetic processes. In J.W. Valley and D. Cole, Eds. *Stable Isotope Geochemistry*, Vol. 43 of Reviews in Mineralogy & Geochemistry, Mineralogical Society of America, Chantilly, VA, pp. 225–278.

Hayes, J.M., Freeman, K.H., Popp, B.N., and Hoham, C.H. 1989. Compound-specific isotopic analyses: a novel tool for reconstruction of ancient biogeochemical processes. *Org. Geochem.* 16: 1115–1128.

Högberg, P. 1997. Tansley Review No. 95: ^{15}N natural abundance in soil–plant systems. *New Phytol*. 137: 179–203.

IAEA. 2001. Use of isotope and radiation methods in soil and water management and crop nutrition. Training Course Series No. 14. International Atomic Energy Agency, Vienna, Austria, 247 pp. Available at: http://www.iaea.org/programmes/nafa/d1/public/tcs-14.pdf (last verified May 2006).

IAEA. 2004. Analytical Quality Control Services Reference Materials Catalogue, 2004–05. International Atomic Energy Agency, Vienna, Austria, 116 pp. Available at: http://www.iaea.org/programmes/aqcs/pdf/catalogue.pdf (last verified May 2006).

Inoue, H.Y. and Mook, W.G. 1994. Equilibrium and kinetic nitrogen and oxygen isotope fractionations between dissolved and gaseous N_2O. *Chem. Geol*. 113: 135–148.

Jansson, S.L. and Persson, J. 1982. Mineralization and immobilization of soil nitrogen. In F.J. Stevenson, Ed. *Nitrogen in Agricultural Soils*. Agronomy Monograph 22. ASA, CSSA, and SSSA, Madison, WI, pp. 229–252.

Jardine, T.D. and Cunjak, R.A. 2005. Analytical error in stable isotope ecology. *Oecologia* 144: 528–533.

Jenkinson, D.S., Coleman, K., and Harkness, D.D. 1995. The influence of fertilizer nitrogen and season on the carbon-13 abundance of wheat straw. *Plant Soil* 171: 365–367.

Jenkinson, D.S., Fox, R.H., and Rayner, J.H. 1985. Interactions between fertilizer nitrogen and soil nitrogen—the so-called priming effect. *J. Soil Sci*. 36: 425–444.

Keeling, C.D. 1958. The concentration and isotopic abundances of atmospheric carbon dioxide in rural areas. *Geochim. Cosmochim. Acta* 13: 322–334.

Keeling, C.D. 1961. The concentration and isotopic abundances of carbon dioxide in rural and marine air. *Geochim. Cosmochim. Acta* 24: 277–298.

Kendall, C. 1998. Tracing nitrogen sources and cycling in catchments. In C. Kendall and J.J. McDonnell, eds. *Isotope Tracers in Catchment Hydrology*. Elsevier, Amsterdam, the Netherlands, pp. 519–576.

Kendall, C. and Caldwell, E.A. 1998. Fundamentals of isotope geochemistry. In C. Kendall and J.J. McDonnell, Eds. *Isotope Tracers in Catchment Hydrology*. Elsevier, Amsterdam, the Netherlands, pp. 51–86.

Kirkham, D. and Bartholomew, W.V. 1954. Equations for following nutrient transformations in soil, utilizing tracer data. *Soil Sci. Soc. Am. Proc*. 18: 33–34.

Kirkham, D. and Bartholomew, W.V. 1955. Equations for following nutrient transformations in soil, utilizing tracer data: II. *Soil Sci. Soc. Am. Proc*. 19: 189–192.

Kohl, D.A., Shearer, G.B., and Commoner, B. 1971. Fertilizer nitrogen: contribution to nitrate in surface water in a Corn Belt watershed. *Science* 174: 1331–1334.

Lajtha, K. and Michener, R.H., eds. 1994. *Stable Isotopes in Ecology and Environmental Science*. Blackwell Scientific Publications, Oxford, UK, 316 pp.

Mayer, B. and Krouse, H.R. 2004. Procedures for sulfur isotope abundance studies. In P.A. de Groot, Ed. *Handbook of Stable Isotope Analytical Techniques*, Vol. 1. Elsevier, Amsterdam, the Netherlands, pp. 538–607.

Meier-Augenstein, W. 1999a. Applied gas chromatography coupled to isotope ratio mass spectrometry. *J. Chromatogr*. A 842: 351–371.

Meier-Augenstein, W. 1999b. Use of gas chromatography–combustion–isotope ratio mass spectrometry in nutrition and metabolic research. *Curr. Opin. Clin. Nutr. Metab. Care* 2: 465–470.

Mengis, M., Walther, U., Bernasconi, S.M., and Wehrli, B. 2001. Limitations of using delta ^{18}O for the source identification of nitrate in agricultural soils. *Environ. Sci. Technol*. 35: 1840–1844.

Nieuwenhuize, J., Maas, Y.E.M., and Middelburg, J.J. 1994. Rapid analysis of organic carbon and nitrogen in particulate materials. *Mar. Chem*. 45: 217–224.

Noggle, G.R. 1951. The use of isotopes in soil research. *Scientific Monthly* 72: 50–56.

Norman, A.G. and Werkman, C.H. 1943. The use of the nitrogen isotope N^{15} in determining nitrogen recovery from plant materials decomposing in soil. *Am. Soc. Agron. J.* 35: 1023–1025.

O'Leary, M.H., Madhavan, S., and Paneth, P. 1992. Physical and chemical basis of carbon isotope fractionation in plants. *Plant Cell Environ.* 15: 1099–1104.

Pennock, D.J. 2004. Designing field experiments in soil science. *Can. J. Soil Sci.* 84: 1–10.

Perez, T. 2005. Factors that control the isotopic composition of N_2O from soil emissions. In L.B. Flanagan, J.R. Ehleringer, and D.E. Pataki, Eds. *Stable Isotopes and Biosphere–Atmosphere Interactions: Processes and Biological Controls*. Elsevier Academic Press, San Diego, CA, pp. 69–84.

Phillips, D.L. and Gregg, J.W. 2001. Uncertainty in source partitioning using stable isotopes. *Oecologia* 127: 171–179.

Phillips, D.L. and Gregg, J.W. 2003. Source partitioning using stable isotopes: coping with too many sources. *Oecologia* 136: 261–269.

Phillips, D.L., Newsome, S.D., and Gregg, J.W. 2005. Combining sources in stable isotope mixing models: alternative methods. *Oecologia* 144: 520–527.

Robinson, D. 2001. $\delta^{15}N$ as an integrator of the nitrogen cycle. *Trends Ecol. Evol.* 16: 153–162.

Rock, L. and Ellert, B.H. 2007. Nitrogen-15 and Oxygen-18 natural abundance of potassium chloride extractable soil nitrate using the denitrifer method. *Soil Sci. Soc. Am. J.* 71: 355–361.

Rock, L. and Mayer, B. 2002. Isotopic assessment of sources and processes affecting sulfate and nitrate in surface water and groundwater of Luxembourg. *Isotopes Environ. Health Stud.* 38: 191–206.

Rock, L. and Mayer, B. 2004. Isotopic assessment of sources of surface water nitrate within the Oldman River Basin, Southern Alberta, Canada. *Water Air Soil Pollut.: Focus* 4: 545–562.

Ryba, S.A. and Burgess, R.M. 2002. Effects of sample preparation on the measurement of organic carbon, hydrogen, nitrogen, sulfur, and oxygen concentrations in marine sediments. *Chemosphere* 48: 139–147.

Sala, O.E., Jackson, R.B., Mooney, H.A., and Howarth, R.W., Eds. 2000. *Methods in Ecosystem Science*. Springer-Verlag, New York, NY, 421 pp.

Santrock, J., Studley, S.A., and Hayes, J.M. 1985. Isotopic analyses based on the mass spectrum of carbon dioxide. *Anal. Chem.* 57: 1444–1448.

Schmidt, H.-L., Werner, R.A., Yoshida, N., and Well, R. 2004. Is the isotopic composition of nitrous oxide an indicator for its origin from nitrification or denitrification? A theoretical approach from referred data and microbiological and enzyme kinetic aspects. *Rapid Commun. Mass Spectrom.* 18: 2036–2040.

Scrimgeour, C.M. 1995. Measurement of plant and soil water isotope composition by direct equilibration methods. *J. Hydrol.* 172: 261–274.

Scrimgeour, C.M. and Robinson, D. 2004. Stable isotope analysis and applications. In K.A. Smith and M.S. Cresser, Eds. *Soil and Environmental Analysis: Modern Instrumental Techniques*, 3rd edn. Marcel Dekker, New York, NY, pp. 381–431.

Sebilo, M., Mayer, B., Grably, M., Billiou, D., and Mariotti, A. 2004. The use of the 'ammonium diffusion' method for $\delta^{15}N\text{-}NH_4^+$ and $\delta^{15}N\text{-}NO_3^-$ measurements: comparison with other techniques. *Environ. Chem.* 1: 99–103.

Shaheen, R. and Hood-Nowotny, R.C. 2005. Effect of drought and salinity on carbon isotope discrimination in wheat cultivars. *Plant Sci.* 168: 901–909.

Sharp, Z. 2007. *Principles of Stable Isotope Geochemistry*. Pearson Prentice Hall, Upper Saddle River, NJ, 344 pp.

Shearer, G. and Kohl, D.H. 1993. Natural abundance of ^{15}N: fractional contribution of two sources to a common sink and use of isotope discrimination. In T.R. Knowles and H. Blackburn, Eds. *Nitrogen Isotope Techniques*. Academic Press, New York, NY, pp. 89–125.

Silva, S.R., Kendall, C., Wilkison, D.H., Ziegler, A.C., Chang, C.C.Y., and Avanzino, R.J. 2000. A new method for collection of nitrate from fresh water and the analysis of nitrogen and oxygen isotope ratios. *J. Hydrol.* 228: 22–36.

Staddon, P.L. 2004. Carbon isotopes in functional soil ecology. *Trends Ecol. Evol.* 19: 148–154.

Stark, J.M. 2000. Nutrient transformations. In O.E. Sala, R.B. Jackson, H.A. Mooney, and R.W. Howarth, Eds. *Methods in Ecosystem Science*. Springer, New York, NY, pp. 215–234.

St-Jean, G. 2003. Automated quantitative and isotopic (^{13}C) analysis of dissolved inorganic carbon and dissolved organic carbon in continuous-flow using a total organic carbon analyzer. *Rapid Commun. Mass Spectrom.* 17: 419–428.

Teece, M.A. and Fogel, M.L. 2004. Preparation of ecological and biochemical samples for isotopic analysis. In P.A. de Groot, Ed. *Handbook of Stable Isotope Analytical Techniques*, Vol. 1. Elsevier, Amsterdam, the Netherlands, pp. 177–202.

Toyoda, S. and Yoshida, N. 1999. Determination of nitrogen isotopomers of nitrous oxide on a modified isotope ratio mass spectrometer. *Anal. Chem.* 71: 4711–4718.

Unkovich, M.J., Pate, J.S., McNeill, A., and Gibbs, D.J., Eds. 2001. *Stable Isotope Techniques in the Study of Biological Processes and Functioning of Ecosystems*. Springer, New York, NY, 289 pp.

Van Groenigen, J.W., Zwart, K.B., Harris, D., and van Kessel, C. 2005. Vertical gradients of $\delta^{15}N$ and $\delta^{18}O$ in soil atmospheric N_2O—temporal dynamics in a sandy soil. *Rapid Commun. Mass Spectrom.* 19: 1289–1295.

Wassenaar, L.I. 1995. Evaluation of the origin and fate of nitrate in the Abbotsford Aquifer using the isotopes of ^{15}N and ^{18}O in NO_3^-. *Appl. Geochem.* 10: 391–405.

Werner, R. and Brand, W. 2001. Referencing strategies and techniques in stable isotope ratio analysis. *Rapid Commun. Mass Spectrom.* 15: 501–519.

Whiticar, M.J. and Snowdon, L.R. 1999. Geochemical characterization of selected Western Canada oils by C_5–C_8 Compound Specific Isotope Correlation (CSIC). *Org. Geochem.* 30: 1127–1161.

VI. SOIL PHYSICAL ANALYSES

Section Editors: Denis A. Angers and F.J. Larney

Chapter 55
Particle Size Distribution

D. Kroetsch and C. Wang
Agriculture and Agri-Food Canada
Ottawa, Ontario, Canada

55.1 INTRODUCTION

Soil textural classes (e.g., loam, clay loam, sandy loam) are estimated in terms of size and distribution of primary particles by sieve and sedimentation analysis. Field estimates of texture are confirmed by laboratory analyses of selected samples. Particle size analysis (PSA) is a measurement of particle size distribution. The Canadian Soil Information System glossary defines particle size distribution as the amounts of the various soil separates in a soil sample, usually expressed as weight percentages (Gregorich et al. 2001).

According to Gee and Or (2002) two major features of PSA are the destruction or dispersion of soil aggregates into distinct units by chemical, mechanical, or ultrasonic means, and the further separation of these particles into size classes by sieving and sedimentation. The proportions are calculated from the relative weights of the particles within defined size classes. The primary particle size classes used in this chapter are defined in the Canadian System of Soil Classification (CSSC) (Soil Classification Working Group 1998) and are given in Table 55.1. The limits of soil particle size classes differ in various commonly used systems (Figure 55.1). The CSSC, the United States Department of Agriculture (USDA), and the International Society of Soil Science (ISSS) systems are used for soil survey data. The American Association of State Highway Officials (AASHO) and the Unified Systems (American Society for Testing and Materials [ASTM]) are used for engineering purposes.

Two common methods of PSA are the pipette and hydrometer methods. In both, the coarser fractions are measured by sieving, and the finer from sedimentation rates based on Stokes' law. Stokes' law states that the amount that a particle sinks depends upon the density of the particle, i.e., denser (larger) particles sink more than less dense (smaller) particles when suspended in a liquid. Sheldrick and Wang (1993) indicate that Stokes' law describes small spherical particles of density, PS, and diameter, D, settling through a liquid of density, PL, and viscosity, n, at a rate of

$$v = D^2 g(\mathrm{PS} - \mathrm{PL})/18n \tag{55.1}$$

TABLE 55.1 Limits of Particle Size Classes Defined in the Canadian System of Soil Classification

Particle size	Diameter (mm)
Very coarse sand	2.0–1.0
Coarse sand	1.0–0.5
Medium sand	0.5–0.25
Fine sand	0.25–0.10
Very fine sand	0.10–0.05
Silt	0.05–0.002
Clay	≤0.002
Fine clay	≤0.0002

Source: Soil Classification Working Group, *The Canadian System of Soil Classification*, Agriculture and Agri-Food Canada Publication 1646 (Revised), Ottawa, Ontario, Canada, 1998.

where g is acceleration due to gravity. It is important to know that all sedimentation tables used for particle size distribution analysis, such as Table 55.2, are on the basis of the following assumptions: (1) soil particles are spherical (most silicate clay particles, in fact, are platy); (2) PS = 2.65 or 2.60 Mg m^{-3} (density could vary from 2.0 to 3.2 Mg m^{-3}); and (3) temperature of H_2O is constant throughout sedimentation (it is important to use H_2O at room temperature and to operate in a temperature-controlled room). It is also assumed that the settling of soil particles in a cylinder is not influenced by other particles or by the cylinder wall.

55.2 PIPETTE METHOD

The following pipette method (Soil Conservation Service 1984) was adapted from the US Soil Survey, Lincoln, NE, and reduces the time required to do the analysis by replacing the numerous centrifuge washing steps with a filter candle system. The data determined using the filter candle system corresponds well with the data from the standard pipette method and centrifuge washing (Sheldrick and Wang 1987).

If centrifuge washing is preferred, the soil samples, after pretreatments, can be washed in 250 mL centrifuge bottles with approximately 50 mL H_2O and centrifuged for 10 min at 500 g. Repeat the washing procedure three times and test for salts as described in step 2 in Removable of Soluble Salts, p. 718.

55.2.1 Material and Reagents

1 Fleakers—300 mL plus plastic caps

2 Ceramic filter candles

3 Shakers

   a. End-over-end (40–60 rpm)

   b. Sieve shaker (500 oscillations per min)

4 Cylinder—soil suspension (1205 mL) marked at 1000 mL

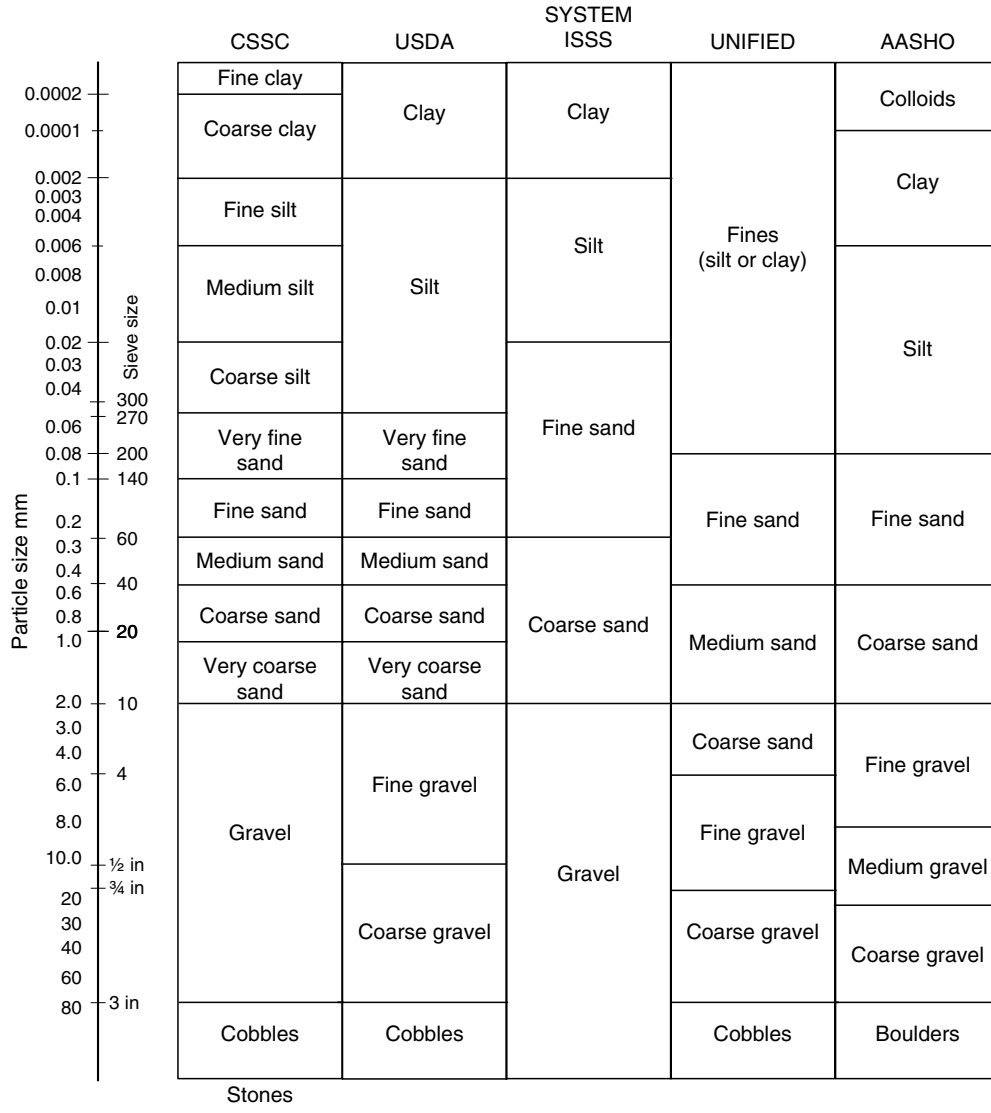

FIGURE 55.1. A comparison of particle size limits in five systems of particle size. (Adapted from Sheldrick and Wang, in M.R. Carter (Ed.), *Soil Sampling and Methods of Analysis*, Canadian Society of Soil Science, Lewis Publishers, Boca Raton, Florida, 1993. Gee and Or, in J.H. Dane and G.C. Topp (Eds), *Methods of Soil Analysis, Part 4—Physical Methods*, Soil Science Society of America, Madison, Wisconsin, 2002.)

5 Racks:

a. Custom-built frame to hold four motor-driven stirrers equipped with propeller-type stirrer and Teflon® guard

b. Shaw pipette rack modified to hold four 25 mL Lowry pipettes

c. Custom-built wood frame to support fleakers, filter candles, and vacuum system

6 Styrofoam pipe insulating cover

TABLE 55.2 Settling Depths for Specific Times and Temperatures for Particle Size = 2 μm

	Time (h)			
	4.5	**5**	**5.5**	**6.5**
Temperature (°C)	**Depth (cm)**			
20	5.79	6.44	7.08	8.37
20.3	5.81	6.48	7.13	8.43
20.5	5.86	6.52	7.17	8.47
20.7	5.89	6.55	7.2	8.51
21	5.93	6.59	7.25	8.57
21.3	5.97	6.64	7.3	8.63
21.5	6.01	6.68	7.33	8.68
21.7	6.04	6.72	7.39	8.73
22	6.09	6.75	7.43	8.78
22.3	6.13	6.8	7.49	8.85
22.5	6.15	6.83	7.51	8.88
22.7	6.18	6.86	7.55	8.92
23	6.22	6.91	7.6	8.98
23.3	6.27	6.96	7.66	9.05
23.5	6.29	6.98	7.68	9.08
23.7	6.33	7.04	7.74	9.15
24	6.37	7.08	7.78	9.2
24.3	6.4	7.12	7.83	9.25
24.5	6.43	7.15	7.86	9.29
24.7	6.45	7.18	7.89	9.33
25	6.51	7.24	7.96	9.41
25.3	6.56	7.28	8.01	9.47
25.5	6.58	7.31	8.04	9.5
25.7	6.61	7.35	8.08	9.55
26	6.66	7.4	8.14	9.62
26.3	6.69	7.44	8.18	9.67
26.5	6.72	7.47	8.22	9.72
26.7	6.76	7.51	8.26	9.76
27	6.81	7.56	8.32	9.83
27.3	6.85	7.61	8.37	9.89
27.5	6.87	7.64	8.4	9.93
27.7	6.91	7.68	8.44	9.98
28	6.97	7.74	8.51	10.06
28.3	7.01	7.79	8.57	10.13
28.5	7.04	7.82	8.61	10.17
28.7	7.07	7.86	8.65	10.22
29	7.12	7.91	8.7	10.28
29.3	7.16	7.95	8.75	10.34
29.5	7.19	7.99	8.79	10.39
29.7	7.22	8.02	8.82	10.43
30	7.27	8.08	8.88	10.5

Source: McKeague, J.A. (Ed.), in *Manual on Soil Sampling and Analysis*, 2nd ed., Canadian Society of Soil Science Ottawa, Ontario, Canada, 1978.

7 100 mL beakers or wide-mouth glass pill bottles

8 Balance (0.1-mg sensitivity)

9 Sieves:

a. 300-mesh, 15 cm

b. Set of sieves, brass, and 6.3 cm diameter. U.S. series or Tyler screen scale equipment designations as follows:

Opening (mm)	U.S. No.	Tyler mesh size
1.00	18	16
0.50	35	32
0.25	60	60
0.105	140	150
0.047	300	300

10 Hydrogen peroxide (30% or 50%)

11 Hydrochloric acid, 1 *M*

12 Citrate–bicarbonate buffer. Prepare a 0.3 *M* solution of sodium citrate (88.4 g L^{-1}) and add 125 mL of 1 *M* sodium bicarbonate (84 g L^{-1}) to each liter of citrate solution

13 Sodium hydrosulfite (dithionite)

14 Saturated sodium chloride solution

15 A solution of sodium metaphosphate with enough sodium carbonate to bring the pH to 10 ($NaPO_3$), 35.7 g L^{-1} + Na_2CO_3 7.9 g L^{-1} is suitable

55.2.2 Procedure for Pretreatments

Removal of Carbonates

1 Weigh 10 g of 2-mm air-dried soil into a 300 mL fleaker (tared to 1 mg). If the sample appears to be sandy, weigh a larger sample (e.g., 30 g).

2 Add 50 mL of water, mix, and add 1 *M* HCl slowly until pH reaches between 3.5 and 4.0 and remains there for 10 min. Stronger HCl can be used to avoid having a large volume of solution in soils high in carbonate content. Soils requiring a large amount of HCl to adjust the pH are washed several times with water to remove excess acid by using the filter candle system.

Removal of Organic Matter

1 Add 10 mL of hydrogen peroxide (H_2O_2, 30% or 50%) to the fleakers cover and allow to stand. If a violent reaction occurs, repeat cold H_2O_2 treatment until no more frothing occurs.

2 When frothing subsides, heat contents of fleakers to 90°C. Continue adding H_2O_2 and continue heating until most of the organic matter is removed (as observed by the color and rate of reaction of the sample).

3 Rinse down the sides of the reaction vessel occasionally. Continue heating the sample for about 45 min after the final addition of H_2O_2 to remove excess H_2O_2.

Note: It may be necessary to transfer samples containing high amounts of organic matter (>5%) to large beakers (e.g., 100 mL tall). If excessive frothing occurs, cool the container either with cold water or by the addition of methyl alcohol to avoid sample loss.

Removal of Soluble Salts

1 Place the fleakers in a rack and filter the remaining peroxide and water off from step 3 to remove organic matter using a filter candle system.

2 Add 150 mL of water in a jet strong enough to stir the sample, and filter the suspension through the filter candle system. Five such washings and filterings are usually enough, except for soils containing large amounts of coarse gypsum. To test for salts, check with silver nitrate ($AgNO_3$) for Cl^- and barium chloride for SO_4^{-2}.

3 Remove soil adhering to the filter candle by applying gentle back pressure and using a rubber-tipped finger to loosen any remaining material.

Note: If iron oxides are to be removed do not complete step 4 at this time.

4 Place the sample in an oven at 105°C overnight, cool in a desiccator, and weigh to the nearest milligram. Use the weight of the oven-dried treated sample as the base weight for calculating the percentages of the various particle size fractions.

Removal of Iron Oxides (Optional)

1 Add 150 mL of citrate–bicarbonate buffer to the samples in the fleakers. Stir and add 3 g of sodium hydrosulfite ($Na_2S_2O_4$) gradually, as some samples may froth.

2 Place fleakers in a water bath at 80°C and stir intermittently for 20 min.

3 Remove fleakers from the bath, place in the holding rack, and filter the suspension through the filter candle system. If the sample remains a brownish color, repeat steps 1 to 3 inclusively. If the samples are completely gray (gleyed) proceed to step 4.

4 Wash five times with a jet of water strong enough to stir the sample and filter the suspension through the filter candle system.

5 To determine the oven-dry weight for calculations, repeat step 4 to remove soluble salts.

55.2.3 Procedure for Particle Size Separation

Dispersion of Sample

1 Add 10 mL of sodium metaphosphate dispersing agent to the fleakers containing the oven-dried treated samples. Add distilled water to make the volume up to 200 mL.

2 Stopper tightly and shake end-over-end (50–60 rpm) overnight.

Separation of Sand Fractions

1 Pour the suspensions through a 300-mesh (47 μm) sieve into a sedimentation cylinder marked at 1000 mL. Place the 300-mesh sieve (14 cm diameter) in a large funnel held above the 1205 mL cylinder by a retort stand.

2 Wash the sand retained on the sieve thoroughly with a fine jet of water and collect the washings in the cylinder until the volume in the cylinder is about 950 mL. Remove the sieve and add water to make the volume up to 1000 mL.

3 Transfer the sand to a 100 mL beaker and oven-dry at 105°C. Weigh the sand and record the weight at this time if only total sand is determined. Otherwise proceed with sand fractionation.

4 Transfer the dried sand to a set of sieves (6 cm diameter) arranged as follows from top to bottom: 1.0 mm (18-mesh), 0.5 mm (30-mesh), 0.25 mm (60-mesh), 0.105 mm (140-mesh), 0.047 (300-mesh), and collecting pan. Pour the sand on to the top sieve, put cover in place, and shake the sieves on a sieve shaker. The time of shaking depends on the type of shaker and the volume of the sand in the sample (usually 5 to 10 min is sufficient). Weigh each sand fraction and record the weight.

Determination of Clay (0–2 μm)

1 Before placing the cylinder in a sedimentation room (vibration-free area equipped with a Shaw pipette rack), stir the material in the sedimentation cylinders for 4 min with a motor-driven stirrer (8 min if suspension has stood for longer than 16 h).

2 Remove from stirrer and place a length of Styrofoam pipe-insulating cover over the sedimentation cylinder. Stir the suspension for 30 s with a hand stirrer using an up-and-down motion. Note the time at the completion of stirring.

3 Sample the 2 μm fraction after a predetermined settling time (usually 4.5 to 6.5 h), varying the depth according to the time and temperature (Table 55.1). About 1 min before sedimentation is complete, lower the tip of a closed Lowry 25 mL pipette slowly into the suspension to the proper depth with a precalibrated Shaw pipette rack. Regulate the filling time of the pipette to about 12 s. Fill the pipette and empty into a tared 90 mL wide-mouth bottle (or 100 mL beaker), and rinse the pipette into the container once.

4 Evaporate the water and dry in an oven at 105°C for at least 24 h. Cool in a desiccator containing phosphorous pentoxide (P_2O_3) or Drierite (calcium sulfate), as a desiccant. Weigh and record the weight.

Determination of Fine Clay (<0.2 μm) (Optional)

1 Pour about 200 mL of suspension from the sedimentation cylinders into 250 mL centrifuge bottles. Shake the suspensions and centrifuge at the appropriate speed for the appropriate time to sediment particles coarser than 0.2 μm to a depth of 5 cm (54 min at 510 *g* at 25°C) on an IEC centrifuge. The formula used is based on Stokes' law:

$$t = \frac{63.0 \times 10^8 n \log R/S}{N^2 D^2 \Delta s} \tag{55.2}$$

where n is the viscosity in poises (cgs unit of dynamic viscosity equal to 1 dyn s cm^{-2}) at the existing temperature, R the radius of rotation (cm) of the top of sediment in the tube, S the radius of rotation (cm) of the surface of the suspension in the tube, N the revolutions per minute, Δs the difference in specific gravity between the particle in solution and the surrounding liquid (usually use $\Delta s = 1.65$), and t the time in minutes.

2 Withdraw a 25 mL aliquot from a depth of 5 cm. Empty the sample into a tared weighing bottle or beaker, rinse pipette, add the rinsing water to the weighing bottle, dry at 105°C, cool in desiccator, weigh, and record weight.

55.2.4 Calculations

1 A = weight (g) of pipetted fraction (2 or 0.2 μm).

B = weight correction for dispersing agent (g).

Note: To determine the correction factor, add 10 mL of the sodium metaphosphate solution to a 1000 mL cylinder, make to volume, stir thoroughly, withdraw duplicate 25 mL samples, dry, and weigh (about 0.012 g):

$$K = \frac{1000}{\text{volume of pipette (mL)}} \tag{55.3}$$

$$D = \frac{100}{\text{pretreated oven-dried total sample (g)}} \tag{55.4}$$

2 Sand fractions (s):

$$\text{Percentage of sand fraction } (s) = \text{weight (g) of fraction on sieve times } D \tag{55.5}$$

Pipetted fraction (s):

$$\text{Percentage of pipetted fractions } (s) = (A - B)KD \tag{55.6}$$

Silt fraction:

$$\text{Percentage of silt} = 100 - (0{-}2\ \mu\text{m clay} + \text{sand}) \tag{55.7}$$

55.3 HYDROMETER METHOD

A hydrometer can be used to measure the density of a soil suspension after various times of settling and, hence, the particle size distribution. Such measurements can be made on suspensions prepared by any of the pretreatments outlined in Section 55.2.2. In reality, however, the hydrometer is commonly used to estimate particle size distribution without any pretreatment, except dispersion with Calgon®. The hydrometer method outlined here is a simplified version of Day (1965).

55.3.1 Materials and Reagents

1 Standard hydrometer, ASTM No. 1. 152H, with Bouyoucos scale in g L^{-1}

2 Electric stirrer

3 Plunger

4 End-over-end shaker

5 Cylinders with 1000 mL mark 36 $\pm$ 2 cm from the bottom of the inside

6 Amyl alcohol

7 Calgon® solution (50 g L^{-1}). Contains sodium hexametaphosphate, a dispersing agent

8 Constant-temperature room

55.3.2 Calibration of Hydrometer

1 Add 100 mL of Calgon® solution to the cylinder and make the volume to 1000 mL with distilled water. Mix thoroughly with plunger and let stand until the temperature is constant (between 20°C and 25°C).

2 Lower the hydrometer into the solution carefully, and determine the scale reading R_L at the upper edge of the meniscus surrounding the stem.

55.3.3 Hydrometer Procedure

1 Weigh 40 g of soil (100 g if loamy sand or sandy soil) into a 600 mL beaker, add 100 mL of Calgon® solution, and 300 mL of distilled water, and allow the sample to soak overnight.

2 Weigh another sample of the same soil (10 g) for determination of oven-dried weight. Dry overnight at 105°C, cool, and weigh.

3 Transfer the Calgon®-treated sample to a dispersing cup and mix for 5 min with an electric mixer (milkshake machine), or transfer the suspension to shaker bottles and shake overnight on an end-over-end shaker.

4 Transfer the suspension to a cylinder and add distilled water to bring the volume to 1000 mL.

5 Allow time for the suspensions to equilibrate to room temperature (between 20°C and 25°C).

6 Insert the plunger and move it up and down to mix contents thoroughly. Dislodge sediment with strong upward strokes of the plunger near the bottom and by

spinning the plunger while the disk is just above the sediment. Finish stirring with two or three slow, smooth strokes. Record the time of completion of stirring. Add a drop of amyl alcohol if the surface of the suspension is covered with foam.

7 Lower the hydrometer carefully into the suspension and take readings after 40 s ($R_{40\,s}$).

8 Remove the hydrometer carefully after the 40 s reading, rinse it, and wipe it dry.

9 Reinsert the hydrometer carefully and take another reading after 7 h ($R_{7\,h}$).

55.3.4 Calculations

$$\text{Sand}\% = 100 - (R_{40\,s} - R_L) \times \frac{100}{\text{oven-dried soil (weight in grams)}} \tag{55.8}$$

$$\text{Clay}\% = (R_{7\,h} - R_L) \times \frac{100}{\text{oven-dried soil (weight in grams)}} \tag{55.9}$$

$$\text{Silt}\% = 100 - (\text{sand}\% + \text{clay}\%) \tag{55.10}$$

55.3.5 Comments

The simplified hydrometer method described in the chapter is not recommended for calcareous or saline soils or soils with greater than 2% organic C. For detailed hydrometer methods please refer to Day (1965).

55.4 SIEVE ANALYSIS (MECHANICAL METHOD)

The grain-size analysis is used in the classification of soils for engineering purposes. The resulting grain-size distribution curves are used as part of the criteria for road engineering, i.e., for road embankment construction or for determining the susceptibility of a soil to frost action.

This grain-size analysis is an attempt to determine the relative proportions of the different grain sizes that make up a given soil mass. This type of analysis has limitations; Day (1965) states that the probability of a particle passing through a sieve in a given time of shaking depends on the nature of the particle, the number of particles of that size, and the properties of the sieve. Gee and Or (2002) suggest that good reproducibility requires careful standardization of the procedure.

55.4.1 Materials and Reagents

1 Sieves and pan (20 cm diameter). Recommended ASTM sieve sizes No. 4 (4.76 mm), No. 10 (2.00 mm), No. 40 (0.42 mm), and No. 200 (0.074 mm)

2 Sieve brush

3 Glass beaker (500 mL)

4 Porcelain evaporation dish (20 cm diameter)

5 Balance (capacity 1000 g; sensitivity 0.1 g)

6 Mortar and rubber-tipped pestle

7 Drying oven (105°C)

8 Sieve shaker

55.4.2 Procedures

1 Thoroughly clean and weigh each sieve to be used to 0.1 g.

Note: Sieves should always be brushed and cleaned from the bottom side. Particles, which are forced through the sieve from the top, may enlarge the openings and reduce the accuracy and life expectancy of the sieve. Particles, which are stuck in the mesh, may be loosened by tapping the side wall of the sieve against the palm of the hand.

2 Select and weigh a representative sample of approximately 500 g, separate the soil into individual soil particles by crushing with fingers or a rubber-tipped pestle.

The size of sample that is considered to be representative is dependent upon the maximum size fragment present or to be analyzed (Gee and Or 2002). Refer to the list below for representative sample guidelines:

Particles up to 5 mm—500 g

Particles up to 20 mm—5 kg

Particles up to 75 mm—20 kg

Note: For fine-grained soils that dry into hard clods or aggregates, the best and most reproducible method to perform sieve analysis is to take a quantity of oven-dried soil, break the sample as fine as possible, wash on a No. 200 sieve, oven-dry, and sieve the residue through a stack of sieves by shaking horizontally mechanically or by hand for 10 min.

3 The initial washing of the soil should be carefully conducted to avoid damaging the sieve or losing any soil by splashing the material out of the sieve. Wash the soil through the sieve using tap water until the wash water runs clear.

4 Using a wash bottle, carefully back-wash the residue into a large porcelain evaporation dish, decant as much excess water as possible, making sure not to lose any of the sample. Oven-dry the remainder of the soil–water suspension for 16 to 24 h at 105°C.

5 Remove sample from the drying oven, place a watch glass on top of the evaporation dish, and allow the dish and contents to cool to room temperature. Record the weight of the sample (S_w).

6 Pass the sample through the stack of sieves, using the following sieve sizes: #4, #10, #40, and #200. It is recommended that #20, #60, #100, and #140 sieves also be included in the stack to improve the fit to the semilogarithmic curve.

7 Shake the sample with the sieve shaker for 10 min, weigh each sieve, and record the weight of the sieve plus soil. Subtract the initial weight of the sieve as determined in step 1 and calculate the amount of the total sample retained on each sieve (as a percentage).

8 Sum the total weight of the sieve residues and compare this to the sample weight (S_w) recorded in step 5. If there is greater than 2% discrepancy, the test should be repeated.

9 Calculate the percentage passing each sieve by starting with 100% and subtracting the percent sample retained on each step as a cumulative procedure.

10 Plot a semilogarithmic grain-size distribution curve. If less than 10% of the total sample passes the #200 sieve, the test is finished; if more than 10% passes, then continue with a particle size distribution method.

11 From the grain-size distribution curve calculate the coefficient of uniformity ($Cu = D_{60}/D_{10}$) where D refers to the effective diameter of the soil particles and subscripts (10 and 60) denote the percent which is smaller. An indication of the spread or range of grain size is given by Cu, with a large Cu value indicating that D_{60} and D_{10} sizes differ appreciably.

55.5 NEWER METHODS

Gee and Or (2002) outlined some newer methods of PSA. These include x-ray attenuation, particle counting (Coulter method), and laser light scattering (diffraction). Elias et al. (1999) and Vaz et al. (1999) discussed gamma-ray attenuation while McTainsh et al. (1997) proposed a composite method of PSA involving sieving (>75 μm), Coulter particle counting (2–75 μm), and pipette (<2 μm).

REFERENCES

Day, P.R. 1965. Particle fractionation and particle size-analysis. In C.A. Black et al., Eds. *Methods of Soil Analysis*. Agronomy No. 9, Part 1. American Society of Agronomy, Madison, WI, pp. 545–567.

Elias, E.A., Bacchi, O.O.S., and Reichardt, K. 1999. Alternative soil particle-size analysis by gamma-ray attenuation. *Soil Till. Res.* 52: 121–123.

Gee, G.W. and Or, D. 2002. Particle-size analysis, In J.H. Dane and G.C. Topp, Eds. *Methods of Soil Analysis, Part 4 — Physical Methods*. Soil Science Society of America, Madison WI, pp. 255–293.

Gregorich, E.G., Turchenek, L.W., Carter, M.R., and Angers, D.A., Eds. 2001. *Soil and Environmental Science Dictionary*. CRC Press, Boca Raton, FL.

McKeague, J.A., Ed. 1978. *Manual on Soil Sampling and Analysis*, 2nd ed. Canadian Society of Soil Science, Ottawa, ON, Canada.

McTainsh, G.H., Lynch, A.W., and Hales, R. 1997. Particle-size analysis of aeolian dusts, soils, and sediments in very small quantities using a Coulter multisizer. *Earth Surf. Proc. Land.* 22: 1207–1216.

Sheldrick, B.H. and Wang, C. 1987. Compilation of data for ECSS reference soil samples. Land Resource Research Centre, Agriculture Canada, Ottawa, ON, Canada.

Sheldrick, B.H. and Wang, C. 1993. Particle size distribution. In M.R. Carter, Ed. *Soil Sampling and Methods of Analysis*. Canadian Society of Soil Science. Lewis Publishers, Boca Raton, FL, pp. 499–511.

Soil Classification Working Group. 1998. *The Canadian System of Soil Classification*. Agriculture and Agri-Food Canada Publication 1646 (Revised), Ottawa, ON, Canada.

Soil Conservation Service. 1984. Soil survey laboratory methods and procedure for collecting soil samples. *Soil Survey Investigations*, Report No. 1. (Revised 1984), U.S. Department of Agriculture, Washington, DC.

Vaz, C.M.P., Naime, J.M., and Macedo, A. 1999. Soil particle size fractions determined by gamma-ray attenuation. *Soil Sci*. 164: 403–410.

Chapter 56
Soil Shrinkage

C.D. Grant
University of Adelaide
Glen Osmond, South Australia, Australia

56.1 INTRODUCTION

Soil shrinkage is the reduction in bulk volume that occurs during drying. It occurs to varying degrees in all soils but most extensively in soils containing appreciable amounts of expanding lattice (smectitic) clays, especially when they are sodic (Parker et al. 1977; Boivin et al. 2004). Also, if a soil shrinks, it can usually swell again, but hysteresis in volume change is common in clays, so shrinkage is not always truly reversible (e.g., Haines 1923; Holmes 1955; Chang and Warkentin 1968). Despite the big differences between shrinkage and swelling processes, however, shrinkage has long been used to indicate a soil's shrink-swell capacity (e.g., Franzmeier and Ross 1968; Ross 1978; De Jong et al. 1992), and to indicate its mechanical workability and its potential for crop performance (Auchinleck 1912). Furthermore, the integrity of engineering structures (Jumikis 1984; Gillot 1986), the potential for pollution of groundwater through cracks (Coles and Trudgill 1985), the regeneration of damaged soil structure (Pillai-McGarry and McGarry 1999), and the availability of soil water under modest overburdens (Groenevelt and Grant 2001; Groenevelt et al. 2001) all depend on the shrink-swell properties of a soil.

Different stages of shrinkage can be identified and the extent of each depends *inter alia* upon whether the soil is poorly or well structured at saturation. For example, when a poorly structured soil begins to lose water from a saturated state, it shrinks. So long as it remains completely saturated during shrinkage, this initial stage of shrinkage is correctly described as ''normal''—the reduction in volume of the soil is exactly equal to the volume of water lost. When interparticle contacts prevent normal shrinkage, cracks form and air enters the soil matrix. Beyond the ''air-entry'' point, shrinkage continues in a manner described as ''residual,'' wherein the reduction in bulk soil-volume gradually declines to values that are less than the volume of water lost. In most soils, shrinkage becomes increasingly restrained and eventually stops beyond the so-called ''shrinkage limit,'' although this ''limit'' may not always occur at a single, clearly defined water content (Groenevelt and Grant 2004). A well-structured soil, however, contains stable macropores, which simply drain and cause little or no loss of bulk volume across a range of water contents known as the ''structural'' shrinkage range. When the structural pores are empty and no further air can enter the soil matrix, it continues to shrink in a proportional fashion such that the reduction in volume is equal to,

or close to, the volume of water lost—this stage is described as ''basic'' (Mitchell 1992) or ''proportional'' shrinkage (Groenevelt and Grant 2001). Beyond this point, well-structured soils continue to shrink in the residual manner described above.

The methods used to measure shrinkage depend upon the purposes for which the data are collected. For example, data on laboratory soil samples differ significantly from data collected in the field, because large differences exist in the scale at which cracks occur between soil in the field and soil contained in laboratory cores (e.g., Crescimanno and Provenzano 1999), and also because lateral and overburden pressures are present *in situ*, whereas, they often are not in the laboratory (Richards 1986). Furthermore, most field-based measures of shrinkage rely on the existence of a conceptual link between one-dimensional and three-dimensional soil movement, such that changes in elevation or height can be related to changes in volume (Aitchison and Holmes 1953). For most purposes, the assumption of equidimensional shrinkage is probably not unreasonable (Yaalon and Kalmar 1972; Yule and Ritchie 1980a,b), but the link may depend upon the range of soil water contents during which measurements of height are taken (Fox 1964) as well as the sample size relative to the representative elementary volume in the field. For example, measurements of height-change in the field ignore horizontal cracks, which can underestimate shrinkage. In the laboratory, measurements of volume change on small samples exclude cracks altogether, which can overestimate shrinkage. Either way, inherent errors must be acknowledged.

The laboratory methods to measure shrinkage are as numerous as those for particle size analysis. We will consider only two methods here—for further coverage of methods, the reader is referred to McGarry (2002). The field methods, while varying in style, virtually all focus on measuring vertical changes of the bulk soil at different points in the profile relative to a fixed reference point.

56.2 FIELD MEASUREMENT OF SOIL SHRINKAGE

Measuring shrinkage in the field relies heavily upon finding an immovable reference point. Such a point is not always easy to find and you may need to excavate the soil to bedrock or at least well below any zones of expansive soil. Alternatively, it is sometimes possible to gain a clear sighting to a distant reference point that is not affected by expansive soil.

56.2.1 Materials

1 Height-sensing rods of desired length and material. These should be cut with extra length so one end can be threaded coarsely for anchoring in concrete at the depth required and the other end can be cut to protrude from the ground so as to be easily located.

2 Open-casing (metal or PVC) to enclose each rod. The casing is fitted into an auger hole in the soil and the height-sensing rod is driven into wet concrete poured down the hole and allowed to set. The space between the rod and the casing is back-filled with either polystyrene beads (to prevent vapor movement) or heavy-duty grease (to prevent water entry where a water table exists)—either of these fillings also prevent movement of the access tube when the soil around it shrinks and swells.

3 Annular floating plate (available from most hardware stores) and depth gauge. The annular floating plate is placed over the open-casing and height-sensing rod to sit on the ground and move independently. The depth gauge is placed on the annular floating plate so the vertical movement of the height-sensing rod can be measured with precision.

4 Dumpy level, surveyor's ruler, and datum.

5 Neutron access tube (and neutron moisture meter). Most changes in vertical soil position over time are related to changes in water content, so a neutron access tube (or other moisture-monitoring system that does not disturb the soil profile) should be installed in the vicinity of the height-sensing rods. Assertions can then be made about the extent to which each point in the soil profile contributes to the overall vertical movement of the soil surface. This is particularly important for foundations and footings of engineered structures. An annular floating plate is placed over each tube to allow correction of the depth for each water content reading in case the access tube moves.

56.2.2 Procedures

1 At appropriate intervals in time, the vertical location of each height-sensing rod is checked relative to the annular floating plate using a dial gauge (Figure 56.1).

2 Vertical location of the annular floating plate is then measured relative to the datum using a dumpy level and surveyor's ruler, the operation of which requires two people (one to operate the dumpy level and one to hold the surveyor's ruler on the datum and on the various annular floating plates).

3 Water content of the soil at the depth of each height-sensing rod is measured using a neutron moisture meter. The depths need to be chosen carefully because the average volume of soil represented by each neutron moisture reading is quite large. This requires the height-sensing rods to be placed well above or below horizon boundaries so that average water contents come from uniform layers and can be interpreted.

56.2.3 Comments

The materials for field measurements will vary according to how long the equipment must stay in the ground and what the budget will allow. Salt-resistant and redox-insensitive materials are best for long burial, but appropriate materials vary hugely in price (stainless steel, Teflon, and Perspex are all relatively expensive). Figure 56.1 shows a schematic of the basic equipment involved, but examples showing photos and other schematics of typical equipment used for various purposes can be found in Aitchison and Holmes (1953), Coquet (1998), Braudeau et al. (1999), and Kirby et al. (2003).

Shrinkage generally occurs close to the soil surface where changes in water content are the greatest, but this is not always the case. If water is extracted by plant roots at different depths,

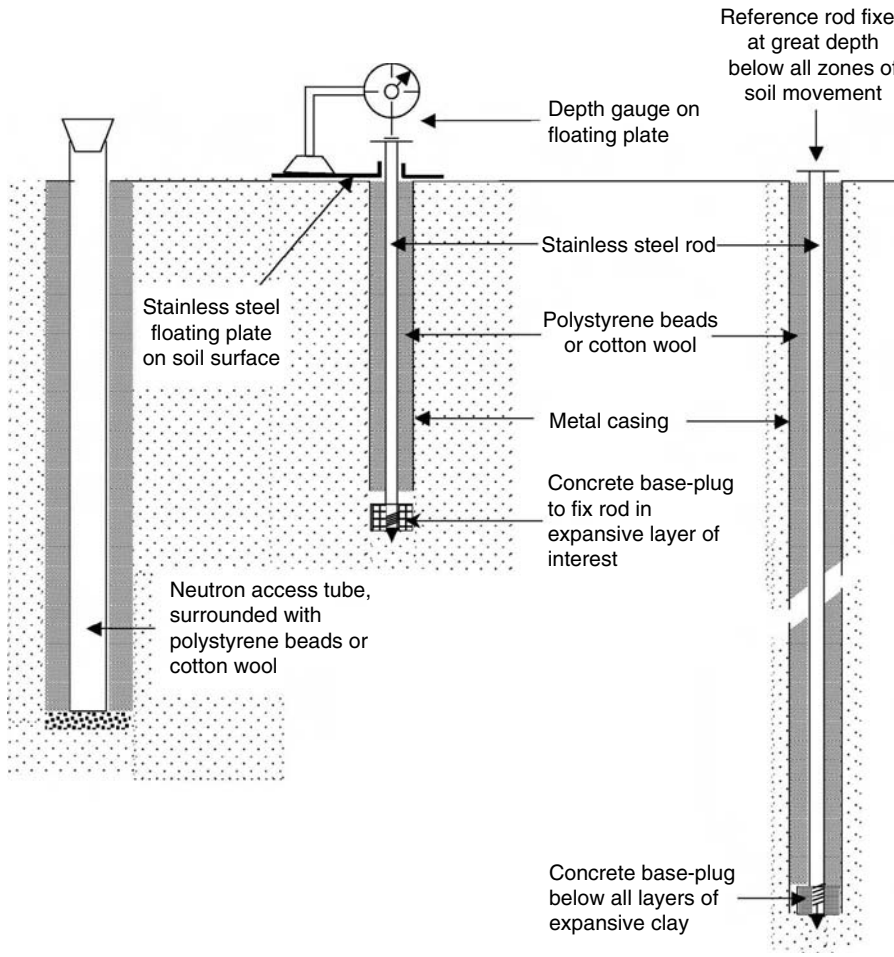

FIGURE 56.1. Schematic of instrumentation used to measure vertical soil movement and water content.

it can be difficult to link water content changes with changes in height unless there is knowledge of the bulk densities of the soil at different depths (such information may be available from calibration of the neutron probe for that soil). With this information, adjustments can be made to the water content profile by taking into account the total depth of soil (material depth) in the saturated state (Ringrose-Voase et al. 2000). It should also be noted that the calibration of neutron probes in expansive soils depends upon bulk density, which changes with water content, so is not linear. Greacen et al. (1981) used the following relation to obtain accurate water contents (θ), from neutron probe readings in swelling soils:

$$\theta = \exp\left(\frac{\mathrm{CR} - c}{m}\right) \tag{56.1}$$

where CR is the count ratio and c and m are dimensionless fitting parameters.

56.3 LABORATORY MEASUREMENT OF SOIL SHRINKAGE

In the laboratory, there are many ways to measure shrinkage depending on equipment available and level of detail required. It is common, however, to measure linear shrinkage because it is simple and repeatable. This involves simply measuring the initial and final lengths of a remolded soil sample as it shrinks from a fixed state of wetness to an oven-dry state. Three-dimensional (volumetric) shrinkage is also measured sometimes, but the procedures involved are more detailed and time-consuming. The choice of method involves balancing the trade-off between rapid and simple procedures, which provide limited information on soil behavior versus more lengthy and complex procedures, which can provide extensive and detailed information from which complex aspects of soil behavior can be extracted (Grant et al. 2002).

56.3.1 Linear Shrinkage

There are several variations of methods to determine linear shrinkage (e.g., McGarry 2002), but a convenient method is to work the soil with water until it reaches a state of consistency known as the Atterberg liquid limit (see Chapter 58). A sample of the remolded soil is then pressed into a special semicylindrical mold of length, L (while tapping to remove air bubbles) and allowed to dry slowly until it reaches a final length at oven-dryness, L_d. The total reduction in length of the sample after drying is expressed as a percentage of the length of the mold, and called ''linear shrinkage'' (LS), as shown in the following equation:

$$\mathrm{LS} = \left(\frac{L - L_d}{L}\right) \times 100 \tag{56.2}$$

Materials

1. Sieve (2 mm), through which the soil should first be passed.
2. Distilled water to mix with soil.
3. Spatula or field knife of appropriate length to work the soil.
4. Large, thick, flat glass plate on which to work the soil.
5. Knowledge of the Atterberg liquid limit (or a device to determine it yourself).
6. Oven, set at 105°C.
7. Semicylindrical mold 2.5 cm internal diameter and 25 cm long (can be shorter), with rectangular ends to contain the wet soil and steady the trough. The mold can be made from any rigid material that will not rust and will not melt at 105°C (e.g., brass or stainless steel). In some cases (e.g., teaching large undergraduate practical classes), such materials may be prohibitively expensive, and it is possible to demonstrate the principles using cheaper materials (e.g., PVC-electrical tubing, split down the middle) so long as the temperature used for oven-drying is not raised above 60°C.

8 Silicone grease to line the mold to reduce sticking and cracking during drying.

9 Ruler (mm graduations).

Procedures

1 If you already know the soil's water content at the Atterberg liquid limit, determine the air-dry water content of the soil material you plan to use.

2 Take a 200 g sample of the air-dry soil and gradually add sufficient distilled water to make up the difference in water contents between the air-dry state and the liquid limit. (If you do not already know the Atterberg liquid limit, then determine this using current standard procedures—see Chapter 58.)

3 Work the mixture thoroughly with a spatula to obtain the liquid limit paste, then cover the mixture in a sealed container and leave it overnight to equilibrate (check the water content next day to ensure it is still at the liquid limit before proceeding—adjust as necessary with additional water and mix well).

4 Grease the inside of the shrinkage mold of length, *L*, shown in Figure 56.2a.

5 Fill the mold with the well-mixed soil paste in such a way as to prevent air gaps, and such that the surface is flat and level with the sides of the mold. Clean the edges of the mold with a moist cloth to prevent the soil from sticking to the edges as the soil shrinks (Figure 56.2b).

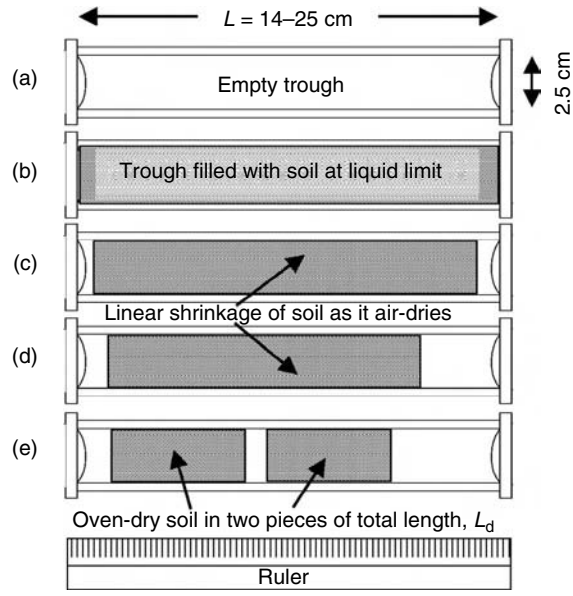

FIGURE 56.2. Trough used to measure linear shrinkage of remolded soil. Letters described in text.

6 Allow the sample to dry slowly over several days at room temperature (Figure 56.2c and Figure 56.2d).

7 Transfer the mold into an oven at 105°C for 24 h (or for PVC molds—60°C for 1 week), then remove it and allow it to cool.

8 Measure the length of the dry soil in the mold, L_d. If the soil has cracked, assemble the pieces carefully and measure their combined length (Figure 56.2e).

Comments

For highly expansive soils, the final shape of the oven-dry soil in the mold may be cracked and distorted, which makes obtaining a good measure of L_d difficult. One way to avoid excessive cracking and distortion is to prevent the sample drying quickly—perhaps in a sealed container open to the air periodically over weeks instead of days. Put the sample into the oven at 105°C only when you are confident most of the water has evaporated. If you cannot wait that long and you are faced with a broken sample, try to reassemble the bits of soil at the crack-faces and measure their combined length using a piece of string.

Various modifications of the linear shrinkage method have been proposed and are widely used (e.g., Mills et al. 1980; McKenzie et al. 1994). Some methods use finer aggregates (e.g., <425 μm) and different procedures to establish the uppermost water content at which shrinkage begins (e.g., equilibration at a certain matric head following a standardized packing procedure). It is thus important to report the details of any such modifications.

Values of LS correlate well with other measures of shrinkage (described below), and can even be correlated with the tendency of nondispersive, expansive soils to exhibit self-mulching behavior (Grant and Coughlan 2002).

56.3.2 Three-Dimensional Shrinkage

If more detailed knowledge of the shrink-swell characteristics of an expansive soil is required, three-dimensional soil shrinkage is measured by observing the change in bulk mass and volume of a sample as it dries from a wet state. A widely used method for this purpose is the coefficient of linear extensibility (COLE), which was developed by Grossman et al. (1968). The method is not described here, however, because it does not deal with shrinkage from saturation, and furthermore, the method is well described elsewhere (Dasog et al. 1988; Warkentin 1993; Soil Survey Staff 1999; McGarry 2002).

This section focuses on the detailed measurement of three-dimensional shrinkage from total saturation to oven-dryness. First, however, a few things need to be appreciated before embarking on this measurement, because to do it well can take many weeks.

Measuring the mass of a soil sample is a trivial matter, at least in concept if not in practice (e.g., very wet samples can be difficult to weigh because they deform easily during handling, but if the sample is stable its mass can easily be recorded). I have found that samples are best contained in Teflon rings to avoid deformation during handling and to prevent samples from sticking to the edges of the ring as they shrink.

The primary challenge in monitoring three-dimensional soil shrinkage is to obtain accurate measures of the bulk volume of a sample. Measuring the linear dimensions of a cube or

cylinder or other regular shape of soil is relatively simple (Schafer and Singer 1976)—good instruments are available for this purpose, such as Vernier callipers, traveling microscopes, and cathetometers to name a few. The volume of a regularly shaped sample can be calculated with reasonable precision and accuracy from the linear dimensions, at least during the early stages of shrinkage. For irregularly shaped samples, however, the error in estimating volume by estimating the linear dimensions increases as the cube of the error in the measured lengths. Most studies simply ignore this problem and do not report linear measurement errors. Remolded samples that start with regular shapes (disks, cubes, etc.) often deform during drying and lose their regular shape—greater errors occur in determining the volume of such samples, particularly if they are small.

Archimedes' principle tells us that when a solid object is immersed in an incompressible fluid (e.g., water), it will displace a mass of the fluid equivalent to the volume of the object. This is because an object experiences buoyancy when immersed, so its mass appears to decline. The apparent weight loss of the solid immersed in the fluid is directly proportional to the volume of the fluid displaced. The sample is usually coated with a thin layer of Saran resin, which prevents liquid water being taken up but allows water vapor to diffuse out during shrinkage (Warkentin 1993). If applied thinly, the correction required for the volume of the Saran coating can be as small as 4.6% (McGarry 2002). The volume of the sample, V_{sample}, can be calculated using the following equation:

$$V_{\text{sample}} = V_{\text{water}} = \frac{M_{\text{sample(air)}} - M_{\text{sample(water)}}}{\rho_{\text{water}}} = \frac{M_{\text{water}}}{\rho_{\text{water}}} \tag{56.3}$$

where V_{water} is the volume of water displaced by soil sample, M_{water} the mass of water displaced by soil sample, $M_{\text{sample(air)}}$ the mass of soil sample measured in air, $M_{\text{sample(water)}}$ the mass of soil sample measured in water, and ρ_{water} the density of water at ambient temperature.

A satisfactory alternative to coating the sample with Saran is to case the sample in a thin rubber membrane such as a balloon or prophylactic (Tariq and Durnford 1993). The apparatus shown in Figure 56.3a through Figure 56.3c, enables the sample to dry slowly

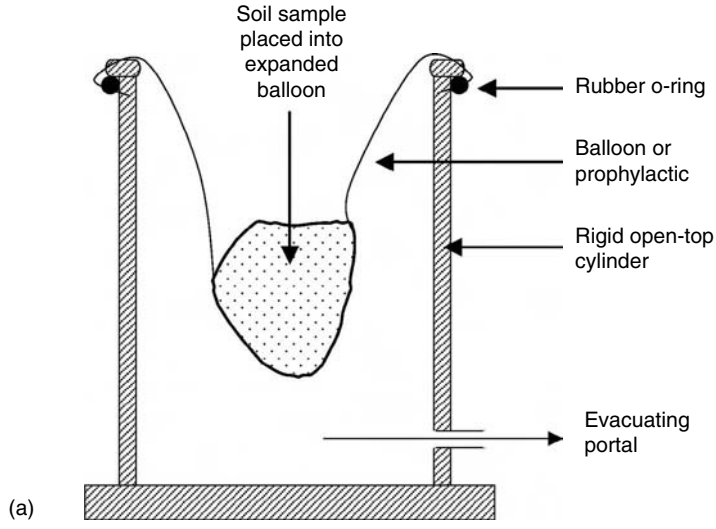

FIGURE 56.3. (a) Suction cylinder used to fit a thin rubber membrane around a soil sample.

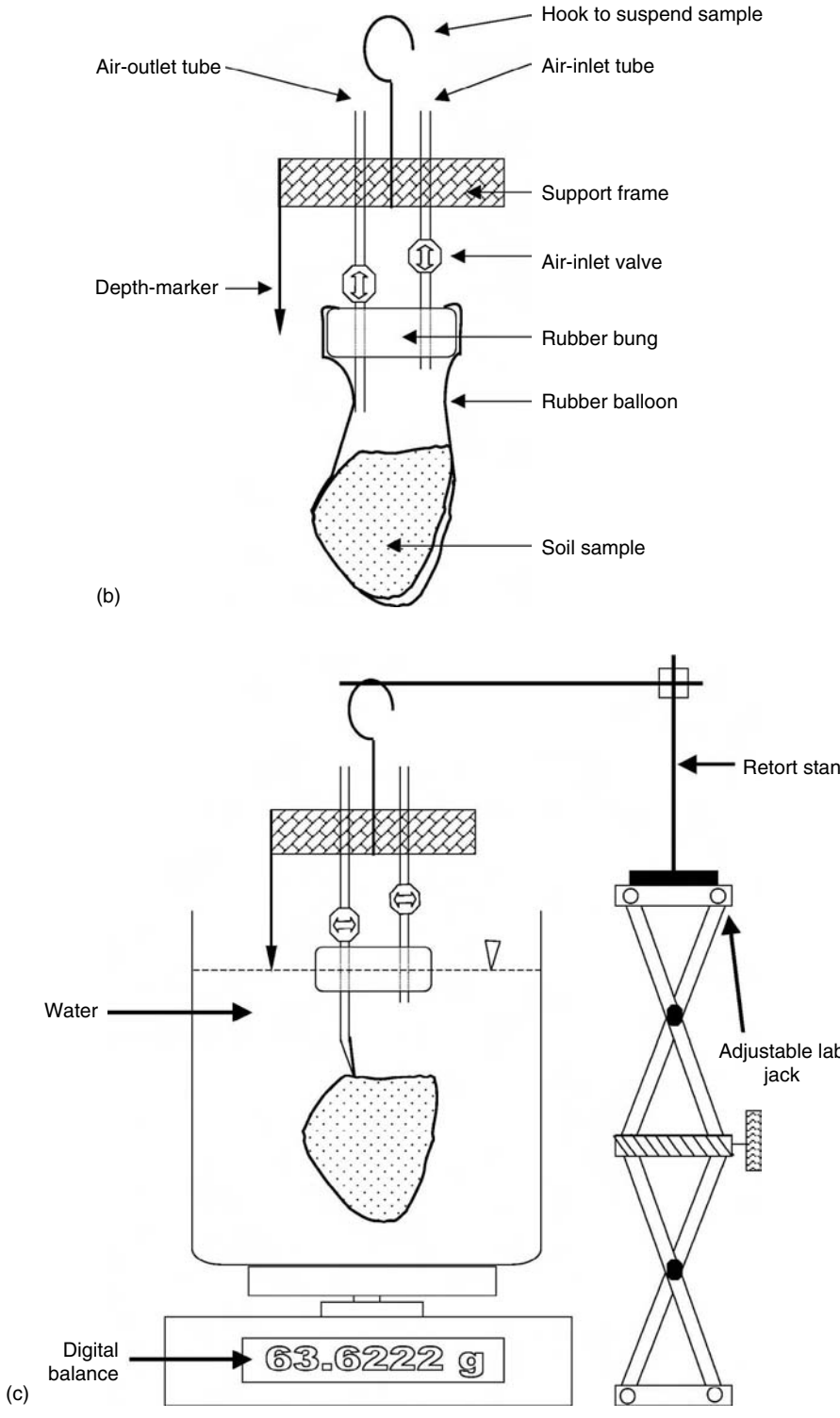

FIGURE 56.3. (continued) (b) Apparatus for supporting the sample and drawing air across it to dry it in its membrane. (c) Assembly to determine the volume of the soil sample by displacement as it shrinks.

without handling it or the membrane at any time during shrinkage, and allows easy removal for obtaining the oven-dry weight.

Materials

1 Rigid (e.g., brass) open cylinder (called a ''suction cylinder'' used by engineers in association with triaxial apparatus) with rubber o-ring at top and an evacuating portal near the base (Figure 56.3a). This needs to be large enough to hold the soil sample yet small enough so that a thin rubber membrane (e.g., balloon or prophylactic) can be stretched over the rim and held firmly by a rubber o-ring.

2 Large, thin-walled balloon or prophylactic. The mass and volume of the rubber membrane, when stretched over the soil sample, are very small and may be negligible.

3 Materials to make up a sample-support structure with rigid air-inlet and -outlet tubes as shown in Figure 56.3b.

4 Laboratory retort stand and adjustable laboratory jack.

5 Digital top-loading balance of 1 kg capacity.

6 1000 mL beaker or other container.

7 Source of dry air, with pressurized adjustable flow rate.

8 Soil clod, of any volume in the range 30–500 cm^3 (larger is better).

9 Water at same temperature as soil sample.

10 Other materials shown in Figure 56.3c.

Procedures

1 Assemble the materials shown in Figure 56.3a through Figure 56.3c.

2 Use the rigid open cylinder and apply a small suction to expand the balloon against the sides of the cylinder while you place the soil sample in it.

3 Release the suction to allow the balloon to fit firmly around the sample, ensuring no air gets entrapped.

4 Remove the sample from the suction cylinder and wrap the neck of the balloon over the rubber bung shown in Figure 56.3b such that the air-inlet and -outlet tubes are not blocked.

5 Close off the air-inlet valve and open the air-outlet valve. Apply suction to exclude all air and to make the balloon fit tightly against the sample.

6 Weigh the sample to obtain the weight in air, $M_{\text{sample(air)}}$.

7 Hang the assembled sample onto the retort stand and lower it into a beaker of water sitting (tared) on a top-loading electronic digital balance. Record the weight, $M_{\text{sample(water)}}$, when you have lowered the sample to a consistent depth indicated by the depth-marker in Figure 56.3c.

8 To dry the sample, lift it from the beaker, open both air valves, and apply a steady, small positive pressure down the air-inlet tube; the air passes over the soil sample and escapes through the air-outlet tube.

9 Control the rate of shrinkage by adjusting the flow of air over the sample.

10 As shrinkage occurs, measure the volume at periodic intervals by repeating procedures 5 to 7.

11 When shrinkage ceases, remove the sample from the membrane, dry it at 105°C and measure the oven-dry mass and volume.

12 Calculate the sample volume for each stage using Equation 56.3. Use the data to calculate the void ratio, e (volume of pores per unit volume of solids) and the moisture ratio, ϑ (volume of water per unit volume of solids) using the following equations:

$$e = \frac{V_{\text{pores}}}{V_{\text{solids}}} \tag{56.4}$$

where

$$V_{\text{pores}} = V_{\text{sample}} - V_{\text{solids}}$$
$$V_{\text{solids}} = \frac{M_{\text{OD solids}}}{\rho_{\text{solids}}}$$

where $M_{\text{OD solids}}$ is the oven-dry weight of sample.

$$\vartheta = \frac{V_{\text{water}}}{V_{\text{solids}}} \tag{56.5}$$

where

$$V_{\text{water}} = \frac{M_{\text{water}}}{\rho_{\text{water}}}$$

where M_{water} is the mass of water remaining in soil sample at each stage of shrinkage and ρ_{water} is the density of water at ambient temperature, often assumed to be 1 g cm^{-3}.

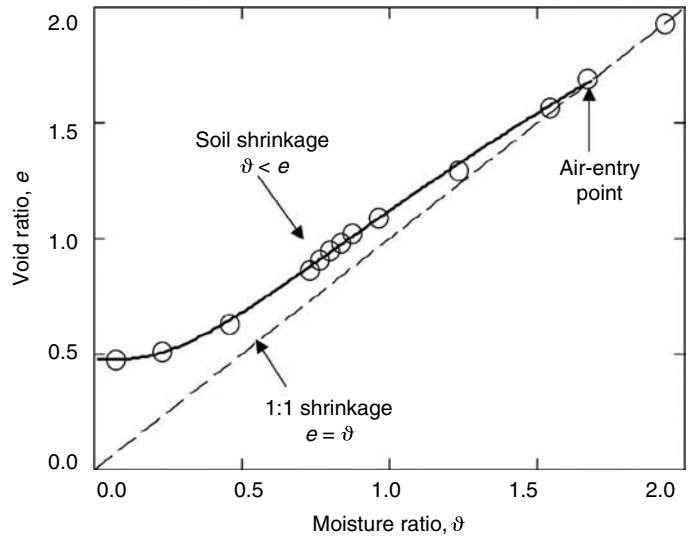

FIGURE 56.4. Typical shrinkage curve showing the air-entry point and the line of shrinkage taken by the soil relative to the 1:1 line.

13 Plot the void ratio as a function of the moisture ratio for each stage of shrinkage. This will produce a ''shrinkage curve,'' which can be superimposed on a 1:1 line to identify the point of air entry as shown in Figure 56.4.

Comments

1 To obtain both the mass and the volume of an irregularly shaped soil sample by direct measurement and without disturbing or handling the sample is a challenging prospect. The method outlined here presents the fewest technical problems in this regard but it is still imperfect. A range of different rubber membranes needs to be kept on hand because sample size and shape vary. The thickness and integrity of the rubber membrane must be sufficiently thin and flexible to hug all external macropores, yet thick enough not to tear. Prophylactics from the supermarket seem to offer as much scope as any rubber material available, but these vary from place to place and with time so it is a tedious exercise to find a suitable range. The suction cylinder helps to obtain a good fit with the soil sample, but practice is required to avoid small gaps.

2 Samples raised from the soil profile and brought into the laboratory to measure shrinkage (e.g., Reeve and Hall 1978; Prebble 1991) behave differently than they would under their natural overburden (Groenevelt et al. 2001). A load equivalent to the natural overburden needs to be applied during measurement of shrinkage in the laboratory; otherwise, the matric head needs to be corrected. It is theoretically possible to correct the matric head using the unloaded shrinkage line (e.g., Groenevelt and Bolt 1972; Stroosnijder 1976; Groenevelt and Kay 1981) but almost no data exist to corroborate this and all of it comes from remolded pastes (e.g., Talsma 1977), not undisturbed soils. To avoid having to correct the matric head, an overburden could be applied to samples using the technique outlined here with only minor modification. It should be possible to encase the entire

apparatus shown in Figure 56.3b and immerse it underwater to a depth equivalent to the overburden. The air-inlet and -outlet tubes would require consideration to keep them open during air flow, or it might also be possible to eliminate the need for one of the tubes by coating the sample with a porous membrane and immerse the sample in a fluid for which the osmotic head can be adjusted (e.g., polyethylene glycol [PEG]). This would achieve a known osmo-matric head (cf. Groenevelt et al. 2004), while at the same time allowing the natural overburden to be applied. A clever student could work out the technical details.

3 The shrinkage curve can be analyzed in a number of ways to obtain shrinkage limits, plastic limits, and other important structural characteristics of expansive soils (cf. Groenevelt and Grant 2002; Peng et al. 2005; Cornelis et al. 2006).

REFERENCES

Aitchison, G.D. and Holmes, J.W. 1953. Aspects of swelling in the soil profile. *Aust. J. Appl. Sci.* 4: 244–259.

Auchinleck, G. 1912. The measurement of shrinkage in soils and its application in agriculture. *West Indian Bull.* 12: 50–61.

Boivin, P., Garnier, P., and Tessier, D. 2004. Relationship between clay content, clay type, and shrinkage properties of soil samples. *Soil Sci. Soc. Am. J.* 68: 1145–1153.

Braudeau, E., Costantini, J.M., Bellier, G., and Colleuille, H. 1999. New device and method for soil shrinkage curve measurement and characterization. *Soil Sci. Soc. Am. J.* 63: 525–535.

Chang, R.K. and Warkentin, B.P. 1968. Volume change of compacted clay soil aggregates. *Soil Sci.* 105: 106–111.

Coles, N. and Trudgill, S. 1985. The movement of nitrate fertiliser from the soil surface to drainage waters by preferential flow in weakly structured soils, Slapton, S. Devon. *Agric. Ecosyst. Environ.* 13: 241–259.

Coquet, Y. 1998. *In situ* measurement of the vertical linear shrinkage curve of soils. *Soil Till. Res.* 46: 289–299.

Cornelis, W.M., Corluy, J., Medina, H., Diaz, J., Hartmann, R., Van Meirvenne, M., and Ruiz, M.E. 2006. Measuring and modelling the soil shrinkage characteristic curve. *Geoderma* 137: 179–191.

Crescimanno, G. and Provenzano, G. 1999. Soil shrinkage characteristic curve in clay soils: measurement and prediction. *Soil Sci. Soc. Am. J.* 63: 25–32.

Dasog, G.S., Acton, D.F., Mermut, A.R., and De Jong, E. 1988. Shrink-swell potential and cracking in clay soils of Saskatchewan. *Can. J. Soil Sci.* 68: 251–260.

De Jong, E., Kozak, L.M., and Stonehouse, H.B. 1992. Comparison of shrink-swell indices of some Saskatchewan soils and their relationships to standard soil characteristics. *Can. J. Soil Sci.* 72: 429–439.

Fox, W.E. 1964. A study of bulk density and water in a swelling soil. *Soil Sci.* 98: 307–316.

Franzmeier, D.P. and Ross, S.J. 1968. Soil swelling: laboratory measurement and relation to other soil properties. *Soil Sci. Soc. Am. Proc.* 32: 573–577.

Gillot, J.E. 1986. Some clay-related problems in engineering geology in North America. *Clay Miner.* 21: 261–278.

Grant, C.D. and Coughlan, K.J. 2002. Estimation of the self-mulching characteristics of surface soils. In N.J. McKenzie, K.J. Coughlan, and H.P. Cresswell, Eds. *Soil Physical Measurement and Interpretation for Land Evaluation*, CSIRO Australia, Melbourne, pp. 370–372.

Grant, C.D., Groenevelt, P.H., and Bolt, G.H. 2002. On hydrostatics and matristatics of swelling soils. In P.A.C. Raats, D.E. Smiles, and A. Warrick,

Eds. *Environmental Mechanics: Water, Mass, and Energy in the Biosphere*. American Geophysical Union, Washington, DC, pp. 95–105.

Greacen, E.L., Correll, R.L., Cunningham, R.B., Johns, G.G., and Nicolls, K.D. 1981. Calibration. In E.L. Greacen, Ed. *Soil Water Assessment by the Neutron Method*. CSIRO Australia, Melbourne, pp. 50–81.

Groenevelt, P.H. and Bolt, G.H. 1972. Water retention in soil. *Soil Sci*. 113: 238–245.

Groenevelt, P.H. and Grant, C.D. 2001. Reevaluation of the structural properties of some British swelling soils. *Eur. J. Soil Sci*. 52: 469–477.

Groenevelt, P.H. and Grant, C.D. 2002. Curvature of shrinkage lines in relation to the consistency and structure of a Norwegian clay soil. *Geoderma* 106: 235–245.

Groenevelt, P.H. and Grant, C.D. 2004. Analysis of soil shrinkage data. *Soil Till. Res*. 79: 71–77.

Groenevelt, P.H., Grant, C.D., and Murray, R.S. 2004. On water availability in saline soils. *Aust. J. Soil Res*. 42: 833–840.

Groenevelt, P.H., Grant, C.D., and Semetsa, S. 2001. A new procedure to determine soil water availability. *Aust. J. Soil Res*. 39: 577–598.

Groenevelt, P.H. and Kay, B.D. 1981. On pressure distribution and effective stress in unsaturated soils. *Can. J. Soil Sci*. 61: 431–443.

Grossman, R.B., Brasher, B.R., Franzmeier, D.P., and Walker, J.L. 1968. Linear extensibility as calculated from natural-clod bulk density measurements. *Soil Sci. Soc. Am. Proc*. 32: 570–573.

Haines, W.R. 1923. The volume-changes associated with variations of water content in soil. *J. Agr. Sci. (Cambr.)* 13: 296–310.

Holmes, J.W. 1955. Water sorption and swelling of clay blocks. *J. Soil Sci*. 6: 200–208.

Jumikis, A.R. 1984. *Soil Mechanics*. R.E. Krieger Publishing, Malabar, FL.

Kirby, J.M., Bernardi, A.L., Ringrose-Voase, A.J., Young, R., and Rose, H. 2003. Field swelling, shrinking, and water content change in a heavy clay soil. *Aust. J. Soil Res*. 41: 963–978.

McGarry, D. 2002. Soil shrinkage. In N.J. McKenzie, K.J. Coughlan, and H.P. Cresswell, Eds. *Soil Physical Measurement and Interpretation for Land Evaluation*. CSIRO Australia, Melbourne, pp. 240–260.

McKenzie, N.J., Jacquier, D.J., and Ringrose-Voase, A.J. 1994. A rapid method for estimating soil shrinkage. *Aust. J. Soil Res*. 32: 931–938.

Mills, J.J., Murphy, B.W., and Wickham, H.G. 1980. A study of three simple laboratory tests for the prediction of soil shrink-swell behaviour. *J. Soil Cons. Serv. NSW* 36: 77–82.

Mitchell, A.R. 1992. Shrinkage terminology: escape from ''normalcy''. *Soil Sci. Soc. Am. J*. 56: 993–994.

Parker, J.C., Amos, D.F., and Kaster, D.L. 1977. An evaluation of several methods of estimating soil volume change. *Soil Sci. Soc. Am. J*. 41: 1059–1064.

Peng, X., Horn, R., Deery, D., Kirkham, M.B., and Blackwell, J. 2005. Influence of soil structure on the shrinkage behaviour of a soil irrigated with saline-sodic water. *Aus. J. Soil Res*. 43: 555–563.

Pillai-McGarry, U.P.P. and McGarry, D. 1999. Structure repair of a compacted vertisol with wet/dry cycles and rotation crops. *Soil Sci. Soc. Am. J*. 63: 201–210.

Prebble, R.E. 1991. Shrinkage, moisture characteristic, and strength of cracking clay soils. *CSIRO Division of Soils*, Divisional Report No.113, Melborne, Australia, 19 pp.

Reeve, M.J. and Hall, D.G.M. 1978. Shrinkage in clayey subsoils of contrasting structure. *J. Soil Sci*. 29: 315–323.

Richards, B.G. 1986. The role of lateral stresses on soil water relations in swelling clays. *Aus. J. Soil Res*. 24: 457–476.

Ringrose-Voase, A.J., Paydar, Z., and Cresswell, H.P. 2000. Swelling soils: problems with access-tube installations. In P. Charlesworth, Ed. *Irrigation Insights No. 1 Soil Water Monitoring*, Land and Water Australia, Canberra, Australia, pp. 54–56.

Ross, G.S. 1978. Relationships of specific surface area and clay content to shrink-swell potential of soils having different clay mineralogical compositions. *Can. J. Soil Sci.* 58: 159–166.

Schafer, W.M. and Singer, M.J. 1976. A new method of measuring shrink-swell potential using soil pastes. *Soil Sci. Soc. Am. J.* 40: 805–806.

Soil Survey Staff 1999. *Soil Taxonomy: A Basic System of Soil Classification for Making and Interpreting Soil Surveys*, 2nd edition. United States Department of Agriculture. Natural Resource Conservation Service. Agricultural Handbook No. 436. USA Government Printing Office, Washington, DC.

Stroosnijder, L. 1976. Infiltration in swelling and shrinking soils. Versl. Landbouwkd. Onderz. (Agric. Res. Rep.) 847: 119–174 (translated into English by T. Talsma).

Talsma, T. 1977. A note on the shrinkage behaviour of a clay paste under various loads. *Aus. J. Soil Res.* 15: 275–277.

Tariq, A.R. and Durnford, D.S. 1993. Soil volumetric shrinkage measurements: a simple method. *Soil Sci.* 155: 325–330.

Warkentin, B.P. 1993. Soil shrinkage. In M.R. Carter, Ed. *Soil Sampling and Methods of Analysis*, Canadian Society of Soil Science, Lewis Publishers, CRC Press, Boca Raton, FL, pp. 513–518.

Yaalon, D.H. and Kalmar, D. 1972. Vertical movement in an undisturbed soil: continuous measurement of swelling and shrinkage with a sensitive apparatus. *Geoderma* 8: 231–240.

Yule, D.F. and Ritchie, J.T. 1980a. Soil shrinkage relationships of Texas vertisols. 1. Small cores. *Soil Sci. Soc. Am. J.* 44: 1285–1291.

Yule, D.F. and Ritchie, J.T. 1980b. Soil shrinkage relationships of Texas vertisols. 2. Large cores. *Soil Sci. Soc. Am. J.* 44: 1291–1295.

Chapter 57
Soil Density and Porosity

X. Hao
Agriculture and Agri-Food Canada
Lethbridge, Alberta, Canada

B.C. Ball
Scottish Agricultural College
Edinburgh, Scotland, United Kingdom

J.L.B. Culley
Agriculture and Agri-Food Canada
Ottawa, Ontario, Canada

M.R. Carter
Agriculture and Agri-Food Canada
Charlottetown, Prince Edward Island, Canada

G.W. Parkin
University of Guelph
Guelph, Ontario, Canada

57.1 INTRODUCTION

Soil is composed of solid particles (minerals and organic matter) of different sizes, usually bound together into aggregates by organic matter, mineral oxides, and charged clay particles. The gaps between the particles are linked together in a complex network of pores of various sizes. The total pore space of a particular soil consists of pores existing both between adjacent soil particles and between soil aggregates. Through this pore space the soil exchanges water and air with the environment. The movement of air and water also allows for heat and nutrients to flow. The number and size of pores vary considerably among soils exhibiting different organic matter content, texture, and structure.

Soil bulk density ($D_b = m_s/V_t$) is the ratio of the mass of oven-dried solids (m_s) to the bulk volume (V_t) of the soil, which includes the volume of the solids and the pore space between the soil particles (Blake and Hartge 1986a). D_b is a widely used physical property; it is a

measure of soil compaction status and is needed for converting water percentage by weight to content by volume, for calculating porosity when particle density is known, and for estimating the weight of a volume of soil too large to weigh conveniently.

The particle density ($D_p = m_s/V_s$) refers to the mass (m_s) of a unit volume of solid soil particles (V_s). No account is taken for the pore space between the particles (Blake and Hartge 1986b). Particle density is used in most mathematical expressions where the volume or weight of a soil sample is being considered. Thus, interrelationships among porosity, bulk density, air space, and rates of sedimentation of particles in fluids depend on particle density.

Porosity (S_t) is the percentage of the soil volume occupied by pore spaces. The types of pores present in a soil are as important as the amount of pore space. Pore spaces are filled with air (F_a, air-filled porosity) or water (WFPS or relative saturation). Pore space is divided into different categories by pore diameter, especially the large soil pores that are associated with the transfer and movement of both water and air (Carter and Ball 1993).

Agricultural activities, which could involve tillage or the wheels of heavy machinery compacting soils, can have a great effect on bulk density and porosity (Gysi et al. 2000; Cameira et al. 2003; Osunbitan et al. 2005). Any management practice that increases organic matter will increase the granular structure of the soil, increase the pore space, and decrease the bulk density (Shaver et al. 2003). Soil density and porosity are the two most important parameters in assessing anthropogenic change in soil.

In the last decade, progress has been made in the determination of soil bulk density and porosity. One of the newer methods is computerized tomography (CT) based on image reconstruction techniques that use x-rays and γ-rays as a source of radiation (Pedrotti et al. 2005). This method has been used to measure soil physical properties, such as bulk density, water content (Crestana and Vaz 1998; Pedrotti et al. 2005), porosity, soil fracture size, geometry and topology of macropore networks (Perret et al. 1999), and micropore size (Macedo et al. 1998). Time domain reflectometry (TDR) probe methods are also being used to simultaneously measure water content, air-filled porosity, and bulk density (Ochsner et al. 2001). However, the focus of this chapter is on presenting common and easy to use methods that require simple and inexpensive equipment.

57.2 SOIL BULK DENSITY

The D_b is a dynamic soil property. D_b differs from D_p in that a measure of bulk density includes all pore space. Unlike D_p, which expresses the density of the solid soil constituents only, D_b is strongly influenced by the quantity and size of the pore spaces as well as the composition of the solid soil materials. As a result, loose, porous soils will have lower bulk densities than more compact soils. Sandy soils, which are relatively low in total pore space and are often low in organic matter content, typically have higher D_b values.

Except for recently tilled soil, D_b is considered to exhibit relatively low spatial variability (Warrick and Neilson 1980). Generally, coefficients of variability for measurements of D_b for a given profile horizon of a soil series do not exceed about 10% of the mean (Grossman and Reinsch 2002). Thus, about four samples per depth and per field of treatment should be sufficient to estimate the mean density to within 10% of the true values, 95% of the time, for a uniform soil type.

Soil D_b can be determined by either sampling or *in situ* methods. For sampling methods, which involve disturbing the soil and removing some of it, the most common is the core method while the clod and excavation approaches are also used. Alternatively, the nuclear radiation method will not disturb the soil being sampled. These four methods are described in this section. Different methods have different personnel and capital costs.

57.2.1 Core Methods

Materials and Supplies

1 Double-cylinder core sampler, either hand operated or hydraulically driven

2 Clean, dry, and uniform cylinder with a known internal diameter d (cm) and height h (cm). The volume V (cm^3) is

$$V = \frac{1}{4}\pi d^2 h \tag{57.1}$$

3 Sharp and rigid knife or spatula

4 Balance sensitive to 0.01 g

5 Drying oven capable of 105°C, preferably equipped with a circulating fan

6 Plastic bags and corrosion-resistant weighing tins large enough to hold the soil sample and the cylindrical core

7 Disks to protect the ends of cores

8 Masking tape

Procedures

1 Label and weigh cylindrical core sampler; record weight as W_1 (g).

2 Label tin bottom and top, weigh together, and record weight as W_2 (g).

3 Prepare a smooth ''undisturbed'' vertical or horizontal surface at the sampling depth.

4 Drive or press core sampler into the soil sufficiently to fill the inner core without inducing compression. Do not rock the sampler. In frictional or dense soils, careful excavation to minimize soil–metal adhesion may help in obtaining a representative core. An application of mineral oil to the core sampler may also be beneficial. Use of oil may affect wetting and drying within the core if it is to be used for water desorption characterization.

5 After careful removal of the undisturbed soil core, examine for signs of shattering or compression. Trim ends of acceptable soil cores flush with the end of the cylinder. Discard and resample if substantial root biomass or large coarse fragments protrude. Remove organic matter thatch at surface before sampling.

6 For cores that completely fill the cylinders, and if only density is to be determined, push the content of the cylinder out into a preweighed tin, which is then closed and weighed (W_3, g).

7 Place samples in an oven set to 105°C. Drying time varies with core size and oven type. Cores of about 350 cm^3 usually require about 72 h of drying in ovens equipped with circulating fans. Smaller cores require less time. After drying and cooling in a desiccator, record the weight of the dry soil plus tin bottom and top as W_5 (g).

Calculations

$$D_b = \frac{W_5 - W_2}{V} \tag{57.2}$$

and volumetric water content θ is

$$\theta = \frac{W_3 - W_5}{W_5 - W_2} \times \frac{D_b}{D_w} \tag{57.3}$$

The wet density (D_{bw}), used in soil mechanics and also for making comparisons between samples of soil that exhibit volume changes on drying, is

$$D_{bw} = D_b + \theta(\text{g cm}^{-3}) \quad \text{or} \quad \frac{W_3 - W_2}{V} \tag{57.4}$$

Density of Partially Filled Cores

1 Tare a graduated cylinder of volume V_{g1} and then fill with glass beads. The weight of the beads is recorded as W_{g1}.

2 Obtain the weight (W_4) of the partially filled soil core, place a disk under one end, and put it on a tray.

3 Pour glass beads onto the soil and level to the top of the cylinder with a spatula.

4 Place a disk over the top of the cylinder, invert the core, and fill the other end with beads. Transfer the core to a preweighed tin (W_2) and dry at 105°C.

5 Return excess glass beads from the tray to the cylinder and record their volume and weight as V_{g2} and W_{g2}, respectively.

6 After drying the sample, cool in a desiccator and weigh (W_5).

7 Calculate soil volume V_s as

$$V_s = V - \frac{W_{g1} - W_{g2}}{C} \tag{57.5}$$

where C is the packing density of the glass beads, which should be verified for each analysis. Beads having a nominal diameter of 260 μm pack to a density

of about 1.50 g cm^{-3}. Alternatively, the volume of beads can be calculated as $V_{g1} - V_{g2}$; so that $V_s = V - (V_{g1} - V_{g2})$.

8 Calculate D_b as

$$D_b = \frac{W_5 - (W_{g1} - W_{g2}) - W_2 - W_1}{V_s} \tag{57.6}$$

and θ as

$$\theta = \frac{W_4 - W_1}{V_s \cdot D_w} \tag{57.7}$$

Correction for Coarse Fragments

For certain applications, the D_b of the fine fraction, defined as those particles less than 2 mm in diameter, is of interest. This density is obtained by sieving the soil through a 2 mm sieve, then oven-drying the soil that passed through. The material retained on the sieve is washed, dried, and weighed (recorded as W_6). The volume of this fraction, V_c, can be determined by measuring the displacement of water in a graduated cylinder when the fragments are added. D_b is then

$$D_b = \frac{W_5 - W_2 - W_1 - W_6}{V - V_c} \tag{57.8}$$

where W_6 is weight and V_c is the volume of oven-dry soil >2 mm in size, and W_1, W_2, W_5, and V are defined in the Section Procedures, pp. 745–746 in steps 1 to 7.

Comments

1 Core compaction accounts for the largest error inherent in this method. To avoid compression or disturbance in heavy, compact, or plastic soils, core diameters should be >7.5 cm with the height of the core not exceeding the diameter. This minimizes disturbance at the core edge, especially when the core samples will be used for further measurement such as pore-size distribution or hydraulic conductivity (Blake and Hartge 1986a). If bulk density is the only parameter being measured, the most common core diameters range from 5 to 7.5 cm.

2 In addition to double cylinders, other tools have been used to obtain soil samples for density determination. For example, McCauley peat augers, which remove a half cylinder, are often used in peat soils.

3 The core method is relatively cheap, requiring only a coring device, a balance, and an oven. Personnel costs are high since sample collection is time-consuming. Sampling deeper into the soil profile often requires two people.

4 Measurements of D_b using destructive sampling methods are influenced by soil water content, particularly, in soil that exhibits high shrinkage and expansion when water content changes. Thus, water content measurement should always accompany D_b determination (Blake and Hartge 1986a).

57.2.2 Clod Method

Blake and Hartge (1986a) and Grossman and Reinsch (2002) have presented details of the clod method. The procedure involves the application of Archimedes' principle to determine clod volume. Bulk density is determined by weighing the clod, coating or saturating it with a water-repellent substance (e.g., paraffin wax or saran resin), and then weighing the coated or saturated clod both in air and while immersed in a liquid of known density and temperature (Campbell and Henshall 2001). A portion of the clod is removed and weighed before and after oven-drying at 105°C to calculate D_b as corrected for water content.

The clod method is time-consuming. Only quite stable (and cohesive) aggregates should be used, and as Blake and Hartge (1986a) pointed out, even then it is not very precise. The whole aggregate, rather than just a subsample, is oven dried at 105°C. The clod method assumes that about 10% of saran initially present is lost on drying. This assumption does not strongly affect results. Shrinkage over specific water content ranges of interest can be determined by equilibrating clods on pressure plate or tension tanks before coating with saran.

Small clods are not appropriate for this method, as the macropore space between clods and the larger fragments of coarser soils are not included in the measurement. Choosing representative clods from disturbed soil layers is difficult because of packing by equipment (Blake and Hartge 1986a).

57.2.3 Excavation Methods

Excavation, developed by soil engineers for bituminous and gravely material, is utilized in tillage and forestry research where loose surface soil and stones prevent the use of core and clod methods (Blake and Hartge 1986a). Bulk density is determined by excavating a quantity of soil, drying and weighing it, and determining the volume of the excavation by filling with an inert substance of known packing density (Blake and Hartge 1986a; Campbell and Henshall 2001; Grossman and Reinsch 2002).

57.2.4 Nuclear Radiation Methods

Nuclear radiation methods provide a rapid means of measuring wet bulk density with suitable calibration. Gardner (1986), Grossman and Reinsch (2002), and Campbell and Henshall (2001) have discussed the principles of γ-ray attenuation to determine soil D_b as well as the sources of error associated with its measurement. Briefly, D_b is determined by measuring the scattering or transmission of γ-rays between a source and detector. This scattering or transmission varies with soil properties, including density. The scattering technique employs a single source and a detector located on either a surface gauge or single probe. Transmission (attenuation) techniques use two rods with the gamma source located on one rod and the Geiger detector on the other. Probes are inserted into access tubes or into predrilled holes in the soil to measure scattered or transmitted radiation. Soil water is measured concurrently to convert D_{bw} to D_b. The dual source (combined gamma–neutron probe) simultaneously measures density and water with corrections required for D_b.

Commercially available gauged methods are increasingly used for determining D_{bw} and water content. For example, the Campbell Pacific Nuclear Dual Probe Strata Gauge MC-S-24

is equipped with two radioactive sources: a Cs_{137} (370 MB_q) gamma-emitter for determination of D_{bw} and an Am_{241}–Be (1900 MB_q) source, emitting fast neutrons, for water content determination. D_{bw} and water content are automatically calculated for direct read-out on the gauge display. The D_b is calculated by subtracting the volumetric water content from D_{bw}.

Manufacturers supply detailed instructions on the safe use of these instruments. Please follow the manufacturer's instructions for determining standard and measured counts. The equipment should be checked for radiation leaks on a regular basis.

Nuclear radiation methods are nondestructive, and are particularly useful when taking intact soil cores is difficult. They are efficient, enabling one person to take many readings in a short time. But this technique has a high capital cost. There is also a need to consider the registration cost for radiation safety monitoring, and requirements for special transport, training for nuclear and safety protocols, and finally, nuclear source disposal.

57.3 SOIL PARTICLE DENSITY

The D_p of a soil represents the composite average of the density of all the particles that comprise the soil. The density of individual soil particles is dependent on their mineralogy and composition. The density of minerals commonly found in soils varies from 2.6 to 2.75 g cm^{-3}. Quartz, feldspars, and colloidal silicates predominate in mineral soils and their densities fall within this range. However, if unusually higher amounts of ''heavy'' minerals such as magnetite, zircon, tourmaline, and hornblende are present in a soil, the particle density of the soil may be greater than 2.75 g cm^{-3}. Particle density can vary widely between soils, even within a soil series. Particle density may also vary with position on a slope, due to the variability in clay mineralogy (Ball et al. 2000) associated with tillage or with variation in type and content of heavy minerals. Ball et al. (2000) recommend that particle density be measured whenever it is to be used in calculating porosities (Section 57.4.1). The particle density of organic matter is far less than mineral particles, typically ranging from 1.3 to 1.5 g cm^{-3}. Thus, relatively small amounts of organic matter can have a considerable effect on a soil's composite particle density. Surface soils, because of their higher organic matter content, usually possess lower particle densities than subsoil.

A soil D_p of 2.65 g cm^{-3} is commonly assumed. This value corresponds to the D_p for quartz. For a soil consisting of three constituents x_1, x_2, and x_3 (fraction expressed by weight) with particle densities of D_{p1}, D_{p2}, and D_{p3}, soil D_p can be calculated as follows (Culley 1993):

$$\frac{1}{D_p} = \frac{x_1}{D_{p1}} + \frac{x_2}{D_{p2}} + \frac{x_3}{D_{p3}} \tag{57.9}$$

The D_p of a soil sample is calculated from two measured quantities, the weight and volume of particles. The weight is determined by weighing and volume by calculation from the weight and density of water (or other fluid) displaced by the sample.

57.3.1 Materials and Supplies

1 Pycnometer (or 100 mL volumetric flask)

2 Distilled water

3 Thermometer

4 Air-dried soil sieved through a 2 mm sieve

5 Balance sensitive to 0.001 g

6 Drying oven capable of 105°C

57.3.2 Procedure

1 Dry duplicate soil samples in a 105°C oven beforehand to determine the gravimetric water content (θ_w) of air-dried soil.

2 Degas distilled water by gently boiling for several minutes and cooling to room temperature. Record the temperature of this water and corresponding density of water (D_w) at this temperature.

3 Fill a pycnometer with the degassed water. Insert the stopper in the pycnometer. Ensure the capillary bore in the stopper is filled. Wipe the pycnometer bottle dry and weigh (W_w).

4 Pour out about half of the water from the pycnometer. Replace the stopper, dry the outside of the bottle, and weigh it.

5 Add approximately 10 g of air-dried soil and again weigh the pycnometer and stopper. (*Note*: the difference in weights obtained in (5) and (4) is the weight of the air-dried soil, W_a). The weight of the oven-dried soil W_s is

$$W_s = \frac{W_a}{1 + \theta_w} \tag{57.10}$$

6 Refill the pycnometer with water. Replace the stopper and again make sure that the capillary bore is filled. Weigh the pycnometer, water, and soil (W_{sw}).

57.3.3 Calculation

$$D_p = \frac{d_w W_s}{W_s - (W_{sw} - W_w)} \tag{57.11}$$

57.3.4 Comments

Note: if a 100 mL volumetric flask is used, add 50 g of air-dried soil and follow all procedures as for a pycnometer.

57.4 SOIL POROSITY

Knowing the number, size, configuration, and distribution of soil pores is useful for assessing the physical condition and structure of the soil (Carter and Ball 1993), but classification of pore sizes lacks standardization. In many cases, pore-size distribution is considered the best indicator

of the soil physical condition. Associated porosity factors, such as macropore volume, pore continuity, and air-filled pore space are also important guides to characterize soil structure.

The texture and arrangement of solid soil particles determines soil porosity. Porosity of sandy surface soils may range from 35% to 50%, whereas finer textured soil typically ranges from 40% to 60%. Compact subsoils may have as little as 25%–30% total pore space. Bulk density values generally reflect soil porosity. In general, the higher the D_b, the lower the porosity. Sandy soils are dominated by large pores. Thus, movement of air and water through sandy soils is relatively unrestricted and rapid in spite of the small amount of total pore space. Fine-textured soils are dominated by micropores, and although total porosity is greater in fine-textured soils compared to soils of coarser texture, the smaller size of the micropores restricts movement of air and water.

Pore-size distribution has proven useful for predicting water infiltration rates, water availability to plants, water storage capacity, aeration status (Cary and Hayden 1973), and classification of soil structure (Thomasson 1978; McKeague et al. 1986). Macropores mainly facilitate the flow of water when soil is saturated. Pore-size distribution is useful for predicting hydraulic conductivity (Suleiman and Ritchie 2001). There is a strong relationship between saturated hydraulic conductivity and macroporosity (effective porosity) (Aimrun et al. 2004).

Pore-size distribution in soil provides descriptive information about the soil pore system, rather than absolute measurements. The techniques are limited by the basic assumptions of the capillary model, which represents soil pores as parallel tubes of varying radii (Ball 1981a), and by nonstandard terminologies for classifying the various pore sizes (Danielson and Sutherland 1986). Pore sizes are thus expressed as equivalent pore diameters (EPD).

Recent developments in computers and image-analysis software make possible the analysis of soil macroporosity with technology such as ultrahigh resolution x-ray tomography (Beaudet-Vidal et al. 1998; Gantzer and Anderson 2002). Micromorphological methods can be used to characterize the actual morphology of soil pores, and are especially useful for studying the shape and continuity of pores above 100 μm in diameter. Morphological techniques are also used to describe large pores and cracks (greater than 2 mm diameter or width) such as wormholes and pores between large structural units.

This section describes the most common and easy to use methods for measuring total porosity, its air- and water-filled fractions, and pore-size distribution from measurements of water desorption using soil cores. The latter is suitable for determination of equivalent pore sizes below 150 μm (Bouma 1991). Indices of pore continuity from measurements of gas diffusion or air permeability are also discussed.

57.4.1 Total Porosity

The total porosity S_t may be calculated from the particle density and bulk density as

$$S_t = 1 - \frac{D_b}{D_p} \tag{57.12}$$

The apparatus and experimental procedures used for measuring D_p and D_b are described in Sections 57.2 and 57.3. Results for S_t can be expressed as a volume fraction or as a percentage. In this chapter, percentages will be used to represent porosity indices.

57.4.2 Macroporosity or Effective Porosity

Macropores are the primary pathway to conduct the flow of water when the soil is saturated. Effective porosity ($Ø_e$) is a measure of this property. It is approximately equal to the difference between total porosity and volumetric water content at 33 kPa of suction or volumetric water content at field capacity (Yu et al. 1993) where heavy clayey soils can be considered at 66 kPa of suction. Deeks et al. (2004) define macropores as those having nominal diameter >50 μm whereas micropores are <50 μm, equivalent to 6 kPa of suction.

The $Ø_e$ could be used to estimate the saturated hydraulic conductivity of soil (Aimrun et al. 2004) since measurement of K_s is time-consuming, labor intensive, and expensive. The $Ø_e$ is a useful index to gauge soil response to different management and tillage systems (Carter 1988). Generally, $Ø_e$ should exceed 10% of the soil volume to maintain optimal soil aeration. However, this can be modified by the degree of pore continuity.

57.4.3 Air-Filled Porosity

Air-filled porosity is a measure of the fraction of the soil bulk volume occupied by air. Soil matric potential information should be given when reporting air-filled porosity. Assuming that the total pore space is filled with water at saturation, the air-filled pore space at −6 kPa matric potential would equal the volume of macropores based on the definition given by Deeks et al. (2004).

Air-filled porosity (F_a), as a percent of total soil volume, can be calculated from the tension table procedure for any specific matric potential using the following equation:

$$F_a = \frac{W_s - W_p}{V_t} \times 100 \tag{57.13}$$

where W_s is the saturated core weight, W_p is the core weight at a specific potential, and V_t is the core volume. The difference method based on bulk density and soil water content can also be used for determining the F_a (volume basis) of a core at any moisture content by calculating total porosity (S_t) using Equation 57.12 and the following equation:

$$F_a = S_t - \theta_w D_b / D_w \tag{57.14}$$

where θ_w is gravimetric moisture content. Ball and Hunter (1988) describe some of the limitations and errors involved in the determination of air-filled porosity.

57.4.4 Water-Filled Pore Space or Relative Saturation

Water-filled pore space (WFPS), sometimes called ''relative saturation,'' expresses the volume of water in the soil relative to the total volume of pores. Thus, it ranges from 0% in a dry soil to 100% under saturated conditions. A relative saturation over 65%–70% can indicate that the soil may become anaerobic (Linn and Doran 1984) and has proved a useful index for porosity studies in wet soils (Carter 1988). Relative saturation is calculated in soil cores as follows:

$$\text{WFPS} = \frac{W_w \Big/ \left(V_t - \dfrac{W_s}{D_p}\right)}{D_w} \tag{57.15}$$

where W_w is the weight of water (g), W_s is the dry weight of soil (g), and V_t, D_p, and D_w are defined as in Section 57.1.

The WFPS index can also be calculated from F_a and S_t (i.e., WFPS $= (S_t - F_a)/S_t$).

57.4.5 Pore-Size Distribution

Pore-Size Classification

Attempts have been made to classify pores in regard to function rather than size alone. Various terminologies for EPD are used to describe the functional properties of pore-size groups as follows: fissures (>500 μm), transmission pores (500–50 μm), storage pores (50–0.5 μm), and residual pores (<0.5 μm). Emphasis has also been placed on large pores (termed ''macropores''), above 50 μm in diameter, which are associated with saturated hydraulic conductivity (Germann and Beven 1981). Generally, the range of pore-size of interest will depend on the purpose of the measurement (Ball and Hunter 1988). For example, soil-survey purposes may require pore-size ranges associated with field capacity (about 50 μm) and the lower limit of readily available water for plants (about 3–1.5 μm). Thomasson (1978) used the soil volume of pores greater than 60 μm diameter (termed ''air capacity'') and the volume occupied by pores of between 60 and 0.2 μm (termed ''available water'') as a classification of soil structural condition. In contrast, soil structure or tillage studies require information about macroporosity (>50 μm). Studies on infiltration and preferential flow of water require information on pores >1 mm EPD in addition to lower pore sizes (Luxmoore et al. 1990).

Pore-Size Distribution

Precise evaluation of the size, configuration, and distribution of the soil pores is essentially impossible due to their complicated nature. However, by making certain assumptions, the size distribution of the larger pores can be measured with at least useful accuracy. Starting with saturated soil samples, drain the soil cores stepwise and measure the volume of water removed between consecutive steps. The volume of water removed can be equated to the soil pore-volume drained. Then, if the size-range of pores drained during each step can be calculated, the pore-size distribution can be determined. In theory, the largest pores should drain first, followed by successively smaller and smaller pores. Actually, the drainage of the linked pore system will be determined by the diameter of the ''bottlenecks'' linking adjacent spores.

Pore-Size Distribution ≤1 mm EPD

Water desorption, using soil cores, has wide application for the determination of pore-size distribution. The method is suitable for undisturbed cores containing relatively small structural units (<2 cm diameter) and for remolded cores. This method is based on the determination of the water desorption curve (moisture characteristic). The curve relates soil moisture content to the energy status of soil water (water potential). The water potential is expressed in terms of matric potential. Based on the assumptions of the capillary model, the volume of water removed from the soil in response to a change in matric potential corresponds to the change in energy status of the soil water and the volume of pores above a specific diameter. Mathematically, this is expressed by the Kelvin equation:

$$d = \frac{4\gamma \cos \alpha}{pgh} \tag{57.16}$$

where d is the diameter (m) of the largest pores that remain full of water after a matric potential (h) in meters of water is applied; γ is the surface tension of water (72.75 mJ m^{-2} at 20°C); α is the contact angle of the water held in the pore (usually taken to be zero); p is the density of water (0.998 Mg m^{-3} at 20°C); and g is the acceleration due to gravity (9.8 m s^{-2}). Equation 57.16 indicates that pores that can maintain a water meniscus against the combined force of pgh have an upper limiting radius. Therefore, applying a negative potential of −1 m of water (equivalent to −0.1 bar or −10 kPa matric potential) will give a diameter of 30 μm at 20°C for the largest pores full of water.

Use of the above procedure, however, requires that decreasing matric potential progressively drains the soil. Otherwise, soil hysteresis influences water content at a given potential. The pore-size distribution must also remain stable during determination of the water desorption curve.

In fine-textured soils (clay content above 30%), shrinkage can change the pore-size distribution over time, whereas in very sandy soils (sand content above 80%), low water adhesion causes gravitational loss of water. Under these conditions, other techniques to determine pore-size distribution such as mercury intrusion and nitrogen sorption have been developed. Both of these methods are based on the cylindrical pore model for pore-size distribution. Danielson and Sutherland (1986) and Flint and Flint (2002) provide details on the mercury intrusion method. The water desorption method described below is best suited for medium textured soils and for both sandy and fine-textured soils. However, the method is applicable in clay soils at relatively high matric potentials (0 to −1 kPa). Generally, the water desorption method is used at low potentials (−1 to −100 kPa) where Equation 57.16 is most applicable.

Methods to determine water desorption between 0 and −20 kPa matric potential use tension table water extraction (Topp and Zebchuk 1979; Ball and Hunter 1988; Romano et al. 2002). Methods to determine water desorption at lower than −20 kPa potential require the use of pressure plate extraction (20–500 kPa) and pressure membrane extraction (100–1500 kPa). These three extraction methods and procedures are described in Chapter 72.

Calculations

To calculate the water desorption curve, plot volumetric moisture content (θ) versus matric potential. Determine volumetric soil moisture content (%) at each matric potential as follows:

$$\theta_v = \frac{W_p - W_2}{V_t} \times 100/D_w \tag{57.17}$$

where W_p is the weight of soil plus core at a specific matric potential and W_2 is the weight of dry soil plus core. Determination of pore-size distribution is based on the information given in Equation 57.17, where the diameter of pores remaining full of water was 30 μm after equilibration at a potential of −1 m (−10 kPa). Thus, the diameter of the smallest pore drained at a specific suction would be

$$D\ (\mu m) = \frac{300}{kPa} \tag{57.18}$$

Calculation of the volume of water removed between two specific pore-size diameters would equal the volume of pore space for that pore-size range.

Comments

1 The pore-size diameters are approximate and therefore designated as EPD. In addition, the contact angle (α) in Equation 57.16 is assumed to be zero; this may not always be correct. Further, the method provides no information on pore continuity or shape. Also, for soil cores with a relatively large volume of macropores (EPD >50 μm), it is difficult to obtain complete saturation by capillary wetting. Under these circumstances, use of vacuum wetting (Ball and Hunter 1988) or estimation of total porosity from bulk density using Equation 57.12 is advised.

2 Use of undisturbed soil cores will prove a problem on recently cultivated soils due to loose cores. Generally some degree of compaction by weathering must occur before intact cores can be obtained.

3 During the saturation procedure, formaldehyde solution (4% w/v) can be sprayed on the surface of the core to remove or suppress the activity of earthworms and other macrofauna (Ball and Hunter 1988).

Pore-Size Distribution $\geq$1 mm EPD

The size and continuity of pores $>$1 mm EPD are particularly important for environmental modeling of infiltration of water and solute solution. Douglas (1986) describes morphological procedures for assessing the dimensions of large macropores. Procedure 1 is recommended for soil that does not shrink measurably on drying. Procedure 2 is recommended for soil that remains stable during saturation.

Procedure 1

Oven dry the core sample. Record the number and diameter of channel-type pores of diameter $\geq$1 mm judged to have openings at both ends of the sample. Measure pore diameter using a set of 1–8 mm rigid aluminium rod gauges.

Douglas (1986) also proposed a method of identification of functional macropores, i.e., those responsible for flow-through samples.

Procedure 2

Saturate the core sample. Pour a solution of Rhodamine-B dye through the samples. After drainage, extrude the lower outflow ends of the cores from their retaining rings for a distance of 1 cm and carefully pick off the extruded 1 cm of soil. The continuous, stained pores thus exposed are traced on to acetate sheets, counted, and measured.

Pore Size and Shape Using Computer Image-Analysis Techniques

Image-analysis techniques not only provide pore-size distribution but also the pore shapes, and could give three-dimensional results. An alternative to staining or direct

measurement techniques is x-ray CT (Rasiah and Aylmore 1998; Gantzer and Anderson 2002). In this technique, CT scanners are used to scan relative pixel density in the undisturbed cores and image-processing software is used to calculate the area, volumes, and three-dimensional measurements (Perret et al. 1999). Another technique is image analysis of soil porosity using difference imagery of stereo photographs (Grevers and De Jong 1990; Sort and Alcańiz 1999).

57.4.6 Pore Continuity or Function Indices

The continuity of soil macropores is particularly important in determining the conductivity of soil for gas movement, water infiltration, and root exploration. Indices of continuity measure the ability of the soil spores to conduct fluid. Gas is commonly the fluid used, because it does not change the soil structure when it diffuses or flows through the soil. Use of gas movement allows measurements to be repeated at different soil moisture contents. This allows assessment of the change of pore continuity with air-filled porosity.

In order to measure pore continuity, measure gas relative diffusivity (D/D_o) and air permeability (K_a) (in units of μm^2) and air-filled porosity (F_a) (volume percentage) in soil cores in the laboratory. Techniques for measuring K_a are given in Chapter 61. In addition, Ball and Smith (1991) present an extensive review of suitable techniques.

In terms of gas relative diffusivity, pore continuity C_d is

$$C_d = \frac{D/D_o}{F_a} \times 100 \tag{57.19}$$

This factor, C_d, derived by Ball (1981b), ranges from 0 for completely blocked pores to 1 for straight tubular pores aligned with the direction of diffusing gas. Schjonning et al. (2002) discuss how large values of C_d can also be interpreted as indicating a large number of marginal pores lying off the arterial pathways for diffusion, a concept of pore function suggested by Arah and Ball (1994).

In terms of air permeability, pore continuity C_k or macropore organization (Groenevelt et al. 1984; Blackwell et al. 1990) is

$$C_k = \frac{K_a}{F_a} \times 100 \tag{57.20}$$

Other indices of pore continuity and pore tortuosity were reviewed by Ball et al. (1988).

REFERENCES

Aimrun, W., Amin M.S.M., and Eltaib, S.M. 2004. Effective porosity of paddy soils as an estimation of its saturated hydraulic conductivity. *Geoderma* 121: 197–203.

Arah, J.R.M. and Ball, B.C. 1994. A functional model of soil porosity used to interpret measurements of gas diffusion. *Eur. J. Soil Sci.* 32: 465–481.

Ball, B.C. 1981a. Modelling of soil pores as tubes using gas permeabilities, gas diffusivities and water release. *J. Soil Sci.* 32: 465–481.

Ball, B.C. 1981b. Pore characteristics of soils from two cultivation experiments as shown by gas diffusivities and permeabilities and air-filled porosities. *J. Soil Sci.* 32: 483–498.

Ball, B.C., Campbell, D.J., and Hunter, E.A. 2000. Soil compactibility in relation to physical and organic properties at 156 sites in UK. *Soil Till. Res.* 57: 83–91.

Ball, B.C. and Hunter, R. 1988. The determination of water release characteristics of soil cores at low suctions. *Geoderma* 43: 195–212.

Ball, B.C., O'Sullivan, M.F., and Hunter, R. 1988. Gas diffusion, fluid flow and derived pore continuity indices in relation to vehicle traffic and tillage. *J. Soil Sci.* 39: 327–339.

Ball, B.C. and Smith, K.A. 1991. Gas movement. In K.A. Smith and C.M. Mullins, Eds. *Soil and Environmental Analysis: Physical Methods*, 2nd ed. Dekker, New York, NY, pp. 499–538.

Beaudet-Vidal, L., Fradin, V., and Rossignol, J.P. 1998. Study of the macroporosity of reconstituted anthropic soils by image analysis. *Soil Till. Res.* 47: 173–179.

Blackwell, P.S., Ringrose-Voase, A.J., Jayawardane, N.S., Olsson, K.A., McKenzie, D.C., and Mason, W.K. 1990. The use of air-filled porosity and intrinsic permeability to characterize structure of macropore space and saturated hydraulic conductivity of clay soils. *J. Soil Sci.* 41: 215–228.

Blake, G.R. and Hartge, K.H. 1986a. Bulk density. In A. Klute, Ed. *Methods of Soil Analysis*. Agronomy No. 9, 2nd ed. American Society of Agronomy, Madison, WI, pp. 363–375.

Blake, G.R. and Hartge, K.H. 1986b. Particle density. In A. Klute, Ed. *Methods of Soil Analysis*. Agronomy No. 9, 2nd ed. American Society of Agronomy, Madison, WI, pp. 377–382.

Bouma, J. 1991. Influence of soil macroporosity on environmental quality. *Adv. Agron.* 46: 1–37.

Cameira, M.R., Fernando, R.M., and Pereira, L.S. 2003. Soil macropore dynamics affected by tillage and irrigation for a silty loam alluvial soil in southern Portugal. *Soil Till. Res.* 70: 131–140.

Campbell, D.J. and Henshall, J.K. 2001. Bulk density. In K.A. Smith and C.M. Mullins, Eds. *Soil and Environmental Analysis: Physical Methods*, 2nd ed. Dekker, New York, NY, pp. 315–348.

Carter, M.R. 1988. Temporal variability of soil macroporosity in a fine sandy loam under mouldboard ploughing and direct drilling. *Soil Till. Res.* 12: 37–51.

Carter, M.R. and Ball, B. 1993. Soil porosity. In M.R. Carter, Ed. *Soil Sampling and Methods of Analysis*. Canadian Society of Soil Science, Lewis Publishers, CRC Press, Boca Raton, FL, pp. 581–588.

Cary, J.W. and Hayden, C.W. 1973. An index for soil pore size distribution. *Geoderma* 9: 249–256.

Crestana, S. and Vaz, C.M.P. 1998. Non-invasive instrumentation opportunities for characterizing soil porous systems. *Soil Till. Res.* 47: 19–26.

Culley, J.L.B. 1993. Density and compressibility. In M.R. Carter, Ed. *Soil Sampling and Methods of Analysis*. Canadian Society of Soil Science, Lewis Publishers, CRC Press, Boca Raton, FL, pp. 529–539.

Danielson, R.E. and Sutherland, P.L. 1986. Soil porosity. In A. Klute, Ed. *Methods of Soil Analysis*. Agronomy No. 9, 2nd Ed. American Society of Agronomy, Madison, WI, pp. 443–461.

Deeks, L.K., Bengough, A.G., Low, D., Billett, M.F., Zhang, X., Crawford, J.W., Chessell, J.M., and Young, I.M. 2004. Spatial variation of effective porosity and its implications for discharge in an upland headwater catchments in Scotland. *J. Hydrol.* 290: 217–228.

Douglas, J.T. 1986. Macroporosity and permeability of some cores from England and France. *Geoderma* 37: 221–231.

Flint, L.E. and Flint, A.L. 2002. Porosity. In J.H. Dane and G.C. Topp, Eds. *Methods of Soil Analysis, Part 4—Physical Methods*. Soil Science Society of America, Madison, WI, pp. 241–254.

Gantzer, C.J. and Anderson, S.H. 2002. Computed tomographic measurement of macroporosity in chisel-disk and no-tillage seedbeds. *Soil Till. Res.* 64: 101–111.

Gardner, W.H. 1986. Water content. In A. Klute, Ed. *Methods of Soil Analysis*. Agronomy 9, 2nd ed. American Society of Agronomy. Madison, WI, pp. 493–544.

Germann, P. and Beven, K. 1981. Water flow in soil macropores III. A statistical approach. *J. Soil Sci*. 32: 31–39.

Grevers, M.C.J. and De Jong, E. 1990. The characterization of soil macroporosity of a clay soil under ten grasses using image analysis. *Can. J. Soil Sci*. 70: 93–103.

Groenevelt, P.H., Kay, B.D., and Grant, C.D. 1984. Physical assessment of soil with respect to rooting potential. *Geoderma* 34: 101–114.

Grossman, R.B. and Reinsch, T.G. 2002. Bulk density and linear extensibility. In J.H. Dane and G.C. Topp, Eds. *Methods of Soil Analysis, Part 4—Physical Methods*. Soil Science Society of America, Madison, WI, pp. 201–228.

Gysi, M., Klubertanz, G., and Vulliet, L. 2000. Compaction of an Eutric Cambisol under heavy wheel traffic in Switzerland—field data and modelling. *Soil Till. Res.* 56: 117–129.

Linn, D.M. and Doran, J.W. 1984. Effect of water-filled pore space on carbon dioxide and nitrous oxide production in tilled and non-tilled soils. *Soil Sci. Soc. Am. J.* 48: 1267–1272.

Luxmoore, R.J., Jardine, P.M., Wilson, G.V., Jones, J.R., and Zelazny, L.W. 1990. Physical and chemical controls of preferred path flow through a forested hillslope. *Geoderma* 46: 139–154.

Macedo, A., Crestana, S., and Vaz, C.M.P. 1998. X-ray microtomography to investigate thin layers of soil clod. *Soil Till. Res.* 49: 249–253.

McKeague, J.A., Wang, C., and Coen, G.M. 1986. Describing and interpreting the macrostructure of mineral soils—a preliminary report. LRRI Contribution No. 84-50 Research Branch, Agriculture Canada, Ottawa, Ontario, Canada, 47 pp.

Ochsner, T.E., Horton, R., and Ren, T. 2001. Simultaneous water content, air-filled porosity, and bulk density measurements with thermo-time domain reflectometry. *Soil Sci. Soc. Am. J.* 65: 1618–1622.

Osunbitan, J.A., Oyedele, D.J., and Adekalu, K.O. 2005. Tillage effects on bulk density, hydraulic conductivity and strength of a loamy sand soil in southwestern Nigeria. *Soil Till. Res.* 82: 57–64.

Pedrotti, A., Pauletto, E.A., Crestana, S., Rodrigues, F.S., Cruvinel, P.E., and Vaz, C.M.P. 2005. Evaluation of bulk density of Albaqualf soil under different tillage systems using the volumetric ring and computerized tomography methods. *Soil Till. Res.* 80: 115–123.

Perret, J., Prasher, S.O., Kantzas, A., and Langford, C. 1999. Three-dimensional quantification of macropore networks in undisturbed soil cores. *Soil Sci. Soc. Am. J.* 63: 1530–1543.

Rasiah, V. and Aylmore, L.A.G. 1998. Characterizing the changes in soil porosity by computed tomography and fractal dimension. *Soil Sci*. 163: 203–211.

Romano, N., Hopmans, J.W., and Dane, J.H. 2002. Suction table. In J.H. Dane and G.C. Topp, Eds. *Methods of Soil Analysis, Part 4—Physical Methods*. Soil Science Society of America, Madison, WI, pp. 692–697.

Schjonning, P., Munkholm, L.J., Moldrup, P., and Jacobsen, O.H. 2002. Modelling soil pore characteristics from measurements of air exchange: the long-term effects of fertilization and crop rotation. *Eur. J. Soil Sci*. 53: 331–339.

Shaver, T.M., Peterson, G.A., and Sherrod, L.A. 2003. Cropping intensification in dryland systems improves soil physical properties: regression relations. *Geoderma* 116: 149–164.

Sort, X. and Alcańiz, J.M. 1999. Modification of soil porosity after application of sewage sludge. *Soil Till. Res.* 49: 337–345.

Suleiman, A.A. and Ritchie, J.T. 2001. Estimating saturated hydraulic conductivity from soil porosity. *Trans. ASAE* 44: 235–239.

Thomasson, A.J. 1978. Towards an objective classification of soil structure. *J. Soil Sci*. 29: 38–46.

Topp, G.C. and Zebchuk, W. 1979. The determination of soil-water desorption curves for soil cores. *Can. J. Soil Sci*. 59: 19–26.

Warrick, A.W. and Neilson, D.R. 1980. Spatial variability of soil physical properties in the filed. In D. Hillel, Ed. *Applications of Soil Physics*. Academic Press, New York, NY, pp. 319–344.

Yu, C., Loureiro, C., Cheng, J.J., Jones, L.G., Wang, Y.Y., Chia, Y.P., and Failance, E. 1993. *Data Collection Handbook to Support Modeling Impacts of Radioactive Material in Soil*. Environmental Assessment and Information Sciences Division, Argonne, National Laboratory, Argonne, IL.

Chapter 58
Soil Consistency: Upper and Lower Plastic Limits

R.A. McBride
University of Guelph
Guelph, Ontario, Canada

58.1 INTRODUCTION

The (Atterberg) consistency limits of soils are used primarily in classifying cohesive soil materials for engineering purposes (ASTM 2000a), and are strongly correlated to other fundamental soil properties (De Jong et al. 1990). They are also used widely in the estimation of other test indices useful for soil engineering interpretations, such as shear strength and bearing capacity, compressibility, swelling potential, and specific surface (reviewed in McBride 1989).

As gravimetric water contents, the shrinkage limit, lower plastic limit (w_P), and upper plastic (liquid) limit (w_L) test indices represent the three major points of transition in soil consistency amongst the solid, semisolid, plastic, and liquid states, respectively. The standard American Society for Testing and Materials (ASTM) test procedures for w_L and w_P determination (ASTM 2000b) are somewhat subjective and arbitrary shear tests, and so are prone to significant operator and mechanical variability. Test reproducibility has not been improved with the introduction of the one-point w_L test method, which reduces the testing time (and cost) as compared to the normally iterative procedures.

Considerable effort has been directed at researching alternative and procedurally unified test methods, including desorption by pressure plate extraction (reviewed in McBride 1989), consolidation of soil–water suspensions (McBride and Bober 1989; McBride and Baumgartner 1992), measurement of paste viscosity, and drop-cone penetration. Some methods have shown very promising results, but only w_L determination by cone penetration has been standardized to date, and is the preferred method of the British Standards Institution (BS 1377:Part 2:1990) (BSI 2000). It appears unlikely, however, that a direct measurement of w_P by the cone penetration method is possible (Harison 1988).

This chapter outlines only those test protocols that have been standardized and that are widely accepted and used. The primary sources for these procedures were AASHTO (2000a,b) ASTM (2000b), BSI (2000), and Sheldrick (1984).

58.2 UPPER PLASTIC (LIQUID) LIMIT

The upper plastic (liquid) limit of a cohesive soil is defined as the gravimetric water content (percentage) corresponding to an arbitrary limit between the liquid and plastic states of consistence when in a remolded condition. In accordance with the standard ASTM (Casagrande) test procedure, it is the water content at which a pat of soil, cut by a standard-sized groove, will flow together for a distance of 13 mm under the impact of 25 blows in a standard ASTM liquid limit device. The undrained cohesion of soils in this consistency state is approximately 1.7 kPa (Wroth and Wood 1978).

58.2.1 Casagrande Method (ASTM D4318-98; AASHTO T89-90; BS 1377:Part 2:1990)

Apparatus and Materials

1 ASTM liquid limit device with grooving tool

2 Metal spatula (7–8 cm in length, 2 cm wide)

3 Evaporating dish (10–12 cm in diameter)

4 Soil sample containers for water content measurement

5 Balance (sensitive to 0.01 g)

6 Drying oven (105°C)

7 Air-dry soil sample of about 100 g and passing a No. 40 (425 μm) sieve

Procedure

1 Place the soil sample in the evaporating dish and thoroughly mix with 15 to 20 mL of distilled water by alternately and repeatedly stirring, kneading, and chopping with a spatula. Make further additions of water in increments of 1 to 3 mL. Thoroughly mix each increment of water with the soil, as previously described, before adding another increment of water.

2 When sufficient water has been thoroughly mixed with the soil to produce a consistency that will require 30 to 35 drops of the cup to cause closure, place a portion of the mixture in the cup above the spot where the cup rests on the base, and squeeze it down and spread it into position with as few strokes of the spatula as possible. Care should be taken to prevent the entrapment of air bubbles within the soil mass. With the spatula, level the soil and at the same time trim it to a depth of 1 cm at the point of maximum thickness. Return the excess soil to the evaporating dish. Divide the soil in the cup by firm strokes of the grooving tool along the diameter through the centerline of the cam follower so that a clean, sharp groove of the proper dimensions will be formed. To avoid tearing of the sides of the groove or slipping of the soil pat on the cup, up to six strokes, from front to back or from back to front counting as one stroke, shall be permitted.

Each stroke should penetrate a little deeper until the last stroke from back to front scrapes the bottom of the cup clean. Make the groove with as few strokes as possible.

3 Lift and drop the cup by turning the crank at the rate of 2 rps, until the two halves of the soil pat come in contact at the bottom of the groove along a distance of about 13 mm. Record the number of drops (N) required to close the groove along a distance of 13 mm.

4 Remove a slice of soil approximately the width of the spatula, extending from edge to edge of the soil pat at right angles to the groove and including that portion of the groove in which the soil flowed together, and place in a suitable tared container. Determine the gravimetric water content.

5 Transfer the soil remaining in the cup to the evaporating dish. Wash and dry the cup and grooving tool, and reattach the cup to the carriage in preparation for the next trial.

6 Repeat steps 2 to 5 for at least two additional trials, with the soil collected in the evaporating dish, to which sufficient water has been added to bring the soil to a more fluid condition. The object of this procedure is to obtain samples of such consistency that the number of drops required to close the groove will be above and below 25. The number of drops should be less than 35 and exceed 15. The test shall always proceed from the drier to the wetter condition of the soil.

Calculations

1 Calculate the gravimetric water content of the soil (w), expressed as a percentage of water in the sample on a dry mass basis (%kg kg^{-1}), as follows:

$$w = \left(\frac{\text{mass of water}}{\text{mass of oven-dry soil}}\right) \times 100 \tag{58.1}$$

2 Plot a flow curve representing the relationship between gravimetric water content and corresponding numbers of drops of the cup on a semilogarithmic graph with w as abscissa on the linear scale, and the number of drops (N) as ordinate on the logarithmic scale. The flow curve is a straight line drawn as nearly as possible through the three or more plotted points.

3 Take the water content corresponding to the intersection of the flow curve with the $N = 25$ ordinate as the upper plastic limit (liquid limit) of the soil. Report the w_L test index to the nearest whole number.

Comments

1 Before testing, inspect the liquid limit device to determine that the device is in good working order, that the pin connecting the cup is not worn sufficiently to permit side play, that the screws connecting the cup to the hanger arm are tight, and that a groove has not been worn in the cup through long usage. Also ensure that the dimensions of the grooving tool are to specification (ASTM 2000b).

2 By means of the gauge on the handle of the grooving tool and the adjustment plate, adjust the height to which the cup is lifted so that the point on the cup that comes in contact with the base is exactly 1 cm above the base. Secure the adjustment plate by tightening the screws. With the gauge still in place, check the adjustment by revolving the crank rapidly several times. If the adjustment is correct, a slight ringing sound will be heard when the cam strikes the cam follower. If the cup is raised off the gauge or no sound is heard, make further adjustments.

3 A motorized version of the liquid limit device with a blow (revolution) counter is commercially available and should be used if possible to minimize operator variability.

58.2.2 One-Point Casagrande Method (ASTM D4318-98; AASHTO T89-90; BS 1377:Part 2:1990)

Procedure

1 This single-point method was based on a study involving regression analysis of a large number of tested soils, and can be used when the available sample size is small or when only an approximation of w_L is needed. The requirements for the apparatus, the soil sample preparation, and the mechanical device adjustments are identical to those under Section 58.2.1.

2 Proceed in accordance with procedural steps 1 through 5 under Section Procedure, p. 762, except that a water content sample shall be taken only for the accepted trial. The accepted trial requires between 20 and 30 drops of the cup to close the groove and at least two consistent consecutive closures are to be observed before taking the water content sample for calculation of the upper plastic limit. The test should always proceed from the drier to the wetter condition of the soil.

Calculations

1 Calculate the percent gravimetric water content (w) of the soil for the accepted trial as per Equation (58.1).

2 Determine the upper plastic limit using the following formula:

$$w_L = w(N/25)^{0.12} \tag{58.2}$$

where N is the number of drops of the cup required to close the groove at the test water content.

3 Report the w_L test index to the nearest whole number.

58.2.3 Drop-Cone Penetrometer Method (BS 1377:Part 2:1990)

Apparatus and Materials

1 Standard drop-cone penetrometer.

2 Cone of stainless steel or duralumin approximately 35 mm long, with a smooth, polished surface and an angle of 30 $\pm$ 1°. The mass of the cone together with its sliding shaft is 80.00 $\pm$ 0.05 g.

3 Noncorrodible airtight container.

4 Metal cup approximately 5.5 cm in diameter and 4.0 cm deep with rim parallel to the flat base.

5 Metal spatula (7–8 cm in length, 2 cm wide).

6 Evaporating dish (10–12 cm in diameter).

7 Soil sample containers for water content measurement.

8 Balance (sensitive to 0.01 g).

9 Drying oven (105°C).

10 Air-dry soil sample of about 200 g and passing a No. 40 (425 μm) sieve.

Procedure

1 A sample weighing at least 200 g is placed on the evaporating dish and mixed thoroughly with distilled water using the spatula until the mass becomes a thick homogeneous paste. This paste is then allowed to stand in the airtight container for about 24 h to allow the water to permeate throughout the soil mass.

2 The sample is then removed from the container and remixed for at least 10 min. If necessary, further water is added so that the first cone penetration reading is approximately 15 mm.

3 The remixed soil is pushed into the cup with a spatula, taking care not to trap air. The excess soil is removed to give a smooth surface. The cone is lowered so that it just touches the surface of the soil. When the cone is in the correct position, a slight movement of the cup will leave a slight mark on the surface of the soil and the reading of the dial gauge is noted to the nearest 0.1 mm. The cone is then released for a period of 5 ± 1 s. If the apparatus is not fitted with an automatic release and locking device, care should be taken to isolate the apparatus from disturbance during these operations. After the cone has been locked in position, the dial gauge is lowered to the new position of the cone shaft and the reading noted to the nearest 0.1 mm. The difference between the readings at the beginning and end of the test is recorded as the depth of cone penetration.

4 The cone is lifted out and cleaned carefully. A little more wet soil is added to the cup and the process repeated. If the difference between the first and second penetration readings is <0.5 mm, the average of the two penetrations is recorded. If the second penetration is >0.5 mm and <1 mm different from the first, a third test shall be carried out. If the overall range is then <1 mm, a water content sample (about 10 g) is taken from the area penetrated by the cone and the water content determined. The average of the three penetrations is recorded. If the overall range is >1 mm, the soil shall be removed from the cup, remixed, and the test repeated until consistent results are obtained.

5 The operations described in steps 3 and 4 are to be repeated at least four times using the same sample to which further increments of distilled water have been added.

The amount of water added shall be chosen so that a range of penetration values of approximately 15 to 25 mm is covered.

Calculations

The relationship between the gravimetric water content and the depth of cone penetration is plotted with the percentage water content as abscissa and the cone penetration as ordinate, both on linear scales. The best straight line fitting the plotted points is drawn through them. The water content corresponding to a cone penetration of 20 mm is taken as the upper plastic limit of the soil and is expressed to the nearest whole number. The method of obtaining the w_L shall be stated (i.e., using the cone penetrometer).

Comments

A version of the drop-cone penetrometer equipped with a digital automatic controller (and direct readout) is commercially available and should be used if possible to minimize operator variability. The 20 mm penetration depth standard should be used with caution, as many studies outside of Britain (including Canada) have documented both under- and over-estimation of the Casagrande w_L using the cone penetration method (cf. McBride and Baumgartner 1992; Leroueil and Le Bihan 1996).

58.3 LOWER PLASTIC LIMIT

The lower plastic limit of a cohesive soil is defined as the gravimetric water content (percentage) corresponding to an arbitrary limit between the plastic and semisolid states of consistence when in a remolded condition. In accordance with the standard ASTM (Casagrande) test procedure, it is the water content at which a soil will just begin to crumble when rolled into a thread approximately 3.2 mm in diameter. The undrained cohesion of soils in this consistency state is approximately 170 kPa (Wroth and Wood 1978).

58.3.1 Casagrande Method (ASTM D4318-98; AASHTO T90-87; BS 1377:Part 2:1990)

Apparatus and Materials

1. Evaporating dish (10–12 cm in diameter)
2. Metal spatula (7–8 cm in length, 2 cm wide)
3. Surface for rolling (e.g., a ground-glass plate)
4. Soil sample containers for water content measurement
5. Balance (sensitive to 0.01 g)
6. Drying oven (105°C)
7. Air-dry soil sample of about 15 g and passing a No. 40 (425 μm) sieve

Procedure

1 If the lower plastic limit only is required, take about 15 g of air-dried soil, place in an evaporating dish and thoroughly mix with distilled water until the mass becomes plastic enough to be easily shaped into a ball. Take a portion of this ball weighing about 8 g for the test sample.

2 If both the upper and lower plastic limits are required, take a test sample weighing about 8 g from the thoroughly wet and mixed portion of the soil prepared for the liquid limit test (see Section 58.2.1). Take the sample at any stage of the mixing process at which the mass becomes plastic enough to be easily shaped into a ball without sticking to the fingers excessively when squeezed.

3 Squeeze and form the 8 g test sample taken in accordance with steps 1 or 2 into an ellipsoidal-shaped mass. Roll this mass between the fingers and the ground-glass plate lying on a smooth horizontal surface with just sufficient pressure to roll the mass into a thread of uniform diameter throughout its length. The rate of rolling shall be between 80 and 90 strokes per min, counting a stroke as one complete motion of the hand forward and back to the starting position again.

4 When the diameter of the thread becomes about 3.2 mm, break the thread into six or eight pieces. Squeeze the pieces together between the thumbs and fingers of both hands into a uniform mass roughly ellipsoidal in shape, and reroll. Continue this alternate rolling to a thread 3.2 mm in diameter, gathering together, kneading, and rerolling, until the thread crumbles under the pressure required for rolling and the soil can no longer be rolled into a thread. The crumbling may occur when the thread has a diameter greater than 3.2 mm. This shall be considered a satisfactory end point, provided the soil has been previously rolled into a thread 3.2 mm in diameter. The crumbling will manifest itself differently with the various types of soil. Some soils fall apart in numerous small aggregations of particles; others may form an outside tubular layer that starts splitting at both ends. The splitting progresses toward the middle, and finally, the thread falls apart in many small platy particles. Heavy clay soils require much pressure to deform the thread, particularly as they approach the lower plastic limit, and finally, the thread breaks into a series of barrel-shaped segments each about 6.4 to 9.5 mm in length. The operator should not attempt to produce failure at exactly 3.2 mm diameter by allowing the thread to reach 3.2 mm, then reducing the rate of rolling or the hand pressure, or both, and continuing the rolling without further deformation until the thread falls apart. It is permissible, however, to reduce the total amount of deformation for marginally plastic soils by making the initial diameter of the ellipsoidal-shaped mass nearer to the required 3.2 mm final diameter.

5 Gather the portions of the crumbled soil together and place in a suitable tared container. Determine the gravimetric water content.

Calculations

1 Calculate the percent gravimetric water content of the remolded soil as per Equation (58.1). Report this value as the w_P test index to the nearest whole number.

2 Calculate the plasticity index of a soil as the difference between its upper and lower plastic limits, as follows:

$$\text{Plasticity index} = w_L - w_P \tag{58.3}$$

3 Report the difference calculated in Equation (58.3) as the plasticity index, except under the following conditions:

(i) When the w_L or w_P test indices cannot be determined, report the plasticity index as NP (nonplastic).

(ii) When the soil is extremely sandy, the w_P test is to be performed before the w_L test. If the w_P cannot be determined, report the plasticity index as NP.

(iii) When the w_P is greater than or equal to w_L, report the plasticity index as NP.

Comments

Test reproducibility and rapidity can be improved by using a soil rolling device of the sort proposed by Bobrowski and Griekspoor (1992) without significantly deviating from the standard manual methods.

REFERENCES

AASHTO. 2000a. Determining the liquid limit of soils (T89-90). In *Standard Specifications for Transportation Materials and Methods of Sampling and Testing*. Part II. American Association of State Highway and Transportation Officials, Washington, DC.

AASHTO. 2000b. Determining the plastic limit and plasticity index of soils (T90-87). In *Standard Specifications for Transportation Materials and Methods of Sampling and Testing*. Part II. American Association of State Highway and Transportation Officials, Washington, DC.

ASTM. 2000a. Standard test methods for liquid limit, plastic limit, and plasticity index of soils (D 4318-98). In *2000 Annual Book of ASTM Standards*, Vol. 04.08, American Society for Testing and Materials, West Conshohocken, PA, pp. 546–558.

ASTM. 2000b. Standard practice for classification of soils for engineering purposes (Unified Soil Classification System) (D 2487-98). In *2000 Annual Book of ASTM Standards*, Vol. 04.08, American Society for Testing and Materials, West Conshohocken, PA, pp. 238–248.

Bobrowski, L.J. and Griekspoor, D.M. 1992. Determination of the plastic limit of a soil by means of a rolling device. *Geotech. Test. J. GTJODF* 15: 284–287.

BSI. 2000. Methods of test for soils for civil engineering purposes: classification tests. *British Standard 1377*: Part 2:1990. British Standards Institution, London.

De Jong, E., Acton, D.F., and Stonehouse, H.B. 1990. Estimating the Atterberg limits of southern Saskatchewan soils from texture and carbon contents. *Can. J. Soil Sci.* 70: 543–554.

Harison, J.A. 1988. Using the BS cone penetrometer for the determination of the plastic limit of soils. *Geotechnique* 38: 433–438.

Leroueil, S. and Le Bihan, J.-P. 1996. Liquid limits and fall cones. *Can. Geotech. J.* 33: 793–798.

McBride, R.A. 1989. A re-examination of alternative test procedures for soil consistency limit determination: II. A simulated desorption procedure. *Soil Sci. Soc. Am. J.* 53: 184–191.

McBride, R.A. and Baumgartner, N. 1992. A simple slurry consolidometer designed for the estimation of the consistency limits of soils. *J. Terramechanics* 29: 223–238.

McBride, R.A. and Bober, M.L. 1989. A re-examination of alternative test procedures for soil consistency limit determination: I. A compression-based procedure. *Soil Sci. Soc. Am. J.* 53: 178–183.

Sheldrick, B.H. 1984. Analytical methods manual 1984. L.R.R.I. Contribution No. 84-30. Land Resource Research Institute, Research Branch, Agriculture Canada, Ottawa, ON, Canada.

Wroth, C.P. and Wood, D.M. 1978. The correlation of index properties with some basic engineering properties of soils. *Can. Geotech. J.* 15: 137–145.

Chapter 59
Compaction and Compressibility

Pauline Défossez
French National Institute for Agricultural Research
Laon, France

Thomas Keller
Swedish University of Agricultural Sciences
Uppsala, Sweden

Guy Richard
French National Institute for Agricultural Research
Olivet, France

59.1 INTRODUCTION

The passage of agricultural and forest machines over soil is the main cause of compaction of cultivated and forest soils. If the load applied during trafficking is larger than the resistance of the soil against compaction (mechanical soil strength), compaction of the soil occurs. Compaction (also referred to as compression) is a reduction of the volume of a given mass of soil. The decrease in soil volume is due to a decrease in the volume of pore space through partial expulsion of soil air and water. When soil is compacted, the porosity is decreased and, conversely, the bulk density is increased. The decrease in porosity due to compaction is accompanied by a modification of the pore geometry, i.e., pore morphology and connectivity. Hence, soil compaction modifies soil structure. Pore geometry, which may also be strongly affected by shearing, is a very important component of soil structure because it greatly affects the properties of water and gas transport in soil.

Soil compaction intensity depends on vehicle and soil characteristics through:

- The stress applied on the soil surface (i.e., at the soil–tire or soil–track interface) and the area of contact between the soil and the tire or track that is determined by loading characteristics (load, tire type, dimension and inflation pressure, track properties) and soil conditions.

- The mechanical soil strength, i.e., the soil resistance against the decrease in soil volume. It is affected by soil type and soil conditions (soil texture, soil organic matter content, soil structure, bulk density, and soil moisture status). For a given

texture, the mechanical soil strength is strongly influenced by soil moisture and bulk density. Generally, soils become stronger with decreasing moisture content and increasing density.

The strength of a soil is obtained from the compressive behavior of soil, which can be measured in a so-called compression test in the laboratory or in the field. The compressive behavior of soil is expressed graphically in the relationship between the logarithm of applied stress and some parameter related to the packing state of the soil, e.g., strain, void ratio, specific volume, or bulk density. This relationship is also referred to as the compression curve.

An idealized soil compression curve is shown in Figure 59.1. Two domains can be defined: a swelling line (SL) (also referred to as recompression line) at a lower stress range and a virgin compression line (VCL) at higher stresses. Both lines are separated by a critical stress, termed the precompression stress (also referred to as preconsolidation stress or preload).

Soil behavior is believed to be mainly elastic in the recompression range and mainly plastic in the virgin compression range. The precompression stress is widely used to characterize the soil-bearing capacity, i.e., the maximum stress that can be applied during trafficking that results in only limited soil compaction.

The slope of the SL is called swelling (or recompression) index, C_s, while the slope of the VCL is termed compression index, C_c (Figure 59.1).

Consequently, three parameters are required to describe the compressive behavior of soil: the precompression stress, σ_p, the compression index, C_c, and the swelling index, C_s.

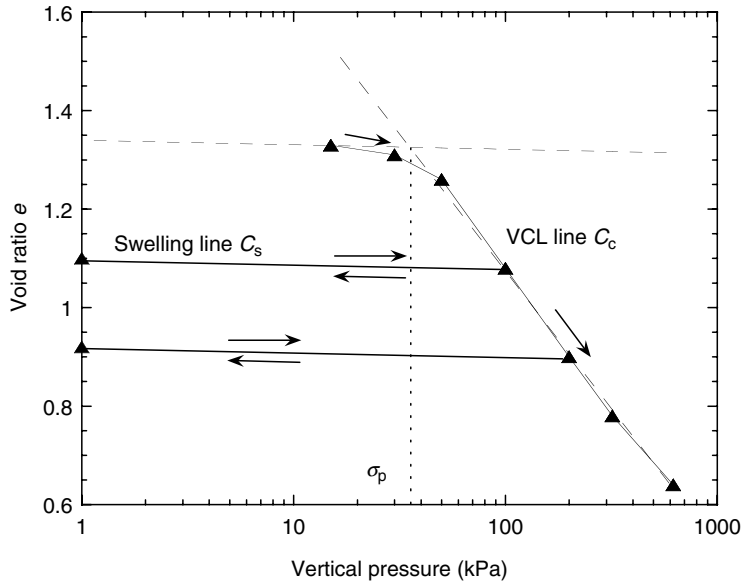

FIGURE 59.1. Stress–strain relationship for a Eutric Cambisol at an initial gravimetric water content of 0.15 g g^{-1} and an initial void ratio, e_0, of 1.34. The swelling index (C_s) was calculated to be 0.009 and the compression index (C_c) to be 0.51. The precompression stress, σ_p, was 36 kPa with the Casagrande method.

These parameters are required input parameters in soil compaction models (Défossez and Richard 2002).

Stress–strain relationships of soils are measured in laboratory and field tests to obtain σ_p, C_c, and C_s. In order to characterize soil compressibility, two easily applicable and commonly used methods are presented here: (1) a laboratory method using the oedometer apparatus and (2) a field method using the plate sinkage apparatus. This is followed by a section on how to determine the precompression stress.

59.2 ONE-DIMENSIONAL LABORATORY TEST: OEDOMETER

The oedometer test is a uniaxial, confined compression test. It simulates vertical loading applied to soil in the field by a tire. The basic setup of the oedometer is shown in Figure 59.2. The soil sample, which is confined in a stiff ring, is loaded uniaxially in a vertical direction. The stiff ring prevents the sample from lateral deformation. During the compression test, axial stress is applied and the resulting soil displacement is measured.

59.2.1 Apparatus

The oedometer apparatus contains a loading device, a compression cell, and devices to record the applied stress and the resulting displacement.

1. Loading device: a uniaxial stress in vertical direction is applied to the soil specimen either by dead weights, by pneumatic methods, or by a step-motor.

2. Compression cell: the cell is usually a circular metal ring (75 mm diameter, 15–20 mm height), which encloses the soil between two porous plates. The ratio of diameter to height should be greater than 3 to minimize the influence of side-wall friction along the cylinder walls.

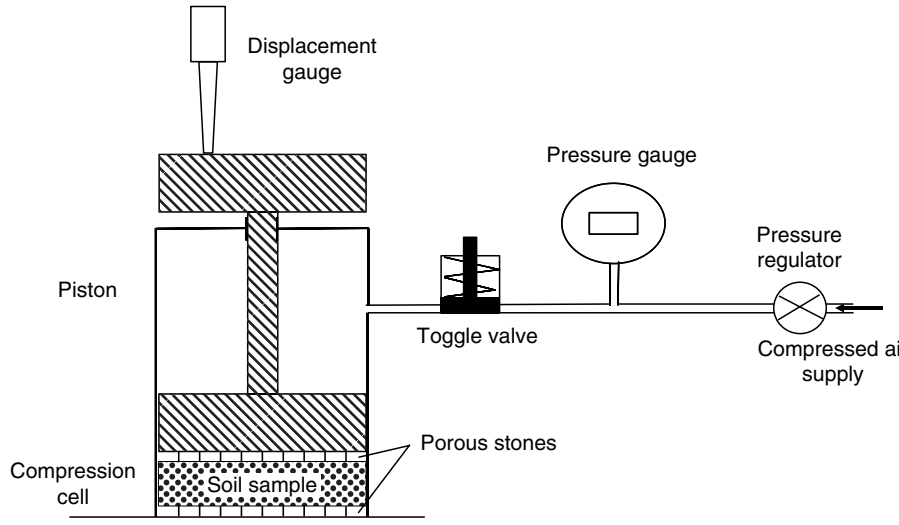

FIGURE 59.2. Oedometer apparatus using a pneumatic loading device.

3 Gauge for measuring applied force or stress (stress is calculated from the force by dividing the applied force by the surface area of the soil sample).

4 Displacement transducer with a range of e.g., 15 mm and an accuracy of 0.002 mm.

5 Optional: an electronic data acquisition system for recording displacement and stress data.

59.2.2 Preparation of Soil Samples

Tests may be performed on intact/undisturbed or on remolded soil samples. Preparation for the latter is described here.

Remolded soil samples are usually prepared from sieved soil. Air-dry soil is sieved through a mesh with a diameter of 2 mm. The gravimetric soil water content of the air-dry soil, w_{airdry}, is determined (see Section ''Soil Water Analysis''). Then, the soil is wetted to the desired soil water content by placing a plastic box containing a mass of air-dry soil, m_{airdry}, on a balance and adding water with a spray. A period of 24 h is allowed for water redistribution.

The mass of water, ${m_{\text{w}}}^{\text{added}}$, which has to be added to the soil in order to obtain the desired gravimetric soil water content, w_{desired}, is

$$ {m_{\text{w}}}^{\text{added}} = m_{\text{airdry}} \frac{(w_{\text{desired}} - w_{\text{airdry}})}{(w_{\text{airdry}} + 1)} \tag{59.1} $$

A soil core at a desired bulk density, ρ_{desired}, is prepared by packing the following mass of soil, m_{soil}, in the compression cell

$$ m_{\text{soil}} = \rho_{\text{desired}} V_{\text{cylinder}} \tag{59.2} $$

where V_{cylinder} is the volume of the oedometer cylinder.

59.2.3 Compression Tests

Soil samples are loaded either sequentially or at constant displacement velocity. Sequential loading (or step loading) is widely used.

Sequential Loading

Sequential loading implies that stress is applied stepwise. Each stress level is hereby applied for a certain loading time. The loading time may be chosen depending upon soil properties and objective of the test. It is typically 30 min in agricultural soil mechanics research and 24 h in geotechnical engineering. However, longer or shorter loading times may be chosen for different reasons. A typical sequence of applied stress levels is 15, 30, 50, 100, 200, 300, and 600 kPa.

Procedure

1 Weigh the soil sample before starting the compression test.

2 Place the cylinder in the oedometer apparatus.

3 Apply stress corresponding to the first stress level and keep this stress constant for the duration of the desired loading time per stress level.

4 After loading for exactly the desired loading time per stress level, measure the displacement.

5 Apply the stress corresponding to the next stress level.

6 Repeat steps 4 and 5 until the last stress level is reached.

7 After removing the cylinder from the oedometer, weigh the sample.

8 Dry the sample in an oven at 105°C for at least 24 h and weigh.

Alternatively, the soil sample may be completely unloaded between steps 4 and 5.

Stress and displacement data may be recorded with high resolution during the compression test. This requires an electronic data acquisition system.

Loading at Constant Displacement Velocity

Loading at constant displacement velocity implies that the piston of the oedometer apparatus (see Figure 59.2) is moving downward at a constant velocity, and the corresponding stress is measured. Measuring at constant displacement velocity requires an electronic data acquisition system for recording displacement and stress data. The procedure is as explained earlier. Instead of steps 3–6, the soil sample is loaded at constant displacement velocity and displacement–stress data are recorded with a data logger.

59.2.4 Calculations

Initial conditions are determined for each specimen. The initial water content, w_0, is calculated as

$$w_0 = \frac{m_0 - m_{\text{dry}}}{m_{\text{dry}}} \tag{59.3}$$

where m_0 is the mass of the soil sample at initial moisture conditions before the compression test and m_{dry} the mass of the oven-dried sample. The initial void ratio, e_0, is calculated as

$$e_0 = \frac{\rho_s}{\rho_0} - 1 = \frac{\rho_s V_0}{m_s} - 1 \tag{59.4}$$

where ρ_s is the density of solids, ρ_0 the initial dry bulk density, and V_0 the initial sample volume (i.e., the volume of the oedometer cylinder).

59.2.5 Presentation of Results

The results of a compression test are presented graphically as the relationship between the logarithm of the applied stress and some parameter related to the packing state of the soil,

e.g., strain, bulk density, or void ratio, as shown in Figure 59.1. Void ratio, e, is calculated from the measured displacement, Δh, as

$$e(\Delta h) = \frac{\rho_s V(\Delta h)}{m_s} - 1 = \frac{\rho_s \pi r^2 (h_0 - \Delta h)}{m_s} - 1 \tag{59.5}$$

where V, r, and h_0 are the volume, radius, and initial height of the cylindrical soil sample, respectively.

From the compression curve (Figure 59.1), C_s, C_c, and σ_p are obtained. The compression index, C_c, i.e., the slope of the VCL, and the swelling index, C_s, i.e., the slope of the SL, are calculated by

$$C_c = \frac{\Delta e}{\log(\Delta\sigma)}; \quad \sigma \in (\text{VCL}) \tag{59.6}$$

$$C_s = \frac{\Delta e}{\log(\Delta\sigma)}; \quad \sigma \in (\text{SL}) \tag{59.7}$$

where e is the void ratio and σ the applied normal stress. Determination of σ_p is explained in detail in Section 59.4.

59.3 *IN SITU* PLATE SINKAGE FIELD TEST: PLATE PENETROMETER

In situ plate sinkage tests are an established procedure used in the prediction of rolling resistance for off-road vehicles. Alexandrou and Earl (1995) showed that the plate sinkage test can be applied for determining soil precompression stress.

An example of a plate penetrometer is shown in Figure 59.3. The plate penetrometer contains a load cell to measure the required force, a depth potentiometer to measure the sinkage of the circular plate, and an electrical motor, which drives the plate downward at a desired plate sinkage (displacement) velocity.

59.3.1 PROCEDURE

1 Excavate the soil to the desired depth (the soil may be subjected to compression at the soil surface, or at any desired depth). Note that the area of excavated soil has to be large enough to place the apparatus within it, and to potentially allow for several measurements (replicates) at the same depth.

2 Level the soil surface at the desired depth in order to allow the penetrometer plate to be driven downward in an exactly vertical direction. When conducting measurements at the soil surface, crop residues should be removed.

3 Put the apparatus in place. The apparatus shown in Figure 59.3 needs two persons acting as counterweights, standing on the footplates on either side of the apparatus.

4 Start the plate sinkage test.

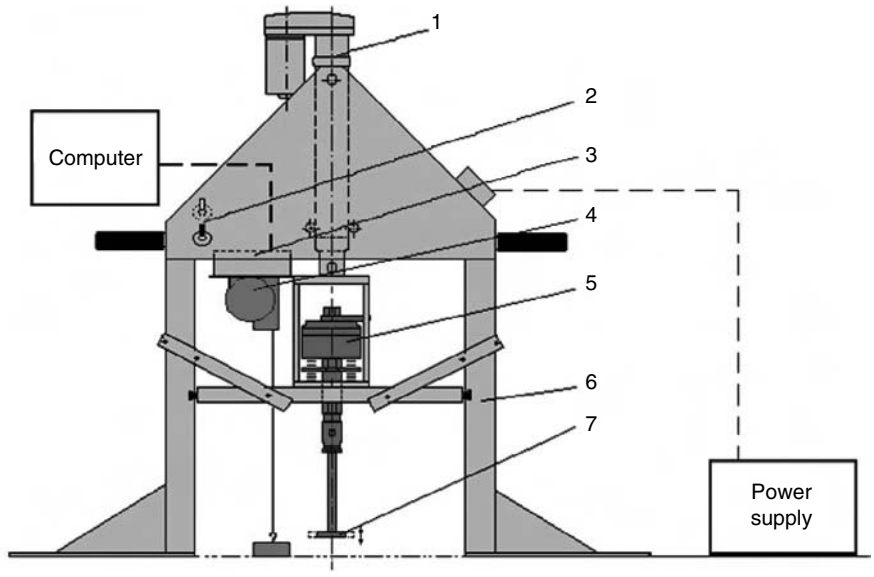

FIGURE 59.3. Side view of a plate penetrometer: (1) electric power unit; (2) switch to record data; (3) data shuttle; (4) depth sensor; (5) load sensor; (6) frame; (7) penetration plate. (From Dawidowski, J.B., Morrison, J.E., and Snieg, M., *Trans. Am. Soc. Agr. Eng.*, 44, 1059, 2001. With permission.)

5 During each test, the vertical normal force and the sinkage (vertical displacement) are recorded (by a data logger) with high resolution (e.g., 100 Hz).

The apparatus used by Dawidowski et al. (2001) and Keller et al. (2004) had the following dimensions:

1 Plate diameter: 49 mm

2 Maximum loading: 4400 N, with a maximum error of $\pm 0.05\%$

3 Maximum error of the depth penetrometer: $\pm 0.1\%$

4 Maximum stroke of the plate: 200 mm

5 Downward velocity of the plate: 7 or 25 mm s^{-1}

6 Maximum frequency of data logging: 1000 Hz

59.3.2 Calculations and Presentation of Results

The recorded data can be plotted in a log σ–displacement diagram, from which the precompression stress, swelling index, and compression index can be obtained as described in Section 59.2.4 and Section 59.2.5.

Note that there is no control over lateral deformations below the penetrometer plate in a plate sinkage test. Therefore, the compression curve obtained from the plate sinkage test is

expressed in a log σ–displacement diagram (whereas the compaction curve from the oedometer test is normally expressed in a log σ–e diagram). Therefore, the expression ''compression index'' is physically inaccurate when applied to the plate sinkage test. However, lateral deformations should be small for small displacements (see also Section 59.5.1).

59.4 DETERMINATION OF THE PRECOMPRESSION STRESS

There are several procedures known for estimating the precompression stress from the compression curve. Some of the most commonly used methods are given in Dias and Pierce (1995).

59.4.1 Casagrande's Method

The procedure developed by Casagrande (1936) is considered as a standard method. The method was developed empirically from a large number of tests on different types of soils.

The procedure consists of six steps (Figure 59.4):

1 Determine the position of the VCL with a sufficient number of data points.

2 Determine the point, *T*, that corresponds to the smallest radius of curvature.

3 Draw a tangent, *t*, to the curve through point *T*.

4 Draw a horizontal line, *h*, through point *T*.

5 Draw the bisecting line, *b*, between the tangent and the horizontal through point *T*.

6 The precompression stress, σ_p, is found as the point of intersection of the bisecting line and the VCL.

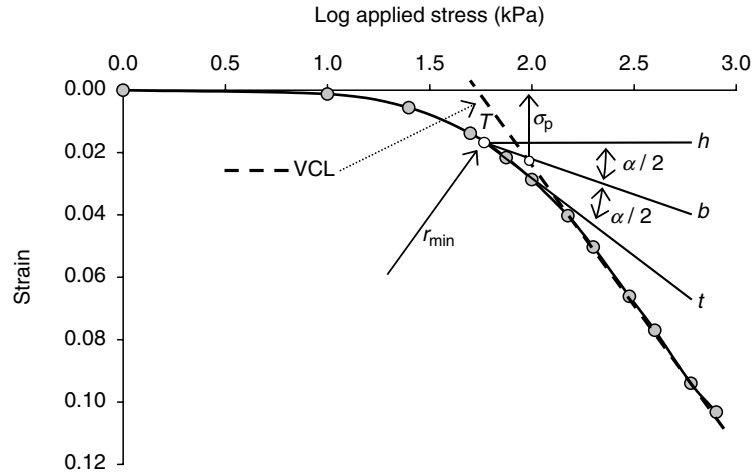

FIGURE 59.4. Determination of the precompression stress according to Casagrande. The procedure and the symbols are described in the text. (Adapted from Casagrande, A., *Proceedings of the International Conference on Soil Mechanics and Foundation Engineering*, Vol. III, Cambridge, UK, 1936.)

The Casagrande procedure is originally a graphical procedure, i.e., the point corresponding to the smallest radius of curvature is determined by visual observation. However, the visual determination is subjective and scale-dependent. Dawidowski and Koolen (1994) developed a mathematical procedure to calculate precompression stress according to Casagrande. Another possibility is to fit the data points to a mathematical equation, from which the above mentioned points 1–6 can be calculated. The data points may be fitted to a logarithmic function (Bailey et al. 1986) to the van Genuchten equation (Baumgartl and Köck 2004) or to a polynomial equation (Arvidsson and Keller 2004).

59.4.2 Other Methods

As the determination of the point that corresponds to the smallest radius of curvature may be difficult, other procedures generally involving regression analysis have been developed for the determination of the precompression stress (Sällfors 1975; Culley and Larson 1987; Jose et al. 1989; Lebert and Horn 1991; Dias and Pierce 1995).

The easiest method is to estimate precompression stress as the intersection of two lines: (1) SL, i.e., the regression line obtained for the points of applied stress sequence in the recompression portion of the compression curve and (2) VCL, i.e., the regression line obtained for the points in the virgin compression portion of the compression curve (Dias and Pierce 1995).

Note that different determination procedures can result in slightly different values for the precompression stress (Arvidsson and Keller 2004).

59.5 GENERAL COMMENTS

59.5.1 Comparison between Confined Laboratory Test and Field Assessment of Soil Compressibility

In an oedometer test (Section 59.2), the lateral (i.e., horizontal) strain is fully prevented by a cylindrical stiff ring in which the sample is enclosed. The plate sinkage test in the field (Section 59.3) takes place in only partly confined conditions, i.e., lateral deformations can take place. Hence, the mechanisms involved in the oedometer test and in the *in situ* plate sinkage test are different (Figure 59.5).

Earl (1997) showed that for small deformations, the data from confined compression tests are similar to those obtained from plate sinkage tests (corresponding to the stress range 0 to ca. 300 kPa in Figure 59.5). It is believed that the precompression stress is identified within this range of deformation (Dawidowski et al. 2001). At greater deformations (corresponding to the stress range >ca. 300 kPa in Figure 59.5), however, the further downward movement of the plate is mainly caused by lateral deformation and not by compaction, whereas in a confined test, the deformation is caused by compaction (Earl 1997).

Therefore, all critical data from plate sinkage tests should be collected before the occurrence of any lateral soil deformation under the penetrometer plate (Dawidowski et al. 2001), i.e., only data associated with relatively small plate sinkage should be considered for determination of the precompression stress. Dawidowski et al. (2001) and Keller et al. (2004) measured precompression stress with a plate sinkage apparatus and an oedometer, respectively, on three different soils with textures ranging from loam to clay. They considered data

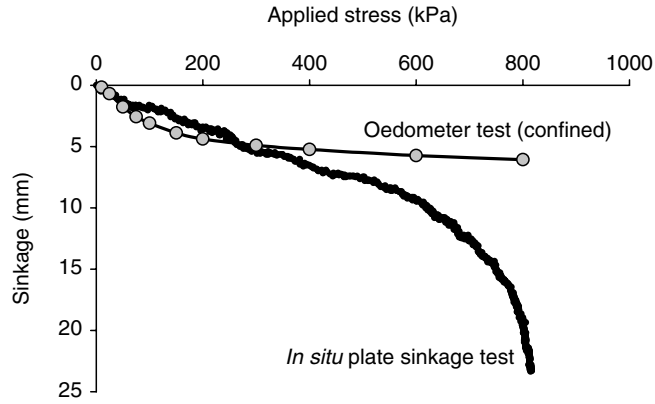

FIGURE 59.5. Experimental curves of axial (vertical) stress versus plate sinkage on a moist silty clay loam for confined oedometer test and *in situ* plate sinkage test; note that stress is plotted on linear scale in this figure in contrast to Figure 59.1 and Figure 59.4.

of plate sinkage <5 mm and found that the precompression stress values derived from the oedometer and the plate sinkage test did generally not differ significantly from one another.

59.5.2 Another Laboratory Method: Triaxial Cell Apparatus

The triaxial cell apparatus is used to measure soil mechanical properties that describe both the compressive and shear behaviors of soil. The former is described by C_s, C_c, and σ_p, while the latter is usually described by the Mohr–Coulomb parameters cohesion and angle of internal friction.

The triaxial cell apparatus allows for applying an axial vertical stress, σ_1 (by a piston) and a lateral confining stress, σ_3 (by hydrostatic pressure). Note that σ_3 is unknown in the oedometer test. Isotropic triaxial compression tests imply that $\sigma_1 = \sigma_3$. In a triaxial cell, the cylindrical soil specimen is enclosed by a rubber membrane and embedded between ceramic plates at the lower and upper faces to allow drainage.

Generally, oedometer tests are preferred to triaxial tests for engineering applications because they are less time-consuming and easier to use.

59.5.3 Range of Variation of Soil Compressibility Parameters

Typical values for precompression stress may vary from 30 to 150 kPa for moist soils, whereas compression indexes may vary from 0.05 to 0.35 (Lebert and Horn 1991).

Precompression stress and compression index have been measured on different soils and under various conditions. As mentioned elsewhere, the mechanical properties of soil are influenced by soil texture, organic matter content and composition, bulk density, soil water potential (water content), and soil structure. Consequently, several authors including Gupta and Larson (1982), McBride (1989), Angers (1990), Lebert and Horn (1991), McBride and Joosse (1996),Veenhof and McBride (1996), Défossez et al. (2003), and Imhoff et al. (2004) have proposed pedotransfer functions for the estimation of soil mechanical parameters from easily measurable soil variables such as soil texture, organic matter content, bulk density, and water content.

REFERENCES

Alexandrou, A. and Earl, R. 1995. *In situ* determination of the pre-compaction stress of a soil. *J. Agric. Eng. Res.* 61: 67–72.

Angers, D.A. 1990. Compression of agricultural soils from Québec. *Soil Till. Res.* 18: 357–365.

Arvidsson, J. and Keller, T. 2004. Soil precompression stress I. A survey of Swedish arable soils. *Soil Till. Res.* 77: 85–95.

Bailey, A.C., Johnson, C.E., and Schafer, R.L. 1986. A model for agricultural soil compaction. *J. Agric. Eng. Res.* 33: 822–825.

Baumgartl, T. and Köck, B. 2004. Modelling volume change and mechanical properties with hydraulic models. *Soil Sci. Soc. Am. J.* 68: 57–65.

Casagrande, A. 1936. Determination of the preconsolidation load and its practical significance. *Proceedings of the International Conference on Soil Mechanics and Foundation Engineering*, 22–26 June 1936, Vol. III, Cambridge, UK, pp. 60–64.

Culley, J.L.B. and Larson, W.E. 1987. Susceptibility to compression of a clay loam Haplaquoll. *Soil Sci. Soc. Am. J.* 51: 562–567.

Dawidowski, J.B. and Koolen, J. 1994. Computerized determination of the preconsolidation stress in compaction testing of field core samples. *Soil Till. Res.* 31: 277–282.

Dawidowski, J.B., Morrison, J.E., and Snieg, M. 2001. Measurement of soil layer strength with plate sinkage and uniaxial confined methods. *Trans. Am. Soc. Agr. Eng.* 44: 1059–1064.

Défossez, P. and Richard, G. 2002. Compaction of tilled topsoil due to traffic: a review of models tested in field conditions. *Soil Till. Res.* 67: 41–64.

Défossez P., Richard G., Boizard H., and O'Sullivan, M., 2003. Modelling change in soil compaction due to traffic as function of soil water content. *Geoderma* 116: 89–105.

Dias Junior, M.S. and Pierce, F.J. 1995. A simple procedure for estimating preconsolidation pressure from soil compression curves. *Soil Tech.* 8: 139–151.

Earl, R. 1997. Assessment of the behaviour of field soils during compaction. *J. Agric. Eng. Res.* 68: 147–157.

Gupta, S.C. and Larson, W.E. 1982. Predicting soil mechanical behaviour during tillage. In *Predicting Tillage Effects on Soil Physical Properties and Processes*. American Society of Agronomy, Special Publication 44, Madison, WI, pp. 151–178.

Imhoff, S., Da Silva, A.P., and Fallow, D. 2004. Susceptibility to compaction, load support capacity, and soil compressibility of Hapludox. *Soil Sci. Soc. Am. J.* 68: 17–24.

Jose, B.T., Sridharan, A., and Abraham, B.M. 1989. Log–log method for determination of preconsolidation pressure. *Geotech. Test. J.* 12: 230–237.

Keller, T., Arvidsson, J., Dawidowski, J.B., and Koolen, A.J. 2004. Soil precompression stress II. A comparison of different compaction tests and stress-displacement behaviour of the soil during wheeling. *Soil Till. Res.* 77: 97–108.

Lebert, M. and Horn, R. 1991. A method to predict the mechanical strength of agricultural soils. *Soil Till. Res.* 19: 275–286.

McBride, R.A. 1989. Estimation of density-moisture-stress functions from uniaxial compression of unsaturated, structured soils. *Soil Till. Res.* 13: 383–397.

McBride, R.A. and Joosse, P.J. 1996. Overconsolidation in agricultural soils: II. Pedotransfer functions for estimating preconsolidation stress. *Soil Sci. Soc. Am. J.* 60: 373–380.

Sällfors, G. 1975. Preconsolidation Pressure of Soft High Plastic Clays, Doctoral Thesis. Department of Geotechnical Engineering, Chalmers University of Technology, Gothenburg, Sweden.

Veenhof, D.W. and McBride, R.A. 1996. Overconsolidation in agricultural soils: I. Compression and consolidation behavior of remolded and structured soils. *Soil Sci. Soc. Am. J.* 60: 362–373.

Chapter 60
Field Soil Strength

G. Clarke Topp and David R. Lapen
Agriculture and Agri-Food Canada
Ottawa, Ontario, Canada

60.1 PRINCIPLES AND PARAMETER DEFINITIONS

Soil strength can occur in various forms or expressions, such as compressive strength, shear strength, and tensile strength, etc. There are many different soil strength measurement techniques, most of which originate from a specific applied soil test requirement. Soil tillage operation will often include a number of directional forces that the soil's strength resists until it breaks. The compressive strength resists tool insertion, the shear strength resists action of crushing soil by lateral forces, and the tensile strength resists the breakage of soil, which involves pulling it apart at the edge of tillage tines. While the ability of the soil to sustain traffic or support a building relates to compressibility and compressive strength, as discussed in Chapter 59, the soil strength associated with root penetration or tillage tool resistance can be conveniently ascertained by a penetrometer, which measures penetration resistance of a device inserted in the soil (most often a vertically oriented measure). The strength of soil to resist landslide and some forms of erosion, for example, is better expressed by techniques that explicitly measure the shear of the soil (a planar measure), such as standard sheargraph techniques.

The coverage in this chapter will be limited to two soil strength measurement approaches: cone penetration resistance and shear strength. Only specific cone resistance and shear strength methods that relate most strongly to manually operated *in situ* agricultural and environmental science evaluations will be discussed hereafter. For information on measuring tensile strength, we recommend the review by Dexter and Watts (2001).

60.2 PENETRATION RESISTANCE

60.2.1 Principles of Operation of Penetrometers

Penetrometers measure the force required to push or drive a device into a soil. The oldest penetrometers in agriculture could well have been animal hooves, where the depth of penetration advised the farmer whether a field was ''trafficable'' for grazing or cultivation. Essentially the principles of modern penetrometers follow the ''cruder'' soil penetration resistance indicators but with the added advantage of standardized measurements, which provide better repeatability and comparability.

A penetrometer consists of a rod or shaft, which is pushed into the soil, usually vertically, using some device to measure the force required to insert the device to a desired depth. The end of the rod, or tip, engaging the soil is commonly conical or flat in shape. Similarly a number of force-sensing methods are used along with a variety of recording devices. Penetrometer data are typically reported as the resistance to soil penetration in terms of penetration force per unit area using units of pressure. For penetrometers using conical tips, the resistance pressure is often referred to as ''cone index'' (CI) and expressed in units of pascal (Pa), kilopascals (kPa), or megapascals (MPa), where $1\ \text{Pa} = 1\ \text{N m}^{-2}$. Most penetrometers use a standardized 30° circular cone with less than 700 mm^2 base area, which allows for manual as well as more mechanized probe insertion into most soil conditions.

Bengough et al. (2001) and Lowery and Morrison (2002) have given extensive and comprehensive reviews of soil penetrometers and penetrability, including background considerations that must be taken into account when undertaking soil penetration studies. Although numerous penetrometers are available, only general criteria for their selection have evolved. Increased data logging and smaller scale motorized drives have enhanced the opportunities for methodology studies comparing different penetrometers from which selection criteria can further evolve (Motavalli et al. 2003). The difficulty in defining objective criteria for penetrometer selection is complicated by (i) number of soil physical factors that influence penetration resistance in the soil and (ii) logistical and operational constraints to measurements (e.g., desired depth, crop damage, transport to in-field locations, measurement goals, cost, etc.).

Soil penetrometers can provide *in situ* data at depth in the soil profile without the need for soil disturbance. Obtaining equivalent soil mechanical measures in a laboratory setting would require major sampling, resulting in a destructive investigation of the soil body. Soil penetrometers fall into two basic categories, ''dynamic'' and ''static.'' Dynamic penetrometers are designed to be driven into the soil using the impact of a hammer or a falling weight. This type of penetrometer is used for highway pavement and roadbed evaluations, but few have automated data acquisition capabilities and are not widely used in soil science investigations. Static penetrometers are designed for insertion into the soil at a slow steady rate to avoid the need to include dynamic effects in the analysis. Only static penetrometers will be discussed in this chapter.

Soil Physical Factors Influencing Penetration Resistance

Soil penetrometers measure the force required to deform soil material, the nature of the deformation depending primarily on the shape of the penetrometer tip and on penetration depth. At the soil surface, the deformation is primarily shear, transforming gradually to a combination of shear and compression with increasing depth. This transition is exhibited as an increasing resistance with depth, where the transition depth is estimated to be between three and five diameters of the probe (Barley et al. 1965; Waldron and Constantin 1970). Beyond this depth, the deformation has been primarily explained using cavity expansion theory (Farrell and Graecen 1966; Vesic 1972). Farrell and Graecen (1966) have assumed compression to occur in two zones, an inner zone with plastic failure surrounded by elastic compression. In addition to shear and compression occurring in the soil there is also the force of friction on the cone/shaft. Thus a penetrometer records some combination of shear, compression deformation, and probe-to-soil friction. The combined effects expressed in

the resistance readings, however, can be used as an indicator of soil strength. These factors, in turn, are influenced by the state of the soil physical conditions such as soil water potential, water content, soil texture, bulk density, structure, and clay mineralogy. The interaction and combination of these factors have a complex effect on subsequent penetration resistance readings. Hence penetration resistance measurements are seldom useful in isolation unless one is simply concerned with identifying the strength of a soil in relation to critical threshold values. However, in most cases, for effective use of penetrometer resistance to characterize soil behavior or soil treatment effects. concurrent independent measurement or control of these complicating factors will be necessary. This is the most important one for monitoring and comparing site conditions.

Tip Designs

The American Society of Agricultural Engineers has established an Engineering Standard, ASAE S313.3 Feb99, for the use of the soil cone penetrometer (American Society of Agricultural Engineers (ASAE) Standards 1999). This standard provides guidelines including purpose, scope, definition, test apparatus, procedure, and interpretation and reporting of data obtained by cone penetrometers. The standard adopts, as its model, a 30° circular stainless steel cone with a driving shaft of smaller diameter to minimize soil friction along the shaft. Penetrometer cones of this type are most common for soil-based activities.

As described by Lowery and Morrison (2002), the size of cone angle determines the relative portions of the cone resistance attributed to the two principal forces: (i) force to deform the soil by the wedge-action of the cone and (ii) soil-to-metal frictional force. For a given base diameter, a decrease in cone angle gives an increase in surface area, and thus an increase in the frictional force component. At an angle of about 30° there is a ''cross over,'' where for angles $<30°$, the cone resistance decreases as the angle increases, and for angles $>30°$ the cone resistance increases as the angle increases.

The cone diameter is an important consideration when measuring in well-aggregated or cracking soils. Cones with small base diameters may produce highly variable data when random measurements are made on soil aggregates, and in the interaggregate pore space or cracks that have lower resistance (Grant et al. 1985). Larger diameter cones may reduce these effects at the expense of greater deformation of aggregates (Jamieson et al. 1988), and potentially affecting measurements on large-scale structural units.

Penetration Rate

Penetration rate for penetrometers has not been standardized because of the potential interaction between rate and cone resistance, especially for finer soils (Freitag 1968). Moreover since soil water potential is a determining factor in soil strength (Busscher et al. 1997), any action to alter the soil water potential during penetrometer measurement potentially influences cone resistance. A cone advancing into soil causing local compression can change the soil water potential also. If the change in potential is not dissipated as quickly as the cone advances, this potential change can manifest as an error in cone resistance. It is important to use a slow, steady rate of penetration in order to compare soils and sites, and to document and record the rate used. The ASAE standard (American Society of Agricultural Engineers (ASAE) Standards 1999) recommends that the rate should not exceed 30 mm s^{-1}. Much slower rates of penetration have been used in other studies (Cockcroft et al. 1969;

Waldron and Constantin 1970; Perfect et al. 1990) in an attempt to emulate plant root elongation rates, which are in the order of 2.78×10^{-4} mm s^{-1}. Such low rates are too slow for practical use in data collection except for specialized research.

Concurrent Measurement of Water Content and Penetration Resistance

Any soil will produce different cone penetration readings at different water contents (Busscher et al. 1997; Lapen et al. 2004). Therefore, water content is critical for interpreting penetration readings especially when comparative studies are made. In recent times, a large number of penetrometers have been developed to measure water content and cone resistance concurrently (e.g., Morrison et al. 2000; Young et al. 2000; Topp et al. 2003; Sun et al. 2004; Hummel et al. 2004). A variety of approaches to water content measurement have been utilized but no single approach has been shown to be superior. Hummel et al. (2004) used a standard cone modified to collect near-infrared reflectance from the soil passing the cone to estimate water content. Other approaches have used high-frequency electromagnetic wave propagation, including time-domain reflectometry (TDR) as a basis for water content measurement. Young et al. (2000), and Topp et al. (2003), used time-domain transmission (TDT) by inserting a transmission line on the periphery of the shaft behind the penetrometer cone (Figure 60.1). The helical wrapped transmission line used by Topp et al. (2003) had an

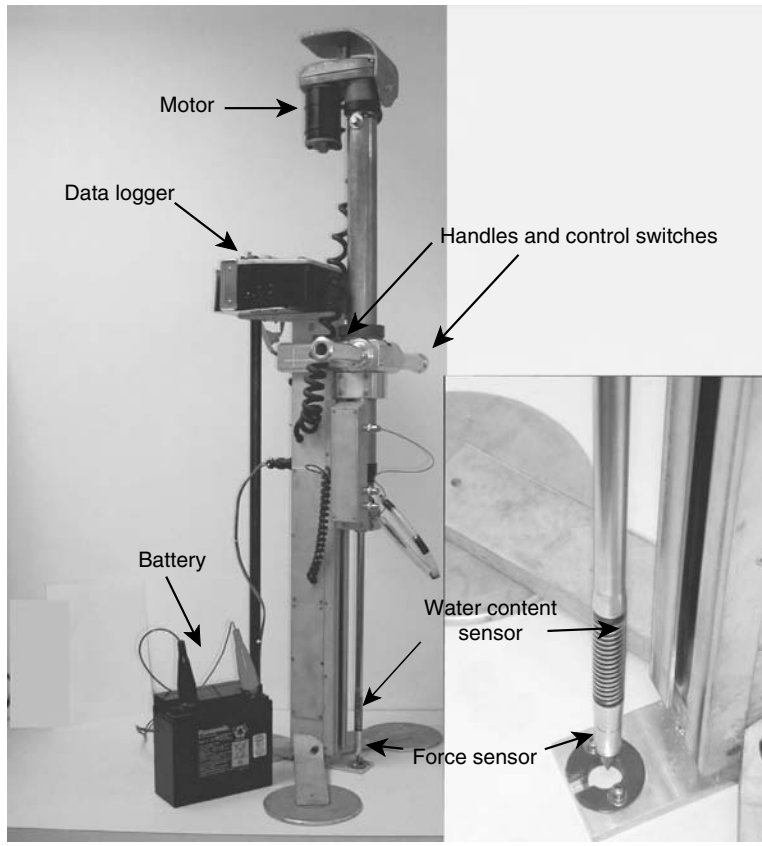

FIGURE 60.1. A motorized portable penetrometer for measuring both cone resistance and water content. (From Topp, G.C., Lapen, D.R., Edwards, M.J., and Young, G.D., *Vadose Zone J.*, 2, 633, 2003. With permission.)

advantage over Young et al. (2000), in that the water measurement zone was reduced to 6 cm along the shaft while maintaining a transmission line length of 30 cm. The reported water content resolution of this shaft-based helical TDT system was ± 0.02 m^3 m^{-3}, which is equivalent to the resolution of a TDR. Morrison et al. (2000) equipped a cone penetrometer with a small TDR transmission line for measuring water content at the cone surface, in which the water content sensor was that described by Starr et al. (2000). Sun et al. (2004) have used a capacitance- or impedance-type sensor at the base of the cone to estimate water content. As these combination penetrometers are relatively new, they have not yet been used extensively to allow ranking or comparative assessments. The principle of operation of some of the above-mentioned electromagnetic sensors is covered in detail in Chapter 70.

60.2.2 Instrumentation

Hand-Push Portable Cone Penetrometers

Portable cone penetrometers are hand-push devices that are about 1.2 m in height allowing for penetration depths to about 0.8 m (some models with rod extensions can provide measurements deeper in the soil). The cones are smoothly machined stainless steel and most commonly have the ASAE recommended 30° cone angle. The cone base and corresponding rods will be usually available in two sizes: (i) 9.5 mm diameter rod with a 12.8 mm diameter cone and (ii) 15.9 mm diameter rod with a 20.0 mm diameter cone for use in ''soft'' soils. The force-sensing devices are located at the upper end of the shaft and use a variety of sensing techniques such as proving ring and dial gauge and strain gauge-based load cells. Depth sensing is achieved by methods such as graded markings on the rod, laser reflectance from the soil surface, a potentiometer, and more. If data logging and data manipulation equipment are employed, they are typically mounted above the load sensors. In most units, two hand-grip handles are conveniently attached to opposite sides of the enclosure for the electronic components. Between the handles on the upper side of the electronics is usually the instrument panel and data display. The insertion rate is operator controlled. Portable cone penetrometers are commercially available from ELE/Soiltest International, Inc., Loveland, Co, USA; Eijkelkamp Agrisearch Equipment BV, Giesbeek, The Netherlands; Spectrum Technologies, Inc., Plainfield, IL, USA; Agridry Rimik Pty Ltd., Toowoomba, QLD, Australia.

Motorized Portable Cone Penetrometers Measuring Water Content

Soil water content is one of the most important factors influencing cone penetration measurements, and for most soil-based applications, it is a mandatory measurement. Penetrometers with simultaneous water content measurement features have developed from portable cone penetrometers and have two added features. The first is to measure water content and the second is to control the rate of penetration. To achieve these improvements, it requires a stand and a frame to support the motor and guide the penetrometer, resulting in a large unit, which approaches the limit of human portability. Nevertheless, the operational advantages of such combination penetrometers warrant their inclusion here.

The general operation of a combination penetrometer with both water content and cone resistance measurements is described by Young et al. (2000) and Topp et al. (2003). The penetrometer system (Figure 60.1) uses a lightweight, 12 V electric motor-driven screw jack assembly to provide a constant velocity for probe insertion of approximately 28 mm s^{-1}. The length of travel is 400 mm. The drive mechanism is mounted on a vertical supporting frame made of lightweight material, which also houses the sensor electronics, data logger, and

motor control switches. The vertical frame is supported by three horizontal legs on which the operators stand to provide a load to hold the equipment in place during operation. The power for the whole system, including the drive motor, is supplied by a 12 V gel-cell battery, which is carried in a backpack. In Topp et al. (2003), the water content sensor on the shaft, a helical transmission line, is connected between 50 Ω coaxial cables to transmit and receive a high-frequency signal along the helix from which the travel time of the signal is used as a measure of water content of the surrounding soil (Figure 60.1). The force sensor at the cone was described previously (Adams et al. 2000).

Sun et al. (2004) described a similar combination penetrometer, but with a shorter capacitance-type sensor for water content. Apart from being at an early stage of development, and less readily portable, the Sun et al. (2004) penetrometer has similar operational properties to that of Topp et al. (2003).

60.2.3 Procedures

The procedural details for the use of penetrometers depend on a number of factors: (i) intended use for the data, (ii) type and capability of the penetrometer, and (iii) soil or field conditions at the time of measurement.

Cone Penetrometers

Cone resistance data are highly variable, necessitating carefully chosen levels of replication to assure high-quality data. Ideally, the degree of replication should be made on the basis of a presampling survey from which one obtains sample variance and mean. From these, the number of replicates required to attain the desired confidence level can be calculated. Cone penetrometers are usually used to indicate conditions within soil profiles. As surface operations on the soil such as tillage and traffic affect the strength distribution in the soil profile, the location of measurement and degree of replication at a field site are the first considerations.

1. Adopt criteria for location of measurement, so that replicated locations can be chosen consistently and in relation to the treatment conditions and objectives of the study. For example, if a comparison of plant row position and wheel traffic are part of the study treatment, locations should be chosen as mid-way between rows in wheel-tracked and/or nontracked rows. In another case, the choice may be only ''in plant rows.''

2. Layout the field sampling program so that replication, data labeling, and site location criteria are specified prior to the initiation of the measurements.

3. Schedule the field measurements to optimize the quality of the data obtained. As cone resistance is highly dependent on water content, it is advisable to aim for simultaneous measurements of water content. In cases where water content cannot be measured as frequently as cone resistance, it is recommended that resistance testing be done at specified water content, such as at ''field-water capacity'' or some equivalent condition that occurs repeatedly either seasonally or within a season.

4 Set up penetrometer to begin data collection. The details of this step depend on the type of penetrometer in use. For gauge type and similar manual penetrometers, this amounts to setting the force indicator to zero. For data logging penetrometers, this step involves initiating the data logger and resetting the data labels.

5 Push the penetrometer into the soil at a uniform rate not to exceed 30 mm s^{-1}. For hand-push penetrometers, the rate control is the responsibility of the operator and some commercial devices have aids to indicate when the desired rate is exceeded. Unsteady rates of insertion often occur as an operator forces the penetrometer tip past occasional harder layers or large pores. This step is more readily achieved satisfactorily with motorized devices.

6 Withdraw the cone from the soil, and wipe it clean, if necessary.

7 Take any necessary steps to ensure that the data have been recorded or retained on the data logger. For fully manual penetrometers, only extreme or limited values of resistance can be recorded, but most data logging penetrometers will automatically carry out this step.

8 Reset the penetrometer and return to step 4 to continue with the predetermined replication schedule for the selected location.

9 Retrieve and download the data as required to meet the objectives of the study.

60.2.4 Calculations and Data Handling

As there is no consistent or standardized protocol for the acquisition or analyses of penetration resistance data, only general considerations will be dealt with here, leaving it to the operator to ensure that reported data have been retrieved and processed properly. Proper calibration of the instrument is required and periodic testing of the stability of the calibration before, during, and immediately following field use is recommended.

Typically calibration applies to three aspects of penetrometry: (i) depth recording and resolution, (ii) force or resistance, and (iii) water content for instruments that include this measurement. In general, the depth indicators and sensing devices are often precise and stable enough to allow infrequent calibration. However, periodic examination of their accuracy is certainly recommended.

Adams et al. (2000) described a method for calibrating the force sensors in the laboratory. Such calibration is critical and should be conducted routinely under controlled laboratory conditions. Methods vary according to design of the device.

Topp et al. (2003) developed in-field procedures for checking the calibration of the force and water content sensors. The general approaches used are applicable to any sensor, but the details will need to be altered depending on specific sensor requirements. Further details on calibration may be obtained from Topp et al. (2003).

Penetrometer calibration is usually achieved using a series of weights acting as loads exerting different forces. The exterted force (N) $= m$ (kg) $\times$ g (9.81 m s^{-2}), where g is the acceleration due to gravity and has a constant value. Penetrometers may record and store data

in different forms, depending on the data-handling capability of the devices used. In cases where resistance is not measured in the units of pressure, it is important that the data are converted to pascals (Pa). Fortunately, most commercially available automated units have internal conversion that present the final values in Pa. The area used in the conversion of force to pressure is the cone base area or the cross-sectional area of the flat-tipped probe of the penetrometers, hence it is important that the tip used is correctly matched for the conversion calculation.

No specific guidelines exist for penetrometer data analysis; therefore, the choice of analyses will depend upon the requirements of the overall study for which the penetrometer data form a component.

60.2.5 Comments

As mentioned in the previous sections, field-based penetration resistance measurements can be highly variable even within similar soil types. Stones, vegetation, soil structure, texture, and trafficking, for instance, contribute to the variability, notwithstanding operator variance. Penetration resistance data have been found to exhibit spatial independence at less than 1 m (O'Sullivan et al. 1987). Lapen et al. (2001) showed that for a clay loam soil under grass, the values had a variable range of spatial dependency based on the direction of field traffic, where shorter distances in spatial correlation were found perpendicular to dominant trafficking patterns. Recommendations on the minimum number of required measurements to achieve desired confidence intervals of averaged values have been put forward (e.g., Bengough et al. 2001). However, such recommendations should not be taken as a strict rule, but rather as a guide, particularly when the required minimum number of measurements cannot be achieved due to logistical or cost constraints. In all situations, a key rule of thumb for penetrometer operators is to acquire as much information about site characteristics as possible to help inform spatial sampling strategies, bearing in mind that there is no single strategy that will meet all requirements for all situations.

Any study attempting to make relative comparisons between soil treatments, for instance, must take into consideration soil water content on the measured cone resistance values. Ideally, the most preferable option is the use of a combination water content/penetrometer. However, if such an instrument cannot be used, an independent measure of soil water content should be made close to the measurement site. In most situations, the relationship between soil water content and cone resistance is negatively correlated. Taking account of this relationship can minimize errors associated with strength–water content interactions, which might otherwise ''mask'' soil management effects on strength properties. Busscher et al. (1997) proposed the general equation (Equation 60.1) to standardize penetration data to a common water content to minimize confounding effects:

$$C_c = C_o + \frac{dC}{dW}(W_c - W_o) \tag{60.1}$$

where C_c is the corrected cone index, C_o the original cone index, W_c the common water content to which the cone indices are being corrected, W_o the original water content of C_o, and dC/dW is the first derivative of any one of the following equations (Equation 60.2 through Equation 60.4) that best fitted a set of cone index values to water content:

$$C = aW^b \tag{60.2}$$

$$C = a(1 - W)^b \tag{60.3}$$

$$C = a\mathrm{e}^{bW} \tag{60.4}$$

where C is the cone index (MPa), W the soil water content on a dry weight basis (g g^{-1}), e the base of the natural logarithm, and a and b are empirical parameters.

In some cases, depending on soil treatments/conditions, the water content vs. cone resistance relationship may vary temporally, for example, soil consolidation over time may change the water content relationship in addition to the strength differences related to different soil treatments or soil condition. For example, Lapen et al. (2004) found temporally consistent water content vs. penetration relationships for nontilled, clay loam soils, but for conventionally tilled soils, the relationships were temporally variable for nearly 3 months after spring planting. Such findings underscore the importance of acquiring as much site information as possible prior to engaging in field monitoring programs.

60.3 SOIL SHEAR STRENGTH

The shear strength of soil is an important consideration for the design of foundations, retaining walls and roadways in civil engineering applications. In agricultural applications, shear strength is expressed during wheel traction and when tillage tools act to fracture the soil. Shear strength is defined as the strength of the soil, just as it ''fails'' or rather when the soil is unable to resist deforming forces applied to it. In the field, most of the forces applied to soil are multidirectional, making it difficult to define the forces that cause the soil to only shear. As a result, there are only a few soil strength methods that are directly applicable to measure soil shear strength in the field. Most shear strength measurements are described for laboratory samples, performed either on remolded soil, or structurally intact soil blocks, or cores. Being a measure of soil strength, shear strength varies with soil water content or more specifically the soil water potential. In general, soil strength increases as the soil dries or the water potential decreases. In a detailed study of laboratory measurement of shear strength of unsaturated soils, Fredlund and Vanapalli (2002) summarized the current state of the research on the importance of soil water potential on soil shear strength. They have also provided many references to a variety of texts and standard guidelines where methods for measuring shear strength are described for engineering specifications.

Field measurement of shear strength has progressed more slowly and few techniques are available. Lloyd and Collis-George (1982) described four types of shear that can occur in structured field soil depending on the relative strength of aggregates and other structural features. Such fracturing detail is difficult to capture and measure after sampling and transport to the laboratory. Lloyd and Collis-George (1982) described a torsional shear box for field measurement of shear strength under near-zero load, as a best estimate of the contribution of cohesion to soil shear strength. A hand-held shear vane, sometimes called a torvane, also measures zero-load shear strength or cohesion at the cylindrical surface enclosing the outer limit of the vane blades (New Zealand Geotechnical Society, Inc., 2001). A similar measurement can be made at the soil surface with a similar torsion head attached to a grouser where vanes are perpendicular to a circular disk and aligned along radii. Some torvane kits include both surface vanes of different diameters for differing strength soils and axial vanes of differing dimensions for soils having different strengths. Surface vane measurements are somewhat difficult as measurement is made at zero-load, which is hard to maintain consistently while applying the shearing torque. In this section, the method

of using the Cohron portable sheargraph, a torsional shear device, for *in situ* measurement of field shear strength (Cohron 1963) is described. Although similar in principle of operation to the torsional shear box and the surface shear vane, the Cohron sheargraph adds the advantage of measuring the normal stress or load applied during shear.

60.3.1 Principles of Measurement

Soil shear strength arises from two characteristics of the soil body: soil cohesion and internal friction. Cohesion in soil arises from the bonding and attraction between particles as well as bonding caused by water films. The resistance that occurs when soil particles interlock and rub against each other during shearing is the frictional component. The shear strength is usually represented as

$$\tau = c + \sigma_n \tan \varphi \tag{60.5}$$

where τ (kPa) is the shear strength, c (kPa) cohesion, σ_n (kPa) the normal stress, and tan φ the friction coefficient, in which φ is the angle of friction. Equation (60.5) is based on an assumed failure mode defined by the Mohr failure envelope and a linear relationship between shear and normal stresses for the failure surface (Ayers 1987). In practice c and tan φ are empirically obtained by measuring the force required to cause shearing of the soil (τ) when subjected to a sequence of varying normal stress (σ_n). From a linear regression of τ against σ_n, both cohesion (c) and the angle of friction, as tan φ, can be determined from the τ-intercept and the slope of the regression, respectively.

The Cohron sheargraph is a torsional shear device used to measure soil strength *in situ*. As with all field torsional shear devices, this device also suffers from the disadvantage that the stress distribution on the shear surface and the exact geometry of the shear plane cannot be determined as well as in laboratory methods. However, the usefulness of this device outweighs any disadvantages (Kirby and Ayers 1993). One of the less attractive operational features of the Cohron sheargraph is the mechanical recording of a graph and subsequent graph digitization (see Section 60.3.3). In addition, there is need to determine water content by the gravimetric method. Recently, we have been modifying the sheargraph to overcome these two difficulties by incorporating TDR measurement of water content and data logging of the stress data directly. These modifications are presented below as an alternative approach under the name of shearlogger.

Ayers (1987) has reported a large number of sheargraph measurements to examine the relationships among cohesion, friction, water content, and density. Further, Kirby and Ayers (1993) have interpreted such measurements in terms of critical state soil mechanics concepts.

60.3.2 Equipment and Supplies

The Cohron sheargraph is available only from custom-designs following the description given by Cohron (1963). Kirby and Ayers (1993) provide a schematic diagram, reproduced here in Figure 60.2, to illustrate the essential components.

The shear head is a 40 mm diameter circular disk with six grouser blades (10 mm depth by 1 mm thick), extending 10 mm perpendicular to the disk, along six equally spaced radial axes

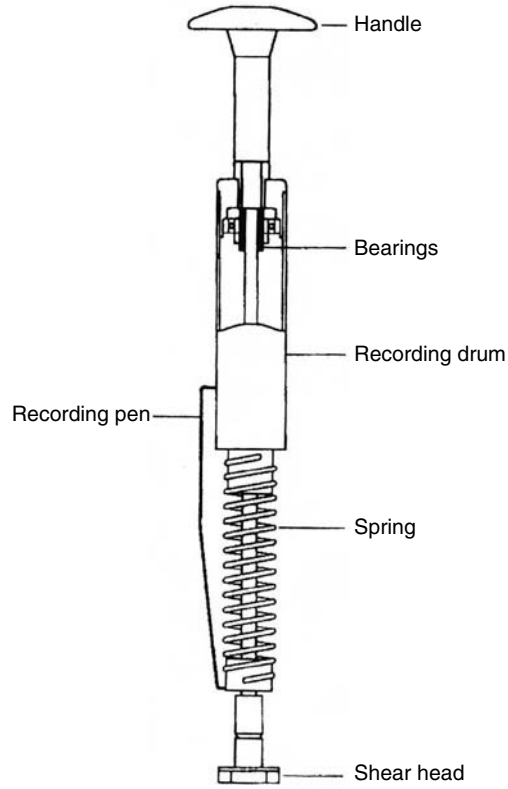

FIGURE 60.2. Schematic drawing of Cohron sheargraph. (Kirby, J.M. and Ayers, P.D., *Soil Till. Res.*, 26, 211, 1993. With permission.)

and into soil. For softer soil, a larger shear head (80 mm diameter) is used. Thus the shearing surfaces (the areas of soil embedded in the shear head) for the 40 and 80 mm diameter heads are 1257 and 5027 mm^2, respectively.

The coil spring allows the recording of both the applied normal stress (the downward force) and the shearing resistance (the torque). A coil spring of 35 mm inside diameter having approximately 10 coils of 3 mm (8 gauge), wire in a 150 mm length provided a maximum normal stress of 300 kPa on the smaller (40 mm diameter), shear head (equivalent to a force of approximately 375 N).

The recording pen consists of a spring-loaded pencil holder such that an inserted pencil records the movement of the spring on user-provided graph paper wrapped around the recording drum. An alternative is to use a combination of a pressure-sensitive graph paper and a spring-loaded scribing point. The handle is used to apply downward forces manually during measurement.

Other required equipment, such as an Instron loading machine (Ayers 1987), is for the calibration of the coil spring both in the axial and torsional or rotational directions, so that axial compression and angular rotation can be converted to units of force.

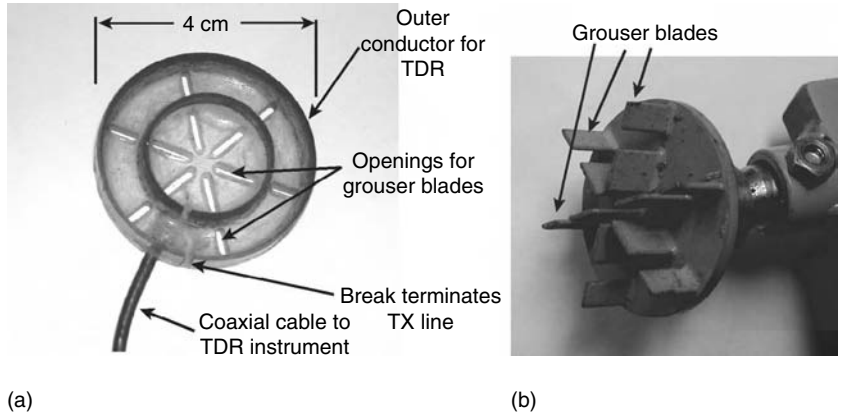

FIGURE 60.3. (a) Water content sensor to be used in conjunction with the Cohron sheargraph or shearlogger, (b) shear head showing grouser blades which insert into and through openings in (a) after the measurement of water content has been completed.

For greater automation during strength measurements, the Cohron sheargraph has been modified in two important ways. One was to provide for the simultaneous measurement of soil water content using TDR and the other was to automate the recording of normal and shear stresses. For use with the TDR, the shear head was modified to include a pair of circular concentric blades of similar depth to the grouser blades and act as TDR transmission (TX) lines (Figure 60.3a). The blades of radii 10 and 20 mm are set in place by a 3 mm thick layer of epoxy resin. The termination of the TX line is achieved by a 2 mm vertical gap in each concentric blade. On each side of the gap, a 5 pf capacitor connected between the two blades provided clear zones in the TDR signal that indicated the ends of the TX line. Figure 60.3a shows slots in the plastic through which the grouser blades of the shear head (Figure 60.3b) are inserted for shear measurements. TDR measurements have been made using the TRASE model instruments (Soilmoisture Equipment Corp., USA) by the authors but other TDR instruments can also be used.

The second modification for automatic recording of stresses was the addition of two strain gauge load cells one to record normal stress and the other to record shear stress, both placed between the shear head and the spring assembly (Figure 60.4). Although the load cell modification minimized the need for the coil spring, the spring was retained to facilitate an estimation of applied stresses by the operator. The voltage signals from the load cells were recorded by a CR510 datalogger (Campbell Scientific, Inc., Canada). Load cells were an S-shaped sensor (0–100 lb, i.e., 45.4 kg load range (Intertechnology Ltd., Canada)) for normal stress and a miniature round beam (50 lb, i.e., 22.7 kg load capacity (Artech Industries, Inc., USA)) for shear stress. As the graphing function was no longer needed, the pencil holder assembly was removed and replaced with two parallel plastic bars along the sides of the arm to which the pencil holder was mounted to transmit the applied torque from the handle to the load cell assembly without using the spring to provide the torque. When the spring was used without the plastic bar restraints, there was a tendency at peak shear stress for the spring to go rapidly and precipitously to the lower stress level. During this rotational ''snap'' of the spring, it was difficult for the operator to maintain consistent normal stress and for the recording of the rapid transition to a lower shear stress value without the restraining bars.

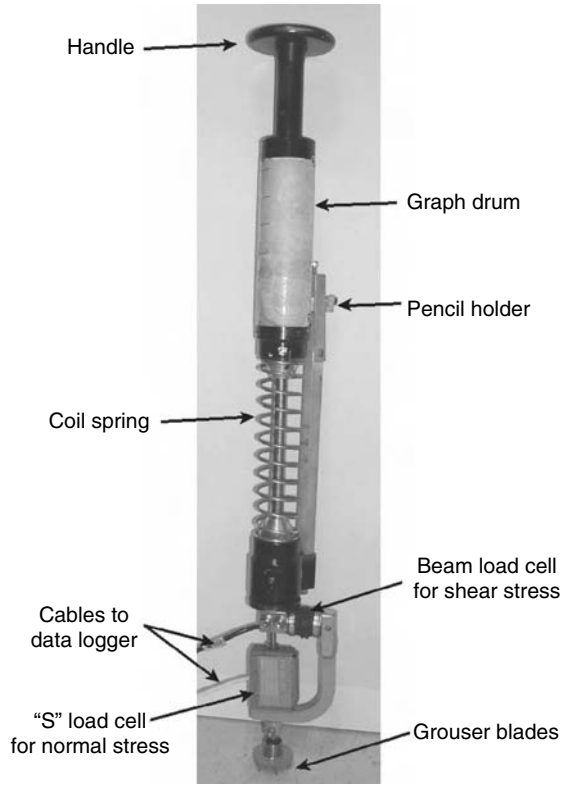

FIGURE 60.4. Shearlogger or Sheargraph as modified to use load cells for recording normal and shear stresses.

60.3.3 Procedures

Both the sheargraph and the shearlogger are custom-designed following Cohron's (1963) description and as a result the procedures are similar. As the shearlogger is more efficient and easier to use, it will be described as the primary method with indicative statements given for use of the sheargraph.

Cohron sheargraph or shearlogger measurements are made on a 50 × 50 mm flat surface for the small shear head; a larger area is used for the large head. The soil surface for measurement is prepared by gently clearing vegetation and producing a level soil surface. Deeper levels in the soil profile are accessed by excavating stepped levels down the side of the soil pit.

The following procedure is carried out for measurement at each location:

1 Water content is measured first. Insert the water content sensor blades into a flat soil surface until the resin (plastic) top is just in contact with the soil surface.

2 Record the water content using the TDR instrument (see Chapter 70 for details).

3 Insert shear head grousers through the openings in the plastic top of the water content sensor, and into the soil below, until the top of the shear head touches the top of the water content sensor (Figure 60.3). Gently clear the soil around the outside of the water sensor using a penknife or spatula.

4 Initiate data logging from the load cells on the shearlogger.

(a) For the sheargraph, install and set graphing chart and pencil for correct alignment and positioning for ''zero''-load condition.

5 Choose three to five levels of normal stress to be applied to the soil, achieved by applying a vertical downward load (pushing) on the handle of the sheargraph/logger. Ayers (1987) used four levels of normal stress: 0, 20, 35, and 70 kPa on repacked soils in the laboratory. The authors used five levels of normal stress on field soils: 60, 100, 150, 200, and 250 kPa (exemplary data for the lower four levels are shown in Figure 60.5).

6 The procedure for applying normal stress and shearing force follows the sequence indicated by numbered arrows in Figure 60.5. The normal stress is increased from zero to one of the preselected values in step 5 above, while the shear stress is zero (following path I in Figure 60.5). This amounts to pressing the handle downward without rotation.

7 The normal stress is maintained constant, while the shear stress is slowly increased by rotating the handle as indicated by the shear head tending to rotate (going along path II in Figure 60.5) until the soil fails. At failure, the point of

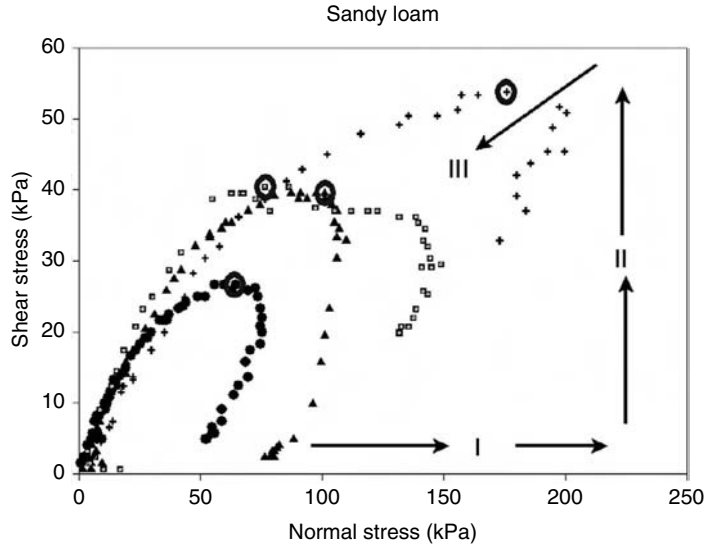

FIGURE 60.5. Normal–shear stress paths recorded during four measurements in a sandy loam soil. The numbered arrows show the sequence along which the normal and shear stresses are applied during each measurement.

maximum shear stress for the soil is reached beyond which shear stress reduces. This step will generally require considerable practice as most operators cannot maintain constant normal stress during rotation of the handle, and the data will show a ''wobbly'' path to maximum shear stress.

8 After failure, normal and shear stresses are decreased together until the normal stress is returned to zero following path III in Figure 60.5. The handle is raised decreasing the normal stress, and the shear head will tend to rotate to decrease the shear stress, which should be allowed by slight rotation of the handle in the direction indicated by rotational tendency of the spring. This completes the shear and normal stress data collection for this step, indicating data logging should stop. Generally three or more replicate measurements should be made at each selected stress level.

(a) During decreasing normal stress level on the sheargraph, the shear head will generally rotate back decreasing the shear stress simultaneously. The graph traced out on the recording drum will consist of the data set for one shear measurement. The data set will depict a closed loop of increasing and decreasing stresses indicating three stages of stress application as shown in Figure 60.5.

9 When using the sheargraph, the water content is determined after shear measurement by collecting soil samples from the shear head and acquired by gravimetric determination.

10 For both shearlogger and sheargraph, it is advisable to collect soil cores adjacent to the measurement site to determine *in situ* bulk density.

11 Download data from the datalogger and apply force sensor calibrations if this was not incorporated in the data logging procedure.

(a) Graph from sheargraph in steps 6, 7, 8(a) is digitized using a method of choice. Generally, this would involve optical scanning to digitize the image and the values converted to stress values based on the calibration information of the coil spring.

12 Plot normal and shear stress patterns as shown in Figure 60.5 and proceed to Section 60.3.4 for calculations.

60.3.4 Calculations and Data Handling

The calculation and data handling are the same for both the Cohron sheargraph and shearlogger as both produce similar data. With data from both devices, it is possible to derive more information than only the maximum shear stress at soil failure. The intent of the procedure in this section is to acquire two further parameters, cohesion and angle of friction, from the series of normal and shear stress data for a soil. As water content affects shear strength, it is important that similar soils at similar water contents are considered together. Thus water content measurement is one basis for grouping data for initial analysis.

1 Plot the normal stress vs. shear stress data to produce curves similar to those in Figure 60.5.

2 From each curve (similar to Figure 60.5), obtain the point of maximum shear stress and the normal stress at which the maximum shear occurred. The circled data points in Figure 60.5 indicate the authors' choice for the data plotted in the figure.

3 Data set of maximum shear stress (τ) vs. normal stress (σ_n), obtained from Figure 60.5, are fitted with a linear regression that satisfies Equation (60.5) from which cohesion (c) and coefficient of friction (tan φ) or friction angle (φ) are obtained from the intercept and slope, respectively.

4 Table 60.1 presents regression results for soils with two different textures. The clay loam data were taken before and after a small rain shower and hence are shown at two water contents.

5 Clay loam soil showed brittle failure in some tests, for example, the solid line data in Figure 60.6. Data such as the solid line in Figure 60.6 may be interpreted for two types of shear strength, referred to as peak, and ultimate strengths (Kirby and Ayers 1993). The peak shear strength is given from the maximum shear stress before the large decrease to a region of lower slope shear stress decline, from which ultimate shear strength is obtained. Although regression parameters are presented in Table 60.1 for peak and ultimate shear strengths (Kirby and Ayers 1993), the detailed procedures are not included here.

6 Water content as measured by the shearlogger is useful for estimating the dependence of shear strength on water content, much as shown by Ayers (1987).

60.3.5 Comments

The data presented above have not been compared or validated against other methods of measurements. The normal and shear stress curves follow similar paths to those shown by Kirby and Ayers (1993) in their laboratory studies. In Figure 60.5, for the sandy loam, maximum shear stress occurs over a range of normal stress (i.e., the curves flatten at the maximum shear stress). Although a range of nearly equal normal stresses were recorded at the maximum shear stress, the authors have used the maximum normal stress for the regression results in Table 60.1. For the clay loam (Figure 60.6), there is a better definition of maximum shear stress, thus the choice for peak stress and corresponding normal stress is more straightforward. The clay loam graphs represent three replicates at the same water content (0.14 $m^3\ m^{-3}$), and some

TABLE 60.1 The Regression Parameters: Cohesion, Angle of Friction, and Water Content (WC) with Standard Deviation (St. Dev.) of Soils from Field Shearlogger Tests

	Cohesion (kPa)		Friction angle (°)		R^2		WC	Standard
Soil	Peak	Ultimate	Peak	Ultimate	Peak	Ultimate	($m^3\ m^{-3}$)	deviation
Sandy loam	9.7	—	12.8	—	0.612	—	0.216	0.027
Clay loam	24.5	7.3	6.7	10.4	0.496	0.824	0.140	0.017
Clay loam	16.3	5.9	18.4	14.4	0.846	0.679	0.207	0.018

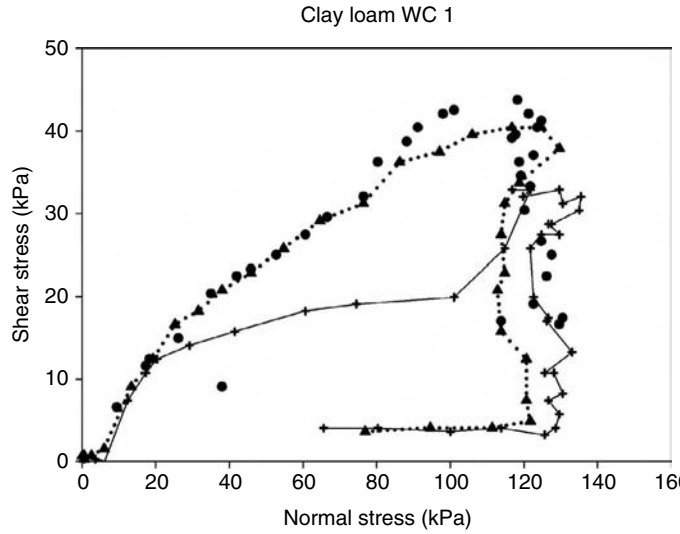

FIGURE 60.6. Normal–shear stress paths recorded during shear measurement in a clay loam soil at low water content. The three measurements are replicates with a targeted maximum normal stress of 120 kPa. The solid line data set indicates both peak and ultimate shear processes have occurred. Note the ''wobbly'' path rising from 120 kPa indicating the difficulty of holding a constant normal stress while applying increasing shear stress.

brittle failure can be detected in the replicate indicated by the solid line data in Figure 60.6. This is not seen in the other two replicates where more plastic failure has occurred.

The difficulty of maintaining constant normal stress as shear stress is increased is evident from Figure 60.6 where, although all measurements were intended to be made at a set normal stress of approximately 120 kPa, each data set showed considerable wobble ($\pm$7 kPa), which tended to increase as the shear stress increased and approached the maximum shear stress at which shearing occurred.

Although the Cohron sheargraph provides useful information in measuring soil shear strength (Ayers 1987; Kirby and Ayers 1993), it has had little use in the last 40 years. The technique involved a high level of operator tedium where acquired data had to be manually digitized to obtain graphical outputs, and the need to work with small number of soil samples, often restricted by gravimetric soil water measurement facilities and labor. The modifications to the sheargraph (shearlogger) presented in this chapter have overcome some of the tedious elements by using TDR to measure water content, and by adding load cells to allow logging of data digitally. This represents considerable time saving, in that, with the present shearlogger, and water content sensor, each stress path determination, and corresponding water content measurement took an average of 6 min in the field for a single operator, and the data collection was automatic and in digital format. Without the modification, using the graphical data from the recording drum, and manual gravimetric sampling for water content required almost twice the time in the field, and further laboratory procedures to get data into numeric format. The precision of the data obtained from the sheargraph, and the shearlogger is comparable and a more definitive evaluation of data quality and operational details of the shearlogger is currently underway.

REFERENCES

Adams, B.A., St-Amour, G., and Topp, G.C. 2000. Evaluation of a piezoelectric load cell for use on cone penetrometers. *J. Agr. Eng. Res.* 76: 205–210.

American Society of Agricultural Engineers (ASAE) Standards. 1999. Soil cone penetrometer. In *Agricultural Engineering Yearbook*. ASAE Standard: ASAE 313.3 February 1999. American Society of Agricultural Engineers, St. Joseph, MI, pp. 832–833.

Ayers, P.D. 1987. Utilizing the torsional shear test to determine soil strength–properties relationships. *Soil Till. Res.* 10: 373–380.

Barley, K.P., Farrell, D.A., and Greacen, E.L. 1965. The influence of soil strength on the penetration of a loam by plant roots. *Aust. J. Soil Res.* 3: 69–79.

Bengough, A.G., Campbell, D.J., and O'Sullivan, M.F. 2001. Penetrometer techniques in relation to soil compaction and root growth. In Smith, K.A. and Mullins, C.E., Eds. *Soil and Environmental Analysis: Physical Methods*, 2nd ed., Marcel Dekker, New York, NY, pp. 377–403.

Busscher, W.J., Bauer, P.J., Camp, C.R., and Sojka, R.E. 1997. Correction of cone index for soil water content differences in a coastal plain soil. *Soil Till. Res.* 43: 205–217.

Cockcroft, B., Barley, K.P., and Greacen, E.L. 1969. The penetration of clays by fine probes and root tips. *Aust. J. Soil Res.* 7: 333–348.

Cohron, G.T. 1963. Soil sheargraph. *Agr. Eng.* 44: 554–556.

Dexter, A.R. and Watts, C.W. 2001. Tensile strength and friability. In Smith, K.A. and Mullins, C.E., Eds. *Soil and Environmental Analysis: Physical Methods*, 2nd ed., Marcel Dekker, New York, NY, pp. 405–433.

Farrell, D.A. and Greacen, E.L. 1966. Resistance to penetration of fine probes in compressible soil. *Aust. J. Soil Res.* 4: 1–17.

Fredlund, D.G. and Vanapalli, S.K. 2002. 2.7 Shear strength of unsaturated soils. In Dane, J.H. and Topp, G.C., Eds. *Methods of Soil Analysis, Part 4—Physical Methods*, Soil Science Society of America, Madison, WI, pp. 329–361.

Freitag, D.R. 1968. Penetration tests for soil measurements. *Trans. Am. Soc. Agr. Eng.* 11: 750–753.

Grant, C.D., Kay, B.D., Groenevelt, P.H., Kidd, G.E., and Thurtell, G.W. 1985. Spectral analysis of micropenetrometer data to characterize soil structure. *Can. J. Soil Sci.* 65: 789–804.

Hummel, J.W., Ahmad, I.S., Newman, S.C., Sudduth, K.A., and Drummond, S.T. 2004. Simultaneous soil moisture and cone index measurement. *Trans. ASAE* 47: 607–618.

Jamieson, J.R., Morris, R.J., and Mullins, C.E. 1988. Effect of subsoiling on physical properties and crop growth on a sandy soil with a naturally compact subsoil. In *Proceedings 11th Int. Conf. Int. Soil Till. Res. Org.*, Vol. 2, ISTRO, Edinburgh, Scotland, UK, pp. 499–503.

Kirby, J.M. and Ayers, P.D. 1993. Cohron sheargraph data: interpretation using critical state soil mechanics. *Soil Till. Res.* 26: 211–225.

Lapen, D.R., Topp, G.C., Gregorich, E.G., and Curnoe, W.E. 2004. Combination cone penetrometer–water content instrumentation to evaluate cone penetration–water content relationships in tillage research. *Soil Till. Res.* 79: 51–62.

Lapen, D.R., Topp, G.C., Hayhoe, H.N., Gregorich, E.G., and Curnoe, W.E. 2001. Stochastic simulation of soil strength/compaction and assessment of corn yield risk using threshold probability patterns. *Geoderma* 104: 325–343.

Lloyd, J.E. and Collis-George, N. 1982. A torsional shear box for determining the shear strength of agricultural soils. *Aust. J. Soil Res.* 20: 203–211.

Lowery, B. and Morrison, J.E., Jr. 2002. Soil penetrometers and penetrability. In Dane, J.H. and Topp, G.C., Eds. *Method of Soil Analysis, Part 4—Physical Methods*, Soil Science Society of America, Madison, WI, pp. 363–388.

Morrison, J.E., Jr., Lowery, B., and Hart, G.L. 2000. Soil penetrometer for sensing soil water

content as in soil characterization for site-specific farming. In *Proc. Agrophysical and Ecological Problems of Agriculture in the 21st Century*. Vol. 2, 2000. International Soil and Till. Research Organization, St. Petersburg, Russia, pp. 121–129.

Motavelli, P.P., Anderson, S.H., Pengthamkeerati, P., and Gantzer, C.J. 2003. Use of soil cone penetrometers to detect the effects of compaction and organic amendments in claypan soils. *Soil Till. Res.* 74: 103–114.

New Zealand Geotechnical Society, Inc. 2001. Test method for determining the vane shear strength of a cohesive soil using a hand held shear vane, 5 pp. www.nzgeotechsoc.org.nz/Shear%20Vane%20Test%20Method%20_Final_.pdf. (verified April 2006).

O'Sullivan, M.F., Dickson, J.W., and Campbell, D.J. 1987. Interpretation and presentation of cone resistance data in tillage and traffic studies. *J. Soil Sci.* 38: 137–148.

Perfect, E., Groenevelt, P.H., Kay, B.D., and Grant, C.D. 1990. Spatial variability of soil penetrometer measurement at the mesoscopic scale. *Soil Till. Res.* 16: 267–271.

Starr, G.C., Lowery, B., and Cooley, E.T. 2000. Soil water content determination using a network analyzer and coaxial probe. *Soil Sci. Soc. Am. J.* 64: 867–872.

Sun, Y., Lammers, P.S., and Ma, D. 2004. Evaluation of a combined penetrometer for simultaneous measurement of penetration resistance and soil water content. *J. Plant Nutr. Soil Sci.* 167: 745–751.

Topp, G.C., Lapen, D.R., Edwards, M.J., and Young, G.D. 2003. Laboratory calibration, in-field validation and use of a soil penetrometer measuring cone resistance and water content. *Vadose Zone J.* 2: 633–641.

Vesic, A.S. 1972. Expansion of cavities in infinite soil mass. *J. Soil Mech. Found. Div., ASCE* 98: 265–290.

Waldron, L.J. and Constantin, G.K. 1970. Soil resistance to a slowly moving penetrometer. *Soil Sci.* 109: 221–226.

Young, G.D., Adams, B.A., and Topp, G.C. 2000. A portable data collection system for simultaneous cone penetrometer force and volumetric soil water content measurements. *Can. J. Soil Sci.* 80: 23–31.

Chapter 61
Air Permeability

C.D. Grant
University of Adelaide
Glen Osmond, South Australia, Australia

P.H. Groenevelt
University of Guelph
Guelph, Ontario, Canada

61.1 INTRODUCTION

Air permeability of soil (and other porous materials) is the coefficient, k_a, governing convective transmission of air through soil under an applied total pressure gradient. The theory for the flow of air through soil is based on Darcy's law, which states that the velocity of a fluid flowing through a porous column is directly proportional to the pressure difference and inversely proportional to the length of the column. This has been investigated thoroughly for both isotropic and anisotropic media (e.g., Maasland and Kirkham 1955; Corey 1986). Importantly, large pores and wide cracks contribute most to air permeability because the volumetric flow of air through a single pore varies as the fourth power of the pore radius. The air permeability coefficient, k_a, has units of m^2 and is also known as the intrinsic permeability to air (Reeve 1953). It can be derived from Darcy's law (for laminar flow of liquids) using simple assumptions about isothermal, nonturbulent flow of a viscous gas (Kirkham 1946).

It has been used since the early part of the twentieth century for describing, defining, and characterizing the structural arrangement and continuity of the pore space in soils (e.g., Green and Ampt 1911; Buehrer 1932; Moldrup et al. 2001). Air permeability is very sensitive to differences in soil structure (Corey 1986; Moldrup et al. 2003) and has been widely used to characterize the changes in structure that result from different soil management practices (e.g., Ball 1981; Groenevelt et al. 1984; Ball et al. 1988; Fish and Koppi 1994; Poulsen et al. 2001). It has even been used to predict other important soil physical properties such as the saturated hydraulic conductivity (e.g., Loll and Moldrup 1999; Iversen et al. 2004).

Measurement of air permeability in the field (as opposed to in the laboratory) is a desirable technical feature (Van Groenewoud 1968; Green and Fordham 1975) but the surface layers of the soil are often structurally anisotropic, so variability is large (and anormally distributed;

McIntyre and Tanner 1959) and the interpretation of field data can be difficult (Janse and Bolt 1960). Considerable work has recently gone into solving the problems associated with field measurements, however, which makes them increasingly useful (e.g., Davis et al. 1994; Fish and Koppi 1994; Iversen et al. 2001, 2003; Jalbert and Dane 2003). Nevertheless, many scientists conduct air permeability measurements in the laboratory because dimensions and geometrical variables are more easily defined (e.g., Iversen et al. 2000; Tartakovsky et al. 2000). Furthermore, a more detailed picture of the pore network can be obtained in the laboratory by taking measurements across a wide range of soil water matric heads (e.g., Buehrer 1932; Moldrup et al. 2003).

Air permeability of soils can be measured in the laboratory in a number of ways (Corey 1986; Ball and Schjønning 2002), but two principal methods will be discussed here, namely the constant pressure gradient method (with a measured flux of air) and the constant flux method (with a measured pressure). The choice of method is usually a matter of convenience, but each method has its own advantages. We will deal here solely with measurement of air permeability under steady-state conditions. For highly impermeable samples where transient-flow conditions may occur, the calculation of air permeability is more complex, and the interested reader is referred to the solution provided by Groenevelt and Lemoine (1987) for guidance.

61.2 CONSTANT PRESSURE GRADIENT METHOD

Numerous variations of the constant pressure gradient method have been used for measuring air permeability (e.g., Grover 1955; Ball et al. 1981; Groenevelt et al. 1984). The method consists of exposing a soil sample in a defined volume (e.g., cylindrical ring) to a large volume of air having constant pressure (above atmospheric), and measuring the volume of air that passes through the soil core with time. The intrinsic permeability to air, k_a (m^2), is calculated for small air pressures (i.e., <0.2 m H_2O):

$$\frac{Q}{A} = k_a \frac{\rho_w g}{\eta} \frac{\Delta h}{L} \tag{61.1}$$

where Q is the volume of air measured at the high-pressure side of the soil core (inlet) passing into the soil core per unit time ($m^3\ s^{-1}$), A the cross-sectional area of the soil core (m^2) orthogonal to direction of airflow, L the length of the soil core (m), $\Delta h = h_i - h_a$ the difference in air pressure expressed (m) across the length of the soil sample between the air-inlet side, i, and the air-outlet side, a, at atmospheric pressure, $h_i = P_i/\rho_w g$ the inlet pressure head (m), $h_a = P_a/\rho_w g$ the outlet pressure head (m), ρ_w the density of water ($kg\ m^{-3}$), g the gravitational acceleration constant (ms^{-2}), and η the viscosity of air ($kg\ m^{-1}\ s^{-1}$).

61.2.1 Materials

Schematic specifications for this apparatus can be found in Tanner and Wengel (1957), but many variations are possible. Only the basics are given here, illustrated in Figure 61.1.

1 Air tank of large volume (i.e., at least 20 L or 200 times larger than the sample volume), made from either stainless steel or nalgene, so long as it is rigid; the tank is partially filled with water to trap air under the float-can.

2 Float-can, which is made of either stainless steel or nalgene.

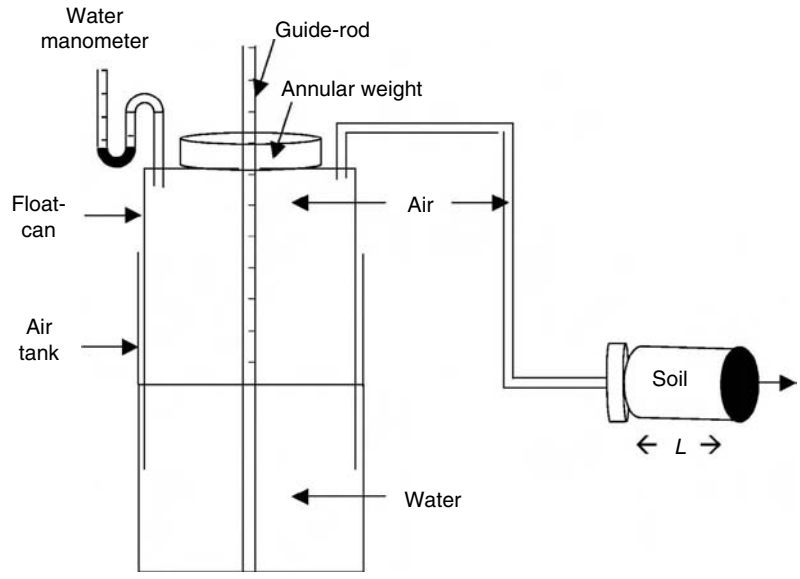

FIGURE 61.1. Constant pressure gradient apparatus to measure air permeability.

3 Guide-rod (calibrated in advance using water to produce a measure of m^3 air mm^{-1} on the guide-rod); this ensures the float-can sinks evenly into the water reservoir in the air tank and also serves as a convenient measuring stick to determine the volume of air flowing out of the air tank into the soil core.

4 Annular dead-weights: These may be required to increase the pressure in the air tank; these are fitted over the guide-rod and placed on the float-can.

5 Pressure gauge: A simple water manometer will suffice.

6 Soil sample: A soil core (at a specified soil water matric head) collected in a rigid cylindrical sample-holder is required.

7 Sample-holder: Depending upon resources, this can be either an elaborate device or a simple one. The simplest construction consists of a short, empty ring of the same (outside) diameter as the ring containing the soil core. A rubber bung and air-supply-tube are fitted to one end of the empty ring and the other end is joined to the soil core using a strip of Parafilm. (More elaborate designs can be conceived, of course, and we generally use a specially constructed brass ring, the diameter of which is just large enough to contain a rubber O-ring fitted snugly around the ring containing the soil core. This avoids the tedium of cutting and stretching multiple strips of Parafilm.)

61.2.2 Procedures

1 Cylinder containing the soil core is connected to the sample-holder using either precut strips of Parafilm or by fitting it directly into a specially constructed brass ring with rubber O-ring to ensure a good seal. The sample-holder is connected to a laboratory retort stand and placed into a shallow bucket of

water such that the connection between the cylinder and its sample-holder is immersed (to check for leaks), while the outflow side of the soil core is left open to the atmosphere.

2 Float-can is allowed to fall freely under its own weight, or with the addition of annular weights to generate higher air pressures maintained throughout the experiment.

3 Guide-rod is monitored with time and when the rate at which the float-can falls becomes constant (steady-state), two readings are selected to calculate the flux of air across the sample under the measured constant pressure difference.

4 Intrinsic permeability is calculated using Equation 61.1.

61.2.3 Comments

This method is ideal for highly permeable samples for which a constant flux is too difficult to maintain, or where you do not wish to allow high pressures to build up (e.g., in wet, highly permeable soils). With this method, the air pressure gradient across the sample can be kept small (e.g., <3 m air m^{-1} soil) to avoid turbulent airflow and so the liquid phase is not altered. In our work, we generally use a difference in pressure head of 0.14 m across a sample length of 0.05 m—this provides a gradient in pressure head of 2.8 m m^{-1}.

Air leaks should be checked for by allowing the float-can to fall and then sealing off the air outlet. The float-can should stop sinking if the system is not leaking. An alternative to the float-can method, which avoids the necessity for calibration, is to measure the flux directly using a flow meter (Green and Fordham 1975).

61.3 CONSTANT FLUX METHOD

With the constant flux method, a constant flux of air is imposed across the soil sample and the resulting air pressure difference is measured. Methods to impose air fluxes are easily constructed and depend only on the resources at hand in the laboratory. A small cylinder and flow meter supplying compressed air, for example, would suffice. Alternatively, Figure 61.2 shows the use of a syringe whose air volume, V, is delivered by a slowly advancing, motor-driven piston. Any other apparatus that can supply a nonvariable and easily measured air flux is adequate.

Steady-state flow of air may or may not occur, and when it does, the pressure difference can become quite large ($\Delta h > 0.2$ m H_2O). For large values of Δh, the intrinsic air permeability, k_a, should be calculated in accordance with the ideal gas law, as follows:

$$\frac{Q}{A} = k_a \frac{\rho_w g}{\eta} \frac{\Delta h}{L} \left[1 - \frac{\Delta h}{2h_i}\right] \tag{61.2}$$

where h_i and the constants ρ_w, g, and η are defined above. If Δh does not exceed 0.2 m H_2O, the second term in parentheses approaches zero, so both terms in parentheses approach unity and may be ignored. In that case Equation 61.2 reduces to Equation 61.1.

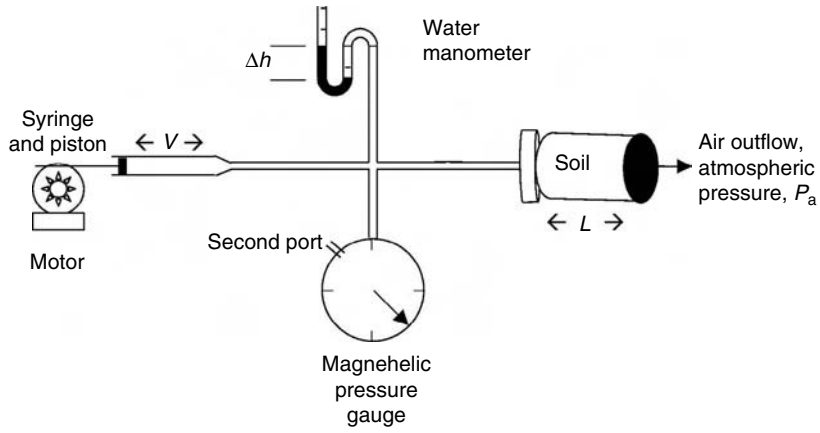

FIGURE 61.2. Constant flux apparatus to measure air permeability.

61.3.1 Materials

The apparatus is shown in Figure 61.2.

1 Syringe: This can be relatively large, having volume, V, anywhere from 35 to 140 cm^3; the inner walls of the syringe can be greased with Vaseline to prevent air leakage. It is convenient to have a range of different sizes of syringes on hand so that the flux of air can be varied easily.

2 Motor-driven piston: The ''piston'' is simply the plunger for the syringe, which is placed on a motor-driven carriage and calibrated for each syringe and motor speed by recording the mass of water delivered per unit marked on the syringe, which delivers air at fluxes set according to the speed of the motor. Groenevelt and Lemoine (1987) and Groenevelt et al. (1984) used a Saga Instruments Model 355 Pump, but any such motorized carriage will do.

3 Pressure gauge: Either a simple water manometer or a Magnehelic pressure gauge (Dwyer Instruments Inc.) is suitable. Conditions for use of each are outlined below.

4 Soil sample: Same as for the constant pressure gradient method discussed in Section 61.2.1.

5 Stiff connection tubing of small inside diameter to minimize the ''dead air'' volume.

61.3.2 Procedures

1 As for the constant pressure gradient method, the soil sample is connected to a rigid holder fitted with a rubber O-ring to ensure a complete seal. The sample-holder is connected to a laboratory retort stand and placed into a shallow bucket of water such that the connection between the cylinder and its sample-holder is immersed (to check for leaks), while the outflow side of the soil core is left open to the atmosphere.

2 Syringe is connected to the soil sample and the motor-driven ''pump'' is set to move at a constant velocity. As it advances, it builds up an air pressure difference across the soil core. This pressure difference is monitored using the Magnahelic pressure gauge shown in Figure 61.2. The actual settings that you choose will depend upon how permeable the soil sample is. Some initial adjustments of the flux with different-sized syringes and pump-settings are often needed prior to data collection. When the pressure difference becomes constant, the mass-flux of air through the soil core also becomes constant.

3 When steady-state flow is established and both the flux and the pressure difference across the soil core are constant, the intrinsic permeability to air can be calculated using Equation 61.2.

4 If steady-state airflow conditions are not reached, the intrinsic permeability to air must be calculated from observations taken during the transient state. In this instance, a water manometer needs to be used rather than the Magnehelic pressure gauge because the Magnahelic pressure gauge ''bleeds'' air until steady-state conditions are reached. The procedures and mathematical tools for calculating the permeability in this case are outlined in detail along with examples in Groenevelt and Lemoine (1987), so it will not be covered in this section.

61.3.3 Comments

The principle advantages of the constant flux method are that the apparatus can be quite simple, and measurements can be made on samples of very low permeability using either steady-state- or transient-state-flow conditions. As indicated above, the analysis of k_a for transient-state airflow is more complicated and is not dealt with here—interested readers should consult Groenevelt and Lemoine (1987). Regardless, the apparatus must be checked carefully for leaks to avoid equipment errors. This can be done by sealing off the air-outlet end of the apparatus and allowing the pressure to build up; shut off the pump, and monitor the pressure, which should stay constant.

REFERENCES

Ball, B.C. 1981. Pore characteristics of soils from two cultivation experiments as shown by gas diffusivities and permeabilities and air-filled porosities. *J. Soil Sci.* 32: 483–498.

Ball, B.C., Harris, W., and Burford, J.R. 1981. A laboratory method to measure gas diffusion and flow in soil and other porous materials. *J. Soil Sci.* 32: 323–333.

Ball, B.C., O'Sullivan, M.F., and Hunter, R. 1988. Gas diffusion, fluid flow and derived pore continuity indices in relation to vehicle traffic and tillage. *J. Soil Sci.* 39: 327–339.

Ball, B.C. and Schjønning, P. 2002. Air permeability. In J.H. Dane and G.C. Topp, Eds. *Methods of Soil Analysis, Part 4*. Soil Science Society of America, Series 5. Madison WI, pp. 1141–1158.

Buehrer, T.F. 1932. The movement of gases through the soil as a criterion of soil structure. *Ariz. Agric. Exp. Sta. Tech. Bull.* 39: 57 pp.

Corey, A.T. 1986. Air permeability. In A. Klute, Ed. *Methods of Soil Analysis, Part 1—Physical and Mineralogical Methods*, 2nd ed. Monograph No. 9. American Society of Agronomy, Madison, WI, pp. 1121–1136.

Davis, J.M., Wilson, J.L., and Phillips, F.M. 1994. A portable air-minipermeameter for rapid *in situ* field measurements. *Ground Water* 32: 258–266.

Fish, A.N. and Koppi, A.J. 1994. The use of a simple field air permeameter as a rapid indicator of functional soil pore space. *Geoderma* 63: 255–264.

Green, R.D. and Fordham, S.J. 1975. A field method for determining air permeability in soil. In *Soil Physical Conditions and Crop Production. Tech. Bull.* 29. HMSO, London, pp. 273–288.

Green, W.H. and Ampt, G.A. 1911. Studies on soil physics. Part 1. The flow of air and water through soils. *J. Agric. Sci.* 4: 1–24.

Groenevelt, P.H., Kay, B.D., and Grant, C.D. 1984. Physical assessment of a soil with respect to rooting potential. *Geoderma* 34: 101–114.

Groenevelt, P.H. and Lemoine, G.G. 1987. On the measurement of air permeability. *Neth. J. Agric. Sci.* 35: 385–394.

Grover, B.L. 1955. Simplified air permeameters for soil in place. *Soil Sci. Soc. Am. Proc.* 19: 414–418.

Iversen, B.V., Moldrup, P., and Loll, P. 2004. Runoff modelling at two field slopes: use of *in situ* measurements of air permeability to characterize spatial variability of saturated hydraulic conductivity. *Hydrol. Process.* 18: 1009–1026.

Iversen, B.V., Moldrup, P., Schjønning, P., and Jacobsen, O.H. 2003. Field application of a portable air permeameter to characterize spatial variability in air and water permeability. *Vadose Zone J.* 2: 618–626.

Iversen, B.V., Moldrup, P., Schjønning, P., and Loll, P. 2001. Air and water permeability in differently textured soils at two measurement scales. *Soil Sci.* 166: 643–659.

Iversen, B.V., Schjønning, P., Poulsen, T.G., and Moldrup, P. 2000. *In situ*, on-site and laboratory measurements of soil air permeability: boundary conditions and measurement scale. *Soil Sci.* 166: 97–106.

Jalbert, M. and Dane, J.H. 2003. A handheld device for intrusive and nonintrusive field measurements of air permeability. *Vadose Zone J.* 2: 611–617.

Janse, A.R.P. and Bolt, G.H. 1960. The determination of the air-permeability of soils. *Neth. J. Agric. Sci.* 8: 124–131.

Kirkham, D. 1946. Field method for determination of air permeability of soil in its undisturbed state. *Soil Sci. Soc. Am. Proc.* 11: 93–99.

Loll, P. and Moldrup, P. 1999. Predicting saturated hydraulic conductivity from air permeability: application in stochastic water infiltration modelling. *Water Res.* 35: 2387–2400.

Maasland, M. and Kirkham, D. 1955. Theory and measurement of anisotropic air permeability in soil. *Soil Sci. Soc. Am. Proc.* 19: 395–400.

McIntyre, D.S. and Tanner, C.B. 1959. Anormally distributed soil physical measurements and nonparametric statistics. *Soil Sci.* 88: 133–137.

Moldrup, P., Olesen, T., Komatsum, T., Schjønning, P., and Rolston, D.E. 2001. Tortuosity, diffusivity, and permeability in the soil liquid and gaseous phases. *Soil Sci. Soc. Am. J.* 65: 613–623.

Moldrup, P., Yoshikawa, S., Olesen, T., Komatsum, T., and Rolston, D.E. 2003. Air permeability in undisturbed volcanic ash soils: predictive model test and soil structure fingerprint. *Soil Sci. Soc. Am. J.* 67: 32–40.

Poulsen, T.G., Iversen, B.V., Yamaguchi, T., Moldrup, P., and Schjønning, P. 2001. Spatial and temporal dynamics of air permeability in a constructed field. *Soil Sci.* 166: 153–162.

Reeve, R.C. 1953. A method for determining the stability of soil structure based upon air and water permeability measurements. *Soil Sci. Soc. Am. Proc.* 17: 324–329.

Tanner, C.B. and Wengel, R.W. 1957. An air permeameter for field and laboratory use. *Soil Sci. Soc. Am. Proc.* 21: 663–664.

Tartakovsky, D.M., Moulton, J.D., and Zlotnik, V.A. 2000. Kinematic structure of minipermeameter flow. *Water Res.* 36: 2433–2442.

Van Groenewoud, H. 1968. Methods and apparatus for measuring air permeability of the soil. *Soil Sci.* 106: 275–279.

Chapter 62
Aggregate Stability to Water

Denis A. Angers
Agriculture and Agri-Food Canada
Quebec, Quebec, Canada

M.S. Bullock
Holly Hybrids
Sheridan, Wyoming, United States

G.R. Mehuys
McGill University
Sainte Anne de Bellevue, Quebec, Canada

62.1 INTRODUCTION

An aggregate is a group of primary particles that adhere to each other more strongly than to surrounding soil particles (Kemper and Rosenau 1986). Aggregate stability can be defined as the resistance to disruption or breakage of the bonds within the aggregates by external forces of impact, shearing, and abrasion and internal forces arising from the escape of entrapped compressed air (slaking) and differential swelling. Methodologies have been developed so that aggregate stability can serve as an indicator of the resistance of soils to water erosion, surface seal or crust formation, compaction leading to decreased infiltration and subsoil aeration, and as a general soil quality indicator (Doran and Parkin 1994; Le Bissonnais and Arrourays 1996; Larney et al. 1996). The methodologies devised for measuring aggregate stability have been numerous and diverse (e.g., Yoder 1936; Hénin et al. 1958; Kemper and Rosenau 1986; Le Bissonnais 1996; Marquez et al. 2004). Nimmo and Perkins (2002) discuss some of the variations or modifications to widely used standardized methods.

Stability measurements can be made at the scale of the whole soil or macroaggregates (>250 μm) or at the scale of clay and silt-size particles. At the macroscopic scale, aggregates or whole soils are exposed to disruptive forces, usually by wet-sieving. The aggregates remaining on one or several sieves represent the stable aggregates. At the scale of clay or silt-size particles, the methods generally consist of characterizing the suspension created as a result of exposing the aggregates to disruptive forces either by turbidimetry or densitometry (e.g., pipetting).

In this chapter, we describe methods for determining the stability of macroaggregates (wet-aggregate stability) (Section 62.3), the size distribution of water-stable aggregates (Section 62.4), and a combined method for wet-aggregate stability and turbidity (Section 62.5).

62.2 FIELD SAMPLING, STORAGE, AND PREPARATION CONSIDERATIONS

Sampling, storage, and pretreatment of soils are as critical to accurate and precise results as the wet-sieving procedure itself. As soil aggregate stability is affected by seasonal climatic conditions (i.e., wetting/drying, freezing/thawing), tillage, cropping systems, and amendments (e.g., Angers and Mehuys 1988; Caron et al. 1992a; Sun et al. 1995), its dynamic nature must be taken into consideration when sampling. Samples are usually taken from the surface soil horizon, but depth of sampling can vary depending on the objective of the study. Generally a square-end shovel or wide diameter (>5 cm) sleeve core apparatus is used to take samples. Care must be taken not to sample areas that are compacted by wheels, shovel, or core pressure, etc. or soil sheared by sampling tools. Wet soils are more sensitive to disruption by external forces such as sampling and presieving than the air-dried soils (Kemper et al. 1987). The water content of the soil at the time of sampling should be measured. Caron et al. (1992b) suggest a covariance statistical analysis be performed if a large variance in water content (covariate) exists between sampling times. Air-drying of field-moist soil can increase aggregate stability (Kemper et al. 1987; Bullock et al. 1988). Stored air-dried soil samples can increase in stability over time; therefore analysis should be done immediately, if possible and definitely within 2 weeks of sampling (Kemper and Rosenau 1984, 1986). Field-moist aggregates must be gently crumbled by hand to pass an 8 or 6 mm sieve for whole soil multiple-sieve analysis or a given sieve size for a specific size fraction single-sieve analysis (e.g., 1–4 mm). The soil is best kept in a rigid-wall plastic container at 4°C in order to minimize microbial activity and water loss, and to avoid compression of the aggregates during storage. Air-drying of field samples for single-sieve analysis should be done immediately by spreading the soil out gently with good air circulation so that the soil is dried within 24 h. Oven-drying is not generally recommended (Kemper and Rosenau 1986; Kemper et al. 1987).

62.3 WET-AGGREGATE STABILITY

Aggregate stability is determined by measuring the proportion of aggregates of a given size (usually 1–2 mm) that do not break down into units smaller than a preselected size (usually 250 μm) under the influence of disruptive forces. The method of Kemper and Rosenau (1986) is considered a standard method (Nimmo and Perkins 2002). It incorporates common wet-sieving methodology that was successfully tested against the more involved multiple-sieve size distribution methods (Kemper and Koch 1966) and has the advantage of giving quick and consistent results. The following method is a typical version of the Kemper and Rosenau (1986) protocol.

62.3.1 Equipment

1 Wet-sieving apparatus and 250 μm sieves (Kemper and Rosenau 1986; Nimmo and Perkins 2002)

2 Vaporizer (commercially available humidifier) modified for vapor wetting soil in the 250 μm sieves (Kemper and Rosenau 1986)

3 Ultrasonic probe or sodium hexametaphosphate solution (0.5%, w/v)

4 Aluminum moisture cans

62.3.2 Procedure

1 Weigh a subsample of 1–2 mm aggregates and oven-dry at 105°C to obtain a gravimetric water content (g g^{-1}) for reference and to calculate the oven-dry soil weight, if needed.

2 If a specified gravimetric water content (g g^{-1}) for the aggregates is required at wet-sieving, calculate the weight of the wetted aggregates plus the tared sieve.

3 Weigh 4 g of 1–2 mm aggregates into tared and numbered sieves.

4 In order to slowly wet the aggregates with a vapor stream, place the sieves into the slot of the humidifier chamber and check periodically until the calculated weight of wetted aggregates plus the tared sieve is reached. Other wetting procedures can be used (see Section 62.6).

5 Fill tared and numbered aluminum moisture cans with low-electrolyte water (<0.01 dS m^{-1}) and place on sieving apparatus beneath sieves.

6 Lower the sieves into water and begin sieving for a specified period of time (generally 3–5 min). Allow the sieves to raise and lower 3.7 cm, 29 times per min for 10 min. Other specifications can be used.

7 Stop sieving apparatus and raise the sieves out of water.

8 Remove aluminum cans containing unstable soil <250 μm and place in the oven at 105°C.

9 Fill another set of tared and numbered aluminum moisture cans with low-electrolyte water (<0.01 dS m^{-1}).

10 Remove the sieves from the sieving apparatus and place each into aluminum cans.

11 Using an ultrasonic probe, disperse the soil remaining on the sieves into the aluminum cans. Remove the cans containing stable soil >250 μm and place them in the oven to dry at 105°C. Sodium hexametaphosphate can also be used to disperse the aggregates as described in Section 62.4.2.

12 Take the aluminum moisture cans out of the oven and obtain a net weight of stable (w_1) and unstable (w_2) aggregates and calculate percent wet-aggregate stability (%WAS) as

$$\%\text{WAS} = \frac{100\ w_1}{w_1 + w_2} \tag{62.1}$$

62.3.3 Comments

Duplicates can be run at the same time to ascertain the variability in the subsamples.

Some researchers have used the 1–4 mm aggregate-size fraction rather than the 1–2 mm aggregate fraction (Bullock et al. 1988; Lehrsch 1998).

The height of the nest of sieves can be adjusted so that the aggregates can either remain totally immersed in water during sieving on the upstroke of the machine or just be covered with water on the downstroke of the machine. The latter introduces additional disruption to the aggregates, i.e., a lapping motion of the water on the aggregates. We recommend that a consistent approach be used in bringing effectively the aggregates out of the water or keeping them immersed.

62.4 SIZE DISTRIBUTION OF WATER-STABLE AGGREGATES

In this method, the entire soil fraction is considered. The size distribution of the aggregates is measured after sieving in water. A correction for coarse primary particles must be made for most soils.

62.4.1 Materials, Equipment, and Reagents

1 A wet-sieving apparatus similar to that described by Bourget and Kemp (1957) or Kemper and Rosenau (1986) with a nest of sieves with openings of 4.0, 2.0, 1.0, 0.5, and 0.25 mm

2 Erlenmeyer flasks of 250 mL capacity

3 Sodium hexametaphosphate solution (0.5% w/v) or an ultrasonic probe

62.4.2 Procedure

1 Weigh 40 g of soil (w_1) that passes an 8 mm sieve (see Section 62.2). Either an air-dry soil or field-moist soil can be used depending on the objective of the study (see Section 62.6).

2 Spread the soil evenly over the top of a nest of sieves.

3 Place the sieves in the wet-sieving apparatus.

4 Lower the sieves into the water until the top sieve is level with the water surface. Allow the soil to wet by capillarity for 10 min. Other wetting procedures can be used (see Section 62.6).

5 Start the motor and allow the sieves to raise and lower 3.7 cm, 29 times per min for 10 min. Other specifications can be used. As mentioned in Section 62.3.3, the height of the nest of sieves can be adjusted so that the aggregates can either remain totally immersed in water during sieving on the upstroke of the machine or be just covered with water on the downstroke of the machine. We recommend that a consistent approach be used.

6 Raise the sieves and wash the stable aggregates on each sieve into tared Erlenmeyers.

7 Dry each fraction of aggregates at 105°C and weigh (w_{2i}).

8 Add approximately 50 mL of sodium hexametaphosphate solution to each Erlenmeyer and shake it well for 45 min. An ultrasonic probe can also be used to disperse the stable aggregates as described in Section 62.3.2.

9 Wash each fraction of dispersed aggregates onto a sieve with the same aperture size as the lower limit of the aggregate-size fraction. Collect the primary particles remaining on each sieve into the corresponding tared Erlenmeyer. Dry at 105°C and weigh (w_{3i}).

10 Weigh a subsample of soil and determine its gravimetric water content (wc) in g g^{-1}.

62.4.3 Calculations

The proportion of water-stable aggregates (WSA_i) in each of the size fractions can be calculated from

$$WSA_i = \frac{w_{2i} - w_{3i}}{\dfrac{w_1}{1 + wc} - \sum_{i=1}^{n} w_{3i}} \tag{62.2}$$

where $i = 1, 2, 3, \ldots, n$ and corresponds to each size fraction.

Several indices can be calculated if it is desired to express the size distribution by a single parameter. The most widely used is the mean weight diameter (MWD):

$$MWD = \sum_{i=1}^{n} x_i \; WSA_i \tag{62.3}$$

where $i = 1, 2, 3, \ldots, n$ and corresponds to each fraction collected, including the one that passes the finest sieve, x_i is the mean diameter of each size fraction (i.e., mean intersieve size), and WSA_i is as defined in Equation 62.2.

Because the size distribution of soil aggregates is approximately lognormal rather than normal (Gardner 1956), the geometric mean weight diameter (GMWD) (Kemper and Rosenau 1986) is also used. Baldock and Kay (1987) used a power function to describe the size distribution and proposed that the power constant be taken as an index of aggregate-size distribution. Perfect and Kay (1991) have proposed that fractal theory be used to characterize soil aggregate-size distribution. Attempts have been made to measure agriculturally valuable aggregates by assigning a weighting value to each aggregate-size range (Dobrzanski et al. 1975; MacRae and Mehuys 1987). Assuming that aggregates between 1 and 5 mm are desirable, weighting values of 3, 8.5, 9.5, 4, and 0 were assigned to the aggregate-size fractions 8–4, 4–2, 2–1, 1–0.25, and <0.25 mm (MacRae and Mehuys 1987).

62.4.4 Comments

The largest source of error in sieving work is in sample preparation. Samples, whether air-dry or field-moist, should be disturbed as little as possible. A representative subsample must be taken for the analysis to be reproducible. The following procedure can be used. Create a cone with the soil to be analyzed. Divide the cone into quarters using a large spatula. Take two subsamples of 40 g, one from each of two quarters. One subsample is used for aggregate-size distribution, the other to determine the sample's water content.

Aggregates passing an 8 mm sieve are commonly used for aggregate-size analysis, but aggregates passing a 6 mm sieve can also be used. In this latter case, the 4 mm sieve can be omitted from the nest of sieves, thus reducing the number of manipulations slightly.

62.5 A COMBINED METHOD FOR WET-AGGREGATE STABILITY AND TURBIDITY

Pojasok and Kay (1990) proposed a method to characterize two different scales of structural units. The method combines the measurement of the stability of macroaggregates (1–2 mm) and turbidity. It is described briefly in Section 62.5.1. The reader is referred to the original paper for more details. Other methods for measuring turbidity only are described by Williams et al. (1966) and Molope et al. (1985).

62.5.1 Procedure

1 Field-moist aggregates are wet under tension (0.1 kPa) and shaken end-over-end in water for 10 min. Other wetting procedures can be used (see Section 62.6).

2 The material is poured through a 250 μm sieve. The aggregates left on the sieve are water-stable and are analyzed further as in Section 62.3.

3 The percent light transmission of the filtrate is measured at a wavelength of 620 nm at a depth calculated from Stokes' law. If desired, the amount of suspended clay particles can be determined using a calibration curve relating percent suspended clay to percent light transmission.

62.5.2 Comments

This method offers the advantage of stability measurements of structural units of different scales and can be easily adapted for routine analysis of a large number of samples with minimum equipment and space. Measurements on whole soils or aggregates of different sizes can also be made.

62.6 GENERAL COMMENTS

The measurement of the stability to water of aggregates of a given size (e.g., 1–2 mm) usually requires less time than a measurement made on the whole soil using a nest of sieves. More information is obtained, however, when the whole soil is considered. For example, management effects such as tillage, cropping, or organic amendments are often detected only in a specific size fraction. Angers and Mehuys (1988) found that cropping had a large effect on the amount of water-stable aggregates in the 2–6 mm size fraction, whereas no effect was

found in the 1–2 mm fraction. Nevertheless, in other studies both fractions have been found to behave similarly (Kemper and Rosenau 1986). Correlations have also been found between turbidity and the stability of large aggregates even though the scales of the measurement differ considerably (Williams et al. 1966; Molope et al. 1985). Molope et al. (1985) also found turbidity to be sensitive to management effects.

Two major factors control the stability of soil aggregates in water: (a) the initial water content of the aggregates and (b) the wetting procedure. When aggregates approaching air-dryness are immersed directly in water, slaking can occur. In some studies, this may be desirable if slaking is of concern: for example, in irrigation studies or if differences among stable soils are to be determined (Angers et al. 1992), or when studying soil organic matter dynamics (Elliott 1986; Angers and Giroux 1996; Six et al. 2004). If slaking is to be avoided, air-dry aggregates should be wet under vacuum, under tension, or using vapor or a fine spray of water. A complete discussion on this subject can be found in Kemper and Rosenau (1986). Measurements can also be made on field-moist aggregates. Under this condition, wetting by capillarity or even by direct immersion can be used with minimal slaking. Comparisons of aggregate stability of samples at different water contents can be confounding (Alderfer 1946) so it may be desirable to wet the samples to similar water contents prior to wet-sieving. In addition to water content at time of sampling, aggregate stability can also be influenced by the antecedent water content prior to rewetting and by the rate at which rewetting takes place (Caron et al. 1992b).

As mentioned earlier, several other methods have been proposed for the determination of aggregate stability. Most are variations of the methods described in this chapter. Variations include the use of chemical pretreatments prior to wet-sieving to characterize bonding mechanisms. For example, aggregates are treated with sodium periodate or hydrogen peroxide (Kemper et al. 1987) to oxidize carbohydrates and organic matter or with sodium pyrophosphate to break cation bridges (Baldock and Kay 1987). Aggregates can also be pretreated in benzene, which induces the formation of a thin hydrophobic layer (Hénin et al. 1958). Le Bissonnais (1996) proposed a unified method that combines prewetting with ethanol (Hénin et al. 1958) and the use of slow wetting, rapid wetting, and mechanical breakdown to separate the effects of various bonding mechanisms. Other approaches also using different aggregate disruptive levels to assess structural stability have been proposed (Van Steenbergen et al. 1991; Marquez et al. 2004).

Because the many variations in sampling, storage, pretreatment, and wet-sieving procedures affect aggregate-stability results, we recommend that all steps in the aggregate-stability analysis be described in great detail when research results are published.

ACKNOWLEDGMENT

We thank Dr. Gary Lehrsch for his helpful suggestions and advice in the preparation of this chapter.

REFERENCES

Alderfer, R.B. 1946. Seasonal variability in the aggregation of Hagerstown silt loam. *Soil Sci.* 62: 151–169.

Angers, D.A. and Giroux, M. 1996. Recently-deposited organic matter in soil water-stable aggregates. *Soil Sci. Soc. Am. J.* 60: 1547–1551.

Angers, D.A. and Mehuys, G.R. 1988. Effects of cropping on macro-aggregation of a marine clay soil. *Can. J. Soil Sci.* 68: 723–732.

Angers, D.A., Pesant, A., and Vigneux, J. 1992. Early cropping-induced changes in soil aggregation, organic matter, and microbial biomass. *Soil Sci. Soc. Am. J.* 56: 115–119.

Baldock, J.A. and Kay, B.D. 1987. Influence of cropping history and chemical treatments on the water-stable aggregation of a silt loam soil. *Can. J. Soil Sci.* 67: 501–511.

Bourget, S.J. and Kemp, J.G. 1957. Wet sieving apparatus for stability analysis of soil aggregates. *Can. J. Soil Sci.* 37: 60.

Bullock, M.S., Kemper, W.D., and Nelson, S.D. 1988. Soil cohesion as affected by freezing, water content, time and tillage. *Soil Sci. Soc. Am. J.* 52: 770–776.

Caron, J., Kay, B.D., and Perfect, E. 1992a. Short-term decrease in soil structural stability following bromegrass establishment on a clay loam soil. *Plant Soil* 145: 121–130.

Caron, J., Kay, B.D., Stone, J.A., and Kachanoski, R.G. 1992b. Modeling temporal changes in structural stability of a clay loam soil. *Soil Sci. Soc. Am. J.* 56: 1597–1604.

Dobrzanski, B., Witkowska, B., and Walczak, R. 1975. Soil-aggregation and water-stability index. *Polish J. Soil Sci.* 8: 3–8.

Doran, J.W. and Parkin, T.B. 1994. Defining and assessing soil quality. In J.W. Doran, D.C. Coleman, D.F. Bezdicek, and B.A. Stewart, Eds. *Defining Soil Quality for a Sustainable Environment*. SSSA Special Publications No. 35, American Society of Agronomy, Madison, WI, pp. 3–21.

Elliott, E.T. 1986. Aggregate structure and carbon, nitrogen, and phosphorus in native and cultivated soils. *Soil Sci. Soc. Am. J.* 50: 627–633.

Gardner, W.R. 1956. Representation of soil aggregate-size distribution by a logarithmic-normal distribution. *Soil Sci. Soc. Am. Proc.* 20: 151–153.

Hénin, S., Monnier, G., and Combeau, A. 1958. Méthode pour l'étude de la stabilité structurale des sols. *Ann. Agron.* 9: 73–92.

Kemper, W.D. and Koch, E.J. 1966. Aggregate stability of soils from western portions of the United States and Canada. *USDA Tech. Bull.* 1355. U.S. Government Printing Office, Washington, DC.

Kemper, W.D. and Rosenau, R.C. 1984. Soil cohesion as affected by time and water content. *Soil Sci. Soc. Am. J.* 48: 1001–1006.

Kemper, W.D. and Rosenau, R.C. 1986. Aggregate stability and size distribution. In A. Klute, Ed. *Methods of Soil Analysis, Part 1, 2nd ed.* American Society of Agronomy, Madison, WI, pp. 425–442.

Kemper, W.D., Rosenau, R.C., and Dexter, A.R. 1987. Cohesion development in disrupted soils as affected by clay and organic matter content and temperature. *Soil Sci. Soc. Am. J.* 51: 860–867.

Larney, F.J., Janzen, H.H., Olson, B.M., Bullock, M.S., and Selinger, L.J. 1996. Aggregate stability: A soil quality indicator for southern Alberta soils. In *Proc. 33rd Annual Alberta Soil Science Workshop*, February 20–22, 1996, Edmonton, AB, Canada, pp. 262–267.

Le Bissonnais, Y. 1996. Aggregate stability and assessment of soil crustability and erodibility: I. Theory and methodology. *J. Soil Sci.* 47: 425–437.

Le Bissonnais, Y. and Arrourays, D. 1996. Aggregate stability and assessment of soil crustability and erodibility: II. Application to humic loamy soils with various organic carbon contents. *J. Soil Sci.* 48: 39–48.

Lehrsch, G.A. 1998. Freeze–thaw cycles increase near-surface aggregate stability. *Soil Sci.* 163: 63–70.

MacRae, R.J. and Mehuys, G.R. 1987. Effects of green manuring in rotation with corn on physical properties of two Québec soils. *Biol. Agric. Hortic.* 4: 257–270.

Marquez, C.O., Garcia, V.P., Cambardella, C.A., Schultz, R.C., and Isenhart, T.M. 2004. Aggregate-size stability distribution and soil stability. *Soil Sci. Soc. Am. J.* 68: 725–735.

Molope, M.B., Page, E.R., and Grieve, I.C. 1985. A comparison of soil aggregate stability tests using soils with contrasting cultivation histories. *Commun. Soil Sci. Plant Anal.* 16: 315–322.

Nimmo, J.R. and Perkins, K.S. 2002. Aggregate stability and size distribution. In J.H. Dane and G.C. Topp, Eds. *Methods of Soil Analysis, Part 4—Physical Methods*. Soil Science Society of America, Madison, WI, pp. 317–328.

Perfect, E. and Kay, B.D. 1991. Fractal theory applied to soil aggregation. *Soil Sci. Soc. Am. J.* 55: 1552–1558.

Pojasok, T. and Kay, B.D. 1990. Assessment of a combination of wet sieving and turbidimetry to characterize the structural stability of moist aggregates. *Can. J. Soil Sci.* 70: 33–42.

Six, J., Bossuyt, H., Degryze, S., and Denef, K. 2004. A history of research on the link between (micro)aggregates, soil biota, and soil organic matter dynamics. *Soil Till. Res.* 79: 7–31.

Sun, H., Larney, F.J., and Bullock, M.S. 1995. Soil amendments and water-stable aggregation of a desurfaced Dark Brown Chernozem. *Can. J. Soil Sci.* 75: 319–325.

Van Steenbergen, M., Cambardella, C.A., Elliott, E.T., and Merckx, R. 1991. Two simple indexes for distributions of soil components among size classes. *Agric. Ecosyst. Environ.* 34: 335–340.

Williams, B.G., Greenland, D.J., Lindstrom, G.R., and Quirk, J.P. 1966. Techniques for the determination of the stability of soil aggregates. *Soil Sci.* 101: 157–163.

Yoder, R.A. 1936. A direct method of aggregate analysis of soils and a study of the physical nature of erosion losses. *J. Am. Soc. Agron.* 28: 337–351.

Chapter 63
Dry-Aggregate Size Distribution

F.J. Larney
Agriculture and Agri-Food Canada
Lethbridge, Alberta, Canada

63.1 INTRODUCTION

Soils containing >15% clay tend to form structural units known as aggregates by both physical and biological processes (Horn and Baumgartl 2000). Kay and Angers (2000) distinguished between aggregates or peds and clods. Peds are naturally formed. The term aggregate and ped may be used interchangeably, where the type of soil structure is granular. Clods are aggregates >100 mm diameter.

Although soil structural units resulting from fragmentation through the application of mechanical energy are widely referred to as aggregates, Díaz-Zorita et al. (2002) believed that the term aggregate should be confined to units formed by ''building-up'' soil processes such as cohesion, organic bonding, inorganic cementation, and influence of roots and fungal hyphae. They advocated the use of the term fragment to define units formed by ''breaking-down'' processes such as tillage, freezing/thawing, slaking, and dispersion. However, they recognized that while the presence of aggregates and fragments on the soil surface indicated the occurrence of opposing soil processes (building-up versus breaking-down), the terms were generally used synonymously to describe soil structure.

Aggregate size distribution (ASD) on the surface of cultivated soils is influenced by management and climatic factors. Management factors include tillage intensity, timing and implement used for seedbed preparation (Larney et al. 1988; Larney and Bullock 1994), as well as cropping (Broersma et al. 1997; Ball-Coehlo et al. 2000) and organic amendment practices (Whalen and Chang 2002). Climatic factors include precipitation form (rain versus snow) and intensity and number of wet-dry, freeze-thaw (Bullock et al. 2001) or freeze-dry cycles (Bullock et al. 1999). ASD influences seedling emergence (e.g., coarse or cloddy seedbeds may lead to reduced or patchy emergence because of lack of seed–soil contact) as well as fluxes of air, water, and solutes. ASD is also a major controlling factor in soil erodibility by wind (Zobeck 1991; Larney et al. 1994; Merrill et al. 1999). Increasing aggregate size decreases wind erosion risk as large aggregates increase surface roughness and slow wind speeds near the soil surface (Chepil 1941). ASD has also been measured on rangeland soils as an index of wind erosion or as related to hydrologic response to grazing intensity (Warren et al. 1986).

It is important to distinguish dry-aggregate size distribution (DASD), dealt within the present chapter, from wet-aggregate size distribution (WASD) covered in Chapter 62. While both methods rely on sieving techniques, the interpretation and application of the resultant ASD data is different. DASD measurement, commonly referred to as dry-sieving, is conducted on air-dry aggregates, and is generally employed in tillage studies to evaluate seedbed structure or in wind erosion studies to assess erosion risk. On the other hand, WASD, or wet-sieving, measures the disruption and breakdown of aggregates sieved in the presence of water. Therefore it is often used as an index of susceptibility to water erosion, crust formation, hardsetting or compaction (Nimmo and Perkins 2002), or in studies on relationships between aggregation and organic matter dynamics (Plante et al. 2002).

Dry-sieving has also been used to describe the heterogeneity of microbial community profiles (Schutter and Dick 2002), carbon, nitrogen and phosphorus contents (Whalen and Chang 2002) and phosphorus desportion (Wang et al. 2001) among soil aggregate size classes. In a tillage soil quality study, Nissen and Wander (2003) elected to use dry-sieved rather than wet-sieved aggregates because their characteristics have been related to seedbed quality, erodibility, and solute transport in structured soils (Perfect et al. 1997). Additionally, unlike measures of wet-aggregate stability, which are difficult to causally link to functionality in intact soils (Young et al. 2001), dry aggregates provide a useful structural surrogate, providing insight into water storage and transport as well as physical protection of organic matter in intact soil. Sainju et al. (2003) chose dry-sieving of soil to determine ASD and associated C and N pools over wet-sieving due to the following reasons: (a) dry-sieving may reduce the disruption of physical habitat of microbial communities compared with wet-sieving (Schutter and Dick 2002); (b) water soluble C and N concentrations can be determined on aggregates separated by dry-sieving, which may not be possible with wet-sieving (Beauchamp and Seech 1990); and (c) aggregates separated by dry-sieving may represent more closely those in the field during the absence of rain or irrigation.

Díaz-Zorita et al. (2002) provide an excellent review of methods for assessing soil structure including indices to quantify the size distribution of aggregates using dry- and wet-sieving procedures.

63.2 DRY-SIEVING METHOD

The method of choice for DASD determination involves rotary sieving, usually with multiple-sieves (Chepil 1942, 1952, 1962; Chepil and Bisal 1943; Lyles et al. 1970) to obtain data on the percent of total soil sample weight retained on each sieve size. Hand-sieving may also be used but is rather time-consuming and may subject the aggregates to higher abrasion losses if overly vigorous. An alternative system is a Ro-Tap Test Sieve Shaker (W.S. Tyler, Mentor, Ohio) which reproduces the circular and tapping motion of hand-sieving but with a mechanical, uniform action on a nest of six 200 mm diameter flat sieves. Usually six or seven sieves are used for DASD, although Hagen et al. (1987) reported a method using only two sieves.

With dry-sieving, the percent of aggregates retained on each sieve is generally of minimal use as conclusive interpretation is difficult. Of greater interest, for evaluating the effect of tillage treatments or climatic processes on DASD, is a single parameter or index (Kemper and Chepil 1965; Kemper and Rosenau 1986). The simplest index of aggregation is percent weight greater or lesser than some specified but arbitrary size. Erodible fraction (EF) which is the percent of aggregates <0.84 mm is widely used in wind erosion research.

Generally soils which have an EF >60% are considered at relatively high-wind erosion risk (Anderson and Wenhardt 1966). Larney et al. (1988) derived a cloddiness ratio by dividing the percentage of aggregates >9.4 mm diameter by the percentage 9.4 mm. The higher the ratio, the cloddier or coarser is the seedbed.

A disadvantage of simple indices, such as EF or cloddiness ratio, is that they use only a part of the available ASD information. van Bavel (1949) proposed that aggregates be assigned an importance or weighting factor that is proportional to their size and called this parameter mean weight diameter (MWD). Later, Gardner (1956) suggested that geometric mean diameter (GMD) and geometric standard deviation (GSD) uniquely characterized a given distribution of aggregates. Kemper and Rosenau (1986) agreed that the use of GMD is supported by Gardner's (1956) finding that ASD in most soils is approximately lognormal rather than normal. For a lognormal distribution Gardner (1956) defined the GMD as the diameter of aggregates corresponding to a cumulative fraction oversize of 0.5 (50%). GMD is a calculated sieve diameter at which 50% of the sample soil mass is oversize and 50% passes, i.e., the median aggregate size on a mass basis. GSD was defined as the log of the ratio of the diameter at 84.13% oversize to that at 50% oversize. GMD and GSD give all possible information concerning an ASD, have statistical meaning, and may be used quantitatively in statistical analyses. Therefore GMD and GSD are the parameters used in the United States Department of Agriculture's Wind Erosion Prediction System (WEPS) Model to describe ASD (Zobeck 1991; USDA-ARS 1996).

In the past, the main disadvantage of expressing DASD data in terms of GMD and GSD was the extensive work involved in obtaining these parameters (Kemper and Rosenau 1986). In the 1950s, GMD and GSD estimation involved manual graphing on log-probability paper, measurement of distances with a ruler and fitting of a regression line by eye. However, numerical algorithms for lognormal fits are now widely available in statistical software (Nimmo and Perkins 2002). Leys et al. (2005) outlined a PC program that allows statistical curve fitting and quantification of composite populations within multimodal particle-size distributions. This may be applied to DASD if enough size (>5) classes are available.

Larney et al. (1994) updated Gardner's (1956) method and derived GMD and GSD from a regression equation of $\log_{10}$ sieve size (y) versus the cumulative fraction oversize (x) transformed by the probit function (SAS Institute Inc. 2005). The rotary sieve employed by Larney et al. (1994) and Bullock et al. (2001) did not have a 0.84 mm sieve. However, simply substituting 0.84 for y in the regression equations for deriving GMD allowed computation of EF. This procedure was quite accurate as the equations had R^2 values >0.9.

Zobeck and Popham (1990) calculated GMD and GSD based on modification of the Gardner (1956) method. They used cumulative percent passing rather than cumulative percent oversize and log sieve size was regressed on the actual cumulative percent passing rather than a probit transformation (linear rather than probability scale on x-axis).

63.2.1 Equipment

1 A flat square-cornered shovel. One may be custom-made with 2.5 cm high sides to ensure even sampling depth.

2 Open trays or paper bags.

3 Rotary sieve or nest of sieves. The rotary sieve at Agriculture and Agri-Food Canada's Lethbridge Research Centre was built in the 1950s to the general specifications of Chepil (1952) but with six sieves instead of 13. It had an upper section of three concentric cylindrical-sieves with openings of 38, 12.6, and 7.1 mm and a lower section of three sieves with openings of 1.9, 1.2, and 0.47 mm. It was initially assumed that the openings were similar to the upper section of the rotary sieve (38.1, 12.7, 6.4, 2.38, 1.19, 0.84, and 0.42 mm) described by Chepil (1952), but caliper measurements revealed otherwise.

4 A balance capable of measuring to two decimal places.

63.2.2 Procedure

1 Using the sampling shovel, sample to a consistent soil depth (e.g., 2.5 cm) across all experimental treatments. The number of subsamples per plot should be adequate to represent a treatment. As an example, Larney et al. (1994) took five samples from 6 × 40 m tillage plots. Samples of about 5 kg (net wt.) are appropriate for rotary sieves and lesser amounts for a nest of flat sieves.

2 Place samples into labeled open trays or paper bags and carefully transport for air-drying at room temperature.

3 After ~7 days of air-drying, introduce samples to rotary sieve hopper or nest of sieves.

4 Weigh soil aggregates passing through each sieve size into collecting pans (rotary sieve) or retained on each sieve (nest of flat sieves).

63.2.3 Calculations

A typical ASD (Table 63.1) generated by sieving a surface sample of tilled soil (Dark Brown Chernozemic clay loam, Lethbridge series) through a rotary sieve at Agriculture and Agri-Food Canada's Lethbridge Research Centre is used as an example.

TABLE 63.1 Dry-Aggregate Size Distribution of a Rotary-Sieved Lethbridge Clay Loam Soil, Showing Data Transformations Required for GMD and GSD Calculation

Sieve diameter (mm)	Cumulative percent oversize[a]	Log_{10} sieve size (y)	Probit transformed cumulative percent oversize or normal equivalent deviate (NED) values (x)
38	17.2	1.58	−0.95
12.6	38.5	1.1	−0.29
7.1	48.7	0.85	−0.03
1.9	64.9	0.28	0.38
1.2	71	0.08	0.56
0.47	81.8	−0.33	0.91

[a] Expressed as fractions, e.g., 0.172, 0.385 etc. in order to perform probit transformation.

63.2.4 Geometric Mean Diameter and Geometric Standard Deviation

A short SAS program (SAS Institute Inc. 2005) included the following steps to calculate GMD and GSD:

1 Assign $\log_{10}$ values to sieve sizes (Table 63.1).

2 Probit transform cumulative percent oversize values, using the probit function. The probit function treats the cumulative fraction oversize (values between 0 and 1) as numeric probability values and returns their normal equivalent deviate (NED) values from the standard normal distribution (Table 63.1).

3 Perform least squares regression analysis with $\log_{10}$ sieve size (y) and probit transformed cumulative percent oversize (x) data. This relationship (Figure 63.1) is similar to the hand-plotted graphs on log-probability paper (Gardner 1956) with y expressed on a $\log_{10}$ scale and x expressed on a probability scale. As well as the percent oversize, the NED values resulting from probit transformation are also displayed for ease of interpretation. The regression analysis for the sieved sample resulted in the equation:

$$y = 0.695 - 1.056x \tag{63.1}$$

having an R^2 value of 0.983.

4 Substitution of the probit transformation value of 0.5 (50% oversize) for x in the regression equation returns a y-value which is the log diameter at 50% oversize which when expressed as 10^y is the GMD (4.95 mm) (Table 63.2). As in Gardner (1956),

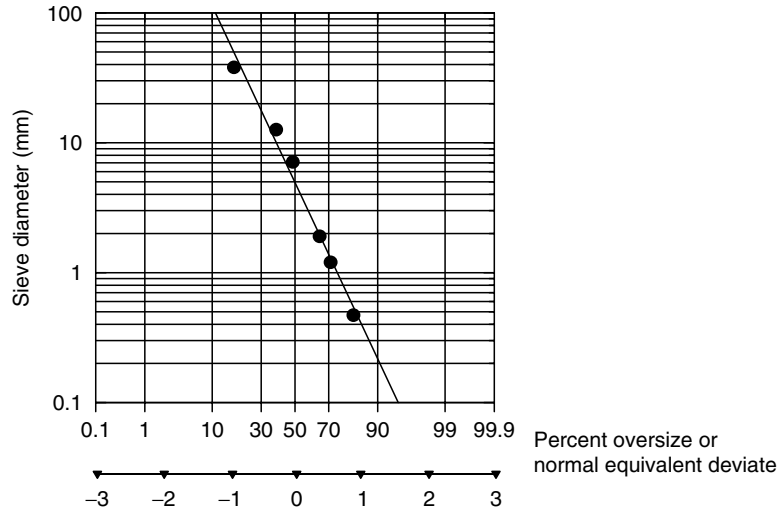

FIGURE 63.1. Regression fit for log of sieve size (y) and probit transformed cumulative percent oversize or normal equivalent deviate (NED) values (x).

TABLE 63.2 Calculations of GMD and GSD from Regression Equation $y = 0.695 - 1.056x$

% Oversize	*x*-value[a]	Solved *y*-value, $\log_{10}$ sieve size	GMD[b] (mm)	GSD[c] log units
50%	0	0.695	4.95	—
84.13%	0.99982	−0.361	—	1.056

[a] Probit transformation of % oversize.
[b] $10^{y\text{-value at 50\% oversize}} = 10^{0.695} = 4.95$.
[c] From Equation 63.3: [log(diam. at 84.13% oversize) – log(diam. at 50% oversize)] $= (-0.361 - 0.695) = -1.056$. Converted to absolute value as logs are positive = 1.056.

GMD may be estimated visually from Figure 63.1 as the *y*-value corresponding to 50% oversize (4.95 mm). Also since the probit transformation of 50% gives an NED value of zero (Table 63.1, Figure 63.1) the GMD is simply 10^y where *y*, having a value of 0.695 is the intercept of the regression equation.

5 Substitution of the probit transformation value of 0.8413 (84.13%) for *x* in the regression equation returns a *y*-value which is the log diameter at 84.13% oversize. GSD is calculated as

$$\log\left[\frac{\text{diam. at 84.13\% oversize}}{\text{diam. at 50\% oversize}}\right] = \tag{63.2}$$

$$[\log(\text{diam. at 84.13\% oversize}) - \log(\text{diam. at 50\% oversize})] \tag{63.3}$$

The absolute value of the difference between the two log values (Equation 63.3) is the GSD of 1.056 (Table 63.2). Gardner (1956) pointed out that GSD, which is a measure of the dispersion of the data, must be kept in log units and that the antilog of GSD has no statistical meaning. Also, the GSD value corresponds to an absolute value (1.056) of the slope of the regression equation. From Figure 63.1 it can be seen that the value of 84.13% oversize corresponds to 1 NED.

The above example updates Gardner's (1956) methodology and as such used cumulative percent oversize. However, identical GMD and GSD values are returned irrespective of whether sieved data are expressed as cumulative percent oversize or cumulative percent passing. An advantage of plotting cumulative percent passing on the *x*-axis is that the slope of the regression equation is positive. For GMD calculations, 50% oversize is the same as 50% passing, so changes are not necessary to the statistical analysis program. However, Equation 63.2 of Gardner (1956) must be adhered to for the correct GSD calculation. Therefore substitution of the probit transformation value of 0.1587 (15.87%) for *x* is required in the regression equation and returns a *y*-value which is the log diameter at 15.87% passing, which is the same as the log diameter at 84.13% oversize.

63.2.5 Mean Weight Diameter

The MWD of an ASD as proposed by van Bavel (1949) assigns weighting factors that are proportional to aggregate size. MWD is equal to the sum of products of (a) the mean diameter of each sieved fraction and (b) the proportion of the total sample weight occurring in the corresponding size fraction. The van Bavel (1949) approach, which involved manual plotting and measurements with a planimeter, was simplified by Youker and McGuinness (1957) who suggested a summation equation:

TABLE 63.3 Calculation of Mean Weight Diameter for Rotary-Sieved Lethbridge Clay Loam Soil

Sieve class diameter (mm)	Midpoint of sieve class, (A) (mm)	% of total weight retained (B)	(A × B)/100
>38	51.5[a]	17.2	8.858
12.6–38	25.3	21.3	5.389
7.1–12.6	9.85	10.2	1.005
1.9–7.1	4.50	16.1	0.725
1.2–1.9	1.55	6.2	0.096
0.47–1.2	0.84	10.7	0.090
<0.47	0.24[b]	18.3	0.044
		$\sum = 100\%$	$\sum = 16.207$ mm

[a] The upper limit of the largest sieve class is determined by measuring the diameter of the largest aggregate prior to sieving. For this soil sample, it was 65 mm, therefore the midpoint was $[(38 + 65)/2] = 51.5$. If the diameter of the largest aggregate is unknown, then the upper limit may be estimated by doubling the size of the largest sieve ($38 \times 2 = 76$) and the midpoint estimated as $[(38 + 76)/2] = 57$.

[b] The lower limit of the smallest sieve class is set at zero. Therefore the midpoint is $[(0 + 0.47)/2] = 0.24$.

$$\sum_{i=1}^{n} \bar{x}_i w_i \tag{63.4}$$

where x_i is the mean diameter of the size fraction and w_i is the proportion of the total sample retained on the sieve. Table 63.3 shows an MWD calculation for the same ASD used in the GMD/GSD example above. The products are summed to a value of 16.207, which is substituted for x in a regression equation

$$y = 0.876x - 0.079 \tag{63.5}$$

to derive y or MWD (Youker and McGuinness 1957). The resulting MWD is 14.12 mm, substantially higher than the GMD (4.95 mm) for the same sample.

63.3 COMMENTS

Dry-field conditions provide better samples of discrete aggregates. If moist samples are taken in the field and then allowed to air-dry too rapidly, aggregates may strengthen beyond their field status. Oven-drying is not recommended for the same reason in that it may cause false strengthening of the aggregates. DASD sampling of a crusted soil may create ''aggregates'' which are really crust fragments. These may be of considerable size and stable enough to resist disintegration during rotary sieving. Bullock et al. (2001) reported increases in GMD as a result of sampling a soil which crusted after snowmelt and evaporative drying in southern Alberta.

The sieving process may cause some aggregate disintegration, but as long as samples are handled gently and sieving is not too prolonged, size distributions should represent field conditions. However, disintegration on sieving can be used to assess resistance to abrasion or dry-aggregate stability. This involves reconstituting the sample after a first sieving and subjecting it to a second sieving (Kemper and Rosenau 1986) or up to a total of four sievings (Chepil 1952). The magnitude of the decrease in GMD between the successive sievings is a

measure of dry-aggregate stability. Eynard et al. (2004) repeatedly sieved the 2–25 mm aggregate size fraction of a soil to measure the rate of disintegration expressed as the slope of the disruption lines.

Díaz-Zorita et al. (2002) discussed the duration of sieving. With rotary sieving, the apparatus is normally operated until separation is complete, which can result in different sieving times, and hence different energy inputs, for different samples. With flat sieves, there is no standard guide as to the duration of the sieving operation with times ranging from 5 s to 100 min. For many soils, sieving for 30 s is often adequate (Braunack and McPhee 1991; Aubertot et al. 1999). Díaz-Zorita et al. (2002) illustrated the change in GMD as a function of sieving duration (15–120 s) for two soils using a nest of flat sieves and vibratory shaking.

It should also be borne in mind that MWD (van Bavel 1949) and GMD/GSD (Gardner 1956) were originally used to characterize ASD from wet-sieving studies where larger aggregates (>8 mm) were removed prior to analysis (van Bavel 1949). As mentioned previously, DASD is carried out on samples with a wider range of aggregate sizes and large aggregates are not removed prior to dry-sieving (unless they are too large to enter the rotary sieve hopper, in which case they are separated and added to the aggregates retained on the largest sieve prior to weighing).

GMD appears to be a more scientifically functional index than MWD for characterizing DASD. MWD is subject to issues of sieve class midpoint or the highly variable determinant of largest aggregate diameter. For example, in Table 63.3 the product of the midpoint of the largest sieve class and the percent of total weight retained on the largest sieve (8.858) represented 55% of the sum of products value (16.207). Therefore any inaccuracy is estimating the largest aggregate diameter has a major influence on the final MWD value.

Although most soil surface samples impacted by tillage result in an ASD that fits a lognormal distribution, some soils may have skewed (e.g., $>50\%$ of cumulative weight is retained on the largest sieve or passes through the smallest sieve) or bimodal (a disproportionate amount of large and small aggregates compared to intermediate ones) distributions. Hagen et al. (1987) pointed out that a deviation from a lognormal distribution would be detected by a low R^2 value for a least squares regression fit to sieved data. In these cases, lognormal fits are less accurate and derived GMD and GSD values may not be very meaningful. Gardner (1956) mentioned that field-sampled ASDs will deviate from a lognormal distribution at the extremes of the diameter range. Wagner and Ding (1994) pointed out that the standard lognormal distribution implies that the smallest aggregate size is zero and the largest aggregate size is infinite. Since agricultural soils exhibit lower and upper aggregate size limits, which account for deviations from lognormality, they suggested use of modified lognormal distributions if the tails of the distributions are important to the application of the ASD data. They presented examples from wind erosion studies where knowledge of the complete DASD is desirable. Small aggregates (<0.84 mm) are considered transportable by wind and emission of even smaller particles (PM_{10}, particulate matter <10 μm diameter) has human health and regulatory implications. At the opposite end of the spectrum, large tillage-induced aggregates (>50 mm diameter) are often brought to the soil surface as an emergency control option when wind erosion is imminent or occurring.

Statistical methods to describe DASD, other than the lognormal distribution, have been outlined by Díaz-Zorita et al. (2002) and Zobeck et al. (2003). These include Gaussian or normal, log hyperbolic, bi- or multimodal, Rosin–Rammler, Weibull and Gaudin–Schuhmann distributions. Additionally, fractal theory has been applied to characterize soil fragment

mass-size distributions (Young and Crawford 1991; Perfect 1997; Perfect et al. 2002). Zobeck et al. (2003) compared lognormal, fractal, and Weibull DASD distributions for over 5,400 soils sampled at 24 locations in six U.S. states. They found the Weibull distribution to be the most precise because the errors were generally smaller than the other distributions over the full range of sieve sizes tested. The fractal distribution had the lowest accuracy.

Methods to characterize DASD, other than by sieving, have been developed. Sandri et al. (1998) compared image analysis, counting of clods >40 mm diameter, and sieving for determining cloddiness in seeded preparation. Aubertot et al. (1999) characterized sugar beet (*Beta vulgaris* L.) seedbeds using soil surface painting, image analysis of soil surface photographs, and stereological analysis of embedded sample sections as well as dry-sieving.

REFERENCES

Anderson, C.H. and Wenhardt, A. 1966. Soil erodibility, fall and spring. *Can. J. Soil Sci.* 46: 255–259.

Aubertot, J.N., Dürr, C., Kiêu, K., and Richard. R. 1999. Characterization of sugar beet seedbed structure. *Soil Sci. Soc. Am. J.* 63: 1377–1384.

Ball-Coehlo, B.R., Roy, R.C., and Swanton, C.J. 2000. Tillage and cover crop impacts on aggregation of a sandy soil. *Can. J. Soil Sci.* 80: 363–366.

Beauchamp, E.G. and Seech, A.G. 1990. Denitrification with different sizes of soil aggregates obtained from dry-sieving and from sieving with water. *Biol. Fert. Soils* 10: 188–193.

Braunack, M.V. and McPhee, J.E. 1991. The effect of initial soil water content and tillage implement on seedbed formation. *Soil Till. Res.* 20: 5–17.

Broersma, K., Robertson, J.A., and Chanasyk, D.S. 1997. The effects of diverse cropping systems on aggregation of a Luvisolic soil in the Peace River region. *Can. J. Soil Sci.* 77: 323–329.

Bullock, M.S., Larney, F.J., Izaurralde, R.C., and Feng, Y. 2001. Overwinter changes in wind erodibility of clay loam soils in southern Alberta. *Soil Sci. Soc. Am. J.* 65: 423–430.

Bullock, M.S., Larney, F.J., McGinn, S.M., and Izaurralde, R.C. 1999. Freeze-drying processes and wind erodibility of a clay loam soil in southern Alberta. *Can. J. Soil Sci.* 79: 127–135.

Chepil, W.S. 1941. Relation of wind erosion to the dry aggregate structure of a soil. *Sci. Agric.* 21: 488–507.

Chepil, W.S. 1942. Measurement of wind erosiveness of soils by dry sieving procedure. *Sci. Agric.* 23: 154–160.

Chepil, W.S. 1952. Improved rotary sieve for measuring state and stability of dry soil structure. *Soil Sci. Soc. Am. Proc.* 16: 113–117.

Chepil, W.S. 1962. A compact rotary sieve and the importance of dry sieving in physical soil analysis. *Soil Sci. Soc. Am. Proc.* 26: 4–6.

Chepil, W.S. and Bisal, F. 1943. A rotary sieve method for determining the size distribution of soil clods. *Soil Sci.* 56: 95–100.

Díaz-Zorita, M., Perfect, E., and Grove, J.H. 2002. Disruptive methods for assessing soil structure. *Soil Till. Res.* 64: 3–22.

Eynard, A., Schumacher, T.E., Lindstrom, M.J., and Malo, D.D. 2004. Aggregate sizes and stability in cultivated South Dakota prairie Ustolls and Usterts. *Soil Sci. Soc. Am. J.* 68: 1360–1365.

Gardner, W.R. 1956. Representation of soil aggregate-size distribution by a logarithmic-normal distribution. *Soil Sci. Soc. Am. Proc.* 20: 151–153.

Hagen, L.J., Skidmore, E.L., and Fryrear, D.W. 1987. Using two sieves to characterize dry soil aggregate size distribution. *Trans. ASAE* 30: 162–165.

Horn, R. and Baumgartl, T. 2000. Dynamic properties of soils. In M.E. Sumner, Ed. *Handbook of Soil Science*. CRC Press, Boca Raton, FL, pp. A19–A51.

Kay, B.D. and Angers, D.A. 2000. Soil structure. In M.E. Sumner, Ed. *Handbook of Soil Science*. CRC Press, Boca Raton, FL, pp. A229–A276.

Kemper, W.D. and Chepil, W.S. 1965. Size distribution of aggregates. In C.A. Black et al., Eds. *Methods of Soil Analysis, Part 1—Physical and Mineralogical Properties Including Statistics of Measurement and Sampling*. Agronomy No. 9, ASA, Madison, WI, pp. 499–510.

Kemper, W.D. and Rosenau, R.C. 1986. Aggregate stability and size distribution. In A. Klute, Ed. *Methods of Soil Analysis, Part 1—Physical and Mineralogical Methods*, 2nd ed., ASA/SSSA, Madison, WI, pp. 425–442.

Larney, F.J. and Bullock, M.S. 1994. Influence of soil wetness at time of tillage and tillage implement on soil properties affecting wind erosion. *Soil Till. Res*. 29: 83–95.

Larney, F.J., Fortune, R.A., and Collins, J.F. 1988. Intrinsic soil physical properties influencing the intensity of cultivation procedures for sugar beet seedbed preparation. *Soil Till. Res*. 12: 253–267.

Larney, F.J., Lindwall, C.W., and Bullock, M.S. 1994. Fallow management and overwinter effects on wind erodibility in southern Alberta. *Soil Sci. Soc. Am. J*. 58: 1788–1794.

Leys, J.F., McTainsh, G.H., Koen, T., Mooney, B., and Strong, C. 2005. Testing a statistical curve-fitting procedure for quantifying sediment populations within multimodal particle-size distributions. *Earth Surf. Proc. Land*. 30: 579–590.

Lyles, L., Dickerson, J.D., and Disrud, L.A. 1970. Modified rotary sieve for improved accuracy. *Soil Sci*. 109: 207–210.

Merrill, S.D., Black, A.L., Fryrear, D.W., Saleh, A., Zobeck, T.M., Halvorson, A.D., and Tanaka, D.L. 1999. Soil wind erosion hazard of spring wheat-fallow as affected by long-term climate and tillage. *Soil Sci. Soc. Am. J*. 63: 1768–1777.

Nimmo, J.R. and Perkins, K.S. 2002. Aggregate stability and size distribution. In J.H. Dane and G.C. Topp, Eds. *Methods of Soil Analysis, Part 4—Physical Methods*. SSSA Book Series No. 5, SSSA, Madison, WI, pp. 317–328.

Nissen, T.M. and Wander, M.M. 2003. Management and soil-quality effects on fertilizer-use efficiency and leaching. *Soil Sci. Soc. Am. J*. 67: 1524–1532.

Perfect, E. 1997. Fractal models for the fragmentation of rocks and soils: a review. *Eng. Geol*. 48: 185–198.

Perfect, E., Díaz-Zorita, M., and Grove, J.H. 2002. A prefractal model for predicting soil fragment mass-size distributions. *Soil Till. Res*. 64: 79–90.

Perfect, E., Zhai, Q., and Blevins, R.L. 1997. Soil and tillage effects on the characteristic size and shape of aggregates. *Soil Sci. Soc. Am. J*. 61: 1459–1465.

Plante, A.F., Feng, Y., and McGill, W.B. 2002. A modeling approach to quantifying soil macroaggregate dynamics. *Can. J. Soil Sci*. 82: 181–190.

Sainju, U.M., Whitehead, W.F., and Singh, B.P. 2003. Cover crops and nitrogen fertilization effects on soil aggregation and carbon and nitrogen pools. *Can. J. Soil Sci*. 83: 155–165.

Sandri, R., Anken, T., Hilfiker, T., Sartori, L., and Bollhalder, H. 1998. Comparison of methods for determining cloddiness in seedbed preparation. *Soil Till. Res*. 45: 75–90.

SAS Institute Inc. 2005. SAS OnlineDoc 9.1.3. SAS Institute Inc., Cary, NC.

Schutter, M.E. and Dick, R.P. 2002. Microbial community profiles and activities among aggregates of winter fallow and cover-cropped soil. *Soil Sci. Soc. Am. J*. 66: 142–153.

USDA-ARS 1996. WEPS Technical Documentation, BETA Release 95-08. USDA-ARS, Wind Erosion Research Unit, Manhattan, KS.

van Bavel, C.H.M. 1949. Mean weight-diameter of soil aggregates as a statistical index of aggregation. *Soil Sci. Soc. Am. Proc*. 14: 20–23.

Wagner, L.E. and Ding, D. 1994. Representing aggregate size distributions as modified lognormal distributions. *Trans. ASAE* 37: 815–821.

Wang, X., Yost, R.S., and Linquist, B.A. 2001. Soil aggregate size affects phosphorus desportion from highly weathered soils and plant growth. *Soil Sci. Soc. Am. J.* 65: 139–149.

Warren, S.D., Thurow, T.L., Blackburn, W.H., and Garza, N.E. 1986. The influence of livestock trampling under intensive rotation grazing on soil hydrologic characteristics. *J. Range Manage.* 36: 491–495.

Whalen, J.K. and Chang, C. 2002. Macroaggregate characteristics in cultivated soils after 25 annual manure applications. *Soil Sci. Soc. Am. J.* 66: 1637–1647.

Youker, R.E. and McGuinness, J.L. 1957. A short method of obtaining mean weight-diameter values of aggregate analyses of soils. *Soil Sci.* 83: 291–294.

Young, I.M. and Crawford, J.W. 1991. The fractal structure of soil aggregates: its measurement and interpretation. *J. Soil Sci.* 42: 187–192.

Young, I.M., Crawford, J.W., and Rappoldt, C. 2001. New methods and models for characterizing structural heterogeneity of soil. *Soil Till. Res.* 61: 33–45.

Zobeck, T.M. 1991. Soil properties affecting wind erosion. *J. Soil Water Conserv.* 46: 112–118.

Zobeck, T.M. and Popham, T.W. 1990. Dry aggregate size distribution of sandy soils as influenced by tillage and precipitation. *Soil Sci. Soc. Am. J.* 54: 198–204.

Zobeck, T.M., Popham. T.W., Skidmore, E.L., Lamb, J.A., Merrill, S.D., Lindstrom, M.J., Mokma, D.L., and Yoder, R.E. 2003. Aggregate-mean diameter and wind-erodible soil predictions using dry aggregate-size distributions. *Soil Sci. Soc. Am. J.* 67: 425–436.

Chapter 64
Soil Air

R.E. Farrell
University of Saskatchewan
Saskatoon, Saskatchewan, Canada

J.A. Elliott
Environment Canada
Saskatoon, Saskatchewan, Canada

64.1 INTRODUCTION

At any point in time, the composition of the soil atmosphere (or soil gas phase) depends upon (i) balance between the rates of production and consumption of various gases in the soil, (ii) rate of exchange between the soil air and the air above the soil surface, and (iii) partitioning of the gases between the gaseous, liquid, and solid phases of the soil. Biological processes (e.g., respiration) normally consume O_2 and produce CO_2, but can also result in the release of other gases such as nitric oxide (NO), nitrous oxide (N_2O), and nitrogen (N_2) during the biological reduction of nitrate in soils. Chemical processes also can produce gases, e.g., the volatilization of ammonia from fertilizers or the release of radon gas from the mineral fraction of the soil.

The soil atmosphere reflects the nature of the soil respiration process (aerobic or anaerobic), and when combined with suitable transport coefficients can provide estimates of the rates with which these processes occur. For example, de Jong et al. (1974) used the CO_2 distribution in the soil to calculate CO_2 fluxes when the diffusion constant of the soil was known; Rolston (1978) and Colbourn et al. (1984) did the same for estimating N_2O fluxes in anaerobic soils. More recently, Tang et al. (2003) estimated the CO_2 efflux from soils using a solid-state sensor for the *in situ* measurement of CO_2 concentration profiles. In this study, steady-state conditions were assumed, and only exchange through gaseous diffusion was taken into account. A complete description of change in the soil atmosphere would have to take into account diffusion, mass flow, and solution and dissolution of various gases in the liquid phase.

Analysis of the soil atmosphere involves collecting a representative gas sample and analyzing the sample for the gas species of interest. In general, sampling approaches can be grouped into four categories: whole-air sampling, sorbent methods, water sampling, and headspace sampling of intact soil cores (Farrell et al. 2002). A further distinction can be

made between *active sampling* (in which the air or water sample is collected under an applied suction) and *passive sampling* (which relies on diffusion of the gas into a sampling chamber). A wide variety of detection systems are available for the determination of gases and vapors in the soil atmosphere—many of which are especially well suited for field-based and *in situ* analyses. In most instances, however, once the sample has been collected the preferred method of analysis is gas chromatography (GC).

64.2 SAMPLING OF THE GASEOUS PHASE

Of the various methods available for soil gas sampling, whole-air sampling is by far the most common. In some studies, ''grab'' samples are taken by inserting a probe to the desired depth in the soil and slowly withdrawing a soil air sample under a gentle vacuum (e.g., using a syringe). Depending on the care used in inserting the probe, the size of the sample and the rapidity of withdrawal, serious contamination can occur from air leaking around the probe or preferential withdrawal of air from the larger pores. At present, grab samples are generally used only for screening purposes—with air samples collected for detailed compositional analysis almost always obtained from air diffusion wells.

Some basic designs for air (diffusion) wells are shown in Figure 64.1. The air inside the well equilibrates with the soil air at the inlet through diffusion. The time required for equilibration depends on the diffusion constant of the soil, the cross-section of the inlet, and the length of the well. Figure 64.1a and Figure 64.1b show the simplest well designs consisting of a piece of polyvinyl chloride (PVC) pipe closed at the top. Wells with smaller inlets (e.g., Figure 64.1b and Figure 64.1c) require longer equilibration times, though the air in the space at the

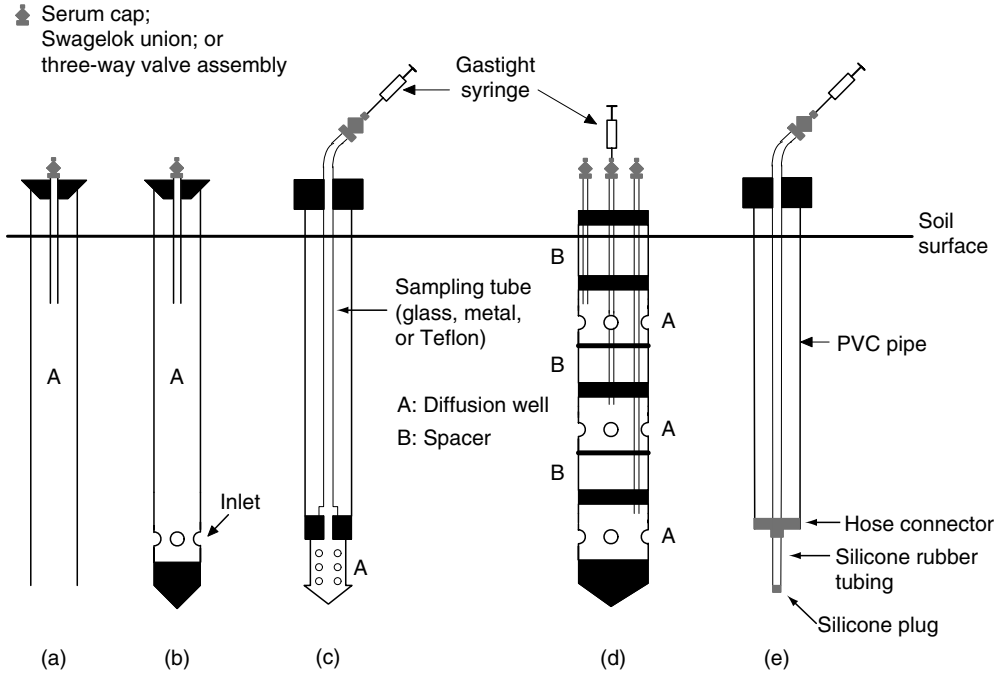

FIGURE 64.1. Air diffusion well designs: (a–c) simple, single-chamber sampling wells; (d) multiple-chamber sampling well; (e) silicone-membrane gas sampling probe for use in waterlogged and flooded soils.

bottom of the well shown in Figure 64.1c would equilibrate more quickly due to the smaller volume of the sampling chamber. Long equilibration times would still be required for the air in the withdrawal tube, though this air can be purged and discarded before taking the sample for analysis. Figure 64.1d shows a design for a multiple-well tube, which has the advantage of providing a similar geometry for each sampling depth and of reducing the number of tubes that have to be inserted in a plot.

Whereas the wells shown in Figure 64.1a through Figure 64.1d can be used to sample the soil atmosphere above the water table (i.e., in well-drained soils under unsaturated conditions), diffusion wells designed for use in waterlogged or temporarily saturated soils also can be constructed (Clark et al. 2001; Kammann et al. 2001). These soil gas samplers make use of silicone tubing that is highly permeable to a number of important soil gases—including CO_2, CH_4, and N_2O—but is impermeable to water (Figure 64.1e). Kammann et al. (2001) demonstrated that equilibration between the inner and outer (soil) atmosphere occurred rapidly, even when the gradient across the silicone membrane was small. The time required to reach 95% of the equilibrium value varied depending on gas species (increasing in the order: $N_2O < CO_2 < CH_4$), wall thickness of the silicone tubing, and temperature.

64.2.1 Sampling Procedures

Materials

Plastic (PVC) tubing is the most common material used to construct air diffusion wells, with the gas withdrawal tubes generally constructed from stainless steel or Teflon tubing. The advantages of PVC include low cost, ease of fabrication, and durability. Serum caps, Swagelok unions, and three-way valves are commonly used to seal the top of the wells or the gas withdrawal tubes. In our experience, translucent plastic tubing used for the withdrawal tube turned brittle with time when exposed to sunlight, though this can be prevented by placing UV-resistant plastic over the samplers. It is also worth noting that rodents occasionally attack this type of tubing.

Installation

Air diffusion wells should be sealed tightly against the surrounding soil. This can be achieved by augering a hole of a slightly smaller diameter than the well and forcing the well into it. Alternatively, the well can be placed into an auger hole slightly larger than the probe and then backfilling the hole with soil around the inlets and with soil or bentonite to the surface. Inserting the well into the soil is facilitated by a pointed tip on the wells, as illustrated in Figure 64.1b through Figure 64.1d. If the wells are installed in a wet soil, shrinkage cracks may develop around the well in clay soils, thus installation in a dry soil is recommended. Wells with a silicone membrane diffusion chamber, such as that illustrated in Figure 64.1e, can be installed using the same basic technique. Wells of the type developed by Kammann et al. (2001) are more difficult to install as they must be installed into the face of a soil pit at the appropriate depth.

Equilibration

van Bavel (1954) estimated that for a soil with $\geq$15% total airspace, a 15 cm long (2.5 cm i.d.), open-ended well (Figure 64.1a) will require up to 1.5 h to equilibrate to within 2% of its final value, and that a 45 cm long well would require up to 8 h to reach a similar stage of equilibrium. Longer equilibration times are required in soils with <15% total airspace and

for wells with smaller inlets (Figure 64.1b through Figure 64.1d). In practice, the gas concentration in the well will always be damped and lagged relative to the actual concentration in the soil air. The shorter the well, the smaller the concentration difference between the sampling chamber and the soil air at the inlet.

Sample Collection and Storage

Samples can be withdrawn from the gas sampling wells using a variety of procedures. Plastic syringes provide an economical method of collecting gas samples, but are not appropriate for storing air samples for more than a few hours (Rochette and Bertrand 2003). In our experience, the most effective and economical method of storing gas samples involves the use of evacuated glass vials (Exetainers; Labco Ltd., High Wycombe, UK; Vacutainers, Becton Dickinson, Oakville, ON). These vials can be reused, and gas leakage can be reduced by adding a second (PTFE/silicone) septum or by covering the tops of the vials with a thin layer of silicone after injecting the sample. Indeed, samples stored under a slight positive pressure can be stored for several weeks (Rochette and Bertrand 2003). In our laboratory, we have found that N_2O samples stored at 200 kPa pressure in Exetainers could be stored for up to 11 weeks, with less than 3% signal loss. Rochette and Bertrand (2003) provide an excellent discussion of soil air sampling and handling using Exetainer vials. Whereas Exetainers can be used ''as is,'' Vacutainers generally require washing to remove contaminants (Covert et al. 1995).

64.3 ANALYSIS OF THE GASEOUS PHASE

Early measurements of soil air composition often relied on absorption techniques, e.g., CO_2 in an alkali and O_2 in pyrogallol. In general, this required the collection of large volumes of soil air (≥ 50 cm^3), which were taken to the laboratory where O_2 and CO_2 were determined by absorption in gas burettes. Today, however, these techniques have been almost universally replaced by methods employing GC analysis of small air samples. Detailed discussions of the principles and practice of modern soil gas analysis are presented in a number of reviews (Smith and Arah 1991; Farrell et al. 2002; Smith and Conen 2004) and will not be discussed here.

64.3.1 Laboratory Analysis by Gas Chromatography

GC is the most versatile method of soil gas analysis, and, thus, remains the methodology of choice in most laboratories. Usually, small gas samples withdrawn from the sampling well by hypodermic syringe (or into Exetainers) are taken to the laboratory for analysis. There, a subsample of the gas is introduced into a flow-regulated *carrier gas* stream through an *injection port*. The sample passes from the injection system onto a *column*, where it is separated into its component gases, which then pass into a *detector* that senses the individual components of the sample gas and produces a signal proportional to the concentration of each component. Signals produced by the detector are then processed and recorded by a data acquisition system, such as a specific-purpose digital electronic integrator or multifunction data station. The column and detector are housed in temperature-controlled environments, and on some GCs temperature changes can be programed to occur during analysis to enhance the performance of the column or detector. A wide range of instruments, detectors, and column packings are currently used in soil atmosphere research (see reviews by Smith

TABLE 64.1 Common Gas Chromatographic Detectors Used to Determine Components of the Soil Atmosphere

Detector	Detection limit (g)	Linear dynamic range	Examples	
			Soil gas	Reference
Thermal conductivity (TCD)	10^{-9}–10^{-6}	10^{4}–10^{5}	O_2, CO_2, CH_4	Kabwe et al. (2005); Sakata et al. (2004); Sitaula et al. (1992); Hall and Dowdell (1981)
Flame ionization (FID)	10^{-10}–10^{-9}	10^{6}–10^{7}	CH_4, C_2H_4	Sakata et al. (2004); Wood (1980); Smith and Dowdell (1973)
Helium ionization (HID)	10^{-12}–10^{-11}	10^{3}–10^{4}	CO_2	Mitchell (1973)
Electron capture (ECD)	10^{-13}–10^{-12}	10^{2}–10^{3}	N_2O, CO_2	Izaurralde et al. (2004); Loftfield et al. (1997); Thomson et al. (1997)
Flame photometric (FPD)	10^{-13}–10^{-11}	10^{3}–10^{4}	S gases	de Souza (1984); Banwart and Bremner (1974)
Ultrasonic	10^{-10}–10^{-9}	10^{5}–10^{6}	O_2, CO_2, N_2O, CH_4	McCarty and Blicher-Mathiesen (1996); Blackmer and Bremner (1977)

Source: Adapted from Farrell, R.E., Elliott, J.A., and de Jong, E. in M.R. Carter (Ed.), *Soil Sampling and Methods of Analysis*, Canadian Society of Soil Science, Lewis Publishers, Boca Raton, Florida, 1993, 663–672; Farrell, R.E., Elliott, J.A., and de Jong, E. in J.H. Dane and G.C. Topp (Eds.), *Methods of Soil Analysis, Part 4—Physical Methods*. Soil Science Society America, Madison, Wisconsin, 2002, 1076–1111.

and Arah 1991; Farrell et al. 2002; Smith and Conen 2004). A list of the more common detectors, their general performance characteristics, and examples of their use in soil gas studies are given in Table 64.1.

Accurate sample injection is important; i.e., errors result if the sample and standard volumes vary. When performing manual injections we have found it useful to use N_2 as an internal standard for the volume of the sample. In well-aerated soils, N_2 should be close to 78% of the total sample, thus any deviation of the internal standard from the expected value can then be used as a scaling factor to correct for variable sample volume. This problem can be avoided by employing a sample loop (Smith and Arah 1991) or autosampler to inject the sample onto the GC column.

In most cases samples are injected directly onto the GC column by the operator, though it is becoming more common to include automated injection systems in the basic GC package. This can result in greater precision while allowing samples to be introduced onto the GC column when an operator is not present—a particularly useful feature when large numbers of samples are being analyzed. A number of designs for automated injection systems are described by Smith and Arah (1991). Commercially available autosamplers that can accommodate a variety of sample storage vials, and which can analyze up to 200 samples are becoming increasingly common. Using a GC equipped with such a system (CombiPAL, CTC Analytics AG, Switzerland), our laboratory at the University of Saskatchewan routinely analyzes 20,000–30,000 gas samples annually—with generally less than 2 h of technician time per day required to operate the system.

Quantitative information from an integrated GC chromatogram is obtained by comparing the peak area (or peak height) of the target gas with those obtained for gas standards having known concentrations. In this way, the gas concentrations in the air sample can be obtained from the least-squares regression equation (linear or nonlinear, depending on the range in concentrations covered by the standards) describing the calibration curve (i.e., concentration versus peak area) prepared for each target gas. Alternatively, an internal standard method of calibration can be used in which a known amount of a standard gas is added to the sample containing the unknowns. An internal response factor (IRF) is first determined by injecting a sample containing known amounts of both the internal standard and the target gas; the IRF is then calculated from the following equation:

$$\mathrm{IRF} = \left(\frac{A_{\mathrm{is}}}{C_{\mathrm{is}}}\right)\left(\frac{C_{\mathrm{tg}}}{A_{\mathrm{tg}}}\right) \tag{64.1}$$

where C_{tg} and C_{is} are the concentrations of the target gas and internal standard, respectively; and A_{tg} and A_{is} are the measured peak areas for the target gas and internal standard, respectively. The unknown sample—spiked with the internal standard—is then injected and the concentration of the target gas calculated by rearranging Equation 64.1 and solving Equation 64.2 for C_{tg}:

$$C_{\mathrm{tg}} = \mathrm{IRF}\left(A_{\mathrm{tg}}\frac{C_{\mathrm{is}}}{A_{\mathrm{is}}}\right) \tag{64.2}$$

The internal standard method has an added advantage in that it accounts for any variability in GC performance. Calibration gases are available commercially, though Lemke et al. (2002) reported that ''careful evaluation and cross referencing of commercially prepared'' standards should be undertaken when preparing a set of ''working standards.''

The number of different column/detector systems used to characterize and quantify components of the soil atmosphere is too numerous to list. Ultimately, however, the choice of a particular system depends on the gases of interest, the sensitivity required, and the cost or availability of a detector. Smith and Arah (1991) provide an excellent overview of column selection and detector capability for GC analysis of the soil atmosphere. Other useful reviews have been prepared by Farrell et al. (2002) and Smith and Conen (2004). References for a variety of GC analyses are provided in Table 64.1; specific examples of several environmentally relevant soil gases (i.e., greenhouse gases) are presented below.

Sitaula et al. (1992) described a GC system for the determination of the major greenhouse gases in soil air (i.e., CO_2, N_2O, and CH_4). They equipped a GC (Fractovap 4200, Carlo Erba, Italy) with three detectors for the determination of CO_2 (thermal conductivity detector, TCD), CH_4 (flame ionization detector, FID), and N_2O (electron capture detector, ECD). Samples are introduced on-column using a 500 μL injection loop, and all separations are achieved isothermally at 35°C on a wide-bore capillary column (Poraplot Q; 25 m × 0.53 mm i.d.). The TCD (operated at 70°C) and FID are connected in series on one line of the detection system, while the ECD (operated at 350°C) is connected via a second line. A six-port valve is used to switch between the two detector lines while maintaining carrier gas flow (7 mL He min^{-1}) in the detectors not connected to the column. Output from both the TCD and ECD is recorded on one channel of the integrator while output from the FID is recorded on the second channel. Supplementary gases are supplied to all three detectors: the TCD

receiving additional He at 7–8 mL min^{-1}; the FID receiving air at 200 mL min^{-1} and H_2 at 20 mL min^{-1}; and the ECD receiving Ar–CH_4 (10:1) at 18 mL min^{-1}. Total analysis time for the three gases was 3.3 min.

The most comprehensive technique for GC analysis of the soil atmosphere was proposed by Blackmer and Bremner (1977). The method allows rapid and precise determination of N_2, O_2, Ar, CO_2, CH_4, and N_2O. Neon, H_2, CO, and NO also are separated along with a composite peak for C_2H_4 and C_2H_2. For the analyses, the GC (a Tracor Model 150G) is fitted with an ultrasonic detector and a dual-phase meter. The gases are separated on two stainless steel columns packed with 50/80 mesh Porapak Q. The sample passes through the first column (4.3 m × 2.1 mm i.d.; maintained at 45°C) into the *A* side of the detector and then enters the second column (7.6 m × 2.1 mm i.d.; submerged in a dry ice–methanol bath) and exits into the *B* side of the detector. The carrier gas (UHP He) flow is maintained at 50 mL min^{-1} by regulating the gas supply at a pressure of 412 kPa and the back pressure regulator on side *B* at 206 kPa. Total analysis time is 6.5 min—though longer run times may be necessary if large amounts of C_2H_4, C_2H_2, or Ne are present in the sample. McCarty and Blicher-Mathiesen (1996) also employed an ultrasonic detector, in a fully automated GC system, for the determination of CO_2, N_2O, O_2/Ar, and N_2 in soil air samples.

Simpler systems are available for studies requiring only basic gas analyses (i.e., N_2, O_2, Ar, CO_2, or CH_4). For example, Anderson (1982) described a system employing two columns (packed with molecular sieve 5A and Porapak R) and a single TCD for the detection of O_2, N_2, and CO_2. Whereas the TCD is the most common detector for CO_2, adequate sensitivity for CO_2 on an ECD can be obtained by reducing the operating temperature of the detector from the N_2O optimum (Loftfield et al. 1997; Thomson et al. 1997).

64.3.2 Alternatives to Gas Chromatography

Whereas GC remains the most versatile method of studying the composition of the soil atmosphere, a number of alternative detection systems suitable for soil gas analysis also are available commercially. These include: colorimetric gas detector tubes for CO_2, NH_3, and volatile organic compounds (VOCs) (Buyanovsky and Wagner 1983; Mayer 1989; DeLaune et al. 2004); infrared gas analyzers (IRGA) for single- and multicomponent determinations of CO_2, CH_4, and N_2O (Deyo et al. 1993; Ambus and Robinson 1998; Fang and Moncrieff 1998; Griffith et al. 2002); paramagnetic, polarographic, and fiber optic sensors for O_2 (van Bavel 1965; Blackwell 1983; Cortassa et al. 2001; Ramamoorthy et al. 2003); electrochemical sensors for O_2 and N_2O (Sexstone et al. 1985; Li and Lundegard 1996); and a variety of detectors for radon gas (Reimer 1991; Monnin and Seidel 1992; Mazur et al. 1999; Yamamoto et al. 2003). These detectors, though generally less sensitive than GC systems, are often better suited for field-based and *in situ* analyses of the soil air, as well as the measurement of gas fluxes between the soil and atmosphere. The basic principles, features, and performance characteristics of various gas detection systems have been reviewed by Saltzman and Caplan (1995), Woebkenberg and McCammon (1995), Farrell et al. (2002), and Smith and Conen (2004).

IRGA are frequently used to measure CO_2 fluxes from the soil to the atmosphere, but can also be used to measure and monitor CO_2 concentrations in the soil air. These analyzers take advantage of the fact that most gases have unique IR absorption signatures in the 2–14 μm region. The basic IRGA system consists of a sample inlet, an IR light source, a sample cell (i.e., a compartment of known optical length), an optical filter, and an IR detector. The optical filter allows the detector to monitor only that part of the IR spectrum specifically affected by the target gas. The amount of IR radiation absorbed by the target gas over the

path length is proportional to its concentration; thus, greater sensitivity and lower detection limits can be achieved by increasing the path length. A detailed explanation of IRGA is given by Woebkenberg and McCammon (1995) and Smith and Conen (2004).

Fang and Moncrieff (1998) used an IRGA to determine CO_2 concentrations in discrete samples collected from ''gas traps'' buried at specified depths in a field soil. Gut et al. (1998) described a novel soil gas sampling system in which an air-permeable hydrophobic polypropylene tube was buried in the soil and CO_2 concentrations in the soil air were measured continuously by circulating the air in the sampling tube through an IRGA placed in series with the sampling tube. Gas sensors based on infrared spectrometry are also finding their way into the realm of soil gas analysis. For example, Hirano et al. (2000) described the use of a silicone-based, nondispersive infrared sensor to measure CO_2 concentrations in the soil atmosphere under a deciduous broad-leaf forest in Japan. Tang et al. (2003) used a newer version of this sensor to continuously monitor soil CO_2 profiles and calculate the soil CO_2 efflux in a Mediterranean savanna ecosystem in California. Nobuhiro et al. (2003) incorporated a similar sensor into a closed static chamber system for measuring the efflux of CO_2 from the soil to the atmosphere.

Another technique that is gaining popularity is isotope ratio mass spectrometry (IRMS). This stems from the fact that many of the elements of importance to environmental and agricultural scientists (i.e., hydrogen, carbon, nitrogen, oxygen, and sulfur) have at least two stable isotopes—with the lighter isotope being the most abundant in natural systems. Because the relative abundance of these isotopes can be obtained using IRMS techniques, stable isotope analysis can provide information regarding the origin and fate of trace gases in the soil atmosphere—information that cannot be obtained from concentration measurements alone. A detailed discussion of IRMS is beyond the scope of this chapter; thus, the reader is directed to reviews by Barrie and Prosser (1996), Platzner (1997), Scrimgeour and Robinson (2004), and Flanagan et al. (2005).

64.4 ANALYSIS OF THE GAS–LIQUID INTERFACE

Our understanding of how aeration influences plant growth and microbial processes is based, in part, on our knowledge of the aeration status of soil at the soil–atmosphere and soil–water interface. Moreover, because soil–water plays such a key role in regulating the composition of the soil atmosphere (i.e., influencing soil biological processes, controlling the rate of exchange between the soil air and atmospheric air, and providing temporary storage of soluble gases) it is also necessary to assess the gas composition of the liquid phase. Of the various types of gas analysis systems described in Section 64.3, electrochemical sensors have proven to be the most useful in terms of measuring *in situ* gas concentrations (partial pressures) and dynamics in both the gaseous and liquid phases. Indeed, electrochemical sensors have been used to measure and monitor oxygen diffusion rate (ODR), O_2 concentration profiles, and O_2 diffusivity in field soils (Patrick 1976; Rolston 1986; Khan et al. 2000), as well as for the *in situ* continuous monitoring of CO_2 concentrations in soil (Jensen et al. 1965) and sediments (Zhao and Cai 1997).

We have chosen to limit our discussion to the platinum (Pt) microelectrode as a tool for measuring the ODR and O_2 concentration in the gaseous and liquid phases of the soil because it is the most common type of electrochemical sensor used to study the soil–air–water interface. Detailed reviews of the theory, validity, and methodology of the Pt microelectrode methods can be found in the literature (Birkle et al. 1964; McIntyre 1971; Phene 1986).

64.4.1 ODR Measurements

Principles and Apparatus

The movement of oxygen from the atmosphere to an actively growing root (or microbial community) involves diffusion through the gaseous phase of the soil, across the gas–liquid phase boundary, and through the water film that permeates the rhizosphere. Thus, by measuring the diffusion of O_2 through the liquid phase of the soil to a reducing surface that approximates a plant root (i.e., a Pt microelectrode), one can obtain a useful measure of the ODR.

The typical ODR measurement system (Figure 64.2) consists of four basic components: (i) Pt microelectrode (the cathode), (ii) nonpolarizable reference electrode (the anode; usually a Ag, AgCl electrode with a KCl-saturated agar salt bridge), (iii) power supply and its associated electrical circuit (to apply an electrical potential between the cathode and anode), and (iv) milliammeter (to measure the output current). The basic ODR measurement system can be adapted to include data acquisition systems that also incorporate soil resistance corrections (see Comments, p. 843), thus allowing rapid sequential measurements of multiple electrodes (Phene et al. 1976; Callebaut et al. 1980).

After insertion in the soil, the electrical potential of the Pt microelectrode is lowered sufficiently with respect to the reference electrode until the O_2 at the electrode surface is electrolytically reduced. In practice, as the applied potential is lowered below about -0.2 V the current increases until the *limiting potential* is reached. At this point, the rate of reduction is controlled by the rate at which O_2 can diffuse to the surface of the cathode and the electrical current (i_{lc}) is proportional to the flux of O_2 at the surface of the Pt microelectrode according to the following equation:

$$i_{lc} = nFAf_{t,a} \tag{64.3}$$

where n is the number of equivalents per mole of O_2 (4), F is the Faraday constant (96,485 coulombs equivalent^{-1}), A is the surface area of the electrode (m^2), and $f_{t,a}$ is the O_2 flux at time t (min) to an electrode with radius a (m). The O_2 flux to the electrode surface (i.e., the ODR; mol m^{-2} s^{-1}) can then be calculated by rearranging Equation 64.3 and solving for $f_{t,a}$:

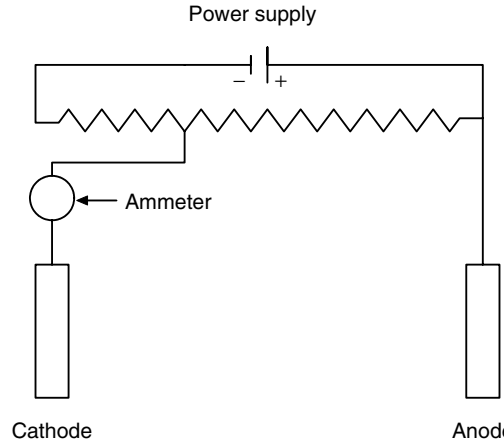

FIGURE 64.2. Basic components of the oxygen diffusion rate (ODR) measurement system.

$$f_{t,a} = \mathrm{ODR} = \left(\frac{i_{lc}}{nFA}\right) \tag{64.4}$$

or, converting the flux to g m^{-2} min^{-1}

$$\mathrm{ODR} = 0.00497\left(\frac{i_{lc}}{A}\right) \tag{64.5}$$

where 0.00497 is a constant with units g A^{-1} min^{-1}, i_{lc} is the measured output current (A), and A is the surface area of the electrode (m^2). [*Note*: the molecular weight of $O_2 = 32$ g mol^{-1}.]

Construction of the Pt Microelectrode

Techniques for constructing Pt microelectrodes suitable for measuring the ODR in soils are too numerous to describe. It is worth noting, however, that electrodes constructed using glass tubing and incorporating liquid Hg junctions have been universally replaced by electrodes that are more rugged and which pose less of an environmental concern. Suitable electrode designs have been described by Letey and Stolzy (1964), Farrell et al. (2002), and Wafer et al. (2004). Platinum microelectrodes used by the authors are fabricated as follows:

1. Insulated, 18 gauge Cu wire is cut to the desired length and about 3 cm of insulation is stripped from both ends of the wire.

2. 1.25 cm length of 20 (or 22) gauge Pt wire (>98% pure) is spot welded to the Cu wire, after which the Cu wire is polished and a small piece of shrink-wrap tubing is slipped over the wire—making sure to cover the Pt–Cu joint—and slowly heated. (*Note*: to provide maximum protection of the Pt–Cu joint, the weld is coated with a small amount of marine epoxy before the shrink-wrap tubing is placed over the wire.)

3. A disposable, 1 mL plastic pipette tip is inserted over the Cu–Pt wire to function as a mold, and, leaving 1.0 mm of the Pt wire exposed, is filled with marine epoxy and left to harden (Farrell et al. 1991). Marine epoxy is used to resist deterioration under saturated conditions.

4. After the epoxy has hardened, a gold-plated pin connector is soldered onto the Cu wire to facilitate connection to the milliammeter, and the Pt tip is cleaned using a jeweller's precious metal cleaner before testing and use.

5. Pt microelectrodes are tested against a Ag, AgCl reference electrode with a 3.5 *M* KCl salt bridge by placing the electrodes in a redox buffer consisting of 3.33 m*M* potassium ferrocyanide, 3.33 m*M* potassium ferricyanide, and 0.1 *M* KCl and recording the cell potential; electrodes are considered acceptable if they exhibit a cell potential of 425 ± 10 mV.

It is worth noting that the use of epoxy to seal the Pt–Cu joint makes it difficult to recover all the platinum, in the event the electrode is faulty. The method described by Wafer et al. (2004) avoids this problem by using a bronze-brazing rod as the body of the electrode, soldering the Pt tip into a small hole drilled into one end of the rod (with the Cu wire connector soldered into a hole in the opposite end), covering the joints with shrink-wrap

tubing, and placing a ridged terminal insulator over the soldered joint (and covering a small portion of the Pt tip). The authors reported that these electrodes were simple to construct, easy to repair when necessary, and exhibited excellent long-term (19 months) stability when used to measure soil redox potential.

Soil Insertion and ODR Measurement

For surface measurements, the Pt microelectrodes are inserted into the soil by hand, taking care not to damage the tip. In general, a small channel is made in the soil using a plastic or metal rod with a diameter slightly smaller than that of the microelectrode. The channel is made slightly (1–2 cm) shallower than the measurement depth to minimize disturbance of the diffusion path in the surrounding soil. For subsurface measurements, the Pt microelectrodes can be buried in place (which is not usually recommended due to the potential of electrode poisoning) or inserted (and removed) using small access tubes that can be sealed just above the electrode with minimal headspace. Access tubes for subsurface placement of Pt microelectrodes have been described by Patrick (1976) and Phene et al. (1976).

Once the Pt microelectrodes are in place, the reference electrode (usually a calomel or Ag, AgCl electrode) is connected to the soil by means of a salt bridge (saturated or 3.5 *M* KCl). If dry, the soil near the salt bridge may be moistened with some distilled water to ensure that there is good contact between the reference electrode and the soil. Reference electrodes are available from numerous manufacturers or can be fabricated as described by Phene (1986), Armstrong and Wright (1976), Blackwell (1983), and Farrell et al. (2002). Veneman and Pickering (1983) described a salt bridge for *in situ* measurements of soil redox potential, and which may be used for ODR measurements.

ODR measurements are obtained by applying a potential between the electrodes (a potential of −0.65 V is often recommended to facilitate standardization) until a steady-state current is achieved (usually 5–10 min after the potential is applied). The steady-state current is recorded and the ODR calculated using Equation 64.2.

Comments

The main factors affecting ODR measurements can be grouped into two categories: (i) electrochemical factors (e.g., choice of the applied potential, establishment of the steady-state current, installation of the electrodes, and poisoning of the Pt electrodes) and (ii) soil factors (e.g., moisture and salt content, O_2 concentration, and temperature). These factors have been discussed in detail by McIntyre (1971), Phene (1986), and Farrell et al. (2002). In general, however, erroneous ODR measurements often can be traced to one of the three causes: (i) selection of an inappropriate applied potential, (ii) poisoning of the Pt microelectrode, or (iii) change in the moisture or salt content of the soil.

1 *Applied potential*: Under ideal conditions, reduction of O_2 at the cathode is initiated at an applied potential of about −0.2 V (the decomposition potential of oxygen). Increasing (negatively) the applied voltage further produces an increase in the current until the limiting potential (the potential at which the rate of reduction is controlled by the rate at which O_2 can diffuse to the surface of the cathode) is reached. At this stage, the plot of current versus applied voltage (i.e., a polarogram) forms a plateau and no further increase in current is observed

until the applied voltage reaches the discharge potential of the hydrogen ion (Armstrong and Wright 1976). Although ODR measurements usually employ an applied potential of −0.65 V (Phene 1986), Armstrong and Wright (1976) and Blackwell (1983) recommended that the applied potential be derived from a current–voltage plot of the limiting potential *in situ* and that this be the first step in any ODR measurement. They further recommended forgoing the ODR measurement if the plateau of the current–voltage plot was absent. Blackwell (1983) reported that the Armstrong and Wright (1976) method yields ODR values which often are an order of magnitude lower than those measured with the standard method (i.e., applied potential = −0.65 V). Hence, considerable thought should be given to the choice of an appropriate applied voltage. Because of the expense and inconvenience involved in making multiple determinations of the limiting potential, it has been suggested that a single measurement obtained at each sampling depth is adequate (Armstrong and Wright 1976).

2 *Electrode poisoning*: Poisoning can be defined as any chemical or physical change to the surface of the Pt microelectrode that interferes with its efficiency to reduce O_2 (Devitt et al. 1989). Poisoning is not usually a factor if the electrodes are removed from the soil after each measurement. If the electrodes are left in place for extended periods, however, poisoning may become a factor. Electrode poisoning can result from the movement of colloidal material to the electrode surface or the precipitation of carbonates or mixed carbonate–aluminosilicates on the surface of the electrode (McIntyre 1971; Devitt et al. 1989). The effects of poisoning can be minimized by removing and cleaning the electrodes every 4 to 8 weeks.

3 *Corrections for soil moisture and salts*: Changes in the moisture or salt content of the soil will be reflected by changes in the electrical resistance of the soil. This, in turn, will affect the ''true'' potential between the Pt and reference electrodes. Thus, because the output current is dependent on the true potential between the electrodes as well as the flux of O_2 to the Pt electrode, the true ODR will depend partly on the soil resistance. Methods of correcting ODRs for changes in the soil resistance have been described by Callebaut et al. (1980).

Despite these problems, as well as some reservations about the theoretical validity of using the Pt microelectrode to measure soil O_2 (McIntyre 1971), it is generally agreed that until a better method is developed, ODR measurements obtained with the Pt microelectrode provide valuable information regarding soil aeration.

64.4.2 O_2 Concentration Measurements

Principles and Apparatus

The basic Clark-type O_2 electrode is an amperometric sensor that consists of a Pt (or Au) cathode and a Ag, AgCl anode (electrically connected to the cathode by an electrolyte, e.g., KCl), which contact the soil through a gas-permeable membrane (Figure 64.3). Theoretical and operational considerations of these electrodes have been reviewed by Phene (1986), Ding and Wang (1993), Hitchman and Berlouis (1995), and Pham and Glass (1997). Briefly, when an appropriate potential is applied between the cathode and anode, the O_2 that diffuses across the gas-permeable membrane is reduced at the cathode, the O_2 concentration at the

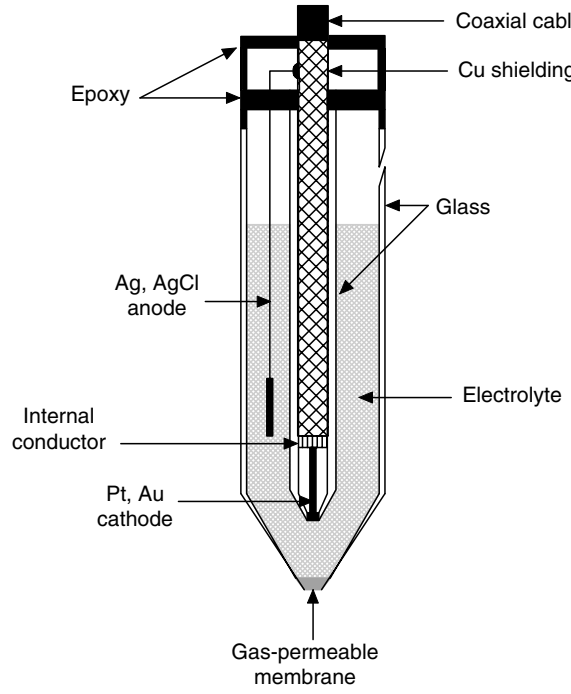

FIGURE 64.3. Clark-type amperometric O_2 microelectrode.

surface of the cathode is zero, and the output current is proportional to the concentration of O_2 reduced at the cathode. Incorporating a thermistor in the basic electrode design allows for temperature compensation. A second gas-permeable membrane, separated from the first by a piece of nylon mesh, is added to the electrode to prevent water from condensing on the membrane adjacent to the Pt cathode. In this way, even though water may condense on the outer membrane, a low-impedance path for the diffusion of O_2 to the cathode exists between the two membranes. Probes such as these are suitable for the determination of O_2 concentrations in both the gaseous and solution phases of the soil. Revsbech (1989) further modified the O_2 microelectrode by incorporating a guard cathode that prevents diffusion of O_2 from the bulk electrolyte to the sensor tip. Electrodes of this design were later used to measure O_2 distribution in bulk and rhizosphere soils (Christensen et al. 1994; Højberg et al. 1994).

Procedures

Oxygen probes incorporating features of the electrodes described above can be fabricated in the laboratory, but also are available commercially. Activation, calibration, and use of the electrodes should be performed according to manufacturer's instructions. In general, these probes require recalibration on a monthly basis, though more frequent recalibration is necessary for studies requiring increased precision. Likewise, to ensure reliable performance it is advisable that the internal electrolyte be changed on a monthly basis. Since the diffusion rate of oxygen in water and air differs slightly, advanced meters apply a correction factor to the water-saturated air calibration value to obtain the correct air-saturated water value. For most Orion probes (Thermo Electron Corporation, Beverly, Massachusetts), the correction factor is 101.7%. When measuring a low-concentration sample (less than 2 $\mu L\ L^{-1}$), a second calibration point for a zero oxygen standard is often required. At zero oxygen

concentration, some more advanced probes generate no current, therefore defining the zero point and making a second calibration step unnecessary.

Comments

The continued development of O_2 electrodes has led to some novel experimental designs. For example, in an attempt to establish the presence of anaerobic microsites within individual soil aggregates and determine the intraaggregate O_2 diffusion coefficient, Sexstone et al. (1985) employed an O_2 microelectrode for the direct measurement of the O_2 concentration profiles within individual soil aggregates. Revsbech et al. (1988) developed a combined electrode for the determination of O_2 and N_2O that was later used by Højberg et al. (1994) to investigate the spatial distribution of O_2 respiration and denitrification in soil aggregates. Although such experiments are not without their difficulties, they would be virtually impossible with any other analytical technique. As well, studies such as these demonstrate the enormous potential presented by the development of other gas-sensing probes.

64.4.3 Miscellaneous Gas-Sensing Probes

Whereas the Clark-type O_2 microsensor is the most frequently and widely used microsensor for environmental applications (Kühl and Revsbech 2001), electrochemical probes for a number of other gases (e.g., CO_2, NH_3, H_2S, SO_2, and CH_4) also have been developed. To date, however, investigations of the soil atmosphere have employed only the potentiometric CO_2 probe (Jensen et al. 1965). Nevertheless, the continuing development of electrochemical and fiber optic sensors and biosensors (Bakker 2004; Wolfbeis 2004) can be expected to yield new opportunities for quantifying the various components of the soil atmosphere and studying its dynamics *in situ*. For example, fiber optic O_2 sensors possess several advantages over the conventional Clark-type sensors in that they can be easily miniaturized for *in situ* applications, are relatively simple to construct, are subject to few interferences, and generally exhibit excellent long-term stability (Kühl and Revsbech 2001).

REFERENCES

Ambus, P. and Robinson, G.P. 1998. Automated near-continuous measurement of carbon dioxide and nitrous oxide fluxes from soil. *Soil Sci. Soc. Am. J.* 62: 394–400.

Anderson, J.P.E. 1982. Soil respiration. In A.L. Page et al. Eds. *Methods of Soil Analysis, Part 2—Chemical and Microbiological Properties*. 2nd ed. American Society of Agronomy, Madison, WI, pp. 831–871.

Armstrong, W. and Wright, E.J. 1976. A polarographic assembly for multiple sampling of soil oxygen flux in the field. *J. Appl. Ecol.* 13: 849–856.

Bakker, E. 2004. Electrochemical sensors. *Anal. Chem.* 76: 3285–3298.

Banwart, W.L. and Bremner, J.M. 1974. Gas chromatographic identification of sulfur gases in soil atmospheres. *Soil Biol. Biochem.* 6: 113–115.

Barrie, A. and Prosser, S.J. 1996. Automated analysis of light-element stable isotopes by isotope ratio mass spectrometry. In T.W. Boutton and S. Yamasaki, Eds. *Mass Spectrometry of Soils*. Marcel Dekker, New York, NY, pp. 1–46.

Birkle, D.E., Letey, J., Stolzy, H., and Szuszkiewicz, T.E. 1964. Measurement of oxygen diffusion

rates with the platinum microelectrode. II. Factors influencing the measurements. *Hilgardia* 35: 555–566.

Blackmer, A.M. and Bremner, J.M. 1977. Gas chromatographic analysis of soil atmospheres. *Soil Sci. Soc. Am. J.* 41: 908–912.

Blackwell, P.S. 1983. Measurements of aeration in waterlogged soils: some improvements of techniques and their application to experiments using lysimeters. *J. Soil Sci.* 34: 271–285.

Buyanovsky, G.A. and Wagner, G.H. 1983. Annual cycles of carbon dioxide level in soil air. *Soil Sci. Soc. Am. J.* 47: 1139–1145.

Callebaut, F., Balcaen, M., Gabriels, D., and De Boodt, M. 1980. Data acquisition system for field determination of redox potential, oxygen diffusion rate and soil electrical resistance. *Mooed. Fac. Landbouwwet. RUG* 45: 15–24.

Christensen, P.B., Revsbech, N.P., and Sand-Jensen, K. 1994. Microsensor analysis of oxygen in the rhizosphere of the aquatic macrophyte *Littorella uniflora* (L.) Ascherson. *Plant Physiol.* 105: 849–852.

Clark, M., Jarvis, S., and Maltby, E. 2001. An improved technique for measuring concentration of soil gases at depth *in situ*. *Commun. Soil Sci. Plant Anal.* 32: 369–377.

Colbourn, P., Harper, I.W., and Iqbal, M.M. 1984. Denitrification losses from 15N-labelled calcium nitrate fertilizer in a clay soil in the field. *J. Soil Sci.* 35: 539–547.

Cortassa, S., Aon, M.A., and Villon, P.F. 2001. A method for quantifying rates of O_2 consumption and CO_2 production in soil. *Soil Sci.* 166: 68–77.

Covert, J.A., Tenuta, M., and Beauchamp, E.G. 1995. Automated analysis of gases stored in Vacutainer vials. *Commun. Soil Sci. Plant Anal.* 26: 2995–3003.

de Jong, E., Schappert, H.J.V., and MacDonald, K.B. 1974. Carbon dioxide evolution from virgin and cultivated soil as affected by management practices and climate. *Can. J. Soil Sci.* 54: 299–307.

de Souza, T.L.C. 1984. Supelpak-S: The GC separating column for sulphur gases. *J. Chromatogr. Sci.* 22: 470–472.

DeLaune, P.B., Moore, P.A. Jr., Daniel, T.C., and Lemunyon, J.L. 2004. Effect of chemical and microbial amendments on ammonia volatilization from composting poultry litter. *J. Environ. Qual.* 33: 728–734.

Devitt, D.A., Stolzy, L.H., Miller, W.W., Campana, J.E., and Sternberg, P. 1989. Influence of salinity, leaching fraction, and soil type on oxygen diffusion rate measurements and electrode ''poisoning.'' *Soil Sci.* 148: 327–335.

Deyo, B.G., Robbins, G.A., and Binkhorst, G.B. 1993. Use of portable oxygen and carbon dioxide detectors to screen soil gas for subsurface gasoline contamination. *Ground Water* 31: 598–604.

Ding, C.P. and Wang, J.H. 1993. Voltammetric methods. In T.R. Yu and G.L. Ji, Eds. *Electrochemical Methods in Soil and Water Research*. Pergamon Press, Oxford, UK, pp. 366–412.

Fang, C. and Moncrieff, J.B. 1998. Simple and fast technique to measure CO_2 profiles in soil. *Soil Biol. Biochem.* 30: 2107–2112.

Farrell, R.E., Elliott, J.A., and de Jong, E. 1993. Soil air. In M.R. Carter, Ed. *Soil Sampling and Methods of Analysis*. Canadian Society of Soil Science. Lewis Publishers, Boca Raton, FL, pp. 663–672.

Farrell, R.E., Elliott, J.A., and de Jong, E. 2002. Gas sampling and analysis. In J.H. Dane and G.C. Topp, Eds. *Methods of Soil Analysis, Part 4—Physical Methods*. Soil Science Society America, Madison, WI, pp. 1076–1111.

Farrell, R.E., Swerhone, G.D.W., and van Kessel, C. 1991. Construction and evaluation of a reference electrode assembly for use in continuous monitoring of *in situ* soil redox potentials. *Commun. Soil Sci. Plant Anal.* 22: 1059–1068.

Flanagan, L.B., Ehleringer, J.R., and Pataki, D.E., Eds. 2005. *Stable Isotopes and Biosphere–Atmosphere Interactions: Processes and Biological Controls*. Elsevier, San Diego, CA.

Griffith, D.W.T., Leuning, R., Denmead, O.T., and Jamie, I.M. 2002. Air-land exchanges of CO_2, CH_4 and N_2O measured by FTIR spectrometry and micrometeorological techniques. *Atmos. Environ.* 36: 1833–1842.

Gut, A., Blatter, A., Fahrni, M., Lehmann, B.E., Neftel, A., and Staffelbach, T. 1998. A new

membrane tube technique (METT) for continuous gas measurements in soil. *Plant Soil* 198: 79–87.

Hall, K.C. and Dowdell, R.J. 1981. An isothermal gas chromatographic method for the simultaneous estimation of oxygen, nitrous oxide and carbon dioxide content of gases in the soil. *J. Chromatogr. Sci*. 19: 107–111.

Hirano, T., Setoyama, H., Tanaka, Y., and Kim, H. 2000. Diffusive CO_2 efflux from the soil surface of a deciduous broad-leaved forest in Hokkaido, Japan. In *Proceedings of the International Workshop for Advanced Flux Network and Flux Evaluation*. Center for Global Environmental Research, National Institute for Environmental Studies, Japan, pp. 113–118.

Hitchman, M.L. and Berlouis, L.E.A. 1995. Electrochemical methods. In F. McLennan and B.R. Kowalski, Eds. *Process Analytical Chemistry*. Blackie Academic & Professional, London, UK, pp. 217–258.

Højberg, O., Revsbech, N.P., and Tiedje, J.M. 1994. Denitrification in soil aggregates analyzed with microsensors for nitrous oxide and oxygen. *Soil Sci. Soc. Am. J*. 58: 1691–1698.

Izaurralde, R.C., Lemke, R.L., Goddard, T.W., McConkey, B., and Zhang, Z. 2004. Nitrous oxide emissions from agricultural toposequences in Alberta and Saskatchewan. *Soil Sci. Soc. Am. J*. 68: 1285–1294.

Jensen, C.R., Van Gundy, S.D., and Stolzy, L.H. 1965. Recording CO_2 in soil root systems with a potentiometric membrane electrode. *Soil Sci. Soc. Am. Proc*. 29: 631–633.

Kabwe, L.K., Farrell, R.E., Carey, S.K., Hendry, M.J., and Wilson, G.W. 2005. Characterizing spatial and temporal variations in CO_2 fluxes from ground surface using three complimentary measurement techniques. *J. Hydrol*. 311: 80–90.

Kammann, C., Grünhage, L., and Jäger, H.-J. 2001. A new sampling technique to monitor concentrations of CH_4, N_2O and CO_2 in air at well-defined depths in soils with varied water potential. *Eur. J. Soil Sci*. 52: 297–303.

Khan, A.R., Chandra, D., Quraishi, S., and Sinha, R.K. 2000. Soil aeration under different soil surface conditions. *J. Agron. Crop Sci*. 185: 105–112.

Kühl, M. and Revsbech, N.P. 2001. Biogeochemical microsensors for boundary layer studies. In B.P. Boudreau and B.B. Jørgensen, Eds. *The Benthic Boundary Layer*. Oxford University Press, New York, pp. 180–210.

Lemke, R., Goddard, T., Hahn, D., Burton, D., Ellert, B., Farrell, R., Monreal, M., and Noot, D. 2002. An inter-laboratory comparison of nitrous oxide analysis in western Canada. *Commun. Soil Sci. Plant Anal*. 33: 2705–2713.

Letey, J. and Stolzy, L.H. 1964. Measurement of oxygen diffusion rates with platinum microelectrodes. I. Theory and equipment. *Hilgardia* 35: 555–566.

Li, D.X. and Lundegard, P.D. 1996. Evaluation of subsurface oxygen sensors for remediation monitoring. *Ground Water Monitor. Remed*. 16: 106–111.

Loftfield, N., Flessa, H., Augustin, J., and Beese, F. 1997. Automated gas chromatographic system for rapid analysis of the atmospheric trace gases methane, carbon dioxide, and nitrous oxide. *J. Environ. Qual*. 26: 560–564.

Mayer, C.L. 1989. Interim guidance document for soil-gas surveying. Contract No. 68-03-3245, U.S. EPA Environmental Monitoring Systems Laboratory, Office of Research and Development, Cincinnati, OH.

Mazur, D., Janik, M., Loskiewicz, J., Olko, P., and Swakolq, J. 1999. Measurements of radon concentration in soil gas by CR-39 detectors. *Rad. Meas*. 31: 295–300.

McCarty, G.W. and Blicher-Mathiesen, G. 1996. Automated chromatographic analysis of atmospheric gases in environmental samples. *Soil Sci. Soc. Am. J*. 60: 1439–1442.

McIntyre, D.S. 1971. The platinum microelectrode method for soil aeration measurement. *Adv. Agron*. 22: 235–283.

Mitchell, M.J. 1973. An improved method for microrespirometry using gas chromatography. *Soil Biol. Biochem*. 5: 271–274.

Monnin, M.M. and Seidel, J.L. 1992. Radon in soil-air and in groundwater related to major geophysical events: a survey. *Nucl. Inst. Meth. Phys. Res*. A314: 316–330.

Nobuhiro, T., Tamai, K., Kominami, Y., Miyama, T., Goto, Y., and Kanazawa, Y. 2003. Development of the IRGA enclosed-chamber system for soil CO_2 efflux measurement and its application to a spatial variation measurement. *J. For. Res.* 8: 297–301.

Patrick, W.H. Jr. 1976. Oxygen content of soil air by a field method. *Soil Sci. Soc. Am. J.* 41: 651–652.

Pham, Q.A. and Glass, R.S. 1997. Characteristics of the amperometric oxygen sensor. *J. Electrochem. Soc.* 144: 3929–3934.

Phene, C.J. 1986. Oxygen electrode measurement. In A.L. Page et al. Eds. *Methods of Soil Analysis, Part 1—Physical and Mineralogical Methods.* 2nd ed. American Society of Agronomy, Madison, WI, pp. 1137–1159.

Phene, C.J., Campbell, R.B., and Doty, C.W. 1976. Characterization of soil aeration *in situ* with automated oxygen diffusion measurements. *Soil Sci.* 122: 271–281.

Platzner, I.T. 1997. *Modern Isotope Ratio Mass Spectrometry*. John Wiley & Sons, Chichester, UK.

Ramamoorthy, R., Dutta, P.K., and Akbar, S.A. 2003. Oxygen sensors: materials, methods, designs and applications. *J. Mater. Sci.* 38: 4271–4282.

Reimer, G.M. 1991. Simple techniques for soil-gas and water sampling for radon analysis. In L.S. Gunderson and R.B. Wanty, Eds. *Field Studies of Radon in Rocks, Soils and Water*. Part 1, Section 1. U.S. Geological Survey Bulletin 1971, Reston, VA, pp. 19–22.

Revsbech, N.P. 1989. An oxygen microelectrode with a guard cathode. *Limnol. Oceanogr.* 34: 474–478.

Revsbech, N.P., Christensen, P.B., Nielsen, L.P., and Sørensen, J. 1988. A combined oxygen and nitrous oxide microsensor for denitrification studies. *Appl. Environ. Microbiol.* 54: 2245–2249.

Rochette P. and Bertrand, N. 2003. Soil air sample storage and handling using polypropylene syringes and glass vials. *Can. J. Soil Sci.* 83: 631–637.

Rolston, D.E. 1978. Application of gaseous-diffusion theory to measurement of denitrification. In D.R. Nielsen and J.G. MacDonald, Eds. *Nitrogen in the Environment*, Vol. 1. Academic Press, New York, NY, pp. 309–335.

Rolston, D.E. 1986. Gas diffusivity. In A.L. Page et al. Eds. *Methods of Soil Analysis, Part 1—Physical and Mineralogical Methods*. Agronomy 9, 2nd ed. American Society of Agronomy, Madison, WI, pp. 1089–1102.

Sakata, T., Ishizuka, S., and Takahashi, M. 2004. A method for measuring fluxes of greenhouse gases from forest soils. *Bull. FFPRI* 3: 259–265.

Saltzman, B.E. and Caplan, P.E. 1995. Detector tubes, direct-reading passive badges, and dosimeter tubes. In B.S. Cohen and S.V. Hering, Eds. *Air Sampling Instruments for Evaluation of Atmospheric Contaminants*, 8th edn. American Conference of Governmental Industrial Hygienists, Cincinnati, OH, pp. 401–437.

Scrimgeour, C.M. and Robinson, D. 2004. Stable isotope analysis and applications. In K.A. Smith and M.S. Cresser, Eds. *Soil and Environmental Analysis: Modern Instrumental Techniques*, 3rd edn. Marcel Dekker, New York, NY, pp. 381–431.

Sexstone, A.J., Revsbech, N.P., Parkin, T.B., and Tiedje, J.M. 1985. Direct measurement of oxygen profiles and denitrification rates in soil aggregates. *Soil Sci. Soc. Am. J.* 49: 645–651.

Sitaula, B.K., Luo, J., and Bakken, L.R. 1992. Rapid analysis of climate gases by wide bore capillary gas chromatography. *J. Environ. Qual.* 21: 493–496.

Smith, K.A. and Arah, J.R.M. 1991. Gas chromatographic analysis of the soil atmosphere. In K.A. Smith, Ed. *Soil Analysis: Modern Instrumental Techniques*, 2nd edn. Marcel Dekker, New York, NY, pp. 505–546.

Smith, K.A. and Conen, F. 2004. Measurement of trace gases. I. Gas analysis, chamber methods, and related procedures. In K.A. Smith and M.S. Cresser, Eds. *Soil and Environmental Analysis: Modern Instrumental Techniques*, 3rd edn. Marcel Dekker, New York, NY, pp. 433–476.

Smith, K.A. and Dowdell, R.J. 1973. Gas chromatographic analysis of the soil atmosphere: automatic analysis of gas samples for O_2, N, Ar,

CO, NO and C–C hydrocarbons. *J. Chromatogr. Sci*. 11: 655–658.

Tang, J., Baldocchi, D.D., Qi, Y., and Xu, L. 2003. Assessing soil CO_2 efflux using continuous measurements of CO_2 profiles in soils with small solid-state sensors. *Agric. For. Met*. 118: 207–220.

Thomson, P.E., Parker, J.P., Arah, J.R.M., Clayton, H., and Smith, K.A. 1997. Automated soil monolith-flux chamber system for the study of trace gas fluxes. *Soil Sci. Soc. Am. J*. 61: 1323–1330.

van Bavel, C.H.M. 1954. Simple diffusion well for measuring soil specific diffusion impedance and soil air composition. *Soil Sci. Soc. Am. Proc*. 18: 229–234.

van Bavel, C.H.M. 1965. Composition of soil atmosphere. In C.A. Black et al., Eds. *Methods of Soil Analysis, Part 1—Physical and Mineralogical Properties*. 1st ed. American Society of Agronomy, Madison, WI, pp. 315–319.

Veneman, P.L.M. and Pickering, E.W. 1983. Salt bridge for field redox potential measurements. *Commun. Soil Sci. Plant. Anal*. 14: 669–674.

Wafer, C.C., Richards, J.B., and Osmond, D.L. 2004. Construction of platinum-tipped redox probes for determining soil redox potential. *J. Environ. Qual*. 33: 2375–2379.

Woebkenberg, M.L. and McCammon, C.S. 1995. Direct reading gas and vapor instruments. In B.S. Cohen and S.V. Hering, Eds. *Air Sampling Instruments for Evaluation of Atmospheric Contaminants*, 8th edn. American Conference of Governmental Industrial Hygienists, Cincinnati, OH, pp. 439–510.

Wolfbeis, O.S. 2004. Fiber-optic chemical sensors and biosensors. *Anal. Chem*. 76: 3269–3284.

Wood, M.J. 1980. An application of gas chromatography to measure concentrations of ethane, propane, and ethylene found in interstitial soil gases. *J. Chromatogr. Sci*. 18: 307–310.

Yamamoto, S., Yoshida, Y., and Iida, T. 2003. Development of an underground radon detector using an optical fiber. *IEEE Trans. Nucl. Sci*. 50: 987–990.

Zhao, P. and Cai, W.-J. 1997. An improved potentiometric pCO_2 microelectrode. *Anal. Chem*. 69: 5052–5058.

Chapter 65
Soil-Surface Gas Emissions

Philippe Rochette and Normand Bertrand

Agriculture and Agri-Food Canada

Quebec, Quebec, Canada

65.1 INTRODUCTION

Measurement of soil-surface gas emissions is useful for several purposes. It is required to fully assess the impact of land management on the atmospheric environment (e.g., ammonia, greenhouse gases, and pesticides), and to develop and test predictive emission models. Also, the short-term rates of several soil biological or chemical reactions can be more easily quantified by measuring the rate of emission of their gaseous products than by monitoring the rate of change in the amounts of soil substrates.

Soil-surface gas emissions can be measured using several techniques but most of them can be categorized based on using chambers, gas diffusion theory, or micrometeorological theory. The reliability of methods based on Fick's first law of diffusion is decreased by imprecision in estimating soil gas diffusivity and by difficulty in determining the vertical gas concentration gradient, especially when gas production or consumption is nonuniformly distributed as a function of soil depth. Micrometeorological techniques are derived from the mathematical description of turbulent mass and energy transport above relatively large, flat, and homogeneous sources. They are nonintrusive and can provide temporally and spatially integrated estimates of the exchange of most gases of interest in agricultural ecosystems. For detailed information about the use of techniques based on gas diffusion theory and micrometeorological theory, readers are referred to other reviews (Rolston 1986; Pattey et al. 2006).

Chamber techniques have been used to estimate soil-surface gas emissions for more than eight decades and remain the most commonly used approach. They permit measurement of very small fluxes, are relatively inexpensive to build and use, and can be adapted to a wide range of field conditions and experimental objectives. Chambers can be grouped into two types according to whether the flux is calculated at constant (steady-state) or changing (nonsteady-state [NSS]) chamber gas concentration (G). The main focus of this chapter is on NSS chambers as most soil-surface gas flux measurements reported in agricultural ecosystems are made using this chamber type.

65.2 NONSTEADY-STATE CHAMBERS

NSS chambers can be used to measure the soil-surface flux of relatively inert gases such as CO_2, CH_4 and N_2O. In NSS chambers, the flux of the gas of interest (F_g; g m^{-2} s^{-1}) is calculated using the rate of change of its concentration (dG/dt; mol $mol^{-1}s^{-1}$) inside the chamber during deployment (Rochette and Hutchinson 2005):

$$F_g = dG/dt \times V/A \times M_{m,g}/V_m \times (1 - e_p/P) \quad (65.1)$$

where G (mol mol^{-1}) is determined in dry air samples, V (m^3) is the chamber volume, A (m^2) is the area covered by the chamber, e_p (kPa) is the partial pressure of water vapor of chamber air, P (kPa) is the barometric pressure, $M_{m,g}$ (g mol^{-1}) is the molecular mass of gas ''g,'' and V_m (m^3 mol^{-1}) is the molecular volume at chamber temperature and barometric pressure. Both e_p and V_m are determined at deployment time $= 0$.

Measurement of G in NSS chambers can be made on-site using a portable gas analyzer. However, use of a portable analyzer is usually limited to gases, such as CO_2, with high fluxes and rapidly changing G. For most other gases, G is determined in the laboratory on air samples previously taken during deployment. Achieving high-quality NSS chamber measurements requires that precautions are taken when handling air samples (sampling, storage, and analysis), when designing and deploying chambers, and when determining dG/dt.

65.2.1 Air Sampling

1 Containers used to store air samples need to be clean, airtight, and made of materials that do not react with the gases of interest. Procedures that follow will refer to commercially available glass vials (12 mL Exetainers, Labco, High Wycombe, UK) that are widely used to handle air samples in soil studies. The rubber septum on the Exetainers provides an adequate seal during storage for most applications. However, the hole left in the septum after pulling a needle off the vial may take a few seconds to close, allowing exchange of air through the septum, especially when the vial is under- or overpressurized. This effect can be reduced by adding a silicone septum (see Table 65.1) on top of the rubber septum (Rochette and Bertrand 2003).

2 Vacuum level in newly purchased vials is variable and we recommend evacuating them with a vacuum line connected to a high-vacuum pump, before usage (1 to >50 needle ports). The vacuum level increases with evacuation time but the evacuation rate is very slow after 3–4 min. Also, the time needed for the needle hole in the septa to close tends to increase with increasing insertion time. Gains in vacuum associated with longer evacuation time can be rapidly lost because of increased leakage when vials are pulled off the line. Users must also evaluate if the gain in vacuum when increasing evacuation time above 3–4 min is worth the loss of efficiency in preparing vials (number of vials per unit of time). The needles connected to the vacuum line should be fine (26G3/8; Becton Dickinson, Rutherford, New Jersey) to minimize damage to the septum and associated leakage. After a first evacuation, vials are flushed with an inert gas such as He (the smaller the molecule, the more rapid and more complete is the flush) followed by a second and final evacuation (3–4 min or more). The whole process

TABLE 65.1 Materials for Nonsteady-State Chambers and Gas Sampling

Chamber	Description
Frame and chamber	Clear acrylic plastic (6.35 mm)
Sampling port	Injectable membrane (Vygon, Ecouen, France) connected to 6.35 mm plastic tubing: Bev-A-Line IV (e.g., Cole-Parmer, Vernon Hills, Illinois)
Cover	Insulated and reflective bubble thermofoil material
Venting tube	25 cm long × 1.5 cm i.d. for a 60 L chamber
Gasket	6.35 mm closed-cell foam (e.g., Lundell Manufacturing Corp., Minneapolis, Minnesota)
Fastener and anchor	Spring-loaded fastener and anchor plate (e.g., Link Lock)
Gas sampling	**Description**
Syringe	Polypropylene syringe (e.g., 20 mL; Becton Dickinson, Rutherford, New Jersey)
Needle	26 gauge needle (e.g., 26G 3/8; Becton Dickinson, Rutherford, New Jersey)
Vials	Glass vials with screw-on caps (e.g., 12 mL Exetainer, Labco Ltd., High Wycombe, UK) An additional septum is recommended (PTFE/silicone 13 mm septa used on top of rubber septum with the Teflon side facing up (e.g., Supelco, Bellefonte, Pennsylvania; see Rochette and Bertrand [2003])

can be performed without removing the vials from the vacuum line by connecting a pressurized tank of the inert gas to the line. A couple of valves allow for successive flushing and evacuation of the vials. Flushing with an inert gas ensures that incomplete evacuation would not result in a contamination of the sample by ambient air gases such as CO_2 or N_2O. Performance of the vacuum line must be checked before evacuating a batch of vials. Vacuum is tested by sipping water into a set of evacuated vials (one per vacuum line unit) using a two-way needle. Rigorous evaluation is made by comparing the mass of tested vials with that of full vials; but can routinely be done by visually evaluating the size of the residual air bubble to detect improper functioning of the vacuum line. When the vacuum is below acceptable level, one should, before inspecting the vacuum line itself, check if caps are adequately screwed on the vials as a leak on one vial can affect the performance of the whole vacuum line. Double-septa vials (Table 65.1) can be used several times (at least seven evacuation–sampling–analysis cycles) (Rochette and Bertrand 2003). For practical reasons (identification of vials, control of the number of times vials were used with a given set of septa, etc.), we recommend using the same batch of vials for a given application (e.g., chamber measurements or soil air samples in a given study). Users must be aware that silicone septa are progressively altered by exposition to ambient air. Accordingly, they should be stored in sealed containers prior to use and replaced after approximately 6 months, regardless of the number of usage cycles. Fully evacuated Exetainers fitted to double-septa caps maintain a vacuum of $\geq$98%, 20 weeks after evacuation (Rochette and Bertrand 2003). Also, syringe needles must be handled carefully to avoid not only personal injury, but also damage to the piercing edges. Since damaged needles can shred septa and cause leaks, needle condition should be monitored and syringe needles should be replaced as required (B.H. Ellert, personal communication, 2005).

3 Correction of flux calculations to account for increasing water vapor concentration inside chambers during deployment requires that gas concentration be determined on dry samples (Rochette and Hutchinson 2005). Air samples can be dried by adding 2–3 mg of magnesium perchlorate ($Mg(ClO_4)_2$) into the vials before evacuation. Magnesium perchlorate is a very efficient desiccant that does not react with most gases of interest. However, it is a strong oxidizing agent and necessary precautions should be taken when handling this product (avoid contact with skin; avoid bringing into contact with acids and organic substances; consult container label and reference manual). For the same reason, vials should be kept upside-up during handling and storage to avoid a prolonged contact of magnesium perchlorate with the rubber septum.

4 At sampling time, a polypropylene syringe (Becton Dickinson, Rutherford, New Jersey; 26G3/8 needle) is inserted into the chamber sampling port and pumped a couple of times to fully flush the syringe and the dead volume of the port (approximately 1 mL) (see Table 65.1). After adequate flushing, 20–24 mL of air is injected into the vial. Injection should be done without applying lateral pressure to avoid deformation of the septa and associated possible alteration of the seal. The resulting positive pressure inside the vials (approximately 200 kPa) minimizes contamination by ambient air ($\sim$0.13% d^{-1}; Rochette and Bertrand 2003), avoids contamination when a subsample is taken for analysis, and can be used to detect leaky vials. Air should not stay longer than a few seconds in the polypropylene syringes to prevent gas leakage and adsorption on the syringe walls (Rochette and Bertrand 2003). Also, a syringe that was used for air at high gas concentrations should not be used for handling samples at low concentrations, as minute residual amounts of the former sample can result in appreciable contamination of the second.

5 On sampling days, a few vials ($\sim$4) are filled with an inert gas (N_2 or He) in the field or in the laboratory before departure for the experimental site using the same procedure as for the experimental samples. Determination of O_2 or CO_2 concentration in these samples (blanks) is used to assess contamination during vials preparation, handling, and storage. There is no benefit in storing air samples at low temperatures, and unpressurized samples (100 kPa) should be kept at a temperature greater or equal to that at sampling time. Containers other than Exetainers should be used only after demonstration of their ability to preserve the integrity of air samples during the required storage period.

6 Determination of gas concentration in air samples is usually done in the laboratory using methods that may vary for each gas and situation. For example, small samples can be analyzed for CO_2 in an infrared analyzer (Parkinson 1981), and ammonia in acid traps is often quantified by colorimetry (Rochette et al. 2001). However, gas chromatography is by far the most often used method for several gases routinely monitored in agricultural systems (CO_2, N_2O, CH_4, O_2) (Smith and Conen 2004). For changes in gas concentration usually encountered during deployment of chambers on agricultural soils, N_2O is measured using an electron capture detector whereas CO_2 (after passing through a methanizer) and CH_4 are analyzed using a flame ionization detector. An example of gas chromatograph specifications and performance for the determination of O_2, CO_2, N_2O, and CH_4 concentrations is given in Figure 65.1 and Table 65.2. With this configuration, duration of the analysis for CO_2 is approximately 5 min but can be as short as

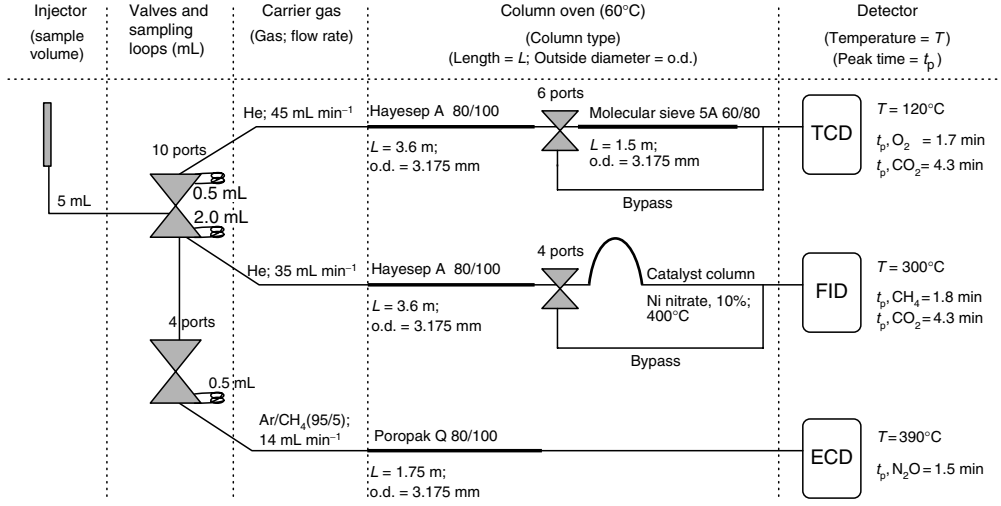

FIGURE 65.1. An example of a gas chromatograph configuration for the determination of CO_2, O_2, N_2O, and CH_4 in air samples.

2 min for N_2O and CH_4. Of course, the performance can be easily modified by changing column or detector temperatures, flow rates, and sample volumes. Calculation of the gas concentration is made using a calibration curve drawn using samples of known gas concentrations (reference gases), and after correction to account for ambient air contamination as determined in blank samples. Reference gases obtained from commercial suppliers should be checked against primary standards obtained from certified laboratories (Lemke et al. 2002). Samples of reference gases are inserted at intervals during the analysis of experimental samples (approximately one every five samples). Injection of samples into a gas chromatograph can be automated using a headspace autosampler when samples are stored in vials.

65.2.2 Chamber Design

1 Chambers can easily be built using rigid materials that do not react with the gases of interest such as acrylic plastic (see Table 65.1). Geometry of the chamber (square, rectangular, or cylindrical) has little impact on its performance as long as adequate air mixing is achieved. Accordingly, users are strongly encouraged to adapt chamber dimensions and shape to the situations where they are deployed and to the objectives of their study. The selection of the right chamber for a given situation is the first and most important step toward optimizing efforts and ensuring high-quality results. For a given F_g, chamber height determines dG/dt and the optimum deployment duration. Chamber heights <5 cm should be avoided as volume determination becomes difficult on uneven soil surfaces. On the other hand, high chambers may require long deployment durations to detect changes in G, allowing alteration of gas exchange rates beyond acceptable levels and resulting in inefficient field work. A chamber height of 15 cm is appropriate

TABLE 65.2 Reproducibility of Gas Concentration Analysis (O_2, CO_2, CH_4, and N_2O) Using a Gas Chromatograph Configured as in Figure 65.2

Detector	Sample volume (μL)	Reproducibility[a] at 200/360/5000/20000 μL CO_2 L^{-1} ($\pm$μL L^{-1})	Reproducibility[a] at 0.15/0.21 L O_2 L^{-1} ($\pm$mL L^{-1})	Reproducibility[a] at 0.3/0.95/10/15 μL N_2O L^{-1} ($\pm$nL L^{-1})	Reproducibility[a] at 1.0/2.0/10.0 μL CH_4 L^{-1} ($\pm$nL L^{-1})
Thermal conductivity	500	8/15 /43 /228	0.17/0.16	NA	NA
Flame ionization + methanizer	2000	0.4/0.7/7/—	NA	NA	9.9/6.0/12.0
Electron capture	500	NA	NA	0.9/2.4/19.6/34.4	NA

[a] Includes variability induced by sampling, handling, and automatic injection into the gas chromatograph (standard deviation of the mean of 20 consecutive analyses).

for most gases in most agricultural situations. Failure to determine dG/dt in 30 min deployments of a 10–15 cm high chamber is an indication that the corresponding F_g is very small and may not be significant in most environmental or agronomic studies. Except when experimental objectives dictate otherwise, chambers should cover an area as large as possible to integrate small-scale spatial variability in F_g. An example of a square chamber adapted for use in crops with wide interrows is presented in Figure 65.1 and Table 65.1. More information on the optimization of chamber design can be found in Rochette and Hutchinson (2005).

2 Forced ventilation inside chambers using small battery-operated fans mounted horizontally inside chambers can be used to ensure adequate mixing of the headspace volume. Chamber headspace mixing reduces variability between successive air samples and minimizes chamber deployment impact on soil-surface gas flux. Ideally, ventilation of chambers should result in mixing intensity similar to ambient levels. This requires adjusting fan speed to local conditions with high intensity in open windy situations and low or no forced ventilation when chambers are deployed under dense canopies.

3 Chambers should be vented to avoid pressure gradients between the inside and outside of chambers and associated alterations of soil-surface gas exchange. Vent design should be such that it transmits barometric pressure fluctuations while minimizing air leakage or contamination (Hutchinson and Mosier 1981; Livingston and Hutchinson 1995). For example, recommended dimensions for the venting tube of a 0.06 m^3 chamber used under typical agricultural field conditions are 24 cm in length and 1.5 cm in diameter (see Figure 65.1 and Table 65.1).

4 Chambers should be covered with a reflective and insulating material to minimize air temperature variations inside the chambers during deployment. This is especially important when chambers are deployed in open environments and for longer periods.

5 Inserting chambers into soil may bias flux measurement by damaging plant roots and altering gas diffusivity. Such perturbation can be avoided by using frames that are inserted into the soil before the measurement (1 h in a dry, bare sandy soil to several weeks when roots need to grow back). Depth of insertion varies with soil conditions and deployment duration but a 10 cm depth is valid for most deployments $\leq$60 min (Rochette and Hutchinson 2005). An airtight seal between the chamber and the frame can be achieved by creating a water barrier or by using a gasket made of rubber or closed-cell foam. Applying weight on top of chamber can ensure good contact between the chamber and frame, but may affect the gas flux if the frame moves (even slightly) under the added weight. An alternative to weighting the chamber is to use a fastener that connects the chamber to an anchor base on the frame (Figure 65.2). At the time of deployment, the fastener pulls the chamber and the frame together, therefore minimizing pressure on soil, deformation of the frame, and associated alteration of soil gas diffusivity. Leakage at the chamber–frame interface or through the venting tube can be tested by injecting a tracer (e.g., high concentrations of CO_2 or N_2O) inside a chamber sealed to a nonemitting surface and monitoring the rate at which the concentration of the tracer changes with time.

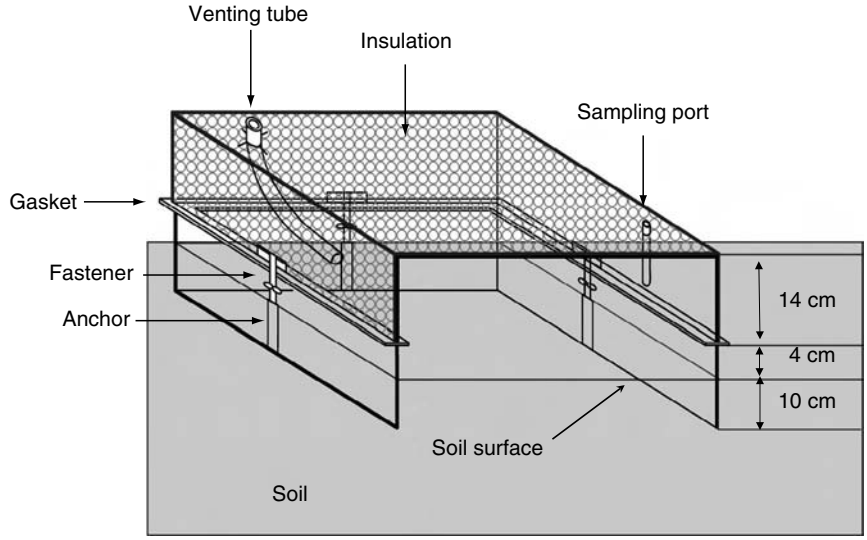

FIGURE 65.2. An example of a nonflow-through nonsteady-state chamber for the measurement of soil-surface gas fluxes.

65.2.3 Chamber Deployment

1 Chamber deployment duration should be the shortest period that allows for a measurable increase in gas concentration between successive air samples and for a statistically valid determination of dG/dt. To achieve this, the number of chambers handled by one operator should be kept low and the chambers deployed at relatively close sites. In the case of measurements made in an experimental design in which treatments are repeated, a group of chambers handled together should represent all replicate treatments. In preparation for the measurements, the chamber, the fasteners, and the sampling syringe (one per chamber) are placed close to each frame. Air temperature and humidity that will be used for flux calculation (Equation 65.1) are then measured immediately above the soil surface. The measurement routine starts when the first chamber is attached to its frame. The first or ''time 1'' air sample is drawn with the syringe as soon as possible after placement of the chamber. The average concentration in a series of ambient air samples taken above the soil surface can be used for all chambers in place of taking a ''time 0'' sample from each chamber. However, we recommend against this practice if the concentration of the gas of interest is variable (in space or time) or can be influenced by operators (e.g., CO_2). The time interval between each chamber depends on its location but is rarely shorter than 60 s.

2 After all chambers are installed and ''time 0'' samples taken, the operator revisits the chambers for successive rounds of air sampling, noting the time when each sample is taken. The time interval between successive visits to the same chamber depends on the number of simultaneously deployed chambers. This interval should be long enough to allow measurable increase in G (see Table 65.2) without inducing a large feedback of the chamber on gas exchange. Deployment duration should not exceed 20 min when F_g is high (most cases

for CO_2) (Rochette and Hutchinson 2005) and 60 min when F_g is low to avoid modifications of F_g beyond acceptable limits. Also, a total of three but preferably four or more samples are needed to adequately determine dG/dt. With such criteria, an operator sampling one chamber every minute will complete the four sampling cycles for a series of eight chambers in a total of 31 min, each chamber being deployed for 24 min. When simultaneously measuring the fluxes of several gases, a compromise must be reached between the sometimes conflicting requirements for the different gases. But under most conditions, deployment duration should not exceed 20 min for CO_2 if only four air samples are taken.

65.2.4 Flux Calculation

Because a change in gas concentration inside the chamber has an immediate impact on the gas flux rate at the soil surface, the value of F_g obtained from Equation 65.1 is often an underestimate of the flux rate that the NSS chamber was intended to measure. Several strategies have been proposed for minimizing bias in the measured value of dG/dt within an NSS chamber (Hutchinson and Mosier 1981; Rayment 2000). The most common is to estimate dG/dt as early as possible during deployment. Usually, a simple mathematical model is used to describe the time-dependence of changes in G, and dG/dt is estimated from the slope of that curve extrapolated to the moment of chamber deployment. This is achieved by obtaining the first derivative of the model and calculating its value at time $= 0$. Gas diffusion theory predicts that a change in G results in a decrease in gas exchange at the soil surface and therefore supports the use of nonlinear model (Hutchinson and Mosier 1981; Anthony et al. 1995; Pedersen 2000). Large underestimation of dG/dt may occur when a linear model is applied to nonlinear data even when the linear fit is very high (underestimation of 28% in Figure 65.3). Nonlinear (quadratic, cubic, exponential) models often yield less biased estimates of dG/dt, but may exhibit extreme sensitivity to measurement imprecision.

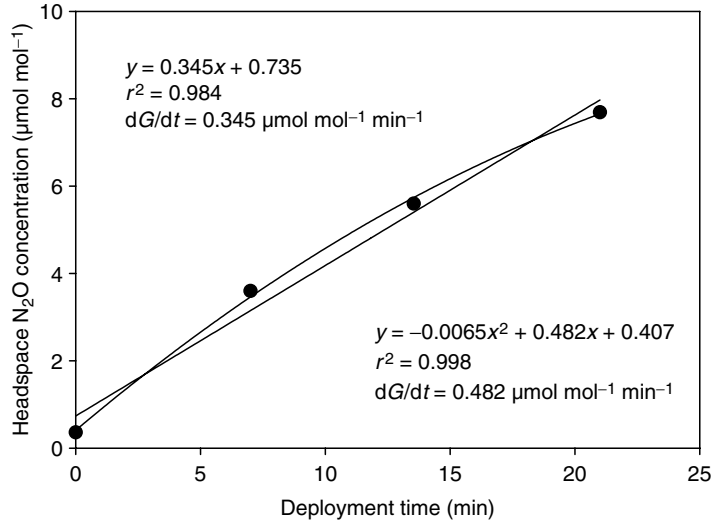

FIGURE 65.3. Determination of dG/dt at deployment time $= 0$ for a nonflow-through non-steady-state chamber using a linear and a nonlinear model.

As a result, the best choice of a model for estimating dG/dt must be a compromise that depends on the deployment duration, as well as the number and precision of G measurements. When in doubt, the linear model should be used because it usually minimizes the errors in flux calculation.

65.2.5 Comments

Gas concentration in NSS chambers can also be monitored using an on-site analyzer. Compared to the determination of gas concentration in discrete air samples, the use of a portable gas analyzer in flow-through NSS chambers provides a more detailed description of the pattern of change in G. The greater number and frequency of G measurements also facilitate using a shorter deployment period. Other advantages include early detection of experimental problems that would ultimately require the resulting data to be discarded, fewer problems related to leakage and lateral diffusion beneath the chamber walls, and smaller changes in air and soil temperature and humidity. Disadvantages of this chamber type include that it is limited to gas species for which a suitable portable analyzer is available, that the short deployment periods seldom allow for the simultaneous measurement of gases with low emission rates (e.g., N_2O, CH_4), and that they focus the sampling effort on the period most likely to exhibit the greatest influence of soil disturbance, changes in the air mixing regime at the soil surface, pressure effects, etc. Flux calculation methods and deployment protocols of flow-through NSS chambers may be found in Rochette and Hutchinson (2005).

65.3 STEADY-STATE CHAMBERS

Flow-through steady-state (SS) chambers offer several advantages compared to NSS chambers. Because they offer control on the chamber gas concentration (G), air temperature, and humidity, flux in SS chambers can be measured under conditions that are closer to ambient. Also, their design lends itself more easily to automation and near-continuous flux monitoring. On the other hand, they are more complex to operate than NSS chambers, require on-site gas analyzers, are usually limited to the measurement of one gas at a time, and their performance is sensitive to pressure gradients between the inside and the outside of the chambers. Consequently, of all the chamber measurements reported in the literature, very few were obtained using flow-through SS chambers. For this reason, they will not be presented in this chapter and readers are referred to recent reviews of chamber methods for more information on this technique (Smith and Conen 2004; Rochette and Hutchinson 2005).

Gas flux measurements at steady-state can also be achieved without air flow through the chamber. Nonflow-through SS chambers have variously been labeled in the past as a static chamber, absorption chamber, or alkali trap chamber. They contain a vessel that is supported above the soil surface and filled with a known amount of a substance that reacts with the gas of interest. Such chambers are typically deployed for long periods, often 12 or 24 h, and the amount of gas trapped by the substance is determined by laboratory analysis. For more information on this type of chamber, the reader is referred to a recent review by Rochette and Hutchinson (2005).

REFERENCES

Anthony, W.H., Hutchinson, G.L., and Livingston, G.P. 1995. Chamber measurement of soil–atmosphere gas exchange: Linear vs. diffusion-based flux models. *Soil Sci. Soc. Am. J.* 59: 1308–1310.

Hutchinson, G.L. and Mosier, A.R. 1981. Improved soil cover method for field measurement of nitrous oxide fluxes. *Soil Sci. Soc. Am. J.* 45: 311–316.

Lemke, R., Goddard, T., Hahn, D., Burton, D., Ellert, B., Farrell, R., Monreal, M., and Noot, D. 2002. An inter-laboratory comparison of nitrous oxide analysis in western Canada. *Commun. Soil Sci. Plant Anal.* 33: 2705–2713.

Livingston, G.P. and Hutchinson, G.L. 1995. Enclosure-based measurement of trace gas exchange: Applications and sources of error. In P.A. Matson and R.C. Harriss, Eds., *Biogenic Trace Gases: Measuring Emissions from Soil and Water*. Blackwell Science, Oxford, UK, pp. 14–51.

Parkinson, D. 1981. An improved method for measuring soil respiration in the field. *J. Appl. Ecol.* 18: 221–228.

Pattey, E., Edwards, G., Strachan, I.B., Desjardins, R.L., Kaharabata, S., and Wagner-Riddle, C. 2006. Towards standards for measuring greenhouse gas flux from agricultural fields using instrumented towers. *Can. J. Soil Sci.* 86: 373–400.

Pedersen, A.R. 2000. Estimating the nitrous oxide emission rate from the soil surface by means of a diffusion model. *Scand. J. Stat.* 27: 385–403.

Rayment, M.B. 2000. Closed chamber systems underestimate soil CO_2 efflux. *Eur. J. Soil Sci.* 51: 107–110.

Rochette, P. and Bertrand, N. 2003. Soil air sample storage and handling using polypropylene syringes and glass vials. *Can. J. Soil Sci.* 83: 631–637.

Rochette, P., Chantigny, M.H., Angers, D.A., Bertrand, N., and Côté, D. 2001. Ammonia volatilization and soil nitrogen dynamics following fall application of pig slurry on canola crop residues. *Can. J. Soil Sci.* 81: 515–523.

Rochette, P. and Hutchinson, G.L. 2005. Measuring soil respiration in situ: Chamber techniques. In J.L. Hatfield and J.M. Baker, Eds., *Micrometeorology in Agricultural Systems*. ASA Monograph. No. 47, American Society of Agronomy, Madison, WI, pp. 247–286.

Rolston, D.E. 1986. Gas flux. In A. Klute, Ed., *Methods of Soil Analysis, Part 1—Physical and Mineralogical Methods*, 2nd ed. Soil Science Society of America, Madison, WI, pp. 1103–1119.

Smith, K.A. and Conen, F. 2004. Measurement of trace gases I: Gas analysis, chamber methods, and related procedures. In K.A. Smith and M.C. Cresser, Eds, *Soil and Environmental Analysis, Modern Instrumental Techniques*, 3rd ed. Marcel Dekker, Inc., New York, pp. 433–476.

Chapter 66
Bulk Density Measurement in Forest Soils

D.G. Maynard
Natural Resources Canada
Victoria, British Columbia, Canada

M.P. Curran
British Columbia Ministry of Forests
Nelson, British Columbia, Canada

66.1 INTRODUCTION

Many of the physical properties important for assessing soils in agricultural systems are the same for forest soils. However, because of the nature of forest soils and terrain associated with forest ecosystems, the most appropriate methods for agricultural soils are not always suitable for forest soils. Coarse fragments, large roots, and steep slopes limit the suitability of some methods for forest soils (Page-Dumroese et al. 1999). In addition, surface organic horizons cover many forest soils and measuring their physical properties such as bulk density requires different sampling methods than mineral soils.

Compaction is one of the key physical processes that is affected by forest management and can influence soil productivity in forest soils (Powers et al. 1998). It has mainly been measured by bulk density but other measurements such as aeration porosity, and soil strength have been used to evaluate the effects of soil compaction. Soil strength can be determined by a cone penetrometer, a device that measures the soil's resistance to penetration by, for example, a root tip (Miller et al. 2001). Determining soil strength by using a cone penetrometer has certain advantages over measuring bulk density, but it is not effective in stony soils (e.g., high variation), a common condition in forest soils (Powers et al. 1998; Miller et al. 2001). Even when a penetrometer is used, bulk density data should be available to provide some interpretation of the readings (e.g., Miller et al. 2001). A recording penetrometer can be very useful in evaluating compaction at depth, such as from forest harvesting equipment traffic. Soil moisture content should be determined each time a penetrometer is used because readings will vary with moisture content, and different soil disturbances will often have different moisture contents (Busscher et al. 1997).

Organic matter plays a dominant role in the bulk density of the soil because of its much lower density than mineral particles and its aggregation effect on soil structure (De Vos et al. 2005). Generally, the higher the organic matter the lower the bulk density. Estimates of bulk density on specific soils have been made from organic matter concentrations using regression equations (e.g., Alexander 1989; Grigal et al. 1989; Huntington et al. 1989; Prevost, 2004). Caution should be used, however, in estimating bulk densities from organic matter content, particularly when applied to soils and environments different than the ones in which the original coefficients were calibrated (De Vos et al. 2005). This technique would only be useful for looking at general trends among soils and would not be appropriate for evaluating the effects of soil disturbance on compaction.

There are a number of factors that need to be considered in determining the most appropriate methods for assessing soil compaction. Quick, less accurate methods may be the most appropriate for field surveys while highly accurate, more expensive, and more time-consuming methods may be needed for research studies (Miller et al. 2001). However, some measure of bulk density is necessary to determine nutrient content (including carbon) on an area basis (kg ha^{-1}).

This chapter presents a bulk density method for surface organic (LFH) and mineral horizons in forest soils. The determination of bulk density on mineral soils is based on the excavation and sand replacement method (Blake and Hartge 1986). This method is particularly relevant to stony forest soils.

66.2 PRINCIPLE

The excavation and volume determination for bulk density is accurate, can be used in forest soils with high coarse fragment contents, and the samples can be used for additional physical and chemical analysis (Page-Dumroese et al. 1999; Maynard and Senyk 2004). The advantages of the excavation method are relative easy of use; it has a low standard error and can give an accurate estimate of coarse fragments (Page-Dumroese et al. 1999). Bulk density is determined on both the total soil and fine fraction (<2 mm). The fine fraction bulk density is critical when converting soil nutrient and carbon data to a mass-per-area basis for nutrient budgets and carbon balance studies in soils with high coarse fragment content, since usually only the fine soil fraction is analyzed for C or N. The main disadvantage of the excavation method is it is more labor-intensive than simple coring or nuclear methods. If sand is used to determine volume, then portability becomes an issue in remote locations; however, this can be partially overcome by using glass beads or polyurethane expanding foam (see Section 66.4.4) rather than sand to determine the volume of the hole.

66.3 SURFACE ORGANIC HORIZON (LFH)

66.3.1 Material and Supplies

1 Square frame (20 × 20 cm)

2 Knife, machete, clippers

3 Tape measure

4 Plastic bags

5 Forced air-dry oven capable of 105°C

66.3.2 Procedure

1 For most forest soils, the bulk density of the LFH is not separated into individual organic layers (e.g., L, F, or H).

2 Place the frame (20 × 20 cm) on the surface of the organic material.

3 Remove green (live), above-ground plant materials like herbs, grasses, and live moss.

4 Cut out the organic material from inside the frame with the knife and put in a labeled plastic bag taking care to avoid contamination from the mineral soil. Small amounts of mineral material can result in large errors in the weight of the material because of the difference in bulk density between organic and mineral soil.

5 Take several measurements to determine the depth of the LFH (e.g., every corner and center of each side yields eight measurements).

6 At the laboratory, oven-dry the sample at 105°C for 24 h and determine the oven-dry weight. If a portion of the sample is going to be used for chemical analysis that requires field moist or air-dried material, then an intermediate step can be included to determine moisture content on a subsample and incorporate that into the procedure.

66.3.3 Calculations

$$V_{\mathrm{LFH}} = 400\ \mathrm{cm}^2\ \mathrm{Dep}_{\mathrm{LFH}}\ (\mathrm{cm}) \tag{66.1}$$

$$D_{\mathrm{b(LFH)}} = \mathrm{Wt}_{\mathrm{(LFH)}}/V_{\mathrm{LFH}} \tag{66.2}$$

where V_{LFH} is the volume of the hole (cm^3), $\mathrm{Dep}_{\mathrm{LFH}}$ the depth of the hole, $D_{\mathrm{b(LFH)}}$ the bulk density of the surface organic horizon, and $\mathrm{Wt}_{\mathrm{LFH}}$ the oven-dry weight of the surface organic material.

66.3.4 Comments

On soils with an Ah horizon under the LFH, distinguishing between the organic and mineral horizon may be difficult. In the field, if any mineral material is detected when a moist sample is smeared between the thumb and forefinger, the sample is likely mineral.

The size of the frame may have to be adjusted depending on the depth of the LFH. For example, if the forest floor is deeper than 20 cm, a smaller frame should be used to limit the volume of organic material collected.

66.4 MINERAL SOILS

66.4.1 Material and Supplies

1 Sand-funnel apparatus—a metal funnel with a valve on the stem to control the flow of sand when the funnel is inverted. The funnel is 10 cm in diameter matching the size of the hole in the template (commercially available).

2 Template is a flat metal plate 30 × 30 cm (ridged) with the 10 cm hole in the center.

3 Sand with uniform particle size that is clean, dry, and free flowing. Ottawa sand (mined in Ottawa, Illinois) is often used because the sand particles are relatively uniform in size and spherically shaped.

4 Field balance sensitive to 0.1 g.

5 Knife, clippers.

6 Tape measure.

7 Plastic bags.

8 Sieves—2 mm.

9 Forced air-dry oven capable of 105°C.

66.4.2 Procedure

1 Fill a density cone bottle with sand and weigh. The weight of sand held in the cone is predetermined in the laboratory. This will be subtracted from the total weight of sand used to fill a hole.

2 When the sampling location is determined, remove moss and other vegetation and any organic horizon material from the surface of the soil.

3 Place a density plate over sampling spot using nails (20 cm in length) to hold it down. Place a plastic sheet under each side of the metal plate.

4 Using spoons, scissors, knife, and small trowel to remove soil in as close to a cylindrical pattern as possible, to the depth required placing the soil in a tared container.

5 Record the depth of the hole (cm). A standard depth of 10 cm is often used but for some conditions and depending on the objectives, sampling may be done by horizon depth.

6 Weigh container with the soil.

7 Place the soil from the container into a labeled plastic bag.

8 Place sand bottle with cone onto metal plate and open stopper to allow the sand to pour into the hole. Ensure a tight fit so that no sand leaks out between the cone and the plate.

9 When the sand stops flowing, close the stopper and remove the sand bottle. Reweigh the sand bottle.

10 Collect the sand left in the hole for reuse. If the sand is dirty or wet, sieve and dry it, or discard it.

11 Refill the sand bottle and weigh it for the next sample.

12 At the laboratory, remove the soil from the bags and air-dry the soil. Sieve the soil (breaking up the soil clumps only) to <2 mm fraction.

13 Weigh the <2 mm fraction of soil, and the coarse material (>2 mm), organic material (e.g., roots), and rock.

14 Oven-dry the <2 mm soil at 105°C for 24 h. If the sample is too large for complete oven-drying, or a portion of the sample is going to be used for chemical analysis that requires field moist or air-dried material, then an intermediate step can be included to determine moisture content on a subsample and incorporate that into the procedure.

15 Determine the oven-dry weight of the sample.

66.4.3 Calculations

The preferred SI unit is Mg m^{-3}, which is numerically equal to g cm^{-3}. Bulk density for fines (<2 mm soil fraction). The volume and weight of large roots may be important and can be determined using the same approach for determining the weight and volume of rock:

$$\text{WSH (g)} = (\text{SWB} - \text{SWA}) - \text{WSC} \tag{66.3}$$

$$\text{VH (cm}^3) = \text{WSH}/D_{\text{b(sand)}} \tag{66.4}$$

$$\text{VR (cm}^3) = \text{WR}/D_{\text{p(rock)}} \tag{66.5}$$

$$\text{VF (cm}^3) = \text{VH} - \text{VR} \tag{66.6}$$

$$\text{BDF (g/cm}^3) = \text{DWF}/\text{VF} \tag{66.7}$$

where

WSH = weight of sand in the hole,
SWB = sand weight before inverting in the hole,
SWA = sand weight after the hole is filled,
WSC = weight of sand in the cone (predetermined in the laboratory),
VH = volume of the hole,
$D_{b(sand)}$ = bulk density of the sand,
VR = volume of the rock,
WR = weight of the rock (>2 mm fraction),
$D_{p(rock)}$ = particle density of the rock (normally 2.65 g cm^{-3}),
VF = volume of the fines,
BDF = bulk density of the fines,
DWF = oven-dry weight of the fines.

Total bulk density

$$TW = DWF + DWC \tag{66.8}$$

$$BDT = TW/VH \tag{66.9}$$

where

TW = total oven-dry weight of material removed from the hole,
DWF = oven-dry weight of the fines,
DWC = dry weight of the coarse fragments,
BDT = total bulk density,
VH = volume of the hole.

66.4.4 Comments

The volume of the hole can also be determined with glass beads or polyurethane foam. If glass beads are used, a plastic bag is used to line the hole, and the bag is filled flush to the surface with the glass beads. The volume is then determined by pouring the beads into a graduated cylinder. If polyurethane expanding foam is used, foam is added to the excavated hole, covered with a piece of cardboard, and held in place with a rock while the foam dries—usually 2 h with fast-drying foam. Foam volume is determined in the laboratory by submersion in water (Muller and Hamilton 1992).

If more than one depth or horizon is to be sampled for bulk density, then it is necessary to dig a trench or small pit below the desired depth. The density plate is located at the edge of the trench. Once the surface bulk density has been sampled, the soil is removed (area of the plate) to the next depth (bottom of the hole) and a flat surface is prepared for the template.

The diameter of the hole in the density plate is usually 10 cm. Plates with larger diameter holes are available. Large diameter holes can reduce sample variability but collecting large samples particularly from remote locations may not be practical.

If a rock fills more than half of the hole, redo the sample.

REFERENCES

Alexander, E.B. 1989. Bulk density equations for southern Alaska soils. *Can. J. Soil Sci.* 69: 177–180.

Blake, G.R. and Hartge, K.H. 1986. Bulk density. In A. Klute, Ed. *Methods of Soil Analysis. Part I*, Agronomy No. 9, American Society of Agronomy, Madison, WI, pp. 464–475.

Busscher, W.J., Bauer, P.J., Camp, C.R., and Sojka, R.E. 1997. Correction of cone index for soil water content differences in a coastal plain soil. *Soil Till. Res.* 43: 205–217.

De Vos, B., Van Meirvenne, M., Quataert, P., Deckers, J., and Muys, B. 2005. Predictive quality of pedotransfer functions for estimating bulk density of forest soils. *Soil Sci. Soc. Am. J.* 69: 500–510.

Grigal, D.F., Brovold, S.L., Nord, W.S., and Ohmann, L.F. 1989. Bulk density of surface soils and peat in the north central United States. *Can. J. Soil Sci.* 69: 895–900.

Huntington, T.G., Johnson, C.E., Johnson, A.H., Siccama, T.G., and Ryan, D.F. 1989. Carbon, organic matter, and bulk density relationships in a forested Spodsol. *Soil Sci.* 148: 380–386.

Maynard, D.G. and Senyk, J.P. 2004. Soil disturbance and five-year tree growth in a montane alternative silvicultural systems (MASS) trial. *Forest. Chron.* 80: 573–582.

Miller, R.E., Hazard, J., and Howes, S. 2001. Precision, accuracy, and efficiency of four tools for measuring soil bulk density or strength. Res. Paper PNW-RP-532: U.S. Department of Agriculture, Forest Service, Pacific Northwest Research Station, Portland, OR.

Muller, R.N. and Hamilton, M.E. 1992. A simple, effective method for determining the bulk density of stony soils. *Commun. Soil Sci. Plant Anal.* 23: 313–319.

Page-Dumroese, D.S., Jurgensen, M.F., Brown, R.E., and Mroz, G.D. 1999. Comparison of methods for determining bulk densities of rocky forest soils. *Soil Sci. Soc. Am. J.* 63: 379–383.

Powers, R.F., Tiarks, A.E., and Boyle, J.R. 1998. Assessing soil quality: practicable standards for sustainable forest productivity in the United States. In J.M. Bigham et al. Eds. *The Contribution of Soil Science to the Development of and Implementation of Criteria and Indicators of Sustainable Forest Management*. Special Publ. No. 53, Soil Science Society of America, Madison, WI, pp. 53–80.

Prevost, M. 2004. Predicting soil properties from organic matter content following mechanical site preparation of forest soils. *Soil Sci. Soc. Am. J.* 68: 943–949.

Chapter 67
Physical Properties of Organic Soils and Growing Media: Particle Size and Degree of Decomposition

L.E. Parent and J. Caron
Laval University
Quebec, Quebec, Canada

67.1 INTRODUCTION

In Canada and in Northern Europe, organic soils are of great importance in vegetable and tree production and for harvesting sphagnum peat moss. They are typically found in wetland environments, rich in wildlife activities, constituting specific ecosystems hosting a unique biodiversity. They have for a long time been recognized as soil systems requiring specific management techniques when used for vegetable and tree production. Some peat bogs are also used for sphagnum peat moss production, a dominant component of growing media around the world. Because of the nature and characteristics of organic soils, specific methodologies related either to the context of wetland use and preservation, to their use for cultivation and tree planting or to the design and manufacturing of organically based growing media have had to be designed over the years. These next two chapters summarize some of these methods.

Methods for determining the physical properties of organic soils and growing media can be divided into three main categories: those related to their particle size distribution and degree of decomposition, those related to the storage of water and air in a structured bulk volume and its wettability, and finally those related to the dynamics of water and air movement in and across the bulk volume. This chapter deals with peat and growing media particle size and degree of decomposition.

67.2 DEGREE OF DECOMPOSITION

The physical properties of peat are of primary importance when using peat in horticulture and for studies on peat hydrology. Measurements of the degree of decomposition are generally well correlated with a number of physical and chemical properties of peat materials. The degree of decomposition of peat materials is thus an important property in relation to classification and evaluation of the material for various uses (Parent 1980). Degree of decomposition or degree of humification of peat materials is assessed by measuring their fiber or humus contents. Fiber and humus contents are conjugate compositional pairs separated by passing peat materials through sieves of 60 or 100 mesh size (0.25 or 0.15 mm openings, respectively). In practice, peat decomposition is determined by a field method, the von Post pressing method (von Post and Granlund 1926; Grosse-Brauckmann 1976), and by laboratory methods, the most commonly used being the fiber volume method (Farnham and Finney 1965; Sneddon et al. 1971; Lynn et al. 1974), the mechanical dispersion and sieving method (Dinel and Lévesque 1976), the centrifugation method for peat standards (Lishtvan and Kroll 1975; Malterer 1988; Malterer et al. 1992), and the Kaila colorimetric method (Kaila 1956; Schnitzer and Desjardins 1966; Lynn et al. 1974).

After drainage and reclamation, the amended, fertilized, and cultivated organic soils undergo physical, chemical, and biological transformations such as irreversible dehydration, darkening, decomposition, and microbial colonization, leading to more granular and dusty organic materials very different from the original peat materials. Such a process has been called muck-forming or moorsh-forming (Okruszko and Ilnicki 2003). The end product of the process is a degraded soil, with fine grains, very susceptible to wind erosion in surface horizons, and the formation of a coke layer below the surface horizons (Okruszko and Ilnicki 2003). Soil structure, generally lamellar in peat materials of a low to medium degree of decomposition, becomes grainy or granular in the surface horizons of the moorsh, and blocky or prismatic underneath the surface horizons and above the original peat layers (Ilnicki and Zeitz 2003). The von Post method and the fiber volume method are not appropriate for moorsh materials.

67.2.1 von Post Pressing Method

This method, introduced by the Swedish scientist Lennart von Post in 1922 (von Post and Granlund 1926), is the most reliable field method for soil and geological surveys.

Procedure

A fresh peat sample is first pressed in the palm of the hand. The color or turbidity of the extruded liquor or mud collected on the dorsum of the other hand, as well as the proportion of extruded matter, are the only criteria for classifying peat materials. Field observations are matched to one of ten humification degrees (H1 to H10) on the von Post scale (Table 67.1).

Comments

The von Post pressing method is not recommended for relatively dry peat materials and for the upper peat layers of drained organic soils, since the humification degree of these less compressible materials is underestimated (Grosse-Brauckmann 1976). The H values can be classified into fibric (H1 to H3), mesic (H5 to H6), and humic (H7 to H10) materials, H4 being fibric in the Canadian scheme and mesic in the German scheme. The von Post method is highly dependent on

TABLE 67.1 The von Post Scale (H) for Assessing the Degree of Peat Decomposition

H	Plant residues	Extruded matter	Residues after pressing
1	Unaltered	Clear water	Nonpasty
2	Distinct	Brown-yellow, clear water	Nonpasty
3	Distinct	Brown turbid water	Nonpasty
4	Distinct	Brown, very turbid water	Nonpasty
5	Distinct	Brown, very turbid water with plant residues	Somewhat pasty
6	Somewhat indistinct[a]	One-third of the peat material extruded	Very pasty
7	Indistinct but recognizable	One-half of the peat material extruded	Very pasty
8	Very indistinct	Two-thirds of the peat material extruded	Few fibers
9	Almost nonrecognizable	Almost all peat material extruded	Few fibers
10	Nonrecognizable	All peat material extruded	No residues

Source: After Grosse-Brauckmann, in K. GöSttlich (Ed.), *Peat Stratification*, Scheizerbart'sche Verlag, Stuttgart, Germany, 1976, 91–133.

[a] Plant residues rather indistinct, but more identifiable in the pressed residue than in the original peat material.

the investigator's skill. Because the von Post scale is based on an ordinal scale, the use of parametric statistical tests has been questioned (Parent et al. 1982), particularly when using the mean instead of the median value for a limited number of replicates.

67.2.2 Fiber Volume Method (Lynn et al. 1974)

This method is an objective alternative to the von Post pressing method to classify peat materials. Fibers are separated from nonfibers by sieving rubbed or unrubbed peat materials through a 100 mesh (0.15 mm) screen.

Materials and Reagents

1. A graduated 5 mL medical half-syringe adjusted for a volume of 2.5 mL (a 5 mL plastic syringe is cut on both sides, longitudinally, to make the half-syringe)
2. Running tap water
3. A 100 mesh sieve (0.15 mm), 8 cm in diameter
4. Absorbing tissue

Procedure

1. Place approximately 25 mL of a wet sample in a piece of absorbing tissue and roll with light pressure to extract excess water. Unroll the tissue and cut the sample into 6 mm long pieces. Mix the subsamples randomly.
2. Pack the half-syringe with randomly selected subsamples and compress just enough to saturate the material, and force out any entrapped air. Do not force

out any water. It is to this water content that the residue must be returned to later when the residue volume is determined.

3 For fiber determination, transfer the 2.5 mL sample to a 100 mesh sieve and wash under running tap water until the effluent appears clear. Remove excess water through the underside of the sieve by blotting with an absorbing tissue. Repack the residue into the half-syringe, and blot further with an absorbing tissue until the water content reaches the state described above. Read the residue volume on the half-syringe and record it as percent unrubbed fiber. Transfer the residue to the 100 mesh sieve and rub between the thumb and forefinger under a stream of running tap water until the effluent is clear. Blot and repack the residue into the half-syringe and proceed as for the unrubbed fiber. Read the volume and record it as percent rubbed fiber.

Comments

Lévesque and Mathur (1979) found that fiber content was well correlated with the relative biodegradability of 26 pristine peat materials ($r = 0.58$). However, the fiber method showed coefficients of variation (CVs) from 12.7% to 22% compared to CVs ranging from 5.0% to 7.2% for the centrifugation method (Malterer 1988; Malterer et al. 1992).

67.2.3 Centrifugation Method (Ministry of Fuel Industry RSFSR 1976)

This method, introduced in 1965 as the Soviet standard, involves separating fibers from the so-called coagulated humus by sieving peat material through a 60 mesh (0.25 mm) screen in a centrifuge. The degree of peat decomposition is determined graphically on a reference nomogram relating the collected sediment volumes before and after sieving. The method is applicable to all natural peat types, but peat materials containing less than 65% H_2O (w/w) require a pretreatment as shown below. This method is not calibrated for processed (milled) peat, since peat fragmentation during processing causes a two- to three-fold increase in the measured degree of decomposition.

Materials and Reagents

1 Electrical centrifuge with a time relay for automatic cutoff 2 min after the switch is closed, sample tube holders and cups to fit either large or small centrifuge test tubes (Figure 67.1). The tubes must be graduated by 0.1 mL up to 1.5 mL.

2 Screen-bottomed cylindrical cups made with a 60 mesh (0.25 mm) screen fixed to a PVC ring 22 mm high and 28 mm I.D. (Figure 67.1). The 60 mesh screen is cemented to the lower wall of the PVC ring with a water-resistant adhesive. The cups must be easily inserted into the large test tubes.

3 Square plate of 25 × 25 cm, sample selector, and plunger. The sample selector is a copper tube, 5 mm in diameter, with an end sharpened to cut through a 3–4 mm peat layer spread over the plate. A plunger is used to push the peat out of the sample selector. All pieces are washed after each sampling.

4 Chemical solutions: 1 *M* NaOH or 1 *M* KOH, 1 *M* HCl, $FeCl_3$ 10%.

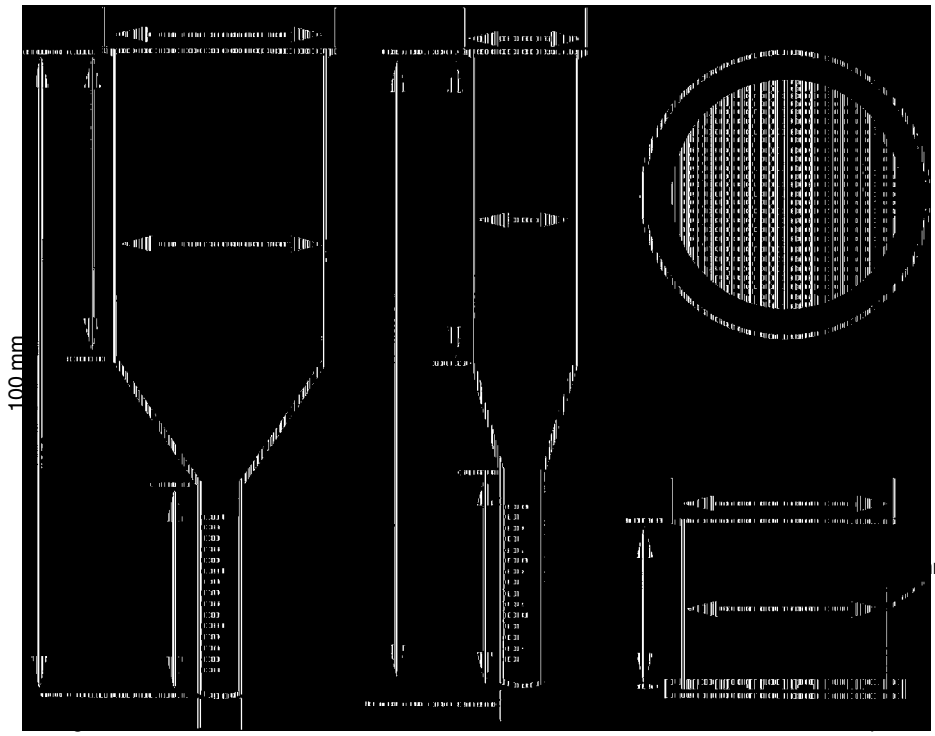

FIGURE 67.1. Tube used for centrifugation method for degree of decomposition.

Procedure for Peat Material Containing More Than 65% H_2O (w/w)

1 A peat sample weighing 100–200 g is spread out gently on the plate in order to obtain a uniform layer 3–4 mm thick. This layer is punched with the sample selector at 10–12 points over the surface, including areas of coarse residues. The sample, approximately 10 mm long, is pushed out with a plunger into the small test tube and covered with water up to 1 cm from the brim. One to two drops of the ferric chloride solution is added, to coagulate humus, and the sample well-mixed with a rod to obtain a homogeneous suspension. At least four parallel determinations are conducted for statistical reliability.

2 The small test tube is spun in a centrifuge for 2 min at 1000 rpm. Relative centrifugal force depends on the rotating radius from the pivot (nearly 200*g* per $r = 17.5$ cm). The volume of sediment, average level estimated by eye, is measured to the nearest 0.01 mL. The supernatant liquid must be clear. If not, add more drops of ferric chloride solution. The volume should be 0.7–1.5 mL (the sample weighs approximately 0.3–0.5 g), but 0.7–1 mL for humic peats.

3 The peat material is suspended again and transferred into a screen-bottomed cup placed on top of the large tube. The small tube is rinsed with 3–4 mL of water. The radius of the screen-bottomed cup is 10 cm. The peat material is centrifuged for 2 min at 1000 rpm. The volume of sediment is measured to the nearest

0.01 mL. The presence of peat clumps on the screen after centrifugation indicates poor peat dispersion; in such a case the analysis should be repeated.

Procedure for Peat Materials Containing Less Than 65% H_2O (w/w)

1 Portions of such peat materials are placed into a porcelain dish so that two-thirds to three-fourths of the cup volume is occupied after peat swelling. The cup is flooded with an alkali solution (1 *M* NaOH or 1 *M* KOH) and equilibrated for 24–30 h. Then, after stirring by hand, peat clumps are broken up. More alkali is added as needed to obtain a uniform mixture. A sample is taken from the dish with the sample selector and put into the small test tube. The small test tube is half-filled with a 1 *M* HCI solution, shaken, and equilibrated for 2–5 min until the neutralization reaction is completed. Then, the small test tube is filled with water up to 1 cm from the brim. Five to eight drops of the ferric chloride solution are added and the mixture is shaken.

2 The small test tube is centrifuged for 2 min at 1000 rpm. After measurement of the volume of sediment to the nearest 0.01 mL, the supernatant liquid is decanted carefully without disturbing the sediment. The test tube is refilled with water and one to two drops of the ferric chloride solution are added and shaken. The sample is further handled at Step 3 as described previously.

Comments

The centrifugation method was the official method for establishing the Soviet peat standards for peat and peatland complex utilization. The rotating speed of the centrifuge should be corrected for rotating radii differing from the 17.5 cm. The relative centrifugal force should be 190*g*–200*g*. The centrifugation method was found more sensitive and repeatable as noted earlier than the fiber volume method (Malterer 1988).

Data Analysis

1 The degree of peat decomposition (*R* in percent) is obtained by reporting the volumes of sediment in the small test tube and in the large test tube on a nomogram (Figure 67.2). The degree of decomposition *R* is read on the right-hand side for each peat type. The higher the degree of decomposition, the higher the *R* value.

2 The degree of decomposition is corrected for values of ash content exceeding 15% (Table 67.2).

3 Analytical precision depends on degree of decomposition and peat water content (Table 67.3).

67.2.4 Colorimetric Method

This method, introduced by the Finnish peat scientist Kaila (1956), is based on the capacity of an alkaline solution of sodium pyrophosphate to extract and solubilize humic

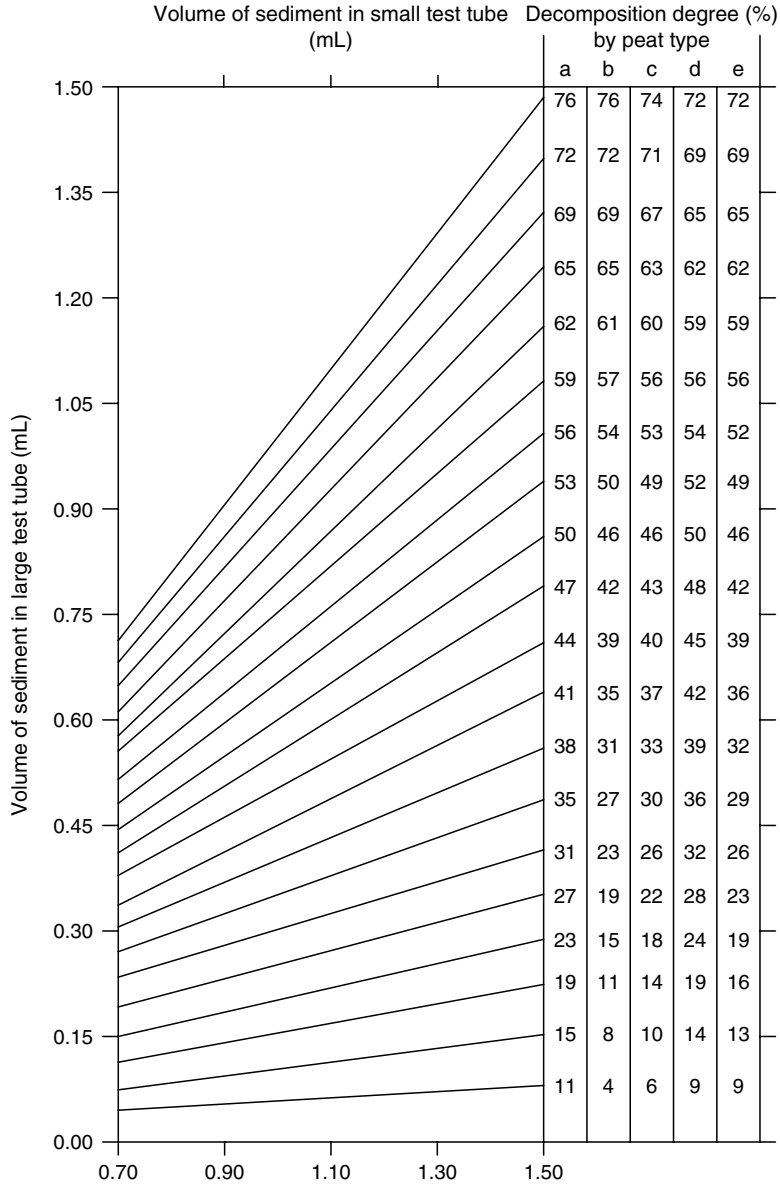

FIGURE 67.2. Nomogram used for the interpretation of degree of decomposition with the centrifugation method. Peat types: a = pine-cottongrass (*Eriophorum*), cottongrass, cottongrass-*sphagnum* highmoor peat types; b = all other highmoor peat types; c = transitional peat types; d = woody peat types; e = all other lowmoor peat types. (Adapted from Ministry of Fuel Industry RSFSR, *The State Standard of the USSR Peat*, Trans. Comm. I Int. Peat Soc.: Working Group for the Classification of Peat, Helsinki, Finland, 1976, 57–66.)

substances. The colorimetric determination of the filtrate at 550 nm or the color of the filtrate matched in a Munsell Color Chart (on the 10 YR page) is a measurement of the degree of decomposition.

TABLE 67.2 The Degree of Decomposition May Be Corrected for Ash Content Exceeding 15% by Subtracting the Following Values from the Calculated Values

Ash content (%)	Subtracting value (%)
≤15	0
15–25	2
25–35	3
35–45	4
45–55	5

Source: Adapted from the Ministry of Fuel Industry RSFSR, *The State Standard of the USSR Peat*, Trans. Comm. I Int. Peat Soc.: Working Group for the Classification of Peat, Helsinki, Finland, 1976, 57–66.

Materials and Reagents

1 A 2.5 mL half-syringe, a 30 mL plastic container, chromatographic paper, Erlenmeyer flasks, reciprocating shaker, funnels, and spectrophotometer

2 Sodium pyrophosphate ($Na_4P_2O_7 \cdot 10H_2O$), as crystals or 0.025 *M* solution (dissolve 11.152 g of $Na_4P_2O_7 \cdot 10H_2O$ per L of distilled water)

Procedure Using the Munsell Color Chart (Lynn et al. 1974)

1 Mix a 2.5 mL half-syringe sample with approximately 1 g of sodium pyrophosphate crystals and 4 mL of water in a 30 mL plastic container, and allow the mixture to stand overnight.

2 Mix again and insert a strip of chromatographic paper (0.5 × 3 cm) to absorb the colored solution. Allow the strip to moisten completely. Tear off the soil end, blot the strip gently on another sheet of chromatographic paper, and compare the colored strip with a Munsell Color Chart (on the 10 YR Munsell page).

3 Calculate a pyrophosphate index (PI) by subtracting the chroma from the value (PI = value − chroma).

4 For taxonomic purposes, a PI of 5 indicates fibric material; a PI of 3 or less is characteristic of sapric materials.

TABLE 67.3 Precision of Determination of the Degree of Decomposition of Peat (%)

	Degree of decomposition (%)			
Water content (% w/w)	1–15	15–30	30–50	>50
>65	1.5	2.0	3.0	5.0
<65	2.0	3.0	5.0	5.0

Source: Adapted from the Ministry of Fuel Industry RSFSR, *The State Standard of the USSR Peat*, Trans. Comm. I Int. Peat Soc.: Working Group for the Classification of Peat, Helsinki, Finland, 1976, 57–66.

Procedure Using Colorimetric Determinations (Schnitzer and Desjardins 1966; Vaillancourt et al. 1999)

1. Weigh 0.5 g of air-dried and 2 mm sieved peat material and transfer into 125 mL flasks.
2. Add 50 mL of 0.025 *M* sodium pyrophosphate solution and shake for 18 h at 300 rpm on an end-over-end shaker at room temperature. Centrifuge sample at 2000 rpm (1118 *g*) for 30 min before filtration. Filter (Whatman no. 1 paper) and dilute filtrate to 250 mL with distilled water.
3. Read absorbance at 550 nm on a spectrophotometer and multiply absorbance by 100 to give cardinal numbers for percent absorbance (PA). Also read absorbance at 465 and 665 nm.
4. Data on a limited number of peat materials indicate that PA < 40 classifies materials as ''peat,'' and that PA > 60 classifies materials as ''muck.'' A ratio of optical densities at 465 and 665 nm (E_4/E_6 ratio) between 2.0 and 5.0 generally indicates high molecular condensation, whereas higher E_4/E_6 ratios are indicative of more open structures (Schnitzer 1970).

Comments

In many cases, pyrophosphate values disagree with other determinations of degree of decomposition (Kaila 1956). PI values are subject to bias due to light intensity and to color perception by different operators (Malterer et al. 1992). The colorimetric methods are semiquantitative and best used to compare peat materials of similar origin and botanical composition, since the humification process and the original polyphenol content depend on peat genesis and peat-forming plant communities (Grosse-Brauckmann 1976; Williams and Yavitt 2003).

67.3 PARTICLE SIZE DISTRIBUTION AND WOOD CONTENT OF PEAT MATERIALS

67.3.1 Particle Size Distribution

Particle size distribution extends the notion of degree of decomposition to more than two particle fractions. The procedure for obtaining particle size distribution was described by Dinel and Lévesque (1976) and Lévesque and Dinel (1977).

Materials and Reagents

1. Reciprocating shaker.
2. 500 mL Erlenmeyer flask.
3. Filter paper (coarse, Whatman no. 1).
4. A 200 mesh sieve.
5. Particle size apparatus. The apparatus consists of a cylinder with an interior diameter of 14.5 cm and a height of 46 cm with a hole near the base for entry of air and an outlet for water. A piece of rubber tubing about 1.5 cm in diameter and

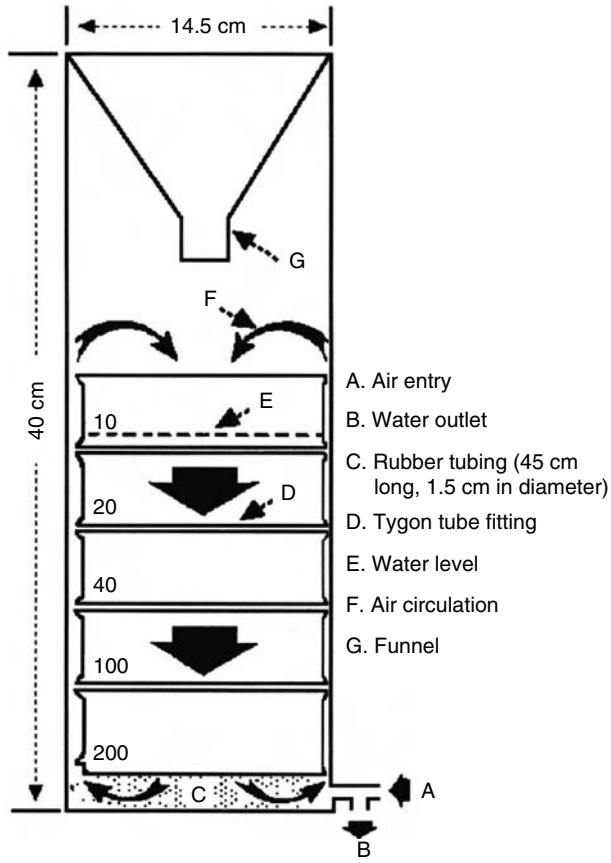

FIGURE 67.3. Apparatus used for the wet sieving of peat material. (From Dinel, H. and Lévesque, M., *Can. J. Soil Sci.*, 56, 119, 1976. With permission.)

45 cm long is formed into a ring and placed at the bottom of the cylinder. A nest of sieves, 13.5 cm in diameter, and in the following order, 10, 20, 40, 100, and 200 mesh, is assembled with a gasket made from thin (2 mm) Tygon tubing positioned between each sieve to provide a seal. The sieves are held together with an elastic band and inserted into the cylinder. The top of the cylinder is closed with a funnel. See Figure 67.3.

6 Drying cans.

7 Oven, preferably ventilated to a fume hood.

8 Preserving solution of the following composition: 10% formaldehyde, 10% acetic acid, 45% ethanol, and 35% distilled water.

9 Glass vials of sufficient size to collect fibers.

Procedure

1 Place 25 g of moist peat sample broken into small pieces into the 500 mL Erlenmeyer flask. Add 300 mL of water and shake the suspension for 16 h at 300 rpm using an end-over-end shaker.

2 Determine the water content of duplicate 25 g samples by weighing when wet, drying at 70°C, and then reweighing when dry. (Note: for both Steps 1 and 2, ensure that the 25 g samples are representative materials. The amount of sample that is used can be adjusted to the requirements of specific studies.)

3 Pour the suspension (Step 1) onto a 200 mesh sieve and wash with water to remove the material finer than 200 mesh.

4 Place the material retained on the 200 mesh into the top sieve (10 mesh sieve) of the particle size apparatus.

5 Fill the cylinder of the particle size apparatus with water to just above the level of the screen of the top sieve.

6 Introduce air into the particle size apparatus through the air-inlet at the base at a rate sufficient to shake the nest of sieves and continue bubbling air vigorously for 1 h.

7 Remove the nest of sieves and recover the fibers remaining on each sieve by washing the fibers onto a funnel fitted with a coarse filter paper (Whatman no. 1).

8 (a) If the fibers are to be examined for botanical composition, remove the fibers from the filter paper and place in vials. Fill the vials with the preserving solution. (b) If the fiber content is to be determined, dry the various fractions at 70°C, weigh, and subtract the weight of the filter paper. Calculate the proportion of the sample in each particle size range as a percentage of the dry weight of the 25 g sample determined in Step 2.

Comments

There seems to be no real advantage in using an electrolyte solution to disperse peat particles, and the long shaking time is not a real inconvenience, since it can be done overnight (Lévesque and Dinel 1977). Experiments, in the Ontario Geological Survey, on fiber determination (100 mesh particle size), mechanical stirring for 10 min gave results similar to the unrubbed fiber method, while mechanical stirring for 16 h produced data comparable to the rubbed fiber method (Riley 1989). Dry sieving is also commonly used in the European and North American industries. However, the output is very dependent on the time and energy of sieving and therefore, these factors are limited to the minimum required to achieve separation of the fractions on small samples (Caron et al. 1997).

67.3.2 Wood Content

Wood content and stumpiness are important characteristics of peat deposits. Stumpiness is the volumetric content of stumps and other woody inclusions to the total volume of the peat deposit (Antonov and Kopenkin 1983). Stumps interfere with drainage and maintenance operations in organic soils and peat fields. In geological surveys, a woody layer occurrence can be quantified by the frequency of intercepting such a layer over a given surface. In pedological surveys, stumpiness is defined volumetrically by estimating the surface occupied by stumps, 10 cm and more in diameter, within a 130-cm-deep control section (Mills et al. 1977). Stumpiness is categorized as null (0%), low (0.5%), medium (0.5%–2%), and high (>2%) for peat extraction (Antonov and Kopenkin 1983), and as none (<1%), moderate (1%–5%), and high (>5%) for peat cultivation (Mills et al. 1977).

REFERENCES

Antonov, V. and Kopenkin, V.D. 1983. *Technology and Complex Mechanization of Peat Production*. Nedra, 2nd ed. Moscow (in Russian).

Caron, J., Blanchet, L., Richard, G., Tardif, P., and Daigle, J.Y. 1997. Guide d'analyse des propriétés physiques, des milieux artificiels, des tourbes et des sols organiques. Conseil des productions végétales du Québec, Québec QC, Canada.

Dinel, H. and Lévesque, M. 1976. Une technique simple pour l'analyse granulométrique de la tourbe en milieu aqueux. *Can. J. Soil Sci*. 56: 119–120.

Farnham, R.S. and Finney, H.R. 1965. Classification and properties of organic soils. *Adv. Agron*. 17: 115–162.

Grosse-Brauckmann, G. 1976. *Peat Stratification*. In K. GöSttlich, Ed. Moor- und Torfkunde. E. Scheizerbart'sche Verlag (NäÜgele und Obermiller), Stuttgart, Germany, pp. 91–133.

Ilnicki, P. and Zeitz, J. 2003. Irreversible loss of organic soil functions after reclamation. In L.E. Parent and P. Ilnicki, Eds. *Organic Soils and Peat Materials for Sustainable Agriculture*. CRC Press, Boca Raton, FL, pp. 15–32.

Kaila, A. 1956. Determination of the degree of humification in peat samples. *Maatal. Tiet. Aikak*. 28: 18–35.

Lévesque, M. and Dinel, H. 1977. Fibre content, particle-size distribution and some related properties of four peat materials in eastern Canada. *Can. J. Soil Sci*. 57: 187–195.

Lévesque, M. and Mathur, S.P. 1979. A comparison of various means of measuring the degree of decomposition of virgin peat materials in the context of their relative biodegradability. *Can. J. Soil Sci*. 59: 397–400.

Lishtvan, I.I. and Kroll, N.T. 1975. Basic Properties of Peat and Methods for Their Determination. Nauka and Tekhnica, Minsk (in Russian).

Lynn, W.C., McKinzie, W.E., and Grossman, R.B. 1974. Field laboratory tests for the characterization of Histosols. In A.R. Aandahl et al., Eds. *Histosols: Their Characterizations, Use, and Classification*. Spec. Publ. No. 6, Soil Science Society of America, Madison, WI, pp. 11–20.

Malterer, T.J. 1988. A comparative analysis of the USDA fiber volume, USSR centrifugation and von Post humification methods for determining fiber content and degree of decomposition (humification). Vol. IV: *Proc. 8th Int. Peat Congr*., Leningrad, USSR, pp. 129–139.

Malterer, T.J., Verry, E.S., and Erjavec, J. 1992. Fiber content and degree of decomposition: a review of national methods. *Soil Sci. Soc. Am. J*. 56: 1200–1211.

Mills, G.F., Hopkins, L.A., and Smith, R.E. 1977. *Organic Soils of the Roseau River Watershed in Manitoba*. Monogr. No. 17, Agriculture Canada, Ottawa, ON, Canada.

Ministry of Fuel Industry RSFSR. 1976. The State Standard of the USSR Peat. Method for the determination of the degree of decomposition: GOST 10650-10672. Trans. Comm. I Int. Peat Soc.: Working Group for the Classification of Peat, Helsinki, Finland, pp. 57–66.

Okruszko, H. and Ilnicki, P. 2003. The moorsh horizons as quality indicators of reclaimed organic soils. In L.E. Parent and P. Ilnicki, Eds. *Organic Soils and Peat Materials for Sustainable Agriculture*. CRC Press, Boca Raton, FL, pp. 1–14.

Parent, L.E. 1980. Guidelines for peat utilization in Quebec and the Maritimes. *Tech. Contr. J*. 826, *Tech. Bull*. 15, Agriculture Canada, Saint-Jean-sur-Richelieu, QC, Canada.

Parent, L.E., Fanous, M.A., and Millette, J.A. 1982. Comments on parametric test limitations for analyzing data on peat decomposition. *Can. J. Soil Sci*. 62: 545–547.

Riley, J.L. 1989. Laboratory methods for testing peat—Ontario peatland inventory project. Ontario Geological Survey Misc. Pap. 145, Ont. Min. North. Dev. Mines, Toronto, ON, Canada.

Schnitzer, M. 1970. Characteristics of organic matter extracted from podzol B horizons. *Can. J. Soil Sci*. 50: 199–204.

Schnitzer, M. and Desjardins, J.G. 1966. Oxygen-containing functional groups in organic soils and their relationship to the degree of humification as determined by solubility in sodium pyrophosphate solution. *Can. J. Soil Sci*. 46: 237–243.

Sneddon, J.I., Farstad, L., and Lavkulich, L.M. 1971. Fiber content determination and the expression of results in organic soils. *Can. J. Soil Sci*. 51: 138–141.

Vaillancourt, N., Parent, L.E., Buteau, P., Parent, V., and Karam, A. 1999. Sorption of ammonia and release of humic substances as related to selected peat properties. *Can. J. Soil Sci*. 79: 311–315.

von Post, L. and Granlund, E. 1926. Soedra Sveriges torvtillgangar. 1. Sver. Geol. Unders. Arsb. 19, Ser. C, No. 335, Stockholm, Sweden (in Swedish).

Williams, C.J. and Yavitt, J.B. 2003. Botanical composition of peat and degree of peat decomposition in three temperate peat lands. *Ecoscience* 10: 85–95.

Chapter 68
Physical Properties of Organic Soils and Growing Media: Water and Air Storage and Flow Dynamics

J. Caron
Laval University
Quebec, Quebec, Canada

D.E. Elrick
University of Guelph
Guelph, Ontario, Canada

J.C. Michel
INH–INRA–University of Angers
Angers, France

R. Naasz
Laval University
Quebec, Quebec, Cananda

68.1 INTRODUCTION

Along with their particle-size distribution and degree of decomposition, the specific properties of growing media and peat substrates require the development of characterization methods specific to their use and behavior. The low wettability of dry peats is a fundamental characteristic that needs to be characterized when assessing peat properties for horticultural use. Other physical properties of peat soils are measured in a similar way to that of mineral soils, but methods developed for mineral soils have been modified to facilitate the standardization of peat materials. This is also the case for growing media, but with even more specificity. Methods have been developed for characterizing growing media because of the importance of disturbance on the analytical results as well as the specific contexts linked to their use: pot configuration, irrigation devices, and type of culture.

When analyzing organic soils and growing media, apart from sample disturbance, careful attention should be paid to wettability and hysteresis effects. Wettability can be dealt with by carefully

rewetting the sample using hot water, a wetting agent, or prewetting well ahead of the final sample preparation. Hysteresis refers to the fact that properties measured during drainage may differ from those measured on rewetting. Some growing media are well known to be hysteretic, and hence particular properties linked to gas diffusivity, water retention, air content, and unsaturated hydraulic conductivity should be performed under rewetting or drainage, depending on sample use (greenhouse or nursery), along with the range of water potentials representative of such use and any other specific conditions (container geometry, irrigation devices, etc.). This chapter presents methods to characterize the physical properties of growing media and organic soils, adapted to reduce disturbance, and acknowledging wettability and hysteretic issues.

68.2 WETTABILITY (OR WATER REPELLENCY)

Peat is well known and is used for its capability of storing large amounts of water. Despite this aspect, air-dried peat is also well known for its hydrophobicity and the nature of this peculiar behavior had been studied extensively (Fuchsman 1986). Commercially, it is overcome by the extensive use of a surfactant or by the addition of mineral components (Michel 1998). However, the wettability of peat-based substrates should be assessed before its use to decide whether or not a wetting agent should be added to the medium.

Organic matter is one constituent affecting the soil's hydrophilicity or hydrophobicity, and thus its behavior during rewetting (Jouany et al. 1992; Dekker et al. 2000; Michel et al. 2001). Water repellency can cause problems because, after drying out, organic soils or growing media show a high heterogeneity in water flow rates, thus requiring a long rewetting time as their physical properties are impaired (Valat et al. 1991; Michel 1998).

Wettability is the ability of a liquid to spread over a surface (Letey et al. 1962). A drop of liquid placed on a solid surface configures itself in a way that depends on the interaction between solid and liquid. The Young (1805) equation describes this system at equilibrium

$$\gamma_L \cos \varepsilon = \gamma_S - \gamma_{SL} \tag{68.1}$$

where γ_S, γ_{SL}, γ_L are the surface tension of the solid, the interfacial tension between the liquid and the solid, and the surface tension of the liquid, respectively, and ε is the contact angle at the solid–liquid–vapor interface.

Wettability can then be estimated from contact angle measurements, knowing that the wettability is high when ε approaches zero (see Data Analysis, p. 888). Most of the time, simple and rapid tests such as the ''water drop penetration time'' (WDPT) (Letey 1969; McGhie and Posner 1980; Dekker and Ritsema 2000), the ''molarity of an ethanol droplet'' (King 1981; De Jonge et al. 1999), etc. are used to estimate the wettability of materials, which provide only a primary (qualitative) evaluation of wettability. However, measurements of the solid–liquid contact angle are the best techniques to precisely evaluate the wettability of materials.

68.2.1 The Water Drop Penetration Time Method

Materials and Reagents

1 Syringe (2 mL maximum) and distilled water

2 Dry surface of soil or substrate

TABLE 68.1 Classification of Soil/Substrate Water Repellency Related to the Water Drop Penetration Time (WDPT)

WDPT	<5 s	5–60 s	60–600 s	600 s–1 h	>1 h
Surface state	Hydrophilic	Weakly hydrophobic	Highly hydrophobic	Severely hydrophobic	Extremely hydrophobic

Source: From Dekker, L.W., Ritsema, C.J., and Oostindie, K. in L. Rochefort and J.-Y. Daigle (Eds.), *Proceedings of the 11th International Peat Congress*, Vol. 2., Edmonton, AB, Canada, 2000, 566–574.

Procedure

1 Apply 10 to 15 drops of distilled water (10 μL each) onto the soil or growing media surface using a syringe.

2 Measure the time for the complete penetration of the drop into the material.

3 Characterize the surface state in relation to the time of penetration, found in Table 68.1.

Comments

Large variations in the measurements can be observed in relation to the roughness and structure of the materials, and also to the heterogeneity of the composition of materials.

68.2.2 Direct Contact Angle Measurement: The Droplet Method

The direct droplet method is by far the most common, and consists of measuring the contact angle between a liquid and a solid surface.

Materials and Reagents

1 Goniometer

2 Hydraulic press for compacting soil or growing media

3 A few grams of air-dried soil or growing media (~1–5 g, depending on the density of material tested)

Procedure

1 Prepare a smooth, planar, homogenous, isotropic surface (Busscher et al. 1984) by compacting the sample of soil or growing media with a hydraulic press at 75 MPa (Valat et al. 1991) or by drying the soil or growing medium liquid suspension on a thin slide.

2 Place a drop of water (10 μL) with a syringe on the material.

3 Measure the contact angle either directly from the profile of the volume of the droplet using an optical goniometer or from the measurement of the geometrical dimensions: volume, height, and length (Letey et al. 1962; Chassin 1979; Good 1979).

Data Analysis

Conventionally, a material can be considered hydrophilic when the contact angle with water is less than 90°, and hydrophobic when the contact angle is more than 90°. The smaller the contact angle, the higher the wettability.

Comments

The necessity of having a smooth and planar surface makes it impossible to measure the wettability of materials related to the water content due to changes in the rugosity (roughness factor) of the surface and the contact angles can only be measured on dried materials.

68.2.3 Indirect Contact Measurement: Capillary Rise Method

Because of the aforementioned constraints, and contrary to the droplet method, the capillary rise method, already used to measure the rewetting time of soils (Letey et al. 1962; Watson and Letey 1970), also can be used to measure contact angles on noncompacted materials, as well as the wettability of materials at different water contents (Michel et al. 2001).

The contact angle is calculated from the modified Washburn (1921) equation, which defines the flow of a liquid through a capillary column by considering that a material can be described as a bundle of capillaries:

$$\frac{l^2}{t} = \frac{\gamma_L(\tau \cdot r)\cos\varepsilon}{2\eta} \tag{68.2}$$

where l represents the height of the wetting front (cm), t is the time (s), η and γ_L are the viscosity (mPa · s) and the surface tension of the liquid (mJ m^{-2}), respectively, r and τ represent the mean radius (cm) and the tortuosity constant (to approximate the tortuosity of the capillaries), respectively, and ε is the contact angle (°).

By replacing the height of the wetting front l by the increase in weight m due to the penetration of the liquid through a bundle of capillaries, the Washburn equation becomes

$$\cos\varepsilon = \left(\frac{m^2}{t}\right)\left(\frac{\eta}{\rho^2\gamma_L c}\right) \tag{68.3}$$

in which

$$c = \frac{1}{2}\Pi^2(\tau r)^5 n^2 \tag{68.4}$$

where m is the mass of the adsorbed liquid (g), ρ is the density of the liquid (g cm^{-3}), and n is the number of capillaries. The term c (cm^5) corresponds to an empirical constant of the porosity and tortuosity of capillaries, which depends on particle size and degree of packing.

Materials and Reagents

1 Glass tube with a porous glass base (around 1 cm diameter 4 cm in height).

2 Microbalance (precision at the millimetric scale).

3 Tensiometer (apparatus for measuring the surface properties of liquid or solid, e.g., surface energy and surface tension). Note: not the tensiometer that measures water potential in soil.

4 Liquids: hexane (extra pure) and distilled water.

5 A few grams of soil or growing media equilibrated at different water contents (~1–5 g, depending on the density of material tested and its water content).

Procedure

The experiment consists of following the capillary rise on a column of soil or growing media with various liquids.

1 Place a sample of soil or growing medium in the glass tube (with a porous glass base).

2 Fix the tube to the microbalance.

3 Place the tube in contact with a receptacle containing a liquid with a very low surface tension (i.e., hexane), which completely wets the sample ($\varepsilon = 0$).

4 Measure automatically the speed of capillary rise, translated by the increase in weight in the sample, in relation to time by a computer.

5 Repeat steps 1 to 4 several times with hexane.

6 Assess the parameter c from the Washburn equation (Equation 68.3).

7 Repeat steps 1 to 4 several times with distilled water.

8 Then, compute the contact angle with water from the above equations.

Comments

The main sources of error come from variations in porosity and permeability of materials, and from the assumption that the geometry of the pores is not affected by wetting, which is not the case for unstable materials. But the most important limitation of the capillary rise method is the inability to measure angles greater than 90° (since there is no capillary rise for a hydrophobic material), and hence the degree of hydrophobicity. It is also impossible to

measure the wettability at very high water potentials (>−10 kPa) because of the absence of capillary rise for quasisaturated materials, but this is of minor importance because materials at water potentials >−100 kPa are already highly hydrophilic (Michel 1998).

68.3 BULK DENSITY

Bulk density (BD) is an easily measured property correlated with many other peat properties and is used for trade and characterization purposes. In organic soils, it is simply determined in the same way as for mineral soils using a cylinder of known volume forced into the soil, then air dried and weighed. Special sampler shapes have been proposed (Sheppard et al. 1993). A cylinder with a sharpened edge can also be used. However, the bottom surface contact area of the core should be very large, as small cores (5 cm diameter and less) can compact the organic soil easily on a ratio of 5, 6, or even 7 to 1 (against about 1.2 to 1 for mineral soil with the same instrument).

For peat-based substrates (as well as other organic growing media), specific methods have been developed to prevent any disturbance, because of their sensitivity to settling and loosening. Therefore, a reliable methodology to prepare samples and measure bulk densities is of great importance. Also, because of this sensitivity, sample preparation should yield BD values close to those obtained under cultivation. Worldwide, two groups of standardized methods exist. The first group uses large-volume samples (20 L) prepared without compaction and have been designed and are used mainly for trade purposes (e.g., CEN method, 12580; Morel et al. 1999). A second group of methods uses smaller volumes (usually less than 1 L), which are naturally drained after saturation or onto which an external pressure is applied in addition to overburden pressure (Hidding 1999). These methods attempt to mimic natural settling conditions in a potted substrate under cultivation and are mainly used for characterization purposes. Additional details on these two groups can be found in Caron and Rivière (2003).

68.3.1 Bulk Density with Cores (for Organic Soils or Loose Substrates)

This method is commonly used with organic soils or on cores filled with loose substrates.

Materials and Reagents

1 Core samplers or McCauley sampler and sharpened knife

2 Forced-air oven

Procedure

1 For organic soils, trim a core of undisturbed peat with a sharpened knife to fit roughly into the core sampler. A core sample can also be extracted with a McCauley sampler.

2 Alternatively, for peat substrates, they should be loosely packed into cores (as described below for the water desorption curves, using the CEN/TC 223 method). Samples should be prepared as for the water desorption procedure with the above part of the cylinder removed (see water desorption), and the

sample wetted from underneath and then saturated again. Then the substrates should be drained on a tension table (see below) at a tension of −1 kPa.

3 Dry samples at 105°C or 70°C, then compute the BD from

$$BD = \frac{SDW}{V} \tag{68.5}$$

where BD is bulk density (mass per unit volume), SDW is the sample dry weight, and V is the core volume.

Comments

Care should be taken in order to minimize peat compression by the cylinder when sampling. The BD of peat materials is affected by water content. Preequilibration of the substrate at −5 kPa before core filling is therefore now a standard practice in Europe (Verdonck and Gabriels 1992). The correlation between BD and ash content is high (Grigal et al. 1989). BD is also highly correlated to the degree of decomposition (Silc and Stanek 1977). The above method, as well as other methods using the oven-dry weight at 105°C (see below), might slightly overestimate the water content of peat, since peat drying at a temperature exceeding 85°C can result in some loss of organic matter (Macfarlane 1969). Hence, drying at 70°C may be preferred. Prior checks should be made with the type of material in order to set a reference drying temperature.

68.3.2 Bulk Density *In Situ*

Techniques have also been developed to measure BD directly in the potted substrates without any substrate manipulation (Paquet et al. 1993). After the compaction process, either natural or artificial, BD is determined using time domain reflectometry (TDR) (Topp et al. 1980) and is calculated from the total porosity (water content at saturation) determination measured on soil cores or cylinders using TDR. The same technique can be used at a saturated depth in the profile (see Section 68.4.2).

68.4 WATER AND AIR STORAGE

68.4.1 Total Porosity

Total porosity is the first point of the water desorption curve since it gives the total volume available for water and air storage. It is one of the important parameters in assessing the quality of commercial growing media (Hidding 1999). It can be measured directly *in situ* for potted growing media or directly in the field for organic soils. Alternatively, it can be measured on soil or substrate cores. For loosely filled substrate cores, samples are prepared the same way as for the water desorption curve (see below).

68.4.2 Total Porosity *In Situ*

The approach is based on the volumetric water content determination on cores or potted substrates slowly rewetted from underneath, and assumes no air entrapment. The same technique can be used at a saturated depth in the profile.

Materials

1 Samples in a pot or in cores or alternatively a saturated depth in the profile.

2 A water bath for slow rewetting from underneath (for pots or cores).

3 Distilled or deionized water.

4 TDR probes of the length equivalent to the desired volume to be sampled.

5 A time domain reflectometer. Alternatively, CS-615 or any other time domain, frequency domain, or capacitive probe could be used, but they tend to be less accurate.

6 An appropriate calibration curve for the probe, if necessary.

Procedure

1 Rewet a sample in a pot or core from underneath by gradual elevation of the water level and immersion for 24 h, with the water level about 1 cm below the top of the substrate. This achieves full saturation of the substrate, without having significant changes in total porosity as a result of the release of the overburden pressure.

2 Insert the TDR probe into the sample. As the TDR technique represents the average water content along the sampling probe, the probe should be made to sample the total pot height (for a vertical sample), desired soil depth (for sampling in peat bogs), or the pot diameter (for horizontal sampling). The probe should be fully inserted into the substrate, or its full length and should sample the whole depth. Additional measurements could be taken, if necessary, by reinserting the probes at other locations within the sample. The TDR apparatus determines the apparent dielectric constant of the medium, from which volumetric water content is derived. The apparatus must be calibrated a priori against volumetric water content determined from weighing, as equations relating the apparent dielectric constant to volumetric water content derived for mineral soils do not apply to organic soils (Paquet et al. 1993). Paquet et al. (1993), Anisko et al. (1994), and Da Sylva et al. (1998) have published different calibration equations for various organic–mineral soil mixtures.

Calculations

Calculate volumetric water content from the dielectric constant measurement. Total porosity is then assumed to be equal to the volumetric water content. BD can be deduced from total porosity estimates, obtained by measuring water content after complete rewetting of the substrate and from particle density (PD) estimates (see next section).

Comments

It is critical with this approach to resaturate slowly (resaturation by slowly raising the water level in the bath to reach full saturation of the sample). This procedure is frequently used for

well-moist blonde peat (Caron et al. 2002), but may lead to serious errors with air-dried white or black peat materials (Wever 1995), and therefore the period of rewetting should be prolonged if necessary. One way to check is to monitor, over a long period of time, the readings obtained with TDR to make sure they do not increase and to deaerate the sample if needed by putting the core in a chamber or the pot within a cell (Nemati et al. 2002). Potted plants, recently cut, with many roots, have been suspected of generating lot of gases, and care should be taken to apply a vacuum when resaturating the sample to avoid any gas entrapment. Gas entrapment (methane) may also occur in field samples (Buttler et al. 1991).

68.4.3 Total Porosity by Calculation

Physical parameters, such as total pore (TP) space, can be calculated from knowing the BD and ash content, after determining the BD obtained on soil cores (see above).

Calculations

Total porosity can be calculated from BD and PD. Particle density is estimated from ash content (Paquet et al. 1993), assuming a PD of 1.55 for the organic fraction (OM) and 2.65 for the mineral fraction (Verdonck et al. 1978):

$$\%\mathrm{OM} = 100\% - \%\mathrm{ash} \tag{68.6}$$

$$\mathrm{PD} = \frac{1}{\frac{F}{1.55} + \frac{1-F}{2.65}} \tag{68.7}$$

where

$$F = \frac{\%\mathrm{OM}}{\%\mathrm{solids}} \tag{68.8}$$

$$\mathrm{TP} = 1 - \frac{\mathrm{BD}}{\mathrm{PD}} \tag{68.9}$$

Alternatively, PD can be measured on samples using kerosene or ethanol and a pycnometer using the classical mineral soil approach (Blake and Hartge 1986).

Comments

Macfarlane (1969) reported that estimates of PD calculated from ash content can deviate up to 18% from the actual value.

68.4.4 Water Desorption Curve on Cores

This method is widely used in Europe and has been adopted by the International Society of Horticultural Science to characterize growing media used in nurseries and greenhouses (Verdonck and Gabriels 1992; Hidding 1999). It provides estimates of the volumetric water content (sometimes referred to as water-holding capacity) at different potentials.

When characterizing peat material, past literature and common use have referred to the water-holding capacity of peat as one characteristic, often obtained by the soak and drain method (Parent and Caron 1993), where water in saturated peat is extracted by gravity. However, since the water potential at which the water-holding capacity is measured is equal to half the height of the peat sample, the value of water-holding capacity is inaccurate as the method does not provide information on the height of the cylinder at which the water content is measured. Hence, much more complete information is provided by the water desorption curve, and this characterization is recommended for obtaining information on the water-holding capacity of materials.

Materials

1 Double rings (5 cm height and 10 cm i.d.) as well as fixing collars made of temperature-resistant polypropylene should be used. Fix the collar at the periphery of the bottom ring of known volume V_R (2 cm high, glued at a height of 1.5 cm on the lower ring, and hence overlapping 0.5 cm on the upper ring).

2 Nylon gauze fitting the bottom of the rings.

3 A sand box or a tension table (Topp and Zebchuk 1979).

4 Large plastic containers, perforated at the bottom.

5 Steel frame and nylon cloth about 30×60 cm.

6 A large plastic water bath (about 5 L or more).

Procedures

1 Transfer around 10 L of material in several containers.

2 Cover the pot with a nylon cloth.

3 Place the pot on a steel frame into the water bath.

4 Fill the bath slowly up to 1 cm under the top of the substrate.

5 Stand overnight.

6 Remove the pot and leave 48 h on the sandbox, applying a potential of -5 kPa pressure head measured from the bottom of the plastic pot.

7 Then fill the assembled rings (with a cheese cloth or very coarse nylon cloth secured at the bottom of the lower ring) with the material using a large spoon in increments of about 100 mL without causing compaction (filling the hollow spaces though) of the removable rings.

8 Cover the upper ring with a nylon cloth to prevent substrate from floating.

9 Transfer the filled double rings to the bath.

10 Flood slowly to 1 cm from the top of the upper ring.

11 Saturate for 24 h.

12 Transfer to the tension table.

13 Cover the table and the sample with a cloth.

14 Apply a pressure head of −1 kPa (10 cm of suction), calculated from the middle of the lower ring.

15 Equilibrate for 48 h.

16 Remove the sample from the table and then the upper ring slowly, exposing the uppermost part to the material.

17 Strike off the excess material keeping a flat surface using a sharp knife without causing compaction. This is a delicate operation that should be performed as precisely as possible. Very fibrous material should be cut with large scissors.

18 Determine the weight of the sample present in the lower ring (W_R).

19 Return the sample for other potential determinations (−2, −5, −10 kPa), leaving them at least 24 h between each measurement. Check for equilibrium (constant weight) at a given potential before applying a new potential.

20 Dry the sample in the oven at 105°C to estimate dry BD and volumetric water content at each corresponding potential. For shrinking material, measurement of height of the substrate within the ring may be useful to correct the volumetric water content by adjusting V_R accordingly. Adjust for cheese cloth weight.

Calculations

1 Volumetric water content at −1 kPa, θ_1, is determined as

$$\theta_1 = \frac{W_1 - W_R}{V_R} \tag{68.10}$$

where W_R is the dry weight of the lower ring and V_R the ring volume. The volumetric water content for other potentials is then determined accordingly by replacing W_1 with the weight corresponding to the potential applied.

2 Air volume (AFP for air-filled porosity) is determined from the difference between total porosity (TP) and θ_1:

$$\text{AFP} = \frac{\text{TP} - \theta_1}{V_R} \tag{68.11}$$

3 Easily available water (EAW) is the water volume between −1 and −5 kPa and is calculated from

$$\text{EAW} = \frac{\theta_1 - \theta_5}{V_R} \tag{68.12}$$

4 Available water (AW) is the water volume between −1 and −10 kPa, and is calculated from

$$\text{AW} = \frac{\theta_1 - \theta_{10}}{V_R} \tag{68.13}$$

5 Buffer capacity (BC) is the water volume between −5 and −10 kPa and is calculated as

$$\text{BC} = \frac{\theta_5 - \theta_{10}}{V_R} \tag{68.14}$$

Comments

Because of pronounced hysteretic effects, the measurements should be performed at different potentials upon rewetting. This is particularly relevant when the substrates are used with subirrigation devices (ebb and flow, gullies, capillary mats) to be more representative of growing conditions.

68.4.5 Water Desorption of Potted Substrates

For diagnostic purposes, in research facilities, nurseries, or greenhouses, attempts have been made to infer properties existing in pots from the water desorption curves measured on independent samples. Paquet et al. (1993) have shown that substrate disturbance alters these properties and Fonteno (1989) exemplified the effects that container size and geometry may have on existing water and air contents in containers. It is also our experience that once potted, substrate physical properties will evolve significantly, as a result of settling and compaction, decomposition, particle reorganization, and root activity (Allaire-Leung et al. 1999). Hence, measurements taken directly in the pot before and during plant growth are advisable for accurate diagnosis and proper characterization.

Materials

1 Potted substrates with the containers open at the bottom

2 TDR apparatus and probe or a weighing scale

3 Polyethylene sheets, a screen or nylon gauze

4 Tension table apparatus (Topp and Zebchuk 1979)

Procedure

1 When using potted substrates with growing plants, first cut off the top part of the plant.

2 Resaturate the substrate from below by slowly increasing the water content to saturate the sample, measuring water content with a vertically inserted probe.

3 Bring the water level up overnight, and finish raising it up to 1 cm below the top of the substrate.

4 Measure the water content during the day to make sure it reaches a constant value. Drift may suggest a high level of entrapped air. Flush trapped air with carbon dioxide if necessary, and then resaturate with deaerated water or put the sample into a vacuum chamber.

5 Determine water content at saturation (it then equals TP).

6 Let the sample drain for about 1.5 to 2 h, and then measure the TDR values vertically at regular intervals during drainage to make sure they have reached a constant value, i.e., the volumetric water content at container capacity, which may differ from that at −1 kPa, since the equivalent applied potential, due to the weight of water, varies with container height (Fonteno 1989). Alternatively, the container can be weighed (in absence of TDR measurements).

7 AFP can then be calculated from the difference between volumetric water content at saturation and that after saturation and drainage (θ_c) using

$$\text{AFP} = \text{TP} - \theta_c \tag{68.15}$$

8 Cover the substrate top surface with a plastic sheet to restrict evaporation.

9 Take a second measurement with a horizontally inserted probe and note the height of the probe to estimate the corresponding potential.

10 Put the substrate in contact with the tension table (Figure 68.1). Make sure a good contact is established between the sample and the tension table by making a slurry if necessary, or by making additional holes at the bottom of the pot and fixing a screen or a gauze, if necessary, to retain the substrate.

11 Apply a series of water potentials, the most common being −1, −2, −5, and −10 kPa, by lowering the opening of the drainage tube of the tension table to a fixed distance (10, 20 cm, etc.) from the probe height. Equilibrate for 24 h between each potential point, measuring the volumetric water content or weigh the pot between each point. For each measurement, record the water content and the corresponding height. Using TDR instead of a weighing balance has the advantage of accuracy at a known height and prevents removal of the potted substrate from the tension table.

12 Measurements should be performed on rewetting and on drainage, as the properties clearly differ because of hysteresis, which affects air content and AW.

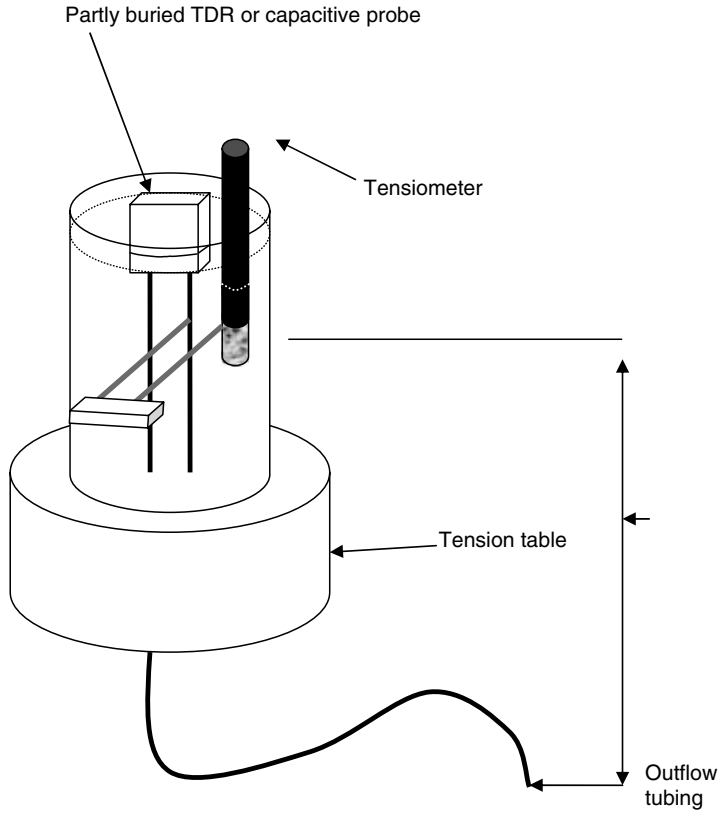

FIGURE 68.1. The system to measure the soil water desorption curve on potted substrates or in cylinders showing horizontally or vertically installed TDR probes. The plant should be cut before putting the pot onto the tension table.

13 Draw the water desorption curves and calculate the parameter as mentioned above (Equation 68.11 through Equation 68.15). In the absence of a TDR, TP should be calculated from the bulk and particle densities, which requires determination of the whole container weight at 105°C for use in the calculation of AFP in Equation 68.15.

Comments

The entrapment of air can be a problem with the tension table method, and care should be taken to avoid breaking the water column. The above procedure has been described in more detail elsewhere for pots (Paquet et al. 1993).

68.4.6 Point of Air Entry

Measurement of point of air entry is critical if an indirect assessment of the gas diffusivity is desired (Caron and Nkongolo 2004). It may also be used for modeling purposes and in the design of growing systems for identifying the height of the water-saturated zone at the bottom of containers, which then may result in oxygen-deficient zones. Caron et al. (2002) and Nemati et al. (2002) carried out a comparison of different approaches to identify the

air-entry value, and the one based on the water desorption curve is presented here (Nemati et al. 2002) for determination of air entry at the bottom of the pot. Nemati et al. (2002) have also proposed and validated another approach based on pressure transducer measurements, which can be automated. Other approaches have been proposed and tested but have yielded inaccurate estimates for a large number of growing media (Caron et al. 2002).

Materials

1 Substrates potted in PVC cylinders or in greenhouse or nursery containers, loosely filled or taken directly from the production area should be used. The walls of cylinders or pots should be perforated with two tapped holes: one for the TDR probe to monitor water content and the other for the tensiometer to monitor matric potential.

2 A TDR probe consisting of three 145-mm long stainless steel rods, 2 mm diameter and spaced 15 mm apart, forming a plane.

3 Minitensiometers approximately 80 mm long $\times$ 8 mm outside diameter.

4 A fast-response tension table, an Erlenmeyer flask, and a metal stand (see Figure 1 in Nemati et al. 2002).

Procedure

1 Before starting the measurements, evaluate the zone of influence of the TDR probe. It can be determined by immersing horizontal probes in water and measuring at what distance from the horizontal position of the probes any changes in water content can be accurately detected.

2 Prepare the substrates in cylinders as mentioned above (see Section 68.4.5) or obtain the containers from the production area.

3 Saturate the sample from the bottom, slowly raising the water level overnight. Bring the water level to about 1 cm from the top of the substrate.

4 Slowly drain the substrate and put the cylinder in contact with the tension table.

5 Insert the TDR probe (30 mm from the bottom of the pot) and the tensiometers horizontally at the precise height corresponding to the top zone of influence of the probe (Nemati et al. 2002), and apply a potential of $+0.2$ kPa to the table (i.e., with a 20 mm height of water on the surface of the tension table).

6 Cover the cylinders or pots to restrict evaporation, but leave small holes to allow air to enter at the surface.

7 Monitor water content and matric potential of the substrates daily after each decrease of water level at the rate of 10 mm per day. This step can be fast or slow depending on the hydrodynamics of the system. An assessment of the dynamics of equilibrium should be performed first by checking (after potential changes) the pace at which the water content changes, by monitoring the water content with the TDR probes at different times.

8 Adjust the matric potential data for the height of the water column in the tensiometer as well as for the distance between the tensiometer and the TDR probe.

9 Plot water content as a function of water potential $\theta(\psi)$. It will result in a curve with at least two distinct zones: an initial zone showing nearly constant water content with decreasing water potential and a second zone showing sharp decrease in water content with water potential (in some cases followed by a third zone of lesser decrease). The air-entry value is estimated from the intersection of the fitted lines for the first two zones as illustrated by Nemati et al. (2002).

68.5 WATER AND GAS MOVEMENT

68.5.1 Saturated Hydraulic Conductivity on Cores or in the Field

This method is preferably used with organic soils and substrate-filled cores. Hydraulic conductivity of organic soils is determined in the same manner as mineral soils (Klute and Dirksen, 1986). One should be aware that organic soils are composed of rather loose materials and that, consequently, the walls of auger holes may be unstable while measuring hydraulic conductivity or the infiltration rate of water in the field. However, measurements *in situ* are obviously more preferable than measurements performed on disturbed cores because of the high sensitivity of the structure. Measurements of saturated hydraulic conductivity (K_s) by the constant-head or the falling-head method may be invalidated by the presence of large particles in the peat sample. Also, mathematical models developed especially to estimate saturated hydraulic conductivity from field measurements might not apply to organic soils (Hemond and Goldman 1985). Verification of the applicability of Darcy's law in peat substrates has however led to the conclusion that low flow is laminar and Darcy's approach applies (Allaire et al. 1994). If so, then measurements made directly in the field using the Guelph permeameter are possible above the water table but may require an independent estimation of α (a parameter used to characterize the unsaturated hydraulic conductivity). Organic soils in our studies have yielded estimates of α of about 9 m^{-1} on internal drainage tests (J. Caron, unpublished data). These values are comparable to that of some peat substrates (about 7–9 m^{-1}) (Caron et al. 1998; Jobin et al. 2004), but may be higher. Saturated hydraulic conductivity values sometimes are comparable to that of sandy loam or loam soils, which is surprising, but may be linked to their low pore effectiveness (Caron and Nkongolo 2004). Readers are referred to K_s measurement procedures for mineral soils (see Section ''Soil Water Analyses'') for further details on K_s determinations, either in the field or in the laboratory (if the decision is made to use cores).

68.5.2 Saturated Hydraulic Conductivity of Potted Growing Media

The particularly sensitive structure of growing media makes it highly advisable to measure the saturated hydraulic conductivity on undisturbed substrates. The measurement is sometimes performed with plants present, which incorporate changes in the structure of decomposition, reorganization, settling, and root enmeshment, all of which are known to affect K_s determinations (Allaire-Leung et al. 1999). The procedure uses constant-head permeameter devices to establish steady-state conditions and obtains flow measurements in a container (Figure 68.2). Since these flow measurements are affected by the container geometry and hole distribution (a 3-D process), the flow is corrected to provide an estimate of the equivalent saturated hydraulic conductivity from Darcy's law as if it was a 1-D process measured in a cylinder. Performing these measurements in a cylinder may be problematic

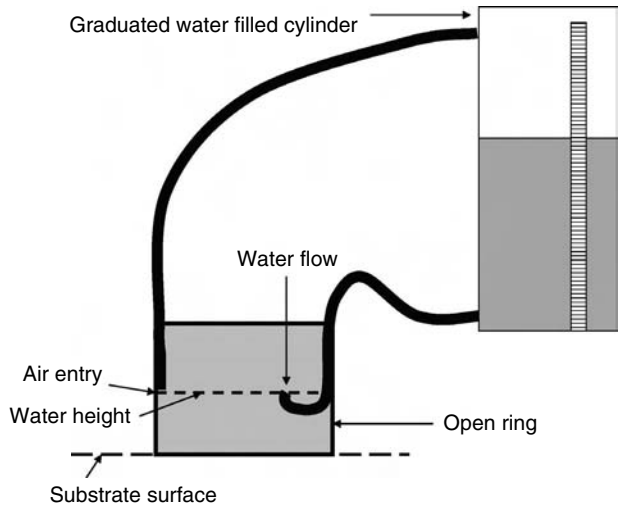

FIGURE 68.2. Schematic representation of the special head of the Côté's infiltrometer to measure saturated hydraulic conductivity.

because of the very sensitive structure, and important deformations affecting the K_s determination have been observed. Allaire et al. (1994) have instead proposed correcting the flow from the measurement performed directly in the pot and have shown this approach to be appropriate. Obviously, the container geometry, hole distribution, and hydraulic gradient affect the correction factor. If no correction factor is available, Allaire et al. (1994) describe an experimental procedure on how to derive it from solving Laplace's equation in 3-D.

Materials

1. A constant-head permeameter (Côté's infiltrometer, Figure 68.2), with a special head that can be moved directly onto a pot surface (Banton et al. 1991)
2. An interpretation chart for different container heights and pot-hole distributions (Allaire et al. 1994)
3. A ruler
4. A substrate field container, with or without the actively growing plant
5. A water pail

Procedure

1. Immerse containers in a distilled-water or tap-water filled bath for 24 h by slowly rewetting the sample from underneath. A prewetting period may be necessary if hydrophobicity is suspected.
2. Take the container slowly off the bath and put it onto a metal stand having a perforated surface.

3 If there is an empty space between the container side and the substrate, fill the gap with bentonite to avoid preferential flow.

4 Cover the substrate surface with a screen or a porous pad (scouring pad) to prevent particles from floating and plugging the opening of the infiltrometer or to reduce particle displacement.

5 Establish steady state when maintaining a known height of water above the substrate surface using the infiltrometer.

6 Measure the water drop in the permeameter as a function of time.

7 Calculate flux after reaching steady-state conditions (Q).

8 Determine the known height of water above the substrate surface (h).

9 Determine the final height after running the experiment (L).

10 Calculate the substrate surface area (A).

11 Find the flux reduction ratio obtained from Figure 5 in Allaire et al. (1994). For 1 L pots with multiple holes (type Ultra) commonly found in greenhouses, we determined that the R_f value is equal to 1.66 with a substrate height of 7 and 3 cm of water head.

12 Calculate the saturated hydraulic conductivity K_s from

$$K_s = \frac{QLR_f}{A(h+L)} \tag{68.16}$$

68.5.3 Unsaturated Hydraulic Conductivity on Soil Cores and Potted Substrates

Instantaneous profile methods (Watson 1966; Wind 1969; Hillel et al. 1972; Vachaud and Dane 2002) have successfully been used in the field at different depths for characterizing the whole-unsaturated hydraulic conductivity curve on both drainage and rewetting. The approach has been used for potted substrates and on soil cores (Naasz et al. 2005) and is presented here. The method is highly variable, close to saturation (−1 to 0 kPa) (Caron and Elrick 2005; Naasz et al. 2005), but provides useful and rapid estimates in the range of water availability (−1 to −20 kPa) in this kind of substrate. Unsaturated hydraulic conductivity (using constant-head methods) is not accurate enough for an adequate characterization at potentials lower than −2 kPa, and therefore is not presented herein.

Materials

1 Two large PVC cylinders (14 cm diameter and 14 cm height).

2 Small PVC cylinders (10 cm diameter and 12 cm height, $V = 942$ cm^3).

3 A TDR system: two TDR miniprobes (three wires, 80 mm long, with 4-mm uncoated stainless steel rods and a spacing of 10 mm). The probes are connected to a Tektronix 1502C system (Tektronix, Beaverton, OR) via a multiplexer run by WINTDR software (Time Domain Reflectometry Soil Sample Analysis Program V. 6.1, Utah State University, Logan, Utah).

4 A tensiometer system: two minitensiometers (2.2 mm diameter and 20 mm length, ceramic cell, SDEC 220 [Société Développement et Commercialization, Reignac, France]) are connected to pressure transducers (differential pressure sensors, precision: ±0.03%, response time: 10^{-3} s) monitored by a real-time multitasking computer to control the measurement and to collect data.

5 Small ventilators to impose top-surface sample evaporation.

6 A Mariotte bottle to maintain a constant-head bottom infiltration.

Procedure

1 Since the physical properties of organic substrates are largely influenced by preparation and, more precisely, by the packing of materials, the procedure of substrates preparation is standardized: manually fill with substrate (but without packing) two large PVC cylinders (14 cm diameter and 14 cm height). Slowly wet cylinders (30 min) from the bottom, saturate with distilled water for 24 h, and allow samples to equilibrate for 48 h to a water potential of −5 kPa (on a tension table). Empty cylinders, homogenize substrate, and fill small PVC cylinders (10 cm diameter and 12 cm height) with substrate without packing. Finally, slowly saturate material from the bottom for 24 h.

2 Horizontally insert (at an angle of 90°) the two pairs of sensors (TDR probes and minitensiometers to determine volumetric water content θ and the water potential ψ, respectively) at two levels, h_1 and h_2, from the bottom of the small PVC cylinder ($h_1 = 9$ cm and $h_2 = 3$ cm, Figure 68.3).

3 Seal the bottom of the column to prevent water loss and then slowly saturate the substrate from the bottom with the Mariotte bottle.

4 When readings (TDR and tensiometers) indicate that the core is in hydrostatic equilibrium (after about 30 min), the evaporation experiment could begin.

5 Impose controlled top-surface sample evaporation with the small ventilators.

6 The evaporation experiment is terminated when the uppermost tensiometer in the substrate core reaches a suction level of approximately −30 kPa.

7 The sample is then subjected to infiltration. During the infiltration experiment, impose three pressure levels (stepwise increases): −15, −5, 0 kPa.

8 The drying–wetting cycle lasts for approximately 1 month and represents ∼8000 sets of water content/water potential data (measurements were taken every 5 min).

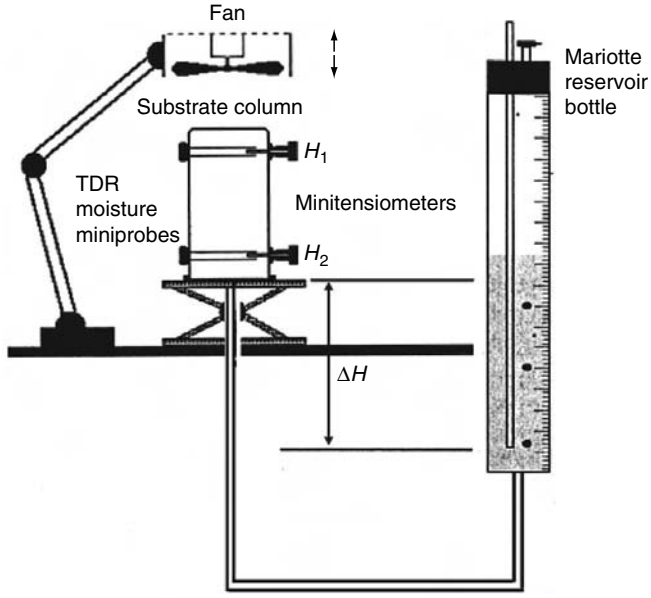

FIGURE 68.3. Schematic representation of the experimental design for measuring the unsaturated hydraulic conductivity in cores. (Redrawn from Naasz, R., Michel, J.-C., and Charpentier, S., *Soil Sci. Soc. Am. J.*, 69, 13, 2005.)

Calculations

Calculate the unsaturated hydraulic conductivity by direct measurement from water content and water pressure data obtained during evaporation and infiltration experiments with the Darcy equation. First, calculate the water flow through the column q from the temporal changes (Δt) in water storage at two depths (h_1 and h_2) as follows:

$$q = -\frac{\Delta\theta_{h_1} - \Delta\theta_{h_2}}{\Delta t} \tag{68.17}$$

where $\Delta t = t_2 - t_1$ is the time interval; t_1 is time 1 and t_2 is time 2. The unsaturated hydraulic conductivity $k(\psi)$ is then obtained by dividing the flux density calculated above with the matric head differences ($d\psi$) at the same positions ($dz = h_1 - h_2$) and times as follows:

$$k(\psi) = \frac{-q}{\left(\dfrac{d\psi}{dz} - 1\right)} \tag{68.18}$$

Comments

The introduction of TDR miniprobes and minitensiometers in the substrate column could possibly lead to a small change in the structure of materials and, as a result, in the hydraulic properties. The volume occupied by all sensors in the column has been calculated and only represents $<1\%$ of the whole substrate core volume.

68.5.4 Unsaturated Hydraulic Conductivity *In Situ*

Organic growing media are almost exclusively used in greenhouse and nursery production and are watered either from above (overhead sprinklers, mist, nozzles) or from below (capillary mats, ebb and flow, gully systems). For subirrigation systems in nurseries, the shape of the unsaturated hydraulic conductivity curve is a very critical factor in assessing their performances (Caron et al. 2005). However, this characterization should be performed *in situ* (in the pot) upon rewetting and very close to saturation. The instantaneous profile (see previous sections) cannot be used in this range. Instead, Caron and Elrick (2005) have proposed a procedure specifically developed for porous media that have a large proportion of macropores, such as organic substrates. It uses a simple tension disk apparatus. At saturation, the procedure also measures the saturated hydraulic conductivity.

Materials

1 A tension disk with a membrane (e.g., nylon fiber) having an air-entry value of approximately −5 kPa of water head (−50 cm).

2 A cylindrical container (e.g., a commercial pot) having a height of at least 15 cm. The bottom should have several holes (for 1-D flow) and a coarse screen used if necessary to contain the substrate (Figure 68.4).

3 A clear container (e.g., acrylic) large enough to contain the substrate-filled container mentioned in step 2.

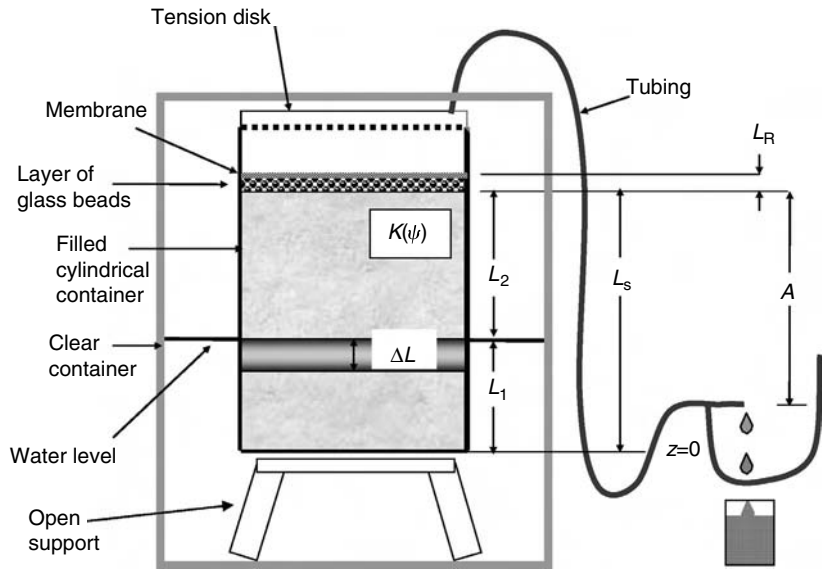

FIGURE 68.4. Schematic of the Laval tension disc for measuring unsaturated hydraulic conductivity upon rewetting on a potted substrate. (Redrawn from Caron, J. and Elrick, D.E., *Soil Sci. Soc. Am. J.*, 69, 794, 2005.)

4 A Mariotte bottle to maintain a constant head.

5 Glass beads (average diameter of 180–120 μm).

6 Plastic tubing and a graduated cylinder to measure the volume of water collected.

Procedure

1 Pack the cylindrical container (pot) as uniformly as possible. Wet the pot from below so that free water is on the surface, then drain and rewet two or more times to obtain a more stable volume. The top of the substrate can be sprayed with water if wetting appears to be a problem. L_s is the depth of the substrate. The substrate can also be taken directly from the production area, but the top part of the plant should be cut first.

2 Put the pot in the larger acrylic box (see Figure 68.4), placing the pot on a support that allows unrestricted flow to the bottom of the pot.

3 A thin layer of glass beads (air-entry value of about -2.5 kPa) should be applied to the surface.

4 The tension disk should be carefully placed on the surface of the substrate (the disk should be slightly smaller in diameter than the inside diameter of the pot). Leave overnight to equilibrate. Note that L_R, the thickness of the membrane system, is $\ll L_s$ (Figure 68.4).

5 Add water to the acrylic box so that the level of the water is about 1 cm above the bottom of the pot. L_1 is the water level in the box measured from the bottom of the pot and L_2 is the distance from the water level in the box to the top of the substrate.

6 Apply suction to the tension disk by lowering the bottom end of the plastic tubing (top end connected to the tension disc) so that the water exiting from the tube is about 2 cm below the water level in the box. Measure the distance between the water level in the container and the exit end of the plastic tube ($A-L_2$). ΔL in Figure 68.4 is the head loss due to Darcy flow in the saturated zone.

7 When steady flow is attained (after about three measurements), record the flow rate in $cm^3\ min^{-1}$ (other units can be used).

8 Raise the water level in the box by about 2 cm; raise the lower end of the plastic tubing about 2 cm; measure the distance between the water level in the container and the exit end of the plastic tube, and then record the steady-state flow rate.

9 Repeat step 8 until the water surface is within 2 cm of the surface and record the steady flow rate.

10 The last step is to raise the water level around the pot to about 1 cm above the substrate level in the pot. The substrate should be saturated. Measure the saturated hydraulic conductivity using Darcy's law for saturated flow.

11 This series of measurements can generally be carried out within 2–3 h.

Calculations

Calculate the saturated hydraulic conductivity, K_s. It may be necessary to correct for the resistance of the tension disk membrane and glass bead system, particularly at high water contents near saturation. Use the formula below to calculate K_s:

$$K_s = \frac{L_s}{\frac{(\Delta H)_T}{J_T} - R_R} \tag{68.19}$$

where L_s is the thickness of the substrate, $(\Delta H)_T = (A - L_2)$ is the measured head drop across the substrate plus the disk system (the combined system), J_T is the measured flux through the combined system, and R_R is the independently measured resistance to flow through the disk system only (Caron and Elrick 2005).

Calculating the unsaturated hydraulic conductivity, $K(\psi)$, where ψ is the soil water pressure head, requires numerical procedures and can best be carried out using a computer program. An Excel program can be used for this purpose and some details are presented by Caron and Elrick (2005).

Comments

This procedure was developed specifically to measure the unsaturated hydraulic conductivity upon rewetting in the high water potential range, for example −2 to 0 kPa of pressure head, which is the range of interest when characterizing organic substrates packed into pots used with subirrigation devices (ebb and flow, capillary mats). It may be useful for Histosols where subirrigation systems are extensively used. The procedure can be applied to high-conductivity mineral soils such as sands or highly structured mineral soils. It can also be used for sand bed systems used in nurseries, or in cranberry production where field subirrigation systems are used. The theoretical justification of the proposed methodology has been presented elsewhere and validated for growing media and sand (Caron and Elrick 2005). The estimates obtained from such an approach have been shown to adequately predict the behavior of the capillary process in soil columns and pot plant production on capillary mats (Caron et al. 2005).

68.5.5 Gas Diffusivity

Gas diffusion is critical for diagnosing aeration problems in growing media as shown in many studies (Allaire et al. 1996; Nkongolo 1996; Nkongolo and Caron 1999; Caron et al. 2001; Caron 2004), and therefore numerous attempts have been made to characterize it. A classical method, used with peat by King and Smith (1987), was presented by Rolston (1986) and the reader is referred to it for greater details. Again, it is important to reemphasize the need for performing this measurement at more than one water content, as this substrate

property is volumetric water content dependent. The chosen water content (or potential) should correspond as closely as possible to the container situation if the gas diffusivity is used as an index to assess plant performance.

In quality control of growing media, the water desorption curve and the saturated hydraulic conductivity are measured. It is thus possible to predict gas diffusivity (and pore connectivity) from the shape of the water desorption curve and the saturated hydraulic conductivity. The approach has been shown to be unbiased for peat substrates and to provide estimates consistent with previously published gas diffusivity data, but it is based on assumptions valid for peat and organic growing media only. This approach appears invalid for mineral soils (Caron and Nkongolo 2004).

Methods

1 Use the results of the saturated hydraulic conductivity measured *in situ* (K_s), the water desorption curve, and the point of air entry, measured as highlighted above, on the same sample, with potted substrates in containers of cylindrical shapes if possible.

2 Commercially available software (capable of handling nonlinear equations) for calculating the different parameters.

Procedure

Fit the water desorption data points, to obtain the value of α, b, and n relationship using the function adapted to horticultural substrates by Milks et al. (1989):

$$\theta = \theta_r + \frac{\theta_s - \theta_r}{[1 + (\alpha\psi)^n]^b} \tag{68.20}$$

where θ is the volumetric water content, θ_s is the mean volumetric water content of the soil at saturation (total porosity), θ_r is the mean volumetric water content at asymptotic residual, ψ is the water potential (kPa), and b, n, and α are empirically fitted parameters.

1 Calculate the dimensionless water content

$$\Theta = \frac{\theta - \theta_r}{\theta_s - \theta_r} \tag{68.21}$$

2 Calculate pore tortuosity from the following equation, using any commercially available software

$$\tau_w = \frac{0.00028\rho g}{\eta K_s} \int_{\theta_r}^{\theta_{ea}} \alpha^2 \left(\Theta^{-1/b} - 1\right)^{-2/n} \mathrm{d}\theta \tag{68.22}$$

where the upper limit of the integral is calculated from the volumetric water content at the point of air entry, θ_{ea}, as this upper limit will correspond to the

radius of the largest pore involved in water flow. The lower limit, θ_r, is calculated from the residual water content at a water potential of −10 kPa. Although the lower limit should theoretically be 0, the contribution to K_s of pores retaining water at water potentials lower than −10 kPa in peat substrates is so small that it is considered to be negligible and can be disregarded for τ_w calculations.

3 Once τ_w is obtained, calculate the pore effective coefficient (γ) from

$$\gamma = \frac{1}{\tau_w} \tag{68.23}$$

Obtain θ_a determined on the same core or potted sample. King and Smith (1987) showed that in peat substrates, the relationship between gas diffusivity (D_s), the proportion of the total volume occupied by air (called AFP, θ_a), and gas diffusivity in the air (D_0) can be expressed as

$$D_s = D_0 \gamma \theta_a \tag{68.24}$$

4. The results of this calculation yield values for tortuosity (or pore efficiency) as well as for gas diffusivity, which can be multiplied by volumetric water content to provide estimates for gas diffusivity across a wide range of water contents based on Equation 68.24.

68.6 INTERPRETATION CHART FOR THE QUALITY OF GROWING MEDIA

Table 68.2 was derived for growers for a wide range of growth problems in the field and when observing the operation of subirrigation systems in greenhouse and nursery experiments. It complements existing data used in the industry for diagnostic purposes and has been obtained from numerous experiments summarized by Caron (2004). It represents values found with best-performing substrates under specific experimental conditions and should therefore be considered indicative only.

TABLE 68.2 Norms for Physical Properties of Growing Media Linked to Gas and Water Storage and Exchange

Properties	Aeration processes			Liquid water transfers		
Parameters	Air-filled porosity (AFP) (–1 kPa)	Gas relative diffusivity (–0.8 kPa)	Easily available water (EAW)	K_s	Unsaturated hydraulic conductivity	
					α_1	ψ_b
Units	$cm^3\ cm^{-3}$	—	$cm^3\ cm^{-3}$	$cm\ s^{-1}$	kPa^{-1}	kPa
Norms	0.15–0.30[a,b]	0.010–0.015[c]	0.20–0.30[b]	0.08[d]	9.6[e]	−0.5[e]

Sources: From [a]Wever, G., *Acta Hort.*, 294, 41, 1991, [b]De Boodt, M. and Verdonck, O., *Acta Hort.*, 26, 37, 1972, [c]Allaire, S., Caron, J., Duchesne, I., Parent, L.E., and Rioux, J.A., *J. Am. Soc. Hort. Sci.*, 121, 236, 1996, [d]Mustin, M., in *Le Compost*, Dubusc, Paris, France, 1987, [e]Caron, J. and Elrick, D.E., *Soil Sci. Soc. Am. J.*, 69, 794, 2005.

REFERENCES

Allaire, S., Caron, J., Duchesne, I., Parent, L.E., and Rioux, J.A. 1996. Air-filled porosity, gas relative diffusivity and tortuosity: indices of *Prunus xcystena* sp. growth in peat substrates. *J. Am. Soc. Hort. Sci.* 121: 236–242.

Allaire, S., Caron, J., and Gallichand, J. 1994. Measuring the saturated hydraulic conductivity of peat substrates in nursery containers. *Can. J. Soil Sci.* 74: 431–437.

Allaire-Leung, S.E., Caron, J., and Parent, L.E. 1999. Changes in physical properties of peat substrates during plant growth. *Can. J. Soil Sci.* 79: 137–139.

Anisko, T., NeSmith, D.S., and Lindstrom, O.M. 1994. Time-domain reflectometry for measuring water content of organic growing media in containers. *Hortscience* 29: 1511–1513.

Banton, O., Côté, D., and Trudelle, M. 1991. Détermination au champ de la conductivité hydraulique saturée à l'aide d'un infiltromètre à charge constante de Côté: théorie et approximations mathématiques. *Can. J. Soil Sci.* 71: 119–126.

Blake, G.R. and Hartge, K.H. 1986. Particle density. In A. Klute, Ed., *Methods of Soil Analysis, Part 1, 2nd ed.* American Society of Agronomy, Madison, WI, pp. 377–381.

Busscher, H.J., van Pelt, A.W.J., De Boer, P., De Jong, H.P., and Arends, J. 1984. The effect of surface roughening of polymers on measured contact angles of liquids. *Colloid Surface* 9: 319–331.

Buttler, A.J., Dinel, H., Lévesque, M., and Mathur, S.P. 1991. The relationship between movement of subsurface water and gaseous methane in a basin bog with a novel instrument. *Can. J. Soil Sci.* 71: 427–438.

Caron, J. 2004. Defining new aeration and capillary rise criteria to assess the quality of growing media. In J. Päivänen, Ed., *Proceedings of the 12th International Peat Congress*, June 5–12, Tempere, Finland, pp. 221–228.

Caron, J. and Elrick, D.E. 2005. Measuring the unsaturated hydraulic conductivity of growing media in pots with a tension disc. *Soil Sci. Soc. Am. J.* 69: 794–806.

Caron, J., Elrick, D.E., Beeson, R., and Boudreau, J. 2005. Defining critical capillary rise properties for growing media in nurseries. *Soil Sci. Soc. Am. J.* 69: 783–793.

Caron, J., Morel, D., and Rivière, L.M. 2001. Aeration in growing media containing large particle sizes. *Acta Hort.* 458: 229–234.

Caron, J. and Nkongolo, N.V.K. 2004. Assessing gas diffusion coefficients in growing media from *in situ* water flow and storage measurements. *Vadose Zone J.* 3: 300–311.

Caron, J. and Rivière, L.M. 2003. Quality of peat substrates. In L.E. Parent and P. Ilnicki, Eds., *Organic Soils and Peat Materials for Sustainable Agriculture*, CRC Press, Boca Raton, FL, pp. 67–93.

Caron, J., Rivière, L.M., Carpentier, S., Renault, P., and Michel, J.C. 2002. Using TDR to estimate hydraulic conductivity and air entry in growing media and sand. *Soil Sci. Soc. Am. J.* 66: 373–383.

Caron, J., Xu, H.L., Bernier, P.Y., Duchesne, I., and Tardif, P. 1998. Water availability in three artificial substrates during *Prunus xcistena* growth: variable threshold values. *J. Am. Soc. Hort. Sci.* 123: 931–936.

Chassin, P. 1979. Détermination de l'angle de contact acides humiques—solutions aqueuses de diols. Conséquences sur l'importance relative des mécanismes de destruction des agrégats. *Annales Agronomiques*, 30: 481–491.

Da Sylva, F.F., Wallach, R., Polak, A., and Chen, Y. 1998. Measuring water content of soil substitutes with time domain reflectometry. *J. Am. Soc. Hort. Sci.* 123: 734–737.

De Boodt, M. and Verdonck, O. 1972. The physical properties of the substrate in horticulture. *Acta Hort.* 26: 37–44.

De Jonge, L.W., Jacobsen, O.H., and Moldrup, P. 1999. Soil water repellency: effects of water

content, temperature, and particle size. *Soil Sci. Soc. Am. J.* 63: 437–442.

Dekker, L.W. and Ritsema, C.J. 2000. Wetting patterns and moisture variability in water repellent Dutch soils. *J. Hydrol.* 231: 148–164.

Dekker, L.W., Ritsema, C.J., and Oostindie, K. 2000. Wettability and wetting rate of Sphagnum peat and turf on dune sand affected by surfactant treatments. In L. Rochefort and J.-Y. Daigle, Eds., Vol. 2, *Proceedings of the 11th International Peat Congress*. Edmonton, AB, Canada, pp. 566–574.

Fonteno, W.C. 1989. An approach to modeling air and water status of horticultural substrates. *Acta Hort.* 238: 67–74.

Fuchsman, C.H. 1986. *Peat and Water: Aspects of Water Retention and Dewatering in Peat*. Elsevier Applied Science Publishers, London, UK.

Good, R.J. 1979. Contact angle and the surface free energy of solids. *Surface Colloid Sci.* 11: 1–29.

Grigal, D.F., Brovold, S.L., Nord, W.S., and Ohmann, L.F. 1989. Bulk density of surface soils and peat in the North Central United States. *Can. J. Soil Sci.* 69: 895–900.

Hemond, H.F. and Goldman, J.C. 1985. On non-Darcian flow in peat. *J. Ecol.* 73: 579–584.

Hidding, A. 1999. Standardization by CEN/TC 223 ''Soil improvers and growing media'' and its consequences. In G. Schmilewski and W.J. Tonnis, Eds., Peat in Horticulture. *Proceedings of the International Peat Conference*, November 1, 1999, Amsterdam, the Netherlands, pp. 21–24.

Hillel, D., Krentos, V., and Stilianou, Y. 1972. Procedure and test of an internal drainage method for measuring soil hydraulic characteristics in-situ. *Soil Sci.* 114: 395–400.

Jobin, P., Caron, J., Bernier, P.Y., and Dansereau, B. 2004. Impact of two hydrophilic polymer on the physical properties of three substrates and the growth of *Petunia hybrida* ''Brilliant pink''. *J. Am. Soc. Hort. Sci.* 129: 449–457.

Jouany, C., Chenu, C., and Chassin, P. 1992. Détermination de la mouillabilité des constituants du sol à partir des mesures d'angles de contact: revue bibliographique. *Science du Sol* 30: 33–47.

King, J.A. and Smith, K.A. 1987. Gaseous diffusion through peat. *J. Soil Sci.* 38: 173–177.

King, P.M. 1981. Comparison of methods for measuring severity of water repellence of sandy soils and assessment of some factors that affect its measurement. *Aust. J. Soil Res.* 19: 275–285.

Klute, A. and Dirksen, C. 1986. Hydraulic conductivity and diffusivity: laboratory methods. In A. Klute, Ed., *Methods of Soil Analysis. Part. 1. 2nd ed.* Agronomy 9, American Society of Agronomy, Madison, WI, pp. 687–734.

Letey, J. 1969. Measurement of contact angle, water drop penetration time, and critical surface tension. In L.F. DeBano and J. Letey, Eds., Water-Repellent Soils. *Proceedings of the Symposium on Water-Repellent Soils*, University of California, Riverside, CA, pp. 43–47.

Letey, J., Osborn, J., and Pelishek, R.E. 1962. Measurement of liquid–solid contact angles in soil and sand. *Soil Sci.* 93: 149–153.

Macfarlane, I.C. 1969. Engineering characteristics of peat. In I.C. Macfarlane, Ed., *Muskeg Engineering Handbook*. University of Toronto Press, Toronto, ON, Canada, pp. 78–126.

McGhie, D.A. and Posner, A.M. 1980. Water repellence of a heavy-textured western Australian surface soil. *Aust. J. Soil Res.* 18: 309–323.

Michel, J.C. 1998. Studies on wettability of organic media used as growing culture media (in French). PhD thesis, Ecole Nationale Supérieure Agronomique de Rennes, Rennes, France.

Michel, J.C., Rivière, L.M., and Bellon-Fontaine, M.N. 2001. Measurement of the wettability of organic materials in relation to water content by capillary rise method. *Eur. J. Soil Sci.* 52: 459–467.

Milks, R.R., Fonteno, W.C., and Larson, R.A. 1989. Hydrology of horticultural substrates: II. Predicting physical properties of media in containers. *J. Am. Soc. Hort. Sci.* 114: 53–56.

Morel, P., Rivière, L.M., and Julien, C. 1999. Measurement of representative volumes of substrates: which method, in which objective? *Acta Hort.* 517: 261–269.

Mustin, M. 1987. Le compost. Editions Francois Dubusc, Paris, France.

Naasz, R., Michel, J.-C., and Charpentier, S. 2005. Measuring hysteretic hydraulic properties of peat and pine bark using a transient method. *Soil Sci. Soc. Am. J.* 69: 13–22.

Nemati, R., Caron, J., Banton, O., and Tardif, P. 2002. Determining air entry in peat substrates. *Soil Sci. Soc. Am. J.* 66: 367–373.

Nkongolo, N.V.K. 1996. Tortuosity of porous space: importance, assessment and effect on plant growth (in French, with English summary). PhD thesis, Université Laval, Sainte-Foy, QC, Canada.

Nkongolo, N.V. and Caron, J. 1999. Bark particle sizes and the modification of the physical properties of peat substrates. *Can. J. Soil Sci.* 79: 111–116.

Paquet, J., Caron, J., and Banton, O. 1993. *In situ* determination of the water desorption characteristics of peat substrates. *Can. J. Soil Sci.* 73: 329–339.

Parent, L.E. and Caron, J. 1993. Physical properties of organic soils. In M.R. Carter, Ed., *Soil Sampling and Methods of Analysis*, CRC Press, Boca Raton, FL, pp. 441–458.

Rolston, D.E. 1986. Gas diffusivity. In A. Klute, Ed., *Methods of Soil Analysis*, *Part 1, 2nd ed.* American Society of Agronomy, Madison, WI, pp. 1089–1102.

Sheppard, M.I., Tarnocai, C., and Thibault, D.H. 1993. Sampling organic soils. In M.R. Carter, Ed., *Soil Sampling and Methods of Analysis*, CRC Press, Boca Raton, FL, pp. 423–439.

Silc, T. and Stanek, W. 1977. Bulk density estimation of several peats in northern Ontario using the Von Post humification scale. *Can. J. Soil Sci.* 57: 75.

Topp, G.C., Davis, J.L., and Annan, A.P. 1980. Electromagnetic determination of soil water content: measurements in coaxial transmission lines. *Water Resour. Res.* 16: 574–582.

Topp, G.C. and Zebchuk, W. 1979. The determination of soil-water desorption curves for soil cores. *Can. J. Soil Sci.* 59: 19–26.

Vachaud, G. and Dane, J.H. 2002. Simultaneous determination of water transmission and retention properties: direct methods: field. In J.H. Dane and G.C. Topp, Eds., *Methods of Soil Analysis*. *Part 4*, Soil Science Society of America Book Series 5. Soil Science Society of America, Madison, WI, pp. 937–945.

Valat, B., Jouany, C., and Rivière, L.M. 1991. Characterization of the wetting properties of air dried peats and composts. *Soil Sci.* 152: 100–107.

Verdonck, O. and Gabriels, R. 1992. Reference method for the determination of physical properties of plant substrates. *Acta Hort.* 302: 169–179.

Verdonck, O.F., Cappaert, T.M., and De Boodt, M.F. 1978. Physical characterization of horticultural substrates. *Acta Hort.* 82: 191–200.

Washburn, E.W. 1921. The dynamics of capillary flow. *Phys. Rev.* 17: 273–283.

Watson, K.K. 1966. An instantaneous profile method determining the hydraulic conductivity of unsaturated porous materials. *Water Resour. Res.* 2: 709–715.

Watson, C.L. and Letey, J. 1970. Indices for characterizing soil-water repellency based upon contact angle–surface tension relationships. *Soil Sci. Soc. Am. J.* 34: 841–844.

Wever, G. 1991. Guide values for physical properties of peat substrates. *Acta Hort.* 294: 41–47.

Wever, G. 1995. Physical analysis of peat and peat-based growing media. *Acta Hort.* 401: 561–567.

Wind, P. 1969. Capillary conductivity data estimated by a simple method. In P.E. Rijtema and H. Wassink, Eds., *Water in the Unsaturated Zone*. Proc. Wageningen Symp. June 1966. Vol. 1. IASAH, Gentbrugge, Belgium, pp. 181–191.

Young, T. 1805. An essay on the cohesion of fluids. *Philos. Trans. R. Soc. Lond.*, 95: 65–87.

VII. SOIL WATER ANALYSES

Section Editors: W.D. Reynolds and G. Clarke Topp

Chapter 69
Soil Water Analyses: Principles and Parameters

W.D. Reynolds
Agriculture and Agri-Food Canada
Harrow, Ontario, Canada

G. Clarke Topp
Agriculture and Agri-Food Canada
Ottawa, Ontario, Canada

69.1 INTRODUCTION

For the uninitiated, soil water analyses can be daunting because they are based on many nonintuitive principles and they use a large number of complex parameters. The primary intent of this chapter is to help alleviate this situation by briefly reviewing the main principles and parameters involved in modern soil water analyses. The chapter also serves as additional background and context for the methods described in Chapter 70 through Chapter 85.

Soil water analyses can be organized into two main groups: (i) analysis of storage properties and (ii) analysis of hydraulic properties. Storage properties refer to the soil's ability to absorb and hold water, and these properties include water content, water potential, and water desorption and imbibition characteristics. Hydraulic properties, on the other hand, refer to the soil's ability to transmit or conduct water, and these include saturated hydraulic conductivity, unsaturated hydraulic conductivity, and various associated capillarity parameters such as sorptivity, flux potential, sorptive number, and flow-weighted mean (FWM) pore diameter. These properties and their interrelationships are discussed in the following sections.

69.2 SOIL WATER CONTENT

Soil water content can be defined on a gravimetric basis (mass of water per unit mass of dry soil) or on a volumetric basis (volume of water per unit bulk volume of dry soil), and it is expressed either as a dimensionless ratio or as a percentage. These two definitions are not equivalent, however, and it is consequently essential to specify the definition used when reporting water content values. It should also be noted that ''bulk volume'' of dry soil refers to the dimensions of the soil sample just before the water volume determination and before

any soil disturbance. Gravimetric water content (i.e., mass water/mass dry soil) is related to volumetric water content (i.e., volume water/bulk volume dry soil) via soil dry bulk density, ρ_b (mg m^{-3}) and pore water density, ρ_w (mg m^{-3}), according to the formula

$$\theta_v = \left(\frac{\rho_b}{\rho_w}\right)\theta_m \tag{69.1}$$

where θ_m is the gravimetric water content ($kg_{water}\ kg_{soil}^{-1}$) and θ_v is the volumetric water content ($m_{water}^3\ m_{soil}^{-3}$).

The volumetric water content is often expressed as ''relative saturation'' (also known as saturation ratio or degree of saturation), which gives the ratio of the measured volumetric water content (θ_v) to the corresponding volumetric water content at full or complete saturation (θ_s). Consequently, relative saturation gives the fraction of the soil pore space that is water-filled, and therefore ranges from a minimum value of 0 (no water in pore space) to a maximum value of 1 (pore space completely water-filled). When the soil pore space is completely water-filled (relative saturation = 1), the soil volumetric water content is equal to the soil porosity, n (porosity is defined as the total volume of soil pore space per unit bulk volume of soil). Relative saturation is frequently expressed as an ''effective saturation,'' S_e, which includes the residual soil water content, θ_r, that is the ''immobile'' water remaining in air-dry soil and retained in small isolated pores. Effective saturation is defined as $S_e = (\theta_v - \theta_r)/(\theta_s - \theta_r)$ and ranges from a minimum value of 0 at residual saturation (i.e., $\theta_v = \theta_r$) to a maximum value of 1 at complete saturation (i.e., $\theta_v = \theta_s$).

Water content measurement techniques are often classified as ''direct'' or ''indirect.'' Direct methods usually alter the sample irrevocably by changing its water content and physical characteristics (i.e., they are ''destructive'' methods); and these methods involve some form of removal or separation of water from the soil matrix with a direct measurement of the amount of water removed. Separation of the water from the soil matrix may be achieved by heating (water vaporization), by water replacement with a solvent (water absorption), or by chemical reaction (water disassociation). The amount of water removed is then determined by measuring the change in soil mass after heating, by collecting and condensing emitted water vapor, by chemical or physical analysis of the extracting solvent, or by quantitative measurement of chemical reaction products. The removal of water by heating is commonly referred to as the thermogravimetric technique (see Topp and Ferré 2002 for details) and it is by far the most common of the direct methods (see Chapter 70). Indirect methods measure some physical or chemical property of soil that depends on its water content. These properties include the relative permittivity (dielectric constant), electrical conductivity, heat capacity, hydrogen content, and magnetic susceptibility. The indirect methods usually alter the sample minimally (or not at all) in that the water content and physical characteristics of the sample are not changed appreciably by the measurement (i.e., they are ''nondestructive'' methods). However, the accuracy and precision of indirect methods depends to a large extent on the accuracy and precision of the relationship between the measured property (e.g., permittivity) and θ_v. In Chapter 70, we limit discussion to the indirect methods that are based on relative bulk soil dielectric permittivity, as they are the most highly developed and versatile.

The electromagnetic (EM) methods discussed in Chapter 70 all arise from analyses based in EM wave propagation or radio frequency (RF) circuits. Measurement of soil water content by these methods involves using the soil as an EM wave-propagating medium or as a resistor or capacitor in a circuit. The time-domain reflectometry (TDR), ground-penetrating radar (GPR), and remote radar (remote sensing) methods use the EM wave-propagation properties

of the soil, whereas the capacitance and impedance methods use the soil as a resistor or capacitor in a circuit.

The unique electrical properties of water (both pure water and soil pore water) form the basis of soil water content measurements by EM wave propagation. The relative dielectric permittivity of water is generally more than an order of magnitude larger than that of other soil components. As a result, the bulk relative dielectric permittivity of soil (ε_{ra}) is almost entirely a function of the soil's volumetric water content (θ_v), with only a slight dependence on the volume fraction of soil solids and the bulk soil electrical conductivity (Topp et al. 1980). For each of the EM methods presented in Chapter 70, a measurement of ε_{ra} is used to infer θ_v.

A single relationship between ε_{ra} and θ_v for all soils does not yet exist because of the complex interactions among EM waves and soil components. Many soils have very similar relationships, however, and thus sufficient accuracy can usually be attained using only a few ''quasigeneral'' relationships, for example, mineral soils, organic soils, saline soils, etc. (Topp et al. 1980; Topp and Ferré 2002). It has further been established that assuming a linear relationship between θ_v and $\sqrt{\varepsilon_{ra}}$ is appropriate for most soil materials (Topp and Reynolds 1998), and that this relationship is predicted by dielectric models employing a three-component mixture of soil solids, soil water, and soil air (Robinson et al. 2005). Thus EM methods are now considered highly reliable for measuring soil volumetric water content.

Water content methods are described in Chapter 70 and include thermogravimetry (oven drying), TDR, GPR, and a general description of the impedance and capacitance techniques. Thermogravimetry based on oven drying is usually considered the ''benchmark'' of accuracy and relevance against which other methods are assessed.

69.3 SOIL WATER POTENTIAL

Total water potential (ψ_t) is classically defined as the amount of work (force $\times$ distance) required to transport, isothermally and reversibly, an infinitesimal quantity of water from a specified reference condition (pool of pure water at specified pressure and elevation) to the system under consideration (Or and Wraith 2002). It is usually more convenient for natural porous materials, however, to consider ψ_t as the amount of work required to transport water away from the material (i.e., remove water rather than add water), as most natural materials are hydrophilic and thereby tend to absorb and retain water in a manner similar to that of a paper towel (nonswelling materials) or sponge (swelling materials).

Water potential is commonly expressed in units of energy per unit mass, U_m (J kg^{-1}), energy per unit volume, U_v (Pa), or energy per unit weight, U_{wt} (m), with the latter two being by far the most prevalent. Conversion amongst the units is achieved using

$$U_m = U_v/\rho_w = gU_{wt} \tag{69.2}$$

where ρ_w is the density of water (1000 kg m^{-3} at 20°C) and g is the acceleration due to gravity (9.81 m s^{-2}).

The total potential, ψ_t, of water in soil or other natural porous materials is usually the sum of four-component water potentials:

$$\psi_t = \psi_m + \psi_\pi + \psi_p + \psi_g \tag{69.3}$$

where ψ_m is the matric potential, ψ_π is the osmotic potential, ψ_p is the pressure potential, and ψ_g is the gravitational potential. The matric potential is negative ($\psi_m \leq 0$) and arises from the various electrostatic forces in the soil matrix that attract water when the soil is unsaturated. The osmotic potential is also negative ($\psi_\pi \leq 0$) and results from dissolved materials (salts) and colloids, which lower the pore water's activity (free energy) below that of pure water. The pressure potential is positive ($\psi_p \geq 0$), and is caused by the hydrostatic pressure of the pore water overlying the measurement point when the soil is saturated. The gravitational potential (ψ_g) arises from the action of the earth's gravitational force field on the pore water and can be either positive or negative depending on whether the datum is below or above the measuring point, respectively. Campbell (1987) reviews the various techniques for measuring matric potential and the type of sensors employed; and the readers are recommended to refer to Passioura (1980) for a more detailed discussion of the meaning of matric potential. A reasonable estimate of osmotic potential can be derived from measurements of electrical conductivity corrected for water content (Gupta and Hanks 1972); however, more reliable measures can be obtained by extracting soil pore water and measuring the osmotic potential directly in a thermocouple psychrometer or by using the combined pressure chamber and thermocouple psychrometer system of Campbell (1987). When the matric, pressure, and gravitational potentials are expressed in units of energy per unit weight (U_{wt}), they are generally called ''heads'' rather than potentials, and they are equivalent to the vertical distance between the measurement point (e.g., piezometer intake, tensiometer cup, etc.) and either the free surface water level (for matric and pressure heads) or the selected reference elevation or datum (for gravitational heads) (Figure 69.1). Water flow can be induced by gradients in all four water potentials, although a gradient in osmotic potential requires the presence of a membrane that is permeable to water but impermeable to selected solutes and colloids (Or and Wraith 2002). Methods for measuring water potential are described in Chapter 71 and include the piezometer method, the tensiometer method, resistance block methods, and selected thermocouple psychrometer methods.

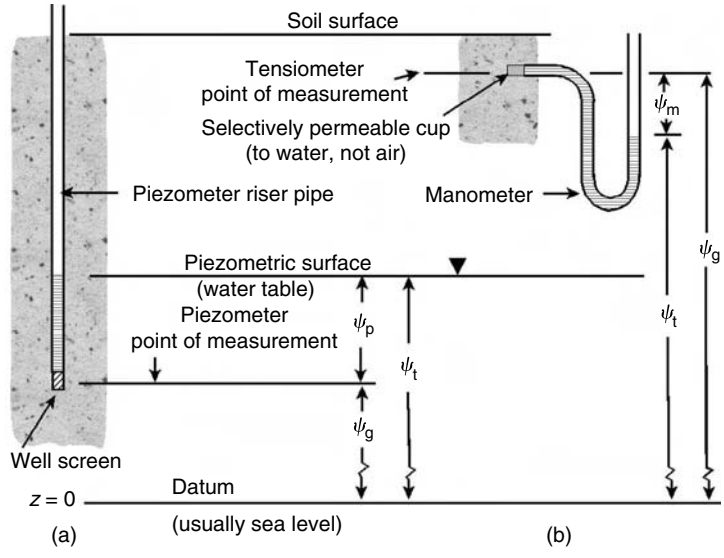

FIGURE 69.1. The operating principles of a piezometer (a) and a tensiometer (b). The piezometer measures pressure potential (ψ_p), and the tensiometer measures matric potential (ψ_m).

69.4 SOIL WATER DESORPTION AND IMBIBITION

Soil water desorption and imbibition curves characterize the relationship between soil volumetric water content, θ_v [L^3L^{-3}] (Chapter 72 through Chapter 74), and pore water matric head, ψ_m [L] (Chapter 71). The desorption curve (also known as the water release characteristic, water retention curve, and soil moisture characteristic) describes the decrease in θ_v from saturation as ψ_m decreases from zero, whereas the imbibition curve describes the increase in θ_v from dryness as ψ_m increases from a large negative value (see Figure 69.2). The two curves generally have different shapes because of hysteretic effects (Hillel 1980); and when a partially drained soil is rewetted, or when a partially wetted soil is redrained, the relationship between θ_v and ψ_m usually follows an intermediate and nonunique path between the desorption and imbibition curves (see Figure 69.2). For this reason, the desorption curve is often referred to as the ''main drainage curve''; the imbibition curve as the ''main wetting curve''; and the intermediate curves as ''scanning curves'' (see Figure 69.2). When the soil has a relatively uniform and narrow pore size distribution (e.g., structureless sandy soil), distinct ''air-entry'' and ''water-entry'' matric heads can occur on the desorption and imbibition curves, respectively (Figure 69.2). The air-entry head or value, ψ_a [L], is the pore water matric head where the saturated soil (i.e., θ_v constant and maximum) suddenly starts to desaturate as a result of decreasing ψ_m; and the water-entry head or value, ψ_w [L], is the pore water matric head where an unsaturated soil suddenly saturates as a result of increasing ψ_m. Both ψ_a and ψ_w are negative, and typically, $|\psi_a| \approx 2|\psi_w|$ (Bouwer 1978). Also note that in Figure 69.2 that the saturated volumetric water content on the imbibition curve (i.e., θ_{fs} at $\psi_m = 0$) is less than the saturated volumetric water content on the desorption curve (i.e., θ_s at $\psi_m = 0$), which is a consequence of air entrapment in soil pores during the wetting process (Bouwer 1978). As implied above, soil water desorption

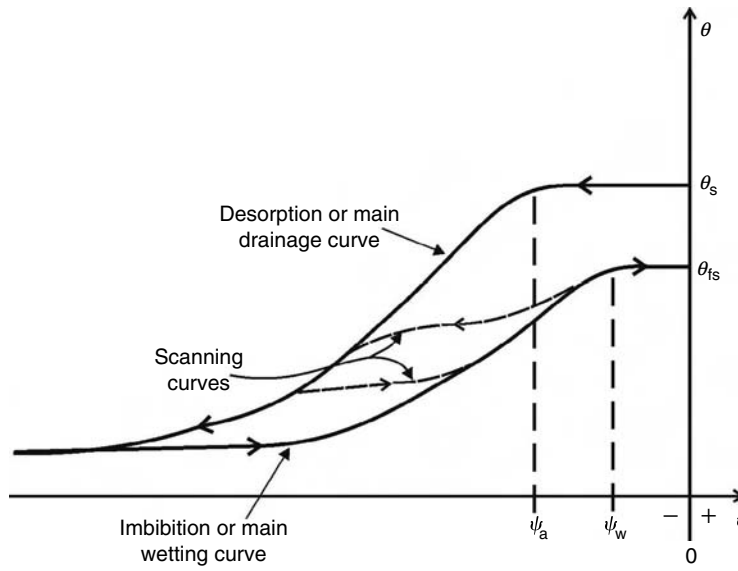

FIGURE 69.2. Desorption, imbibition, and scanning curves, $\theta(\psi)$, for a hysteretic soil. The arrows indicate the direction of the drainage and wetting processes. Note that the saturated volumetric water content for the imbibition curve, θ_{fs}, is less than that for the desorption curve, θ_s, due to air entrapment upon rewetting. Note also that the water-entry matric head, ψ_w [L], is greater (less negative) than the air-entry matric head, ψ_a [L].

and imbibition is a complicated process that is difficult and time-consuming to characterize in detail. Fortunately, it is usually not necessary to measure the scanning curves and Chapter 72 through Chapter 74 consequently focus on determination of only the desorption (main drainage) curve and the imbibition (main wetting) curve.

69.4.1 Application of Desorption and Imbibition Curves

The shape and magnitude of desorption and imbibition curves depends on the number and size distribution of the soil pores, which in turn depends on texture, porosity, structure, organic matter content, and clay mineralogy. Figure 69.3 gives schematic examples of desorption curves for a representative coarse-textured, unstructured soil (e.g., uniform sandy soil), and for a representative fine-textured soil (e.g., clayey soil) with and without structure, where ''structure'' refers to the presence of aggregates, peds, and macropores (i.e., large cracks, root channels, worm holes, etc.). Note that the coarse-textured (sandy) soil retains less water than the fine-textured (clayey) soil (i.e., lower θ_v values), and it also releases its water in a different manner (i.e., different curve shape). Note also that soil structure can increase the saturated water content (if the bulk density decreases) and it can cause the wet-end of the desorption curve to be very steep relative to a structureless condition when aggregates, peds, and macropores are not present.

Soil water desorption and imbibition curves are important for determining soil pore size distribution, for interpreting soil strength data, and for determining the transmission and

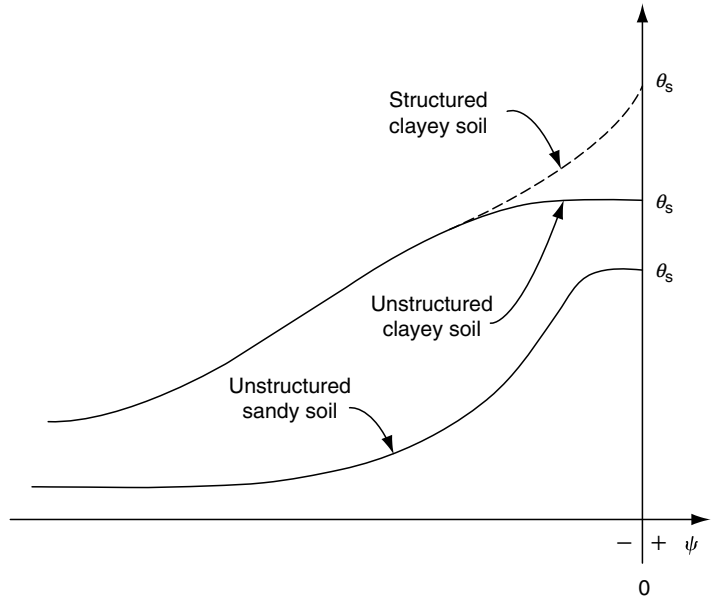

FIGURE 69.3. Soil water desorption curves for a ''representative'' unstructured sandy soil, and a representative clayey soil with and without structure. θ_s [L^3L^{-3}] is the saturated volumetric water content and ψ [L] is pore water matric head. Note that the increase in θ_s for the structured clayey soil relative to the unstructured clayey soil implies a decrease in soil bulk density. If bulk density remains constant, the presence of structure changes only the shape of the curve and not the value of θ_s.

storage of fluids (liquids, gases) in the soil profile. The sizes of soil pores relevant to the storage and transmission of fluids are determined from desorption and imbibition curves via the Kelvin or ''capillary rise'' equation. Soil strength relationships, such as cone penetration resistance and vane shear, are highly dependent on the antecedent soil water content at the time of the measurement, and must therefore be related to the desorption and imbibition curves before detailed analyses can be conducted. With respect to water and solute transmission, the desorption and imbibition curves are required for defining the water capacity relationship in the water transport (Richards) equation, and various solute sorption–desorption relationships in the solute transport (convection–dispersion) equation. With respect to water and air storage, the desorption and imbibition curves are used to determine saturated and field-saturated soil water contents, field capacity water content, permanent wilting point water content, air capacity, and plant-available water capacity. These water/air storage parameters and other quantities derived from these parameters are defined and briefly discussed in the following sections.

69.4.2 Water and Air Storage Parameters

The volumetric water content, θ_v [L^3L^{-3}], for a rigid soil (i.e., no shrinkage or swelling) is defined by

$$\theta_v = V_w/V_b \tag{69.4}$$

where V_w [L^3] is the volume of soil water per unit bulk volume of dry soil, V_b [L^3] (see Section 69.2). When the soil is completely saturated (i.e., no entrapped air), V_w = volume of pore space and thus $\theta_v = \theta_s$ = soil porosity. When the soil is ''field-saturated'' (entrapped air present), $V_w <$ volume of pore space and $\theta_v = \theta_{fs} <$ soil porosity, usually by 2–5 percentage points (Bouwer 1978). For most field applications where wetting and drying are involved, θ_{fs} is a more relevant measure of the maximum soil volumetric water content than θ_s or porosity because entrapped air is almost always present.

Field water capacity (more commonly known as field capacity, FC) is formally defined as the amount of water retained in an initially saturated or near-saturated soil after 2–3 days of free gravity drainage without evaporative loss (Hillel 1980; Townend et al. 2001). For application purposes, however, FC is usually defined as the equilibrium volumetric water content, θ_{FC}, at a specified matric head, ψ_{FC}. For intact soil containing normal field structure, $\psi_{FC} = -1$ m is most often used, although values as high as $\psi_{FC} = -0.5$ m have been recommended for wet soils with a shallow water table, and as low as $\psi_{FC} = -5$ m for dry soils with a very deep water table (Cassel and Nielsen 1986). If the soil has been disturbed and repacked, use of $\psi_{FC} = -3.3$ m is usually considered to provide θ_{FC} values that are comparable to intact soil values.

The permanent wilting point (PWP) is defined as the soil water content at which growing plants wilt and do not recover when the evapotranspirative demand is eliminated by providing a water vapor–saturated atmosphere for at least 12 h (Hillel 1980; Romano and Santini 2002). Once the soil water decreases to the PWP value, plants are permanently damaged and may even die if water is not added quickly. In this respect, the PWP water content also represents the amount of ''plant-unavailable'' water; i.e., water that is too strongly held by the soil to be extracted by plant roots. Although the true PWP can vary widely with plant species, plant growth stage, and soil type, it has been found that the equilibrium volumetric water content, θ_{PWP}, at the matric head, $\psi_{PWP} = -150$ m, is a

suitable working definition (Soil Science Society of America 1997). This is because water content becomes relatively insensitive to matric head (i.e., water content is nearly constant) in the $\psi_m \leq -150$ m range for most agricultural soils (Romano and Santini 2002).

Plant growth and performance is critically dependent on adequate supplies of air and water in the root zone. Convenient and popular measures of the soil's ability to store and provide air and water for plant use are the so-called air capacity and plant-available water capacity. Air capacity (AC) is defined as

$$AC = \theta_s - \theta_{FC} \tag{69.5}$$

and proposed minimum values for adequate root-zone aeration are 0.10 $m^3\ m^{-3}$ for loamy soils (Grable and Siemer 1968), 0.15 $m^3\ m^{-3}$ for clayey soils (Cockroft and Olsson 1997), and about 0.20 $m^3\ m^{-3}$ for horticultural substrates (Verdonck et al. 1983; Bilderback et al. 2005). Field soils that have AC values appreciably below these minimums are susceptible to periodic and damaging root-zone aeration deficits. Plant-available water capacity (PAWC) is defined as

$$PAWC = FC - PWP \tag{69.6}$$

and it represents the maximum amount of water that a fully recharged soil can provide to plant roots. This definition is based on the concept that soil water at $\psi_m > \psi_{FC}$ drains away too quickly to be captured by plant roots, whereas water at $\psi_m < \psi_{PWP}$ is held too strongly by the soil to be extracted by the roots (compare PWP discussion). The proposed minimum PAWC for optimum plant growth and minimum susceptibility to droughtiness is 0.20–0.30 $m^3\ m^{-3}$ (Verdonck et al. 1983; Cockroft and Olsson 1997; Bilderback et al. 2005).

Recent research (Olness et al. 1998; Reynolds et al. 2002) suggests that the optimal balance between root-zone soil water and soil air is achieved in rain-fed crops when

$$FC/Porosity = 0.66 \tag{69.7}$$

or alternatively, when

$$AC/Porosity = 0.34 \tag{69.8}$$

These criteria are based on the finding that maximum production of crop-available nitrogen by aerobic microbial mineralization of organic matter occurs when about 66% of the soil pore space in the root zone is water-filled, or alternatively, when 34% of the pore space is air-filled (Skopp et al. 1990). The rationale for applying Equation 69.7 and Equation 69.8 to rain-fed crops is that root-zone soils with these ratios are likely to have desirable water and air contents (for good microbial production of nitrogen) more frequently and for longer periods of time (especially during the critical early growing season) than root-zone soils that have larger or smaller ratios.

69.4.3 Determination of Desorption and Imbibition Curves

The generally accepted ''ideal'' for obtaining soil water desorption and imbibition curves is to collect simultaneous field-based measurements of volumetric water content, θ_v, and

matric head, ψ_m, in an undisturbed vertical profile under conditions of steady drainage (desorption) or steady wetting (imbibition). Several approaches are available for achieving this (e.g., Bruce and Luxmoore 1986), with the most popular approach being the ''instantaneous profile'' method (see Chapter 83). Several factors inhibit or complicate the field-based methods, however, including complex and poorly controlled boundary conditions (e.g., varying water table depth, strong and varying temperature gradients); limited instrumentation for determining ψ_m (e.g., tensiometers have a narrow operating range and often fail after a period of time); difficulty in maintaining continuous wetting or drainage throughout the soil profile (e.g., periodic rainfalls can induce hysteretic effects); complicated and labor-intensive experimental setups (e.g., installation of many pairs of θ_v and ψ_m sensors over a substantial depth range with minimum soil disturbance, equipment for applying large volumes of water to saturate the soil profile, complex electronics and data logging equipment for simultaneous and long-term monitoring of θ_v and ψ_m, limited ability for spatial replication); and potentially very long measurement times (it can take several weeks to months to obtain adequate desorption or imbibition curve over the required soil depth because of slow wetting and drainage rates). As a result, experimentally determined desorption and imbibition curves are usually obtained in the laboratory on relatively small soil cores or columns where θ_v and ψ_m sensors are more easily installed and maintained, and where initial and boundary conditions can be precisely defined and controlled. Desorption and imbibition curves can also be estimated from basic soil data via pedotransfer functions (see Chapter 84); from flow experiments, such as the evaporation method (see Chapter 81) and the instantaneous profile method (see Chapter 83); or from inverse modeling procedures (Hopmans et al. 2002).

Laboratory determination of desorption and imbibition curves that are representative of field conditions requires (i) the collection of soil cores or columns that are large enough to adequately sample the antecedent soil structure and (ii) use of collection, handling, and analysis procedures that maintain the soil structure intact. Bouma (1983, 1985) suggests that the volume encompassed by the core/column should include at least 20 soil structural units (e.g., peds, worm holes, abandoned root channels, etc.), which is especially important for the $\psi_m > -3.3$ m range and if saturated hydraulic conductivity (see Chapter 75) is to be determined on the same sample. For relatively structureless sandy soils, the minimum recommended core/column inside diameter and length is on the order of 7.6 cm, whereas structured loamy and clayey soils should use a core length and diameter of at least 10 cm (McIntyre 1974). The samples should be collected when the soil is near its field capacity water content, θ_{FC}, which generally makes the soil strong enough to resist compaction and structural collapse during core/column insertion, but still plastic enough to prevent shattering and breakage of peds. Recommended procedures for the collection of minimally disturbed soil samples are given in McIntyre (1974) and Chapter 80. Excavated soil cores should be trimmed flush with the ends of the sampling cylinder, capped to prevent damage of the core ends, wrapped in plastic to prevent evaporation, and transported to the laboratory in cushioned coolers to minimize vibration-induced damage and large temperature-changes. Sample storage before analysis should be in darkened facilities maintained at $0°C-4°C$, which is cold enough to inhibit faunal–bacterial–fungal–algal activity, but not so cold as to cause freezing and ice lens formation.

Soil water desorption–imbibition methods are described in Chapter 72 through Chapter 74 and include the tension table, tension plate, and pressure extractor methods (Chapter 72), the long column method (Chapter 73), and the dew point psychrometer method (Chapter 74). The approximate matric head ranges of these methods are compared in Figure 69.4.

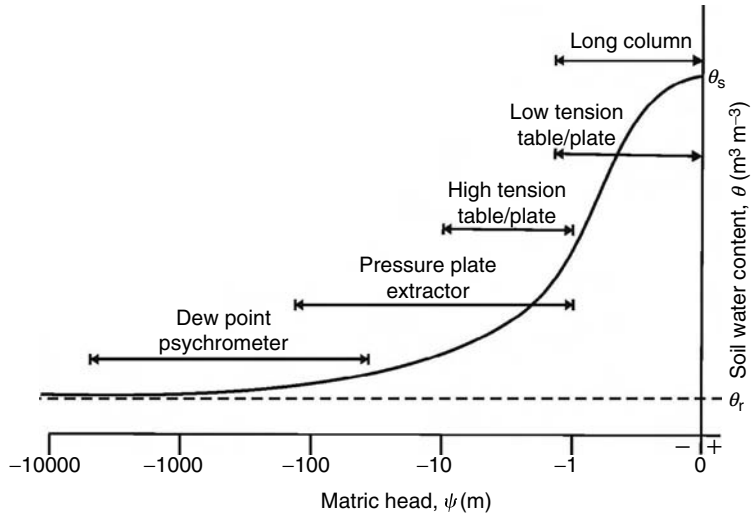

FIGURE 69.4. Approximate matric head ranges of the long column, tension table, tension plate, pressure extractor, and dew point psychrometer methods for measuring desorption and imbibition curves. θ_s is the saturated water content and θ_r is the residual water content. These methods are described in Chapter 72 through Chapter 74.

69.5 SATURATED HYDRAULIC PROPERTIES

The saturated hydraulic properties are used to describe and predict water movement in permeable porous material (e.g., soil, building fill, sand, rock, etc.) when the pore water pressure (or matric) head in the material is greater than or equal to the water-entry value or air-entry value (see Section 69.4 for explanation of water-entry and air-entry values). The saturated soil hydraulic properties of greatest relevance include saturated hydraulic conductivity, field-saturated hydraulic conductivity, and the so-called capillarity parameters such as matric flux potential, sorptivity, sorptive number, Green–Ampt wetting front pressure head, and FWM pore size and pore number. Saturated hydraulic conductivity, K_s [LT^{-1}], and field-saturated hydraulic conductivity, K_{fs} [LT^{-1}], are measures of the ''ease'' or ''ability'' of a permeable porous medium to transmit water. The K_s parameter applies when the water-conducting pores in the porous medium are completely water-filled (saturated), and the K_{fs} parameter applies when the water-conducting pores contain entrapped or encapsulated bubbles of air or gas (field-saturated). The capillarity parameters measure various aspects of the suction or ''capillary pull'' that unsaturated soil exerts on infiltrating water; and measurement or estimation of the soil's capillarity is usually required when K_s or K_{fs} are measured in initially unsaturated soil (e.g., soil above the water table). The K_s and K_{fs} parameters are discussed below and the capillarity parameters are discussed in Section 69.6 (unsaturated hydraulic properties).

The K_s and K_{fs} parameters are defined by Darcy's law, which may be written in the form

$$q = K_{sat} i \tag{69.9}$$

where q is the water flux density through the porous medium (volume of water flowing through a unit cross-sectional area of porous medium per unit time), i is the hydraulic head gradient in the porous medium (dimensionless), and $K_{sat} = K_s$ or K_{fs}, depending on whether

the porous medium is completely saturated or field-saturated, respectively. As implied by Equation 69.9, the dimensions of K_{sat} are the same as those for q (i.e., volume of water per unit cross-sectional area of flow per unit time); however, these dimensions are usually simplified to length per unit time so that K_{sat} may be expressed in the more convenient (but physically incorrect) units of velocity (i.e., cm s^{-1}, cm s^{-1}, cm h^{-1}, m $days^{-1}$, etc.). The K_{sat} value is a constant when the porous medium is rigid, homogenous, isotropic, and stable; when *in-situ* biological activity such as earthworm burrowing and algal/fungal growth are negligible; and when the flowing water maintains constant physical and chemical properties (e.g., temperature, viscosity, dissolved air content, dissolved salt content, etc.) and does not chemically or physically interact with the porous medium. The primary factors determining the magnitude of K_{sat} include the physical characteristics of the porous medium and the physical and chemical characteristics of the flowing water (discussed further below).

The physical characteristics of the porous medium affecting K_{sat} include the size distribution, roughness, tortuosity, shape, and degree of interconnectedness of the water-conducting pores. For soils, K_{sat} increases greatly with coarser texture (larger grain sizes), increasing numbers of biopores (e.g., worm holes, root channels), and increasing structure (e.g., aggregates, interpedal spaces, shrinkage cracks), as these factors increase the number of water-conducting pores that are relatively large, straight (i.e., low tortuosity), smooth, rounded, and interconnected. Soils and other porous media that are coarse-textured, structured, and bioporous consequently tend to have larger K_{sat} values than those that are fine-textured, structureless, and devoid of biopores. In addition, texture, structure, and biopores can interact in such a way that it is not uncommon for a fine-textured material with structure or biopores (e.g., a clay soil with shrinkage cracks or worm holes) to have a substantially larger K_{sat} than a coarse-textured material that is devoid of structure and biopores (e.g., single-grain sandy soil). An important implication of this texture–structure–biopore interaction is that the physical condition of the porous medium must be preserved by the measuring technique in order for the measured K_{sat} value to be representative of the porous medium in its ''natural'' or *in-situ* condition.

Hydraulic conductivity is inversely related to water viscosity, which is inversely related to temperature (Bouwer 1978, p. 43). Consequently, the measured value of K_{sat} will increase with the temperature of the water used; and an increase in water temperature from 10°C to 25°C will result in a 45% increase in K_{sat}, all other factors remaining equal. Temperature effects can be important if the water used in a field measurement differs greatly in temperature from that of the resident soil water or groundwater, or if laboratory measurements of field samples (e.g., intact cores) are conducted at temperatures that differ greatly from the field temperature. Precise measurements and comparisons of K_{sat} values should therefore always be referenced to a specific water temperature, which is usually 20°C (Bouwer 1978, p. 43), as it yields a water viscosity of nearly 1 cP. Note in passing that the temperature of ''deep'' soil water and shallow groundwater is fairly constant and close to the local mean annual air temperature, for example, about 10°C at 40°N–45°N latitude (Bouwer 1978, p. 378).

The concentration and speciation of dissolved salts in the water can affect K_{sat} through swelling, flocculation, or dispersion of silt and clay within the porous medium, and through the creation or dissolution of precipitates. The K_{sat} value will usually increase if silt and clay particles are flocculated, or if precipitates are dissolved, as this tends to increase the size and interconnectedness of water-conducting pores. Alternatively, formation of precipitates and swelling/dispersion of silt and clay particles will usually decrease K_{sat} through narrowing and plugging of pores. Reduction in K_{sat} most commonly occurs in silt- and clay-rich soils

when the cationic speciation is changed or the concentration of the resident soil water is diluted by incoming rainfall, irrigation water, or groundwater. The relative concentrations of sodium, calcium, and magnesium in solution and sorbed onto the porous medium exchange sites are particularly important in this respect (Bouwer 1978, p. 44). In extreme cases, such as when water low in dissolved salts (e.g., rainwater) is introduced into saline soil, the resulting silt and clay dispersion can reduce K_{sat} to virtually zero. The water used for measuring the K_{sat} of a natural porous medium should therefore be either ''native'' water extracted from the porous medium, or a laboratory ''approximation,'' which has about the same major ion composition and concentrations as the native water. Local municipal tap water is often an adequate approximation to native soil water, although this should always be checked as some municipal water treatment facilities can change major ion chemistry radically. Distilled or deionized water should never be used for measuring the K_{sat} of a natural porous medium, as it will almost always induce clay swelling or dispersion of silt and clay particles.

Entrapped bubbles tend to constrict or block the water-conducting pores in a porous medium. As a result, K_{fs} (i.e., field-saturated K_{sat}) is usually less than K_s (i.e., completely saturated K_{sat}) with the degree of reduction largely dependent on the mechanism responsible for bubble formation. Bubbles can become encapsulated in pores through physical entrapment of resident air during wetting of an initially unsaturated porous medium (Bouwer 1966); by accumulation of biogases (e.g., methane) as a result of microbial activity (Reynolds et al. 1992); and by ''exsolution'' of dissolved air as a result of changes in the temperature or chemistry of the pore water (Bouwer 1978, p. 45). Air encapsulation as a result of rapid wetting (e.g., ponded infiltration) often causes K_{fs} to be on the order of 0.5 K_s (Bouwer 1966; Stephens et al. 1987; Constantz et al. 1988), while gradual accumulation of biogases and exsolved air can cause much greater reductions (Bouwer 1978; Reynolds et al. 1992).

Further information concerning the theoretical basis and other aspects of K_s, K_{fs}, and their associated capillarity parameters can be obtained from Bouwer (1978), Koorevaar et al. (1983), Smith (2002), Reynolds and Elrick (2005), and references contained therein. Saturated hydraulic property methods are described in Chapter 75 through Chapter 79 and Chapter 84; and they include the constant and falling head core methods (Chapter 75), selected constant and falling head well permeameter methods (Chapter 76), selected constant and falling head ring infiltrometer methods (Chapter 77), the auger hole method (Chapter 78), the piezometer method (Chapter 79), and selected estimation methods (Chapter 84).

69.6 UNSATURATED HYDRAULIC PROPERTIES

Unsaturated hydraulic properties are used to describe and predict water movement in permeable porous material (e.g., soil, building fill, sand, rock, etc.) that is only partially saturated and has a pore water matric head that is less than the material's air-entry value or water-entry value (see Section 69.4 for explanation of air-entry and water-entry values). The unsaturated hydraulic properties of greatest relevance include unsaturated hydraulic conductivity, $K(\psi)$ or $K(\theta)$ [LT^{-1}], sorptivity, $S(\psi)$ [$LT^{-1/2}$], sorptive number, $\alpha^*(\psi)$ [L^{-1}], flux potential, $\phi(\psi)$ [L^2T^{-1}], FWM pore diameter, PD(ψ) [L], and the number of FWM pores per unit area, NP(ψ) [L^{-2}]. The $K(\psi)$ or $K(\theta)$ parameter quantifies the ability of an unsaturated porous material to transmit water as a result of a hydraulic head gradient, while $S(\psi)$ measures the ability of the material to imbibe water as a result of capillarity forces (Philip 1957). The $\alpha^*(\psi)$ parameter, on the other hand, indicates the relative magnitudes of gravity and capillarity forces during unsaturated flow (Raats 1976),

while the $\phi(\psi)$ parameter relates to the ''potential'' for water flow (Gardner 1958). The PD(ψ) parameter represents the effective equivalent mean pore size conducting water during constant head infiltration, and NP(ψ) indicates the number of PD(ψ) pores that are active (Philip 1987). These parameters and their interrelationships are discussed briefly below.

Vertical water flow in rigid, homogeneous, variably saturated porous material (e.g., soil) can be described by (Richards 1931)

$$\frac{\partial\theta}{\partial t} = \frac{\partial}{\partial z}\left[K(\psi)\frac{\partial H}{\partial z}\right] = \frac{\partial}{\partial z}\left[K(\theta)\frac{\partial H}{\partial z}\right]; \quad H = \psi + z \tag{69.10}$$

where θ [L^3L^{-3}] is volumetric water content, t[T] is time, $K(\psi)$ [LT^{-1}] is the hydraulic conductivity (K) versus pore water matric head (ψ) relationship, $K(\theta)$ [LT^{-1}] is the hydraulic conductivity (K) versus volumetric water content (θ) relationship, H [L] is hydraulic head, and z [L] is elevation or gravitational head above an arbitrary datum (positive upward). (Note that the ''v'' and ''m'' subscripts on θ and ψ, respectively, have been dropped to simplify the nomenclature.) Equation 69.10 indicates that the rate of water flow through the porous medium is determined by the magnitude of the hydraulic head gradient, $\partial H/\partial z$, and by the hydraulic conductivity function, $K(\psi)$ or $K(\theta)$. The $K(\psi)$ or $K(\theta)$ term is the porous material's water transmission relationship, and it gives the permeability of the porous material to water as a function of either pore water matric head, ψ [L], or volumetric water content, θ [L^3L^{-3}].

The $K(\psi)$ and $K(\theta)$ relationships depend strongly on the magnitude and shape of the pore water desorption–imbibition relationship, $\theta(\psi)$ [L^3L^{-3}], which itself describes the change in volumetric water content with changing pore water matric head (Section 69.4). As a result, the $K(\psi)$ and $K(\theta)$ relationships decrease from the K_{sat} maximum (Section 69.5) as ψ and θ decrease from their respective maximum values at porous medium saturation (i.e., $\psi = 0$ and $\theta = \theta_s$). Through their connection with the $\theta(\psi)$ relationship, $K(\psi)$ and $K(\theta)$ depend on the number and size distribution of the porous medium pores, which in turn depend on porosity, structure, texture, organic matter content, and clay mineralogy. Unlike $\theta(\psi)$, however, $K(\psi)$ and $K(\theta)$ also depend on pore morphology parameters such as tortuosity, roughness, connectivity, and continuity. These various dependencies cause $K(\psi)$ and $K(\theta)$ to change by many orders of magnitude over the range in ψ applicable to plant growth (i.e., $\approx -150\ \text{m} \le \psi \le 0$).

Due to the extreme sensitivity of unsaturated hydraulic conductivity to pore size and pore morphology, the magnitude and shape of the $K(\psi)$ and $K(\theta)$ relationships change substantially with the texture and structure of the porous medium. Figure 69.5 gives schematic examples of $K(\psi)$ and $K(\theta)$ relationships for a representative ''sandy'' soil, and for a representative ''loamy'' soil with and without structure, where structure refers to the presence of aggregates, peds, cracks, root channels, worm holes, etc. For convenience, the structured loam was assumed to have the same $\theta(\psi)$ relationship as the unstructured loam. Note in these figures that for a rigid (nonswelling) porous material, $K(\psi)$ and $K(\theta)$ are maximum and constant when the material is saturated, i.e.,

$$K(\psi) = K(\theta) = \text{constant} = K_{sat}; \quad \psi \ge \psi_e, \quad \theta = \theta_{sat} \tag{69.11}$$

where K_{sat} [LT^{-1}] is the saturated or field-saturated hydraulic conductivity, ψ_e [L] is the air-entry or water-entry matric head, and θ_{sat} [L^3L^{-3}] is saturated or field-saturated volumetric water content (see Section 69.4 and Section 69.5). Note also that the near-saturated hydraulic

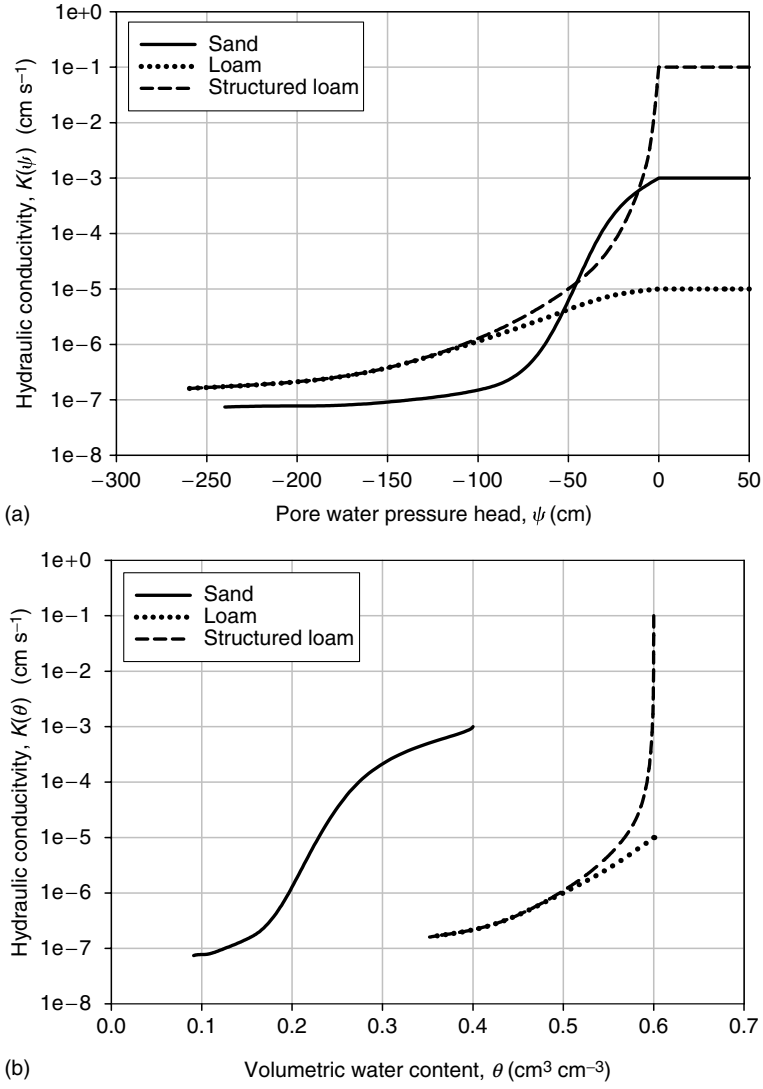

FIGURE 69.5. (a) Hydraulic conductivity, $K(\psi)$, versus pore water matric (or pressure) head, ψ and (b) hydraulic conductivity, $K(\theta)$, versus volumetric water content, θ, for a representative sandy soil (Sand), and a representative loamy soil with structure (structured loam) and without structure (loam).

conductivity relationship in a structured porous medium can change very rapidly (by orders of magnitude) with only small changes in ψ or θ, and that the hydraulic conductivity of a fine-textured material with structure can be either greater than or less than the hydraulic conductivity in a coarse-textured material, depending on the value of ψ or θ. Texture and structure effects are also illustrated in the K_{sat} values, where it is seen that the K_{sat} of the sandy soil is two orders of magnitude greater than the K_{sat} of the unstructured loam (texture effect), but two orders of magnitude less than the K_{sat} of the structured loam (structure effect).

The sorptivity parameter, $S(\psi)$ [$LT^{-1/2}$], is related to $K(\psi)$ and $\phi(\psi)$ by (Philip 1957; White and Sully 1987)

$$S(\psi_0) = \left[\gamma[\theta(\psi_0) - \theta(\psi_i)] \int_{\psi_i}^{\psi_0} K(\psi) d\psi\right]^{1/2} = [\gamma[\theta(\psi_0) - \theta(\psi_i)]\phi(\psi_0)]^{1/2};$$
$$\theta(\psi_i) \le \theta(\psi_0) \le \theta_s, \quad \psi_i \le \psi_0 \le 0 \tag{69.12}$$

where it is seen that the matric flux potential, $\phi(\psi_0)$ [$L^2\ T^{-1}$], is defined by (Gardner 1958)

$$\phi(\psi_0) = \int_{\psi_i}^{\psi_0} K(\psi) d\psi; \quad -\infty < \psi_i \le \psi_0 \le 0 \tag{69.13}$$

In Equation 69.12 and Equation 69.13, ψ_0 [L] is the pore water matric head at the infiltration (sorption) surface, ψ_i [L] is the background or antecedent pore water matric head in the porous medium at the time of the infiltration measurement, $\theta(\psi_0)$ [L^3L^{-3}] is the porous medium volumetric water content at $\psi = \psi_0$, $\theta(\psi_i)$ [L^3L^{-3}] is the porous medium volumetric water content at $\psi = \psi_i$, and $\gamma = 1.818$ is a dimensionless empirical constant (White and Sully 1987) related to the shape of the wetting (or drainage) front ($\gamma = 1.818$ for wetting, but may be smaller for drainage). The shape and magnitude of the $S(\psi_0)$ and $\phi(\psi_0)$ relationships is thus controlled by the shape and magnitude of the $K(\psi)$ relationship, as well as the magnitude of ψ_i. Figure 69.6 gives the $S(\psi_0)$ and $\phi(\psi_0)$ relationships corresponding to the $K(\psi)$ (and $\theta(\psi)$) relationships for our three representative soils, and it is seen that $S(\psi_0)$ and $\phi(\psi_0)$ are essentially ''subdued replicas'' of $K(\psi)$. Note from Equation 69.12 and Equation 69.13, however, that $S(\psi_0) = \phi(\psi_0) = 0$ when $\theta(\psi_0) = \theta(\psi_i)$ or when $\psi_0 = \psi_i$; and that $S(\psi_0)$ and $\phi(\psi_0)$ do not exist for positive pore water pressure heads (i.e., $\psi_p > 0$).

If the $K(\psi)$ relationship is represented by the Gardner (1958) exponential function

$$K(\psi) = K_{sat} \exp(\alpha\psi); \quad \psi \le 0 \tag{69.14}$$

then Equation 69.13 becomes

$$\phi(\psi_0) = \left[\frac{K(\psi_0) - K(\psi_i)}{\alpha(\psi_0)}\right]; \quad \psi_i < \psi_0, \quad K(\psi_i) < K(\psi_0) \tag{69.15}$$

where the ''alpha parameter,'' $\alpha(\psi_0)$ [L^{-1}] gives the slope of $\ln K$ versus ψ. For most natural porous materials at field capacity or dryer, $K(\psi_i) \ll K(\psi_0)$, and Equation 69.15 can consequently be simplified to

$$\phi(\psi_0) \approx \frac{K(\psi_0)}{\alpha^*(\psi_0)}; \quad K(\psi_i) \ll K(\psi_0) \tag{69.16}$$

which defines the ''sorptive number,'' $\alpha^*(\psi_0)$ [L^{-1}]. The $\alpha^*(\psi_0)$ parameter is generally used rather than $\alpha(\psi_0)$ because it avoids having to determine $K(\psi_i)$ in Equation 69.15, which can be extremely difficult or impossible. Large $\alpha(\psi_0)$ and $\alpha^*(\psi_0)$ values indicate dominance of the gravitational force (gravity) over the porous medium adsorption forces (capillarity) during infiltration, whereas small $\alpha(\psi_0)$ and $\alpha^*(\psi_0)$ values indicate the reverse (Raats 1976). The $\alpha(\psi_0)$ relationships corresponding to our three representative soils are given in

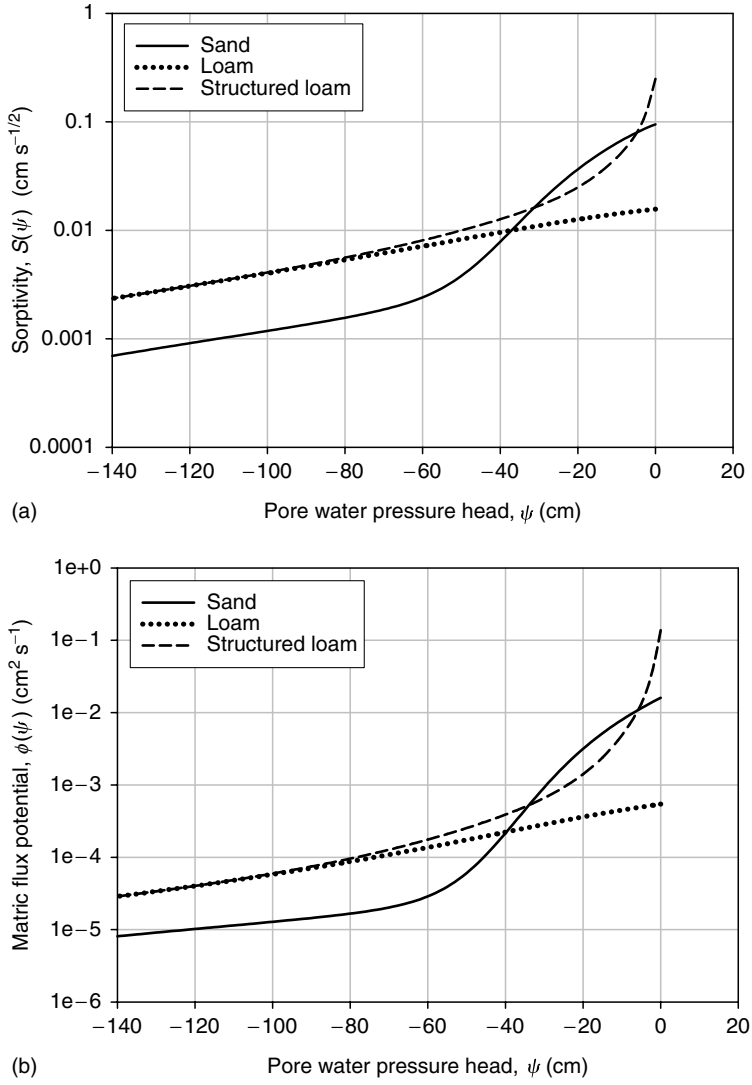

FIGURE 69.6. (a) Sorptivity, $S(\psi)$, versus pore water matric (or pressure) head, ψ, and (b) matric flux potential, $\phi(\psi)$, versus pore water matric head, ψ, for a representative sandy soil (sand), and a representative loamy soil with structure (structured loam) and without structure (loam).

Figure 69.7a; and generally speaking, $\alpha(\psi_0)$ increases as ψ_0 increases, indicating an increase in the importance of the gravity component of infiltration relative to the capillarity component as the soil gets wetter. Note, however, that the $\alpha(\psi_0)$ relationships have complex slopes, and the sand and unstructured loam produce curves with local maxima and minima. This occurs because $\alpha(\psi_0)$ is based on the exponential $K(\psi)$ function (i.e., Equation 69.14), whereas the actual $K(\psi)$ relationships were not exponential, especially those for the sand and unstructured loam (see Figure 69.5a). Generally speaking, the closer the $K(\psi)$ relationship is to a monotonic exponential function (i.e., Equation 69.14), the closer the $\alpha(\psi_0)$ relationship is to a single constant value. Figure 69.7b compares $\alpha^*(\psi_0)$ to $\alpha(\psi_0)$ for the

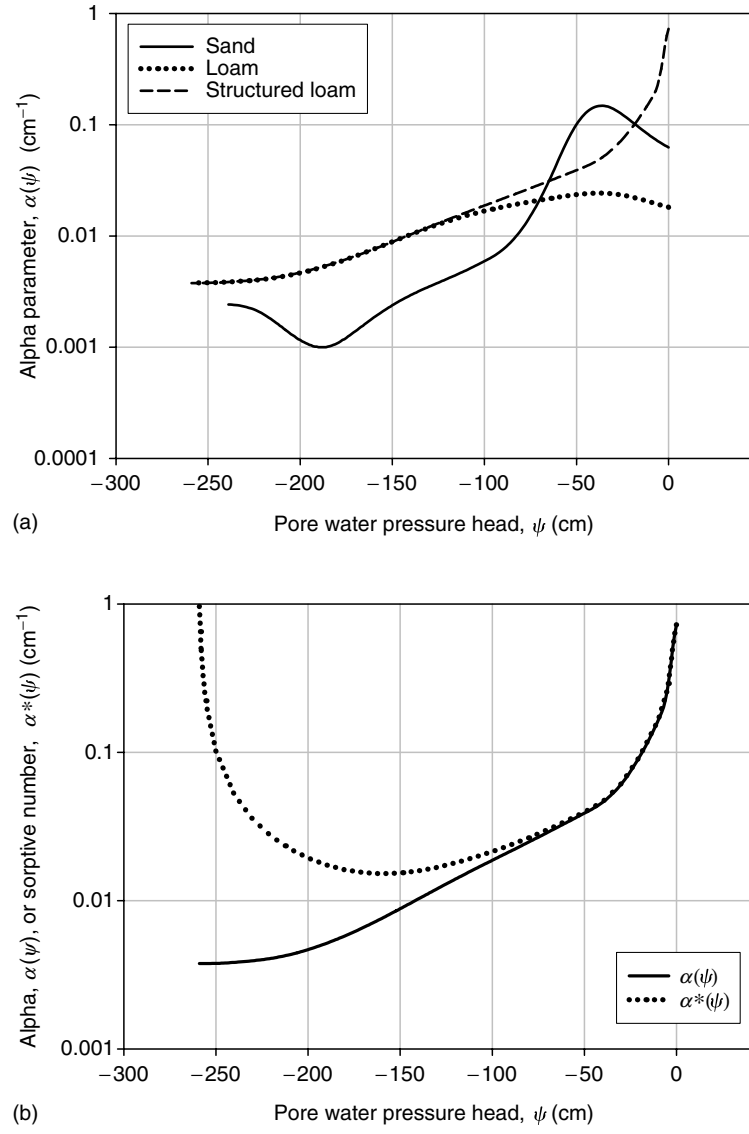

FIGURE 69.7. (a) Alpha parameter, $\alpha(\psi)$, versus pore water matric (or pressure) head, ψ, for a representative sandy soil (sand) and a representative loamy soil with structure (structured loam) and without structure (loam) and (b) alpha parameter, $\alpha(\psi)$, and sorptive number, $\alpha^*(\psi)$, versus pore water pressure head, ψ, for the structured loamy soil.

structured loam, where it is seen that $\alpha^*(\psi_0)$ diverges progressively for $\psi_0 < -50$ cm. This occurred because $K(\psi_i) = K(-260\text{ cm})$ in this scenario, and the assumption $K(\psi_i) \ll K(\psi_0)$ became progressively more incorrect as ψ_0 decreased, resulting in increasing error in $\alpha^*(\psi_0)$ with smaller (more negative) ψ_0 values. The $\alpha^*(\psi_0)$ parameter (and relationships based on the $\alpha^*(\psi_0)$ parameter) must consequently be used with caution when $K(\psi_i)$ is not substantially less than $K(\psi_0)$, such as might occur in very wet porous materials, or in fine-textured materials where $K(\psi)$ does not decrease rapidly with decreasing ψ.

Substituting Equation 69.16 into Equation 69.12 produces

$$S(\psi_0) = \left[\gamma[\theta(\psi_0) - \theta(\psi_i)]\frac{K(\psi_0)}{\alpha^*(\psi_0)}\right]^{1/2} \tag{69.17}$$

which shows that the ability of a porous medium to imbibe water (i.e., its sorptivity as indicated by the magnitude of $S(\psi_0)$) depends on the available water-storage capacity ($\theta(\psi_0) - \theta(\psi_i)$), the $K(\psi)$ relationship, and the $\alpha^*(\psi_0)$ relationship. Hence, a porous material's sorptivity decreases with increasing antecedent water content (i.e., decreasing available water-storage capacity), decreasing hydraulic conductivity, and increasing sorptive number. Note also that the accuracy of Equation 69.17 will depend strongly on the accuracy of the $\alpha^*(\psi_0)$ relationship, as discussed above.

The FWM pore diameter, $PD(\psi_0)$ [L], is defined as (Philip 1987)

$$PD(\psi_0) = \frac{2\sigma K(\psi_0)}{\rho g \phi(\psi_0)} = \frac{2\sigma\alpha^*(\psi_0)}{\rho g} \tag{69.18}$$

where σ [MT^{-2}] is the air–pore water interfacial surface tension, ρ [ML^{-3}] is the pore water density, and g [LT^{-2}] is the acceleration due to gravity. The $PD(\psi_0)$ parameter is often referred to as the effective ''equivalent mean'' pore diameter conducting water when infiltration occurs at ψ_0 (White and Sully 1987). It may be more accurate, however, to view $PD(\psi_0)$ as an index parameter that represents the mean ''water-conductiveness'' of the hydraulically active pores, rather than an actual pore size. This is because the $PD(\psi_0)$ parameter is derived from a flow measurement (associated with the measurement of $K(\psi_0)$; Equation 69.18), and must consequently reflect in some way the combined sizes, tortuosities, roughnesses, and connectivities of all water-conducting pores at $\psi = \psi_0$ (Reynolds et al. 1997). Associated with $PD(\psi_0)$ is the ''concentration'' of pore sizes, $NP(\psi_0)$ (number of pores L^{-2}), which may be derived from Poiseuille's law for flow in smooth, cylindrical capillary tubes (Philip 1987):

$$NP(\psi_0) = \frac{128\mu K(\psi_0)}{\pi\rho g[PD(\psi_0)]^4} \tag{69.19}$$

where μ [$ML^{-1}\ T^{-1}$] is the dynamic viscosity of water and the other parameters are as defined above. The $NP(\psi_0)$ parameter is an indicator of the number of hydraulically active pores per unit area of infiltration surface, which have FWM diameter, $PD(\psi_0)$. The relationships among $PD(\psi_0)$, $NP(\psi_0)$, and $K(\psi_0)$ for the structured loam soil are illustrated in Figure 69.8, where it is seen that a two-order of magnitude increase in flow-weighted mean pore diameter, $PD(\psi_0)$, corresponded to about a six-order of magnitude increase in $K(\psi_0)$, and about a four-order of magnitude decrease in $NP(\psi_0)$.

Equation 69.14 through Equation 69.19 also apply when measuring saturated flow parameters in unsaturated porous materials (see Section 69.5). In this case, ψ_0 is at its maximum value in the equations (i.e., $\psi_0 = 0$), and consequently the $K(\psi)$, $\phi(\psi_0)$, $\alpha^*(\psi_0)$, $\theta(\psi_0)$, $S(\psi_0)$, $PD(\psi_0)$, and $NP(\psi_0)$ relationships become maximum-valued constants, which are indicated by K_{sat} (i.e., K_s or K_{fs}), ϕ_m, α^*, θ_{sat} (i.e., θ_s or θ_{fs}), S, PD, and NP, respectively. As mentioned in Section 69.5, the matric flux potential (ϕ_m), sorptive number (α^*), and sorptivity (S) are measures of the capillary suction/pull or ''capillarity'' that unsaturated hydrophilic porous materials exert on infiltrating water. Mathematically, ϕ_m is the area under the $K(\psi)$ curve between $\psi = \psi_0 = 0$ and $\psi = \psi_i$ (Equation 69.13); and as a result, the magnitude of a

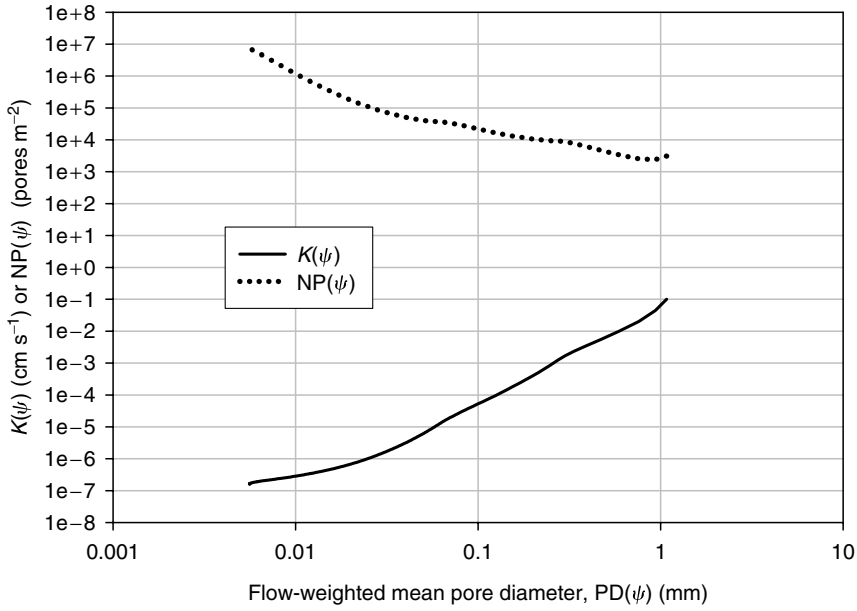

FIGURE 69.8. Hydraulic conductivity, $K(\psi)$, and number of FWM pores per unit area, NP(ψ), versus FWM pore diameter, PD(ψ), for the structured loamy soil.

material's capillarity depends on the shape and magnitude of the $K(\psi)$ curve, and on the antecedent pore water matric head, ψ_i. Porous media that are coarse-textured, structured, bioporous, or wet consequently tend to have lower capillarity (i.e., smaller area under the $K(\psi)$ curve) than porous media that are fine-textured, structureless, dry, or devoid of biopores. Furthermore, all porous media (regardless of texture or structure) have zero capillarity (i.e., $\phi_m = 0$) when they are saturated or field-saturated because under that condition, $\psi_0 = \psi_i = 0$ in Equation 69.13. If the $K(\psi)$ function is represented by Equation 69.14, it can be shown that for porous materials at field capacity or drier (Mein and Farrell 1974; Scotter et al. 1982; Reynolds et al. 1985; see also Section 69.4):

$$\alpha \approx \alpha^* \equiv (K_{sat}/\phi_m) \approx -\psi_f^{-1}; \quad \psi_f < 0 < \alpha^* \tag{69.20}$$

where α^* [L^{-1}] is the maximum sorptive number (for the material in question) and ψ_f [L] is the Green–Ampt wetting front matric head (negative quantity). Near-zero ψ_f (large α^*) occurs primarily in porous materials that are coarse-textured and/or highly structured and/or highly bioporous, while large negative ψ_f (small α^*) occurs primarily in materials that are fine-textured or structureless or devoid of biopores. When $\psi_0 = 0$, the S, ϕ_m, K_{sat}, α^*, and ψ_f parameters are related by

$$S = [\gamma(\theta_{fs} - \theta_i)\phi_m]^{1/2} = \left[\gamma(\theta_{fs} - \theta_i)\frac{K_{sat}}{\alpha^*}\right]^{1/2} = [\gamma(\theta_i - \theta_{fs})K_{sat}\psi_f]^{1/2} \tag{69.21}$$

where θ_{fs} [L^3L^{-3}] is the field-saturated volumetric water content (Section 69.4), θ_i [L^3L^{-3}] is the initial or antecedent volumetric water content, and the other parameters are as previously defined. Note that in Equation 69.21, S decreases to zero as θ_i increases to θ_{fs}, indicating (as expected) that field-saturated porous material has no ability to absorb or store

additional water. The PD and NP parameters (Equation 69.18 and Equation 69.19, respectively) are often used to quantify temporal and management-induced changes in porous medium structure as they relate to water flow (e.g., White et al. 1992; Reynolds et al. 1995).

In structured porous materials, it is often important to distinguish between ''matrix'' flow parameters and ''macropore'' flow parameters, given that macropores (e.g., large cracks, worm holes, abandoned root channels, large interaggregate spaces, etc.) can have a substantial effect on near-saturated water flow and solute transport. Matrix pores are defined as all pores that are small enough to remain water-filled at a specified pore water matric head, ψ_{mat} [L], whereas macropores are pores that are too large to remain water-filled at ψ_{mat}. The value of ψ_{mat} is not yet agreed upon (i.e., various values have been proposed such as -3, -5, -10 cm); however, growing experimental evidence suggests that $\psi_{mat} = -10$ cm is appropriate (Jarvis et al. 2002), which corresponds to an equivalent pore diameter of 0.3 mm according to classical capillary rise theory (Or and Wraith 2002). Using this criterion, all pores with equivalent diameters $\leq$0.3 mm ($\psi \leq \psi_{mat} = -10$ cm) are matrix pores, whereas those with equivalent diameters $>$0.3 mm ($\psi > \psi_{mat} = -10$ cm) are macropores. The various ''total porous medium'' flow parameters described above (i.e., Equation 69.11 through Equation 69.21 that apply to all pore sizes) can be recast as matrix flow parameters by simply restricting ψ_0 to the range, $\psi_i < \psi_0 < \psi_{mat}$. Macropore flow parameters can be similarly defined by restricting ψ_0 to the range, $\psi_{mat} < \psi_0 < 0$; however, the hydraulic conductivity relationships must be rewritten as

$$K_p(\psi) = K(\psi) - K(\psi_{mat}); \quad \psi_{mat} \leq \psi \leq 0 \tag{69.22}$$

$$K_p(\theta) = K(\theta) - K[\theta(\psi_{mat})]; \quad \theta(\psi_{mat}) \leq \theta \leq \theta_s \tag{69.23}$$

where the subscript ''p'' denotes the macropore flow domain, and $K(\psi)$ and $K(\theta)$ refer to the total porous medium (i.e., both matrix pores and macropores). As a result of these definitions, the flow parameters in the matrix domain are at their maximum values when $\psi_0 = \psi_{mat}$; whereas the flow parameters in the macropore domain are either zero ($K_p(\psi) = K_p(\theta) = \phi(\psi_0) = S(\psi_0) = 0$) or undefined (PD($\psi_0$) and NP($\psi_0$)) when $\psi_0 = \psi_{mat}$. Figure 69.9 and Figure 69.10 illustrate selected flow parameter relationships for the matrix, macropore, and total porous medium flow domains in our representative structured loam soil. Note in these figures that the matrix and total porous medium flow parameters are coincident when $\psi_0 \leq \psi_{mat}$ because the macropores are empty, and thus only the matrix pores are water-conducting. Note also that the macropore relationships produce complex patterns and may have values that are greater than, equal to, or less than the corresponding matrix and total porous medium values, depending on the value of ψ_0.

The primary physical and chemical factors affecting the above unsaturated flow parameters include porous medium texture and structure, pore water viscosity, the concentration and speciation of dissolved salts in the pore water, and porous medium hydrophobicity. All of the unsaturated flow parameters are highly sensitive to porous medium texture and structure (compare Figure 69.5 through Figure 69.7), and hence measuring techniques must preserve the porous medium in its natural/*in-situ*/antecedent condition to as great an extent as possible. The effects of pore water viscosity and dissolved salts on the unsaturated flow parameters are similar to those described for saturated and field-saturated hydraulic conductivity (see Section 69.5). A hydrophobic soil is nonwetting (i.e., it partially or completely repels water rather than attracts water), and this in turn impedes infiltration because of reduced (or even negative) capillarity. Soil hydrophobicity can be caused by accumulation of certain naturally water-repelling organic constituents (such as pine tree

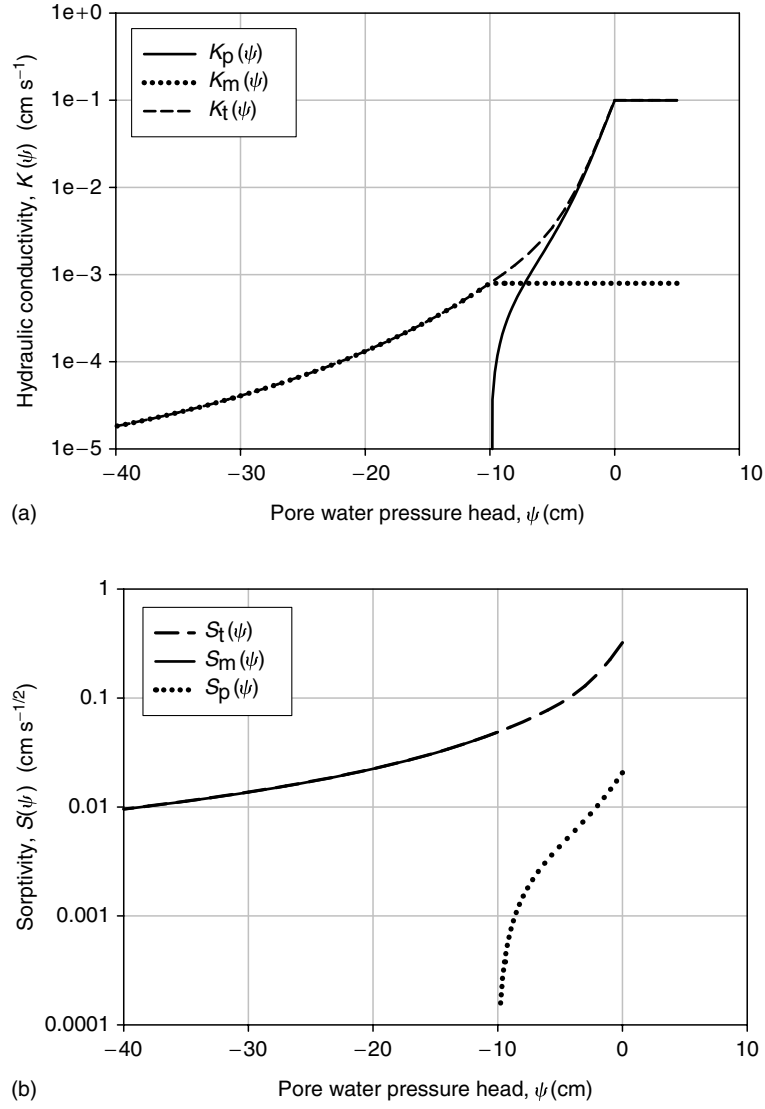

FIGURE 69.9. For the structured loamy soil: (a) hydraulic conductivity, $K(\psi)$, versus pore water matric (or pressure) head, ψ, in the total soil ($K_t(\psi)$), matrix flow domain, ($K_m(\psi)$), and macropore flow domain ($K_p(\psi)$) and (b) sorptivity, $S(\psi)$, versus pore water pressure head, ψ, for the total soil ($S_t(\psi)$), matrix flow domain ($S_m(\psi)$), and macropore flow domain ($S_p(\psi)$).

needles), or by extreme or prolonged drying (such as after a long drought or after a forest fire), which causes certain organic materials and mineral oxides lining the soil pores to become partly or completely water-repellent. Hydrophobicity reduces the capillarity parameters (i.e., $\phi(\psi_0)$, $\alpha(\psi_0)$, $\alpha^*(\psi_0)$, $S(\psi_0)$, PD(ψ_0), NP(ψ_0)) relative to a hydrophilic (water-wetting) situation, all other factors remaining equal. Although soil hydrophobicity can be initially strong enough to prevent infiltration of even shallow-ponded water, it usually breaks down over time, allowing normal soil capillarity to eventually return. Further information on soil hydrophobicity and its impacts on soil hydraulic processes and properties

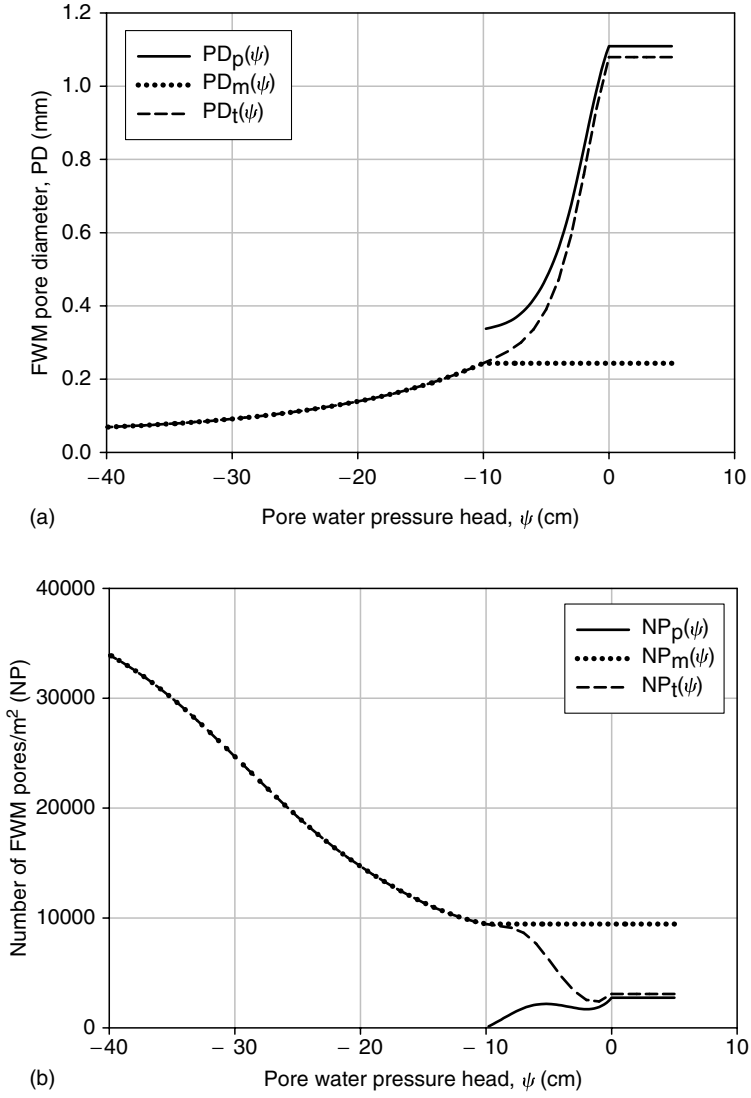

FIGURE 69.10. For the structured loamy soil: (a) FWM pore diameter (PD), versus pore water matric (or pressure) head, ψ, in the total soil ($PD_t(\psi)$), matrix flow domain ($PD_m(\psi)$), and macropore flow domain ($PD_p(\psi)$) and (b) number of FWM pores per unit area, NP, versus pore water pressure head, ψ, in the total soil ($NP_t(\psi)$), matrix flow domain ($NP_m(\psi)$), and macropore flow domain ($NP_p(\psi)$).

can be found in Bauters et al. (1998, 2000), Nieber et al. (2000), and references contained therein.

Unsaturated hydraulic property methods are described in Chapter 80 through Chapter 84 and include the laboratory tension infiltrometer (Chapter 80), the evaporation method (Chapter 81), the field tension infiltrometer (Chapter 82), the instantaneous profile method (Chapter 83), and selected estimation methods (Chapter 84).

REFERENCES

Bauters, T.W.J., DiCarlo, D.A., Steenhuis, T.S., and Parlange, J.-Y. 1998. Preferential flow in water repellent sands. *Soil Sci. Soc. Am. J.* 62: 1185–1190.

Bauters, T.W.J., Steenhuis, T.S., DiCarlo, D.A., Nieber, J.L., Dekker, L.W., Ritsema, C.J., Parlange, J.-Y., and Haverkamp, R. 2000. Physics of water repellent soils. *J. Hydrol.* 231–232: 233–243.

Bilderback, T.E., Warren, S.L., Owen, J.S., and Albano, J.P. 2005. Healthy substrates need physicals too! *HortTechnology* 15: 747–751.

Bouma, J. 1983. Use of soil survey data to select measurement techniques for hydraulic conductivity. *Agric. Water Manage.* 6: 177–190.

Bouma, J. 1985. Soil variability and soil survey. In J. Bouma and D.R. Nielsen, Eds. *Proceedings of Soil Spatial Variability Workshop.* PUDOC, Wageningen, The Netherlands, pp. 130–149.

Bouwer, H. 1966. Rapid field measurement of air-entry value and hydraulic conductivity of soil as significant parameters in flow system analysis. *Water Resour. Res.* 2: 729–738.

Bouwer, H. 1978. *Groundwater Hydrology.* McGraw-Hill, Toronto, ON, Canada.

Bruce, R.R. and Luxmoore, R.J. 1986. Water retention: Field methods. In A. Klute, Ed., *Methods of Soil Analysis, Part I—Physical and Mineralogical Methods.* 2nd ed. American Society of Agronomy, Madison, WI, pp. 663–683.

Campbell, G.S. 1987. Soil water potential measurement. In R.J. Hanks and R.W. Brown, Eds., *Proceedings of International Conference on Measurement of Soil and Plant Water Status*, Vol. 1. Logan, UT, July 1987, pp. 115–119.

Cassel, D.K. and Nielsen, D.R. 1986. Field capacity and available water capacity. In A. Klute, Ed., *Methods of Soil Analysis, Part 1—Physical and Mineralogical Methods.* 2nd ed. American Society of Agronomy, Madison, WI, pp. 901–926.

Cockroft, B. and Olsson, K.A. 1997. Case study of soil quality in south-eastern Austrialia: management of structure for roots in duplex soils. In E.G Gregorich and M.R. Carter, Eds., *Soil Quality for Crop Production and Ecosystem Health.* Developments in Soil Science, Vol. 25. Elsevier, New York, pp. 339–350.

Constantz, J., Herkelrath, W.N., and Murphy, F. 1988. Air encapsulation during infiltration. *Soil Sci. Soc. Am. J.* 52: 10–16.

Gardner, W.R. 1958. Some steady-state solutions of the unsaturated moisture flow equation with application to evaporation from a water table. *Soil Sci.* 85: 228–232.

Grable, A.R. and Siemer, E.G. 1968. Effects of bulk density, aggregate size, and soil water suction on oxygen diffusion, redox potentials, and elongation of corn roots. *Soil Sci. Soc. Am. Proc.* 32: 180–186.

Gupta, S.C. and Hanks, R.J. 1972. Influence of water content of electrical conductivity of the soil. *Soil Sci. Soc. Am. Proc.* 36: 855–857.

Hillel, D. 1980. *Applications of Soil Physics.* Academic Press, Toronto, ON, Canada.

Hopmans, J.W., Simunek, J., Romano, N., and Durner, W. 2002. Simultaneous determination of water transmission and retention properties: inverse methods. In J.H. Dane and G.C. Topp, Eds., *Methods of Soil Analysis, Part 4—Physical Methods*, Soil Science Society of America, Madison, WI, pp. 963–1004.

Jarvis, N.J., Zavattaro, L., Rajkai, K., Reynolds, W.D., Olsen, P.-A., McGechan, M., Mecke, M., Mohanty, B., Leeds-Harrison, P.B., and Jacques, D. 2002. Indirect estimation of near-saturated hydraulic conductivity from readily available soil information. *Geoderma* 108: 1–17.

Koorevaar, P., Menelik, G., and Dirksen, C. 1983. *Elements of Soil Physics.* Elsevier, *New York, 228 pp.*

McIntyre, D.S. 1974. Soil sampling techniques for physical measurements. In J. Loveday, Ed., *Methods for Analysis of Irrigated Soils. Tech.*

Commun. No. 54, Commonwealth Agricultural Bureau, Australia, pp. 12–20.

Mein, R.G. and Farrell, D.A. 1974. Determination of wetting front suction in the Green–Ampt equation. *Proc. Soil Sci. Soc. Am*. 38: 872–876.

Nieber, J.L., Bauters, T.W.J., Steenhuis, T.S., and Parlange, J.-Y. 2000. Numerical simulation of experimental gravity-driven unstable flow in water repellent sand. *J. Hydrol*. 231–232: 295–307.

Olness, A., Clapp, C.E., Liu, R., and Palazzo, A.J. 1998. Biosolids and their effects on soil properties. In A. Wallace and R.E. Terry, Eds., *Handbook of Soil Conditioners*. Marcel Dekker, New York, pp. 141–165.

Or, D. and Wraith, J.M. 2002. Soil water content and water potential relationships. In A.W. Warrick, Ed., *Soil Physics Companion*. CRC Press, Boca Raton, FL, pp. 49–84.

Passioura, J.B. 1980. The transport of water from soil to shoot in wheat seedlings. *J. Exp. Bot*. 3: 1161–1169.

Philip, J.R. 1957. The theory of infiltration. 4: Sorptivity and algebraic infiltration equations. *Soil Sci*. 84: 257–264.

Philip, J.R. 1987. The quasilinear analysis, the scattering analog, and other aspects of infiltration and seepage. In Y.S. Fok, Ed., *Infiltration, Development and Application*. Water Resources Research Centre, Honolulu, HI, pp. 1–27.

Raats, P.A.C. 1976. Analytical solutions of a simplified flow equation. *Trans. ASAE* 19: 683–689.

Reynolds, W.D., Bowman, B.T., Drury, C.F., Tan, C.S., and Lu, X. 2002. Indicators of good soil physical quality: density and storage parameters. *Geoderma* 110: 131–146.

Reynolds, W.D., Brown, D.A., Mathur, S.P., and Overend, R.P. 1992. Effect of in-situ gas accumulation on the hydraulic conductivity of peat. *Soil Sci*. 153: 397–408.

Reynolds, W.D., Bowman, B.T., and Tomlin, A.D. 1997. Comparison of selected water and air properties in soil under forest, no-tillage, and conventional tillage. In J. Caron, D.A. Angers, and G.C. Topp, Eds., *Proceedings of 3rd Eastern Canada Soil Structure Workshop*. Université Laval, Sainte-Foy, Quebec, Canada, pp. 235–248.

Reynolds, W.D. and Elrick, D.E. 2005. Measurement and characterization of soil hydraulic properties. In J. Alvarez-Benedi and R. Munoz-Carpena, Eds., *Soil–Water–Solute Process Characterization: An Integrated Approach*. CRC Press, Boca Raton, FL, pp. 197–252.

Reynolds, W.D., Elrick, D.E., and Clothier, B.E. 1985. The constant head well permeameter: effect of unsaturated flow. *Soil Sci*. 139: 172–180.

Reynolds, W.D., Gregorich, E.G., and Curnoe, W.E. 1995. Characterization of water transmission properties in tilled and untilled soils using tension infiltrometers. *Soil Till. Res*. 33: 117–131.

Richards, L.A. 1931. Capillary conduction of liquids in porous mediums. *Physics* 1: 318–333.

Robinson, D.A., Jones, S.B., Blonquist, J.M. Jr., and Friedman, S.P. 2005. A physically derived water content/permittivity calibration model for coarse-textured, layered soils. *Soil Sci. Soc. Am. J*. 69: 1372–1378.

Romano, N. and Santini, A. 2002. 3.3 Water Retention and Storage, 3.3.3 Field. In J.H. Dane and G.C. Topp, Eds., *Methods of Soil Analysis, Part 4—Physical Methods*. Soil Science Society of America, Madison, WI, pp. 721–738.

Scotter, D.R., Clothier, B.E., and Harper, E.R. 1982. Measuring saturated hydraulic conductivity and sorptivity using twin rings. *Aust. J. Soil Res*. 20: 295–304.

Skopp, J., Jawson, M.D., and Doran, J.W. 1990. Steady-state aerobic microbial activity as a function of soil water content. *Soil Sci. Soc. Am. J*. 54: 1619–1625.

Smith, R.E. 2002. *Infiltration Theory for Hydrologic Applications*. Water Resources Monograph 15, American Geophysical Union, Washington, DC, 212 pp.

Soil Science Society of America. 1997. *Glossary of Soil Science Terms*. Soil Science Society of America, Madison, WI.

Stephens, D.B., Lambert, K., and Watson, D. 1987. Regression models for hydraulic conductivity and field test of the borehole permeameter. *Water Resour. Res.* 23: 2207–2214.

Topp, G.C., Davis, J.L., and Annan, A.P. 1980. Electromagnetic determination of soil–water content: Measurement in coaxial transmission lines. *Water Resour. Res.* 16: 574–582.

Topp, G.C. and Ferré, Ty. P.A. 2002. 3.1 Water content. In J.H. Dane and G.C. Topp, Eds., *Methods of Soil Analysis, Part 4—Physical Methods*. Soil Science Society of America, Madison, WI, pp. 417–545.

Topp, G.C. and Reynolds, W.D. 1998. Time domain reflectometry: a seminal technique for measuring mass and energy in soil. *Soil Till. Res.* 47: 125–132.

Townend, J., Reeve, M.J., and Carter, A. 2001. Water release characteristic. In K.A. Smith and C.E. Mullins, Eds., *Soil and Environmental Analysis: Physical Methods*, 2nd ed. Marcel Dekker, New York, pp. 95–140.

Verdonck, O., Penninck, R., and De Boodt, M. 1983. Physical properties of different horticultural substrates. *Acta Hortic.* 150: 155–160.

White, I. and Sully, M.J. 1987. Macroscopic and microscopic capillary length and time scales from field infiltration. *Water Resour. Res.* 23: 1514–1522.

White, I., Sully, M.J., and Perroux, K.M. 1992. Measurement of surface-soil hydraulic properties: disk permeameters, tension infiltrometers, and other techniques. In G.C. Topp, W.D. Reynolds, and R.E. Green, Eds., *Advances in Measurement of Soil Physical Properties: Bringing Theory into Practice*. SSSA Special Publication No. 30, Soil Science Society of America, Madison, WI, pp. 69–103.

Chapter 70
Soil Water Content

G. Clarke Topp
Agriculture and Agri-Food Canada
Ottawa, Ontario, Canada

G.W. Parkin
University of Guelph
Guelph, Ontario, Canada

Ty P.A. Ferré
University of Arizona
Tucson, Arizona, United States

70.1 INTRODUCTION

Water in soil is a vital link in the hydrological cycle that controls exchange with the atmosphere above and with the groundwater below. Water in soil acts both as a lubricant and as a binding agent among the soil particulate materials, thereby influencing the structural stability and strength of soil and geologic materials. The high heat capacity of water causes a moderation of diurnal and seasonal temperature cycles at the soil surface. Chemically, water serves as the transport agent for the dissolved inorganic chemicals and suspended biological components that are involved in the processes of soil development and degradation. Biological production from soil, either as forest products or agricultural crops, is influenced primarily by water availability. The measurement of soil water content then is important directly for quantifying water balance, for estimates of plant water status, and for characterizing most soil physical, chemical, and biological processes.

The measurement of soil water content has undergone revolutionary advancements in the last 20 years. From having gravimetric sampling and neutron moderation as the primary field methods in the early 1980s, we now have numerous options, such as time-domain reflectometry (TDR), capacitance (and impedance) devices, ground penetrating radar (GPR), airborne/satellite active radar, and passive microwave methods (Gardner et al. 2001; Topp and Ferré 2002). These five newer methods are all based on electromagnetic (EM) measurements. Information on EM properties of soil and their use in soil water content measurements can be found in Topp et al. (1980), Ferré and Topp (2002), and Topp and Reynolds (1998). All of the EM methods make use of the high relative permittivity (dielectric constant) of the

water (80) in soil compared with the permittivities of the other soil components, which range from one for air to 3–5 for typical soil solids. Due to this contrast, methods that measure the bulk dielectric permittivity of soil are effective for the measurement of volumetric water content. A selection of EM methods is the focus of this chapter, as these offer a variety of sample geometries and spatial coverage, are minimally site disruptive, collect data digitally allowing real- or near real-time information, and measure on volumetric basis directly. In Section 69.2 the basic water content parameters and expressions for water content are defined, such as volumetric, gravimetric, and degree of saturation. In addition, the principles behind the use of EM methods, including how dielectric permittivity relates to water content appear in Section 69.2.

70.2 GRAVIMETRIC WITH OVEN DRYING

The thermogravimetric method is conceptually simple. Initially, a moist soil sample is weighed. The sample is then oven dried at 105°C and reweighed. The gravimetric water content is defined as the ratio of the mass lost, attributed to water initially present in the sample, to total mass of the fully dried soil. The method is apparently straightforward and is commonly thought to yield absolute results. In fact, this is not so for several reasons. Water is retained by the components of the soil at a wide range of energy levels and there is no absolute time at which the soil reaches a ''dry'' state when maintained at 105°C. Soil samples continue to decrease in mass slowly at 105°C for many days (Gardner 1986). In addition, many soil samples contain organic materials, some of which are volatile at 105°C, so some of the decrease in mass may be due to volatilization of components other than water. Finally, there is the problem of temperature control. Although the drying ovens in common use in most soil laboratories can maintain temperatures in the range of 100°C–110°C with careful adjustment, temperatures within the oven vary depending on the location in the oven chamber. Given that the actual temperature of the soil sample is not measured, this variability can lead to differential heating among soils placed in the same oven for the same amount of time. In spite of these imperfections, however, the oven-drying method is a commonly used and convenient method to obtain a good estimate of soil water content. The use of microwave ovens is not as rigorously standardized, as in the case of incandescent heating ovens. A more complete discussion of the procedures and limitations of the gravimetric method are given in many standard texts (e.g., Topp and Ferré 2002).

70.3 TIME-DOMAIN REFLECTOMETRY

It was just 30 years ago that TDR was first applied to measurement in soil and earth materials (Davis and Chudobiak 1975). Since those first measurements, TDR has been used to measure water content at many scales and under a broad range of conditions (Topp and Reynolds 1998; Robinson et al. 2003a), and has become a standard method of water content measurement. The popularity of the method for soil/environmental monitoring and research arises from a combination of its accuracy in a wide range of soils and its relative ease of use compared with many other available techniques. TDR provides real-time, *in-situ* soil water content measurements. Measurement systems can be multiplexed and data-logged, allowing for remote automated monitoring. For most soils, the accuracy of measurements of volumetric water content change is within $\pm 0.02\ m^3\ m^{-3}$ without the need for soil-specific calibration, and better absolute water contents can be achieved with calibration. There is considerable flexibility in the design and placement of TDR probes, allowing users to modify water content measurement networks to conform to the requirements of any specific study. Finally, because TDR determines the volumetric water content, the data are directly applicable

to hydrologic water balance analyses with no need for the measurement of supporting soil parameters such as bulk density.

70.3.1 Material and Instruments

TDR instrumentation consists of four basic components: a timing circuit, a pulse generator, a sampling receiver, and a display or recording device. It is the pulse generator, which launches a pulse or wave whose travel is analyzed. Most commercial instruments have all components in a single unit, which also performs analyses of the TDR traces, displaying and recording the interpreted water contents. Any of these instruments can be used to measure water content as long as they provide stable low noise readings with high time base accuracy, typically with a pulse transition time of $\leq$0.2 ns (Hook and Livingston 1995).

For custom analyses involving highly precise applications, the capability to record the entire waveform is necessary. An additional useful feature is the ability to provide automated water content analysis. The capability of displaying the actual TDR trace, and manually interpreting it, is very useful for assuring that the instrument is operating properly and that the automated interpretation is reasonable. Connection of the TDR instrument to a multiplexer for sequential measurement at a number of locations increases greatly the efficiency of data collection possibilities.

The initial and still widely used TDR instrument is the portable cable tester (Model 1502 B or C, Tektronix). In this instrument, the trace is displayed and analyses may be performed, and recorded manually, or data may be recorded and analyzed digitally on a PC (Or et al. 2003). The cable tester and a PC were incorporated into a number of custom systems designed to achieve automated TDR trace analysis, and multiplexing (Ferré and Topp 2002). Most commercial instruments now offer automated analysis as a part of the basic instrument with the multiplexing capability as an option. Some of the features of commercially available instruments are listed in Table 70.1.

The basic elements of a TDR probe are conductive components, often parallel metallic rods, which act as wave-guides, and the soil material in which the wave or signal propagates (Figure 70.1). Currently, the most common soil probes are of the balanced pair transmission line, consisting of two parallel rods, with rods that vary in length, depending on the measurement requirement, from 0.1 to 1.0 m and with probe separations from 0.01 to 0.1 m (Topp and Davis 1985). The minimum practical probe length for standard equipment is 0.1 m. The upper limit on length of probe is largely determined by electrical conductivity, clay content, and maximum water content expected. Although no firm guide can be offered, Dalton (1992) showed that probe lengths will have to be reduced to 0.2 m in clayey soil of EC > 0.1 S m^{-1}. Coated probes, discussed later, overcome this limitation to some extent. Zegelin et al. (1989) introduced multipronged probes where one prong or wire is centrally located and variable numbers of prongs are located circumferentially around the central wire. These configurations, even with only two outer prongs, act electrically to emulate a coaxial transmission line and result in a marginally improved TDR reflection. The extra rods, however, make for greater installation difficulty and associated soil disturbance than from a parallel pair. The configuration of the wave-guide or probe determines the extent and shape of the measured soil sample. Earlier experimental and theoretical analyses have demonstrated that the distribution along the length of probes has an effect, which is represented by a linear-weighted average (Hook and Livingston 1995). Specific refinements may be required for layered soils (Robinson et al. 2003b).

TABLE 70.1 TDR Instruments, Listing Options and Capabilities

Supplier	Model	Data logging	Multiplexing	Soil probes	Waveform	EC
Environmental Sensors, Inc.	MP917	Internal option	Yes	MP917 compatible, with shorting diodes	No	No
Tektronix	1502B/C	No	No	Custom	Yes	Yes
Campbell Scientific, Inc.	TDR100	CR10X or CR23X	SDMX50	Custom	Yes	Yes
Soilmoisture Equipment Corp.	TRASE	Internal	TRASE 6003	TRASE compatible	Yes	Yes
Dynamax, Inc.	Uses Tek 1502 B/C	PC-based	TR-200	Custom	Yes	No
MESA Systems Co.	TRIME TDR	PC-based	TRIME-MUX6	TRIME compatible	No	No

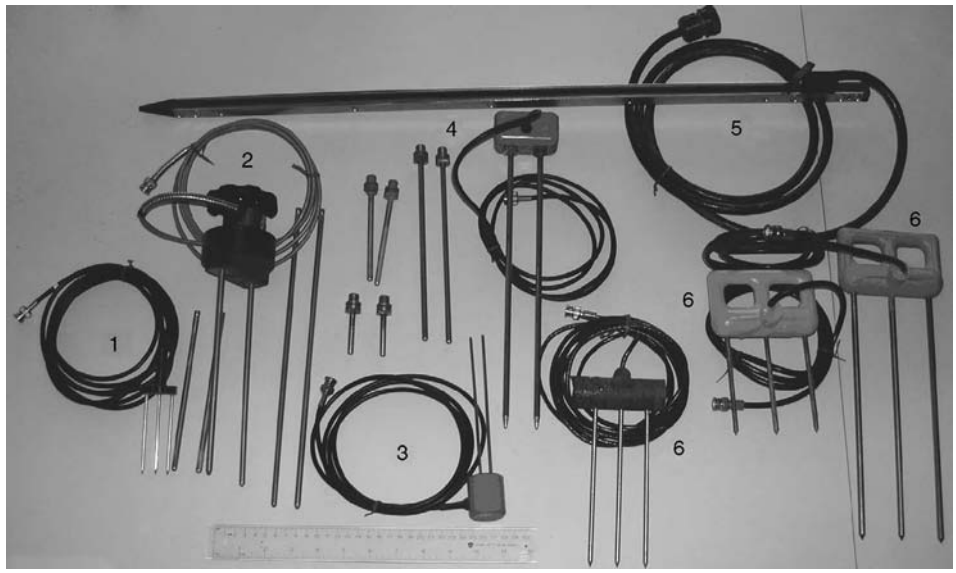

FIGURE 70.1. A collection of TDR from a limited number of suppliers. The numbers indicate the sources of those shown as: 1 and 2 are from Soilmoisture Equipment Corp.; 3, 4, and 5 are from Environmental Sensors Inc. (ESI); 6 are custom design developed in our laboratory.

For the lateral distribution, the situation is more complex. Knight (1992) and Knight et al. (1994) examined theoretically the spatial weighting function for parallel pair and multiwire acoaxial probes inserted in a medium of nearly uniform permittivity. The analytical expressions and approaches from Knight (1992) form the basis for probe design specifications and for evaluation of probe performance. For example, Knight (1992) showed that the ratio of the wire or prong spacing to the wire diameter in a soil probe is an important geometric descriptor of all TDR probes and should be considered for design and installation purposes. Knight (1992) proposed that the ratio of wire spacing to wire diameter should not exceed 10. It is reasonable that the wire diameter should be at least 10 times the representative pore size or particle diameter to provide sensible averages. One important finding of this analytical investigation is that the sample area of TDR is independent of the water content of the medium. We have found that 6 mm diameter rods spaced at 50 mm have worked well in a variety of studies in tilled and untilled agricultural soil. Many other probe configurations have come into current use and these can be used successfully with due consideration of the limitation applying to each probe type.

70.3.2 Procedure

The TDR method is straightforward but varies for different types of applications such as laboratory or field; surficial or at depth; point specific or spatially referenced; and so on.

Insert Soil Probe or Transmission Line into the Soil Sample

The installation of TDR probes is also important for high-quality measurements. Air gaps around the probes can cause erroneously low water content measurements. However, Knight et al. (1997) and Ferré et al. (1998) applied a numerical analysis to show

that partial air gaps, surrounding only a fraction of the probe perimeter, will not adversely affect the measured relative permittivity. Rods of the probe should be installed in parallel; however, minor deviations from parallel alignment will not lead to significant errors unless the rods come into contact with each other. Installation by insertion of nonparallel or poorly aligned rods or probes may lead to air gaps along the rods; this should be avoided at all times. Care should be taken to minimize disturbance of the soil when inserting the rods, especially in compressible media. In laboratory and near-surface field measurements, it is important that the cross-section and length of the probe be chosen so that the EM field associated with the TDR signal is contained within the soil sample (Knight 1992). In addition, the maximum probe length is limited by excessive conductive loss in the soil.

Connect Probe to TDR Instrument Using Coaxial Cable and Initiate Signal Transmission and Recovery of the TDR Waveform

The length of cable connecting probe, and instrument is best limited to 25 m to achieve acceptable signal-to-noise ratio and prevent excessive signal attenuation. Some instruments have introduced compensation for signal loss due to cable length allowing the use of greater cable lengths. Choice of acceptable cable length should be based on signal quality from the measurements in the wettest, most conductive conditions. The use of multiplexers introduces additional signal deterioration and may restrict additionally the separation between probe and instrument.

Analyze the Waveform to Determine the Time of Travel of the Signal in the Soil, Which Serves to Determine the Relative Permittivity

Of interest for water content determination is the two-way travel time of the TDR signal in the soil in and surrounding the probe. Two times are measured; the time of arrival of signal reflected from the probe-to-soil interface (t_1 in Figure 70.2) and the time of arrival of the signal reflected from the end of the probe (t_2 in Figure 70.2). The TDR waveform in Figure 70.2 shows the recommended way of estimating the two times. The intersection of tangential lines on either side of the identifying signal reflection is the most precise indication of the desired times. The time difference ($t_2 - t_1$) is a measure of the two-way travel time for the pulse or wave along the length of the rods. For some probes, the choice of where to pick t_1 may be difficult under some conditions. Robinson et al. (2003b) present a method for probe calibration using only water and air, claiming this to be highly accurate.

Periodic Measurements in a Reference Liquid to Detect Instrument Drift and Malfunction

Reference liquids of known dielectric permittivity are useful to check measurement repeatability and instrument drift. We have used repeated measurements with the TDR probe immersed in isopropyl alcohol or water and recorded at hourly intervals during field measurement. It is important to ensure that the container is sufficiently large to contain the signal entirely within the reference fluid.

70.3.3 Calculations

For many instruments calculations of volumetric water content are made within the instrument. The simple calculation sequence given here applies to those instruments where travel time measurement is made explicit.

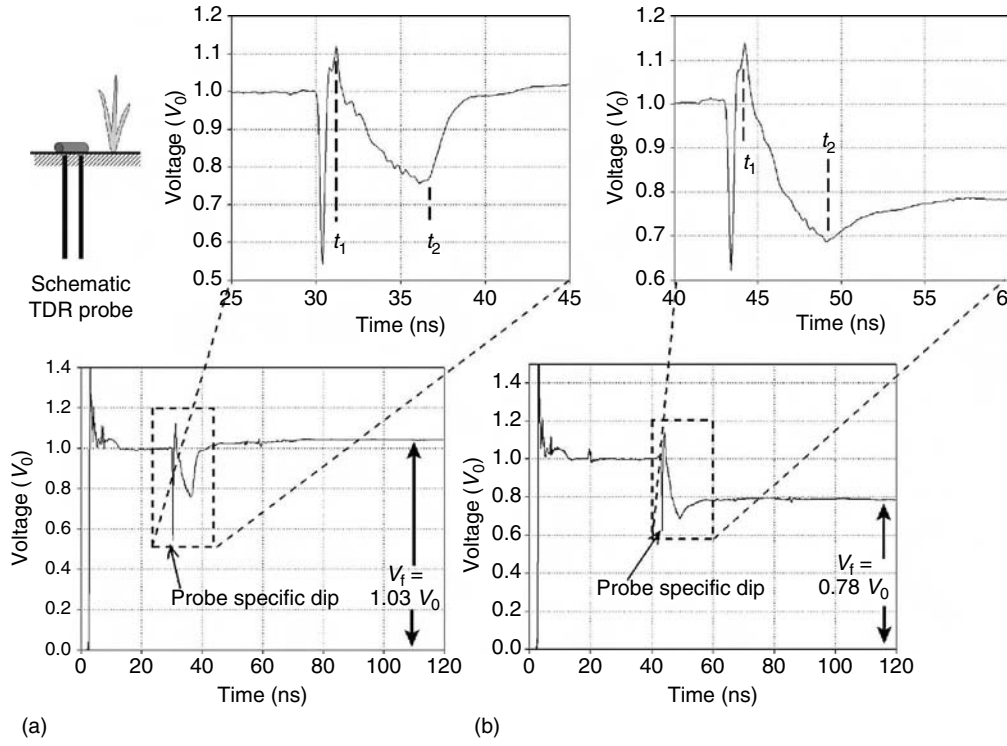

FIGURE 70.2. Two TDR curves from 20 cm probes in silty clay loam soil. The soils are at similar water content but the soil solution is more conductive in (b), giving a smaller return reflection and resulting lower V_f. In (a) $\theta_v = 0.304$ m^3 m^{-3} and $\sigma_0 = 57$ mS m^{-1} and in (b) $\theta_v = 0.271$ m^3 m^{-3} and $\sigma_0 = 95$ mS m^{-1}. (From Topp, G.C. and Ferré, Ty P.A., in D. Hillel et al. (Eds.), *Encyclopedia of Soils in the Environment*, Vol. 4, Elsevier, Oxford, UK, 2004, 174–181. With permission.)

Convert Travel Time to Relative Permittivity

The travel time $(t_2 - t_1)$ from second section, p. 944, is converted to propagation velocity and then to apparent relative permittivity as follows:

$$(t_2 - t_1) = \frac{2L}{v} = \frac{\sqrt{\varepsilon_{ra}}}{c} \tag{70.1}$$

where L is the length of the probe, v is the velocity of propagation, ε_{ra} is the apparent relative permittivity, and c is the velocity of light or other EM waves in vacuum (3×10^8 m s^{-1}).

Convert $\sqrt{\varepsilon_{ra}}$ to Volumetric Water Content Using a Selected Calibration Relationship

Although calibration relationships should be validated for each soil, experience has shown that the empirical relationship given by Topp et al. (1980) is widely applicable. The simpler-to-use linear relationship is recommended for soil where a calibration has not been developed:

$$\theta_v = 0.115\sqrt{\varepsilon_{ra}} - 0.176 \quad (70.2)$$

Soils where it may become advisable to develop a specific calibration include those high in clay and/or salt and having organic matter above 0.05 kg kg^{-1}. The effect of high clay cannot be made specific as its effect depends on grain size and mineralogy of the clay. The high clay, salt, and organic matter alter the slope (0.115) of Equation 70.2 and may introduce curvature as well (Topp et al. 2000). Dense soils may influence the intercept (−0.176) in Equation 70.2, as the magnitude of that term is dependent on the soil solids composition.

70.3.4 Comments

Measuring Water Content Profiles in the Field

For profiles near to (approximately 1.5 m depth) and extending to the surface, three general approaches have been used (Ferré and Topp 2002). Each offers certain advantages along with some limitations.

With a series of differing length probes, vertically installed from the surface, it is possible to segregate the water into layers in the profile. Water in each layer is assumed evenly distributed over the appropriate length interval. Spatial variability laterally contributes to the uncertainty or error associated with this type of profile determination, which can be as large as ± 0.03 m^3 m^{-3} (Topp 1987). The longest probes are useful for water balance calculation, where a single measurement gives the total water quantity over the depth spanned and is not dependent on the depth distribution of the water. Vertically installed rods tend to generate cracks in the soil between them at the surface and/or gaps around the individual rods. These soil openings each affect the infiltration of rainfall or irrigation and also affect the TDR reading. Vertical rods will tend to be moved vertically out of the soil during winter by the processes of frost-heave.

A second method involves installation of a number of horizontally oriented probes, one at each measured depth. These provide a more precise profile of water content that is not influenced strongly by lateral spatial variations, but these cannot compensate for major discontinuities in the vertical water content distribution. The total profile storage for water balance estimates involves sums of values measured at each depth, being less precise than from a single vertical probe. Horizontally installed probes generally require opening a pit or hole into the soil, creating the possibility of disturbance to the region to be measured. Additionally the cable and probe connection must be hermetically sealed.

An optimized profiling option uses parallel rods installed from the soil surface but 45° off the vertical. These can be placed so that the resulting water content profile is a single vertical profile, and affected less by lateral variability and each depth increment provides for equal magnitude lateral and vertical integration. Schwartz and Evett (2003) give an evaluation of 30° installations for wetting front evaluation in a soil column. The two disadvantages of angled installations are the greater difficulty of making installations at an angle with the required precision to know the actual depth at the end of the installed rods. The increased probe length to achieve an angled installation decreases the total vertical depth that can be measured in clayey soils.

Hook et al. (1992) describe the use of diode shorting to segment probes, which are constructed as profiling probes for use with model MP917 TDR instrument from Environmental Sensors, Inc. These probes allow for determination of water content profiles having the same accuracy for each segment of ± 0.01 m^3 m^{-3}. The EM field for TDR measurement propagates both in the resin comprising the probe, and in the surrounding soil, with more of the field in soil in wet than in dry soil, meaning that the sampling volume changes with water content. Installation of this type of probe is of critical importance as any disturbance of the soil adjacent to the probe is in the most sensitive of the measured region. These edge effect factors have not been adequately evaluated to allow specific quantification.

Recently, a number of attempts have been made to determine the water content profile using waveform analysis (Todoroff and Luk 2001; Heimovaara et al. 2004). With additional research and development, this approach may become the method of choice to overcome limitations cited above.

Coated-Rod Probes

Applying electrically resistive coatings to the rods can minimize the signal attenuation and loss of signal in conductive soils. Ferré et al. (1996) extended the work of Annan (1977) to show that coated rods do not measure the arithmetic average of the dielectric permittivities of the coatings and the surrounding medium. Because common coating materials have low dielectric permittivities, coated rods are more sensitive to lower water contents than to higher water contents. One result of this variable sensitivity is that, unlike uncoated rods, coated rod probes do not measure the correct length-weighted average water content along their length if the water content varies along their length. Therefore, probes that measure the water content through coatings should be installed in a manner that minimizes water content differences throughout their sample volume. In addition, the reduced sensitivity of coated rods to conductive losses reduces the usefulness of these probes for electrical conductivity measurement.

70.4 GROUND PENETRATING RADAR

GPR has been widely applied in the geosciences (Neal 2004) and methods have recently been developed for measuring soil volumetric water content (Davis and Annan 2002; Huisman et al. 2003). GPR methods offer the advantage of providing data from larger spatial regions than for TDR. Another significant advantage of surface and airborne GPR methods over TDR is that both methods are nonintrusive. The borehole GPR method is intrusive requiring installation of GPR transmitter and receiver in horizontal or vertical boreholes (Parkin et al. 2000; Rucker and Ferré 2003). Surface and airborne GPR methods are most appropriate for root zone investigations, whereas borehole methods are more appropriate for deeper vadose zone applications. This discussion is limited to above ground methods, which offer greater spatial coverage than downhole methods. However, many of the concepts presented are equally applicable to borehole GPR.

The physics of the GPR method is identical to TDR (Weiler et al. 1998). Both methods rely on measuring the travel time or amplitude of EM wave fields. Energy emitted from the GPR transmitter travels through air and soil to the receiver. Depending on the method used, the

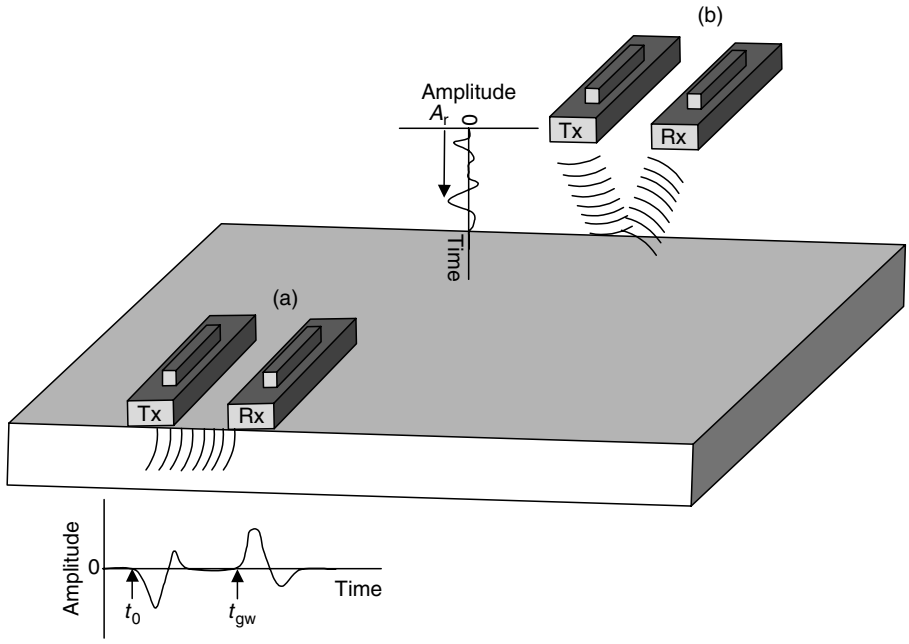

FIGURE 70.3. A schematic diagram showing two different GPR antennae configurations for measuring soil water content. (a) Surface GPR, direct ground wave, (b) Air-launched surface reflectivity. Tx and Rx are GPR transmitter and receiver antennae, respectively.

travel time or amplitude of energy from reflected or direct pathways is measured and converted to the soil relative permittivity. Equation 70.2 (or a soil-specific calibration) is then used to convert the measured relative permittivity to volumetric water content. More details on the principles of using GPR to measure soil water content are found in Davis and Annan (2002) and Huisman et al. (2003).

Figure 70.3 shows two of the GPR antenna configurations that have been used to measure soil water content of which the methods are described herein. The air-launched surface reflectivity method has the advantage over the surface method in that the antenna can be suspended above the land surface, with the energy directed downwards. The chosen antenna frequency and height above ground will depend on the desired size of the energy footprint (area sampled) on the ground. For example, Huisman et al. (2003) show that when using 1 GHz and 225 MHz antenna systems elevated 1 m above the ground, approximate footprint areas are 0.79 m by 0.79 m and 1.76 m by 1.76 m, respectively. The following equation (Davis and Annan 2002; Redman et al. 2002) calculates the soil relative permittivity from the amplitude of the reflected energy, A_r, relative to a maximum amplitude, A_m, from a perfect reflector such as a metal sheet placed on the ground, which has a reflection coefficient of -1:

$$\varepsilon_r = \frac{\left(1 + \frac{A_r}{A_m}\right)^2}{\left(1 - \frac{A_r}{A_m}\right)^2} \tag{70.3}$$

Active microwave remote sensing (synthetic aperture radar or SAR) operates on the same principle as air-launched surface reflectivity GPR. As SAR operates at a higher frequency (above 1 GHz) there are additional complications caused by soil surface roughness and growing plants. One of the primary motivations behind SAR satellites is to be able to estimate surface soil conditions, including water content. Mapping soil water content with SAR has been extensively researched and several projects have demonstrated the feasibility of deriving water content using SAR. As the methods continue to be under development microwave remote sensing is not given detailed coverage in this manual. McNairn et al. (2002) prepared a state of the art summary of the SAR approach as a method for the measurement of soil water content.

The surface GPR method differs from the air-launched in that the antennae are placed in direct contact with the ground surface and the relative permittivity is determined by measuring the GPR wave velocity. The velocity of direct or reflected waves between the GPR transmitter and receiver is converted to relative permittivity and water content as shown above for TDR. For either method, fixed or multiple antennae separation distances (offsets) can be used to collect velocity data. Multiple offset methods include wide-angle reflection and refraction (WARR) and common midpoint (CMP). A WARR survey involves keeping the receiver antenna at a fixed location and moving the transmitter antenna away from the receiver a set increment, measuring the ground wave velocity at each offset. A CMP begins with the transmitter and receiver placed very close together, and then incrementally moving them in opposite directions, again measuring the ground wave velocity at each offset. The ground wave velocity is more straightforward to measure when using the two multiple offset methods as opposed to the fixed offset (FO) method. The FO method requires picking the arrival time of the direct ground wave, whereas the WARR and CMP methods can use ground wave peak amplitude arrival times at different offsets to measure ground wave velocity.

70.4.1 Material and Instruments

There are no commercially available GPR instruments designed specifically for measuring soil water content. Davis and Annan (2002) give GPR manufacturers whose equipment can be adapted for measuring soil water content. The procedures described forthwith assume that users are familiar with the basic operational methods, licensing requirements, and potential health and safety issues of their GPR equipment and will therefore not be repeated.

70.4.2 Procedure

Air-Launched Surface Reflectivity

1 Position the GPR transmitter and receiver about 1 m above the ground surface using a cart or vehicle (Davis and Annan 2002; Huisman et al. 2003). Use at least a 10 MHz system so that the electrical conductivity of the ground does not substantially influence the electrical current flow (Davis and Annan 2002).

2 Place a metal sheet, larger than the energy footprint on the ground, under the GPR antennae. Measure A_m, the maximum amplitude of the energy reflected from the metal sheet.

3 Measure A_r over the soil of interest and then use Equation 70.3 to calculate ε_r. Finally, Equation 70.2 or a soil-specific calibration can be used to convert ε_r to soil volumetric water content.

Surface GPR (Direct Ground Wave, Fixed Offset)

The following procedure is adapted after the studies by Grote et al. (2003), and Galagedara et al. (2003, 2005), and the review by Huisman et al. (2003):

1 Perform a WARR survey to determine the GPR system airwave velocity calibration (time zero, t_0), to identify clearly the ground wave on the GPR output of energy versus time, and to select the best antennae offset distance for the FO survey. Time zero is defined as the start of the transmitter pulse, which may vary due to thermal drift and flexing of the fiber optic cables of the GPR system. It is critical to determine, using Equation (70.4), an accurate t_0 calibration using the airwave velocity measurement from the WARR survey as all direct ground wave arrival times are measured relative to it:

$$t_{ab} = t_{gw} - t_0 \tag{70.4}$$

where t_{ab} is the absolute ground wave arrival time, and t_{gw} is the measured ground wave arrival time (leading edge of the ground wave). For more information on time zero, and other issues related to this method see Galagedara et al. (2003). As a general recommendation, Galagedara et al. (2005) suggest using seven offsets (from 0.5 to 2.0 m) for the WARR survey.

2 After selecting the best offset (one for which the ground wave is clearly separated from reflected waves), perform the FO survey by keeping the GPR antennae at the selected offset (Galagedara et al. 2005 recommend 1.5–2.0 m) and moving along the survey line (Huisman et al. 2003). Measurements can be taken at a very small time increment (few seconds), depending on the speed at which the antennae are moving, and the desired measurement resolution. Synchronizing the GPR measurements with a GPS system facilitates analysis of spatial variability of soil water content.

3 Measure the travel time of the direct ground wave by picking its leading edge arrival time with a 5% threshold, for example.

4 Convert the measured travel time to velocity using the fixed antenna offset distance. Then determine the apparent relative permittivity from the velocity using Equation 70.1; then use Equation 70.2 or a soil-specific calibration to determine the soil water content.

Surface GPR (Direct Ground Wave, Multiple Offsets)

Either the WARR or CMP methods can be used to gather data on the velocity of the direct ground wave. Huisman et al. (2001) found that soil water contents measured with the WARR method were more accurate than those measured with the FO method. The WARR and CMP methods do not rely on an accurate measurement of t_0 or picking of the leading edge of the ground wave; they only depend on the slope of the peak arrival time versus antenna offset relationship:

1 Perform WARR or CMP measurements as discussed above.

2 Select the arrival times of the peak amplitude of the ground wave for each antenna offset.

3 Measure the velocity of the ground wave using the slope of the peak arrival time versus antennae offset distance data.

4 Repeat step 4 given under the first section on p. 950.

Surface GPR (Reflected Ground Wave, Single and Multiple Offsets)

The single offset method relies on knowing the depth to a subsurface reflector, whereas the multiple offset method only requires the presence of reflecting horizons at depth in the soil profile, such as the water table, lithologic boundaries, and buried objects (Davis and Annan 2002). For the multioffset method, the average soil water content between the ground surface and the reflector, and the depth to the reflector can be estimated since multiple travel pathways occur. See Greaves et al. (1996) for an example using this method:

1 Perform single or multiple offset GPR surveys.

2 Convert measured travel times of reflected energy to velocity using the known distance to the reflector (single offset method) or measured depth to the reflector (multiple offset method).

3 Determine the relative permittivity from the velocity using Equation 70.1; then use Equation 70.2 or a soil-specific calibration to determine the soil water content.

70.4.3 Comments

The GPR-based methods described above seem straightforward; however, data processing is not routine and would be very difficult to automate (Davis and Annan 2002). The major questions/limitations surrounding the GPR-based methods are:

1 Potential users of any of the GPR-based methods are advised to contact their local regulatory agency for any limitations on the use of EM energy emitting devices.

2 The surface methods work best in soils of low signal loss (low electrical conductivity, EC). For instance, the direct ground wave method works best when soil EC is less than 20 mS m^{-1} (Davis and Annan 2002).

3 Depth of penetration of the direct ground wave is a function of many variables including the GPR frequency, antennae offset distance, soil EC and water content, and soil heterogeneities.

4 Little is known about the effects of surface roughness, and soil water heterogeneities on the value of the reflection coefficient, and the depth of penetration in the air-launched method (Huisman et al. 2003).

5 Methods that rely on subsurface reflectors may be limited by nature of reflectors and conductive loss.

6 The larger sample volume with GPR over TDR may be an advantage or disadvantage depending on the purpose of the investigation.

Notwithstanding the aforementioned questions/limitations surrounding the GPR methods, they do hold great promise as a means of rapidly determining soil water content variability at the field scale. Although GPR-based methods remain largely at the research and development stage, it may one day be the standard method of measuring soil water content at the field scale, if GPR technology advances occur as for TDR over the past 25 years.

Active microwave remote sensing radar (SAR) operates on the same principle as air-launched GPR but at 1.4 and 6 GHz frequencies. Although relative permittivity (water content) is the main factor influencing radar backscatter, the soil and surface factors also have major influence on radar backscatter, especially, the surface geometry of the soil (random roughness related to tillage; soil aggregation; tillage row direction; and micro-topography), and the vegetation characteristics (size and geometry of the leaves; stalks and fruits; and the vegetation water content). Other soil properties, such as texture, and bulk density have a minor effect. The relationships between radar backscatter and soil water content are usually based on regression analyses as surface and plant factors cannot be characterized adequately. Getting reliable soil data as ''ground truth'' for the regression analyses is complicated by the shallow depth of penetration of the radar wave ($<$20 mm for C-band radar for soil above 0.2 m^3 m^{-3}). The difficulty of getting precise volumetric samples for gravimetric analysis over a 20 mm depth implies a significant advantage for specifically designed TDR probes (Lapen et al. 2004). The large disparity between radar footprint area ($\approx$100 to 1000 m^2) and ground truth sample size ($\leq$0.0025 m^2) is a huge challenge for adequate calibration. In spite of the difficulties effort will be directed toward improving the capability of using SAR data for spatial estimation of soil water content.

70.5 IMPEDANCE AND CAPACITANCE METHODS

Impedance and capacitance devices are EM instruments operating at frequencies within the range of TDR and GPR. The soil probe forms part of an electronic circuit. The soil within and/or in the vicinity of the probe also becomes part of the circuit by virtue of its proximity to the probe. A water content determination is possible because the impedance or capacitance values are influenced by water as was discussed above. The equation of importance for soil measurement is the impedance, Z, having the form

$$Z = \frac{g_1}{\sqrt{\varepsilon_{ra}}} = f(\theta_v) \tag{70.5}$$

where g_1 is the geometric shape factor pertaining to the probe. In principle, g_1 can be calculated. For most probe geometries, however, the cumbersome calculation has resulted in the use of the more straightforward approach of using liquids, such as water, of known relative permittivity and measuring g_1 directly (Gaskin and Miller 1996). After g_1 has been determined for a particular rod-type probe, it is possible to use Equation 70.2 as a calibration.

As the name implies, capacitance devices determine the apparent capacitance of a probe placed in or near a soil (Dean et al. 1987; Robinson et al. 1998; Gardner et al. 2001;

Kelleners et al. 2004b). The capacitance probe (along with the soil) forms part of an inductance–capacitance (LC) resonant circuit with a specific resonance frequency that depends upon the water content of the soil near the probe. The probe capacitance, C, is expressed as (Starr and Paltineanu 2002)

$$C = g_2 \varepsilon_{\mathrm{ra}} \tag{70.6}$$

where g_2 is the geometrical constant for the electrode configuration of the probe. With appropriate choice of inductance L, it is possible to establish the resonant frequency for soil probes in the frequency range of 100–150 MHz where salt and other conductivity factors are minimized. The oscillation frequency, F, is an inverse square root function of capacitance and a function of water content:

$$F = (2\pi\sqrt{LC})^{-1} = f(\theta_{\mathrm{v}}) \tag{70.7}$$

In principle, inserting Equation 70.6 into Equation 70.7 leads directly to a calibration equation for capacitance probes based on the relative permittivity as (Robinson et al. 1998)

$$F = \frac{1}{2\pi\sqrt{Lg_2}\sqrt{\varepsilon_{\mathrm{ra}}}} = \frac{g_3}{\sqrt{\varepsilon_{\mathrm{ra}}}} \tag{70.8}$$

where g_3 is a constant combining geometric and circuit inductance factors. Equation 70.8 is a linear relationship between F and $1/\sqrt{\varepsilon_{\mathrm{ra}}}$, a convenient calibration relationship, and of similar algebraic form to Equation 70.5. In practice, however, such a calibration approach has not proven universally applicable, particularly with conductive soils, making direct soil calibrations a very common requirement (Kelleners et al. 2004a).

Thus the theory in support of both impedance and capacitance devices results in straightforward calibration equations and the current state-of-the-art circuit manufacture makes these devices easy to use. The similarity in operation means that these devices are grouped here for convenience of presentation. Starr and Paltineanu (2002) have given specific procedures for calibration and use of capacitance probes and they have given limited mention of impedance devices.

70.5.1 Material and Instruments

A system for making capacitance and impedance measurements consists of probes within the soil, associated electronic equipment, datalogger, and associated software. Supplementary supplies and apparatus are required for calibrations and for making installations, such as soil augers. As the physical arrangement between probes and electronic circuitry can alter geometric factors g_1 and g_2, most commercially available instruments have a major portion (all radio frequency parts) of the electronics built into the probe to assure the geometrical integrity. Table 70.2 presents some of the more common instruments, with no intention to imply preferential treatment by the authors.

Capacitance instruments can be adapted to use different electrode configurations. Impedance instruments have more rigorous constraints and until recently used probes of two or more parallel rods. Capacitance probes generally fall into two categories, two or more parallel rods constructed to be pushed into, or buried in, the soil or one or more pairs of cylindrical metal

TABLE 70.2 Examples of Capacitance and Impedance Instruments Along with Probe and Operational Information

Supplier, country	Model	Frequency (MHz)	C or I[a]	Usage[b]	Probe type[c]	Data logging	EC correction	Temp. correction
Sentek Ltd Pty, Australia	EnviroSCAN	150	C	S	CR	Yes	No	No
Delta-T Devices, UK	Theta Probe	100	I	P, B	PR	Yes	No	No
Troxler Inc. USA	Sentry 200 AP	50	C	P	CR	Yes	No	No
Decagon Devices, Inc. USA	ECH_2O	—	C?	B	—	Yes	No	No
Stevens Water Monitoring Systems, USA	Hydra Probe	50	C	P, B	PR	Yes	No	No
SDEC France, France	HMS 9000	38	C	P, B	PR	Yes	Yes	Yes
Geneq Inc. Canada	AQUA-TEL-TDR	—	C?	S	—	Yes	No	No
Aquapro-Sensors, USA	AP Moisture Probe	—	C	B	CR	Yes	No	No

[a] C or I: capacitance or impedance.
[b] B: buried in soil, P: portable probe, S: semipermanent installation.
[c] CR: cylindrical rings placed inside PVC access pipe, PR: parallel rods.

rings separated by a nonconducting plastic ring and mounted on a cylindrical support that is inserted into a previously installed PVC access pipe. The zone of influence or sensor sampling volume for rod-type capacitance probes is similar to that of a TDR probe using the same rods as a probe. That is, it is integrated along the length of the rods, and largely contained between the electrode rods. These probes are best suited for surface or burying near surface, providing soil disturbance by installation is minimized. Capacitance probes configured as one or more pairs of cylindrical metal rings are well suited for discrete depth interval measurements in the soil profile. The zone of influence of the EM field in the metal ring probes includes the plastic separating the rings, the PVC access pipe, and the surrounding soil, which is in a fringe field of the capacitor. As a result, the sample area is limited to the region immediately adjacent to the access tubes.

The supplier for each instrument provides a list of materials that are required for each particular instrument, which should be consulted for assembly to allow most effective measurement procedure.

70.5.2 Procedure

Instruments listed in Table 70.2 will include operation and use instructions to which adherence should be given for optimal operation of the instrument. General procedures with particular considerations will be given here. The article by Starr and Paltineanu (2002) can be consulted for more detailed information, if needed.

The optimum procedure has three phases: sensor normalization, calibration, and measurement. The normalization process minimizes instrument-dependent sensor readings, enables one calibration equation to cover all the sensors, and allows one sensor or probe to be replaced at the same field position without loss of data continuity. Robinson et al. (1998) described the sensor normalization procedure based on the use of two reference fluids of known permittivity, such as air and water. Responses of different instruments are compared in terms of relative permittivity. Accurate measures of the soil water content with capacitance probes require calibration for specific type soils due to EM effects of soil materials and the varying effect of electrical conductivity.

70.5.3 Calibration

In theory, calibration using soil is not necessary, i.e., the normalization procedure is in effect a calibration. Robinson et al. (1998) have shown that soil-based calibration is necessary only if electrical conductivity cannot be taken into account by calculation and when soil bulk electrical conductivity is > 0.03 S m^{-1}, hence a soil-based calibration procedure follows.

Calibration procedures will vary with the electrode configuration of the capacitance sensor. Laboratory and field calibrations are the same and only a laboratory procedure is given. Although the gravimetric method is the usual standard, a more convenient standard for these calibrations is TDR. TDR measures on a volumetric basis as do capacitance and impedance instruments. When using the gravimetric method, it is necessary to make additional measurements of bulk density to convert gravimetric mass basis values to volumetric:

1 Choose a container size and shape to accommodate the sensor's primary zone of influence. Minimum container volume can be estimated using the general

procedure described by Starr and Paltineanu (2002). For ring-type sensors, the container diameter is ~25 cm. In addition, there should be 5 cm of uniform soil above the uppermost sensor and below the lowermost sensor to assure adequate sample size.

2 Screen the required mass of soil through a 5 mm sieve.

3 Thoroughly mix the soil after air-drying.

4 Weigh the desired mass of soil for a 2 cm soil depth to be packed to the chosen soil density.

5 Pack the soil carefully to the desired bulk density (i.e., to give the desired depth increment).

6 Repeat steps 4 and 5 until the container is filled.

7 Install the probe carefully in the soil so that there are no air gaps between the probe and soil and so that soil density is not altered by the probe installation.

8 Record capacitance probe reading in the container.

9 Record a matching TDR value in the container, if TDR is the reference method. If gravimetric method is the reference method, a series of additional steps are required as follows:

   a. Record weight of container plus soil, to be used for bulk density measurement.

   b. Take a minimum of three subsamples for wet and dry weights for mass basis values.

   c. If soil packing was done with adequate precision, subsampling for bulk density is not required. If assurance of density uniformity is required, obtain carefully a minimum of three subsamples using bulk density cylinders near the location of the probe.

10 Prepare the soil for the next calibration point. This step includes selecting the wetting increments so that four or five discrete soil water contents will result; and adding water and mixing the soil to distribute the water uniformly. Spread soil uniformly on a plastic sheet or large tray (a thickness not greater than 4 cm is ideal). Mist-spray one measured volume of water on the soil in several stages, mixing the soil after each stage. The mixing may be accomplished at each stage by lifting and turning with a flat lifter or by allowing the soil to cascade over itself, caused by lifting the plastic sheet from one corner toward its diagonal opposite and so on from other corners.

11 Repeat steps 4 to 10 for each calibration point.

12 Record the data for use in calculating a calibration equation.

70.5.4 Measurement

Good results require that great care be given to probe installation to ensure a tight fit of the electrodes or access pipe to the soil (i.e., no air gaps along the electrodes or access pipe), and with minimal soil disturbance (i.e., change of soil density or structure, in or near the sensing volume). Rod-type probes are pushed carefully into the soil surface, or into the wall of a soil pit for probes that are to be buried, without creating air gaps along the rods or compressing the soil with the electrode housing:

1(a) Connect probe to impedance instrument to measure impedance, following the operations manual.

1(b) Connect probe to capacitance instrument to measure resonant frequency as directed by the operations manual.

2 For monitoring involving data storage, initiate the data logging capability to retrieve the measured data.

3 Transmit or retrieve stored data for calculation and analysis.

70.5.5 Calculations

The first calculation step is to convert measured impedance or capacitance (frequency) values to either apparent relative permittivity or water content depending on adopted calibration procedure. As most instruments have a voltage output as indicative of impedance or capacitance, these calculations will adopt that assumption.

Normalization

Here it is convenient to represent voltage output from the impedance measurements as V_Z and that from the capacitance measurements as V_F:

1 Plot and/or perform a linear regression of $1/V_Z$ or $1/V_F$ against $\sqrt{\varepsilon_{ra}}$ for air and water, along with any other liquids that were used for the normalization measurements.

2 If the above does not automatically give a zero intercept, then the normalization involves subtracting the intercept to get equations having similar form of Equation 70.5 and Equation 70.8. This normalizes the data to air as the lowest reading.

3 Calibration can be achieved by substituting this simple regression relationship into Equation 70.2 or an equivalent relationship between $\sqrt{\varepsilon_{ra}}$ and water content.

For soils needing additional soil-based calibration another step is required.

Calibration Using Soil

1 Plot and/or perform a regression of $1/V_Z$ or $1/V_F$ against θ_v. For soils of low electrical conductivity, this relationship is expected to be linear. Increasing electrical conductivity will contribute curvature to the relationship.

2 The resulting calibration relationship can be used to convert all measurements to water content on a volume basis.

70.5.6 Comments

The zone of influence of the rod-type sensors is similar to that of equivalent TDR probes. The cylindrical ring sensors, however, have a limited zone of influence in the soil. The zone of influence has both axial (vertically along the sensor) and radial (perpendicular to the sensor) components. The electric field giving rise to the capacitance measure is most heavily weighted to the region between the rings and drops off very rapidly, both axially and radially, from that point. Research aimed at quantifying the electric field strength and radial weighting of the capacitance is ongoing. Commercial suppliers have claimed radial reach upto 10 cm, and axial reach at ±5 cm, which are seldom accompanied by quantitative verification. The electric field diminishes radically in the access pipe, and adjacent soil. Therefore, it is imperative that installation is tight-fitting and soil disturbance around the access pipe is minimized. Electrical conductivity has a major influence on capacitance measurements (Robinson et al. 1998; Kelleners et al. 2004b). Although Robinson et al. (1998) and Kelleners et al. (2004b) show that corrections can be made to the affected capacitance measurement, one needs additional circuit and probe information and an estimate of bulk electrical conductivity. As electrical conductivity varies with water content, the error from unknown conductivity will be greater at higher water contents. This is not likely to be a discernable problem at conductivity below 0.03 S m^{-1}.

REFERENCES

Annan, A.P. 1977. Time domain reflectometry—air gap problem for parallel wire transmission lines. Report of Activities, Part B. Geological Survey of Canada. Paper 77-1B: 59–62.

Dalton, F.N. 1992. Development of time-domain reflectometry for measuring soil water content and bulk soil electrical conductivity. In G.C. Topp et al., Eds. *Advances in Measurement of Soil Physical Properties: Bringing Theory into Practice*. Soil Science Society of America, Madison, WI, pp. 143–167.

Davis, J.L. and Annan, A.P. 2002. Ground penetrating radar to measure soil water content. In J.H. Dane and G.C. Topp Eds. *Methods of Soil Analysis, Part 4—Physical Methods*, Soil Science Society of America, Madison, WI, pp. 446–463.

Davis, J.L. and Chudobiak, W.J. 1975. *In situ* meter for measuring relative permittivity of soils. *Geol. Surv. Can. Pap*. 75–1A: 75–79.

Dean, T.J., Bell, J.P., and Bary, A.J.B. 1987. Soil moisture measurement by an improved capacitance technique. Part 1. Sensor design and performance. *J. Hydrol*. 93: 67–78.

Ferré, P.A., Rudolph, D.L., and Kachanoski, R.G. 1996. Spatial averaging of water content by time domain reflectometry: Implications for twin rod probes with and without dielectric coatings. *Water Resour. Res*. 32: 271–279.

Ferré, P.A., Rudolph, D.L., and Kachanoski, R.G. 1998. The water content response of a profiling time domain reflectometry probe. *Soil Sci. Soc. Am. J*. 62: 865–873.

Ferré, P.A. (Ty) and Topp, G.C. 2002. Time domain reflectometry. In J.H. Dane and G.C. Topp Eds. *Methods of Soil Analysis, Part 4—Physical Methods*, Soil Science Society of America, Madison, WI, pp. 434–446.

Galagedara, L.W., Parkin, G.W., and Redman, J.D. 2003. An analysis of the GPR direct ground wave

method for soil water content measurement. *Hydrol. Process.* 17: 3615–3628.

Galagedara, L.W., Parkin, G.W., Redman, J.D., von Bertoldi, P., and Endres, A.L. 2005. Field studies of the GPR ground wave method for estimating soil water content during irrigation and drainage. *J. Hydrol.* 301: 182–197.

Gardner, C.M.K., Robinson, D., Blyth, K., and Cooper, D. 2001. Soil water content. In K.A. Smith and C.E. Mullins Eds. *Soil and Environmental Analysis: Physical Methods*, 2nd ed., Marcel Dekker, New York, NY, pp. 1–64.

Gardner, W.H. 1986. Water content. In A. Klute Ed. *Methods of Soil Analysis, Part 1—Physical and Mineralogical Methods*, 2nd ed. American Society of Agronomy, Soil Science Society of America, Madison, WI, pp. 493–544.

Gaskin, G.J. and Miller, J.D. 1996. Measurement of soil water content using a simplified impedance measuring technique. *J. Agric. Eng. Res.* 63: 153–160.

Greaves, R.J., Lesmes, D.P., Lee, J.M., and Toksoz, M.N. 1996. Velocity variations and water content estimated from multioffset, ground-penetrating radar. *Geophysics* 61: 683–695.

Grote, K., Hubbard, S., and Rubin, Y. 2003. Field-scale estimation of volumetric water content using ground-penetrating radar ground wave techniques. *Water Resour. Res.* 39(11): 1321–1335.

Heimovaara, T.J., Huisman, J.A., Vrugt, J.A., and Bouten, W. 2004. Obtaining the spatial distribution of water content along a TDR probe using the SCEM-UA Bayesian inverse modeling scheme. *Vadose Zone J.* 3: 1128–1145.

Hook, W.R. and Livingston, N.J. 1995. Propagation velocity errors in time domain reflectometry measurements. *Soil Sci. Soc. Am. J.* 59: 92–96.

Hook, W.R., Livingston, N.J., Sun, Z.J., and Hook, P.B. 1992. Remote diode shorting improves measurement of soil water by time domain reflectometry. *Soil Sci. Soc. Am. J.* 56: 1384–1391.

Huisman, J.A., Hubbard, S.S., Redmond, J.D., and Annan, A.P. 2003. Measuring soil water content with ground penetrating radar: A review. *Vadose Zone J.* 2: 476–491.

Huisman, J.A., Sperl, C., Bouten, W., and Verstraten, J.M. 2001. Soil water content measurements at different scales: Accuracy of time domain reflectometry and ground penetrating radar. *J. Hydrol.* 245: 48–58.

Kelleners, T.J., Soppe, R.W.O., Ayars, J.E., and Skaggs, T.H. 2004a. Calibration of capacitance probe sensors in a saline silty clay soil. *Soil Sci. Soc. Am. J.* 68: 770–778.

Kelleners, T.J., Soppe, R.W.O., Robinson, D.A., Schaap, M.G., Ayars, J.E., and Skaggs, T.H. 2004b. Calibration of capacitance probe sensors using electric circuit theory. *Soil Sci. Soc. Am. J.* 68: 430–439.

Knight, J.H. 1992. The sensitivity of time domain reflectometry measurements to lateral variations in soil water content. *Water Resour. Res.* 28: 2345–2352.

Knight, J.H., Ferré, P.A., Rudolph, D.L., and Kachanoski, R.G. 1997. A numerical analysis of the effects of coatings and gaps upon relative dielectric permittivity measurement with time domain reflectometry. *Water Resour. Res.* 33: 1455–1460.

Knight, J.H., White, I., and Zegelin, S.J. 1994. Sampling volume of TDR probes used for water content monitoring. In K.M. O'Connor et al., Eds. *Time Domain Reflectometry in Environmental Infrastructure and Mining Applications*. U.S. Bureau of Mines, Minneapolis and Northwestern University, Evanston, Spec. Publ. SP 19–94: 93–104.

Lapen, D.R., Topp, G.C., Bugden, J.L., and Pattey, E. 2004. A new TDR probe for evaluating airborne SAR data for soil water content estimates. In Baoji Wang, Quanzhong Huang, Qing Li, Jianhan Lin, Yu Chen, Feng Mei, Qing Wei, and Jieqiang Zhuo Eds. *Proceedings of the 2004 CIGR International Conference* (Agricultural Engineering), Bejing, China. Oct. 11–14. (Published on CD-ROM).

McNairn, H., Pultz, T.J., and Boisvert, J.B. 2002. Active microwave remote sensing methods. In J.H. Dane and G.C. Topp Eds. *Methods of Soil Analysis, Part 4—Physical Methods*. Soil Science Society of America, Madison, WI, pp. 475–488.

Neal, A. 2004. Ground-penetrating radar and its use in sedimentology: Principles, problems, and progress. *Earth Sci. Rev*. 66 (3–4): 261.

Or, D., Jones, S.B., VanShaar, J.R., and Wraith, J.M. 2003. WinTDR 6.0 Users Guide (Windows-based TDR program for soil water content and electrical conductivity measurement). Available at: http://129.123.13.101/soilphysics/wintdr/documentation.htm (posted Fall 2003; verified 6 June 2004). Utah Agric. Exp. Stn. Res., Logan, UT.

Parkin, G., Redman, D., von Berotldi, P., and Zhang, Z. 2000. Measurement of soil water content below a waste water trench using ground penetrating radar. *Water Resour. Res.* 36: 2147–2154.

Redman, J.D., Davis, J.L., Galagedara, L.W., and Parkin, G.W. 2002. Field studies of GPR air launched surface reflectivity measurements of soil water contents. Proceedings of Ninth Conference on Ground Penetrating Radar. *SPIE* 4758: 156–161.

Robinson, D.A., Gardner, C.M.K., Evans, J., Cooper, J.D., Hodnett, M.G., and Bell, J.P. 1998. The dielectric calibration of capacitance probes for soil hydrology using an oscillation frequency response mode. *Hydrol. Earth Sys. Sci*. 2: 83–92.

Robinson, D.A., Jones, S.B., Wraith, J.M., Or, D., and Friedman, S.P. 2003a. A review of advances in dielectric and electrical conductivity measurements in soils using time domain reflectometry. *Vadose Zone J*. 2: 444–475.

Robinson, D.A., Schaap, M., Jones, S.B., Friedman, S.P., and Gardner, C.M.K. 2003b. Considerations for improving the accuracy of permittivity measurement using TDR: Air/water calibration, effects of cable length. *Soil Sci. Soc. Am. J*. 67: 62–70.

Rucker D.F. and Ferré, Ty.P.A. 2003. Near-surface water content estimation with borehole ground penetrating radar using critically refracted waves. *Vadose Zone J*. 2: 247–252.

Schwartz, R.C. and Evett, S.R. 2003. Conjunctive use of tension infiltrometry and time-domain reflectometry for inverse estimation of soil hydraulic parameters. *Vadose Zone J*. 2: 530–538.

Starr, J.L. and Paltineanu, I.C. 2002. Capacitance devices. In J.H. Dane and G.C. Topp Eds. *Methods of Soil Analysis, Part 4—Physical Methods*, Soil Science Society of America, Madison, WI, pp. 463–474.

Todoroff, P. and Luk, J. 2001. Calculation of *in situ* soil water content profiles from TDR signal traces. *Measure. Sci. Technol*. 12: 27–36.

Topp, G.C. 1987. The application of time-domain reflectometry (TDR) to soil water content measurement. In *Proceedings of International Conference on Measurement of Soil and Plant Water Status*. Logan, Utah, pp 1: 85–93.

Topp, G.C. and Davis, J.L. 1985. Measurement of soil water content using TDR: A field evaluation. *Soil Sci. Soc. Am. J*. 49: 19–24.

Topp, G.C., Davis, J.L., and Annan, A.P. 1980. Electromagnetic determination of soil-water content: Measurement in coaxial transmission lines. *Water Resour. Res.* 16: 574–582.

Topp, G.C. and Ferré, Ty.P.A. 2002. Water content. In J.H. Dane and G.C. Topp Eds. *Methods of Soil Analysis, Part 4—Physical Methods*, Soil Science Society of America, Madison, WI, pp. 417–545.

Topp, G.C. and Ferré, Ty.P.A. 2004. Time-domain reflectometry. In D. Hillel et al., Eds. *Encyclopedia of Soils in the Environment*, Vol. 4, Elsevier, Oxford, UK, pp. 174–181.

Topp, G.C. and Reynolds, W.D. 1998. Time domain reflectometry: A seminal technique for measuring mass and energy in soil. *Soil Till. Res*. 47: 125–132.

Topp, G.C., Zegelin, S.J., and White, I. 2000. Impacts of the real and imaginary components of relative permittivity on TDR measurements in soils. *Soil Sci. Soc. Am. J*. 64: 1244–1252.

Weiler, K.W., Steenhuis, T.S., Boll, J., and Kung, K.-J.S. 1998. Comparison of ground penetrating radar and time-domain reflectometry as soil water sensors. *Soil Sci. Soc. Am. J.* 62: 1237–1239.

Zegelin, S.J., White, I., and Jenkins, D.R. 1989. Improved field probes for soil water content and electrical conductivity measurement using time domain reflectometry. *Water Resour. Res.* 25: 2367–2376.

Chapter 71
Soil Water Potential

N.J. Livingston
University of Victoria
Victoria, British Columbia, Canada

G. Clarke Topp
Agriculture and Agri-Food Canada
Ottawa, Ontario, Canada

71.1 INTRODUCTION

Soil water potential may be considered as the ''energy status'' of the water in the soil pores, relative to some standard reference condition or datum. Soil water potential is defined along with the units of measurement now in common practice (see Section 69.3). Soil water potential is used primarily for determining the direction and rate of water flow between locations with differing potentials (i.e., flow due to a potential gradient or hydraulic head gradient). The potential of soil pore water varies over several orders of magnitude, ranging from positive values in saturated soil to extremely negative values in dry soil. There are numerous instruments and techniques for direct and indirect measurement of soil water potential, but no single approach applies for the entire water potential range commonly found in soils or other natural porous materials. Direct measurement of soil water potential involves determining water pressure or water surface elevation relative to a datum (e.g., pressure transducer, standpipe water level, etc.), while indirect measurement involves measuring some surrogate property that correlates with water potential (e.g., electrical resistance or conductivity, water vapor pressure, water content, plant xylem potential, etc.). For example, a direct determination of positive pore water potential is obtained from the elevation of the water surface in a piezometer pipe, while an indirect determination of negative water potential can be obtained from electrical resistance or relative humidity.

This chapter focuses on selected direct and indirect methods for measuring soil water potential, which are well established and commonly used, namely the piezometer method for saturated soils, and the tensiometer, resistance block, and psychrometer methods for unsaturated soils. The emphasis is on basic principles and practical application. More detailed descriptions of these methods and other methods for measuring soil pore water potential can be found in Richards (1965), Brown and van Haveren (1972), Hanks and Brown (1987), Young (2002), Young and Sisson (2002), Andraski and Scanlon (2002),

Scanlon et al. (2002), and Strangeways (2003). A more general overview of measuring water potential and flow is given in Kramer and Boyer (1995).

71.2 PIEZOMETERS

Piezometers are generally of small diameter ($\approx 0.01-0.1$ m), nonpumping wells, which are used primarily to determine water potential (hydraulic head) and the direction of saturated water flow (Young 2002), but can also be used as water quality sampling wells and as a technique for *in situ* measurement of saturated hydraulic conductivity. We focus here on the measurement of water potential.

Piezometers consist essentially of a subsurface intake connected to the bottom of a standpipe or riser pipe which extends above the surface (Figure 71.1) (see also Figure 69.1 for principles of operation of piezometers). The intake in the soil may consist of a prefabricated well screen, a slotted section of the standpipe, or simply the open end of the standpipe. A piezometer operates by allowing water to move freely in or out through the intake in response to imposed changes in standpipe water level, and/or natural changes in piezometric surface elevation, water table elevation, or barometric pressure. The top of the piezometer is normally fitted with a vented cap to maintain atmospheric pressure within the pipe and to prevent unintended entry of water and foreign materials.

Piezometers measure the total water potential (ψ_t) and pressure potential (ψ_p) in saturated porous materials. If units of energy per unit weight are used, then ψ_t is equivalent to the total

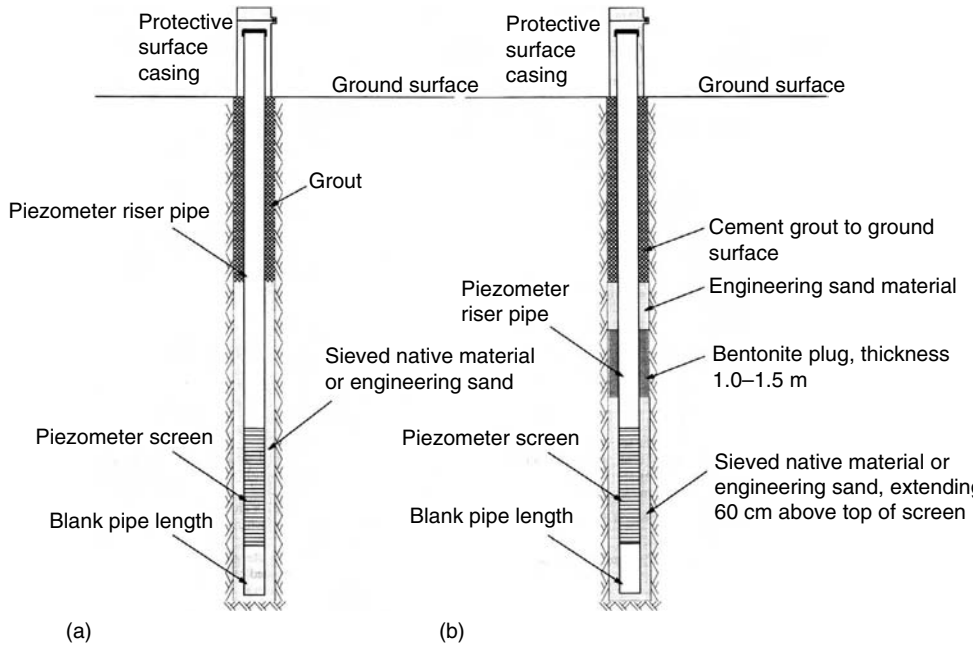

FIGURE 71.1. A piezometer that is not hydrologically isolated (a) and a piezometer that is hydrologically isolated (b), with isolation being achieved through installation of an impermeable bentonite ''plug''. (From Young, M.H. and Sisson, J.B., in J.H. Dane and G.C. Topp (Eds.), *Methods of Soil Analysis, Part 4—Physical Methods*, Soil Science Society of America, Madison, WI, 2002. With permission.)

elevation of the water surface (piezometric surface) in the piezometer standpipe and the ψ_p is equivalent to the depth of water in the piezometer standpipe (see Figure 69.1). Piezometers do not measure matric potential, which does not exist in saturated materials (see Section 69.3), and the gravitational potential (ψ_g) is determined by measuring the elevation difference between the midpoint of the piezometer intake and an arbitrary datum, such as mean sea level (see Figure 69.1).

Note that a ''water table well'' may be viewed as a special case piezometer where the intake (e.g., slotted section) extends from the piezometer base to near the porous medium surface. A water table well is used primarily to measure the elevation of the water table in unconfined aquifers.

71.2.1 Material and Supplies

Pipe Materials

Piezometer pipes are constructed from iron, aluminum, stainless steel, acrylonitrile butadiene styrene (ABS) plastic, and other materials. ABS plastic is most commonly used, as it is inexpensive and easily handled. If measurements of pore water chemistry or electrical conductivity are planned, care should be taken to ensure that the selected pipe materials will not affect the results through leaching, adsorption, or electrical interferences. The diameter of the pipe must be greater than the diameter of the devices, selected for measuring ψ_p (often referred to as the ''piezometric head'' or ''pressure head'') and for collecting water samples if required.

Piezometer Intake

The piezometer intake is usually constructed by attaching a length of prefabricated well screen, or by cutting a series of saw slots along the pipe at the desired position (which is usually at the base of the pipe) and covering the slots with a filter cloth (e.g., tile sock). In stable, highly permeable soils (usually coarse-textured sandy materials), a simple wire mesh and/or filter cloth covering the open base of the pipe provides a sufficient intake.

Drilling Capability

Drilling requirements depend largely on the depth of installation, diameter of the hole, and soil conditions (e.g., texture, density, stoniness, etc.). Options include drill rigs, which are used primarily for stony soils, deep boreholes, or large-diameter boreholes, impact hammers (e.g., Cobra rock drill), which are used for vibrating piezometer pipes into place (work best in saturated medium-coarse sandy materials), and various motorized or manual augers, which are designed for specific soil types and conditions.

Surveying Capability

To obtain measures of total water potential, the elevation (measured relative to mean sea level or relative to some arbitrarily selected datum) of the piezometer intake and/or ground surface adjacent to the piezometer must be determined to account for variations in surface topography and depth of piezometer installation. Piezometric water levels (i.e., pressure potentials or heads) are usually collected as depth of water from the ground surface and then converted to elevation using the known depth of the piezometer intake.

Measurement and Monitoring

Water levels can be monitored using either manual or automated devices. Manual collection of water levels from piezometers is most often accomplished using electronic water level indicators, electric tapes, or simple measuring tapes fitted with a ''popper.'' A popper is simply a small cube or cylinder of closed pore foam (e.g., Styrofoam), split lengthwise, and screwed or cemented around the end of the measuring tape, so that the zero end of the tape floats at the water level. Automated sensors are usually electronic and combined with a data logger. A variety of automated sensors are available, most being pressure-sensing devices based on piezoresistive, strain gauge, or vibrating wire diaphragms, or nonpressure-sensing devices based on sonic, radar, or time-domain reflectometry (TDR) technologies. Young (2002) gives a detailed discussion of the setup and use of automated water level sensors. The main advantages of manual water level devices are that they are simple, inexpensive, rugged, and easily portable so that many piezometers can be measured using a single device. Important advantages of automated water level devices include greatly improved temporal resolution and acquisition of data in a format that can be directly downloaded into a computer spreadsheet.

Water Extraction Equipment

Manual bailer, hand pump, or motorized pump.

Sealing Material

Bentonite pellets, grout, or cement for preventing ''short circuit'' flow (see Piezometer Installation, p. 969).

Backfill Material

Sieved soil from the installation sites may be used. Sandy material is often chosen because of its ''fluidity'' for pouring around the pipe.

Selected Hand Tools and Consumables

Pipe wrenches, saw, rope, shovels, glue, couplings, etc. are needed for construction and installation of the piezometers.

71.2.2 Procedure

Piezometer Selection and Construction

As indicated above, a wide variety of materials are used for piezometers along with a variety of intake designs. The intake is usually tailored to soil conditions to ensure unimpeded water flow, for example, high-hydraulic conductivity soils require less intake area than low-conductivity soils. As a result, sandy soils often use piezometers that are open only at the bottom. Large artificial gravel packs are not normally placed around piezometer intakes (unlike water supply wells), as this can decrease the accuracy of water potential readings, especially when hydraulic gradients exist.

Borehole Construction

Construct the borehole using an appropriate technology (e.g., drill rig, hand/motorized auger, impact hammer, etc.). Young (2002) gives a summary of the approaches commonly used for piezometer installation, and the shallow boreholes typically required for agri-environmental applications are amenable to small, mobile drill rigs, impact hammers, and various hand/motorized augers designed for specific soil types and conditions. In loose, sandy materials, installation of shallow piezometers is sometimes possible without digging a borehole, i.e., a conical tip is fitted to the bottom of the piezometer pipe (below the intake), and the pipe is then simply pushed (using a drill rig) or vibrated (using an impact hammer) to the required depth.

Piezometer Installation

There are two installations under piezometer installations namely the single installations and the nested installations. Single installations are those where one piezometer is installed in the borehole, and nested installations are those where several piezometers are installed at different depths in the borehole. Single installations may be hydrologically ''isolated,'' where a bentonite or grout seal is placed just above the intake, or ''nonisolated,'' where no seal is used. Nested installations almost always require hydrologic isolation of each piezometer intake by placement of bentonite, grout or cement seals, above and below ea!ch intake (Figure 71.1). The objective of hydrologic isolation is to prevent short-circuit water flow (i.e., direct water flow between nested intakes, water flow along the standpipe wall and through the backfill material, leakage from the surface), which can invalidate measurements.

1. Connect the piezometer intake (e.g., well screen, slotted pipe section) to the bottom of the first section of standpipe. Lower the intake and standpipe into the borehole, add additional standpipe sections as required to reach the bottom of the hole.

2. Place backfill material into the borehole using either a shovel or funnel, or a tremie tube to fill the hole around the intake to 0.3–0.6 m above the intake (ASTM 1995). A tremie tube is a small-diameter pipe lowered to the bottom of the borehole, into which air-dried and granulated backfill material is poured to provide more uniform and more accurate placement of backfill material. If the piezometer is nonisolated, backfilling is continued to the surface. Backfill should be tamped as much as possible during placement to prevent settlement, and also mounded at the surface to prevent collection of surface water around the standpipe.

3. For isolated piezometers, a seal of bentonite, grout, or cement (see ASTM 1995 for cement compositions) is applied just above each intake in an annular ring around the piezometer standpipe (1–1.5 m thickness) to prevent short-circuit water flow (see above). Tamped backfill is placed between each seal, and once the seal is in place, backfilling is continued to the surface as for nonisolated piezometers.

4. Place a vented cap on the piezometer to maintain ambient atmospheric pressure inside the pipe and prevent entry of rain water or foreign materials.

71.2.3 Piezometer Response Time and Development

Piezometer response time is the time required for the water level in the piezometer standpipe to re-equilibrate after an imposed change in pipe water level (as a result of bailing or slug testing), or after a change in the surrounding piezometric surface or water table elevation (as a result of precipitation, drainage, or groundwater extraction). Piezometer response time should reflect the permeability of the porous medium, not the permeability of the intake or the adjacent borehole wall. The installation process often causes partial plugging of the intake with fine particles, and also smearing and compaction of the borehole wall. To ensure that the piezometer response time reflects the permeability of the porous medium, newly installed piezometers are often ''developed,'' which involves ''surging'' and rapid extraction of the piezometer water. A pump or bailer can be used to extract water, and surging can be conveniently accomplished by ''bouncing'' the bailer in and out of the water before removal. Surging seems to be particularly effective at washing off smeared or compacted borehole surfaces and dislodging fines from the intake. Surging and water extraction are continued until the extracted water is free of suspended silt and clay.

71.2.4 Monitoring and Data Acquisition

1 Establish for each piezometer a ''reference height'' against which the piezometric head will be measured over time, and determine (by surveying or other means) the elevation of each reference height. The top of the piezometer standpipe is often chosen as the reference height.

2 Check the calibration and operation of the chosen manual or automatic water level monitoring device, and operate as directed in the operator's manual.

3 Initiate the data collection as required by the study.

71.2.5 Calculation Considerations

The use of piezometers to calculate total water potential (i.e., $\psi_t = \psi_p + \psi_g$) and total potential gradient (i.e., $\Delta\psi_t/\Delta\psi_g$) involves summations, subtractions, and divisions of values that are often of dissimilar magnitude (e.g., $\psi_g = 300$ m, $\psi_p = 2$ m). This can greatly magnify measurement errors, and it is therefore critically important that substantial effort be expended in ensuring that the ψ_p and ψ_g measurements are as precise and accurate as possible.

71.3 TENSIOMETERS

Tensiometers are instruments for *in situ* measurement of total pore water potential in unsaturated porous materials, where the total potential, ψ_t, is the summation of the negative matric potential, ψ_m, and the gravitational potential, ψ_g (i.e., $\psi_t = \psi_m + \psi_g$) (refer to Figure 69.1 for the similarities and the differences between piezometer and tensiometer operation). Tensiometers are used widely in the determination of water potential, water potential gradients, aeration, and water availability to plants. They are relatively inexpensive, simple, and easy to install—particularly well suited to studies where large numbers of measurements

may be required. Tensiometers are used primarily in unsaturated porous materials, and thus complement piezometers, which operate only in saturated porous materials.

Tensiometers typically consist of a water-filled plastic tube, which has a saturated porous cup (usually made from fired ceramic or porous metals) sealed to the bottom, a removable cap, rubber stopper, or rubber septum sealed to the top, and some device for measuring matric potential (e.g., manometer, pressure gauge, pressure transducer) (Figure 71.2). When installed in unsaturated soil, the saturated porous cup prevents air entry into the tensiometer, and provides hydraulic connection between the tensiometer water and the soil water. Hence, the matric potential of the tensiometer water equilibrates to the negative matric potential of the soil water, which is recorded by the measuring device. As solutes pass freely through the porous cup, tensiometers are insensitive to osmotic potential, ψ_π.

As the matric potential decreases (becomes more negative), the water in the tensiometer tends to gradually degas and vaporize. Degassing can reduce or prevent tensiometer response by forming obstructive bubbles, whereas progressive vaporization will cause the tensiometer to empty gradually, which can cause erroneous matric potential readings and eventual failure

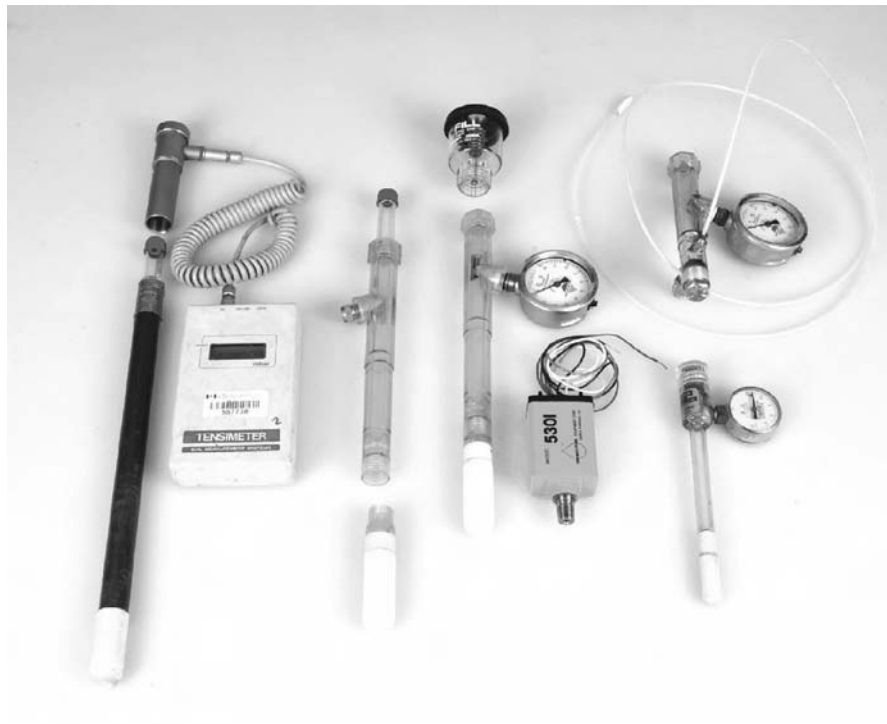

FIGURE 71.2. Some selected tensiometers. From left to right: tensimeter® fitted with septum cap and tensimeter readout device; customized tensimeter modified to accept a gauge or pressure transducer readout; tensiometer showing two optional screw caps and a manual gauge readout; pressure transducer for use as an alternative to a manual gauge; tensiometer fitted with a flexible ''spaghetti'' tubing and a mini porous cup; scaled-down tensiometer with midsized cup. Note that all the porous cups are ceramics, which is the most popular and least expensive of the available porous materials.

of the tensiometer. As a result, the effective measurement range of tensiometers is about -0.08 MPa $\leq \psi_m \leq 0$. Methods for dealing with air bubbles are discussed by Miller and Salehzadeh (1993).

71.3.1 Material and Supplies

Tensiometer Cups, Tubes, and Caps

Fully assembled tensiometers are available from suppliers, such as Soil Measurement Systems, Soilmoisture Equipment Corp., and Irrometer Co. (Figure 71.2). It is also possible to purchase component parts and assemble tensiometers for specific applications. A detailed list of the materials required and the procedures necessary to construct tensiometers are available from Soil Measurement Systems.

Pressure-Indicating or Recording Devices

The companies listed above also provide a variety of pressure-sensing devices. Soil Measurement Systems offers a tensimeter, which uses a hypodermic needle and a battery-powered pressure transducer to measure the partial vacuum above the water in the tensiometer tube (upper left in Figure 71.2). The other two companies use either mechanical pressure gauges or electronic pressure transducers, depending on the requirement of the application. U-tube manometers containing heavy liquids (e.g., mercury) were used frequently in the past, but are now avoided because of inconvenience, health and environmental concerns.

Pressure Readout Devices

Mechanical gauges and manometers must be read and recorded manually. Pressure transducers are usually battery-powered and some (e.g., the tensimeter) have a digital readout, while others require data logging.

Selected Hand Tools

Hand-operated vacuum pump, wrenches, shovels, and augers, etc.

71.3.2 Procedure

Filling the Tensiometer

Saturate the tensiometer cup in de-aired, temperature equilibrated water, a process that can be quickened by applying a slight vacuum (suction) to the tensiometer tube. Once the ceramic tip is saturated (water appears in the tensiometer tube), fill the tensiometer to the prescribed level by removing the cap or septum and directly pouring de-aired temperature equilibrated water into the top of the tube. Attach the pressure-indicating device and assure that its tubing and connection are water-filled. Note that the tensimeter requires a small airspace below the rubber septum, while other pressure-indicating devices respond more effectively in the absence of air.

Field Installation

For relatively shallow installations (say, $\leq$1 m) in relatively stone-free soils, bore a hole to the desired depth using an auger with the same outside diameter as the tensiometer (sliding fit without gap), and then carefully insert the tensiometer, ensuring good hydraulic

connection between the tensiometer cup and the soil at the bottom of the hole. Two approaches are recommended for establishing good hydraulic connection between the soil and the cup: (i) place a small amount of water-slurried soil (all stones and grit are removed) in the bottom of the hole before tensiometer insertion and (ii) fully insert the tensiometer, then wet the soil immediately surrounding the cup by removing the cap/septum to allow a small amount of water outflow. After the tensiometer is installed, refill the tensiometer and replace the cap (if required), and then wait for the tensiometer to equilibrate to the matric potential of the soil. Note that the time required for initial equilibration increases with the amount of water-slurried soil used, or the amount of water outflow allowed, when establishing the hydraulic connection between soil and cup. For a full description of field installed tensiometers equipped with pressure gauges, see Marthaler et al. (1983). For relatively deep installations (say, >1 m) and unstable soils, an access tube (metal or hard plastic) can be installed, and then the tensiometer inserted through the access tube until the porous cup protrudes below the access tube and about 0.05–0.1 m into the soil. In stoney soils, considerable care is required to avoid damaging the porous cup during tensiometer installation and placement of stone-free, water-slurried soil in the bottom of the hole is usually necessary to establish good hydraulic connection between the soil and the cup. Above ground, tubing should be kept to a minimum to reduce bubble formation, and it should also be shielded to avoid damage and solar heating effects.

Recording the Pressures

After the initial equilibration, the tensiometer pressure is a continuous indication of soil matric potential. Data logged transducers are easily programmed to sample at the desired frequency and time of day, whereas manual readings taken early in the morning in order to minimize temperature and solar heating effects are considered to be best.

Tensiometer Maintenance

Dissolved air diffuses slowly through the porous cup and can exsolve inside the tensiometer tube, forming undesirable bubbles, which impede water movement and thereby impair (increase) response time. To maintain optimum performance, it is necessary to remove exsolved air periodically, which accumulates more rapidly as the matric potential approaches the low end of the tensiometer operating range (i.e., −0.08 MPa). If the matric potential decreases below −0.1 MPa, then the tensiometer rapidly fills with exsolved air and becomes operative again only after it is recharged with water, which can be done in place when the soil water matric potential is again greater than −0.08 to −0.1 MPa.

71.3.3 Calculation Considerations

Tensiometer readout devices usually give matric potential directly, and thus no additional calculations are necessary. As tensiometers are often used to determine gradients in potential, they are subjected to the same accuracy and precision concerns as piezometers, which in turn influences the choice of readout device and the required frequency of recalibration.

71.3.4 Comments

1 For a vertically installed tensiometer, the absolute pressure head measured by the tensiometer gauge, P (positive quantity), is given by

$$P = A + \psi_m - h \tag{71.1}$$

where ψ_m is the negative matric potential (head) at the tensiometer cup (negative quantity), h is the vertical height of the gauge above the tensiometer cup (positive quantity), and A is the ambient atmospheric pressure head (positive quantity). The minimum measurable ψ_m is therefore given by

$$\psi_m = -A + h \tag{71.2}$$

as this corresponds to $P = 0$ (i.e., complete vacuum) at the tensiometer gauge; and the measurable range of ψ_m is consequently

$$(-A + h) \leq \psi_m \leq 0 \tag{71.3}$$

Given that the average atmospheric pressure is $A = 10$ m, then $h < 10$ m is required to provide a usable range of ψ_m and for most field applications, $h = 4$ m is the practical maximum, as this yields a measurable matric potential range of -6 m $\leq \psi_m \leq 0$ according to Equation 71.3. As a result, matric potential measurements at depths greater than about 3.5 m are best achieved using short, buriable transducer-based tensiometers, which are fitted with wire leads that extend to the surface, to allow monitoring.

2 It is advisable to incorporate a short section of a clear plastic tubing at the upper end of the tensimeter tube if the tensiometer readout system is to be used (Figure 71.2). The clear plastic allows the headspace (air gap) at the top of the tensiometer to be seen so that one can ensure that the tensimeter needle is inserted into air and not into water.

3 Tensiometers can provide accurate and reliable measurements of soil water matric potential in moist soils (i.e., -0.08 MPa $\leq \psi_m \leq 0$), with a precision of about ± 0.0001 MPa if the pressure-sensing devices are well maintained and calibrated.

4 If a large number of tensiometers are required, costs can be reduced by using a single-pressure transducer to read several tensiometers via an automated switching (scanning) valve and a data logging system.

71.4 RESISTANCE BLOCK

Resistance blocks are a relatively inexpensive means of providing a continuous estimate of the negative matric potential, ψ_m, of relatively dry soil (i.e., $\psi_m \leq -0.05$ MPa). They are typically composed of an engineered matrix of hydrophilic porous materials, such as gypsum, fiberglass, or nylon, within which two electrodes are embedded. The blocks are buried at the desired depth in the soil, where they absorb or desorb water until the energy status of the block water equals that of the soil water. Soil matric potential is then inferred by measuring the electrical conductivity (or resistance) across the two embedded electrodes, and then applying a conductivity (or resistance) versus matric potential calibration curve. The electrical conductivity of a dry block is effectively zero, and it normally increases with block water content in a nonsaline environment. Note, however, that resistance blocks do not work well in saline environments (e.g., saline soils; saline irrigation water) as electrical conductivity later becomes insensitive due to changes in water content.

Resistance blocks react relatively slowly to changes in soil water potential (because they equilibrate by absorbing or desorbing water), and should therefore not be used to track the movement of wetting fronts. In addition, very large measurement errors can arise if the blocks are not in complete equilibrium with the soil, or if they are subjected to large temperature variations (Carlson and El Salam 1987).

71.4.1 Material and Supplies

Resistance Blocks and Readout Devices

Blocks of various materials are commercially available from a wide variety of suppliers. Each supplier offers compatible voltage supply and data logger or readout alternatives. General data loggers and power supplies having a.c. voltage output may also be used with most resistance blocks.

Hand Tools

Selected hand tools used primarily for block installation (e.g., shovels, augers, etc.).

71.4.2 Procedure

Calibration

The logarithmic calibration curve that relates soil water matric potential to electrical conductivity or resistance is usually hysteretic and specific to each block and soil type. Hence, each block should be individually calibrated for wetting up and drying down using the same soil from which the field or laboratory measurements will be collected. It is further recommended that the pressure plate apparatus can be used to conduct the calibration, as it operates well within the measurement range of resistance blocks, and it allows electrical conductance, water content, and matric potential to be measured simultaneously. Note also that resistance blocks tend to degrade over time (e.g., due to slow gypsum dissolution; formation of small water-conducting cracks), and therefore need recalibration at approximately 3 month intervals.

Installation

Before installation, presoak the blocks for at least 24 h using water slurry made from the appropriate soil. Considerable care should be taken during installation to ensure minimum soil disturbance and good hydraulic connection between the block and soil. Note that soil disturbance (e.g., compaction) or damage to surface vegetation can lead to dramatic changes in the original soil water balance.

71.4.3 Calculation Considerations

The resistance block calibration curves can often be programmed into data logger and readout devices, which consequently allows direct readout of soil water potential (and sometimes also water content) without further manipulation. The precision of resistance block ψ_m data is rather low (typically ranging from ± 0.1 to ± 0.5 MPa), which precludes their use for determining gradients in water potential. They are also sensitive to temperature

(i.e., matric potential changes by approximately 1.5% for each Kelvin change in temperature), although partial temperature correction is possible if block temperature is monitored using thermistors or thermocouples.

71.4.4 Comments

An important and unique advantage of resistance blocks is that they can provide a continuous and automated measure of both matric potential and water content for dry soil. On the other hand, equally important disadvantages include the requirement for regular laboratory recalibration (which usually means laborious and careful removal and reinstallation), slow equilibration, and generally low precision (which precludes their use for estimating potential gradients).

71.5 THERMOCOUPLE PSYCHROMETERS

Thermocouple psychrometers provide an excellent complement to tensiometers in that they operate in the $\psi_t \leq -0.1$ MPa water potential range, whereas tensiometers operate in the -0.08 MPa $\leq \psi_t \leq 0$ range. There are both field-based psychrometer systems that measure water potential *in situ* (e.g., Wescor, Inc., Logan, Utah) and laboratory-based systems that measure water potential in intact or disturbed samples (e.g., Decagon Devices, Inc., Pullman, Washington).

Thermocouple psychrometers operate by relating the total potential of the liquid water in the sample to the equilibrium water vapor pressure in the air above the sample. The relation between water potential and relative water vapor pressure at thermodynamic equilibrium is given by

$$\psi_t = \left(\frac{RT}{V_w}\right) \ln\left(\frac{e}{e_s}\right) \tag{71.4}$$

where R is the universal gas constant (J mol^{-1} K^{-1}), T is the absolute temperature (K), e is the water vapor pressure of the air (Pa), and e_s is the saturation vapor pressure (Pa) at the air temperature. The dimensionless ratio, e/e_s, is the relative water vapor pressure or ''relative humidity.''

71.5.1 *In Situ* Soil Psychrometers

Rawlins and Dalton (1967), Lang (1968), and Weibe et al. (1971) describe soil psychrometer devices that can measure soil water potential *in situ*. A soil psychrometer usually consists of a small porous cup (about 1 cm in diameter and 1 cm in length) that contains a single thermocouple (50–100 μm in diameter). The cup is usually made of porous ceramic, brass, or stainless steel (3–30 μm pore size), which allows water vapor to diffuse between the soil and the inside of the cup until vapor pressure equilibrium is established. The sensing junction of the thermocouple is constructed of very fine, welded chromel and constantan wires, while the reference junction is connected to much larger (>0.40 mm diameter) copper wires. The open end of the porous cup is sealed with a Teflon plug, and in some psychrometers (Szietz 1975), another thermocouple is embedded in this region to provide a measure of the psychrometer temperature.

Modes of Operation

Psychrometric Mode of Operation

When an appropriate current is applied to the sensing junction in a thermally equilibrated psychrometer system, the junction cools by the Peltier effect. With continued cooling, the junction temperature falls below the dew point of the air in the porous cup so that a drop of water condenses on the junction. The maximum cooling is about 5°C below the ambient cup temperature. When the soil water potential is less than 0 MPa, the relative humidity inside an equilibrated porous cup will be less than 100% and the water drop will consequently re-evaporate and cool the junction to a temperature that can be related to the relative humidity inside the cup. This decline in temperature can be measured with a voltmeter that has microvolt or nanovolt sensitivity, and the output voltage is typically about 5 μV MPa^{-1}. The temperature of the psychrometer is also measured so that the soil water potential can be calculated from Equation 71.4. The relationship between psychrometer output voltage and water potential can be obtained by immersing the psychrometer in a range of constant temperature salt solutions with varying water potentials (Lang 1967).

Very small temperature depressions are generated at the sensing junction during measurements so that any temperature gradient between the sensing junction and the reference junction will lead to large errors. For example, a temperature difference of 0.001°C corresponds to an error of 0.01 MPa (0.1 bar). It is therefore imperative that there are no temperature gradients across the sensor or leads, and as a result, soil psychrometers usually cannot be used where large temperature gradients exist (e.g., within 0.15–0.30 m of the soil surface).

There have been numerous attempts to design thermocouple psychrometers that can accurately measure soil water potential in the presence of temperature gradients. For example, Campbell (1979) designed a psychrometer containing both high thermal conductivity materials to minimize temperature gradients and symmetrically arranged ceramic ''windows'' to improve vapor exchange with the soil and thereby reduce internal condensation. These improvements reduced measurement errors due to temperature gradients to about one-third of those for earlier designs.

Dew Point Mode of Operation

Many psychrometers can be used in a ''continuous feedback'' dew point mode (Neumann and Thurtell 1972), which is often referred to as the ''dew point hygrometer'' system. Here, Peltier cooling is again used to condense a water droplet on the sensing junction; however, the cooling current is continuously adjusted so that there is no net gain or loss of water vapor. In unsaturated soil conditions, the dew point temperature will be below ambient and this temperature difference will be measured as a differential voltage between the reference junction and the sensing junction when no current is flowing.

Although dew point hygrometers are still sensitive to internal temperature gradients, they are much less sensitive than psychrometers to changes in ambient temperature, and therefore require no temperature correction. In addition, they provide a relatively large output signal with a sensitivity of approximately 0.75 μV MPa^{-1}, which is about 50% greater than that provided by psychrometers. Further, since there is no net movement of water from the thermocouple junction to the chamber at the dew point, the signal is stable for long periods and the vapor equilibrium in the chamber is not disturbed.

Apparatus and Procedures

1 Psychrometers have two main components: the porous cup with its contained sensing and reference junctions and the instrument for generating the electrical current and measuring the psychrometer output. Wescor Inc. offers soil psychrometers, combined psychrometer–hygrometer systems, and various data logging systems for continuous monitoring.

2 To minimize thermal gradients, psychrometers should be installed with the axis of the sensor parallel to the soil surface, and *in situ* psychrometers should not be installed at depths shallower than 0.15–0.30 m. To reduce heat conduction along lead wires, at least two loops of wire (about 0.04 m long) should be wrapped up behind the psychrometer sensing head and buried at the same depth. Rundel and Jarrell (1989) recommend that if continuous data records are required, extra psychrometers should be installed to replace those that fail or are removed for calibration checks. Use of psychrometers to measure the water potential in greenhouse or outdoor pots is often not successful because of large temperature gradients that are difficult to control.

Psychrometer Maintenance

For valid and accurate results, it is critically important that thermocouple psychrometer components remain free of contamination and corrosion, as contaminated and corroded surfaces dramatically delay vapor equilibration, and also invalidate the calibration relationship by causing a nonuniform internal vapor concentration and nonconstant evaporation from the sensing junction. Unfortunately, the porous nature of the psychrometer cup allows contamination of its internal surfaces and structures by allowing the entry of dissolved soil salts that form precipitates and promote corrosion. Hence, all internal surfaces in the psychrometer cup must be cleaned periodically. Simply running water over the cups for several hours can sometimes effect adequate cleaning, although most commercial units are now easily disassembled for more thorough cleaning. It is often recommended that thermocouples and their mounts be cleaned by immersion in steam or solvents (such as reagent grade acetone or 10% ammonium hydroxide solution), then thoroughly rinsed in distilled or deionized water (especially if solvent cleaners were used). Wescor Inc. strongly recommends that the water used for rinsing should be pure enough to have an electrical resistance of at least 1 megohm ($10^6\ \Omega$) cm^{-3}. Psychrometers should be dried by blowing with clean (filtered) air. Savage et al. (1987) further recommend that the screen cage covers attached to commercially available soil psychrometers be removed and soaked in a 10:1 mixture of water and hydrochloric acid to remove any traces of rust. This is particularly important if the devices were calibrated in salt solutions. The screens should then be soaked in acetone to reduce the possibility of fungal growth. Psychrometers fabricated from stainless steel are highly resistant to internal corrosion, but are generally much more expensive than those made from brass. Corrosion resistance of brass psychrometers can be quite improved considerably by chrome or nickel plating. In saline soils, psychrometers should be checked frequently for corrosion of the fine thermocouple wires.

71.5.2 Laboratory Dew Point Psychrometers

The dew point psychrometer, which was first developed for the food industry, has been adapted to soils applications (Scanlon et al. 2002) as it is much less sensitive to temperature

effects than the thermocouple psychrometer. It operates by measuring the dew point temperature inside a chamber, which is in thermal and vapor pressure equilibrium with a soil sample. Laboratory dew point psychrometers are commercially available, and this section will focus on the system offered by Decagon Devices Inc., known as the WP4 ''Dewpoint PotentiaMeter.''

The WP4 Dewpoint PotentiaMeter uses a sealed chamber to equilibrate the liquid-phase water of the sample with the vapor-phase water in the headspace above the sample. A mirror situated in the headspace above the sample is Peltier-cooled until the dew point is reached, which is detected as a sudden decrease in mirror reflectance because of condensation. The dew point and sample temperatures are then recorded and used to calculate the headspace water vapor pressure (e) and the saturated water vapor pressure (e_s), respectively. Water potential is then calculated using Equation 71.4.

Apparatus and Procedures

1 Load each sample (≈7 mL volume) into a separate psychrometer sample holder. Slightly compress using a rubber stopper or square-ended metal rod to produce a flat surface and a uniform thickness of ≈0.5 cm (surface leveling and slight compression tends to produce more reliable results—Gee et al. 1992). The loaded sample holders should be sealed in vapor-tight containers to prevent loss or gain of water before analysis.

2 Insert one loaded sample holder into the psychrometer and start the measuring process (samples are inserted and measured one at a time). The WP4 Dew point PotentiaMeter requires ≈5 min per measurement and displays both soil water matric potential and sample temperature after internal calculations.

Comments

1 The operating range of the WP4 is about -40 MPa $\leq \psi_t \leq -0.1$ MPa. A precision of ± 0.1 MPa can be achieved if the difference between the sample temperature and the dew point temperature is known within ± 0.005°C, and if the sample temperature is within ± 0.5°C of the chamber temperature. Hence, the temperature sensors of the instrument must be extremely accurate, and it is advisable to house the prepared samples and psychrometer instrument together in a constant temperature room (e.g., 20°C ± 1°C).

2 With a precision limit of ± 0.1 MPa, the WP4 instrument is most effectively applied to very dry soils, i.e., $\psi_t \leq -0.4$ MPa. When working with disturbed field samples at such low potentials, the main source of measurement error arises from changes in sample water content (and thereby water potential) during sample collection, transport, and storage. This is because the soil water characteristic curve is very flat in this water potential range, and thus a very small change in water content can produce a very large change in water potential. Hence, great care must be taken to prevent water evaporation or condensation when the samples are collected, transported, and stored.

71.6 CONCLUDING REMARKS

1 Selection of the most appropriate devices for measuring water potential depends strongly on the anticipated water potential range (i.e., positive, slightly negative, strongly negative), the intended use of the data, and the limitations of the devices (e.g., operating range, accuracy, etc.). Furthermore, all devices must be carefully installed and maintained, else incorrect and misleading data will likely result.

2 Note that a tensiometer is capable of operating as a piezometer (i.e., record positive water potentials in saturated porous materials), but its response time may be impractically or unacceptably slow because of flow impedance by the porous cup.

3 Piezometers remain the simplest and most reliable method for measuring saturated porous materials with positive water potentials (i.e., $\psi_p > 0$), while tensiometers are recommended for wet but unsaturated materials (i.e., -0.08 MPa $\leq \psi_m \leq 0$). Measurements in dry porous materials (i.e., $\psi_m \leq -0.1$ MPa) are best achieved using thermocouple psychrometers, thermocouple hygrometers, and dew point psychrometers.

Note, however, that great care should be taken when using thermocouple-based devices since very large errors can occur if they are incorrectly calibrated, poorly maintained, or subjected to strong temperature gradients. Moisture blocks should only be used to obtain a general indication of water potential, even when they are carefully installed and maintained.

REFERENCES

Andraski, B.J. and Scanlon, B.R. 2002. Thermocouple psychrometry. In J.H. Dane and G.C. Topp, Eds. *Methods of Soil Analysis, Part 4—Physical Methods*, Soil Science Society of America, Madison, WI, pp. 609–642.

ASTM (American Society for Testing and Materials). 1995. Standard practice for design and installation of ground water monitoring wells in aquifers—Method D5092-90(1995)e1. ASTM, West Conshohocken, PA.

Brown, R.W. and van Haveren, B.P. 1972. Psychrometry in water relations research. *Proceedings of the Symposium on Thermocouple Psychrometers*. Utah Agricultural Experimental Station, Utah State University, Logan, UT, pp. 1–27.

Campbell, G.S. 1979. Improved thermocouple psychrometers for measurement of soil water potential in a temperature gradient. *J. Phys. E. Sci. Instrum.* 12: 739–743.

Carlson, T.N. and El Salam, J. 1987. Measurement of soil moisture using gypsum blocks. In R.J. Hanks and R.W. Brown, Eds. *Proceedings of International Conference on Measurement of Soil and Plant Water Status*. Vol. 1. Logan, Utah State University, UT, July 1987, pp. 193–200.

Gee, G.W., Campbell, M.D., Campbell, G.S., and Campbell, J.H. 1992. Rapid measurement of low soil water potentials using a water activity meter. *Soil Sci. Soc. Am. J.* 56: 1068–1070.

Hanks, R.J. and Brown, R.W. 1987. Eds. *Proceedings of International Conference on Measurement of Soil and Plant Water Status*, Vol 1, Logan, UT, July 1987, pp. 115–119.

Kramer, P.J. and Boyer, J.S. 1995. *Water Relations of Plants and Soil*. Academic Press, San Diego, CA.

Lang, A.R.G. 1967. Osmotic coefficients and water potentials of sodium chloride solutions from 0 to 40°C. *Aust. J. Chem.* 20: 2017–2023.

Lang, A.R.G. 1968. Psychrometric measurement of soil water potential in situ under cotton plants. *Soil Sci*. 106: 460–464.

Marthaler, H.P., Vogelsanger, W., Richard, F., and Wierenga, P.J. 1983. A pressure transducer for field tensiometers. *Soil Sci. Soc. Am. J*. 47: 624–627.

Miller, E.E. and Salehzadeh, A. 1993. Stripper for bubble-free tensiometry. *J. Soil Sci. Soc. Am*. 57: 1470–1473.

Neumann, H.H. and Thurtell, G.W. 1972. A Peltier cooled thermocouple dewpoint hygrometer for *in situ* measurement of water potential. In R.W. Brown and B.P. van Haveren, Eds. *Psychrometry in Water Relations Research*. Utah Agricultural Experimental Station, Logan, Utah State University, UT, pp. 103–112.

Rawlins, S.L. and Dalton, F.N. 1967. Psychrometric measurements of soil water potential without precise temperature control. *Soil Sci. Soc. Am. Proc*. 31: 297–300.

Richards, L.A. 1965. Physical conditions of water in soil. In C.A. Black et al., Eds. *Methods of Soil Analysis*. American Society of Agronomy, Madison, WI, pp. 128–152.

Rundel, P.W. and Jarrell, W.R. 1989. Water in the environment. In R.W. Pearcy, J. Ehleringer, H.A. Mooney, and P.W. Rundel, Eds. *Plant Physiological Ecology*. Chapman and Hall, New York.

Savage, M.J., Ritchie, J.T., and Khuvutlu, I.N. 1987. Soil hygrometers for obtaining water potential. In R.J. Hanks and R.W. Brown, Eds. *Proceedings of International Conference on Measurement of Soil and Plant Water Status*. Vol. 1. Logan, Utah State University, UT, July 1987, pp. 119–124.

Scanlon, B.R., Andraski, B.J., and Bilskie, J. 2002. Miscellaneous methods for measuring matric or water potential. In J.H. Dane and G.C. Topp, Eds. *Methods of Soil Analysis, Part 4—Physical Methods*, Soil Science Society of America, Madison, WI, pp. 643–670.

Strangeways, I. 2003. *Measuring the Natural Environment*. Cambridge University Press, Cambridge, UK.

Szietz, G. 1975. Instruments and their exposure. In J.L. Monteith, Ed. *Vegetation and the Atmosphere*. Vol. 1. Academic Press, London.

Weibe, H.H., Campbell, G.S., Gardner, W.H., Rawlins, S., Cary, J.W., and Brown, R.W. 1971. Measurement of plant and water status. *Utah Agricultural Experimental Bulletin* 484. Utah State University, Logan, UT.

Young, M.H. 2002. Piezometry. In J.H. Dane and G.C. Topp, Eds. *Methods of Soil Analysis, Part 4—Physical Methods*, SSSA Book Series No. 5, Soil Science Society of America, Madison, WI, pp. 547–573.

Young, M.H. and Sisson, J.B. 2002. Tensiometry. In J.H. Dane and G.C. Topp, Eds. *Methods of Soil Analysis, Part 4—Physical Methods*, Soil Science Society of America, Madison, WI, pp. 575–608.

Chapter 72
Soil Water Desorption and Imbibition: Tension and Pressure Techniques

W.D. Reynolds
Agriculture and Agri-Food Canada
Harrow, Ontario, Canada

G. Clarke Topp
Agriculture and Agri-Food Canada
Ottawa, Ontario, Canada

72.1 INTRODUCTION

Soil water desorption refers to the decrease in soil volumetric water content with decreasing pore water matric head (drainage), while imbibition refers to the increase in volumetric water content with increasing matric head (wetting). A discussion of the principles and parameters associated with the determination of desorption and imbibition curves is given in Chapter 69. This chapter describes the tension table, tension plate, and pressure extractor methods for measuring soil water desorption and imbibition curves. Alternative methods include the long column (Chapter 73), dewpoint psychrometer (Chapter 74), soil core evaporation (Chapter 81), instantaneous profile (Chapter 83), and estimation techniques (Chapter 84).

72.2 TENSION TABLE AND TENSION PLATE

The tension table and tension plate methods are used primarily for soil cores that are less than 20 cm diameter by 20 cm long, although larger samples can be used. These methods involve establishing a continuous hydraulic connection between the sample and the tension medium or plate, and then sequentially equilibrating the sample to a series of preselected matric heads set on the table or plate. The water content of the sample after equilibration represents one point on the desorption or imbibition curve. If the soil sample is initially saturated and the preselected matric heads are set in a descending sequence (i.e., successively more negative), a desorption curve is obtained. If the soil sample is initially dry and the preselected matric heads are set in an ascending sequence (successively less negative), an imbibition curve is obtained. Scanning curves are obtained by reversing the sequence of matric heads

(i.e., from ascending to descending or vice versa) at some intermediate point along the desorption or imbibition curves (see Chapter 69 for details).

72.2.1 Materials and Supplies

1 *Tension table*: A tension table (Figure 72.1a) consists of a circular or rectangular tank containing a saturated layer of tension medium, a port for allowing water inflow and outflow, and an apparatus for changing and controlling the matric head, ψ_m, of the pore water in the tension medium (Stakman et al. 1969). The tension medium has an air-entry value, ψ_a (see Chapter 69), that is lower (more negative) than the minimum matric head set on the medium, plus a high-saturated hydraulic conductivity to minimize sample equilibration time (Topp and Zebchuk 1979). For convenience and improved equilibration times, ''low-tension'' and ''high-tension'' tables are often set up, with low-tension tables operating in the range of $-1\ \text{m} \leq \psi_m \leq 0\ \text{m}$, and high-tension tables operating in the $-5\ \text{m} \leq \psi_m \leq -1\ \text{m}$ range (Topp and Zebchuk 1979). The tension medium in low-tension tables is usually natural fine sand (<50 μm particle diameter), fine glass beads (42 μm mean particle diameter), or silica flour ($10-50$ μm particle diameter), while the high-tension tables generally use glass bead powder (25 μm mean particle diameter) or aluminum oxide powder (9 μm mean particle diameter) (see also Table 72.1). Beneath the tension medium is a water inflow–outflow port that is connected to the apparatus for setting and maintaining matric head, a drainage system to facilitate water movement into or out of the tension medium, and a fine mesh retaining screen to prevent loss of tension medium through the inflow–outflow port. The top of the tension medium may be protected by a cloth cover (nylon mesh) to prevent the tension medium from adhering to the soil core samples. Two main tension table designs are currently in use: (i) a rectangular perspex (acrylic) tank with a drainage system comprised of a glass microfiber retaining screen overlying a network of channels cut into the tank bottom (Ball and Hunter 1988) and (ii) a cylindrical polyethylene or PVC tank (Figure 72.1a) with a drainage system comprised of a retaining screen made of fine-grade nylon mesh ($6-20$ μm openings depending on fineness of tension medium) overlying a coarse mesh woven stainless steel screen (≈ 3 mm openings) placed on the tank bottom (Topp and Zebchuk 1979). Both designs should have loose-fitting, opaque lids for the following reasons: (i) to allow easy air exchange, and thereby prevent possible buildup of vacuum or pressure when the matric head is changed; (ii) to prevent evaporative water loss from the sample surfaces during the course of the measurements; and (iii) to omit light to inhibit fungal/algal/microbial growth on and in the samples during the course of the measurements.

The tank needs to be stiff enough to resist flexing over the applied matric head range, as this can result in air entry due to cracking of the tension medium or breaking of the seal between the tension medium and tank wall (for cylindrical polyethylene or PVC tanks, a wall and base thickness of at least 0.5 cm is recommended for the low-tension system, and at least 1.5 cm for the high-tension system). A 60 cm diameter tension tank can accommodate up to 30 cores with a 7.6 cm diameter, and up to 12–15 cores with a 10 cm diameter. Although tension tables are relatively easy and inexpensive to construct, they can require frequent maintenance as a result of algal growth and periodic plugging of the retaining screen or tension medium with silt and clay; and they can also be unreliable at

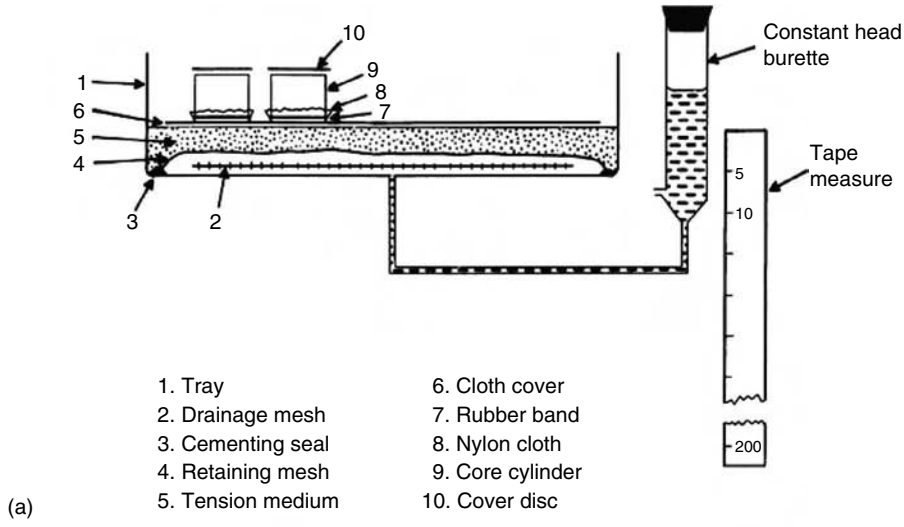

1. Tray
2. Drainage mesh
3. Cementing seal
4. Retaining mesh
5. Tension medium
6. Cloth cover
7. Rubber band
8. Nylon cloth
9. Core cylinder
10. Cover disc

(a)

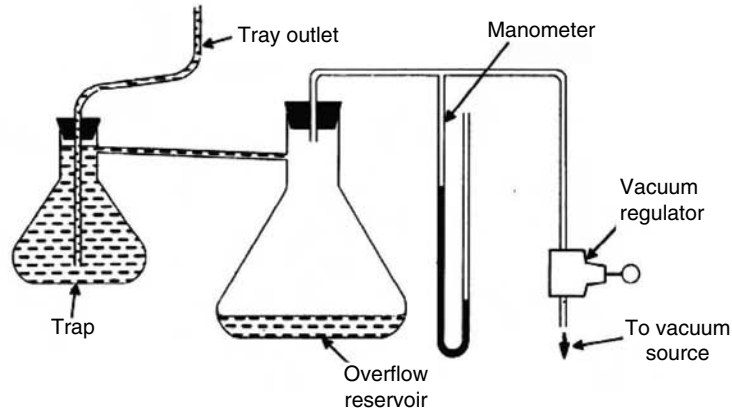

(b)

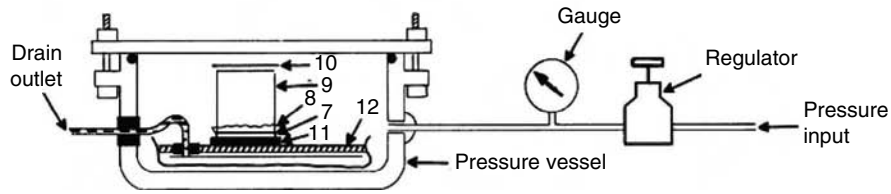

11. Hydraulic contact slurry
12. Ceramic plate

(c)

FIGURE 72.1. Tension table/plate and pressure extractor systems: (a) a low-tension table with matric head control by constant head burette; (b) a controlled vacuum system for use with high-tension tables or plates; and (c) a pressure extractor system. Note that the burette reservoir and trap (storage) flask are the water sources for the imbibition curve.

TABLE 72.1 Approximate Equilibration Times (Days) for Desorption from Saturation. The Tension Table and Tension Plate Times Apply to 7.6 cm Long Intact (Undisturbed) Soil Cores, or 10 cm Long Intact Cores (Bracketed Values). The Pressure Extractor Times Refer to 7.6 cm Long Intact Cores (First Column) or 1.0 cm Thick Samples that Have Been Granulated to ≤2 mm (Second Column)

	Tension table or tension plate with corresponding tension medium or contact material					
Matric head, ψ_m (m)	Glass beads (42 μm mean particle diameter)	Glass beads (25 μm mean particle diameter)	Aluminum oxide (9 μm mean particle diameter)	Silica flour (10–50 μm particle diameter)	Pressure extractor (intact core)	Pressure extractor (granulated sample)
0	0.5 (1)	—	—	—	—	—
−0.05	1 (2)	—	—	—	—	—
−0.1	1 (2)	—	—	4 (5)	—	—
−0.2	1 (2)	—	—	5 (6)	—	—
−0.3	2 (3)	—	—	6 (7)	—	—
−0.4	3 (4)	—	—	7 (8)	—	—
−0.5	3 (4)	—	—	8 (9)	—	—
−0.6	3 (4)	—	—	9 (10)	—	—
−0.75	4 (5)	—	—	9 (10)	—	—
−0.8	4 (5)	—	—	9 (10)	—	—
−1.0	6 (7)	—	—	10 (11)	—	—
−1.5	—	8 (9)	—	11 (12)	—	—
−2.0	—	10 (11)	—	12 (13)	—	—
−3.3	—	12 (13)	12 (13)	14 (15)	≥10[a]	—
−5.0	—	—	14 (15)	—	≥11[a]	—
−10	—	—	—	—	≥12[a]	≥3[a]
−40	—	—	—	—	≥15[a]	≥7[a]
−150	—	—	—	—	≥20[a]	≥10[a]

[a] Equilibration times for pressure extractors are very sensitive to sample and plate hydraulic characteristics, and to the degree of hydraulic connection between sample and plate. Hence, determination of equilibration is best achieved by monitoring plate outflow (e.g., Figure 72.3).

matric heads < -1 m due to air entry and air accumulation problems (Topp and Zebchuk 1979; Townend et al. 2001).

2 *Tension plate*: An alternative to the tension table is the so-called ''tension plate'' (Figure 72.2). The essential difference between a tension plate and a tension table is that the tension plate uses a large-diameter ceramic disc or ''plate'' (e.g., ≥50 cm diameter) instead of tension medium. The ceramic plate is usually designed to have a relatively high saturated hydraulic conductivity and minimum operating matric heads of −5 to −10 m. Although tension plates are more expensive than tension tables and must usually be purchased from a commercial supplier (e.g., Soilmoisture Equipment Corp., California), they are very reliable and much easier to operate and maintain. Good hydraulic connection between the plate and the core samples is established and maintained using a thin layer (≈0.5 cm) of saturated ''contact material'' made of fine-grade glass beads (42 μm

FIGURE 72.2. Example of tension plate apparatus (high-tension system) loaded with 10 cm inside diameter by 11 cm long intact soil cores. The cores are resting on a nylon cloth (15 μm pore size), which overlies a 0.5 cm thick layer of glass bead tension medium (25 μm mean particle diameter), which in turn overlies a 53 cm diameter ceramic disk (−10 m bubbling pressure) sealed within a PVC backing plate. To minimize biological growth and evaporative water loss, the cores are loosely capped with opaque plastic lids and the entire tension plate is covered with an acrylic lid. The trap (small flask) and overflow reservoir (large flask) for the vacuum system (Figure 72.1b) can be seen below the plates. Tygon tubing (1/4-in. i.d. by 1/8-in. wall) connects the trap to the inflow–outflow port of the tension plate via a hole drilled through the bench top.

mean particle diameter for the ''low-tension'' system; 25 μm mean particle diameter for the ''high-tension'' system) topped with fine-mesh nylon cloth (15 μm openings) to prevent the contact material from adhering to the samples. To minimize biological growth and evaporative water loss, the samples are loosely capped with opaque plastic lids and the entire tension plate is covered with an acrylic lid (Figure 72.2). A 50 cm diameter tension plate can accommodate up to 20–22 cores of 7.6 cm diameter, and up to 10–11 cores of 10 cm diameter.

3 *Matric head control*: Control of the matric head (ψ_m) applied to the water saturating the tension medium/plate and the coincident drainage/uptake of water by the samples is achieved using a hanging water column–constant head burette system (Figure 72.1a), or a regulated vacuum—manometer/transducer system (Figure 72.1b). The constant head burette system is recommended for low-tension tables/plates ($-1\ \text{m} \leq \psi_m \leq 0$), while the vacuum system is recommended for high-tension tables/plates ($-5\ \text{m} \leq \psi_m \leq -1\ \text{m}$). For desorption

curve measurements, water removed from the samples drains out the burette outflow or into the overflow flask; and for imbibition curve measurements, water taken up by the samples is extracted from the burette reservoir or trap (storage) flask. Both systems are fitted with shutoff valves so that water flow can be stopped when needed (see Section 72.3.1). The matric head datum can be set at the top, bottom, or mid height position on the soil cores; however, the mid height position is most logical as it locates the average matric head in the core once equilibrium is established. For the constant head burette system, the mid-core datum position is most easily established by simply setting the zero point of the measuring scale (i.e., the top of the tape measure in Figure 72.1a) at the height, $L/2$, above the tension medium or contact sand surface, where L is the length of the soil core.

4 *Appropriately collected and prepared soil cores*: Collect soil cores (as recommended in Chapter 69), then trim the soil flush with the bottom end of the sampling cylinder using a sharp, thin-bladed knife or hacksaw blade to prevent smearing and loss of material. If there are gaps or holes at the bottom of the soil sample, fill them with fine-grade sand or glass beads (e.g., $25-42$ μm mean particle diameter) so that hydraulic contact between the sample and the tension medium or plate is maximized. Place a piece of nylon cloth (53 μm openings) over the bottom end of the core and hold in place with a stout, elastic band. The upper end of the core is covered with a loose-fitting disc to prevent losses or gains of soil and water.

5 *Rake (tension table) or putty knife (tension plate)*: Use a small handheld rake or similar implement suitable for raking and leveling the tension medium surface. Use a wide plastic putty knife or similar implement for scraping contact material off the tension plate. Do not use metal implements to scrape the tension plate, as they may damage the ceramic surface.

6 *Balance*: A weigh balance with the appropriate range (usually 0–3 kg) and sensitivity (usually 0.1–0.01 g).

7 *Controlled temperature*: Temperature controlled room ($20°C \pm 1°C$) for housing the tension tables or plates, sample preparation, and sample weighing.

8 *Drying oven*: Forced air or convection oven for drying soil cores at $105°C \pm 5°C$.

9 *Cooling box*: Box with water vapor-tight seal suitable for cooling soil cores and other samples from oven temperature to room temperature in the presence of a desiccant.

72.2.2 Procedure

Desorption Curve

(i) Saturate the soil cores at room pressure and temperature ($20°C \pm 1°C$) using deaired, temperature equilibrated water. Convenient procedures for deairing water include the following: (a) boiling or autoclaving in large-vacuum flasks (4 L), then applying airtight seals to the flasks and cooling, (b) filling a vacuum desiccator with water and applying a 65 kPa vacuum for 45 min, and (c) direct application of vacuum (via vacuum pump or tap aspirator) to water in

large-vacuum flasks. An advantage of autoclaving is that the water is also sterilized, which helps to reduce biological growth in the samples and in the tension medium or plate. Water used for saturation should have similar major ion speciation and concentrations as the native soil water to prevent aggregate slaking and dispersion/aggregation of silt and clay. Local tap water is often adequate, but this should always be checked. Saturate the cores by placing them in an empty ''wetting tank'' (Chapter 75), and submerge one-third and subsequent thirds of the core length each 24 h period, so that the ponded water is at the top of the core by the third day. This promotes more complete saturation of the sample (e.g., reduces air entrapment within the sample), and allows time for fine-textured soils to swell completely. Leave the cores in the wetting tank until free water appears on the core surface. Weigh the saturated core by (a) weighing it under water (using a cradle) or (b) quickly removing the core from the wetting tank and placing it in a tared weigh boat so that the weight of rapidly drained macropore water is included in the total core weight. Record the saturated core weight, $M_c(\psi_1)$, where $\psi_1 = 0$ is the first (and largest) ψ_m value on the desorption curve, which yields the saturated water content value, θ_s.

(ii) Place the saturated cores on the presaturated tension table or plate with the constant head burette set to yield $\psi_m = 0$ m at the tension medium surface (tension table) or contact material surface (tension plate). Close the burette inflow–outflow valve to prevent water flow. Establish good hydraulic connection between the bottom of the cores and the tension medium or contact material by pushing and twisting the cores slightly to deform the material to the shape of the core base. Open the burette valve and allow the cores to equilibrate, then remove and weigh to obtain core weight, $M_c(\psi_2)$, where $\psi_2 = -L/2$ is the second ψ_m value on the desorption curve and L is the core length. The time required for equilibration (equilibration time) depends on the matric head (equilibration time increases with decreasing head due to decreasing soil core hydraulic conductivity); the height of the soil core (equilibration time increases roughly as the square of the core length because of increased flow path); the quality of the hydraulic connection between soil core and tension medium or contact material (equilibration time increases as the contact area between core and medium decreases); and the saturated hydraulic conductivity of the tension medium/contact material (equilibration time may be somewhat greater for high-tension media relative to low-tension media). Approximate equilibration times for 7.6 cm long soil cores are given in Table 72.1, and 1–2 days are generally added to these times for 10 cm long cores. Note that the times are approximate only, and individual equilibration time tests are recommended for accurate work with any particular soil.

Imbibition Curve

(i) Weigh the unsaturated soil cores to obtain, $M_c(\psi_i)$, where ψ_i is the initial ψ_m value of the samples. This weight will be used later to determine the initial soil water content of the cores.

(ii) Presaturate the tension table (or tension plate and contact material) using deaired, temperature-equilibrated water (see desorption curve procedures for details), and

set the constant head burette or vacuum to produce the desired minimum (most negative) matric head relative to the chosen datum (e.g., mid-core height), and close the water inflow–outflow valve. Establish contact between the soil cores and the tension table or plate by wetting the bottom of the cores, then firmly placing the cores on the tension medium or contact material with a slight push and twist to establish a good hydraulic connection. Open the inflow–outflow valve and allow the cores to equilibrate (imbibe water), then remove and weigh to obtain core weight, $M_c(\psi_1)$, where ψ_1 is the first (and most negative) ψ_m value on the imbibition curve. Equilibration times for imbibition are generally longer than those for desorption because rewet soil hydraulic conductivity is usually less than drainage hydraulic conductivity due to hysteretic and air entrapment effects. Unfortunately, equilibration time guidelines for imbibition curves are not yet established, hence preliminary equilibration tests are required.

Desorption and Imbibition Curves

(i) *Next matric head* (ψ_m) ≥ -1 *m (low-tension system)*: After $M_c(\psi_1)$ is measured, close the water inflow–outflow valve. To reestablish hydraulic connection between the cores and the tension table or plate, dampen the tension medium or contact material surface using a spray bottle (desorption curve), or wet the bottom of the cores (imbibition curve), and then return the cores to the same locations used for the previous head using a slight push and twist to ensure good core contact. Set the next desired head (i.e., ψ_2) by adjusting the height of the constant head burette, and then open the water inflow–outflow valve. Allow the soil cores to equilibrate, then remove and weigh to obtain, $M_c(\psi_2)$.

Low-tension tables and plates usually do not accumulate significant exsolved air (within and under the tension medium or plate) for matric heads ≥ -1 m. It is always advisable, however, to flush low-tension systems periodically to prevent possible buildup of exsolved air over time. This is most conveniently accomplished by closing the inflow–outflow valve, setting the matric head at -1 m, ponding 3–6 L of deaired temperature-equilibrated water on the surface, opening the inflow–outflow valve to allow the water to drain through, and then resetting the matric head to zero at the surface. At the end of a sequence of low-tension measurements on a batch of soil cores (e.g., cores successively equilibrated to $\psi_m = 0, -0.05, -0.1, -0.3, -0.5, -0.75, -1$ m), it is advisable to ''purge'' the low-tension table or plate using the procedures given below for the high-tension system. It is also advisable to replace the contact material at the end of each sequence of low-tension measurements to prevent potential plugging of the ceramic plate by silt and clay; and to replace the tension medium when the tank drainage rate starts to decline, which usually signals incipient plugging of the medium by silt and clay. Idle tanks and plates should always be left with a small amount of ponded water on the surface, the matric head set to near-zero, and the inflow–outflow valve closed.

(ii) *Next matric head* (ψ_m) < -1 *m (high-tension system)*: Tension table: close the water inflow–outflow valve; add 1–2 cm depth of deaired, temperature-equilibrated water onto the tension medium surface; rake and level the top 1–2 cm of the

medium (to produce a soft, smooth, and flat surface for easier establishment of good hydraulic connection between core and medium); then purge exsolved air that usually accumulates within and under the tension medium (procedure given below). Tension plate: scrape the contact material off the plate; purge exsolved air that usually accumulates within and under the plate (procedure given below); pond 1–2 cm of deaired, temperature-equilibrated water on the plate surface; then replace and level the contact material ($\approx$0.5 cm depth).

The high-tension systems usually accumulate exsolved air over time, which should be ''purged'' between tensions as air bubbles can impede, or even stop, drainage and imbibition. The following procedure seems effective for purging exsolved air from within and under the tension medium or plate: (a) close the inflow–outflow valve and pond a shallow depth (3–5 cm) of deaired, temperature-equilibrated water on the surface; (b) set a low-matric head (e.g., -3 to -5 m) on the tension table or plate; (c) open the inflow–outflow valve quickly to produce sudden rapid drainage through the tension medium or plate. The hydraulic ''shock'' produced by rapid opening the valve generally dislodges exsolved air within and under the tension medium or plate, and the ensuing rapid drainage forces the air out the outflow port; and (d) after about 1 min of flow, close the inflow–outflow valve for a few minutes, then repeat step (c). Most, if not all, exsolved air can generally be removed by a few repetitions of steps (c) and (d), as evidenced by few air bubbles coming out the outflow port. During this procedure, care must be taken to maintain ponded water on the surface so the air cannot reenter the tension medium or plate as a result of the low-matric head set in step (b). Idle tanks and plates should always be left with a small amount of ponded water on the surface, the matric head set to near-zero, and the inflow–outflow valve closed.

After removing exsolved air, close the water inflow–outflow valve, install the core samples as done for the low-tension system, set the next desired matric head (i.e., ψ_2) by adjusting the vacuum, and then slowly open the water inflow–outflow valve. Allow the soil cores to equilibrate, then remove and weigh to obtain, $M_c(\psi_2)$.

(iii) Repeat step (i) or (ii) for each desired point on the desorption or imbibition curve (i.e., θ for ψ_3, ψ_4, ψ_5, etc.). The matric head settings depend on the intended use of the data (see Comment 1 in Section 72.4). If changing water content causes the soil in intact cores to shrink (desorption curve) or swell (imbibition curve), the soil volume must be determined at a specific matric head, which is usually the field capacity head; e.g., $\psi_{FC} = -1$ m for intact core samples and $\psi_{FC} = -3.3$ m for disturbed samples.

(iv) Proceed to the analysis section if no additional curve points (i.e., $\theta(\psi_m)$ values) are required. If matric heads lower (more negative) than -5 m are required for the desorption curve, proceed to the pressure extractor method. At present, obtaining points on the imbibition curve at matric heads more negative than -5 m is difficult and rare, as it requires specialized materials and equipment.

72.3 PRESSURE EXTRACTOR

The pressure extractor method (Figure 72.1c) can provide points on the soil water desorption curve over the matric head range, -150 m $\leq \psi_m \leq -1$ m. However, the method is most commonly used for the more limited range, -150 m $\leq \psi_m \leq -3.3$ m, as the tension table

and tension plate methods are more efficient for greater heads (i.e., the tension table and plate methods have greater capacity and faster equilibration). The pressure extractor method applies gas pressure (rather than water tension) to push water from the soil sample, and thereby allows matric heads much lower (more negative) than the −5 to −8 m limit of the tension table or plate method. The pressure extractor method includes a ''low-pressure'' ($-50\ \text{m} \leq \psi_m \leq -1\ \text{m}$) and a ''high-pressure'' system ($-150\ \text{m} \leq \psi_m \leq -50\ \text{m}$), with the main difference being the air-entry pressure head (ψ_a) of the ceramic plate, and the size and strength of the pressure vessel. The use of pressure restricts the size of the extractor vessel, which in turn limits the size and number of intact soil cores that can be processed at one time. Standard commercial extractors can usually desorb no more than six 7.6 cm diameter soil cores at a time, and the cores cannot be longer than about 7.6 cm. Due to the restrictions on sample size/number and the long equilibration times associated with very low-matric heads, pressure extractors are used primarily for desorbing disturbed (granulated) soil samples that are only about 1–3 cm thick (see also Comment 2 in Section 72.4).

72.3.1 Materials and Supplies

1 *Pressure vessels*: The pressure vessels should be designed and built specifically for this application (e.g., Soilmoisture Equipment Corp., California), as the low-pressure vessels must withstand pressures up to 500 kPa (≈73 psi), and the high-pressure vessels must withstand pressures up to 1500 kPa (≈220 psi).

2 *Ceramic plates*: Porous ceramic plates with attached drainage system and three maximum pressure head ratings (10, 50, 150 m) are available commercially (e.g., Soilmoisture Equipment Corp., California).

3 *Pressurized air or nitrogen gas*: Regulated air compressor or commercial compressed gas cylinder containing compressed air or industrial grade nitrogen. Compressed nitrogen gas in a cylinder is often preferred due to the following reasons: (i) nitrogen is less soluble in water than air and thereby produces less gas accumulation under the porous plate and less evaporative water loss from the soil samples; (ii) nitrogen excludes oxygen from the pressure vessel and thereby reduces biological activity in the soil samples; and (iii) a compressed gas cylinder allows a simpler pressure control system than an air compressor, and it is not affected by power outages.

4 *Pressure regulator, pressure hose, gas shutoff valve, needle valve, and pressure gauge*: A bleed-off type regulator should be used if the pressure source is an air compressor; a nonbleeding type regulator should be used if the pressure source is a compressed gas cylinder. Use appropriately rated flexible pressure hose and gas shutoff valves. Plumb an accurate and sufficiently detailed pressure gauge into the line between the pressure source and pressure vessel to allow setting and monitoring the vessel pressure. Connect a needle valve to the pressure vessel exhaust to allow slow release of gas pressure when the soil samples are ready to be removed from the vessel.

5 *Contact material*: Fine particulate material, such as kaolin, is often (but not always) used to establish and maintain a good hydraulic connection between the ceramic plate and intact soil cores or samples of granulated soil. Equilibration times may be increased substantially if contact material is not used.

6 *Appropriately collected and prepared soil cores or granulated soil samples*: Intact soil cores should be collected and prepared as recommended in Chapter 69. Granulated soil samples are prepared by placing ≈1 cm depth of air-dried, granulated soil (≤2 mm particle size) in preweighed (0.01 g precision) 2.8–4.7 cm diameter by 2.0–4.0 cm long noncorroding rings (e.g., aluminum, brass, acrylonitrile butadiene styrene (ABS) plastic, etc.) which have either high-flow, ashless filter paper (e.g., Whatman no. 42) or nylon cloth (15 μm openings) wrapped over the bottom end and held in place by a stout elastic band. Record the weight of air-dry soil plus ring plus filter paper or cloth plus elastic band (0.01 g precision). Place loose-fitting cover plates on top of the cores or rings to minimize evaporative water loss while equilibrating in the pressure vessel.

7 *Balance, controlled temperature room, drying oven, and cooling box*: See Section 72.2.1 for specifications and details.

72.3.2 Procedure

1 Saturate the ceramic plates by immersion in deaired, temperature equilibrated tap water overnight and drain ponded water from the plate before placing the plate into position inside the pressure vessel. A wire or string cradle allows more convenient placement and removal of plates from pressure vessels. Connect the plate drainage outlet to the feed-through of the pressure vessel (Figure 72.1c). Some practitioners place a small volume of water (e.g., 50 mL) at the bottom of the pressure vessel (below the ceramic plate) to maintain high-relative humidity and thereby reduce evaporative water loss from the samples and porous plate.

2 (a) *Intact soil cores*: After completion of the tension table or plate desorption measurements (Section 72.2), spread a 1–3 mm thick layer of saturated contact material (e.g., kaolin) onto the cloth-covered base of the cores and immediately place this end of the cores on the ceramic plate. Place loose-fitting cover plates on top of the cores to reduce evaporative water loss.

(b) *Granulated samples*: Saturate the air-dry samples by placing in 1–2 cm depth of deaired, temperature-equilibrated water for 24 h, so that water infiltrates through the filter paper or cloth and upward into the soil. Spread a 1–3 mm thick layer of saturated contact material (e.g., kaolin) on the ceramic plate, then immediately place the saturated soil samples on the plate. Place loose-fitting cover plates on top of the rings to reduce evaporative water loss.

3 Close the pressure vessel and pressurize slowly (to avoid potential disruption of sample-plate contact) to the desired pressure head, noting that a pressure head of x m is equivalent to a matric head of $-x$ m. Monitor water outflow from the vessel until sample equilibration is achieved, as evidenced by cessation of water flow. Given that water outflow often approaches zero asymptotically (especially for low-matric heads), detection of equilibration (or virtual equilibration) can be assisted by plotting cumulative outflow volume versus inverse time (Figure 72.3). Approximate pressure extractor equilibration times are given in Table 72.1, although it must be recognized that actual times can vary substantially.

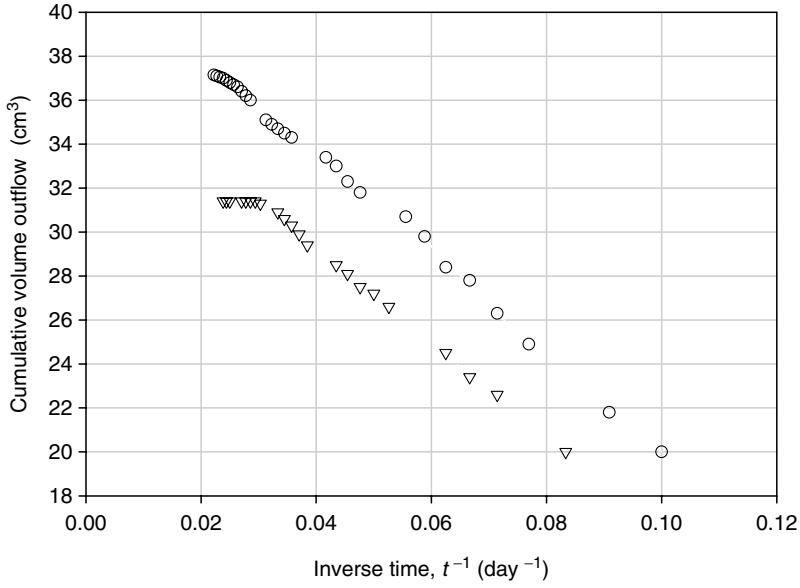

FIGURE 72.3. Cumulative volume outflow versus inverse time (t^{-1}) for equilibration of two sets of granulated clay loam soil samples (1 cm thickness) at $\psi_m = -150$ m using the pressure extractor method. One set of samples reached equilibrium after 34 days (triangles), while the other was still not equilibrated after 40 days (circles).

For example, Gee et al. (2002) found that 1.5 cm thick samples of granulated sandy, silty, and clayey soils pressurized to $\psi_m = -150$ m were still far from equilibrium after 10 days; and one author (W.D. Reynolds) routinely finds that equilibration to $\psi_m = -150$ m of 1.0 cm thick clay loam samples requires 30–60 days (see Comment 3 in Section 72.4).

4 Slowly bleed the pressure from the vessel (by closing the valve to the pressure source and opening the needle valve on the vessel exhaust) and remove the samples once the pressure has reached atmospheric. Remove the cover plate and all contact material adhering to the base of the sample, then weigh immediately (before significant evaporative water loss can occur) to obtain $M_c(\psi_m)$ (intact cores) or $M_s(\psi_m)$ (granulated samples).

5 Repeat steps 2, 3, and 4 for each selected matric head, but do not resaturate granulated samples.

6 After the final matric head and sample weights are attained, place the samples (minus the cover plates) in the drying oven at 105°C ± 5°C until oven-dry (≈72 h for 7.6 cm high intact cores; ≈96 h for 10 cm high intact cores; ≈24 h for 1 cm high granulated samples), then place in the cooling box until equilibrated to room temperature.

7 Weigh the cooled intact cores to a precision of 0.1 g, or the cooled granulated samples to a precision of 0.01 g, to obtain the oven-dry sample weight, M_d [M].

72.3.3 Analysis and Example Calculations

Intact Soil Cores

1 Calculate the mass of water in the soil, M_w [M], at each matric head, ψ_m [L], using

$$M_w(\psi_m) = M_c(\psi_m) - M_d \tag{72.1}$$

2 Calculate the volumetric water content, θ_v [L^3L^{-3}], at each matric head, ψ_m [L], using

$$\theta_v(\psi_m) = \frac{M_w(\psi_m)}{\rho_w V_b} \tag{72.2}$$

where V_b [L^3] is the bulk volume of the soil, and ρ_w [ML^{-3}] is the pore water density at the temperature of the room (e.g., $\rho_w = 0.9982$ g cm^{-3} at 20°C). The bulk soil volume, V_b, is calculated using

$$V_b = V_c - V_h = \pi a^2(l_c - \Delta l) \tag{72.3}$$

where V_c [L^3] is the volume of the core sampling cylinder, V_h [L^3] is the ''head-space'' volume between the top of the soil core and the top of the cylinder, a [L] is the cylinder inside radius, l_c [L] is the length of the sampling cylinder, and Δl [L] is the distance between the soil surface and the top of the sampling cylinder. If changing water content causes the soil in the intact cores to shrink (desorption curve) or swell (imbibition curve), Δl must be measured at a specific head, which is usually the field capacity value, i.e., $\psi_m = \psi_{FC} = -1$ m for intact soil cores, or -3.3 m for disturbed soil cores.

3 For among soil comparisons, the degree of water saturation, $S(\psi_m)$, is often useful

$$S(\psi_m) = \frac{\theta_v(\psi_m)}{\theta_{sat}} \tag{72.4}$$

where θ_{sat} [L^3L^{-3}] is the saturated soil volumetric water content, i.e., θ_v at $\psi_m = 0$.

4 If the mass of oven-dry soil is determined, one can also calculate gravimetric soil water content and soil bulk density. The mass of oven-dry soil, M_{ods} [M], is determined using

$$M_{ods} = M_d - M_{cce} \tag{72.5}$$

where M_{cce} [M] is the weight of the sampling cylinder plus cloth plus elastic band, after the removal of all adhering soil. The gravimetric soil water content, $\theta_g(\psi_m)$ [MM^{-1}], is then determined using

$$\theta_g(\psi_m) = \frac{M_w(\psi_m)}{M_{ods}} \tag{72.6}$$

and bulk density, ρ_b [ML^{-3}], is calculated from

$$\rho_b = \frac{M_{ods}}{V_b} \tag{72.7}$$

Granulated Samples

1 Calculate the mass of water in the soil, M_w [M], at each matric head, ψ_m [L], using

$$M_w(\psi_m) = M_s(\psi_m) - M_d \tag{72.8}$$

2 Calculate the mass of oven-dry soil, M_{ods} [M], using

$$M_{ods} = M_d - M_{rfe} \tag{72.9}$$

where M_{rfe} [M] is the weight of the ring plus filter paper or cloth plus elastic band, after all adhering soil has been removed.

3 Calculate gravimetric soil water content, $\theta_g(\psi_m)$ [L^3L^{-3}], using Equation 72.6.

4 Calculate the volumetric soil water content, θ_v [L^3L^{-3}], using

$$\theta_v(\psi_m) = \frac{\theta_g(\psi_m) \times \rho_b}{\rho_w} \tag{72.10}$$

where ρ_b [ML^{-3}] is the soil dry bulk density (Equation 72.7) and ρ_w [ML^{-3}] is the soil water density (e.g., $\rho_w = 0.9982$ g cm^{-3} at 20°C). Note that when granulated soil samples are used, V_b is best obtained as the average value from several replicate intact soil cores collected close to where the granulated samples were obtained.

5 Calculate degree of saturation, $S(\psi_m)$, using Equation 72.4.

Soil water desorption and imbibition curves are often presented as graphical relationships, where the matric head is plotted on a logarithmic x-axis (Figure 72.4). Example calculations for a desorption curve are given in Table 72.2.

72.4 COMMENTS

1 The choice of matric head (ψ_m) settings is best made in relation to the intended use of the data. For example, agronomic surveys may require only the three heads needed to determine soil air capacity and plant-available water capacity (i.e., $\psi_m = 0$, -1, -150 m, see Chapter 69 for details), while highly detailed characterization of management and texture effects on pore size distribution or water relations may require many heads (e.g., $\psi_m = 0$, -0.05, -0.1, -0.3, -0.5, -0.75, -1, -2, -3.3, -15, -50, -150 m). A common selection of heads for characterizing soil structure effects on water transmission and storage is $\psi_m = 0$, -0.05, -0.1, -0.3, -0.5, -1, -3.3 m.

2 The pressure extractor method was originally designed and used for determining the water desorption characteristics of small granulated soil samples (McKeague

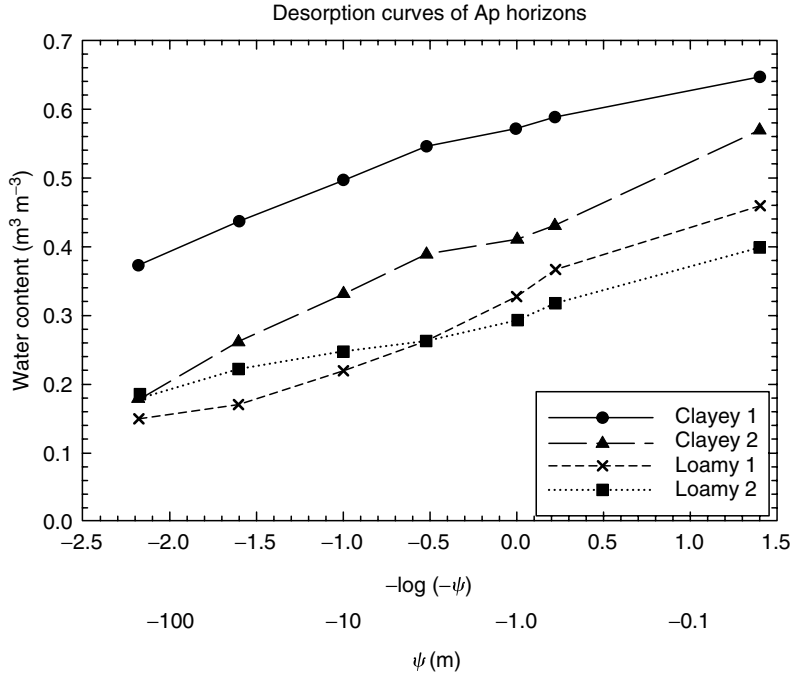

FIGURE 72.4. Example soil water desorption curves for clayey and loamy soils. Note in this example that the first matric head was set at $\psi_m = -0.04$ m, rather than at $\psi_m = 0$.

1978; Sheldrick 1984; Klute 1986). It is being increasingly used, however, for desorption of intact soil cores to matric heads below the limit of tension tables and tension plates (Section 72.2), thereby providing more complete descriptions of undisturbed pore-size distributions and soil structure, soil water-strength relationships, and water content relations for use in water–solute transport models.

3 Sample equilibration time depends primarily on the unsaturated hydraulic conductivity relationship of the sample, the length of the sample, the set matric head, the hydraulic conductivity of the tension medium or ceramic plate, and the quality of the hydraulic connection between the sample and the tension medium or ceramic plate. Generally speaking, equilibration time increases as the hydraulic conductivity of the sample, tension medium or ceramic plate decreases; as matric head decreases; as the quality of the hydraulic connection between sample and tension medium or ceramic plate decreases; and as sample length increases (equilibration time often increases as the square of the sample length). As a result, fine-textured soils and long samples tend to equilibrate much more slowly than coarse-textured soils and short samples; samples at low (more negative) matric heads equilibrate more slowly than samples at high-matric heads; samples on low-permeability tension media or ceramic plates equilibrate more slowly than those on high-permeability media or plates; and samples with poor hydraulic connection to the tension medium or ceramic plate equilibrate more slowly than samples with good connection. A discussion of the

TABLE 72.2 Example Calculation of Desorption Curve Water Contents and Degree of Saturation Using the Tension Table/Plate Method and the Pressure Extractor Method

Core or sample number	Matric head, ψ_m (m)	M_c[a] (g)	M_w[b] (g)	θ_v[c] (cm^3 cm^{-3})	θ_g[d] (g g^{-1})	S[e] (%)
280[f]	0	2925.7	460.7	0.520	0.393	100.0
280	−0.05	2869.7	404.7	0.457	0.345	87.8
280	−0.1	2859.6	394.6	0.445	0.336	85.7
280	−0.3	2846.5	381.5	0.431	0.325	82.8
280	−0.5	2841.2	376.2	0.425	0.321	81.7
280	−1	2827.0	362.0	0.409	0.309	78.6
280	−2.25	2805.2	340.2	0.384	0.290	73.8
280	−3.5	2790.5	325.5	0.367	0.277	70.7
25[g]	−150	55.32	2.88	0.220	0.166	42.3

Intact soil core cylinders: 11.0 cm long × 10.4 cm inside diameter.
Granulated sample rings: 4.0 cm long × 4.7 cm inside diameter.
Oven-dry mass of intact soil plus cylinder plus cloth plus elastic band, $M_d = 2465.0$ g.
Oven-dry mass of granulated sample plus ring plus filter paper plus elastic band, $M_d = 52.44$ g.
Mass of oven-dry soil, intact core, $M_{ods} = 1173.4$ g (Equation 72.5).
Mass of oven-dry soil, granulated sample, $M_{ods} = 17.35$ g (Equation 72.9).
Soil water density, $\rho_w = 0.9982$ g cm^{-3} (20°C).
Soil core bulk volume, $V_b = 887.71$ cm^3 (Equation 72.3); soil dry bulk density, $\rho_b = 1.32$ g cm^{-3} (Equation 72.7).

Note: The θ_v value at $\psi_m = 0$ gives the saturated volumetric water content, θ_s. For highly accurate work, the amount of water retained in the cloth or filter paper should be measured and subtracted from the M_w determination. This is usually important only for small granulated samples where the mass of water retained by the filter paper or cloth can be large enough to affect the calculated soil water contents.

[a] M_c = Mass of soil plus water plus cylinder/ring plus cloth/filter paper plus elastic band.
[b] M_w = Mass of water in soil (Equation 72.1 or Equation 72.8).
[c] θ_v = Volumetric soil water content (Equation 72.2).
[d] θ_g = Gravimetric soil water content (Equation 72.6).
[e] S = Percent water saturation (Equation 72.4).
[f] 280 = Intact core i.d. number.
[g] 25 = Granulated sample i.d. number.

effects of ceramic plate permeability on equilibration time can be found in Gee et al. (2002).

4 The approximate equilibration times given in Table 72.1 for intact soil cores were estimated by extrapolating core drainage rates during the 48–200 h period to the time where drainage was deemed negligible (Topp et al. 1993). This approach was taken because drainage from saturated intact soil cores is usually rapid during the first 24–48 h, and then becomes much slower.

5 Some practitioners (e.g., Klute 1986) recommend ''loading'' the soil samples with lead weights (≈700 g for a 5 cm diameter core sample) to maintain consistent hydraulic connection between the sample and the tension medium and/or porous

plate as the sample desorbs or imbibes water. Breakdown or degradation of the hydraulic connection between the sample and the tension medium or porous plate can greatly increase sample equilibration time, or even entirely prevent equilibration. Topp and Zebchuk (1979) found, however, that the desorption–imbibition curve procedures listed above (i.e., use of appropriate contact media, rewetting base of sample before replacement on contact medium) provided adequate hydraulic connection (and reconnection) without sample loading. On the other hand, loading appears to be necessary for samples of swelling soil collected from the subsurface (as these materials can give unrepresentative desorption and imbibition curves if they are not confined and loaded in a way that mimics their original overburden pressure Collis-George and Bridge 1973).

6 Figure 69.4 (Chapter 69) gives the approximate matric head ranges of the tension table, tension plate, and pressure extractor methods.

REFERENCES

Ball, B.C. and Hunter, R. 1988. The determination of water release characteristics of soil cores at low suction. *Geoderma* 43: 195–212.

Collis-George, N. and Bridge, B.J. 1973. The effect of height of sample and confinement on the moisture characteristic of an aggregated swelling clay soil. *Aust. J. Soil Res*. 11: 107–120.

Gee, G.W., Ward, A.L., Zhang, Z.F., Campbell, G.S., and Mathison, J. 2002. The influence of hydraulic nonequilibrium on pressure plate data. *Vadose Zone J*. 1: 172–178.

Klute, A. 1986. Water retention: laboratory methods. In A. Klute, Ed. *Methods of Soil Analysis, Part I—Physical and Mineralogical Methods*. Agronomy Monograph No. 9, 2nd ed. American Society of Agronomy, Madison, WI, pp. 635–662.

McKeague, J.A., Ed. 1978. *Manual on Soil Sampling and Methods of Analysis*, 2nd ed. Canadian Society of Soil Science, Ottawa, ON, Canada, 212 pp.

Sheldrick, B.S., Ed. 1984. *Analytical Methods Manual 1984*. Land Resource Research Institute, LRRI Report No. 84-30. Agriculture Canada, Ottawa, ON, Canada. pp. 35/1–36/2.

Stakman, W.P., Valk, G.A., and van der Harst, G.G. 1969. Determination of soil moisture retention curves: I. Sand-box apparatus—range pF 0 to 2.7. Institute for Land and Water Management Research. Wageningen, The Netherlands.

Topp, G.C., Galganov, Y.T., Ball, B.C., and Carter, M.R. 1993. Soil water desorption curves. In M.R. Carter, Ed. *Soil Sampling and Methods of Analysis*. Lewis Publishers, CRC Press, Boca Raton, FL, pp. 569–579.

Topp, G.C. and Zebchuk, W.D. 1979. The determination of soil-water desorption curves for soil cores. *Can. J. Soil Sci*. 59: 19–26.

Townend, J., Reeve, M.J., and Carter, A. 2001. Water release characteristic. In K.A. Smith and C.E. Mullins, Eds. *Soil and Environmental Analysis: Physical Methods*, 2nd ed. Marcel Dekker, New York, NY, pp. 95–140.

Chapter 73
Soil Water Desorption and Imbibition: Long Column

W.D. Reynolds
Agriculture and Agri-Food Canada
Harrow, Ontario, Canada

G. Clarke Topp
Agriculture and Agri-Food Canada
Ottawa, Ontario, Canada

73.1 INTRODUCTION

Soil water desorption refers to the decrease in soil volumetric water content with decreasing pore water matric head (drainage), while imbibition refers to the increase in volumetric water content with increasing matric head (wetting). A discussion of the principles and parameters associated with the determination of desorption and imbibition curves is given in Chapter 69. This chapter describes the long column method for measuring soil water desorption and imbibition curves. Alternative methods include the tension table, tension plate and pressure extracter (Chapter 72), the dewpoint psychrometer (Chapter 74), soil core evaporation (Chapter 81), instantaneous profile (Chapter 83), and estimation techniques (Chapter 84).

The long column method provides static equilibrium volumetric water content values (θ_v) at selected elevations along an upright column of soil, following either drainage from saturation (desorption curve) or wetting from dryness (imbibition curve) (Figure 73.1). The water contents are most conveniently measured using time-domain reflectrometry (TDR), capacitance, and impedance probes (see Chapter 69 and Chapter 70 for details) installed through the wall of the column at the selected elevations. Matric head (ψ_m) at the selected elevations is equivalent to the elevation head above a constant head device (e.g., constant head burette, controlled vacuum). The constant head device is usually set to yield $\psi_m = 0$ at or near the column base, although negative heads can also be set if the column base is fitted with tension medium or a porous plate or membrane to prevent air entry (Chapter 72). In essence, the method involves setting a constant matric head at some position along the column (usually near the column base), allowing the column to drain or wet under the imposed hydraulic head gradient until static equilibrium (no flow) is achieved and then measuring the water content and corresponding matric head at chosen elevations. The soil column can be uniform,

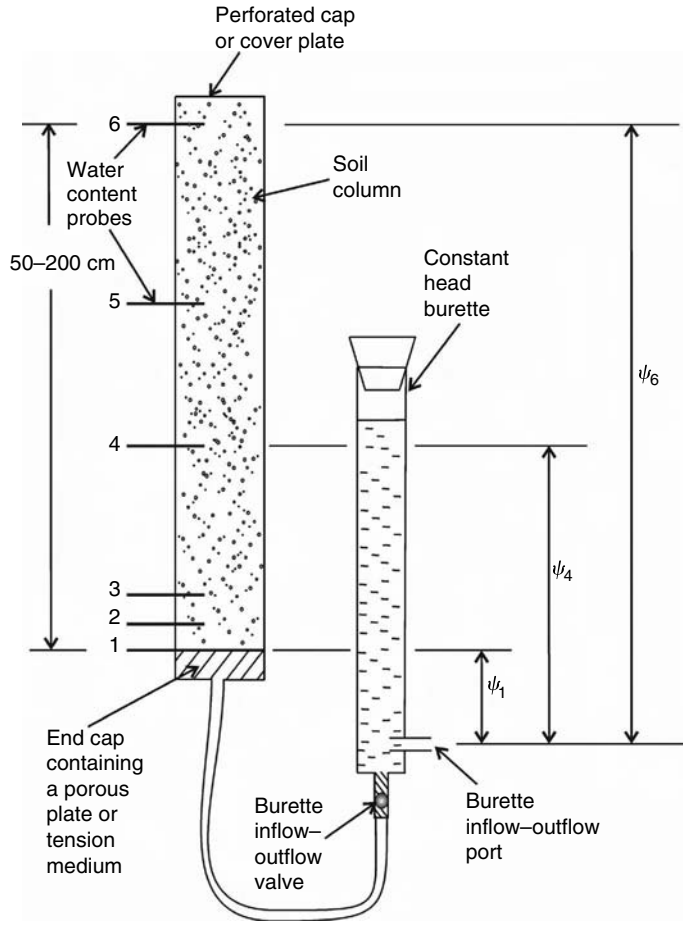

FIGURE 73.1. The long column method for measuring desorption and imbibition curves. The water content probes (labelled 1,2,3,4,5,6) are most conveniently based on TDR, capacitance, or impedance technologies, although gamma ray attenuation can also be used. After equilibration (i.e., no flow into or out of column and constant water content at all probe locations), matric head, ψ_i, applies to the water content (θ_v) measured at probe i, where $i = 1,2,3,4,5,6$.

layered, intact, or repacked. The column method is most commonly used for detailed characterization of near-saturated desorption and imbibtion curves (i.e., $\psi_m \geq -1$ m) in quasiundisturbed soil columns that are ≤ 2 m long.

73.2 MATERIALS AND SUPPLIES

1 *Column*: Column of cylindrical, square, or rectangular cross-section suitable for collecting soil cores or monoliths, usually 0.5–2.0 m long. If soil water content will be measured using TDR, capacitance, or impedance probes, the column should be nonconductive (e.g., ABS or PVC plastic, plaster of Paris) and the internal width or diameter should be ≥ 8 cm. Water content can also be measured using gamma ray attenuation (Topp 1969; Dane and Hopmans 2002).

2 *End cap*: Column end cap with an inflow–outflow connection to a constant head device and provision for tension medium or a porous plate with an air-entry value sufficient to allow application of the minimum (most negative) desired matric head to the base of the soil core or monolith (Figure 73.1). The end cap must make a water-tight seal with the column, as it serves to both add and remove water and to apply tension to the base of the soil core or monolith.

3 *Constant head device*: A constant head device capable of adding or removing water from the soil core or monolith under constant matric head (e.g., constant head burette). If a constant head burette is used, the flexible tube connecting the end cap to the burette should be long enough to allow the burette inflow–outflow port (Figure 73.1) to be level with the top of the column so that saturation of the soil core or monolith can be achieved by upward wetting. The burette should be large enough to allow column saturation without having to interrupt wetting to refill the burette reservoir.

4 *Column cap*: A loose-fitting or perforated cap for the top of the column to minimize evaporative water loss from the soil surface while still allowing easy air exchange.

5 *Water content probes*: Water content probes for measuring volumetric soil water content at preselected positions along the column (Figure 73.1). The selection of positions and the spacing between probes will depend on soil profile characteristics (e.g., presence of layers), the zone of influence of the probes, the desired matric heads, and the number of probes that can be monitored with the available instrumentation. Two-wire TDR probes (Chapter 70) are well-suited for this application, as they are easily installed via access holes drilled through the column wall; they can have a small zone of influence (≈twice the between-wire spacing) to allow short between-probe distances, and multiple probes are easily monitored either manually or electronically. Cores or monoliths of uniform soil might have a uniform probe spacing, while layered cores or monoliths might have at least one probe per layer and variable probe spacing.

6 *Controlled temperature room*: As soil desorption and imbibition curves are temperature-sensitive, the measurements should be conducted at constant temperature, usually 20°C ± 1°C. See Chapter 69 and Chapter 72 for further details.

73.3 PROCEDURE

1 Collect the soil core or monolith. Procedures for collecting relatively undisturbed cores or monoliths from the field are discussed in Chapter 72 and Chapter 75. For relatively short soil cores (e.g., ≤1 m), the sampling column can sometimes be fitted with a cutting edge and hydraulically jacked or driven into the soil, although this can cause soil compaction or shattering. Repacked columns of sieved soil are adequate for some applications or highly uniform soils. For uniform soil columns, install the same number of water content probes as the desired number of matric heads, locating the first probe (probe 1) near the column base, and spacing the remaining probes at distances numerically equivalent to the desired matric head values; e.g., if the desired matric heads are $\psi_m = 0, -0.05, -0.1, -0.3, -0.5,$

TABLE 73.1 Example Calculation of Near-Saturated Desorption and Imbibition Curves for a Uniform Soil Using the Long Column Method (See Figure 73.1)

			Desorption curve	Imbibition curve
Water content probe number (lowest probe = number 1)	**Probe elevation relative to lowest probe (cm)**	**Equivalent equilibrium matric head, ψ_m (m)**	**Equilibrium soil water content, θ_v (m^3 m^{-3})**	**Equilibrium soil water content, θ_v (m^3 m^{-3})**
1	0	0	0.488	0.461
2	5	−0.05	0.451	0.388
3	10	−0.1	0.429	0.358
4	30	−0.3	0.387	0.312
5	50	−0.5	0.310	0.241
6	75	−0.75	0.247	0.191
7	100	−1	0.211	0.165

Column length = 1.1 m; Soil type = uniform loam; Number of water content (TDR) probes = 7. Equilibration achieved with inflow–outflow port of burette level with the lowest water content probe.

Initial soil water content at lowest water content probe, desorption curve = 0.488 m^3 m^{-3} (saturation). Initial condition obtained by raising burette inflow–outflow port to top of column to saturate entire soil core; equilibrium condition produced by lowering burette inflow–outflow port to the lowest water content probe position (probe 1 in Figure 73.1).

Initial soil water content at lowest water content probe, imbibition curve = 0.211 m^3 m^{-3} ($\psi_m = -1$ m). Initial condition obtained by lowering burette inflow–outflow port to 1 m below lowest water content probe position (probe 1 in Figure 73.1); equilibrium condition produced by raising burette inflow–outflow port to the lowest water content probe position (probe 1 in Figure 73.1).

and −1 m, then install probes 2–6 at 0.05, 0.1, 0.3, 0.5, and 1 m, respectively, above probe 1 (Table 73.1, Figure 73.1). For layered soil columns, install at least one water content probe per major layer if it is desired to take layer effects into account.

2 Saturate the tension medium or porous plate in the end cap by connecting it to the constant head device, and then install the end cap on the bottom end of the column, ensuring good hydraulic connection between soil and end cap. The inflow–outflow valve of the constant head device should be open so that water can either enter or exit the soil core or monolith, depending on the soil's initial water content and the matric head set on the constant head device. Stand the column upright.

3 Slowly wet the soil core or monolith to saturation or field-saturation. If complete soil saturation is desired (i.e., no entrapped air), replace the air in the core or monolith with water-soluble carbon dioxide (by slow injection of carbon dioxide from a compressed gas cylinder), then saturate the core or monolith with de-aired, temperature-equilibrated water that is either native soil water or water that has about the same major ion speciation and concentrations as the native water. If field-saturation is desired (i.e., entrapped air present, which may be more representative of actual field conditions), saturate the column with aerated, temperature-equilibrated water. Saturation or field-saturation is most easily achieved by initially setting the water inflow–outflow port of a constant head burette at the column base,

and then slowly raising the burette in stages (e.g., 10 cm h^{-1}) until the burette's inflow–outflow port is level with the soil surface at the top of the column. The soil is saturated or field-saturated when free water appears on the soil surface.

4 For a uniform soil core or monolith, the desorption curve is obtained by: (i) lowering the constant head burette in one step to produce zero matric head at the lowest water content probe (e.g., the burette inflow–outflow port is lowered in one step from the top of the column to the probe nearest the column base); (ii) waiting until outflow stops, which signals equilibration—this may require hours to weeks (equilibration is also signified by constant water content at all probe locations); (iii) recording the soil water content at each probe position; and (iv) obtaining the matric head at each probe position by measuring the vertical distance between the probes and the inflow–outflow port of the constant head burette. For water content probes distributed over a 1 m length of soil column, this approach produces a maximum matric head of $\psi_m = 0$ at the lowest probe, and a minimum matric head of $\psi_m = -1$ m at the highest probe (see Section 73.4).

For a layered soil core or monolith, the desorption curve is obtained by lowering the constant head burette in a succession of steps, waiting until equilibration is achieved at each step, then measuring water content and matric head at each probe position using the same procedure as for the uniform soil case. The sequence of distances that the burette is lowered should match the intended matric heads; e.g., if the matric heads, $\psi_m = 0, -0.05, -0.1, -0.3, -0.5, -0.75, -1$ m are desired at a particular water content probe position, then the burette inflow–outflow port should be set successively at 0, 0.05, 0.1, 0.3, 0.5, 0.75, and 1 m below that probe position.

5 To obtain an imbibition curve, the soil core or monolith is initially equilibrated with the inflow–outflow port of the constant head burette lowered to some distance below the lowest water content probe (e.g., 1 m below the lowest probe). If the core or monolith is uniform, the burette inflow–outflow port is then raised in one step to the same level as the lowest probe, and the rewet water content and matric head determined as in Step 4 for uniform soil. If the core or monolith is layered, the burette inflow–outflow port is raised from its initial position (e.g., 1 m below the lowest probe) in a succession of equilibrating steps, and the water content and matric head determined as in Step 4.

73.4 ANALYSIS AND EXAMPLE CALCULATIONS

For each probe position, record the equilibrium soil water content (θ_v) and the corresponding elevation of the probe above the inflow–outflow port of the constant head burette (or equivalent constant head device). Convert the elevations to matric head (e.g., an elevation of $+0.5$ m at a particular probe converts to the matric head, $\psi_m = -0.5$ m, at the probe). For a uniform soil core or monolith where a single change in burette height is made, each water content probe position produces a single point (i.e., (θ_v, ψ) data pair) along the soil's desorption curve or imbibition curve. For a layered soil core or monolith where multiple changes in burette height are made, each probe position produces data points along desorption or imbibition curves that are specific to that position in the core or monolith (i.e., several position-specific desorption and imbibition curves are produced). Example calculations for a desorption curve and an imbibition curve are given in Table 73.1.

73.5 COMMENTS

1 Installing tension medium or a tension plate in the column end cap effectively amalgamates the tension table or plate method and the long column method, in that matric heads much lower (more negative) than the column length can be applied, thus allowing a more complete description of desorption and imbibition curves.

2 Due to the near-asymptotic equilibration of soil wetting and drainage, the long column method is most practicable for high permeability materials and column lengths of $\leq$1 m. Note also that upward wetting of soil tends to be a much slower process than drainage (due to gravity, hysteresis, and air entrapment effects), and as a consequence, equilibration times for imbibition curves can be impractically long, especially for columns approaching 1 m in length.

3 An important advantage of the long column method is that it provides measures of θ_v and ψ_m that apply to the same location (or nearly the same location) in the soil sample. Most other methods, on the other hand, yield ''average'' θ_v values that apply to the whole sample, but ψ_m values that apply to a specific location in the sample (e.g., tension table, tension plate, pressure extractor—Chapter 72). Coupling ''sample-average'' θ_v with ''position-specific'' ψ_m can introduce appreciable error in desorption and imbibition curves when θ_v changes very rapidly with ψ_m, such as might occur in very coarse or highly structured porous media, or when solutes or immiscible fluids change the effective air–pore fluid interfacial tension. For example, when Dane et al. (1992) used the long column method to determine desorption and imbibition of trichloroethylene in a sandy soil, they found that trichloroethylene content changed from its saturation level to its residual level and vice versa after only 2.5–10 cm change in equivalent pore water matric head, ψ_m. Hence, use of the usual core sample length of 5–10 cm and a method that gives sample-average θ_v and position-specific ψ_m would likely yield misleading results in this case, as sample-average trichloroethylene content would be obtained while the top section of the core may actually be at the residual level and the bottom section at the saturation level.

4 A useful variation on the long column method, described in Topp (1969) and elsewhere, uses transient water flow and regulated air pressure. The main advantages of this approach are that it allows detailed and highly accurate characterization of desorption, imbibition, and scanning curves, as well as determination of the unsaturated soil hydraulic conductivity relationship (see Chapter 69). An important disadvantage, on the other hand, is the need for much more complicated equipment, and highly controlled experimental conditions.

5 Figure 69.4 (Chapter 69) gives the practicable matric head range of the long column method.

REFERENCES

Dane, J.H. and Hopmans, J.W. 2002. Water retention and storage, long column. In J.H. Dane and G.C. Topp, Eds. *Methods of Soil Analysis, Part 4—Physical Methods*. Soil Science Society of America, Madison, WI, pp. 690–692.

Dane, J.H., Oostrom, M., and Missildine, B.C. 1992. An improved method for the determination of capillary pressure–saturation curves involving TCE, water, and air. *J. Contam. Hydrol.* 11: 69–81.

Topp, G.C. 1969. Soil–water hysteresis measured in a sandy loam and compared with the hysteretic domain model. *Proc. Soil Sci. Soc. Am.* 33: 645–651.

Chapter 74
Soil Water Desorption and Imbibition: Psychrometry

W.D. Reynolds
Agriculture and Agri-Food Canada
Harrow, Ontario, Canada

G. Clarke Topp
Agriculture and Agri-Food Canada
Ottawa, Ontario, Canada

74.1 INTRODUCTION

Soil water desorption refers to the decrease in soil volumetric water content with decreasing pore water matric head (drainage), while imbibition refers to the increase in volumetric water content with increasing matric head (wetting). A discussion of the principles and parameters associated with the determination of desorption and imbibition curves is given in Chapter 69. This chapter briefly describes the psychrometer method (specifically the laboratory-based dewpoint psychrometer) for measuring soil water desorption and imbibition curves. Alternative methods include the tension table, tension plate and pressure plate extractor (Chapter 72), long column (Chapter 73), soil core evaporation (Chapter 81), instantaneous profile (Chapter 83), and estimation techniques (Chapter 84).

Psychrometric methods for measuring soil water desorption and imbibition curves use a psychrometer to measure soil water matric head, ψ_m [L], and weight change upon oven-drying to measure gravimetric water content, θ_g [MM^{-1}]. Determination of volumetric water content, θ_v [L^3L^{-3}] requires independent measurement of soil dry bulk density, ρ_b [ML^{-3}], and water density, ρ_w [ML^{-3}], i.e., $\theta_v = \theta_g\rho_b/\rho_w$. The psychrometer method uses small disturbed samples ($\approx$7–15 mL, $\approx$10–20 g), and applies primarily at the ''dry ends'' of the water desorption and imbibition curves (i.e., $\psi_m \leq -20$ to -40 m). One psychrometer measurement of equilibrated soil produces one point on the desorption or imbibition curve.

74.2 THEORY AND PRINCIPLES

Psychrometry determines pore water matric head, ψ_m, by measuring the equilibrium relative water vapor pressure, or relative humidity, of the soil air (Andraski and Scanlon 2002; Scanlon et al. 2002). The equilibrium relationship between ψ_m and relative water vapor pressure (e/e_s) is described by the Kelvin equation,

$$\psi_m = \frac{RT}{V_w} \ln\left(\frac{e}{e_s}\right) \tag{74.1}$$

where R is the ideal gas constant (8.314 J mol^{-1} K^{-1}), T is the Kelvin temperature (°K), V_w is the molecular volume of water (1.8×10^{-5} m^3 mol^{-1}), e is the water vapor pressure of the soil air (Pa) at temperature, T, and e_s is the saturation water vapor pressure of the soil air (Pa) at temperature, T.

Psychrometer measurements of relative water vapor pressure (i.e., relative humidity) in soil are accomplished using two main techniques, namely thermocouple psychrometry (Chapter 71) and dewpoint psychrometry. Thermocouple psychrometers operate by measuring the temperature depression of a ''wet bulb'' thermocouple as soil water condensed on the thermocouple (via Peltier cooling) re-evaporates into the soil air. Dewpoint psychrometers, on the other hand, operate by measuring the temperature depression required to condense soil water vapor onto a Peltier-cooled mirror, which was previously temperature-equilibrated with the soil air. Although both methods are frequently used to measure ψ_m, we will focus here on the dewpoint technique, as it measures a wider range of ψ_m, it is slightly less sensitive to temperature gradients, and it provides a much faster measurement than the thermocouple system.

In the dewpoint psychrometer technique, a soil sample is placed in a small, sealed chamber, and the headspace air above the sample is allowed to equilibrate with the vapor pressure and temperature of the soil water (Figure 74.1). The chamber contains a mirror with attached thermocouple, a light beam, a photodetector cell, an infrared thermometer, and a small fan to speed equilibration of the mirror to the temperature and water vapor pressure of the sample (Figure 74.1). The light beam is directed onto the mirror and reflected back into the photodetector cell. A measurement is made by first recording the equilibrated temperature of the sample and chamber via the infrared thermometer. The mirror is then Peltier-cooled until

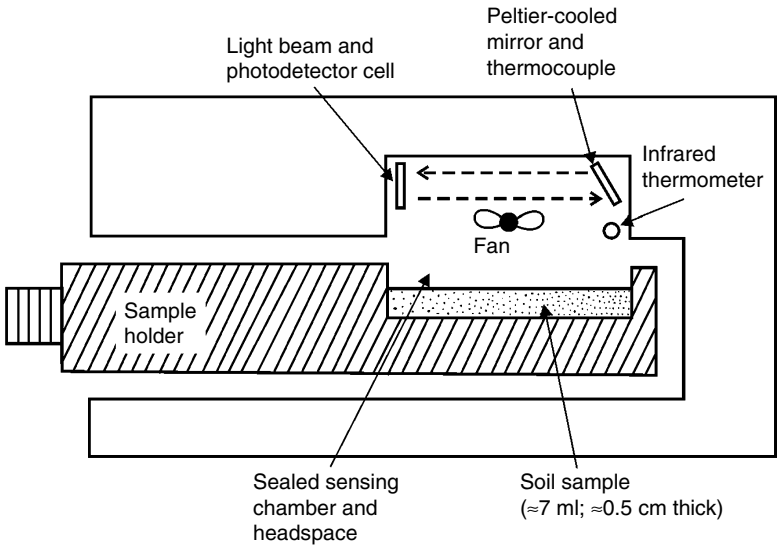

FIGURE 74.1. A dewpoint psychrometer for measuring the dry end of desorption and imbibition curves (Decagon Devices, Inc. ''WP4''). (From Gee, G.W., Campbell, M.D., Campbell, G.S., and Campbell, J.H., *Soil Sci. Soc. Am. J.*, 56, 1068, 1992. With permission.)

water vapor condenses onto the mirror's reflective surface. The photodetector senses the change in mirror reflectance when condensation first occurs, which then signals the thermocouple to record the mirror temperature, which is equivalent to the ''dewpoint'' temperature of the soil air. The dewpoint and sample temperatures are then used to determine (e/e_s) via

$$\left(\frac{e}{e_s}\right) = \exp\left[\frac{bc(T_d - T_s)}{(T_d + c)(T_s + c)}\right] \tag{74.2}$$

where T_d is the dewpoint temperature, T_s is the sample and headspace temperature, and b and c are constants (Buck 1981). The soil water matric head, ψ_m, is then readily calculated via Equation 74.1.

74.3 APPARATUS AND PROCEDURES

1 Laboratory dewpoint psychrometers are commercially available, such as the ''WP4 Dewpoint PotentiaMeter'' marketed by Decagon Devices, Inc., Pullman, Washington, and comparable instruments marketed by Wescor, Inc., Logan, Utah. We will focus here on the Decagon WP4 unit.

2 To obtain points in the dry end of a desorption or imbibition curve, soil samples must be prepared at a range of water contents. Imbibition curves are most often determined in the laboratory by starting with air-dry or oven-dry soil, thoroughly mixing in progressive amounts of water, and then equilibrating the soil–water mixture in vapor-tight containers held at constant temperature (usually 20°C). Recommended minimum equilibration times range from as little as 16 h for coarse-textured soils to as much as 1 week for fine-textured soils (Andraski and Scanlon 2002; Decagon Devices, Inc. 2005). As might be expected, desorption curves are determined by reversing the imbibition procedure, i.e., by progressively drying initially moist soil. The amount of water added to (or removed from) each sample will depend on soil texture and the desired range of soil water contents and matric heads; and this usually requires some preliminary trial-and-error testing. Samples might also be collected directly from the field as the soil either dries under evapotranspiration or wets under mild rainfall or irrigation. Field samples must be sealed in vapor-tight containers immediately after collection to prevent water loss or gain before analysis in the laboratory.

3 Load each soil sample (≈7 mL volume or ≈10 g mass for the Decagon WP4 unit) into a separate, preweighed psychrometer sample holder or cup (M_c), and slightly compress using a rubber stopper or square-ended metal rod to produce a flat surface and a uniform thickness of ≈0.5 cm (surface leveling and slight compression tend to produce more reliable and repeatable results—Gee et al. 1992). Immediately seal each loaded sample holder in a separate vapor-tight container to prevent water loss or gain before analysis.

4 Remove the first loaded sample holder from its vapor-tight container and immediately insert into the psychrometer (to minimize water loss or gain) and start the measuring process (samples are inserted and measured one at a time). The WP4 Dewpoint PotentiaMeter requires ≈0.5 min per measurement and displays both soil water matric head (ψ_m) and sample temperature. Matric head is calculated internally using Equation 74.1 and Equation 74.2.

5 After ψ_m is obtained, remove the sample from the meter, and weigh immediately (to minimize water loss or gain) to obtain the weight of the sample holder plus soil plus soil water (M_{c+s+w}). Oven-dry the sample for 24–48 h at 105°C ± 5°C, cool in a cooling box (Chapter 72) until the ambient temperature is attained, and then reweigh to obtain the weight of the sample holder plus oven-dry soil (W_{c+s}). Calculate gravimetric water content, θ_g, using

$$\theta_g = \frac{(W_{c+s+w} - W_{c+s})}{(W_{c+s} - W_c)} \tag{74.3}$$

Note that $(W_{c+s+w} - W_{c+s})$ is the weight of water in the soil sample, and $(W_{c+s} - W_c)$ is the weight of dry soil (see Chapter 69 for definition of gravimetric soil water content).

6 Calculate volumetric water content, θ_v, using

$$\theta_v = \theta_g \rho_b / \rho_w \tag{74.4}$$

where ρ_b [ML^{-3}] and ρ_w [ML^{-3}] are independently measured soil dry bulk density and water density, respectively. The calculated θ_v (or θ_g) versus ψ_m data pair provides one point on the desorption or imbibition curve; an example determination of an imbibition curve appears in Decagon Devices, Inc. (2005).

74.4 COMMENTS

1 The range of dewpoint psychrometers is approximately $-6000 \text{ m} \leq \psi_m \leq -40$ m, with an uncertainty of about ±10 m from $-1000 \text{ m} \leq \psi_m \leq -40$ m, and an uncertainty of about ±1% from $-6000 \text{ m} \leq \psi_m \leq -1000$ m (Gee et al. 1992; Decagon Devices, Inc. 2005). Although these uncertainty values may seem alarmingly large, they have little effect on predicted soil water contents due to the extreme ''flatness'' of desorption and imbibition curves within the ψ_m range of psychrometers (Figure 69.4, Chapter 69).

2 Psychrometric measurements are extremely sensitive to the difference between the sample temperature and the dewpoint temperature, i.e., $\Delta T = (T_d - T_s)$ (Equation 74.2); and an accuracy of ±0.005°C in ΔT is required to obtain an accuracy of ±10 m in ψ_m. Hence, the psychrometer temperature sensors must be extremely accurate, and the sample and chamber temperatures should be within ±0.5°C of each other at the time of the measurement. It is consequently advisable to house the prepared samples and psychrometer instrument together in a constant temperature room (e.g., 20°C ± 1°C).

3 Prior to sample analysis, instrument accuracy and calibration should be checked (and corrected if necessary) by measuring the water matric head of standard salt solutions of known osmotic potential. Salt solution standards can be prepared (e.g., Table 3.2.3–1, Andraski and Scanlon 2002) or obtained commercially (e.g., Decagon Devices, Inc.).

4 The necessity for temperature and vapor pressure equilibrium throughout the sample chamber usually requires that the soil samples be disturbed and small

(e.g., ≈7–15 mL). Sample disturbance disqualifies the method for characterizing soil structure, bulk density, and hysteresis effects on desorption and imbibition curves, although these effects are often negligibly small in the ''dry end'' ψ_m range measured by psychrometers. The small sample size may greatly increase the replication required to adequately characterize the extensive spatial–temporal variability of natural field soils. Notwithstanding the usual need for disturbed samples, dewpoint psychrometry has successfully estimated the desorption curve of small intact rock samples (Flint et al. 1999).

5 The single greatest source of error with laboratory psychrometer techniques appears to be water loss (by evaporation) or gain (by absorption or condensation) during sample collection, preparation, and measurement; and this is especially critical when working with coarse-textured soils or dry soils. Hence, steps must be taken to prevent or minimize water loss or gain—which generally involves diligent use of water vapor-tight sample storage containers, plus temperature equilibration between the samples and the dewpoint psychrometer instrument at the time of measurement.

6 Figure 69.4 compares the matric head range of the dewpoint psychrometer to other methods for measuring desorption and imbibition curves.

REFERENCES

Andraski, B.J. and Scanlon, B.R. 2002. Thermocouple psychrometry. In J.H. Dane and G.C. Topp, Eds. *Methods of Soil Analysis, Part 4—Physical Methods*. Soil Science Society of America, Inc., Madison, WI, pp. 609–642.

Buck, A.L. 1981. New equations for computing vapor pressure and enhancement factor. *J. Appl. Meteorology* 20: 1527–1532.

Decagon Devices, Inc. 2005. www.decagon.com/wp4/wptheory.html. Last verified July 2006.

Flint, L.E., Hudson, D.B., and Flint, A.L. 1999. Unsaturated hydraulic parameters determined from direct and indirect methods. In M.Th. van Genuchten et al., Eds. *Characterization and Measurement of the Hydraulic Properties of Unsaturated Porous Media: Part 1*. University of California, Riverside, CA.

Gee, G.W., Campbell, M.D., Campbell, G.S., and Campbell, J.H. 1992. Rapid measurement of low soil water potentials using a water activity meter. *Soil Sci. Soc. Am. J.* 56: 1068–1070.

Scanlon, B.R., Andraski, B.J., and Bilskie, J. 2002. Miscellaneous methods for measuring matric or water potential. In J.H. Dane and G.C. Topp, Eds. *Methods of Soil Analysis, Part 4—Physical Methods*. Soil Science Society of America, Inc., Madison, WI, pp. 643–670.

Chapter 75
Saturated Hydraulic Properties: Laboratory Methods

W.D. Reynolds
Agriculture and Agri-Food Canada
Harrow, Ontario, Canada

75.1 INTRODUCTION

The most important saturated hydraulic property measured in the laboratory is the saturated hydraluic conductivity, K_s [LT^{-1}]. Laboratory measurement of K_s uses samples of intact or disturbed porous materials that were removed from the field. Field or *in situ* methods, on the other hand, measure K_s directly in the field.

The primary strengths of laboratory methods (relative to field methods) are that the water flow boundaries and flow field are well defined and controlled (e.g., constant and accurately known hydraulic head, one-dimensional rectilinear flow), the flow environment can be specified and maintained (e.g., constant temperature, pressure, water chemistry), K_s is determined using the equation by which it is defined (i.e., Darcy's law—Equation 75.1), and the work environment is comfortable and convenient (e.g., no need to contend with inclement outside weather, flexible timing of measurements, etc.). Additional advantages specific to the laboratory core methods described here (Section 75.2 and Section 75.3) are that large numbers of K_s determinations can be made rapidly and economically (thus making large-area coverage, high replication and spatial–temporal analyses more meaningful and feasible), and the same samples are readily used for water desorption–imbibition measurements (Chapter 72). On the other hand, important weaknesses of laboratory methods relative to field methods include: (i) generally small sample sizes that may not be representative of the *in situ* porous medium; (ii) loss of hydraulic contact with the porous medium from which the sample was collected; (iii) imposed flow field (e.g., one-dimensional rectilinear flow) that may be unrealistic or inappropriate for the *in situ* condition (e.g., the *in situ* flow field may be anisotropic); and (iv) sample disturbance during the collection process (e.g., vibration-induced shattering of aggregates or collapse of macrostructure, friction-induced compression), which may result in unrepresentative K_s determinations. The decision to use laboratory methods for measuring K_s will consequently be based on the overwhelming need for the methods' ''pros,'' while being able to minimize or live with the ''cons.''

By far the most popular laboratory methods include the ''constant head core'' and ''falling head core'' methods, which are described below in Section 75.2 and Section 75.3, respectively. The core methods are not always feasible, however, and Section 75.4 gives brief descriptions of the alternative laboratory ''ped'' and ''monolith'' methods, which may be preferable under certain conditions. *In situ* or field methods for determining saturated hydraulic conductivity are given in Chapter 76 through Chapter 79. Selected methods for estimating saturated hydraulic conductivity from surrogate porous medium properties are given in Chapter 84. A discussion of the principles and parameters associated with the determination of saturated hydraulic conductivity is given in Chapter 69.

75.2 CONSTANT HEAD CORE

This method determines the saturated hydraulic conductivity, K_s [LT^{-1}], of core samples. The cores may have virtually any cross-sectional shape and a wide range of widths and lengths; however, cylindrical cores that are 4–20 cm in diameter and 4–20 cm long are most practical. The cores are first wetted to saturation, and then water is allowed to flow through the cores at a steady rate under constant hydraulic head gradient. A rectangular ''conductivity'' tank (adapted from Elrick et al. 1981) is recommended to increase the speed and efficiency with which the cores can be processed; however, numerous other arrangements are possible (e.g., Youngs 2001). The method described below is designed to complement the falling head core method described in Section 75.3, and it uses some of the same apparatus and procedures. The range of K_s that can be measured using the constant head method is about 10^0 to 10^{-5} cm s^{-1}. The complementary falling head core method (Section 75.3) can measure a K_s range of about 10^{-4} to 10^{-7} cm s^{-1}.

75.2.1 Apparatus and Procedures (for Cylindrical Cores)

1 Collect the porous medium (e.g., soil) samples in cylinders made of a material that will neither break or deform during the sampling process, nor corrode in water (i.e., use cylinders made of aluminum, brass, stainless steel, high density plastics, etc.). If the K_s measurements are intended to be representative of field conditions, then the sampling cylinders should be large enough to adequately sample the antecedent structure (e.g., peds, aggregates, cracks, biopores, intergranular packing, etc.); and procedures should be used that minimize disruption of the structure during the sampling process. Criteria for selecting an adequate sample (core) size plus procedures for minimizing soil disturbance and preferential (short circuit) flow along the core walls can be found in Chapter 80, and in McIntyre (1974), Bouma (1985), Rogers and Carter (1986), Amoozegar (1988), Lauren et al. (1988), and Cameron et al. (1990). At both ends of the sampling cylinder, trim the porous medium flush with the cylinder and remove any evidence of smearing or compaction (i.e., expose ''undisturbed'' porous medium surfaces). Also, remove any material adhering to the outside of the sampling cylinder. Cover the top end of the cylinder with 270 mesh (53 μm pore size) woven nylon ''bolting'' cloth, held in place with a stout elastic band (Figure 75.1). Attach a transparent (e.g., acrylic) end cap onto the bottom end of the cylinder (see Comment 2) and make a watertight seal. Various end cap designs are possible—the design in Figure 75.1 is easily and quickly sealed to the cylinder using an ''MJ'' cast iron–plastic–plastic pipe coupling with an internal rubber sleeve. It may also be possible to seal the

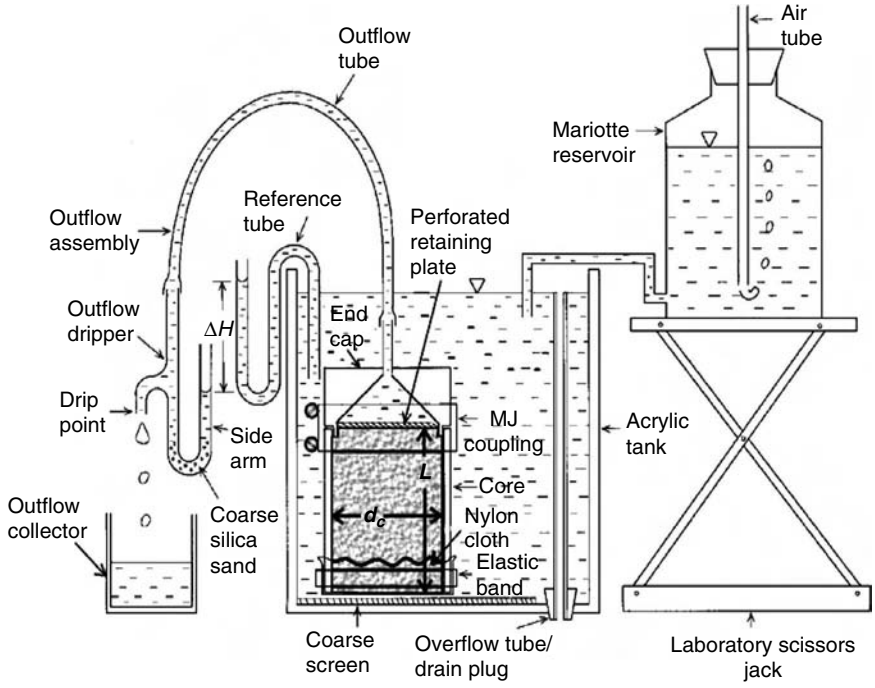

FIGURE 75.1. The constant head core (tank) method. (From Reynolds, W.D. and Elrick, D.E. in J.H. Dane and G.C. Topp (Eds.), *Methods of Soil Analysis, Part 4—Physical Methods*, Soil Science Society of America, Madison, Wisconsin, 2002. With permission.)

end cap to the cylinder by brushing melted (100°C) paraffin wax over the joint, although this approach is slow and not always effective.

2 Place the prepared cores in an empty tank, which has a coarse mesh (≥2 mm openings) woven nylon, brass, or stainless steel screen in the bottom (Figure 75.1) to allow unrestricted wetting of the core through the nylon cloth. The tank walls should be approximately 30 cm high so that a wide range of hydraulic head gradients can be applied to the cores (discussed further below). A combined overflow tube–drain plug prevents overfilling and also facilitates drainage of the tank at the end of the measurements (Figure 75.1).

3 Saturate the cores slowly over a four-day period by adding temperature-equilibrated water (either native water or a laboratory approximation—see Chapter 69). Submerge an additional one-third of the length of the core for each of the first three days, and then add water to the full tank level (top of the overflow tube, Figure 75.1) on the fourth day (alternative saturation procedures can be found in Ball and Hunter 1988 and Townend et al. 2001). It may be advisable for some soils to add algicide or fungicide to the water to prevent excessive growth of microorganisms both within the cores and in the tank. Growth of algae and fungi in the sample or on the nylon cloth can restrict flow and thereby produce an unrepresentative K_s value. During the saturation process, the end cap outflow tubes should be held vertical to prevent their open ends from becoming immersed

in the water, as this may restrict air escape from the core and thereby impede porous medium saturation and the filling of the end cap with water. At the end of the four-day saturating period, the end caps should be filled with water. If the end caps or their outflow tubes are only partially water-filled (which may occur if the porous medium has a low hydraulic conductivity), the filling process is easily completed by using a syringe to inject water directly into the end cap via a small-diameter ''spaghetti'' tube inserted through the outflow tube. Occasionally, the conductivity is so low that no ponded water appears on the porous medium surface at the end of the four-day saturation period. If this occurs, the saturation period should be extended until ponded water appears.

4 Fill a Mariotte reservoir (25 L carboy) with the same type of water that was used to fill the tank, connect its outflow to the tank using large-diameter tubing (about 8 mm internal diameter [I.D.]), and adjust the height of the reservoir or Mariotte air tube so that the equilibrium water level is 1–3 cm below the top of the tank wall and coincident with the top of the overflow tube (Figure 75.1). Placing the reservoir on a laboratory scissors jack allows for convenient height adjustment. The Mariotte reservoir maintains a constant water level in the tank during the measurements (required by the theory) by supplying water to the tank at the same rate at which it is being withdrawn through the outflow drippers. It is not recommended that water collected from the drippers be poured back into the tank, as this may add suspended sediment (e.g., silt and clay) to the tank water, which may subsequently plug the nylon cloth or influent end of the cores.

5 Using a syringe, fill the water outflow assembly with water and then clamp. Fill the end cap outflow tube with water by submerging it in the tank. Connect the outflow assembly and the end cap outflow tube, making sure that there are no air bubbles trapped within the tubing or outflow assembly. Fill the reference tube with water by submerging it in the tank, and set it up as indicated in Figure 75.1.

6 Arrange the water outflow assembly such that the drip point of the outflow dripper is 1–2 cm below the water level in the reference tube. Unclamp the outflow assembly slowly and carefully so that air is not sucked into the dripper. Adjust the elevation of the outflow dripper so that a drop falls no faster than one every 0.25–0.5 s and no slower than every 1–2 min. Flow rates faster or slower than these are difficult to measure accurately. Once the desired dripper elevation is set, allow flow through the core to ''equilibrate'' for a few minutes (i.e., come to steady state) before starting the flow rate measurements. If the minimum possible dripper elevation (i.e., maximum difference in elevation between the drip point and the water level in the tank) produces less than one drop every 1–2 min, then the measurement should be repeated using the falling head core method (Section 75.3, see also Comment 4).

7 Determine the flow rate through the core either by measuring the volume (or weight) of water collected in a set period of time (a 30–120 s time interval is convenient), or by measuring the time required to collect a set volume of water (a 5–20 mL volume is convenient). It is recommended that about four to five flow rate determinations are made and the results averaged to reduce the effects of measurement-to-measurement variability. Concurrent with the flow rate measurements (i.e., when the dripper is set at the desired level and water

is flowing), the difference in hydraulic head (ΔH) between the top and bottom of the core (sample) is determined by using a scale with 1 mm graduations to measure the difference in elevation between the water level in the reference tube and the water level in the side arm of the outflow dripper (Figure 75.1).

75.2.2 Analysis and Example Calculations

Calculate K_s [LT^{-1}] using Darcy's law in the form

$$K_s = Q_s/(Ai) \tag{75.1}$$

where Q_s [L^3T^{-1}] is the steady flow rate through the core, A [L^2] is the cross-sectional area of the core perpendicular to flow, and i (LL^{-1}) is the hydraulic head gradient across the core. For a cylindrical core, Equation 75.1 becomes

$$K_s = \frac{4VL}{\pi \Delta t\, \Delta H {d_c}^2} \tag{75.2}$$

where V [L^3] is the volume of water collected during time interval, Δt [T], L [L] is the core length, ΔH [L] is the difference in elevation between the water level in the reference tube and the water level in the side arm of the outflow dripper (equivalent to the change in hydraulic head across the core), and d_c [L] is the diameter of the core (equivalent to the inside diameter of the sampling cylinder). (See also Comment 7).

An example data sheet and calculation are given in Table 75.1, where it is seen that water volume (V) was conveniently obtained by measuring water weight at timed intervals (60 s in this example) and then dividing by the appropriate water density (ρ) for the measured water temperature (T). Given that temperature affects both the density and viscosity of water (see Chapter 69), it is recommended that K_s measurements be conducted at constant temperature.

TABLE 75.1 Example Data Sheets and K_s Calculations for the Constant Head and Falling Head Core Methods

Constant head core	Falling head core
Core number: 708	Core number: 170
Sample length, $L = 9.8$ cm	Sample length, $L = 9.0$ cm
Core (sample) diameter, $d_c = 10.0$ cm	Core (sample) diameter, $d_c = 10.0$ cm
Timing interval, $\Delta t = 60$ s	Standpipe inside diameter, $d_s = 1.13$ cm
Change in hydraulic head, $\Delta H = 27.1$ cm	Water temperature, $T = 20°C$
Water temperature, $T = 20°C$	$H_1 = 70.2$ cm, $t_1 = 0$ min
Water density, $\rho = 0.9982$ g cm^{-3}	$H_2 = 69.2$ cm, $t_2 = 8$ min, $\Delta t_{1,2} = 480$ s[a]
$V_1 = (1.63\ g/\rho) = 1.63$ cm^3	$H_3 = 68.2$ cm, $t_3 = 16$ min, $\Delta t_{2,3} = 480$ s
$V_2 = 1.68$ cm^3	$H_4 = 67.3$ cm, $t_4 = 24$ min, $\Delta t_{3,4} = 480$ s
$V_3 = 1.63$ cm^3	$H_5 = 66.4$ cm, $t_5 = 32$ min, $\Delta t_{4,5} = 480$ s
$V_4 = 1.65$ cm^3	$K_{1,2} = 3.44 \times 10^{-6}$ cm s^{-1} (Equation 75.3)
$V_5 = 1.66$ cm^3	$K_{2,3} = 3.49 \times 10^{-6}$ cm s^{-1}
$V_{aver} = 1.65$ cm^3	$K_{3,4} = 3.18 \times 10^{-6}$ cm s^{-1}
$K_s = 1.27 \times 10^{-4}$ cm s^{-1} (Equation 75.2)	$K_{4,5} = 3.22 \times 10^{-6}$ cm s^{-1}
	$K_{aver} = 3.33 \times 10^{-6}$ cm s^{-1}

[a] The timing interval (Δt) need not be constant, although this is usually more convenient.

75.2.3 Comments

1 Cone-shaped interior of the end cap illustrated in Figure 75.1 prevents entrapment of air bubbles in the outflow assembly and thus ensures an unrestricted and continuous hydraulic connection between the outflow dripper and the sample. The removable perforated acrylic (or PVC) retaining plate in the end cap prevents possible lifting of the sample during the measurements (the retaining plate should be about 3 mm thick, the perforations should have diameter of about 3 mm, and the perforated area should be about 26% of total plate area). The small inside lip on the end cap projects into the sampling cylinder and thus serves the dual function of centering the end cap on the cylinder and reducing ''short circuit'' flow along the inside wall of the cylinder. Filter paper should not be used on either end of the core, as it is susceptible to gradual plugging with suspended sediment during the flow measurements.

2 Because water flows upward in this method, one may wish to place the end cap on the bottom of the core (i.e., the core is ''upside down'' in the tank) so that water flows from the top of the porous medium sample to the bottom. For most porous media, however, K_s is the same regardless of whether flow is upward or downward, and thus core orientation usually does not matter.

3 Outflow dripper is designed to allow accurate determination of the hydraulic head difference (ΔH) across the core. This is particularly important for highly permeable samples when the head difference is usually small (e.g., $\Delta H = 0.5-1$ cm). The dripper side arm accounts for the pressure required for drop formation, which can cause the level of true zero pressure (i.e., the water level in the side arm) to be as much as 0.6 cm above the drip point. The coarse silica sand (1–2 mm grain size) in the dripper elbow damps out the pressure pulses of drop formation and drip, which could otherwise induce a 0.5–1 cm oscillation of the side arm water level. The outflow dripper and reference tube should be made of the same material (e.g., glass, plastic) and have the same I.D. in order to cancel out capillary rise effects. It is recommended that all flow tubing (i.e., end cap outflow port, outflow tubing, dripper, reference tube) has an I.D. of at least 6 mm to facilitate removal of air bubbles and to minimize possible flow restrictions.

4 As mentioned earlier, if the flow through a core is too slow for the constant head method, the falling head method (Section 75.3) can be set up quickly with minimum effort. It is also possible with the tank approach to run the constant head and falling head methods concurrently on separate cores if core-to-core variability in K_s is extreme.

5 Advantages of this ''tank'' approach include:

(i) A 122 cm long by 46 cm wide tank can conveniently saturate up to sixty 7.6 cm diameter cores (or up to twenty-four 10.0 cm diameter cores) at a time, and one operator can measure the K_s of several cores simultaneously by using several outflow assemblies. The method is, thus, well suited for ''high volume'' projects.

(ii) A wide range of K_s (about 10^0–10^{-5} cm s^{-1}) can be measured, as the hydraulic head difference (ΔH) can be conveniently adjusted from a low of

about 0.5 cm to a high of about 30 cm (it is recommended that the tank be placed on a 10–15 cm high platform, and the tank wall be about 30 cm high).

(iii) Use of 270 mesh nylon cloth allows the cores to be moved directly to a tension (suction) table or plate or pressure extractor for measurement of soil water desorption and imbibition relationships (Chapter 72).

(iv) Tanks of various dimensions can be built to suit various core dimensions and designs. The flanged stainless steel rings of the pressure infiltrometer method (Chapter 77) provide convenient cores for the tank method, although a different end cap design from that described above would be required (e.g., an acrylic end cap containing an O-ring and bolt holes so that the end cap can be clamped down using wing bolts to make a water-tight seal against the ring's flange).

(v) The tank approach can accommodate the falling head method (Section 75.3) as well as the constant head method.

6 A disadvantage of the tank method might be that it requires more equipment than some other laboratory core methods (see e.g., Klute and Dirksen 1986; Youngs 2001).

7. For some low-permeability soils and engineered geomaterials, it may be advisable to obtain K_s from the linear regression slope of several i versus Q_s measurements, i.e. $y = mx + b$ where $y = i$, $m = 1/K_s$, $x = Q_s/A$, and $b = i$-axis intercept (see Equation 75.1). This approach avoids possible ''threshold gradient'' errors (i.e. $b \neq 0$) associated with material swelling, pore blockage, nonlinear gradients, and experimental artifacts during the flow measurements (personal communication, D.G. Chandler).

75.3 FALLING HEAD CORE METHOD

This method determines the saturated hydraulic conductivity, K_s [LT^{-1}], of core samples. The cores may have virtually any cross-sectional shape and a wide range of widths and lengths; however, cylindrical cores, which are 4–20 cm in diameter and 4–20 cm long, are most practical. The cores are first wetted to saturation and then water is allowed to flow through the samples under a falling head condition. Although many falling head setups are possible (e.g., Klute and Dirksen 1986; Youngs 2001), the method described below is designed to complement the constant head ''tank'' method described in Section 75.2. The range of K_s that can be conveniently measured with this falling head method is about 10^{-4} to 10^{-7} cm s^{-1} (see also Comment 3).

75.3.1 Apparatus and Procedures (for Cylindrical Cores)

Collect and prepare the core samples as indicated for the constant head core method (Section 75.2), except for the following changes:

1 Reverse the ends of the core to which the end cap and nylon cloth are attached, i.e., the end cap is attached to the top end of the core and the nylon cloth to the

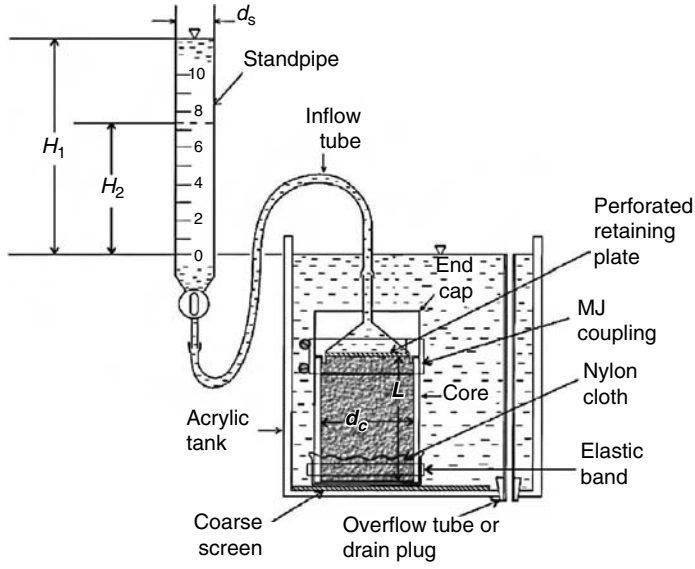

FIGURE 75.2. Schematic of the falling head core (tank) method. (From Reynolds, W.D. and Elrick, D.E. in J.H. Dane and G.C. Topp (Eds.), *Methods of Soil Analysis, Part 4—Physical Methods*, Soil Science Society of America, Madison, WI, 2002. With permission.)

bottom end of the core. This causes water to flow from the top of the sample to the bottom during the measurement rather than vice versa (see also Comment 1).

2 Place the prepared cores in the empty conductivity tank, and saturate using the procedures given in Step 3, Section 75.2. Ensure that the end cap is water-filled with no entrapped air bubbles (see also Comment 2).

3 Fill the end cap tube with water by submerging it in the tank. Connect the tube to a falling head standpipe, which is filled with the same water as used in the tank (Figure 75.2). A particularly convenient falling head standpipe has a 50–100 mL capacity, a basal stopcock, and a scale with 1 mm graduations that increase upward, rather than downward (Figure 75.2). Make sure that the water level in the tank is at the maximum allowed by the overflow tube (Figure 75.2). Adjust the height of the standpipe so that the zero point of its scale corresponds with the water level in the tank—the constant water level in the tank then serves as a convenient datum, and the standpipe scale gives a direct reading of the height of the standpipe water level (H_i) above the datum (Figure 75.2).

4 Open the standpipe stopcock and measure the time for the water level to fall from H_1 to H_2, H_3, H_4, etc. (Figure 75.2). The initial water level in the standpipe should be somewhat above the level chosen for H_1 so that initial, short-term transient effects are not included in the measurements. Such effects are due primarily to the sudden hydrostatic pressure-induced expansion of the flexible end cap tubing or compression of air inside the end cap, when the standpipe stopcock is opened. Successive measurement of about 5 H-levels (i.e., H_1, H_2, H_3, H_4, H_5) is recommended, starting at $H_1 = 50$–100 cm (see Comment 2).

5 If the standpipe water level falls too quickly to allow reading H_i to the nearest millimeter, then either install a larger diameter standpipe to reduce the rate of fall of the water level or use the constant head core method (Section 75.2), which is set up to complement the falling head method. Note also that the rate of water level fall depends on H, i.e., rate of fall decreases as H decreases.

75.3.2 Analysis and Example Calculations

Calculate K_s [LT^{-1}] using

$$K_{i,\,i+1} = \left(\frac{d_s}{d_c}\right)^2 \left(\frac{L}{\Delta\, t_{i,i+1}}\right) \ln\left(\frac{H_i}{H_{i+1}}\right); \quad i = 1, 2, 3, 4, 5 \tag{75.3}$$

where d_s [L] is the inside diameter of the standpipe, d_c [L] is the diameter of the core (which is equivalent to the inside diameter of the sampling cylinder), L [L] is the length of the core, H [L] is the height of water in the standpipe relative to the datum and $\Delta t_{i,\,i+1}$ [T] is the time required for the water level in the standpipe to fall from H_i to H_{i+1}. Successive measurement of 5 H-levels allows four individual K_s values to be determined (i.e., $K_{1,2}$, $K_{2,3}$, $K_{3,4}$, $K_{4,5}$), which may then be averaged to obtain a mean K_s value. The standpipe may also be refilled to obtain additional K_s measurements. An example data sheet and calculation are given in Table 75.1. Equation 75.3 is rather sensitive to the magnitude of H (as can be demonstrated using the data in Table 75.1), and thus H_i and H_{i+1} must be measured as accurately as possible. Note in Table 75.1 that water temperature (T) is recorded, although it does not appear in Equation 75.3. This is done because of the substantial effect that T can have on K_s (Chapter 69).

75.3.3 Comments

1 Note that water flows downward in the falling head method, but upward in the constant head method (Section 75.2). Hence, if consistent downward flow is desired (as occurs for infiltration and drainage), then attach the end cap to the top of the core for the falling head method and to the bottom of the core for the constant head method. Under most circumstances, however, the direction of water flow through the sample (i.e., upward or downward) has no significant effect on the K_s calculation. Consequently, core orientation is usually of little concern, and more importantly, the end cap usually does not need to be moved to the opposite end of the core when switching from the constant head method to the falling head method or vice versa.

2 As the water level in the standpipe falls during a measurement, any air entrapped within the end cap will expand in response to the declining hydrostatic pressure. This can introduce significant errors into the K_s calculation (Equation 75.3) if either the volume of entrapped air or the (H_i/H_{i+1}) ratio, or both are large. It is therefore recommended that the volume of air in the end cap and associated tubing be kept to a practical minimum (preferably zero), and that the (H_i/H_{i+1}) ratio be no greater than about 1.1 for each timing interval. The initial standpipe water level can be adjusted to obtain a convenient rate of water level decline.

3 The Range of K_s that can be measured practically using the above described falling head method is about 10^{-4} to 10^{-7} cm s^{-1}. This range can be extended

somewhat by adjusting the diameter of the standpipe. Increase the standpipe diameter for a larger maximum K_s and decrease the diameter for a smaller minimum K_s. Keep in mind, however, that very small diameter standpipes may introduce significant capillary rise or flow impedance effects, or both, which may, in turn, cause errors in the K_s calculations.

4 As mentioned earlier, the falling head method described here is designed to complement the constant head method described in Section 75.3. When flow through a core is found to be too slow for the constant head method, the falling head method can be set up quickly with minimum effort. The tank approach will also allow both falling head and constant head methods to be run concurrently on separate cores, if core-to-core variability in K_s is extreme. The two methods, therefore, constitute a versatile ''package,'' which allows rapid and convenient measurement of K_s values ranging from about 10^0 to 10^{-7} cm s^{-1}.

75.4 OTHER LABORATORY METHODS

Many variations on the above core methods (Section 75.2 and Section 75.3) can be found in various manuals and reference texts, along with other less-used laboratory methods (e.g., Bouwer 1978; Klute and Dirksen 1986; Youngs 2001). Although some of these methods may be simpler than those described here, they may also be less versatile and/or slower and/or less accurate. In this respect, it should be ensured that a method's sample size, K_s range, speed, accuracy, and equipment characteristics are compatible with the needs and objectives of the study.

When porous medium characteristics prevent the collection of good, undisturbed (intact) core samples (e.g., massive, high density material; material with very fragile structure), the so-called ''ped'' or ''monolith'' methods may be viable alternatives.

The ped method involves the collection of an intact, naturally occurring ped of material (e.g., a soil ped or clod approximately 10–15 cm diameter); trimming the ped to a cylindrical or cuboid shape; encasing the sides of the ped in paraffin wax and installing end caps; saturating the ped in water; and determining K_s using standard constant head or falling head procedures (Section 75.2 and Section 75.3). An important practical disadvantage of this method is the difficulty in trimming the ped to a cylindrical or cuboid shape without breakage. In addition, the measured K_s value may not be representative of the whole porous medium because intact peds usually do not contain the full range of macrostructure—most notably, the interpedal cracks and pores. Details of the ped method may be found in Sheldrick (1984), where it is referred to as the ''clod'' method.

The monolith method involves carving either a block or cylindrical column of undisturbed porous medium out of the wall of a sampling pit. The monolith can be virtually any size, although practicality usually dictates that blocks are on the order of 10–50 cm on a side (the vertical and horizontal cross-sections can be square or rectangular), and that columns are 10–50 cm in diameter and 10–50 cm long. The vertical surfaces of the monolith are sealed using paraffin wax, resin, gypsum, or plaster of Paris. A perforated plate is attached to the base of the monolith to prevent slumping of the material, and the monolith is set on an effluent collection apparatus (e.g., funnel and graduated cylinder, end cap, and outflow dripper). A small, constant depth of water ($\approx$0–3 cm) is ponded on the upper surface of the monolith, and infiltration measured until the flow rate into the top of the monolith equals the flow rate out the bottom, which signals saturation or field-saturation (Chapter 69).

At steady flow, the hydraulic head gradient will be near unity if the monolith is homogeneous, but possibly different from unity if the monolith contains heterogeneities (e.g., layering, horizonation). Heterogeneous monoliths should consequently have at least two tensiometers (Chapter 71) installed (one within about 5 cm of the inflow surface and one within about 5 cm of the outflow surface) to allow calculation of the average hydraulic head gradient across the monolith (i.e., hydraulic head gradient, i = difference in hydraulic head between the two tensiometers divided by the distance between the tensiometers). It may also be advisable to install time domain reflectometer (TDR) probes (Chapter 70) adjacent to the tensiometers to determine the degree of monolith saturation. The average K_s value (or field-saturated hydraulic conductivity value, K_{fs}—Chapter 69) of the monolith can then be determined using Equation 75.1. If the variation in K_s or K_{fs} along the length (depth) of the monolith is desired, multiple tensiometers can be installed (either uniformly spaced or placed at observed layer or horizon boundaries), then hydraulic head gradient, i, calculated for each tensiometer pair, and then Equation 75.1 applied to each tensiometer pair, given that Q_s in Equation 75.1 is a constant because of steady flow. If measurement of flow out the base of the monolith is inconvenient, one can also obtain average hydraulic conductivity values or profiles using the ''interceptor drain'' technique of Youngs (1982). An important advantage of the monolith approach is that the size of the monolith can be adjusted to ensure that the full range of variability (i.e., structure, biopores, layering, etc.) is included in each sample (e.g., Lauren et al. 1988 suggested that porous medium samples should be large enough to include at least 20 structural elements). In addition, smearing and compaction of clayey and low strength materials is minimized because carving a monolith out of a pit avoids the pressure and vibration associated with inserting a core sampling cylinder. When the monolith is in the form of a cuboid block, the anisotropy in K_s or K_{fs} (i.e., K in the x-, y-, and z-directions) can be measured within a single sample by alternately rotating the block and flowing water through the side walls (after sealing off the block ends and opening up the appropriate sides). Disadvantages of the monolith method are that it is slow, labor-intensive, highly destructive (large pits must be dug), and the monoliths can be difficult to saturate. Further detail on the undisturbed monolith method may be found in Bouma (1977), Bouma and Dekker (1981), and Youngs (1982).

REFERENCES

Amoozegar, A. 1988. Preparing soil cores collected by a sampling probe for laboratory analysis of soil hydraulic properties. *Soil Sci. Soc. Am. J.* 52: 1814–1816.

Ball, B.C. and Hunter, R. 1988. The determination of water release characteristics of soil cores at low suctions. *Geoderma* 43: 195–212.

Bouma, J. 1977. Soil survey and the study of water in unsaturated soil. *Soil Survey Paper No. 13*. Netherlands Soil Survey Institute, Wageningen, The Netherlands, pp. 1–107.

Bouma, J. 1985. Soil variability and soil survey. In J. Bouma and D.R. Nielsen, Eds. *Soil Spatial Variability Workshop*. PUDOC, Wageningen, The Netherlands, pp. 130–149.

Bouma, J. and Dekker, L.W. 1981. A method for measuring the vertical and horizontal K_{sat} of clay soils with macropores. *Soil Sci. Soc. Am. J.* 45: 662–663.

Bouwer, H. 1978. *Groundwater Hydrology*. McGraw-Hill, Toronto, 480 pp.

Cameron, K.C., Harrison, D.F., Smith, N.P., and McLay, C.D.A. 1990. A method to prevent edge-flow in undisturbed soil cores and lysimeters. *Aust. J. Soil Res.* 28: 879–886.

Elrick, D.E., Sheard, R.W., and Baumgartner, N. 1981. A simple procedure for determining the hydraulic conductivity and water retention of putting green soil mixtures. In *Proc. IV International Turfgrass Research Conference*, Guelph, ON, Canada, pp. 189–200.

Klute, A. and Dirksen, C. 1986. Hydraulic conductivity and diffusivity: Laboratory methods. In A. Klute, Ed. *Methods of Soil Analysis, Part 1—Physical and Mineralogical Methods*, 2nd ed. Agronomy 9. American Society of Agronomy, Madison, WI, pp. 687–734.

Lauren, J.G., Wagenet, R.J., Bouma, J., and Wösten, J.H.M. 1988. Variability of saturated hydraulic conductivity in a Glassaquic Hapludalf with macropores. *Soil Sci*. 145: 20–28.

McIntyre, D.S. 1974. Procuring undisturbed cores for soil physical measurements. In J. Loveday, Ed. *Methods for Analysis of Irrigated Soils*. Commonwealth Agricultural Bureaux. Wilke and Company Ltd., Clayton, Australia, pp. 154–165.

Reynolds, W.D. and Elrick, D.E. 2002. Saturated and field-saturated water flow parameters: Laboratory methods. In J.H. Dane and G.C. Topp, Eds. *Methods of Soil Analysis, Part 4—Physical Methods*. Soil Science Society of America, Madison, WI, pp. 802–817.

Rogers, J.S. and Carter, C.E. 1986. Soil core sampling for hydraulic conductivity and bulk density. *Soil Sci. Soc. Am. J*. 51: 1393–1394.

Sheldrick, B.H. 1984. In Analytical Methods Manual. Land Resource Research Institute, Agriculture Canada, Ottawa, ON, Canada, pp. 38/1–38/2.

Townend, J., Reeve, M.J., and Carter, A. 2001. Water release characteristic. In K.A. Smith and C.E. Mullins, Eds. *Soil and Environmental Analysis: Physical Methods*, 2nd ed. Marcel Dekker, Inc., New York, NY, pp. 95–140.

Youngs, E.G. 1982. The measurement of the variation with depth of the hydraulic conductivity of saturated soil monoliths. *J. Soil Sci*. 33: 3–12.

Youngs, E.G. 2001. Hydraulic conductivity of saturated soils. In K.A. Smith and C.E. Mullins, Eds. *Soil and Environmental Analysis: Physical Methods*, 2nd ed. Marcel Dekker, Inc., New York, NY, pp. 141–181.

Chapter 76
Saturated Hydraulic Properties: Well Permeameter

W.D. Reynolds
Agriculture and Agri-Food Canada
Harrow, Ontario, Canada

76.1 INTRODUCTION

The well or borehole permeameter method (also known in the engineering literature as the shallow well pump-in method) is used primarily for *in situ* or field measurement of field-saturated hydraulic conductivity, K_{fs} [LT^{-1}], in unsaturated porous materials (e.g., soil, fill, etc.). It can also be used, however, for *in situ* estimation of the capillarity parameters: matric flux potential, ϕ_m [L^2T^{-1}], sorptive number, α^* [L^{-1}], the effective Green–Ampt wetting front pressure head, ψ_f [L], sorptivity, S [$LT^{-1/2}$], flow-weighted mean pore diameter, PD [L], and number of PD pores per unit area, NP [L^{-2}] (Chapter 69). The most common form of this method uses wells on the order of 4–10 cm in diameter and 10–100 cm deep, although greater well diameters and depths are possible. Both constant-head and falling-head approaches are available (described in Section 76.2 and Section 76.3, respectively). Other field methods for measuring K_{fs} include the ring infiltrometer (Chapter 77), the auger hole (Chapter 78), and the piezometer (Chapter 79) methods. Laboratory methods for measuring saturated hydraulic conductivity, K_s, are described in Chapter 75; and selected methods for estimating K_s from surrogate porous medium properties are given in Chapter 84. A discussion of the principles and parameters associated with determination of K_{fs} and the capillarity parameters appears in Chapter 69.

The overall strengths of the well permeameter methods include: (1) simple and robust equipment and procedures (e.g., easily portable equipment, no requirement for electronics or specialized materials); (2) relatively rapid measurements with generally low water consumption (e.g., measurements completed within minutes to hours using only a few liters of water); (3) easy and rapid depth profiling and spatial–temporal replication of measurements; (4) ability to use in a wide range of porous medium textures including moderately stony soils; and (5) general acceptance in the science and engineering communities because of long-term usage. Perhaps the primary weaknesses of the well permeameter methods include potential parameter underestimation due to smearing or compaction and siltation of the infiltration surface (e.g., well wall or base); potential difficulty in obtaining

representative parameter values in porous materials where vertical flow is controlled primarily by isolated macropores (e.g., limited interception by the well of discrete worm holes and root channels in fine textured soils); and potentially reduced accuracy for the capillarity parameters (ϕ_m, S, α^*, ψ_f, PD, NP) because ponded infiltration maximizes the hydrostatic pressure and gravity components of flow at the expense of the capillarity component of flow.

76.2 CONSTANT-HEAD WELL PERMEAMETER

The constant-head well permeameter method involves ponding one or more constant depths (heads) of water in an uncased well, and measuring the flow out of the well and into unsaturated porous material. The flow rate declines rapidly during an initial early-time transient and then becomes steady, which is the desired measurement. If well diameter and ponding depth are kept small (e.g., 4–10 cm well diameter; 5–50 cm head), steady flow can usually be reached within minutes to hours, and water consumption is generally limited to a few liters per measurement. As infiltration from the uncased well is three-dimensional, the measured water transmission parameters (i.e., K_{fs}, ϕ_m, S, α^*, ψ_f, PD, NP) (see Chapter 69) are relevant to combined vertical–horizontal flow, as occurs during infiltration from wastewater leach fields or drainage into tile lines. The vertical–horizontal weighting of the water transmission parameters increases toward the horizontal direction as the depth of ponding in the well increases. Single-head, two-head, and multiple-head analyses are available for this method. Although there are several constant-head well permeameter designs (see Comment 7), only the ''in-hole Mariotte bottle'' system will be illustrated here. Note, however, that the equations and analyses apply regardless of permeameter design.

76.2.1 Apparatus and Procedures

1 Using a screw-type auger or bucket auger, excavate a 4–10 cm diameter ''well'' to the desired depth (Figure 76.1). The well should be cylindrical and flat-bottomed, as this shape is assumed in the well permeameter analysis (flat-faced ''bottoming'' or ''sizing'' augers are commercially available for producing flat-bottomed wells). The bottom of the well should be at least 20 cm above the water table or capillary fringe (Figure 76.2) to avoid possible interference caused by ''mounding'' of the water table up into the well, which is not accounted for in the analysis. Auger-induced smearing and compaction of the well surfaces in fine textured materials should be minimized within the measurement zone (Figure 76.1), as this can result in unrepresentative K_{fs}, ϕ_m, α^*, ψ_f, S, PD, or NP values. Smearing and compaction can be minimized by not augering when the material is very wet (e.g., clayey soils should not be augered when they are wet enough to be ''sticky''), by using a very sharp auger, by applying very little downward pressure on the auger, and by taking only small bites with the auger before emptying it out. The ''two-finger/two-turn'' rule for augering within the measurement zone seems to work reasonably well: once the top of the measurement zone is reached, use only two fingers on each hand to apply downward pressure on the auger (i.e., the weight of the auger provides most of the downward pressure), and make only two complete turns of the auger before emptying it out. If inspection of the well reveals smearing/compaction within the measurement zone (a smeared and/or compacted surface generally appears ''smooth and polished'' under the light of a flashlight), steps should be taken to remove it. This can be accomplished reasonably well by running a small, spiked roller

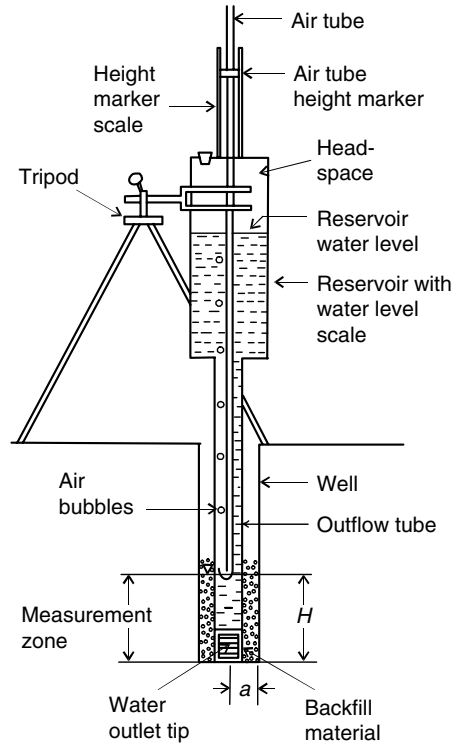

FIGURE 76.1. In-hole Mariotte bottle system for use in the constant-head well permeameter method. (From Reynolds, W.D., in M.R. Carter (Ed.), *Soil Sampling and Methods of Analysis*, Canadian Society of Soil Science, Lewis Publishers, Boca Raton, Florida, 1993. With permission.)

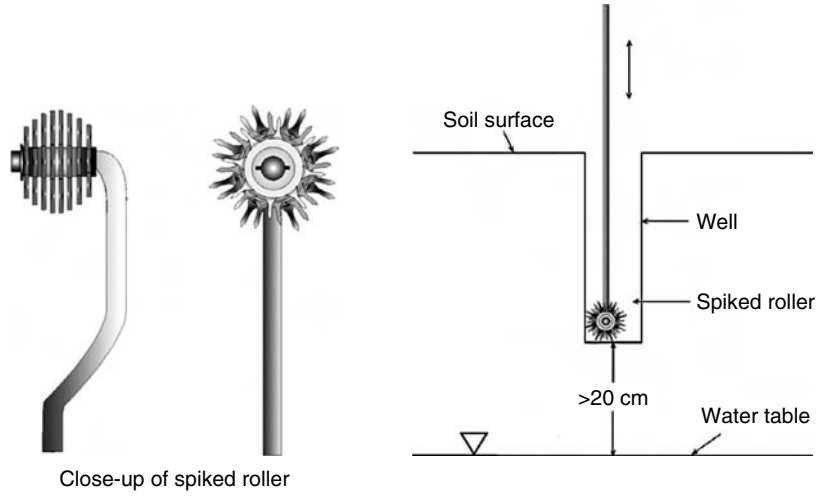

FIGURE 76.2. Roller-type desmearing–decompaction apparatus for the constant-head well permeameter method. (From Reynolds, W.D. and Elrick, D.E., in J.H. Dane and G.C. Topp (Eds.), *Methods of Soil Analysis, Part 4—Physical Methods*, Soil Science Society of America, Madison, Wisconsin, 2002. With permission.)

(Figure 76.2) up and down the measurement zone (Figure 76.1) several times to break up and pluck off the smeared/compacted surface (Reynolds and Elrick 1986). Other implements that have been used for removing smeared and compacted surfaces include a stiff cylindrical brush (available from many commercial auger and well/borehole permeameter suppliers), a pick-like ''plucking'' instrument (Campbell and Fritton 1994; Bagarello 1997), and soil peels made from quick-setting resin (Koppi and Geering 1986) (see Comment 1). If the removal of smeared or compacted surfaces results in an appreciable increase in well radius, this new radius should be measured and used in the calculations (Section 76.2.2).

2 Stand the empty permeameter in the well and attach it to some kind of stabilizing apparatus (here we refer specifically to ''vertical'' permeameters based on in-hole Mariotte bottle systems as illustrated in Figure 76.1—other systems may not require stabilizing). The stabilizing apparatus should hold the permeameter upright, give the permeameter good stability against wind, and carry the weight of the permeameter (when full of water) so that the water outlet tip (Figure 76.1) does not sink into the base of the well during the measurements. A simple tripod (similar to a surveyor's transit or camera tripod) that clamps solidly to the permeameter reservoir works very well for this purpose (Figure 76.1). To prevent possible collapse of the well when measuring unstable porous materials, it is advisable to install a well screen, or to backfill around the permeameter to the top of the measurement zone using pea gravel or coarse sand (Figure 76.1). Backfill material (which must have a much greater permeability than the material tested to avoid flow impedance effects) also helps to reduce siltation (see Comment 1), as well as produce faster and more uniform bubbling of the Mariotte bottle when measuring low-permeability materials (i.e., porous materials with low hydraulic conductivity).

3 Close the water outlet of the Mariotte bottle by pushing the air tube down into the outlet tip and then fill the bottle with water (Figure 76.1). Use water at ambient temperature to minimize the accumulation within the reservoir of bubbles of degassed air, which can obscure the reservoir scale. Do not use distilled or deionized water, as this may encourage clay/silt dispersion and subsequent siltation of the well surface during the measurement (see also Chapter 69). In many cases, local tap water can be used, as its major ion speciation and concentrations are often sufficient to prevent clay and silt dispersion. In porous media that are particularly susceptible to siltation (primarily materials with high silt content), it may be necessary to use native water (i.e., water extracted from the porous medium), or water with flocculent added. Fill the permeameter reservoir to the top, leaving no air space. This minimizes overfilling of the well when flow is started (see Comment 2).

4 Lift the air tube out of the outlet tip to establish and maintain the desired depth (head) (H) of water in the well (Figure 76.1). The air tube should be raised slowly to prevent a sudden rush of water against the well surface. A sudden rush of water can erode the well (especially if backfill material has not been used), promote well siltation by stirring silt and clay into suspension, and cause excessive air entrapment within the porous medium. Perforated well liners and screens have also been used to protect the well surface and prevent collapse

(Bagarello 1997). The desired head (H) is obtained by setting the base of the air tube at the appropriate level, which is usually accomplished using a calibrated height marker and scale (Figure 76.1). The Mariotte bottle is operating properly when air bubbles rise regularly up through the outflow tube and into the reservoir (Figure 76.1).

5 The rate of water flow or discharge (Q) out of the Mariotte bottle and into the porous medium is measured by monitoring the rate of fall, R, of the water level in the reservoir. This can be accomplished using a scale attached to the reservoir (Figure 76.1) and a stopwatch, or an automated pressure transducer–data logger system similar to that described by Ankeny (1992). The rate of fall, R, decreases with increasing time and approaches a constant value (R_s) as the flow rate becomes quasisteady (Q_s). Quasisteady flow is usually assumed when effectively the same R value (R_s) is obtained over four or five consecutive R measurements (Section 76.2.2).

6 If the single-head analysis is to be used, proceed to Section 76.2.2. If the two-head analysis is desired, raise the air tube again to obtain steady flow for a second head (H_2); and if the multiple-head analysis is required, raise the air tube two or more times to obtain steady flows at H_2, $H_3, \ldots$, and so on. For both the two-head and multiple-head analyses, H_1 must be ponded first with $H_1 < H_2 < H_3 < \cdots$, and the water level in the well must not be allowed to fall when switching from one head to the next higher head.

76.2.2 Analysis and Example Calculations

The original constant-head well permeameter analysis is based on the approximate Glover relationship (Zangar 1953)

$$K_{fs} = C_G Q_s / (2\pi H^2) \tag{76.1}$$

where Q_s [L^3T^{-1}] is the quasisteady flow rate out of the permeameter and into the porous medium, H [L] is the steady depth (head) of water in the well (set by the height of the air tube), and C_G is a dimensionless shape factor given by

$$C_G = \sinh^{-1}\left(\frac{H}{a}\right) - \left[\left(\frac{a}{H}\right)^2 + 1\right]^{1/2} + \left(\frac{a}{H}\right) \tag{76.2}$$

where a [L] is the radius of the well. In Mariotte-type permeameters (such as the one illustrated in Figure 76.1), Q_s is conveniently obtained by measuring the quasisteady rate of fall of the water level in the reservoir, R_s [LT^{-1}], and then multiplying by the reservoir cross-sectional area, A [L^2] (i.e., $Q_s = AR_s$). Although the Glover analysis (i.e., Equation 76.1 and Equation 76.2) is simple and easy to use, it is seriously limited because only K_{fs} is calculated; and of the three components of flow out of the well (i.e., pressure, gravity, and capillarity), only the pressure component is taken into account (Reynolds et al. 1985). As a consequence, α^*, ϕ_m, ψ_f, S, PD, and NP cannot be determined with this analysis, and the K_{fs} value can be overestimated by an order of magnitude or more in dry, fine-textured materials (Philip 1985; Reynolds et al. 1985). The accuracy of the Glover analysis tends to improve with increasing H/a ratio, however; Amoozegar and Wilson (1999) suggest that the systematic overestimate of K_{fs} by Equation 76.1 and Equation 76.2

can usually be reduced to reasonable levels by maintaining $H/a \geq 5$, although the original work of Zangar (1953) indicates that $H/a \geq 10$ is required.

Extended and improved well permeameter analyses have been developed, which include single-head, two-head, and multiple-head procedures (Reynolds et al. 1985; Reynolds and Elrick 1986; Elrick et al. 1989). These updated analyses account for all three components of flow out of the well (i.e., pressure, gravity, and capillarity); and as a result, they yield more accurate K_{fs} values, plus simultaneous estimates of the capillarity parameters. The extended single-head analysis (which is directly comparable to the original single-head Glover analysis) determines K_{fs} using

$$K_{fs} = \frac{C_w Q_s}{[2\pi H^2 + C_w \pi a^2 + (2\pi H/\alpha^*)]} \tag{76.3}$$

where the α^* parameter is visually estimated using the texture–structure categories in Table 76.1 (see Comment 6), and the dimensionless shape parameter, C_w, is determined by using (Zhang et al. 1998)

$$C_w = \left(\frac{H/a}{2.074 + 0.093(H/a)}\right)^{0.754} \quad \text{for} \quad \alpha^* \geq 0.09 \text{ cm}^{-1} \tag{76.4a}$$

$$C_w = \left(\frac{H/a}{1.992 + 0.091(H/a)}\right)^{0.683} \quad \text{for} \quad \alpha^* = 0.04 \text{ cm}^{-1} \tag{76.4b}$$

$$C_w = \left(\frac{H/a}{2.081 + 0.121(H/a)}\right)^{0.672} \quad \text{for} \quad \alpha^* = 0.01 \text{ cm}^{-1} \tag{76.4c}$$

Once α^* is estimated and K_{fs} calculated, estimates of ϕ_m, S, PD, NP, and ψ_f can be obtained using Equation 69.16 through Equation 69.21, recognizing that for this case (field-saturated flow) $K(\psi_0) = K_{fs}$, $\alpha^*(\psi_0) = \alpha^*$, $\theta(\psi_0) = \theta_{fs}$, $\theta(\psi_i) = \theta_i$, $PD(\psi_0) = PD$, and $NP(\psi_0) = NP$.

TABLE 76.1 Texture–Structure Categories for Visual Estimation of α^*

Texture–structure category	α^* (cm^{-1})
Compacted, structureless, clayey, or silty materials such as landfill caps and liners, lacustrine, or marine sediments, etc.	0.01
Porous materials that are both fine textured and massive; include unstructured clayey and silty soils, as well as fine structureless sandy materials	0.04
Most structured and medium textured materials; include structured clayey and loamy soils, as well as unstructured medium sands. This category is generally the most appropriate for agricultural soils	0.12
Coarse and gravelly sands; may also include some highly structured soils with large and numerous cracks and biopores	0.36

Source: Adapted from Elrick, D.E., Reynolds, W.D., and Tan, K.A., *Ground Water Monit. Rev.*, 9, 184, 1989.

The two-head analysis (two heads ponded successively in the well) and the multiple-head analysis (three or more heads ponded successively in the well) allow simultaneous calculation of both K_{fs} and α^*, i.e., the α^* parameter does not have to be estimated. The two-head and multiple-head approaches make use of (Reynolds and Elrick 1986)

$$C_{wi}Q_{si} = P_1H_i^2 + P_2H_i + P_3; \quad i = 1, 2, 3, \ldots, n; \quad n \geq 2 \tag{76.5a}$$

which is least squares fitted to C_wQ_s versus H data (C_wQ_s on Y-axis; H on X-axis), where Q_{si} is the steady flow rate corresponding to steady ponding head, H_i, the C_{wi} parameter is the C_w value corresponding to H_i/a (Equation 76.4), and

$$P_1 = 2\pi K_{fs}; \quad P_2 = 2\pi\frac{K_{fs}}{\alpha^*}; \quad P_3 = Y\text{-axis intercept} \tag{76.5b}$$

For the two-head approach, $n = 2$ in Equation 76.5a (i.e., H_1, H_2; Q_1, Q_2; C_{w1}, C_{w2}), and for the multiple-head approach, $n \geq 3$ in Equation 76.5a (i.e., $H_1, H_2, H_3, \ldots$; $Q_1, Q_2, Q_3, \ldots$; $C_{w1}, C_{w2}, C_{w3}, \ldots$). Equation 76.5 can be solved for K_{fs} and α^* using a custom-built computer program (see Reynolds and Elrick 1986, for working equations), or using the regression function of a computer spreadsheet (quadratic curve). The two-head approach can also be solved using simultaneous equations presented in Reynolds et al. (1985) and Reynolds and Elrick (1986). Once K_{fs} and α^* are determined, the ϕ_m, S, PD, NP, and ψ_f parameters are calculated as above for the extended single-head analysis. Further detail on the extended single-head, two-head, and multiple-head techniques can be found in Reynolds et al. (1985), Reynolds and Elrick (1986), and Reynolds and Elrick (2002). All three of the extended analyses prevent the systematic overestimation of K_{fs} that occurs with the Glover analysis (illustrated in Table 76.2).

Example data sheets and calculations for the single-head, two-head, and multiple-head analyses are given in Table 76.2 and Table 76.3.

76.2.3 Comments

1 Because water flows out of the well and into the porous medium in the constant-head well permeameter method, any significant smearing, compaction, or siltation of the porous medium in the measurement zone (Figure 76.1) can result in unrepresentative (inaccurate) K_{fs}, ϕ_m, S, α^*, ψ_f, PD, or NP values. In wet, structured silty clay soils, for example, the K_{fs} and ϕ_m values can be reduced by more than an order of magnitude if ''normal'' augering techniques are used, rather than the ''two-finger/two-turn'' rule. Proper and careful augering of the well is therefore essential in materials susceptible to smearing, compaction, and siltation. Removal of any smeared or compacted areas in the measurement zone is also strongly recommended, although it appears that none of the currently available methods are completely effective in susceptible materials (i.e., silty and clayey soils).

2 If the Mariotte bottle does not respond after the air tube has been raised to the desired H-level (i.e., no bubbling), the well may be overfilled with water (i.e., the water level in the well is above the base of the air tube). To remedy this, withdraw water from the well until bubbling starts, which indicates that the set H-level has been reached. One way to accomplish this is to tape a small-diameter ''extraction

TABLE 76.2 Example Data Sheet and K_{fs} Calculations for the Constant-Head Well Permeameter Method, Single-Head Approach (Equation 76.1 through Equation 76.4)

Cumulative time, t (min)	Reservoir scale reading, L (cm)	Rate, R ($\Delta L/\Delta t$) (cm/2 min)
0	5.8	—
2	8.6	2.8
4	10.6	2.0
6	12.4	1.8
8	14.1	1.7
10	15.7	1.6
12	17.2	1.5
14	18.7	1.5
16	20.1	1.4
18	21.5	1.4
20	22.9	1.4
22	24.3	1.4
24	25.7	1.4

Well radius, $a = 5$ cm; well depth, $d = 50$ cm; depth of ponding, $H = 10$ cm.
Mariotte reservoir cross-sectional area, $A = 12.57$ cm^2.
Porous material type: structureless clay loam soil (estimated $\alpha^* = 0.04$ cm^{-1} from Table 76.1).

$\theta_{fs} = 0.65$; $\theta_i = 0.40$; $\gamma = 1.818$.
The R value is the rate of fall of water level in the Mariotte reservoir.
$R_s = \Delta L/\Delta t = 1.4$ cm/2 min $= 0.7$ cm/min $= 1.1667 \times 10^{-2}$ cm s^{-1}.
$Q_s = AR_s = (12.57 \text{ cm}^2)(1.1667 \times 10^{-2} \text{ cm s}^{-1}) = 1.4665 \times 10^{-1}$ cm^3 s^{-1}.

Glover analysis	Extended analysis
$C_G = 0.8256$ (Equation 76.2)	$C_w = 0.9446$ (Equation 76.4b)
$K_{fs} = 1.93 \times 10^{-4}$ cm s^{-1} (Equation 76.1)	$K_{fs} = 6.09 \times 10^{-5}$ cm s^{-1} (Equation 76.3)

Note: 1. The K_{fs} from the Glover analysis overestimates the K_{fs} from the extended analysis by a factor of 3.2.
2. Any convenient timing interval can be used, and it need not be constant.

tube'' to the outflow tube (Figure 76.1) before the Mariotte bottle is inserted into the well, and then connect a syringe to the top of the extraction tube to withdraw the excess water from the well. Alternatively, one can simply wait for the water level to fall and the Mariotte bottle will start itself when the H-level is eventually reached. A slowly bubbling Mariotte bottle means that the porous medium has low hydraulic conductivity or the well is smeared/compacted/silted up. In low hydraulic conductivity materials where the Mariotte bottle bubbles slowly, it is advisable to shade the reservoir from direct, hot sun in order to minimize solar heating of the headspace (Figure 76.1) above the water surface. Thermal expansion of the air in the headspace can prevent bubbling. In addition, extreme solar heating of the water in the reservoir will cause a significant reduction in water viscosity, which will introduce calculation errors if not corrected (see Chapter 69 for details). A Mariotte-based permeameter that will not bubble but still registers flow (i.e., dropping water level in the reservoir) may have an air (vacuum) leak in the reservoir.

TABLE 76.3 Example Data Sheet and Calculations for the Constant-Head Well Permeameter Method, Two-Head and Multiple-Head Analyses (Equation 76.5)

H_1 = 3 cm			H_2 = 9 cm			H_3 = 15 cm		
Cumulative time, t (min)	**Reservoir scale reading, L (cm)**	**Rate, R ($\Delta L/\Delta t$) (cm/2 min)**	**Cumulative time, t (min)**	**Reservoir scale reading, L (cm)**	**Rate, R ($\Delta L/\Delta t$) (cm/2 min)**	**Cumulative time, t (min)**	**Reservoir scale reading, L (cm)**	**Rate, R ($\Delta L/\Delta t$b) (cm/2 min)**
0	3.0	—	26	17.8	—	50	41.0	—
2	4.1	1.1	28	19.6	1.8	52	43.9	2.9
4	5.0	0.9	30	21.3	1.7	54	46.8	2.9
6	5.8	0.8	32	22.9	1.6	56	49.6	2.8
8	6.5	0.7	34	24.4	1.5	58	52.2	2.6
10	7.3	0.8	36	25.9	1.5	60	54.6	2.4
12	8.0	0.7	38	27.3	1.4	62	56.9	2.3
14	8.8	0.8	40	28.8	1.5	64	59.1	2.2
16	9.5	0.7	42	30.2	1.4	66	61.3	2.2
18	10.3	0.8	44	31.6	1.4	68	63.5	2.2
20	11.0	0.7	46	33.0	1.4	70	65.7	2.2
22	11.8	0.8	48	34.4	1.4	—	—	—
24	12.5	0.7	—	—	—	—	—	—
$R_1 = 0.75$ cm/2 min $= 0.00625$ cm s^{-1}			$R_2 = 1.4$ cm/2 min $= 0.01167$ cm s^{-1}			$R_3 = 2.2$ cm/2 min $= 0.01833$ cm s^{-1}		
$Q_{s1} = AR_1 = 0.225$ cm^3 s^{-1}			$Q_{s2} = AR_2 = 0.42$ cm^3 s^{-1}			$Q_{s3} = AR_3 = 0.66$ cm^3 s^{-1}		
$C_{w1} = 0.3847$ (Equation 76.4a)			$C_{w2} = 0.8476$ (Equation 76.4a)			$C_{w3} = 1.2010$ (Equation 76.4a)		

Well radius, $a = 5$ cm; well depth, $d = 50$ cm.
Mariotte reservoir cross-sectional area, $A = 36.0$ cm^2.
Porous material type: structured clay loam soil.
$\theta_{fs} = 0.65$; $\theta_i = 0.40$; $\Delta\theta = 0.25$; $\gamma = 1.818$.
The R value is the rate of fall of water level in the Mariotte reservoir.

(continued)

TABLE 76.3 (continued) Example Data Sheet and Calculations for the Constant-Head Well Permeameter Method, Two-Head and Multiple-Head Analyses (Equation 76.5)

Two-Head Analysis (Equation 76.5)		
H_1, H_2	$K_{fs} = 3.06 \times 10^{-4}$ cm s^{-1}	$\alpha^* = 0.0959$ cm^{-1} ≈ 0.10 cm^{-1}
H_1, H_3	$K_{fs} = 3.35 \times 10^{-4}$ cm s^{-1}	$\alpha^* = 0.1098$ cm^{-1} ≈ 0.11 cm^{-1}
H_2, H_3	$K_{fs} = 3.63 \times 10^{-4}$ cm s^{-1}	$\alpha^* = 0.1397$ cm^{-1} ≈ 0.14 cm^{-1}
Multiple-Head Analysis (H_1, H_2, H_3) (Equation 76.5)		
$K_{fs} = 3.54 \times 10^{-4}$ cm s^{-1}		$\alpha^* = 0.1288$ cm^{-1} ≈ 0.13 cm^{-1}
$\phi_m = 2.75 \times 10^{-3}$ cm^2 s^{-1}		(Chapter 69, Equation 69.16)
$\psi_f = -7.76$ cm		(Chapter 69, Equation 69.20)
$S = 3.53 \times 10^{-2}$ cm s$^{-1/2}$		(Chapter 69, Equation 69.17)
$PD = 0.0191$ cm		(Chapter 69, Equation 69.18)
$NP = 1.11 \times 10^6$ pores m^{-2}		(Chapter 69, Equation 69.19)

Note: 1. The two-head results can also be used to calculate ϕ_m, ψ_f, S, PD, and NP.
2. For the PD and NP calculations: $\sigma = 72.75$ g s^{-2}; $\rho = 0.9982$ g cm^{-3} (20°C); $g = 980.621$ cm s^{-2}; $\mu = 1.002$ g cm^{-1} s^{-1} (20°C).

3 The time required for a well permeameter to reach quasisteady flow (equilibration time) is determined primarily by the hydraulic conductivity of the material tested, but also by the antecedent water content of the material, the radius of the well, and the depth of water in the well. Generally speaking, equilibration time increases with decreasing hydraulic conductivity, decreasing antecedent water content, increasing well radius, and increasing depth of water ponding (Reynolds and Elrick 1986). Equilibration times range from about 5 to 60 min in moderate to highly permeable materials ($K_{fs} \geq 10^{-4}$ cm s^{-1}) to as much as two or more hours in low permeability materials ($K_{fs} \leq 10^{-5}$ cm s^{-1}). The range of K_{fs} that can be measured practically with a Mariotte bottle permeameter is on the order of 10^{-2}–10^{-6} cm s^{-1}, although this range can be extended somewhat with careful use and adjustments in the size of the reservoir, outflow tube, and air tube.

4 The C_w value (shape factor) relationships given in Equation 76.4 are calibrated for approximately 1 cm $\leq a \leq$ 5 cm, 0.5 cm $\leq H \leq$ 20 cm, and 0.25 cm $\leq H/a \leq$ 20 cm. They are based on discrete data points obtained from numerical solution of Richards' equation for steady, three-dimensional saturated–unsaturated flow around the well (Reynolds and Elrick 1987). If a, H, or H/a values substantially outside these ranges are required, it is recommended that new C_w values be calculated using the procedures in Reynolds and Elrick (1987). Note that Equation 76.4a applies for all $\alpha^* \geq 0.09$ cm^{-1} (because of the decreasing influence of capillarity with increasing α^*), and is thus the appropriate C_w versus H/a relationship for the $\alpha^* = 0.12$ cm^{-1} category and the $\alpha^* = 0.36$ cm^{-1} category in Table 76.1.

5 The primary advantage of the two-head and multiple-head approaches is that simultaneous measurements of the K_{fs}, ϕ_m, S, α^*, ψ_f, PD, and NP parameters can be obtained. An important limitation, however, is that heterogeneity in the form of layering, horizonation, cracks, worm holes, root channels, etc. can result in unrealistic and invalid (e.g., negative) parameter values (Elrick et al. 1989). This occurs because both the infiltration surface and the wetted bulb around the well increase with increasing H, which increases the likelihood of encountering heterogeneities. In addition, the coefficient matrices in the two-head and multiple-head analyses are ill-conditioned, which further increases sensitivity to heterogeneity (Philip 1985). When the two-head or multiple-head analysis produces a negative K_{fs} and ϕ_m value, or when the calculated α^* value falls substantially outside the physically realistic range of 0.01 $cm^{-1} \leq \alpha^* \leq 1$ cm^{-1}, then the extended single-head analysis (Equation 76.3 and Equation 76.4) should be applied to each head (H value) and the resulting K_{fs} and capillarity averaged (Elrick and Reynolds 1992). Further discussion on analyzing constant-head well permeameter data can be found in Amoozegar (1993) and Elrick and Reynolds (1993).

6 Relative to the two-head and multiple-head approaches (Equation 76.5), the primary advantages of the updated single-head analysis (Equation 76.3) include time saving and avoidance of negative K_{fs} values, as a result of using only one ponded head and site estimation of α^*, as illustrated in Table 76.1. Disadvantages include lack of simultaneous calculation of ϕ_m, S, α^*, ψ_f, PD, and NP, and potentially reduced parameter accuracy through inappropriate selection of α^* from Table 76.1. Fortunately, the categories are broad enough in Table 76.1

that one should not be in error by more than one α^* category when visually estimating the texture and structure at the measurement site. This in turn introduces an ''error'' into the K_{fs} and ϕ_m calculations, which is generally less than a factor of 2 and often less than $\pm 25\%$ (Reynolds et al. 1992). This is sufficient accuracy for many practical applications, given the inherent variability of these parameters. In addition, the sensitivity of K_{fs} and ϕ_m to the choice of α^* can be reduced further by adjusting the *H*-level. The sensitivity of K_{fs} to the choice of α^* decreases as *H* increases, while the sensitivity of ϕ_m to α^* decreases as *H* decreases (Reynolds et al. 1992). Consequently, if one is interested primarily in K_{fs}, then the *H*-level used for the single-head approach should be as large as possible. On the other hand, if interest is primarily in ϕ_m or the other capillarity parameters, then the *H*-level should be as small as possible. It should also be kept in mind, however, that ϕ_m, *S*, α^*, ψ_f, *PD*, and *NP* can be of low accuracy when obtained using ponded infiltration techniques (regardless of analysis procedure) because of the usual dominance of the pressure and gravity components of flow over the capillarity component of flow in a ponded environment.

7 Alternative constant-head well permeameter designs, which are based on various Mariotte bottle or float valve arrangements, can be found in Amoozegar and Warrick (1986), Koppi and Geering (1986), Stephens et al. (1987), Jenssen (1989), Bell and Schofield (1990), and Amoozegar (1992). Alternative procedures for collecting and analyzing constant-head well permeameter data may be found in Philip (1985), Amoozegar and Warrick (1986), Stephens et al. (1987), Amoozegar (1992), Elrick and Reynolds (1992), Reynolds et al. (1992), and Xiang (1994). Further discussion of the apparatus and analyses presented here may be found in Reynolds and Elrick (1986), Elrick et al. (1989), and Elrick and Reynolds (1992).

76.3 FALLING-HEAD WELL PERMEAMETER

The falling-head well permeameter method involves ponding a known head (depth) of water in a tightly cased well, and monitoring the decline in head with time as water flows out through the base of the casing and into the unsaturated porous material (Figure 76.3). The diameter and shape of the well are usually similar to those of the constant-head well permeameter method (i.e., 4–10 cm diameter, flat bottom), although there are no theoretical restrictions on well diameter. As flow is entirely through the bottom of the well, the calculated water transmission parameters (K_{fs}, ϕ_m, *S*, α^*, ψ_f, *PD*, *NP*) are primarily relevant to vertical flow, as occurs during infiltration or near-surface drainage.

Overall strengths of the falling-head method relative to steady flow methods include greatly reduced measurement times in low-permeability materials, and the ability to measure lower K_{fs} values than what is practical with the steady flow (e.g., constant head) approaches. Overall weaknesses include the necessity for a watertight seal between the well liner (casing) and the well wall (which can be difficult or impossible in some porous materials), and limited comparison to more established methods.

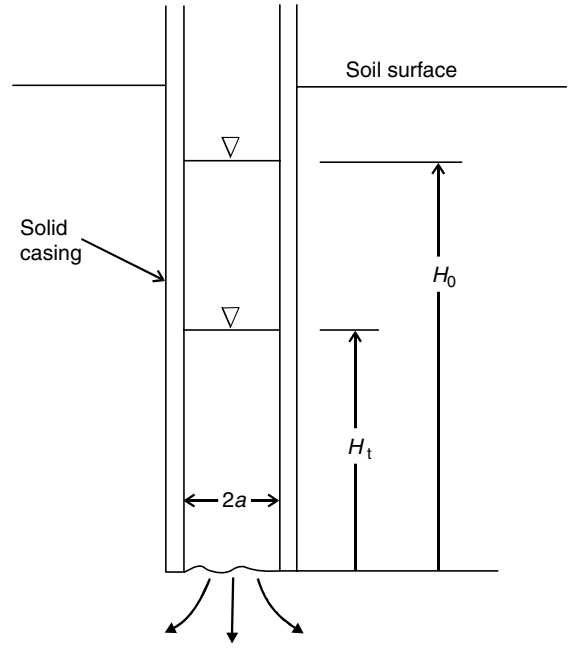

FIGURE 76.3. Schematic of the falling-head well permeameter method, cased well. (From Reynolds, W.D. and Elrick, D.E., in J. Alvarez-Benedi and R. Munoz-Carpena (Eds.), *Soil–Water–Solute Process Characterization*: *An Integrated Approach*, CRC Press, Boca Raton, Florida, 2005. With permission.)

76.3.1 Apparatus and Procedures

1 Construct a cylindrical, flat-bottomed well using the procedures given for the constant-head well permeameter method (Section 76.2). The bottom of the well should be sufficiently above the water table or capillary fringe to avoid ''ground-water mounding'' up into the well, which is not accounted for in the analysis. Use the procedures in Section 76.2 and Chapter 78 (auger hole method) to remove smearing or compaction from the well base, as these conditions can result in unrepresentatively low values for K_{fs} and the capillarity parameters.

2 Slide a solid casing (i.e., solid-walled pipe open only at its ends) down to the bottom of the well (Figure 76.3). The casing must be tight-fitting in the well to prevent water ''leakage'' between the casing and the well wall (required by theory) (see Comment 1). The casing should extend at least to the surface, but may extend above the surface to accommodate the desired initial water depth (H_0) at the start of the measurement (Figure 76.3).

3 Quickly add a calibrated volume of water into the casing to produce the desired water level, $H = H_0$, at time $t = 0$ (Figure 76.3). This may be accomplished by simply pouring the water into the casing, or alternatively, by adding the water through a tube that extends to the well base. It may be necessary in some porous materials (e.g., silty and clayey soils) to place a screen (≈2 mm openings) or layer of pea gravel (≈5 cm thickness) in the bottom of the casing to prevent both

erosion of the well base when water is first added, and subsequent siltation of the well base by the eroded material as water flows out of the casing and into the porous medium (Figure 76.3). The hydraulic conductivity of the screen or pea gravel must be substantially greater than that of the porous medium to prevent flow impedance, which may cause unrepresentative results. After the water is added, measure the decline in water level (H) with time (t) and calculate the various hydraulic parameters as indicated below.

76.3.2 Analysis and Example Calculations

The decline in water level with time is given by (Philip 1993)

$$t = \frac{\pi^2 a}{8K_{\mathrm{fs}}}\left[\begin{array}{l}\left(1+\dfrac{1}{2A}\right)\ln\left(\dfrac{A^3-1}{A^3-\rho_t^3}\right)-\dfrac{3}{2A}\ln\left(\dfrac{A-1}{A-\rho_t}\right)\\ +\dfrac{\sqrt{3}}{A}\left[\arctan\left(\dfrac{A+2\rho_{\mathrm{t}}}{\sqrt{3}A}\right)-\arctan\left(\dfrac{A+2}{\sqrt{3}A}\right)\right]\end{array}\right] \tag{76.6a}$$

where

$$A^3 = \frac{3\left(H_0+\dfrac{1}{\alpha^*}+\dfrac{\pi^2 a}{8}\right)}{a(\Delta\theta)}+1 \tag{76.6b}$$

$$\rho_t{}^3 = \frac{3(H_0-H_t)}{a(\Delta\theta)}+1 \tag{76.6c}$$

where t [T] is the time since initiation of flow out of the well, a [L] is the inside radius of the casing (Figure 76.3), $\Delta\theta = (\theta_{\mathrm{fs}} - \theta_{\mathrm{i}})$ [$\mathrm{L^3L^{-3}}$] is the difference between the field-saturated volumetric water content (θ_{fs}) and the antecedent volumetric water content (θ_{i}) of the porous medium, H_0 [L] is the initial water depth in the well (at $t = 0$), H_t [L] is the depth of water in the well at time, t, and the arctan functions are in radian measure. Equation 76.6 thus describes the time-dependent decline in water level (H_t versus t) as water flows out through the bottom of the cased well and into the porous medium. For simultaneous determination of K_{fs} and α^* using Equation 76.6, a minimum of two H versus t data points are required, which Philip (1993) and Munoz-Carpena et al. (2002) chose as t at $H = H_0/2$ and t at $H = 0$. An alternative (and perhaps more robust) approach is to numerically curve-fit Equation 76.6 to a sequence of H_t versus t data points. The θ_{fs}, θ_{i}, and H_0 parameters must be measured independently. Once K_{fs} and α^* are determined, ϕ_{m}, S, PD, NP, and ψ_{f} are calculated using Equation 69.16 through Equation 69.21, recognizing that for this case (field-saturated flow) $K(\psi_0) = K_{\mathrm{fs}}$, $\alpha^*(\psi_0) = \alpha^*$, $\theta(\psi_0) = \theta_{\mathrm{fs}}$, $\theta(\psi_{\mathrm{i}}) = \theta_{\mathrm{i}}$, $PD(\psi_0) = PD$, and $NP(\psi_0) = NP$.

If only K_{fs} is of interest, Equation 76.6a and Equation 76.6c can be simplified to (Elrick and Reynolds 2002)

$$K_{\mathrm{fs}} = \frac{\pi^2 a}{8t_{\mathrm{b}}}\left[\begin{array}{l}\left(1+\dfrac{1}{2A}\right)\ln\left(\dfrac{A^3-1}{A^3-\rho_{\mathrm{b}}{}^3}\right)-\dfrac{3}{2A}\ln\left(\dfrac{A-1}{A-\rho_{\mathrm{b}}}\right)\\ +\dfrac{\sqrt{3}}{A}\left[\arctan\left(\dfrac{A+2\rho_{\mathrm{b}}}{\sqrt{3}A}\right)-\arctan\left(\dfrac{A+2}{\sqrt{3}A}\right)\right]\end{array}\right] \tag{76.7a}$$

$$\rho_b{}^3 = \frac{3(H_0 - H_b)}{a(\theta_{fs} - \theta_i)} + 1 \tag{76.7b}$$

where A is defined by Equation 76.6b and H_b [L] is the measured water level in the casing at time, t_b [T]. In Equation 76.7a and Equation 76.7b, the initial water level at zero time (H_0) is preset by adding a calibrated volume of water to the well, and the α^* parameter is site-estimated using the texture–structure categories in Table 76.1. The simplified K_{fs} calculation thus requires measurements of t_b, H_b, θ_{fs}, and θ_i, remembering that H_0 (i.e., H at $t = 0$) is already known because a calibrated volume of water was added to the well. If the well empties within a reasonable amount of time (due to favorable well dimensions or adequate permeability of the porous medium), it is feasible to set t_b as the time required for the well to empty, in which case $H_b = 0$ in Equation 76.7b and only t_b, θ_{fs}, and θ_i need to be measured. The simplifications also allow K_{fs} to be obtained directly from Equation 76.7a without resorting to simultaneous equation or numerical curve-fitting methods.

Elrick and Reynolds (1986) developed a falling-head analysis for an uncased well, which is derived from the constant-head well permeameter method (Equation 76.3). Although simultaneous determination of K_{fs} and α^* (and thereby ϕ_m, S, ψ_f, PD, and NP as well) is possible with this method, numerical curve fitting to a sequence of H versus t data points is required (i.e., no simplified analytical expressions are available), and steady flow at $H = H_0$ must be attained before the falling-head phase is started. This approach is also susceptible to the sensitivity and heterogeneity problems discussed under the two-head and multiple-head approaches for the constant-head method (Section 76.2).

Further details on the falling-head well permeameter methods can be found in Elrick and Reynolds (1986, 2002), Munoz-Carpena et al. (2002), and Reynolds and Elrick (2005). Example calculations based on Equation 76.6 and Equation 76.7 are given in Figure 76.4 and Table 76.4, respectively.

76.3.3 Comments

1. It is critically important to obtain a watertight seal between the casing and the well wall, as ''short circuit'' flow in this area can cause substantial overestimation of K_{fs} and the capillarity parameters. One way of accomplishing this is to use an auger that fits snugly (1–2 mm clearance) inside a sharpened, thin-walled metal casing, and advance the slightly oversized casing as the well is being dug (see Chapter 79 and Amoozegar 2002 for details). Other possible approaches include applying grease to the outside of the casing, or attaching an inflatable ''packer'' to the base of the casing that can then be expanded once the casing is in place. The measurement should be abandoned if leakage of free water occurs between the casing and well wall.

2. As indicated in Equation 76.7b, H_b can be any value less than H_0, including zero (i.e., empty well), although setting $H_b = 0$ may result in impractically long t_b times. Generally speaking, the most practical H_b values are $\geq H_0/2$. Note also that one can measure the decline in water level using either specified t_b and measured H_b or specified H_b and measured t_b.

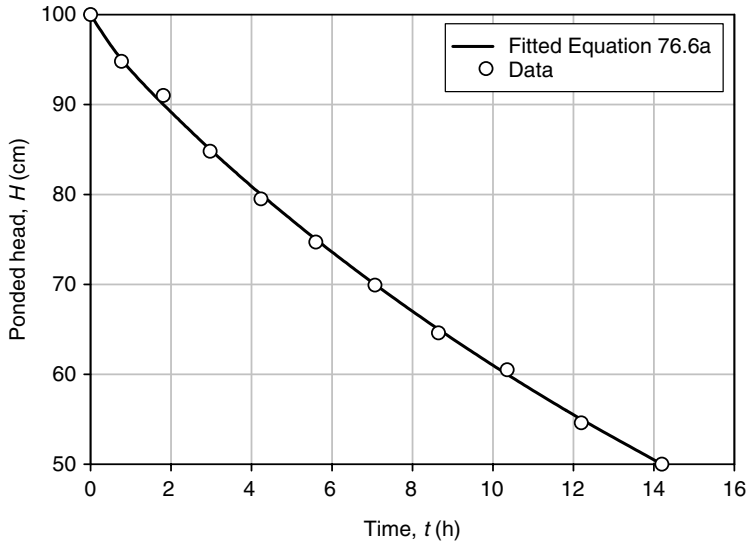

FIGURE 76.4. Curve-fit of Equation 76.6a to H versus t for the falling-head well permeameter method. Input parameters: $a = 2$ cm; $H_0 = 100$ cm; $\Delta\theta = 0.25$. Fitted parameters: $K_{fs} = 2.29 \times 10^{-5}$ cm s^{-1}; $\alpha^* = 0.12$ cm^{-1}. Calculated parameters: $\phi_m = 1.91 \times 10^{-4}$ cm^2 s^{-1} (Chapter 69, Equation 69.16); $\psi_f = -8.3$ cm (Chapter 69, Equation 69.20); $S = 9.31 \times 10^{-3}$ cm s$^{-1/2}$ (Chapter 69, Equation 69.17); $PD = 0.0178$ cm (Chapter 69, Equation 69.18); $NP = 9.51 \times 10^4$ pores per m^2 (Equation 69.19).

3 Equation 76.6 and Equation 76.7 are relatively insensitive to $\Delta\theta$, e.g., a change of a factor of 2 in $\Delta\theta$ often results in less than 20% change in K_{fs}. It may consequently be feasible in some situations (e.g., when only ''ball park'' K_{fs} values are required) to further simplify the method by using a single ''field average'' $\Delta\theta$ rather than individual values. The field average $\Delta\theta$ could be obtained from a series of TDR measurements (Chapter 70), or perhaps even estimated from average texture and antecedent wetness.

TABLE 76.4 Example Data Sheet and K_{fs} Calculation for the Falling-Head Well Permeameter Method, Simplified Analysis (Equation 76.6 and Equation 76.7)

Cumulative time, t (h)		Water height above well base, H (cm)	
0	(t_0)	100	(H_0)
3	(t_b)	85	(H_b)
$A^3 = 665.8044$	(Equation 76.6b)		
$\rho_b{}^3 = 91.0$	(Equation 76.7b)		
$K_{fs} = 2.27 \times 10^{-5}$ cm s^{-1}	(Equation 76.7a)		

Well radius, $a = 2$ cm; well depth, $d = 50$ cm.
Initial ponded head, $H_0 = 100$ cm.
Water volume required to produce $H_0 = 1.257$ L.
Porous material type: structured silt loam soil (estimated $\alpha^* = 0.12$ cm^{-1} from Table 76.1).
$\theta_{fs} = 0.65$; $\theta_i = 0.40$; $\Delta\theta = 0.25$

4 The falling-head cased permeameter method often overestimates K_{fs} and α^* relative to other methods (Munoz-Carpena et al. 2002). The reasons for this are unclear at this time, but may be related to simplifying assumptions in the falling-head theory (Philip 1993), to differing flow geometries and sampling volumes among methods, or to experimental problems such as leakage between the casing and well wall.

REFERENCES

Amoozegar, A. 1992. Compact constant head permeameter: a convenient device for measuring hydraulic conductivity. In G.C. Topp et al., Eds. *Advances in Measurement of Soil Physical Properties: Bringing Theory into Practice*. SSSA Special Publication, 30. Soil Science Society of America, Madison, WI, pp. 31–42.

Amoozegar, A. 1993. Comments on ''Methods for analyzing constant-head well permeameter data.'' *Soil Sci. Soc. Am. J.* 57: 559–560.

Amoozegar, A. 2002. Piezometer method (saturated zone). In J.H. Dane and G.C. Topp, Eds. *Methods of Soil Analysis, Part 4—Physical Methods*. Soil Science Society of America, Madison, WI, pp. 859–878.

Amoozegar, A. and Warrick, A.W. 1986. Hydraulic conductivity of saturated soils: field methods. In A. Klute, Ed. *Methods of Soil Analysis, Part 1—Physical and Mineralogical Methods*. Agronomy 9, Soil Science Society of America, Madison, WI, pp. 758–763.

Amoozegar, A. and Wilson, G.V. 1999. Methods for measuring hydraulic conductivity and drainable porosity. In R.W. Skaggs and J. van Schilfgaarde, Eds. *Agricultural Drainage*. Agron. Monogr. 38. American Society of Agronomy, Crop Science Society of America, and Soil Science Society of America, Madison, WI, pp. 1149–1205.

Ankeny, M.D. 1992. Methods and theory for unconfined infiltration measurements. In G.C. Topp et al., Eds. *Advances in Measurement of Soil Physical Properties: Bringing Theory into Practice*. Soil Science Society of America. Special Publication, 30. Soil Science Society of America, Madison, WI, pp. 123–141.

Bagarello, V. 1997. Influence of well preparation on field-saturated hydraulic conductivity measured with the Guelph permeameter. *Geoderma* 80: 169–180.

Bell, R.W. and Schofield, N.J. 1990. Design and application of a constant head well permeameter for shallow high saturated hydraulic conductivity soils. *Hydrol. Process*. 4: 327–342.

Campbell, C.M. and Fritton, D.D. 1994. Factors affecting field-saturated hydraulic conductivity measured by the borehole permeameter technique. *Soil Sci. Soc. Am. J*. 58: 1354–1357.

Elrick, D.E. and Reynolds, W.D. 1986. An analysis of the percolation test based on three-dimensional, saturated–unsaturated flow from a cylindrical test hole. *Soil Sci*. 142: 308–321.

Elrick, D.E. and Reynolds, W.D. 1992. Methods for analyzing constant-head well permeameter data. *Soil Sci. Soc. Am. J*. 56: 320–323.

Elrick, D.E. and Reynolds, W.D. 1993. Reply to ''Comments on 'Methods for analyzing constant-head well permeameter data' ''. *Soil Sci. Soc. Am. J*. 57: 560–563.

Elrick, D.E. and Reynolds, W.D. 2002. Measuring water transmission parameters in vadose zone using ponded infiltration techniques. *Agri. Sci*. 7: 17–22.

Elrick, D.E., Reynolds, W.D., and Tan, K.A. 1989. Hydraulic conductivity measurements in the unsaturated zone using improved well analyses. *Ground Water Monit. Rev*. 9: 184–193.

Jenssen, P.D. 1989. The constant head percolation test—improved equipment and possibilities of assessing the saturated hydraulic conductivity. In H.J. Morel-Seytoux, Ed. *Unsaturated Flow in Hydrologic Modeling: Theory and Practice*. NATO ASI Series C: Mathematical and Physical Sciences, Vol. 275, Kluwer Academic Publishers, the Netherlands, pp. 481–488.

Koppi, A.J. and Geering, H.R. 1986. The preparation of unsmeared soil surfaces and an improved

apparatus for infiltration measurements. *J. Soil Sci*. 37: 177–181.

Munoz-Carpena, R., Regalado, C.M., Alvarez-Benedi, J., and Bartoli, F. 2002. Field evaluation of the new Philip-Dunne Permeameter for measuring saturated hydraulic conductivity. *Soil Sci*. 167: 9–24.

Philip, J.R. 1985. Approximate analysis of the borehole permeameter in unsaturated soil. *Water Resour. Res*. 21: 1025–1033.

Philip, J.R. 1993. Approximate analysis of falling-head lined borehole permeameter. *Water Resour. Res*. 29: 3763–3768.

Reynolds, W.D. 1993. Saturated hydraulic conductivity: field measurement. In M.R. Carter, Ed. *Soil Sampling and Methods of Analysis*. Canadian Society of Soil Science, Lewis Publishers, Boca Raton, FL, pp. 599–613.

Reynolds, W.D. and Elrick, D.E. 1986. A method for simultaneous in situ measurement in the vadose zone of field-saturated hydraulic conductivity, sorptivity and the conductivity–pressure head relationship. *Ground Water Monit. Rev*. 6: 84–95.

Reynolds, W.D. and Elrick, D.E. 1987. A laboratory and numerical assessment of the Guelph permeameter method. *Soil Sci*. 144: 282–299.

Reynolds, W.D. and Elrick, D.E. 2002. Constant head well permeameters (vadose zone). In J.H. Dane and G.C. Topp, Eds. *Methods of Soil Analysis, Part 4—Physical Methods*. Soil Science Society of America, Madison, WI, pp. 844–858.

Reynolds, W.D. and Elrick, D.E. 2005. Measurement and characterization of soil hydraulic properties. In J. Alvarez-Benedi and R. Munoz-Carpena, Eds. *Soil–Water–Solute Process Characterization: An Integrated Approach*. CRC Press, Boca Raton, FL, pp. 197–252.

Reynolds, W.D., Elrick, D.E., and Clothier, B.E. 1985. The constant head well permeameter: effect of unsaturated flow. *Soil Sci*. 139: 172–180.

Reynolds, W.D., Vieira, S.R., and Topp, G.C. 1992. An assessment of the single-head analysis for the constant head well permeameter. *Can. J. Soil Sci*. 72: 489–501.

Stephens, D.B., Lambert, K., and Watson, D. 1987. Regression models for hydraulic conductivity and field test of the borehole permeameter. *Water Resour. Res*. 23: 2207–2214.

Xiang, J. 1994. Improvements in evaluating constant-head permeameter test data. *J. Hydrol*. 162: 77–97.

Zangar, C.N. 1953. Theory and problems of water percolation. U.S. Department of the Interior, Bureau of Reclamation, Eng. Monogr. No. 8, Denver, CO.

Zhang, Z.F., Groenevelt, P.H., and Parkin, G.W. 1998. The well shape-factor for the measurement of soil hydraulic properties using the Guelph permeameter. *Soil Till. Res*. 49: 219–221.

Chapter 77
Saturated Hydraulic Properties: Ring Infiltrometer

W.D. Reynolds
Agriculture and Agri-Food Canada
Harrow, Ontario, Canada

77.1 INTRODUCTION

The ring infiltrometer methods are used primarily for *in situ* or field measurement of field-saturated hydraulic conductivity, K_{fs} [LT^{-1}], in unsaturated porous materials (e.g., soil). They can also be used, however, for *in situ* determination of the capillarity parameters: matric flux potential, ϕ_m [L^2T^{-1}], sorptive number, α^* [L^{-1}], the effective Green–Ampt wetting front pressure head, ψ_f [L], sorptivity, S [$LT^{-1/2}$], flow-weighted mean pore diameter, PD [L], and the number of PD pores per unit area, NP [L^{-2}]. A discussion of the principles associated with determination of K_{fs} and the capillarity parameters appears in Chapter 69.

Ring infiltrometers are thin-walled, open-ended metal or plastic cylinders with the bottom end sharpened to ease insertion into the porous medium. Most ring infiltrometers are 5–20 cm long by 10–50 cm in diameter, although much smaller and much larger ring diameters have been used for special-purpose applications (e.g., Youngs et al. 1996; Leeds-Harrison and Youngs 1997). Ring infiltrometers are operated by inserting one or more rings into the soil (usually to a depth of 3–10 cm), ponding one or more known heads of water inside the rings, and measuring the rate of water flow out of the rings and into the unsaturated porous medium. Both constant head and falling head analyses are available. Other field methods for measuring K_{fs} and the associated capillarity parameters include the well permeameter (Chapter 76), auger hole (Chapter 78), and piezometer (Chapter 79). Laboratory methods for measuring saturated hydraulic conductivity, K_s, are described in Chapter 75. Selected methods for estimating K_s from surrogate porous medium properties are given in Chapter 84.

The overall strengths of ring infiltrometer methods include: (i) accurate measures of vertical K_{fs}; (ii) simple and robust equipment and procedures; (iii) relatively easy and rapid spatial/temporal replication of measurements; (iv) ability to measure water transmission parameters at the porous medium surface; and (v) widespread acceptance by the science and engineering communities because of long-term usage in a vast range of porous materials. The general weaknesses of ring methods include: (i) difficult use in stony porous media

(rings difficult to insert); (ii) potential disturbance/alteration of the measured porous medium volume during the ring insertion process; (iii) inconvenience for subsurface measurements (relatively large access pits have to be dug); and (iv) capillarity parameter determinations (i.e., ϕ_m, S, α^*, ψ_f, PD, NP) of potentially reduced accuracy because ponded infiltration maximizes the hydrostatic pressure and gravity components of flow at the expense of the capillarity component of flow.

77.2 SINGLE RING INFILTROMETER

The single ring infiltrometer involves inserting a solitary cylinder into unsaturated porous medium, ponding one or more heads of water in the cylinder, and measuring the rate of water flow out of the cylinder and into the porous medium. Data analysis options include the single constant head approach, the multiple constant head approach, and the falling head approach. The single constant head approach involves ponding one constant head of water in the cylinder, and measuring the quasisteady rate of water flow out of the cylinder (Figure 77.1a).

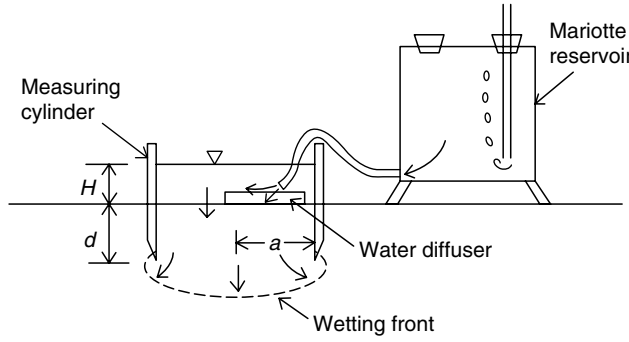

Single ring infiltrometer (cross section)

(a)

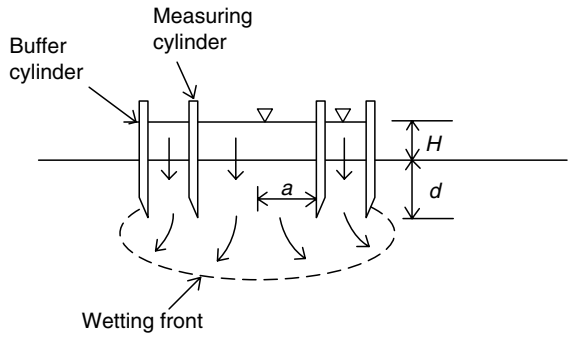

Double or concentric ring infiltrometer (cross section)

(b)

FIGURE 77.1. A single ring constant head infiltrometer (a) and double/concentric ring constant head infiltrometer (b). (From Reynolds, W.D., Elrick, D.E., and Youngs, E.G., in J.H. Dane and G.C. Topp (Eds.), *Methods of Soil Analysis, Part 4—Physical Methods*, Soil Science Society of America, Madison, Wisconsin, 2002. With permission.)

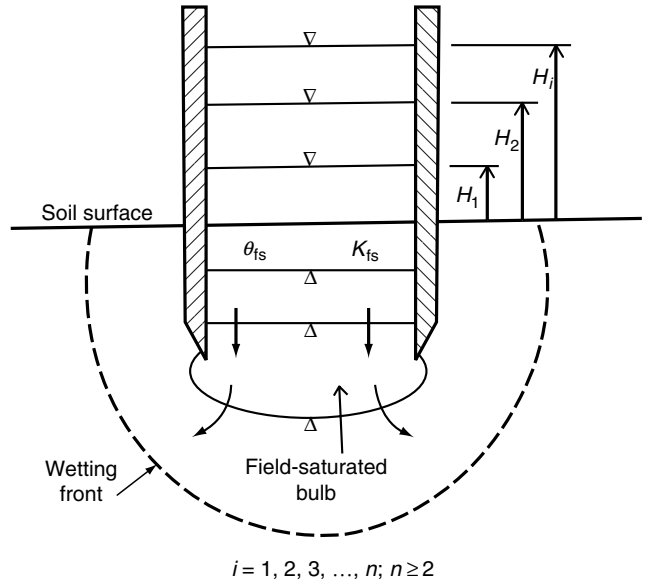

FIGURE 77.2. The single ring, multiple constant head infiltrometer. (From Reynolds, W.D. and Elrick, D.E., in J. Alvarez-Benedi and R. Munoz-Carpena (Eds.), *Soil–Water–Solute Process Characterization: An Integrated Approach*, CRC Press, Boca Raton, Florida, 2005. With permission.)

The multiple constant head approach extends the single head analysis in that it ponds two or more constant heads in succession, and measures the corresponding quasisteady flow rates for each head (Figure 77.2). The falling head approach, on the other hand, monitors the fall of water level with time from an initial ponded head (Figure 77.3), (see also Comment 4 in Section 77.2.3).

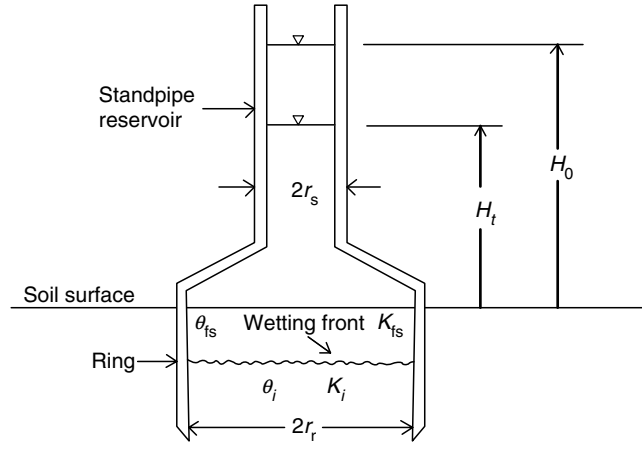

FIGURE 77.3. The single ring, falling head infiltrometer with attached standpipe reservoir. (From Reynolds, W.D. and Elrick, D.E., in J. Alvarez-Benedi and R. Munoz-Carpena (Eds.), *Soil–Water–Solute Process Characterization: An Integrated Approach*, CRC Press, Boca Raton, Florida, 2005. With permission.)

77.2.1 Apparatus and Procedures

1 The single ring infiltrometer is typically 10–20 cm long by 10–50 cm in diameter, although diameters as large as 100 cm are used occasionally (see Comment 1 in Section 77.2.3). The cylinder should be sturdy (e.g., made of metal or high-density plastic), but thin-walled (e.g., 1–5 mm wall thickness) with a sharp outside beveled cutting edge at the base to minimize resistance and porous medium compaction/shattering during cylinder insertion. Using an appropriate insertion technique (e.g., drop-hammer apparatus, hydraulic ram, etc.), insert the cylinder into the porous medium to a depth of 3–10 cm. The cylinder should be held as straight (vertical) as possible during the insertion process to ensure one-dimensional vertical flow through the porous medium. To allow the desired water ponding heights, *H*, the top of the inserted cylinder should either extend to at least the maximum *H*-level above the porous medium surface (Figure 77.1 and Figure 77.2), or the cylinder should be coupled to a standpipe attachment (Figure 77.3) or a Mariotte bottle attachment (Figure 77.4). Scraping, leveling, or similar disturbance

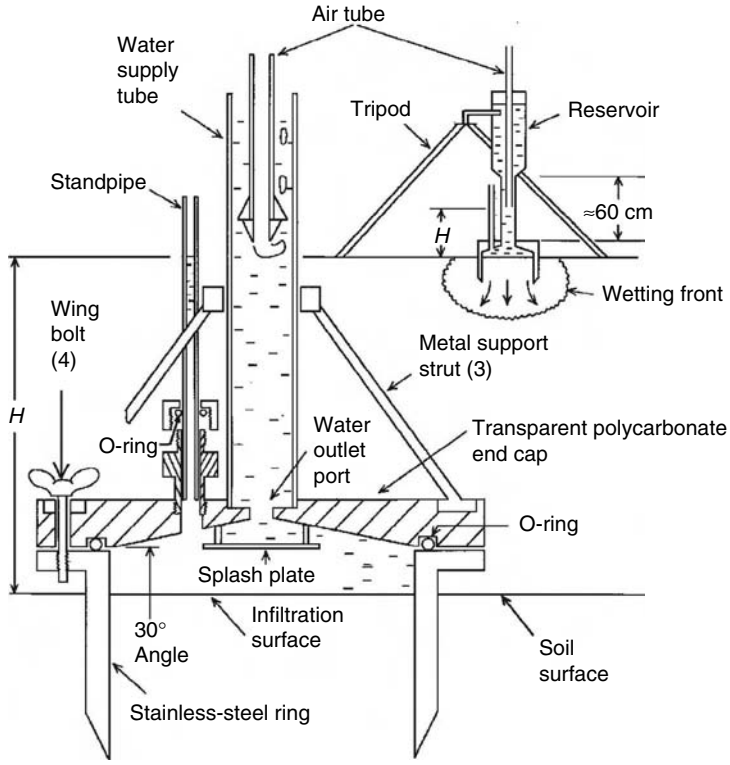

FIGURE 77.4. The single ring "pressure infiltrometer" apparatus, which uses a combined standpipe—Mariotte bottle system to allow single constant head, multiple constant head or falling head analyses. (From Reynolds, W.D., in M.R. Carter (Ed.), *Soil Sampling and Methods of Analysis*, Canadian Society of Soil Science, Lewis Publishers, Boca Raton, Florida, 1993. With permission.)

of the infiltration surface is not recommended, as this may alter the porous medium's hydraulic properties and thereby produce unrepresentative results.

2 Prevent short circuit flow or leakage around the cylinder wall by lightly tamping the contact between the porous medium and the inside surface of the cylinder. Larger gaps between the porous medium and the cylinder wall should be backfilled with powdered bentonite or fine clay.

3 For a single constant head approach, pond a constant head (depth) of water inside the cylinder (H), and monitor the rate at which water infiltrates the porous medium until the infiltration rate becomes steady (Figure 77.1a). The depth of water ponding is usually in the order of 5–20 cm. For the multiple constant head approach, repeat the single head process for each head (H_1, H_2, H_3, ...), starting with the smallest head (i.e., $H_1 < H_2 < H_3 \ldots$) (Figure 77.2). A Mariotte reservoir provides a simple and convenient method for simultaneously maintaining a constant head and measuring the infiltration rate (Figure 77.1a through Figure 77.4); i.e., the height of the Mariotte bubble tube sets the depth of ponding, and the rate of fall of the water level in the Mariotte reservoir can be used to calculate the steady infiltration rate, q_s [LT^{-1}], or discharge rate, Q_s [L^3T^{-1}]. Alternative constant head approaches include the use of a float valve arrangement connected via flexible tubing to a gravity-feed reservoir (often useful for high infiltration rates), and simple manual addition of water (often useful for low infiltration rates). In the manual approach, some kind of pointer or ''hook gauge'' is positioned above the infiltration surface, and when the water surface in the cylinder drops to the pointer/hook gauge level, water is manually added to bring the water surface back up to a preset mark on the cylinder wall. Average infiltration rate in the manual approach is determined using the volume of water added, and the time interval between additions. The depth of water ponding is estimated as the mid-way elevation between the mark on the cylinder wall and the height of the pointer or hook gauge. In the falling head approach, water is quickly added (within a few seconds) to the cylinder to attain the desired initial head, $H = H_0$ at $t = 0$, and then the fall of water level with time (H vs. t) is measured (Figure 77.3).

4 Constant head infiltration through a cylinder into unsaturated porous material normally decreases through an early-time transient and becomes quasisteady within finite time. The time required to reach quasisteady flow (equilibration time), generally increases with finer porous medium texture, decreasing porous medium structure, increasing depth of water ponding (H), increasing depth of cylinder insertion (d), and increasing cylinder radius (a). For the single constant head approach (or the initial head of the multiple constant head approach), equilibration times can be as short as 10–60 min for relatively small cylinders (e.g., 5–10 cm diameter) and/or materials that are coarse textured or well structured (Scotter et al. 1982), to as long as several hours or days for large cylinders (e.g., 30–60 cm diameter and larger) and/or materials, which are moderate to fine textured and unstructured (Scotter et al. 1982; Daniel 1989). Generally speaking, the equilibration times for the succeeding constant heads in the multiple head approach (i.e., H_2, H_3, etc.) are substantially less than that for the initial head (H_1). The falling head approach obviously does not have an equilibration time, as infiltration rate is entirely transient due to the falling head.

77.2.2 Analysis and Example Calculations

Single Constant Head

Calculate K_{fs} using (Reynolds and Elrick 1990)

$$K_{fs} = \frac{q_s}{[H/(C_1 d + C_2 a)] + \{1/[\alpha^*(C_1 d + C_2 a)]\} + 1} \tag{77.1}$$

where $q_s = Q_s/\pi a^2$ [LT^{-1}] is the quasisteady infiltration rate out of the cylinder, Q_s [L^3T^{-1}] is the corresponding quasisteady flow rate, a [L] is the inside radius of the cylinder, H [L] is the steady depth (head) of ponded water in the cylinder, d [L] is the depth of cylinder insertion into the porous medium, α^* [L^{-1}] is the sorptive number of the porous medium (estimated from Chapter 76, Table 76.1 or measured independently—see Comment 2 in Section 77.2.3), and $C_1 = 0.316\pi$ and $C_2 = 0.184\pi$ are dimensionless quasiempirical constants that apply for $d \geq 3$ cm and $H \geq 5$ cm (Reynolds and Elrick 1990; Youngs et al. 1993). Once α^* is estimated and K_{fs} calculated, estimates of ϕ_m, S, PD, NP, and ψ_f can be obtained using Equation 69.16 through Equation 69.21, recognizing that for this case (field-saturated flow) $K(\psi_0) = K_{fs}$, $\alpha^*(\psi_0) = \alpha^*$, $\theta(\psi_0) = \theta_{fs}$, $\theta(\psi_i) = \theta_i$, $PD(\psi_0) = PD$, and $NP(\psi_0) = NP$.

Note in Equation 77.1 that the magnitude of K_{fs} depends not only on flow rate, but also on depth of ponding (H), cylinder radius (a), depth of cylinder insertion (d), and porous medium capillarity (α^*). As a result, the traditional constant head ring infiltrometer analysis,

$$K_{fs} = q_s \tag{77.2}$$

overestimates K_{fs} to varying degrees, depending on the magnitudes of H, a, d, and α^* (Reynolds et al. 2002). The accuracy of Equation 77.2 improves as H decreases, and as a, d, and α^* increase, although d and a must generally be impractically large before Equation 77.2 is sufficiently accurate (Table 77.1).

An example data sheet and calculations based on Equation 77.1 and Equation 77.2 are given in Table 77.1.

TABLE 77.1 Example Data Sheet and K_{fs} Calculation for the Single Ring Infiltrometer Method, Single Constant Head (Equation 77.1 and Equation 77.2)

Cylinder radius, $a = 15$ cm
Depth of cylinder insertion, $d = 5$ cm
Depth of ponding, $H = 10$ cm
Porous material type: Unstructured clay loam soil
(estimated $\alpha^* = 0.04$ cm^{-1}—Table 76.1, Chapter 76)
Quasiempirical constant, $C_1 = 0.316\pi = 0.9927$
Quasiempirical constant, $C_2 = 0.184\pi = 0.5781$
Measured quasisteady infiltration rate, $q_s = Q_s/\pi a^2 = 8.56 \times 10^{-5}$ cm s^{-1}

Extended analysis (Equation 77.1)	***Traditional analysis (Equation 77.2)***
$K_{fs} = 2.40 \times 10^{-5}$ cm s^{-1}	$K_{fs} = 8.56 \times 10^{-5}$ cm s^{-1}

Note: The traditional analysis overestimates the extended analysis by a factor of 3.6. The degree of overestimation by the traditional analysis is systematic and depends on the values of α^*, H, d, and a.

Multiple Constant Head

Ponding two or more constant heads allows simultaneous calculation of both K_{fs} and α^*, i.e., the α^* parameter does not have to be estimated as in the single constant head analysis (see analysis above).

If two heads are ponded, K_{fs} and α^* can be determined using the two simultaneous equations (Reynolds and Elrick 2005)

$$K_{fs} = \frac{T(q_2 - q_1)}{(H_2 - H_1)} \tag{77.3a}$$

$$\alpha^* = \frac{(q_2 - q_1)}{[q_1(H_2 + T) - q_2(H_1 + T)]} \tag{77.3b}$$

where

$$T = C_1 d + C_2 a \tag{77.3c}$$

and q_1 is q_s at H_1; q_2 is q_s at H_2; $q_1 < q_2$; $H_1 < H_2$; and the other parameters are as defined in Equation 77.1.

For two or more ponded heads, q_s is linearly related to H via the relationship (Reynolds and Elrick 2005)

$$q_i = \left(\frac{K_{fs}}{T}\right) H_i + K_{fs}\left[\left(\frac{1}{\alpha^* T}\right) + 1\right]; \quad i = 2, 3, 4, \ldots, n; \quad n \geq 2 \tag{77.4a}$$

where T is given by Equation 77.3c. Least squares fitting procedures can consequently be used to obtain K_{fs} from the regression *slope*,

$$K_{fs} = T \times slope \tag{77.4b}$$

and α^* from the regression *intercept*,

$$\alpha^* = K_{fs}/[T(intercept - K_{fs})] \tag{77.4c}$$

of the q_i vs. H_i data points (q_i on Y-axis; H_i on X-axis). Once K_{fs} and α^* are determined, the capillarity parameters, ϕ_m, S, PD, NP, and ψ_f are calculated using Equation 69.16 through Equation 69.21, recognizing that for this case (field-saturated flow) $K(\psi_0) = K_{fs}$, $\alpha^*(\psi_0) = \alpha^*$, $\theta(\psi_0) = \theta_{fs}$, $\theta(\psi_i) = \theta_i$, $PD(\psi_0) = PD$, and $NP(\psi_0) = NP$. Note that Equation 77.3 and Equation 77.4 yield identical results for two ponded heads because linear regression is equivalent to simultaneous equations when only two q_s vs. H data points are used.

Example data sheets and calculations based on Equation 77.3 and Equation 77.4 are given in Table 77.2.

Falling Head

Falling head infiltration through a solitary cylinder into unsaturated porous material can be described by (Elrick et al. 2002)

TABLE 77.2 Example Data Sheet and Calculation of K_{fs} and the Capillarity Parameters for the Single Ring Infiltrometer Method, Multiple Constant Heads (Equation 77.3 and Equation 77.4)

Cylinder radius, $a = 15$ cm
Depth of cylinder insertion, $d = 5$ cm
Steady depth of ponding, H: $H_1 = 5$ cm, $H_2 = 10$ cm, $H_3 = 20$ cm
Porous material type: Structured loam soil
Quasiempirical constant, $C_1 = 0.316\pi = 0.9927$
Quasiempirical constant, $C_2 = 0.184\pi = 0.5781$
$T = C_1 d + C_2 a = 13.635$
$\theta_{fs} = 0.65$, $\theta_i = 0.40$
Measured quasisteady infiltration rates, q_s:
$q_1 = 6.53 \times 10^{-4}$ cm s^{-1}, $q_2 = 7.74 \times 10^{-4}$ cm s^{-1}, $q_3 = 10.16 \times 10^{-4}$ cm s^{-1}

***Two-head analysis* (*Equation* 77.3)**	***Regression analysis* (*Equation 77.4*)**
Using (H_1, q_1) and (H_3, q_3)	Regress q_1, q_2, q_3 (Y-axis) against H_1, H_2, H_3 (X-axis)
$K_{fs} = 3.3 \times 10^{-4}$ cm s^{-1} (Equation 77.3a)	Regression *slope* $= 2.42 \times 10^{-5}$ s^{-1}
$\alpha^* = 0.12$ cm^{-1} (Equation 77.3b)	Regression *intercept* $= 5.32 \times 10^{-4}$ cm s^{-1}
	$K_{fs} = 3.3 \times 10^{-4}$ cm s^{-1} (Equation 77.4b)
	$\alpha^* = 0.12$ cm^{-1} (Equation 77.4c)
$\phi_m = K_{fs}/\alpha^* = 2.75 \times 10^{-3}$ cm^2 s^{-1}	(Chapter 69, Equation 69.16)
$\psi_f = -1/\alpha^* = -8.3$ cm	(Chapter 69, Equation 69.20)
$S = [\gamma(\theta_{fs} - \theta_i)\phi_m]^{1/2} = 3.54 \times 10^{-2}$ cm s$^{-1/2}$	(Chapter 69, Equation 69.17)
$PD = 0.0178$ cm	(Chapter 69, Equation 69.18)
$NP = 1.37 \times 10^6$ pores m^{-2}	(Chapter 69, Equation 69.19)

For the S calculation, $\gamma = 1.818$ was assumed.
For the PD and NP calculations, $\sigma = 72.75$ g s^{-2}; $\rho = 0.9982$ g cm^{-3} (20°C); $g = 980.621$ cm s^{-2}; $\mu = 1.002$ g cm^{-1}s^{-1} (20°C).

Note: In this example, the two-head analysis produces the same result regardless of which combination of two (H, q) data pairs is used. The regression analysis can also be used when only two (H, q) data pairs are available.

$$t = \frac{\Delta\theta}{CK_{fs}}\left[\frac{R(H_0 - H_t)}{\Delta\theta} - \frac{\left(H_0 + \frac{1}{\alpha^*}\right)}{C}\ln\left(1 + \frac{CR(H_0 - H_t)}{\Delta\theta\left(H_0 + \frac{1}{\alpha^*}\right)}\right)\right]; \quad C \neq 0 \qquad (77.5)$$

where t [T] is the time since initiation of ponded infiltration, $\Delta\theta = (\theta_{fs} - \theta_i)$ [L^3L^{-3}] is the difference between the field-saturated volumetric water content (θ_{fs}) and the antecedent volumetric water content (θ_i) of the porous medium, $C = 1 - (\Delta\theta/R) = \text{constant}$, H_0 is the depth of ponding at $t = 0$, H_t [L] is the depth of ponding at time, t, and $R = A_s/A_c$ is the cross-sectional area of the standpipe reservoir ($A_s = \pi r_s^2$) divided by the cross-sectional area of the cylinder ($A_c = \pi r_c^2$) (Figure 77.3). Note that Equation 77.5 is both implicit and nonlinear in H_t, and, as a result, simultaneous determination of K_{fs} and α^* is best achieved by curve-fitting the equation to a sequence H_t vs. t data points using numerical optimization procedures (e.g., Figure 77.5). The $\Delta\theta$, R, and H_0 parameters in Equation 77.5 must be measured independently, although $R = 1$ if water is ponded directly in the cylinder without using a standpipe reservoir. Once K_{fs} and α^* are obtained, ϕ_m, S, PD, NP, and ψ_f are determined using Equation 69.16 through Equation 69.21 (see Figure 77.5).

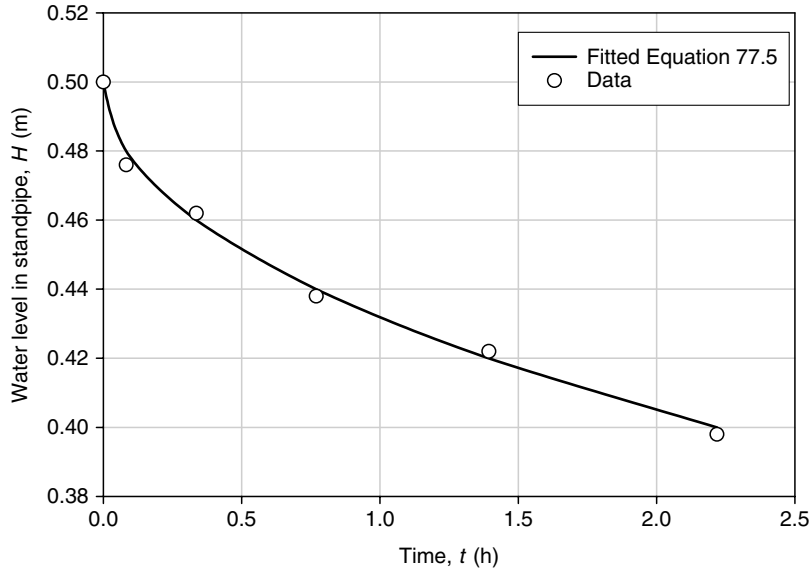

FIGURE 77.5. Curve-fit of Equation 77.5 to H vs. t data for the falling head ring infiltrometer method. Input parameters $\Delta\theta = 0.50$; $R = 0.0278$; $C = -16.9856$; $H_0 = 0.50$ m. Fitted parameters: $K_{fs} = 1.41 \times 10^{-7}$ cm s^{-1}; $\alpha^* = 0.04$ cm^{-1}. Calculated parameters: $\phi_m = 3.53 \times 10^{-6}$ cm^2 s^{-1} (Chapter 69, Equation 69.16); $\psi_f = -25$ cm (Chapter 69, Equation 69.20); $S = 1.79 \times 10^{-3}$ cm s$^{-1/2}$ (Chapter 69, Equation 69.17); $PD = 0.0059$ cm (Chapter 69, Equation 69.18); $NP = 4.85 \times 10^4$ pores m^{-2} (Chapter 69, Equation 69.19).

If K_{fs} is the primary interest, Equation 77.5 can be rewritten in the form (Bagarello et al. 2003)

$$K_{fs} = \frac{\Delta\theta}{Ct_a}\left[\frac{R(H_0 - H_a)}{\Delta\theta} - \frac{\left(H_0 + \dfrac{1}{\alpha^*}\right)}{C}\ln\left(1 + \frac{CR(H_0 - H_a)}{\Delta\theta\left(H_0 + \dfrac{1}{\alpha^*}\right)}\right)\right]; \quad C \neq 0 \qquad (77.6)$$

where H_a [L] is the measured standpipe water level at time, t_a [T]. The initial standpipe water level at zero time (i.e., H_0) is preset by adding a calibrated volume of water to the reservoir, and the α^* parameter is estimated using the texture–structure categories in Table 76.1. These simplifications reduce the number of required measurements to only three (i.e., H_a, t_a, and $\Delta\theta$), and also allow K_{fs} to be obtained directly from Equation 77.6 without resorting to numerical optimization procedures. Even further simplification can be achieved when it is feasible to allow the standpipe water level to fall all the way to the porous medium surface to produce $H_a = 0$ at $t = t_a$. Equation 77.6 can then be solved for K_{fs} using only two measurements (t_a and $\Delta\theta$) because H_a is now 0. An example data sheet and calculation based on Equation 77.6 is given in Table 77.3.

77.2.3 Comments

1 Bouma (1985) suggests that the volume encompassed by a ring infiltrometer (i.e., infiltration surface area multiplied by depth of ring insertion) must include at least 20 structural units (e.g., soil peds delineated by a polygonal cracking pattern,

TABLE 77.3 Example Data Sheet and K_{fs} Calculation for the Single Ring Infiltrometer Method, Simplified Falling Head Analysis (Equation 77.6)

Cylinder radius, $r_c = 15$ cm
Depth of cylinder insertion, $d = 10$ cm
Standpipe (reservoir) radius, $r_s = 2.5$ cm
Initial ponded head, $H_0 = 50$ cm
Porous material type: Unstructured clay loam soil (estimated $\alpha^* = 0.04$ cm^{-1}—Table 76.1, Chapter 76)
$\theta = 0.70$; $\theta_i = 0.20$

Cumulative time, t (s)		Water level in standpipe, H (cm)	
0	(t_0)	50	(H_0)
8000	(t_a)	40	(H_a)

$R = A_s/A_c = \pi r_s^2/\pi r_c^2 = 0.0278$
$\Delta\theta = \theta_{fs} - \theta_i = 0.50$
$C = 1 - (\Delta\theta/R) = -16.9856$
$K_{fs} = 1.41 \times 10^{-7}$ cm s^{-1} (Equation 77.6)

large aggregates, worm holes, abandoned root channels, etc.) before representative measures of water transmission parameters are obtained. Limited field data in Youngs (1987), Lauren et al. (1988), Richards (1987), and Bouma (1985) suggest that cylinder diameters need to be ≥5–10 cm for single-grain sandy material and uniform structureless materials (e.g., compacted landfill liners); ≥30 cm for stony/heterogeneous sands, structured sandy loams, and structured silty loams; and ≥50 cm for structured clays and clay loams.

2 Estimation (rather than measurement) of α^* using the texture–structure categories in Table 76.1 (Chapter 76) may introduce some error into the single constant head and simplified falling head calculations (Equation 77.1 and Equation 77.6), given that α^* varies continuously with porous medium capillarity. The error (or potential for error) can be decreased, however, by reducing the importance of the α^* terms in Equation 77.1 and Equation 77.6 relative to the other terms. For the single constant head approach (Equation 77.1), the importance of the α^* term is reduced by making the cylinder radius (a), and the water ponding depth (H) as large as practicable. For the simplified falling head approach (Equation 77.6), the importance of the α^* terms is reduced by making both H_0 and H_a as large as practicable. The maximum potential error introduced in K_{fs} by estimating α^* via Table 76.1 can be determined by recalculating Equation 77.1 or Equation 77.6 using the α^* category immediately above and immediately below the selected category. The categories in Table 76.1 are broad enough that visual estimation of the appropriate category will not likely be in error by more than ±1 category. If the estimated maximum potential error in K_{fs} (and corresponding capillarity parameters) is unacceptably large, then the importance of the α^* terms should be further reduced, or an alternative analysis used, such as the multiple head approach (Equation 77.3 or Equation 77.4), or the complete falling head approach (Equation 77.5). Incorrect estimation of α^* by ±1 texture–structure category in Table 76.1 generally introduces an error of ≤50% and capillarity parameter calculations, which is usually of no great concern given the high natural variability of these parameters.

3 The falling head analysis (Equation 77.5 and Equation 77.6) is based on the Green–Ampt model for transient ponded infiltration, which assumes

one-dimensional vertical flow with a step-function wetting front that is horizontal, stable, and downward migrating (Guyonnet et al. 2000; Reynolds and Elrick 2005). The falling head analysis consequently requires that the wetting front remain distinct, horizontal, and within the cylinder during the falling head measurements (i.e., no divergent flow out through the bottom of the cylinder). As a result, the falling head method is often not practical in coarse textured and highly structured materials (e.g., coarse and medium single-grain sands; loams and clays with many shrinkage cracks and biopores), as the wetting front either reaches the base of the cylinder too quickly to allow sufficient H vs. t measurements, or the wetting front is unstable and discontinuous (due to preferential or finger flow). An approximation of the maximum time available for H vs. t measurements can be obtained from

$$t_d = \frac{\Delta\theta}{CK_{fs}}\left[d - \frac{\left(H_0 + \frac{1}{\alpha^*}\right)}{C}\ln\left(1 + \frac{Cd}{\left(H_0 + \frac{1}{\alpha^*}\right)}\right)\right]; \quad H_0 > \frac{\Delta\theta}{R}d \tag{77.7}$$

where t_d [T] is the time required for the Green-Ampt wetting front to migrate from the infiltration surface to the base of the cylinder, d [L] is the depth of cylinder insertion, and the other parameters are as previously defined. The constraint on H_0 in Equation (77.7) ensures that the standpipe does not run dry before d is reached. Equation (77.7) is applied by specifying R, H_0 and d, and then calculating t_d for likely values (or likely ranges) of $\Delta\theta$, C, K_{fs} *and* α^*.

4 The so-called ''pressure infiltrometer'' is a convenient and commercially available apparatus (Soilmoisture Equipment Corp., Goleta, CA) that is capable of applying the single constant head, multiple constant head, and falling head approaches to single ring infiltrometer measurements. The apparatus consists essentially of a Mariotte-based dual reservoir system (one small inner reservoir for slow flows located inside a larger outer reservoir for rapid flows), and an end cap that clamps onto the infiltrometer cylinder (Figure 77.4). During operation, water flows out of the reservoir, through the end cap, and into the cylinder. The Mariotte system can be engaged (Mariotte bottle mode) to apply the single constant head or multiple constant head approaches, or it can be disengaged (standpipe mode) to apply the falling head approach. Infiltration rates are determined by measuring the rate of fall of the water level in the inner or outer reservoir. Detailed discussions of the apparatus and its application appear in Reynolds (1993) and Reynolds et al. (2002), where the equations provided are different forms of those given here.

5 Strengths of the steady (constant head) analyses include reasonably accurate and robust determination of vertical K_{fs}, extensive field testing, relatively simple measurements (q_s, H, d, a, α^*), and relatively large sample volume (often comparable to ring volume). Weaknesses of the steady analyses include potentially long equilibration times and extensive water consumption for large rings or highly structured/permeable porous materials. Exacerbating these weaknesses is the fact that ring diameters may need to be $\geq$10 cm in single-grain sands and uniform structureless materials, $\geq$30 cm in heterogeneous sands and structured loams, and $\geq$50 cm in structured clays and clay loams to obtain truly representative measures of K_{fs} and the capillarity parameters. The main strengths of the transient (falling

head) analyses (relative to steady analyses) include reduced measurement time (especially in low-permeability soils) and potentially simpler equipment. Weaknesses of the transient analyses include potentially small sample volume (sampled volume depends on the rate of wetting front migration and measurement duration), the need to measure $\Delta\theta$, which requires separate collection of soil samples or use of expensive *in situ* techniques (e.g., see TDR; Chapter 70), and questionable usability in coarse textured and/or highly structured porous materials (due to rapid flow and potentially unstable wetting fronts).

77.3 OTHER RING INFILTROMETER METHODS

Other important ring infiltrometer methods include the ''double'' or ''concentric'' ring infiltrometer, the ''twin'' or ''dual'' ring infiltrometer, the ''multiple'' ring infiltrometer, and the ''air-entry'' permeameter.

The double/concentric ring infiltrometer consists of an inner ''measuring'' cylinder placed concentrically inside an outer ''guard'' or ''buffer'' cylinder (Figure 77.1b). It is an established ASTM standard method, where the measuring cylinder and buffer cylinder have set diameters of 30 and 60 cm, respectively (Lukens 1981). Inclusion of the outer buffer cylinder is an attempt to improve the accuracy of Equation 77.2 by reducing flow divergence under the measuring cylinder, which results from ponding (H), finite cylinder radius (a), and porous medium capillarity (α^*). However, laboratory sand tank studies (Swartzendruber and Olsen 1961) and numerical simulation studies (Wu et al. 1997; Smettem and Smith 2002) have shown that the double ring system still systematically overestimates K_{fs} when Equation 77.2 is applied, although the degree of overestimation tends to be decreased somewhat relative to the single ring infiltrometer. The overestimate continues to occur because the physical barrier provided by the outer buffer cylinder is not effective for eliminating flow divergence. There is consequently no real advantage gained by using the double ring infiltrometer over the single ring infiltrometer, and Equation 77.2 should be avoided regardless of cylinder arrangement.

The twin/dual ring and multiple ring infiltrometers employ adjacent cylinders with a single constant head (H) but different cylinder diameters. Two adjacent cylinders are used in the twin ring system, and three or more adjacent cylinders are used in the multiple ring system. The cylinders are typically 5–50 cm in diameter by 5–20 cm long, and are installed individually (not concentrically as in the double ring infiltrometer) with just enough separation to prevent the wetting fronts from merging before steady infiltration is achieved. Both infiltrometer systems can determine K_{fs}, ϕ_m, S, α^*, ψ_f, PD, and NP (via constant head steady flow analyses); however, they are not widely used because they are more labor-intensive than the single ring approaches (e.g., two or more cylinders vs. one cylinder) and they are highly sensitive to lateral heterogeneity. Further detail on the twin ring and multiple ring infiltrometer methods can be found in Scotter et al. (1982), Reynolds et al. (2002), and Reynolds and Elrick (2005).

The air-entry permeameter includes a single cylinder connected to a constant head reservoir. The method estimates K_{fs} and α^* from measurements of the constant head infiltration rate (q_s), the time (t_f) required for the wetting front to reach a specified depth within the cylinder (wetting front depth, z_f, must be less than or equal to the cylinder insertion depth, d), and an estimate of the Green–Ampt wetting front pressure head (ψ_f), which is based on a measurement of the porous medium's air-entry pressure head (ψ_a). This method is not extensively used because of

awkward and delicate equipment, somewhat complicated procedures, and frequent difficulty in estimating z_f and ψ_f accurately. Further information on the air-entry permeameter method can be found in Topp and Binns (1976) and Reynolds and Elrick (2005).

REFERENCES

Bagarello, V., Iovino, M., and Elrick, D.E. 2003. A simplified falling-head technique for rapid determination of field-saturated hydraulic conductivity. *Soil Sci. Soc. Am. J.* 68: 66–73.

Bouma, J. 1985. Soil variability and soil survey. In J. Bouma and D.R. Nielsen, Eds. *Proc. Soil Spatial Variability Workshop*. PUDOC, Wageningen, The Netherlands, pp. 130–149.

Daniel, D.E. 1989. *In situ* hydraulic conductivity tests for compacted clay. *J. Geotech. Eng.* 115: 1205–1226.

Elrick, D.E., Angulo-Jaramillo, R., Fallow, D.J., Reynolds, W.D., and Parkin, G.W. 2002. Infiltration under constant head and falling head conditions. In P.A.C. Raats, D. Smiles, and A.W. Warrick, Eds. *Environmental Mechanics: Water, Mass and Energy Transfer in the Biosphere*. Geophysical Monograph 129, American Geophysical Union, Washington, DC, pp. 47–53.

Guyonnet, D., Amraoui, N., and Kara, R. 2000. Analysis of transient data from infiltrometer tests in fine-grained soils. *Ground Water* 38: 396–402.

Lauren, J.G., Wagenet, R.J., Bouma, J., and Wösten, J.H.M. 1988. Variability of saturated hydraulic conductivity in a Glassaquic Hapludalf with macropores. *Soil Sci.* 145: 20–28.

Leeds-Harrison, P.B. and Youngs, E.G. 1997. Estimating the hydraulic conductivity of soil aggregates conditioned by different tillage treatments from sorption measurements. *Soil Till. Res.* 41: 141–147.

Lukens, R.P. Ed. 1981. *Annual Book of ASTM Standards, Part 19: Soil and Rock*. American Standards of Materials and Testing. Washington, DC, pp. 509–514.

Reynolds, W.D. 1993. Saturated hydraulic conductivity: field measurement. In M.R. Carter, Ed. *Soil Sampling and Methods of Analysis*. Canadian Society of Soil Science. Lewis Publishers, Boca Raton, FL, pp. 605–611.

Reynolds, W.D. and Elrick, D.E. 1990. Ponded infiltration from a single ring: I. Analysis of Steady Flow. *Soil Sci. Soc. Am. J.* 54: 1233–1241.

Reynolds, W.D. and Elrick, D.E. 2005. Measurement and characterization of soil hydraulic properties. In J. Alvarez-Benedi and R. Munoz-Carpena, Eds. *Soil–Water–Solute Process Characterization: An Integrated Approach*. CRC Press, Boca Raton, FL, pp. 197–252.

Reynolds, W.D., Elrick, D.E., and Youngs, E.G. 2002. Ring or cylinder infiltrometers (vadose zone). In J.H. Dane and G.C. Topp, Eds. *Methods of Soil Analysis, Part 4—Physical Methods*. Soil Science Society of America, Madison, WI, pp. 818–843.

Richards, N.E. 1987. A comparison of three methods for measuring hydraulic properties of field soils. MSc thesis. University of Guelph, Guelph, ON, Canada.

Scotter, D.R., Clothier, B.E., and Harper, E.R. 1982. Measuring saturated hydraulic conductivity and sorptivity using twin rings. *Aust. J. Soil Res.* 20: 295–304.

Smettem, K.R.J. and Smith, R.E. 2002. Field measurement of infiltration parameters. In R.E. Smith, Ed. *Infiltration Theory for Hydrologic Applications*. Water Resources Monograph 15, American Geophysical Union, Washington, DC, pp. 135–157.

Swartzendruber, D. and Olsen, T.C. 1961. Model study of the double ring infiltrometer as affected by depth of wetting and particle size. *Soil Sci.* 92: 219–225.

Topp, G.C. and Binns, M.R. 1976. Field measurements of hydraulic conductivity with a modified air-entry permeameter. *Can. J. Soil Sci.* 56: 139–147.

Wu, L., Pan, L., Robertson, M.L., and Shouse, P.J. 1997. Numerical evaluation of ring-infiltrometers under various soil conditions. *Soil Sci.* 162: 771–777.

Youngs, E.G. 1987. Estimating hydraulic conductivity values from ring infiltrometer measurements. *J. Soil Sci.* 38: 623–632.

Youngs, E.G., Elrick, D.E., and Reynolds, W.D. 1993. Comparison of steady flows from infiltration rings in ''Green and Ampt'' soils and ''Gardner'' soils. *Water Resour. Res.* 29: 1647–1650.

Youngs, E.G., Spoor, G., and Goodall, G.R. 1996. Infiltration from surface ponds into soils overlying a very permeable substratum. *J. Hydrol.* 186: 327–334.

Chapter 78
Saturated Hydraulic Properties: Auger Hole

G. Clarke Topp
Agriculture and Agri-Food Canada
Ottawa, Ontario, Canada

78.1 INTRODUCTION

The auger-hole method is a field technique for measuring the *in situ* saturated hydraulic conductivity, K_s [LT^{-1}], of porous materials within the saturated zone (i.e., below the water table); and it is perhaps the most reliable and trusted means of obtaining K_s values for the design of subsurface tile drainage systems. An alternative *in situ* method for K_s measurement in the saturated zone is given in Chapter 79 (piezometer), while several laboratory and estimation techniques for K_s determination are given in Chapter 75 and Chapter 84, respectively. A discussion of the principles and parameters associated with the determination of K_s appears in Chapter 69.

The auger-hole method is based on an application of Darcy's law (Chapter 69) where the initial equilibrium or ''static'' water level in the auger hole (the static water level is usually equivalent to the water table level) is rapidly raised or lowered, and then the recovery to the static level is monitored through time as water flows between the auger hole and the surrounding porous material. The method and most of the equipment are similar to the piezometer method (Chapter 79).

The K_s value is determined using (Boast and Kirkham 1971; Youngs 2001)

$$K_s = C_{AH}\frac{\Delta y}{\Delta t} \tag{78.1}$$

where Δy (cm) is the change in water level in the auger hole (relative to the initial static water level) during time interval, Δt (s), and C_{AH} is a dimensionless shape factor. The C_{AH} parameter is related to the radius of the auger hole, r_c, the depth of the auger hole below the static water level, H, and the depth from the base of the auger hole to an impermeable or highly permeable porous medium layer, F (Figure 78.1). The C_{AH} values can be obtained

Auger-hole data sheet			
Location:		Date:	
Site:		Operator:	
Notes:			
$T = 19°C$	$h_c = 27$ cm	$r_c = 5$ cm	$r = 3.65$ cm
$F' = \infty$	$F = (F' - D - E) = \infty$		$F/H = \infty$

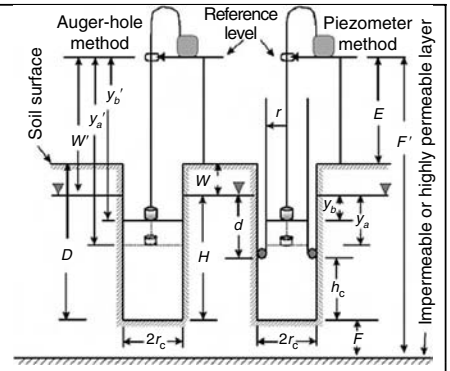

$W' = 49$ cm	$E = 41$ cm	$W = (W' - E) = 8$ cm		$W' =$ cm	$E =$ cm	$W = (W' - E) =$ cm	
$D = 50$ cm	$H = (E + D - W') = 42$ cm		$y_i = (y_i' - E)$	$D =$ cm	$H = (E + D - W') =$ cm		$y_i = (y_i' - E)$
i	t (s)	y' (cm)	$\Delta y/\Delta t$	i	t (s)	y' (cm)	$\Delta y/\Delta t$
1	0	85.5		1			
2	15	84.8	0.0467	2			
3	30	84.1	0.0467	3			
4	45	83.4	0.0467	4			
5	60	82.7	0.0467	5			
6	75	82.1	0.04	6			
$t_b - t_a = 75$	$(y_a' - y_b') = 85.5 - 82.1$		0.0453	$t_b - t_a =$	$(y_a' - y_b') =$		
$H/r_c = 8.4$		Average $y/H = 0.829$		$H/r_c =$		Average $y/H =$	
$C_{AH} = 25.1 \times 10^{-3}$	$K_s = C_{AH}(y_a' - y_b')/(t_b - t_a)$ cm s^{-1}			$C_{AH} =$	$K_s = C_{AH}(y_a' - y_b')/(t_b - t_a)$ cm s^{-1}		
$K_s = 1.14 \times 10^{-3}$ cm s^{-1}				$K_s =$		cm s^{-1}	

FIGURE 78.1. Data sheet for the auger-hole method, including schematic diagrams of the equipment for the auger-hole method and the piezometer method (Chapter 79).

from Table 78.1 (Boast and Kirkham 1971; Youngs 2001), or from graphs (van Beers 1970; Bouwer and Jackson 1974), or empirical equations (Ernst 1950; Amoozegar 2002).

The auger hole must be large enough to sample a sufficient volume of porous medium to yield representative K_s values. Unfortunately, the complexity of both the flow regime and auger hole geometry precludes a precise determination of the volume of porous medium sampled, although it is clear that the porous material adjacent to the wall and base of the auger hole exerts by far the greatest influence on the results. Generally speaking, the larger the auger hole diameter, the more representative the K_s measurements; and auger hole diameters of 10 cm or more are typical. Most analyses assume flat-bottomed auger holes (i.e., right cylindrical geometry), and it is generally recommended that the bottom of the hole be at least 30 cm below the static water level (water table).

The basic procedure for making an auger-hole measurement is as follows: (i) auger a hole that extends to at least 30 cm below the static water level; (ii) allow the water in the auger

TABLE 78.1 Values of $C_{AH} \times 10^3$ for the Auger-Hole Method (Equation 78.1) with an Underlying Impermeable or Highly Permeable Layer[a]

		F/*H* for underlying impermeable layer								*F*/*H*	*F*/*H* for underlying impermeable or highly permeable layer			
H/r_c	*y*/*H*	0	0.05	0.1	0.2	0.5	1	2	5	∞	5	2	1	0.5
1	1	518	490	468	435	375	331	306	296	295	292	280	247	193
	0.75	544	522	503	473	418	376	351	339	338	335	322	287	230
	0.5	643	623	605	576	521	477	448	441	440	437	416	376	306
2	1	215	204	193	178	155	143	137	135	133	133	131	123	106
	0.75	227	216	208	195	172	160	154	152	152	151	148	140	123
	0.5	271	261	252	240	218	203	196	194	194	193	190	181	161
5	1	60.2	56.3	53.6	49.6	44.9	42.8	41.9		41.5		41.2	40.1	37.6
	0.75	63.6	60.3	57.9	54.3	49.5	47.6	46.6		46.4		45.9	44.8	42.1
	0.5	76.7	73.5	71.1	67.4	62.5	60.2	59.1		58.8		58.3	57.1	54.1
10	1	21.0	19.6	18.7	17.5	16.4	15.8	15.5		15.5		15.4	15.2	14.6
	0.75	22.2	21.0	20.2	19.1	18.0	17.4	17.2		17.2		17.1	16.8	16.2
	0.5	27.0	25.9	24.9	23.9	22.6	22.0	21.8		21.7		21.6	21.3	20.6
20	1	6.86	6.41	6.15	5.87	5.58	5.45	5.40		5.38		5.36	5.31	5.17
	0.75	7.27	6.89	6.65	6.38	6.09	5.97	5.90		5.89		5.88	5.82	5.67
	0.5	8.90	8.51	8.26	7.98	7.66	7.52	7.44		7.44		7.41	7.35	7.16
50	1	1.45	1.37	1.32	1.29	1.24	1.22			1.21			1.19	1.18
	0.75	1.54	1.47	1.42	1.39	1.35	1.32			1.31			1.30	1.28
	0.5	1.90	1.82	1.79	1.74	1.69	1.67			1.66			1.65	1.61
100	1	0.43	0.41	0.39	0.39	0.38	0.37			0.37			0.32	0.36
	0.75	0.46	0.44	0.42	0.42	0.41	0.41			0.41			0.39	0.39
	0.5	0.57	0.54	0.52	0.52	0.51	0.51			0.51			0.50	0.50

Source: From Boast, C.W. and Kirkham, D., *Soil Sci. Soc. Am. Proc.* 35, 365, 1971, as modified by Youngs, E.G., in K.A. Smith and C.E. Mullins (Eds.), *Soil and Environmental Analysis: Physical Methods*, 2nd ed., Marcel Dekker, New York, New York, 2001, 157–160.

[a] r_c = Radius of the auger hole, H = depth of water in the hole at static level, y = average distance from the water level in the hole to the static level for two consecutive measurements, and F = distance from the bottom of the borehole to an impermeable or highly permeable layer.

hole to equilibrate to the static level; (iii) add or remove water from the auger hole to initiate water flow into or out of the hole; and (iv) monitor the early-time change in water level in the auger hole as it reequilibrates to the static level.

78.2 APPARATUS AND SUPPLIES

1 *Soil auger(s) of 10 cm diameter or larger.* A variety of designs are available for specific porous medium conditions; for example, ''dutch/mud'' augers are often best in clayey soils, while ''bucket/sand'' or ''screw'' augers are usually best for sandy and stony soils. Once a hole is augered to the desired depth, a ''planer'' auger can be used to produce the flat bottom assumed in the auger hole analysis (see e.g., Figure 29.11 in Amoozegar and Warrick 1986).

2 *Equipment for producing a rapid change in auger hole water level.* This usually involves rapid addition or removal of water. Rapid removal of water from the auger hole is easily achieved using a bailer or water pump (e.g., Figure 3.2.1.6 in Young 2002). If a pump is used, it should have a pumping rate > 0.5 L s^{-1} so that water level decline occurs quickly. Rapid addition of water can be accomplished by simply pouring water into the hole (see Comment 3 in Section 78.5). If addition or removal of water is problematic, a rapid initial increase in water level can be produced by quickly submerging a ''slug'' (see Procedure 5; Comment 3, Section 78.5).

3 *Timer.* A stopwatch or equivalent timer (graduated in seconds) for timing the rise or fall of the water level in the auger hole.

4 *Water level measuring device.* Several possibilities exist depending either on the rate of rise or fall of the water level. If water level change is relatively slow (e.g., <1 mm s^{-1}), manual readings are often made using electric water level tapes, ''popper'' tapes, or float systems (e.g., Figure 3.2.1.7 in Young 2002). A particularly convenient float system consists of a ''Styrofoam'' cylinder attached to the end of a flexible metal measuring tape (Figure 78.1), as it allows the tape to extend straight up out of the hole past a conveniently selected datum or reference level. If the rate of water level change is greater than about 3 mm s^{-1}, it may be necessary to use fast-acting automated systems, such as a quick-response pressure transducer placed at the bottom of the hole and connected to a data logger (e.g., Figure 3.2.1.8 in Young 2002).

5 *Hole liner.* For porous materials that are unstable when saturated (e.g., saturated sands, silts, and organic soils), it may be necessary to line the auger hole with a length of thin-walled perforated pipe (e.g., a section of well screen) to prevent caving before or during the measurement.

6 *Data sheet.* A one-page data sheet similar to the one presented in Figure 78.1 will speed up data collection, and also facilitate accurate, on-site calculation of K_s. The form of Figure 78.1 can be modified to suit individual needs and alternative K_s calculation methods.

78.3 PROCEDURE

1 *Bore the auger hole.* Using the optimum auger for the porous medium (e.g., bucket auger, dutch auger, screw auger, etc.), bore a hole with minimum disturbance

to at least 30 cm below the static water level. It is important to minimize smearing and compaction of the borehole wall, and to achieve right cylindrical geometry (i.e., cylindrical cross section, flat bottom), which may require use of a planer auger.

2 *Initial data collection*. Allow adequate time for the water level in the auger hole to ''equilibrate'' (rise or fall) to the static water level. Measure the auger hole radius in the measurement zone (r_c). Set a reference level or datum (E) at a convenient height centered above the hole. Measure the depth of the auger hole (D) and the depth to the static water level ($W = W' - E$) (Figure 78.1). Estimate the depth from the bottom of the auger hole to any effectively impermeable (or highly permeable) layer ($F = F' - D - E$) from existing information or other boreholes near the measurement site (the error in K_s resulting from ''guesstimating'' $F < 3\%$ for cases where $H/r_c \geq 5$ and $F/H \geq 1$). Determine the initial depth of water in the auger hole ($H = D - W$), and calculate the H/r_c and F/H values. Record the above information in the appropriate locations on the data sheet (Figure 78.1).

3 *Condition the auger hole*. To minimize the effect of auger-induced smearing and compaction of the auger hole wall and base, bail or pump the hole dry several times until the water removed no longer contains appreciable suspended silt and clay. Water removed during this ''conditioning'' process should be disposed of several meters from the hole to prevent rapid re-entry via overland flow or infiltration. After the auger hole has been conditioned, allow the water in the hole to re-equilibrate to the static water level.

4 *Decide on a data collection strategy*. This step collects data for $(\Delta y'/\Delta t)$ or $(\Delta y/\Delta t)$ (Figure 78.1). Using $\Delta y' = (y'_i - y'_{i+1})$ and $\Delta t = (t_{i+1} - t_i)$ is convenient for water level rise, where $i = 0, 1, 2, \ldots$. Time intervals should be long enough to allow a water level change >1 cm per interval, but short enough that several measurements can be made while $y/H \geq 0.5$. Intervals of 10–20 s are usually optimal.

5 *Produce a rapid change in water level*. Once the water level returns to its static level after the auger hole conditioning process, quickly lower or raise the water level in the hole to initiate water level change. Lowering the water level is achieved using a ''bailer'' or pump (e.g., Figure 3.2.1.6 in Young 2002) to remove water; raising the water level by a known distance can be accomplished by rapidly submerging a ''slug'' (solid cylinder of known volume suspended on a rope), or by simply adding water to the borehole. Water removal or use of a slug is usually preferred over water addition (see Comment 3 in Section 78.5). Dispose removed water well away from the auger hole (or place it in a container) so that it cannot perturb the measurements by re-entering the auger hole or disturbing the static water level.

6 *Record the rate of water level rise or fall*. Quickly place the water level recorder in the auger hole and initiate monitoring the change in water level with time (some water level recording systems, e.g., pressure transducers, can be placed in the auger hole before step 5). Record t_i and y'_i as illustrated in Figure 78.1, and attempt to obtain several values before $y/H = 0.5$. At least five times of water level readings are recommended. Step 5 and step 6 can be repeated to obtain additional or confirming measurements.

78.4 CALCULATIONS

1 Calculate $\Delta y/\Delta t$ following the example on the left in Figure 78.1. These values are expected to decrease monotonically with time for water level rise. If $\Delta y/\Delta t$ is constant or decreasing consistently, then either a single timing interval or multiple timing intervals may be chosen for the next step.

2 Choose a time interval $(t_b - t_a)$ and corresponding $(y_a' - y_b')$, then calculate $\Delta y/\Delta t$, the average y/H, and H/r_c (see Figure 78.1). Note that the average water level depth relative to the static level for two consecutive measurements is $y = [(y_a' + y_b')/2] - W'$.

3 Estimate C_{AH} from Table 78.1 using graphical interpolation for maximum accuracy.

4 Calculate K_s using Equation 78.1; calculate C_{AH} and $\Delta y/\Delta t$, as illustrated in Figure 78.1.

78.5 COMMENTS

1 The auger-hole method offers a reliable and relatively rapid procedure for determining the K_s of a relatively large volume of porous material in the saturated zone (Amoozegar 2002). For large values of H/r_c, the auger-hole method approaches a measure of the horizontal K_s. Amoozegar (2002) provides a detailed method for using the auger-hole method in layered soils.

2 The example calculation given in Figure 78.1 uses Table 78.1 to find C_{AH} via linear interpolation between adjacent table entries. The C_{AH} coefficient is not linearly dependent on H/r_c and y/H, however, and greater precision in C_{AH} is usually obtained via nonlinear graphical interpolation based on simulation modeling results and quasiempirical regression relationships. For the example in Figure 78.1, applying nonlinear graphical interpolation resulted in a 20% reduction in K_s relative to linear interpretation, which may or may not be important depending on the intended K_s application. Nonlinear graphical interpolation of the C_{AH} values in Table 78.1 is recommended for maximum K_s accuracy (see van Beers 1970; Bouwer and Jackson 1974).

3 In principle, the auger-hole method works equally well regardless of whether the rise or fall of water is recorded. Adding water to the hole to achieve a decline in water level is not recommended, however, as rapid addition of water may introduce silt and clay into suspension (e.g., through erosion of the borehole wall); and this entrained material can cause progressive siltation (partial plugging) of the auger hole and thereby result in unrepresentative low K_s values.

4 The terms ''highly permeable layer'' and ''impermeable layer'' in Figure 78.1 do not indicate absolute K_s values or ranges, but rather large differences in K_s relative to the K_s of the zone being measured. For example, Amoozegar (2002) specifies that an ''impermeable layer'' has K_s, that is $\leq$20% of the K_s in the zone being measured.

REFERENCES

Amoozegar, A. 2002. Auger-hole method (saturated zone). In J.H. Dane and G.C. Topp, Eds. *Methods of Soil Analysis, Part 4—Physical Methods.* Soil Science Society of America, Madison, WI, pp. 859–869.

Amoozegar, A. and Warrick, A.W. 1986. Hydraulic conductivity of saturated soils: field methods. In A. Klute, Ed. *Methods of Soil Analysis, Part 1: Physical and Mineralogical Methods*, 2nd ed. Soil Science Society of America, Madison, WI, pp. 735–770.

Boast, C.W. and Kirkham, D. 1971. Auger hole seepage theory. *Soil Sci. Soc. Am. Proc.* 35: 365–373.

Bouwer, H. and Jackson, R.D. 1974. Determining soil properties. In J. van Schilfgaarde, Ed. *Drainage for Agriculture*. American Society of Agronomy, Madison, WI, pp. 611–672.

Ernst, L.F. 1950. Een nieuwe formule voor de berekening van de doorlaatfactor met deboorgatenmethode. Groningen, The Netherlands. Rap. Landbouwproefsta. en Bodemkundig Inst. T.N.O.

van Beers, W.F.J. 1970. The auger-hole method: a field measurement of the hydraulic conductivity of soil below the water table. International Institute for Land Reclamation and Improvement (ILRI), Bull No. 1. H. Veenman and Zonen, Wageningen, the Netherlands.

Young, M.H. 2002. Water Potential. In J.H. Dane and G.C. Topp, Eds. *Methods of Soil Analysis, Part 4—Physical Methods*. Soil Science Society of America, Madison, WI, pp. 547–573.

Youngs, E.G. 2001. Hydraulic conductivity of saturated soils. In K.A. Smith and C.E. Mullins, Eds. *Soil and Environmental Analysis: Physical Methods*, 2nd ed. Marcel Dekker, New York, NY, pp. 157–160.

Chapter 79
Saturated Hydraulic Properties: Piezometer

G. Clarke Topp
Agriculture and Agri-Food Canada
Ottawa, Ontario, Canada

79.1 INTRODUCTION

The piezometer method is a well-established field technique for measuring the *in situ* saturated hydraulic conductivity, K_s [LT^{-1}], of porous materials within the saturated zone (i.e., below the water table). An alternative *in situ* method for K_s measurement in the saturated zone is given in Chapter 78 (Auger Hole), while several laboratory and estimation techniques for K_s determination are given in Chapter 75 and Chapter 84, respectively. A discussion of the principles and parameters associated with the determination of K_s appears in Chapter 69.

The piezometer method measures K_s through an open-ended pipe or casing inserted into a borehole that extends into the saturated zone of a confined or an unconfined aquifer (Figure 79.1). The pipe may extend to the bottom of the borehole, or it may terminate above the bottom leaving a cylindrical ''piezometer cavity'' (Figure 79.1). Often the borehole is flat-bottomed, although other shapes can be used (Youngs 1968). It is important that the pipe is sealed against the borehole wall so that leakage or short-circuit flow along the outside wall of the pipe is prevented (Figure 79.1). The principle of piezometer operation is the same as that of the auger-hole method (Chapter 78), which is explained as follows: first, it consists of allowing the water level in the piezometer pipe to equilibrate to the static or equilibrium water level, then quickly changing the water level in the pipe (usually by adding or removing water), and then monitoring the return of the water level back to the static level. The static water level is the water table elevation in unconfined aquifers, and the phreatic surface in confined aquifers.

For water level rise in the piezometer, the saturated hydraulic conductivity is given by (Figure 79.1)

$$K_s = \frac{\pi r^2 \ln(y_a/y_b)}{C_P(t_b - t_a)} \tag{79.1}$$

Piezometer data sheet			
Location:	Date:		
Site:	Operator:		
Notes:			
T = 19°C	h_c = 27 cm	r_c = 5 cm	r = 3.65 cm
$F' = \infty$	$F = (F' - D - E) = \infty$	$F/H = \infty$	

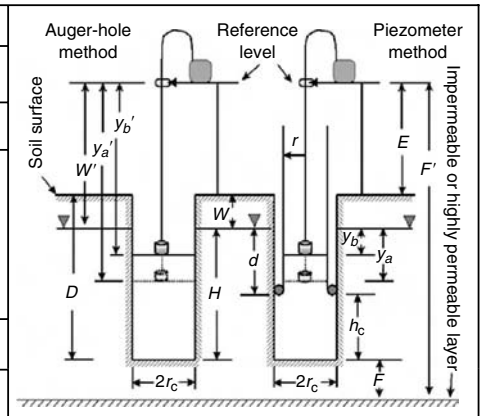

W' = 51.5 cm	E = 44 cm	$W = (W' - E)$ = 7.5 cm	W' = cm	E = cm	$W = (W' - E)$ = cm		
$d = (H - h_c) = (E + D - W' - h_c)$ = 57 cm		$y_i = (y_i' - E)$	$d = (H - h_c) = (E + D - W' - h_c)$ = cm			$y_i = (y_i' - E)$	

I	t (s)	y' (cm)	y_i (cm)	y_i / y_{i+1}	I	t (s)	y' (cm)	y_i (cm)	y_i / y_{i+1}
1	0	95	51	1.06	1				
2	60	92.3	48.3	1.06	2				
3	120	89.7	45.7	1.05	3				
4	180	87.6	43.6	1.06	4				
5	240	85	41	1.06	5				
6	300	82.8	38.8		6				

$t_b - t_a$ = 300	y_b / y_a = 51/38.8 = 1.31	$\ln(y_b/y_a)$ = 0.273	$t_b - t_a$ =	y_b / y_a =	$\ln(y_b/y_a)$ =	
h_c / r_c = 7.4	d / r_c = 15.6	$F / r_c = \infty$	h_c / r_c =	d / r_c =	F / r_c =	
C_P / r_c = 27	$K_s = \pi r^2 \ln(y_b/y_a) / C_P (t_b - t_a)$ (cm s^{-1})		C_P / r_c =	$K_s = \pi r^2 \ln(y_b/y_a) / C_P (t_b - t_a)$ (cm s^{-1})		
C_P = 7.40	$K_s = 9.65 \times 10^{-3}$ cm s^{-1}		C_P =	K_s = cm s^{-1}		

FIGURE 79.1. Data sheet for the piezometer method, including schematic diagrams of the equipment for the piezometer method and the auger-hole method (Chapter 78).

where y_a and y_b are the water depths below the static level at times t_a and t_b, respectively; r is the inside radius of the pipe, and C_P is a shape factor (Table 79.1) that depends on the height of the static water level above the end of the pipe (d), on the length (h_c), on the radius (r_c) of the piezometer cavity, and on the distance below the bottom of the borehole to a layer of greatly different hydraulic conductivity (F) (Youngs 1968, 2001; Amoozegar 2002).

79.2 APPARATUS AND SUPPLIES

1 *Soil augers of 10 cm diameter or larger.* A variety of designs are available for specific porous medium conditions; for example, ''dutch/mud'' augers are often best for clayey soils, while ''bucket/sand'' or ''screw'' augers are usually best for

TABLE 79.1 Values of C_P/r_c for the Piezometer Method (Equation 79.1) with an Impermeable or Highly Permeable Layer below the Borehole[a]

		F/r_c for impermeable layer							F/r_c for highly permeable layer						
h_c/r_c	d/r_c	∞	8.0	4.0	2.0	1.0	0.5	0	∞	8.0	4.0	2.0	1.0	0.5	0
0	20	5.6	5.5	5.3	5.0	4.4	3.6	0	5.6	5.6	5.8	6.3	7.4	10.2	∞
	16	5.6	5.5	5.3	5.0	4.4	3.6	0	5.6	5.6	5.8	6.4	7.5	10.3	∞
	12	5.6	5.5	5.4	5.1	4.5	3.7	0	5.6	5.7	5.9	6.5	7.6	10.4	∞
	8	5.7	5.6	5.5	5.2	4.6	3.8	0	5.7	5.7	5.9	6.6	7.7	10.5	∞
	4	5.8	5.7	5.6	5.4	4.8	3.9	0	5.8	5.8	6.0	6.7	7.9	10.7	∞
															∞
0.5	20	8.7	8.6	8.3	7.7	7.0	6.2	4.8	8.7	8.9	9.4	10.3	12.2	15.2	∞
	16	8.8	8.7	8.4	7.8	7.0	6.2	4.8	8.8	9.0	9.4	10.3	12.2	15.2	∞
	12	8.9	8.8	8.5	8.0	7.1	6.3	4.8	8.9	9.1	9.5	10.4	12.2	15.3	∞
	8	9.0	9.0	8.7	8.2	7.2	6.4	4.9	9.0	9.3	9.6	10.5	12.3	15.3	∞
	4	9.5	9.4	9.0	8.6	7.5	6.5	5.0	9.5	9.6	9.8	10.6	12.4	15.4	∞
															∞
1.0	20	10.6	10.4	10.0	9.3	8.4	7.6	6.3	10.6	11.0	11.6	12.8	14.9	19.0	∞
	16	10.7	10.5	10.1	9.4	8.5	7.7	6.4	10.7	11.0	11.6	12.8	14.9	19.0	∞
	12	10.8	10.6	10.2	9.5	8.6	7.8	6.5	10.8	11.1	11.7	12.8	14.9	19.0	∞
	8	11.0	10.9	10.5	9.8	8.9	8.0	6.7	11.0	11.2	11.8	12.9	14.9	19.0	∞
	4	11.5	11.4	11.2	10.5	9.7	8.8	7.3	11.5	11.6	12.1	13.1	15.0	19.0	∞
															∞
2.0	20	13.8	13.5	12.8	11.9	10.9	10.1	9.1	13.8	14.1	15.0	16.5	19.0	23.0	∞
	16	13.9	13.6	13.0	12.1	11.0	10.2	9.2	13.9	14.3	15.1	16.6	19.1	23.1	∞
	12	14.0	13.7	13.2	12.3	11.2	10.4	9.4	14.0	14.4	15.2	16.7	19.2	23.2	∞
	8	14.3	14.1	13.6	12.7	11.5	10.7	9.6	14.3	14.8	15.5	17.0	19.4	23.3	∞
	4	15.0	14.9	14.5	13.7	12.6	11.7	10.5	15.0	15.4	16.0	17.6	20.1	23.8	∞
															∞
4.0	20	18.6	18.0	17.3	16.3	15.3	14.6	13.6	18.6	19.8	20.8	22.7	25.5	29.9	∞
	16	19.0	18.4	17.6	16.6	15.6	14.8	13.8	19.0	20.0	20.9	22.8	25.6	29.9	∞
	12	19.4	18.8	18.0	17.1	16.0	15.1	14.1	19.4	20.3	21.2	23.0	25.8	30.0	∞
	8	19.8	19.4	18.7	17.6	16.4	15.5	14.5	19.8	20.6	21.4	23.3	26.0	30.2	∞
	4	21.0	20.5	20.0	19.1	17.8	17.0	15.8	21.0	21.5	22.2	24.1	26.8	31.5	∞

(continued)

TABLE 79.1 (continued) Values of C_P/r_c for the Piezometer Method (Equation 79.1) with an Impermeable or Highly Permeable Layer below the Borehole[a]

		F/r_c for impermeable layer							F/r_c for highly permeable layer						
h_c/r_c	d/r_c	∞	8.0	4.0	2.0	1.0	0.5	0	∞	8.0	4.0	2.0	1.0	0.5	0
															∞
8.0	20	26.9	26.3	25.5	24.0	23.0	22.2	21.4	26.9	29.6	30.6	32.9	36.1	40.6	∞
	16	27.4	26.6	25.8	24.4	23.4	22.7	21.9	27.4	29.8	30.8	33.1	36.2	40.7	∞
	12	28.3	27.2	26.4	25.1	24.1	23.4	22.6	28.3	30.0	31.0	33.3	36.4	40.8	∞
	8	29.1	28.2	27.4	26.1	25.1	24.4	23.4	29.1	30.3	31.2	33.8	36.9	41.0	∞
	4	30.8	30.2	29.6	28.0	26.9	25.7	24.5	30.8	31.5	32.8	35.0	38.4	43.0	∞

Source: From Youngs, E.G., *Soil Sci.*, 106, 235, 1968.

[a] d = Length of piezometer pipe below the static water level, r_c = radius of the piezometer cavity, h_c = length of the piezometer cavity, and F = depth from the base of the piezometer cavity to an impermeable or highly permeable layer (see Figure 79.1).

sandy and stony soils. Once a hole is augered to the desired depth, a ''planer'' auger can be used to produce the flat bottom assumed in the piezometer analysis (see e.g., Figure 29.11 in Amoozegar and Warrick 1986).

2 *Equipment for producing a rapid change in piezometer water level*. This usually involves rapid addition or removal of water. Rapid water removal is easily achieved using a bailer or water pump (see e.g., Figure 3.2.1.6 in Young 2002). If a pump is used, it should have a pumping rate >0.5 L s^{-1} so that water level decline occurs quickly. Water addition involves simply pouring water into the piezometer pipe, although this approach is not recommended (see Comment 3 in Section 79.5). One can also change the piezometer water level by quickly lowering a ''slug'' (solid cylinder of known volume) into the piezometer to displace the water level a known distance upward, or quickly removing a slug (after the static level is reestablished) to displace the water level a known distance downward.

3 *Timer*. A stopwatch or equivalent timer (graduated in seconds) for timing the rise or fall of water in the pipe.

4 *Water level measuring device*. Several possibilities exist depending somewhat on the rate of rise or fall of the water level. If water level change is relatively slow (e.g., <1 mm s^{-1}), manual readings are often made using electric water level tapes, ''popper'' tapes, or float systems (see e.g., Figure 3.2.1.7 in Young 2002). A particularly convenient float system consists of a Styrofoam cylinder attached to the end of a flexible metal measuring tape (Figure 79.1), as it allows the tape to extend straight up out of the piezometer past a conveniently selected datum or reference level. If the rate of water level change is greater than about 3 mm s^{-1}, it may be necessary to use fast-acting automated systems, such as a quick-response pressure transducer placed at the bottom of the hole and connected to a data logger (see e.g., Figure 3.2.1.8 in Young 2002).

5 *Piezometer pipe*. Two types of piezometer pipes are used: (i) a thin-walled, open-ended pipe with the same internal diameter as the auger diameter (most frequently used) and (ii) a pipe similar to the above but smaller diameter and fitted with an inflatable packer (sealing device) at the bottom end (see e.g., Figure 79.1). Topp and Sattlecker (1983) describe two types of packers for use in the piezometer method.

6 *Data sheet*. A one-page data sheet similar to the one presented in Figure 79.1 will speed up data collection, and also facilitate accurate, on-site calculation of K_s. The form of Figure 79.1 can be modified to suit individual needs and alternative K_s calculation methods.

79.3 PROCEDURE

79.3.1 Piezometer Pipe Fitted with a Packer

1 *Excavate the borehole*. Using an appropriate auger, bore an oversized hole with minimum disturbance to a depth of at least 30 cm plus depth h_c (Figure 79.1)

below the static water level (as mentioned above, the static level is the water table level for an unconfined aquifer and the phreatic surface level for a confined aquifer). The borehole should be sufficiently oversized to allow easy insertion of the deflated packer, as well as insertion of a water level monitoring device (e.g., electric water level tape) down the annulus between the piezometer pipe and the borehole wall (see step 2). The piezometer cavity should be devoid of smearing and compaction, and have a right cylindrical shape (i.e., circular cross section, flat bottom).

2 *Install the piezometer pipe*. Insert the pipe into the hole to depth, *d*, below the static water level and inflate the packer (Figure 79.1). Allow the water level to equilibrate to the static level on both the inside and outside of the pipe. Check the packer seal by raising the water level on the inside of the pipe (by adding water) and then monitoring the water level on the outside of the pipe using a water level monitoring device (e.g., electric water level tape, popper tape). The packer seal leaks if the water level outside the pipe starts rising (within a couple of minutes or less) above the static level; and if this occurs the packer must be reset or replaced. Once the integrity of the packer seal is verified, allow the static water level to re-establish on both the inside and outside of the piezometer pipe.

79.3.2 Piezometer Pipe without Packer

1 *Excavate the hole*. Bore a 10–20 cm deep vertical hole with the auger and push the sharpened end of the piezometer pipe into the hole. Insert the auger into the piezometer pipe and excavate an additional 10–15 cm from beneath the end of the pipe. Remove the auger and soil cuttings from the pipe and push the pipe into the freshly excavated section of the borehole. Repeat the above steps until the bottom end of the pipe is at the desired depth, *d*, below the static water level (Figure 79.1).

2 *Excavate the piezometer cavity*. Using the auger, excavate the piezometer cavity to the desired distance, h_c, below the end of the inserted pipe (Figure 79.1).

79.3.3 Piezometer with or without Packer

1 *Initial data collection*. Allow adequate time for the water level in the piezometer pipe to ''equilibrate'' (rise or fall) to the static water level. Record both the radius of the piezometer cavity (r_c) and the inside radius of the pipe (r) (if different from r_c such as when a packer system is used) on the data sheet (Figure 79.1). Set a measurement reference level or datum (E) at a convenient position above the piezometer pipe. Measure the length of the piezometer cavity (h_c) and the depth to the static water level ($W = W' - E$) (Figure 79.1). Measure the depth from the static water level to the bottom of the piezometer pipe (d). Determine the initial depth of water in the borehole ($H = D - W$). Estimate the depth to any effectively impermeable (or highly permeable) layer below the borehole ($F = F' - D - E$) from existing information or by borings at nearby locations. Note that the terms ''highly permeable layer'' and ''impermeable layer'' in Figure 79.1 do not

indicate absolute K_s values or ranges, but rather large differences in K_s relative to the K_s of the layer or zone being measured (see Chapter 78 for further detail). Enter the above data in the data sheet (Figure 79.1); calculate and record the d/r_c, h_c/r_c, and F/r_c values.

2 *Condition the piezometer cavity*. To minimize the effect of auger-induced smearing and compaction of the piezometer cavity, bail or pump the piezometer dry several times until the water removed no longer contains appreciable suspended silt and clay (this process is known as ''conditioning''). Water removed in this process should be disposed off several meters from the piezometer to prevent rapid re-entry of the water via overland flow or infiltration. After the piezometer cavity has been conditioned, allow the water in the piezometer to re-equilibrate to the static water level.

3 *Decide on a data collection strategy*. Before collecting the y_i and t_i data ($i = 0, 1, 2, \ldots$), conduct preliminary trial and error tests to establish an appropriate timing interval (i.e., $\Delta t = t_{i+1} - t_i$). The timing interval should be long enough to allow a water level change of more than 1 cm (for accurate water level measurements), but also short enough that several measurements can be made before the water returns to its static level. Timing intervals of 10–20 s are often adequate.

4 *Produce a rapid change in water level*. Once the water level has returned to its static position after conditioning the piezometer cavity, quickly lower or raise the water level in the pipe using a bailer, pump, slug, or by water addition (see Comment 3 in Section 79.5). Dispose removed water far away from the piezometer (or place it in a container) so that it cannot perturb the results by affecting the static water level during the measurement period.

5 *Record the rate of water level rise or fall*. Quickly place the water level recorder in the piezometer and initiate monitoring the change in water level with time (some water level recording systems, for example, fast-response pressure transducers, can be placed in the piezometer before step 6). Record t_i and y_i' as illustrated in Figure 79.1, and attempt to obtain several readings before the water level returns to the static level. At least five times of the water level readings are recommended. Step 6 and step 7 can be repeated to obtain additional or confirming measurements.

79.4 CALCULATIONS

1 Calculate y_i and (y_i/y_{i+1}) following the example in Figure 79.1. These values should decrease monotonically with time if water was initially removed from the piezometer. If (y_i/y_{i+1}) is constant or decreasing consistently, either constant or variable time intervals may be chosen for step 2 below. If (y_i/y_{i+1}) shows a consistent pattern, it is advisable to use a large time interval to minimize measurement error.

2 Choose an appropriate time interval, $\Delta t = (t_b - t_a)$, and measure the corresponding y_a and y_b values.

3 Estimate C_P/r_c from Table 79.1 and calculate C_P.

4 Calculate K_s using Equation 79.1, C_P, $(t_b - t_a)$, and (y_a/y_b). Note that this calculation produces K_s in cm s^{-1} (Figure 79.1).

79.5 COMMENTS

1 The length of the piezometer cavity, h_c, determines whether the measured K_s represents the horizontal, three-dimensional, or vertical saturated hydraulic conductivity within the measurement zone. When h_c is relatively large (e.g., $4r_c \leq h_c \leq 8r_c$), the measured K_s primarily represents the horizontal hydraulic conductivity of the porous material adjacent to the piezometer cavity. As h_c approaches r_c, the measured K_s becomes a combination of the horizontal and vertical hydraulic conductivity, and when $h_c = 0$, K_s represents the vertical hydraulic conductivity of the porous medium along the bottom of the piezometer pipe. Topp and Sattlecker (1983) developed a packing device by which the horizontal and vertical K_s of a shallow aquifer can be measured in a single borehole via the piezometer method.

2 The piezometer method is not practical for rocky and gravelly soils, as advancing a piezometer pipe or establishing a seal between the pipe and the soil are usually problematic. The packing devices depicted by Topp and Sattlecker (1983) can be used provided the seal to the wall of the borehole is sufficient to prevent appreciable short-circuit flow (leakage) past the packer. To speed the process of installing deep piezometers, bore an oversized hole (i.e., a borehole larger than the outside diameter of the piezometer pipe or inflated packer) to just above the water table. Lower the piezometer pipe into the borehole and then continue installation through the bottom of the oversized borehole using the procedures described above. If a packer system is not being used, the gap between the piezometer pipe and the oversized borehole should be backfilled with excavated material and/or bentonite to assure stability of the pipe.

3 It is recommended that the initial change in piezometer water level is produced by rapid water removal or use of a slug, rather than by rapid water addition. Water addition may introduce silt and clay into suspension, which in turn can cause progressive siltation (partial plugging) of the piezometer cavity and thereby unrepresentatively low K_s results.

REFERENCES

Amoozegar, A. 2002. Piezometer method (saturated zone). In J.H. Dane and G.C. Topp, Eds. *Methods of Soil Analysis, Part 4—Physical Methods*. Soil Science Society of America, Madison, WI, pp. 870–877.

Amoozegar, A. and Warrick, A.W. 1986. Hydraulic conductivity of saturated soils: field methods. In A. Klute, Ed. *Methods of Soil Analysis, Part 1: Physical and Mineralogical Methods*, 2nd ed. Soil Science Society of America, Madison, WI, pp. 735–770.

Topp, G.C. and Sattlecker, S. 1983. A rapid measurement of horizontal and vertical components of saturated hydraulic conductivity. *Can. J. Agric. Eng*. 25: 193–197.

Young, M.H. 2002. Water Potential. In J.H. Dane and G.C. Topp, Eds. *Methods of Soil Analysis,*

Part 4—Physical Methods. Soil Science Society of America, Madison, WI, pp. 547–573.

Youngs, E.G. 1968. Shape factors for Kirkham's piezometer method for determining the hydraulic conductivity of soil in situ for soils overlying an impermeable floor or infinitely permeable stratum. *Soil Sci*. 106: 235–237.

Youngs, E.G. 2001. Hydraulic conductivity of saturated soils. In K.A. Smith and C.E. Mullins, Eds. *Soil and Environmental Analysis: Physical Methods*, 2nd ed. Marcel Dekker, New York, NY, pp. 160–164.

Chapter 80
Unsaturated Hydraulic Conductivity: Laboratory Tension Infiltrometer

F.J. Cook

Commonwealth Scientific and Industrial Research Organization

Indooroopilly, Queensland, Australia

80.1 INTRODUCTION

The laboratory tension or disk infiltrometer method is used primarily to measure ''near-saturated'' sorptivity, $S(\psi)$ [$LT^{-1/2}$], and hydraulic conductivity, $K(\psi)$ [LT^{-1}], in the laboratory on undisturbed (intact) cores retrieved from the field. It is also usable, however, for the determination of near-saturated desorption or imbibition curves, $\theta(\psi)$ [L^3L^{-3}], sorptive number, $\alpha^*(\psi)$ [L^{-1}], flow-weighted mean pore diameter, $PD(\psi)$ [L], and the number of flow-weighted mean pores per unit area, $NP(\psi)$ [L^{-2}] (see Chapter 69 for details). By near-saturated, we mean measurements at pore water matric heads (ψ) in the range $\approx -100 \text{ mm} \leq \psi \leq 0$ (Ward and Hayes 1991).

In essence, the laboratory tension infiltrometer method involves collecting an intact core of unsaturated porous material, setting the core on a perforated platform or constant head device (e.g., Buchner funnel), and then setting a tension infiltrometer on top of the core and measuring either early-time transient infiltration (sorptivity measurement) or steady-state infiltration (hydraulic conductivity measurement) under a constant matric head, ψ_0. The method uses the CSIRO tension infiltrometer (Figure 80.1) and a modification of the analysis developed by Clothier and White (1981).

An alternative laboratory core method for $K(\psi)$ determination in the ''wet end'' (i.e., $-7000 \leq \psi \leq -100$ mm) is given in Chapter 81. Field (*in situ*) methods for $K(\psi)$ or $S(\psi)$ determination are given in Chapter 82 and Chapter 83. Selected methods for estimating $K(\psi)$ from surrogate porous medium properties are given in Chapter 84. A discussion of the principles and parameters associated with the determination of $K(\psi)$ and the capillarity relationships [i.e., $S(\psi)$, $\alpha^*(\psi)$, $PD(\psi)$, $NP(\psi)$] appear in Chapter 69. Given that flow from the laboratory tension infiltrometer is confined by the core to one dimension, the measured $K(\psi)$ and capillarity relationships are most relevant to one-dimensional flow.

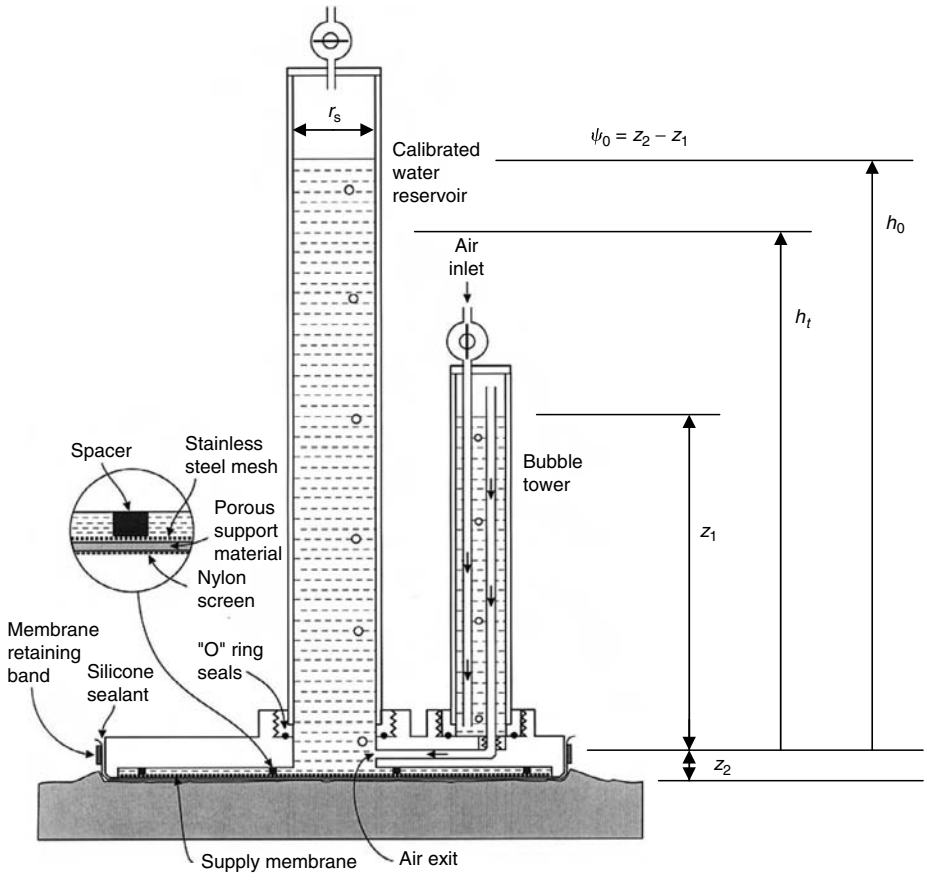

FIGURE 80.1. Tension infiltrometer. Note that z_2 is the vertical distance from the supply membrane to the air exit of the bubble tower. Note also that the datum for h_0 and h_t is arbitrary because $(h_0 - h_t)$ is used in Equation 80.8. (Adapted from Perroux, K.M. and White, I., *Soil Sci. Soc. Am. J.* 52, 1205, 1988.)

80.2 CALCULATING NEAR-SATURATED SORPTIVITY

Constant head infiltration into initially dry soil can be represented by (Philip 1957, 1969)

$$I = S(\psi_0)\sqrt{t} + At \tag{80.1a}$$

which can be rearranged into (Smiles and Knight 1976)

$$\frac{I}{\sqrt{t}} = A\sqrt{t} + S(\psi_0) \tag{80.1b}$$

where I [L] is cumulative infiltration, $S(\psi_0)$ [$LT^{-1/2}$] is soil sorptivity at constant matric head ψ_0 [L], A [LT^{-1}] is a parameter related to soil hydraulic conductivity, and t [T] is time. Philip (1957) showed that

$$\lim_{t \to 0} I \to S(\psi_0)\sqrt{t} \tag{80.2}$$

because the soil's capillarity forces dominate all other forces in dry soil at early time. This indicates in turn that

$$S(\psi_0) \approx I/\sqrt{t} \tag{80.3}$$

for early-time I vs. $\sqrt{t}$ data. Consequently, an early-time plot of I vs. $\sqrt{t}$ (Equation 80.1a) produces a straight line with zero intercept and slope equal to $S(\psi_0)$, whereas an early-time plot of $I/\sqrt{t}$ vs. $\sqrt{t}$ (Equation 80.1b) produces a straight line with zero slope and Y-axis intercept equal to $S(\psi_0)$.

Contact sand is often required to establish and maintain a hydraulic connection between the infiltrometer and the soil. Unfortunately, this material perturbs the early-time I vs. $\sqrt{t}$ behavior (Figure 80.2a, Region 1), and its effects must be eliminated before valid values of $S(\psi_0)$ can be obtained via Equation 80.1a or Equation 80.1b. This can be achieved by plotting $I/\sqrt{t}$ vs. $\sqrt{t}$, which produces a variable slope relationship during the initial wetting of the contact sand (Figure 80.2b, Region 1), and then becomes constant when infiltration is controlled by the soil (Figure 80.2b, Region 2). Equation 80.1a and Equation 80.1b are consequently applicable for $t \geq t_0$, where t_0 is the time when the contact sand is fully wetted and no longer influencing early-time infiltration (i.e., Region 2 of Figure 80.2a and Figure 80.2b) (see also Comment 3 in Section 80.9). An alternative early-time approach to eliminating contact sand effects is provided by Vandervaere et al. (2000a,b) (see also Comment 3 in Section 80.9 and Chapter 82).

In addition to perturbing early-time infiltration, contact sand can also introduce artifacts related to flow impedance and hydraulic head loss across the contact sand layer. A description of these artifacts, and methods to compensate for them, are given in Chapter 82 (see Section 82.3.3).

80.3 CALCULATING NEAR-SATURATED HYDRAULIC CONDUCTIVITY

In the original method of Clothier and White (1981), water was supplied to the top of the undisturbed soil core by the tension infiltrometer (Figure 80.1), while the bottom was left open to the atmosphere (Figure 80.3). As a result, the steady-state flux density of water passing through the core, q [LT^{-1}], occurred while the top of the core was at the matric head set on the infiltrometer (ψ_0), and the bottom of the core was at a matric head of zero (Figure 80.3). Clothier and White (1981) then calculated the near-saturated hydraulic conductivity using

$$K(\psi_0/2) = \frac{qL}{(\psi_0 + L)} \tag{80.4}$$

where L [L] is the length of the soil core, and $(\psi_0/2)$ is the assumed average matric head throughout the core. Equation 80.4 can overestimate the true value of $K(\psi_0/2)$, however,

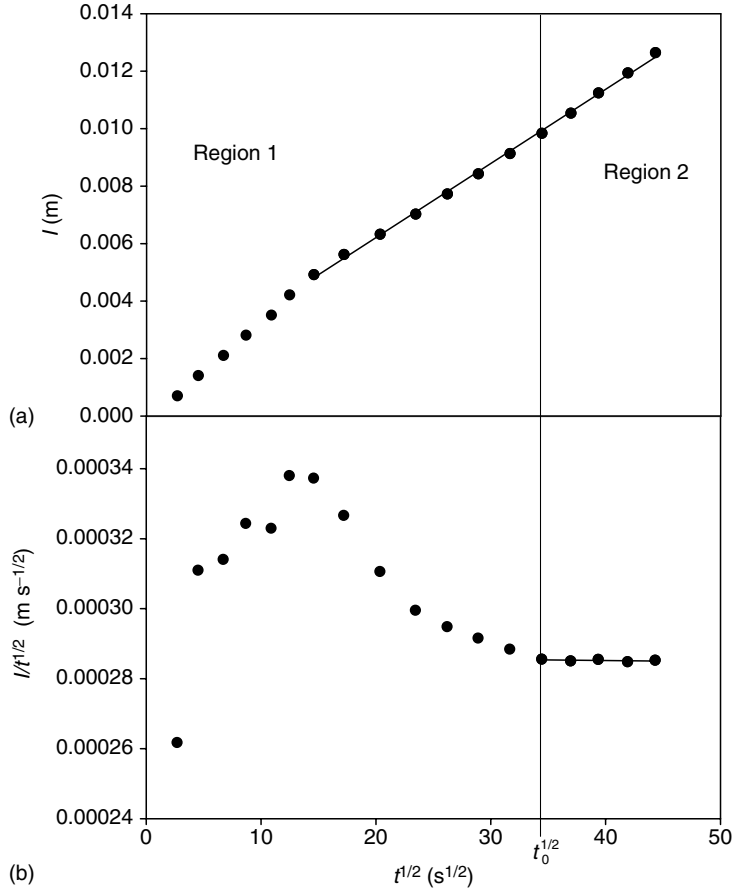

FIGURE 80.2. Plot of (a) I vs. $t^{1/2}$ and (b) $I/t^{1/2}$ vs. $t^{1/2}$, where I [L] is cumulative infiltration and t [T] is time. Region 1 is influenced by sorption in the contact sand, and Region 2 is due solely to sorption by the soil. As shown in the figure, Region 2 is difficult to distinguish when using I vs. $t^{1/2}$, but easily distinguished when using $I/t^{1/2}$ vs. $t^{1/2}$. The apparently linear data in plot (a) spans Regions 1 and 2, and the corresponding regression based on Equation 80.1a yields $S(\psi_0) = 0.000258$ m s$^{-1/2}$, which is inaccurate. Using only the data in Region 2 (i.e., $t^{1/2} \geq t_0^{1/2}$) produces the more accurate and effectively equivalent results, $S(\psi_0) = 0.000283$ m s$^{-1/2}$ (Equation 80.1a) and $S(\psi_0) = 0.000287$ m s$^{-1/2}$ (Equation 80.1b).

because the matric head gradient in the core can be highly nonlinear. Cook (1991) developed a more accurate $K(\psi_0)$ analysis for the Clothier and White (1981) method; however, the saturated hydraulic conductivity of the core must also be measured. A more straightforward alternative approach is to simply apply the same matric head, ψ_0, to both the top and bottom of the core (Figure 80.4). This simplifies the analysis to

$$K(\psi_0) = q \tag{80.5}$$

where q [LT^{-1}] is the steady water flux density through the core, which corresponds to both the steady infiltration rate from the tension infiltrometer and the steady specific discharge rate from the Buchner funnel when $\psi = \psi_0$.

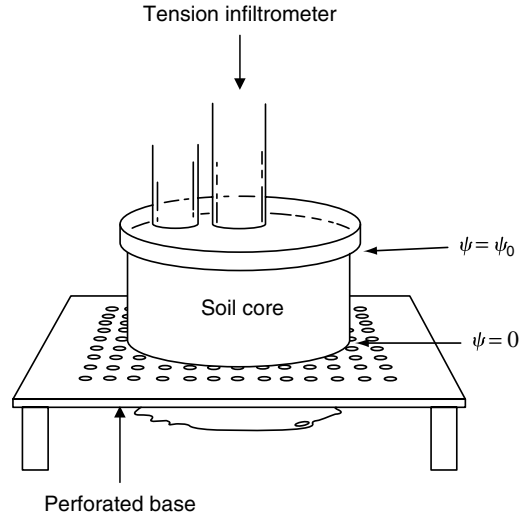

FIGURE 80.3. Near-saturated hydraulic conductivity apparatus after Clothier, B.E. and White, I., *Soil Sci. Soc. Am. J.* 45, 241, 1981.

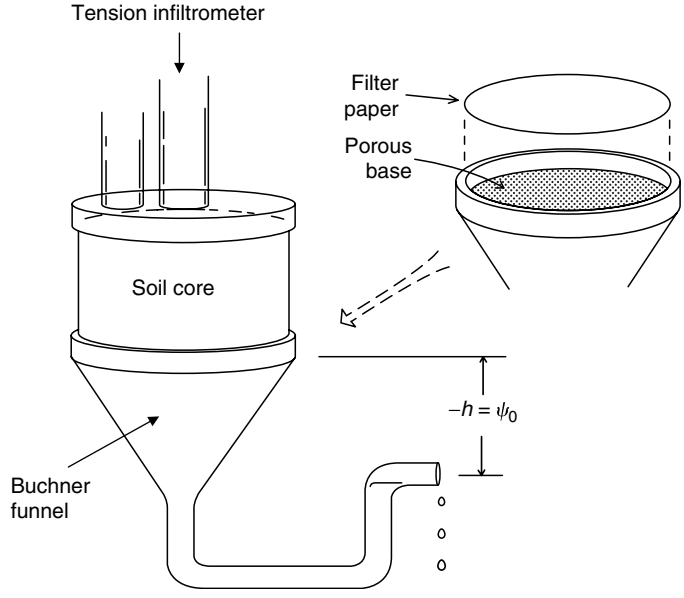

FIGURE 80.4. Buchner funnel as used to apply the matric head, ψ_0, to the bottom of the soil core while the tension infiltrometer maintains ψ_0 at the top. This produces one-dimensional, near-saturated flow through the core under unit hydraulic head gradient. The porous base in the funnel must have an air-entry matric head, ψ_a (bubble point) that is more negative than the minimum ψ_0 set on the infiltrometer and the Buchner outflow. The permeability of the porous base and filter paper or contact sand must be large enough to prevent flow impedance, as this would cause unrepresentative $S(\psi_0)$ and $K(\psi_0)$ results.

80.4 CORE SAMPLING

Successful acquisition of undisturbed (intact) soil cores requires techniques that avoid (or at least minimize) disturbance to the soil's structure and matrix during core collection, preparation, and transport. It is recommended that cores are taken using the following procedure:

1 Small amount of light grease is smeared on the inside bottom 20 mm of the core cylinder. This reduces sliding friction (and thereby core compression) and can prevent preferential flow along the cylinder wall if the core is also used to measure saturated hydraulic conductivity.

2 Core cylinder is placed on the surface of the soil from which the core sample is to be taken. This may be the soil surface or an exposed soil horizon at some depth. The cylinder is then manually pushed a small distance into the soil (say, 5–10 mm). A soil pedestal about 20 mm in height and of slightly larger radius than the cylinder is then carefully carved out with a sharp knife (Figure 80.5a).

3 Cylinder is carefully pushed downwards about 15–20 mm (Figure 80.5b).

4 Steps 2 and 3 are repeated until the soil is approximately 5 mm below the top of the cylinder (Figure 80.5c).

5 Soil in the cylinder is subsequently cut off carefully below the bottom of the cylinder using a large spatula or paint scraper (Figure 80.5c). The excess soil on the bottom is then trimmed smooth and flush with the base of the cylinder using a sharp knife. Snap-off blade knives are useful for this task. Any excess grease on the top rim of the core should be carefully removed with a spatula.

6 Seal the cylinder and its contained core in a plastic bag (or wrapped in self-adhesive plastic film) to prevent soil loss and evaporation. Use a foam-lined carrying-case to minimize temperature changes, jarring, and vibration (which can alter soil structure) during transport to the laboratory.

The cores are usually stainless steel (see Comment 4 in Section 80.9) with a radius of 50 mm and a length of 75 mm. Other core materials and dimensions are possible, however, to meet chemical or size criteria dictated by specific soil conditions or the diameter of the

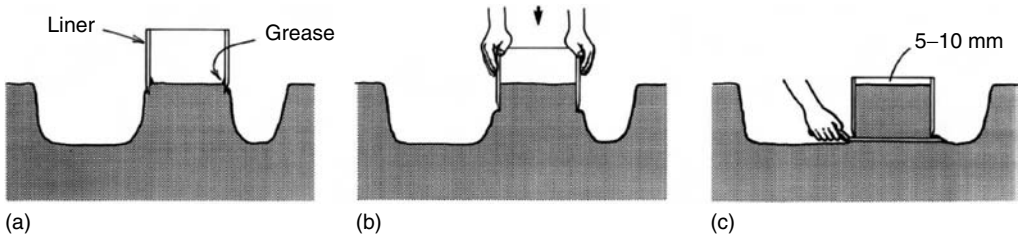

FIGURE 80.5. Taking an intact (undisturbed) soil core: (a) adding grease to the bottom of the liner (sampling cylinder), starting the cylinder, and carving a soil pedestal; (b) pushing the sampling cylinder down over the pedestal; and (c) soil core removal.

infiltrometer membrane. To ensure one-dimensional flow throughout the core, the diameter of the tension infiltrometer supply membrane (Figure 80.1) should be the same as the inside diameter of the core sampling cylinder.

80.5 MEASURING NEAR-SATURATED SORPTIVITY

80.5.1 Materials

1 Contact sand consisting of uniform, fine-grade natural sand, diatomaceous earth, or fine-grade glass beads. This material is used to provide good hydraulic connection between the soil core and the membrane at the bottom of the infiltrometer. Details on the required properties of contact sand can be found in Perroux and White (1988), Reynolds and Zebchuk (1996), and Chapter 82.

2 Soil core, obtained by the method described in Section 80.4.

3 Tension infiltrometer with the appropriate diameter.

4 Stand or table as shown in Figure 80.3.

5 Stopwatch or automated water height measuring device, such as data-logging pressure transducers or TDR probes (Dawes et al. 2003; Moret et al. 2004).

6 Recording sheet.

80.5.2 Procedure

1 Weight of the soil core and its volume are recorded for later determination of the core's initial volumetric water content, $\theta(\psi_i)$. Soil core volume can be determined by calculating the ''headspace'' volume between the soil and the top of the sampling cylinder, and then subtracting from the total volume of the cylinder, i.e.,

$$V_s = V_c - V_h = \pi r_c^2 (l_c - \Delta l) \tag{80.6}$$

where V_s [L^3] is the volume of soil, V_c [L^3] is the volume of the cylinder, V_h [L^3] is the headspace volume, r_c [L] is the inside radius of the cylinder, l_c [L] is the length of the cylinder, and Δl [L] is the distance between the soil surface and the top of the cylinder. The headspace volume can also be estimated from the volume of contact sand applied (see step 2 below).

2 Contact sand is placed on top of the soil core and leveled flush with the top of the sampling cylinder. If the required volume of sand is measured carefully (e.g., via a graduated cylinder), it can be used as a measure of the headspace volume ($V_h = \pi r_c^2 \Delta l$) in step 1 above.

3 Tension infiltrometer (Figure 80.1) is filled by placing the base in a container of de-aired, temperature-equilibrated water, opening the valve on the top of the

reservoir, and sucking water into the infiltrometer until the reservoir is full. The tension infiltrometer is set to the required matric head

$$\psi_0 = z_2 - z_1 \tag{80.7}$$

by adjusting the water level in the bubble tower (z_1) (see Figure 80.1). Remove all air bubbles from the cavity between the supply membrane and the infiltrometer base (Figure 80.1).

4 Sorptivity is measured by placing the core on a perforated surface with the base open to the atmosphere (Figure 80.3). The initial water level in the infiltrometer reservoir is recorded. The infiltrometer is placed on the contact sand with a slight twisting motion to ensure good hydraulic contact, a stopwatch (manual method) or data-logging system (automated method) is started, and reservoir water level recorded with time. Since infiltration rates can vary substantially, it is advisable (and perhaps more accurate) to record the time for every 10–20 mm drop in reservoir water level, rather than record water level at a set time interval. Collect measurements until sufficient data are obtained to clearly define soil-controlled infiltration (Region 2, Figure 80.2).

5 Cumulative infiltration rate, I, is calculated by

$$I = \frac{(h_0 - h_t)r_s^2}{{r_c}^2} \tag{80.8}$$

where h_0 [L] is the initial water level (height) in the infiltrometer reservoir, h_t [L] is the water level at time t [T], r_s is the internal radius of the infiltrometer reservoir [L], and r_c is the radius of the soil core [L] (Figure 80.1). Either I or $I/t^{1/2}$ is plotted against $t^{1/2}$ (Figure 80.2), and the portion of the graph associated with infiltration into the soil is used to calculate $S(\psi_0)$ via Equation 80.3. For example, the data in Region 2 of Figure 80.2a yield

$$S(\psi_0) = \frac{\Delta I}{\Delta\sqrt{t}} = \frac{(0.0125 - 0.0097)}{(44.2553 - 34.2553)} = 0.000283 \text{ m s}^{-1/2}$$

and the data in Region 2 of Figure 80.2b yield effectively the same value, i.e., $S(\psi_0) = Y$-axis intercept $= 0.000287$ m s$^{-1/2}$, which is best obtained by regressing $I/\sqrt{t}$ against $\sqrt{t}$ for $t \geq t_0$.

6 Infiltrometer is carefully slid off the core. The core is then transferred to the Buchner funnel (Figure 80.4) for measurement of hydraulic conductivity.

80.6 MEASURING NEAR-SATURATED HYDRAULIC CONDUCTIVITY

80.6.1 Materials

1 Soil core from sorptivity measurements (Section 80.5).

2 Buchner funnel apparatus (Figure 80.4). Alternative methods using sand columns are presented by McKenzie and Cresswell (2002).

3 ''Fast-flow'' filter paper, 270 mesh (53 μm pore size) nylon bolting cloth, or contact sand.

4 Tension infiltrometer with appropriate diameter.

5 Stopwatch or automated water height measuring device.

6 Recording sheet.

80.6.2 Procedure

1 Place the Buchner funnel in a rack or stand (Figure 80.6) and place a fast-flow filter paper or nylon cloth on the porous base plate (Figure 80.4). If plugging of the filter paper or nylon cloth with suspended silt and clay is a concern, one might replace them with contact sand. Use a squeeze bottle to completely fill the outflow tubing and funnel with de-aired, temperature-equilibrated water, ensuring that there is a small depth of water ponded on top of the filter paper (or nylon cloth or contact sand) to ensure complete saturation (Figure 80.6). After removing the squeeze bottle, lower the outflow tubing to drain off the ponded water and establish the desired matric head:

$$\psi_0 = -h \tag{80.9}$$

where h is defined in Figure 80.4. The core is then placed on the filter paper (or nylon cloth or contact sand) in the Buchner funnel.

2 Tension infiltrometer is filled by the method described in procedure step 3, Section 80.5.2 (see also Chapter 82), and set to the desired matric head, $\psi_0 = -h$. The initial water level in the infiltrometer reservoir (h_0) is recorded.

3 Infiltrometer is placed on the core (i.e., contact sand layer) with a slight twisting motion to ensure good hydraulic contact (Figure 80.4). A stopwatch or automated

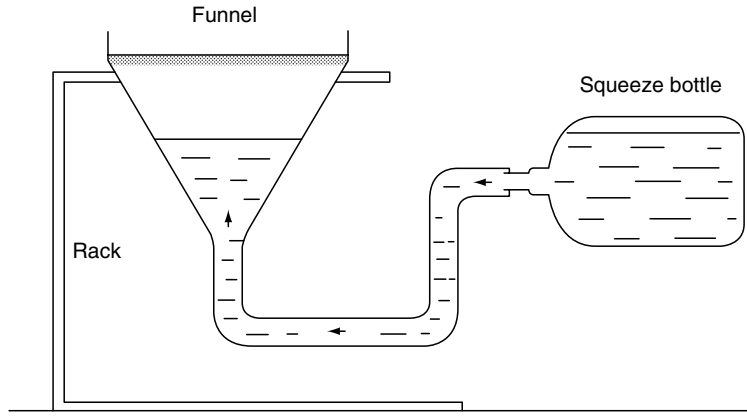

FIGURE 80.6. Procedure for saturating the Buchner funnel in preparation for measuring $S(\psi_0)$ and $K(\psi_0)$ on an intact soil core.

TABLE 80.1 Example Data for Laboratory Measurement of $K(\psi_0)$ on an Intact Soil Core Using a Tension Infiltrometer and Buchner Funnel

Time, t (min)	Water level in reservoir, h_t (mm)	$-\Delta h/\Delta t$ (mm/min)	Comments
0	93	—	Wetting of contact sand begins
5	53	8	—
10	38	3	—
15	34	0.8	—
20	31	0.6	—
30	27	0.4	Steady soil-controlled flow begins
40	23	0.4	—
50	18	0.5	—
60	14	0.4	—
70	10	0.4	—

Soil type = transitional red-brown earth (Typic Natrixeralf, Soil Survey Staff 1990); core dimensions = 98 mm diameter by 75 mm long; $\psi_0 = -20$ mm; $h_0 = 93$ mm.

recording device (e.g., Moret et al. 2004) is started, and periodic measurements of the water level in the reservoir are made, as exemplified in Table 80.1. From these data, the water flux density (q) can be calculated and the onset of steady flow determined (e.g., steady flow occurred at 30 min in the example in Table 80.1). The progression to steady flow is nonlinear, and depends on ψ_0, the soil's antecedent water content, and the soil's $K(\psi)$ relationship. Hence, the time taken to reach steady state can vary from minutes to hours, and it is consequently more convenient (and perhaps more accurate) to record the time for every 10 or 20 mm drop in the reservoir water level (h_t), rather than record water level at a set time interval.

4 Once steady flow is attained, hydraulic conductivity $K(\psi_0)$ is calculated using Equation 80.5 in the form

$$K(\psi_0) = q = -\frac{r_s^2(h_2 - h_1)}{r_c^2(t_2 - t_1)} = -\frac{r_s^2}{r_c^2}\frac{dh}{dt} \tag{80.10}$$

where h_1 and h_2 are the water levels (heights) in the tension infiltrometer reservoir at times t_1 and t_2, respectively, during steady-state flow; r_s is the internal radius of the tension infiltrometer reservoir; r_c is the radius of the soil core; and dh/dt is the rate of water level fall during steady flow if an automated water height measuring device is used. An example calculation using the data from Table 80.1 is given below.

Given,

$$r_s = 9.5 \text{ mm} \quad r_c = 49 \text{ mm}$$

$$t_1 = 30 \text{ min} \quad h_1 = 27 \text{ mm}$$

$$t_2 = 70 \text{ min} \quad h_2 = 10 \text{ mm}$$

then,

$$K(\psi_0) = -\frac{(9.5)^2 \cdot (10 - 27)}{(49)^2 \cdot (70 - 30)}$$
$$= 1.60 \times 10^{-2} \text{ mm min}^{-1}$$
$$= 2.66 \times 10^{-7} \text{ m s}^{-1}$$

where $\psi_0 = -20$ mm.

5 After the steady flow measurement is completed, the infiltrometer and contact sand are quickly removed and core weight is recorded. Proceed to Section 80.7.

80.7 CALCULATING $\theta(\psi_0)$ OR MEASURING ADDITIONAL $S(\psi_0)$ AND $K(\psi_0)$ VALUES

If $S(\psi_0)$ and $K(\psi_0)$ for a sequence of matric heads (ψ_0) are required, repeat the above procedures starting at step 1 of Section 80.5.2. If only additional $K(\psi_0)$ values are required, set the Buchner funnel at the next ψ_0 value (Equation 80.9), refill the tension infiltrometer, and repeat the above procedure starting at step 3 of Section 80.6.2. Note that $S(\psi_0)$ depends on the antecedent water content at the time of the measurement (Chapter 69). Hence, the first $S(\psi_0)$ measurement is relative to the initial water content of the soil core, $\theta(\psi_i)$, whereas all succeeding measurements are relative to the water content established from the previous $S(\psi_0)$ measurement, $\theta(\psi_0)$. When a sequence of matric heads are used, they should be increased or decreased monotonically to avoid the possible introduction of hysteresis effects into the $S(\psi_0)$ and $K(\psi_0)$ results (Chapter 69).

Following the last measurement, the whole core is oven dried and the weight recorded. The core bulk density, initial volumetric water content, $\theta(\psi_i)$, and the volumetric water content associated with each ψ_0 value, $\theta(\psi_0)$, can then be calculated. Use the $\theta(\psi_0)$ vs. ψ_0 data to plot the core's desorption or imbibition curve within the range of ψ_0 values used (see Chapter 69 for details). Proceed to Section 80.8 if capillarity parameters are required.

80.8 CALCULATING CAPILLARITY PARAMETERS

Once $S(\psi_0)$, $K(\psi_0)$, and $\theta(\psi_0)$ are determined for the desired ψ_0 values, the capillarity parameters, $\alpha^*(\psi_0)$, $PD(\psi_0)$, and $NP(\psi_0)$, can be estimated using Equation 69.17 through Equation 69.19, respectively.

80.9 COMMENTS

1 Method described here is generally used to make measurements of hydraulic conductivity and sorptivity for matric heads ranging between 0 and −100 mm, although the lower limit can be reduced to −400 mm by using special nuclepore membranes (R. Sides, personal communication).

2 Main advantage of this laboratory approach is that a large number of intact cores can be taken quickly in the field, and the measurements of $S(\psi_0)$, $K(\psi_0)$, and capillarity parameters can be made later under controlled laboratory conditions.

3 Precise identification of t_0 (i.e., the time when infiltration becomes soil-controlled) is critical for accurate determination of $S(\psi_0)$; and as illustrated in Figure 80.2, plotting $I/t^{1/2}$ vs. $t^{1/2}$ identifies t_0 much more clearly than plotting I vs. $t^{1/2}$. An alternative method for identifying t_0 was developed by Vandervaere et al. (2000a, b) which involves differentiating Equation 80.1a with respect to $t^{1/2}$ (see Chapter 82). However, applying the Vandervaere et al. (2000a, b) approach to ''noisy'' data can be problematic, because the differentiation process can obscure the location of t_0 by greatly magnifying the random noise.

4 Core sampling cylinder should be noncorroding and strong enough to not deform or break during insertion. Cylinders made from PVC, aluminum, or stainless steel are usually acceptable, although stainless steel is recommended because of its high strength, ability to retain a sharp cutting edge, and longevity.

5 Details on saturating and calibrating tension infiltrometers can be found in Chapter 82.

REFERENCES

Clothier, B.E. and White, I. 1981. Measurement of sorptivity and soil water diffusivity in the field. *Soil Sci. Soc. Am. J.* 45: 241–245.

Cook, F.J. 1991. Calculation of hydraulic conductivity from suction permeameter measurements. *Soil Sci.* 152: 321–325.

Dawes, L., Sweeney, C., Cook, F.J., Bristow, K.L., Elridge, S., Biggs, J., and Thorburn, P.J. 2003. *Soil Hydraulic Properties of the Fairymead Soils, Bundaberg*. CRC Sugar Technical Publication, CRC for Sustainable Sugar Production, Townsville, Australia, 24 pp.

McKenzie, N.J. and Cresswell, H.P. 2002. Laboratory measurement of hydraulic conductivity. In N.J. McKenzie et al., Eds. *Soil Physical Measurements and Interpretation for Land Evaluation*. CSIRO Publishing, Australia, pp. 150–162.

Moret, D., Lopez, M.V., and Arrue, J.L. 2004. TDR application for automated water level measurement from Mariotte reservoirs in tension disc infiltrometers. *J. Hydrol.* 297: 229–235.

Perroux, K.M. and White, I. 1988. Designs for disc permeameters. *Soil Sci. Soc. Am. J.* 52: 1205–1215.

Philip, J.R. 1957. The theory of infiltration. 4. Sorptivity and algebraic infiltration equations. *Soil Sci.* 84: 257–264.

Philip, J.R. 1969. The theory of infiltration. *Adv. Hydrosci.* 5: 215–296.

Reynolds, W.D. and Zebchuk, W.D. 1996. Use of contact material in tension infiltrometer measurements. *Soil Technol*. 9: 141–159.

Smiles, D. and Knight, J.H. 1976. A note on the use of Philip infiltration equation. *Aust. J. Soil Res*. 14: 103–108.

Soil Survey Staff 1990. *Keys to Soil Taxonomy*. Virginia Polytechnic Institute and State University, Blacksburg, VA.

Vandervaere, J.-P., Vauclin, M., and Elrick, D.E. 2000a. Transient flow from tension infiltrometers: I. The two-parameter equation. *Soil Sci. Soc. Am. J*. 64: 1263–1272.

Vandervaere, J.-P., Vauclin, M. and Elrick, D.E. 2000b. Transient flow from tension infiltrometers: II. Four methods to determine sorptivity and conductivity. *Soil Sci. Soc. Am. J*. 64: 1272–1284.

Ward, R.D. and Hayes, M.J. 1991. Measurement of near-saturated hydraulic conductivity of undisturbed cores by use of the permeameter tube. DSIR Land Resources, Technical Record 20, New Zealand. 6 pp.

Chapter 81
Unsaturated Hydraulic Properties: Laboratory Evaporation

O.O.B. Wendroth
University of Kentucky
Lexington, Kentucky, United States

N. Wypler
Leibniz-Centre for Agricultural Landscape Research
Müncheberg, Germany

81.1 INTRODUCTION

The laboratory-based ''evaporation'' or ''Wind'' method (Wind 1968) is used primarily for determining the unsaturated hydraulic conductivity relationship [$K(\psi)$ or $K(\theta)$] and the pore water desorption relationship [$\theta(\psi)$] on cores or columns of soil. It is also potentially useful, however, for estimating the so-called capillarity relationships, i.e., sorptivity, $S(\psi)$, sorptive number, $\alpha^*(\psi)$, flow-weighted mean pore diameter, $PD(\psi)$, and the number of flow-weighted mean pores per unit area, $NP(\psi)$ (Chapter 69). An alternative laboratory method for determining near-saturated $K(\psi)$, $K(\theta)$, and $\theta(\psi)$ is given in Chapter 80. Field methods for determining $K(\psi)$, $K(\theta)$, or $\theta(\psi)$ are given in Chapter 82 and Chapter 83. Selected methods for estimating $K(\psi)$, $K(\theta)$, and $\theta(\psi)$ from surrogate porous medium properties are given in Chapter 84. A discussion of the principles and parameters associated with the determination of $K(\psi)$, $K(\theta)$, $\theta(\psi)$, and the capillarity relationships appears in Chapter 69.

In essence, the evaporation method involves installing probes for measuring pore water matric head (ψ) and volumetric water content (θ) at selected positions along a core or column, and then monitoring the decrease in ψ and θ with time from near-saturation as water evaporates from the exposed upper surface of the core or column. Given that the method is based on evaporative water loss and flow is confined by the column walls, the $K(\psi)$, $K(\theta)$, $\theta(\psi)$, and capillarity relationships obtained are most relevant to one-dimensional drainage or evaporation. The method applies for the matric head range, $\approx$–700 cm $\leq \psi \leq -10$ cm; and it includes a ''simplified'' analysis, where the theoretical minimum of two tensiometers is used to determine the change in ψ with time, and a ''comprehensive'' analysis, where three or more tensiometers are monitored. Here, the

simplified analysis is referred to as the ''2T'' setup (i.e., two tensiometers are monitored), and the comprehensive analysis is referred to as the ''5T'' setup (i.e., five tensiometers are monitored).

81.2 MATERIALS

1 Cylindrical core sampling ring or column (metal, plastic) with two access holes (2T setup) or several access holes (e.g., 5T setup) predrilled through the wall to allow insertion of tensiometer cups (Chapter 71). The access holes should be slightly larger in diameter than the tensiometer cups to facilitate damage-free insertion.

2 Base plate (metal, plastic) that is rigid, lightweight, and impermeable.

3 Cable holders for mounting the tensiometers (Figure 81.1).

4 Plumber lute for sealing the soil core or column to the base plate.

5 Fast-equilibrating tensiometers (one for each core access hole), which sample a substantial cross-section of the soil core or column and have a wide operating range. The preferred tensiometers are fitted with 0.6 cm diameter by 6–7 cm long ''high-flow'' porous ceramic cups with an air entry matric head of about −800 cm. Either manual or electronic tensiometer systems can be used (Chapter 71), although systems based on electronic pressure transducers are usually preferred, for they can provide rapid and automated data collection. The transducers should be

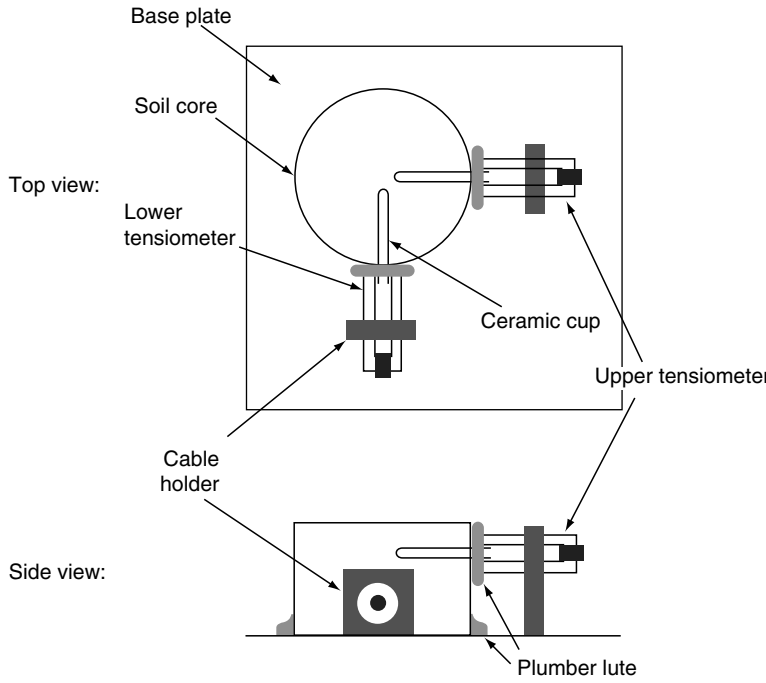

FIGURE 81.1. The ''2T'' (two tensiometer) setup for the evaporation and Wind method.

calibrated prior to the measurements (e.g., using a hanging water column) and recalibrated periodically to correct for drift. The measurements should be conducted under constant temperature (e.g., 20°C ± 1°C) to minimize temperature effects on pressure transducer calibration, soil water desorption, and soil water flow (see Chapter 69).

6 Scale with a range of at least 2 kg (2T setup) or 3 kg (5T setup), and a sensitivity of ±0.01 g.

7 A data logger for automated recording of tensiometer and scale readings is not required but makes the operation less labor-intensive.

8 Timer (±1 s accuracy).

9 Rotary drill with a bit diameter slightly smaller than the ceramic tensiometer cups.

10 When measuring coarse-textured porous materials, fine silt slurry to establish and maintain hydraulic contact between the material and the tensiometer cup; large size medical syringe for injecting silt slurry.

11 Basin or tank for sample saturation (see e.g., Chapter 75).

12 Constant temperature room (preferably 20°C ± 1°C).

13 Drying oven (105°C ± 5°C).

14 Computer for data analysis.

Figure 81.1 gives a schematic of the 2T setup using a 6 cm high by 8 cm diameter soil core, with tensiometer cups inserted at 1.5 and 4.5 cm below the core surface and offset laterally by 90°. The 5T setup is an extension of the 2T setup; and in the example given here, a 10 cm high by 10 cm diameter core has tensiometers located at 1, 3, 5, 7, and 9 cm below the core surface, with each tensiometer offset laterally from the adjacent tensiometers by 20°–25° (spiral pattern) to facilitate installation (setup not shown).

81.3 PROCEDURE

81.3.1 Sample Preparation

1 The 2T or 5T sample cylinder is used to collect an intact (undisturbed) soil core from the field, or to prepare a repacked laboratory sample, and the core or sample should be flushed with the ends of the sample cylinder. The cylinder and its contained core are placed upright on the base plate, and the rotary drill used to excavate tensiometer installation holes via the access holes predrilled through the cylinder wall. Drilling should be performed gently, at low rpm, and in small steps to minimize smearing and compaction of the soil. To ensure good hydraulic contact between the soil and the tensiometer cup, the hole should not extend beyond the end of the cup, and it should have a slightly smaller diameter than the cup; e.g., if a 0.6 cm diameter tensiometer cup is used, a 0.5 cm diameter hole should be drilled in fine-medium textured soil, and a 0.4 cm diameter hole drilled

in coarse-textured soil. More accurate hydraulic property results may be achievable if a drilling guide is used to produce completely horizontal tensiometer holes with very accurate elevations, diameters, and depths.

2 Once the tensiometer holes are completed, the tensiometers are inserted through the cylinder access holes and into the soil. This should be done incrementally and slowly to minimize air entrapment in the soil or tensiometer cup, which could affect both soil properties and tensiometer performance. As it can be difficult in some sandy soils to obtain good hydraulic contact between soil and tensiometer cup, it is often advisable to inject a silt-water slurry into the tensiometer hole (using the large syringe) just prior to tensiometer insertion. The silt will not affect the equilibrium tensiometer readings, although it may reduce tensiometer response time slightly.

3 Once the tensiometers are inserted in the soil, the upright sample is slowly saturated from the bottom upward using deaired temperature-equilibrated water, which has about the same major ion speciation and concentrations as the native soil water (see Chapter 75 for details on recommended saturation procedures). After saturation, the water table in the basin is lowered below the bottom of the soil sample, and the sample is removed carefully from the basin, using the base plate to give support. The top of the sample is covered with a lid to prevent evaporative water loss. Plumber lute is placed on the cylinder wall around the tensiometers to prevent evaporative water losses through the access holes (Figure 81.1). At this time, some water may continue to leak out between the bottom of the cylinder and base plate, and it should be soaked up until flow stops. During this time, the tensiometers should yield increasingly more negative values; and once a matric head reading of ≤ -5 cm occurs at the bottom tensiometer, and ≤ -8 cm (2T setup) or ≤ -14 cm (5T setup) occurs at the top tensiometer, the bottom of the core or column is sealed to the base plate with plumber lute (Figure 81.1).

4 At this point, the sample should be left standing long enough for hydrostatic equilibrium to be established within the soil, which is indicated by steady tensiometer readings that correspond with the height difference between the tensiometers (i.e., zero hydraulic head gradient). For example, the upper tensiometer in the 2T setup should yield a steady matric head that is 3 cm lower (more negative) than the steady matric head at the lower tensiometer (Figure 81.1). When pressure transducer-based tensiometers are used, false nonzero hydraulic head gradients can occur at hydrostatic equilibrium because of offsets in the calibration curves. This can be rectified using the following procedure (see Table 81.1). For the 2T case, we obtain (for example) uncorrected soil water matric head readings, ψ_u, of -7.4 cm at the upper tensiometer (1.5 cm below soil surface), and -5.2 cm at the lower tensiometer (4.5 cm below soil surface) once flow has ceased. We assume that both tensiometer calibrations contribute equally, but in opposite directions, to the apparent deviation from hydrostatic equilibrium. Hence, the average soil water matric head, $\psi_{avg} = [-7.4 + (-5.2)]/2 = -6.3$ cm, is correct for the midcore elevation of -3 cm (elevation defined as positive upward with zero elevation at the top of the core). The corrected matric heads, ψ_c, that we expect under hydrostatic equilibrium consequently correspond to the difference in elevation between midcore and the level of each tensiometer. For the upper tensiometer, we thus obtain $\psi_c = [(-6.3 \text{ cm}) - 1.5 \text{ cm}] = -7.8$ cm; and for the lower tensiometer

TABLE 81.1 Initial Matric Head (ψ) Readings at Hydrostatic Equilibrium (Zero Hydraulic Head Gradient), and Adjustment of Transducer Calibration Curve Intercepts to Zero Offset

Depth below surface (cm)	ψ_u (cm)	ψ_{avg} (cm)	ψ_c (cm)	Intercept adjustment, $\Delta\psi$ (cm)
2T setup				
−1.5	−7.4	−6.3	−7.8	−0.4
−4.5	−5.2		−4.8	+0.4
5T setup				
−1.0	−11.4	−5.18	−9.18	+2.22
−3.0	−4.2		−7.18	−2.98
−5.0	−6.2		−5.18	+1.02
−7.0	−3.1		−3.18	−0.08
−9.0	−1.0		−1.18	−0.18

ψ_u = Initial, unadjusted soil water matric head.
ψ_{avg} = Average unadjusted soil water matric head.
ψ_c = Required soil water matric head for zero offset.
$\Delta\psi$ = Adjustment in ψ_u required to obtain zero offset in the calibration curve intercept.

$\psi_c = [(-6.3\text{ cm}) - (-1.5\text{ cm})] = -4.8$ cm. The resulting correction constants that need to be added to the tensiometer readings during the evaporation experiment are consequently $[-7.4\text{ cm} - (-7.8\text{ cm})] = -0.4$ cm for the upper tensiometer, and $[-4.8\text{ cm} - (-5.2\text{ cm})] = +0.4$ cm for the lower tensiometer. According to our experience, the magnitude of this adjustment (i.e., ±0.4 cm) is relatively common; although it can be larger, as in the 5T example (Table 81.1), where ψ_u values of −11.4, −4.2, −6.2, −3.1, and −1.0 cm were obtained at the cessation of flow for the tensiometers at −1, −3, −5, −7, and −9 cm depth, respectively, yielding an average value $\psi_{avg} = [-11.4 + (-4.2) + (-6.2) + (-3.1) + (-1.0)]/5 = -5.18$ cm. This value is again assumed to be valid at core midheight, i.e., −5.0 cm. The values for ψ_c are derived in the same way as for the 2T setup and the resulting correction constants to be added to the tensiometer readings are +2.22, −2.98, +1.02, −0.08, and −0.18 cm for the tensiometers at −1, −3, −5, −7, and −9 cm depth, respectively (Table 81.1).

81.3.2 Data Collection

1 After establishing the initial ψ values, the evaporation process is initiated (at $t = t_0$) by removing the lid from the top of the core sample. The initial sample weight, $W(t_0)$, needs to be recorded immediately. If the sample remains on the weigh scale for the entire experiment, $W(t)$ needs to be recorded either manually or by a data logger. If two or more core samples are to be measured using the same scale, the wires to the pressure transducers need to be disconnected and the base plate with the sample and tensiometers gently placed on the scale for weighing, then placed back on the lab bench, and transducers reconnected. If weighing involves moving the core samples, the tensiometers should be read immediately before weighing, as even gentle movement can cause temporary disturbance of tensiometer readings, especially when ψ is close to zero.

2 Depending on the soil type, tensiometer, and sample weight readings [$W(t)$] should be taken at 1–4 h intervals. For the early stage of an experiment with a

sandy soil, when soil water matric head decreases very slowly with decreasing water content, time intervals can be relatively long, e.g., 4 h. Fine-textured soils, on the other hand, require more frequent measurements throughout their water content range (e.g., at 1 or 2 h intervals), as matric head in these soils often decreases rapidly with decreasing water content.

3 The evaporation is terminated when the top tensiometer reaches a matric head of $\psi \approx -700$ cm. At this time, the final matric heads and core weight, $W(t_{end})$, are recorded and the core is capped to stop further evaporation. The tensiometers and base plate are then removed, the bottom of the core immediately covered with another cap, and the core weight, W_w, is determined again, i.e., weight of the moist soil, the cylinder, and the two end caps. The core with the two end caps removed is then oven-dried (105°C ± 5°C) and weighed a third time (W_d) to allow determination of soil dry bulk density and water content at the end of evaporation.

4 Measured laboratory evaporation rates (E) are usually on the order of 0.1 to 0.2 cm d^{-1}. For sandy soils, this rate may be impractically slow when the soil is close to saturation, as the soil's large near-saturated hydraulic conductivity can maintain the hydraulic head gradient at virtually zero for a considerable period of time. If this occurs, a fan can be used to blow air at room temperature across the top surface of the soil sample, producing an evaporation rate between 0.5 and 1.2 cm d^{-1}. This accelerated evaporation should be terminated (by putting the cap back on top of the sample) when the hydraulic head gradient reaches a value of approximately -3 cm cm^{-1}. Time is then allowed for re-establishment of hydrostatic equilibrium (i.e., zero hydraulic head gradient), which usually occurs within a few hours. After this, the intercepts of the pressure transducer calibration curves should be rechecked for offset at hydrostatic equilibrium (and readjusted if necessary using correction constants, as explained in Section 81.3.1), and then evaporation without the fan resumed. The accelerated evaporation must be interrupted to prevent excessive hydraulic head gradients and to ensure a linear matric head gradient between adjacent tensiometers, as assumed by theory.

5 For fine-textured soils, on the other hand, the evaporation rate may need to be restricted from the beginning of the experiment to maintain a linear matric head gradient between adjacent tensiometers. This is easily achieved by placing a perforated lid on the top of the sample during evaporation to reduce air turbulence and thereby reducing evaporation rate. According to our experience, a perforated lid reduces the evaporation rate to approximately 0.08 cm d^{-1}.

81.4 CALCULATIONS

81.4.1 Calculation of the Water Desorption Curve, 2T Setup

The total mass of water initially in the sample is calculated using

$$M(t_0) = (W_w - W_d) + [W(t_0) - W(t_{end})] \quad (81.1)$$

where the first term on the right ($W_w - W_d$) represents the water remaining in the sample at the end of the evaporation experiment, and the second term $[W(t_0) - W(t_{end})]$ represents the water removed during the evaporation experiment. The mass of water remaining in the core sample at each measurement time, $M(t)$, is determined using

$$M(t) = M(t_0) - \Delta M = M(t_0) - [W(t_0) - W(t)] \tag{81.2}$$

which may then be converted to total volumetric water content, θ ($cm^3\ cm^{-3}$), by

$$\theta(t) = \frac{M(t)}{\rho_w V_t} \tag{81.3}$$

and to total water storage, S (cm), by

$$S(t) = \theta(t) \cdot L = \frac{M(t)}{\rho_w A} \tag{81.4}$$

where ρ_w is the density of water ($g\ cm^{-3}$), V_t is the total soil bulk volume (cm^3), which is the core volume minus the volume of the holes drilled for the ceramic cups, A is the cross-sectional area of the core (cm^2), and L is the length (cm) of the core, i.e., 6 cm for the 2T setup and 10 cm for 5T setup in our examples.

An example for the calculations is illustrated in the following and in Table 81.2. The evaporation experiment ran from $t = 0$ min to $t = 3960$ min. The pore water matric head at both measurement depths and the total weight of the sample are recorded every 2 h. The total mass of the sample and tensiometers at the beginning and end of the measurements is $W(t_0) = 882.98$ g and $W(t_{end}) = 852.89$ g, respectively (Table 81.2). The tensiometers, plumber lute, and base plate are then removed and sample wet weight, $W_w = 681.49$ g, recorded immediately. The sample is then oven-dried (105°C ± 5°C) and the sample dry weight, $W_d = 580.81$ g, recorded. After subtracting the tare of the metal sampling cylinder (220.62 g), the weight of dry soil is known and used for the calculation of dry bulk density (i.e., $W_s = W_d - 220.62$ g = 360.19 g).

The mass of water in the sample at the beginning of the experiment, $M(t_0)$, was 130.77 g. The mass of water in the sample, $M(t)$, and the water storage in the sample, $S(t)$, at each measurement time are calculated from Equation 81.2 and Equation 81.4, respectively. The data obtained so far are collectively presented in the first part of Table 81.2.

Next, an iterative procedure is initiated for calculating the van Genuchten (1980) $\theta(\psi)$ function:

$$\theta = \theta_r + \frac{\theta_s - \theta_r}{\left[1 + |\alpha\psi|^n\right]^{(1-(1/n))}} \tag{81.5}$$

where θ_s, θ_r, α, and n are fitting parameters. The θ_s and θ_r parameters are related to the saturated and residual volumetric water contents, respectively, and the α (cm^{-1}) and n parameters are related to curve shape. Other quasiphysical $\theta(\psi)$ functions can be used besides the van Genuchten (1980) function (e.g., Campbell 1974; Groenevelt and Grant 2004); and even empirical polynomials of the third or higher order might be applied (Wind 1968).

TABLE 81.2 Example Calculation of the Water Retention Curve, $\psi(\theta)$, for the 2T Setup (Measurements Were Collected for 3960 min, but for Brevity Only the First 1800 min Are Given)

						Initialization $\alpha = 0.0400$ $n = 1.200$ $\theta_s = 0.4500$ $\theta_r = 0.0500$						1st Iteration $\alpha = 0.03905$ $n = 1.0926$ $\theta_s = 0.4381$ $\theta_r = 0.0440$					
	Measured information																
Time min	$\psi 1.5$ cm	$\psi 4.5$ cm	$W(t)$ g	$M(t)$[a] g	$S(t)$[b] cm	$\theta 1.5$[c] cm^3 cm^{-3}	$\theta 4.5$[d] cm^3 cm^{-3}	$S_c(t)$[e] cm	$S(t)\ S_c(t)^{-1}$	$\theta_{up}1.5$ cm^3 cm^{-3}	$\theta_{up}4.5$ cm^3 cm^{-3}	$\theta 1.5$ cm^3 cm^{-3}	$\theta 4.5$ cm^3 cm^{-3}	$S_c(t)$ cm	$S(t)\ S_c(t)^{-1}$	$\theta_{up}1.5$ cm^3 cm^{-3}	$\theta_{up}4.5$ cm^3 cm^{-3}
0	−7.8	−4.8	882.98	130.77	2.5970	0.4251	0.4348	2.5796	1.0068	0.4280	0.4377	0.4302	0.4332	2.5901	1.0027	0.4313	0.4344
120	−10.9	−6.9	881.95	129.74	2.5765	0.4160	0.4279	2.5319	1.0176	0.4234	0.4355	0.4272	0.4311	2.5748	1.0007	0.4275	0.4313
240	−14.1	−10.0	880.94	128.73	2.5565	0.4076	0.4186	2.4786	1.0314	0.4204	0.4317	0.4244	0.4281	2.5573	0.9997	0.4242	0.4279
360	−17.2	−13.2	879.91	127.70	2.5358	0.4003	0.4099	2.4308	1.0432	0.4176	0.4276	0.4218	0.4252	2.5409	0.9980	0.4210	0.4243
480	−21.4	−17.3	878.91	126.70	2.5160	0.3916	0.4001	2.3750	1.0593	0.4148	0.4239	0.4186	0.4217	2.5211	0.9980	0.4178	0.4209
600	−26.7	−21.5	877.96	125.75	2.4971	0.3820	0.3914	2.3200	1.0763	0.4111	0.4212	0.4149	0.4185	2.5004	0.9987	0.4144	0.4180
720	−30.9	−25.7	876.99	124.78	2.4778	0.3753	0.3837	2.2770	1.0882	0.4084	0.4175	0.4123	0.4156	2.4836	0.9977	0.4113	0.4146
840	−36.1	−30.9	876.06	123.85	2.4593	0.3680	0.3753	2.2301	1.1028	0.4059	0.4139	0.4093	0.4123	2.4646	0.9979	0.4084	0.4114
960	−42.4	−35.1	875.15	122.94	2.4413	0.3603	0.3694	2.1890	1.1152	0.4018	0.4119	0.4059	0.4098	2.4473	0.9975	0.4049	0.4088
1080	−48.7	−40.4	874.23	122.02	2.4230	0.3535	0.3626	2.1485	1.1278	0.3987	0.4090	0.4029	0.4070	2.4296	0.9973	0.4018	0.4058
1200	−56.1	−46.6	873.30	121.09	2.4043	0.3466	0.3557	2.1068	1.1412	0.3955	0.4059	0.3997	0.4039	2.4109	0.9973	0.3986	0.4028
1320	−64.5	−52.9	872.40	120.19	2.3864	0.3397	0.3495	2.0673	1.1544	0.3921	0.4034	0.3964	0.4011	2.3925	0.9975	0.3954	0.4000
1440	−73.9	−59.2	871.51	119.30	2.3688	0.3329	0.3439	2.0304	1.1666	0.3884	0.4012	0.3931	0.3985	2.3748	0.9975	0.3921	0.3975
1560	−83.4	−66.5	870.60	118.39	2.3507	0.3269	0.3381	1.9952	1.1782	0.3852	0.3984	0.3901	0.3957	2.3575	0.9971	0.3890	0.3946
1680	−96.0	−74.9	869.72	117.51	2.3332	0.3200	0.3322	1.9568	1.1924	0.3816	0.3962	0.3866	0.3928	2.3381	0.9979	0.3858	0.3920
1800	−109.7	−84.3	868.80	116.59	2.3149	0.3135	0.3264	1.9198	1.2058	0.3781	0.3936	0.3831	0.3899	2.3189	0.9983	0.3824	0.3892

	2nd Iteration $\alpha = 0.04071$ $n = 1.09106$ $\theta_s = 0.4380$ $\theta_r = 0.0457$						3rd Iteration $\alpha = 0.04078$ $n = 1.09103$ $\theta_s = 0.4380$ $\theta_r = 0.0458$					
Time min	$\theta 1.5$ cm^3 cm^{-3}	$\theta 4.5$ cm^3 cm^{-3}	$S_c(t)$ cm	$S(t)\ S_c(t)^{-1}$	$\theta_{up}1.5$ cm^3 cm^{-3}	$\theta_{up}4.5$ cm^3 cm^{-3}	$\theta 1.5$ cm^3 cm^{-3}	$\theta 4.5$ cm^3 cm^{-3}	$S_c(t)$ cm	$S(t)\ S_c(t)^{-1}$	$\theta_{up}1.5$ cm^3 cm^{-3}	$\theta_{up}4.5$ cm^3 cm^{-3}
0	0.4299	0.4329	2.5884	1.0033	0.4313	0.4344	0.4299	0.4330	2.5884	1.0033	0.4313	0.4344
120	0.4269	0.4308	2.5729	1.0014	0.4275	0.4314	0.4269	0.4308	2.5729	1.0014	0.4275	0.4314
240	0.4240	0.4277	2.5551	1.0005	0.4242	0.4279	0.4240	0.4277	2.5552	1.0005	0.4242	0.4279
360	0.4214	0.4248	2.5386	0.9989	0.4210	0.4243	0.4214	0.4248	2.5386	0.9989	0.4210	0.4243
480	0.4182	0.4213	2.5186	0.9990	0.4178	0.4209	0.4182	0.4213	2.5186	0.9989	0.4178	0.4209
600	0.4145	0.4181	2.4979	0.9997	0.4144	0.4180	0.4145	0.4181	2.4979	0.9997	0.4144	0.4180
720	0.4119	0.4152	2.4811	0.9987	0.4113	0.4146	0.4119	0.4152	2.4811	0.9987	0.4113	0.4146
840	0.4089	0.4119	2.4621	0.9989	0.4084	0.4114	0.4089	0.4119	2.4621	0.9989	0.4084	0.4114
960	0.4056	0.4094	2.4449	0.9985	0.4050	0.4088	0.4056	0.4094	2.4449	0.9985	0.4050	0.4088
1080	0.4026	0.4066	2.4274	0.9982	0.4018	0.4058	0.4026	0.4066	2.4273	0.9982	0.4018	0.4058
1200	0.3994	0.4035	2.4087	0.9982	0.3987	0.4028	0.3994	0.4035	2.4087	0.9982	0.3986	0.4028
1320	0.3961	0.4007	2.3905	0.9983	0.3955	0.4000	0.3961	0.4007	2.3905	0.9983	0.3955	0.4000
1440	0.3929	0.3981	2.3730	0.9982	0.3922	0.3974	0.3929	0.3981	2.3730	0.9982	0.3922	0.3974
1560	0.3899	0.3954	2.3559	0.9978	0.3890	0.3945	0.3899	0.3954	2.3559	0.9978	0.3890	0.3945
1680	0.3864	0.3925	2.3367	0.9985	0.3858	0.3920	0.3864	0.3925	2.3367	0.9985	0.3858	0.3919
1800	0.3830	0.3896	2.3178	0.9988	0.3825	0.3892	0.3830	0.3896	2.3178	0.9988	0.3825	0.3892

[a] Calculated using Equation 81.2.
[b] Calculated using Equation 81.4.
[c] $\theta 1.5$ = water content for tensiometer located at depth, −1.5 cm.
[d] $\theta 4.5$ = water content for tensiometer located at depth, −4.5 cm.
[e] Calculated using Equation 81.6.

The iteration procedure is first initialized by estimating Equation 81.5 using an arbitrary set of fitting parameter values (Table 81.2) and then the measured matric heads, ψ, are input to calculate the corresponding volumetric water content values, θ, at the two tensiometer elevations (columns $\theta 1.5$ and $\theta 4.5$ in Table 81.2). The total water storage in the sample, $S_c(t)$, may then be estimated for each measurement time using

$$S_c(t) = [\theta 1.5(t) + \theta 4.5(t)]\Delta z \tag{81.6}$$

where Δz refers to the difference in elevation (or depth) between the two tensiometers (3 cm in this example). The iterations then proceed by (i) updating the water content at each depth and time ($\theta_{up}1.5$, $\theta_{up}4.5$, Table 81.2) by multiplying by $S(t)/S_c(t)$; (ii) curve fitting Equation 81.5 to the updated water contents to get a new set of fitting parameters (i.e., θ_s, θ_r, α, and n in this example); (iii) calculating a new set of water contents and $S_c(t)$ values; and (iv) returning to step (i). The results of the initialization and three successive iterations are illustrated in Table 81.2. In this example, the iteration process was set to terminate (converge) when the maximum change in calculated water content, $\Delta\theta$, was $<10^{-4}$ cm^3 cm^{-3} for all depths and measurement times (other convergence criteria can be specified). Successive curve-fitting of Equation 81.5 to each updated set of water contents can be achieved using specialized programs such as RETC (van Genuchten et al. 1991; see also Chapter 84), or using established curve-fitting algorithms such as the ''downhill simplex'' method (Press et al. 1990). In this example, the downhill simplex method was applied, and curve-fitting based on minimizing the squared deviations between successive estimates of water content (code available from the senior author). Note: for the example in Table 81.2, the maximum change in calculated water contents declined to 10^{-5} cm^3 cm^{-3} after only three iterations, which is not uncommon for reasonably homogeneous soil samples. Convergence to the correct solution (i.e., the correct fit of Equation 81.5 to the data) is indicated by $S(t)/S_c(t) \approx 1$ for all times and depths (Table 81.2). Results of the iterative estimation of $\theta(\psi)$ are illustrated in Figure 81.2 for the 2T and 5T setups, where it is seen that convergence was nearly immediate, regardless of the initial fitting parameter estimates.

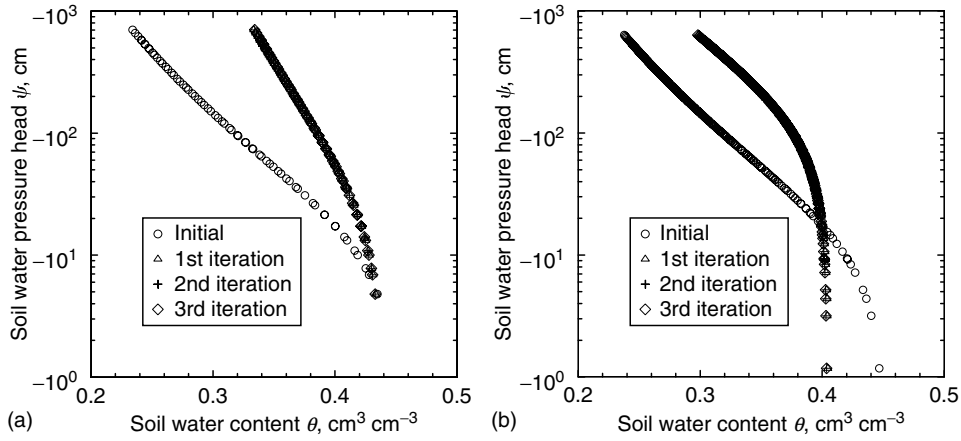

FIGURE 81.2. Iterative estimation of the water desorption curve, $\theta(\psi)$, for the 2T setup (a) and the 5T setup (b) of the evaporation or Wind method. The data for the 2T setup also appear in Table 81.2.

81.4.2 Calculation of the Hydraulic Conductivity Relationship, 2T Setup

The hydraulic conductivity relationship, $K(\psi)$ or $K(\theta)$, is calculated from the water flux density between the two tensiometers, q [LT^{-1}], and the corresponding hydraulic head gradient. The water flux density is given by (see Figure 81.3)

$$q = \frac{q_1 + q_2}{2} \tag{81.7a}$$

with

$$q_1 = \frac{\Delta S_1}{\Delta t}, \qquad q_2 = \frac{\Delta S_1 + \Delta S_2 + \Delta S_3}{\Delta t} \tag{81.7b}$$

and

$$\Delta S = \Delta\theta \cdot \Delta z \tag{81.7c}$$

where $\Delta\theta$ refers to the change in water content during a time step (i.e., between two successive collections of tensiometer readings and corresponding column weights). If it is assumed that $\Delta\theta$ increases linearly with depth within each time step, it can be shown that (Wendroth et al. 1993)

$$\begin{aligned} q_T &= \frac{(2.5\Delta\theta 4.5 - 0.5\Delta\theta 1.5)\Delta z + (\Delta\theta 4.5 + \Delta\theta 1.5)\Delta z}{2\Delta t} \\ &= \frac{(3.5\Delta\theta 4.5 + 0.5\Delta\theta 1.5)\Delta z}{2\Delta t} \end{aligned} \tag{81.7d}$$

The hydraulic head gradient, grad, at time t_i is (see Figure 81.3)

$$\text{grad}(t_i) = \frac{(\psi 1.5 + z1.5) - (\psi 4.5 + z4.5)}{(z1.5 - z4.5)}; \quad i = 1, 2, 3, \ldots \tag{81.8}$$

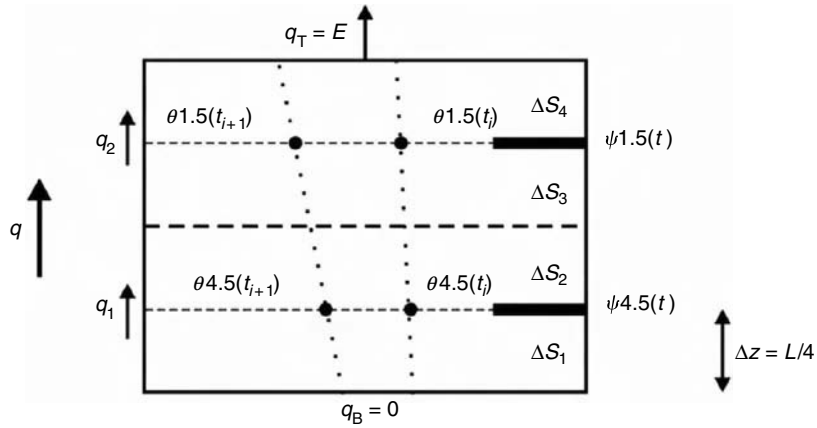

FIGURE 81.3. Flux calculation scheme for the 2T setup of the evaporation or Wind method. L = total column length (6 cm in this example).

For example, at $t_4 = 360$ min (Table 81.3), the following hydraulic head gradient is obtained:

$$\text{grad (360 min)} = \frac{[-17.2 \text{ cm} + (-1.5 \text{ cm})] - [(-13.2 \text{ cm}) + (-4.5 \text{ cm})]}{[-1.5 \text{ cm} - (-4.5 \text{ cm})]} = -\frac{1}{3} \text{ cm cm}^{-1}$$

The hydraulic head gradient causing flux during time interval, $\Delta t = (t_{i+1} - t_i)$ (i.e., time between two successive measurements) is the average gradient during Δt,

$$\overline{\text{grad}} = \frac{\text{grad}(t_i) + \text{grad}(t_{i+1})}{2} \tag{81.9}$$

Consequently, the hydraulic conductivity, K, for a given Δt is

$$K = -\frac{q}{\overline{\text{grad}}} \tag{81.10}$$

which applies for the geometric mean matric head, $\overline{\psi}$:

$$\overline{\psi} = 10^{\gamma} \tag{81.11a}$$

where

$$\gamma = \frac{[\log_{10} \psi 1.5(t_i) + \log_{10} \psi 1.5(t_{i+1}) + \log_{10} \psi 4.5(t_i) + \log_{10} \psi 4.5(t_{i+1})]}{4} \tag{81.11b}$$

and for the arithmetic mean volumetric water content, $\overline{\theta}$:

$$\overline{\theta} = \frac{\theta 1.5(t_i) + \theta 1.5(t_{i+1}) + \theta 4.5(t_i) + \theta 4.5(t_{i+1})}{4} \tag{81.12}$$

The resulting $K(\psi)$ relation (Figure 81.4a) corresponds well with tension infiltrometer measurements (Chapter 80 and Chapter 82) made on the same soil sample for $\psi = -1$, -5, and -10 cm (Wendroth and Simunek 1999).

81.4.3 Calculation of the Water Desorption Curve, 5T Setup

For the 10 cm high soil column with tensiometers at five levels, the water retention curve is estimated iteratively in the same way as for the 2T case. The calculated water storage at each of the five depths, $S_c(t)$, is integrated and compared to the measured total water storage, $S(t)$. The iterative estimation of curve parameters is repeated until the specified convergence criterion is met (e.g., $\Delta\theta < 10^{-4}$ cm^3 cm^{-3}). Example results are given in Figure 81.2b and Table 81.4 for the first two days of the experiment. As for the 2T setup, only three iterations were required to reach convergence at all depths.

81.4.4 Calculation of the Hydraulic Conductivity Relationship, 5T Setup

Because there are multiple depth intervals (tensiometers), the calculation of fluxes and hydraulic conductivities does not require the assumption of linearly increasing water flux between the top and bottom of the sample during a time interval, Δt, as required in the 2T setup.

TABLE 81.3 Example Calculation of the Hydraulic Conductivity Relationship, $K(\overline{\psi})$ and $K(\overline{\theta})$, for the 2T Setup (see Figure 81.3)

Time min	ψ1.5 cm	ψ4.5 cm	θ1.5 $cm^3\ cm^{-3}$	θ4.5 $cm^3\ cm^{-3}$	$S(t)$[a] cm	E[b] $cm\ d^{-1}$	grad[c] $cm\ cm^{-1}$	$\overline{\text{grad}}$[d] $cm\ cm^{-1}$	K[e] $cm\ d^{-1}$	$\overline{\psi}$[f] cm	$\overline{\theta}$[g] $cm^3\ cm^{-3}$
0	−7.8	−4.8	0.4299	0.4330	2.5970		0.00				
120	−10.9	−6.9	0.4269	0.4308	2.5765	0.2455	−0.33	−0.17	4.93E − 01	−7.3	0.4301
240	−14.1	−10.0	0.4240	0.4277	2.5565	0.2407	−0.37	−0.35	3.11E − 01	−10.2	0.4273
360	−17.2	−13.2	0.4214	0.4248	2.5358	0.2479	−0.33	−0.35	2.97E − 01	−13.4	0.4245
480	−21.4	−17.3	0.4182	0.4213	2.5160	0.2384	−0.37	−0.35	3.52E − 01	−17.0	0.4214
600	−26.7	−21.5	0.4145	0.4181	2.4971	0.2264	−0.73	−0.55	2.14E − 01	−21.5	0.4180
720	−30.9	−25.7	0.4119	0.4152	2.4778	0.2312	−0.73	−0.73	1.43E − 01	−26.0	0.4149
840	−36.1	−30.9	0.4089	0.4119	2.4593	0.2217	−0.73	−0.73	1.61E − 01	−30.7	0.4119
960	−42.4	−35.1	0.4056	0.4094	2.4413	0.2169	−1.43	−1.08	8.51E − 02	−35.9	0.4089
1080	−48.7	−40.4	0.4026	0.4066	2.4230	0.2193	−1.77	−1.60	6.45E − 02	−41.4	0.4060
1200	−56.1	−46.6	0.3994	0.4035	2.4043	0.2241	−2.17	−1.97	5.59E − 02	−47.6	0.4030
1320	−64.5	−52.9	0.3961	0.4007	2.3865	0.2145	−2.87	−2.52	4.10E − 02	−54.7	0.3999
1440	−73.9	−59.2	0.3929	0.3981	2.3688	0.2121	−3.90	−3.38	2.83E − 02	−62.2	0.3970
1560	−83.4	−66.5	0.3899	0.3954	2.3507	0.2169	−4.63	−4.27	2.33E − 02	−70.2	0.3941
1680	−96.0	−74.9	0.3864	0.3925	2.3332	0.2097	−6.03	−5.33	1.99E − 02	−79.5	0.3911
1800	−109.7	−84.3	0.3830	0.3896	2.3149	0.2193	−7.47	−6.75	1.58E − 02	−90.3	0.3879

[a] Calculated using Equation 81.4.
[b] Calculated from soil column weight change with time.
[c] Calculated using Equation 81.8.
[d] Calculated using Equation 81.9.
[e] Calculated using Equation 81.10.
[f] Calculated using Equation 81.11.
[g] Calculated using Equation 81.12.

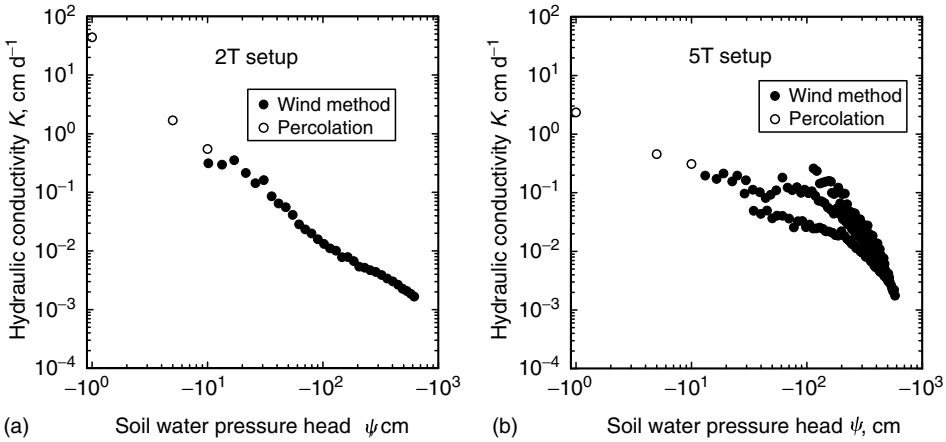

FIGURE 81.4. Hydraulic conductivity, K, as a function of soil water pressure or matric head, ψ, for the 2T setup (a) and the 5T setup (b) of the evaporation or Wind method. The open symbols represent tension infiltrometer measurements at $\psi = -1, -5$, and -10 cm.

The scheme for calculating fluxes conceptually divides the soil column into five compartments (Watson 1966), with a tensiometer located in the center of each compartment (Figure 81.5). Therefore, it is assumed that the measured matric heads and calculated soil water contents represent average values for their respective compartments at each measurement time. The bottom boundary is again zero flux, i.e., $q_B = 0$. The water flux, q_1, leaving the bottom compartment of the sample during time interval, Δt, is equivalent to the change in water storage in the compartment, ΔS_1, i.e.,

$$q_1 = \frac{\Delta S_1}{\Delta t} = \frac{[\theta 9(t_i) - \theta 9(t_{i+1})]\Delta z}{\Delta t} \tag{81.13}$$

where the depth increment, Δz, is 2 cm (see Figure 81.5). The flux, q_1, is caused by the hydraulic head gradient between the -7 cm and the -9 cm depths, which is calculated using $\psi 7(t)$ and $\psi 9(t)$, and averaged over Δt in the same way as for the 2T setup.

Flux, q_2, is the integral of the water storage changes below the 6 cm depth,

$$q_2 = \frac{\Delta S_1 + \Delta S_2}{\Delta t} = q_1 + \frac{\Delta S_2}{\Delta t} \tag{81.14}$$

and is due to the hydraulic head gradient between the -5 and -7 cm depths averaged over Δt, and is based on $\psi 5(t)$ and $\psi 7(t)$. The fluxes for the above compartments (i.e., compartments 3, 4, and 5) are calculated in a similar manner. Adding the change in water storage in the uppermost compartment at each time step, ΔS_5, to q_4 (i.e., the water flux entering this uppermost compartment from below), produces the total flux, q_T, which is theoretically equal to the measured evaporative water flux (E) out through the top of the column (Figure 81.5). Average matric head $\overline{\psi}$ and water content $\overline{\theta}$ values are calculated as in the 2T setup.

TABLE 81.4 Example Calculation of Hydraulic Conductivity for the 5T Setup. Data for Hydraulic Head Gradients and *K* Values Are Shown Only for the Upper Four Compartments (Figure 81.5)

Time min	$\psi 1$ cm	$\psi 3$ cm	$\psi 5$ cm	$\psi 7$ cm	$\psi 9$ cm	$\theta 1$ cm^3 cm^{-3}	$\theta 3$ cm^3 cm^{-3}	$\theta 5$ cm^3 cm^{-3}	$\theta 7$ cm^3 cm^{-3}	$\theta 9$ cm^3 cm^{-3}	$S(t)$ cm	g1−g[a] cm cm^{-1}	g3–5 cm cm^{-1}	g5–7 cm cm^{-1}	$K1–3$[b] $cm\ d^{-1}$	$K3–5$ $cm\ d^{-1}$	$K5–7$ $cm\ d^{-1}$
0	−9.18	−7.18	−5.18	−3.18	−1.18	0.4017	0.4022	0.4027	0.4031	0.4035	4.0667						
120	−15.48	−12.38	−9.38	−8.38	−4.38	0.4000	0.4009	0.4017	0.4019	0.4029	4.0381	−0.28	−0.25	0.25	3.65E − 01	2.74E − 01	−1.77E − 01
240	−21.78	−17.68	−14.58	−13.68	−10.68	0.3983	0.3994	0.4003	0.4005	0.4013	4.0122	−0.80	−0.53	0.53	1.72E − 01	1.96E − 01	−1.33E − 01
360	−27.98	−23.98	−20.88	−18.88	−16.98	0.3965	0.3977	0.3985	0.3991	0.3996	3.9910	−1.03	−0.55	0.28	1.56E − 01	2.13E − 01	−2.73E − 01
480	−35.28	−29.28	−26.18	−24.08	−22.28	0.3943	0.3961	0.3970	0.3976	0.3981	3.9711	−1.50	−0.55	−0.03	9.67E − 02	1.97E − 01	2.86E + 00
600	−41.58	−33.48	−30.28	−29.28	−26.48	0.3925	0.3949	0.3958	0.3961	0.3969	3.9521	−2.53	−0.58	0.23	4.90E − 02	1.64E − 01	−2.91E − 01
720	−46.78	−38.68	−34.48	−33.48	−31.68	0.3909	0.3933	0.3946	0.3949	0.3954	3.9337	−3.05	−0.85	0.50	4.35E − 02	1.13E − 01	−1.32E − 01
840	−51.98	−43.98	−39.78	−38.68	−36.98	0.3894	0.3918	0.3930	0.3933	0.3938	3.9160	−3.03	−1.10	0.48	4.95E − 02	1.02E − 01	−1.57E − 01
960	−57.18	−48.18	−43.98	−42.88	−41.18	0.3879	0.3905	0.3918	0.3921	0.3926	3.8999	−3.25	−1.10	0.45	3.67E − 02	8.14E − 02	−1.33E − 01
1080	−62.38	−53.48	−49.18	−48.08	−45.38	0.3864	0.3890	0.3902	0.3906	0.3914	3.8833	−3.48	−1.13	0.45	4.06E − 02	9.21E − 02	−1.48E − 01
1200	−71.78	−59.78	−55.48	−53.38	−51.68	0.3837	0.3871	0.3884	0.3890	0.3895	3.8649	−4.23	−1.15	0.20	4.04E − 02	1.10E − 01	−4.10E − 01
1320	−83.28	−67.18	−63.78	−61.68	−58.98	0.3804	0.3850	0.3860	0.3866	0.3874	3.8404	−6.03	−0.93	−0.05	3.63E − 02	1.81E − 01	2.19E + 00
1440	−86.38	−73.48	−69.08	−66.88	−65.28	0.3796	0.3832	0.3844	0.3851	0.3855	3.8208	−6.25	−0.95	−0.08	2.55E − 02	1.23E − 01	1.07E + 00
1560	−94.78	−80.88	−76.38	−73.18	−71.58	0.3773	0.3811	0.3824	0.3833	0.3837	3.7997	−5.70	−1.23	−0.35	3.27E − 02	1.11E − 01	2.47E − 01
1680	−103.08	−88.18	−83.68	−81.58	−78.98	0.3751	0.3791	0.3803	0.3809	0.3816	3.7785	−6.20	−1.25	−0.33	3.29E − 02	1.25E − 01	3.29E − 01
1800	−109.38	−94.48	−89.98	−87.78	−85.28	0.3734	0.3774	0.3786	0.3792	0.3799	3.7595	−6.45	−1.25	−0.08	2.57E − 02	9.98E − 02	1.11E + 00

[a] g1–3, g3–5, g5–7 refer to the hydraulic head gradients between the tensiometers located at the −1 and −3 cm depths, the −3 and −5 cm depths, and the −5 and −7 cm depths, respectively.

[b] *K*1–3, *K*3–5, *K*5–7 refer to calculated hydraulic conductivity for the −1 to −3 cm depth, the −3 to −5 cm depth, and the −5 to −7 cm depth, respectively.

Note: The water content values were calculated after the iterative estimation of the water retention curve (Equation 81.5, Figure 81.2b), which yielded $\alpha = 0.0057$, $n = 1.2094$, $\theta_s = 0.4037$, and $\theta_r = 0.0001$. Data are shown only for the first 1800 min of the experiment.

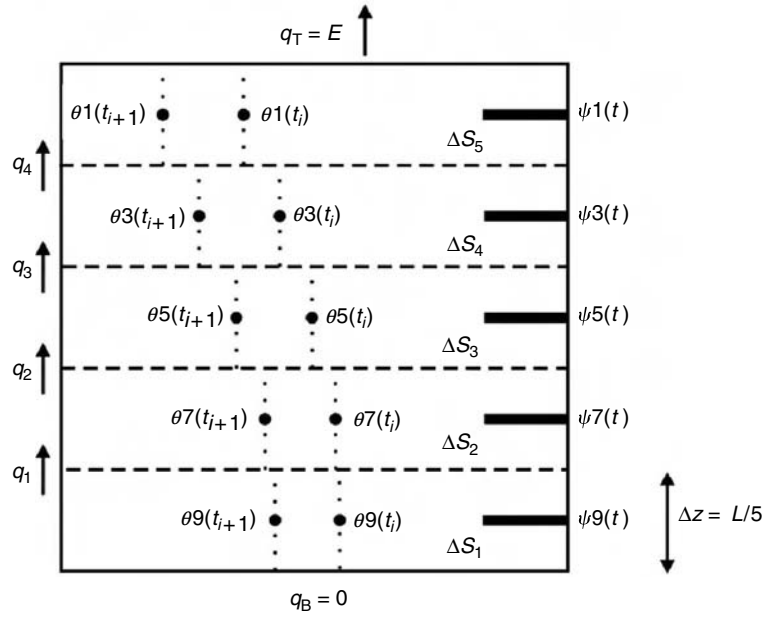

FIGURE 81.5. Flux calculation scheme for the 5T setup of the evaporation or Wind method. L = total column length (10 cm in this example).

The calculated $K(\psi)$ values are presented in Table 81.4 and plotted in Figure 81.4b. Although soil layering has caused the data to be much noisier than for the 2T case, the resulting $K(\psi)$ relationships still correspond well with tension infiltrometer measurements collected at $\psi = -1$, -5, and -10 cm.

81.4.5 Calculation of Capillarity Relationships

It should be possible to estimate the capillarity relationships, $\alpha^*(\psi)$, $S(\psi)$, $PD(\psi)$, and $NP(\psi)$ from the $K(\psi)$ and $\theta(\psi)$ results (see Chapter 69). This would likely involve (i) fitting an appropriate function to the $K(\psi)$ data; (ii) integrating under the fitted $K(\psi)$ function to obtain $\phi(\psi)$ via Equation 69.13; (iii) calculation of $\alpha^*(\psi)$ via Equation 69.16 [i.e., the $\alpha^*(\psi)$ values are ''integrally correct'']; and (iv) using $\alpha^*(\psi)$, $K(\psi)$, and $\theta(\psi)$ in Equation 69.17 through Equation 69.19 in Chapter 69 to obtain $S(\psi)$, $PD(\psi)$, and $NP(\psi)$, respectively. The success of this would probably depend on how well the $K(\psi)$ function fits the $K(\psi)$ data.

81.5 COMMENTS

1 *Measurement range and uncertainty*: The measurement range of the Wind and evaporation method is about -700 cm $\leq \psi \leq -10$ cm. Below $\psi \approx -700$ cm, tensiometers often fail due to loss of hydraulic contact with the soil, or air entry into the tensiometer cup. Although $\theta(\psi)$ can still be determined accurately for -10 cm $\leq \psi \leq 0$, hydraulic head gradients (grad) in this ψ range are often too close to zero (e.g., -1 cm cm^{-1} $\leq$ grad ≤ 0) for accurate determination of $K(\psi)$, and the $K(\psi)$ values can be in error by a factor of 100 or more. In the examples given here (Table 81.3 and Table 81.4; Figure 81.4), $K(\psi)$ was not determined for grad > -0.3 cm cm^{-1} in the 2T setup, and for grad > -0.5 cm cm^{-1}

in the 5T setup, these thresholds being determined by experience and by the accuracy and precision of the pressure transducers. Other methods, such as the tension infiltrometer (Chapter 80 and Chapter 82), should be used to obtain $K(\psi)$ in the -10 cm $\leq \psi \leq 0$ range (Wendroth and Simunek 1999).

2 *Method assumptions*: Critical assumptions of the method are that changes in water content and pore water matric head between adjacent tensiometers are linear, which further implies that water flow is steady and the soil sample is homogeneous and isothermal. Wendroth et al. (1993) validated these assumptions for the 2T setup over the range, -650 cm $\leq \psi \leq 0$, and also avoided potential sample boundary effects (Becher 1975) by locating the tensiometers away from the sample ends. Some attempts have been made to extend the method into the ''dry soil'' range (i.e., $\psi < -700$ cm) by installing gypsum blocks or other devices (e.g., Becher 1971a,b). This is not advisable for the 2T setup, however, as the assumption of linear water flux profile would likely be violated, and the hydraulic head gradient causing flux may not be adequately represented by ψ measurements at only two depths. Moreover, allowing evaporation to continue would eventually produce a downward-migrating ''drying front,'' which would cause a substantial decrease in evaporation rate as well as invalidate the application of Darcy's law for liquid water flow (Idso et al. 1974). A relatively steady evaporation rate is generally a good indicator that the quasisteady liquid water flow regime required by theory has been achieved (Willis 1960).

3 *Additional information*: Additional information on experimental procedures using two or more tensiometers is given in Schindler (1980) and Tamari et al. (1993). The optimum sample diameter or length and number of tensiometers depend on the soil condition, the objective of the investigation, and operator experience. On the one hand, it is not advisable to install many tensiometers in short samples, as the optimum tensiometer spacing for accurate determination of hydraulic head gradient is 2–3 cm. On the other hand, increasing sample length to accommodate more tensiometers often invalidates the assumption of sample homogeneity, which may complicate the results (e.g., Figure 81.4b). Sample diameters of 8–10 cm, sample lengths of 5–10 cm, and installation of two to five tensiometers with 2–3 cm spacing are used most commonly and most successfully. The top and bottom tensiometers should be installed at least 1–2 cm from the ends of the sample to avoid possible end effects. Criteria for minimum representative sample size in structured and unstructured soils are given in Chapter 69.

REFERENCES

Becher, H.H. 1971a. Ein Verfahren zur Messung der ungesättigten Wasserleitfähigkeit. *Z. Pflanzenern. Bodenkd*. 128: 1–12.

Becher, H.H. 1971b. Ergebnisse von Wasserleitfähigkeitsmessungen im wasserungesättigten Zustand. *Z. Pflanzenern. Bodenkd*. 128: 227–234.

Becher, H.H. 1975. Bemerkungen zur Ermittlung der ungesättigten Wasserleitfähigkeit unter nichtstationären Bedingungen. *Z. Pflanzenern. Bodenkd*. 132: 1–12.

Campbell, G.S. 1974. A simple method for determining conductivity from moisture retention data. *Soil Sci*. 117: 311–314.

Groenevelt, P.H. and Grant, C.D. 2004. A new method for the soil-water retention curve that solves the problem of residual water contents. *Eur. J. Soil Sci.* 55: 479–485.

Idso, S.B., Reginato, R.J., Jackson, R.D., Kimball, B.A., and Nakayama, F.S. 1974. The three stages of drying of a field soil. *Soil Sci. Soc. Am. Proc.* 38: 831–837.

Press, W.H., Flannery, B.P., Teukolsky, S.A., and Vetterling, W.T. 1990. *Numerical Recipes*. Cambridge University Press. New York, NY, 702 pp.

Schindler, U. 1980. Ein Schnellverfahren zur Messung der Wasserleitfähigkeit im teilgesättigten Boden an Stechzylinderproben. *Arch. Acker-Pflanzenbau Bodenkd.* 24: 1–7.

Tamari, S., Bruckler, L., Halbertsma, J., and Chadoeuf, J. 1993. A simple method for determining soil hydraulic properties in the laboratory. *Soil Sci. Soc. Am. J.* 57: 642–651.

van Genuchten, M.Th. 1980. A closed-form equation for predicting the hydraulic conductivity of unsaturated soils. *Soil Sci. Soc. Am. J.* 36: 380–383.

van Genuchten, M.Th., Leij, F.J., and Yates, S.R. 1991. The RETC code for quantifying the hydraulic functions of unsaturated soils, Version 1.0. EPA Report 600/2-91/065, U.S. Salinity Laboratory, USDA, ARS, Riverside, CA.

Watson, K.K. 1966. An instantaneous profile method for determining the hydraulic conductivity of unsaturated porous materials. *Water Resour. Res.* 2: 709–715.

Wendroth, O., Ehlers, W., Hopmans, J.W., Kage, H., Halbertsma, J., and Wösten, J.H.M. 1993. Reevaluation of the evaporation method for determining hydraulic functions in unsaturated soils. *Soil Sci. Soc. Am. J.* 57: 1436–1443.

Wendroth, O. and Simunek, J. 1999. Soil hydraulic properties determined from evaporation and tension infiltration experiments and their use for modeling field moisture status. In Van Genuchten, M.Th. and F.J. Leij, Eds. *Proceedings of the International Workshop on ''Characterization and Measurement of the Hydraulic Properties of Unsaturated Porous Media,''* Riverside, CA, pp. 737–748.

Willis, W.O. 1960. Evaporation from layered soils in the presence of a water table. *Soil Sci. Soc. Am. Proc.* 24: 239–242.

Wind, G.P. 1968. Capillary conductivity data estimated by a simple method. In P.E. Rijtema and H. Wassink, Eds. *Water in the Unsaturated Zone*. Proceedings of the Wageningen Symposium. June 1966. Vol. 1, IASAH, Gentbrugge, Belgium, pp. 181–191.

Chapter 82
Unsaturated Hydraulic Properties: Field Tension Infiltrometer

W.D. Reynolds
Agriculture and Agri-Food Canada
Harrow, Ontario, Canada

82.1 INTRODUCTION

The tension or disk infiltrometer is used primarily for field (*in situ*) measurement of near-saturated hydraulic conductivity, $K(\psi)$ [LT^{-1}], and sorptivity, $S(\psi)$ [$LT^{-1/2}$]. It can also be used, however, to determine near-saturated sorptive number, $\alpha^*(\psi)$ [L^{-1}], flow-weighted mean pore diameter, $PD(\psi)$ [L], and number of flow-weighted mean pores per unit area, $NP(\psi)$ [L^{-2}]. By ''near-saturated'' we mean measurements at pore water matric heads (ψ) within the range, ≈ -20 cm $\leq \psi \leq +2$ cm, although some infiltrometers can operate at matric heads as low as -40 cm. An alternative field method for $K(\psi)$ determination in the ''wet-end'' (i.e., -200 cm $\leq \psi \leq 0$) is given in Chapter 83. Laboratory methods for $K(\psi)$ or $K(\theta)$ determination are given in Chapter 80 and Chapter 81. Selected methods for estimating $K(\psi)$ from surrogate porous medium properties are given in Chapter 84. A discussion of the principles and parameters associated with the determination of $K(\psi)$ and the capillarity relationships [i.e., $S(\psi)$, $\alpha^*(\psi)$, $PD(\psi)$, $NP(\psi)$] appears in Chapter 69. Given that flow from field-based tension infiltrometers is three dimensional, the measured $K(\psi)$ and capillarity relationships are most relevant to three-dimensional flow.

Tension infiltrometers consist essentially of a 10–20 cm diameter ''infiltrometer plate'' containing a hydrophilic porous disk (e.g., ceramic, porous plastic, porous metal) or membrane (e.g., nylon mesh, sieve screen) connected to a water reservoir and a Mariotte-type bubble tower. The reservoir supplies water to the disk/membrane and the bubble tower determines the water matric head, ψ_0, on the disk/membrane ($\approx -20 \leq \psi_0 \leq +2$ cm). When the infiltrometer is placed on an unsaturated porous medium, the capillarity of the porous medium ''sucks'' the water out of the infiltrometer such that water infiltrates the porous medium under matric head, ψ_0. A layer of contact sand is frequently placed under the infiltrometer to ensure good hydraulic connection between the disk/membrane and the porous medium. Tension infiltrometer measurements can usually be obtained within a few minutes to several hours, depending on the type of analysis used and number of matric heads (ψ_0) set on the disk/membrane. Several steady-flow and transient-flow analyses are

available, which involve single, twin, or multiple infiltrometers and single or multiple matric heads (e.g., Elrick and Reynolds 1992; White et al. 1992; Clothier 2000; Smettem and Smith 2002). We will focus here, however, on one steady-flow analysis and one transient-flow analysis—both are physically based, practical, well established, and applicable to a single disk and one or more matric heads (see Section 82.4.6). We will also focus on the ''overhead reservoir'' infiltrometer design (e.g., the ''CSIRO'' or ''Guelph'' tension infiltrometers), notwithstanding that other valid designs exist (see Section 82.4.6).

82.2 APPARATUS AND PROCEDURES

1 For a measurement at the porous medium surface, choose a level site (or cut a level ''bench'' if on a continuous hillslope), which is at least as large as the retaining ring for the contact material (Figure 82.1) (see Section 82.4.5). Clip vegetation flush with the surface and remove all debris that are both loose and ''large'' (e.g., plant residues, stones, etc., which are more than about 0.4 cm high), as this material may cause poor contact between the porous medium and the contact sand. Avoid measurement sites containing large ''attached'' debris, such as partially exposed roots, partially buried plant residues and stones, large clods, etc., which are greater than about 0.4 cm high. The disruption of the porous medium caused by removal of attached debris or extraction of plant roots may change the hydraulic properties of the infiltration surface. For a subsurface measurement (or measurement on a bench cut into a hillslope), the site should

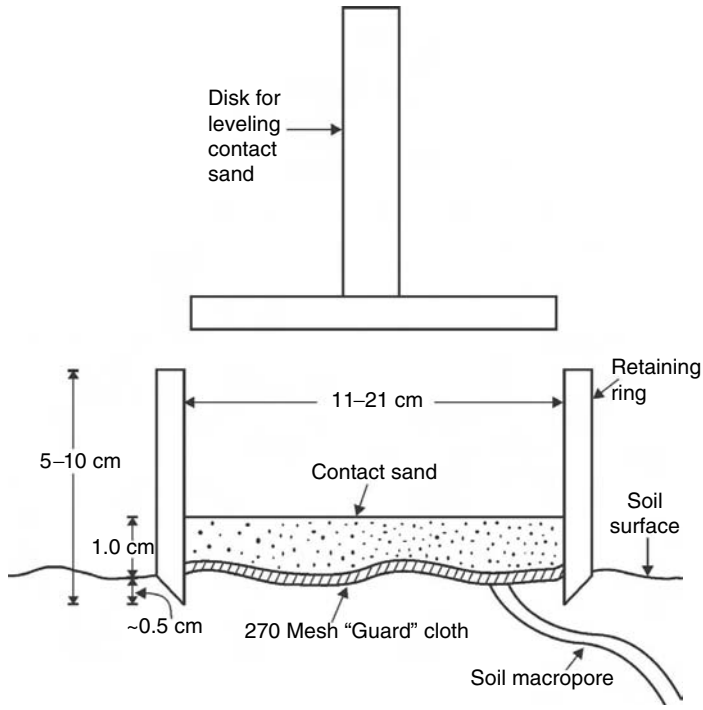

FIGURE 82.1. Schematic of the retaining ring, leveling disk, contact sand, and guard cloth for use in the tension infiltrometer method. (Adapted from Reynolds, W.D., in M.R. Carter (Ed.), *Soil Sampling and Methods of Analysis*, Canadian Society of Soil Science, Lewis Publishers, Boca Raton, Florida, 1993. With permission.)

be excavated using procedures that minimize smearing and compaction, which can also alter hydraulic properties.

2 Gently press a sharpened ''retaining ring'' into the infiltration surface to a depth of about 0.5 cm (Figure 82.1) (see Section 82.4.1). The retaining ring, which is conveniently constructed from PVC sewer pipe, should be just large enough to allow the chosen size of infiltrometer (10–20 cm diameter) to fit inside (Figure 82.2).

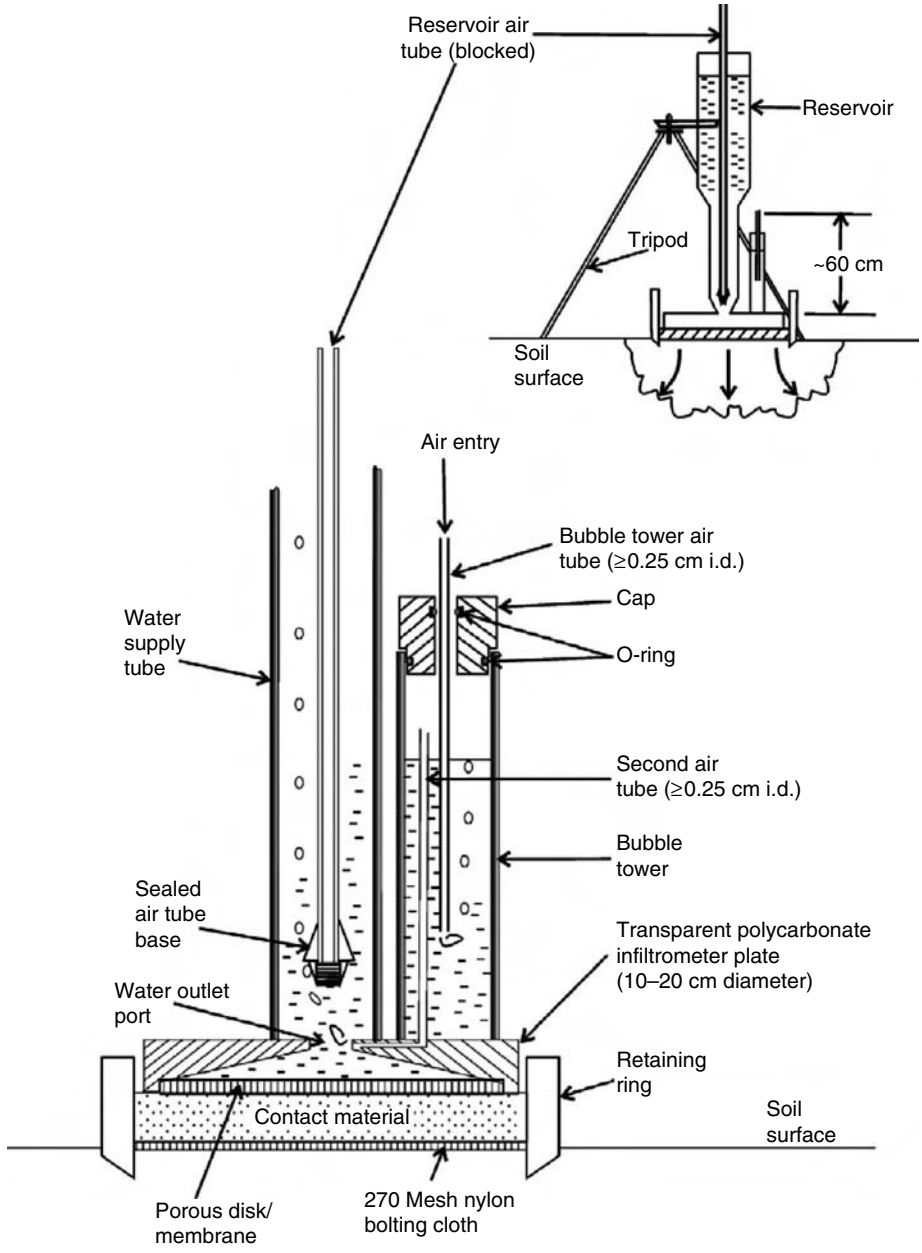

FIGURE 82.2. Schematic of the tension infiltrometer apparatus—''Guelph'' version with concentric overhead reservoirs. (Adapted from Reynolds, W.D., in M.R. Carter (Ed.), *Soil Sampling and Methods of Analysis*, Canadian Society of Soil Science, Lewis Publishers, Boca Raton, Florida, 1993. With permission.)

3 Lay a circle of flexible 270 mesh ''guard'' cloth (e.g., 53 μm pore size, ''Nitex'' nylon bolting cloth, precut to the same inside diameter as the retaining ring) on the infiltration surface inside the ring (see Section 82.4.1). Pour air-dry contact sand (discussed further below) on top of the cloth to an average depth of 1 cm (a 1 cm reference line on the inside of the retaining ring helps achieve this). Level, smooth, and lightly tamp the contact sand using a wooden disk or similar device (Figure 82.1).

4 Attach the presaturated infiltrometer plate and supply tube assembly (see Section 82.4.2 for details concerning the construction and saturation of the infiltrometer plate) to the water reservoir (e.g., see Chapter 76) and stand upright with the infiltrometer disk submerged in a flat-bottomed pail below a few centimeters of water. Support the infiltrometer using a large tripod (Figure 82.2). Close the water outlet of the infiltrometer plate by firmly pushing the base of the reservoir air tube down into the outlet port, and then fill the reservoir to the top with water. The base of the reservoir air tube should be sealed (clear silicon caulking or a small rubber bung works well for this), so that the bubble tower air tube provides the only source of air (Figure 82.2). Using a syringe (illustrated in Figure 82.6), adjust the water level in the bubble tower to establish the minimum (most negative) desired matric head. Open the water outlet of the infiltrometer plate by lifting the base of the reservoir air tube out of the water outlet port (as indicated in Figure 82.2). The water used in the infiltrometer should meet the same specifications as given for the well permeameter method (see Chapter 76).

5 Lift the infiltrometer out of the bucket and tilt slightly to remove water from the upper surface of the infiltrometer plate. Carefully lower the infiltrometer plate onto the contact sand, using a slight twist to ensure contact. Use the tripod to hold the infiltrometer in place and to carry the weight of the reservoir and water (Figure 82.2, inset). When initial contact with the contact sand is made, air bubbles should rise rapidly in the bubble tower and up into the reservoir, indicating rapid saturation of the contact sand. Air bubbles should not appear from any location other than the bubble tower air tube and the connection between the bubble tower and the water supply tube (Figure 82.2; see also Section 82.4.2). The infiltrometer is operating properly when air bubbles rise regularly up into the reservoir from the connection between the bubble tower and the supply tube.

Measurements should be limited to porous materials, which are at field capacity or drier (i.e., antecedent pore water matric head, $\psi_i \leq -50$ to -100 cm), otherwise there may be insufficient capillarity in the porous medium to draw water out of the infiltrometer against the tension applied by the bubble tower. Also, tension infiltrometer theory (Chapter 69) requires that the porous medium be sufficiently dry (i.e., $\psi_i \leq -50$ to -100 cm) to ensure that the antecedent $K(\psi)$ value is negligibly small relative to the minimum $K(\psi)$ being measured (steady-flow analysis), and that the early-time transient-flow phase is long enough to provide relevant measurements (transient-flow analysis). Working with ''wet'' porous materials may consequently require preliminary measurement of ψ_i (e.g., using a portable/handheld tensiometer—Chapter 71) to ensure that the material is ''dry'' enough for tension infiltrometer application.

6 The rate of water flow or discharge (Q) out of the infiltrometer and into the porous medium is measured by monitoring the rate of fall, R [LT^{-1}], of the water level in

the infiltrometer reservoir. This can be accomplished using a handheld stopwatch and a scale attached to the reservoir, or via an automated pressure transducer–data logger system similar to that described by Ankeny (1992). For the transient-flow analysis, start measurements as soon as the infiltrometer plate touches the contact sand, and collect frequent early-time measurements (e.g., after 0, 5, 10, 20, 40, . . . s). This ensures that sufficient flow data are collected to both identify contact sand effects and delineate the time period over which the transient analysis is applicable. For the steady-flow analysis, measurements do not need to be started immediately, as only the steady-flow rate is required.

7 For the transient-flow analysis, collect a small disturbed sample (only a few millimeters deep) from the infiltration surface immediately after infiltration is stopped (by quickly removing the infiltrometer and contact sand), and collect a second sample adjacent to the infiltration surface but just outside the wetted zone. Seal these samples in water vapor–tight containers and transport to the laboratory for water content determination (Chapter 70). The difference in water content between the wetted and unwetted (background) soil, $\Delta\theta = \theta(\psi_0) - \theta(\psi_i)$, is required to determine $K(\psi_0)$ from the transient-flow analysis, and $S(\psi_0)$ from the steady-flow analysis (see Section 82.3). Small *in situ* TDR probes (Chapter 70) have also been used to obtain $\Delta\theta$ (e.g., Vogeler et al. 1996; Wang et al. 1998).

8 Calculate the near-saturated $K(\psi)$ and capillarity parameters as indicated below.

82.3 ANALYSIS AND EXAMPLE CALCULATIONS

82.3.1 Steady Flow

Under a constant matric head, ψ_0, the rate of fall of the water level in the infiltrometer reservoir, R [LT^{-1}], normally decreases with increasing time, and approaches a constant value, R_s, as the flow rate becomes quasisteady (Q_s). Quasisteady flow is usually assumed when effectively the same R-value (R_s) is obtained over four or five consecutive R measurements (i.e., R constant within about $\pm 1\%$–5% with no trend evident—see Table 76.3, Chapter 76, for example R_s and Q_s calculations; see also Section 82.4.3). Once steady flow is attained at the current matric head (e.g., ψ_1), the water level in the bubble tower is adjusted to obtain the next desired matric head (e.g., ψ_2), and flow is again monitored until the next steady-flow rate is attained. The method requires that at least two matric heads (ψ_1, ψ_2) are set sequentially on the infiltrometer plate (by adjusting the water level in the bubble tower), and measurement of the corresponding steady-flow rates [$Q_s(\psi_1)$, $Q_s(\psi_2)$]. The matric heads should be set in ascending order of magnitude (i.e., $\psi_1 < \psi_2 < \psi_3, \ldots$), with the first and most negative matric head (ψ_1) no less than about -20 cm, and the last and largest matric head (ψ_n) at or near zero. It is recommended that 3–5 matric heads be used to provide adequate definition of the various near-saturated flow parameters (see also Section 82.4.4). Once Q_s is obtained for the desired number of matric heads, the $K(\psi_0)$, $\alpha^*(\psi_0)$, $S(\psi_0)$, $PD(\psi_0)$, and $NP(\psi_0)$ relationships can be calculated as described below.

Steady constant-head infiltration from the tension infiltrometer can be described using the Wooding (1968) ''shallow pond'' relationship written in the form

$$Q_s(\psi_0) = \pi a^2 K(\psi_0) + \frac{a}{G}\phi(\psi_0) \tag{82.1}$$

where $Q_s(\psi_0)$ [L^3T^{-1}] is the steady-flow rate out of the infiltrometer and into the porous medium when $\psi = \psi_0$ [L] on the infiltration surface, a [L] is the inside radius of the retaining ring, $K(\psi_0)$ [LT^{-1}] is the hydraulic conductivity at the infiltration surface, $G = 0.237$ is a shape factor constant (Reynolds and Elrick 1991), and $\phi(\psi_0)$ [L^2T^{-1}] is the matric flux potential at the infiltration surface (see Equation 69.13, Chapter 69). Substituting the Gardner (1958) exponential $K(\psi)$ relationship (Equation 69.14, Chapter 69) into Equation 82.1 and assuming $K(\psi_i) \ll K(\psi_0)$ produces

$$Q_s(\psi_0) = \left(\pi a^2 + \frac{a}{\alpha^*(\psi_0)}\right) K_{fs} \exp\left[\alpha*(\psi_0)\psi_0\right] \tag{82.2}$$

where $\alpha^*(\psi_0)$ [L^{-1}] is the sorptive number (Equation 69.16, Chapter 69) and K_{fs} [LT^{-1}] is the field-saturated hydraulic conductivity (Equation 69.9, Chapter 69) of the porous medium.

If it is assumed that $\alpha^*(\psi_0)$ is constant between any two adjacent matric heads set on the infiltrometer plate (ψ_0), Equation 82.2 can be written in the form (Reynolds and Elrick 1991):

$$\ln Q_s(\psi_0) = \alpha'_{x,x+1}\psi_0 + \ln\left[\left(\pi a^2 + \frac{a}{\alpha'_{x,x+1}G}\right)K'_{x,x+1}\right]; \quad x = 1, 2, 3, \ldots, n-1; \quad n \geq 2 \tag{82.3}$$

where n is the total number of matric heads set on the infiltrometer plate, ψ_x and ψ_{x+1} are matric heads set in succession on the plate (first ψ_x, then ψ_{x+1}, with ψ_x more negative than ψ_{x+1}), and $\alpha'_{x,x+1}$ and $K'_{x,x+1}$ are parameters related to $\alpha^*(\psi_0)$ and $K(\psi_0)$, respectively. Equation 82.3 describes a piece-wise linear plot of $\ln Q_s(\psi_0)$ versus ψ_0, from which $\alpha'_{x,x+1}$ is determined from the piece-wise slope:

$$\alpha'_{x,x+1} = \frac{\ln\left[Q_s(\psi_x)/Q_s(\psi_{x+1})\right]}{(\psi_x - \psi_{x+1})} \tag{82.4}$$

and $K'_{x,x+1}$ is determined from the piece-wise intercept:

$$K'_{x,x+1} = \frac{G\alpha'_{x,x+1}\, Q_s(\psi_x)}{a(1 + G\alpha'_{x,x+1}\pi a)[Q_s(\psi_x)/Q_s(\psi_{x+1})]^P} \tag{82.5}$$

where $P = \psi_x/(\psi_x - \psi_{x+1})$. For the intermediate ψ_0 values ($\psi_2, \psi_3, \ldots, \psi_{n-1}$) the $K(\psi_0)$ values are calculated using

$$K(\psi_x) = \frac{\left[K'_{x-1,x}\exp\left(\alpha'_{x-1,x}\psi_x\right) + K'_{x,x+1}\exp\left(\alpha'_{x,x+1}\psi_x\right)\right]}{2} \tag{82.6}$$

while $K(\psi)$ for the first ψ_0 value (i.e., ψ_1) is given by

$$K(\psi_1) = K'_{1,2}\exp\left(\alpha'_{1,2}\psi_1\right) \tag{82.7}$$

and $K(\psi)$ for the last ψ_0 value (i.e., ψ_n) is given by

$$K(\psi_n) = K'_{n-1,n}\exp\left(\alpha'_{n-1,n}\psi_n\right) \tag{82.8}$$

Once the $K(\psi_0)$ values are calculated, the corresponding $\alpha^*(\psi_0)$ values are determined by solving Equation 82.1 for $\phi(\psi_0)$, then substituting in Equation 69.16 (Chapter 69) to produce

$$\alpha^*(\psi_0) = \frac{aK(\psi_0)}{G[Q(\psi_0) - \pi a^2 K(\psi_0)]} \tag{82.9}$$

The $S(\psi_0)$, $PD(\psi_0)$, and $NP(\psi_0)$ relationships can then be calculated using Equation 69.17 through Equation 69.19, respectively, in Chapter 69. Note that the $S(\psi_0)$ calculation requires independent determination of $\Delta\theta = \theta(\psi_0) - \theta(\psi_i)$, which for multiple head analyses, would require installation of an *in situ* water content measuring device (e.g., TDR probe—Chapter 70) under the infiltrometer plate to avoid interrupting flow and destructive sampling of the infiltration surface.

82.3.2 Transient Flow

Under a constant matric head, early-time transient flow out of the infiltrometer can be described using a two-term infiltration equation similar in form to that developed by Philip (1957) for one-dimensional infiltration:

$$I(\psi_0) = E_1 t^{1/2} + E_2 t \tag{82.10}$$

where $I(\psi_0)$ [L^3L^{-2}] is cumulative infiltration from the infiltrometer at $\psi = \psi_0$, t [T] is time, and E_1 and E_2 are constants related to the porous medium hydraulic properties. Equation 82.10 is applied by differentiating with respect to $t^{1/2}$ to produce (Vandervaere et al. 2000a)

$$\frac{dI(\psi_0)}{dt^{1/2}} = E_1 + 2E_2 t^{1/2} \tag{82.11}$$

which implies that a plot of $dI(\psi_0)/dt^{1/2}$ versus $t^{1/2}$ should be linear with a Y-axis intercept of E_1 and a slope of $2E_2$. Haverkamp et al. (1994) showed that for three-dimensional infiltration at short-to-medium times (not approaching steady state)

$$E_1 = S(\psi_0) \tag{82.12}$$

and

$$E_2 = \left(\frac{2-\beta}{3}\right)K(\psi_0) + \frac{\omega S(\psi_0)^2}{a[\theta(\psi_0) - \theta(\psi_i)]} \tag{82.13}$$

where $\beta \approx 0.6$ (Haverkamp et al. 1994), $\omega = 0.75$ (Smettem et al. 1994), $S(\psi_0)$ [$LT^{-1/2}$] is porous medium sorptivity at $\psi = \psi_0$, $\theta(\psi_0)$ is porous medium volumetric water content at $\psi = \psi_0$, and $\theta(\psi_i)$ is the antecedent volumetric water content at the antecedent pore water matric head, ψ_i. Next, Equation 82.11 is discretized to produce (Vandervaere et al. 2000a)

$$\frac{dI(\psi_0)}{dt^{1/2}} \approx \frac{\Delta I(\psi_0)}{\Delta t^{1/2}} = \frac{(I_{j+1} - I_j)}{({t_{j+1}}^{1/2} - {t_j}^{1/2})} = E_1 + 2E_2 {}^*{t_j}^{1/2} \tag{82.14}$$

where $j = 1, 2, 3, \ldots (n-1)$, n is the number of $\Delta I(\psi_0)/\Delta t^{1/2}$ versus $t^{1/2}$ data points, and ${}^*{t_j}^{1/2}$ is calculated as the geometric mean of ${t_j}^{1/2}$ and ${t_{j+1}}^{1/2}$ $\left(\text{i.e., } {}^*{t_j}^{1/2} = \sqrt{{t_{j+1}}^{1/2} \cdot {t_j}^{1/2}}\right)$. Then, simple linear regression is used to calculate both the magnitudes and standard errors of

E_1 and E_2, noting that calculation of $K(\psi_0)$ from E_2 (Equation 82.13) requires independent measurement of $\Delta\theta = \theta(\psi_0) - \theta(\psi_i)$. Vandervaere et al. (2000b) showed that determination of $K(\psi_0)$ from Equation 82.13 is most accurate when

$$\frac{\omega {E_1}^2}{a[\theta(\psi_0) - \theta(\psi_i)]} < \frac{E_2}{2} \tag{82.15}$$

and determination of $S(\psi_0)$ from Equation 82.12 is most accurate when the porous medium sorptivity is close to a so-called optimal value given by

$$S(\psi_0)_{opt} = \sqrt{\frac{a[\theta(\psi_0) - \theta(\psi_i)](2-\beta)K(\psi_0)}{3\omega}} \tag{82.16}$$

Both of these criteria minimize the interference (masking effect) of source geometry (finite disk radius) in the $K(\psi_0)$ and $S(\psi_0)$ calculations, and are best achieved by using large infiltrometer plates. Selecting relatively wet antecedent moisture conditions further assists in achieving the $K(\psi_0)$ criterion (i.e., Equation 82.15), whereas selecting relatively dry antecedent moisture conditions further assists in achieving the $S(\psi_0)$ criterion (i.e., Equation 82.16). Once $K(\psi_0)$ and $S(\psi_0)$ are calculated, $\alpha^*(\psi_0)$, $PD(\psi_0)$, and $NP(\psi_0)$ can be determined via Equation 69.17 through Equation 69.19, respectively, in Chapter 69.

An important and elegant feature of Equation 82.14 is the ease with which the transient analysis can be validated; that is, a plot of $\Delta I(\psi_0)/\Delta t^{1/2}$ versus $t^{1/2}$ must be linear with both E_1 (intercept) and $2E_2$ (slope) positive. If these criteria are not met, the basic assumptions of the method (i.e., constant-head infiltration into rigid, homogeneous, isotropic porous medium with uniform antecedent water content) are seriously violated and the calculated E_1 and E_2 values are not likely to have physical meaning. Vandervaere et al. (2000a) also showed that Equation 82.14 provides a convenient and sensitive means for detecting loss of hydraulic contact between the infiltrometer disk/membrane and the porous medium, and for eliminating flow data perturbed by contact sand (see Section 82.3.3).

The transient-flow approach is limited to varying degrees in its ability to apply a succession of ψ_0 values to a single infiltration surface. This is because the transient analysis is valid only for early-time flow not approaching steady state, and the transition toward steady state can start very soon after the initiation of flow, depending on the ψ_0 value, the infiltrometer radius, and the texture, structure, and antecedent water content of the porous medium. Applying a succession of ψ_0 values to a single infiltration surface would also require installation of an *in situ* water content measuring device (e.g., TDR probe—Chapter 71) under the infiltrometer plate to obtain $\Delta\theta$ without interrupting flow or destructive sampling of the infiltration surface. Routine determination of $K(\psi_0)$, $S(\psi_0)$, $\alpha^*(\psi_0)$, $PD(\psi_0)$, and $NP(\psi_0)$ for a range of ψ_0 values may consequently require the use of several adjacent infiltration surfaces (rather than a single infiltration surface), which may in turn increase the uncertainty of the results because of small-scale spatial variability.

82.3.3 Accounting for Contact Sand

A layer of ''contact sand'' (usually natural sand, uniform glass beads, or some other fine particulate material) should be placed under the tension infiltrometer to establish and maintain good hydraulic connection or linkage between the disk/membrane and the porous medium. This should be done regardless of whether the porous medium surface has been

smoothed, leveled, or left undisturbed (e.g., Perroux and White 1988; Bagarello et al. 2001; Vandervaere 2002; Smettem and Smith 2002), and regardless of whether steady-state or transient analyses are used (Vandervaere 2002). The contact sand layer can introduce artifacts, however, which must be accounted for in tension infiltrometer analyses (Reynolds and Zebchuk 1996).

For both steady state and transient flow, the saturated hydraulic conductivity of the contact sand, K_{cs} [LT^{-1}], must be greater than the maximum measured $K(\psi_0)$ of the porous medium. Also, the water-entry matric head of the contact sand, ψ_w [L] (i.e., the matric head at which the contact sand spontaneously saturates from a dry state), must be smaller (more negative) than the minimum matric head set on the infiltrometer plate, ψ_0. If these criteria are not met, the hydraulic conductivity of the contact sand may fall below that of the porous medium at one or more of the set ψ_0 values, and the sand layer may consequently restrict the flow and cause the infiltrometer measurements to be unrepresentative of the porous medium. Reynolds and Zebchuk (1996) recommend a fine glass bead material with $\psi_w = -30$ cm and $K_{cs} = 10^{-2}$ cm s^{-1}, which should be adequate for $\psi_0 \geq -20$ cm and for use on most agricultural soils.

For steady flow, elevation and hydraulic head-loss effects induced by the contact sand layer can produce an important difference (or offset) between the matric head set on the infiltrometer plate (ψ_0) and the matric head actually applied to the soil surface (ψ_s). If the contact sand layer is contained within a retaining ring (Figure 82.2), flow through the sand layer is steady, saturated, and rectilinear, which allows the ψ_s value to be estimated accurately using Darcy's law in the form (Reynolds and Zebchuk 1996):

$$\psi_s = \psi_0 + \left[1 - \frac{Q(\psi_0)}{\pi a^2 K_{cs}}\right] T_{cs} \tag{82.17}$$

where $Q(\psi_0)$ [L^3T^{-1}] is the flow rate out of the infiltrometer at $\psi = \psi_0$, K_{cs} [LT^{-1}] is the saturated hydraulic conductivity of the contact sand layer, T_{cs} [L] is the mean thickness of the contact sand layer (Figure 82.1), and a [L] is the inside radius of the retaining ring. The value of ψ_s thus depends on ψ_0, $Q(\psi_0)$, K_{cs}, T_{cs}, and a. Using numerical simulations and controlled laboratory experiments, Reynolds and Zebchuk (1996) determined that ψ_s during steady flow can range between $\psi_s \approx \psi_0$ and $\psi_s \approx (\psi_0 + T_{cs})$ when $K_{cs} \geq K_{fs}$. Given that $T_{cs} = 1.0$ cm is often considered a practical minimum for field studies due to the roughness of undisturbed soil surfaces (Thony et al. 1991), the ψ_s value can differ from ψ_0 by 1.0 cm or more. Tension infiltrometer analyses based on steady flow should consequently use ψ_s (calculated using Equation 82.17) rather than ψ_0 to maintain accuracy when contact sand is used.

The contact sand layer can also introduce substantial artifact effects into transient infiltration from the tension infiltrometer, although this may be difficult to detect from plots of cumulative infiltration versus time (e.g., Figure 82.3), or infiltration flux versus time (Vandervaere et al. 2000a). Plotting infiltration data according to Equation 82.14, however, reveals a distinct early-time negative slope region followed by a later-time positive slope region (Figure 82.4). The nonlinear negative slope region indicates contact sand effects, whereas the linear positive slope region represents infiltration into the porous medium (Vandervaere et al. 2000a; Vandervaere 2002). Thus, only the data in the linear positive slope region are used for the determination of $K(\psi_0)$ and $S(\psi_0)$. Inclusion of the contact sand–affected data, even when the sand layer is only a few millimeters thick, can result in large errors and/or physically meaningless (e.g., negative) $K(\psi_0)$ and $S(\psi_0)$ values (Vandervaere et al. 2000a). Equation 82.14 consequently provides an easy and convenient means for identifying contact sand

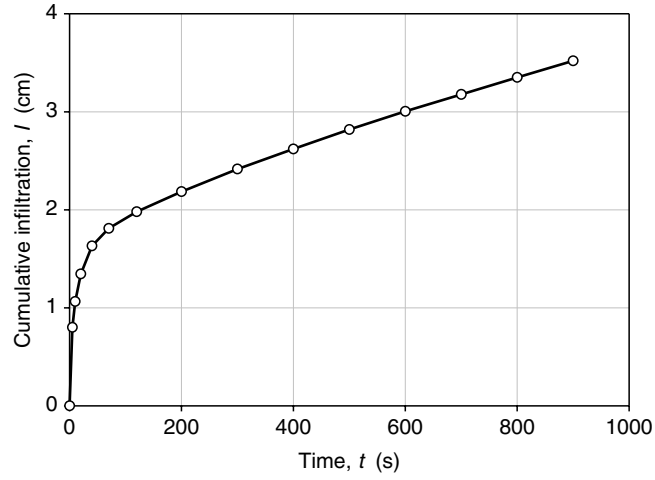

FIGURE 82.3. Example of cumulative tension infiltration, I, versus time, t, into a layer of air-dry contact sand placed over an unsaturated loamy sand soil. The matric head set on the infiltrometer membrane was $\psi_0 = -3$ cm. Contact sand thickness and saturated hydraulic conductivity were $T_{cs} = 1$ cm and $K_{cs} = 1.0 \times 10^{-2}$ cm s^{-1}, respectively. The cumulative infiltration versus time data also appear in Table 82.2.

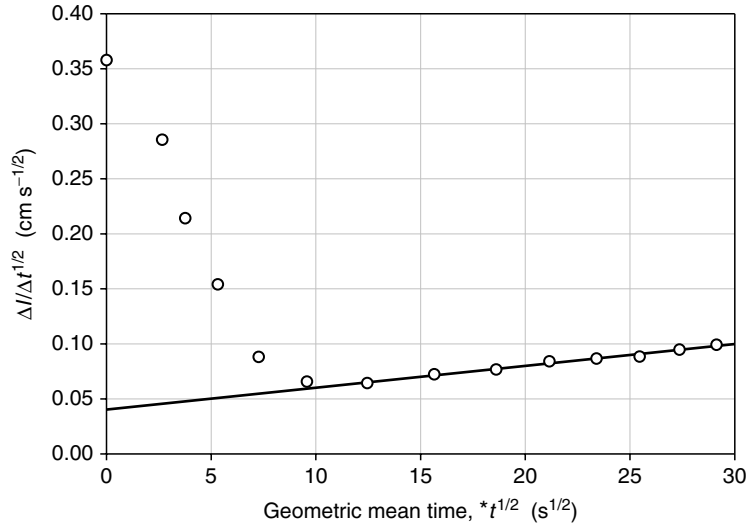

FIGURE 82.4. The previous figure plotted as infiltration rate, $\Delta I/\Delta t^{1/2}$, versus geometric mean square root time, $*t^{1/2}$ (see Equation 82.14). The initial negative slope portion (first six data points) represents wetting and saturation of the contact sand, and the linear positive slope portion represents infiltration into the unsaturated loamy sand soil. The solid straight line is a least squares regression through the linear data (final eight data points), from which near-saturated soil sorptivity, $S(\psi_0)$, and near-saturated soil hydraulic conductivity, $K(\psi_0)$, can be calculated using Equation 82.12 and Equation 82.13, respectively. In this example, $S(\psi_0) = 4.03 \times 10^{-2}$ cm s$^{-1/2}$ and $K(\psi_0) = 1.08 \times 10^{-3}$ cm s^{-1}, with $\psi_0 = -3$ cm. The infiltration rate versus geometric mean square root time data also appear in Table 82.2.

effects, and for eliminating these data from the transient analysis. As with the steady-state analyses, ψ_s should be used in place of ψ_0 in Equation 82.12 and Equation 82.13 to account for elevation and head-loss effects caused by the contact sand layer, especially when the layer must be thick due to surface roughness. This is somewhat less straightforward for transient analyses, however, because $Q(\psi_0)$ changes with time, and this may in turn cause ψ_s to change with time. For example, Figure 82.5 illustrates the predicted change in ψ_s with K_{cs} and time (using Equation 82.17) for the same transient infiltration data used to generate Figure 82.3 and Figure 82.4, but after the contact sand layer was fully wetted (i.e., for times greater than 150 s). Note that when K_{cs} is an order of magnitude greater than the $K(\psi)$ of the porous medium, ψ_s is effectively constant (as required by the transient analysis), but offset from ψ_0 by $\approx +0.8$ cm; hence, use of ψ_0 instead of ψ_s in the flow parameter calculations would introduce substantial error. On the other hand, when K_{cs} is equal to the $K(\psi)$ of the porous medium, ψ_s not only is offset substantially from ψ_0 (by about -1.6 to -0.7 cm), but also changes with time (by about 20%), which violates the constant-head requirement of the transient analysis. Successful application of the transient analysis with contact sand consequently requires both accounting for the offset between ψ_s and ψ_0 (via Equation 82.17) and ensuring that K_{cs} is sufficiently greater than the $K(\psi)$ of the porous medium to maintain ψ_s constant.

Another important consequence of using contact sand is that ψ_s can be slightly positive when ψ_0 is close to zero. Given that the tension infiltrometer relationships apply only for $\psi_s \leq 0$, then either ψ_0 must be adjusted to prevent $\psi_s > 0$ (e.g., by accounting for the thickness of the contact sand layer in the bubble tower calibration and/or setting the maximum $\psi_0 < 0$),

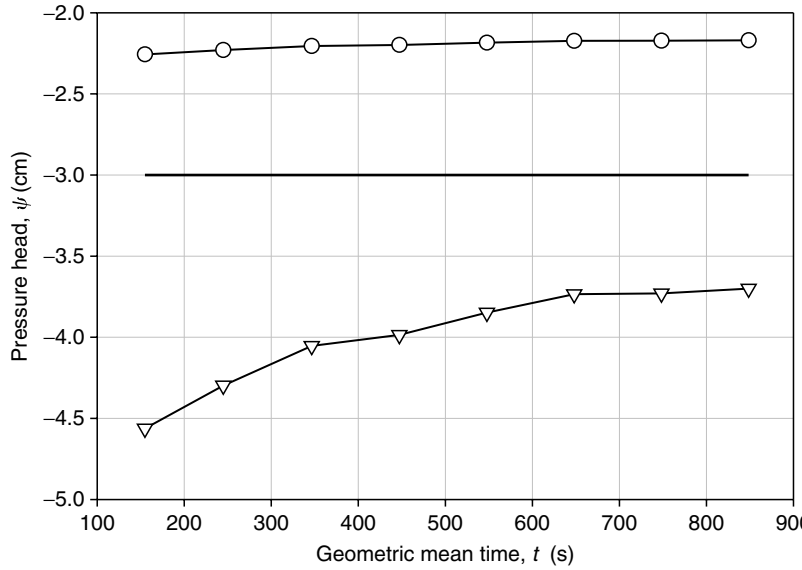

FIGURE 82.5. Impact of transient, constant-head tension infiltration, and contact sand on the matric head at the infiltration surface, ψ_s. The ψ_s values were calculated using Equation 82.17 and the infiltration rate data in Figure 82.4 (and Table 82.2) for a loamy sand soil. The heavy solid line represents the matric head set on the infiltrometer membrane, $\psi_0 = -3$ cm; the circles give ψ_s when $K_{cs} = 1.0 \times 10^{-2}$ cm s^{-1}; and the triangles give ψ_s when $K_{cs} = 1.0 \times 10^{-3}$ cm s^{-1}. The $K(\psi_0)$ of the soil is 1.08×10^{-3} cm s^{-1}, and the contact sand thickness is $T_{cs} = 1$ cm.

TABLE 82.1 Example $K(\psi)$, $S(\psi)$, $\alpha^*(\psi)$, $PD(\psi)$, and $NP(\psi)$ Calculations for the Tension Infiltrometer Method, Steady-Flow Analysis, Overhead Reservoir System (Figure 82.2). The Tension Infiltrometer Data Collection Sheet Is Similar in Format to Table 76.3, Chapter 76

Retaining ring inside radius, $a = 12.5$ cm
Contact sand: thickness, $T_{cs} = 1$ cm; saturated hydraulic conductivity, $K_{cs} = 10^{-2}$ cm s^{-1}
Porous material type: loamy sand soil
$\beta = 0.6$; $\omega = 0.75$; $\gamma = 1.818$; $\theta(\psi_i) = 0.10$

ψ_0[a] (cm)	Q_s[b] (cm^3 s^{-1})	ψ_s[c] (cm)	α'[d] (cm^{-1})	K'[e] (cm s^{-1})	$K(\psi_s)$[f] (cm s^{-1})	$\alpha^*(\psi_s)$[g] (cm^{-1})	$\theta(\psi_s)$ (cm^3 cm^{-3})	$S(\psi_s)$[h] (cm s$^{-1/2}$)	$PD(\psi_s)$[i] (mm)	$NP(\psi_s)$[j] (p m^{-2})
−16	0.90	−15.1667	0.04043	9.2562E−04	5.01E−04	0.040	0.22	5.2008E−02	0.060	1.60E + 08
−11	1.10	−10.2037	0.06975	1.7973E−03	7.47E−04	0.054	0.24	5.9479E−02	0.080	7.64E + 07
−6	1.55	−5.2871	0.13299	3.5281E−03	1.49E−03	0.097	0.26	6.7095E−02	0.14	1.47E + 07
−4	2.00	−3.3704	0.21307	5.5542E−03	2.48E−03	0.167	0.28	6.9660E−02	0.25	2.70E + 06
−2	2.95	−1.5463	0.35826	8.0451E−03	4.31E−03	0.272	0.31	7.7733E−02	0.40	6.70E + 05
−1	3.95	−0.7315	0.42748	8.7914E−03	6.31E−03	0.390	0.33	8.2204E−02	0.58	2.32E + 05
0	5.40	−0.00007			8.79E−03	0.427	0.35	9.6679E−02	0.64	2.25E + 05

Note: Air-pore water interfacial surface tension, $\sigma = 72.75$ g s^{-2}.
Assumed pore water density, $\rho = 0.9982$ g cm^{-3}.
Assumed pore water viscosity, $\mu = 1.002$ g cm^{-1} s^{-1}.
Acceleration due to gravity, $g = 980.621$ cm s^{-2}.

[a] Pressure head set on infiltrometer disk or membrane.
[b] Calculated from steady rate of fall of water level, R_s (as in Table 76.3, Chapter 76).
[c] Calculated using Equation 82.17.
[d] Calculated using Equation 82.4.
[e] Calculated using Equation 82.5.
[f] Calculated using Equation 82.6, Equation 82.7, or Equation 82.8 depending on ψ_0.
[g] Calculated using Equation 82.9.
[h] Calculated using Equation 69.17, Chapter 69.
[i] Calculated using Equation 69.18, Chapter 69.
[j] Calculated using Equation 69.19, Chapter 69.

or alternative relationships must be used. Reynolds and Zebchuk (1996) provide approximate steady-flow expressions for determining $K(\psi_s)$ from tension infiltrometer data when $\psi_s > 0$.

Example data sheets and calculations for the steady-state and transient-flow methods are given in Table 82.1 and Table 82.2, respectively.

TABLE 82.2 Example Data Sheet and $K(\psi_0)$, $S(\psi_0)$, $\alpha^*(\psi_0)$, $PD(\psi_0)$, and $NP(\psi_0)$ Calculations for the Tension Infiltrometer Method, Transient-Flow Analysis, Overhead Reservoir System (see Figure 82.2)

Reservoir inside radius, $r = 5$ cm; retaining ring or disk radius, $a = 10$ cm
Initial height of water in reservoir, $h_0 = 30$ cm
Pressure head on infiltrometer disk or membrane, $\psi_0 = -3$ cm
Contact sand: thickness, $T_{cs} = 1$ cm; saturated hydraulic conductivity, $K_{cs} = 10^{-2}$ cm s^{-1}
Porous material type: loamy sand; $\theta(\psi_0) = 0.35$; $\theta(\psi_i) = 0.10$
$\beta = 0.6$; $\omega = 0.75$; $\gamma = 1.818$

Time, t_j (s)	Reservoir scale reading, L_j (cm)	Flow rate, Q_j[a] (cm^3 s^{-1})	Cumulative infiltration, I_j[b] (cm^3 cm^{-2})	Square root time $t_j^{1/2}$(s$^{1/2}$)	Geometric mean time, t_j^{GM}[c] (s)	Geometric mean square root time, $^*t_j^{1/2}$[d] (s$^{1/2}$)	$\Delta I_j/\Delta t_j^{1/2}$[e] (cm s$^{-1/2}$)
0[f]	0	50.2655	0	0	0	0	0.3578
5	3.20	16.6096	0.800	2.24	7.07	2.66	0.2854
10	4.26	8.8085	1.064	3.16	14.14	3.76	0.2141
20	5.38	4.4809	1.345	4.47	28.28	5.32	0.1540
40	6.52	1.8850	1.630	6.32	52.92	7.27	0.0881
70	7.24	1.0681	1.810	8.37	91.65	9.57	0.0657
120	**7.92**	**0.8050**	**1.980**	**10.95**	**154.92**	**12.45**	**0.0643**
200	**8.74**	**0.7219**	**2.185**	**14.14**	**244.95**	**15.65**	**0.0723**
300	**9.66**	**0.6452**	**2.415**	**17.32**	**346.41**	**18.61**	**0.0766**
400	**10.48**	**0.6237**	**2.620**	**20.00**	**447.21**	**21.15**	**0.0841**
500	**11.27**	**0.5807**	**2.819**	**22.36**	**547.72**	**23.40**	**0.0866**
600	**12.01**	**0.5450**	**3.004**	**24.49**	**648.07**	**25.46**	**0.0884**
700	**12.71**	**0.5435**	**3.177**	**26.46**	**748.33**	**27.36**	**0.0947**
800	**13.40**	**0.5341**	**3.350**	**28.28**	**848.53**	**29.13**	**0.0991**
900	**14.08**		**3.520**	**30.00**			

Note: Values for σ, ρ, μ, and g are given in Table 82.1. The accuracy criteria for hydraulic conductivity (Equation 82.15) and sorptivity (Equation 82.16) were both met in this example.

[a] $Q_j = [(L_{j+1} - L_j)/(t_{j+1} - t_j)](\pi r^2)$; $j = 1, 2, 3, \ldots, n-1$; $n = 15$ = number of measurements.
[b] $I_j = L_j(r^2/a^2)$.
[c] $t_j^{GM} = [t_{j+1} \times t_j]^{1/2}$.
[d] $^*t_j^{1/2} = [t_{j+1}^{1/2} \times t_j^{1/2}]^{1/2}$.
[e] $\Delta I_j/\Delta t_j^{1/2} = (I_{J+1} - I_j)/(t_{j+1}^{1/2} - t_j^{1/2})$.
[f] Regular font refers to the initial wetting and saturation of the contact sand layer; bold font refers to wetting of the unsaturated porous medium under the contact sand.

Plot $\Delta I_j/\Delta t_j^{1/2}$ versus $^*t_j^{1/2}$ and determine the *Y*-axis intercept and slope for the data in bold (Figure 82.4): Intercept $= 4.0293 \times 10^{-2}$ cm s$^{-1/2}$; Slope $= 1.9849 \times 10^{-3}$ cm s^{-1}.
Sorptivity, $S(\psi_0)$ = Intercept $= 4.03 \times 10^{-2}$ cm s$^{-1/2}$ (Equation 82.12).
Hydraulic conductivity, $K(\psi_0) = 1.08 \times 10^{-3}$ cm s^{-1} (Equation 82.13).
Sorptive number, $\alpha^*(\psi_0) = 0.303$ cm^{-1} (Equation 69.17, Chapter 69).
Flow-weighted mean pore diameter, $PD(\psi_0) = 0.451$ mm (Equation 69.18, Chapter 69).
Number of flow-weighted mean pores, $NP(\psi_0)$
$= 1.09 \times 10^5$ pores m^{-2} (Equation 69.19, Chapter 69).

82.4 COMMENTS

82.4.1 Purpose of Retaining Ring and Guard Cloth

The purpose of the retaining ring is to (i) ensure that the flow cross-section is circular and that flow within the contact sand is vertical and rectilinear (required by theory); (ii) prevent development of ''horizontal wicks'' caused by slumping or spillage of contact sand beyond the edge of the infiltrometer plate; and (iii) prevent possible horizontal leakage of free water from under the infiltrometer plate when zero or slightly positive matric heads occur at the infiltration surface. Note that the small depth of ring insertion (≈ 0.5 cm) causes negligible disturbance and has no appreciable effect on flow within the porous medium (Reynolds and Elrick 1991; Reynolds and Zebchuk 1996). The primary purpose of the guard cloth is to prevent the contact sand from infilling cracks, worm holes, and other macropores present in the infiltration surface (Figure 82.1). Significant infilling of macropores can change the hydraulic properties of the porous medium, as well as increase greatly the amount of contact sand required. The guard cloth can be omitted if macropores are not present, although the cloth provides a very convenient and effective means for reclaiming the contact sand from the infiltration surface for subsequent reuse at other sites (after air-drying and sieving to remove entrained debris). In loose, single-grain materials (e.g., loose sandy soils), the contact sand, guard cloth, and retaining ring may not be necessary (i.e., the infiltrometer plate can be placed directly on the infiltration surface), although some work suggests that contact sand should always be used (Bagarello et al. 2001).

82.4.2 Design, Saturation, Leak Testing, and Calibration

The tension infiltrometer consists essentially of a porous disk or membrane covering a conical or hemispherical cavity in the underside of a transparent plastic plate (Figure 82.2 and Figure 82.6). Water is supplied to the infiltrometer via the water supply tube. Tension is set on the porous disk/membrane via the bubble tower.

The seal between the porous disk or membrane and the infiltrometer plate (often made using epoxy, resin glue, or a tight-fitting O-ring) must be airtight or it will leak air when tension is applied. The porous disk or membrane must be hydrophilic (water wettable) and have an air-entry matric head that is more negative than the minimum matric head set by the bubble tower. If the air-entry matric head is exceeded, air will leak through the disk/membrane and appear as a stream of bubbles entering the cavity above the disk/membrane. Porous disks may be constructed of porous metal (stainless steel, brass), sintered glass, high-flow ceramic, or porous plastic that has been treated to make it hydrophilic. Membranes are usually made of fine-mesh (270 mesh or smaller) nylon cloth or metal sieve screen. The wettability of the disk or membrane can often be enhanced by first cleaning it with a solvent (e.g., ethanol, dithionite–citrate solution, dilute bleach solution) to remove hydrophobic oils, oxides, organic matter, etc., and then treating it with a wetting agent (e.g., a solution of isopropyl alcohol, distilled water, and commercial surfactant). Porous disks and membranes should have an air-entry matric head ≤ -20 cm and a saturated hydraulic conductivity of 10^{-1} to 10^{-3} cm s^{-1}. The porous disk or membrane is saturated by submerging the entire infiltrometer plate in a water bath containing several centimeters of deaired, temperature-equilibrated water, and then drawing the water up through the disk/membrane (by sucking through a one-way valve inserted into the top of the water supply tube) until the cavity and supply tube are full (Figure 82.6). The bubble tower should also be filled to the maximum level with water (discussed below). Leave the infiltrometer standing in the water bath for a couple of days

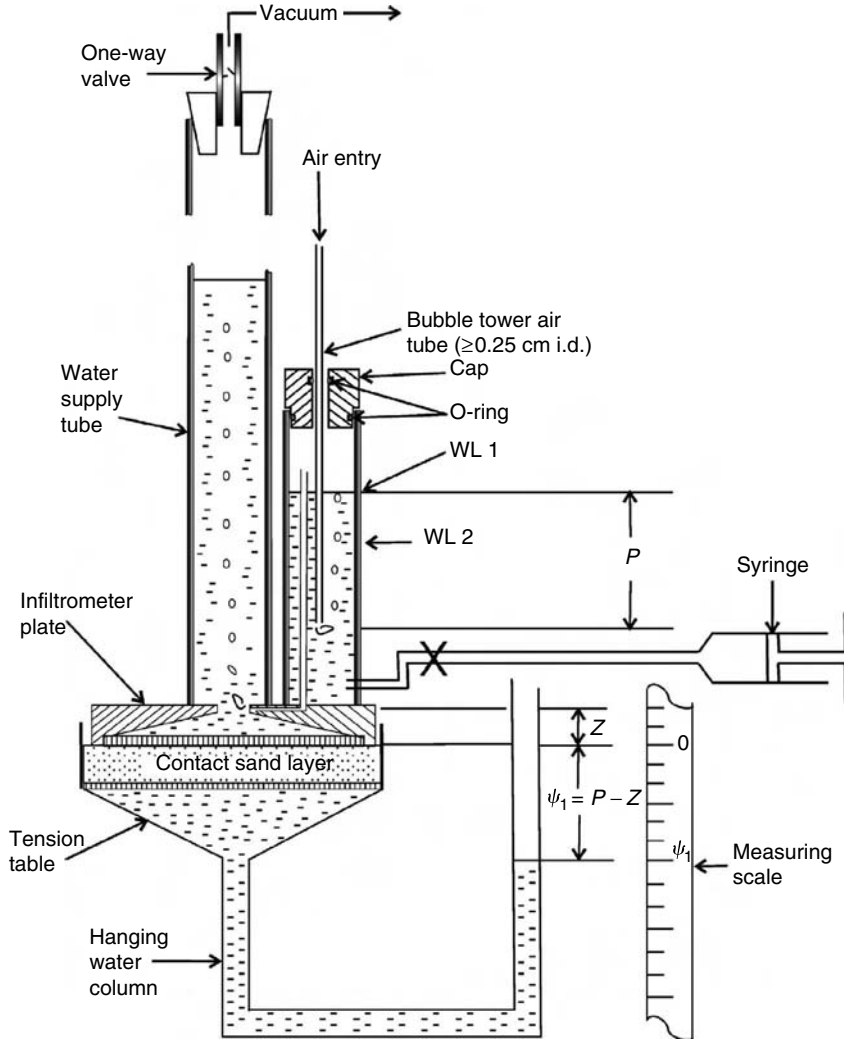

FIGURE 82.6. Calibration of a tension infiltrometer using a vacuum source and a tension table–hanging water column system. (Adapted from Reynolds, W.D., in M.R. Carter (Ed.), *Soil Sampling and Methods of Analysis*, Canadian Society of Soil Science, Lewis Publishers, Boca Raton, Florida 1993. With permission.)

periodically jarring the plate against the wall of the water bath to remove air that may be entrapped in the disk/membrane.

Test the infiltrometer by removing it from the water bath and setting it on several layers of dry paper towel. Air bubbles should rise rapidly from the air tube and up into the supply tube as water flows out of the infiltrometer and into the paper towel. If air bubbles rise from the disk/membrane itself, then the infiltrometer is not completely saturated or contains a hole/large pore or there is a break in the seal between the disk/membrane and the plate. Repeating the above procedures should stop the leak if incomplete saturation is the problem. The leak will persist if it is due to a hole in the disk/membrane, or to a break in the seal. Such holes and breaks can usually be plugged using a couple of drops of epoxy/resin glue,

although membranes with several holes may need to be replaced. To prevent damage and maintain saturation during transport, place the infiltrometer on padding (e.g., sponge, water-resistant carpet underlay, etc.) in a flat-bottomed pail with the plate submerged below several centimeters of water. For long-term storage, the infiltrometer should be air-dried to prevent algal growth, corrosion, etc.

The bubble tower should be calibrated to ensure that the matric heads applied to the infiltration surface are correct and accurate. This can be accomplished using a tension table–hanging water column arrangement (Figure 82.6). Adjust the water level in the bubble tower (using a syringe) so that it is about 2 cm below the top of the second air tube (the ''second tube'' is identified in Figure 82.2). Lower the bubble tower air tube until its bottom end is about $P = (\psi_1 + Z)$ cm below the water surface, where ψ_1 is the minimum (most negative) matric head to be set on the disk/membrane and Z is the height of the bubble point above the disk/membrane (Figure 82.6). Place the saturated infiltrometer on a prewetted tension table/Buchner funnel, which is set at zero matric head (Figure 82.6). Attach a one-way air valve to the supply tube and gently draw air through the bubble tower air tube and into the water supply tube by applying a vacuum (Figure 82.6). Using the syringe, ''fine-tune'' the water level in the bubble tower (by adding or removing water) until the minimum (most negative) matric head to be set on the disk/membrane (ψ_1) is established, as indicated by the water elevation in the hanging water column (i.e., $\psi_1 = P - Z$ in Figure 82.6). Mark and label the water level on the side of the bubble tower (WL 1 in Figure 82.6), then remove water to find and mark the next desired matric head (WL 2 in Figure 82.6). Repeat this procedure until all desired matric heads have been marked. Note that if the bubble tower and air tubes are highly uniform in diameter, the change in matric head is equal to the change in water level in the bubble tower, which allows the succeeding water levels (i.e., WL 2, WL 3, etc.) to be obtained by simply using a ruler to measure downward from WL 1. A matric head sequence of $\psi_1 = -15$ cm, $\psi_2 = -10$ cm, $\psi_3 = -5$ cm, $\psi_4 = -3$ cm, $\psi_5 = -1$ cm, $\psi_6 = 0$ cm is often used.

82.4.3 Equilibration Times, Reservoir Refilling, and Evaporative Losses

Deciding when steady flow (R_s) is attained is somewhat arbitrary (as seen in the procedures section), and it will depend to some extent on the experience of the operator. Nevertheless, steady flow is usually reached within 15–120 min for the first (and most negative) matric head set on the infiltrometer; and the succeeding (less negative) matric heads usually require less time. At lower matric heads (say -20 to -5 cm), the steady-flow rates are often slow enough to require use of the smaller of the two concentric reservoirs in order to obtain adequate measurement accuracy. When the small reservoir is used, it will require periodic refilling. This is best accomplished at the end of a measurement for a given matric head. Adjust the reservoir valve to allow slow flow of water from the large reservoir into the small reservoir. At the same time, slowly lower the water level in the bubble tower (by withdrawing water via the syringe) to establish the next matric head. This technique accomplishes refilling, while at the same time ensuring that the change from one matric head to the next is monotonic, thereby preventing possible hysteresis effects. Details on switching between the two concentric reservoirs are given in the Soilmoisture Equipment Corp. procedure manual for the Guelph permeameter.

An infiltrometer that is bubbling slowly is susceptible to solar heating effects, and the procedures for minimizing these adverse effects (as well as for general ''troubleshooting'') are similar to those given in Section 76.2. The base of the infiltrometer should be covered with a plastic sheet or transparent lid to prevent evaporative water loss from the annulus

between the retaining ring and infiltrometer plate (Figure 82.2), as such losses can be sufficient to perturb the measurements when flow is slow and atmospheric evaporative demand is high.

82.4.4 Factors Affecting Accuracy and $K(\psi)$ Range

As discussed in Section 82.3, the steady-flow approach determines $K(\psi_0)$ values by fitting an exponential curve segment between successive (ψ_0, Q_s) data pairs. Since $K(\psi)$ relations are generally exponential over only small ranges, then the accuracy of the $K(\psi_0)$, $\alpha^*(\psi_0)$, $S(\psi_0)$, $PD(\psi_0)$, and $NP(\psi_0)$ values tends to increase with the number of matric heads (and thereby the number of exponential curve segments) used within a particular matric head range; and as a consequence, the steeper the $K(\psi)$ curve of the porous medium, the greater the number of matric heads required to maintain flow parameter accuracy (see Reynolds and Elrick 1991). Note as well that Reynolds and Zebchuk (1996) provide steady-flow expressions for the determination of $K(\psi_0)$ from a single ψ_0 value when a priori knowledge of $\alpha^*(\psi_0)$ is available.

The range of $K(\psi_0)$ values that can be measured conveniently with 10–20 cm diameter tension infiltrometers appears to be on the order of 10^{-2} to 10^{-6} cm s^{-1}. Excessive restriction of flow by the contact sand can occur at $K(\psi_0)$ values greater than 0.008–0.01 cm s^{-1} (Reynolds et al. 2000). For the steady-flow analysis, impractically slow flows (and correspondingly long equilibration times) can occur when $K(\psi_0) < 10^{-6}$ cm s^{-1}.

Both the steady-flow and transient-flow analyses will occasionally yield unrealistic or invalid (e.g., negative) parameter values. This is usually caused by porous medium heterogeneities or strong water content gradients. The steady-flow method can also produce unrealistic results if the matric head set on the infiltrometer is changed to the next head before steady flow is achieved. Sometimes, the tension infiltrometer measurement can be salvaged by eliminating obviously aberrant data points, such as a steady-flow rate measurement that decreased with increasing matric head, or a transient infiltration rate measurement that deviates from linearity with $t^{1/2}$.

Other factors affecting the accuracy of tension infiltrometer measurements include macrostructure collapse under the infiltrometer during the infiltration measurement, and inadequate or changing hydraulic connection between the infiltrometer and the infiltration surface. Macrostructure collapse is caused by the weight of the infiltrometer combined with a decline in porous medium strength as the porous medium wets up. Inadequate or changing hydraulic connection is usually caused by wind-induced vibration of the infiltrometer, and by the decreasing weight of the infiltrometer as the water empties out of the reservoir. Both of these problems can be reduced by supporting the infiltrometer with a large tripod (as recommended above), which clamps solidly to the reservoir.

82.4.5 Sensitivity to Calibration and Slope

Near-saturated soil hydraulic properties are often extremely sensitive to small changes in pore water matric head, e.g., $K(\psi)$ often changes by 2–3 orders of magnitude over the range, $-15 \text{ cm} \leq \psi \leq 0$ (Reynolds and Elrick 1991; Thony et al. 1991; Reynolds et al. 1995). It is consequently important that the infiltrometer is accurately calibrated (using a precise calibration method such as in Section 82.4.2); and that the infiltrometer plate is level when making a measurement (gravity effects cause the ''high'' and ''low'' sides of a sloping plate

to have different ψ_0 values than the value set by the bubble tower). Placement of contact sand is the best approach for leveling (and smoothing) rough or undulating surfaces (Figure 82.1), as it also ensures good hydraulic contact over the entire infiltration surface, and it does not alter surface hydraulic properties. For continuously sloping surfaces (e.g., hillslopes), it is generally recommended that the infiltrometer is placed on a level bench cut into the slope. It has recently been found, however, that infiltrometers as large as 20 cm diameter can still yield valid results when placed without leveling on slopes as great as 20% (Bodhinayake et al. 2004). Evidently, the difference in matric head (and thereby infiltration rate) between the upslope and downslope sides of the infiltrometer tends to be compensating as long as the infiltration surface has reasonably uniform hydraulic properties.

82.4.6 Alternative Designs and Analyses

Additional information concerning the tension infiltrometer method, including several alternative infiltrometer designs and analyses, may be found in Smettem and Clothier (1989), Ankeny (1992), Elrick and Reynolds (1992), White et al. (1992), Vandervaere et al. (2000b), Clothier and Scotter (2002), and Smettem and Smith (2002). Although many of these designs and analyses have specific advantages, the apparatus presented here (Figure 82.2) tends to be the most versatile, and single disk analyses usually yield the most stable, accurate, and repeatable results (e.g., Hussen and Warrick 1993). Commercial manufacturers of tension infiltrometers include Soil Measurement Systems, Tucson, Arizona; and Soilmoisture Equipment Corp., Goleta, California.

82.5 STRENGTHS AND WEAKNESSES OF TENSION INFILTROMETER METHODS

An important strength of the tension infiltrometer method is that the apparatus is simple, inexpensive, portable, easily applied in both field and laboratory studies, and requires only small volumes of water. Hence, laboratory or greenhouse studies, detailed investigations of spatial variability, field studies in areas with difficult access, and large-scale surveys are more feasible with this method than with many other methods. The apparatus also does not require soil disturbance such as augering a well or deep insertion of a ring, and can thus provide highly plausible estimates of the hydraulic properties of fragile aggregates and soil macropores.

Perhaps the main theoretical strength of the method is its ability to determine a number of important water transmission parameters (e.g., $K(\psi_0)$, $S(\psi_0)$, $\alpha^*(\psi_0)$, $PD(\psi_0)$, $NP(\psi_0)$) in the near-saturated range, $\approx -0.20 \text{ m} \leq \psi_0 \leq 0$, where both parameter values and water/solute movement can change dramatically with even small changes in ψ_0. The tension infiltrometer method consequently has the ability to relate ''macropore'' and ''matrix pore'' flow parameters to changes in soil condition or soil management. For example, changes in $PD(\psi_0)$ have been used to quantify the effects of macrostructure collapse and macropore infilling (White et al. 1992), soil cracking (Thony et al. 1991), tillage practices (Sauer et al. 1990; White et al. 1992; Reynolds et al. 1995), root growth (White et al. 1992), and sediment erosion-deposition (White et al. 1992). Measurements of near-saturated $K(\psi_0)$ and $S(\psi_0)$ have been used to quantify changes in water transmission as a result of different tillage procedures (Sauer et al. 1990; Reynolds et al. 1995), faunal activity (Clothier et al. 1985), soil structural changes during the growing season (Messing and Jarvis 1993), soil textural changes (Jarvis and Messing 1995), wheel trafficking (Ankeny et al. 1991), and development

of soil hydrophobicity (Clothier et al. 1996, 2000; Hallett et al. 2004). Tension infiltrometers have also been used to characterize near-saturated mobile–immobile soil water contents (Clothier et al. 1992; Angulo-Jaramillo et al. 1997), solute transport characteristics (Jaynes et al. 1995; Clothier et al. 1996; Vogeler et al. 1996), solute sorption isotherms (Clothier et al. 1995), and the hydraulic properties of surface crusts (Vandervaere et al. 1997).

Perhaps the primary weaknesses of the tension infiltrometer method are the potential difficulties associated with working on sloped surfaces, and the need to use contact sand to establish and maintain good hydraulic connection between the infiltrometer and the porous medium surface. Tension infiltrometer measurements on hillslopes may require cutting a level bench so that the applied matric head is the same at all points on the infiltration surface, although some recent work suggests that benches may not be necessary for slopes $\leq 20\%$ (see Section 82.4.5). The requirement for cutting a bench would obviously preclude measuring intact (undisturbed) hillslope surfaces. The contact sand must meet specific and somewhat restrictive performance criteria, and the presence of contact sand must be accounted for in the data analysis procedures. Specifically, the saturated hydraulic conductivity, K_{cs}, and water-entry matric head, ψ_w, of the contact sand must be such that the sand never restricts flow into the porous medium. Recommended values are $K_{cs} \geq 10^{-2}$ cm s^{-1}, which is greater than the K_{fs} of most unstructured agricultural soils, and $\psi_w \leq -20$ cm, which is less than the minimum matric head set on most infiltrometer plates. The K_{cs} and ψ_w values should also be stable with a narrow standard deviation to minimize contact sand–induced variations. The contact material should be strongly hydrophilic and single grain with a narrow particle-size distribution so that it levels easily and readily establishes good hydraulic connection. The material should also be easily obtained, inexpensive, and reusable. Most natural soil materials cannot meet all of the above performance criteria; however, the glass bead material proposed by Reynolds and Zebchuk (1996) appears to be a good choice according to field tests conducted by Bagarello et al. (2000, 2001).

The steady-state and transient tension infiltrometer analyses also have strengths and weaknesses. Important strengths of the steady-flow, multiple-head approach (Equation 82.4 through Equation 82.9) include well-established and tested theory, robustness, provision of measurements at several matric heads on a single infiltration surface, relatively large (and thereby more representative) sample volumes, and the ability to accurately account for the effects of a contact sand layer. Weaknesses of the steady-flow analysis include potentially long equilibration times and potentially greater susceptibility to error associated with porous medium heterogeneities (e.g., layering) and nonuniform water contents (due to large sample volume). Some recent simulation studies suggest, however, that the steady-flow approach may be far less sensitive to near-surface layering than previously supposed (Smettem and Smith 2002). The main strengths of the transient analysis (Equation 82.12 through Equation 82.16) include shorter measurement-times (because steady flow is not required), simple but effective procedures for determining valid results and for eliminating flow perturbations caused by contact sand, and straightforward use of linear regression to obtain the hydraulic conductivity and sorptivity values. On the other hand, important weaknesses of the transient analysis include imprecise knowledge of the β parameter and the matric head at the porous medium–contact sand interface (ψ_s), and limited ability to obtain measurements on a single infiltration surface for a sequence of ψ_0 values. Generally speaking, steady-flow analyses are more effective for determining $K(\psi_0)$, whereas transient analyses are more effective for determining $S(\psi_0)$.

REFERENCES

Angulo-Jaramillo, R., Moreno, F., Clothier, B.E., Thony, J.L., Vachaud, G., Fernandez-Boy, E., and Cayuela, J.A. 1997. Seasonal variation of hydraulic properties of soils measured using a tension disk infiltrometer. *Soil Sci. Soc. Am. J.* 61: 27–32.

Ankeny, M.D. 1992. Methods and theory of unconfined infiltration measurements. In G.C. Topp, W.D. Reynolds, and R.E. Green, Eds., *Advances in Measurement of Soil Physical Properties: Bringing Theory into Practice*, SSSA Special Publication No. 30, Soil Science Society of America, Madison, WI, pp. 123–141.

Ankeny, M.D., Ahmed, M., Kaspar, T.C., and Horton, R. 1991. Simple field method for determining unsaturated hydraulic conductivity. *Soil Sci. Soc. Am. J.* 55: 467–470.

Bagarello, V., Iovino, M., and Tusa, G. 2000. Factors affecting measurement of the near saturated soil hydraulic conductivity. *Soil Sci. Soc. Am. J.* 64: 1203–1210.

Bagarello, V., Iovino, M., and Tusa, G. 2001. Effect of contact material on tension infiltrometer measurements. *Trans. Am. Soc. Agric. Eng.* 44: 911–916.

Bodhinayake, W., Si, B.C., and Noborio, K. 2004. Determination of hydraulic properties in sloping landscapes from tension and double-ring infiltrometers. *Vadose Zone J.* 3: 964–970.

Clothier, B.E. 2000. Infiltration. In K.A. Smith and C.E. Mullins, Eds., *Soil and Environmental Analysis: Physical Methods*. Marcel Dekker, Inc., New York, pp. 239–280.

Clothier, B.E., Green, S.R., and Katou, H. 1995. Multidimensional infiltration: points, furrows, basins, wells, and disks. *Soil Sci. Soc. Am. J.* 59: 286–292.

Clothier, B.E., Kirkham, M.B., and McLean, J.E. 1992. *In situ* measurement of the effective transport volume for solute moving through soil. *Soil Sci. Soc. Am. J.* 56: 733–736.

Clothier, B.E., Magesan, G.N., Heng, L., and Vogeler, I. 1996. *In situ* measurement of the solute adsorption isotherm using a disc permeameter. *Water Resour. Res.* 32: 771–778.

Clothier, B.E. and Scotter, D.R. 2002. Unsaturated water transmission parameters obtained from infiltration. In J.H. Dane and G.C. Topp, Eds., *Methods of Soil Analysis, Part 4—Physical Methods*. Soil Science Society of America, Madison, WI, pp. 879–898.

Clothier, B.E., Scotter, D.R., and Harper, E. 1985. Three-dimensional infiltration and trickle irrigation. *Trans. Am. Soc. Agric. Eng.* 28: 497–501.

Clothier, B.E., Vogeler, I., and Magesan, G.N. 2000. The breakdown of water repellency and solute transport through a hydrophobic soil. *J. Hydrol.* 231: 255–264.

Elrick, D.E. and Reynolds, W.D. 1992. Infiltration from constant-head well permeameters and infiltrometers. In G.C. Topp, W.D. Reynolds, and R.E. Green, Eds., *Advances in Measurement of Soil Physical Properties: Bringing Theory into Practice*, SSSA Special Publication No. 30, Soil Science Society of America, Inc., Madison, WI, pp. 1–24.

Gardner, W.R. 1958. Some steady-state solutions of the unsaturated moisture flow equation with application to evaporation from a water table. *Soil Sci.* 85: 228–232.

Hallett, P.D., Nunan, N., Douglas, J.T., and Young, I.M. 2004. Millimeter-scale spatial variability in soil water sorptivity. *Soil Sci. Soc. Am. J.* 68: 352–358.

Haverkamp, R., Ross, P.J., Smettem, K.R.P., and Parlange, J.-Y. 1994. Three-dimensional analysis of infiltration from the disc infiltrometer: 2. Physically based infiltration equation. *Water Resour. Res.* 30: 2931–2935.

Hussen, A.A. and Warrick, A.W. 1993. Alternative analyses of hydraulic data from disc tension infiltrometers. *Wat. Resour. Res.* 29: 4103–4108.

Jarvis, N.J. and Messing, I. 1995. Near-saturated hydraulic conductivity in soils of contrasting texture measured by tension infiltrometers. *Soil Sci. Soc. Am. J.* 59: 27–34.

Jaynes, D.B., Logsdon, S.D., and Horton, R. 1995. Field method for measuring mobile/immobile water content and solute transfer rate coefficient. *Soil Sci. Soc. Am. J.* 59: 352–356.

Messing, I. and Jarvis, N.J. 1993. Temporal variation in the hydraulic conductivity of a tilled clay soil as measured by tension infiltrometers. *J. Soil Sci.* 44: 11–24.

Perroux, K.M. and White, I. 1988. Designs for disc permeameters. *Soil Sci. Soc. Am. J.* 52: 1205–1215.

Philip, J.R. 1957. The theory of infiltration. 4. Sorptivity and algebraic infiltration equations. *Soil Sci.* 84: 257–264.

Reynolds, W.D. 1993. Saturated hydraulic conductivity: Field measurement. In M.R. Carter, Ed., *Soil Sampling and Methods of Analysis.* Canadian Society of Soil Science. Lewis Publishers, Boca Raton, FL, pp. 599–613.

Reynolds, W.D., Bowman, B.T., Brunke, R.R., Drury, C.F., and Tan, C.S. 2000. Comparison of tension infiltrometer, pressure infiltrometer, and soil core estimates of saturated hydraulic conductivity. *Soil Sci. Soc. Am. J.* 64: 478–484.

Reynolds, W.D. and Elrick, D.E. 1991. Determination of hydraulic conductivity using a tension infiltrometer. *Soil Sci. Soc. Am. J.* 55: 633–639.

Reynolds, W.D., Gregorich, E.G., and Curnoe, W.E. 1995. Characterization of water transmission properties in tilled and untilled soils using tension infiltrometers. *Soil Till. Res.* 33: 117–131.

Reynolds, W.D. and Zebchuk, W.D. 1996. Use of contact material in tension infiltrometer measurements. *Soil Tech.* 9: 141–159.

Sauer, T.J., Clothier, B.E., and Daniel, T.C. 1990. Surface measurements of the hydraulic properties of a tilled and untilled soil. *Soil Till. Res.* 15: 359–369.

Smettem, K.R.J. and Clothier, B.E. 1989. Measuring unsaturated sorptivity and hydraulic conductivity using multiple disc permeameters. *J. Soil Sci.* 40: 563–568.

Smettem, K.R.J., Parlange, J.-Y., Ross, P.J., and Haverkamp, R. 1994. Three-dimensional analysis of infiltration from the disc infiltrometer: 1. A capillary-based theory. *Water Resour. Res.* 30: 2925–2929.

Smettem, K.R.J. and Smith, R.E. 2002. Field measurement of infiltration parameters. In R.E. Smith, Ed., *Infiltration Theory for Hydrologic Applications.* Water Resources Monograph 15, American Geophysical Union, Washington, DC, pp. 135–157.

Thony, J.-L., Vachaud, G., Clothier, B.E., and Angulo-Jaramillo, R. 1991. Field measurement of the hydraulic properties of soil. *Soil Tech.* 4: 111–123.

Vandervaere, J.-P. 2002. Early-time observations. In J.H. Dane and G.C. Topp, Eds., *Methods of Soil Analysis, Part 4—Physical Methods.* Soil Science Society of America, Madison, WI, pp. 889–894.

Vandervaere, J.-P., Peugeot, C., Vauclin, M., Angulo-Jaramillo, R., and Lebel, T. 1997. Estimating hydraulic conductivity of crusted soils using disc infiltrometers and minitensiometers. *J. Hydrol.* 188: 203–223.

Vandervaere, J.-P., Vauclin, M., and Elrick, D.E. 2000a. Transient flow from tension infiltrometers: I. The two-parameter equation. *Soil Sci. Soc. Am. J.* 64: 1263–1272.

Vandervaere, J.-P., Vauclin, M., and Elrick, D.E. 2000b. Transient flow from tension infiltrometers: II. Four methods to determine sorptivity and conductivity. *Soil Sci. Soc. Am. J.* 64: 1272–1284.

Vogeler, I., Clothier, B.E., Green, S.R., Scotter, D.R., and Tillman, R.W. 1996. Characterizing water and solute movement by time domain reflectometry and disk permeametry. *Soil Sci. Soc. Am. J.* 60: 5–12.

Wang, D., Yates, S.R., and Ernst, F.F. 1998. Determining soil hydraulic properties using tension infiltrometers, time domain reflectometry, and tensiometers. *Soil Sci. Soc. Am. J.* 62: 318–325.

White, I., Sully, M.J., and Perroux, K.M. 1992. Measurement of surface-soil hydraulic properties: disk permeameters, tension infiltrometers, and other techniques. In G.C. Topp, W.D. Reynolds, and R.E. Green, Eds., *Advances in Measurement of Soil Physical Properties: Bringing Theory into Practice.* SSSA Special Publication No. 30, Soil Science Society of America, Madison, WI, pp. 69–103.

Wooding, R. 1968. Steady infiltration from a shallow circular pond. *Water Resour. Res.* 4: 1259–1273.

Chapter 83
Unsaturated Hydraulic Properties: Instantaneous Profile

W.D. Reynolds
Agriculture and Agri-Food Canada
Harrow, Ontario, Canada

83.1 INTRODUCTION

The instantaneous profile method (also known as the internal drainage method) is used primarily for direct (*in situ*) field measurement of the hydraulic conductivity (K) versus matric head (ψ) relationship, $K(\psi)$ [LT^{-1}], and/or the hydraulic conductivity versus volumetric water content (θ) relationship, $K(\theta)$ [LT^{-1}]. It is also occasionally used for *in situ* determination of $\theta(\psi)$ desorption curves; and it may potentially be useful for *in situ* estimation of the capillarity relationships (Chapter 69), although this has not yet been attempted (see Comment 7 in Section 83.4). An alternative field method for determining near-saturated $K(\psi)$ and capillarity relationships is given in Chapter 82. Laboratory methods for $K(\psi)$ or $K(\theta)$ determination are given in Chapter 80 and Chapter 81. Selected methods for estimating $K(\psi)$, $K(\theta)$, and $\theta(\psi)$ from surrogate porous medium properties are given in Chapter 84. A discussion of the principles and parameters associated with the determination of $K(\psi)$, $K(\theta)$, $\theta(\psi)$, and the capillarity relationships appears in Chapter 69.

The instantaneous profile method involves installing probes for *in situ* measurement of volumetric water content, θ [L^3L^{-3}] (e.g., time-domain reflectometer (TDR) probes, Chapter 70), and pore water matric head, ψ [L] (e.g., tensiometers, Chapter 71), at selected depths below the porous medium surface. The porous medium is then wetted to field saturation, and the $K(\psi)$ and $K(\theta)$ relationships are derived from periodic measurements of θ and ψ during drainage, which coincidentally provides an *in situ* $\theta(\psi)$ desorption curve (Chapter 69). The resulting $K(\psi)$, $K(\theta)$, and $\theta(\psi)$ relationships are most relevant for one-dimensional vertical flow and are usually limited to the ''wet end'' matric head range of about $-200 \leq \psi \leq 0$ cm (Dirksen 2001). Although the method may be somewhat involved and laborious, it is often considered the ''benchmark'' of precision and relevance against which other field-based $K(\psi)$, $K(\theta)$, and $\theta(\psi)$ methods are evaluated (Vachaud and Dane 2002).

83.2 APPARATUS AND PROCEDURES

1 Enclose a level area $\geq$12 m^2 in the field using a lined earthen berm, wooden planking, or other materials that will allow ponding of water. The area should be large enough that the initial infiltration and subsequent drainage are effectively vertical in the center of the enclosure (see also Comment 1 in Section 83.4). Clear the enclosed area of vegetation by clipping level with the soil surface.

2 In the center of the enclosed area, install the water content (θ) and matric head (ψ) probes at the desired depths below the surface (see Chapter 70 and Chapter 71 for probe designs; see also Comment 2 in Section 83.4). The θ and ψ probes should be fast-acting (e.g., response time of $\leq$1–2 min) to accurately portray the potentially rapid changes in porous medium water content and matric head at the start of measurements. Depth increments of 15–30 cm are often recommended, with at least one pair of θ–ψ probes per porous medium layer or soil horizon. Installation procedures should be used that prevent ''short-circuit'' flow down the probe access holes, e.g., use of tight-fitting access holes, or backfilling oversized access holes with powdered bentonite and/or clay. In some cases, it may also be feasible to use inclined access holes so that any leakage down the hole is diverted into the porous medium matrix before contact with the probe sensors. Even small amounts of short-circuit flow/leakage to the probe sensors may cause erroneous results. The antecedent water content of the porous medium or soil profile should be low enough that a wide range of θ and ψ can be measured between antecedent and field-saturated conditions. The porous medium should not be so dry, however, that the pore water matric head probes (e.g., tensiometers) lose hydraulic contact with the porous material (which usually occurs for porous ceramic cup tensiometers when the antecedent ψ falls below about -800 to -900 cm).

3 The enclosed area is flooded with water until the porous material is either field-saturated (i.e., $\theta = \theta_{fs}$, $\psi \geq 0$—see Chapter 69), or θ and ψ are constant at all instrumented depths. The area is then insulated and covered (e.g., straw/bark mulch laid down and a plastic sheet placed on top) to impose gravity drainage under a surface boundary condition of zero flux and constant temperature. Gravity drainage causes θ and ψ to decrease with time throughout the initially wetted volume of porous material.

4 Collect θ versus time and ψ versus time data at all depths from the time when flooding stops ($t = 0$) until θ and ψ decreases to effectively constant values, a time period that can extend from hours to months, depending on the porous medium. Data collection often needs to be frequent (or even continuous) for the first hour or so after irrigation is stopped, as initial drainage rates are often quite rapid, which in turn causes rapid decreases in θ and ψ. Data collection can be much less frequent as drainage slows, however; and it is often recommended that the later-time collection intervals follow geometric time increments (e.g., at 3, 6, 12, 24 h after irrigation is stopped) to better define the often exponential-like decline of θ versus time. If the field setup is maintained, replicate measurements can be made over several wetting/drainage cycles and/or at different times of the year.

83.3 ANALYSIS AND EXAMPLE CALCULATIONS

The amount of water, W [L], stored in the porous medium profile at time, t [T], is given by

$$W(z,t) = \int_0^z \theta(z,t)\mathrm{d}z; \quad 0 \le z \le L \tag{83.1}$$

where z [L] is depth below the porous medium surface ($z = 0$ at surface), and L [L] is the depth to the deepest pair of θ and ψ probes. Given that a no-flow boundary is imposed on the porous medium surface, the flux density, q [LT^{-1}], for drainage at any depth and time in the measurement zone is given by

$$q(z,t)_z = \frac{\int_0^z \theta(z,t)\mathrm{d}z}{\partial t} = \left.\frac{\partial W(z,t)}{\partial t}\right|_z \tag{83.2}$$

which states that the time rate of decrease in water storage between the porous medium surface and depth, z, equals the drainage flux density at depth, z. Darcy's law for water flow at any depth and time in the porous medium profile can be written as

$$q(z,t)_z = K(\theta)_z \left.\frac{\partial H(z,t)}{\partial z}\right|_z \tag{83.3}$$

where $H(z,t) = \psi(z,t) - z$ is hydraulic head (z positive downward), and $K(\theta)_z$ [LT^{-1}] is the hydraulic conductivity–volumetric water content relationship at depth, z. Substituting Equation 83.2 in Equation 83.3 and solving for $K(\theta)_z$ produces

$$K(\theta)_z = \left.\frac{\partial W(z,t)}{\partial t}\right|_z \Big/ \left.\frac{\partial H(z,t)}{\partial z}\right|_z \tag{83.4}$$

which indicates that $K(\theta)_z$ at depth, z, can be determined from the time rate of decrease in water storage between the porous medium surface and depth, z, divided by the hydraulic head gradient at depth, z. The $\theta(\psi)_z$ and $K(\psi)_z$ relationships can also be determined because both $\theta(z,t)$ and $\psi(z,t)$ are measured at each depth, i.e., replace θ with the corresponding ψ in $K(\theta)_z$ to produce $K(\psi)_z$.

The accuracy of Equation 83.4 is obviously dependent on the accuracy with which $\partial H(z,t)/\partial z$ and $\partial W(z,t)/\partial t$ can be determined. The accuracy of $\partial H(z,t)/\partial z$ is improved by careful calibration of the pore water matric head probes (tensiometers) and by minimizing the depth increments between the probes. The accuracy of $\partial W(z,t)/\partial t$, on the other hand, is improved by curve-fitting empirical, time-differentiable expressions to $W(z,t)$ versus t data in order to better describe both the very rapid decrease in $W(z,t)$ at early time and the very slow decrease in $W(z,t)$ at late time. It has been found, for example, that the empirical relationships (Vachaud and Dane 2002)

$$W(t) = a \ln t + b \tag{83.5}$$

or

$$W(t) = ct^d \tag{83.6}$$

can often provide good fits to a wide range of porous medium data, where a, b, c, and d are curve-fitting constants. These expressions are then differentiated with respect to time and substituted into Equation 83.4 to produce

$$K(\theta)_z = [a/t]_z \Big/ \left[\left.\frac{\partial H(z,t)}{\partial z}\right|_z\right] \tag{83.7}$$

or

$$K(\theta)_z = [cdt^{(d-1)}]_z \Big/ \left[\left.\frac{\partial H(z,t)}{\partial z}\right|_z\right] \tag{83.8}$$

where Equation 83.7 incorporates Equation 83.5, and Equation 83.8 incorporates Equation 83.6.

The determination of $K(\theta)$ can be simplified substantially if the porous medium profile is homogeneous over the depth range of interest. In this special case, drainage produces $\partial H(z,t)/\partial z \approx -1$ and thus tensiometer measurements of $\psi(z,t)$ are not required. In addition, $\partial W(z,t)/\partial t$ can be represented by

$$\left.\frac{\partial W(z,t)}{\partial t}\right|_z = z\left.\frac{\partial \overline{\theta}(t)_z}{\partial t}\right|_z = zm\left.\frac{\partial \theta(t)_z}{\partial t}\right|_z \tag{83.9}$$

where $\overline{\theta}(t)_z$ is the average water content from the porous medium surface to depth, z (see Comment 3 in Section 83.4), which can be represented by the empirical relationship (Libardi et al. 1980)

$$\overline{\theta}(t)_z = m\theta(t)_z + n \tag{83.10}$$

where $\theta(t)_z$ is the measured water content at depth, z, and m and n are curve-fitting constants (m is generally close to 1). It has also been established that the empirical relationship (Vachaud and Dane 2002)

$$\theta(t)_z = \tau \cdot t^{\mu} \tag{83.11}$$

applies for drainage in homogeneous profiles, where τ and μ are coefficients obtained from a regression analysis of θ versus t data at each depth, z. Substituting Equation 83.9 through Equation 83.11 into Equation 83.4 and remembering that $\partial H(z,t)/\partial z \approx -1$ produces a simplified $K(\theta)$ analysis

$$K(\theta)_z = -zm\tau^{(1/\mu)}\mu\theta_z^{[(\mu-1)/\mu]} \tag{83.12}$$

which provides a simple analytic relationship between $K(\theta)_z$ and θ_z at any depth, z, in a homogeneous porous medium profile, and avoids direct estimation of uncertain time and space derivatives associated with $W(z,t)$ and $H(z,t)$, respectively. Further details on the justification and derivation of Equation 83.9 through Equation 83.12 can be found in Libardi et al. (1980) and Vachaud and Dane (2002).

Although the simplified analysis (Equation 83.12) is technically restricted to homogeneous porous media, some applications suggest that it can still provide useful results in profiles that

are moderately heterogeneous with depth (Hillel et al. 1972; Vachaud and Dane 2002). In addition, the simplified analysis avoids serious error propagation problems associated with inaccurate tensiometer readings (e.g., insufficient equilibration when ψ is changing rapidly; lack of sensitivity when ψ is close to zero; partial or complete loss of hydraulic contact when ψ is low), and with inaccurate estimation of hydraulic head gradients (Flühler et al. 1976). It may consequently be advisable to apply the simplified analysis even when tensiometer data are available. A comparison of the complete analysis (Equation 83.7 and Equation 83.8) and the simplified analysis (Equation 83.12) is given in Vachaud and Dane (2002). An example data sheet and calculation for the simplified analysis is given in Table 83.1 and Figure 83.1 through Figure 83.3.

TABLE 83.1 Example Data Sheet and Calculation of $K(\theta)$ for the Instantaneous Profile Method, Simplified Analysis (Equation 83.12). Analysis Based on Volumetric Water Content Data Obtained from a Probe Located at Depth, $z = 50$ cm

Table (a): θ versus t at depth, $z = 50$ cm (Figure 83.1)

Time, t (min)	ln (t)	θ (cm^3 cm^{-3})	ln (θ)
1	0	0.50	−0.6932
3	1.0986	0.47	−0.7550
10	2.3026	0.44	−0.8210
20	2.9957	0.42	−0.8675
40	3.6889	0.40	−0.9163
80	4.3820	0.39	−0.9416
160	5.0752	0.37	−0.9943
320	5.7683	0.36	−1.0217
640	6.4615	0.34	−1.0788
1280	7.1546	0.33	−1.1087
2560	7.8478	0.32	−1.1394
5120	8.5409	0.31	−1.1712
8100	8.9996	0.30	−1.2040

Regression fit of Equation 83.11 to data in Table (a):
Intercept $= \ln\tau = -0.6964$.
Therefore, $\tau = 0.4984$.
Slope $= \mu = -0.0569$.
$R^2 = 0.9979$.

Table (b): $\overline{\theta}(t)_z$ versus $\theta(t)_z$ at depth, $z = 50$ cm (Figure 83.2)

$\theta(t)_z$ (cm^3 cm^{-3})	$\overline{\theta}(t)_z$ (cm^3 cm^{-3})
0.50	0.47
0.48	0.46
0.44	0.42
0.40	0.38
0.38	0.36
0.34	0.34
0.30	0.30

Regression fit of Equation 83.10 to data in Table (b). The $\theta(t)_z$ values were measured at depth, z, and the $\overline{\theta}(t)_z$ values were calculated to depth, z, using Equation 83.13:
Intercept $= n = 0.0401$.
Slope $= m = 0.8624$.
$R^2 = 0.9929$.

(continued)

TABLE 83.1 (continued) Example Data Sheet and Calculation of $K(\theta)$ for the Instantaneous Profile Method, Simplified Analysis (Equation 83.12). Analysis Based on Volumetric Water Content Data Obtained from a Probe Located at Depth, $z = 50$ cm

Table (c): $K(\theta)_z$ versus θ_z at depth, $z = 50$ cm (Figure 83.3)

θ_z (cm^3 cm^{-3})	$K(\theta)_z$ (cm min^{-1})	$K(\theta)_z$ (cm s^{-1})
0.50	1.30×10^{0}	2.16×10^{-2}
0.47	4.11×10^{-1}	6.85×10^{-3}
0.44	1.21×10^{-1}	2.01×10^{-3}
0.42	5.09×10^{-2}	8.48×10^{-4}
0.40	2.06×10^{-2}	3.43×10^{-4}
0.39	1.29×10^{-2}	2.14×10^{-4}
0.37	4.83×10^{-3}	8.06×10^{-5}
0.36	2.91×10^{-3}	4.84×10^{-5}
0.34	1.00×10^{-3}	1.67×10^{-5}
0.33	5.77×10^{-4}	9.62×10^{-6}
0.32	3.26×10^{-4}	5.43×10^{-6}
0.31	1.81×10^{-4}	3.01×10^{-6}
0.30	9.83×10^{-5}	1.64×10^{-6}

$K(\theta)_z$ values in Table (c) are calculated using Equation 83.12:
$z = 50$ cm.
$m = 0.8624$.
$\tau = 0.4984$.
$\mu = -0.0569$.
The above process is repeated for each measurement depth/probe.

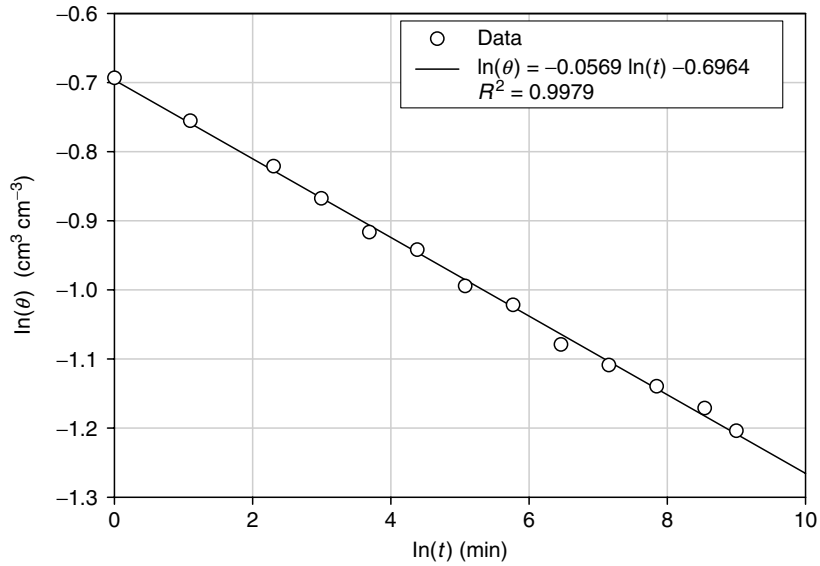

FIGURE 83.1. Example measurements of decrease in volumetric water content, θ, with time, t, at depth, z, for the instantaneous profile method. The straight line is a regression through the data to obtain the coefficients in Equation 83.11. The data appear in Table 83.1a.

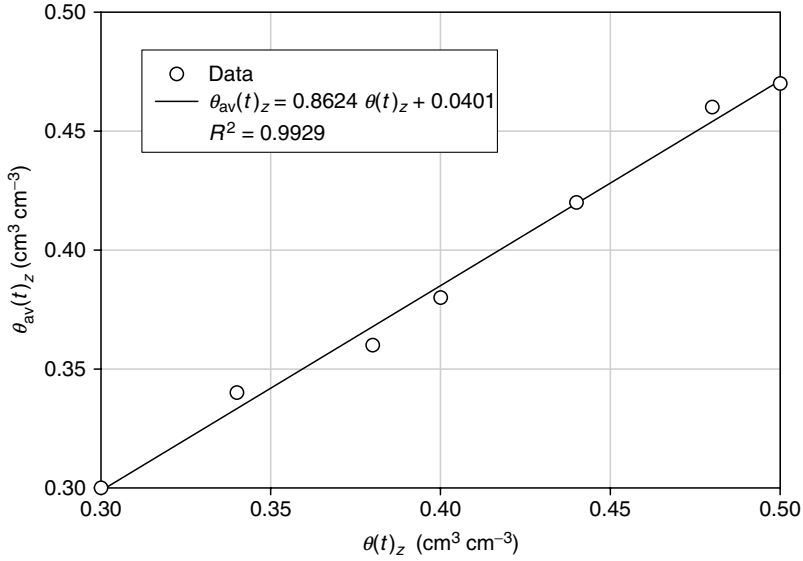

FIGURE 83.2. Example of average volumetric water content to depth z, $\theta_{av}(t)_z$, versus measured volumetric water content at depth z, $\theta(t)_z$, for the instantaneous profile method. The straight line is a regression through the data to obtain the coefficients in Equation 83.10. The data appear in Table 83.1b.

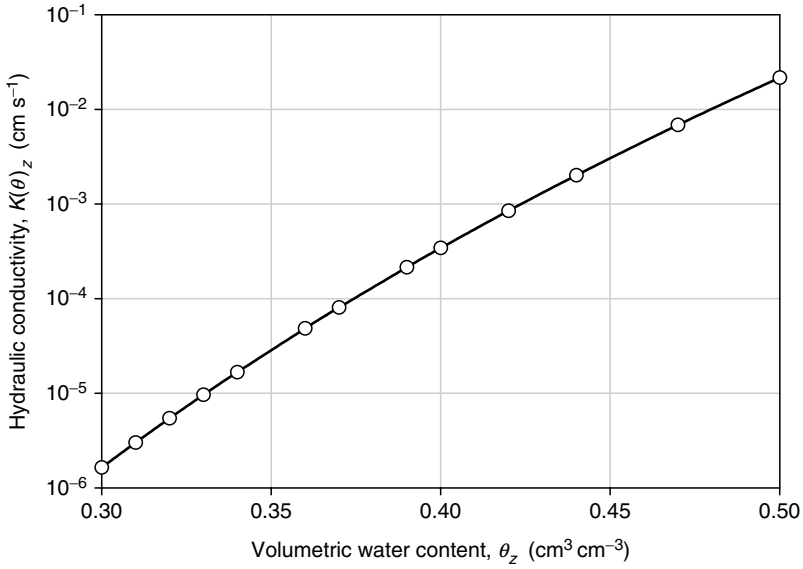

FIGURE 83.3. Example calculation of hydraulic conductivity, $K(\theta)_z$, versus volumetric water content, θ_z, at depth z using the instantaneous profile method (Equation 83.12). The data appear in Table 83.1c.

83.4 COMMENTS

1 A critical requirement of the method is that flow be entirely vertical and due only to gravity drainage. Hence, situations that induce lateral flow (e.g., presence of subsurface flow-impeding layers; presence of a shallow water table), or upward flow (e.g., surface evaporation/transpiration) must be avoided.

2 Use of single tube, multidepth matric head probes (e.g., multilevel tensiometers) and water content probes (e.g., TDR or neutron probes that slide down an access tube) may be advisable in the instantaneous profile method because they can reduce the number of access holes to as few as two (i.e., one for matric head and the other for water content), which in turn minimizes profile disturbance and potential pathways for short-circuit flow to the sensors.

3 If the vertical spacing between the water content probes is highly variable (as might be required to accommodate subsurface layers, horizons, etc.), it may be advisable to calculate $\overline{\theta}(t)_z$ as a weighted arithmetic mean, with the weights determined by the depths of the water content probes; i.e.,

$$\overline{\theta}(t)_z = \frac{1}{z}\sum_{i=1}^{n}\theta(t)_i T_i; \quad i = 1, 2, 3, \ldots, n; \qquad n > 1 \tag{83.13}$$

where z [L] is the depth (probe) under consideration, n is the number of water content probes between the surface and depth z, $\theta(t)_i$ [L^3L^{-3}] is the water content versus time values measured at probe i, and T_i is the weighing factor at probe i which is given by

$$T_i = \frac{(d_{i+1} - d_{i-1})}{2}; \quad i = 2, 3, 4, \ldots, (n-1) \tag{83.14a}$$

$$T_1 = \frac{(d_1 + d_2)}{2}; \quad i = 1 \tag{83.14b}$$

$$T_n = \frac{(d_n - d_{n-1})}{2}; \quad i = n \tag{83.14c}$$

where d_i [L] is the depth from the surface to water content probe i, d_1 is the depth to the shallowest water content probe ($i = 1$), and d_n ($i = n$) corresponds to the depth (z) of the water content probe under consideration. When the probe under consideration is the shallowest probe ($i = 1$), or in the special case when only one water content probe was installed ($n = 1$), then $T_1 = d_1 = z$, and $\overline{\theta}(t)_z = \theta(t)_z$.

4 The complete analysis (Equation 83.7 and Equation 83.8) is generally incapable of determining the $K-\theta-\psi$ relationship reliably within the top 20–30 cm of the porous medium surface because the near-surface hydraulic head gradient is very low, and actually goes to zero at the surface because $q(z,t) = 0$ is imposed at the surface (see Equation 83.2). The simplified analysis (Equation 83.12) applies at all depths, however; and ''at surface'' estimates of $K(\theta)$ are also possible via timed collection of core samples from the porous medium surface and subsequent determination of θ by oven-drying.

5 The instantaneous profile method may not yield realistic representations of $K(\theta)$, $K(\psi)$, and $\theta(\psi)$ in highly structured or low-permeability materials. In highly structured materials, flow through preferential flow zones (e.g., worm holes, cracks, finger-flow zones, etc.) may be missed partially or completely by the relatively small θ and ψ probes. In low-permeability materials, the time required for profile saturation and drainage can be impractically long.

6 The empirical relationships between $W(t)$ and t (Equation 83.5 and Equation 83.6), and between $\theta(t)_z$ and t (Equation 83.11) are not fixed. Alternative empirical relationships that provide better fits to particular data sets are permissible; however, $W(t)$ versus t must be differentiable by t, and $\theta(t)_z$ versus t must be both differentiable by t and explicitly solvable in terms of t.

7 Although not yet attempted, it should be possible to estimate the capillarity relationships, $\alpha^*(\psi)$, $S(\psi)$, $PD(\psi)$, and $NP(\psi)$ (see Chapter 69), from instantaneous profile determinations of $K(\psi)$ and $\theta(\psi)$. This would likely involve the following: (i) fitting an appropriate function to the $K(\psi)$ data; (ii) integrating under the fitted $K(\psi)$ function to obtain $\phi(\psi)$ via Equation 69.13; (iii) calculation of $\alpha^*(\psi)$ via Equation 69.16 (i.e., the $\alpha^*(\psi)$ values are ''integrally correct''); and (iv) using $\alpha^*(\psi)$, $K(\psi)$, and $\theta(\psi)$ in Equation 69.17 through Equation 69.19 to obtain $S(\psi)$, $PD(\psi)$, and $NP(\psi)$, respectively. The success of this would probably depend on how well the $K(\psi)$ function fits the $K(\psi)$ data. The capillarity relationships obviously cannot be determined if the simplified analysis is used (i.e., Equation 83.12), as no ψ measurements are available in that case.

83.5 STRENGTHS AND WEAKNESSES OF THE INSTANTANEOUS PROFILE METHOD

The main strengths of the instantaneous profile method are that it can yield simultaneous *in situ* estimates of $K(\theta)$, $K(\psi)$, and $\theta(\psi)$ for a number of depths and horizons during active drainage, and it does not require assuming any particular functional form for $K(\theta)$, $K(\psi)$, and $\theta(\psi)$. No other method is capable of doing this. On the other hand, important weaknesses of the method include the need for complex and delicate equipment (e.g., TDR probes, tensiometers) installed at various depths below the surface; measurement times that can run from hours to months; the potential need for large volumes of water to effect profile saturation; extensive effort required for replication (because of extensive equipment, time, and water requirements); and determination of only the wet end ($\approx -200 \leq \psi \leq 0$ cm) of the $K(\theta)$, $K(\psi)$, and $\theta(\psi)$ relationships.

Particular strengths of the simplified approach for homogeneous porous materials (i.e., Equation 83.9 through Equation 83.12) include avoidance of ''finicky'' pore water matric head probes (e.g., tensiometers); no requirement to evaluate uncertain water content and hydraulic head gradients; and provision of a straightforward analytical relationship between $K(\theta)_z$ and θ_z (Equation 83.12) that applies at all depths. Disadvantages of the simplified approach include loss of useful $\theta(\psi)$ and capillarity parameter data (because ψ is not measured); potentially inadequate representations of the data by the available empirical relationships; and limited applicability to nonuniform (e.g., layered) porous medium profiles.

REFERENCES

Dirksen, C. 2001. Unsaturated hydraulic conductivity. In K.A. Smith and C.E. Mullins, Eds. *Soil and Environmental Analysis: Physical Methods*. Marcel Dekker, Inc., New York, NY, pp. 218–219.

Flühler, H., Ardakani, M.S., and Stolzy, L.H. 1976. Error propagation in determining hydraulic conductivities from successive water content and pressure head profiles. *Soil Sci. Soc. Am. J.* 40: 830–836.

Hillel, D., Krentos, V.D., and Stylianou, Y. 1972. Procedure and test of an internal drainage method for measuring soil hydraulic characteristics in situ. *Soil Sci.* 114: 395–400.

Libardi, P.L., Reichardt, K., Nielsen, D.R., and Biggar, J.W. 1980. Simple field methods for estimating soil hydraulic conductivity. *Soil Sci. Soc. Am. J.* 44: 3–7.

Vachaud, G. and Dane, J.H. 2002. Instantaneous profile. In J.H. Dane and G.C. Topp, Eds. *Methods of Soil Analysis, Part 4—Physical Methods*. Soil Science Society of America, Madison, WI, pp. 937–945.

Chapter 84
Estimation of Soil Hydraulic Properties

F.J. Cook
Commonwealth Scientific and Industrial Research Organization
Indooroopilly, Queensland, Australia

H.P. Cresswell
Commonwealth Scientific and Industrial Research Organization
Canberra, Australian Capital Territory, Australia

84.1 INTRODUCTION

Soil hydraulic properties should be directly measured whenever possible, as they are critically important to the transport and storage of water and solutes (see other chapters in the Section Soil Water Analysis), and they are highly variable in space and time. However, direct measurement is not always feasible, due to restrictive budgets, insufficient time, and substantial difficulty associated with certain measurements, such as the dry end of the unsaturated hydraulic conductivity relationship. In these situations, the only practical option may be to estimate soil hydraulic properties from more easily measured parameters, such as texture, bulk density, porosity, and soil water desorption–imbibition relationships. Although the prudence of estimating soil hydraulic properties has been questioned (particularly when predicting or modeling water–solute movement; Philip 1991; Addiscott 1993; Passioura 1996), it can nonetheless provide insights that would otherwise be difficult to achieve; and it also allows extrapolation beyond the specific soil conditions under which measurements must be conducted.

A plethora of methods have been developed over the years for estimating the saturated or field-saturated hydraulic conductivity and water content, the soil water desorption–imbibition relationships, and the unsaturated hydraulic conductivity relationships (e.g., Mackenzie and Cresswell 2002). We will restrict ourselves here, however, to the well-established and versatile methods of Cresswell and Paydar (1996), Minasny et al. (1999), Saxton et al. (1986), and van Genuchten et al. (1991).

84.2 SOIL WATER DESORPTION–IMBIBITION RELATIONSHIPS

The soil water desorption relationship describes the release of water from soil, while the imbibition relationship describes the uptake of water. These so called $\theta(\psi)$ relationships are

usually represented by empirical or quasiempirical functions or ''models'' describing the change in soil volumetric water content, θ [L^3L^{-3}], with soil pore water pressure or matric head, ψ [L].

84.2.1 Brooks–Corey (1964) $\theta(\psi)$ Model

One of the most popular quasiempirical $\theta(\psi)$ models is the modified Brooks and Corey (1964) function (Campbell 1974; Hutson and Cass 1987):

$$\frac{\theta_i}{\theta_{sat}} = \frac{2b}{1+2b}; \quad b > 0 \tag{84.1a}$$

$$\frac{\theta}{\theta_{sat}} = \left(\frac{|\psi|}{a}\right)^{-1/b}; \quad a > 0; \quad \theta \le \theta_i; \quad \psi \le \psi_i < 0 \tag{84.1b}$$

$$\frac{\theta}{\theta_{sat}} = 1 - \frac{\psi^2\left(1 - \frac{\theta_i}{\theta_{sat}}\right)}{a^2\left(\frac{\theta_i}{\theta_{sat}}\right)^{-2b}}; \quad \psi_i < \psi \le 0 \tag{84.1c}$$

where θ_{sat} [L^3L^{-3}] is the saturated or field-saturated soil volumetric water content, a [L] is a constant analogous to the air-entry pressure head of the desorption curve or the water-entry pressure head of the imbibition curve, b is a dimensionless empirical constant, and (ψ_i, θ_i) is the point of inflexion on the desorption–imbibition relationship (represented by Equation 84.1a) where the power curve component of the relationship (represented by Equation 84.1b) joins the parabolic curve component (represented by Equation 84.1c). The advantage of this form of the Brooks and Corey (1964) equation is that it avoids a mathematical discontinuity when $|\psi| = a$.

The parameters in Equation 84.1a through Equation 84.1c are obtained using three main approaches: (i) least-squares fitting of Equation 84.1b when water content and matric head data are available over the appropriate range of $\theta(\psi)$; (ii) the ''two-point'' method where only two widely spaced data points on the $\theta(\psi)$ curve are required; and (iii) the ''surrogate data'' method where the parameters are derived from other soil data such as texture, bulk density, average particle density, etc. These approaches are described further below.

Regression Method for Brooks–Corey $\theta(\psi)$

Rewriting Equation 84.1b into the form

$$\log_{10}\theta = -\frac{1}{b}\log_{10}|\psi| + C_1; \qquad \theta \le \theta_i; \quad \psi \le \psi_i \tag{84.2a}$$

where

$$C_1 = \log_{10}\theta_{sat} + \frac{1}{b}\log_{10} a \tag{84.2b}$$

describes a straight line with slope $-1/b$, and a y-axis intercept of C_1. The b and C_1 values are consequently found by least-squares regression of $\log_{10}\theta$ against $\log_{10}|\psi|$. Once b is known,

θ_i is readily determined from Equation 84.1a. Given that Equation 84.1b and Equation 84.2a apply for θ_i and ψ_i, then ψ_i can be obtained by rearranging Equation 84.2a into

$$\log_{10}|\psi_i| = -b(\log_{10}\theta_i - C_1) \tag{84.2c}$$

which in turn allows a to be obtained by rewriting Equation 84.1b in the form

$$a = |\psi_i|\left(\frac{\theta_i}{\theta_{\text{sat}}}\right)^b \tag{84.2d}$$

Example calculations are given in Section 84.4.

Two-Point Method for Brooks–Corey $\theta(\psi)$ (Cresswell and Paydar 1996)

Estimate θ_{sat} using

$$\theta_{\text{sat}} = C_2\left(1 - \frac{\rho_{\text{b}}}{\rho_{\text{s}}}\right) \tag{84.3a}$$

where ρ_{b} [Mg m^{-3}] is the dry bulk density of the soil sample, $\rho_{\text{s}} = 2.65$ Mg m^{-3} is the average soil particle density, and $C_2 = 0.93$ is a coefficient accounting for entrapped air, which is usually present in saturated (or field-saturated) soil.

Measure two widely spaced points on the sample's desorption or imbibition curve within the range of validity of Equation 84.1b, i.e., (ψ_1, θ_1) and (ψ_2, θ_2) where ψ_1 and ψ_2 are $\leq\psi_i$, and θ_1 and θ_2 are $\leq\theta_i$. This assumes that $\log_{10}\theta$ vs. $\log_{10}\psi$ is roughly linear in the range of validity of Equation 84.1b.

Calculate b using

$$b = \frac{-\Delta x}{\Delta y} = \frac{-(\log_{10}|\psi_1| - \log_{10}|\psi_2|)}{\log_{10}\theta_1 - \log_{10}\theta_2} \tag{84.3b}$$

Note that b is the negative inverse slope of the straight line between the two points (Figure 84.1).

Back substitute θ_{sat} and b into Equation 84.1a to obtain θ_i. Calculate ψ_{i} by rearranging Equation 84.3b into

$$\log_{10}|\psi_i| = -b(\log_{10}\theta_i - \log_{10}\theta_1) + \log_{10}|\psi_1| \tag{84.3c}$$

where the data point, (ψ_1, θ_1), falls within the range of validity of Equation 84.1b.

Example calculations are given in Section 84.4.

Surrogate Data Method for Brooks–Corey $\theta(\psi)$ (Saxton et al. 1986)

The surrogate data method of Saxton et al. (1986) employs empirical regression relationships based on soil texture. The θ_{sat}, b, and a parameters in Equation 84.1a through Equation 84.1c are given by

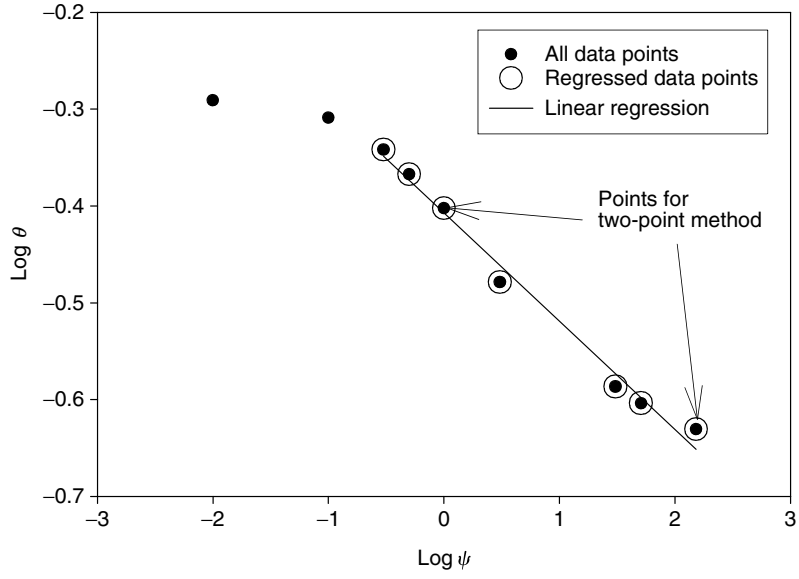

FIGURE 84.1. Soil water content (θ) vs. pore water matric head (ψ) relationship for the data in Table 84.3. The data points used in the Brooks–Corey ''regression'' and ''two-point'' methods are indicated.

$$\theta_{sat} = A + B(\text{Sa}) + D\ln(\text{Cl}) \tag{84.4a}$$

$$b = E + F(\text{Cl})^2 + G(\text{Sa})^2(\text{Cl}) \tag{84.4b}$$

$$a = 100\exp\left[H + I(\text{Cl}) + J(\text{Sa})^2 + L(\text{Sa})^2(\text{Cl})\right] \Big/ \theta_{sat}^{b}\ [\text{kPa}] \tag{84.4c}$$

where $A, B, D, E, F, G, H, I, J, L$ are dimensionless empirical coefficients (Table 84.1), Cl is the % clay by weight (<2 μm) in the soil sample, and Sa is the percent sand by weight in the soil sample (0.05–2 mm). Note that the sand particle size range corresponds to the USDA system, which differs from both the British system (British Standards Institution 1984) and the Australian system. (An interpolated textural adjustment is given in the example calculation below, see Table 84.4.) Note also in Equation 84.4c that the units for a are kPa.

An alternative formula for determining a is

$$a = 100(M + N\theta_{sat}) \tag{84.4d}$$

TABLE 84.1 Parameters for Determining the Brooks–Corey $\theta(\psi)$ Using the Saxton et al. (1986) Soil Texture Method

Parameter	Value	Parameter	Value	Parameter	Value
A	0.332	F	2.22×10^{-3}	J	-4.880×10^{-4}
B	-7.251×10^{-4}	G	3.484×10^{-5}	L	-4.285×10^{-5}
D	0.0555	H	−4.396		
E	3.140	I	−0.0715		

where $M = -0.108$ and $N = 0.341$ are dimensionless empirical coefficients.

Note that Equation 84.4a through Equation 84.4d are applicable only for soils with a clay content between 5% and 60% by weight, and a sand content of more than 5% by weight (Saxton et al. 1986).

Example calculations are given in Section 84.4.

84.2.2 van Genuchten (1980) $\theta(\psi)$ Model

The van Genuchten (1980) quasiempirical function estimates $\theta(\psi)$ using

$$\theta = \theta_r + \frac{\theta_{sat} - \theta_r}{[1 + (\alpha_v|\psi|)^n]^m} \tag{84.5a}$$

where α_v [L^{-1}] is an empirical parameter related to the air or water-entry value, θ_{sat} [L^3L^{-3}] is the saturated or field-saturated soil volumetric water content, θ_r [L^3L^{-3}] is the residual soil volumetric water content, and n and m are dimensionless empirical constants.

Regression Method for van Genuchten $\theta(\psi)$

When measured $\theta(\psi)$ data are available, the RETC program (van Genuchten et al. 1991) can be used to determine the parameters in Equation 84.5a by a nonlinear least-squares optimization method. The program allows various fitting options, including independent fitting of α_v, m, and n; setting $m = 1 - (1/n)$; and setting $m = 1 - (2/n)$. The θ_{sat} and θ_r parameters can be either specified input or additional fitting parameters.

Example calculations are given in Section 84.4.

Surrogate Data Methods for van Genuchten $\theta(\psi)$

Many methods have been developed to obtain the parameters in Equation 84.5a from surrogate soil data. Some of the more recent and popular methods include the ROSETTA analysis system (Schaap 1999), which is based on the international (but mostly North American) UNSODA database (Leij et al. 1999); the Minasny et al. (1999) algorithm that is based on Australian soils; and the Rajkai et al. (2004) algorithm, which is based on Hungarian soils. The ROSETTA and Minasny et al. methods are described further below.

ROSETTA Methods

ROSETTA estimates K_{sat} and the parameters in the van Genuchten $\theta(\psi)$ and $K(\psi)$ models. It uses a hierarchical system of five pedotransfer functions (PTFs) that allow prediction based on increasing amounts of available soil data, i.e., PTF1: soil textural class only; PTF2: soil texture data only (weight percent sand, silt, and clay); PTF3: soil texture plus bulk density data; PTF4: soil texture plus bulk density plus volumetric water content at −3.3 m matric head; and PTF5: soil texture plus bulk density plus volumetric water content at both −3.3 and −150 m matric heads. The main advantage of the hierarchical approach is that it allows maximal use of available data. The first PTF (PTF1) uses a simple lookup table (based on the

UNSODA database) that provides representative ''class average'' hydraulic parameters for each USDA soil textural class. The PTF2–PTF5 functions, on the other hand, use a neural network approach, with each higher PTF level providing a more accurate prediction (at least in theory) because it uses a greater amount of soil information. Uncertainty estimates are included with each parameter value to allow an assessment of the reliability of the prediction. Example calculations are given in Section 84.4.

Minasny et al. (1999) Methods

McKenzie and Cresswell (2002) updated the Minasny et al. (1999) method to obtain

$$\theta_r = A_v(\mathrm{Cl}) + B_v(\mathrm{PWP}) + D_v(\mathrm{Si}) + E_v \tag{84.5b}$$

$$\theta_{sat} = F_v(\mathrm{Cl}) + G_v(\mathrm{POR}) \tag{84.5c}$$

$$\alpha_v = H_v + I_v d_g \tag{84.5d}$$

$$n = J_v + L_v \sigma_g \tag{84.5e}$$

where Cl is the % clay by weight in the soil sample (<2 μm), Si is the % silt by weight (2–20 μm), POR [L^3L^{-3}] is the soil porosity, PWP [L^3L^{-3}] is the permanent wilting point water content given by θ at $\psi = -150$ m, d_g (mm) is the geometric mean particle diameter, σ_g (mm) is the geometric standard deviation of the particle size distribution, and the other coefficients are given in Table 84.2 for three different estimation methods known as

TABLE 84.2 Parameter Values Used in the McKenzie and Cresswell (2002) Update of the Minasny et al. (1999) Methods for Estimating the Empirical $\theta(\psi)$ Function of van Genuchten (1980)

Parameter	ENR2	ENR6	ENR7	Soil texture for ENR7
A_v	−0.00092	0.00427	−0.00156	—
B_v	1.17748	0	1.22333	—
D_v	0	0.00267	0	—
E_v	0	−0.00733	0	—
F_v	0.00112	0.00110	0.00149	—
G_v	0.8331	0.82607	0.81851	—
H_v	0.1561	0.1361	0.0984	Sandy
			0.1787	Loamy
			0.3186	Clayey
I_v	1.7046	1.6929	1.5607	Sandy
			0.4152	Loamy
			18.1363	Clayey
J_v	1.3978	1.4062	1.4990	Sandy
			1.3373	Loamy
			1.2433	Clayey
L_v	0.0027	−0.0050	−0.0024	Sandy
			0.0053	Loamy
			0.00156	Clayey

''ENR2,'' ''ENR6,'' and ''ENR7'' (McKenzie and Cresswell 2002). The d_g and σ_g parameters are obtained using

$$\begin{aligned} d_g &= \exp(a_p); \qquad i = 1, 2, 3, \ldots, T \\ a_p &= 0.01 \sum_{i=1}^{T} f_i \ln W_i \end{aligned} \tag{84.5f}$$

and

$$\begin{aligned} \sigma_g &= \exp(b_p) \\ b_p &= \sqrt{0.01 \sum_{i=1}^{T} \ln^2 W_i - a_p{}^2} \end{aligned} \tag{84.5g}$$

where T is the number of soil particle size fractions, and f_i is the percentage of the total soil mass having a diameter $\leq W_i$ (mm).

Note that the three estimation methods in Table 84.2 (ENR2, ENR6, and ENR7) generally yield similar parameter values. Note also that the UNSODA database and ROSETTA may be more applicable for Canadian soils, as the Minasny et al. (1999) method is based solely on Australian soils. Example calculations are given in Section 84.4.

84.3 UNSATURATED HYDRAULIC CONDUCTIVITY RELATIONSHIPS

The unsaturated hydraulic conductivity relationship describes the change in soil hydraulic conductivity, K [LT^{-1}], with changing soil volumetric water content, θ [L^3L^{-3}], or changing soil pore water matric head, ψ [L]. These $K(\theta)$ and $K(\psi)$ relationships are generally represented by empirical or quasiempirical models because direct measurement is often difficult and time-consuming. Direct measurement can also be very inaccurate (or even impossible) for small values of θ and ψ.

84.3.1 Brooks–Corey (1966) $K(\theta)$ Model

The modified Brooks and Corey (1966) $K(\theta)$ function has the form (Campbell 1974):

$$K(\theta) = K_{sat}\left(\frac{\theta}{\theta_{sat}}\right)^{2b+3} \tag{84.6}$$

where K_{sat} [LT^{-1}] is the saturated or field-saturated hydraulic conductivity, θ_{sat} [L^3L^{-3}] is the saturated or field-saturated soil volumetric water content, and b is the dimensionless empirical constant described in Equation 84.1a and Equation 84.1b.

The most straightforward application of Equation 84.6 is to simply plug in measured or calculated values of K_{sat}, θ_{sat}, and b, where b was determined from the corresponding Brooks–Corey $\theta(\psi)$ function Equation 84.1. Use of K_{sat} may introduce considerable uncertainty into the $K(\theta)$ function, however, as K_{sat} values are often highly variable due to extreme sensitivity to soil macopores, texture, and structure. Bruce (1972) suggests that better results are obtained by using a K value determined at a slightly negative matric head, rather than K_{sat}.

Rawls et al. (1982) found that Equation 84.6 does not fit hydraulic conductivity data well for average soil textural classes, and Saxton et al. (1986) recommend using the texture-based relationship:

$$K(\theta) = \kappa\left\{\exp\left[\beta + \gamma(\mathrm{Sa}) + \left(\delta + \varepsilon(\mathrm{Sa}) + \varphi(\mathrm{Cl}) + \lambda(\mathrm{Cl}^2)\right)/\theta\right]\right\} \tag{84.7}$$

where

$\kappa = 2.778 \times 10^{-6}$ m s^{-1}
$\beta = 12.012$
$\gamma = -0.0755$
$\delta = -3.895$
$\varepsilon = 0.03671$
$\varphi = -0.1103$
$\lambda = 8.8546 \times 10^{-4}$

and Sa and Cl are, respectively, the percents by weight of sand and clay in the soil.

Attempts have also been made to estimate the likely range (extreme values) of K_{sat} from visual estimates of soil morphology such as pedality, structure, and the number and size of macropores (McKeague et al. 1984; McKenzie et al. 1991; Griffiths et al. 1999). From an applications point of view, such an approach is perhaps most useful for scenario testing or interpreting model output. Note, however, that the effort involved in obtaining the morphological data can often be greater than making the K_{sat} measurements, although morphology-based estimation is usually less costly.

Example calculations for the Saxton et al. (1986) method are given in Section 84.4.

84.3.2 Mualem–van Genuchten $K(\theta)$ and $K(\psi)$ Models

Mualem (1976) developed a method for predicting unsaturated soil hydraulic conductivity by integrating the soil–water desorption or imbibition function. This approach can be combined with the van Genuchten (1980) $\theta(\psi)$ model to give

$$\begin{aligned} K(\theta) &= K_{\mathrm{sat}}\Theta^{l}\left[1 - \left(1 - \Theta^{1/m}\right)^{m}\right]^{2} \\ \Theta &= \frac{\theta - \theta_r}{\theta_{\mathrm{sat}} - \theta_r} \end{aligned} \tag{84.8}$$

and

$$K(\psi) = K_{\mathrm{sat}}\frac{\left[(1 + |\alpha_v\psi|^{n})^{m} - |\alpha_v\psi|^{(n-1)}\right]^{2}}{\left[1 + |\alpha_v\psi|^{n}\right]^{m(l+2)}} \tag{84.9}$$

where α_v [L^{-1}] is an empirical parameter related to the air-entry or water-entry value, l is a dimensionless pore connectivity parameter, and n and m are dimensionless empirical constants. The van Genuchten parameters (θ_{r}, θ_{sat}, α_v, n, and m) are obtained by fitting the model to data using the RETC program, or by estimation via the ROSETTA system of pedotransfer functions.

Mualem (1976) proposed $l = 0.5$ based on an analysis of 45 data sets. Subsequent work suggests, however, that l tends to be soil-specific. The appropriateness of the $l = 0.5$ assumption for a particular model-data fit can be assessed by calculating $K(\theta_{FC})$ or $K(\psi_{FC})$ (using Equation 84.8 or Equation 84.9, respectively), and comparing the result to the ''global'' field capacity hydraulic conductivity of $K_{FC} = 1 \times 10^{-8}$ m s^{-1} (N. Huth, personal communication). If the calculated K is substantially greater than or less than K_{FC} (say, by more than about an order of magnitude), then the $l = 0.5$ assumption is probably invalid. A more appropriate value for l can be calculated if θ_{FC} or ψ_{FC} are either known, estimated, or assumed. Under this condition, l is obtained by rearranging Equation 84.8 to

$$l = \frac{\ln\left\{K_{FC}/\left(K_{sat}\left[1-\left(1-\Theta_{FC}^{1/m}\right)^{m}\right]^{2}\right)\right\}}{\ln \Theta_{FC}} \qquad (84.10)$$

$$\Theta_{FC} = \frac{\theta_{FC} - \theta_r}{\theta_{sat} - \theta_r}$$

or by rearranging Equation 84.9 to

$$l = \frac{1}{m}\,\frac{\ln\left\{K_{sat}\left[(1+|\alpha_v\psi_{FC}|^{n})^{m} - |\alpha_v\psi_{FC}|^{n-1}\right]^{2}/K_{FC}\right\}}{\ln(1+|\alpha_v\psi_{FC}|^{n})} - 2 \qquad (84.11)$$

where K_{FC} replaces $K(\theta_{FC})$ in Equation 84.10 or $K(\psi_{FC})$ in Equation 84.11. One can then either accept the existing α_v, n, and m values along with the new l-value, or refit the van Genuchten model using the new l-value to obtain updated α_v, n, and m values. Setting $K_{FC} = 1 \times 10^{-8}$ m s^{-1}($\approx$1 mm day^{-1}) is justified on the basis that soil drainage from saturation effectively stops (becomes negligible) once K has declined to about this value.

The fitted values of m, n, and α_v produced by RETC for $K(\theta)$ or $K(\psi)$ tend to be more realistic or reliable when both $\theta(\psi)$ and $K(\theta)$ data are input.

ROSETTA can be used to estimate K_{sat} when only limited physical data are available, although such an estimate is usually highly uncertain. If only textural data are available, UNSODA or Equation 84.7 can be used to estimate K_{sat}.

Example calculations are given in Section 84.4.

84.4 EXAMPLE CALCULATIONS

The desorption, bulk density, hydraulic conductivity, and texture data (Table 84.3 and Table 84.4) used in the example calculations are from a Sulfuric, Redoxic, Hydrosol soil (Australian Soil Classification System; Isbell 1996). The texture is clay loam from 0 to 30 cm, fine sandy clay from 30 to 90 cm, and silty clay below 90 cm. The data were collected from the 2–7 cm depth.

Note that the following example calculations are for illustrative purposes only, and should not be considered as a comparison of the various methods.

TABLE 84.3 Soil Water Desorption, $\theta(\psi)$, Bulk Density, $\rho_b = 1.03$ Mg m^{-3}, Particle Density, $\rho_s = 2.65$ Mg m^{-3}, and Saturated Hydraulic Conductivity, $K_{sat} = 1.7 \times 10^{-5}$ m s^{-1}, in the 2–7 cm Depth of a Clay Loam Soil

ψ (m)	$\text{Log}_{10}\lvert\psi\rvert$	θ (m^3 m^{-3})	$\text{Log}_{10}\theta$
−0.01	−2	0.512	−0.291
−0.10	−1	0.491	−0.309
−0.30	−0.52288	0.455	−0.342
−0.50	−0.30103	0.429	−0.367
−1.00	0	0.396	−0.402
−3.06	0.485721	0.332	−0.479
−30.6	1.485721	0.259	−0.587
−51	1.70757	0.249	−0.604
−153	2.184691	0.234	−0.631

Source: From Cook, F.J., Dobos, S.K., Carlin, G.D., and Millar, G.E. *Aust. J. Soil Res.*, 42, 499, 2004.

84.4.1 Brooks–Corey $\theta(\psi)$ and $K(\theta)$ Functions

Regression Method

The θ_{sat} is estimated using the soil bulk density, ρ_b, particle density, ρ_s (see Table 84.3), and Equation 84.3a:

$$\theta_{sat} = 0.93[1 - (1.03/2.65)] = 0.569 \tag{84.12}$$

The value of b is obtained via Equation 84.2a using data points where $\psi \leq \psi_i$ (Figure 84.1). The slope of the regression is $-1/b = -0.112$, the intercept is $C_1 = -0.407$, and the regression coefficient is $R^2 = 0.988$. Thus, $b = 8.929$, and θ_i is calculated using Equation 84.1a:

$$\theta_i = (0.569)(2)(8.929)/[1 + (2)8.929] = 0.539 \tag{84.13}$$

Substitution of the θ_i value into Equation 84.2c gives the value of ψ_i:

$$\log_{10}|\psi_i| = (-8.929)[\log_{10}(0.539) - (-0.407)] = -1.2375 \tag{84.14a}$$

$$\psi_i = -0.0579 \text{ m} \tag{84.14b}$$

TABLE 84.4 Particle Size Distribution in the 2–7 cm Depth of a Clay Loam Soil

Texture	Particle size range (mm)	Weight (% of total sample weight)
Coarse sand	0.2–2	8.4
Fine sand	0.02–0.2	43.2
Silt	0.002–0.02	27.9
Clay	<0.002	20.6

Source: From Cook, F.J., Dobos, S.K., Carlin, G.D., and Millar, G.E. *Aust. J. Soil Res.*, 42, 499, 2004.

The value of a is obtained via Equation 84.2d and substitution of the calculated values for b, θ_i, θ_{sat}, and ψ_i:

$$a = 0.0579(0.539/0.569)^{8.929} = 0.0357 \text{ m} \tag{84.15}$$

The hydraulic conductivity function, $K(\theta)$, is then obtained by substitution of K_{sat}, θ_{sat}, and b into Equation 84.6:

$$K(\theta) = 1.7 \times 10^{-5}(\theta/0.569)^{[2(8.929)+3]} = 2.179\theta^{20.858} \text{ m s}^{-1} \tag{84.16}$$

Two-Point Method

Calculate θ_{sat} using Equation 84.3a and the data in Table 84.3:

$$\theta_{sat} = 0.93[1 - (1.03/2.65)] = 0.569 \tag{84.17}$$

Calculate b using Equation 84.3b and two appropriate data points in Table 84.3, e.g., $(\psi_1, \theta_1) = (-1 \text{ m}, 0.396)$ and $(\psi_2, \theta_2) = (-153 \text{ m}, 0.234)$:

$$b = \frac{-(\log_{10}|-1| - \log_{10}|-153|)}{\log_{10}(0.396) - \log_{10}(0.234)} = 9.562 \tag{84.18}$$

Calculate θ_i using Equation 84.1a and the calculated values for θ_{sat} and b:

$$\theta_i = (0.569)(2)(9.562)/[1 + (2)(9.562)] = 0.541 \tag{84.19}$$

Calculate ψ_i using Equation 84.3c and one appropriate data point in Table 84.3, e.g., $(\psi_1, \theta_1) = (-1 \text{ m}, 0.396)$:

$$\begin{aligned} \log_{10}|\psi_i| &= -9.562[\log_{10}(0.541) - \log_{10}(0.396)] + \log_{10}|-1| = -1.2957 \\ \psi_i &= -0.0506 \text{ m} \end{aligned} \tag{84.20}$$

Calculate a by back substitution of ψ_i, θ_i, and b into Equation 84.2d:

$$a = 0.0506(0.541/0.569)^{9.562} = 0.0312 \text{ m} \tag{84.21}$$

The hydraulic conductivity function, $K(\theta)$, is then obtained by substitution of K_{sat}, θ_{sat}, and b into Equation 84.6:

$$K(\theta) = 1.7 \times 10^{-5}(\theta/0.569)^{[(2)(9.562)+3]} = 4.450\theta^{22.124} \tag{84.22}$$

The Brooks–Corey $K(\theta)$ function obtained using the regression and two-point methods is compared in Figure 84.2.

Saxton et al. (1986) Surrogate Data Method

To use the Saxton et al. (1986) texture-based method, we must move the sand–silt boundary to 0.05 mm for the USDA system. This was achieved in Table 84.4 by interpolation, which

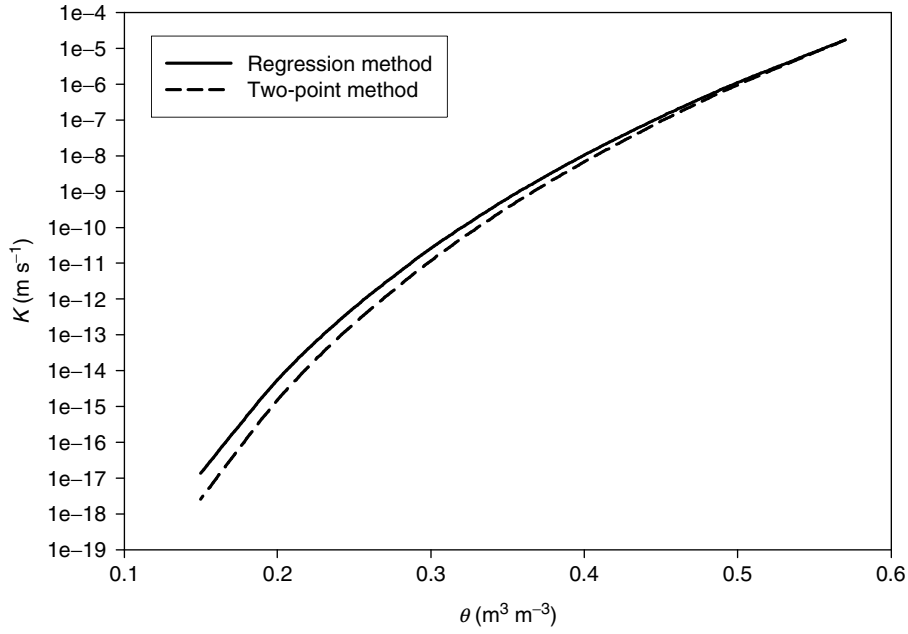

FIGURE 84.2. Hydraulic conductivity (K) vs. water content (θ) relationship for the Brooks–Corey model (Equation 84.6) with parameters obtained using the data in Table 84.3 and the ''regression'' and ''two-point'' fitting methods.

resulted in a silt content, Si = 45.0%, a sand content, Sa = 34.4%, and a clay content, Cl = 20.6%. The Brooks–Corey $\theta(\psi)$ parameters (Equation 84.4a through Equation 84.4c) are then

$$\theta_{sat} = 0.332 + (-7.251 \times 10^{-4})(34.4) + 0.0555 \ln(20.6) = 0.475 \tag{84.23}$$

$$b = 3.140 + (2.22 \times 10^{-3})(20.6^2) + (3.484 \times 10^{-5})(34.4^2)(20.6) = 4.93 \tag{84.24}$$

$$\begin{aligned} a =& 100 \exp[-4.396 + (-0.0715)(20.6) + (-4.880 \times 10^{-4})(34.4^2) \\ &+ (-4.285 \times 10^{-5})(34.4^2)(20.6)]/0.475^{4.93} = 2.19 \text{ kPa} \end{aligned} \tag{84.25}$$

or alternatively, Equation 84.4d:

$$a = 100[-0.108 + (0.341)(0.475)] = 5.40 \text{ kPa} \tag{84.26}$$

The value of θ_i is obtained via Equation 84.1a:

$$\theta_i = (0.475)(2)(4.93)/[1 + (2)(4.93)] = 0.431 \tag{84.27}$$

and ψ_i is obtained via Equation 84.2d:

$$|\psi_i| = 2.19(0.431/0.475)^{-4.93} = 0.354 \text{ m} \quad \text{(using Equation 84.25)} \tag{84.28}$$

or

$$|\psi_i| = 5.40(0.431/0.475)^{-4.93} = 0.872 \text{ m} \quad \text{(using Equation 84.26)} \tag{84.29}$$

The hydraulic conductivity function, $K(\theta)$, is estimated using Equation 84.7:

$$\begin{aligned} K(\theta) &= 2.778 \times 10^{-6}\{\exp[12.012 + (-0.0755)(34.4) \\ &\quad + (-3.895 + (0.03671)(34.4) + (-0.1103)(20.6) \\ &\quad + (8.8546 \times 10^{-4})(20.6^2))/\theta]\} \\ &= 2.778 \times 10^{-6}\{\exp[9.415 + (-4.5286/\theta)]\} \text{ m s}^{-1} \end{aligned} \tag{84.30}$$

which can also be used to estimate K_{sat} by inputting θ_{sat}:

$$\begin{aligned} K_{sat} &= 2.778 \times 10^{-6}\{\exp[9.415 + (-4.5286/0.475)]\} \\ &= 2.47 \times 10^{-6} \text{ m s}^{-1} \end{aligned} \tag{84.31}$$

84.4.2 van Genuchten $\theta(\psi)$, $K(\theta)$, and $K(\psi)$ Functions

Least-Squares Fitting with RETC

The RETC version 6.0 program is USDA freeware that can be downloaded along with a users manual from the US Salinty Laboratory (2006) Web site.

The program was used to fit Equation 84.5a to the $\theta(\psi)$ data in Table 84.3, with the fitting parameters being θ_r, θ_{sat}, n, m, and α_v. The resulting parameter values are given in Table 84.5, and the RETC input and output files are shown in Appendix 84.1. Note that the RETC-generated fit to the data is very good, as indicated by a coefficient of regression, $R^2 = 0.997$. For comparison purposes, RETC was run again with the restriction, $m = 1 - (1/n)$, which produced somewhat different parameter values and a slightly better fit, $R^2 = 0.9996$ (Table 84.5). Note, however, that the two fitted $\theta(\psi)$ curves are virtually indistinguishable (Figure 84.3).

To ensure that the true global minimum in the objective function has been found, RETC should be run several times using different initial values for the fitted parameters.

TABLE 84.5 van Genuchten $\theta-\psi-K$ Function Parameters and R^2 Values Obtained Using RETC

Fitting parameters plus K_{sat} and R^2 value	All five parameters fitted	Four parameters fitted with $m = 1-(1/n)$
θ_r (m^3m^{-3})	0.211	0.194
θ_{sat} (m^3m^{-3})	0.515	0.511
n	1.034	1.331
m	0.428	Not applicable
α_v (m^{-1})	2.255	3.710
K_{sat} (m s^{-1})	2.9×10^{-6}	2.9×10^{-6}
R^2	0.9998	0.9996

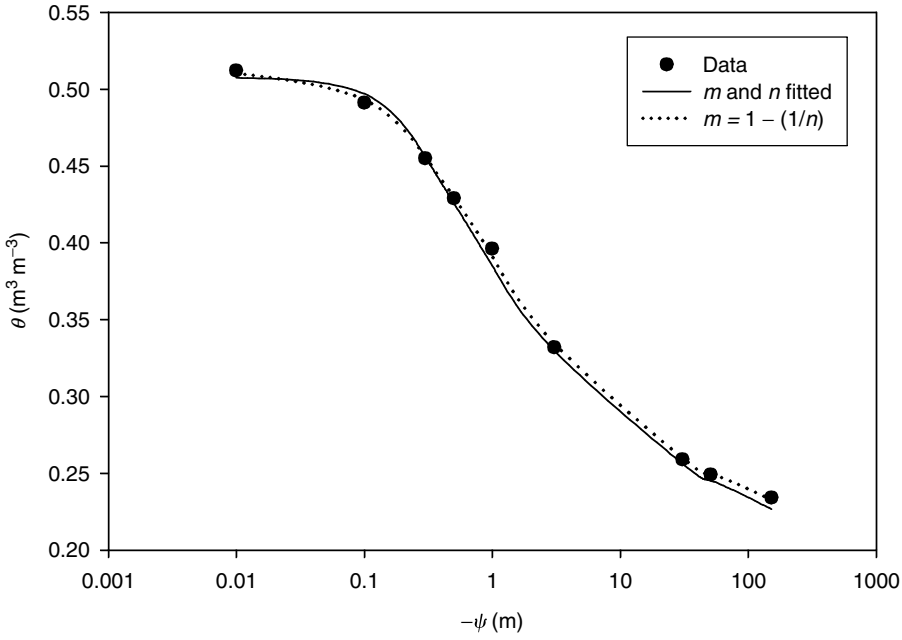

FIGURE 84.3. Prediction of the soil water content (θ) vs. pore water matric head (ψ) relationship (Table 84.3) using the van Genuchten model and RETC with both m and n fitted (solid line) and with $m = 1-(1/n)$ (dotted line).

The estimated K_{sat} is 2.9×10^{-6} m s^{-1}, which is less than the measured value of 1.7×10^{-5} m s^{-1}. The predicted values of K in the appendix can be scaled by the ratio of the measured to the predicted K_{sat} values ($1.7 \times 10^{-5}/2.9 \times 10^{-6} = 5.86$) to give values based on the measured K_{sat}. When this scaling is done, the hydraulic conductivity predicted at the field capacity matric head ($\psi_{FC} = -1$ m) by the fitted van Genuchten function is $K(\psi_{FC}) = 2.1 \times 10^{-8}$ m s^{-1}. As this value is close to the proposed ''global'' field capacity conductivity of $K_{FC} = 1 \times 10^{-8}$ m s^{-1} (see above), the assumption, $l = 0.5$, in the van Genuchten model is appropriate for this soil.

If $K_{sat} = 2.9 \times 10^{-6}$ m s^{-1} is used, however, then the fitted van Genuchten function yields $K(\psi_{FC}) = 3.5 \times 10^{-9}$ m s^{-1}, which is almost a factor of 3 lower than K_{FC}. For illustrative purposes, an updated value for l is calculated below using Equation 84.10 and Equation 84.11.

Using the four fitted parameters in the right-hand column of Table 84.5, m is determined via

$$m = 1 - (1/n) = 1 - (1/1.331) = 0.249$$

θ_{FC} is calculated via Equation 84.5a to yield

$$\theta_{FC} = 0.194 + \frac{(0.511 - 0.194)}{[1 + (3.71|-1|)^{1.331}]^{0.249}} = 0.391$$

and the relative field capacity water content, Θ_{FC}, is given by

$$\Theta_{FC} = (\theta_{FC} - \theta_r)/(\theta_{sat} - \theta_r) = (0.391 - 0.194)/(0.411 - 0.194) = 0.621$$

Using Equation 84.10, the *l*-parameter is

$$l = \frac{\ln\left\{1 \times 10^{-8} / \left[2.9 \times 10^{-6}\left(1 - (1 - 0.621^{1/0.249})^{0.249}\right)^2\right]\right\}}{\ln(0.621)} = -1.720$$

which is very different from the commonly assumed value of 0.5. Note that the same result for *l* is obtained using Equation 84.11.

If the five fitted parameters in the left-hand column of Table 84.5 are used for the same field capacity conditions as above, Equation 84.11 yields

$$l = \frac{1}{0.428} \frac{\ln\left\langle\left\{2.9 \times 10^{-6}\left[\left(1 + |(2.255)(-1)|^{1.034}\right)^{0.428} - |(2.255)(-1)|^{0.034}\right]^2 / 1.0 \times 10^{-8}\right\}\right\rangle}{\ln\left(1 + |(2.255)(-1)|^{1.034}\right)} - 2$$

$$= 7.32$$

whereas Equation 84.10 gives $l = 3.45$. Equation 84.10 and Equation 84.11 yield different *l*-values in this case because both *n* and *m* were obtained by fitting to soil water desorption data, i.e., *m* is independent from *n* in this case. As with the above example, however, the calculated values for *l* are very different from the commonly assumed value of 0.5.

Surrogate Data Methods

ROSETTA Methods

The PTF2–PTF5 pedotransfer functions in ROSETTA were used to determine the van Genuchten parameters with four different levels of data input, i.e., PTF2: particle size fractions only (i.e., sand, silt, and clay content on % weight basis—SSC); PTF3: particle size fractions plus bulk density (ρ_b); PTF4: particle size fractions plus bulk density plus volumetric water content at 3.3 m matric head ($\theta_{3.3}$); and PTF5: particle size fractions plus bulk density plus volumetric water content at both 3.3 and 150 m (θ_{150}) matric heads. For these calculations, $\theta_{3.3} = 0.328$ was obtained by interpolating the log-transformed volumetric water content and matric head data in Table 84.3.

Note in Table 84.6 that some parameter values are relatively insensitive to prediction level (e.g., θ_r, θ_{sat}, n), whereas others are highly sensitive (e.g., α_v, K_{sat}). The resulting van Genuchten model predictions (Figure 84.4) vary substantially, but the model-data fits tend

TABLE 84.6 Estimation of the van Genuchten θ–ψ–K Parameters Using PTF2–PTF5 in ROSETTA

Parameter	PTF2 Sand, silt, clay (SSC)	PTF3 SSC + ρ_b	PTF4 SSC + ρ_b + $\theta_{3.3}$	PTF5 SSC + ρ_b + $\theta_{3.3}$ + θ_{150}
θ_r (m^3m^{-3})	0.062	0.070	0.060	0.109
θ_{sat} (m^3m^{-3})	0.394	0.513	0.516	0.548
n	1.383	1.454	1.306	1.287
α_v (m^{-1})	2.05	1.36	1.72	5.17
K_{sat} ($m\ s^{-1}$)	1.69×10^{-6}	1.12×10^{-5}	1.70×10^{-5}	1.82×10^{-5}

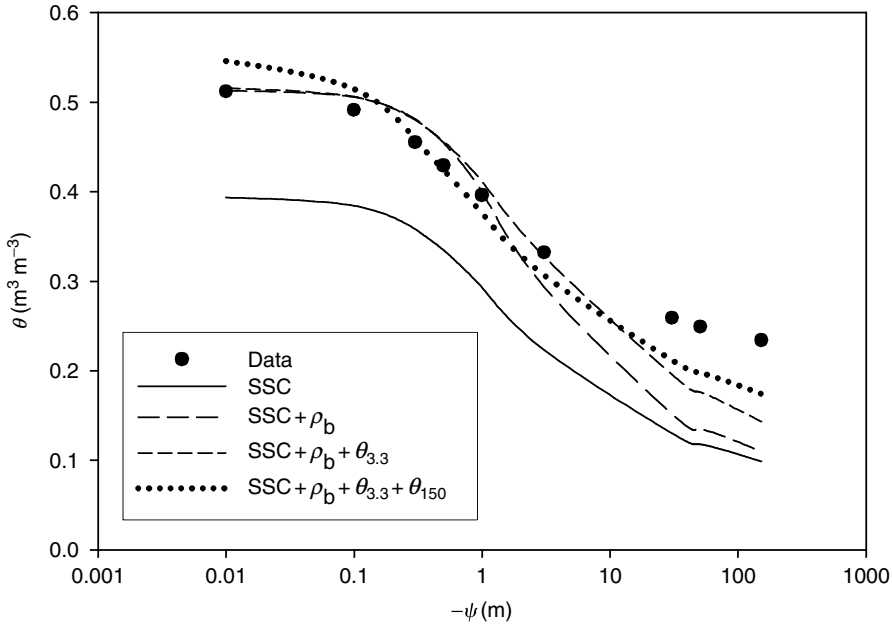

FIGURE 84.4. Prediction of the soil water content (θ) vs. pore water matric head (ψ) relationship (Table 84.3) using the van Genuchten model fitted via the ROSETTA surrogate data system and the parameter values in Table 84.6. SSC = weight percent sand–silt–clay, ρ_b = bulk density, $\theta_{3.3}$ = volumetric water content at 3.3 m matric head, and θ_{150} = volumetric water content at 150 m matric head.

to improve with increasing ROSETTA prediction level, although all fits are clearly very approximate relative to the RETC fits (Figure 84.3).

Minasny et al. Methods

The Minasny et al. (1999) methods were also used to estimate the van Genuchten parameters (Table 84.7). The required soil data were obtained from Table 84.3 and Table 84.4, with

$$d_g = 0.142 \text{ mm} \tag{84.32}$$

$$\sigma_g = 1.806 \text{ mm} \tag{84.33}$$

$$\text{POR} = [1 - (\rho_b/\rho_s)] = 0.611 \tag{84.34}$$

TABLE 84.7 van Genuchten Parameters Obtained Using the Minasny et al. (1999) Method. The Required Soil Data Were Obtained from Table 84.3 and Table 84.4, and the Minasny Coefficients from Table 84.2

Parameter	ENR2	ENR6	ENR7
θ_r (m^3m^{-3})	0.257	0.155	0.254
θ_{sat} (m^3m^{-3})	0.533	0.529	0.532
n	1.403	1.397	1.494
α_v (m^{-1})	0.189	0.168	0.128

Note that although the parameter values are similar among the various estimation methods in this example (Table 84.7), other scenarios may result in substantial differences among the estimation methods.

84.5 COMMENTS

1 The van Genuchten $K-\theta-\psi$ models fitted via the RETC least-squares optimization method generally produce the most accurate model-data fits (e.g., Figure 84.3), and as a result, this approach is most often used. The van Genuchten–RETC system is not always successful, however, and the other models and fitting methods can sometimes produce good (or at least acceptable) model-data fits when the van Genuchten–RETC system cannot.

2 Use of surrogate data methods to estimate K–θ–ψ relationships is always ''risky,'' as illustrated in Figure 84.4, and they should be used only when insufficient hydraulic data are available. In addition, the methods are very dependent on the soil data from which they were derived—those presented here being based primarily on North American and Australian soils. As a result, $K-\theta-\psi$ relationships obtained using surrogate data methods should be viewed as only nominal representations of the actual relationships (as is evident in Figure 84.4). A very important feature of the surrogate data methods, however, is that they can provide quasiphysically based hydraulic property input to water–solute transport models when no other options are available.

REFERENCES

Addiscott, T.M. 1993. Simulation modelling and soil behaviour. *Geoderma* 60: 15–40.

British Standards Institution. 1984. BS3406. Methods for determination of particle size distribution, Part 2—Recommendations for gravitational liquid sedimentation methods for powders and suspensions, BSI: London.

Brooks, R.H. and Corey, A.T. 1964. Hydraulic properties of porous media. Hydrology Paper 3, Civil Engineering Department, Colorado State University, Fort Collins, CO.

Brooks, R.H. and Corey, A.T. 1966. Properties of porous media affecting fluid flow. *J. Irrig. Drainage Div*. 92: 61–88.

Bruce, R.R. 1972. Hydraulic conductivity evaluation of the soil profile from soil water retention relations. *Soil Sci. Soc. Am. J*. 36: 555–561.

Campbell, G.S. 1974. A simple method for determining unsaturated hydraulic conductivity from moisture retention data. *Soil Sci*. 117: 311–314.

Cook, F.J., Dobos, S.K., Carlin, G.D., and Millar, G.E. 2004. Oxidation rate of pyrite in acid sulfate soils: In situ measurements and modelling. *Aust. J. Soil Res*. 42: 499–507.

Cresswell, H.P. and Paydar, Z. 1996. Water retention in Australian soils. I. Description and prediction using parametric functions. *Aust. J. Soil Res*. 34: 195–212.

Griffiths, E., Webb, T.H., Watt, J.P.C., and Singleton, P.L. 1999. Development of soil morphological descriptors to improve field estimation of hydraulic conductivity. *Aust. J. Soil Res*. 37: 971–982.

Hutson, J.L. and Cass, A. 1987. A retentivity function for use in soil water simulation models. *J. Soil Sci*. 38: 105–113.

Isbell, R.F. 1996. *The Australian Soil Classification*. CSIRO Publishing: Collingwood, Victoria, Australia.

Leij, F.J., Alves, W.J., van Genuchten, M.Th., and Williams, J.R. 1999. The UNSODA unsaturated

soil hydraulic conductivity database. In Users Manual version 1. USEPA, EPA/600/R-96/095.

McKeague, J.A., Eilers, R.G., Thomasson, A.J., Reeve, M.J., Bouma, J., Grossman, R.B., Favrot, J.C., Renger, M., and Strebel, O. 1984. Tentative assessment of soil survey approaches to the characterisation and interpretation of air–water properties of soils. *Geoderma* 34: 69–100.

McKenzie, N.J. and Cresswell, H.P. 2002. Estimating soil physical properties using readily available data. In N.J. McKenzie, K.I. Coughlan and H.P. Cresswell, Eds. *Soil Physical Measurement and Interpretation for Land Evaluation*. CSIRO Publishing. Melbourne, Victoria, Australia, pp. 292–316.

McKenzie, N.J., Smettem, K.R.J., and Ringrose-Voase, A.J. 1991. Evaluation of methods for inferring air and water properties of soils from field morphology. *Aust. J. Soil Res*. 29: 587–602.

Minasny, B., McBratney, A.B., and Bristow, K.L. 1999. Comparison of different approaches to the development of pedotransfer functions for water-retention curves. *Geoderma* 93: 225–253.

Mualem, Y. 1976. A new model for predicting the hydraulic conductivity of unsaturated porous media. *Water Resour. Res*. 12: 513–522.

Passioura, J.B. 1996. Simulation models: Science, snake oil, education, or engineering. *Agronomy J*. 88: 690–694.

Philip, J.R. 1991. Soils, natural science, and models. *Soil Sci*. 151: 91–98.

Rajkai, K., Kabos, S., and van Genuchten, M.Th. 2004. Estimating the water retention curve from soil properties: comparison of linear, nonlinear and concomitant variable methods. *Soil Till. Res*. 79: 145–152.

Rawls, W.J., Brakensiek, D.L., and Saxton, K.E. 1982. Estimation of soil water properties. *Trans. ASAE* 25: 1316–1320, 1328.

Saxton, K.E., Rawls, W.J., Romberger, J.S., and Papendick, R.I. 1986. Estimating generalized soil-water characteristics from texture. *Soil Sci. Soc. Am. J*. 50: 1031–1036.

Schaap, M.J. 1999. Rosetta 1.0. http://www.ussl.ars.usda.gov/MODELS/rosetta/rosetta.htm. (Accessed April 2006).

US Salinty Laboratory. 2006. Web site. www.ussl.ars.usda.goc/models/modelsmenu.htm. (Accessed July 2006).

van Genuchten, M.Th. 1980. A closed-form equation for predicting the hydraulic conductivity of unsaturated soils. *Soil Sci. Soc. Am. J*. 44: 892–898.

van Genuchten, M.Th., Leij, F.J., and Yates, S.R. 1991. The RETC Code for Quantifying the Hydraulic Functions of Unsaturated Soils, Version 1.0. EPA Report 600/2-91/065, U.S. Salinity Laboratory, USDA, ARS, Riverside, CA.

APPENDIX 84.1

Output from the computer program, RETC (v.6), for fitting the van Genuchten $K-\theta-\psi$ functions to the data in Table 84.3. Output File 1 fits all five van Genuchten parameters ($\theta_r, \theta_{sat}, \alpha_v$, n, m), while Output File 2 fits only the first four parameters and assumes $m = 1 - (1/n)$.

Output File 1 Please Check

Analysis of soil hydraulic properties
Welcome to RETC
Variable n and m (Mualem-theory for K)
Analysis of retention data only
MType = 1 Method = 3

Initial values of the coefficients

No.	Name	Initial value	Index
1	ThetaR	.0780	1
2	ThetaS	.4300	1
3	Alpha	3.6000	1
4	*n*	1.5600	1
5	*m*	.3590	1
6	*l*	.5000	0
7	*Ks*	.0000	0

Observed data

Obs. No.	Pressure head	Water content	Weighting coefficient
1	.010	.5120	1.0000
2	.100	.4910	1.0000
3	.300	.4550	1.0000
4	.500	.4290	1.0000
5	1.000	.3960	1.0000
6	3.060	.3320	1.0000
7	30.600	.2590	1.0000
8	51.000	.2490	1.0000
9	153.000	.2340	1.0000

NIT	SSQ	ThetaR	ThetaS	Alpha	*n*	*m*
0	.16044	.0780	.4300	3.6000	1.5600	.3590
1	.00017	.2111	.5126	3.6505	1.2580	.2939
2	.00004	.2023	.5133	2.9479	1.1408	.3251
3	.00002	.2054	.5136	2.7591	1.1164	.3519
4	.00002	.2073	.5139	2.6086	1.0911	.3725
5	.00002	.2086	.5141	2.5028	1.0737	.3880
6	.00002	.2095	.5143	2.4285	1.0616	.3994
7	.00002	.2102	.5144	2.3763	1.0531	.4077
8	.00002	.2116	.5146	2.2652	1.0348	.4254
9	.00002	.2117	.5147	2.2552	1.0336	.4277
10	.00002	.2117	.5147	2.2548	1.0336	.4278
11	.00002	.2117	.5147	2.2548	1.0336	.4278

Correlation matrix

	ThetaR	ThetaS	Alpha	*n*	*m*
	1	2	3	4	5
1	1.0000				
2	.3590	1.0000			
3	−.9054	−.4619	1.0000		
4	−.7297	−.6984	.9101	1.0000	
5	.9094	.5636	−.9889	−.9403	1.0000

R^2 for regression of observed vs. fitted values = 0.99981919

Nonlinear least-squares analysis: final results

		95% Confidence limits			
Variable	**Value**	**S.E. Coeff.**	***T*-Value**	**Lower**	**Upper**
ThetaR	0.21172	0.00819	25.86	0.1890	0.2345
ThetaS	0.51466	0.00263	195.81	0.5074	0.5220
Alpha	2.25484	0.61642	3.66	0.5435	3.9662
n	1.03355	0.10666	9.69	0.7374	1.3297
m	0.42777	0.10433	4.10	0.1381	0.7174

Observed and fitted data

No.	***P***	**Log *P***	**WC-Obs**	**WC-Fit**	**WC-Dev**
1	.1000E − 01	−2.0000	.5120	.5121	−.0001
2	.1000E + 00	−1.0000	.4910	.4905	.0005
3	.3000E + 00	−.5229	.4550	.4551	−.0001
4	.5000E + 00	−.3010	.4290	.4309	−.0019
5	.1000E + 01	.0000	.3960	.3931	.0029
6	.3060E + 01	.4857	.3320	.3339	−.0019
7	.3060E + 02	1.4857	.2590	.2581	.0009
8	.5100E + 02	1.7076	.2490	.2488	.0002
9	.1530E + 03	2.1847	.2340	.2346	−.0006

Sum of squares of observed vs. fitted values

	Unweighted	**Weighted**
Retention data	.00002	.00002
Cond/Diff data	.00000	.00000
All data	.00002	.00002

Soil hydraulic properties (MType = 1)

WC	*P*	Log *P*	Cond	Log *K*	Diff	Log *D*
.2125	−.3254E + 06	5.512	.9866E − 27	−27.006	.9394E − 18	−18.027
.2133	−.6784E + 05	4.831	.1284E − 24	−24.892	.1274E − 16	−16.895
.2148	−.1415E + 05	4.151	.1670E − 22	−22.777	.1729E − 15	−15.762
.2179	−.2949E + 04	3.470	.2173E − 20	−20.663	.2345E − 14	−14.630
.	.	.	.	.	.	.
.	.	.	.	.	.	.
.	.	.	.	.	.	.
.	.	.	.	.	.	.
.5144	−.1289E − 02	−2.890	.7820E − 07	−7.107	.3160E − 06	−6.500
.5146	−.1387E − 03	−3.858	.1459E − 06	−6.836	.6333E − 06	−6.198
.5147	−.1495E − 04	−4.825	.2274E − 06	−6.643	.1064E − 05	−5.973
.5147	.0000E + 00		.2889E − 05	−5.539		

End of problem

Output File 2 Please Check

Analysis of soil hydraulic properties
Welcome to RETC
Mualem-based restriction, $m = 1 - (1/n)$
Analysis of retention data only
MType = 3 Method = 3

Initial values of the coefficients

No.	Name	Initial value	Index
1	ThetaR	.0780	1
2	ThetaS	.4300	1
3	Alpha	3.6000	1
4	*n*	1.5600	1
5	*m*	.3590	0
6	*l*	.5000	0
7	*K*s	.0000	0

Observed data

Obs. No.	Pressure head	Water content	Weighting coefficient
1	.010	.5120	1.0000
2	.100	.4910	1.0000
3	.300	.4550	1.0000
4	.500	.4290	1.0000
5	1.000	.3960	1.0000
6	3.060	.3320	1.0000
7	30.600	.2590	1.0000
8	51.000	.2490	1.0000
9	153.000	.2340	1.0000

NIT	SSQ	ThetaR	ThetaS	Alpha	*n*
0	.16044	.0780	.4300	3.6000	1.5600
1	.00059	.2103	.5117	3.8335	1.3345
2	.00004	.1935	.5112	3.7159	1.3300
3	.00004	.1936	.5112	3.7101	1.3311
4	.00004	.1936	.5112	3.7101	1.3311

Correlation matrix

	ThetaR	ThetaS	Alpha	*n*
	1	2	3	4
1	1.0000			
2	−.3438	1.0000		
3	−.7350	.7033	1.0000	
4	.9626	−.4079	−.8487	1.0000

R^2 for regression of observed vs. fitted values = 0.99956634

Nonlinear least-squares analysis: final results

		95% Confidence limits			
Variable	Value	S.E. Coeff.	*T*-Value	Lower	Upper
ThetaR	.19363	.00865	22.40	.1714	.2159
ThetaS	.51120	.00260	196.63	.5045	.5179
Alpha	3.71012	.35931	10.33	2.7865	4.6337
N	1.33108	.02808	47.40	1.2589	1.4033

Observed and fitted data

No.	*P*	Log *P*	WC-Obs	WC-Fit	WC-Dev
1	.1000E − 01	−2.0000	.5120	.5102	.0018
2	.1000E + 00	−1.0000	.4910	.4930	−.0020
3	.3000E + 00	−.5229	.4550	.4560	−.0010
4	.5000E + 00	−.3010	.4290	.4300	−.0010
5	.1000E + 01	.0000	.3960	.3913	.0047
6	.3060E + 01	.4857	.3320	.3343	−.0023
7	.3060E + 02	1.4857	.2590	.2599	−.0009
8	.5100E + 02	1.7076	.2490	.2496	−.0006
9	.1530E + 03	2.1847	.2340	.2325	.0015

Sum of squares of observed vs. fitted values

	Unweighted	**Weighted**
Retention data	.00004	.00004
Cond/Diff data	.00000	.00000
All data	.00004	.00004

Soil hydraulic properties (MType = 3)

WC	***P***	**Log *P***	**Cond**	**Log *K***	**Diff**	**Log *D***
.1944	−.1834E + 08	7.263	.1268E − 8	−28.897	.8674E−18	−18.062
.1953	−.2261E + 07	6.354	.4724E − 26	−26.326	.1991E−16	−16.701
.1969	−.2786E + 06	5.445	.1759E − 23	−23.755	.4569E−15	−15.340
.2001	−.3434E + 05	4.536	.6553E − 21	−21.184	.1049E − 13	−13.979
.	.	.	.	.	.	.
.	.	.	.	.	.	.
.	.	.	.	.	.	.
.	.	.	.	.	.	.
.5109	−.4347E−02	−2.362	.1604E − 05	−5.795	.1620E − 04	−4.790
.5112	−.7694E−03	−3.114	.2118E − 05	−5.674	.3779E − 04	−4.423
.5112	−.1364E−03	−3.865	.2439E − 05	−5.613	.7715E − 04	−4.113
.5112	.0000E+00		.2889E − 05	−5.539		

End of problem

Chapter 85
Analysis of Soil Variability

B.C. Si
University of Saskatchewan
Saskatoon, Saskatchewan, Canada

R.G. Kachanoski
University of Alberta
Edmonton, Alberta, Canada

W.D. Reynolds
Agriculture and Agri-Food Canada
Harrow, Ontario, Canada

85.1 INTRODUCTION

Soil properties characteristically vary from location to location and from time to time, and understanding their spatial and temporal variability has important applications in the soil and hydrological sciences. Data collected at a number of locations at one point in time (or within a small time frame) are called a space series, and data collected through time at one location (or within a small area) are called a time series. The methods for analyzing space and time series are similar, and are usually referred to as spatial analysis and temporal analysis, respectively.

There are many spatial and temporal analysis methods, including geostatistics, spectral analysis, wavelet analysis, multifractal analysis, state-space analysis, fuzzy-set analysis, and others. Of these, geostatistics, spectral analysis, wavelet analysis, and multifractal analysis are the most commonly used in geosciences. Geostatistics provides a means for describing the common observation that sample values, which are close in space or time, tend to be more similar than sample values that are far away in space or time (Jongman et al. 1995; Goovaerts 1997; Nielsen and Wendroth 2003). Spectral analysis (Koopmans 1974; Webster 1977; Kachanoski et al. 1985) partitions the total variation (or variance) of sample values into spatial frequency scales, thus identifying the dominant spatial scales of the variations. Wavelet analysis, on the other hand, partitions the sample variation into position (or location) and frequencies (Si 2003; Si and Farrell 2004; Si and Zeleke 2005). Geostatistical, spectral, and wavelet analyses deal primarily with variance and covariance, whereas multifractal analysis (Zeleke and Si 2004, 2005, 2006) includes the higher statistical moments

(e.g., skewness, kurtosis, etc.), and examines how the different moments change with scale in space or time. Unfortunately, spectral, wavelet, and multifractal analyses require very large and dense datasets, which often limit their use in the soil and hydrological sciences. We will therefore focus here on geostatistical analysis, which is both well established and not restricted to large datasets.

85.2 GEOSTATISTCAL ANALYSIS

A geostatistical description of the spatial or temporal variability of a dataset is based on four quantities: the mean, the variance, the probability distribution, and a description of the similarity between values at different space or time scales. As the mean, variance, and probability distribution are well described in many elementary statistics texts, only the similarity in space or time will be discussed further. Note also that the following discussion is focused primarily on spatial variability (space series), but is equally applicable to temporal variability (time series).

For most soil properties, measurements that are made close together in space or time tend to be more similar than measurements that are far from each other in space or time. For example, the similarity (or correlation) in organic carbon content between two soil samples tends to be high when the samples are closely spaced, and decreases as the distance between the two samples increases. As a result, contour maps of soil properties (e.g., soil organic carbon content, texture, density, etc.) tend to show patterns rather than randomness, i.e., low values tend to be near other low values and high values tend to be near other high values. Therefore, to understand spatial or temporal variability and its patterns, we need to know how a measurement at two locations (or times) varies with the spatial (or temporal) separation between them. This two-point ''covariation'' (or covariance), as a function of separation or ''scale,'' is often referred to as ''structure'' (Goovaerts 1997). Determining the spatial or temporal structure of a variable (e.g., soil organic carbon content, soil density, etc.) is useful in the following ways:

1. One of the basic assumptions of standard parametric (i.e., Fisher) statistics is that sample values are independent of each other, i.e., a measurement (e.g., soil organic carbon content) on any particular sample must not be related to (or ''autocorrelated'' with) the same measurement on any other sample. Consequently, knowledge of the spatial or temporal structure can be used to ensure that the distance or time between replicate samples (or treatments or field plots) is great enough to prevent intersample dependence or autocorrelation.

2. Describing spatial or temporal structure reveals the existence of patterns in the data and the scales at which these patterns are expressed—a first step toward determining the underlying reasons or processes that generated the pattern.

3. Spatial distribution of a soil variable is often dependent on a number of dynamic processes operating over different spatial–temporal scales. Examining the change in the spatial variance structure with time is a powerful method of identifying the spatial scales of major processes operating over the sample time periods.

4. Prediction at unsampled locations or times is more accurate (i.e., estimation errors are minimized and unbiased), if the interpolation function takes into account the

spatial/temporal structure via kriging (Deutsch and Journel 1998; Nielsen and Wendroth 2003).

5 Knowing spatial or temporal structure allows (i) better design of experimental plots (shape, size, and orientation) (Fagroud and van Meirvenne 2002) and monitoring networks (Prakash and Singh 2000); (ii) selection of more appropriate methods for data analysis and interpretation (Lambert et al. 2004); and (iii) better assessment of simulation and uncertainty analyses (Papritz and Dubois 1999). For example, if the spatial structure is directional (anisotropic), rectangular experimental plots will be more efficient than square plots. A pure nugget semivariogram model indicates that the traditional (Fisher) analysis of variance is appropriate, whereas a nonpure nugget semivariogram model indicates that an alternative analysis is advisable (such as the SAS ''Proc Mixed'' procedure).

85.3 MEASURING SPATIAL OR TEMPORAL STRUCTURE

There are generally three relative ''scales'' of variation for soil space or time series: small-, medium-, and large-scale. Spatial or temporal structure is usually determined by the medium-scale variation, which is the scale at which the data are autocorrelated as a result of spatial or temporal continuity (i.e., intersample dependence). Structure or pattern at scales less than the sampling interval cannot be identified and behaves like random measurement or observation errors. Large-scale variation (i.e., variation that occurs at scales that are large relative to the size of the sampling domain) appears as a pattern or ''trend'' (which is usually linear, curvilinear, or sinusoidal); and it is caused by large-scale factors not related to medium-scale autocorrelation (e.g., sloping land surface; climate shift; sinusoidal variation due to regularly repeating farm-management operations). When the appropriate minimum sampling interval is used, small-scale variation occurs at distance or time intervals less than the sampling interval, and need not be considered further. Trends associated with large-scale variation must be removed from the data before the medium-scale variation can be analyzed to obtain the underlying spatial or temporal structure (discussed further below). Analysis of medium-scale variation to determine spatial or temporal structure is usually achieved using autocovariance, autocorrelation, or semivariance procedures, which are briefly described below.

85.3.1 Structural Analysis by Autocovariance and Autocorrelation

The autocovariance function, $C(h)$, and the autocorrelation function, $\eta(h)$, measure the degree of similarity, or correlation, between pairs of data values as the distance or time separating the values, h, increases. The $C(h)$ function is defined by

$$C(h) = \frac{1}{N(h)} \sum_{i=1}^{N(h)} [(z(x_i) - m_{-h}) \cdot (z(x_i + h) - m_{+h})] \tag{85.1a}$$

where $N(h)$ is the number of data pairs within distance or time h, $z(x_i)$ is the sample value at location or time, x_i,

$$m_{-h} = \frac{1}{N(h)} \sum_{i=1}^{N(h)} z(x_i) \tag{85.1b}$$

is the mean of the dataset that is $-h$ apart from $z(x_i)$ (known as the ''tailset'' data), and

$$m_{+h} = \frac{1}{N(h)} \sum_{i=1}^{N(h)} z(x_i + h) \tag{85.1c}$$

is the mean of the dataset that is $+h$ apart from $z(x_i)$ (known as the ''headset'' data). The autocorrelation function, $\eta(h)$, is essentially a normalized form of the autocovariance function and it is obtained by dividing the autocovariance by the geometric mean variance of the tail-set and headset data, i.e.,

$$\eta(h) = \frac{C(h)}{\sqrt{\sigma^2_{-h}\sigma^2_{+h}}} \tag{85.2a}$$

where

$$\sigma^2_{-h} = \frac{1}{N(h)} \sum_{i=1}^{N(h)} [z(x_i) - m_{-h}]^2 \tag{85.2b}$$

is the variance (or lag variance) of the tail-set data, and

$$\sigma^2_{+h} = \frac{1}{N(h)} \sum_{i=1}^{N(h)} [z(x_i + h) - m_{+h}]^2 \tag{85.2c}$$

is the variance (or lag variance) of the headset data. Ideally, the autocovariance function (i.e., a plot of $C(h)$ versus h) yields the total variance (σ^2) of the dataset at zero separation (i.e., $C(h) = \sigma^2$ at $h = 0$), and decreases with increasing separation between the samples in space or time (increasing h), reaching zero when the sample values are sufficiently separated to be truly independent of each other (i.e., $C(h) \to 0$ as h gets large). Correspondingly, the autocorrelation function (i.e., $\eta(h)$ versus h) is unity at zero separation (i.e., $\eta(h) = 1$ at $h = 0$), and decreases toward zero as h increases (i.e., $\eta(h) \to 0$ as h gets large) (Figure 85.1a). In practice, however, the endpoints for $C(h)$ and $\eta(h)$ often differ from those indicated above as a result of random variability, incomplete stationarity, and other factors (see Section 85.3.3). Note also that when samples are collected on a spatial grid/transect or at time intervals, it is often convenient to set h as the minimum sample separation (or minimum average separation if the space or time intervals are irregular), and to express all greater separations as multiples of h. This is known as ''lag'' format, where lag $= 1$ corresponds to separation h, lag $= 2$ corresponds to separation $2h$, etc. (Figure 85.1a). Function values at lag $= h = 0$ are obtained by extrapolating to the origin (discussed further below).

85.3.2 Structural Analysis by Semivariogram

The autocovariance and autocorrelation functions measure the similarity between pairs of data points as a function of the distance or time separating the points, whereas the semivariogram measures the average dissimilarity between the pairs of data points. Semivariance is computed as half the average squared difference between the headset and tailset data (Matheron 1962):

$$\gamma(h) = \frac{1}{2 \cdot N(h)} \sum_{k=1}^{N(h)} [z(x_k) - z(x_k + h)]^2 \tag{85.3}$$

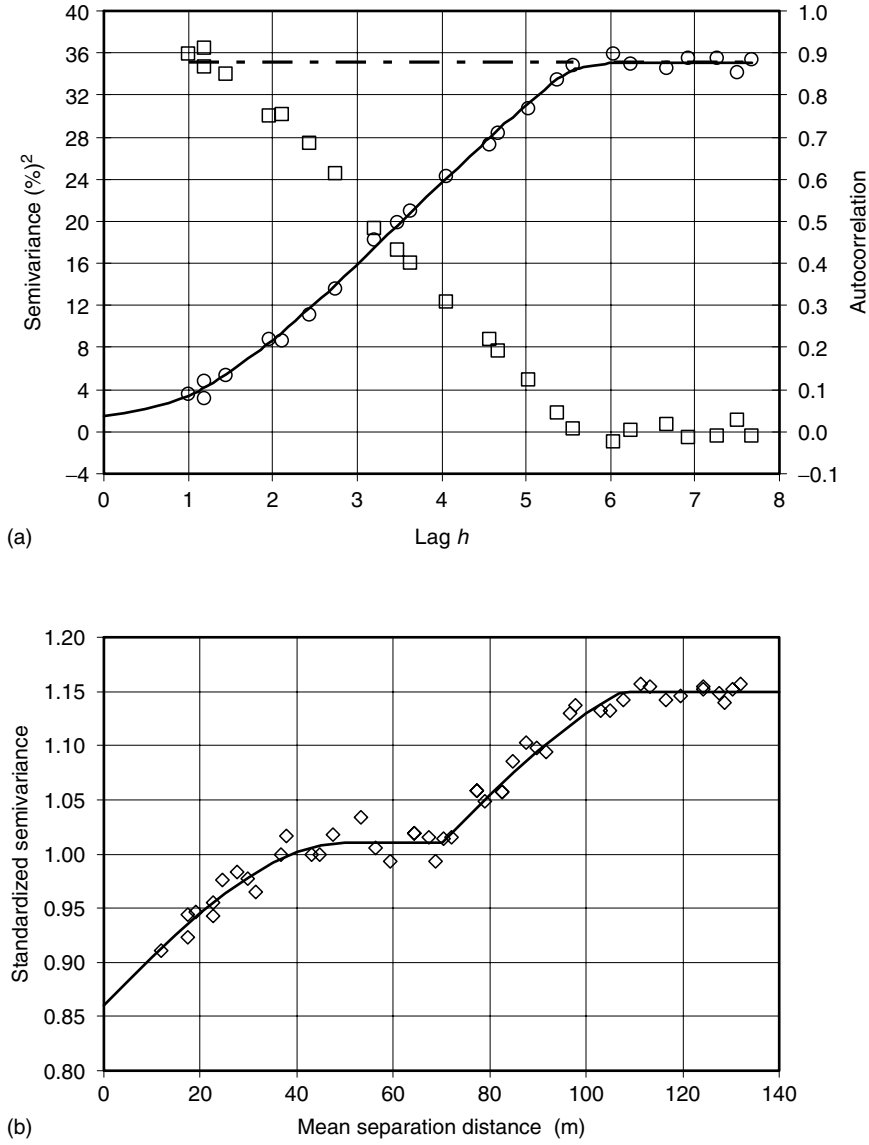

FIGURE 85.1. (a) Illustration of autocorrelation (open squares) and semivariance (open circles) for soil water content data (vol%). The horizontal dashed line indicates dataset variance. The solid line is a fitted semivariogram model: nugget (c_0) = 1.5%^{2}, scale (c) = 33.5%^{2}, sill ($c_0 + c$) = 35%^{2}, range (a) = lag 6 = 60 m. Autocorrelation = 1 at zero lag only for zero nugget; (b) illustration of nested semivariogram structure with fitted models: nugget = 0.86, first sill = 1.01, first range = 50 m, second sill = 1.15, second range = 110 m. Note that ''standardized'' semivariance and mean separation distance were used here instead of semivariance and lag, respectively.

where $z(x_k)$ is property, z (e.g., soil organic carbon content), at location or time, x_k, and $z(x_k + h)$ is property z at location or time $(x_k + h)$. A plot of semivariance, $\gamma(h)$, as a function of h or lag is known as a semivariogram (or experimental semivariogram) (Figure 85.1a). For soil data, a well-behaved semivariogram increases from a minimum value at the smallest lag

(i.e., lag = 1) until a plateau is reached where semivariance remains constant with increasing lag. The extrapolated minimum semivariance at lag = 0 is referred to as the ''nugget''; the lag at which the semivariance becomes maximum and constant is called the ''range''; and the semivariance value at the range is called the ''sill'' (Figure 85.1a). Some semivariograms exhibit ''nested structure,'' which is the appearance of two or more distinct ranges and sills with increasing lag (Figure 85.1b). A nested structural pattern represents distinct processes occurring at different space or time scales (e.g., small-scale spatial variation due to soil macropores, nested within a larger-scale variation due to soil texture, nested within a still larger-scale variation due to elevation). Poorly behaved semivariograms are those where the range and sill are partially or completely obscured because of large scatter in the semivariance values.

When analyzing the spatial or temporal structure of variables with different units, variances, or ranges, it is often convenient to use the ''standardized'' or ''lag-standardized'' semivariogram, $\gamma^*(h)$ (Rossi et al. 1992), which is simply the semivariogram divided by the geometric mean variance of the headset and tailset data at the corresponding lag h:

$$\gamma^*(h) = \frac{\gamma(h)}{\sqrt{\sigma^2_{-h}\sigma^2_{+h}}} \tag{85.4}$$

where σ^2_{-h} and σ^2_{+h} are defined by Equation 85.2b and Equation 85.2c, respectively. The main advantage of standardized semivariograms is that they facilitate comparison of spatial/temporal structures by allowing variograms of different variables to be plotted on the same graph. This can also be achieved using the so-called relative semivariogram where each $\gamma(h)$ is divided by either the lag mean (Goovaerts 1997) or the dataset variance (Vieira et al. 1988).

85.3.3 Stationarity Requirements

The autocovariance, autocorrelation, and semivariogram analyses require ''stationarity'' assumptions about the spatial or temporal data, where stationarity essentially means that a particular aspect or feature of the dataset (e.g., mean, variance) is constant throughout the space/time region of interest. Theoretically, the autocovariance and autocorrelation analyses require that the dataset exhibits ''second-order stationarity,'' which in practical terms means that: (i) the statistical distribution of the dataset is normal; (ii) the mean and variance of the dataset are finite and constant for all locations and directions or times; and (iii) the autocovariance and autocorrelation values are independent of location, direction, or time and are only a function of the separation between data pairs (lag). The semivariogram, on the other hand, requires the much less-stringent dataset assumption of ''intrinsic stationarity,'' which effectively means that the dataset possesses a normal or near-normal statistical distribution, and that only the difference between data pairs at a given lag needs to have a finite and constant variance throughout the space/time region of interest. A dataset with a trend (i.e., the dataset exhibits a continual, large-scale change in mean or variance across the space/time region) does not have second-order stationarity, but it may still have intrinsic stationarity. Hence, autocovariance and autocorrelation cannot be used when the dataset contains a trend, whereas the semivariogram may still be useable when a trend is present (although detrending is required—see below). Datasets that have second-order stationarity also have intrinsic stationarity, but datasets with intrinsic stationarity do not necessarily have second-order stationarity.

For datasets exhibiting second-order stationarity, the autocovariance, autocorrelation, and semivariance are related by

$$\gamma(h) = C(0)[1 - \eta(h)] \tag{85.5}$$

where $C(0)$ is the autocovariance at $h = 0$, i.e., the variance of the total dataset.

From a practical standpoint, the stationarity (or degree of stationarity) of a dataset is perhaps best determined in the following manner: (i) determine if the data exhibit a ''normal'' statistical distribution, i.e., the frequency distribution of the data is approximately ''bell shaped,'' and the mean (arithmetic average value), mode (most frequently occurring value), and median (value at the midpoint of the distribution) are all approximately coincident; and (ii) subdivide the dataset into several nonoverlapping subsets, which are more or less evenly spaced throughout the space/time region under consideration, then calculate the mean and variance of the data in each subset to determine if either change consistently (monotonically) across the region. The normality (or degree of normality) of a dataset's statistical distribution can be determined formally via the Kolmogorov–Smirnov, Shapiro–Wilk, Cramer–von Mises, and Anderson–Darling tests (Press et al. 1992); or it can be estimated by simply inspecting a plot of the dataset's frequency distribution. If the dataset is found to be substantially nonnormal (due to high-end or low-end skewing, or peakedness that is excessive or insufficient), it can often be ''normalized'' (made normal) by applying a transform to the data values. For soil data, the most commonly applied transforms include the log-transform (natural or common logarithms of the data are calculated) and the square-root transform (square roots of the data are calculated). If normalization of the dataset is required, the autocovariance, autocorrelation, and semivariance calculations must be conducted on the transformed data, rather than on the raw data.

If a trend is detected (i.e., mean or variance changes continually and monotonically across the space/time region), it must be removed before further analysis can proceed. Trends are usually linear or polynomial in shape and are generally removed (a process called detrending) using linear regression, polynomial regression, or *n*th order differencing techniques (see Cressie 1993, for procedures). An example of spatial data containing a trend might be the variation of surface roughness down a hillslope, i.e., the continuous, large-scale change in hillslope elevation superimposes a trend on top of the small-scale changes in surface roughness. Detrended data should be retested to determine if second-order or intrinsic stationarity were achieved. Generally speaking, data possessing second-order stationarity produces a semivariogram, which levels off to a distinct range and sill, whereas data containing a trend produces a semivariogram that continually increases at a rate $\geq \text{lag}^2$.

85.4 MEASURING JOINT VARIABILITY

Joint variability is the covariation between two parameters (e.g., soil permeability and sand content) over space or time; and its main application is to determine if and how one parameter varies with another within the space/time region of interest. The autocovariance, autocorrelation, and semivariance functions can be readily extended to two parameters and are known as the cross-covariance, cross-correlation, and cross-semivariance, respectively.

The cross-covariance, $C_{yz}(h)$, is defined as (Goovaerts 1997)

$$C_{yz}(h) = \frac{1}{N(h)} \sum_{i=1}^{N(h)} [(y(x_i) - my_{-h}) \cdot (z(x_i + h) - mz_{+h})] \tag{85.6a}$$

where

$$my_{-h} = \frac{1}{N(h)} \sum_{i=1}^{N(h)} y(x_i) \tag{85.6b}$$

and

$$mz_{+h} = \frac{1}{N(h)} \sum_{i=1}^{N(h)} z(x_i + h) \tag{85.6c}$$

$y(x_i)$ is the headset data for one parameter, $z(x_i + h)$ is the tailset data for the other parameter, and the other variables are as previously defined. The cross-covariance is not necessarily symmetric, i.e., $C_{yz}(h) \neq C_{zy}(h)$.

The cross-correlation, $\eta_{yz}(h)$, can be defined as

$$\eta_{yz}(h) = \frac{C_{yz}(h)}{\sqrt{\sigma y^2_{-h} \sigma z^2_{+h}}} \tag{85.7a}$$

where

$$\sigma y^2_{-h} = \frac{1}{N(h)} \sum_{i=1}^{N(h)} [y(x_i) - my_{-h}]^2 \tag{85.7b}$$

and

$$\sigma z^2_{+h} = \frac{1}{N(h)} \sum_{i=1}^{N(h)} [z(x_i + h) - mz_{+h}]^2 \tag{85.7c}$$

The cross-semivariance, $\gamma_{yz}(h)$, measures how the increment of one parameter (e.g., soil permeability) over a given lag is dissimilar to the increment of another variable (e.g., sand content) over the same lag, and is defined as

$$\gamma_{yz}(h) = \frac{1}{2N(h)} \sum_{k=1}^{N(h)} [y(x_k) - y(x_k + h)] \cdot [z(x_k) - z(x_k + h)] \tag{85.8}$$

where, for example, y represents soil permeability and z represents sand content. The cross-semivariogram (cross-semivariance versus h) is symmetric (i.e., $\gamma_{yz}(h) = \gamma_{zy}(h)$; $\gamma_{yz}(-h) = \gamma_{yz}(h)$); and like the semivariogram, it normally increases with increasing space or time separation (lag), indicating that the greater the separation between the two parameters, lesser is the correlation between them. The cross-semivariogram can be normalized to produce the codispersion coefficient, $\xi_{yz}(h)$:

$$\xi_{yz}(h) = \frac{\gamma_{yz}(h)}{\sqrt{\gamma_y(h)\gamma_z(h)}} \tag{85.9}$$

where, $\gamma_y(h)$ and $\gamma_z(h)$ are the semivariograms for variables y and z, respectively. Goovaerts and Chiang (1993) used the codispersion coefficient to examine the scale-dependent relationships between soil mineralizable nitrogen and various other soil properties.

85.5 INDICATOR SEMIVARIOGRAM

Structural analysis of categorized parameters (e.g., impact versus no impact; presence versus absence) is possible via the so-called indicator semivariogram. Here, the data are transformed into ''indicator coding'' and the codes (rather than the original data) are used to calculate ''indicator semivariances.'' Indicator coding is obtained by selecting one or more ''threshold'' values, then specifying one or more rules (e.g., $=$, $<$, $>$, $\geq$, $\leq$, etc.) for using the thresholds to assign indicator codes to the dataset values, and then systematically replacing each dataset value with the appropriate indicator code. The form of the indicator coding system depends on the number of thresholds and the assignment rules specified; for example, for multiple thresholds and the single assignment rule, ''$<$,'' the coding system has the form

$$i_j(T_k) = \begin{cases} 1 & \text{if } z_j < T_k \\ 0 & \text{otherwise} \end{cases} \quad k = 1, 2, \ldots, K \quad K \geq 1 \tag{85.10}$$

where $i_j(T_k)$ are the coded indicators, T_k are the specified threshold values, K is the number of thresholds, and z_j are dataset values at positions j in the space/time region. To illustrate Equation 85.10, suppose we measure soil electrical conductivity (EC), in a field at six different locations to obtain the dataset $z_1 = 0.5$, $z_2 = 1.5$, $z_3 = 0.2$, $z_4 = 2.1$, $z_5 = 3.0$, $z_6 = 0.1$ dS m^{-1}, and we are interested in the effect of EC (salinity) on crop growth. We know that EC $= 2$ dS m^{-1} is the threshold value for crop growth, i.e., EC < 2 dS m^{-1} does not affect crop growth, while EC ≥ 2 dS m^{-1} adversely affects crop growth. Using Equation 85.10, we have a single threshold, $T_1 = 2$ dS m^{-1}, and the above z_j data are thereby transformed into the numerical indicators, i_j (i.e., $i_1 = 1$, $i_2 = 1$, $i_3 = 1$, $i_4 = 0$, $i_5 = 0$, $i_6 = 1$), which indicate for each measurement location, j, whether crop growth is affected ($i_j = 0$) or not ($i_j = 1$). The semivariance is then calculated using the set of numerical indicators, i_j, rather than the original EC data (z_j). The thresholds can be based on virtually any meaningful quantity, including cumulative probability levels such as 25%, 50%, 75%, etc. By selecting appropriate indicator-thresholds, data with a highly skewed probability distribution or a strong trend can sometimes be converted into data with a near-normal distribution and no appreciable trend (Yates et al. 2006). Care should be taken in assigning the threshold magnitudes, however, as they can have a large impact on the resulting indicator semivariogram because spatial or temporal structure may change with the magnitude of the threshold (e.g., small threshold values may vary continuously in space or time, whereas large threshold values may be random, Goovaerts 1997). It is therefore advisable to recalculate the indicator semivariogram using a range of threshold magnitudes to ensure that the most realistic and relevant semivariogram is obtained.

85.6 CALCULATING SPATIAL OR TEMPORAL STRUCTURE

Calculating spatial or temporal structure is sufficiently involved that it almost always requires the use of computer software. Fortunately, many statistics software packages are now available for convenient calculation of autocovariance, autocorrelation, and semivariance, such as GeoEas (US Environmental Protection Agency), GSLIB (Deutsch and Journel 1998), GS+ (Gamma Design Software, LLC, Plainwell, Michigan), SAS (SAS Institute Inc.,

Cary, North Carolina), Surfer (Golden Software, Inc., Golden, Colorado), and VarioWin (Pannatier 1996). High-level programming languages (e.g., Mathcad, Mathsoft Inc., Cambridge, Massachusetts; Matlab, Mathworks Inc., Novi, Michigan) are also amenable to these calculations, and even standard spreadsheets are easily used if the sample collection scheme is simple. Example procedures for calculating semivariance and semivariograms are given below.

85.6.1 Regularly Spaced One-Dimensional Datasets

The spatial structure of uniformly spaced data collected on a straight-line transect can be readily determined using a standard computer spreadsheet, as illustrated below:

1 Input the coordinate data (location in space or time) into spreadsheet column I and the corresponding variable data (e.g., soil organic carbon content) into column II. Copy the variable data into column III. As the data are uniformly spaced, the sampling interval, d, is constant. Set M equal to the number of coordinate locations (i.e., rows of data values). Note that the coordinate data (column I) are only for reference purposes and are not involved in the calculations below.

2 Shift column III down by one row relative to columns I and II. This produces data pairs in columns II and III that have a uniform separation distance, h, equal to the sampling interval, d.

3 In spreadsheet column IV, calculate the squared difference between the data values in columns II and III for each row where there are data in both rows.

4 Sum the squared differences, then divide the sum by twice the number of data pairs, $TD = 2(M - 1)$, to obtain the semivariance value for $h = 1d$ or lag 1.

5 To obtain $h = 2d$, copy column III into column V, shift the data down by one row, repeat step 3 using columns II and V, place the result in column VI, and then repeat step 4 using $TD = 2(M - 2)$ to obtain the semivariance value for $h = 2d$ (i.e., lag 2).

6 Repeat the above sequence for $h = 3d, 4d, \ldots, nd$, where n is an integer $\leq 0.6\ M$. The $n \leq 0.6\ M$ criterion ensures that each semivariance value is derived from an adequate number of data pairs (i.e., each semivariance value should include ≥ 30 data pairs).

7 Experimental semivariogram is then obtained by plotting the calculated semivariances as a function of h or lag.

85.6.2 One-Dimensional Datasets with Nonuniform Sample Spacing or Datasets Collected in Two Dimensions

The procedure described in Section 85.6.1 is not applicable to irregularly spaced transect data or data collected in two dimensions, as the separations (in distance or time) between pairs of data points are not simple multiples of a single sampling interval. Instead, we must

group the data pairs into a sequence of lag ''bins'' that consist of a specified separation and separation tolerance. For example, if bin 1 (lag 1) has a specified separation of 100 m and a separation tolerance of ±50 m, then it contains all data pairs separated by 50–150 m. The separation distance corresponding to this lag is the average separation distance of all the data pairs that happen to fall within the bin. The separation tolerance is frequently half the specified separation, as this usually ensures that sufficient data pairs are included for valid semivariance calculations, and it often produces the optimal semivariogram in terms of detail and smoothness. Increasing separation tolerance produces a smoother but less detailed semivariogram, whereas decreasing separation tolerance produces not only more detailed but also more random scatter. Some practitioners advise that semivariogram optimization procedures should include testing a range of separation tolerances. The semivariogram may be calculated as follows:

1. Calculate the separation distances between all pairs of sampling locations.
2. Define lag bins using specified separations and separation tolerances.
3. For each bin, determine the number of data pairs within the bin, the sum of the separations in the bin, and the sum of squared differences between paired values in the bin. The average separation between data pairs in the bin is then calculated as the sum of the separations divided by the number of data pairs. The semivariance value for each bin is then determined as the sum of the squared differences divided by twice the number of data pairs.
4. Plot semivariance versus lag bin to produce the semivariogram. Here, lag x = mean data-pair separation for bin x, where $x = 1, 2, 3, \ldots$

Although the above procedure can be implemented using a spreadsheet, the complexity involved (especially for irregular sample spacing) warrants use of statistics software or a programming language, such as one of those mentioned above. A Mathcad implementation of the procedure is available from the senior author.

Note also that two-dimensional datasets (e.g., datasets with X and Y coordinates) may exhibit ''isotropy'' or ''anisotropy'' with respect to spatial structure. An isotropic structure means that the calculated semivariogram is the same (i.e., produces effectively the same nugget, range, and sill) regardless of whether the calculations are restricted to spatial separations in the X direction, the Y direction, or at some angle to the X and Y directions. An anisotropic structure, on the other hand, causes the magnitude of the nugget and/or range and/or sill to change with direction. For anisotropic datasets, one has the option of calculating a single ''omnidirectional'' semivariogram, which is based on spatial separations in all directions, or a number of ''directional'' semivariograms that are based on spatial separations in specific directions. An example of a simple anisotropic dataset might be variation in soil texture on a hillslope, i.e., the spatial structure of the texture data parallel to the slope differs from that perpendicular to the slope, and as a result, the appropriate spatial analysis depends on whether the objective is to determine down-slope textural variation (via a down-slope directional semivariogram), across-slope variation (directional semivariogram at 90° to the down-slope semivariogram), or overall variation (omnidiretional semivariogram). Most geostatistical software packages contain modules for directional semivariogram analysis (e.g., GeoEas, GSLIB, VarioWin, and GS+).

85.6.3 Practical Guidelines for Semivariogram Calculation

When calculating semivariances, the following general guidelines should be observed:

1 Generally speaking, the reliability of a semivariance value increases with the number of data pairs used in its calculation (the suggested minimum number is usually 30 data pairs).

2 Chosen lag (minimum data-pair separation) should be no greater than 1/4–1/2 the semivariogram range. As lag and range are not completely independent, several trial-and-error iterations may be required to meet this criterion.

3 Semivariograms are susceptible to artifact effects not related to the natural variability of the sample values. Artifact effects can stem from sample separation (lag size), number of data points, presence of data outliers, sampling pattern, measurement precision, sample volume, and the size of the spatial or temporal domain. Typically, the strength of the spatial or temporal structure in the data (see Section 85.8) decreases artificially with an increase in minimum lag size, a decrease in the total number of data points, the presence of data outliers, and a decrease in measurement precision or sample volume. In addition, small sample numbers, an irregular sampling pattern (e.g., variable sample spacing), data outliers, and low measurement precision can cause an unstable or ''noisy'' semivariogram (see item 4 below). Irregular sample spacing can also cause data ''clustering,'' which imparts an artificial skew in the data's probability distribution (e.g., a disproportionate representation of high or low values) and necessitates specialized semivariogram analysis procedures (Goovaerts 1997; Deutsch and Journel 1998). It is consequently important to minimize artifact effects, and this is usually achieved most effectively by setting measurement precision, sample numbers, and sample volume to their maximum practicable values, by removing data outliers (Hawkins 1980), and by using a regular sampling grid with minimum practicable spacing.

4 Very noisy (visually erratic) semivariograms can obscure the underlying spatial/temporal structure, and cause inaccurate model fits or the fitting of inappropriate models. Noise reduction or ''smoothing'' can often be achieved by (i) use of data transforms (e.g., log-transform), which mitigates the effects of extreme values; (ii) removal of data outliers (i.e., obviously erroneous or unrealistic values), which can add greatly to semivariogram scatter; (iii) use of a larger lag tolerance to increase the number of data pairs per semivariance value (but still strive for the minimum lag spacing that gives a reasonable number of data pairs); and (iv) use of overlapping lags, which operates like a ''running average'' in terms of noise reduction. Additional information on semivariogram smoothing can be found in Pannatier (1996).

85.7 FITTING MODELS TO SEMIVARIANCE DATA

Models are fitted to semivariogram data for two main reasons: (i) to separate random ''noise'' or ''static'' in semivariance results from the underlying structural pattern and (ii) to allow interpolation and mapping analyses such as kriging (Deutsch and Journel 1998). Fitting models to semivariogram data is generally not straightforward, however, as it requires several decisions regarding appropriate semivariogram models, and this in turn requires a

TABLE 85.1 Permissible Semivariogram Models, $\gamma(h)$, Commonly Used in the Geosciences[a]

Name	Equation[b]
Pure nugget	$\gamma(h) = \begin{cases} 0 & h = 0 \\ c_0 & h > 0 \end{cases}$
Linear-plateau with nugget	$\gamma(h) = c_0 + \begin{cases} c\left[\dfrac{h}{a}\right] & 0 \le h < a \\ c & h \ge a \end{cases}$
Spherical with nugget	$\gamma(h) = c_0 + \begin{cases} c\left[1.5\dfrac{h}{a} - 0.5\left(\dfrac{h}{a}\right)^3\right] & 0 \le h < a \\ c & h \ge a \end{cases}$
Exponential[c] with nugget	$\gamma(h) = c_0 + c\left[1 - \exp\left(-\dfrac{h}{a}\right)\right] \quad h \ge 0$
Gaussian[c] with nugget	$\gamma(h) = c_0 + c\left\{1 - \exp\left[-\left(\dfrac{h}{a}\right)^2\right]\right\} \quad h \ge 0$
Linear with nugget	$\gamma(h) = c_0 + (m \cdot h) \quad h \ge 0$
Power with nugget	$\gamma(h) = c_0 + (m \cdot h^p) \quad h \ge 0; \quad 0 < p < 2$

[a] Other possible models include: quadratic (Alfaro 1980), rational quadratic (Cressie 1991), wave/hole effect (Cressie 1991), logarithmic (Kitanidis 1997), pentaspherical (Olea 1999), and cubic (Olea 1999).

[b] γ = semivariance; h = lag; a = range; c_0 = nugget; c = scale; $(c_0 + c)$ = sill; $m = p$ = empirical fitting parameters.

[c] Given that the exponential and Gaussian models approach their sills asymptotically, the effective range is defined as the lag at which the model semivariance is 95% of the sill. It is not difficult to prove that the effective range is 3a for experimental model and $\sqrt{3}$a for Gaussian model.

good understanding of the data itself and the likely processes responsible for the observed spatial or temporal structures. Furthermore, only certain semivariogram models are permissible (see Table 85.1), as they must be ''positive-definite'' to ensure nonnegative covariance values (Isaaks and Srivastava 1989; Goovaerts 1997; Deutsch and Journel 1998). Recommended background reading for fitting semivariogram models includes Cressie (1985, 1993), Isaaks and Srivastava (1989), Pannatier (1996), and Goovaerts (1997). The discussion below includes only the basics of model fitting to semivariance data.

85.7.1 Fitting Criteria and Procedures

The semivariogram model should not be fitted to semivariance data at separations greater than 1/2–2/3 the largest distance or time in the study region. This is because data at larger separations are likely to be more representative of the variability at the edges (or beyond the edges) of the space/time region than the variability inside the region.

The weighted nonlinear least squares approach is the most popular method for fitting models to semivariance data, as it is usually the most robust and reliable (Cressie 1985). Depending on the semivariogram model selected (see Table 85.1), the weighted nonlinear least squares method adjusts the nugget, sill, and range values simultaneously to minimize the sum of squared errors (SSE) between the semivariance data and the model using

$$\text{SSE} = \sum_{i=1}^{m} w_i[\tilde{\gamma}_i - \gamma_i]^2 \tag{85.11}$$

where m is the number of lags, $\tilde{\gamma}_i$ are the semivariance values for each lag, γ_i are the corresponding model predictions, and w_i are weighting factors, which are usually defined by (Cressie 1985)

$$w_i = N_i \tag{85.12a}$$

$$w_i = N_i/\tilde{\gamma}_i^2 \tag{85.12b}$$

or

$$w_i = 1 \tag{85.12c}$$

where N_i is the number of data pairs used to calculate $\tilde{\gamma}_i$ at each lag. The weighting schemes given by Equation 85.12a and Equation 85.12b assign small-lag semivariances (i.e., semivariances calculated using large numbers of data pairs) more weight (importance) than large-lag semivariances, while Equation 85.12c assigns equal weight to all semivariances. The justification for Equation 85.12a and Equation 85.12b is that the reliability of a semivariance value should increase with the number of data pairs used in its calculation, i.e., the greater the number of data pairs the greater the weight. Implementation of weighted nonlinear least squares fitting is most conveniently achieved using commercial software packages, such as Mathcad, Matlab, Surfer, and SAS (Gotway 1991) (see Section 85.6). An example fitting scheme using Mathcad is available from the senior author.

85.7.2 Selecting the Best Semivariogram Model

The ''best'' semivariogram model is often defined as the model that has the least number of parameters (McBratney and Webster 1986) and the smallest SSE (Equation 85.11). Alternatives to SSE include the so-called root mean squared error (RMSE), $\text{RMSE} = \sqrt{\sum_{i=1}^{n} \frac{(y_i - \hat{y}_i)^2}{n}}$, and mean relative error (MRE), $\text{MRE} = \frac{1}{n} \sum_{i=1}^{n} \left| \frac{y_i - \hat{y}_i}{y_i} \right|$, where y_i are the data and $\hat{y}_i$ are the model estimates. The SSE, RMSE, and MRE criteria may not be optimal, however, as they apply only to the averaged differences of the data pairs comprising each lag, and therefore do not account for the ''scatter'' in the individual differences that make up the averages.

Alternative approaches for determining the best model fit include the so-called cross-validation or jack-knifing analyses, which determine the kriged surface that provides the most accurate fit to the original measured values (Isaaks and Srivastava 1989; Goovaerts 1997). These analyses consist of successively removing one datum point (cross-validation) or several data points (jack-knifing) at a time from the original dataset (e.g., soil organic carbon content), then recalculating a kriged estimate of the values from the remaining data by successively using each of the permissible semivariogram models (e.g., Table 85.1). The estimated values ($\hat{y}_i$, $i = 1, 2, \ldots, n$) and the actual values (y_i) are compared, and the semivariogram model that yields the most accurate overall predictions is deemed the best semivariogram model (as indicated by regression statistics such as coefficient of determination, r^2, standard error, RMSE, MRE, etc.) (see also Comment 8, Section 85.10).

85.7.3 Model Fitting to Nested Semivariogram Structure

Obtaining an appropriate model fit to nested semivariogram data is usually best achieved by a linear combination of two or more of the basic semivariogram models (see Table 85.1),

a process known as ''linear regionalization'' (Isaaks and Srivastava 1989; Goovaerts 1997; Morisette 1997). For example, if a calculated semivariogram shows a nugget and structural dependence at two different separations (e.g., Figure 85.1b), the regionalized semivariogram model might take the form

$$\gamma(h) = b_0 g(h) + b_1 \mathrm{SP}_1(h, a_1) + b_2 \mathrm{SP}_2(h, a_2) \tag{85.13}$$

where $g(h)$ is the pure nugget model (see Table 85.1), SP_1 and SP_2 are two spherical models with zero nuggets, unit sills, and two different ranges (a_1, a_2) (Table 85.1), and $b = (b_0, b_1, b_2)$ are empirical constants (or weights) related to the relative importance of the three models. To fit the regionalized model to semivariogram data, it is recommended that the individual models are first fitted at their relevant separations to obtain the individual scales and ranges, and then the combined model fitted using the b values as fitting parameters. Note that fitting a regionalized cross-semivariogram model to data with nested structure is subject to restrictions designed to guarantee that the component models are still permissible (see Isaaks and Srivastava 1989).

85.8 INTERPRETATION OF THE NUGGET, RANGE, SCALE, AND SILL

The nugget is the intercept on the semivariance axis of the fitted semivariogram models; the range is the minimum lag (separation) at which the semivariogram model is maximum and constant; the sill is the semivariance value at the range and the scale is the still value minus the nugget value (Figure 85.1a). In some cases, the semivariance data at small lags are sufficiently smooth and close to the semivariance axis that a nugget value can be determined visually, and then used as a specified constant when fitting a semivariogram model. Physically, the nugget represents an amalgamation of random measurement errors and natural variability at scales smaller than the minimum sample separation (i.e., at lags <1). The sill and range, on the other hand, define the structure of the data, i.e., samples at lags greater than or equal to the range are independent of each other (i.e., completely random or not autocorrelated), whereas samples at lags less than the range are not independent of each other (i.e., the sample values are at least partially dependent on each other, or autocorrelated). The ratio of the nugget semivariance (V_N) to the sill semivariance (V_S) gives a measure of the strength or degree of spatial or temporal structure in the data. Generally speaking, $V_N/V_S < 25\%$ indicates strong spatial or temporal structure, $25\% \leq V_N/V_S \leq 75\%$ indicates moderate structure, and $V_N/V_S > 75\%$ indicates virtually no structure (i.e., near randomness) (Cambardella et al. 1994). Note that the semivariogram scale and sill are identical when the nugget is zero. Note also that although the semivariogram sill is often similar to the sample variance, there is no requirement for the two to be equal (Barnes 1991).

85.9 EXAMPLE CALCULATIONS

85.9.1 Spatial Analysis of Soil Hydraulic Conductivity and Sand Content

Table 85.2 shows the saturated soil hydraulic conductivity (K_s) and sand content (Sa), measured from 128 intact soil cores collected at 3 m intervals along a 384 m linear transect (Zeleke and Si 2005). Included below are some basic steps involved in spatial analysis of these data.

TABLE 85.2 Saturated Hydraulic Conductivity (K_s) and Sand Content (Sa) Obtained from Core Samples along a Linear Transect, Where *X* Is Sample Location Relative to the Origin of the Transect

X (m)	K_s (cm h^{-1})	Sa (wt%)	*X* (m)	K_s (cm h^{-1})	Sa (wt%)	*X* (m)	K_s (cm h^{-1})	Sa (wt%)	*X* (m)	K_s (cm h^{-1})	Sa (wt%)
0	4.7	69	96	4.7	71	192	4.2	59	288	4.3	69
3	7.0	66	99	3.8	67	195	5.1	56	291	3.8	59
6	5.7	65	102	3.1	76	198	6.1	69	294	1.6	53
9	8.2	69	105	3.6	62	201	6.4	71	297	1.4	59
12	5.3	64	108	3.9	70	204	2.9	65	300	2.2	64
15	4.9	56	111	1.6	65	207	5.5	69	303	2.9	55
18	6.0	66	114	3.0	66	210	1.8	57	306	3.9	59
21	6.7	66	117	2.1	66	213	5.1	56	309	2.2	58
24	6.2	66	120	2.1	55	216	1.7	59	312	4.0	66
27	7.4	69	123	3.8	55	219	1.1	59	315	1.4	59
30	4.7	71	126	0.6	61	222	1.9	56	318	1.5	59
33	4.0	74	129	1.3	61	225	2.3	56	321	2.0	66
36	4.9	74	132	2.1	59	228	2.8	70	324	2.1	57
39	5.1	72	135	1.2	59	231	4.2	69	327	2.6	58
42	2.9	64	138	3.8	58	234	3.7	69	330	2.9	58
45	3.4	79	141	1.9	64	237	5.5	66	333	3.1	58
48	5.4	79	144	4.7	66	240	4.8	63	336	1.5	58
51	3.3	75	147	1.2	64	243	3.8	66	339	2.4	60
54	4.0	70	150	1.4	66	246	0.9	58	342	4.2	62
57	4.2	73	153	4.9	66	249	1.3	59	345	1.5	58
60	4.3	75	156	2.0	64	252	2.4	54	348	1.4	66
63	3.0	69	159	3.3	64	255	2.6	64	351	3.7	63
66	3.5	73	162	3.5	58	258	2.8	54	354	2.5	65
69	4.4	74	165	1.3	66	261	2.1	59	357	2.5	65
72	2.3	74	168	1.6	58	264	2.2	61	360	4.7	66
75	1.8	71	171	2.9	66	267	1.9	59	363	4.6	68
78	3.5	76	174	1.7	61	270	4.1	66	366	4.6	59
81	2.9	74	177	1.7	57	273	3.2	63	369	6.1	68
84	3.4	69	180	2.3	61	276	3.4	64	372	5.8	58
87	2.6	71	183	2.2	58	279	3.9	69	375	5.4	74
90	4.3	70	186	5.6	64	282	3.9	61	378	5.4	70
93	4.7	76	189	3.6	56	285	4.0	59	381	5.5	66

Source: From Zeleke, T.B. and Si, B.C., *Soil Sci. Soc. Am. J.*, 69, 1691, 2005.

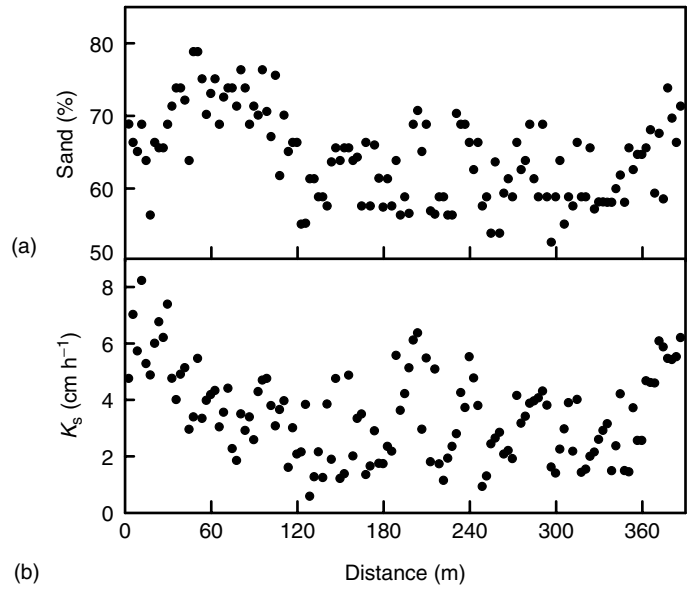

FIGURE 85.2. Plots of the spatial distribution of sand content (Sa) (a) and saturated hydraulic conductivity (K_s) (b) measured at 3 m intervals along a 384 m linear transect.

Step 1. Check for nonstationarity and nonnormal probability distributions. Determine if either dataset is nonstationary (contains a trend), or has a substantially skewed (non-normal) probability distribution. Plots of K_s and Sa versus distance along the transect show no large-scale trends with distance, and there are no obvious outliers (Figure 85.2). Furthermore, when the transect is divided into several segments (say 4–5 segments), the mean and variance of the K_s and Sa data remain similar among segments (data not shown). Note also from Figure 85.2 that high and low K_s and Sa values tend to fall close to other high and low values, respectively, indicating that both datasets contain spatial structure. Histogram plots of K_s and Sa are not substantially skewed (data not shown), and thus the K_s and Sa probability distributions are already approximately normal and do not require transformation. Hence, the stationarity assumption required for semivariogram analysis is satisfied.

Step 2. Select appropriate lag increment, lag tolerance, and maximum lag distance. For this example, we set lag = sampling interval = 3 m. The lag tolerance was also set to 3 m (sampling interval), as the data were collected on a linear transect with constant sample spacing. The maximum lag distance is set to 200 m, which is roughly half the length of the transect (384 m). A Mathcad program (available from the senior author) was used to determine the semivariograms, cross-semivariogram, and codispersion coefficients for K_s and Sa (Figure 85.3; Table 85.3). Note that the K_s semivariogram is highly variable (which often occurs for this parameter) but reaches a plateau at about 100 m, whereas the Sa semivariogram is much smoother and plateaus at about 90 m (Figure 85.3a). The cross-semivariogram and codispersion coefficients plateau at about 100 m, indicating that K_s and Sa have a scale-dependent correlation at separation distances $<$100 m (Figure 85.3b).

Step 3. Selection and fitting of semivariogram models to semivariance data. As mentioned above, selecting appropriate semivariogram models often involves careful inspection of the

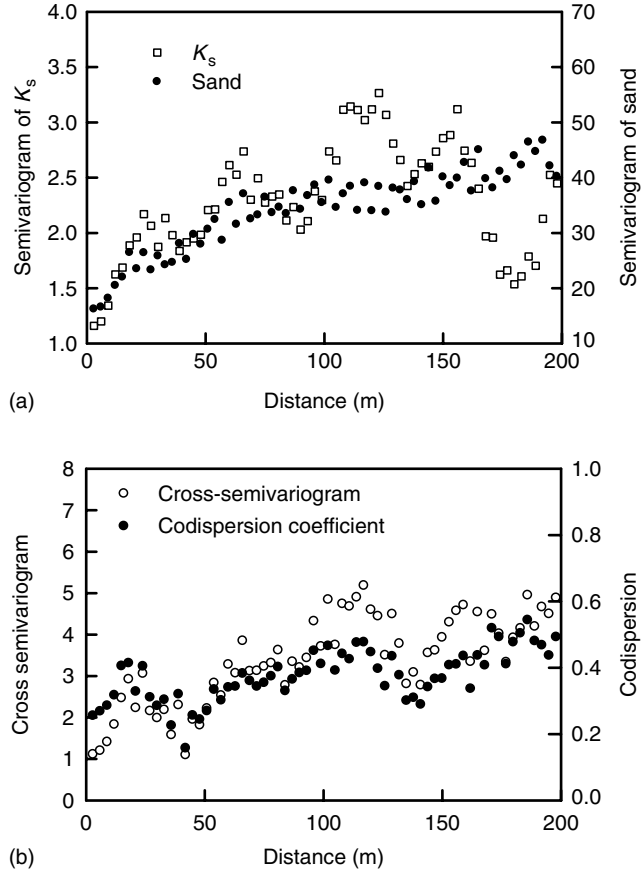

FIGURE 85.3. Spatial analysis of the saturated hydraulic conductivity (K_s) and sand content (Sa) data shown in Table 85.2 and Figure 85.2: (a) semivariograms; (b) cross-semivariogram and codispersion coefficient.

semivariogram data and identification of trends or patterns. Inspection of the K_s semivariogram data (Figure 85.3a) suggests a linear portion at distances less than about 20 m, a curvilinear portion at distances from about 20–90 m, and a plateau for distances greater than 90 m. This suggests that the data contain a ''nested'' structure, which implies in turn that some combination of semivariogram models is more appropriate than any single model. To illustrate this, a single linear-plateau model and a single spherical model (see Table 85.1) were fitted individually to the data (Figure 85.4a) using a Mathcad program. The fitted linear-plateau model gave nugget, sill, and range values of 1.3 $cm^2\ h^{-2}$, 2.6 $cm^2\ h^{-2}$, and 66 m, respectively, while the fitted spherical model gave nugget, sill, and range values of 1.4 $cm^2\ h^{-2}$, 2.7 $cm^2\ h^{-2}$, and 109 m, respectively. The sum squared differences between the fitted model and the data (indicator of goodness of fit) were 157 $cm^2\ h^{-2}$ and 153 $cm^2\ h^{-2}$ for the linear-plateau and spherical models, respectively. Note that although the predicted nugget and sill values were similar between the two models, the ranges were greatly different, and the goodness of fit was equally poor for both models (large sum squared differences). Note also that both models produced poor fits at the distances <25 m, which is problematic as good fits at small distances are essential for identifying nugget values and for providing accurate kriged interpolations. Hence, single model fits were

TABLE 85.3 Selected Semivariance, Cross-Semivariance, and Codispersion Coefficients for Saturated Hydraulic Conductivity (K_s) and Sand Content (Sa) for the Transect in Table 85.1

Number of data pairs	Location, X (m)	K_s Semivariance ($cm^2\ h^{-2}$)	Sa Semivariance $(wt\%)^2$	Cross-semivariance	Codispersion coefficient
127	3	1.2	16.2	1.1	0.26
126	6	1.2	16.6	1.2	0.27
125	9	1.3	18.2	1.4	0.29
123	15	1.7	22.0	2.5	0.40
121	21	2.0	23.5	2.2	0.33
119	27	2.1	23.3	2.2	0.31
117	33	2.1	24.2	2.2	0.30
115	39	1.8	28.1	2.3	0.32
113	45	1.9	29.7	1.9	0.26
111	51	2.2	30.6	2.2	0.27
109	57	2.5	28.6	2.5	0.30
107	63	2.5	31.6	3.1	0.34
105	69	2.3	32.5	3.1	0.36
103	75	2.3	36.4	3.2	0.35
101	81	2.3	34.6	3.6	0.40
99	87	2.2	37.6	3.3	0.36
97	93	2.1	36.7	3.4	0.39
95	99	2.3	35.5	3.7	0.41
93	105	2.7	34.6	3.7	0.39
91	111	3.1	38.4	4.7	0.43
89	117	3.0	39.0	5.2	0.48
87	123	3.3	38.4	4.4	0.40
85	129	2.8	38.1	4.5	0.43
83	135	2.4	36.0	2.8	0.30
81	141	2.6	35.1	2.8	0.29

rejected in favor of fitting a combination of a pure nugget model, $g(h, C_0)$, and two spherical models, $SP_1(h, C_1, a_1)$ and $SP_2(h, C_2, a_2)$:

$$\gamma(h) = b_0 g(h) + b_1 SP_1(h, C_1, 20) + b_2 SP_2(h, C_2, 90) \tag{85.14}$$

which produced a much better fit to the data (Figure 85.4b; sum squared differences = 130.36 $cm^2\ h^{-2}$). Note also that the fitted model weights ($b_0 = 0.923$, $b_1 = 0.565$, $b_3 = 1.081$) are indicators of the relative importance of the three models, and the sum of the weights (2.57) is roughly equivalent in magnitude to the sill for the nested semivariance data ($V_S = 2.48\ cm^2\ h^{-2}$).

Step 4. Interpretation and application of semivariogram parameters. For the K_s semivariance data, $V_N = 1.3\ cm^2\ h^{-2}$ and $V_S = 2.57\ cm^2\ h^{-2}$; hence, $V_N/V_S = 50\%$, which indicates only moderate spatial structure. This result is relatively common for K_s data, as the precision of K_s measurements is inherently low, and there was likely extensive small-scale variability (i.e., at distances less than the sampling interval of 3 m) in the form of macropores, root channels, etc., that increased the nugget value. Selective subsampling at smaller sample spacings would determine the importance and impact of the small-scale variability.

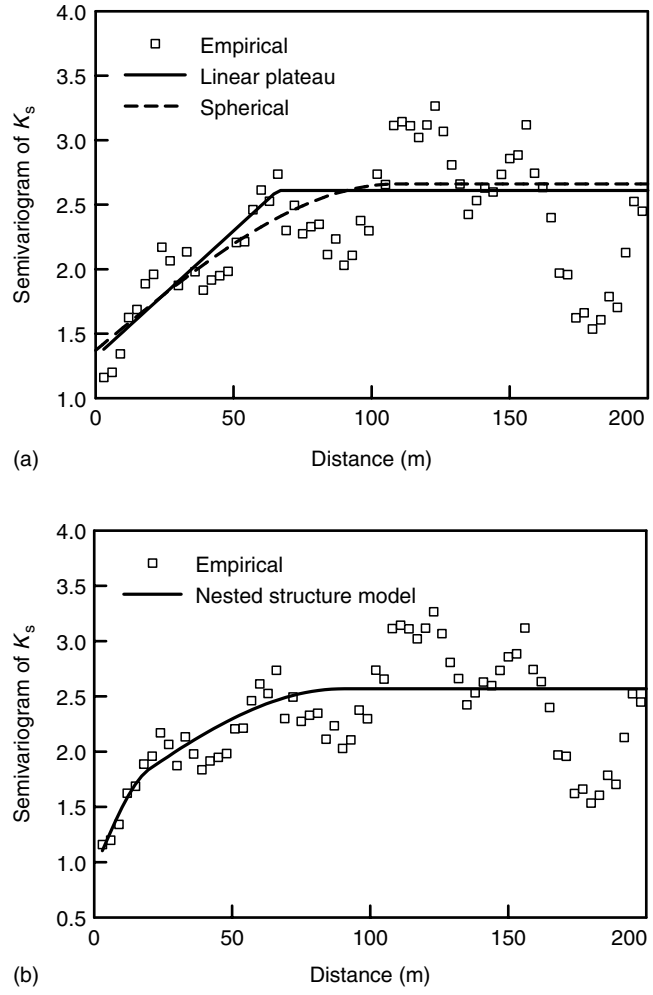

FIGURE 85.4. Model fits to the saturated hydraulic conductivity (K_s) semivariogram in Figure 85.3a: (a) linear-plateau and spherical models; (b) linear combination of a pure nugget and two spherical models.

The range of the nested model is 109 m, which indicates that K_s measurements at this site need to be at least 109 m apart before they can be considered truly independent of each other and admissible for use in Fisher-type statistical analyses.

85.9.2 Spatial Analysis of Elevation, Texture, Organic Carbon Content, Water Content, and Hydraulic Conductivity

Surface elevation (El), sand content (Sa), clay content (Cly), organic carbon content (OC), water content (θ_a), and field-saturated hydraulic conductivity (K_{fs}) were measured at 164 grid points (10 m spacing) in a triangular ''paddock'' under continuous grass-legume pasture (Figure 85.5) (Vieira et al. 1988). The soil was a well structured silty clay (moderate-strong, fine-medium, subangular blocky), and the measurements were collected at the 35–50 cm depth. At each grid point, K_{fs} was measured *in situ* using a Guelph permeameter (GP) (see Chapter 76), and θ_a was measured *in situ* using a down-hole TDR probe (see Chapter 70).

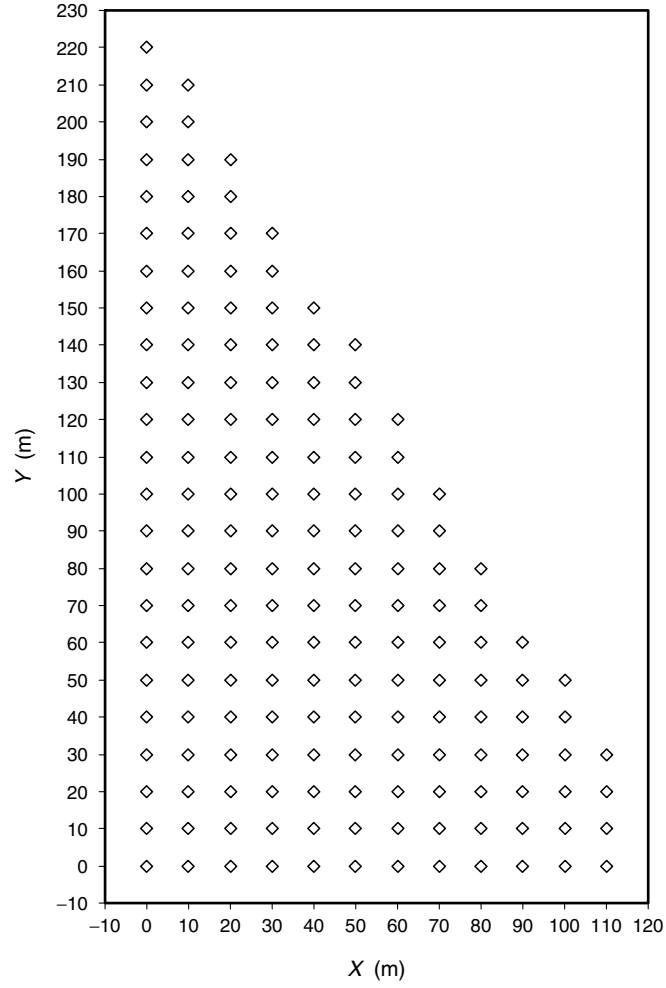

FIGURE 85.5. Schematic of the triangular paddock field site with sampling locations (diamonds) and X–Y coordinates ($n = 164$).

The Sa and Cly contents and OC concentrations were obtained from the GP auger cuttings, and El was measured relative to an arbitrary datum using a surveyor's transit. The θ_a measurements were collected in the GP wells just before the K_{fs} measurements, and thus represent the antecedent soil volumetric water content at the time of the K_{fs} readings.

Step 1. Test for nonnormal probability distributions. All six parameters exhibit nonnormal statistical distributions, as evidenced by the Anderson–Darling test for normality (Table 85.4a). The skewness and kurtosis values indicate, however, that only the Sa, OC, and K_{fs} distributions are seriously nonnormal (due to extensive high-end skewing and extreme peakedness), while the El, θ_a, and Cly distributions are near normal (near-zero skewness and kurtosis). Hence, only the Sa, OC, and K_{fs} distributions need to be normalized; and this was adequately accomplished via log-transformation, as shown by the resulting small skewness and kurtosis values, and the substantial reductions in CV (Table 85.4b). As a result, the log-transforms of Sa, OC, and K_{fs} were used in place of the raw data for all further analyses.

TABLE 85.4 Summary Statistics for the Measured Parameters at the Paddock Field Site ($n = 164$) (See Vieira et al. 1988 for Background)

(a) Raw Data

Statistic	El (cm)	θ_a (vol%)	Sa (wt%)	Cly (wt%)	OC (wt%)	K_{fs} (cm s^{-1})
Mean	77.13	39.51	14.12	41.91	0.42	6.46×10^{-4}
Minimum	0	16.9	0.93	8.9	0.11	1.51×10^{-6}
Maximum	122	53.6	78.9	58.4	1.8	7.12×10^{-3}
CV[a] (%)	33.08	18.21	83.44	21.05	69.62	139.69
Skewness[b]	−0.93	−0.33	2.46	−0.61	2.34	3.65
Kurtosis[c]	0.89	−0.38	7.37	0.22	7.29	18.86
Distribution[d]	NN	NN	NN	NN	NN	NN

(b) Log-Transformed Data

Statistic	ln Sa (wt%)	ln OC (wt%)	ln K_{fs} (cm s^{-1})
Mean	11.07[e]	0.35[e]	2.59×10^{-4e}
Minimum	0.93	0.11	1.51×10^{-6}
Maximum	78.9	1.8	7.12×10^{-3}
CV[a] (%)	28.26	−54.21	−19.91
Skewness[b]	0.17	0.47	−0.79
Kurtosis[c]	1.17	0.07	0.16
Distribution[d]	NN	NN	NN

[a] CV = coefficient of variation.
[b] Negative, low-end skewed distribution; zero, normal distribution; positive, high-end skewed distribution.
[c] Negative, flat-topped distribution; zero, normal distribution; positive, peaked distribution.
[d] Anderson–Darling test for distribution normality: NN, nonnormal; N, normal.
[e] Geometric mean.

Step 2. Test for data trends and nonstationarity. Plots of El, θ_a, ln Sa, Cly, ln OC, and ln K_{fs} versus station number (Figure 85.6) showed no important patterns or large-scale trends, hence detrending was not necessary. Plots of parameter means and variances, on the other hand, showed varying degrees of variation with location in the field (data not shown). Elevation (El) was substantially nonstationary (i.e., its variance changed substantially and systematically with field location), whereas the other parameters had at least limited stationarity (i.e., mean and variance did not change greatly or systematically with field location). Hence, the El data would likely produce meaningless autocovariance and autocorrelation results.

Step 3. Calculate and interpret semivariograms. The standardized omnidirectional semivariograms (see Equation 85.4) of θ_a, ln K_{fs}, Cly, ln OC, and ln Sa all produced distinct sills (Figure 85.7), which implies second-order stationarity of the respective datasets and is consistent with the lack of large-scale trends (see Figure 85.6). The semivariogram of El, on the other hand, did not produce a sill (data not shown), which implies a lack of second-order stationarity.

The standardized semivariograms of θ_a and ln K_{fs} were similar (Figure 85.7a); and the standardized semivariograms for Cly and ln OC were virtually identical, but different

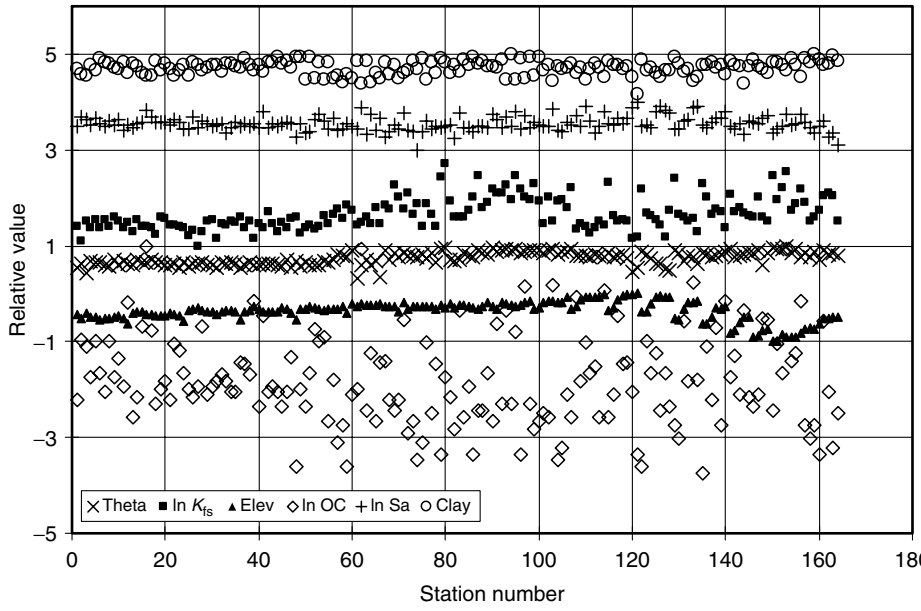

FIGURE 85.6. Measured parameter versus grid station number: Theta = antecedent volumetric water content (θ_a), ln K_{fs} = log field-saturated hydraulic conductivity (ln K_{fs}), Elev = elevation (El), ln OC = log organic carbon content (ln OC), ln Sa = log sand content (ln Sa), Clay = clay content (Cly). To allow data separation and plotting on a single scale, each dataset was normalized by dividing by its maximum value, then offset by adding or subtracting a constant. The grid stations were numbered from left to right in Figure 85.5, with station 1 corresponding to *X*–*Y* coordinate (0,0) and station 20 corresponding to *X*–*Y* coordinate (70,10).

from that for ln Sa (Figure 85.7b). Hence, θ_a and ln K_{fs} had similar spatial structure, while Cly and ln OC had spatial structure that was nearly identical but substantially different from that for θ_a, ln K_{fs}, and ln Sa. The semivariograms for θ_a and ln K_{fs} indicate that both of these parameters were spatially dependent for separation distances <70–80 m, and that their spatial structures were very strong ($V_N/V_S = 16.7\%$). The Cly and ln OC parameters, on the other hand, were spatially dependent for separation distances <50 m, and their spatial structures were very weak ($V_N/V_S = 83.3\%$). The ln Sa parameter was moderately structured ($V_N/V_S = 64.2\%$) and spatially dependent for separations <72 m. The similar spatial structure between Cly and ln OC, along with the fact that ln Sa had a different spatial structure, suggests that soil texture effects on OC were controlled by clay content and not by sand content. The similar spatial structure between ln K_{fs} and θ_a, coupled with the fact that Cly, ln OC, and ln Sa had different spatial structures, suggests that ln K_{fs} and θ_a were affected by a parameter other than the amount of sand, clay, or OC present. Given that the θ_a measurement was determined via *in situ* TDR in unsaturated soil just before the K_{fs} measurement, it is suspected that both parameters were controlled by soil macrostructure in the form of cracks and biopores. That is, the greater the number of cracks and biopores intercepted by the GP well, the lower the θ_a measured by the *in situ* TDR probe and the greater the corresponding K_{fs} measured by the GP. A controlling macrostructure effect would also explain why the geometric mean K_{fs} at this site (2.59×10^{-4} cm s^{-1}; Table 85.4b) was substantially larger than one might expect for a silty clay soil (by 1–2 orders of magnitude).

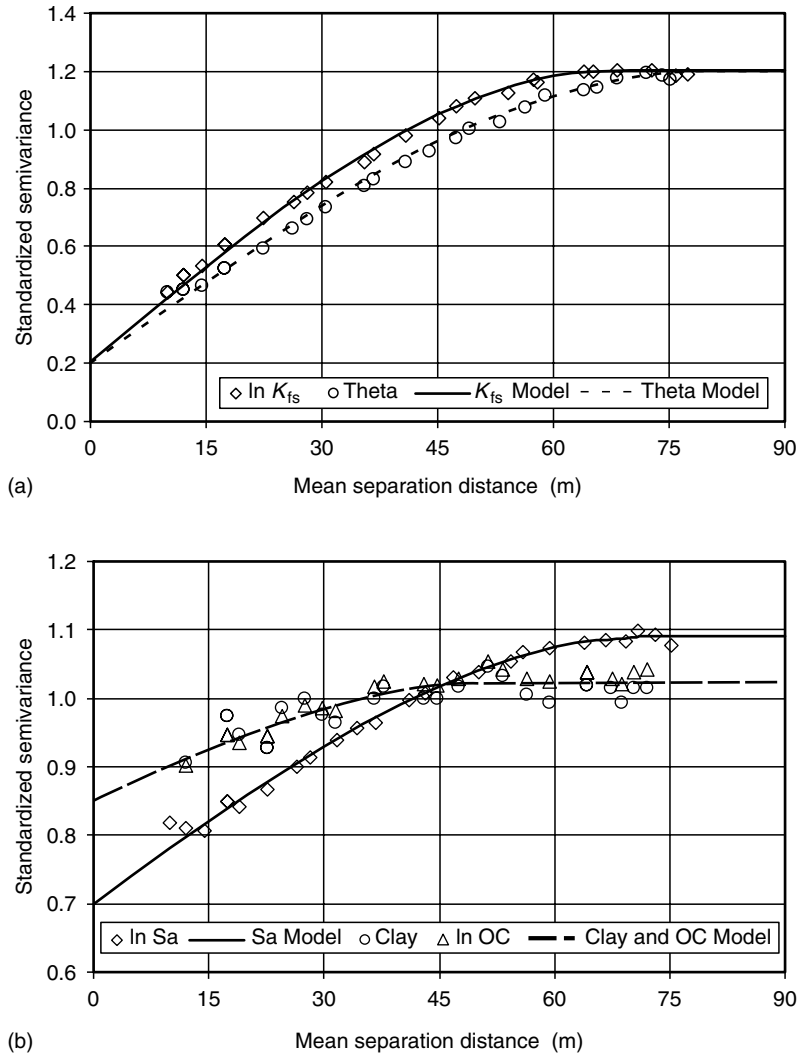

FIGURE 85.7. Standardized omnidirectional semivariance (Equation 85.4) versus mean separation distance: (a) ln K_{fs} = log field-saturated hydraulic conductivity (K_{fs}) plus fitted model (K_{fs} Model), Theta = antecedent volumetric water content (θ_a) plus fitted model (Theta Model); (b) ln Sa = log sand content (Sa) plus fitted model (Sa Model), Clay = clay content (Cly), ln OC = log organic carbon content (OC), Clay and OC Model = fitted joint model.

Step 4. Calculate and interpret kriged surfaces. The fitted semivariogram models were used to calculate kriged surfaces (via Surfer) to illustrate the spatial variability of ln K_{fs}, θ_a, ln OC, and Cly across the field site, and to also determine the two-dimensional spatial relationships between ln K_{fs} and θ_a (Figure 85.8), and between ln OC and Cly (Figure 85.9). The ln K_{fs} and θ_a surfaces (Figure 85.8) show numerous small-scale features in the form of isolated ''knolls and closed depressions,'' which are superimposed on a larger-scale sequence of roughly parallel ''ridges and troughs'' that run nearly perpendicular to the Y-axis (i.e., at $Y \approx 0$–30 m, at $Y \approx 70$–80 m, at $Y \approx 120$–140 m, and at $Y \approx 160$–180 m). The ln OC and Cly surfaces (Figure 85.9) differ from the ln K_{fs} and θ_a surfaces in that small-scale

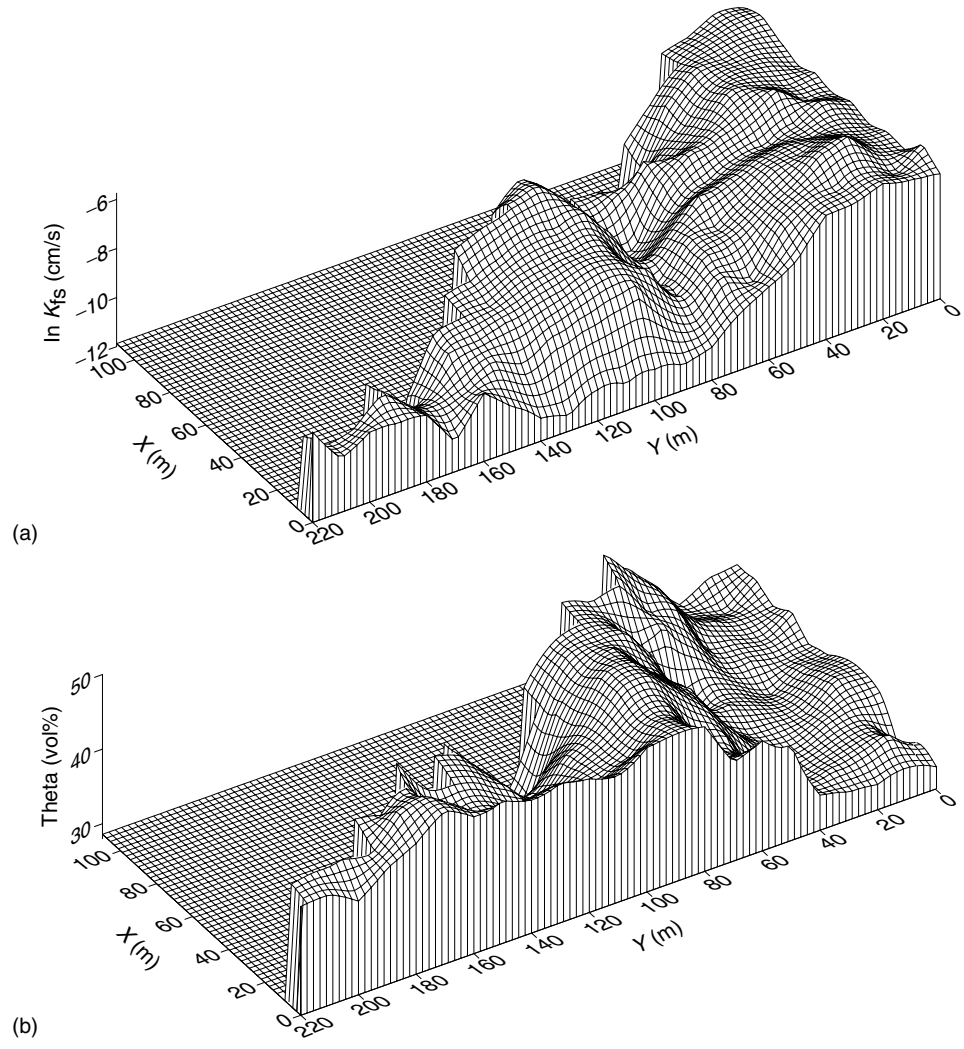

FIGURE 85.8. Kriged surfaces for (a) log field-saturated hydraulic conductivity, ln K_{fs}, and (b) antecedent volumetric water content, θ_a, based on the semivariogram models shown in Figure 85.7a.

features are far fewer and much less pronounced (which is due in part to their larger nuggets—Figure 85.7b), and the large-scale features consist of randomly positioned ''hills and valleys'' rather than a sequence of parallel ridges and troughs. Note also the approximate inverse relationship between the ln K_{fs} and θ_a surfaces (see Figure 85.8), and between the ln OC and Cly surfaces (see Figure 85.9), i.e., large ln K_{fs} or ln OC generally corresponds with low θ_a or Cly. This occurs because of strong negative correlations ($P < 0.0001$) for ln K_{fs} versus θ_a and for ln OC versus Cly.

Step 5. Application of semivariograms and kriged surfaces. As mentioned above, the information provided by the semivariograms and kriged surfaces has several practical applications. For example, the standardized semivariograms (see Figure 85.7) indicate that K_{fs} and θ_a at the 35–50 cm depth in the paddock field site have a very strong spatial structure

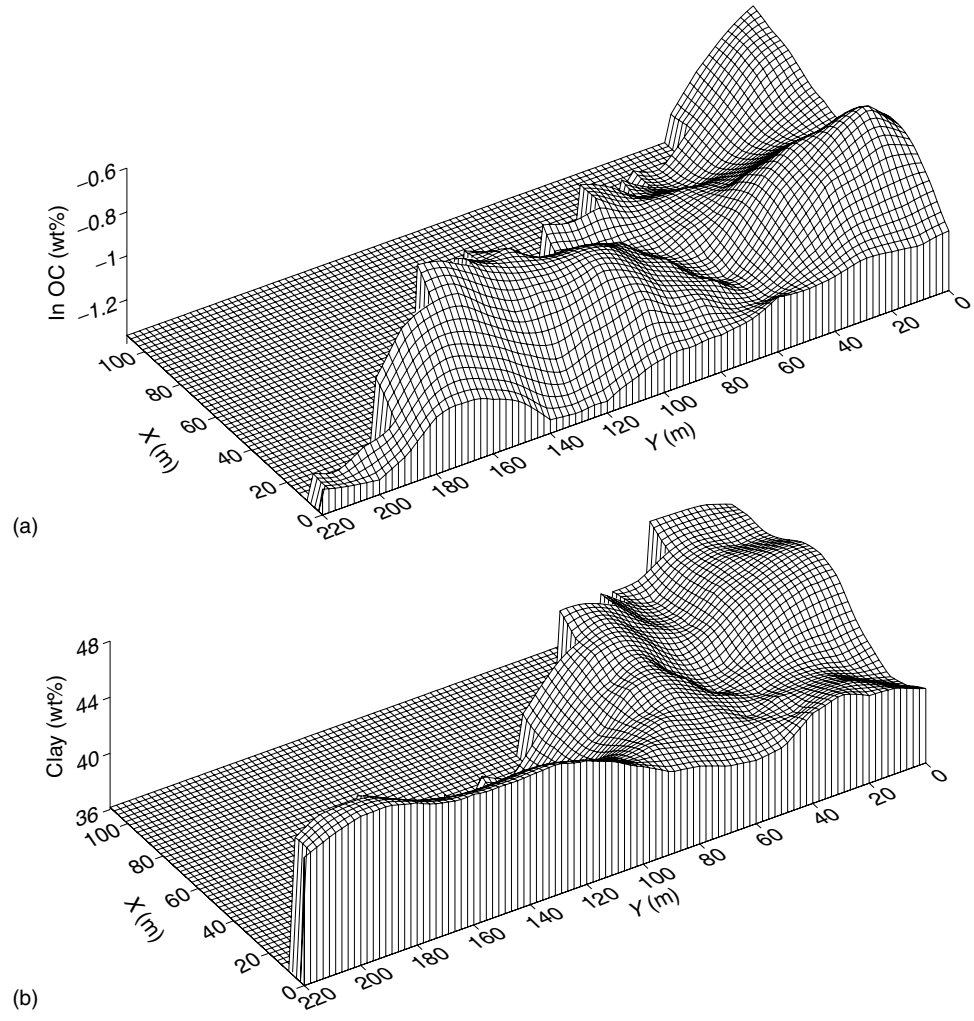

FIGURE 85.9. Kriged surfaces for (a) log organic carbon content, ln OC, and (b) clay content, Cly, based on the semivariogram model shown in Figure 85.7b.

(i.e., $V_N/V_S = 16.7\%$), whereas OC and Cly have a weak spatial structure ($V_N/V_S = 83.3\%$). Hence, K_{fs} and θ_a at the 35–50 cm depth are much less randomly distributed across the field site than OC and Cly. Furthermore, measurements of K_{fs} and θ_a must be at least 70–80 m apart before they are admissible for Fisher-type statistical analysis, while measurements of OC and Cly need to be at least 50 m apart. The kriged surface for ln K_{fs} (see Figure 85.8a) shows two distinct ''plateaus'' of high and relatively uniform K_{fs} and two distinct ''troughs'' of low K_{fs}. This type of information would be essential for understanding the drainage characteristics of the field site, for designing the optimum tile drainage network, and for locating experimental subplots requiring uniform K_{fs}. Similarly, the kriged surface for θ_a (Figure 85.8b) shows a ''plain'' of relatively uniform low water content (presumably due to extensive soil macrostructure) at about $X = 0$–110 m, $Y = 0$–35 m, and a ''plateau'' of relatively uniform high water content (presumably due to reduced soil macrostructure)

at about $X = 0–70$ m and $Y = 70–100$ m. Such information would be necessary for optimum location of experimental subplots requiring relatively uniform antecedent soil water content, soil macrostructure, or soil aeration. The kriged surface for ln OC (see Figure 85.9a), on the other hand, indicates that there are no areas at the 35–50 cm depth with uniform soil OC content, whereas the kriged surface for Cly (see Figure 85.9b) indicates only two small areas of relatively uniform clay content: one at about $X = 60–110$ m and $Y = 0–30$ m and other at about $X = 40–80$ m and $Y = 60–80$ m. Hence, experiments requiring spatially uniform soil OC content or clay content at the 35–50 cm depth might be inadvisable at this site.

85.10 COMMENTS

1 Stationarity and approximate normality of the frequency distributions are critical dataset requirements for the semivariogram and autocorrelation functions, as nonstationarity and substantial nonnormality render the nugget, sill, range, and autocorrelation values difficult to interpret. Datasets that cannot be normalized because of extreme skews and/or the presence of negative or zero values may still be analyzable using the indicator semivariogram approach (see Section 85.5; Isaaks and Srivastava 1989; Goovaerts 1997).

2 Calculate the omnidirectional variogram before directional variograms. There is no reason to expect structure in the directional variograms if the omnidirectional variogram is very noisy.

3 If the dataset has limited nonstationarity or contains outliers, the ''robust'' semivariogram analysis (Cressie 1993; Lark 2000) or ''madogram'' analysis (Deutsch and Journel 1998) can be used to obtain an estimate of range and anisotropy.

4 Semivariogram nugget, range, and sill are most accurately determined when there is a relatively uniform distribution of small sampling intervals and large sampling intervals.

5 If the dataset is quite small, unbiased semivariogram model parameters are best obtained by fitting to the semivariogram map, rather than to the semivariogram (Faulkner 2002).

6 For second-order stationary data, autocovariance, autocorrelation, and semivariance are essentially equivalent for illustrating spatial or temporal structure. However, semivariance is usually more useful as it can also be used (via semivariogram models and kriging) to generate theoretically defensible plots of parameter variation over space or time (e.g., Figure 85.8 and Figure 85.9).

7 Although not yet used extensively, bivariate and multivariate spatial/temporal analyses (e.g., cokriging, cross-variograms) are proving increasingly useful for estimating difficult soil parameters and for determining how two or more soil processes are interrelated. For example, cokriging can provide a means for using a soil property that is easily measured to improve the spatial estimate of a correlated soil property that is very difficult to measure, or only sparsely measured. Cross-variogram analysis, on the other hand, can show how the variability of one soil parameter relates to the variability of another parameter

(e.g., Figure 85.3b). A good introduction to the application of cokriging and cross-variograms in the soil and agricultural sciences is given in Nielsen and Wendroth (2003).

8 Although cross-validation, jack-knifing, and statistical criteria have the important advantages of being objective and repeatable, they are also limited in that they can neither directly assess how well the models represent the sill and nugget nor assess the accuracy of the models at the semivariogram origin (see Goovaerts 1997). Hence, some practitioners recommend that model selection should be based on subjective, study-specific criteria. For example, if the purpose is to obtain a kriging interpolation, the best semivariogram model depends on the kriging neighborhood, as it is essential to obtain a good variogram model fit for the lag distances being used in the kriging matrix.

REFERENCES

Alfaro, M. 1980. The random coin method: solution of the problem of the simulation of a random function in the plane. *Math. Geol.* 12: 25–32.

Barnes, R.J. 1991. The variogram sill and the sample variance. *Math. Geol.* 23: 673–678.

Cambardella, C.A., Moorman, T.B., Novak, J.M., Parkin, T.B., Karlen, D.L., Turco, R.F., and Konopka, A.E. 1994. Field-scale variability of soil properties in central Iowa soils. *Soil Sci. Soc. Am. J.* 58: 1501–1511.

Cressie, N. 1985. Fitting variogram models by weighted least squares. *J. Int. Assoc. Math. Geol.* 17: 563–586.

Cressie, N. 1991. *Statistics for Spatial Data*, 1st ed. John Wiley & Sons, New York.

Cressie, N. 1993. *Statistics for Spatial Data*, 2nd ed. John Wiley & Sons, New York.

Deutsch, C.V. and Journel, A.G. 1998. *GSLIB Geostatistical Software Library and User's Guide*, 2nd ed. Oxford University Press, New York.

Fagroud, M. and van Meirvenne, M. 2002. Accounting for soil spatial autocorrelation in the design of experimental trials. *Soil Sci. Soc. Am. J.* 66: 1134–1142.

Faulkner, B.R. 2002. Java classes for nonprocedural variogram modeling. *Comput. Geosci.* 28(3): 387–397.

Goovaerts, P. 1997. *Geostatistics for Natural Resources Evaluation*. Oxford University Press, New York.

Goovaerts, P. and Chiang, C. 1993. Temporal persistence of spatial patterns for mineralizable nitrogen and selected soil properties. *Soil Sci. Soc. Am. J.* 57: 397–414.

Gotway, C.A. 1991. Fitting semivariogram models by weighted least squares. *Comput. Geosci.* 117: 171–172.

Hawkins, D.M. 1980. *Identification of Outliers*. Chapman and Hall, London, UK.

Isaaks, E. and Srivastava, R. 1989. *An Introduction to Applied Geostatistics*. Oxford University Press, Oxford, New York.

Jongman, R.H.G., Ter Braak, C.J.F., and van Tongeren, O.F.R. 1995. *Data Analysis in Community and Landscape Ecology*, 2nd ed. Cambridge University Press, Cambridge, UK.

Kachanoski, R.G., Rolston, D.E., and de Jong, E. 1985. Spatial and spectral relationships of soil properties and microtopography: I. Density and thickness of A horizon. *Soil Sci. Soc. Am. J.* 49: 804–812.

Kitanidis, P. 1997. *Introduction to Geostatistics—Applications in Hydrosciences*. Cambridge University Press, New York.

Koopmans, L.H. 1974. *The Spectral Analysis of Time Series*. Academic Press, New York, 366 pp.

Lambert, D.M., Lowenberg-Deboer, J., and Bongiovanni, R. 2004. A comparison of four spatial regression models for yield monitor data: a case study from Argentina. *Precis. Agr*. 5: 579–600.

Lark, R.M. 2000. A comparison of some robust estimators of the variogram for use in soil survey. *Eur. J. Soil Sci*. 51: 137–157.

Matheron, G. 1962. Traité de Géostatistique Appliqué, Tome 1. Memoires du Bureau de Recherches Géologiques et Minières, Paris.

McBratney, A.B. and Webster, R. 1986. Choosing functions for semivariograms of soil properties and fitting them to sampling estimates. *J. Soil Sci*. 37: 617–639.

Morisette, J. 1997. Examples using SAS to fit the model of linear coregionalization. *Comput. Geosci*. 23 (3): 317–323.

Nielsen, D.R. and Wendroth, O. 2003. *Spatial and Temporal Statistics: Sampling Field Soils and Their Vegetation*. Catena Verlag GMBH, Reiskirchen, Germany, 398 pp.

Olea, R.A. 1999. *Geostatistics for Engineers and Earth Scientists*. Kluwer Academic Publishers. Boston, MA.

Pannatier, Y. 1996. *VARIOWIN: Software for Spatial Data Analysis in 2D*. Springer-Verlag, New York.

Papritz, A. and Dubois, J.P. 1999. Mapping heavy metals in soil by (non-) linear kriging: an empirical validation. In J. Gómez-Hernández, A. Soares, and R. Froidevaux, Eds. *geoENV II—Geostatistics for Environmental Applications*. Kluwer Academic Publishing, Dordrecht, The Netherlands, pp. 429–440.

Prakash, M.R. and Singh, V.S. 2000. Network design for groundwater monitoring—a case study. *Environ. Geol*. 39: 628–632.

Press, W.H., Teukolsky, S.A., Vetterling, W.T., and Flannery, B.P. 1992. *Numerical Recipes in C. The Art of Scientific Computing*. Cambridge University Press, New York.

Rossi, R.E., Mulla, D.J., Journel, A.G., and Franz, E.H. 1992. Geostatistical tools for modeling and interpreting ecological spatial dependence. *Ecol. Monogr*. 62: 277–314.

Si, B.C. 2003. Spatial and scale-dependent soil hydraulic properties: a wavelet approach. In Y. Pachepsky, D.E. Radcliffe, and H.M. Selim, Eds. *Scaling Methods in Soil Physics*. CRC Press, New York, pp. 163–178.

Si, B.C. and Farrell, R.E. 2004. Scale-dependent relationship between wheat yield and topographic indices: a wavelet approach. *Soil Sci. Soc. Am. J*. 68: 577–587.

Si, B.C. and Zeleke, T.B. 2005. Wavelet coherency to relate soil saturated hydraulic conductivity and physical properties. *Water Resour. Res*. 41: 11. Doi.10.1029/2005WR004118.

Vieira, S.R., Reynolds, W.D., and Topp, G.C. 1988. Spatial variability of hydraulic properties in a highly structured clay soil. In P.J. Wierenga and D. Bachelet, Eds. *Validation of Low and Transport Models for the Unsaturated Zone: Conference Proceedings*. May 23–26, 1988, Ruidoso, NM, pp. 471–483.

Webster, R. 1977. Spectral analysis of gilgai soil. *Aust. J. Soil Res*. 15: 176–194.

Yates, T., Si, B.C., Farrell, R.E., and Pennock, D. 2006. Probability distribution and spatial dependence of nitrous oxide emission: temporal change in hummocky terrain. *Soil Sci. Soc. Am. J*. 70: 753–762.

Zeleke, T.B. and Si, B.C. 2004. Scaling properties of topographic indices and crop yield: multifractal and joint multifractal approaches. *Agron. J*. 96: 1082–1090.

Zeleke, T.B. and Si, B.C. 2005. Scaling relationships between saturated hydraulic conductivity and soil physical properties. *Soil Sci. Soc. Am. J*. 69: 1691–1702.

Zeleke, T.B. and Si, B.C. 2006. Characterizing scale-dependent spatial relationships between soil properties using multifractal techniques. *Geoderma* 134: 440–452.

Appendix A

Site Description

G.T. Patterson
Agriculture and Agri-Food Canada
Truro, Nova Scotia, Canada

J.A. Brierley
Agriculture and Agri-Food Canada
Edmonton, Alberta, Canada

A1 INTRODUCTION

A site description is a record of observations for a specific locale, where soil and landscape attributes are to be evaluated. A site can be of any size ranging from under a square meter to several square kilometers or more in extent.

The amount of data recorded at a site as well as the required precision is dependent upon the purpose of the project. The purpose also determines the selection of an appropriate site. For example, demonstration plots must be easily accessible and preferably visible from the road (Maguire and Jensen 1997). Although there are exceptions, sites are generally chosen to be representative of a typical soil–climate–landscape situation.

Information about the site serves as the link between the actual location, associated landscape and soil characteristics, and corresponding relevance of the samples. A site description provides the context for the various soil properties to be analyzed and may help in the final evaluation and interpretation of analytical results (North Dakota State University [NDSU] Extension Service 1998; Schoeneberger et al. 2002). A good site description also defines how information gained at one location can be extrapolated to other areas.

Site information can be classified into three categories: basic sampling data, such as (a) who did the sampling, where, when, and why; (b) information about the landscape; and (c) a summary of the soil horizon data (Soil Survey Staff 1951; Taylor and Pohlen 1962; Walmsley et al. 1980; Day 1983; Knapik et al. 1988; USDA 2002). As mentioned previously, the specific site attributes collected depend upon the nature of the project, and thus

there can be no definitive list. However, as a minimum, the first two categories should be always included. If the results of a study are to be scaled-up to broader areas or interpreted within a regional context, then soil horizon data are necessary in order to apply soil classification systems (Soil Survey Staff 1975; Webster and Butler 1976; Soil Classification Working Group 1998).

Various methods are available for measuring site attributes. Consider location, for example. Latitude–longitude measurements of location based upon National Topographic Survey maps may be appropriate at the national level, while legal descriptions might be more appropriate at the farm level. Where more precise location coordinates are required, geographic positioning systems (GPS) are readily available devices for accurately locating a site (latitude, longitude, and elevation) to within submeter confidence. The list of GPS Web sites at the end of this chapter is a sample of what is available; it is not an endorsement of one product over another.

All site data are not necessarily measured in the field. Soil survey reports, surficial, and bedrock geology maps, hydrology reports can provide valuable background information on the landscape and associated soils.

A2 SITE ATTRIBUTES

Tables A1 through A3 provide a list of site attributes applicable to soil-related studies. Table A1 is a list of basic information related to sample site and sampling method. Landscape and soil profile attributes are listed in Table A2 and Table A3, respectively.

TABLE A1. A List of Basic Sampling Data

Project ID
Regional setting
1. Purpose, e.g.,
   a. Fertility status
   b. Environmental assessments (well-site, pipeline)
   c. Long-term monitoring
2. Location, e.g.,
   a. Latitude–longitude
   b. Legal description
   c. Latitude–longitude in decimal degrees (GPS)
3. Sampling plan, e.g.,
   a. Random
   b. Grid
   c. Purposeful
   d. Single/composite
4. Sampling date
5. Name of sampler
6. Sampling method, e.g.,
   a. Probe or auger
   b. Core
7. Horizon or depth sampled
8. Vegetative cover (native, crop)

TABLE A2. A List of Landscape Attributes

1. Ecological setting
2. Climate
3. Land use
4. Landform
5. Parent material
   a. Particle size
   b. Mode of deposition including petrology
6. Topography
   a. Aspect
   b. Elevation
   c. Steepness of slope
   d. Slope length
   e. Shape/curvature
   f. Site position
   g. Slope pattern
7. Soil moisture regime (e.g., drainage, seepage, perviousness)
8. Stoniness class
9. Rockiness class
10. Flooding events

TABLE A3. A List of Soil Profile Attributes

1. Thickness of layers/horizons
2. Organic layers
   a. Thickness
   b. Organic material composition
   c. von Post scale of decomposition
3. Depth to free carbonates
4. Depth to saline conditions
5. Depth to water table
6. Depth to bedrock
7. Rooting zone
   a. Thickness
   b. Particle size
8. Root-restricting layer
   a. Thickness
   b. Kind
   c. % Area affected

REFERENCES

Day, J.H. Ed. 1983. The Canada Soil Information System (CanSIS). Manual for describing soils in the field. Expert Committee on Soil Survey. LRRC #82-52. Ottawa, Canada, 97 pp.

GPS Web sites (last verified January 2007). http://www.trimble.com/gps http://www.garmin.com./about GPS/ http://www.omnistar.com

Knapik, L.J., Russell, W.B., Riddell, K.M., and Stevens, N. 1988. Forest Ecosystem Classification and Land System Mapping Pilot Project. Duck Mountain, Manitoba. Canadian Forest

Services and MB Forest Br., Ottawa, Canada 129 pp.

Maguire, T. and Jensen, T. 1997. Guide to Field Experimentation in Agriculture: Site Location. Last verified January, 2007. http://www1.agric.gov.ab.ca/$department/deptdocs.nsf/all/sag3025

North Dakota State University (NDSU) Extension Service 1998. Soil sampling as a basis for fertilizer application. Last verified January 2007. http://www.ext.nodak.edu/extpubs/plantsci/soilfert/sf-990-3.htm

Schoeneberger, P.J., Wysocki, D.A., Benham, E.C., and Broderson, W.D. Eds., 2002. Field Book for Describing and Sampling Soils, Version 2.0. Natural Resources Conservation Service, National Soil Survey Center, Lincoln, NE.

Soil Classification Working Group. 1998. The Canadian System of Soil Classification. Agriculture and Agri-Food Canada Publication, 1646 (Revised), Ottawa, Canada. 187 pp.

Soil Survey Staff. 1951. Soil Survey Manual. SCS. U.S. Department of Agriculture Handbook 18, Washington, DC, 503 pp.

Soil Survey Staff. 1975. Soil Taxonomy. SCS. U.S. Department of Agriculture Handbook 436, Washington, DC, 754 pp.

Taylor, N.H. and Pohlen, I.J. 1962. Soil Survey Method. A New Zealand Handbook for the Field Study of Soils. Soils Bureau Bulletin 25. Taita Exp. Sta., Hutt Valley, New Zealand. 241 pp.

USDA. 2002. Field Book for Describing and Sampling Soils. National Soil Survey Centre, Resources Conservation Service. Washington, DC, 228 pp.

Walmsley, M., Utzig, G., Vold, T., Moon, D., and van Barneveld, J. 1980. Describing Ecosystems in the Field. RAB Technical Paper 2. Land Management Report No. 7. Ministry of Environment and Ministry of Forests, Victoria, BC, Canada. 224 pp.

Webster, R. and Butler, B.E. 1976. Soil Classification and survey studies and Ginninderra. *Aust. J. Soil Res.* 14: 1–24.

Appendix B
General Safe Laboratory Operation Procedures

P. St-Georges
Agriculture and Agri-Food Canada
Ottawa, Ontario, Canada

B1 GENERAL SAFETY PROCEDURES

Inform yourself:

- Consult the material safety data sheets (MSDS) to learn the hazards of each chemical (MSDS can be obtained from chemical suppliers).
- It is highly recommended (and may be mandatory) that all supervisors, employees, students, and volunteers get Workplace Hazardous Materials Information System (WHMIS) certification. This system informs workers of commonly used warning labels and symbols for chemicals and other agents used in the workplace.
- Follow all policies, regulations, and safety procedures (municipal, provincial/state, and federal) detailed for your workplace.
- Verify that the appropriate personal protection equipment (PPE) is available and used as prescribed.
- Special attention is required if there are any level 4 hazards listed on the chemical's National Fire Protection Association (NFPA) label regarding health (blue), fire (red), or reactivity (yellow). Level 4 hazards indicate extreme hazard potential. Special training or safety requirements must be attained before handling these chemicals.

Label chemical bottles and containers when received and opened, as per WHMIS guidelines. Most chemicals have a shelf life. Some of these chemicals may become unsafe and/or unstable after the expired date.

Ensure that there is an adequate supply of the reagents before starting any procedure.

Do not carry glass bottles only by the finger-ring on the neck of the bottle. This ring is meant to help grip bottle when pouring its contents. Transport the bottle using both hands or use an appropriate rubber/plastic bottle holder.

Store chemicals in an appropriate location as directed in MSDS. Pay special attention to noncompatible chemicals, shelf life, and ventilation. Make sure chemicals are properly labeled and an accurate chemical inventory is kept.

B2 BASES

General Characteristics and Precautions

Bases are caustic and some have low surface tensions, making them difficult to wash off.

Eye contact: Causes severe eye burns. May cause irreversible eye injury.

Skin contact: Causes skin burns. May cause deep, penetrating ulcers of the skin.

Ingestion: Causes gastrointestinal tract burns. May cause perforation of the digestive tract.

Bases and acids should be stored separately due to incompatibilities (i.e., potentially violent reaction).

Strong bases include the following: LiOH (lithium hydroxide), NaOH (sodium hydroxide), KOH (potassium hydroxide), RbOH (rubidium hydroxide), and CsOH (cesium hydroxide).

Unique Hazards

Ammonium Hydroxide

- Volatile: Produces ammonia fumes which are pungent and toxic. This chemical must be used in a fume hood.

Sodium Hydroxide, Lithium Hydroxide, and Potassium Hydroxide

- Substances are hygroscopic (i.e., absorb water from the atmosphere).
- Must be stored in plastic bottles since these bases can fuse glass.
- These bases are exothermic when dissolved/diluted with water. LiOH may boil if 10 *M* stock solution is made; NaOH and KOH will heat up significantly. There is a small risk of skin burns.

Sodium Hypochlorite (Bleach)

- Toxic if ingested in sufficient quantities.
- Avoid skin contact as this can cause irritation.
- Avoid inhaling excessive quantities of vapor.

- Strong oxidizer: This chemical has several incompatibilities (i.e., acids, ammonia-based compounds, hydrogen peroxide, and flammables).

B3 ACIDS

General Characteristics and Precautions

Most acids are volatile and produce acidic fumes.

Corrosive to most metals; this reaction can form explosive hydrogen gas.

Eye contact: Causes severe eye burns. May cause irreversible eye injury.

Skin contact: Causes skin burns. May cause deep, penetrating ulcers of the skin.

Ingestion: Causes gastrointestinal tract burns. May cause perforation of the digestive tract. Does not induce vomiting.

Inhalation: May be fatal if inhaled. Effects may be delayed. May cause irritation of the respiratory tract with burning pain in the nose and throat, coughing, wheezing, shortness of breath, and pulmonary edema.

Chronic effects: Repeated inhalation may cause chronic bronchitis.

Reacts exothermically with water, sometimes violently. Always add acid to water when making up solutions.

Store acids and bases separately.

Strong acids include: HCl (hydrochloric acid), HNO_3 (nitric acid), H_2SO_4 (sulfuric acid), HBr (hydrobromic acid), HI (hydroiodic acid), and $HClO_4$ (perchloric acid).

Unique Hazards

Acetic Acid

- Highly volatile: Strong pungent, vinegar-like odor.
- Flammable in its concentrated form (i.e., glacial).

Hydrochloric Acid

- Volatile: Releases toxic chlorine gas. Vapors are visible in high humidity.

Nitric Acid

- Strong oxidizer: Reacts violently with some chemicals.
- Volatile: Vapors are visible, especially in high humidity.

Sulfuric Acid

- Hygroscopic: Absorbs moisture from the air. Keep tightly sealed.
- Strong inorganic acid. Mists containing sulfuric acid may cause cancer.
- Sulfuric acid reacts vigorously, violently, or explosively with many organic and inorganic chemicals, and with water.

Formic Acid

- Flash Point is 69°C. Both liquid and vapor are combustible.
- Strong reducing agent: Fire and explosion risk if in contact with oxidizing agents. Keep refrigerated. (Store below 4°C.)
- Lachrymator (i.e., a substance that produces the flow of tears).

Hydrofluoric Acid

- Poison, Extremely hazardous liquid and vapor. Special safety training recommended.
- Neutralizing HF gel (2.5% calcium gluconate gel) must be kept on your person both at and away from the workplace. A person's reaction to exposure may be delayed by 8 h or longer, depending on the concentration of the acid. Fluoride ions readily penetrate skin, causing deep tissue and bone damage and can be fatal. Any exposure requires hospital care, even after neutralizing gel application.
- Hydrofluoric acid must be stored in plastic bottles, since HF can dissolve glass.

B4 FLAMMABLES AND COMBUSTIBLES

General Characteristics and Precautions

These substances can result in a fire or explosion if in contact with a heat or ignition source.

Most flammables are volatile and considered to be toxic. Many flammable solvents affect the central nervous system.

To avoid potential contact with ignition sources, it is important to determine whether fumes are lighter or heavier than air (e.g., chloroform is heavier than air, while natural gases are lighter than air).

Some flammables can become unstable through time due to peroxide formation, resulting in auto ignition (e.g., diethyl ether, tetrahydrofuran).

Safety Precautions

Store in a vented cabinet or room.

Store away from ignition, heat, or oxidizer sources (including sunlight and room heaters).

If flammables need to be stored cold, they must be stored in a fridge which has been specifically designed by the manufacture to be suitable for the storage of flammables. The fridge must be labeled as such.

Reduce routine handling of large volumes of flammable or combustible materials by dispensing into smaller WHMIS-labeled containers. Ensure that metal containers are grounded to prevent static discharge.

Dispense and use flammable or combustible materials in properly working fume hoods or well-ventilated areas. Certification of fume hoods is often mandatory to ensure that adequate airflow is available for safe working conditions.

Do not use the laboratory as a storage place. Return all containers to the volatile materials storage facility.

Store flammables separately from other chemicals: It is especially important to store flammables separately from oxidizers.

B5 COMPRESSED GAS CYLINDERS

General Characteristics and Precautions

Some gases support combustion (e.g., oxygen).

Some gases are flammable (e.g., acetylene, hydrogen, propane).

Some gases are asphyxiants (e.g., carbon dioxide, carbon monoxide).

All gases (except air and oxygen) can displace breathable air if they are exhausted into nonvented, closed areas.

Incorrect use of pressure regulators can cause fires or explosions.

High temperatures can cause a buildup of pressure in cylinders.

Safety Precautions

Label all cylinders clearly. Do not use a cylinder if its contents cannot be unequivocally identified.

Keep all unused cylinders well sealed.

Use appropriate PPE while handling cylinders.

Ventilate storage areas.

Secure cylinders individually by using chains or straps.

Do not store cylinders near open flame or heat source.

Ground all flammable gas cylinders.

O_2 (oxygen) tanks: Ensure all surfaces on the tank and regulator are absolutely free of grease or any other lubricant.

Transportation of Gas Cylinders

The appropriate cap must be in place.

Person(s) transporting the cylinder should wear gloves and safety shoes or boots (steel-toed or equivalent).

Prior to transport: Ensure that suitable tie-down chains or straps are available immediately upon arrival at the destination place.

Use freight elevators (where available) to transport cylinders.

Person(s) transporting compressed gases in vehicles often requires specific (and mandatory) training and licensing.

Connection of Pressure Regulators

Once the cap has been removed from the cylinder, inspect the threads for damage and dirt. Do not use any cylinder or regulator if the threads have been damaged. Use a cloth to clean any dirt or grease from the threads.

Use only the pressure regulator which has been designed for the particular cylinder and type of gas. Regulators and gas cylinders are designed so that the fittings (compressed gas association, CGA fittings) are unique and must match. If the fittings are correct, they will matchup and assemble easily. Do not use force when putting fittings together.

Prior to opening the regulator, turn off the low-pressure side of the regulator. Do this by turning the valve counter clockwise. Failure to turn off the low-pressure side may force the high-pressure gas into the low-pressure side, resulting in explosion.

When opening the high-pressure side, a person should face away from the valve gauges. Open the valves slowly. An explosion could result if the regulator malfunctions, letting high-pressure gas enter the low-pressure side of the valve.

Check for leaks in fittings by applying a leak detection solution (e.g., warm soapy water).

Do not direct the compressed gas towards your body or any other person's body.

If using multiple compressed gases, consider labeling (e.g., color coding) the gas lines.

When a cylinder is empty, it must be labeled as such. If returning a partially used cylinder to the supplier, the cylinder must be labeled as being partially full.

B6 PATHOGENS AND VECTORS

General Characteristics and Precautions

Precautions are primarily related to human pathogens from untreated fecal waste (e.g., *E. coli*).

Workspace (laboratory) areas should have restricted access, in order to limit traffic flow.

Antibiotics are often used in labs handling pathogens. Antibiotics should be treated as if they were toxic.

Most microbes can form airborne particles and therefore should be handled in fume hoods.

Avoid skin and eye contact. Wear appropriate PPE. Wash hands frequently. Lab coats used in these areas should be restricted to the laboratory in order to quarantine potentially dangerous microbes.

Safety Precautions

Lab coats should be dedicated to this workspace and never leave the lab without being autoclaved or disinfected.

Lab strains of *E. coli* are attenuated (i.e., weakened) and therefore not pathogenic; however, care should be taken to avoid any contamination of these organisms, including direct skin contact, inhalation, or ingestion.

All bacteria, including transgenic lines (e.g., carrying an antibiotic resistance gene), must be maintained and handled in an aseptic manner to avoid environmental contamination.

Before disposal, organisms must be killed using a suitable procedure (such as bleach, autoclaving, or 70% ethanol). Workspace and equipment should be decontaminated or sterilized at the end or between procedures. If in doubt, consult your laboratory supervisor.

Before lighting a Bunsen burner, make sure that there are no open flammable chemicals in the vicinity. If diethyl ether is being used anywhere in the laboratory, burners must not be used at all.

BIBLIOGRAPHY

Canadian Centre for Occupational Health and Safety (CCOHS). 2006. Occupational health and safety resource. Available at: www.ccohs.ca/ (verified 14 July 2006). 135 Hunter St. East, Hamilton, ON, Canada.

Health Canada. Environment and Workplace Health—WHMIS guidelines. Available at: www.hc-sc.gc.ca/ewh-semt/occup-travail/whmis-simdut/index_e.html (last updated 12 June 2006; verified 14 July 2006). 1010 Somerset St. West, Ottawa, ON, Canada.

National Fire Protection Association (NFPA). 2006. Frequently asked questions (FAQs) dealing with NFPA 704—addressing the labeling of hazardous materials for health, flammability, reactivity and special related hazards. Available at: www.nfpa.org/faq.asp?categoryID = 928 (verified 14 July 2006). 1 Batterymarch Park, Quincy, MA.

Public Health Agency of Canada. 1996. Laboratory Biosafety Guidelines, 2nd Edition 1996. Available at: www.phac-aspc.gc.ca/publicat/lbg-ldmbl-96 (last updated 10 June 1996; verified 14 July 2006). 130 Colonnade Rd., Ottawa, ON, Canada.

Shugar, G.J. and Ballinger, J.T. 1996. Chemical Technicians Ready Reference Handbook. McGraw-Hill, Inc., New York.

Windholz, M., Budavari, S., Blumetti, R.F., and Otterbein, E.S. 1983. The Merck Index, Merck and Co., Inc., Rahway, NJ.

Index

INDEX

I

K

L

M

N

O

Q

R

S

T

U

V